



Introduction

The FeSBE Annual Meeting is one of the most traditional events in Brazilian science. We will have an attractive congress for scientists from different fields who are looking for the latest news in their respective field. But we also invite who are interested in the more general and comprehensive framework of the biological sciences. This will be the 34th FeSBE meeting and the themes will cover Cellular Biology, Biophysics, Biochemistry, Molecular Biology, Nuclear Biosciences, Endocrinology, Physiology, Pharmacology, Immunology, Clinical Research and Neurosciences. In addition, the 2019 FeSBE will host the “3rd Australia-Brazil-Chile Regenerative Medicine and Developmental Biology Symposium”.

Hernandes F. Carvalho
President of FeSBE

INDEX

Organization	03
General Announcements.....	05
3 rd Symposium ABC	06
FeSBE Jovem 2019	09
Program Schedule	12
Program.....	13
Poster Session I - Sept.10.2019.....	34
Poster Session II - Sept.11.2019	115
Poster Session III - Sept.12.2019	179
Author Index	243

Organizing Committee

FeSBE Board of Directors

Hernandes F. Carvalho
President of FeSBE

Claudia do Ó Pessoa
1° Vice-President of FeSBE

João Gustavo P. Amarante-Mendes
2° Vice-President of FeSBE

Ana Paula Couto Davel
1st Secretary FeSBE

Marcel Frajblat
2nd Secretary FeSBE

Ana Carolina T. Takakura
Treasurer FeSBE

Presidents of FeSBE Affiliated Societies

Augusto Paranhos
President of BRAVO

Patrícia Gama
President of SBBC

Antônio Jose da Costa Filho
President of SBBf

Sílvia Maria Velasques de Oliveira
President of SBBN

Selma Maria Bezerra Jerônimo
President of SBBq

Eduardo Colombari
President of SBFis

André Sampaio Pupo
President of SBFTE

Claudia Ida Brodskyn
President of SBI

Adriana Castello Costa Girardi
President of SBIC

Anderson Manoel Herculano
President of SBNeC

Juliana da Silva
President of MutaGen-BRASIL

Célio Fernando De Sousa Rodrigues
President of SBA

Luis Mochizuki
President of SBB

Ekaterina Akimovna Botovchenco Rivera
President of SBCAL

Maria Izabel Chiamolera
President of SBEM

Daniel Lorscheitter Baptista
President of SBMM

José Roberto Machado e Silva
President of SBP

Edmundo Carlos Grisard
President of SBPz

Tânia Marcourakis
President of SBTox

Yara Cury
President of SBTx

Fernando Rosado Spilki
President of SBV

Luciane Marinoni
President of SBZ

FeSBE former Presidents

1985-1987 Eduardo Moacyr Krieger
1987-1989 Eduardo Moacyr Krieger
1989-1991 Eduardo Moacyr Krieger
1991-1993 Sergio Henrique Ferreira
1993-1995 Sergio Henrique Ferreira
1995-1997 Dora Fix Ventura
1997-1999 Dora Fix Ventura
1999-2001 Dora Fix Ventura
2001-2003 Antonio Carlos Campos de Carvalho
2003-2005 Gerhard Malnic
2005-2007 Gerhard Malnic
2007-2009 Luiz Eugenio Araujo de Moraes Mello
2009-2011 Luiz Eugenio Araujo de Moraes Mello
2011-2013 Walter Araújo Zin
2013-2015 Walter Araújo Zin
2015-2017 Dalton Valentim Vassallo

Financial support

Conselho Nacional de Desenvolvimento Científico e Tecnológico (CNPq)

Coordenação de Aperfeiçoamento de Pessoal de Nível Superior (CAPES)

Fundação de Amparo à Pesquisa do Estado de São Paulo (FAPESP)

Secretary

FeSBE - Federação de Sociedades de Biologia Experimental
USP - ICB III, Av. Prof. Lineu Prestes 2415
CEP 05508-000, São Paulo, SP
Fone: (11) 3091-7369 e 3814-8266
Weber Minoru Yoshioka
weber@fesbe.org.br

Event organization

CWY Eventos
Cristiane Yoshizato
Email: fesbe@cwyeventos.com.br

Support

Science Pro

KLONELIFE

Brain Support

ADInstruments

ALESCO

General Announcements

Secretaria / Secretary

O horário de funcionamento da Secretaria do Congresso é das 08h00 às 18h00. Haverá entrega do crachá para os pré-inscritos e novas inscrições serão realizadas durante todo o Congresso. Somente será permitida a entrada no local do evento de posse do crachá de identificação. Em caso de extravio, será cobrada uma taxa de emissão de 2ª via do crachá. Entre os dias 09 a 13 de setembro de 2019, a Secretaria da FeSBE atenderá apenas no Campos do Jordão Convention Center, Av. Macedo Soares, 499 – Capivari, Campos do Jordão-SP.

FeSBE secretary will be working from 8:00 am to 6:00 pm on September 09 - 13 2019 at Campos do Jordão Convention Center, Av. Macedo Soares, 499 – Capivari, Campos do Jordão-SP. Check-in will be available during secretary hours. Meeting badge will be required for admittance in the event.

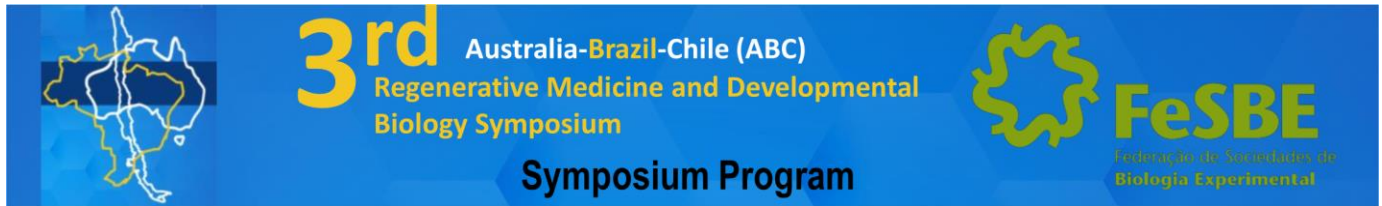
Cursos/ Courses

- Os cursos estão incluídos no valor da sua inscrição. Não é necessário fazer nenhum pagamento adicional.
 - Existem 2 Grupos de Cursos: os cursos do Grupo I serão ministrados no período da manhã (8:00 – 8:50h) e os cursos do Grupo II serão ministrados no período da (19:10-20:00h).
 - Cada congressista pode se inscrever em 1 curso do Grupo I e 1 curso do Grupo II.
 - Não é possível fazer dois cursos do mesmo Grupo. Não será possível trocar de curso no dia do evento.
 - Para receber o certificado de participação será necessário ter 100% de presença.
 - Tempo de Tolerância: 15 (quinze) minutos após o início do curso. Após esse tempo a presença não será registrada.
 - A programação completa de cada curso está disponível no site: <http://www2.fesbe.org.br/eventos/fesbe-anual-2019/>
 - Vagas limitadas!
-
- *There is no additional cost for Courses participation.*
 - *There are 2 groups of Courses: Group I in the mornings (8:00-8:50 am) and Group II in the afternoons (7:10-8:00 pm).*
 - *A maximum of two courses are allowed for each participant.*
 - *For the certificate a 100% presence is mandatory.*
 - *Limited vacancies.*
 - *For more information visit our website: <http://www2.fesbe.org.br/eventos/fesbe-anual-2019/>*

Certificados / Certificate

Certificados de participação geral, painéis e cursos estarão disponíveis no prazo de 10 dias nas áreas reservadas no sistema de inscrição durante 6 meses. Certificados de Menção Honrosa serão encaminhados por e-mail no prazo de 15 dias.

Certificates will be available on-line for 6 months. Awards certificate will be emailed in 15 days.



Day 1: Monday 9 September 2019

9:00 - 9:15 h - Opening Ceremony

Hernandes Carvalho (director FeSBE) and Silvio Tiziani (director External Strategy and Planning, Australian Regenerative Medicine Institute)

Session I: Genetic and molecular control of development and regeneration

Chair: Lucia Elvira Alvares (Unicamp, Brazil)

9:15 - 9:45 **“Telling a tale of tails: The Hox13 genes and the specification of the posterior vertebrae and tail in the zebrafish”**

Miguel Allende (FONDAP Center for Genome Regulation (CGR), Universidad de Chile, Chile)

9:45 - 10:15 **“Insights from Developmental Pathways on the Evolution of Snakelike phenotypes in Tetrapoda”**

Tiana Kohlsdorf (University of Sao Paulo - Ribeirao Preto, Brazil)

10:15 - 10:45 **“Deciphering the cardiac gene regulatory network”**

Mirana Ramialison (Australian Regenerative Medicine Institute, Australia)

10:45 - 11:15 Coffee Break

11:15 - 11:45 **“Gene regulation in early cell fate decisions and digit regeneration in mice”**

Henrique Marques Souza - University of Campinas (Unicamp)

11:45 - 12:15 **“When the inhibitor also helps: Cactus/I κ B protein function in Drosophila embryogenesis and immunity”**

Helena Araujo (Federal University of Rio de Janeiro, Brazil)

12:15 - 12:45 **“Effect of tRNA composition in ORF selection and proteostasis in Drosophila”**

Alvaro Glavic (Universidad de Chile, Chile)

12:45 - 14:30 Lunch

Session II: Nervous System development and regeneration

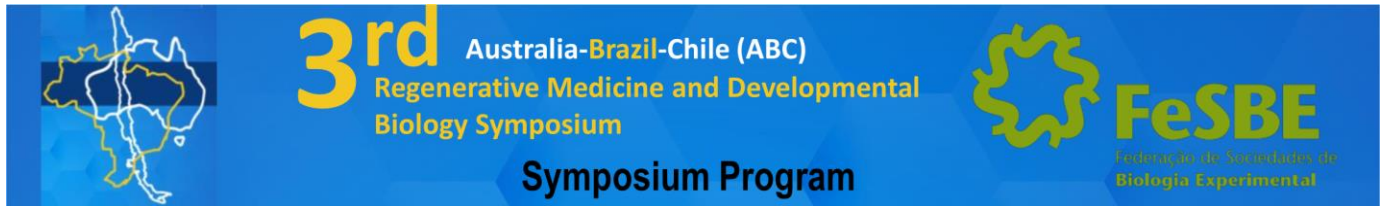
Chair: Alvaro Glavic (Universidad de Chile, Chile)

14:30 - 15:00 **“New insights on AP axis and neural induction”**

Jose Garcia Abreu Junior (Federal University of Rio de Janeiro, Brazil)

15:00 - 15:30 **“Pre and pos transcriptional regulation of cSCRATCH2 gene expression in neural embryogenesis”**

Irene Yan (University of Sao Paulo, Brazil)



15:30 - 16:00 Coffee Break

16:00 - 16:30 **"Make do and make new: how zebrafish rapidly regenerates CNS injury"**

Jan Kaslin (Australian Regenerative Medicine Institute, Australia)

16:30 - 17:00 **"Cellular and Molecular Mechanisms of Zebrafish Spinal Cord Regeneration"**

Hozana Castillo (Brazilian Biosciences National Laboratory (LNBio/CNPEN), Brazil)

18:00 - 18:30 FeSBE Opening Ceremony

18:30-19:30 - Plenary Conference

"Understanding skeletal muscle regeneration using zebrafish models"

Peter Currie (Australian Regenerative Medicine Institute, Australia)

Day 2: Tuesday 10 September 2019

Session III: Stem cells and disease

Chair: Laura Galvis (Institut NeuroMyoGène, France and Australian Regenerative Medicine Institute, Australia)

9:00 - 9:30 **"Can you model breast cancer using human induced pluripotent stem cells?"**

Andrew Laslett (Australian Regenerative Medicine Institute and Commonwealth Scientific and Industrial Research Organisation, Australia)

9:30 - 10:00 **"Stem cell therapy in lung diseases"**

Patricia Rocco (Federal University of Rio de Janeiro, Brazil)

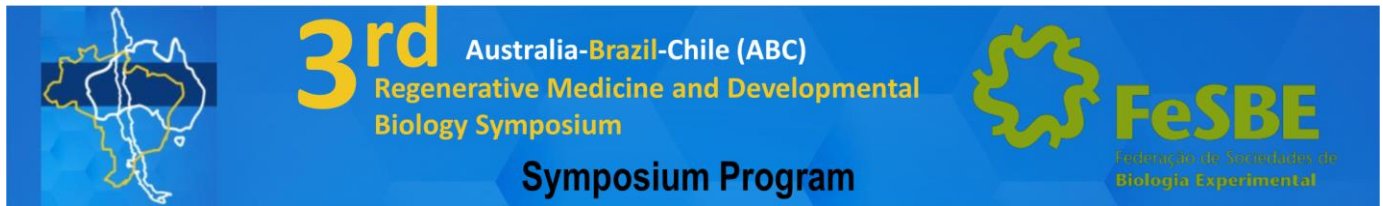
10:00 - 10:30 **"JAM-A is critical for HSC trafficking and maintenance of their quiescence in the stem cell niche"**

Susie Nilsson (Australian Regenerative Medicine Institute and Commonwealth Scientific and Industrial Research Organisation, Australia)

10:30 - 11:00 **"iPSC: a powerful modeling tool to study diseases"**

Bruno Torres (Brazilian Biosciences National Laboratory (LNBio/CNPEN), Brazil)

11:00 - 11:30 Coffee Break



11:30 - 12:30 FeSBE Plenary Conference

“What lies ahead of the frontier in cardiac development and evolution?”

José Xavier Neto – Federal University of Ceara (UFC)

12:30 - 14:30 Lunch

Session IV: **Molecular control of muscle development**

Chair: Hozana Castillo (Brazilian Biosciences National Laboratory, Brazil)

14:30 - 15:00 **“Sonic hedgehog signaling during chick myogenesis”**

Claudia Mermelstein (Federal University of Rio de Janeiro, Brazil)

15:00 - 15:30 **“Elucidating the role of Fgfr4 in skeletal muscle development and metabolism”**

Laura Galvis (Institut NeuroMyoGène, Université Claude Bernard, France and Australian Regenerative Medicine Institute, Australia)

15:30 - 16:00 **“DACT1 is a nucleocytoplasmic protein expressed during amniote myogenesis and modulated in human skeletal muscle disease”**

Lucia Alvares - University of Campinas (Unicamp)

16:00 - 18:00 Poster Session

18:00 - 18:30 Poster Prize Announcement and Closing Remarks



FESBE JOVEM 2019 - MEIO AMBIENTE E SAÚDE

Tradicionalmente, durante suas reuniões regionais e anuais, temos oferecido um espaço para estudantes do Ensino Médio, chamada de FeSBE Jovem, onde acontecem palestras com cientistas e apresentação de painéis, os quais são avaliados e premiados.

Para 2019, a proposta é abordar a temática Meio Ambiente e Saúde, contemplando a segunda competência da BNCC-EM. A unidade temática Vida e evolução propõe o estudo de questões relacionadas aos seres vivos (incluindo os seres humanos), suas características e necessidades, e a vida como fenômeno natural e social, os elementos essenciais à sua manutenção e à compreensão dos processos evolutivos que geram a diversidade de formas de vida no planeta. Estudam-se características dos ecossistemas destacando-se as interações dos seres vivos com outros seres vivos e com os fatores não vivos do ambiente, com destaque para as interações que os seres humanos estabelecem entre si e com os demais seres vivos e elementos não vivos do ambiente. Abordam-se, ainda, a importância da preservação da biodiversidade e como ela se distribui nos principais ecossistemas brasileiros.

Nos anos iniciais, as características dos seres vivos são trabalhadas a partir das ideias, representações, disposições emocionais e afetivas que os alunos trazem para a Escola. Esses saberes dos alunos vão sendo organizados a partir de observações orientadas, com ênfase na compreensão dos seres vivos do entorno, como também dos elos nutricionais que se estabelecem entre eles no ambiente natural. Nos anos finais, a partir do reconhecimento das relações que ocorrem na natureza, evidencia-se a participação do ser humano nas cadeias alimentares e como elemento modificador do ambiente, seja evidenciando maneiras mais eficientes de usar os recursos naturais sem desperdícios, seja discutindo as implicações do consumo excessivo e descarte inadequado dos resíduos. Contempla-se, também, o incentivo à proposição e adoção de alternativas individuais e coletivas, ancoradas na aplicação do conhecimento científico, que concorram para a sustentabilidade socioambiental. Assim, busca-se promover e incentivar uma convivência em maior sintonia com o ambiente, por meio do uso inteligente e responsável dos recursos naturais, para que estes se recomponham no presente e se mantenham no futuro.

Outro foco dessa unidade é a percepção de que o corpo humano é um todo dinâmico e articulado, e que a manutenção e o funcionamento harmonioso desse conjunto dependem da integração entre as funções específicas desempenhadas pelos diferentes sistemas que o compõem. Além disso, destacam-se aspectos relativos à saúde, compreendida não somente como um estado de equilíbrio dinâmico do corpo, mas como um bem da coletividade, abrindo espaço para discutir o que é preciso para promover a saúde individual e coletiva, inclusive no âmbito das políticas públicas.

Referência bibliográfica: Lei nº 13.415, de 16 de fevereiro de 2017. Define a Base Nacional Comum Curricular. Ministério da Educação, MEC, Brasília, DF, 2018.



PROGRAMA - FESBE JOVEM 2019

Quarta-feira, 11 de setembro de 2019

Sala 5

08:00 - 10:30 h - Curso

“A proteção do ser humano em situações de acidentes biológicos, químicos e radioativos e em ataques terroristas”

Módulo 01: **Aplicações da Física Nuclear e possíveis impactos para o ser humano**

Silvia Maria Velasques de Oliveira (Sociedade Brasileira de Biociências Nucleares)

10:30 - 11:30 h - Palestra

“Mudanças no cérebro e sua importância na aprendizagem escolar”

Lucianne Frigel (Universidade Federal Fluminense)

11:30 - 12:30 h - Conferência Plena

Vide programação geral da FeSBE

12:30 - 14:00 h - Intervalo para o almoço

14:00 - 16:00 h - Workshop CEPID-FAPESP

“Experimentação animal no estudo da obesidade e diabetes”

Centro de Pesquisa em Obesidade e Comorbidades (OCRC)

“Adote um cientista”

Centro de Terapia Celular (CTC)

16:00 - 18:00 h - Sessão de Painéis



Quinta-feira, 12 de setembro de 2019

Sala 5

08:00 - 10:30 h - Curso

“A proteção do ser humano em situações de acidentes biológicos, químicos e radioativos e em ataques terroristas”

Módulo 02: **Experiências de remediação do impacto ambiental em acidentes nucleares**

Horst Monken-Fernandes (Nuclear Energy Department/International Atomic Energy Agency)

10:30 - 11:30 h - Palestra

“Transgênicos e Biossegurança: O risco de comunicar mal o risco”

Natalia Pasternak (Universidade de São Paulo)

11:30 - 12:30 h - Conferência Plena

Vide programação geral da FeSBE

12:30 - 14:00 h - Intervalo para o almoço

14:00 - 16:00 h - Workshop CEPID-FAPESP

“Aula Tech 4.0: uma abordagem inovadora sobre tecnologia e saúde em sala de aula”

Centro de Pesquisa em Doenças Inflamatórias (CRID)

16:00 - 18:00 h - Sessão de Painéis

Sexta-feira, 13 de setembro de 2019

Sala 5

08:00 - 10:30 h - Curso

“A proteção do ser humano em situações de acidentes biológicos, químicos e radioativos e em ataques terroristas”

Módulo 03: **Como funcionam os laboratórios de Defesa Nuclear, Biológica, Química e Radiológica**

Edson Ramos de Andrade (Instituto de Engenharia Nuclear, IEN/CNEN)

10:30 - 11:30 h - Palestra

“Uma quimera chamada poluição”

Walter Araujo Zin (Universidade Federal do Rio de Janeiro)

Room 1

11:30 - 13:00 h - Cerimônia e Conferência de Encerramento/ Premiações

Vide programação geral da FeSBE

PROGRAM SCHEDULE

Monday - Sept.09.2019

9:00 - 17:00 - 3rd Australia-Brazil-Chile Regenerative Medicine and Developmental Biology Symposium
13:00 - 17:30 - “Escola de Ciências na FeSBE”
18:00 - 18:30 - Opening Ceremony
18:30 - 19:30 - Opening Lecture

Tuesday - Sept.10.2019

8:00-9:00 – Opening Session
9:00 - 11:30 - 3rd Australia-Brazil-Chile Regenerative Medicine and Developmental Biology Symposium
9:30 - 11:30 - Sessions
11:30 - 12:30 - Plenary Lecture
12:30 - 14:00 - Lunch
14:00 - 16:00 - Sessions
14:30 - 16:00 - 3rd Australia-Brazil-Chile Regenerative Medicine and Developmental Biology Symposium
16:00 - 18:00 - Poster Session I
18:00 - 19:00 - Lectures
19:10 - 20:00 - Courses II (1st class)

Wednesday - Sept.11.2019

8:00 - 9:00 - Courses I (1st class) / “FeSBE Jovem - 25 anos”
9:00 - 9:30 - Coffee Break
9:30 - 11:30 - Sessions / “FeSBE Jovem - 25 anos”
11:30 - 12:30 - Plenary Lecture
12:30 - 14:00 - Lunch
14:00 - 16:00 - Sessions / “FeSBE Jovem - 25 anos”
16:00 - 18:00 - Poster Session II
18:00 - 19:00 - Lectures
19:10 - 20:00 - Courses II (2nd class)
20:00 - 21:00 - FeSBE General Assembly

Thursday - Sept.12.2019

8:00 - 9:00 - Courses I (2nd class) / “FeSBE Jovem - 25 anos”
9:00 - 9:30 - Coffee Break
9:30 - 11:30 - Sessions / “FeSBE Jovem - 25 anos”
11:30 - 12:30 - Plenary Lecture
12:30 - 14:00 - Lunch / Technical Lecture
14:00 - 16:00 - Sessions / “FeSBE Jovem - 25 anos”
16:00 - 18:00 - Poster Session III
18:00 - 19:00 - Lectures
19:10 - 20:00 - Courses II (3rd class)

Friday - Sept.13.2019

8:00 - 9:00 - Courses I (3rd class) / “FeSBE Jovem - 25 anos”
9:00 - 9:30 - Coffee Break
9:30 - 11:30 - Sessions / Affiliated Societies Awards / “FeSBE Jovem - 25 anos”
11:30 - 13:30 - Closing ceremony and Awardees announcement

FeSBE Annual Meeting 2019
September 9- Monday

9:00-17:00 h – Symposium

Room 1

3rd Australia-Brazil-Chile Regenerative Medicine and Developmental Biology Symposium

“Understanding skeletal muscle regeneration using zebrafish models”

Peter Currie (Australian Regenerative Medicine Institute, Australia)

13:00-17:30 h – Escola de Ciências

Room 4

Escola de Ciências na FeSBE – Edição 2019

14:00-17:00 h – Cursos/Courses

Room 2

Marketing para cientistas: da bancada a concursos

Coordenador: Helder Nakaya (USP-SP)

Aula 1 - **Mitos e fatos na carreira científica**

Helder Nakaya (USP-SP)

Aula 2 - **Escrita científica e fazendo figuras impactantes**

Helder Nakaya (USP-SP)

Aula 3 - **Desenvolvendo sua carreira científica**

Helder Nakaya (USP-SP)

Room 3

Aspectos fisiológicos e comportamentais nas pesquisas com fêmeas

Coordenadora: **Fabiana C. Vilela Giusti** (UNIFAL-MG)

Aula 1 - **Aprendendo a trabalhar com fêmeas**

Bruna Kalil (UNIFAL-MG)

Aula 2 - **Lactação e comportamento materno**

Fabiana C. Vilela Giusti (UNIFAL-MG)

Aula 3 - **O funcionamento do sistema circadiano em fêmeas**

Maristela de Oliveira Poletini (UFMG)

18:00-19:30 h - FeSBE Opening Ceremony

Room 1

18:00-18:30 h

Opening Ceremony

18:30-19:30 h

Opening Lecture

FeSBE Annual Meeting 2019

September 10 - Tuesday

8:00-9:00 h – Opening Session

Room 2

Title: To be announced

Marcelo M Morales (SEFAE-MCTIC)

9:00-11:30 h – Symposium and Sessions

Room 1

3rd Australia-Brazil-Chile Regenerative Medicine and Developmental Biology Symposium

Room 2

Pharmacological changes in cell senescence and consequences for the aging process and neurodegenerative diseases

Chair: Tânia Viel (USP)

Cellular senescence is induced by the environmental neurotoxin paraquat and contributes to neuropathology linked to Parkinson's disease

Julie Kay Andersen (Buck Institute for Research on Aging)

Gedunin Inhibits Oligomeric A β 1-42-Induced Microglia Activation Via Modulation of Nrf2-NF- κ B Signaling

Shankar Chinta (Touro University)

Bradykinin treatment increased the longevity of hippocampal organotypic cultures from old mice

Hudson de Sousa Buck (FCMSCSP)

Translational evidence of microdose lithium effects for central nervous system healthy aging

Tânia Viel (EACH-USP)

Room 3

Advances in endocrine pancreas physiology and metabolic programming

Chair: Everardo Magalhães Carneiro (UNICAMP)

Advances and future perspectives for the study of the human pancreas

Alejandro Caicedo (University of Miami)

Metabolic programming and obesity

Patrícia Cristina Lisboa (UERJ)

OP: 04.027 - Characterization of the mouse lieno-pancreatic artery reactivity. Guizoni

DM, Carneiro EM, Davel AP - Departamento de Biologia Estrutural e Funcional – UNICAMP

OP: 07.036 - Early in vitro amino acid restriction leads to impairment of mitochondrial metabolism and reduction of pancreatic β cell viability when exposed to fatty acids. Araujo TR, Vettorazzi JF, Guimarães DSPSF, Carneiro EM - Biologia Funcional e Molecular - UNICAMP

Room 4

Heart failure-induced cardiorenal diseases: potential targets.

Chair: Adriana C. C. Girardi (InCor- HC-FMUSP)

Cardioprotection conferred by antidiabetic drugs in heart failure: a renal proximal tubule perspective.

Adriana C. C. Girardi (InCor-HC-FMUSP)

The potential benefits of exercise training on vascular disorders induced by heart failure

Luciana V. Rossoni (ICB-USP)

OP: 17.004 - New DPP-4 inhibitor attenuates metabolic disturbance and improves cardiovascular function in Zucker diabetic fatty rats. Montagnoli TL, Costa GC, Alencar AKN, Da Silva JS, Silva MMC, Alves BEO, Gamba LER, Lima LM, Barreiro EJ, Sudo RT, Zapata-Sudo G - Programa de Pós-graduação em Farmacologia e Química Medicinal – UFRJ; Programa de Pós-graduação em Cardiologia – UFRJ; Programa de Pesquisa em Desenvolvimento de Fármacos – UFRJ

OP: 08.015 - Endothelial function profiles in resistance arteries in two different mouse models orthologous to autosomal dominant polycystic kidney disease type 1. Dourado VC, Rossoni LV, Onuchic LF - Departamento de Fisiologia e Biofísica - USP, Departamento de Clínica Médica - USP

Room 5

Balance control and visual function: basic and applied approaches

Chair: Givago da Silva Souza (UFPA)

The role of the visual information in balance control

Ana Francisca Rozin Kleiner (UFSCar)

FeSBE Annual Meeting 2019

September 10 - Tuesday

Balance control in low-vision patients

Givago da Silva Souza (UFPA)

OP: 24.009 - The influence of visual functions on school performance of children. Silva FMC, Sousa MDR, Oliveira MC, Cortes MIT, Souza GS, Lacerda EMCB - Laboratório de Neurociência e comportamento - Ceuma Centro de Ciências da Saúde - UFMA Centro de Ciências da Saúde – UNIFAP; Núcleo de Medicina Tropical - UFPA

OP: 24.016 - Dark-adapted rod thresholds in Duchenne muscular dystrophy patients. Dias SL, Silva LA, Oliveira TA, Nagy BV, Zatz M, Pavanello R, Costa MF, Grossklaus LF, Barboni MTS, Ventura DF - Psicologia Experimental – USP; Centro de Pesquisa sobre o Genoma Humano e Células-Tronco – USP; Neurociências e Comportamento – USP; Setor de investigação de doenças neuromusculares – UNIFESP.

11:30-12:30 h - Plenary Lecture

Room 1

What lies ahead of the frontier in cardiac development and evolution?

Chair: Hernandez F. Carvalho (UNICAMP)

Speaker: José Xavier-Neto (UFC)

12:30-14:00 h – Lunch

13:00-14:00 h - Technical Lecture

Room 3

Quantitative 3D imaging, cell and tissue ultrastructure

Speaker: Tara Nylese (Thermo Fischer)

14:00-16:00 h – Symposium and Sessions

Room 1

3rd Australia-Brazil-Chile Regenerative Medicine and Developmental Biology Symposium

Room 2

Therapies with stem cells and extracellular vesicles in chronic degenerative diseases

Chair: Pedro Leme (UFRJ) / Patricia Rocco (UFRJ)

Therapies with stem cells and extracellular vesicles in respiratory diseases

Patricia Rocco (UFRJ)

Extracellular vesicles therapy in kidney diseases

Danilo Cândido de Almeida (UNIFESP/USP)

Stem cells therapy in pulmonary arterial hypertension: a new perspective

Pedro Leme (UFRJ)

Challenges for cardiac repair and regeneration after myocardial infarction

José Eduardo Krieger (Incor-HC-USP)

Room 3

Transgenics and Biosafety

Chair: Anibal E. Vercesi (UNICAMP)

Impacts of adopting OGMs

Edivaldo Velini (UNESP)

OGMs: a mobile target

Carlos Orsi (Instituto Questão de Ciência)

The risk of miscommunicating risks

Natalia Pasternak (ICB-USP)

History and importance of the Brazilian biosafety law

Walter Colli (IQ-USP)

Room 4

Several aspects of zebrafish as a research model

Chair: Maria Izabel Chiamolera (UNIFESP)

Unraveling microRNAs function in zebrafish: strategies and advances

Arthur Casulli de Oliveira (UNESP)

Congenital hypopituitarism and its multiple presentation in different species *Homo sapiens*, *Mus musculus* and *Danio rerio*

Luciani Renata Silveira de Carvalho (HC-FMUSP)

Sanitary control in zebrafish and its implication in experimental results

Bianca Ventura (FMUSP-SP)

Room 5

Neuroscience of learning and Brazilian education

FeSBE Annual Meeting 2019

September 10 - Tuesday

Chair: Camilo Lellis-Santos (UNIFESP)

Universal design for learning: accommodating individual learning differences

Claudia Berlim de Mello (UNIFESP)

The day that elementary school students have built a pH meter themselves

Eduardo Galembeck (UNICAMP)

OP: 25.007 - The peer instruction method is time-consuming but promotes learning in physiology classes for low-income students.

Sá VA, Cunha AV, Lellis-Santos C - Ciências Biológicas- UNIFESP

OP: 25.011 - Unraveling multiple intelligences in the traveling science center science under tents.

Capistrano RL, Alves GH, Azeredo TV, Correa RP, Fragel-Madeira L - Neurobiologia – UFF; Pós-Graduação em Ensino em Biociências e Saúde – Fiocruz; Graduação em Ciências e Biotecnologia – UFF; Pós-Graduação em Ensino em Biociências e Saúde - Fiocruz

Hotel 1

New challenges to blindness treatment

Chair: Hilda Petrs-Silva (UFRJ)

Modulation of Endocannabinoid system induce neuroprotection in a murine model of retinitis pigmentosa

Lucianne Fragel Madeira (UFF)

Micro-RNAs and the regulation of stem cells and retinal degeneration

Carolina Beltrame Del Debbio (USP)

Non-viral vectors for retinal degeneration gene therapy

Marcela Coelho (UFMG)

Gene therapy for retinal ganglion cells - is it feasible?

Hilda Petrs-Silva (UFRJ)

16:00-18:00 h - Poster Session I and coffee break

18:00-19:00 h - Lectures

Room 1

The wide spectrum of hypothalamic abnormalities in obesity

Chair: Everardo M. Carneiro (UNICAMP)

Speaker: Licio A. Velloso (UNICAMP)

Room 2

A Chimera Named Pollution

Chair: Patricia Rocco (UFRJ)

Speaker: Walter Araujo Zin (UFRJ)

Room 3

Hypertensive neuropathy: a new clinical disease?

Chair: Ana Carolina T. Takakura (ICB-USP)

Speaker: Valéria Paula S. Fazan (FMRP-USP)

19:10-20:00 h - Curso II (1ª aula) / Courses II (1st class) (will be held in Portuguese or English)

Room 1

Desreguladores endócrinos

Coordenadora: Maria Izabel Chiamolera (UNIFESP)

Aula 1 - **Intrduction aos Desreguladores Endócrinos**

Andrea Claudia Freitas Ferreira (UFRJ)

Room 2

Molecular pathways in cell death subroutines

Chair: Giselle Zenker Justo (UNIFESP)

Class 1 - **Overview of cell death: Regulated and accidental cell death; classification of cell death subroutines**

Giselle Zenker Justo (UNIFESP)

Room 3

Avaliação cardiovascular: adequando o método à hipótese

Coordenadora: Luciana V. Rossoni (ICB- USP)

Aula 1 - **Avaliando a função cardíaca**

Dalton Valentim Vassallo (UFES/ EMESCAM)

Room 4

How to make the most of optical microscopy

Chair: Manoel Luis Costa (UFRJ)

Class 1 - **Identifying the major variables in optical microscopy**

FeSBE Annual Meeting 2019
September 10 - Tuesday

Manoel Luis Costa (UFRJ)

Room 5

Modelagem animal: o que preciso fazer para ter Results precisos

Coordenador: Marcel Frajblat (UFRJ)

Aula 1 - **Ciência e modelagem animal**

Marcel Frajblat (UFRJ)

Hotel 1

Ritmos Biológicos: mais próximo da sua pesquisa que você imagina

Coordenadora: Fernanda Gaspar do Amaral (UNIFESP)

Aula 1 - **Análises Rítmicas na Pesquisa Experimental**

Fernanda Gaspar do Amaral (UNIFESP)

Hotel 2

Proteomics for everyone

Chair: Giuseppe Palmisano (ICB-USP)

Class 1 - **Proteomics tools and applications to biology**

Giuseppe Palmisano (ICB-USP) / Jose Cesar Rosa (USP-RP)

Hotel 3

Modelos animais em psicofarmacologia

Coordenador: Helena M Tannhauser Barros (UFCSPA)

Aula 1: **Noções básicas de neuroanatomia, neurofisiologia, etologia e psicofarmacologia**

Helena M Tannhauser Barros (UFCSPA)

FeSBE Annual Meeting 2019

September 11 - Wednesday

8:00-9:00 h - Curso I/ Courses I

Room 1

Redação Científica: Artigos, Projetos e Ética

Coordenador: Walter Araujo Zin (UFRJ)

Aula 1 - **Redação de Artigo Científico**

Walter Araujo Zin (UFRJ)

Room 2

Revisiting the Physiology Teaching

Chair: Maria Tereza Nunes (ICB- USP)

Class 1 – “Who am I?” a game-based teaching tool to promote endocrine physiology learning

Maria Tereza Nunes (ICB- USP) e João Kleber Neves Ramos (ICB- USP)

Room 3

O tecido muscular esquelético: da estrutura a aspectos adaptativos

Coordenador: Anselmo Moriscot (ICB- USP)

Aula 1 - **Aspectos estruturais do músculo estriado esquelético e correlações com a função**

Anselmo Moriscot (ICB- USP)

Room 4

Advanced tissue-based techniques in drug development, with emphasis on toxicologic pathology and safety pharmacology applications

Chair: Gilberto De Nucci (UNICAMP/USP)

Class 1 - Formalin-fixed paraffin-embedded (FFPE) tissue blocks/sections: review of molecular pathology techniques (relevance and limitations)

Frédéric Gervais (Citoxlab, France)

Hotel 1

Canais para íons em membranas celulares

Coordenador: Antônio Carlos Cassola (ICB- USP)

Aula 1 - **Técnicas para a observação experimental de canais unitários: “Patch Clamp” e Análise de Ruído**

Antônio Carlos Cassola (ICB- USP)

Hotel 2

Imagens de Bases Moleculares

Coordenador: Valbert Nascimento Cardoso (UFMG)

Aula 1 - **Imagens cintilográficas (SPECT e PET)**

Simone Odilia Antunes Fernandes (UFMG)

Hotel 3

Bioimpressão 3D na Medicina Regenerativa

Coordenadora: Marimelia Porcionatto (UNIFESP)

Aula 1 - **Imprimindo tecidos e órgãos: biotintas e células**

Marimelia Porcionatto (UNIFESP)

9:30-11:30 h - Sessions

Room 1

Advances in muscle physiology

Chair: Flavia Bloise (UFRJ)

Skeletal muscle physiology during the nonthyroidal illness syndrome

Flavia Bloise (UFRJ)

Muscle mitochondrial function in a model of dystrophic mice

Claudia Mermelstein (UFRJ)

OP: 07.001 - Maternal vitamin D deficiency selectively affects fiber-II rich skeletal muscle phenotype in adult offspring rats.

Reis NG, Gonçalves DAP, Silveira WA, Lautherbach NES, Almeida LF, Assis AP, Zanon NM, Heck LC, Coimbra TM, Kettelhult IC, Navegantes LCC - Fisiologia – FMRP/USP; Bioquímica e Imunologia – FMRP/USP; Educação Física UFMG

OP: 16.010 - Overexpression of miR 29c as a regulator of skeletal muscle mass.

Silva WJ, Graça FA, Oliveira AC, Silvestre JGO, Alves PKN, Lima GS, Yan CYI, Miyabara EH, Labeit S, Wang D, Moriscot AS - Department of Cell Biology and Development – USP; Institute for Integrative Pathophysiology – Department of Cardiology – HMS; Department of Anatomy – USP

Room 2

Mechanotransduction in biological systems

Chair: Ayumi Aurea Miyakawa (InCor-USP)

Mechanotransduction at the cell-matrix interface

Christoph Ballestrem (The University of Manchester)

Crp3 and vascular remodeling by mechanical stress

Ayumi Aurea Miyakawa (InCor-USP)

OP: 04.004 - Cysteine and glycine-rich protein 3 (crp3) absence impairs focal adhesion signaling and force generation in aortic smooth muscle cells. Ribeiro-Silva JC, Ferraz MSA, Silva TG, Alencar AM, Ballestrem C, Krieger JE, Miyakawa AA - Heart Institute, University of Sao Paulo Medical School – FMUSP; Physics Institute, University of Sao Paulo – USP; The University of Manchester

OP: 22.033 - Cell contractility drives mechanical memory of oral squamous cell carcinoma. De Campos PS, Matte BF, Placone JK, Engler AJ, Lamers ML - Patologia Bucal – UFRGS; Departamento de Ciências Morfológicas – UFRGS; Department of Bioengineering – UCS

Room 3

New insights into thyroid hormones and TSH actions

Chair: Rodrigo Soares Fortunato (UFRJ)

Is there a role of TSH on thyroid and breast cancer?

Rodrigo Soares Fortunato (UFRJ)

Autocrine actions of thyroid hormone

Rafael Benjamin Araújo Dias (UNINOVE)

OP: 06.012 - TSH induces miRNA expression changes in thyroid follicular cells. Fuziwara CS, de Santalnez DC, Sousa ISMA, Saito KC, Kimura ET - Departamento de Biologia Celular e do Desenvolvimento – USP

Room 4

Mechanisms conditioning the beneficial effects of exercise in cardiovascular diseases

Chair: Lisete C Micheline (ICB-USP)

Autonomic dysfunction in heart and cerebral ischemic diseases: Effects of exercise

Bruno Rodrigues (FEF-UNICAMP)

Molecular mechanisms in the genesis of hypertension: Exercise benefits

Gustavo Santos Masson (ICB-USP)

OP: 11.002 - Effect of moderate physical training on the oxidative balance in the brainstem of young rats submitted to maternal protein restriction. Bernanrdo EM, Pereira AR, Silva SCDA, Braz GRF, Ferreira DJS, Pedroza AADS, Lagranha CJ - Laboratory of Exercise Biochemistry and Molecular Biology – UFPE; Post-Graduate Program in Biochemistry and Physiology – UFPE; Neuropsychiatry and Behavior Science Graduate Program – UFPE; Federal University of Sao Francisco Valley – UNIVASF

OP: 11.014 - Skeletal myopathy in heart failure: changes in muscle regeneration capacity and therapeutic effects of aerobic physical training. Vieira JS, Bacurau AVN, Cunha TF, Carrascoza LS, Dourado PMM, Brum PC - Biodinâmica do Movimento Humano - Universidade de São Paulo; Instituto do Coração - InCor-FMUSP

Hotel 1

Use of noise to mask color and luminance contrast

Chair: Eliza M. C. Brito Lacerda (CEUMA University)

Detection of luminance noise: influence of the stimulus parameters

Eliza M. C. Brito Lacerda (CEUMA University)

Color and luminance discrimination masked by luminance noise

Terezinha M. Gonçalves de Loureiro (UFPA)

OP: 24.011 – Light adaptation of the pseudo-random electrogram. Brasil A, Assis JB, Loureiro TMG, Souza GS - Núcleo de Medicina Tropical – UFPA

OP: 24.008 - Characterization of melanopsin expression in owl retinas. Naman MJV, Assis LVM, Hauzman E, Castrucci AML, Ventura DF, Baron J, Bonci DMO - Departamento de Psicologia Experimental – USP; Departamento de Fisiologia e Biofísica – UFMG; Departamento de Fisiologia - USP

FeSBE Annual Meeting 2019

September 11 - Wednesday

11:30-12:30 h - Plenary lecture

Room 1

The cholesterol war: fake news vs. scientific based evidences

Chair: Helena Coutinho F. Oliveira (UNICAMP)

Speaker: Eder C. R. Quintão (FMUSP)

12:30-14:00 h - Lunch

14:00-16:00 h - Sessions

Room 1

Microenvironment and cell behavior

Chair: Patricia Gama (USP)

Mechanotransduction in tumor cells

Marcelo Lazzaron Lamers (UFRGS)

Hyperglycemic environment and cell behavior

Marinilce Fagundes dos Santos (ICB-USP)

Scaffolds and brain injury

Marimelia A Porcionatto (UNIFESP)

Room 2

Inflammation-induced alterations of the neurovascular unit

Chair: Daniel Adesse (Fiocruz)

Microvessel alterations in Toxoplasma gondii infected mice

Daniel Adesse (Fiocruz)

Alcohol exposure during gestation impairs endothelial-astrocyte interactions in the embryonic cerebral cortex

Joice Stipursky (UFRJ)

Zika virus hampers blood vessels development in a murine model of congenital infection

Patrícia Pestana Garcez (UFRJ)

The role of TLR4 in the microvascular cerebral dysfunction in a model of metabolic syndrome

Nathalie Obadia Pereira (Fiocruz)

Room 3

New aspects of endocrine disruptors

Chair: Maria Izabel Chiamolera (UNIFESP)

Experience with the European Commission for Endocrine Disruptors

Maria Tereza Nunes (ICB-USP)

Zebrafish as an alternative method for toxicity assessment of emerging environmental contaminants

Bianca Sales (UNESP-Botucatu)

Endocrine disruptors and intrauterine programming of thyroid dysfunctions

Caroline Serrano do Nascimento (Hospital Albert Einstein)

Endocrine disruptors and the brain

Gisele Giannocco (UNIFESP-Diadema)

Room 4

Purinergic Signaling in Development and Disease

Chair: Henning Ulrich (IQ-USP)

Regulation of Type 1 Equilibrative Nucleoside Transporters (ENT1) in lipid rafts and by microRNA-124 in the retina

Alexandre Rodrigues (UFF)

Purinergic signaling in sepsis-induced liver injury

Robson Coutinho-Silva (UFRJ)

Purinergic Signaling in the Developing Retina

Ana Lucia Marques Ventura (UFF)

Therapeutic effects of purinergic receptors in neurodegenerative diseases

Henning Ulrich (IQ-USP)

Hotel 1

Why scientists should share their discoveries through different media not only by publishing papers?

Chair: Camilo de Lellis Santos (UNIFESP)

Science and Citizenship

Natália Pasternak (ICB-USP)

Podcasts, a simple way to connect scientists and public

Leandro A. Lobo (UFRJ)

Who's afraid of media exaggeration?

Carlos Orsi (Instituto Questão de Ciência)

FeSBE Annual Meeting 2019
September 11 - Wednesday

**Science in the media, science in the class:
the fight against misconceptions**

Camilo de Lellis Santos (UNIFESP)

Luciana Venturini Rossoni (ICB- USP)

16:00-18:00 h - Poster Sessions II

Room 4

How to make the most of optical microscopy

Chair: Manoel Luis Costa (UFRJ)

**Class 2 - Choosing the best procedure for
each inquiry in optical microscopy**

João Ricardo Lacerda de Menezes (UFRJ)

18:00-19:00 h - Lectures

Room 1

**Discussing the Relationship (DR): The bi-
directional communication between tumor and
stroma**

Chair: Patricia Gama (ICBUSP)

Speaker: Christina Barja Fidalgo (UERJ)

Room 5

**Modelagem animal: o que preciso fazer para
ter Results precisos**

Coordenador: Marcel Frajblat (UFRJ)

**Aula 2 - Fatores que afetam os Results de
uma pesquisa**

Marcel Frajblat (UFRJ)

Room 2

**Non-coding RNAs: pathophysiological role and
clinical application in the cardiovascular system**

Chair: Alice Cristina Rodrigues (ICB-USP)

Speaker: Da-Zhi Wang (Harvard Medical School)

Hotel 1

**Ritmos Biológicos: mais próximo da sua
pesquisa que você imagina**

Coordenadora: Fernanda Gaspar do Amaral
(UNIFESP)

Aula 2 - Análises Rítmicas na Pesquisa Clínica
Maria Paz Hidalgo (UFRGS)

Room 3

**Melatonin as a Hormone: New Physiological
and Clinical Insights**

Chair: Fernanda Gaspar do Amaral (UNIFESP)

Speaker: José Cipolla Neto (ICB-USP)

Hotel 2

Proteomics for everyone

Chair: Giuseppe Palmisano (ICB-USP)

**Class 2 - Mass spectrometry and
bioinformatics for protein identification and
quantification**

Giuseppe Palmisano (ICB-USP) / Jose Cesar
Rosa (USP-RP)

19:10-20:00h - Cursos II (2ª aula) / Courses II
(2nd class)

Room 1

Desreguladores endócrinos

Coordenadora: Maria Izabel Chiamolera
(UNIFESP)

**Aula 2 - Contaminantes Organoestênicos e o
Sistema Endócrino e Reprodutor**

Jones B. Graceli (UFES)

Hotel 3

Modelos animais em psicofarmacologia

Coordenador: Helena M Tannhauser Barros
(UFCSPA)

**Aula 2: Modelos animais em depressão e
estresse pós-traumático**

Helena M Tannhauser Barros (UFCSPA)

Room 2

Molecular pathways in cell death subroutines

Chair: Giselle Zenker Justo (UNIFESP)

**Class 2 - Molecular pathways of major
regulated cell death modalities**

Giselle Zenker Justo (UNIFESP)

20:00-22:00 h - Assembly

Hotel 1

FeSBE General Assembly

Room 3

**Avaliação cardiovascular: adequando o método à
hipótese**

Coordenadora: Luciana V. Rossoni (ICB- USP)

Aula 2 - Avaliando a função vascular

FeSBE Annual Meeting 2019

September 12 – Thursday

8:00-9:00 h - Curso I / Courses I

Room 1

Redação Científica: Artigos, Projetos e Ética

Coordenador: Walter Araujo Zin (UFRJ)

Aula 2 - **Ética na Redação e Publicação de um Artigo**

Walter Araujo Zin (UFRJ)

Room 2

Revisiting the Physiology Teaching

Chair: Maria Tereza Nunes (ICB- USP)

Class 2 - **Dramatization in Physiology teaching: date to do different**

Lucila Ludmila Paula Gutierrez (UFCSPA)

Room 3

O tecido muscular esquelético: da estrutura a aspectos adaptativos

Coordenador: Anselmo Moriscot (ICB- USP)

Aula 2 - **Mecanismos celulares e moleculares controladores da massa muscular esquelética**

Dawit A. Pinheiro Goncalves (EEFFTO-UFMG)

Room 4

Advanced tissue-based techniques in drug development, with emphasis on toxicologic pathology and safety pharmacology applications

Chair: Gilberto De Nucci (UNICAMP/USP)

Class 2 - **Advanced in situ hybridization techniques: RNAScope**

Frédéric Gervais (Citoxlab, France)

Hotel 1

Canais para íons em membranas celulares

Coordenador: Antônio Carlos Cassola (ICB- USP)

Aula 2 - **Análise estocástica de canais unitários**

Antônio Carlos Cassola (ICB- USP)

Hotel 2

Imagens de Bases Moleculares

Coordenador: Valbert Nascimento Cardoso (UFMG)

Aula 2 - **Nanoformulações para diagnóstico por imagens**

Valbert Nascimento Cardoso (UFMG)

Hotel 3

Bioimpressão 3D na Medicina Regenerativa

Coordenadora: Marimelia Porcionatto (UNIFESP)

Aula 2 - **Bioimpressão 3D como ferramenta para recapitular o desenvolvimento e doenças**

Marimelia Porcionatto (UNIFESP)

9:30-11:30 h – Sessions

Room 1

Noncoding RNAs in health and disease

Chair: Alice Cristina Rodrigues (ICB-USP)

Modulation of Muscle Development and Disease by Noncoding RNAs

Da-Zhi Wang (Harvard Medical School)

Integration of Transcriptomics and MicroRNA Analyses in Cancer Cachexia

Robson Francisco Carvalho (UNESP)

MicroRNAs mediate beneficial effects of exercise on the cardiovascular system

Edilamar Menezes de Oliveira (EEFE-USP)

Exosomal microRNAs as mediators of intertissue communication in obesity

Alice Cristina Rodrigues (ICB-USP)

Room 2

Influence of microenvironment on tumor development

Chair: João Alfredo de Moraes (UFRJ)

Clues from the tumor-derived extracellular matrix to neighbor cells in the microenvironment

Christina Barja-Fidalgo (UERJ)

Neutrophil extracellular traps (NETs) as mediators of tumor progression

Robson de Queiroz Monteiro (UFRJ)

Adipose tissue derived extracellular vesicles modify tumoral cells behavior

Mariana Renovato Martins (UFF)

Effect of melanoma extracellular vesicles on neutrophil polarization

João Alfredo de Moraes (UFRJ)

FeSBE Annual Meeting 2019

September 12 – Thursday

Room 3

Immunomodulators and intestinal homeostasis

Chair: Valbert Nascimento Cardoso (UFMG)

Probiotic Bacteriophages- A novel strategy to control infection and inflammation.

Belchiolina Beatriz Fonseca (UFU)

Use of lactic acid bacteria genetically modified as immunomodulators to promote intestinal homeostasis

Vasco Ariston Carvalho de Azevedo (UFMG)

Lipids as immunomodulatory agents

Tatiani Uceli Maioli (UFMG)

Room 4

Pathogenesis of Chagas Disease

Chair: João Santana da Silva (FMRP-USP)

The Yin-and-Yang of the immune response: keeping the balance to decrease the burden of Chagas heart disease

Walderez O. Dutra (UFMG)

Consequences of controlling inflammation during *Trypanosoma cruzi* infection

Fabiana Simão Machado (UFMG)

The involvement of lipid kinases in the pathogenesis of *Trypanosoma cruzi* infection

Maria Claudia Silva (FMRP-USP)

Omics analysis in Chagas disease cardiomyopathy: a mitochondrial disease?

Edecio Cunha Neto (USP)

Hotel 1

Content versus process in modern cell biology teaching

Chair: Manoel Luis Costa (UFRJ)

On the basic concepts in cell biology

Manoel Luis Costa (UFRJ)

On the impact of technology in biology teaching methodologies

Miriam Struchiner (UFRJ)

The impact of recent process in cell biology teaching

Mauricio Roberto Pinto da Luz (Fiocruz)

Survey of major topics in cell biology

Claudia Mermelstein (UFRJ)

Hotel 2

BRAVO Award

11:30-12:30 h - Plenary Lecture

Room 1

“A política como Ciência, a Ciência na política”

Chair: Marcel Frajblat (UFRJ)

Speaker: Celso Pansera (Iniciativa para a Ciência e Tecnologia no Parlamento - ICTP.br)

12:30- 13:30 h - Technical Lecture

Room 2

Como melhorar seu protocolo de purificação de proteínas

Speaker: Fellipe Bronze-Assessor Científico da Sinapse Biotecnologia LTDA.

12:30-14:00 h - Lunch

14:00-16:00 h - Sessions

Room 1

Immunology in health and disease

Chair: Marcelo T. Bozza (UFRJ)

Regulation of CD8 T cell differentiation and function by Polycomb group (PcG) proteins during acute and chronic infections

Renata Pereira (UFRJ)

Mucosal inflammation: quantitative vs. qualitative aspects of Treg cell imbalance

Fabio Barrozo do Canto (UFF)

Immunological scarring: understanding chronic effects of acute infections

Denise Moraes da Fonseca (USP)

Combining in vivo imaging and high dimensional phenotyping to understand immune and metabolic development during life

Gustavo Batista de Menezes (UFMG)

Room 2

Risks to the environmental and health due to the uranium mining in Brazil

Chair: Silvia Maria Velasques de Oliveira (SBBN) and Claudia Laje (IBCCF-UFRJ)

FeSBE Annual Meeting 2019

September 12 – Thursday

Environmental remediation in uranium mining and naturally occurring radioactive material waste

Horst Monken-Fernandes (Nuclear Energy Department/International Atomic Energy Agency)

Relevant aspects in the environmental modelling according the radiobiological perspective

Dunstana Melo (Melohill Technology)

Potential hazards in chemical, biological, nuclear and radiological exposures

Edson Andrade (Instituto Militar de Engenharia-IME/Instituto de Engenharia Nuclear-IEN)

Biological effects of chronic exposures in the neighborhood of nuclear fuel cycle facilities

Carlos Eduardo Brandão (UNIRIO / UFRJ)

Room 3

Regulation of muscle mass: cellular and molecular aspects

Chair: Claudia Mermelstein (UFRJ)

Calcium and calpain in muscle dystrophy

Claudia Mermelstein (UFRJ)

Role of miR-29 family in skeletal muscle mass control

Anselmo Moriscot (ICB-USP)

Does insulin/IGF-1 signaling mediate the effects of beta2-adrenergic agonists on skeletal muscle remodeling and function?

Dawit A. Pinheiro Goncalves (EEFFTO-UFMG)

The role of extracellular matrix during myoblast migration

Ingo Riederer (FIOCRUZ)

Room 4

Renin, angiotensins, bradykinin, noradrenaline, acetylations and oxidative stress: friends or foes in cardiorenal syndromes? In honor to the memory of Margarida de Mello Aires

Chair: Adalberto Vieyra (UFRJ)

Cardiorenal syndrome: the long road from kidney to heart

Marcela Sorelli Carneiro Ramos (UFABC)

Novel role of bradykinin and B2-receptors: regulation of collecting duct renin

Lucienne da Silva Lara (UFRJ)

The role of oxidative stress in the renal alterations underlying the onset of hypertension programmed by intrauterine undernutrition

Leucio Duarte Vieira (UFPE)

Renin-angiotensin system and acetylations: key elements in the cardiorenal alterations provoked by undernutrition and obesity

Humberto Muzi Filho (UFRJ)

Hotel 1

Photobiomodulation and its applications

Chair: Marucia Chacur (ICB-USP)

Application of photobiomodulation in different animal models.

Marucia Chacur (ICB-USP)

Effect of photobiomodulation in different models of orofacial pain

Daniel de Oliveira Martins (ICB-USP)

Is there for the use of photobiomodulation in the treatment of pain in medicine?

Hazem A. Ashmawi (FMUSP)

Light to treat pain: biophysics of the mechanisms of action and how to perform clinical and experimental procedures

Marcelo Victor P de Sousa (Bright Photomedicine)

Photobiomodulation Therapy as a tool to improve the quality of life in patients in different types of pain

Nathali Cordeiro Pinto (FMUSP)

16:00-18:00 h - Poster Session III

18:00-19:00 h - Lectures

Room 1

Aerobic exercise training as therapy for skeletal myopathy: relevance to heart failure and cancer

Chair: Ana Paula C. Davel (UNICAMP)

Speaker: Patricia C. Brum (EEFE-USP)

FeSBE Annual Meeting 2019

September 12 – Thursday

Room 2

The Immune-Pineal Axis – a chronopharmacological approach for integrating the timing in Physiology and Pathology

Chair: André Sampaio Pupo (UNESP)

Speaker: Regina P. Markus (USP)

19:10-20:00h- Cursos II 3ª aula/Courses II (3rd class)

Room 1

Desreguladores endócrinos

Coordenadora: Maria Izabel Chiamolera (UNIFESP)

Aula 3 - **Plasticantes, Herbicidas e Metais Pesados**

Glaecir Roseni Mundstock Dias (UFRJ)

Room 2

Molecular pathways in cell death subroutines

Coordenadora: Giselle Zenker Justo (UNIFESP)

Class 3 - **Metabolic control of cell death.**

Giselle Zenker Justo (UNIFESP)

Room 3

Avaliação cardiovascular: adequando o método à hipótese

Coordenadora: Luciana V. Rossoni (ICB- USP)

Aula 3 - **Avaliando a efetividade dos protocolos de treinamento físico**

Patrícia C. Brum (EEFE-USP)

Room 4

How to make the most of optical microscopy

Chair: Manoel Luis Costa (UFRJ)

Class 3 - **Demonstration of the possibilities and limitations in optical microscopy and image processing**

Manoel Luis Costa (UFRJ)

Room 5

Modelagem animal: o que preciso fazer para ter Results precisos

Coordenador: Marcel Frajblat (UFRJ)

Aula 3 - **Como será a pesquisa com animais em 2040**

Marcel Frajblat (UFRJ)

Hotel 1

Ritmos Biológicos: mais próximo da sua pesquisa que você imagina

Coordenadora: Fernanda Gaspar do Amaral (UNIFESP)

Aula 3 - **Discussão guiada de projetos - onde estão os ritmos e como lidar com eles?**

Maria Paz Hidalgo (UFRGS)

Hotel 2

Proteomics for everyone

Chair: Giuseppe Palmisano (ICB-USP)

Class 3 - **Identification of protein phosphorylation by proteomics approaches**

Giuseppe Palmisano (ICB-USP) / Jose Cesar Rosa (USPRP)

Hotel 3

Modelos animais em psicofarmacologia

Coordenador: Helena M Tannhauser Barros (UFCSPA)

Aula 3: **Modelos animais em ansiedade e dependência química**

Luana Freese (UFCSPA)

FeSBE Annual Meeting 2019

September 13 – Friday

8:00-9:00 h - Curso I (3ª aula) / Courses I (3rd class)

Room 1

Redação Científica: Artigos, Projetos e Ética

Coordenador: Walter Araujo Zin (UFRJ)

Aula 3 - **Elaboração de Projeto de Pesquisa**

Dalton Valentim Vassallo (UFES / EMESCAM)

Room 2

Revisiting the Physiology Teaching

Chair: Maria Tereza Nunes (ICB- USP)

Class 3 - **Using arts to foster the learning of scientific concepts**

Camilo Lellis-Santos (UNIFESP)

Room 3

O tecido muscular esquelético: da estrutura a aspectos adaptativos

Coordenador: Anselmo Moriscot (ICB- USP)

Aula 3 - **Mecanismos celulares e moleculares envolvidos na resposta regenerativa muscular**

Anselmo Moriscot (ICB- USP)

Room 4

Advanced tissue-based techniques in drug development, with emphasis on toxicologic pathology and safety pharmacology applications

Chair: Gilberto De Nucci (UNICAMP/USP)

Class 3 - **Core techniques in the development of therapeutic oligonucleotides**

Cécile Sobry (Citoxlab, France)

Hotel 1

Canais para íons em membranas celulares

Coordenador: Antônio Carlos Cassola (ICB- USP)

Aula 3 - **Topologia de canais para cátions assemelhados aos canais dependentes de voltagem**

Antônio Carlos Cassola (ICB- USP)

Hotel 2

Imagens de Bases Moleculares

Coordenador: Valbert Nascimento Cardoso (UFMG)

Aula 3 - **Nanoformulações para tratamento**

Valbert Nascimento Cardoso (UFMG)

Hotel 3

Bioimpressão 3D na Medicina Regenerativa

Coordenadora: Marimelia Porcionatto (UNIFESP)

Aula 3 - **Desafios e Perspectivas da Bioimpressão 3D**

Marimelia Porcionatto (UNIFESP)

09:30-11:30 h - Sessions and Awards

Room 1

Development, aging and cell functions

Chair: Patricia Gama (ICB-USP)

Development, diet and hepatic functions

Gustavo Batista de Menezes (UFMG)

Breastfeeding and the priming of gastric cell functions

Patricia Gama (ICB-USP)

OP: 05.001 - Effect of anti-TNF α on enteric neurons and enteric glial cells in experimental ulcerative colitis. Souza RF, Machado FA, Castelucci P. Anatomia – ICB.

OP: 05.002 - Early weaning triggers transient effects on TGF beta and FGF10 levels in the rat gastric mucosa Silva, K. M. , Rattes, I. C. , Costa, A. V. , Rigonati, C. A. M. , Gama, P. Departamento de Biologia Celular e do Desenvolvimento - USP

Room 2

A tribute to Margarida de Mello Aires, the leading lady of renal physiology

Chair: Maria Oliveira de Souza (ICB-USP)

Small extracellular vesicles and kidney disease models: a tribute to the leading lady of renal physiology

Adalberto Vieyra (IBCCF & CENABIO-UFRJ)

Everything started in the kidney... but ended in the heart... A trajectory through the Renin-Angiotensin System

Maria Luiza Barreto Chaves (ICB-USP)

Glucose - an energetic substrate that modifies proximal reabsorption and, in excess, impairs renal function and promotes fetal programming

Guiomar Nascimento Gomes (UNIFESP)

Margarida de Mello Aires: Physiologist, scientist, teacher and friend

Maria Oliveira de Souza (ICB/ USP) and Gerhard Malnic (ICB-USP)

FeSBE Annual Meeting 2019
September 13 – Friday

Room 3

New approaches in animal vision research

Chair: Leonardo Dutra Henriques (USP)

Evaluation of New World monkeys color vision with an adaptation of Cambridge Colour Test

Leonardo Dutra Henriques (USP)

Suprathreshold chromatic discrimination in tufted capuchin monkeys (*Sapajus apella*)

Letícia Miquilini de Arruda Farias (UFPA)

OP: 24.003 - SWS1 opsin gene duplication confers sensitivity to UV and violet light in the aquatic colubrid snake *Helicops modestus*.

Hauzman E, Bhattacharyya N, Chang BSW, Ventura DF - Psicologia Experimental – USP; Ecology & Evolutionary Biology – UofT; Cell & Systems Biology - UofT

OP: 24.018 - A novel uveitis model induced by BCG in rabbits.

Castro BFM, Vieira LC, Silva LM, Santos DVV, Fialho SL, Cotta OAL, Paiva MRB, Guerra MCA, Silva-Cunha A - Faculty of Pharmacy – UFMG; Faculty of Medicine – UFMG; Pharmaceutical Research and Development – FUNED; Cell Biology Laboratory - FUNED

Room 4

SBEM Award

11:30 -13:30 h - Closing Ceremony

Room 1

“Science Service Award - FeSBE 2019”

A instabilidade no sistema federal de fomento à Ciência e Tecnologia

Wanderley de Souza (UFRJ)

Awardees Announcement:

FeSBE Affiliated Societies awards

“Prêmio Professor de Ciências do Ano FeSBE 2019”

Poster Presentation Prize

Closing Remarks

FeSBE Annual Meeting 2019
Poster Sessions and Abstracts

Poster Session I - Sept.10.2019 - 16:00 - 18:00 h

1 - Ambiental Biology, Evolution and Comparative Biology.....	001 - 006
3 - Laboratory Animal Science.....	001 - 005
4 - Cardiovascular Biology and Diseases	001 - 010
5 - Gastrointestinal Biology and Diseases	001 - 002
6 - Endocrine System	001 - 006
7 - Nutrition and Metabolism.....	001 - 017
8 - Renal Biology and Diseases	001 - 006
9 - Respiratory Biology and Diseases	001 - 005
10 - Neurobiology	001 - 014
11 - Physical Training Responses.....	001 - 007
13 - Cell differentiation, growth and death	001 - 009
15 - Optical and Mechanical Technologies for Health.....	001 - 004
16 - Gene and Cell Therapy, Omics Biology	001 - 005
17 - Basic & Clinical Pharmacology.....	001 - 005
18 - Neuropsychopharmacology	001 - 005
19 - Toxicology.....	001 - 009
20 - Pain and Inflammation.....	001 - 008
22 - Cancer Signaling and Therapeutics	001 - 013
23 - Regenerative Medicine and Developmental Biology.....	001 - 026
24 - Vision and Ophthalmology	001 - 006
25 - Education, Science History and Philosophy, Science Communication.....	001 - 005

FeSBE Annual Meeting 2019

Poster Sessions and Abstracts

1 - Ambient Biology, Evolution and Comparative Biology

01.001 - METALLOTHIONEINS MRNA EXPRESSION IN HEPATOPANCREAS OF BLUE CRABS CALLINECTES DANAE FOLLOWING PB EXPOSURE. Bordon IC, Emerenciano AK, Souza FC, Joviano WR, Santos LN, Favaro DIT, Abessa DMS, Silva JRM, - Biologia Celular - USP NEPEA - UNESP CRPq - CNEN

Introduction: In Brazil, the blue crab *Callinectes danae* Smith, 1869 (Crustacea, Decapoda, Portunidae) represent an important fishing resource, especially for traditional communities. Previous studies have assessed metal concentrations in *C. danae* tissues for biomonitoring purposes and some have reported that different metals may present different target tissues and bioaccumulate differently in distinct tissues. More recently, a study has reported that lead (Pb) bioaccumulation and total metallothionein-like induction are related to the uptake pathway and the type of tissue of *C. danae*.

Aim:

Due to this complexity related to metal exposure and toxicity in aquatic organisms, this study aimed to assess the expression of mRNA metallothionein (MT) isoforms in hepatopancreas of blue crabs *Callinectes danae* following single and combined dietary and waterborne Pb exposures.

Methods:

Male *C. danae* individuals were collected in the south area of the Cananéia-Iguape-Peruíbe Protected Area (APA-CIP), in São Paulo, Brazil. After an acclimatization period, exposure assays were performed during 24h, 48h and 96 h, at [Pb]= 2.0 µg ml⁻¹ in 4 treatments: 1) control; 2) contaminated water only; 3) contaminated food only; 4) contaminated water and food. After each period of exposure, samples of hepatopancreas were dissected and transferred to microtubes containing RNALater (Invitrogen). Total RNA was extracted, and cDNA synthesis was performed by reverse transcription. Assumptions of homology to *Callinectes sapidus* metallothioneins sequences (CuMT II; CdMT I e II) were considered in order to design species-specific primers for *C. danae*. Then, the obtained cDNA was quantified by quantitative PCR (qPCR). Transcriptional profile was calculated following $\Delta\Delta CT$. To detect significant differences in mRNA expression values regarding the treatment and the time of exposure, the analysis of variance test (ANOVA 2-way) was applied, followed by Fisher LSD post hoc test.

Results:

CuMTII: compared to control treatment, the mRNA expression declined after 96h of contaminated food exposure. The increasing of the CuMTII mRNA expression was detected only after 24 h of combined exposure. However, it declined to control levels in 48 h exposure; CdMTI: the declining of mRNA expression was observed after 96 h of combined exposure; CdMTII: compared to control treatment, the mRNA expression increased after 48h and subsequently decreased after 96h of contaminated water exposure. In contaminated food exposure, the CdMTII mRNA expression decreased after 24h, achieving control levels after 48h of exposure and subsequently increasing after 96h of exposure. In combined treatment, the mRNA increased after 24h of exposure, decreasing to control levels after 48h of exposure.

Conclusion:

In general, it could be inferred that metallothionein mRNA expression respond to Pb exposure. Specifically, the CdMTII mRNA expression was affected by all treatments, suggesting that it could be applied as a molecular biomarker, indicating the predominance of a single or combined pathways of Pb uptake in *C. danae*.

Financial support:

FAPESP, Capes

01.002 - MUSCLE GROWTH SIGNALING PATHWAYS ACT DIFFERENTLY BETWEEN FISH SUPERORDERS OSTARIOPHYSI AND ACANTHOPTERYGII. Duran BOS, Garciadelaserrana D, Zanella BTT, Mareco EA, Santos VB, Carvalho RF, Dal-Pai-Silva M, - Morphology - São Paulo State University (UNESP) Cell Biology, Physiology and Immunology - University of

Barcelona Biology - University of Western São Paulo (UNOESTE) - - São Paulo Agency for Agribusiness Technology (APTA)

Introduction:

Whole genome duplication (WGD) events are considered a major feature of the evolution of eukaryotic genomes, increasing complexity and, eventually, biological diversity of organisms. Around 450-320 million years ago, teleost fish had a specific WGD on the base of the lineage, with estimated 15-21% retention of the originated paralogue genes. Recent studies have shown differential paralogue retention between the superorders Ostariophysi and Acanthopterygii, but the identification of these lineage-specific paralogues (LSPs) and their roles remain mostly unknown. We hypothesized that distinct mechanisms of sub-functionalization and/or neo-functionalization occurred between Ostariophysi and Acanthopterygii, which caused a differential retention of LSPs.

Aim:

During this work we compared the expression of a subset of LSPs related to muscle growth between pacus (*Piaractus mesopotamicus* - Ostariophysi) and tilapias (*Oreochromis niloticus* - Acanthopterygii), for a better understanding of their evolutionary divergence.

Methods:

Ethical committee protocol 705. Juvenile pacus and tilapias were fasted for 4 days and then refed for 3 days, to manipulate muscle growth. Muscle samples were collected from the epaxial region before the fasting period (-4d), daily during fasting (-3d, -2d, -1d and 0d) and during refeeding (6h, 12h, 1d, 2d and 3d). The identification of LSPs was achieved by comparison of peptide sequences between Ostariophysi and Acanthopterygii species (Ensembl Browser 89 and BioEdit Sequence Alignment Editor) and generation of phylogenetic trees (MEGA7 software). LSPs expression were evaluated using Quantitative PCR (n=6 per species). After Shapiro-Wilk normality test, data was analyzed using a one-way ANOVA followed by Tukey's test or Kruskal-Wallis followed by Dunn's test, with statistical significance at 5% (p<0.05).

Results:

From a list of 238 genes related to myogenesis, protein synthesis and degradation, we identified 20 LSPs differently retained. Some pacu paralogues increased their expression after 4 days of fasting (0d), and maintained high expression during 1 day of refeeding (up to 2-fold increase). In contrast, orthologues genes for the pacu paralogues in tilapias decreased their expression immediately after 1 day of fasting (-3d) (up to 2-fold decrease), increasing again 1 day after refeeding (up to 2-fold increase). This indicates that these genes are differently regulated between the superorders in response to nutritional inputs. For example, the follistatin a (*fsta*) in tilapias was highly upregulated during protein degradation (3-fold increase), whereas in pacus both *fsta* and *fstb* had high expression during protein synthesis (4-fold increase). Moreover, some LSPs also showed different expression between their paralogue copies within the same species, as was the case of the ras-related gtp binding c (*rragc*). After refeeding, there was an upregulation of *rragca* (2-fold increase) and a downregulation of *rragcb* (0.5-fold decrease) in tilapias. These variations indicate the existence of LSPs sub-functionalization.

Conclusion:

Our results revealed differential transcription between Ostariophysi and Acanthopterygii LSPs in response to feeding status, showing that the evolutionary history of pacus and tilapias culminated with divergent gene regulatory mechanisms. Focus should be given on these LSPs in future research, for improvement of pacus and tilapias farming and to understand what adaptive advantages this differential retention and distinct expression profiles have brought to each of the lineages.

Financial support:

São Paulo Research Foundation (FAPESP), grants #2015/03234-8 and #2016/05009-4.

01.003 - OSMOIONIC HOMEOSTASIS IN BIVALVES MOLLUSCS INHABITANTS OF DIFFERENT OSMOTIC NICHES. Medeiros IPM, Faria SC,

FeSBE Annual Meeting 2019

Poster Sessions and Abstracts

Souza MM, - Instituto de Ciências Biológicas - FURG Programa de Pós-Graduação em Ciências Fisiológicas - FURG Instituto de Biociências - USP

Introduction:

In the aquatic environment, the salinity is recognized as one of the main abiotic factors that influences the physiology of organisms. Although the physiological patterns and challenges imposed by each occupied environment are distinct, they tend to converge to osmotic oscillations on them.

Aim:

From a comparative perspective, we aimed to characterize the osmoregulatory patterns and identify the main osmotic effectors used in intracellular isosmotic regulation (IIR) of bivalve molluscs freshwater *Corbicula largillierti* (purple Asian cockle), estuarine *Erodona mactroides* (lagoon cockle) and marine *Amarilladesma mactroides* (white clam) - inhabitants of different osmotic niches - when submitted to hypo- and/or hyperosmotic variations of salinity.

Methods:

Specimens of the bivalves *C. largillierti*, *E. mactroides* e *A. mactroides* was sampled in the State of Rio Grande do Sul (Brazil) and acclimated (7-days; constant aeration; 21 °C; 12 h light:12 h dark photoperiod; feeding with microalgae; natural habitat salinities: 0, 11 and 28 g/L, respectively). For the osmotic shock experiment the bivalves were subjected to conditions of 25% above and/or below the acclimation salinity (*C. largillierti* - 0, 5, 10 and 15 g/L; *E. mactroides* - 8, 11 and 14 g/L; *A. mactroides* - 21, 28 and 35 g/L) during 96 h (5≤N≤7) under the same laboratory conditions, but not feeding. Subsequently, the hemolymph, mantle, adductor muscle and gills were sampled. Finally, were determined the hemolymph osmotic and ionic (Na^+ , K^+ and Cl^-) concentration, tissue hydration and the IIR capacity from the use of osmolytes (organic and inorganic). We used the non-parametric analysis of Kruskal-Wallis variance, followed by Dunns post-hoc to detect statistically different means ($p \leq 0.05$), and Mann-Whitney U-test for independent samples (physiological vs. osmotic and ionic concentrations of the exposure solutions).

Results:

Hemolymphatic analyzes support the osmoconformer profile of the three species. Both ionoregulation and ionoconformation patterns were observed in the evaluated species ($p < 0.05$). The reflexes of the variation in hemolymph osmotic concentration could be visualized by the decrease in water content in all tissues of *C. largillierti* (10-37%; $p < 0.05$), but not in *E. mactroides* and *A. mactroides* when compared to the acclimation condition. About intracellular osmotic effectors, *C. largillierti* increases $[\text{Na}^+]$ ($\leq 150\%$), $[\text{K}^+]$ ($\leq 250\%$) and $[\text{Cl}^-]$ ($\leq 220\%$), $p < 0.05$, as well as organic osmolytes in all tissues ($\leq 1500\%$). On the other hand, *E. mactroides* varied only $[\text{Na}^+]$ (-21%; +28%) and $[\text{K}^+]$ ($\leq 260\%$) in their tissues, while *A. mactroides* mobilized Na^+ (-24%; +36%), $p < 0.05$. In both estuarine and marine species, the concentration of free amino acids in the evaluated tissues were either punctual or did not vary in face of the osmotic shock experienced.

Conclusion:

Physiological profiles of osmotic conformation, as well as patterns of regulation and ionic conformation were verified in freshwater, estuarine and marine bivalves. In addition, the investigated bivalve species showed greater use of inorganic osmolytes, which vary according to the osmotic niche occupied by each species, compared to the participation of organic molecules in the IIR in the evaluated tissues.

Financial support:

CAPES

01.004 - ACUTE TOXICITY TEST WITH TRIBUTYLTLIN (TBT) IN THE BLUE CRAB CALLINECTES SAPIDUS. Simões LAR, Vogt ÉL, Amaral M, Vinagre AS, - Departamento de Fisiologia - UFRGS

Introduction:

Tributyltin (TBT) is an organostannic compound widely used in the painting of boat hulls to prevent fouling by marine organisms. Consequently, large amounts of TBT have been released into aquatic ecosystems indirectly through ship hull waste. Studies have demonstrated the action of this compound as a potent endocrine disruptor, causing metabolic and reproductive system disorders. Estuarine environments are commonly affected due to the activities of boat traffic. Crustaceans may become contaminated by the diffusion of water with TBT through gills, sediment contact, or the ingestion of contaminated food. The blue crab *Callinectes sapidus* (Rathbun, 1896) is a benthic species found in oceanic or estuarine waters, with great ecological and socioeconomic importance. Decapod crustaceans are considered excellent animal models for toxicological studies of xenobiotics.

Aim:

The objective of this study was to verify the acute effects of sublethal concentrations of TBT in the metabolism of *C. sapidus* after different exposure periods.

Methods:

The animals were captured in Imbé, RS, with hollow nets and transported to the laboratory, where they were acclimatized for 7 days in 10‰ water, natural photoperiod and at 24°C. After this period of acclimation, the animals were kept individually in aquaria and divided into three groups (n = 10 per group) and exposed to different TBT concentrations: control group (without TBT), 100 or 1000 ng/L of TBT for 48 or 96 hours. Subsequently, the animals were cryoanesthetized and hemolymph was collected with syringes containing anticoagulant (potassium oxalacetate). Glucose, cholesterol and triglyceride concentrations were evaluated using commercial kits (Labtest®, São Paulo, Brazil). Statistical analysis was performed using Kruskal-Wallis test, followed by Dunn's post-test. The differences were considered significant when $p < 0.05$.

Results:

The levels of cholesterol and triglycerides in the hemolymph were not affected by TBT or time of exposure. Hemolymph glucose levels were not affected by TBT after 48h of treatment (22.83 ± 10.38 control; 37.12 ± 32.05 TBT 100, 24.60 ± 11.78 TBT 1000). After 96h of treatment (24.40 ± 12.58 control; 32.88 ± 26.68 TBT 100, 50.20 ± 22.15 TBT 1000), glucose levels were significantly increased in all groups in relation to 48h. No significant differences were observed between treatments in both periods of treatment.

Conclusion:

This increase in glycemia may indicate that a longer exposure period may generate an increase in stress. Other studies corroborate these findings indicating that increased stress in these animals may increase glycemia. There was no change in the lipid metabolism of these animals. However, this study presents preliminary data and further analyses with different periods of exposure and dosages to TBT will be conducted to investigate possible damage caused by this compound in this crustacean.

Financial support:

CNPq

01.005 - CHARACTERIZATION OF SIRTUINS IN AEDES AEGYPTI. Melo MM, DoVal-Amorim J, Serafim SC, Jablonka W, Atella GC, - Laboratório de Sinalização Celular - Universidade Federal do Rio de Janeiro

Introduction:

The *Aedes aegypti* mosquito is a vector of several tropical diseases, such as dengue, zika, chikungunya and yellow fever. *A. aegypti* females can transmit these viruses during blood feeding, which is rich in amino acids important for the reproduction. The female can also feed on nectar and sap, where polyphenols are present between different compounds. Our group showed that resveratrol (a polyphenol) activates AMPK, reducing the mosquito's microbiota and increasing longevity. However, the effect on lifetime does not seem to be related

FeSBE Annual Meeting 2019

Poster Sessions and Abstracts

only to the activation of AMPK, since AICAR (a pharmacological activator of AMPK) does not increase the life time of the mosquito (unpublished). Resveratrol is also an allosteric regulator of Sirtuins, a family of evolutionarily conserved proteins, classically related to the aging process. Currently, they are characterized as special sensors, which regulate metabolic pathways, dependent on the availability of NAD⁺. In addition, there are studies that show that sirtuins are antiviral factors and this function are conserved from bacteria to mammals (Koyuncu et al, 2014). Until now, there are no studies on this family of proteins in insect vectors.

Aim:

Our objective is to characterize *A. aegypti* sirtuins and to understand their role in mosquito physiology.

Methods:

Several databases were used to identify the sirtuins present in the *A. aegypti* genome. The expression of sirtuins were observed using qPCR analysis in different tissues of males and females sucrose feeding. And also in different tissues of the female under the conditions: sucrose feeding and during oogenesis.

Results:

We identified four Sir2 orthologous sequences of *Saccharomyces cerevisiae* (AAEL005816, AAEL011473, AAEL006655, AAEL004004) in the *Aedes aegypti* genome. We also observed that these sequences exhibit the catalytic domains and catalytic amino acids which are characteristics of Sirtuins. Afterwards, qPCR analysis shows the expression of the 4 sequences in the mosquito, and which, in the whole body, are most expressed in males. While in the female's tissues we have noticed that the ovary seems to present higher expression compared to the others, there was no effect observed in the male when compared with the testis. After this data, we decided to analyze the expression during oogenesis in the female and, in general, the sirtuins tend to increase in the ovary 24 hours after the blood feeding, a pattern followed by the other organs.

Conclusion:

We've observed the expression of the 4 sirtuins sequences in males and females of *A. aegypti*, and that this expression is tissue-specific, and also modulated by the blood feeding in females. One of the perspectives is to silence, through RNAi, the sirtuins of *A. aegypti* and to observe its effects on metabolic pathways and vector capacity of this mosquito. From this project, we believe that these proteins can contribute with new strategies to control the vector.

Financial support:

FAPERJ

01.006 - THE FLOOD PULSE OF MIDDLE RIO NEGRO BASIN AS AN ENVIRONMENTAL DRIVE FOR THE REPRODUCTION OF ADULT FEMALES OF AMAZONIAN FRESHWATER STINGRAY (POTAMOTRYGON WALLACEI). Morales-Gamba RD, Araújo MLG, Barcellos JFM, Marcon JL, - Ciências Fisiológicas - UFAM Programa de Pós-Graduação em Zoologia - UFAM Departamento de Engenharia de Pesca e Aquicultura - UFS Departamento de Morfologia - UFAM

Introduction:

At the end of 1980s, Wolfgang Junk and his colleagues launched the Flood Pulse Concept for rivers and floodplain systems, highlighting that the dynamic of aquatic biota is strongly driven by annual cyclic phenomenon of flooding and drought that occur in these areas. In Amazon basin, these natural variations in water level dramatically change the extent and persistence of water bodies along its main tributaries, including the Rio Negro basin. The cururu stingray *Potamotrygon wallacei* is endemic from this black water river system in the Brazilian Amazon and have high habitat specificity, living preferentially in areas of flooded forests (igapós) that are influenced by these annual pulses of flooding.

Aim:

Given the particular features of these aquatic/terrestrial transitional environments, allied to the reproductive strategy of this Amazonian stingray species, we hypothesized that morphological development of gonads in females are correlated to plasma profile of steroid hormones in different phases of the reproductive cycle, that for your time, are prompted by the pulsing period of flooding in its natural habitats.

Methods:

A total of 34 adult females were captured in the middle Rio Negro basin (0o50'28'' S, 62o46'5'' W) by ornamental fishermen during the flooding period (January to May 2017). Each stingray was measured, sexed and classified according to the maturational state for elasmobranchs. The present study received the approval from the Ethics Committee on Animal Use for Research of the Federal University of Amazonas (no 002/2017). The changes in size of vitelogenic follicles, the activity of oviducal glands and uterine activity were associated with the gonad macroscopic characteristics to validate the maturation stages. The morphological data were also compared with the circulating levels of steroid hormones in plasma. Concentrations of progesterone (P4), testosterone (T) and 17 β -estradiol (E2) were determined with enzyme-linked immunosorbent (ELISA) assays (kits DRG®, Germany).

Results:

Elevated levels of P4 occurred in all development stages, with the highest peak observed at the beginning of pregnancy in May. In addition, the P4 has a positive correlation with T concentrations showing its precursor function in females. In March during the rising water, the follicular development and growing were corresponded by increasing concentrations of T and E2 until ovulation event that occurred in the beginning of the high-water level in May. Estradiol showed no differences along the studied period. The eminent values of P4 were associated with the maintenance of the trofonemata in a period when no females in reproductive rest have been reported. In addition, these high levels could be interpreted as a response mechanism to the preparation of a new reproduction when favorable conditions arise. The pulsing behavior of Rio Negro observed in March initiated the development and growing of follicles that were followed by increasing concentrations of steroid hormones until the ovulation event that occurred in the higher water level in May.

Conclusion:

The present investigation was able to confirm the above tested hypothesis and demonstrates that reproductive period of *P. wallacei* is strongly synchronized with the annual cycling event of flooding in the Rio Negro basin.

Financial support:

CNPq, process number: 484566/2013-0

3 - Laboratory Animal Science

03.001 - IMPROVED SKELETAL QUALITY AND BONE HEALING IN ALOX5 KNOCKOUT AGED FEMALE MICE. Biguetti CC, Mahamoud R, Custódio IC, Simionato GB, Andreo JC, Oliva AH, Silva ACR, Brotto M, Matsumoto MA, - Departamento de Ciências Básicas - FOA-UNESP Departamento de Ciências da Saúde - USC Departamento de Ciências Biológicas - FOB-USP Bone-Muscle Research Center - UTA

Introduction:

Aging plays a critical role in affecting bone metabolism and skeletal homeostasis in which deterioration of bone microarchitecture is prevalent in elderly females. In this context, intramembranous bone healing post tooth extraction is a concerning factor in particular in the rehabilitation of elderly patients that require dental implants. Bone healing involves a transient and low degree inflammatory response, which involves the participation of various inflammatory factors like leukotrienes and prostaglandins, both from arachidonic acid metabolism by arachidonate 5-lipoxygenase (Alox5) and cyclooxygenases, respectively. While prostaglandins production (e.g PGE2) has been positively associated with angiogenesis and bone

FeSBE Annual Meeting 2019

Poster Sessions and Abstracts

formation, leukotrienes production has been associated with increased bone loss. Of note, disruption of Alox5 expression in Alox5KO young male mice leads to accelerated bone healing in endochondral fractures and attenuation of periodontal bone loss in mice, indicating that Alox5 impairs bone healing and bone homeostasis in certain experimental mice models. However, the function of Alox5 in skeletal maintenance and bone healing along aging remains poorly understood.

Aim:

Therefore, the aim of this study is to investigate skeletal bone quality and local bone healing post tooth extraction in 18-month-old 129 Sv female wild-type mice (WT) vs Alox5 Knockout (KO) mice (129-Alox5tm1Fun/J).

Methods:

Thus, twenty mice (n=10 WT and n=10 Alox5KO) were subjected to upper right incisor extraction and were euthanized after 7 and 21 days post surgeries (CEUA #8516040518). Maxillae containing alveolar socket were removed for microtomographic analysis (MicroCT), as well histological, birefringence and immunohistochemical (TRAP and Runx2) analysis. L5 vertebrae and femur were removed for additional skeletal bone evaluation by micro-CT. Mann-Whitney test was used to detect significant differences ($p < 0.05$) between quantitative data from WT vs Alox5KO groups in different time points.

Results:

For skeletal bone quality, a significantly increased percentage of bone volume (BV/TV, %) was detected in the L5-vertebra body and femur distal metaphysis in Alox5KO vs WT mice. Regarding the alveolar sockets, Alox5KO mice showed a significantly increase percentage of BV/TV compared to WT mice at 7 days, as well an increased trabecular thickness (Tb.Th, mm) at 7 and 21 days. Birefringence analysis by picrosirius red stained sections revealed more organized collagen content on Alox5KO compared to WT mice. The H&E histological staining and histomorphometric analysis in both WT and Alox5KO showed a transient inflammatory response at 7 days, with the increased initial bone formation at 7 days in Alox5KO compared to WT mice ($p < 0.05$). No differences were observed in the quantity of Runx2+ cells, while the number of TRAP+ osteoclasts was significantly increased in WT alveolar sockets compared to the Alox5KO mice at 21 days.

Conclusion:

In summary, these results support the current literature and indicate that targeted disruption of Alox5 also improves skeletal bone quality and accelerates the intramembranous bone healing in Alox5KO aged female mice.

Financial support:

FAPESP #2018/08913-9

03.002 - AGING OF THE REPRODUCTIVE SYSTEM: MORPHOLOGY AND CITOLOGY IN C57BL/6 FEMALE MICE. Schimdt TCG, Acioli LT, Silva GMF, Perez PLV, Bottino CFS, - Departamento de Ciências Básicas - UFF

Introduction:

The female reproductive system is versatile in both mouse and human, with variable morphological appearance due to the hormonal influence during the estrous/menstrual cycle and ovarian senescence as well. Also, studies suggest that the deterioration of adipose tissue (AT) metabolism with aging contributes to the deterioration of energy metabolism, and that sex hormones have a role in this process.

Aim:

Investigate the morphological changes in the reproductive system of female C57BL/6 mice during aging.

Methods:

The study protocol was approved by the Ethics Committee (CEUA UFF 446/2014). Animals were allocated into five groups according to age: 3, 6, 12, 18 and 24 months. Before euthanasia, body mass (BM), fasting blood glucose and vaginal cytology were evaluated. After anesthesia, blood was collected, and also the white (WAT) and visceral adipose tissue (VAT), brown adipose tissue (BAT), liver, uterus, and ovary for

morphometric analysis. Data were tested with respect to normality and homoscedasticity by the ANOVA one-way test with Tukey post-test. The distribution of animals per group among different classification systems was evaluated by the chi-square test. All analyzes were performed on GraphPad Prism 6.0.

Results:

Presented as mean \pm SD. Categorical data are expressed as median and 95% confidence intervals. BM increased progressively at ages of 3, 6, 12, 18 and 24 months (18.7 \pm 1.6g, 22.7 \pm 1.5g, 24.7 \pm 2.3g, 26.8 \pm 2.8g and 27.3 \pm 4.8g, respectively). WAT (visceral) deposits increased with the ages of 3, 6, 12, 18 and 24 months (198.6 \pm 97.31g; 278.1 \pm 162.2g; 482.6 \pm 211.5g; 512.3 \pm 233.9g e 741.0 \pm 527.1g, respectively), as well as the WAT (subcutaneous) (243.6 \pm 173g; 132.3 \pm 72.31g; 372.2 \pm 206g; 211.2 \pm 53g e 493.1 \pm 379.1g, respectively). No difference in BAT mass. The relation g. visceral /g. subcutaneously increased with age (1.1 \pm 0.7g, 2.2 \pm 0.8g, 1.6 \pm 0.9g, 2.3 \pm 0.9g and 1.8 \pm 0.9g) in the morphological quantification, there was an increase in adipocyte diameter in the genital fat (45.4 \pm 4.1 μ m, 52.6 \pm 10.8 μ m, 47.7 \pm 9.7 μ m, 63.9 \pm 5.6 μ m and 51.5 \pm 12.6 μ m) and inguinal (30.3 \pm 4.4 μ m, 42.2 \pm 5.6 μ m, 37.2 \pm 1.2 μ m, 46.5 \pm 1.5 μ m and 52.1 \pm 12.7 μ m). No difference in the diameter of brown fat adipocytes, however, it was observed that the smaller diameter lipid droplets are more prevalent in animals with greater age, 3 months 1.0(1.0-2.0); 6 months 1.0(1.0-4.0); 12 months 1.0(1.0-2.0); 18 months 1.0(1.0-4.0) and 24 months 1.0(3.0-4.0). Liver weight increased at the age of 18 months (1.0 \pm 0.1g). No difference between the ages for glycemia, serum and hepatic triglycerides. In the cytological analysis, it was observed that the animals lost cyclicity at 12 months of age (7% cycling), corroborating with the histomorphometric findings of the ovary analysis, where there was a decrease in the number of follicles (26.0 \pm 27.3; 30 \pm 15.3; 3.3 \pm 3.3; 1.5 \pm 2.3 and 0 \pm 0), as well as in the uterus, where the sectional area increased at the age of 12 months. (0.5 \pm 0.1 μ m; 0.6 \pm 0.1 μ m; 1.4 \pm 0.4 μ m; 0.8 \pm 0.6 μ m and 0.4 \pm 0.1 μ m).

Conclusion:

During aging in female C57BL/6 mice, several stages of reproductive system development are found (mature and senescent), and the loss of cycling at 12 months of age. It is crucial to analyze reproductive status with age in female animals since it might affect the evaluation and interpretation of scientific findings.

Financial support:

Faperj

03.003 - RECOMBINANT GROWTH FACTORS BMP7 (BONE MORPHOGENETIC PROTEIN 7) AND E PDGF-BB (PLATELET DERIVED GROWTH FACTOR BB) AIMING OSTEOPOROSIS TREATMENT IN OVARIECTOMIZED RATS. Reis TG, Koga BAA, Azzi CM, Sogayar MC, Carreira ACO, - NUCEL- CLÍNICA MÉDICA - USP CIRURGIA - USP BIOTECNOLOGIA - USP

Introduction:

Osteoporosis is a common degenerative disease caused by the imbalance between bone formation and resorption. It is characterized by a decrease in bone mineral density and loss of tissue's trabecular microarchitecture, causing difficulty in tissue repair and regeneration, what results in patient's morbidity and mortality. It affects a large number of patients in Brazil and worldwide. Furthermore, this number tends to increase as the population is aging and the disease affects mainly postmenopausal women and elderly men. The growth factors (GF) are among the proteins responsible for osteogenesis' regulation and stimulation, they include bone morphogenetic proteins (BMPs) and the platelet derived growth factor (PDGF). These proteins play a very important role in the maintenance of bone homeostasis and have tissue repair activity, therefore they are candidates with high potential for the treatment of osteoporosis.

Aim:

FeSBE Annual Meeting 2019

Poster Sessions and Abstracts

Thus, the objective of the present work is to perform the treatment of osteoporotic rats with recombinant BMP7 (rBMP7) and PDGF-BB (rPDGF-BB) aiming at disease regression.

Methods:

For this, Sprague Dawley rats at 12 weeks were separated into three groups: 1- Control- in which no surgery was performed; 2- Sham group- in which the animals' ovaries were exposed and then relocated into the abdominal cavity; and 3- Ovariectomy group in which both ovaries were removed. After 100 days, a subgroup of ovariectomized animals (N=4) were euthanized to confirm the model establishment and animals' osteoporotic condition. The other ovariectomized animals were subdivided into: one ovariectomy control group (N=4), receiving only the vehicle, and seven treatment groups (N=4) to received the protein injections systemically through the ocular plexus of the animals (30µg / kg rBMP-7 1 or 2 times per week; 20µg / kg rPDGF-BB 1 or 2 times per week; or the combination of the two proteins rBMP7+rPDGF-BB 1 or 2 times weekly). The injections were carried out during five weeks and the animals were euthanized 15 days after the end of the injections. Blood samples were collected for biochemical tests before (0 day) and during treatment (15 and 30 days) and in the day of euthanasia (50 days). The osteoporosis was analyzed by bone densitometry at 0 and 100 days after surgery, and in the day of euthanasia (50 days after treatments). After euthanasia, the animals' organs were collected for histological analysis. Statistical analyzes will be performed using GraphPad 8 and values of $p < 0.05$ were considered statistically significant.

Results:

The results show that after 100 days of ovariectomy the animals develop osteoporosis. The body mass of ovariectomized rats is significantly higher compared to the other groups, which indicates that the surgery was effective. In addition, histological results show degradation of trabecular microarchitecture of these animals' femurs and their BMD is significantly smaller when compared to the control and sham groups.

Conclusion:

Thus, it is concluded that performing ovariectomy and waiting 100 days is an effective protocol osteoporosis' induction in Sprague Dawley rats and the effectiveness of GF treatments is under analysis. We wait to contribute to new clinical and therapeutic protocols for osteoporosis with this innovative treatment.

Financial support:

CNPq, CAPES, FINEP, BNDES, MCT, MS-DECIT, INCT-Regenera.

03.004 - EFFECT OF REPEATED STIMULATION OF COLD RECEPTORS - TRPM8 IN BODY MASS IN OB/OB MICE AND OBESE RATS. Armentano GM, Vizin RCL, Carrettiero DC, Almeida MC, - Centro de Ciências Naturais e Humanas - Universidade Federal do ABC

Introduction:

The understanding of the neural pathways involved in thermoregulatory response to cold advanced after the discovery of temperature sensitive TRP channels. Menthol mimics the sensation of cold and activates thermoregulatory mechanisms of cold defense in mammals, promoting hyperthermia and increasing energy expenditure. For this reason, menthol has been suggested as an anti-obesity drug, as it increases metabolism without affecting food intake, resulting in lower body mass gain in lean rodents. The effects of menthol on obese animals however, is unknown. Thus, this study aimed at investigating the effects of menthol in both obese ob/ob mice and high-fat diet (HFD) obese rats.

Aim:

To evaluate whether the chronic stimulation of the peripheral TRPM8 channels changes the weight and food consumption in ob / ob mice treated with menthol; To verify the influence of the chronic stimulation of the TRPM8 channels on the Tc as well as the locomotor activity of these animals; To analyze histological alterations in white adipose

tissue in animals submitted to chronic treatment with agonist of TRPM8 channels.

Methods:

Menthol was dissolved in propyleneglycol at a concentration of 5% (w/v). HFD-induced obesity was obtaining by feeding Wistar rats with high fat chow (Rhoister) for 10 weeks. Both obese (ob/ob or HFD) and lean (C57Bl mice and lean wistar rats) were topically treated with menthol or PPG for 9 consecutive or alternate days. Throughout experiment abdominal temperature, total activity and body mass were monitored. Data were analyzed by two-way ANOVA or t-test.

Results:

In lean animals (C57Bl or lean Wistar rats) repeated application of menthol resulted in a decrease in body mass gain, which agree with our previous report in lean Wistar rats (Vizin et al, 2018). Menthol treatment was accompanied by a hyperthermic response in both mice and rats (nearly 1°C increase in body temperature compared to control animals), which most probably accounted for the increased energy expenditure that allowed body mass reduction. In obese HFD rats, mentol treatment resulted in a decrease in 20g +/- 1,2g in mean body weight, which corresponds to a 5% reduction in body mass. However, in obese ob/ob mice repeated application of menthol was not sufficient to cause a significant reduction on body mass gain. Interestingly, the hyperthermic response of ob/ob mice to menthol was reduced as compared to C57Bl.

Conclusion:

We have confirmed our previous results that short-term treatment with topical menthol results in less body mass gain in lean rodents due to a persistent increase in energy expenditure, with limited compensatory thermoregulatory adaptations and, most unexpectedly, without affecting food intake (Vizin et al, 2018). Here, we tested the effects of topical menthol (5%) treatment on body weight gain and body temperature on both genetic obese ob/ob mice and in high fat diet (HFD)-induced obesity in rats. Although topical menthol was not efficient to reduce body mass in ob/ob mice, it reduced body mass in obese HFD rats. Our data supports the suggestion that menthol is a promising drug not only for obesity prevention but also for obesity treatment.

Financial support:

FAPESP, UFABC

03.005 - APPLICATION OF MACHINE LEARNING TECHNIQUES IN THE ESTROUS CYCLE AND SEXUAL MATURATION OF RATS EXPOSED TO DIFFERENT LIGHTING PATTERNS. Constantino DB, Tonon AC, Xavier NB, Oliveira MAB, Freitas JJ, Rodriguez GA, Silva LF, Idiart M, Hidalgo MP, - Programa de Pós-Graduação em Psiquiatria e Ciências do Comportamento - HCPA

Introduction:

Modern lifestyle is characterized by constant exposure to artificial light, which can lead to alterations in biological rhythms and abnormalities to reproductive cycles. Considering that female reproductive cycle is maintained by the intact circadian regulation of the hypothalamic-pituitary-gonadal axis, which is sensitive to several external stimuli, especially the light-dark cycle, we hypothesized that females exposed to artificial light would develop earlier puberty. Since the classification of the stages of the estrous cycle can be a useful measure of the cycling patterns of rodents, we developed, in a second study, a machine learning algorithm able to classify images of estrous cycle.

Aim:

To evaluate the effect of four different lighting patterns on pubertal development of female Wistar rats and, as a secondary objective, to develop a machine learning algorithm able to classify images of estrous cycle in the right stage of the cycle.

Methods:

This project was approved by the ethical committee (#HCPA 16-0378). Females were obtained from a process of mating within a photoperiod

FeSBE Annual Meeting 2019 Poster Sessions and Abstracts

station, so that they were exposed to different lighting patterns since gestation. Thus, they were divided into four groups: RGB color combination (red, green, blue) varying their spectral composition throughout the day (RGB-v; N = 14), RGB with a fixed light color temperature (RGB-f; N = 13) during the whole photoperiod, constant darkness (DD; N = 13) and constant fixed light (LL; N = 15). The experiments were performed in females from the postnatal day (PND) 22 to 50. Vaginal smears were taken daily at the same hour (5 p.m) once vaginal opening occurred. Statistical comparisons between groups were evaluated by two-way ANOVA, followed by Tukey's test. Kruskal-Wallis was used to compare non-parametric data. Statistical difference was accepted as $p < 0.05$. After optical microscopic initial evaluation, pictures were taken using a mobile phone and the images classified by human experts according to the estrous phase cycle. The dataset of images was used to train and test an automatic classifier based on convolutional neural networks (implemented by the Python package Keras.) First, 80 images were selected, 80% of pictures was used for training and 20% for test. Second, it was used a major database, using 500 new images, to improve previous results.

Results:

In the first study, no significant differences were found in the age of vaginal opening, however the RGB-v group showed significant lower number of complete and consecutive cycles. Also, RGB-f group showed first complete estrous cycle significantly earlier than RGB-v group. In the second study, the first database resulted in 91% training accuracy and 60% test accuracy, what indicates some degree of overfitting. In the second phase, each photo was divided into 4 photos of 400x400 pixels, in order to improve training speed. The result was more robust with 73% of training accuracy and 69% when testing the algorithm for novel images.

Conclusion:

Our experiment suggests that changes in lighting quality could affect pubertal development. Also, the algorithm was capable to identify the different stages of estrous cycle with 69% accuracy. Application of these results might be constructive to improve the algorithm accuracy and develop tools capable of identifying biological processes and other types of cells.

Financial support:

CAPES, FIPE/HCPA, CNPQ

4 - Cardiovascular Biology and Diseases

04.001 - HYPEROXIA PROMOTES ANTIOXIDANT ENZYMES ACTIVITY IMBALANCE IN HEART OF BALB/C MICE WITHOUT OXIDATIVE DAMAGE. Silva BL, Santos-Silva MA, Bezerra FS, Lanzetti M, Valença SS, deMoraesSobrinhoPorto LC, Nagato AC, - Departamento de Fisiologia - UFJF Centro de Ciências da Saúde - UFRJ Laboratório de Histocompatibilidade e Criopreservação - UERJ Departamento de Ciências Biológicas - UFOP Centro de Ciências da Saúde - UNI VASSOURAS

Introduction:

Oxygen is a lipophilic molecule able to spread by any biological microenvironment. Clinically, oxygen inhalation therapy (hyperoxia) is required to reverse hypoxemia. However, hyperoxia is known for inducing ROS, RNS, redox imbalance, oxidative damage and inflammation. In response to oxidative stress, enzymatic antioxidants are produced to defend the biological microenvironment.

Aim:

Here we evaluated enzymatic antioxidant activities in heart of BALB/c mice after hyperoxia.

Methods:

The experimental design was approved by the Ethics Committee of the Instituto de Biologia Roberto Alcântara Gomes (CEA-010/09). Male BALB/c mice were exposed to hyperoxia (100% oxygen) during 12 (12h group), 24 (24h group) or 48 hours (48h group) by using an inhalation

chamber (n=10 per group). Control-group was sham-exposed (n=10). Mice were euthanized right after oxygen exposure. Hearts were removed and homogenized for biochemical analyses (catalase-CAT, glutathione peroxidase-GPx and malondialdehyde-MDA). The data were presented as the mean \pm standard error of the mean (SEM). One-way ANOVA followed by the Student-Newman-Keuls post hoc test was used and the significance level was 5%.

Results:

The results shown an increased ($\approx 60\%$; $p < 0.001$) CAT activity (U/mg ptm) after 24h ($0,53 \pm 0,02$) of hyperoxia compared to the control group ($0,32 \pm 0,02$). Hyperoxia increased ($p < 0.001$) GPx activity ($\mu\text{M}/\text{min}/\text{mg ptm}$) after 12h ($\approx 449\%$; $0,094 \pm 0,008$), 24h ($\approx 518\%$; $0,109 \pm 0,009$) and 48h ($\approx 583\%$; $0,123 \pm 0,014$) of exposure when compared to the control group ($0,021 \pm 0,002$). Hyperoxia did not change CAT activity at 24h and 48h as well as MDA levels at any time of exposure.

Conclusion:

Our results suggest that 100% of oxygen exposure during 48 hours can triggers oxidative stress in hearts of BALB/c mice without oxidative damage. Adverse effects of hyperoxia on heart might be considered before prescription to humans.

Financial support:

This work was supported by grants from FAPERJ and CNPq. ACN and ML received a bursary from Coordenação de Aperfeiçoamento de Pessoal de Ensino Superior (CAPES).

04.002 - THE CARDIOVASCULAR EFFECT OF EMPAGLIFLOZIN IN AN EXPERIMENTAL MODEL OF METABOLIC SYNDROME. Cotrin JC, Silva TIP, Souza-Mello V, Barbosa-da-Silva S, - Anatomia - UERJ

Introduction:

Cardiovascular disease (CVD) remains the number 1 cause of morbidity and mortality globally. Obesity, hypertension and diabetes are risk factors for CVD, and in the presence of both type 2 diabetes and CVD increases the risk of death. Empagliflozin, one sodium-glucose cotransporter 2 inhibitor, also has favorable effects in some risk factors for CVD, like reducing hyperglycemia, visceral adiposity and blood pressure. The present study hypothesized that treatment with empagliflozin may improve left ventricular remodeling in an experimental model that presented CVD risk factors.

Aim:

This study aimed to evaluate the effects of empagliflozin on cardiovascular parameters of mice fed a high-fat diet to induce metabolic alterations (Hyperglycemia, obesity, hypercholesterolemia, hypertension).

Methods:

This study was approved for the local ethical committee (031/2017). 40 male mice C57BL6 were used, metabolic alterations were induced in mice by providing them free access to a high-fat diet (HF) for 10 weeks. After that, the mice were subjected to the empagliflozin treatment (10mg/kg/day), during 5 weeks, totalizing 4 groups, control group (C), control with empagliflozin (CE), High-fat group (HF), High-fat empagliflozin (HFE). Body weight (BW) was determined once a week, and food intake was evaluated daily. Oral Glucose tolerance test (OGTT) and the insulin measured are used to calculate the HOMA-IR. Systolic blood pressure (SBP) was monitored once a week using a calibrated insight tail cuff system. Blood samples were obtained via cardiac puncture through the right atrium and stored at -80°C . The heart was dissected, and the left ventricle (LV) volume were determined by Scherle's method. The LV was fixed and stained with hematoxylin and eosin. The cross-sectional area of LV cardiomyocytes was estimated by stereology $A[\text{car}]$. The LV thickness was calculated. The plasma cholesterol and the urinary uric acid were determined with appropriate commercial kits. The data were statistically analyzed with T-Student test or OneWay ANOVA with Tamhane pos-test (mean \pm standard deviation, significant p-value < 0.05).

Results:

FeSBE Annual Meeting 2019

Poster Sessions and Abstracts

The HFE group showed a decrease in BW -5% (g, HF:28.5±1.49; HFE:27.2±1.12), while increased food intake +13% (KJ, HF:44.16±5.23; HFE: 49.66±5.31). Total cholesterol presented significant reduction about -17% (mg/dL, HF:132.8±5.4; HFE:110.2±9.7). The urinary uric acid increased +53% (mg/24h, HF:5744±1535; HFE:8763±793.4). There is no effect observed in triglyceride levels (mmol/L, HF:51.2±3.23; HFE:59.72±5.3). Data from LV, showed lower LV thickness in HFE -15% when compared with HF group (μm , HF:1337±38.89; HFE:1133±34.65), as well as reduced LV weight -9% (mg, HF:0.081±0.0028; HFE:0.073±0.0036) and regarding cardiomyocyte area of the HFE group, showed reduction compared with HF group, A[car] -27% (HF:1307±665.5; HFE:958.5±447.9), in addition was observed significant reduction in SBP of the HFE group -16% (mmHg, HF:153.90±10.34; HFE:129.60±5.14). Concerning carbohydrate metabolism, area under the curve of OGTT was -5% lesser in HFE than HF (a.u., HF:1028±25.88; HFE:973.30±20.13) and the HOMA-IR decreased -63% (HF:35.78±4.94; HFE:13.24±1.17).

Conclusion:

This study shows positive effects of empagliflozin in an experimental model of metabolic syndrome. The empagliflozin reduced CVD risk factors by reducing BW, the total cholesterol, uric acid and SBP. Equivalently there was VE remodeling after the treatment decreasing LV thickness and A[car].

Financial support:

CAPES

04.003 - BRONCHIAL VASCULAR REMODELING IS ATTENUATED BY ANTI-IL17 IN MICE WITH CHRONIC ALLERGIC INFLAMMATION EXACERBATED BY LPS. Camargo LN, Santos TM, Martins MA, Prado CM, Leick EA, Righetti RF, Tibério IFLC, Tibério IFLC, - Ciências Médicas - FMUSP

Introduction:

Although the major asthmatic alterations are related to airways there is also evidence of the importance of peribronchial vascular inflammation and remodeling in its pathophysiology

Aim:

To estimate the effects of anti-IL17 therapy on peribronchial vessels of an asthma model exacerbated by LPS

Methods:

This study was approved by CAPPesq FMUSP (Process nº 141/16). Thirty-six male BALB / c mice repeatedly exposed to ovalbumin and treated or not with anti IL17 were used. Chronic allergic pulmonary inflammatory model: A) SAL group: Inhalations with sterile saline (SF) (n = 8); B) OVA group: Inhalations with ovalbumin solution (n = 8); C) SAL + anti-IL-17 group: Inhalations with sterile SF and treatment with IL-17 monoclonal antibody (n = 8); D) OVA + anti-IL-17 group: Inhalations with OVA solution and treatment with anti-IL-17 monoclonal antibody (n = 8). LPS exacerbated chronic allergic lung inflammation model: E) OVA + LPS group: Inhalations with ovalbumin solution and LPS instillation (n = 8); F) OVA + LPS + anti-IL-17 group: Inhalations with ovalbumin solution, LPS instillation and treatment with anti-IL-17 monoclonal antibody (n = 8). Twenty-four hours before the end of the experimental protocol, one group received LPS (0.1mg/ml-intratracheally) OVA + LPS and OVA + LPS + anti-IL-17. After the end of the experimental protocol. We evaluated inflammation, remodeling, oxidative stress, perivascular edema, angiogenesis, NFKB and ROCK1 and ROCK2.

Results:

OVA-LPS anti-IL17 showed a decrease in inflammation: CD4+(9.3±0.5vs5.3±0.3), CD8+(14.5±1.1vs11.1±0.9), IL-2(18.3±3.0 vs 4.9±1.1),IL-4(7.7±0.6 vs 0.8±0.1),IL-6(14.0±1.1 vs 2.2±0.2), IL-10(9.7±0.8 vs 2.1±0.1),and IL-17(23.6±1.5 vs 9.4±1.2) positive cells/104 μm^2 , perivascular edema (11.8±0.9 vs 3.5±0.2) and angiogenesis (7.2±0.4 vs 5.7±0.5) μm^2 . Remodelling: MMP-9(14.5±1.4 vs 7.8±1.0), MMP-12(14.0±1.2 vs 8.6±0.6),TIMP-1(15.6±1.6 vs 6.3±0.6) and TGF- β (27.6±1.7 vs 20.5±1.1) positive cells/104 μm^2 and volume fraction of

collagen I (21.8±3.6 vs 17.0±3.0), collagen III (16.2±3.7 vs 16.7±1.4). Oxidative Stress: iNOS(14.7±0.7 vs 7.6±0.3) positive cells/104 μm^2 and volume fraction of PGF2 α (22.3±2.7 vs 21.0±2.4). Signaling Pathways: FOXp3(15.3±0.9 vs 6.9±1.7), dendritic cells(20.0±1.8 vs 10.9±0.9), NFKB(23.4±2.1 vs 7.9±1.0), ROCK1(14.5±1.3 vs 7.8±0.3), ROCK2(10.4±0.7 vs 4.7±0.6) positive cells/104 μm^2 compared to OVA-LPS, p<0.05.

Conclusion:

In this model of asthma exacerbated by LPS inhibition of IL17 represents a promising therapeutic strategy, since it contributes to bronchial vascular control of Th2 and Th17 responses, remodeling and oxidative stress pathway activation. This effect may be associated with the control of signaling pathways

Financial support:

FAPESP, CNPq, LIM-20-FMUSP

04.004 - CYSTEINE AND GLYCINE-RICH PROTEIN 3 (CRP3) ABSENCE IMPAIRS FOCAL ADHESION SIGNALING AND FORCE GENERATION IN AORTIC SMOOTH MUSCLE CELLS. Ribeiro-Silva JC, Ferraz MSA, Silva TG, Alencar AM, Ballestrem C, Krieger JE, Miyakawa AA, - Heart Institute, University of Sao Paulo Medical School - FMUSP Physics Institute, University of Sao Paulo - USP The University of Manchester -

Introduction:

We have previously demonstrated that cysteine and glycine-rich protein 3 (CRP3) interaction with focal adhesion kinase (FAK) modulates the vascular response to injury. As FAK is central to focal adhesion (FA) signaling (the structure connecting the extracellular matrix to the actin cytoskeleton), and CRP3 has been implicated as an actin regulatory protein, we hypothesized that CRP3 would be a FA protein in control of aortic smooth muscle cell mechanoresponse.

Aim:

To test the hypothesis that CRP3 is a focal adhesion protein in charge of aortic smooth muscle cell mechanoresponse.

Methods:

Immunoprecipitation: AoSMC protein extracts were used to both immunoprecipitate and analyze the expression of FA proteins via immunoblotting. Immunofluorescence: AoSMCs were seeded in glass coverslips coated with gelatin or fibronectin, exposed to angiotensin II (Ang II 1 μM) or ROCK inhibitor (ROCKi, 3 μM), immunostained for FAs and analyzed via confocal microscopy. Optical Magnetic Twisting Cytometry: cell-attached RGD-coated ferrimagnetic beads were exposed to a magnetic field to deform the adjacent cytoskeleton in the baseline and in response to Ang II or cytochalasin D (5 μM). Contraction Assay: AoSMCs were mixed with a collagen I solution, forming a collagen disk whose diameter was analyzed at time 0 and 24h in the presence of Ang II or Ri. Statistical Analysis: data expressed as mean±standard deviation and compared via Student's t test or two-way analysis of variance, followed by Tukey's post hoc test. P values <0.05 were considered statistically significant.

Results:

Immunoprecipitation and colocalization studies revealed CRP3 as a new FA protein. AoSMCs from CRP3 knockout (KO) displayed increased FA mean size regardless of the substratum (gelatin WT 2.4 μm^2 ±0.7/CRP3KO 2.7 μm^2 ±0.7 n=78; fibronectin WT 1.7 μm^2 ±0.3/CRP3KO 2 μm^2 ±0.4 n=73). Upon stimulation with angiotensin II, CRP3KO cells failed to mature FA when compared to WT (WT Basal 1.9 μm^2 ±0.4 Ang II 2.5 min 2.3 μm^2 ±0.6 24h 2.1 μm^2 ±0.5/CRP3KO Basal 2.2 μm^2 ±0.4 Ang II 2.5 min 2.2 μm^2 ±0.6 24h 2.1 μm^2 ±0.6 n=85), what could be associated with the reduced expression of FAK (WT 1±0.2/CRP3KO 0.6±0.1 n=8), paxillin (WT 1.1±0.21/CRP3KO 0.7±0.1 n=6), and MLC2 (WT 1±0.1/CRP3KO 0.5±0.2 n=8) in CRP3KO cells. Increased stiffness was also observed in CRP3KO AoSMCs (WT Basal 1.5Gp±0.3 Ang II 1.9Gp±0.5 CytD 0.8Gp±0.6/CRP3KO Basal 1.6Gp±0.4 Ang II 2.2Gp±0.4 CytD 0.9Gp n=1419), accompanied of reduced contractile capacity at the baseline and in response to Ang II or

FeSBE Annual Meeting 2019

Poster Sessions and Abstracts

ROCKi (WT Basal 27%±3 Ang II 47%±9 Ri 13%/CRP3KO Basal 7%±1 Ang II 24%±2 Ri 0% n=4).

Conclusion:

CRP3 behaves as a focal adhesion protein, regulating its size and signaling in aortic smooth muscle cells. The absence of CRP3 at FAs increases cell stiffness and reduces force generation, which are key features of smooth muscle cell physiology. Altogether, our findings support the idea that CRP3 is a key modifier of aortic smooth muscle cell mechanoresponse.

Financial support:

FAPESP (2013/17368-0; 2015/11139-5; 2017/50298-7) and CNPQ (130142/2016-6)

04.005 - INDUCTION OF A CELLULAR MODEL OF ENDOTHELIAL DYSFUNCTION BY INHIBITION OF NITRIC OXIDE PRODUCTION. Silva FC, Araújo BJ, Correia MC, Martins IC, Guerra JFC, Araújo TG, Fürstenau CR, - Programa de Pós-Graduação em Biotecnologia - UFU Centro de Ciências Naturais e Humanas - UFABC Graduação em Biotecnologia - UFU Programa de Pós-Graduação em Ciências Farmacêuticas - UFG

Introduction:

Endothelial cells perform important functions in the vasculature, ranging from the regulation of cell proliferation and adhesion to thrombosis, inflammation in vessel lumen and regulation of vessel tone. These effects are mediated by the production of important biomolecules, such as nitric oxide (NO). Endothelial dysfunction is a condition characterized by an imbalance in the production/bioavailability of those biomolecules, mainly due to a significant reduction in the bioavailability of NO. Endothelial dysfunction is present in a number of metabolic and cardiovascular diseases, including diabetes, atherosclerosis, and hypertension, however, only few in vitro models are available to study such condition.

Aim:

This study aimed to develop and validate an in vitro protocol for the induction of a condition similar to endothelial dysfunction in endothelial cells of the tEnd.1 lineage.

Methods:

Cells were used between 4 and 8 passages and were challenged with L-NAME (1, 10, 100 µM or 1 mM), an inhibitor of nitric oxide synthase; and 100 µM L-arginine, a substrate for the synthesis of NO (negative control) for 12, 24, 48, 72, 96 and 120 hours without retreatment and for 48, 72, 96 and 120 hours with retreatment every 24 hours. Cell viability was evaluated by MTT method and nitrite measurements were made with Griess reagent kit.

Results:

The results obtained are still preliminary. However, in general, we observe that: 1) cellular viability in response to L-arginine is best achieved by changing the medium every 24 hours (retreatment), since the percentage of cell viability does not differ from the control group (no treatment) in any of the evaluated times. The exception is for the group 72 hours, in which there was cell death (73.86 ± 10.58 % cell viability); 2) regarding L-NAME treatment, cellular viability was not altered only at 72 hours without retreatment and at 96 hours with retreatment; 3) nitrite measurements showed that in L-arginine tends to increase NO concentration all treatments when compared to control, and the most significant increases were observed in the treatments for 96, 120 and 72 hours without retreatment, being 61.90%, 62.68% and 21.98%, respectively (p <0.0001). On the other hand, L-NAME tends to reduce nitrite level in a dose-dependent manner, best observed in treatments at a concentration of 10 µM (29.65%), 100 µM (70.83%), and 1 mM (91.37%) (p <0.0001) for 72 hours without retreatment, and at 10 µM (32.62%), 100 µM (51.47%) and 1 mM (94.30%) (p <0.0001) of L-NAME for 96 hours with retreatment.

Conclusion:

To date, results obtained with tEnd.1 cells treated with 10 µM and 100 µM L-NAME for 72 hours without retreatment and 96 hours with

retreatment seem to be more promising in the development of an in vitro model of endothelial dysfunction since there is no change in cell viability, but there is inhibition of NO production, one of the hallmarks of this condition. These results, however, need to be confirmed and further analyses such as the dosage of oxidizing molecules and eNOS gene and protein expression are planned.

Financial support:

CAPES e CNPq (Projeto 446747/2014-9)

04.006 - MYELOPEROXIDASE AND HDL-C AS CARDIOVASCULAR RISK MARKERS IN PRE-PUBERTAL PRETERM CHILDREN. Schoeps DO, Holzer S, Suano-Souza FI, Fonseca FLA, Sarni ROS, Hix S, - Bioquímica - FMABC Pediatría - FMABC Laboratório de Análises Clínicas - FMABC

Introduction:

Prematurity occurs in 11.1% of the world's live births, corresponding to 14.9 million births before 37 weeks of gestation. Complications resulting from premature birth account for one million yearly deaths. Short- and long-term complications in the preterm group include stunting, increased risk of infections, developmental impairment, and death in childhood. The consequences of prematurity may, however, persist throughout the adulthood life, increasing the likelihood of future cardiovascular, renal and metabolic syndrome. The early identification of cardiovascular risk markers in pre-term born children may therefore prevent or reduce the likelihood of morbidity and mortality due to cardiovascular disease in adulthood. In addition to classical lipid biomarkers, the use of apolipoproteins (Apo A1 and B), paraoxonases (PON), high sensitivity C-reactive protein (hs-CRP) and myeloperoxidase (MPO) are increasing in importance on cardiovascular risk.

Aim:

To evaluate the biomarkers related to cardiovascular risk in pre-pubertal preterm children with a birth weight of less than 1,500g and relate them to current nutritional status, insulin resistance and inflammation

Methods:

This is a cross-sectional, controlled study with pre-pubertal preterm children between 5 and 9 years of age with a birth weight of less than 1,500 grams (Preterm group, n=44) compared to full term children of adequate weight for gestational age (Control group, n=30). Clinical evaluation: anthropometry and pubertal staging. Laboratory tests were performed using standard laboratory methods: total cholesterol and fractions, triglycerides, paraoxonase 1, apolipoproteins A1 and B, myeloperoxidase (MPO), high sensitivity C-reactive protein (hs-CRP), glycemia and insulin (to calculate HOMA-IR). Statistical analysis was performed using SPSS 24.0 (IBM®), and the variables are presented as absolute number and percentage, mean value and standard deviation for normal distribution or median and interval for non-parametric data. The comparison of the variables was performed using t-Student and Mann-Whitney tests. The study was approved by the Ethics Committee: CAAE 35175614.6.0000.0082

Results:

The preterm group showed lower concentrations of HDL-c (60.1±10.1 vs. 69.0±10.0 mg/dL; p<0.001); higher concentrations of hs-CRP [0.55 mg/dL (0.30;39.4) vs. 0.30 mg/dL (0.30;10.80); p=0.043], of MPO [21.1 ng/mL (5.7;120.0) vs. 8.1 ng/mL (2.6;29.6); p<0.001] and of MPO/HDL-c ratio [0.39 (0.09;2.07) ng/mg vs. 0.11 (0.05; 0.58)]. The MPO/HDL-c ratio was the variable that showed the best discriminatory power between the groups (AUC=0.878; 95% CI; 0.795-0.961). MPO concentrations in the preterm group were correlated with those of hs-CRP (r=0.390; p=0.009), insulin (r=0.448; p=0.002) and HOMA-IR (r=0.462; p=0.002).

Conclusion:

Pre-pubertal preterm children show high MPO concentrations and MPO/HDL-c ratio that are associated with inflammation and oxidative stress, which, in turn, may be associated with atherosclerosis

Financial support:

FeSBE Annual Meeting 2019 Poster Sessions and Abstracts

NEPAS

04.007 - IMPAIRMENT IN THE VASCULAR REACTIVITY OF MESENTERIC RESISTANCE ARTERIES BY TIME OF EXPOSURE TO TESTOSTERONE IS REVERSED BY GONADECTOMY. Rouver WN, Delgado NTB, Santos RL, - Department of Physiological Sciences - UFES

Introduction:

Testosterone levels has been associated with an increased risk of cardiovascular diseases, but this relationship is not fully elucidated. Our hypothesis is that the presence of testosterone can modulate the vascular reactivity of mesenteric resistance arteries.

Aim:

Thus, this study was designed to investigate age-related changes in vascular reactivity of mesenteric resistance arteries in sham and orchietomized rats.

Methods:

All procedures were approved by the Ethics Committee on Animal Use of the Federal University of Espirito Santo under protocol #07/2016. Wistar male rats (eight weeks old) were divided into Sham and orchietomized (ORX). Sham and ORX groups were evaluated after 2 and 10 weeks of surgery. The vascular reactivity was assessed through resistance myograph system. The third-order mesenteric arteries were identified, isolated and dissected from the adjacent tissue after euthanasia. The artery segments were cut into 2-mm rings and mounted (using a tungsten wires with 40 μm in diameter) inside the chambers filled with Krebs solution heated to 37 $^{\circ}\text{C}$ and aerated with carbogenic mixture (95 % O_2 and 5 % CO_2). After stabilization a concentration-response curves were obtained by cumulative doses of ACh (0,1 nM – 10 μM) in pre-contracted arteries (Phe, 3 μM) before and after the use of NOS (L-NAME, 300 μM) or COX inhibitors (indomethacin, 10 μM), individually or in combination. Arteries were also submitted to a concentration-response curve by cumulative doses of Phe (1 nM a 100 μM). The systolic blood pressure (SBP) was measured throughout 10 weeks by tail-cuff plethysmography. Data were expressed as mean \pm SEM. Student's t-test and 2-way ANOVA followed by Bonferroni post hoc test were used ($p < 0.05$).

Results:

Sham 10 weeks rats showed an impairment in the endothelium-dependent relaxation (AUC, 240 \pm 12 vs 150 \pm 27 a.u., n=6-8) and a greater contractile response (AUC, 26 \pm 1 vs 37 \pm 2 a.u., n=6-7) when compared to Sham 2 weeks rats. Relaxation response was not altered at 2 weeks after orchietomy (AUC, 242 \pm 11 vs 230 \pm 10 a.u., n=9), but gonadectomy avoided the impairment found in Sham 10 weeks rats (AUC, 150 \pm 27 vs 225 \pm 13 a.u., n=6-8). COX metabolites do not seem to be involved in ACh-induced relaxation. Nevertheless, the associated inhibition (L-NAME + Indomethacin) revealed an important participation of NO in all groups. There were no changes in the contractile response evoked by Phe in Sham and ORX groups evaluated after 2 weeks (AUC, 26 \pm 1 vs 27 \pm 1 a.u., n=7), while after 10 weeks of gonadectomy there was an improvement in the Phe-induced contraction (37 \pm 2 vs 30 \pm 2 a.u., n=6). Despite the modulation found in both relaxation and contraction response, we found no change in SBP throughout 10 weeks (Sham 127 \pm 2 and ORX 126 \pm 2 mmHg, n=7-10).

Conclusion:

Our data show that the time of testosterone exposure, by age, seems to play an important role in the development of vascular changes in the vascular reactivity of mesenteric arteries that were reversed by gonadectomy. Thus, we believe that testosterone seems to be involved in the development of vascular changes that may participate in the onset of age-related cardiovascular diseases.

Financial support:

PPGCF-UFES/PROAP

04.008 - ANTIHYPERTENSIVE EFFECT OF N-ACYLHYDRAZONIC DERIVATIVES IN SPONTANEOUSLY HYPERTENSIVE RATS. ROCHA BS, daSILVA JS, PEDREIRA JGB, BARREIRO EJ, SUDO RT, ZAPATA-SUDO G, -

PROGRAMA DE PESQUISA EM DESENVOLVIMENTO DE FÁRMACOS - UFRJ

Introduction:

Arterial hypertension is one of the main risk factors for cardiovascular diseases, which are the leading cause of death in the world. It is a multifactorial clinical condition, characterized by elevated blood pressure, which can be persistent after using three antihypertensive drugs. Thus, it is important to identify new therapeutic alternative to the resistant hypertension and prevent the evolution to heart failure.

Aim:

This work investigated the antihypertensive action of new derived N-acylhydrazones.

Methods:

Protocols were approved by the Animal Care and Use Committee at Federal University of Rio de Janeiro (#DFBICB049). Vascular reactivity was evaluated by recording the isometric tension of thoracic aorta from male Wistar rats (200-220 g). Aortic rings pre-contracted with phenylephrine (10 μM , n=5) was exposed to increasing concentrations (0.1-100 μM) of either LASSBio-A, LASSBio-B, LASSBio-C or LASSBio-D. Blood pressure (BP) and heart rate (HR) were determined following intravenous administration of 10 and 30 $\mu\text{mol/kg}$ of compounds in spontaneously hypertensive rats (SHR, 12-14 wks).

Results:

LASSBio-A, LASSBio-B, LASSBio-C and LASSBio-D promoted vasodilator activity in a concentration dependent manner with maximum relaxation of 84.4 \pm 4.1; 94.8 \pm 2.1; 59.2 \pm 14.7; and 92.9 \pm 2.6% after exposure to 100 μM . The concentration of those compounds to produce 50% vascular relaxation was 14.7 \pm 5.2; 14.6 \pm 2.9; 104.8 \pm 35.1 and 8.7 \pm 3.3. Intravenous injection of LASSBio-A (30 $\mu\text{mol/kg}$) reduced the systolic and diastolic pressures in SHR from 174.0 \pm 15.1 to 131.2 \pm 1.2 mmHg and from 107.3 \pm 13.1 to 68.5 \pm 14.0 mmHg, respectively, indicating its antihypertensive effect. HR was also reduced from 226.3 \pm 12.7 to 132.5 \pm 36.8 bpm. Similar results were observed after intravenous administration of LASSBio-B. It produced reduction of systolic and diastolic pressures from 147.6 \pm 2.5 to 109.0 \pm 8.4 mmHg and from 94.0 \pm 3.8 to 49.8 \pm 6.8 mmHg.

Conclusion:

The antihypertensive effect of new N-acylhydrazone compounds in SHR is probably caused by their vasodilator action.

Financial support:

CNPq, FAPERJ, CAPES, INCT-INOVAR

04.009 - SEX DIFFERENCES IN PROGESTERONE-INDUCED RELAXATION IN THE CORONARY BED FROM NORMOTENSIVE RATS. Giesen JAS, Rouver WN, Costa ED, Lemos VS, Santos RL, - Department of Physiological Sciences - UFES Department of Physiology and Biophysics - UFMG

Introduction:

Progesterone seems to exert a physiological role in cardiovascular physiology since its receptors are found in endothelial cells. However, little is known about its action on the coronary circulation.

Aim:

Thus, the purpose of this study was to investigate the acute effect of progesterone and the involvement of possible endothelial mediators in the action of this hormone on the coronary bed from normotensive rats of both sexes.

Methods:

We used Wistar rats of both sexes on the protocols approved by the Ethics Committee on Animal Use of the Federal University of Espirito Santo (#64/2017). The experimental protocols were conducted by the modified Langendorff method. The vascular reactivity of the coronary vascular bed was evaluated by dose response curve of progesterone (1-50 μM , in bolus) in isolated hearts from female and male rats. CPP was determined and the progesterone effect was assessed before and after perfusion with N ω -nitro-L-arginine methyl ester (L-NAME, 100 μM), indomethacin (2.8 μM), clotrimazole (0,75 μM), catalase (1000 u/mL),

FeSBE Annual Meeting 2019

Poster Sessions and Abstracts

Tiron (1 mM), and apocynin (30 μ M). The analysis of nitric oxide (NO) and superoxide anion ($O_2^{\bullet-}$) levels and were performed by DAF-2 and DHE, respectively, with progesterone stimulation in the presence of L-NAME (300 μ M) and Tiron (10 μ M). The data were expressed as the mean \pm standard error of the mean (SEM). The comparisons of coronary perfusion pressure (CPP) among groups were performed through the unpaired Student t-test and the vasodilator effect of progesterone was evaluated through two-way analysis of variance (two-way ANOVA) followed by Bonferroni post hoc test. The fluorescence microscopy analysis was evaluated through one-way analysis of variance (one-way ANOVA) followed by Tukey post hoc test ($p < 0.05$).

Results:

The sexual difference in CPP was confirmed and females had a higher CPP when compared with males (female, $F = 87.39 \pm 2.4$ mmHg, $n=10$; male, $M = 69.04 \pm 2.7$ mmHg, $n=9$). However, progesterone showed similar vasodilatation in both sexes ($F = 10.8 \pm 1.1$ %, $n=10$; $M = 10.2 \pm 1.7$ %, $n=9$). After inhibition of NO synthesis, both females and males had an increased vasodilatory response when compared to the curve performed in the absence of inhibitor ($F = 10.8 \pm 1.1$ % to 23.5 ± 4.4 %, $n=10$; $M = 10.2 \pm 1.7$ % to 26.6 ± 3.4 %, $n=9$). The fluorescence analysis showed that after progesterone stimulation the NO production was increased in both sexes. After inhibition of prostanoids synthesis, only males had a reduced response ($F = 10.8 \pm 1.1$ % to 11.5 ± 2.4 %, $n=8$; $M = 10.2 \pm 1.7$ % to 4.3 ± 1.0 %, $n=8$). When the participation of hydrogen peroxide (H_2O_2) was verified, only the females had the response to attenuated progesterone ($F = 10.8 \pm 1.1$ % to 6.7 ± 2.4 %, $n=8$; $M = 10.2 \pm 1.7$ % to 17.0 ± 2.6 %, $n=7$). In addition, $O_2^{\bullet-}$ appears to be involved in this response in females, considering that $O_2^{\bullet-}$ production ($n=4$ per group) was increased in female group after stimulation with progesterone.

Conclusion:

These results suggest a protective role of progesterone, which promotes relaxation in the coronary vascular bed from normotensive rats of both sexes. Nevertheless, the mediators involved in this action appear to be different between sexes.

Financial support:

PPGCF-UFES

04.010 - GPER AGONIST (G-1) RELAXES RESISTANCE MESENTERIC ARTERIES FROM SPONTANEOUSLY HYPERTENSIVE RATS OF BOTH SEX. Delgado NTB, Rouver WN, Santos RL, - Pós-graduação em Ciências Fisiológicas - UFES

Introduction:

Hypertension is considered the risk factor for cardiovascular diseases with greater susceptibility in men when compared to premenopausal women. However, this difference is lost after menopause, indicating the cardioprotective effects of estrogen that are mediated by classical receptors and G protein-coupled receptors (GPER). However, little is known about the GPER actions in hypertension.

Aim:

The objective of our study was to evaluate the response mediated by GPER using the specific agonist. We hypothesized that GPER agonist induces a relaxing response in resistance mesenteric arteries.

Methods:

The present study was approved by the Ethics Committee of the Federal University of Espírito Santo #048/2016. Adult spontaneously hypertensive rat (10–12 weeks old) of both sexes were used. For the first protocol, third-order mesenteric arteries were isolated, and concentration-response curves were plotted following the cumulative addition of the G-1 (1 nM – 10 μ M) following induction of contraction with phenylephrine (3 μ M). The G-1 effects were assessed before and after incubation for 30 min with L-NAME (300 μ M) and indomethacin (10 μ M) isolated or combined with clotrimazole (0.75 μ M), catalase or with tetraethylammonium-TEA (5 mM). For the second protocol, the responses were observed in increasing and cumulative doses of

acetylcholine (0.1 nM - 0.1 mM) or phenylephrine (0.1 nM - 0.1 mM) with G-1 incubations (0.1 μ M, 1 μ M, and 10 μ M G-1). Data were expressed as mean \pm SEM. The response was assessed by two-way analysis of variance (ANOVA) followed by the Sidak post-hoc test. $p < 0.05$.

Results:

G-1 induced a relaxing response similarly in both sexes (Female control curve = 85 ± 3.5 % and Male control curve = 80 ± 3.2 %). In females, the presence of inhibitors for NO synthase and the prostanoid pathway not changed the relaxing response. However, the presence of the inhibitor of a probable EDHF pathway promoted a reduction in this response (47 ± 12.5 %). In males, the use of inhibitors for NO synthase and a probable EDHF pathway reduced (50 ± 6 % and 54 ± 8 %, respectively) and the inhibition of prostanoid pathways potentialized (94 ± 2 %) the relaxing response. Thus, the G-1 response in females, unlike males, does not depend on the NO and prostanoid pathways, but there was an involvement of the EDHFs, such as H_2O_2 in both sexes. According to our second protocol, the G-1 was able to modulate only the phenylephrine response in both sexes (Female Curve = 13 ± 1 %, 10 μ M G-1 = 7 ± 0.7 % and Male Curve = 11.5 ± 0.4 %, 0.1 μ M G-1 = 14 ± 1 % and 1 μ M G-1 = 14 ± 1.2 %).

Conclusion:

The present findings show that GPER agonist can induce the relaxing response in mesenteric arteries from hypertensive rats similarly between the sexes, however, with the participation of different endothelial mediators. These results may be important to understand about the GPER activation on the vascular reactivity of resistance mesenteric arteries and suggest as a potential therapeutic target for the cardiovascular system in hypertension.

Financial support:

Conselho Nacional de Desenvolvimento Científico e Tecnológico (CNPq)

5 - Gastrointestinal Biology and Diseases

05.001 - EFFECT OF ANTI-TNFA ON ENTERIC NEURONS AND ENTERIC GLIAL CELLS IN EXPERIMENTAL ULCERATIVE COLITIS. Souza RF, Machado FA, Castelucci P, - Anatomia - ICB

Introduction:

The inflammatory bowel disease (IBD) is a disorder that involves chronic inflammation in the digestive tract such as ulcerative colitis (UC) and Crohn's disease (CD), furthermore, has a main pro-inflammatory cytokine involved, the tumour necrosis factor alpha (TNF α).

Aim:

This work aimed to study the effects of anti-TNF α , adalimumab (ADA), in the myenteric plexus of mice submitted to experimental ulcerative colitis.

Methods:

Male mice were used (*Mus musculus*). Colitis was induced by adding 3% Dextran sodium sulfate (DSS) to drinking water for 7 days ($n=5$) (DSS and DSS+ADA groups). The status of the animals was monitored by general examination and body weight evolution. The Sham group received water through the same period and received saline injection in second day. The DSS+ADA group received the anti-TNF α (50 mg/kg+saline injection) in second day of ingestion of DSS. The animals were euthanized after 7 days and distal colon was removed. This study was accordance with the Ethics Committee on Animal Use of the University of São Paulo, Brazil. Tissues were prepared by immunohistochemical methods with double labelling of the nitric oxide synthase neuronal (NOSn), acetyl choline transferase (ChAT), TNF Receptor 2 (TNFR2), protein gene product 9.5 (PGP 9.5) and glial fibrillary acidic protein (GFAP). The number of NOSn-immunoreactive (ir) neurons (neuron/ganglion), ChAT-ir, TNFR2-ir, PGP 9.5-ir and glial cells positive for GFAP-ir were counted. Additionally, profile area (μ m²) of NOSn-ir and ChAT-ir neurons were obtained.

Results:

FeSBE Annual Meeting 2019

Poster Sessions and Abstracts

The NOSn-ir neurons/ganglion in the DSS group (5.7 ± 0.2) decreased by 28.8% compared to that in the Sham group (8.0 ± 0.1), and in the DSS+ADA group (7.3 ± 0.1) increased by 28.2% compared to that in DSS group ($p < 0.05$); ChAT-ir neurons/ganglion of DSS group (6.2 ± 0.4) decreased by 38.6% compared to that in the Sham group (10.2 ± 0.2), and in the DSS+ADA group (8.3 ± 0.2) increased by 32% compared to that in the DSS group ($p < 0.05$). The TNFR2-ir/ganglion in the DSS group (30.3 ± 0.0) increased by 11.2% compared to that in the Sham group (27.3 ± 0.1) and in the DSS+ADA group (19.1 ± 0.3) decreased by 36.9% compared to that in the DSS group ($p < 0.05$). The PGP 9.5-ir/ganglion of DSS group (15.2 ± 0.3) decreased 20.9% compared to that in the Sham group (19.2 ± 0.1), and in the DSS+ADA group (17.4 ± 0.2) increased by 14.7% compared to that in DSS group ($p < 0.05$). The GFAP-ir/ganglion shows no differences among the number of neurons of DSS group (13.0 ± 0.2) and Sham group (12.1 ± 0.2) were detected, and DSS+ADA group (14.9 ± 0.3) increased by 14.2% compared to that in DSS group ($p < 0.05$). The profile area of the NOSn-ir neurons shows no differences in the profile area between the DSS group (166.0 ± 27.5) and DSS+ADA group (158.9 ± 6.8) were detected, and DSS+ADA group decreased by 32.3% compared to that in the Sham group (235.0 ± 10.2) ($p < 0.05$). No differences in the profile area of the ChAT-ir neurons were detected among Sham, DSS and DSS+ADA groups.

Conclusion:

Our data conclude that myenteric neurons were immunoreactive to TNFR2 receptor and, treatment with anti-TNF α seems to be an effective treatment in experimental ulcerative colitis.

Financial support:

FAPESP, CAPES

05.002 - EARLY WEANING TRIGGERS TRANSIENT EFFECTS ON TGF BETA AND FGF10 LEVELS IN THE RAT GASTRIC MUCOSA. Silva KM, Rattes IC, Costa AV, Rigonati CAM, Gama P, - Departamento de Biologia Celular e do Desenvolvimento - USP

Introduction:

During the first three postnatal weeks, the rat gastric mucosa grows rapidly, and there is an endogenous production of biologically active peptides, such as the transforming growth factor beta (TGF β) that controls the development of the stomach, and fibroblast growth factor (FGF10), which is fundamental for gastric morphogenesis. During this phase, breastfeeding acts an important agent in growth programming, and feeding disturbances lead to imbalances in gastric development.

Aim:

Because it is known that early weaning (EW) disturbs gastrointestinal functional maturation and differentiation, at first, we evaluated how it regulates the expression of genes involved in growth control and inflammatory responses. From this screening, we selected growth factors from TGF beta and FGF families, and so our current aim was to study their levels and distribution in the gastric mucosa of EW rats. Moreover, we compared immediate and late responses in order to investigate whether EW effects were maintained lately during adult life.

Methods:

On the 15th day, Wistar rats were divided into two groups: suckling control (S) and early weaning (EW). The control group was allowed to suckle regularly until 21 days, when they were weaned, while EW rats were separated from their mothers. At 15, 18, 30 and 60 days, mucosa gastric corpus samples were collected for analyses of RT-qPCR, Western Blot and Immuno-histochemistry (IHC).

Results:

We observed that whereas EW decreased Tgfb2 at 18 days and augmented Tgfb1 and Tgfb3 at 60 days, it only affected protein levels at 18 days through a decrease of TGF β 1. TGF beta signals after binding receptors T β RI and T β RII, and we found that EW reduced Tgfb2 at 18 and 30 days, whereas T β RII protein levels only decreased at 18 days. TGF β signals through Smads cascade and we detected constant

Smad2/3 immunolabelin in the cytoplasm of epithelial cells. This protein is activated and translocated to the nucleus (Smad2P), but levels remain constant both in IHQ and immunoblot tests. We also evaluated FGF10 and FGFR2, and we observed low expression of Fgf10 in pups and at 30 days after EW, whereas this gene increased in EW-rats at 60 days. Fgfr2 was reduced only at 18 days. The encoded proteins were not affected by EW. Lastly, in the FGF distribution studies, we did not observe changes in the number of cells immunolabeled for FGF10 and FGFR2 and both proteins were detected in the cytoplasm of epithelial cells at 60 days. Both, growth factor and receptor were not identified in pups.

Conclusion:

We suggest that EW induces transient effects on TGFbeta and FGF genes and proteins as differential responses were detected in pups and adult rats.

Financial support:

This study was financed in part by the Coordenação de Aperfeiçoamento de Pessoal de Nível Superior – Brasil (CAPES)- Finance Code 001; FAPESP processes: 2014/21449-9; 2018/07782-8.

6 - Endocrine System

06.001 - PLACENTAL MULTIDRUG RESISTANCE TRANSPORTERS EXPRESSION AND OFFSPRING BEHAVIORAL ANALYSES AFTER GESTATIONAL ADMINISTRATION OF THE VIRAL MIMETIC POLY(I:C) IN THE MOUSE. Monteiro VRS, Gomes HR, Reginatto MW, Fontes KN, Andrade CBV, Bloise FF, Império GE, Spiess DA, Junior WR, Stephen M, Bloise E, Pimentel-Coelho PM, Ortiga-Carvalho TM, - Instituto de Biofísica Carlos Chagas Filho - UFRJ Departamento de Morfologia - UFMG Department of Physiology - UofT

Introduction:

The placenta is responsible for establishing a maternal-fetal interface to supply the physiological needs of the fetus. Besides that, placenta features a barrier replete with the multidrug resistance ABC transporters P-glycoprotein (P-gp, encoded by Abcb1a and Abcb1b genes) and breast cancer resistance protein (BCRP, Abcg2). Current evidence show that gestational infection has the potential to alter the placental expression and function of these transporters. As such, we used the viral mimetic polyinosinic-polycytidylic acid (poly (I:C)), a synthetic analogue of double stranded RNA, widely used to model viral infection through TLR-3 activation. We hypothesized that poly (I:C) may functionally disrupt placental ABC transporters as well as behavioral parameters in the offspring.

Aim:

To evaluate the expression of selected placental ABC transporters, and behavioral changes in the offspring in a murine model of viral infection mimicked by poly (I:C).

Methods:

Pregnant mice (CEUA-CCS: 036/16) were intravenously administered with poly (I:C) or PBS (control group) on gestational day (GD) 13.5. For the behavioral analysis, adult offspring from 5 pregnancies were subjected to the Rotarod performance test after 54 and 93 days of birth and the T-water maze test after 96 days ($n=15-22$). For placental analysis, 6 female subjects from each group were euthanized at GD18.5. Three ABC transporters were evaluated by qPCR analysis: the Abcb1a and Abcb1b genes, Abcg2 and Abca1 (a lipid transporter). T-Student test ($p < 0.05$) was used for statistical analysis.

Results:

A decreased expression in Abcb1a (control: $1,002 \pm 0,1626$ N=7; poly(I:C): $0,5101 \pm 0,08828$ N=8; $P < 0.01$), Abcb1b (control: $0,9997 \pm 0,1613$ N=7; poly(I:C): $0,6284 \pm 0,07877$ N=5; $P < 0.05$) and Abcg2 (control: $1,000 \pm 0,1611$ N=7; poly(I:C): $0,5134 \pm 0,08935$ N=8; $P < 0.01$) was observed following poly (I:C) administration when compared with the control group. The offspring exhibited an impaired performance in

FeSBE Annual Meeting 2019

Poster Sessions and Abstracts

the Rotarod test after 54 days in females (control: 328,9 ± 26,54 N=28; poly(I:C): 217,9 ± 22,80 N=22; P<0.01) and males (control: 278,2 ± 25,35 N=20; poly(I:C): 160,4 ± 21,34 N=18; P<0.01), and also after 93 days in females (control: 369,2 ± 30,61 N=28; poly(I:C): 248,5 ± 15,96 N=22; P<0.01) and males (control: 392,1 ± 20,80 N=20; poly(I:C): 222,0 ± 24,16 N=18; P<0.0001). An impaired performance was also observed in T-water maze task after 96 days in females (control: 20,54 ± 2,103 N=26; poly(I:C): 29,71 ± 2,912 N=22; P<0,05) and males (control: 22,63 ± 1,656 N=19; poly(I:C): 31,94 ± 4,135 N=18; P<0.05).

Conclusion:

Viral infection during pregnancy impairs the expression of placental multidrug resistance transporters encoding genes and has the potential to increase fetal exposure to drugs and toxins; this effect was associated with motor and cognitive deficits in the adult offspring.

Financial support:

FAPERJ, CAPES, CNPq, Bill & Melinda Gates Foundation

06.002 - THE ROLE OF CAMP SIGNALING IN THE ACTIVATION OF HEPATIC GLUCONEOGENESIS INDUCED BY SYMPATHETIC INNERVATION IN THE SETTING OF COLD. Morgan HJN, Delfino HBP, Silva CLA, Kettelhut IC, Navegantes LCC, - Fisiologia - USP Bioquímica e Imunologia - USP Hemocentro - USP

Introduction:

The second messenger cAMP stimulates the expression of numerous genes via the PKA-mediated phosphorylation of the CREB and dephosphorylation of the cAMP-regulated CREB coactivator CRT2. We have previously shown that in the cold state, increases in hepatic norepinephrine promote hepatic glucose production through induction of the gluconeogenic program. However, the role of cAMP in such adrenergic effect remains unknown.

Aim:

Therefore, we aimed to investigate the participation of CREB/CRT2 signaling in the activation of hepatic gluconeogenesis induced by sympathetic innervation.

Methods:

Neonate male C57BL/6 mice (ethical committee nº183/2015) were submitted to pharmacological sympathectomy (6-OH-Dopamine; 100 mg.kg⁻¹.dia⁻¹ at P0, P2 and P7). In adulthood, animals were exposed to cold stimulus (4°C) for 3 and 6 h and the liver was harvested for enzymatic activity, western blot, and Rt-PCR analysis. The transcriptional activity of CREB in vivo was evaluated by an imaging system (IVIS) in transgenic animals that expresses the reporter for CRE-luciferase. Norepinephrine was estimate by HPLC and hormones by ELISA. The results are expressed as means ± SEM and were submitted to appropriate statistical analysis considering the level of significance of p<0.05.

Results:

In innervated mice, cold exposure (6h) increased plasma levels of glucose (1332±34 vs 899±26 in controls; AUC) and glucagon (65.5±9.9 vs 10.5±1.3 in control; ug/dl) but suppressed insulinemia. Cold also induced increases of 60.6% and 112%, respectively in the activity and mRNA levels of liver PEPCK, a key gluconeogenic enzyme. Similar findings were observed with Glucose-6-Pase (G6Pase). These effects were associated with an increase in the levels of norepinephrine (240.3±38 vs 94.7± 17.5 in control; ng/g), cAMP (1359±61.7 vs 1225±80.8 in control; fmol/mg), PKA substrates (1.42±0.05 vs 1±0.07 in control; AU), phosphorylation of CREB at Ser-133 (2.04±0.14 vs 1±0.12 in control; AU) and dephosphorylation of CRT2 at Ser-171. Additionally, using CRE-luciferase reporter mice, we demonstrate that the in vivo transcriptional activity of CREB was increased by cold (1.1e12±5e11 vs 3.49e8±1e8 in controls; p/s) and in response to a single injection of norepinephrine (1.9e8±3.14e7 vs 1.38e7±9.4e6 in controls; p/s). The majority of cold effects on gluconeogenesis enzymes and cAMP/PKA/CREB signaling was abolished or attenuated in

denervated mice. However, the sympathectomy did not affect the cold-induced CRT2 dephosphorylation.

Conclusion:

These results suggest that the hepatic sympathetic nerves acutely stimulate the gluconeogenesis in response to cold through the transcriptional activation of CREB without the involvement of CRT2. These findings may be helpful for the better understanding of metabolic diseases that cause changes in glycemic homeostasis.

Financial support:

Fapesp (2018/10089-2)

06.003 - EGG WHITE HYDROLYSATE AS A POSSIBLE THERAPEUTIC AGENT AGAINST THE WHITE ADIPOSE TISSUE DYSFUNCTION IN RATS EXPOSED TO MERCURY. Piagette JT, Rizzetti DA, Corrales P, Gómez MGM, Ocio JAU, Peçanha FM, Miguel M, Wiggers GA, - Cardiovascular Physiology Laboratory, - Universidade Federal do Pampa Metabolic Phenotyped of Animals Experimentation Laboratory - Universidad Rey Juan Carlos Bioactivity and Food Analysis Laboratory - CIAL

Introduction:

Mercury (Hg) is a well-known heavy metal related to toxic effects in several organs. White adipose tissue (WAT) dysfunction has been reported after chronic exposure to Hg, which is considered as a central mechanism to metabolic disorders. In this context, Egg White Hydrolysate (EWH) bioactive peptides present antioxidant and antidiabetogenic effects and could be beneficial to counteract the harmful effects of Hg exposure.

Aim:

To investigate if EWH protects the WAT against the toxic effects of chronic Hg exposure at low doses in rats.

Methods:

Male Wistar rats (200-250 g) were treated for 60 days in: a) Untreated (saline solution, i.m. plus tap water by gavage); b) Mercury (mercury chloride, i.m. - 1st dose 4.6 µg/kg, subsequent doses 0.07 µg/kg/day plus tap water by gavage); c) Hydrolysate (saline solution, i.m. plus EWH by gavage - 1 g/kg/day); d) Hydrolysate-Mercury. At the end of the treatment, histological assays, Hg levels measurement and GRP78, CHOP, PPARα, PPARγ, leptin, and adiponectin mRNA expression were performed in epididymal WAT. Plasma levels of glucose, triglycerides, total cholesterol, and insulin were also measured.

Results:

EWH co-treatment prevented the reduced absolute and relative eWAT weights, adipocytes size, plasma insulin levels, antioxidant defenses, and the increased plasma glucose and triglyceride levels and CHOP, Leptin and PPARα mRNA expressions induced by Hg exposure. However, this co-treatment did not alter the increased GRP78, PPARγ and adiponectin mRNA expressions in Hg-treated animals. These results corroborate that the reduction in adipocytes size is related to the impaired antioxidant defenses, endoplasmic reticulum (ER) stress, the disrupted PPARs, and adipokines mRNA expression induced by the metal in WAT and suggest that the antioxidant and antidiabetogenic properties of EWH were able to prevent its toxic effects.

Conclusion:

EWH could be considered as an alternative treatment tool for Hg-induced WAT damage.

Financial support:

National Council for Scientific and Technological Development – CNPq (203440/2014-5; 307399/2017-2), and a Spanish Government (MINECO - AGL2012-32387; CSIC – Intramural 2015701028

06.004 - DIFFERENT FORMS OF ANDROGEN ABLATION CAUSE CHANGE IN MORPHOLOGY AND IN EXTRACELLULAR MARKERS IN THE PROSTATE OF MONGOLIAN GERBILS. COLLETA SJ, Antoniassi JQ, Vilamaior PSL, Góes RM, TABOGA SR, - Departamento de Biología - UNESP

Introduction:

FeSBE Annual Meeting 2019

Poster Sessions and Abstracts

The prostate is a gland of the reproductive system regulated by androgens and estrogens. The balance between these hormones is important for the maintenance of prostatic homeostasis and also for development of diseases. Finasteride is a 5 α -reductase effective inhibitor. The 5 α -reductase is responsible for converting testosterone to dihydrotestosterone. Finasteride is also commonly used in treatment of prostatic lesions, alopecia, and acne. Chrysin is a flavonoid found in various vegetal species. It has been widely studied for presenting antioxidant and anti-inflammatory properties. This compound has inhibitory effects on activity of aromatase enzyme, responsible for aromatization of testosterone in estradiol.

Aim:

The current study was conducted to recognize, quantify and describe stromal cells, in addition, extracellular matrix elements associated with prostatic reactive stroma in gerbils submitted to different forms of androgen ablation: orchiectomy, 5 α -reductase and aromatase enzyme inhibition.

Methods:

We used 90 days old male Gerbil (*Meriones unguiculatus*). The animals were divided into the following experimental groups: Control- animals free of any manipulation; Castrated- bilaterally orchiectomized animals; Chrysin- animals that received 50mg/kg of chrysin in 0,1ml corn oil weekly via gavage; Finasteride- animals that received 10mg/kg of finasteride in 0.1ml of corn oil weekly via gavage. At 1 year and 3 months old, the animals were euthanized, prostates were collected and processed for histological analysis.

Results:

Assumed the morphology of adult gerbils ventral prostate (90 days old), the 1 year and 3 months old gerbil present ventral prostate with some morphological aspects different. Acini are voluminous with increased luminal space, epithelial cells and stromal compartment becomes atrophied. Prostatic secretion reduced considerably. Stromal microenvironment is altered, with increases in TGF- β , MMP-2, MMP-9, CD163, and CD68 macrophages. Were observed an increase of clear cells and atypical nucleus in epithelium, appearance of inflammatory cells in the acinar region and the presence of prostatic intraepithelial neoplasia (PINs). The castrated animals exhibited stromal, collagen and vessels increased. The lumen, epithelial and prostate secretion atrophied. The TGF- β and CD163 immunostaining showed an increase. The finasteride administration caused stromal and epithelial compartments hypertrophied. Collagen accumulated in subepithelial layer. Immunostaining to TGF- β , MMP9 and CD163, CD68 and CD34 macrophages increased. An increase in MMP2 was also observed. These results show that finasteride altered the prostatic microenvironment, leading to morphological and molecular alterations in the prostatic stromal, establishing a reactive stroma. Chrysin was shown to have a protective effect on the hormonal imbalance observed in senile animals, structural changes were less common in these animals than in control animals. Epithelial compartment became atrophied, while stromal hypertrophied. There were no infiltrates of inflammatory cells and PINs, common in senile animals. Acinar secretion decreased. Some regions of CML rupture were observed. There was a decrease in MMP-2 and increased of TGF- β , MMP9, CD163 and CD68 macrophages immunostaining.

Conclusion:

The current study showed that finasteride and chrysin are not capable of causing glandular regression as observed in surgically castrated animals. The treatment with chrysin proved to be protective for development of lesions and treatment with finasteride proved to be an enhancer of the development of the reactive stroma.

Financial support:

FAPESP (2014/26660-0)/CAPES

06.005 - REDUCED IMMUNOSTAINING OF VAMP-2 IN ISLETS OF ADULT MICE FROM OFFSPRING OF DAMS FED A HIGH FAT DIET DURING PREGNANCY AND LACTATION. Sales DC, Fontes CC, Zanella AP, CARVALHO CPF, - Departamento de Biotecnologia - Universidade Federal de São Paulo

Introduction:

Metabolic programming refers to a critical window during the ontogenesis, when the development of each organ or system is particularly sensible to environmental factors, such as feeding. Animal studies show that offsprings of diabetic females or dams fed a high-fat (HF) or low protein diets during pregnancy and lactation can present glucose homeostasis perturbations and increased risk to obesity and type 2 diabetes (T2D) development at long-term.

Aim:

The aim of this work was to study the later repercussion of the metabolic programming with HF diet during pregnancy and lactation for the secretory function of pancreatic β -cell of mice offsprings at adult age (12-week-old mice).

Methods:

C57BL/6 female mice after vaginal plug identification were divided in two groups: control (fed a control diet containing 4.5% lipids in g) and HFD (34% lipids in g) during pregnancy and lactation. After weaning, male mice from both groups were fed a control diet until euthanasia. This study was approved by the Committee for Ethics in Animal Experimentation (CEUA – UNIFESP Nº: 1306150817). Some metabolic parameters were evaluated, such as: body weight, postprandial glycemia, visceral fat mass (gonadal, retroperitoneal and mesenteric), glucose tolerance test (GTT) and insulin tolerance test (ITT). We also investigated, using phalloidin assays, the intensity of F-actin staining exhibited by islets in pancreas sections of both groups. The cellular distribution and fluorescence degree of VAMP-2 (vesicle associated membrane protein-2) immunolabeling was measured in islets of pancreas sections for both groups.

Results:

The mice from HFD group presented increased body weight at weaning (CON: 8.46 \pm 0.21 vs HFD: 11.29 \pm 0.25g; N=25-35; p<0.0001), but at adult age (12 week-old) the weight was decreased, compared to the control group (CON: 27.06 \pm 0.36 vs HFD: 25.36 \pm 0.45g, N=25-34, p<0.004). The postprandial glycemia was increased in HFD group at weaning (CON: 129.7 \pm 3.36 vs HFD: 169 \pm 5,9 mg/dL, N=22-35, p<0.0001). However, the final glycemia was not different (CON: 162.2 \pm 2.802 vs HFD: 162.8 \pm 4.6 mg/dL, N=26-33). We didn't find significant differences between groups in visceral fat depots (gonadal, retroperitoneal and mesenteric). We also didn't observe difference in area under the curve (AUC) of GTT. However, the AUC of ITT, expressed as a percentage of the initial glycemia value, was increased for HFD group (CON: 1284 \pm 40,56 vs HFD: 1542 \pm 69,69; N=13/group; p<0,004). Mice from HFD group showed increased labeling intensity for F-actin, compared to control group (CON: 24.7 \pm 0.2 vs HFD: 27.29 \pm 0.2 pixels; N=5/group; p<0.0001). The immunostaining of VAMP-2 was decreased in islets of HFD group (CON: 251129 \pm 2866 vs HFD: 236994 \pm 3317 pixels, N=5/group, p<0.0001).

Conclusion:

The HF diet administration during pregnancy and lactation induced some metabolic perturbations to the male offspring at adult age, predisposing them to (T2D) development with age or other metabolic challenges. These findings are accompanied to the reduced immunostaining of an islet SNARE protein, the VAMP-2, a protein important to insulin exocytosis in pancreatic islets.

Financial support:

FAPESP, CNPq and CAPES.

FeSBE Annual Meeting 2019

Poster Sessions and Abstracts

06.006 - TIME RESTRICTED FEEDING DURING THE RESTING PHASE ALTERS HEPATIC CLOCK IN FEMALE RATS: THE ROLE OF OVARIAN STEROIDS. Cardoso TSR, Horta NAC, Fernandes P, Poletini MO, - Fisiologia e Biofísica - UFMG

Introduction:

In male rodents, time restricted feeding (TRF) alters the phase of clock gene expression in metabolic tissues such as the liver. In female rodents, on the other hand, the ovarian steroids are able to alter the circadian rhythms in behavior and the clock gene expression.

Aim:

Therefore, the present study evaluated the effect of ovarian steroids on the entrainment of the liver clock by TRF.

Methods:

Regular chow was offered ad libitum or in a TRF protocol (food available from lights on (7 am) to lights off (7 pm)) to female adult rats displaying regular estrous cycles (Intact) and to ovariectomized (OVX) rats. After 21 days, the rats were euthanized at 8 am and at 7 pm for liver collection. Per1, Bmal1 and Reverb- α mRNA levels were evaluated by qRT-PCR. The results were analyzed by delta-delta-CT method, expressed as arbitrary units (au), and presented as mean \pm SEM. The comparisons of gene expression found within ad libitum- or TRF-subjected animals at different times were performed by t-Student test. UFMG's Ethics Commission for the Use of Animals approved the experimental protocols (n^o117/2018).

Results:

In intact rats under ad libitum regimen, Reverb- α expression was lower at 8 am than at 7 pm (1.26 au \pm 0.44 vs 5.39 au \pm 1.05) and the opposite was observed after TRF protocol, in which the expression was lower at 7 pm (1.00 au \pm 0.07 vs 0.07 \pm 0.02). OVX abolished the response of Reverb- α expression to TRF in the liver. As such, in ad libitum OVX rats, Reverb- α expression was also lower at 8 am. (1.10 au \pm 0.29 vs 3.01 au \pm 0.67) and after TRF protocol, it was kept lower at 8 am (1.02 au \pm 0.12 vs 3.82 au \pm 1.97). Bmal1 expression was higher at 8 am than at 7 pm, in both intact (1.15 au \pm 0.32 vs 0.06 au \pm 0.02) and OVX (1.19 au \pm 0.36 vs 0.03 au \pm 0.01) rats under ad libitum. TRF abolished the temporal differences found in both intact rats (1.06 au \pm 0.20 vs 1.86 au \pm 0.44) and OVX rats (1.31 au \pm 0.55 vs 2.25 \pm 0.87). In intact rats under ad libitum, Per1 expression was lower at 8 am than at 7pm (0.95 au \pm 0.23 vs 1.87 au \pm 0.36), and TRF inverted this relationship, as such, the expression was higher at 8 am than at 7 pm (1.05 \pm 0.22 vs 0.14 \pm 0.02). Per1 expression did not differ between times in OVX rats under ad libitum (2.03 au \pm 0.57 vs 1.15 au \pm 0.22) neither in OVX rats under TRF protocol (1.04 \pm 0.11 vs 0.93 \pm 0.25).

Conclusion:

Therefore, the temporal alterations induced by TRF in the expression of Reverb- α in the liver depend on the ovarian steroids of female rats. On the other hand, ovarian steroids are essential to keep the temporal pattern of Per1 expression in both feeding protocols, whereas they are unnecessary for Bmal1 expression. These hormones may contribute to TRF entrainment of the liver clock.

Financial support:

CAPES, FAPEMIG, CNPq

7 - Nutrition and Metabolism

07.001 - MATERNAL VITAMIN D DEFICIENCY SELECTIVELY AFFECTS FIBER-II RICH SKELETAL MUSCLE PHENOTYPE IN ADULT OFFSPRING RATS. Reis NG, Gonçalves DAP, Silveira WA, Lautherbach NES, Almeida LF, Assis AP, Zanon NM, Heck LC, Coimbra TM, Kettelhult IC, Navegantes LCC, - Fisiologia - FMRP-USP Bioquímica e Imunologia - FMRP-USP Educação Física - UFMG

Introduction:

Although it is well established that maternal vitamin D (Vit. D) deficiency (VDD) may have long-lasting consequences on offspring

metabolic health, little information is available on the impact of maternal VDD on offspring skeletal muscle development.

Aim:

To characterize the effects of VDD in utero and early postnatal life on offspring metabolic, hormonal and muscular phenotypic alterations in adulthood.

Methods:

Twelve 5-week-old female Wistar Hannover rats were fed either a standard diet (VDS; AIN93G with 1000 IU vitamin D3/kg diet) or VDD diet (0 IU vitamin D3/kg diet) for six weeks and then bred to male rats. Females were maintained on the diets throughout gestation and lactation. The efficiency of the diet was evaluated by the serum calcidiol concentration. At weaning, male offsprings were separated in two groups: offspring standard (O-SD) (n = 6; pups of dams with VDS-diet) and offspring VDD (O-VDD) (n=5; pups of dams treated with VDD-diet). Offsprings received a normal diet (Nuvilab) until 180 days of age, at which point serum and skeletal muscle (EDL and Soleus) were harvested for histological and immunohistochemical analysis. * P \leq 0,05

Results:

O-VDD rats weighed less at weaning than O-SD but recovered weight in the 60 days post weaning and acquired a greater body mass (490 \pm 19 vs 432 \pm 12 g in the O-SD) and mass of white adipose tissue (epididymal: 11 \pm 1 vs 8 \pm 0.7 g in the O-SD and retroperitoneal: 11 \pm 0.7 vs 7 \pm 0.8 in the O-SD), and brown adipose tissue (278 \pm 10 vs 536 \pm 28 mg in the O-SD) in the 180 days. At this age, O-VDD group showed a reduction in the calcidiol serum concentration (23 \pm 1 vs 40 \pm 2 ng/ml in the O-SD) without alteration in serum calcium (2,3 \pm 0,06 vs 2,3 \pm 0,008 mmol/L in the O-SD) and PTH (197 \pm 113 vs 144 \pm 33 pg/ml in the O-SD). Additionally, these animals had a higher plasma concentration of angiotensin II (56 \pm 6 vs 20 \pm 2 pg/ml in the O-SD) as well as increased blood glucose (110 \pm 3 vs 95 \pm 2 mg/dL in the O-SD) and serum insulin (6.7 \pm 0.6 vs 3.5 \pm 0.5 ng/ml in the O-SD*) suggesting insulin resistance. The morphological analysis of the EDL showed a significant increase in the area of the muscle fibers IIA (1228 \pm 50 vs 1026 \pm 27 μ m² in the O-SD), IIAx (1402 \pm 57 vs 1155 \pm 45 μ m² in the O-SD), and IIB (3952 \pm 186 vs 3356 \pm 161 μ m² in the O-SD) accompanied by a lower number of total fibers (2244 \pm 222 vs 2814 \pm 105 in the O-SD) and a reduction in the oxidative capacity as estimated by SDH activity (0.90 \pm 0.009 vs 0.99 \pm 0.03 AU in the O-SD). These alterations were not found in Soleus muscle.

Conclusion:

Maternal VDD during pregnancy and lactation results in a metabolic syndrome phenotype accompanied by a selective increase in the area of type II fibers of glycolytic muscle (EDL) in adult offspring rats.

Financial support:

FAPESP: 18/10089-2 and CNPq

07.002 - MATERNAL HIGH-FAT DIET INDUCES SEX-SPECIFIC CHANGES OF TYPE-1 CANNABINOID RECEPTOR (CNR1) EXPRESSION AND BINDING OF SEX HORMONE RECEPTORS IN WHITE ADIPOSE TISSUE OF ADULT RAT OFFSPRING. Almeida MM, Dias-Rocha CP, Gomes CFR, Wang H, Pazos-Moura CC, Cordeiro A, Joss-Moore L, Trevenzoli IH, - Department of Pediatrics - University of Utah Centro de Ciências da Saúde - Universidade Federal do Rio de Janeiro

Introduction:

Perinatal maternal high-fat diet dysregulates the endocannabinoid signaling in the adipose tissue of offspring at weaning. Endocannabinoid system (ECS) consists of the type-1 and type-2 cannabinoid receptors (coded by Cnr1 and Cnr2 genes) and the ECS-metabolizing enzymes fatty acid amide hydrolase and the monoacylglycerol lipase (coded by Faah and Mgl1 genes). ECS stimulates lipogenesis in visceral (VAT) and subcutaneous (SAT) white adipose tissue.

Aim:

We aimed to investigate the hypothesis that maternal HFD would induce sex-specific changes in the ECS in VAT and SAT of adult offspring

FeSBE Annual Meeting 2019

Poster Sessions and Abstracts

associated with changes in epigenetic markers, such as histone acetylation, and sex hormone signaling.

Methods:

All procedures were approved by the Animal Care and Use Committee of the Health Science Center of the Federal University of Rio de Janeiro (process number 095/17). Female rats received a standard diet (C; 9% fat) or a HFD (28% fat) 8 weeks before mating, during gestation and lactation. Male and female offspring were fed C diet from weaning and adulthood (180 days old), when rats were killed for tissue harvest. We assessed body weight, adiposity, plasma levels of 17 β -estradiol and testosterone, mRNA levels of Cnr1, Cnr2, Faah and Mgl1 in VAT and SAT of male and female offspring. We also investigated histone acetylation, ER α and AR binding to Cnr1 promoter by chromatin immunoprecipitation. Data were analyzed employing two-way ANOVA with maternal diet and offspring sex as factors, followed by within sex pairwise comparisons using Bonferroni post hoc test.

Results:

Maternal HFD increased weight body (+6.0%, $p < 0.05$), VAT (+18.6%, $p < 0.05$) and SAT (+31.9%, $p < 0.05$) mass in the offspring. Maternal HFD decreased plasma levels of 17 β -estradiol in female (-28.1%, $p < 0.05$) and testosterone in male (-59.1%, $p < 0.05$) offspring. In VAT, maternal HFD increased Cnr1 mRNA levels (+46.5%, $p < 0.05$) without changes in histone acetylation, ER or AR binding to Cnr1 promoter. In VAT, maternal HFD decreased Cnr2 mRNA levels (+70.0%, $p < 0.05$) in male adult offspring. In SAT, maternal HFD increased Cnr1 mRNA levels (+87.6%, $p < 0.05$) associated with increased ER α binding (+2.3-fold, $p < 0.05$) to Cnr1 promoter and without changes in histone acetylation in female offspring. In SAT, maternal HFD decreased AR binding (-45.4%, $p < 0.05$) to Cnr1 promoter.

Conclusion:

Maternal HFD induced sex-specific changes in the ECS in the SAT and VAT of adult offspring rats, with female offspring more affected. Maternal HFD decreased 17 β -estradiol plasma levels in adult female offspring, impairing estrogen signaling and leading to increased ER α binding to Cnr1 promoter, which may contribute to up-regulated Cnr1 mRNA in SAT.

Financial support:

CNPq, CAPES and FAPERJ

07.003 - PERINATAL MATERNAL HIGH-FAT DIET UP-REGULATES TYPE-1 CANNABINOID RECEPTOR IN SUBCUTANEOUS WHITE ADIPOSE TISSUE AND DOWN-REGULATES 17 β -ESTRADIOL PLASMA ONLY IN ADULT FEMALE OFFSPRING RATS. Reis-Gomes CF, Almeida MM, Dias-Rocha CP, Pazos-Moura CC, Trevenzoli IH, - Instituto de Biofísica Carlos Chagas Filho - UFRJ

Introduction:

Maternal high-fat diet (HFD) programs obesity in the offspring throughout life. Obesity is characterized by an overactivation of the endocannabinoid system (ECS), however the role of the ECS in the developmental origins of obesity is the mostly unknown. ECS consists of receptors, the cannabinoid type-1 and 2 (CB1 and CB2) and ECS-metabolizing enzyme, as the monoacylglycerol lipase (MAGL). In subcutaneous (SAT) white adipose tissue, ECS stimulates lipogenesis. Estrogen receptor (ER) response elements were reported in ECS promoters, suggesting the differential contribution of sex hormones on ECS activation.

Aim:

We aimed to investigate the hypothesis that maternal HFD induced sex-specific changes in the ECS in SAT of adult offspring in association with changes in the circulating levels of estrogen.

Methods:

All procedures with animals were approved by CEUA/CCS/UFRJ (protocol 095/17). Female rats, 60 days old, were assigned to experimental groups (n=15/group): control group (C), which received standard diet (9% fat) and HFD group, which received HFD (29% fat).

Diets were isocaloric and offered for 8 weeks before mating and during gestation and lactation. During all life, offspring were fed C. At 180-days-old, we assessed body weight, SAT mass, plasma levels of 17 β -estradiol and the CB1, CB2 and MAGL protein contents in SAT. Data were analyzed employing two-way ANOVA with maternal diet and offspring sex as factors, followed by within sex pairwise comparisons using Bonferroni post hoc test. To investigate the role of estrogen plasma levels on ECS in SAT, a new set of 80-day-old female rats were underwent a bilateral ovariectomy and were divided into OVX, treated with soy oil (vehicle), and OVXE, treated with estradiol, both for 7 days. We evaluated the plasma levels of 17 β -estradiol and the CB1, CB2, MAGL and ER α protein contents in SAT from OVX and OVXE groups. Data were analyzed employing Student's unpaired t test.

Results:

Maternal HFD increased weight body (+6.0%, $p < 0.05$) and SAT (+31.9%, $p < 0.05$) mass in the offspring. Maternal HFD decreased plasma levels of 17 β -estradiol only in female offspring (-28.1%, $p < 0.05$). In SAT, maternal HFD increased CB1 protein content (+85.6%, $p < 0.05$) only in adult female offspring while it did not change CB2 and MAGL protein contents. To investigate if plasma estrogen levels can modulate ECS in SAT, we developed the ovariectomy model. As expected, we observed higher estradiol levels in OVXE compared with OVX rats (+19-fold, $p < 0.05$). OVX female rats presented increased CB1 (+46.05%, $p < 0.05$), MAGL (+36.03%, $p < 0.05$) and ER α (+45.48, $p < 0.05$) protein contents in SAT, while there was no change in CB2 protein content.

Conclusion:

Maternal HFD induces sex-specific changes in the CB1 content in SAT of adult offspring rats associated with reduced circulating 17 β -estradiol only in female pups. As the low 17 β -estradiol plasma levels induced by maternal HFD or ovariectomy are related to increased CB1 protein content in the SAT, we speculate that the impaired estrogen signaling may contribute to up-regulation of CB1 in SAT of females.

Financial support:

CNPq, CAPES and FAPERJ

07.004 - DIFFERENTIAL EFFECTS OF PPAR-ALPHA ON THE WHITENING OF BROWN ADIPOSE TISSUE IN HIGH-FAT OR HIGH-FRUCTOSE FED MICE. Miranda CS, Silva-veiga FM, Oliveira DAS, Cordeiro BO, Rachid TL, SOUZA-MELLO V, - Programa de Pós-Graduação em Biologia Humana e Experimental - UERJ

Introduction:

Nutritional imbalance causes the accumulation of larger lipid droplets as a result of a poor vascularization, a phenomenon called whitening. Conversely, PPAR-alpha activation is able to activate the thermogenesis pathway. Our hypothesis is that PPAR-alpha activation can reverse BAT whitening in mice fed with a high-fat or a high-fructose diet.

Aim:

To examine the differential effects of PPAR-alpha activation on energy expenditure, thermogenic and inflammatory mediators involved in brown adipose tissue whitening in mice fed a high-fat or high-fructose diet.

Methods:

All procedures were approved by the local ethics committee (CEUA 041/2018). C57BL/6 mice (3 months old) received a control diet (C, 10% of energy as lipids, n=10), high-fat diet (HF, 50% of energy as lipids, n=10) or high-fructose diet (HFRU, 50% of energy as fructose, n=10) for 12 weeks. Afterward, groups were redivided to a 5 week-treatment: C, HF, HF-a (HF diet plus PPAR-alpha), HFRU e HFRU-a (HFRU diet plus PPAR-alpha). PPAR-alpha agonist (WY14643, Sigma-Aldrich) was mixed with the diet (2.5 mg/Kg body mass). Body mass food intake, oral glucose tolerance test (OGTT) and indirect calorimetry were assessed. BAT was evaluated using light microscopy, electron microscopy, immunofluorescence, and qPCR. Data are expressed as mean and

FeSBE Annual Meeting 2019

Poster Sessions and Abstracts

standard deviation and were analyzed with Brown-Forsythe and Welch ANOVA and Tamhane (T2) post hoc test.

Results:

HF animals showed overweight ($31.11g \pm 0.66$ in HF group vs. $27.43g \pm 0.27$ in C group, +13.41%, $P < 0.0001$), which was reduced in both treated groups ($28.65g \pm 0.30$ in HF-a group vs. $31.11g \pm 0.66$ in HF group, -7.91%, $P = 0.0033$; $22.04g \pm 0.25$ in HFRU-a vs. $26.58g \pm 0.24$ in HFRU group, -17.09%, $P < 0.0001$), without alteration in food intake. The OGTT showed that the HF group and the HFRU had glucose intolerance ($1038 \text{ a.u.} \pm 17.64$ in HF group vs. $731 \text{ a.u.} \pm 38.29$ in C group, +45.58%, $P = 0.0012$; and $869.8 \text{ a.u.} \pm 18.22$ in HFRU group vs. $731 \text{ a.u.} \pm 38.29$ in C group, +18.99%, $P = 0.0241$). The treatment alleviated the glucose intolerance in the HF-a group ($882.5 \text{ a.u.} \pm 15.43$ in HF-a group vs. $1038 \text{ a.u.} \pm 17.64$ in HF group, -14.98%, $P < 0.0001$), whereas it rescued the glucose intolerance in the HFRU-a group. HF group showed decreased UCP1 immunostaining and a pattern of lipid droplet accumulation that resembled the white adipose tissue, suggesting the whitening phenomenon. The treatment reduced expressively the size of lipid droplets in BAT from the HF-a group, resembling the C group, suggesting enhanced thermogenesis. Excessive fructose also diminished the UCP1 immunoreaction and enhanced lipid accumulation in BAT, but treatment could reverse these adverse remodeling in the HFRU-a group. Both treated groups also showed a lower respiratory exchange ratio than untreated groups, suggesting that lipids were used as fuel for the enhanced thermogenesis.

Conclusion:

PPAR-alpha activation rescued the whitening of BAT in the HF group, whereas it attenuated the morphological alterations caused by the HFRU diet. These beneficial effects seem to be mediated by the enhanced thermogenesis observed by the high UCP1 expression coupled with the reduced lipid droplets size after the treatment. The next steps will shed light on the possible mechanisms underlying these findings through the evaluation of the mitochondrial remodeling and gene expression of thermogenesis and inflammatory markers.

Financial support:

Faperj E-26/202.657/2018

07.005 - LINAGLIPTIN INDUCES BROWNING OF SUBCUTANEOUS WHITE ADIPOSE TISSUE AND THERMOGENESIS IN HIGH-FAT-FED C57BL/6 MICE. Correia BRO, Rachid TL, Silva AF, Santana ACM, Martins FF, Souza-Mello V, - Anatomia - UERJ

Introduction:

Dipeptidyl peptidase 4 inhibitors (DPP-4i) act on carbohydrate metabolism and stimulate PGC1-alpha, which is a thermogenic marker and master regulator of mitochondrial biogenesis. Drugs that increase energy dissipation as heat emerge as alternatives to manage the metabolic abnormalities from obesity. We tested the hypothesis that linagliptin could induce the formation of beige adipocytes in mice fed with a high-fat diet.

Aim:

To examine the effects of linagliptin (DDP-4i) on the subcutaneous white adipose tissue (sWAT) remodeling in diet-induced obese mice, focusing on the thermogenesis stimulation.

Methods:

All procedures were approved by the local ethics committee (CEUA 053/2016). Forty animals were randomly assigned to receive a control diet (C, 10% lipids) or a high-fat diet (HF, 50% lipids) for ten weeks. Each group was re-divided to begin the five-week treatment, totalizing four experimental groups: C, C-L (C plus linagliptin), HF and HF-L (HF plus linagliptin). Linagliptin was mixed with the respective diet (30mg/kg BM). Body mass and food intake were monitored. Oral glucose tolerance test and indirect calorimetry were performed prior to sacrifice. At sacrifice, blood was collected to determine insulin levels and the sWAT was harvested to be evaluated using light microscopy, confocal microscopy, and q-PCR techniques. Data are expressed as

mean and standard deviation and were analyzed with One-way ANOVA and Holm-Sidak post hoc test.

Results:

HF animals showed overweight ($31.11 \pm 3.28g$ in HF group vs. $26.68 \pm 0.42g$ in C group, +16.60%, $P < 0.0037$), glucose intolerance verified by a great area under the curve for OGTT ($928.80 \pm 47.40 \text{ a.u.}$ in HF group vs. $754.00 \pm 15.76 \text{ a.u.}$ in C group, +23.18%, $P < 0.0001$), and a greater cross-sectional area of adipocytes ($97.39 \pm 28.15 \mu\text{m}^2$ in HF group vs. $60.6 \pm 22.22 \mu\text{m}^2$ in C group, +60.71, $P < 0.0001$). The treatment with linagliptin was able to reduce the BM ($27.82 \pm 0.543g$ in HF-L vs. $31.11 \pm 3.28g$ in the HF group, -10.58%, $P = 0.0356$), restore the glucose tolerance ($732.60 \pm 67.22 \text{ a.u.}$ in HF-L group vs. $928.80 \pm 47.40 \text{ a.u.}$ in HF group, -21.12%, $P < 0.0001$) and the cross-sectional area of adipocytes ($46.26 \pm 7.33 \mu\text{m}^2$ in HF-L group vs. $97.39 \pm 28.15 \mu\text{m}^2$ in HF group, -52.50%, $P < 0.0001$). These observations comply with the observation of UCP1-positive multilocular adipocytes in the sWAT of treated animals. Both treated groups (C-L and HF-L) showed high expression of thermogenic and type 2 cytokines genes, which agree with the enhanced body temperature ($35.04 \pm 0.50 \text{ }^\circ\text{C}$ in C-L vs. $33.81 \pm 0.72 \text{ }^\circ\text{C}$ in C group, +3.64%, $P < 0.0001$; and $35.04 \pm 0.45 \text{ }^\circ\text{C}$ in HF-L vs. $34.32 \pm 0.522 \text{ }^\circ\text{C}$, +2.10%, $P = 0.0221$) and the lower respiratory exchange ratio (0.900 ± 0.040 in C-L vs. 0.981 ± 0.001 in C, -8.26%, $P < 0.0001$; and 0.678 ± 0.040 in HF-L vs. 0.898 ± 0.030 in HF, -24.50%, $P < 0.0001$) implying enhanced thermogenesis with the use of lipids as fuel.

Conclusion:

The reduced BM, the enhanced body temperature, and the presence of positive UCP1 beige cells in the sWAT point to the activation of the browning cascade on the sWAT of linagliptin-treated mice, and hence, linagliptin could induce the thermogenic pathway as a pleiotropic effect that can have translational potential.

Financial support:

E-26/202.657/ 2018 (Faperj for V.S.-M.)

07.006 - MATERNAL HIGH-FAT DIET ALTERS ENDOCANNABINOID AND DOPAMINERGIC SYSTEM COMPONENTS IN THE CENTRAL NERVOUS SYSTEM OF MALE AND FEMALE ADULT RAT OFFSPRING. Dias-Rocha CP, Almeida MM, Costa JCB, Pazos-Moura CC, Trevenzoli IH, - Laboratório de Endocrinologia Molecular - UFRJ

Introduction:

Maternal high-fat diet (HF) during the perinatal period induces obesity in the offspring. Obesity is associated with unbalanced energy metabolism and endocannabinoid system (ECS) over activation. ECS components include the cannabinoid receptors (CB1 and CB2) and metabolizing enzymes of endocannabinoids (FAAH and MAGL). ECS activation in the central nervous system (CNS) is associated with increased homeostatic and hedonic eating, resulting in hyperphagia and higher motivation for palatable foods. Food intake homeostatic and hedonic regulation includes communications between several CNS regions, as such lateral hypothalamus area (LHA) and accumbens nucleus (Acc), and the dopaminergic system activity. We hypothesized that maternal HF diet changes ECS and dopaminergic system components expression in LHA and Acc of male and female adult offspring in a sex-specific manner, programming the feeding behavior and contributing to obesity.

Aim:

The objective of this study is to evaluate the effects of maternal high fat diet on the ECS and dopaminergic system expression in specific regions of CNS and its influence on homeostatic and hedonic regulation of food intake among adult male and female offspring.

Methods:

All procedures with animals were approved by CEUA/CCS/UFRJ (protocol 095/17). Female rats received standard diet (C; 9% fat) or high-fat diet (HF; 28% fat) during 8 weeks before mating, gestation and lactation. We assessed body weight and food intake of male and female offspring throughout life, and at 150-day-old we performed the food

FeSBE Annual Meeting 2019

Poster Sessions and Abstracts

preference test with C, HF and high-sucrose diets. At 180-day-old, we evaluated adiposity, leptinemia (radioimmunoassay) and protein content of ECS components in LHA and Acc and dopaminergic markers in Acc of male and female offspring (western blotting). The ANOVA two-way test was used with the maternal diet and offspring sex as the main factors, and multiple comparisons are assessed by Tukey's post hoc test, with significance of * $p < 0.05$.

Results:

Maternal HF diet increased food intake, body weight and adiposity in male and female offspring, but only HF male offspring presented hyperleptinemia (+50%). Maternal HF diet programmed male and female offspring to higher food preference for HF diet (+2 fold* and +1.2 fold*, respectively). In LHA, maternal HF diet did not change the components of ECS. In Acc, maternal HF diet increased CB1 content (male: +23,3%* and female: +25%*) and decreased CB2 (male: -22,4%* and female: -31%*) and MAGL content (male: -22,2%* and female: -28,6%*) in offspring, without alterations in FAAH content. Maternal HF diet increased the dopaminergic receptor 2 (D2R) content in female (+30.8%*) and it was decreased in male (-26.3%*) offspring. Besides that, maternal HF diet increased the tyrosine hydroxylase enzyme (TH) content in male (+12%*) and it was decreased in female (-62.7%*) offspring.

Conclusion:

We demonstrated that maternal HF diet induced adult offspring overweight, increased adiposity and hyperphagia accompanied by higher preference for HF diet. We observed alterations in ECS in a sex independent manner induced by maternal HF. These data contribute to understand the relationship between metabolic programming, ECS, dopaminergic system and feeding behavior.

Financial support:

CAPES, CNPq e FAPERJ

07.007 - PPAR-BETA AGONIST ALLEVIATES HEPATIC ENDOPLASMIC RETICULUM STRESS BY IMPROVING HEPATIC ENERGY METABOLISM IN HIGH-FAT DIET FED MICE. Monteiro IMLV, Veiga FMS, Oliveira L, Glauser JSO, Graus-Nunes F, Souza-Mello V, - Departamento de anatomia - UERJ

Introduction:

Endoplasmic reticulum (ER) stress and hepatic steatosis are intertwined with insulin resistance. PPARs are at the crossroads of these pathways and PPAR-beta has been previously associated with a preference for the use of lipids as fuel. Our hypothesis was that the treatment with PPAR-beta agonist could alleviate the ER stress through improved hepatic energy metabolism and the consequent augmented sensitivity to insulin.

Aim:

This study aimed to investigate the effects of GW0742 (PPAR-beta agonist) on hepatic energy metabolism and ER stress in a murine diet-induced obesity model.

Methods:

All procedures were approved by the local ethics committee (CEUA 053/2016). Forty animals were randomly assigned to receive a control diet (C, 10% lipids) or a high-fat diet (HF, 50% lipids) for ten weeks. Each group was re-divided to begin the four-week treatment, totalizing four experimental groups: C, C-B (C plus PPAR-beta agonist, GW0742, Cayman Chemicals), HF and HF-B (HF plus PPAR-beta agonist). GW0742 was mixed with the respective diet (1mg/kg BM). Body mass and food intake were monitored. Oral glucose tolerance test was performed prior to sacrifice. At sacrifice, blood was collected to determine insulin levels and the liver was harvested to be evaluated using light microscopy, transmission electron microscopy, immunofluorescence, immunoblotting, and q-PCR techniques. Data are expressed as mean and standard deviation and were analyzed with One-way ANOVA and Holm-Sidak post hoc test.

Results:

HF diet caused overweight ($33.61 \pm 2.32g$ in HF vs. $28.96 \pm 1.65g$ in C, +16%, $P=0.0017$), hyperinsulinemia ($1326 \pm 253.40pg/mL$ in HF group vs. $756.50 \pm 199.30pg/mL$ in C, +75,28%, $P=0.0009$) and hepatic inflammation through increased NF-Kb protein expression ($0.50 \pm 0.08a.u.$ corrected by beta-actin in HF vs. $0.25 \pm 0.01a.u.$ in C, +100%, $P=0.0001$), and TNF-alpha ($2.38 \pm 0.61a.u.$ corrected by beta-actin in HF vs. $1.18 \pm 0.16a.u.$ in C, +102%, $P=0.0113$) and IL-6 gene expression ($1.46 \pm 0.25a.u.$ in HF vs. $0.92 \pm 0.23a.u.$, +59%, $P=0.0105$). HF also exhibited favored hepatic lipogenesis verified by high FAS gene expression (2.16 ± 0.31 in HF vs. $0.85 \pm 0.58a.u.$ in C, +272%, $P=0.0022$), leading to ER stress, with ultrastructural and molecular alterations, ending up in proapoptotic stimulus. GW0742 rescued the overweight ($26.64 \pm 1.07g$ in HF-B vs. $33.61 \pm 2.32g$ in HF, -20.74%, $P<0.0001$) and the hyperinsulinemia ($471.60 \pm 151.60pg/mL$ in HF-B vs. $1326 \pm 253.40pg/mL$ in HF, -64.43%, $P<0.0001$), tackled hepatic inflammation by an expressive reduction in NF-Kb protein expression ($0.28 \pm 0.06a.u.$ in HF-B vs. $0.50 \pm 0.08a.u.$ in HF, -44%, $P=0.0004$) and favored hepatic beta-oxidation (CPT1a gene expression: $1.77 \pm 0.42a.u.$ in HF-B vs. $0.41 \pm 0.09a.u.$ in HF, +332%, $P=0.0004$) over lipogenesis (FAS gene expression: $0.62 \pm 0.24a.u.$ in HF-B vs. 2.16 ± 0.31 in HF, -71.30%, $P=0.0005$). These results comply with ER ultrastructure improvement, which exhibited in the HF-B group continuous cisternae, without fission or any sign of enlargement as the HF group did. These observations imply an alleviation of ER stress and apoptosis in treated animals.

Conclusion:

Our results indicate that the PPAR-beta activation alleviated the ER stress by improving the insulin sensitivity and maximizing the hepatic energy metabolism with a shift towards beta-oxidation. PPAR-beta activation could be an essential tool to avoid NAFLD progression and other obesity constraints.

Financial support:

FAPERJ, E-26/ 202.888/2015 for Vanessa Souza-Mello.

07.008 - EFFECT OF FRUCTOSE INTAKE ON SKELETAL MUSCLE OF ADULT MALE OFFSPRING FROM DAMS FED A HIGH-FAT DIET. Woyames J, Souza AFP, Oliveira LS, Caetano BG, Miranda RA, Cordeiro A, Trevenzoli IH, Souza LL, Moura CCP, - Laboratório de Endocrinologia Molecular - UFRJ Laboratório de Fisiologia Endócrina - UERJ

Introduction:

Metabolic programming by perinatal maternal high-fat diet (HFD) changes the pattern of metabolic responses of the offspring, increasing their susceptibility to obesity. Skeletal muscle is important to energy metabolism and is susceptible to metabolic stress.

Aim:

We hypothesized that perinatal maternal HFD would influence skeletal muscle of adult offspring in a fiber type manner and affect their response to a challenge with fructose in adult life.

Methods:

The study design was previously approved by ethical committee (process number 118/15). Female Wistar rats received standard diet (STD: 9% fat) or isocaloric high-fat diet (HFD: 29% fat) 8 weeks prior and throughout pregnancy and lactation. After weaning, male offspring received a standard diet and, between 120-150 days of age, half of the animals from each group received fructose in drinking water (F: 15%). The highly oxidative soleus and highly glycolytic extensor digitorum longus (EDL) muscles were collected at 150 days.

Results:

Fructose increased lipid content in EDL muscle (+1.4x; $p=0.05$) without affecting lipogenic markers, which were increased by HFD, such as increased protein expression of FAS ($p=0.04$) and SCD1 mRNA (+1.4x; $p=0.02$). We observed a suggestive increase in fatty acid uptake, since fructose increased FATP1 transporter mRNA only in STD (+1.3x, $p=0.05$). In addition, both HFD ($p=0.03$) and fructose ($p=0.01$) increased the protein expression of FABP4 transporter, and its expression was higher in the HFD-F group (+1.8x; $p=0.03$ versus STD-F), which conversely had

FeSBE Annual Meeting 2019

Poster Sessions and Abstracts

lower expression of lipoprotein LPL mRNA (-29%; $p=0.02$). However, HFD increased mRNA levels of the lipid oxidation transcription factor PPAR δ (+1.5x; $p=0.03$), justifying the non-alteration of lipid content observed. We also identified alteration in endocrine function of EDL muscle, suggested by the lower protein expression of FNDC5 in HFD ($p=0.05$) and F group ($p=0.02$), and its expression was lower in HFD-F (-54%; $p=0.01$ versus STD). Conversely, in soleus muscle, we observed no difference in FNDC5 protein expression. However, HFD increased the expression of lipogenic markers, such as SREBP1 mRNA (+1.4; $p=0.03$), its active protein form (cleaved/precursor) (+2.2x; $p=0.05$) and SCD1 mRNA ($p=0.03$). Interestingly, HFD increased mRNA expression of the transporters FATP4 ($p=0.004$) and FATP1 ($p=0.002$), and the latter was higher in the HFD-F group (+0.8x, $p=0.05$ versus STD-F). However, we did not observe difference in lipid content in the soleus muscle, which could be justified by the possible increase of lipid oxidation, since HFD increases the expression of PPAR α mRNA (+1.2x; $p=0.007$) and PPAR δ mRNA ($p=0.002$) and its protein levels (+1.4x; $p=0.02$), in addition to CPT1a protein ($p=0.02$).

Conclusion:

Our data suggest that maternal HFD increased lipid uptake and the lipogenic capacity of EDL muscle, besides compromising its endocrine function, in contrast, we observed an overload in the oxidative capacity of the soleus muscle. Taken together, maternal diet alters muscle lipid metabolism and endocrine function depending on the fiber type, effects that seem to be enhanced by the fructose intake in adult life.

Financial support:

CNPq, FAPERJ, CAPES

07.009 - COLD EXPOSURE EXACERBATES THE BODY METABOLIC RATES IN CETP EXPRESSING MICE COMPARED TO CONTROLS. Castelli JZ, Raposo HF, Oliveira HCF, - Departamento de Biologia Estrutural e Funcional - UNICAMP

Introduction:

Plasma cholesteryl ester transfer protein (CETP) promotes the transfer of cholesterol from HDL to the apoB containing lipoproteins. This action may enhance the atherosclerosis risk because of the reduction of HDL-cholesterol plasma levels. However, the use of CETP inhibitors failed to prove benefits in reducing cardiovascular disease mortality. We have identified that CETP has a novel function of reducing adiposity. Under standard condition (chow diet, housing temperature of 22 °C), CETP expressing mice are leaner and show increased lipolysis, brown adipose tissue (BAT) activity and body energy expenditure compared to non-transgenic controls.

Aim:

The aim of this study was to evaluate how CETP mice would modulate their body temperature during cold exposure being leaner and having higher BAT activity.

Methods:

Two independent strains of CETP transgenic mice were used: hCETP - mice expressing a human CETP minigene under the control of its natural promoter and sCETP mice overexpressing the simian CETP cDNA under the control of the metallothionein promoter. Their non-transgenic (NTg) littermates were used as controls. Mice (female, 5-month-old) were exposed to cold (4 °C; 7 days, singly caged, no bedding, 12 h light/dark cycle, free access to water and chow diet). Food intake and body weight were evaluated 3 times during the experimental period. Body temperature (rectal temperature) were measured daily. The temperature of interscapular (iBAT) and inguinal (iWAT) adipose depot areas were determined with a thermosensitive camera FLIR T450sc every other day. Oxygen consumption (VO₂) in response to intraperitoneal injection of isoproterenol (10 mg/kg BW) was evaluated in anesthetized mice before and immediately after the experiment. The comparisons between the groups were analyzed by unpaired Student's t test and the level of significance was set at $P < 0.05$.

Results:

The cold resistance (after 6 hours at 4 °C) was not different in CETP expressing mice compared to NTg. The rectal temperature, body weight and food intake were similar between CETP expressing mice and NTg along the whole period at 4 °C. sCETP mice showed higher iBAT temperature after 24 hs of cold exposure. However, from day 2 to 7 at 4 °C no significant differences were detected. iWAT temperatures did not differ between groups. The oxygen consumption in response to isoproterenol in hCETP was 21% higher before the cold experiment and 41% higher than in NTg at the end of the cold exposure period. In sCETP group an increase of 15% in BAT mass was observed.

Conclusion:

CETP expressing mice are able to maintain their body temperature during cold exposure due to their capacity to increase body metabolic rates (VO₂) 50% above the level of control (NTg) mice.

Financial support:

FAPESP and CNPq.

07.010 - EFFECT OF MATERNAL HIGH FAT DIET ON HEPATIC ENDOCANNABINOID SYSTEM OF NEWBORN RAT OFFSPRING. Fassarella LB, Miranda RA, Almeida MM, Rocha CPD, Moura CCP, Trevenzoli IH, - Laboratório de Endocrinologia Molecular - UFRJ

Introduction:

Perinatal maternal overnutrition induces obesity in the offspring. Obesity is associated with changes in endocannabinoid system (ECS). The ECS is composed by endocannabinoids that regulate energy and lipid metabolism via cannabinoid receptors (CB1 and CB2) and are degraded by fatty acid amide hydrolase (FAAH) and monoacylglycerol lipase (MAGL). We have recently shown that the maternal high-fat (HF) diet induces sex-specific alterations of the ECS on liver of adult male and female offspring. Our hypothesis is that these alterations on hepatic ECS of the offspring originate in gestation. Therefore, we tested whether maternal HF diet changes the expression of the ECS components in the liver of male and female offspring at birth, contributing to the development of obesity throughout life.

Aim:

To investigate the effect of maternal HF diet on ECS in liver of the male and female newborn rat offspring.

Methods:

All procedures with animals were approved by CEUA/CCS/UFRJ (protocols 095/17). 60 days old female Wistar rats received standard diet (C; 9% fat) or high-fat diet (HF; 28% fat) during 8 weeks before mating and during gestation. At birth, we evaluated the ECS components expression in liver of C and HF offspring by western blotting. Data were analyzed using two-way ANOVA with the maternal diet and the offspring sex as main factors, followed by pair comparisons per each sex using the Bonferroni post-test.

Results:

The maternal diet or sex of offspring did not change the hepatic content of CB1 and CB2 in the offspring at birth. On the other hand, newborn female offspring presented higher FAAH expression (+ 43%, $p < 0.05$) compared to males, demonstrating the influence of sex.

Conclusion:

Maternal high-fat diet did not alter the hepatic expression of CB1, CB2 and FAAH in offspring at birth. As we have already shown alterations of these components in the liver of adult offspring, we speculate that such modifications may arise in other phases of life, such as weaning and adolescence. Characterizing the moment when these changes occur is important for understanding the periods of plasticity of the endocannabinoid system in the offspring exposed to maternal nutritional insults.

Financial support:

CNPq, CAPES and FAPERJ

FeSBE Annual Meeting 2019

Poster Sessions and Abstracts

07.011 - CLONING OF MOUSE ALDOSE REDUCTASE (AKR1B3) IN MAMMALIAN EXPRESSION VECTOR PCINEO TO STUDY HEPATIC GLUCOSE METABOLISM IN INSULIN RESISTANCE. Nascimento-Sales M, Christoffolete MA, - Laboratório de Fisiologia Metabólica - UFABC

Introduction:

Insulin resistance in humans and rodents evokes compensatory hyperinsulinemia in order to ensure normal utilization of glucose by the insulin target tissues. Aldose reductase are cytosolic monomeric enzymes which catalyzes the NADPH-dependent conversion of glucose to sorbitol, the first step in polyol pathway of glucose metabolism. The second and last step in the pathway is catalyzed by sorbitol dehydrogenase, which catalyzes the NAD-linked oxidation of sorbitol to fructose. In liver, resistance to insulin action leads glucose metabolism to divert from glycolysis to other pathways, such as sorbitol synthesis, which in overproduction lead to accumulation of triglycerides in hepatic steatosis.

Aim:

Cloning Akr1b3 gene (*Mus musculus*) in pCINEO vector system (Invitrogen), with green fluorescent protein as molecular marker.

Methods:

Total RNA from liver of FVB/N male mice was extracted with TriReagent (Sigma Aldrich) following fabricant instructions. cDNA was obtained by Reverse transcriptase (Life Technologies). The aldose reductase (Akr1b3) coding sequence was cloning by conventional PCR, using specific primers, purified and recovered by QiaQuick gel extraction Kit (Qiagen). The insert was cloned into pGEM-t easy vector system (Promega) and subcloned into pCINEO (Promega) plus internal ribosome entry site (IRES) and enhanced green fluorescent protein sequence (EGFP). Cell lines HepG-2 and HEK-293 were transfected with lipofectamine 2000 (Invitrogen). After 48 hours of expression, fluorescence microscopy images were captured, total protein was recovered and analyzed by western Blotting using specific antibody anti AKR1B3 (Cusabio).

Results:

The integrity of the total RNA, the transcribed cDNA and the amplification of the 956Kbp fragment corresponding to aldose reductase were confirmed by agarose gel electrophoresis. After receiving the plasmid by heat shock and being seeded in a selective medium with Ampicillin, we obtained 30 CFU positive of DH5 α bacteria for pGEM-T-Akr1b3 and 4 CFU of pCINEO CMV IRES EGFP Akr1b3, confirmed by double digestion with strategic restriction enzymes and Sanger sequencing. Plasmid recovering was by miniprep kit (Qiagen), yielding 10 μ g of each purified constructs. Transfection success was achieved in 30% of the HepG2 and HEK293 cell lines, which showed Akr1b3 overexpression after 48 hours.

Conclusion:

We successfully cloned the Akr1b3 gene into mammalian expression vector with GFP as molecular marker, proving expression efficiency in two distinct cell lines, which will allow us to better understand its role in glucose metabolism in an in vitro model of hepatic insulin resistance.

Financial support:

FAPESP, CNPQ

07.012 - CAPSICUM BACCATUM VAR. PENDULUM: MODULATION OF DIFFERENT CONDITIONS ASSOCIATED WITH METABOLIC SYNDROME. Leonardi B, Benin T, Gosmann G, Zimmer AR, - Laboratório de Fitoquímica e Síntese Orgânica - Faculdade de Farmácia - UFRGS

Introduction:

Capsicum baccatum var. pendulum is a highly consumed red pepper and little explored regarding its chemical composition and pharmacological properties (Chiou, K. L. et al. Econ. Bot. 2014, 68, 316-336). In previous studies conducted by our research group, antioxidant and anti-inflammatory properties were demonstrated for different extracts obtained from this pepper (Zimmer A. R. et al. J. Ethnopharmacol. 2012). It is known that there is an important

correlation between inflammation of adipose tissue, obesity and metabolic diseases (Reilly S. M. and Saltiel A. R. Nat. Rev. 2017, 13, 633-643). Metabolic syndrome, characterized by the association of obesity, insulin resistance, dyslipidemia and hypertension, is reaching epidemic proportions worldwide and result in an increased risk of heart disease and early mortality (IDF, 2005).

Aim:

This study aimed to evaluate the influence of *C. baccatum* var. pendulum on metabolism of mice submitted to a hypercaloric diet.

Methods:

To obtain the extract, fruits of *C. baccatum* were extracted as previously described (Zimmer A. R. et al. J. Ethnopharmacol. 2012). The extract underwent a column fractionation process to obtain one purified fraction. In vivo assays were performed on C57BL/6 male mice fed with a standard diet (SD) or a hyperpalatable diet (HPD) to induce metabolic disorders (CEUA/UFRGS - 19446). Mice were treated with extract (200 mg/kg) or purified fraction (50 mg/kg) of *C. baccatum* during 120 days by gavage. After the treatment period, all animals were submitted to a glucose tolerance test, then euthanized and blood sampling for other biochemical analysis. Statistical analysis was performed by two-way ANOVA followed by Tukey's post-hoc test, considering as significant difference $p < 0.05$.

Results:

The consumption of a HPD resulted in a significantly weight gain compared to SD group which was prevented by the administration of the purified fraction of *C. baccatum*. The treatment of the C57BL/6 mice with the extract and purified fraction significantly decreased visceral adiposity accumulation in 35% and 53%, respectively, and prevented the increase in hepatic cholesterol and triglycerides levels in the animals fed with HPD compared to the SD group. Furthermore, the administration of *C. baccatum* prevented the development of a glucose intolerance profile and the rise in plasma insulin and leptin levels, induced by HPD consumption, showing no significant difference concerning SD group.

Conclusion:

These results showed the beneficial effects of *C. baccatum*, preventing important changes in biological parameters related to the metabolic syndrome, attesting its promising therapeutic potential in this field.

Financial support:

Capes, CNPq, Fapergs

07.013 - ASCORBIC ACID SUPPLEMENTATION ACCELERATES SKELETAL MUSCLE RESPONSES TO REFEEDING AFTER FASTING IN FISH. Zanella BTT, Magiore IC, Duran BOS, Valente JS, Salomão RAS, Mareco EA, Paula TG, Dal-Pai-Silva M, - Departamento de Biologia - UNOESTE Departamento de Morfologia - UNESP

Introduction:

Skeletal muscle in fishes comprises 60% of total body weight, representing a major amino acids source; besides, external conditions can affect its phenotype. Nutrients restriction are common through fish's life, both in natural and artificial environments. Fasting periods, in addition to lead to muscle degradation, may trigger a physiological stress and reactive oxygen species (ROS) production, which in high amounts can cause cell damage disturbing muscle growth. Compounds that act as antioxidants, as the ascorbic acid (AA), may present an alternative to prevent the harm caused by ROS, rescuing muscle phenotype.

Aim:

We aimed to evaluate the AA supplementation effects on refeeding in skeletal muscle of pacu (*Piaractus mesopotamicus*) after a fasting period. Our initial hypothesis was that the AA supplementation would enhance muscle recovery by inhibiting catabolic and increasing anabolic and myogenic genes, besides neutralizing ROS and stimulating antioxidant enzymes.

Methods:

FeSBE Annual Meeting 2019

Poster Sessions and Abstracts

Pacu juvenile (\cong 30g) were distributed (n: 8/group) in: Control (continuous feeding - 200 mg/kg of AA), Fasting (15 days of fasting) and three groups of refeeding for 6 hours after fasting; Low (100 mg/kg of AA), Medium (200 mg/kg of AA) and High (400 mg/kg of AA); (ethical committee protocol 1050). RT-qPCR and biochemistry analyses were performed to determine gene expression and antioxidant enzymes activity. To statistical analyzes, T-test was applied to the comparison between Control and Fasting groups and ANOVA one-way to the comparison between Control and refeeding groups ($p > 0,05$).

Results:

We found an increase of 36x and 3x, respectively, in catabolic genes *mafb*x and *murf1a* expression, in the Fasting compared to the Control group. Besides, *pgc1a* expression, a gene related to mitochondrial biogenesis, increased 0.52x, in the fasting situation. After refeeding, the *mafb*x expression remained higher in all refeeding groups (\cong 14x), while *murf1a* expression decrease 0.86x, compared to Control. The anabolic genes expression, *igf1*, *igfbp5*, and *mtor* had a decrease in Fasting group of 0.52x, 0.63x and 0.20x, respectively, compared to Control, while after refeeding, only the *igfbp5* expression presented a 0.75x increase in the High group compared to Control. The *myod* expression, a gene related to myoblast proliferation, had a 0.25x decrease in Fasting compared to Control group, while *myogenin* expression, a gene related to myoblast differentiation, did not change. After refeeding, *myogenin* expression remained similar between the groups and *myod* had a 0.30x increase in the High group compared to Control. The activity of antioxidant enzymes, superoxide dismutase (*Sod*), catalase (*Cat*) and glutathione peroxidase (*GPx*) was similar between Control and Fasting groups. The *Sod* activity, after refeeding, remained similar between groups; *GPx* activity had a 6x increase in refeeding groups compared to Control, and *Cat* activity had a 7x decrease in Medium and High groups compared to Low group.

Conclusion:

Our results suggest that the fasting period led to muscle degradation and growth inhibition and, that the AA supplementation promoted a faster response to recovery muscle growth by neutralizing ROS effects and stimulating myogenic and anabolic genes. In conclusion, our work may present an approach to minimize the negative stress effects on muscle phenotype.

Financial support:

FAPESP 2017/26346-1; CNPq 148108/2018-0.

07.014 - EFFECTS OF AEROBIC PHYSICAL TRAINING IN LIPID METABOLISM OF RATS FED A HYPERLIPIDIC DIET SINCE POST-WEANING. Correia LA, Pereira RO, Azevedo CEA, Araujo IC, Evangelista FS, Farah V, Fiorino P, - Medicina Translacional - UNIFESP Escola de Artes, Ciências e Humanidades - USP Laboratório de Fisiopatologia Metabólica Cardiovascular e Renal - MACKENZIE Medicina Translacional/Laboratório de Fisiopatologia Metabólica Cardiovascular e Renal - UNIFESP/MACKENZIE

Introduction:

Overweight and obesity are usually associated with excessive food consumption rich in saturated fat and sedentary lifestyle. This situation is more alarming when the consumption of high fat foods begins in childhood, increasing the susceptibility to the development of chronic degenerative diseases in the young adult phase. Data from our laboratory demonstrated that adult rats fed a hyperlipidic diet (HD) since post-weaning increased total cholesterol (TC), VLDL, LDL and triglycerides (TG). In contrast, aerobic physical training (APT) had a positive effect on body weight control, prevents insulin resistance and intrarenal fat accumulation. Therefore, the aim of this study was to test the hypothesis that APT is efficient to prevent dyslipidemia in rats fed a HD since post-weaning.

Aim:

The aim of this study was to test the hypothesis that APT is efficient to prevent dyslipidemia in rats fed a HD since post-weaning.

Methods:

Post-weaning male Wistar rats (40-60g) were randomly divided into 2 groups (n=4/group) and followed during 12 weeks: HD and sedentary (HDS, 30% lipids) and HD and trained (HDT, 30% lipids). APT was performed since the 5th week and consisted of 8 week running sessions of 60 minutes at 60% of maximal speed, 5 days/week. At the end of the protocol, animals were killed with anesthetic overload. Epididymal fat pad was removed, weighted and normalized by the body weight. The blood was collected through the inferior vena cava using a vacuum system and centrifuged at 2000 rpm during 15 minutes. The lipid profile (HDL, triglycerides and total cholesterol) was determined in collected serum samples and analyzed in a spectrophotometer using colorimetric kits. VLDL (TG/5) and LDL (TC - HDL - LDL) levels were calculated. All the procedures following the rules of the Committee of Research and Ethics of the Mackenzie University (N°166/03/2018). The results were analyzed by Student's t test and presented as mean \pm standard error of the mean (SEM). The results were significantly different only when $p \leq 0.05$.

Results:

APT did not change body weight significantly (HDS: 342 ± 7 g; HDT: 324 ± 19 g). However, visceral fat pad was 33% reduced in HDT compared to HDS group (HDS: $0,015 \pm 0,001$ g; HDT: $0,010 \pm 0,002$ g). A significant decrease was observed in the triglycerides concentration of HDT group (63 ± 1 mg/dL) when compared with HDS group (93 ± 11 mg/dL). In addition, a significant reduction in VLDL concentration of HDT animals ($13 \pm 0,2$ mg/dL) was also observed when compared with HDS group (19 ± 2 mg/dL). However, total cholesterol, HDL and LDL analyzes had no significant differences between groups.

Conclusion:

Our data suggests that aerobic physical training was efficient to reduce the fat pad accumulation and also to prevent dyslipidemia in rats fed hyperlipidic diet since post-weaning.

Financial support:

Mackpesquisa

07.015 - INFLUENCE OF PHENOLIC MICROBIAL FERMENTATION ON THE GROWTH AND SURVIVAL OF YEAST EXPRESSING A-SYNUCLEIN. Prudêncio ER, Pereira MD, Castro RN, Riger CJ, - Departamento de Bioquímica - UFRJ Laboratório de Química Medicinal e Laboratório de Química do Mel (LabMed & LabMel), Departamento de Química Orgânica - UFRJ Laboratório de Estresse Oxidativo em Microorganismos (LEOM), Departamento de Bioquímica - UFRJ

Introduction:

Parkinson's disease is a neurodegenerative disorder associated with aging and its pathogenicity is attributed to the loss of α -synuclein (α -syn) protein function that acts on the signaling of dopaminergic neurons. Studies indicate that the bioavailability of polyphenols and their accumulation in brain tissue may contribute to the prevention or even reversal of cognitive decline seen in neurodegenerative diseases. Significant amount of phenolic compounds becomes bioavailable after metabolism by the intestinal microbiota, leading to the belief that this microbiological transformation may influence its neuroprotective effect.

Aim:

The aim of this study was to verify the influence of phenolics and their microbial fermentation on the survival and growth of yeasts expressing α -syn.

Methods:

Phenolic fermentation was conducted for 168 h at 36 °C with an probiotic blend. Aliquots were withdrawn every 24 hours and submitted to HPLC analysis. As a biological model, was used *Saccharomyces cerevisiae* containing α -syn human gene plasmids with the regulation of GAL1 inducible promoter. A pre-inoculum (OD600 0.5 ± 0.1 - log growth phase) was prepared in synthetic complete medium SC-Glu [0.67% (w/v) yeast nitrogen base without amino acids

FeSBE Annual Meeting 2019

Poster Sessions and Abstracts

(Difco), 2% (w/v) glucose and 0.79 g.L⁻¹ solution of histidine, leucine and methionine] under shaking at 30 °C. Then, were diluted to OD600 0.03 in the medium SC-GAL (SC with 1% (w/v) galactose instead of glucose) and supplemented with caffeic acid phenethyl ester (CAPE) and mangiferin phenolics; CAPE and mangiferin fermented by probiotic blend, all of them 0.1 mM; medium fermented by probiotic blend and a control with only SC-GAL. Cells were then incubated at 30 °C with shaking for 40 h. Yeast growth was kinetically monitored by measuring the OD600nm. For spot assays, cells in log growth phase were incubated in the same treatment above for 6 hours. After, were adjusted to OD600nm 0.05±0.005, diluted and 3 µL of each dilution was spotted in SC-Glu (Control, α-Syn OFF) and SC-GAL (α-Syn ON) and grown for 3 days at 30 °C. Assays were conducted in triplicate.

Results:

Chromatograms obtained by HPLC indicate that 50% of CAPE was converted to its precursors caffeic acid and quinic acid, probably due to esterases produced by the bacteria. On the other hand, only 0.3% of mangiferin was converted into other products. Comparing the maximum optical density obtained in the growth curves, it was observed that fermented supernatant promoted the highest yeast growth in SC-GAL medium, reaching an average OD of 1.512 ±0.014, ie, the supernatant of bacteria appears to reduce toxicity associated with α-syn aggregation. Then, fermented phenolics promoted similar curves of each other, with maximum OD values close to 1.400, but higher than control (OD 1.147 ±0.13). For unfermented phenolics, mangiferin had similar growth to control while CAPE was highly toxic, inhibiting yeast growth. Differences in CAPE toxicity clearly shows that fermentation influences the bioactivity of the phenolic compound. The spot plating confirmed CAPE toxicity, however, no difference was observed between the other treatments.

Conclusion:

Therefore, it was concluded that microbial fermentation is capable of altering the bioactivity of phenolic compounds and these are promising in combating toxicity caused by synucleopathies.

Financial support:

FAPERJ, CNPq

07.016 - BRAZIL NUT (BERTHOLLETIA EXCELSA H.B.K.) EFFECT ON WHITE ADIPOSE TISSUE OF MALE WISTAR RATS. Campos JM, Almeida PP, Costa NS, Brito ML, Pereira AD, Cruz BO, Magliano DC, Stockler-Pinto MB, - Departamento de Morfologia - MMO - UFF Departamento de Nutrição e Dietética - MND - UFF

Introduction:

White Adipose Tissue (WAT) is already considered an important endocrine organ on metabolism regulation. Several nutritional interventions have been tested to control the body mass (BM) in experimental models, however, literature doesn't show studies about the influence of Brazil nut supplementation in rodents.

Aim:

Thus, our objective was to evaluate the composition of BM and WAT of rats that consumed an enriched diet with 10% of Brazil nut.

Methods:

2 months aged male Wistar rats were kept in an equipped room with controlled temperature and light-dark cycle. The animals were allocated in two experimental groups: control group (CG, n=10), which received a control diet, and the Brazil nut group (N10, n=10), which received a diet enriched with 10% of Brazil nut, both ad libitum. The animals received the diets during 8 weeks. The BM was measured weekly as well as the diet consumption. At the end of the experiment, fasting glycemia and plasmatic malondialdehyde levels were analyzed, and the epididymal, inguinal and retroperitoneal WAT were weighed.

Results:

In relation to the CG (352.7±7.3g, p<0.0001), N10 (280.7±5.5g, p<0.0001) presented a decrease in final BM. The diet consumption decreased in N10 group (11.4±0.4g/day/animal, p<0.0001) compared to

CG (21.6±0.4g/day/animal, p<0.0001). Glycemia levels showed no difference (CG: 73.6±1.8mg/dL, N10: 75.6±2.5mg/dL, p=0.5299). Concerning to malondialdehyde levels, the N10 (0.9±0.2nmol/mL, p=0.0138) presented lower levels compared to CG (2.7±0.6nmol/mL, p=0.0138). Regarding the adipose tissues, epididymal decreased in N10 (0.8±0.03g, p=0.0054) compared to CG (1.04±0.05g, p=0.0054); inguinal showed no difference between CG (0.5±0.03g, p=0.2075) and N10 (0.4±0.05g, p=0.2075) and retroperitoneal adipose tissue decreased in N10 (0.6±0.06g, p=0.0020) compared to CG (0.9±0.02g, p=0.0020).

Conclusion:

The results suggest that an enriched diet with 10% of Brazil nut supplementation is able to reduce BM, plasma lipid peroxidation and adipose tissues in male Wistar rats.

Financial support:

CAPES, CNPq e FAPERJ

07.017 - PENTOXIFYLLINE IMPROVED THE INSULIN SENSITIVITY AND THE GLUCOSE TOLERANCE, AND ATTENUATES GLYCOXIDATIVE STRESS IN HIGH-FAT DIET-INDUCED OBESITY IN MICE. Inácio MD, Costa MC, Lima TFO, Figueiredo ID, Assis RP, Brunetti IL, Baviera AM, - Departament of Clinical Analysis - UNESP

Introduction:

Obesity is a major public health problem and a risk factor for the development of insulin resistance and type 2 diabetes mellitus (DM), which lead to hyperglycemia. Chronic hyperglycemia accounts for the onset and maintenance of microvascular and macrovascular complications of DM, mainly triggered by glycoxidative stress, characterized by increased formation of advanced glycation end-products (AGEs). Pentoxifylline (PTX) is a methylxanthine, non-selective phosphodiesterase inhibitor; PTX has been used for intermittent claudication; however preclinical studies have demonstrated its efficacy on improve the insulin resistance and obesity-associated complications.

Aim:

This study was performed to investigate the changes in physiometabolic parameters and glycoxidative stress biomarkers in mice under an experimental model of high-fat diet-induced obesity and treated with PTX.

Methods:

C57BL/6 male mice were fed for 14 weeks with a standard diet (P, 3.85 kcal/g, 4% lipids) and a high-fat diet (HFD, 5.40 kcal/g, 35% lipids). P and HFD mice were treated with vehicle (saline; 0.85% NaCl), and HFD mice were treated with 50 mg/kg PTX (HPTX), intraperitoneally, from 8th to 14th weeks. Body weight was monitored weekly. Oral glucose tolerance test (OGTT) was performed at week 12. At the end of the treatments (week 14), animals were fasted, anesthetized (16 mg/kg xylazine and 90 mg/kg ketamine). Some animals received insulin (3.8 units/kg, intraperitoneally), and other animals received saline; after 10 min, epididymal white adipose tissues (eWAT) were removed, weighed and snap-frozen (-80°C) for further analysis of the changes in the AKT phosphorylation (Ser-473 residue). Then, blood samples were collected by cardiac puncture, and plasma samples were used to determine the activity of paraoxonase 1 (PON1), and plasma levels of thiobarbituric acid reactive substances (TBARS) and of fluorescent AGEs. Results were expressed as mean ± standard error and considered statistically different with p<0.05 (One-Way ANOVA followed by Student-Newman-Keuls).

Results:

HFD mice had increases in the body weight gain (HFD, 18.3±0.54 vs P, 12.2±1.07, g) and eWAT mass (HFD, 0.11±0.005 vs P, 0.03±0.002, g/mm tibia), increased plasma levels of TBARS (HFD, 18.3±0.54 vs P, 12.2±1.07, µmol/L) and AGEs (HFD, 83.5±4.14 vs P, 56.6±5.23, UA/ mg protein), as well glucose intolerance (HFD, 26444±557 vs P, 22062±581, mg/dL, AUC of OGTT). Glucose intolerance was corroborated by the decreased levels of both basal and insulin-stimulated AKT phosphorylation levels in adipose tissue of HFD mice. In comparison

FeSBE Annual Meeting 2019

Poster Sessions and Abstracts

with HFD mice, HPTX mice had minor body weight gain (22%) and eWAT mass (23%). Furthermore, HPTX mice showed decreases in plasma levels of TBARS (20%) and AGEs (28%), and increased PON1 activity (32%). Glucose tolerance was also improved in HPTX animals (17%), which was corroborated by the increases in both basal (59%) and insulin-stimulated (32%) AKT phosphorylation in eWAT.

Conclusion:

The treatment with PTX attenuated various metabolic disturbances observed in obesity, with emphasis on the reduction in markers of glycoxidative damage, increased antioxidant defenses, and improved the insulin sensitivity and the glucose tolerance. These findings highlight PTX as a promising candidate to be further studied for its repositioning for the treatment of obesity and its complications.

Financial support:

FCFAR/UNESP, CAPES, CNPq, FAPESP (16/23644-9).

8 - Renal Biology and Diseases

08.001 - CHRONIC KIDNEY DISEASE IN WISTAR RATS AS A CONSEQUENCE OF ACUTE KIDNEY INJURY (AKI) EVENTS DURING AGING. Silva RC, Quintas LE, Morcillo LSL, - Farmacologia e Química Medicinal - UFRJ

Introduction:

Among the biological process of aging, the progressive loss of the structure and function of the kidney strictly impact body homeostasis in the elderly. The understanding of the pathophysiological mechanisms is important for the identification of new pharmacological interventions.

Aim:

The aim of this work is to determine the mechanism by which repeated episodes of ischemia/reperfusion (I/R) renal _ characteristics of acute kidney injury (AKI) _ during aging process accelerate the progression of chronic kidney disease (CKD).

Methods:

Male Wistar rats were submitted to bilateral ischemia for 30 min followed by 24 h of reperfusion at ages 90, 180 and 365 days (n=5/group). Renal physiologic parameters were compared to rats that underwent natural senescence (n=5 for each respective age). The model used was approved by the Ethics Committee for the Use of Animals (ECUA) of the Federal University of Rio de Janeiro (059/17).

Results:

We observed that during the aging period the rats presented no difference in the glomerular filtration rate (GFR) after each I/R intervention. However, the accumulation of blood urea nitrogen (BUN) and proteinuria was progressively higher in the aging I/R rats. At 365 days, 4 out of 15 rats subjected to I/R presented expressive increase of the dimensions with irregular surfaces of one of the kidneys with normal contralateral kidney. During senescence, cortical (Na⁺K⁺)ATPase protein content decreased 42% and its activity increased in 140% at 410 days of life. The I/R procedure applied in the young rat decreased (Na⁺K⁺)ATPase protein content and increased by 135% at the elderly rat (410 days of life). The enzymatic activity in the elderly rat was also higher (148%, 410 days of life). The ratio of the protein content of the salt-induced kinase (SIK1) and its active form (pSIK1/SIK1) was 44% reduced at 90 days for the I/R group, increased in 24% at 180 days and sustained higher at 410 days of life. The overall O-glycosylation profile of proteins was reduced with senescence (reduction of 18% at 180 days and another 27% at 410 days, setting approximately 45% reduction throughout the evaluated period). The interference of the I/R accentuated this effect being maximal at 410 days of life (a reduction in 27%) only at the rat that presented kidney injury.

Conclusion:

Taken together, these results suggest that episodes of AKI during aging lead to CKD, by a mechanism that involves increased activity of SIK1 and

decreased intracellular O-glycosylation levels. These mechanism maybe related with an increased (Na⁺K⁺)ATPase activity in the elderly.

Financial support:

Capes, Faperj

08.002 - EFFECTS OF ACETAZOLAMIDE IN THE POTASSIUM REABSORPTION IN PROXIMAL TUBULE OF RATS. Silva BS, Castelo-Branco RC, Malnic G, - Fisiologia e Biofísica - USP

Introduction:

Acetazolamide (AZT) is a diuretic inhibitor of carbonic anhydrase (AC) present in the proximal tubule (PT) converting water and CO₂ into carbonic acid (H₂CO₃). Its inhibition reduces the concentration of both and leads to the excretion of Na⁺ and H₂O. PT reabsorbs most of the filtered K⁺ by the paracellular pathway by solvent drag and electro diffusion. S3226 is an inhibitor of the Na⁺/H⁺ exchanger isoform 3 (NHE3) present in PT, important for pH and volume regulation.

Aim:

The objective of the project is to evaluate the effects of AZT and S3226 on the K⁺ reabsorption in PT.

Methods:

Renal function using metabolic cages (Control 24h/AZT 2h). The ministration of AZT (200mg/kg/2h) was intraperitoneal in Wistar rats. Microperfusion method in vivo to measuring the intratubular K⁺ using potassium sensitive microelectrodes and calculating the potassium reabsorption flow (JK) by the equation $\{k \frac{[(K^+)i - (K^+)s]}{r/2}\}$, where "k" is the luminal potassium reduction constant $[k = \ln 2 / (t/2)]$, "r" is the tubule radius and (K⁺)_i and (K⁺)_s are the concentrations of injected K⁺ in the level stationary K, respectively. All data of metabolic cages were analyzed by t-test and the data of microperfusion were by One-Way ANOVA followed by Bonferroni post-test. All data analyzed were carried out in GraphPad software version 5. Statistical significance was set as *p<0.005.

Results:

The group treated with AZT for two hours presented higher urinary flow $[18 \pm 1.4 \mu\text{l}/\text{min}/100\text{g}/2\text{h}$ (n=3)] when compared to the control group $[4.3 \pm 0.7 \mu\text{l}/\text{min}/100\text{g}/24\text{h}$ (n=4)], excreted loads of Na⁺ $[3.209 \pm 0.57 \text{ mEq}/100\text{g}/2\text{h}$ (n=2)] and K⁺ $[1.575 \pm 0.04 \text{ mEq}/100\text{g}/2\text{h}$ (n=2)] of AZT group were higher than control group $\{\text{Na}^+ [0.672 \pm 1.29 \text{ mEq}/100\text{g}/24\text{h}$ (n=4)] and K⁺ $[1.152 \pm 0.17 \text{ mEq}/100\text{g}/24\text{h}$ (n=4)]\}. The plasma concentrations of Na⁺ $[136 \pm 1 \text{ mEq}/\text{L}$ (n=2)] and K⁺ $[3.4 \pm 0.7 \text{ mEq}/\text{L}$ (n=2)] of the AZT group were significantly decreased when compared to the control group $\{\text{Na}^+ [142 \pm 2 \text{ mEq}/\text{L}$ (n=4)] and K⁺ $[4.9 \pm 0.2 \text{ mEq}/\text{L}$ (n=4)]\}. So, our data are showing that in Wistar rats the AZT causes a higher excretion of K⁺ consistent with the literature. In Wistar rats, the mean control value of JK was $1.10 \pm 0.10 \text{ nmol}\cdot\text{cm}^2\cdot\text{s}$ (n= 08), the treatment with AZT $[200\text{mg}/\text{kg}/2\text{h}]$ caused a significant increase of the JK to $1.66 \pm 0.14 \text{ nmol}\cdot\text{cm}^2\cdot\text{s}$ (09); S3226 $[10^{-6} \text{ M}]$ in lumenally perfused tubules caused a significant decrease of the JK to $0.66 \pm 0.04 \text{ nmol}\cdot\text{cm}^2\cdot\text{s}$ (08). So, our data are showing that the effects of AZT on JK modulates the paracellular way and that JK is dependent of NHE3 activity in proximal tubule.

Conclusion:

The results of microperfusion in vivo, indicated that the inhibition of NHE3 by S3226 (acute) in the PT, affects the reabsorption of the paracellular pathway of K⁺. In basal situation the NHE3 represents the main mechanism of generation of the electrochemical gradient for the reabsorption of H₂O and Na⁺, creating a perfect process for the transport of K⁺ by the paracellular path. The interaction between the transcellular pathway by NHE3 and the paracellular pathway by K⁺ reabsorption in PT may represent an important mechanism of physiological regulation of intra-extracellular volume.

Financial support:

FAPESP

FeSBE Annual Meeting 2019

Poster Sessions and Abstracts

08.003 - EFFECTS OF AEROBIC EXERCISE TRAINING ON RENAL EXTRACELLULAR MATRIX ACCUMULATION IN RATS FED A HIGH-FAT DIET SINCE POST-WEANING. Pereira RO, Komoni G, Correia LA, Evangelista FS, Fiorino P, Farah V, - Medicina Translacional - Universidade Federal de São Paulo (UNIFESP) Laboratório de Fisiologia Metabólica Cardiovascular e Renal - Universidade Presbiteriana Mackenzie Escola de Artes, Ciências e Humanidades - EACH - USP Medicina Translacional / Laboratório de Fisiologia Metabólica Cardiovascular e Renal - UNIFESP / Mackenzie

Introduction:

High-fat intake since childhood may predict several morphofunctional abnormalities in adulthood. Data from our group showed that adult SHR and Wistar rats developed renal dysfunction and morphological alterations when fed high-fat diet since post-weaning. It is well known that physical training is efficient to prevent several metabolic diseases. However, the role of aerobic exercise training (AET) in the prevention of renal morphofunctional alterations in response to a high-fat diet needs more investigation.

Aim:

Thus, the aim of this study was to test the hypothesis that AET is efficient to prevent renal extracellular matrix accumulation in rats fed a high-fat diet since early period of life.

Methods:

Male post-weaned Wistar rats (40-50g) were divided into 4 groups (n=4/group) and followed during 12 weeks: normal diet and sedentary (NS); High-fat diet and sedentary (HFS, 30% lipids); normal diet and trained (NT); High-fat diet and trained (HFT). AET was performed since the 5th week of protocol and consisted of 8 week running sessions of 60 minutes at 60% of maximal speed, 5 days/week. After euthanasia, the left kidney and visceral fat pads were removed, weighted and normalized by the body weight and by the tibia length, respectively. Ethics Committee of Mackenzie (166/03/2018) and UNIFESP (7005180516). The left kidney was fixed with 4% buffered formaldehyde and embedded in paraffin. Sections from the kidney (5µm) were stained with Picrosirius Red for collagen fibers quantification. Sections from the kidney (4µm) were incubated with antibodies anti-Fibronectin (Abcam, ab45688) and anti-Collagen IV (Abcam, ab6586) and counterstained with hematoxylin. Digital images were taken (microscope Leica DM 1000) and analyzed using Image Pro-Plus 4.1 software. Results were presented as mean ± standard error of the mean. Statistical analysis was performed using two-way ANOVA and Tukey post-hoc test (P≤0.05).

Results:

The weight of the kidney was reduced in the sedentary group fed a high-fat diet compared to NS, NT and HFT groups. Retroperitoneal fat pad (HFS: 1.7 ± 0.1; HFT: 1.1 ± 0.3; NT: 0.3 ± 0.1 vs. NS: 0.6 ± 0.1 g) and epididymal fat pad (HFS: 1.4 ± 0.1; HFT: 0.8 ± 0.2; NT: 0.3 ± 0.1 vs. NS: 0.5 ± 0.1 g) were increased in the HFS group compared to NS group and AET prevented this increase. Immunohistochemistry showed that HFS group increased significantly renal fibronectin immunorepression (0.91 ± 0.01 %/area) compared to NS group (0.32 ± 0.01 %/area). AET was able to prevent this increase in HFT group (0.52 ± 0.11 %/area). Despite immunohistochemistry measurement revealed no difference in the renal collagen IV, histological analysis showed that HFS significantly increased the renal fibrillary collagen compared to NS group, and this increase was not observed in trained groups (HFS: 3.7 ± 0.4; HFT: 1.6 ± 0.2; NT: 1.0 ± 0.1 vs. NS: 1.1 ± 0.1 %/area).

Conclusion:

Our results suggest that high-fat diet intake since early period of life induces renal extracellular matrix accumulation and the AET was efficient to prevent this damage.

Financial support:

CAPES and Mackpesquisa

08.004 - DOXYCYCLINE ATTENUATES ISCHEMIA-REPERFUSION-INDUCED RENAL INJURY BY PREVENTING THE PROGRESSION OF ENDOPLASMIC RETICULUM STRESS. Cortes AL, Mello BP, Valença SS, Lindoso RS, Melo PA, Lara LS, - Farmacologia e Química Medicinal - UFRJ Instituto de Biofísica Carlos Chagas Filho - UFRJ

Introduction:

Doxycycline (Dc) is an antibiotic in the tetracycline family that has been noted for its pleiotropic action (antioxidant and metalloproteinase inhibitor, MMP) and its repositioning for the treatment of ischemic diseases. We demonstrated that treatment with 3 mg/Kg of Dc prevents the reduction of glomerular and tubular functions caused by bilateral renal ischemia-reperfusion (I/R). Stress of the endoplasmic reticulum (ER stress) is one of the major pathophysiological mechanisms associated with AKI.

Aim:

The main objective of this work was to determine the mechanism of action of Dc upon ER stress of activated RE during renal I/R.

Methods:

Male Wistar rats were divided into 4 groups (n = 5 / group, CEUA 133/18): (a) control (false operated); (b) I/R: ischemia was induced by applying a non-traumatic vascular clamp to the renal pedicles for 30 min, followed by reperfusion for 24 h, (c) I/R+Dc: two hours before ischemia, Dc (3 mg/Kg) was administered intraperitoneally and (d) Dc: control rats were treated with 3 mg/kg Dc. In addition, immortalized mesangial mouse cells (IMC) and inner medullary collecting duct cells (IMCD) were divided into the following groups: (a) control, (b) Hc/R: cells submitted to the process of chemical hypoxia and reperfusion (Hc/R), (c) Hc/R+Dc 1, 5 or 10: 1h prior to hypoxia the cells were treated with different Dc concentrations (1, 5 or 10 µM), (d) H/R: cells subjected to chamber hypoxia and reperfusion for 24 h (Hc/R), (E) H/R + Dc10: hypoxia immediately before the cells were treated with 10 uM Dc.

Results:

In the in vivo model, Dc treatment prevented the I/R- increase in protein content of MMPs 2 and 9, preserving renal morphology and decreasing fibronectin deposition and TGFβ1 immunostaining. In this model of injury induced by I/R, the activation of ER stress was characterized by increased expression of GRP78 (142%) (resident protein of ER, which is master regulator for ER stress), p-eIF2α (168%) and pro-apoptotic proteins: CHOP (100%), caspase-3 (144%) and caspase-12 (150%). Immunolocalization has shown that the proteins are mainly located in the glomeruli and distal tubules. Treatment with Dc prevented the increase of the protein content of these proteins. In the in vitro model, it was observed that Dc promotes increase in cell viability of IMCs and IMCD submitted to the process of chemical and oxygen depletion. IMCD cells subjected to oxygen depletion presented increase GRP78 expression (156%). We observed an increase in the expression of monomeric TGFβ1 (154%), HIF1α (142%) and pro-apoptotic protein caspase-12 (139%). Dc treatment prevented the increase of these proteins. Moreover, under this condition Dc increased the anti-apoptotic Bcl2 protein by 50%.

Conclusion:

These results suggest that Dc prevents AKI by attenuating ER stress and increasing renal cell viability. We propose that Dc interacts with GPR 78-modulated protein folding in ER, opening up new perspectives for the pharmacological treatment of AKI.

Financial support:

CNPq / FAPERJ

08.005 - SALT-INDUCIBLE KINASE (SIK) AS A PHARMACOLOGICAL TARGET OF SALT-SENSITIVE HYPERTENSION. Gomes DS, Visniauskas B, Prieto MC, Lara LS, - Programa de Pesquisa em Farmacologia e Inflamação - UFRJ Department of Physiology and Renal Hypertension Center of Excellence - TU

Introduction:

FeSBE Annual Meeting 2019

Poster Sessions and Abstracts

Salt-inducible kinase (SIK) is a serine/threonine kinase that acts as an intracellular Na⁺ sensor, related to tissue injury in pathological development by high salt intake, such as hypertension.

Aim:

In the present study we tested the hypothesis that SIK inhibition decreases blood pressure and renal function in a salt-sensitive hypertension model.

Methods:

Adult C57BL/6J mice (20-25g) were randomly submitted or not to intraperitoneal injection of SIK inhibitor (iSIK - YKL-05-099, 20 mg/Kg) associated to normal or high-sodium diet (4% NaCl): Normal Salt (NS), High Salt (HS), NS+iSIK and HS+iSIK (n=6/group; CEUA: 013/19). Systolic (SBP), diastolic (DBP), mean blood pressures (MBP), and heart rate (HR) were measured by radio telemetry method during 15 days. On days 9th and 14th, mice were allocated in metabolic cages to collect urine. At the end of the treatment, they were euthanized, blood and kidneys were collected to analyze renal function and to obtain renal cortex homogenate, respectively. The data was analyzed using Two-way ANOVA with Bonferroni's post-test. A value of P<0.05 was regarded as significant.

Results:

SIK activity in the kidney cortex was 7 x higher in HS group, and the treatment with iSIK blocked this effect. It was observed an increased in 20% of SBP at daytime (from 114±1 mmHg, NS to 136±1 mmHg, HS) and nighttime (from 127±3 mmHg, NS to 141±4 mmHg, HS) starting on the 5th day. The iSIK prevented salt-sensitive SBP increased. No significant changes were observed in DBP, MBP and HR. No differences were found in body weight, food intake, kidney indexes, plasma osmolality, Na⁺ and K⁺ plasma concentrations, proteinuria, and blood urea nitrogen (BUN) among the groups. On day 10th of treatment, water intake (13,51±1,8 vs. NS 7.31±0,7 ml) and urine volume (1,8±0,1 vs. NS 0,99±0,14 mL/12h) were high in HS group. Urinary excretion of Na⁺ was 4 x higher on groups HS (359±11 vs. NS 71,7±3,8 mmol/L) and HS+iSIK (311±15,8 vs. NS+iSIK 59±2,3 mmol/L) and urinary excretion of K⁺ were 50% lower (124±2,3 mmol/L NS vs 57±1,1 mmol/L HS; 127±4 mmol/L HS+iSIK vs. 54,7±0,2 mmol/L HS+iSIK). After 15 days of treatment, the iSIK prevented the increase in urine osmolality (40%) observed in HS group (1692±14 mOsm/Kg H₂O vs. 1104±34 mOsm/Kg H₂O HS+iSIK), but not prevented a decrease in urine creatinine levels (14±1,9 mg/dL vs. 14±1,7 mg/dL in HS+iSIK). The level of monocyte chemoattractant protein type 1 (MCP-1, an indicator of renal injury) was 30% lower in plasma of the animals treated with iSIK (58±7 pg/dL to NS+iSIK and 51±2 pg/dL to HS+iSIK vs 81±9 pg/dL NS and 79±7 pg/dL HS). In the kidney, iSIK blocked high salt diet-dependent macrophages infiltration and reactive oxygen species, and decreased TGF-β protein expression content by 33% (1,9±0 A.U. HS vs. 1,467±0,25 A.U. HS+iSIK).

Conclusion:

These data characterize the initial phase of the HS diet action due to the increase in PS, without modification of renal function. We conclude, in this phase, occurs the activation of an inflammatory mechanism associated with oxidative stress, which is sensitive to the inhibition of SIK in the kidney.

Financial support:

The Enhancement Career Award of the American Society of Physiology funded this work. FAPERJ and CAPES supported carrying out this work.

08.006 - CHARACTERIZATION OF THE ACUTE RENAL INJURY MODEL INDUCED BY BOTHROPS JARARACUSSU VENOM. ROMANELLI MA, Silva PAS, Melo PA, LARA LS, - Farmacologia e Química Medicinal - UFRJ

Introduction:

Snakebite accidents represent a serious public health problem in tropical regions due to their high incidence and associated morbidity and mortality. The Brazilian Ministry of Health predicts that occurs around 20,000 snakebites per year, being caused in the majority by snakes of the genus Bothrops. The clinical picture is pain, edema,

muscle injury, myonecrosis and systemic manifestations, such as acute kidney injury (AKI). The pathophysiology of AKI caused by ophidian accidents has not been fully elucidated.

Aim:

Therefore, the main objective of this work is to characterize the AKI model induced by administration of Bothrops jararacussu (Bj) venom by the intramuscular (im), intraperitoneal (ip) and intravenous (iv) routes.

Methods:

Male Wistar rats were randomly assigned to two groups were blood and urine were collected 24 or 72 h after Bj administration. In each group, the rats were randomly subdivided into 3 different routes of administration (n=8/group): (1) Bj-im: animals received 3.5 mg/kg Bj im; (2) Bj-ip: animals received 2,0 mg/kg Bj ip; (3) Bj-iv: animals received 0,6 mg/kg Bj iv. For each group there was a corresponding control group where saline 0.9% was administered (Ctrl-IM, Control-IP and Ctrl-IV). The data obtained were compared through the program GraphPad Prism 5.0. Statistical analysis was performed using the One-Way ANOVA and Tukey post-test, considering P<0.05.

Results:

We observed that after 24 h administration of Bj, independent of the route applied, the venom provoked blood urea nitrogen (BUN) accumulation, proteinuria and decreased plasma creatinine and urinary creatinine ratio (CrP/CrU) (increase in BUN: Bj-IM 40%, Bj-IP 10% and Bj-IV 23%; increase in proteinuria: Bj-IM 50%, Bj-IP 52% and Bj-IV 23% and decrease in CrP/CrU: Bj-IM 53%, Bj-IP 38% and Bj-IV 50%). Although water intake did not change in any kind of administration route, in the im venom administration there was an augmented urine volume, thus increasing the glomerular filtration rate (GFR). After 72 h of venom administration, most of the renal physiological parameters were attenuated (e.g. BUN and proteinuria). GFR remained low in the im and ip administration of the venom (70 and 43%, respectively), but was higher in the iv administration (75% of increase) due to augmented urine volume.

Conclusion:

The results obtained in this study allowed us to conclude that experimental intoxication with Bj venom (3.5 mg/kg) provoked AKI in the first 24 h of administration independent of the route of administration. This observation suggests that the impairment of kidney function is a consequence of the systemic action of the venom caused by the isolated or combined action of different ischemic or nephrotoxic mechanisms. Taken together, the results demonstrate that the administration of venom induces AKI, which is self-limited until 72 h. Because im route is similar to that occurs during the snakebites we suggested this route as the closest to the clinical cases.

Financial support:

CAPES, CNPq, FAPERJ

9 - Respiratory Biology and Diseases

09.001 - HYPEROXIA INDUCES ANTIOXIDANT ENZYMES EXPRESSION IN HIPPOCAMPUS OF BALB/C MICE. Batista BLV, Cunha RS, Aarestrup FM, Aarestrup BJV, Bezerra FS, Nagato AC, - Fisiologia - UFJF

Introduction:

Oxygen is a lipophilic molecule able to spread by any biological microenvironment and it is required clinically in supraphysiological concentration to reverse hypoxemia, especially in brain hypoxia. However, experimental evidences shown hyperoxic reperfusion after hypoxia promotes hippocampal neuronal death [Hazelton, 2010]. Hyperoxia is known for inducing oxidants enzymatic responses accelerating the reactive oxygen and nitric reactive species formation, causing redox imbalance and oxidative damage.

Aim:

Here we evaluated nitric oxide synthase (iNOS) expression in hippocampal tissue slices after hyperoxia.

Methods:

FeSBE Annual Meeting 2019 Poster Sessions and Abstracts

The study was approved by the Ethics Committee of Federal University of Ouro Preto (UFOP)-No.092/2012. Groups of female BALB/c mice (8 weeks old; 24.53±0.31g) were divided randomly in two experimental groups: control (Air room) - remained to air room and O₂ group was exposed to 100% oxygen in a chamber for 24h. Histopathological, histomorphometric, and stereologic analysis were performed in brain tissue sections stained with Hematoxylin and Eosin, Toluidine blue (Acidic Polysaccharides) and Ferric Hematoxylin (myelin). Immunohistochemical analysis for detection of iNOS expression in tissue paraffin section were performed through avidin-biotin peroxidase-anti-peroxidase complex method. All tissue sections were examined by light microscopy. The data were presented as the mean and standard error of the mean (SEM). Continuous data were analyzed by one-way ANOVA followed by the Student Newman Keuls post hoc test. Non continuous data were analyzed by Kruskal Wallis test followed by the Dunns post hoc test. The significance level was set at 5% (P < 0.05).

Results:

Hyperoxia increased iNOS expression in hippocampal tissue slices of BALB/c mice (p<0.05) when compared to control (Air room). The exposed to oxygen decreased cells number in O₂ group (p<0.001) when compared to control (Air room). Hyperoxia did not change the volume density of myelin and acidic polysaccharides.

Conclusion:

We suggest that hyperoxia-induced oxidants enzymatic responses is involved with the reduction of the cells number in hippocampal tissue slices of BALB/c mice, especially by over expression of iNOS.

Financial support:

This work was supported by grants from Rede Mineira de Bioterismo/FAPEMIG 31/11, TOXIFAR 26/11, and CNPq. ACN received a bursary from Coordenação de Aperfeiçoamento de Pessoal de Ensino Superior (CAPES). The authors would like to express their gratitude to the UFOP and this work was supported by the UFOP (# 23109.003267/2017-01 and # 23109.003268/2017-47) and CAPES [Bolsista CAPES - PVEX - Process # 88881.172437/2018-01] to FSB. AT credits CNPq for the fellowship of research productivity. FSB is doing a Post-Doctoral Fellow in the Interdepartmental Division of Critical Care Medicine, St. Michael's Hospital, University of Toronto, Toronto, ON, Canada.

09.002 - THERAPEUTIC POTENTIAL OF G. BRASILIENSIS IN A SMOKING MODEL: MORPHOLOGICAL, PHYSIOLOGICAL AND INFLAMMATORY PROFILES. Possebon L, Costa SS, Souza HR, Pilon MMI, Moreno AH, Oliani SM, Girol AP, - Biociências - UNESP Biociências - UNIFIPA Biociências - UNESP e UNIFIPA

Introduction:

Background: Smoking is associated with chronic obstructive pulmonary disease (COPD), with important respiratory alterations. Various inflammatory and systemic diseases may use medicinal herbs as treatment. Here, we emphasize *Garcinia brasiliensis* as a therapeutic alternative to the alterations caused by smoking.

Aim:

Objective: to analyze the *G. brasiliensis* alcoholic extract administration on morphological, physiological and inflammatory profiles in a COPD model.

Methods:

methods: Wistar rats (CEUA-UNIFIPA, number 06/17) were divided into three groups (n=7/group). The control group was exposed only to compressed air. The two other groups were exposed to 10 cigarettes/2x a day for 8 weeks. One of them was treated with *G. brasiliensis* leaves alcoholic extract, (exsicate deposited in the herbarium IRINA DELANOVA GEMTCHUJNICOV (BOTU) number:33511, bacupari), at 4% concentration. The treatment was performed by gavage (1ml), 3x/week. Physiological evaluations were performed: 1) weekly weighing; 2) blood pressure noninvasive measurements in the first and

last weeks of the exposure protocol, 3) plethysmography to study pulmonary volume, frequency and ventilation and 4) pulmonary measurements by X-ray images. After euthanasia, bronchoalveolar lavage (BAL) was obtained from the left lung, which was then macerated. The intact right lung was processed for the histopathological analysis. Levels of IL-1 β , IL-6, IL-10, TNF- α , and MCP-1 were quantified in the supernatant of the macerated lung and BAL by MAGPIX. The means±S.E.M were compared by one-way ANOVA for lung measurements obtained from radiographs, plethysmography, BAL quantification, and cytokine levels. ANOVA with repetitions was used for blood pressure and two-way ANOVA for weighing data. Bonferroni post-test was used in all analysis

Results:

Results: from the second week of experimental protocols weight gain was observed in both cigarette smoke-exposure groups, treated (380.2±35.81) or not (380.2±35.81), with the *G. brasiliensis* extract compared to controls (358.3±46.52). Arterial pressure was elevated in untreated animals (106.3±3.067; p<0.01) compared to control (90.60±0.2405) and treated (92.95±0.2207) groups. Radiographic images revealed right lung enlargement in untreated smoke-exposed rats (495.2±4.320) in relation to controls (430.6±19.78; p<0.01). Plethysmography showed increased pulmonary volume (9.054±0.8343; p<0.001), frequency (168.5±2.862; p<0.01) and ventilation (837.8±126.8; p<0.001) in the smoke-exposed animals compared to controls (volume:1.655±0.3934, frequency:151.4±4.307, ventilation:318.9±64.93), with reduction of these variables (p<0.001) in the smoke-exposed and treated animals (volume:1.735±0.1081; frequency:156.5±0.9899, ventilation:301.5±24.68). Histopathological studies indicated larger intra-alveolar spaces in the lungs of the untreated smoke-exposed rats. BAL analyses pointed increase of macrophages (11.14±2.348; p<0.05) and lymphocytes (47.61±2.942; p<0.01) compared to control. But *G. brasiliensis* treatment reduced the inflammatory cells into BAL (p<0.05) (macrophages:4.250±0.9805; lymphocytes:25.43±3.293). Higher levels of IL-1 β (555.7±39.21; p<0.001) TNF- α (3.837±0.2290; p<0.001) and MCP-1 (30.41±0.3131; p<0.05) were observed in BAL and lung supernatant of the untreated-smoke-exposed animals in relation to controls (IL-1 β :305.4±36.55; TNF- α :1.739±0.2542; MCP-1:25.22±1.000). Reduction of these cytokines occurred with *G. brasiliensis* treatment (IL-1 β :434.2±32.66; TNF- α :2.100±0.2253; MCP-1:27.00±1.665, p<0.001). Differently, decreased IL-10 levels were found in the lung supernatant of the untreated smoke-exposed group (p<0,001; 9.266±1.945) compared to the control group (31.12±3.112) but treatment increased the IL-10 levels (p<0.05; 22.32±4.144).

Conclusion:

Conclusion: administration of *G. brasiliensis* extract promoted important morphological, physiological and anti-inflammatory effects in animals exposed to cigarette smoke with interesting therapeutic perspectives.

Financial support:

CAPES and UNIFIPA

09.003 - EFFECTS OF SIGH DURING MECHANICAL VENTILATION IN HEALTHY WISTAR RATS. Souza ABF, Silva ACL, Matos NA, Cândido LS, Castro TF, Cangussú SD, Bezerra FS, - Departamento de Ciências Biológicas - UFOP

Introduction:

Mechanical Ventilation (MV) is an important tool used for the treatment of patients with acute or chronic respiratory failure, considered as a non-physiological resource and can cause metabolic disorders. However, in clinical practice, there are recruitment maneuvers, techniques as sighing, gradual inflation, variable ventilation recognized for their protective effect on the lungs.

Aim:

FeSBE Annual Meeting 2019 Poster Sessions and Abstracts

This study aimed to analyze the effects of sigh on lung oxidative stress in healthy adult Wistar rats submitted to MV.

Methods:

31 male Wistar rats were divided into four groups: control (CG), mechanical ventilation (MVG), mechanical ventilation set at 20 sighs/hour (MV20) and mechanical ventilation set at 40 sighs/hour (MV40). Animals from CG were maintained under spontaneous ventilation for 1h, and MVG, MV20, and MV40 were sedated, anesthetized, paralyzed and mechanically ventilated for 1h (Inspira Advanced Safety Ventilator, Harvard Apparatus) at a tidal volume of 7mL/kg in volume controlled ventilation; respiratory rate of 80 breaths/minute, and positive end-expiratory pressure (PEEP) of 3 cmH₂O. After ventilation, all animals were euthanized and bronchoalveolar lavage fluid (BALF), arterial blood and lungs were collected for further analysis. The Ethics Committee of the Federal University of Ouro Preto (UFOP) approved the experiments, according to the Protocol nº 2018/13. Statistical analyses were performed using GraphPad Prism, data were expressed as mean ± SEM or median, minimum and maximum value and p <0.05 was considered statistically significant.

Results:

In arterial blood at the end of mechanical ventilation, no changes were observed in O₂ saturation and blood pH between experimental groups. Animals from MV40 group presented higher partial pressure of oxygen (PO₂) (mmHg) (100.2 ± 3.62) and lower partial pressure of carbon dioxide (PCO₂) (mmHg) (28.68 ± 0.80) compared to CG (82.17 ± 4.15; 35.37 ± 2.31). The levels of bicarbonate (HCO₃) (mmol/L) in the MV20 group (18.10 ± 0.59) were lower compared to the CG (21.65 ± 1.55). The ratio between PO₂ and inspired a fraction of oxygen (PO₂/FIO₂) was higher in MVG (474.4 ± 18.70) and MV40 (479.2 ± 17.31) compared to CG (393.2 ± 19.87). The cell influx in BALF (x10⁵/mL) was higher in MVG (20.94 ± 1.51) compared to CG (13.75 ± 1.34). Analysis of thiobarbituric acid reactive substances (TBARS) (nmol/mg PTN) showed higher oxidation of lipids in MVG (1.69 ± 0.02) compared to CG (0.54 ± 0.15), MV20 (1.08 ± 0.14), MV40 (1.17 ± 0.18). Protein oxidation (nmol/mg PTN) was higher in the mechanical ventilation group (16.70 ± 2.71) when compared to MV40 (8.42 ± 1.44). The superoxide dismutase (SOD) activity (U/mg PTN) was higher in MVG (30.04 ± 1.70) when compared to CG (15.66 ± 2.59), MV20 (19.34 ± 1.47) and MV40 (16.42 ± 3.36). The catalase (CAT) activity (U / mg PTN) was also higher in MVG (2.27 ± 0.31) compared to CG (1.27 ± 0.19), MV20 (1.30 ± 0.17) and MV40 (1.17 ± 0.17).

Conclusion:

Our data suggest that use of the sigh plays a protective role in the lung decrease the oxidative damages and lung inflammation caused by MV.

Financial support:

CNPq, CAPES, FAPEMIG, UFOP and Nova Biomedical Corporation

09.004 - ACTION OF PIPERLONGUMINE IN A MODEL OF PULMONARY EXPOSURE TO CARCINOGEN BENZOPYRENE. Ashino TEB, Yoshikawa AH, Iyomasa MM, Possebon L, Costa SS, Silva JM, Girol AP, - Biologia - UNESP Biotécnicas - UNIFIPA

Introduction:

Air pollution and cigarette smoking are the major exposure sources to carcinogenic agents, such as polycyclic aromatic hydrocarbons. Benzopyrene is one of the main polycyclic aromatic hydrocarbons present in the environment, and is highly carcinogenic; therefore, it is used in experimental in vivo models. Studies have shown that anti-inflammatory drugs may reduce lung cancer incidence. The natural bioactive extracts (NBE), such as terpenes and flavonoids, stand out in this scenario because of their many properties, like inflammation reduction, immune system stimulation and modulation of detoxification enzymes. Among the NBE, we highlight the piperlongumine (PL), an alkaloid/amide of long pepper (Piper longum) which may be a possible preventive treatment for lung cancer.

Aim:

To study the effect of PL administration on a pulmonary carcinogenesis model. To evaluate the physiological, macroscopic, histopathological, immunohistochemical and biochemical aspects in control and benzopyrene-induced animals treated or not with PL.

Methods:

Balb/c mice were divided in 3 groups (n=10/group): control (sham, 10% DMSO); induced by benzopyrene (100 mg/kg in 10% DMSO) administered intraperitoneally (i.p.) and not treated (BaP); and induced by benzopyrene and treated with PL (2 mg/kg in 10% DMSO, i.p., BaP/PL) from the 8th week post induction onwards. The animals were daily weighed. Plethysmography (lung volume, frequency and ventilation) was performed at the last week of the protocol (12th week). After euthanasia, materials were collected and processed for the quantification of inflammatory cells in bronchoalveolar lavage (BAL), blood hemoglobin levels, lung histopathological analysis and immunohistochemical studies of anti-inflammatory protein annexin A1 (AnxA1), proinflammatory enzyme cyclooxygenase 2 (COX-2), anti-apoptotic protein Bcl-2 and nuclear transcription factor NFκB.

Results:

There was no difference in weight among groups. Lung volume (Sham 2,356±0,120; BaP 7,505±0,065; BaP/PL 2,411±0,194), respiratory rate (Sham 157,9±1,908; BaP 190,5±0,712; BaP/PL 154,5±1,274) and pulmonary ventilation (Sham 374,3±22,65; BaP 1439±7,976; BaP/PL 371,2±31,56) were elevated in BaP animals compared to Sham (p<0.001). A significant reduction of these pulmonary parameters was observed in PL-treated rats (p<0.001). Increased lymphocytes (25.92 ±2.46, p <0.001), monocytes (9.10±0.64, p<0.001) and neutrophils (6.50±0.29, p<0.001) occurred in BAL of BaP group compared to Sham (lymphocytes: 9.78 ± 1.28, monocytes: 3.75±0.94; neutrophils:0.60±0.40). But PL reduced the number of these cells (lymphocytes 16.57±2.44, p<0.05; monocytes 5.20±1.32, p<0, 05; neutrophils 4.2 ±0.75; p<0.05). Similarly, higher hemoglobin blood levels were found in BaP group (13.94±0.26; p<0.01) compared to Sham (12.19±0.36) with reduction in BaP/PL animals (11.47±0.68 p<0.01). PL treatment also preserved the pulmonary architecture compared to the untreated animals. Moreover, expressions of AnxA1 (142,4±7,220 p<0.01), COX-2 (152,6±3,711 p<0.001), Bcl-2 (157,9±6,608 p<0.01) and NFκB (164,2±4,548 p<0.001) were elevated in BaP group in relation to Sham (AnxA1 114,8±6,106; COX-2 123,6±2,606; Bcl-2 129,1±1,539; NFκB 134,7±3,310). The anti-inflammatory and protective effect of PL was observed by the significant reduction of COX-2 (136,7±5,754 p<0.05), Bcl-2 (133,5±5,428 p<0.01) and NFκB (120,7±4,532p <0.001) expressions and maintenance of AnxA1 high levels (143,7±4,027).

Conclusion:

These data show the potential of PL and open perspectives for new studies on the therapeutic application of PL in pulmonary carcinogenesis.

Financial support:

University Center Pe. Albino (UNIFIPA), Catanduva/SP

09.005 - HIGH TIDAL VOLUME INDUCES OXIDATIVE STRESS AND PULMONARY INFLAMMATION IN WISTAR RATS SUBMITTED TO MECHANICAL VENTILATION. Cândido LS, Matos NA, Castro TF, Paula LC, Chirico RN, Cangussú SD, Bezerra FS, - Departamento de Ciências Biológicas - UFOP

Introduction:

Mechanical ventilation (MV) is an essential strategy in the treatment of critical patients such as acute respiratory distress syndrome and aims to provide adequate gas exchange may exacerbate or initiate lung injury. However, the effects of the low and high tidal volume in healthy lungs must need to investigate.

Aim:

FeSBE Annual Meeting 2019

Poster Sessions and Abstracts

This study aimed to evaluate the effects of mechanical ventilation with different tidal volumes on redox imbalance and pulmonary inflammatory response in healthy rats.

Methods:

The Ethics Committee of the Federal University of Ouro Preto approved the experiments, according to the Protocol nº 2017/42. Male Wistar rats were divided into 4 groups: Control group (CG) exposed to ambient air and others rats were anesthetized, paralyzed, tracheotomized and then submitted to MV (Harvard Apparatus) with the following ventilatory parameters: VCV mode, low tidal volume 4 mL/kg (MV4) or 8 mL/kg (MV8) or high 12 mL/kg (MV12), PEEP of 0cmH₂O, Respiratory Rate: 70 bpm, I:E ratio of 1:2 and FiO₂ of 21%, during 1 hour. Throughout the experiment, ventilatory and hemodynamic parameters were monitored. After this, arterial blood, bronchoalveolar lavage fluid (BALF) and lung tissue were collected for analysis. Statistical analyzes were performed using GraphPad Prism software version 5.00. Data were expressed as mean ± SEM and p <0.05 were considered statistically significant.

Results:

In BALF, MV with high tidal volume increased neutrophils (x10³/mL) in the MV12 group (1.62±0.24) compared to CG (0.41±0.28), MV4 (0.82±0.14) and MV8 (0.73±0.13). We observed an increase of TNF-α (pg/ml) in MV12 (1572.0±50.71) compared to CG (1293.0±83.66) and MV4 (1263.0±38.35). The biochemical parameters showed an increase in the SOD activity (U/mg PTN) in MV12 (33.96±5.50) compared to CG (18.59±1.00) and MV4 (18.01±2.50), in relation to CAT (U/mg PTN) we also observed an increase in this activity in the MV12 (5.39±0.76) compared to CG (3.09±0.43). The damage in lung parenchyma was evaluated by carbonylated proteins (nmol/mgPtn) and TBARS (nM/mgptn), we observed an increase of TBARS in the MV12 (1.74±0.25) compared to CG (0.80±0.09), MV4 (0.71±0.18) and MV8 (0.71±0.05), as also increase of carbonylated protein in MV12 (17.69±1.40) compared to CG (6.41±0.77) and MV4 (6.68±0.83). The stereological analysis of the alveolar airspace volume density values (Vv [a]) and the volume densities of the alveolar septa (Vv [sa]) showed alterations in MV12 compared to CG and MV4. We observed an increase of Vv [a] in MV12 (60.12 [55.95-63.99]) compared to CG (36.56 [31.88-42.81]) and MV4 (40.18 [36.01-43.45]) and a decrease of Vv [sa] in MV12 (39.88 [36.01-44.05]) compared to CG (63.44 [56.88-68.13]) and MV4 (59.82 [56.55-63.99]). In the analysis of arterial blood gases, we observed that pCO₂ (mmHg) MV12 (17.27±1.26) was lower than CG (35.98±1.69), MV4 (64.16±1.67) and MV8 (31.56±2.06), about HCO₃ this parameter also lower in MV12 (13.08±0.29) compared to CG (22.77±1.06), MV4 (28.08±0.85) and MV8 (20.43±0.52). However, the pO₂ (mmHg) was lower in VM4 (50.98±2.45) compared to CG (72.73±6.74).

Conclusion:

Our present findings suggest that the effects of a low and intermediate tidal volume ventilation strategy can be protective and high tidal volume in healthy rats promoted lung inflammation, redox imbalance, leading tissue damage.

Financial support:

CNPq, CAPES, FAPEMIG, UFOP and Nova Biomedical Corporation.

10 - Neurobiology

10.001 - PROTEIN LEVELS OF APP IN PLATELETS OF SUBJECTS WITH ALZHEIMER'S DISEASE AND MILD COGNITIVE IMPAIRMENT. Cordeiro AMT, - Laboratório Neurociências - IPQ

Introduction:

Introduction: The clinical diagnosis of Alzheimer's disease (AD) is a probabilistic formulation that may lack accuracy particularly at early stages of the dementing process as Mild Cognitive Impairment, that are a continuum and noticeable deterioration in cognitive skills and memory, becoming a growing risk of progress to AD. Beta-amyloid

peptide (AB) accumulation is one of the hallmarks of Alzheimer's disease. It is well-known that the main mechanism of AB production is from abnormalities in amyloid-beta precursor protein (APP) metabolism. APP is an integral transmembrane protein widely expressed in neuronal and peripheral tissues. The enzymatic machinery needed to process APP in neurons is also present in platelets.

Aim:

Objective: The aim of the present study was to compare the protein level of the Amyloid Precursor Protein (APP) to discriminate cases of AD and MCI from controls.

Methods:

Methodology: The present study was conducted at the Laboratory of Neuroscience (LIM-27), Institute of Psychiatry, University of Sao Paulo, Brazil, according to the tenets of the Helsinki declaration. It was designed to include a cross-sectional assessment of the whole sample at baseline. The APP protein levels were measured in platelets from non-medicated older adults with AD (n=10), MCI (n=17) and healthy elders (n=12) by western blotting. The densitometries of 130kDa and 110kDa were used to estimate the levels of APP and APP -ratio. Each sample was analyzed in duplicate and for normalization of platelet assay values we used β-actin as loading (internal) control (IC). All statistical analyses were performed with the aid of the software Statistical Package for the Social Sciences (SPSS) - version 22. Differences in sociodemographic characteristics and platelets APP concentrations at baseline were analyzed by non-parametric tests (Kruskal-Wallis) among groups.

Results:

Results: There was no difference regarding gender distribution or age among the three groups (p=0.310 and p=0.088, respectively). We found a down expression of 110kDa-APP-fragment in AD compared to MCI and controls. In contrast, there was no difference nor in 130kDa-APP-fragment (p=0.212) either APPratio (p=0.736).

Conclusion:

Conclusion: Our findings indicate that 110kDa-APP-fragment is down regulated in AD and may be a marker of altered APP metabolism in platelets since MCI state when compared to controls.

Financial support:

CAPES

10.002 - KETAMINE PROMOTES AGGRESSION AND MEMORY DEFICITS WITHOUT ALTERING LOCOMOTION AND BRAIN ACETYLCHOLINESTERASE ACTIVITY IN ADULT ZEBRAFISH. Marion JC, Michelotti P, Franscescon F, Pereira ME, Rosemberg DB, - Bioquímica e Biologia Molecular - UFMS

Introduction:

Ketamine, a derivative of phencyclidine, is a potent non-competitive antagonist of N-methyl-D-aspartate (NMDA) receptors widely used in clinical and veterinary for anesthesia. At sub-anesthetic concentrations, ketamine causes analgesia. The administration of ketamine in experimental models are associated with changes in memory, anxiety, and depression-like behaviors. The zebrafish (*Danio rerio*) is an experimental model to assess various behavioral phenotypes due to its extensive behavioral repertoire, which has been characterized elsewhere.

Aim:

Considering the neurochemical effects of ketamine in the vertebrate brain as NMDA antagonist and a possible correlation with a modulatory role on cholinergic signaling, we hypothesize that ketamine modulates aggression, causes memory deficits and influences brain acetylcholinesterase activity. Thus, the main goal of this study was to investigate the acute effects of ketamine on aggressive behavior (using the mirror-induced aggression test), memory consolidation (using an inhibitory avoidance apparatus), and brain acetylcholinesterase activity in zebrafish.

Methods:

FeSBE Annual Meeting 2019

Poster Sessions and Abstracts

Animals were exposed to sub-anesthetic concentrations of ketamine (2, 20, and 40 mg/L) for 20 min. Then, aggressive behavior (n=12) was assessed in animals individually placed in an apparatus with an inclined mirror (22.5°) touching the tank wall. The number and duration of aggressive episodes were counted. Aggressive display was considered when fish swam directly to their own image reflected in the mirror. For memory assessment (n=21-22), ketamine exposure was performed immediately after training session, in which animals were individually placed in the white side of a black/white tank and received a mild electric shock (125 mA, 3 ± 0.2 V AC at 100 Hz frequency) for 5 s after entering in the black compartment. Animals were tested 24 h, except that no shock was given. Moreover, fish were placed in a novel tank to verify whether ketamine could affect locomotion (n=12). Results were expressed as means ± standard error of the mean (S.E.M.) and differences among control and ketamine groups were determined by one-way ANOVA followed by Student-Newman-Keuls multiple comparison test when appropriate. Non-parametric data (latency to enter the black compartment) were expressed median ± interquartile range. Latencies to enter the black side in training and test sessions (inhibitory avoidance protocol) were analyzed by Wilcoxon matched-pairs signed rank test. Results were considered significant when $p \leq 0.05$. All protocols were approved by the Ethics Commission on Animal use of the Federal University of Santa Maria (protocol number 6894010616).

Results:

Animals exposed to 40 mg/L ketamine did not show differences in the latency to enter the dark compartment between training and test sessions ($W = 107$, $p = 0,0635$), suggesting that ketamine impairs memory consolidation. Importantly, the respective treatment did not alter the locomotion. Moreover, zebrafish showed exacerbated aggression at 2 mg/L ketamine ($F(3,44) = 4.399$, $p = 0.0086$), while 20 and 40 mg/L reduced aggressive behaviors ($F(3,44) = 43.95$, $p < 0.0001$). No differences in brain acetylcholinesterase activity were detected among treatment groups.

Conclusion:

Overall, ketamine induces aggression and impairs memory consolidation in zebrafish. These data reinforce the use of this aquatic species as a promising tool to assess the neurobehavioral effects of sub-anesthetic concentrations of ketamine in a vertebrate model organism. Although more studies are needed to understand the mechanisms of action of ketamine in the zebrafish brain, our data, demonstrate a lack of association between changes in acetylcholinesterase activity with behavioral responses observed here.

Financial support:

CNPq, CAPES.

10.003 - LOW AND MODERATE INTENSITY EXERCISE ATTENUATES SPINAL CORD INFLAMMATORY AREAS IN A MURINE MODEL OF MULTIPLE SCLEROSIS. Leoni GH, Oliveira ARL, Bernardes D, - Programa de Pós-Graduação em Ciências Biomédicas - Centro Universitário da Fundação Hermínio Ometto. Laboratório de Regeneração Nervosa - LRN - UNICAMP.

Introduction:

Multiple sclerosis (MS) is an incurable disorder characterized by an autoimmune activation that targets myelin, an essential component of the central nervous system, which is responsible for the acceleration of the action potential propagation. Experimental autoimmune encephalomyelitis (EAE) is an animal model used to understand the disease as well as therapies associated mechanisms. Some recent data have provided useful information regarding a modulatory effect from regular physical exercise on the neuroinflammatory response of EAE mice. However, little is known about the best intensity of regular exercise that is necessary to provide such a benefit.

Aim:

Therefore, the present study investigated the effects of low, moderate and high intensity of treadmill exercise on clinical presentation and spinal cord inflammation in EAE animals.

Methods:

After the ethics committee approval (3844-1/2015), the Multidisciplinary Center for Biological Research (CEMIB/UNICAMP, Campinas, SP, Brazil) supplied the 22 female C57BL/6J mice (4–6 weeks old) used in the present study. The animals were maintained on a 12/12 h light/dark cycle and, were provided with food and water ad libitum. After a week of environment adaptation, 5 of these animal were kept on sedentary condition while the remainder 17 were forced to exercise in one of three different treadmill exercise intensity (low: 10.68 m/min [n=6]; moderate: 18.78m/min [n=6]; high: 26.8 m/min [n=5]). In all cases, exercise was performed for 1 hour a day, 5 days a week. After 5 weeks of physical exercise, all animals were immunized for EAE model by subcutaneous injection of an emulsion containing MOG35-55 peptide. Exercise protocols were maintained until 10 days post induction (dpi), completing 6 weeks. All animals were followed regarding the clinical presentation from induction day to 16 dpi when they were submitted to cardiac perfusion. The lumbosacral spinal cord of each animal was collected and prepared for paraffin embedding. At the micromorphology laboratory of the University Center of Hermínio Ometto Foundation – FHO, spinal cords were sectioned transversally and stained using hematoxylin and eosin (HE). Afterward, the images were captured and analyzed for the areas of the inflammatory infiltrate using the free Java image processing software ImageJ. The clinical score data as well the inflammatory infiltrate areas data were analyzed by Student t-test with significance level established at $P < 0.05$ using GraphPad Prism software.

Results:

The clinical presentation of the disease was not different among the groups (EAE: 2.80 ± 0.20 ; EAE-Low: 2.75 ± 0.25 ; EAE-Moderate: 3.42 ± 0.16 ; EAE-High: 3.20 ± 0.20 ; $P > 0.05$). However, low and moderate intensity exercises were effective in to promote reduction of the percentage of inflammatory infiltrate areas in the lumbosacral spinal cords from EAE animals (EAE: $16.30 \pm 1.52\%$; EAE-Low: $9.21 \pm 2.10\%$ with $P < 0.05$ vs EAE; EAE-Moderate: $10.76 \pm 1.18\%$ with $P < 0.05$ vs EAE and; EAE-High: $9.14 \pm 4.33\%$ with $P > 0.05$ vs EAE).

Conclusion:

Our data show that low and moderate intensity exercises, both performed for 1 hour a day, 5 days a week, by 6 weeks, were effective in to reduce the percentage of inflammatory infiltrate areas in the lumbosacral spinal cords from EAE animals.

Financial support:

FAPESP; CNPq; PIC-FHO

10.004 - HISTOQUÍMICA PARA NADPH DIAFORASE E ATIVAÇÃO ASTROCÍTICA NO CÓRTEX VISUAL DE RATOS APÓS INTOXICAÇÃO POR METILMERCÚRIO. Freire MAM, Gomes-Leal W, Lima RR, Pereira A, - Faculdade Nova Esperança de Mossoró - Universidade do Estado do Rio Grande do Norte Instituto de Ciências Biológicas - Universidade Federal do Pará Instituto de Tecnologia - Universidade Federal do Pará

Introduction:

O mercúrio (Hg) é um elemento que oferece grande risco à saúde humana, sendo ainda empregado na mineração de ouro artesanal ao redor do mundo. O metilmercúrio (MeHg), sua forma orgânica, é produzido ambientalmente pela biometilação do mercúrio inorgânico presente em sedimentos aquáticos, levando à sua acumulação na cadeia alimentar. O Sistema Nervoso Central (SNC), devido a sua alta taxa metabólica, é um dos principais alvos da ação do Hg.

Aim:

No presente estudo, investigamos o impacto da intoxicação crônica por MeHg sobre a enzima NADPH diaforase (NADPH-d) e na ativação de astrócitos no córtex visual do rato.

Methods:

FeSBE Annual Meeting 2019

Poster Sessions and Abstracts

Ratos Wistar adultos (210±15g, n=16), foram divididos em dois grupos. Os animais tratados (n = 8) foram intoxicados oralmente por gavagem com cloreto de MeHg (diluído em óleo de girassol) a uma taxa de 0,04 mg/kg/dia durante 45 dias. O grupo controle (n = 8) recebeu apenas o veículo, pelo mesmo esquema de tratamento (óleo de girassol, no mesmo volume administrado ao grupo MeHg) (ID # BIO 225-14-CEPAE-UFPA). Após perfusão, o córtex visual foi testado para medição dos níveis de Hg, histoquímica para NADPH-d e imunohistoquímica para astrócitos (GFAP).

Results:

A intoxicação crônica pelo MeHg promoveu um depósito significativo de Hg no córtex visual (0,0437 ± 0,002795 µg/g) quando comparado ao grupo controle (0,0018 ± 0,0002117 µg/g; ***p<0,0001, teste t de Student), associado a uma redução da reatividade enzimática no neurópila reativa a NADPH-d em animais intoxicados quando comparados aos controles (intoxicados: 0,604 ± 0,0267; controles: 0,471 ± 0,0088; **p<0,01, teste t de Student). A análise morfométrica revelou que os neurônios reativos a NADPH-d foram poupados da ação lesiva do MeHg (área de corpo celular - controle: 255,43 ± 10,10 µm²; intoxicado: 249,98 ± 9,92 µm², p>0,05; área do campo dendrítico - controle: 26,99 ± 1,001 x 10³ µm²; intoxicado: 28,33 ± 0,97 x 10³ µm², p>0,05; dimensão fractal - controle: 1,204; intoxicado: 1,276, p>0,05; teste t de Student para todas as comparações). Animais intoxicados apresentaram ativação astrocítica em relação ao grupo controle.

Conclusion:

Tanto a síntese quanto o transporte da enzima NADPH-d podem ser prejudicados após intoxicação crônica por MeHg, o que pode estar relacionado a distúrbios metabólicos associados à ação lesiva do Hg no SNC. A resistência relativa dos neurônios NADPH-d reativos à intoxicação crônica por MeHg pode estar associada a um metabolismo não usual dessas células ou a um papel protetor do óxido nítrico, salvaguardando este grupo celular dos efeitos deletérios do Hg.

Financial support:

CNPq, FAPESPA, PROPESP (UFPA)

10.005 - THE ROLE OF ASTROCYTES IN DEEP BRAIN STIMULATION FOR PARKINSON'S DISEASE: AN IN VITRO AND IN VIVO APPROACH. Campos ACP, Kikuchi DS, Paschoa AFN, Lassengè B, Kuroki MA, Fonoff ET, Griendling KK, Hamani C, Hernandez MS, Pagano RL, - Division of Neuroscience - Hospital Sírio Libanês Division of Cardiology - Emory University Division of Functional Neurosurgery - University of São Paulo Division of Neurosurgery - Sunnybrook Health Sciences Centre

Introduction:

The underlying mechanisms of high frequency stimulation (HFS), as used in deep brain stimulation (DBS), remain largely unknown, especially on control of inflammatory response. Reactive astrocytes displaying pro-inflammatory (A1 subtype) may oscillate to neuroprotective/anti-inflammatory (A2 subtype) phenotypes.

Aim:

Our aim was to investigate the anti-inflammatory mechanisms of DBS/HFS in a rodent model of Parkinson's disease and in cultured astrocytes.

Methods:

Male Wistar rats injected with 6-hydroxydopamine (6-OHDA) or saline in the striatum were implanted with stainless steel electrodes in the subthalamic nucleus (STN). Controls had no electrodes implanted. Seven days later, animals were divided in: saline, 6-OHDA, 6-OHDA + DBS OFF and 6-OHDA + DBS ON. DBS ON animals were stimulated for 5 days during 2 h (130 Hz, 60 µs, 0,1 mA) and then, submitted to the bar test. GFAP immunostaining and cytokines expression were evaluated in the globus pallidus (GP) (CEUA P2016-04). In vitro, cultured astrocytes were stimulated with HFS for 6 h, and then activated with TNF-α in the last 1 h (for IL-6 and MCP-1 expression) or 15 min (for NFκ-B activation by IκB-α degradation and p65 nuclear translocation). In vitro conditions were as follows: no TNF-α, TNF-α + HFS OFF and TNF-α + HFS ON.

Statically analyses were performed using analysis of variance and the significance was defined as p ≤ 0.05.

Results:

The DBS-treated animals presented less immobility in the bar (n = 8 per group; 7.5 ± 4.3 of DBS ON to 38.5 ± 4.5 of 6-OHDA, p < 0.0001). Six-OHDA animals showed increase of GFAP in the GP (n = 4 per group; 99.8 ± 10.3 of 6-OHDA to 38 ± 9.1 of saline, p < 0.001), which was partially decreased by DBS (70.5 ± 6.2 of DBS ON to 99.75 ± 10.3 of 6-OHDA, p < 0.01). Despite the astrocytic activation, DBS ON decreased IL-1β (n = 4 per group; 13 ± 2.2 of DBS ON to 29 ± 15.8 of 6-OHDA, p < 0.05), IL-10 (n = 4 per group; 7.2 ± 0.6 of DBS ON to 36.8±9 of 6-OHDA, p < 0.001) and IFN-γ (n = 4 per group; 4.5 ± 3.4 of DBS ON to 650.6 ± 227.9 of 6-OHDA, p < 0.001) expression in the GP. In vitro model (n = 5 independent experiments per group), HFS ON astrocytes showed decreased MCP-1 expression in both cell lysate (143.2 ± 37.9 of HFS ON to 369.4 ± 63.7 of TNF-α, p < 0.001) and supernatant (52.2 ± 4.0 of HFS ON to 88.2 ± 7.7 of TNF-α, p < 0.01), together with the prevention of IκB-α degradation (102.6 ± 30.3 of HFS ON to 38.4 ± 8.6 of TNF-α, p < 0.05) and p65 translocation into the nuclear fraction (59.1 ± 31.6 of HFS ON to 174.2 ± 39.7 of TNF-α, p < 0.05) induced by TNF-α.

Conclusion:

We suggest that DBS/HFS can inhibit the A1-inflammatory pattern of astrocytes which inhibits M1 microglia attraction by inhibiting MCP-1 reflecting in the attenuation of the INF-γ/IL-10 disbalance. Suggesting an anti-inflammatory action of DBS/HFS.

Financial support:

FAPESP 2016/07168-2; FAPESP 2017/14020-4; AHA 17sdg33410777

10.006 - MOLECULAR EVALUATION OF NEUROPROTECTION AFTER TREATMENT OF MICE WITH MICRODOSING LITHIUM AND SUBMISSION TO ENRICHED ENVIRONMENT. Malerba H, Ruiz A, Buck H, Viel T - Pharmacology - USP Department of Physiological Sciences - FCMSCSP Laboratory of Biogerontology - USP

Introduction:

With increase in longevity, there is also increase in chronic diseases sometimes with debilitating conditions. Lately our research team have been showing the benefits of enriched environment and microdosing lithium for keeping memory of mice and human beings, which can lead to healthspan. In a previous work it was shown that combination of these strategies promoted better memory and reduction in anxiety behavior in senescence-associated mice prone (SAMP-8).

Aim:

In this way, the aim of this study was to verify the effectiveness of microdosing lithium combined or not with enriched environment for neuroprotection of SAMP-8.

Methods:

Male SAMP-8, 2 months old were divided into four groups: SAMP-8 (no treatment), Lithium (Li: Li₂CO₃, 0.25mg/kg, p.o.), Enriched Environment (EE: change of objects in cage 2-3 times a week) and Li+EE (combined strategies). Senescence-associated mice resistant (SAMR-1) were used as controls. When animals were 10 months old, they were anesthetized and killed by decapitation. The brain was removed and freeze-dried. Hippocampus samples were obtained in a cryostat (20 µm, -21°C) and submitted to immunofluorescence for evaluation of neuronal density (using NeuN antibody), density of amyloid plaques (with tioflavine-T labelling) and neurodegeneration (with fluorojade C labelling). Density of synaptophysin was assessed by western-blotting. Data were expressed as means ± SEM and analyzed by one-way ANOVA followed by Bonferroni's test. Ethical committee approved number ICB/USP: 949/2018.

Results:

When compared to SAMR-1, SAMP-8 showed reduced density of neurons in dentate gyrus (DG, 69.84%, p<0.001), CA1 (49.67%, p<0.05) and CA3 (57.60%, p<0,0001). Also, an increase in neurodegeneration in the three areas was also observed (60.98%, p<0.01; 42.52%, p<0.01;

FeSBE Annual Meeting 2019

Poster Sessions and Abstracts

59.88%, $p < 0.01$, respectively). SAMP-8 also presented increased density of senile plaques in DG, CA1 and CA3 (74.60%, 94.10% and 94.73%, respectively, $p < 0.05$) and decreased density of synaptophysin (58.65%, $p < 0.001$). The use of microdosing lithium, enriched environment or both strategies were effective in restore the density of neurons and synaptophysin and decrease neurodegeneration, but the effects of the combined strategies were more evident. In this way, when compared to untreated SAMP-8 mice, Li+EE group presented an increase of 69.33% ($p < 0.001$) in the neuronal density in GD, as well as 81.69% decrease in neurodegeneration ($p < 0.05$). In CA1 area an increase of 50.99% ($p < 0.01$) in neuronal density was observed as well as a decrease of 83.29% ($p < 0.01$) in neurodegeneration. In CA3, an increase of 60.85% ($p < 0.001$) in neuronal density and a decrease of 83.4% ($p < 0.001$) in neurodegeneration were also observed. Combined strategies also reduced in 92.06% and 98.57% ($p < 0.0001$) the density of senile plaques in GD and CA1. Li+EE group also presented an increase of 43.64% ($p < 0.001$) in the density of synaptophysin.

Conclusion:

SAMP-8 mice is a model of accelerated aging and Alzheimer's disease and showed, at 10 months of age, a decrease in neuronal density. In the present work it was possible to conclude that combined strategies are significantly effective in maintaining neuroprotection and integrity of synapses when applied along the aging process. These data corroborate previous works showing that multiple strategies are effective to promote brain resilience and healthy aging.

Financial support:

CAPES- Coordenação de Aperfeiçoamento de Pessoal de Nível Superior, FAPESP- Fundação de Amparo a Pesquisa do Estado de São Paulo

10.007 - SENESCENCE-ACCELERATED MICE PRESENTED REDUCTION IN LONG-TERM POTENTIATION MARKERS AND NEUROPROTECTIVE MECHANISMS RELATED TO THE A7 NICOTINIC CHOLINERGIC RECEPTOR. Pereira AAR, Abrão GS, Malerba HN, Toricelli M, Buck HS, Viel TA, - Farmacologia - USP Ciências fisiológicas - FCMSCSP

Introduction:

The aging process is a relevant area for research, once it is frequently followed by debilitating conditions as Alzheimer's disease. Memory formation and keeping is subjected to modulation of many neurotransmitter systems, including the cholinergic system. It is already known that activation of $\alpha 7$ nicotinic cholinergic receptors (nAChR) leads to neuroprotection mediated by PI3k-Akt-BDNF pathway, resulting in neuronal plasticity and cellular resilience. In previous work it was shown that female senescent-accelerated mice prone (SAMP-8, a model for Alzheimer's disease) presented reduction in spatial and aversive-related memories, when compared to their age-matched control, senescence-accelerated mice resistant (SAMR-1).

Aim:

The aim of this work was to evaluate if there were changes in the levels of proteins involved in long-term potentiation (LTP) and in the $\alpha 7$ nAChR neuroprotective signalling that are involved in the modulation of memory in hippocampal samples from old SAMP-8.

Methods:

Ten months old, female, SAMP-8 were anesthetized and the brains were extracted and immediately freeze-dried. Under ice-cold saline (0.9%), the hippocampus was isolated and homogenized in lysis buffer (50 mM Tris-HCl buffer, pH 7.4, containing 0.1% Triton X-100, 4 mM EGTA, 10 mM EDTA and a tablet of proteases and phosphatases inhibitors). The same protocol was applied to ten months old, female, SAMR-1 hippocampus (control group). The density of $\alpha 7$ nAChR, Akt, phosphoAkt, NMDA receptor, PSD-95 and synaptophysin were evaluated by western-blotting. The relationship of phosphoAkt/Akt was used to estimate the activity of the enzyme. The density of BDNF was verified using an ELISA commercial kit. Data were analyzed with Student-t test and only p values < 0.05 were considered statistically

significant. Seven to eight animals were used in each group. Ethical committee approved number FCMSCSP: 12/2016.

Results:

It was observed that hippocampal samples obtained from SAMP-8 presented significant reduction of 60.0% in the density of NMDA receptor, 45.0% in the density of NMDA anchoring protein PSD-95 and reduction of 21.0% in synaptophysin, when compared to SAMR-1 (1.17 ± 0.66 A.U., 1.08 ± 0.19 A.U. and 1.03 ± 0.19 A.U., respectively). This suggests dysfunction in LTP mechanism and synapse stability. In addition, a significant decrease of 33.5% in $\alpha 7$ nAChR and 20.0% reduction in phosphoAkt/Akt relationship was verified, when compared to control animals (1.17 ± 0.26 A.U. and 1.09 ± 0.07 A.U., respectively), suggesting a down-regulation of the neuroprotective pathway related to $\alpha 7$ receptors, although no significant changes in BDNF density was verified between both groups.

Conclusion:

It is suggested that the reduction of proteins related to LTP and synaptic structure may be the causal factors of the intracellular signaling impairment that could result in the memory disruption previously observed in SAMP-8, when compared to SAMR-1. Also, it is suggested that the neuroprotective pathway related to the $\alpha 7$ nAChR is also impaired, contributing to the observed behavioral condition.

Financial support:

FAPESP and CAPES

10.008 - NEUROPROTECTIVE EFFECTS OF KININ B2 RECEPTOR IN ORGANOTYPIC HIPPOCAMPAL CULTURES OF MIDDLE-AGED MICE. Toricelli MP, Evangelista SR, Oliveira LR, Viel TA, Buck SH, - Fisiologia - FCMSCSP EACH - USP

Introduction:

Aging is a multifactorial phenomenon that results in several changes at cellular and molecular levels and is considered the main risk factor for some neurodegenerative diseases. Several evidences show the participation of the kallikrein kinin system in neurodegeneration and this system has been associated with inflammation and immunogenic responses in the central and peripheral systems by the activation of B1 and B2 receptors. Previous work of our group suggested that bradykinin and the B2 receptor played a possible role in neuroprotection.

Aim:

The objective of this study was to evaluate the participation of B2 receptors in cell viability, neuroinflammatory response and neuroplasticity in organotypic hippocampal cultures of 6 and 12-month-old mice.

Methods:

Eighteen male C57Bl/6 mice (6- and 12-month-old; $n = 9$ per age) were obtained from the FCMSCSP Animal Facilities, Sao Paulo, Brazil. The experimental protocols were approved by the Animal Ethics Committee from Santa Casa de Sao Paulo School of Medical Sciences, Nº. 003/18. Slices were treated with 300pM of bradykinin (BK) or 300pM of BK plus 200pM of B1 antagonist (BK+AntB1) (AntB1: [desArg10]-Hoe140) (3-4hydroxyphenyl-propionyl-des-Arg9-D_Arg [Hyp3, Thi5, D-Tic7, Oic8]_BK). Cell death was analyzed by propidium iodide staining. Protein expression was analyzed by Western Blotting assay. The inflammatory profile was quantified by Magnetic Luminex® Assay (R&D System. S100b and BDNF analysis by Elisa).

Results:

In the dentate gyrus, where it was observed greater cellular loss when compared to the other hippocampal areas, BK significantly reduced cell death in both the 6- and 12-OHC (30.1%, $p < 0.01$ and 42.5%, $p < 0.001$, respectively). In the samples from 6-month-old mice, incubation with BK or BK+AntB1 significantly decreased the density of NeuN in hippocampal cells (by 24.8% and 71.6% respectively, $p < 0.0001$). However, in the 12-month-old samples the effect was the opposite, as BK and BK+AntB1 significantly increased the neuronal density 1.0 fold ($p < 0.01$) and 1.2 fold ($p < 0.0001$). It was observed that

FeSBE Annual Meeting 2019 Poster Sessions and Abstracts

activation of the B2 receptor by bradykinin decreased the inflammatory response in 12 months old slices. Conversely, there was an increase in the inflammatory response in the six-months old slices. The untreated 6-OHC show higher levels of BDNF than 12-OHC (2-fold; $p < 0.001$). In samples from 6-OHC treated with BK and BK+AntB1 a greater cell damage was observed when compared to the control group (55.5%, $p < 0.01$ and 98%, $p < 0.0001$, respectively). However, in untreated 12-OHC the levels of cell damage are three-fold higher in relation to untreated 6-OHC, as expected. Interestingly, treatments with BK and BK + AntB1 were able to significantly decrease S100b release in 12-OHC (16%, $p < 0.05$ and 37.7% $p < 0.001$), indicating that the KKS confers a neuroprotective role only in middle-aged animals where a neuroinflammatory process is already present. Bradykinin or Bk+AntB1 do not alter BDNF levels in 6-OHC. However, BDNF levels in 12-OHC treated with BK increased 45.8% ($p < 0.05$).

Conclusion:

This data suggests that the function of the kinin B2 receptor in the hippocampus is modulated by age, providing neuroprotective action in old age.

Financial support:

FAPESP (2013/13656-1, 2016/07115-6, 2017/21655-6), CNPq (303283/2014-9, 425838/2016-1, 307252/2017-5), CAPES (086/2013, 005/17) and FAP-FCMSCSP (010/2018).

10.009 - LOW LITHIUM DOSAGE DECREASED SENESCENCE-ASSOCIATED SECRETED PHENOTYPES (SASPs) IN HUMAN iPSCS-DERIVED ASTROCYTES. Maia J, Chinta S, Rane A, Chamoli M, Andersen JK, Viel T, - Sem departamento - The Buck Institute for Research on Aging Gerontologia - USP

Introduction:

Cellular senescence is a process that causes growth arrest and the release of SASPs, characterized by chemokines, cytokines, cell growth factors and metalloproteases secretion and also the increase in senescence-associated beta-galactosidase (SA-beta-gal) activity, leading to a tissue condition that may precipitate cancers and neurodegenerative processes. In the last few years our research group showed that lithium carbonate (Li2CO3) at microdose levels was able to stabilize memory and change neuropathological characteristics of Alzheimer's disease (AD).

Aim:

The aim of this work was to evaluate the effects of low lithium treatment for the release of SASPs in human induced pluripotent stem cells (iPSCs)-derived astrocytes.

Methods:

Human iPSCs-derived astrocytes, donated by a young human with no previous conditions, were bought from CDI Company (Novato, CA). Cells were plated in 1% Matrigel and maintained in DMEM buffer containing 10% fetal bovine serum (FBS), 1% N-2 supplement and 2% penicillin-streptomycin. After 90% confluence, cells were treated with 2.5 μ M, 10.0 μ M and 25.0 μ M Li2CO3 for 24 hours. Culture media was changed for DMEM buffer containing 1% FBS to induce the release of SASPs. After more 24 hours, the media and cells were collected and frozen. IL-6 and IL-8 were analyzed in conditioned media with ELISA kits (R&D technologies). SA-beta-gal activity was analyzed using a staining solution containing X-gal (Biocompare) and positive (blue) cells were expressed as a percentage of total cell number. RNA was extracted from cells and qPCR for the SASPs IL-1 α , p16 and p21 was performed. Data are related to three biological replicates and were analyzed using one-way ANOVA followed by Dunnett test.

Results:

It was observed that iPSCs-derived astrocytes showed detected levels of IL-6 and IL-8, which were considered 100% labeling. Treatment with 2.5 μ M and 10 μ M Li2CO3 promoted a significant decrease of 57.6% and 47.5% ($p < 0.05$) in the release of IL-6 and 54.2% and 49.6% ($p < 0.05$) in the release of IL-8. Incubation of 25 μ M Li2CO3 did not change the

release of both cytokines. Incubation of astrocytes with 2.5 μ M and 10 μ M Li2CO3 also significantly decreased the activity of SA- β -gal in 34.7% ($p < 0.001$) and 27.9% ($p < 0.01$), when compared to untreated cells. qPCR data for SASPs indicated no statistical difference concerning IL-1 α genes. However, a significant decrease of 29.6% ($p < 0.05$) was observed in gene expression of p-16 with incubation of 2.5 μ M Li2CO3. Besides 2.5 μ M and 25 μ M Li2CO3 also promoted significant decrease of 21.5% and 18.4%, respectively ($p < 0.05$), when compared to control cells. The lack of effects with the highest concentration is still under investigation.

Conclusion:

It is already known that senescent cells accumulate along aging and are able to cause or intensify age-related diseases that can be related to degeneration or hyperplasia. Astrocytes derived from a young woman iPSCs also showed some of the SASP factors by themselves and microdose lithium was efficient in reduce them with acute treatment, suggesting that microdose lithium could protect cells from senescence and development of aging-related conditions. This was the first time that acute effects of microdose lithium was registered.

Financial support:

FAPESP 2018/05288-6

10.010 - THE ROLE OF GLIAL CELLS IN ACTIVE AVOIDANCE TEST. Antunes GF, Venetucci F, Kuroki MA, Santos LCT, Campos ACP, Seno MDJ, Oliveira CC, Pagano RL, Martinez RCR, - Division of Neuroscience - Sirio Libanes Hospital

Introduction:

Impairments in learning, memory and cognitive functions have been suggested to be mediated by inflammatory response, which could be mostly attributed to glial cells. In the two-way active avoidance test, two distinct subpopulations are identified based on the number of avoidance responses: good and poor performers.

Aim:

The goal of our project was to investigate the correlation between glial activation, cytokine release and avoidance response with the hypothesis that there is an inflammatory profile in the poor performers.

Methods:

The expression of plasma cytokines, such as TNF-alpha, interleukin (IL)-1 beta, IL-6, IL-10, IL-17, cytokines neutrophil chemo attractants (CINC)-1 were evaluated by ELISA comparing control, poor and good performers, in the prefrontal cortex, hippocampus and amygdala. The data was analyzed by One Way ANOVA, followed when appropriated by Newman-Keuls post hoc test.

Results:

Our data showed that in the prefrontal cortex there was a reduction in the levels of IL-1 beta (control 152.05 \pm 5.29, poor 130.05 \pm 5.60, good 129.73 \pm 4.17-F(2.45)=3.58; $P < 0.05$), TNF-alfa (control 170.84 \pm 12.01, poor 108.07 \pm 3.34, good 99.76 \pm 6.31-F(2.45)=26.48; $P < 0.001$) and CINC-1 (control 61.18 \pm 2.52, poor 40.05 \pm 1.58, good 42.68 \pm 2.70-F(2.45)=17.48; $P < 0.001$) in the good and poor performers in comparison with control animals. The good performers showed higher levels of IL-6 (control 833.56 \pm 29.07, poor 790.65 \pm 32.05, good 1090.77 \pm 49.37-F(2.45)=17.86; $P < 0.001$), in comparison with the other groups. The poor performers showed reduction in levels of IL-10 (control 220.72 \pm 7.47, poor 188.82 \pm 10.49, good 249.49 \pm 11.02-F(2.45)=8.89; $P < 0.001$) in comparison with the other groups. The good performers showed higher levels of IL-17 in comparison with poor performers (control 137.38 \pm 12.90, poor 122.03 \pm 7.00, good 160.03 \pm 11.10-F(2.45)=3.90; $P < 0.05$). In the hippocampus, there was no statistical difference among the groups considering the levels of IL-1 beta (control 136.89 \pm 8.51, poor 122.80 \pm 4.84, good 143.87 \pm 6.33-F(2.45)=3.23; $P > 0.05$); TNF-alfa (control 176.21 \pm 12.14, poor 149.61 \pm 7.90, good 169.81 \pm 8.83-F(2.45)=2.39; $P > 0.05$); CINC-1 (control 66.30 \pm 3.42, poor 59.86 \pm 3.13, good 64.81 \pm 3.61-F(2.45)=1.04; $P > 0.05$); IL-6 (control 1269.01 \pm 83.37, poor 1131.11 \pm 95.23, good 1294.23 \pm 59.21-F(2.45)=1.06; $P > 0.05$); IL-10 (control 220.78 \pm 6.74, poor 205.11 \pm 11.29,

FeSBE Annual Meeting 2019

Poster Sessions and Abstracts

good 231.30±7.49-F(2.45)=1.88; P>0.05) and IL-17 (control 178.72±13.49, poor 156.26±9.79, good 191.53±10.70-F(2.45)=2.55; P>0.05). In the amygdala, good performers showed higher levels of IL-1beta (control 78.93±4.85, poor 100.89±2.98, good 72.46±5.19-F(2.45)=14.99; P<0.05); TNF-alfa (control 73.19±8.07, poor 111.81±5.49, good 65.76±8.20-F(2.45)=14.00; P<0.05) in comparison with poor performers group. There was no statistical differences considering the levels of CINC-1 (control 37.18±3.53, poor 30.51±2.24, good 31.59±2.49-F(2.45)=1.63; P>0.05); IL-6 (control 621.55±34.93, poor 559.86±38.48, good 573.71±28.35-F(2.45)=0.74; P>0.05); IL-10 (control 258.45±17.78, poor 255.78±8.83, good 266.90±14.51-F(2.45)=0.16; P>0.05) and IL-17 (control 88.50±5.90, poor 95.18±2.93, good 73.99±10.80-F(2.45)=3.04; P>0.05).

Conclusion:

Our findings highlight the pre-frontal cortex as a mediator of stress response and an increase of anti-inflammatory cytokines IL-1beta and TNF-alfa on amygdala suggesting alteration of the nervous system associated with impairment of learning and memory.

Financial support:

Hospital Sírio Libanês e CAPES

10.011 - VDACC1 INHIBITION PROTECTS SPINAL CORD FROM DEMYELINATION AND RESTORE LOCOMOTOR FUNCTION AFTER INJURY. Morena BC, Correia FF, Paschon V, Santos GB, Cristante AF, Kihara AH, - Núcleo de Cognição e Sistemas Complexos - UFABC Instituto de Ortopedia e Traumatologia - FMUSP

Introduction:

Paraplegia is a debilitating condition caused by spinal cord injury (SCI), a central nervous system organ responsible for motor and sensory functions. After the primary insult, several processes are activated in an attempt to maintain homeostasis, and some of them may be harmful to neuronal regeneration, such as glial scar formation, inflammation, and increased calcium concentration. The voltage-dependent anion channel 1 (VDACC1) is mainly present in the mitochondrial membrane, with an important role on of apoptosis intrinsic pathway. This protein has an N-terminal portion that externalizes when the formation of oligomers occurs during apoptosis, being fundamental for the release of cytochrome C and inducing apoptosis inducing factor.

Aim:

The aim of this project was to evaluate the importance of VDACC1 in the neuronal tissue damage, death spread and locomotor recovery after SCI in rats.

Methods:

Male Wistar rats with 60 postnatal days were subjected to spinal cord compression on T8 level and pharmacological treatment with DIDS, VDACC1 blocker, or PBS (vehicle) after 1h. Motor recovery was evaluated for 6 weeks using the BBB scale. Spinal cord was collected for immunofluorescence (IF), TUNEL and Western Blot (WB) assays 24h and 6 weeks after SCI. Results were evaluated through Anova Two-Way.

Results:

IF showed an increase of VDACC1 N-term labeling (sham 7,4 ± 0,4; SCI 11,78 ± 2), and VDACC1 PORIN labeling 24h after SCI (sham 6,5 ± 0,3; SCI 16,9 ± 2). WB showed that VDACC1 protein levels did not alter after SCI (sham 16,4 ± 3,6; SCI 16,36 ± 7). TUNEL revealed that PBS group had more TUNEL positive cells than DIDS group (190,6 ± 120 vs. 69,6 ± 43). Double labeling with TUNEL+OSP on DIDS group was significantly smaller than on PBS group (7,25% ± 7,25 vs. 22,8% ± 2,2). Double labeling with TUNEL+NCP showed that the percentage of cells labelling both markers on DIDS and PBS group (25,8% ± 9 vs. 28,3% ± 10,7) was the same. GFAP labeling in sagittal cuts showed that DIDS animals had larger injury area than PBS animals (24,3 ± 4,3 vs. 39,3 ± 12) 6 weeks after SCI. Radial analysis of apoptosis showed that DIDS animals has less apoptotic cells close from the injury epicenter, mainly at ventral horn, related to movement. BBB test showed that DIDS group had a better motor recovery (PBS 8,6 ± 2,2; DIDS 19 ± 1).

Conclusion:

IF results relate to an increased externalization of N-terminal region and the oligomerization process, essential to cell death spread. TUNEL showed that DIDS is effective in decreasing cell death after SCI, maybe by altering the physical conformation of VDACC1, and preventing molecules responsible for apoptosis from leaving the mitochondria. TUNEL double labelling revealed that the blockade decreased death of oligodendrocytes, but not neurons, suggesting that they undergo different apoptosis pathways. Also, oligodendroglia death reduction on ventral horn could impair on initiation and movement control, improve tissue response to degeneration and support axonal remyelination, promoting a minor tissue cavity and improving locomotor function recovery, as confirmed on BBB test.

Financial support:

FAPESP

10.012 - PRESENCE OF AN ALPHA-SYNUCLEIN LIKE IN CENTRAL NERVOUS SYSTEM OF A CRUSTACEAN. Santos RR, Gomes CABA, Vitorino LC, Wajsenzon IJ, Silva WAB, Correa CL, Foguel D, Allodi S, - Centro de Ciências da Saúde - PUC Neurobiologia - UFRJ Bioquímica - UFRJ

Introduction:

Alpha synuclein is a protein widely distributed in the central nervous system (CNS) throughout vertebrates. The main function is related with synaptic regions, as a SNARE-like protein. Additionally, it acts as a negative regulator of neurotransmitter release, synaptogenesis and as a chaperone. However, despite these functions, this protein is more known by its relation with Parkinson's disease (PD), because it forms Lewy bodies. It is considered as conserved in vertebrates, nevertheless, it has never been described in invertebrates. Alternative invertebrate models have been used to study neurodegeneration due to easy manipulation and maintenance, low cost and short cell cycle. Crustaceans, specifically, have low rate mutations, and because crabs dwell in mangroves with high concentration of metals, they are fit to studies on neuronal degeneration.

Aim:

To evaluate the presence of alpha-synuclein in the crustacean *Ucides cordatus* CNS and effects of the neurotoxin 6-hydroxydopamine (6-OHDA) on alpha-synuclein cells in vitro.

Methods:

This work was approved by IBAMA, #14689-1/IBAMA/2008. We carried out immunohistochemistry (4 crabs), western blotting and simple immunoprecipitation (60 crabs) to verify the content and localization of alpha-synuclein in the CNS. The simple immunoprecipitation was used to concentrate the protein extract to posterior proteomic analysis. Next, we analyzed cell cultures (180 crabs), to verify the content of alpha-synuclein in control and experimental groups (1, 3 or 5 days of exposure to 6-OHDA). The in vitro experiments were analyzed by Student's T Test to compare experimental conditions with time-matched control groups, and One Way Anova, to analyze between experimental conditions.

Results:

Ex vivo results showed alpha-synuclein-positive cells in CNS regions associated with sensorial processing, motor control, memory and neurogenesis. The molecular weight was 76kDa, which indicates a tetramer. The in vitro study showed, in all experimental conditions, that there were more alpha-synuclein-positive cells (p < 0,001 and p < 0,05) than the time-matched control groups.

Conclusion:

These results showed alpha-synuclein in the crustacean CNS, and that 6-OHDA affects cells similarly to vertebrates. Therefore, *U. cordatus* is appropriate to study neurodegeneration, focusing on cellular physiology and evolution.

Financial support:

CNPq and FAPERJ

FeSBE Annual Meeting 2019

Poster Sessions and Abstracts

10.013 - THE BRAIN-GUT AXIS: ROLE OF THE GUT MICROBIOMA IN THE OUTCOME AND PROGRESSION OF IDIOPATHIC PARKINSON'S DISEASE. AmorimNeto DP, Bosque BP, Meneses DD, Fonseca MC, - LNBio - CNPEM Facultad de Ciencias Químicas y Farmaceuticas - U.de Chile

Introduction:

Parkinson's disease is a debilitating pathology marked by motor and cognitive impairment. A hallmark of this synucleinopathy is the accumulation of α -synuclein (α -syn) in the substantia nigra of the brain. Recent studies have shown that innumerable patients with non-genetic (idiopathic) Parkinson's disease showed aggregate forms of α -syn in the enteroendocrine gut cells which are in direct communication with sympathetic nerve terminals. Patients also present unbalanced intestinal mucin synthesis and intestinal microbiota dysbiosis, with greater abundance of the specie *Akkermansia muciniphila* when compared to healthy patients. This data suggest a connection towards a microbiota-intestine-brain triad. However, the mechanisms by which the microbiota may modulate the expression and folding of α -syn in the intestine are so far barely exploited.

Aim:

Our aim was to evaluate how/whether *A. muciniphila* secretome can induce α -syn overexpression and/or aggregation in the enteroendocrine cells in order to establish a pathological connection between the gut microbiome and the outcome of idiopathic Parkinson's disease.

Methods:

A. muciniphila was cultured in pure BHI medium, BHI supplemented with 0.4% mucin in anaerobic chamber until the peak of bacteria growth. After 44hs, the media were centrifuged, the supernatant collected and concentrated through 3kDa Centricons for the obtention of the Conditioned Media (CM). Secretomes were analyzed under mass spectrometry. STC-1 cell line was cultivated in complete DMEM medium with 10%FBS and 1%PSA. Cells were cultivated in the presence of bacterium secretome (1 and 10%v/v) for 48hrs and proceeded to immunofluorescence and western blotting procedures for detection of α -syn. Intracellular Ca^{2+} -signaling assays were also conducted on STC-1 cells using confocal microscopy and Fluo-4/AM probe. At least 3 individual experiments were performed for each condition and $p < 0.05$ was considered.

Results:

Mucin supplementation expanded the growth curve of *A. muciniphila* when compared to mucin-free medium. The intracellular Ca^{2+} -signaling assay revealed that nonconditioned media used as stimuli had no effect on STC-1 cells. However, BHICM and BHICM+0.4% mucin, containing the bacteria secretome, lead to an increase on intracellular Ca^{2+} signal, the BHICM even leading to a more prominent increase on Ca^{2+} signal when compared to BHICM+0.4% (BHICM: 200% vs BHICM+0.4% mucin: 100%). Interestingly, when we used *E. coli* BHICM as a control, we observed an increase on Ca^{2+} signal comparable to BHICM+0.4% mucin (BHICM: 100%). We next aimed to answer whether bacteria secretome could lead increased α -syn expression on STC-1 cells. BHICM from *A. muciniphila* induced α -syn increase in STC-1 cells after 48hrs of incubation with 1% or 10% (v/v) when evaluated by immunofluorescence (1%BHI: 2% and BHICM: 25%; 10%BHI: 3% and BHICM: 55%) and western blotting (1%BHI: 1,3A.U and BHICM: 4A.U; 10%BHI: 1,3A.U and BHICM: 6A.U). None of the techniques evidenced a difference in α -syn expression in cells incubated with non-conditioned media, BHICM+0.4% mucin or with BHICM from *E. coli*. Therefore, α -syn increase seems to be specifically caused by *A. muciniphila* secretome in a mucin-free condition.

Conclusion:

STC-1 cells stimulated with *A. muciniphila* secretome cultured in pure mucin-free media present augmented intracellular Ca^{2+} -signaling and α -synuclein expression. The data suggest the formation of a microenvironment conducive to the development of α -synuclein aggregates and cell spreading, similar to the pathological condition of sporadic Parkinson's disease, making *A. muciniphila* a possible biological inhibition target for early disease control. Our next goals are to go

further into α -syn aggregation process inside intestinal cells and spreading to neurons.

Financial support:

FAPESP (2018/20014-0); CNPq; MCTIC

10.014 - DISEASE-RELATED MUTANT DDX3X INDUCES ITS INTRACELLULAR AGGREGATION AND TOXICITY IN NEUROBLASTOMA CELL LINE. Bosque BP, Oliveira JF, Canateli C, AmorimNeto DP, Prado PFV, Borges AC, Portugal RV, Krepischi ACV, Rosenberg C, Franchini KG, Fonseca MC, - Genetics and Evolutionary Biology - USP LNBio - CNPEM LNNano - CNPEM

Introduction:

Previous reports estimate that between 1-3% of females with unexplained intellectual disability (ID) may have de novo nonsense, frameshift, splice site or missense mutations in DDX3X. DDX3X encodes an RNA-binding protein of the DEAD-box family. Although this protein is broadly implicated in mRNA metabolism, DDX3X is also described as a translational regulator, being a component of RNA-protein granules, including neuronal transport granules and cytoplasmic stress granules, which are RNA-protein foci induced by stress.

Aim:

Therefore, the aim of this work was to evaluate the cell effects of a new described mutation (L556S) on DDX3X protein, found on a girl with severe ID.

Methods:

In vitro tests in cells were performed with plasmid constructs containing the full-length sequence of wild-type (WT) or the mutant variant (L556S) of DDX3X protein, both with a GFP-tag. Human neuroblastoma cell line SH-SY5Y was transfected with 3 μ g of DNA in liposomal system and incubated for 48hrs for the expression of the construct. Then, the cells were directed to FRAP or immunofluorescence experiments, after heat (43°C) or chemical treatment for evaluation of stress granules and their motility, both under confocal microscopy. The GFP was excited with 488nm and the emission detected at 520nm. Cell viability was assessed by MTT. For the experiments with isolated protein, the protein portion containing the domains D1 and D2 was obtained by expression in *E. coli*. In vitro characterization of aggregates was evaluated by Fluorimetry based on light scattering at 350nm, ThT fluorescence and cryo-EM (negative staining). The enzymatic activity was evaluated by degradation of ATP and quantified by colorimetry (Abs 620nm).

Results:

It was observed, that in normal conditions of temperature (37°C), the WT protein is distributed homogeneously along the cytoplasm and the L556S mutant appears aggregated. DDX3X-granules of WT or L556S proteins were assembled either under thermal or chemical treatment and colocalized with stress granules markers. The FRAP assay showed that after 20 min of heat-stress, the WT DDX3X almost granule completely recovered the fluorescence after photobleaching, while the L556S mutant recovered only 17%, indicating that protein motility was reduced (% of recovery WT: 75 \pm 2,2 and L556S: 17 \pm 5,7%). In addition, after 2 hours of heat stress, the WT DDX3X granule recovered only 25% of fluorescence meanwhile no recovery was observed after photobleaching for the mutant protein (% of recovery WT: 25 \pm 6,2% and L556S: 1 \pm 0,5%). The MTT assay indicated that the mutation reduced ~15% of cell viability when compared to the WT protein (% of viable cells WT: 82 \pm 2,3 and L556S: 65 \pm 3). The experiments with purified, isolated protein showed that only the mutant variant aggregates spontaneously with time (Light scattering at 350nm, WT: 11800 a.u.; L556S: 45500 a.u./ ThT fluorescence, WT: 1970 a.u.; L556S: 19000 a.u.). The electronic cryo-EM evidenced the aggregation in amyloid fibers by the mutant protein. Finally, it was found that the aggregation impairs the ATPase activity of the protein, since the L556S dimers, after the reaction, showed levels of phosphate approximately 60 μ M, the mutant monomers of 90 μ M and the wild-type monomers of 200 μ M.

FeSBE Annual Meeting 2019

Poster Sessions and Abstracts

Conclusion:

Therefore, DDX3X-L556S mutation affects protein motility, state of aggregation and, consequently, its activity in neuronal cells, forming toxic aggregates. Thereby, this mutation can be directly involved in the genesis of neurodevelopment disorders and therefore, be a possible pharmacological target.

Financial support:

FAPESP 2018/20014-0, MCTIC

11 - Physical Training Responses

11.001 - EFFECT OF PHYSICAL TRAINING DURING CHILDHOOD ON THE MITOCHONDRIAL BIOENERGETICS AND METABOLIC REGULATION OF MALE WISTAR RATS EXPOSED TO MATERNAL LOW PROTEIN DIET. PEDROZA AADS, BERNANRDO EM, PEREIRA AR, FERNANDES MSDS, BRAZ GRF, SILVA SCDA, FERREIRA DJS, LAGRANHA CJ, - Post-Graduate Program in Biochemistry and Physiology - UFPE Laboratory of Exercise Biochemistry and Molecular Biology - UFPE Neuropsychiatry and Behavior Science Graduate Program - UFPE Federal University of Sao Francisco Valley - UNIVASF

Introduction:

Epidemiological and experimental studies have demonstrated a close relationship between nutritional insults during development and subsequent genesis of cardiovascular diseases, wherein mitochondrial dysfunction underpins their pathophysiology. Otherwise, it is well known that moderate exercise promotes cardiac health by improving heart metabolism.

Aim:

To evaluate whether the moderate physical training is capable of reverse the detrimental effects of a maternal protein restriction on the heart of male rats.

Methods:

Pregnant rats were divided into two groups: Control (C=17% casein) and undernourished (U=8% casein). Both groups received the diet throughout gestation and lactation period. At weaning, offspring started to receive laboratory chow, and, at 30 days of life, male offspring from the undernourished group were subdivided into undernourished sedentary (U) and undernourished+exercise (UT) groups. Treadmill exercise was performed as follow: (4 weeks, 5 days/week, 60 min/day at 50% of maximal running capacity). 24 hours after the last exercise session, hearts were collected for the following biochemical analyses: Mitochondrial oxygen consumption (MOC), Respiratory control ratio (RCR), Citrate synthase activity (CS), and SIRT3 protein expression. The experimental procedures were in accordance with the Brazilian Committee of Animal Experimentation and approval by UFPE Animal Care Committee (Process number: 23076.017806/2014-62). The results were analyzed by ANOVA One-Way test and followed by Tukey post-test. Data were expressed as mean \pm SEM, considering $p \leq 0.05$.

Results:

Our analysis demonstrated that in the low energy states of MOC(nmol/min/mg prot), no differences were observed between C and U groups (State2: C=2.450 \pm 0.1646, N=4 vs. U=3.220 \pm 0.4689, N=3; $p=0.7792$; and State4: C=2.360 \pm 0.3532, N=4 vs. U=4.540 \pm 1.271, N=3; $p=0.7063$). However, in the states that mitochondria increase their O₂ consumption, the U group was beneath (State3: C=22.10 \pm 1.119, N=4 vs. U=10.22 \pm 2.390, N=3; $p=0.008$; uncoupling state: C=13.50 \pm 2.140, N=4 vs. U=4.850 \pm 1.419, N=3; $p=0.05$; and RCR: C=9.240 \pm 0.8695, N=4 vs. U=3.075 \pm 0.4689, N=3; $p=0.0008$). Once the undernourished animals had trained, their MOC increased significantly (State2: U=3.220 \pm 0.4689, N=3 vs. UT=10.79 \pm 2.319; N=3; $p=0.011$; State3: U=10.22 \pm 2.390, N=4 vs. UT=24.07 \pm 1.120, N=4; $p=0.002$), increase in uncoupling state (U=4.850 \pm 1.419, N=4 vs. UT=12.09 \pm 0.3097, N=4; $p=0.0$; and RCR: U=3.075 \pm 0.2353, N=4 vs. UT=7.250 \pm 1.079, N=4; $p=0.02$). Our results also showed that protein restriction decreased CS activity (U/mg prot

(C=0.8969 \pm 0.06092, N=5 vs. U=0.3458 \pm 0.1776, N=4; $p=0.023$) although moderate physical training restored it (U=0.3458 \pm 0.1776, N=4 vs. UT=1.198 \pm 0.07917, N=3, $p=0.004$). Undernutrition also decreased SIRT3 expression (2DDCt) (C=1.594 \pm 0.4211, N=3 vs. U=0.2301 \pm 0.04879, N=3; $p=0.02$), where physical training demonstrated to be newly protective (U=0.2301 \pm 0.04879, N=3 vs. UT=1.061 \pm 0.003643, N=3; $p=0.05$).

Conclusion:

Taken together, our results demonstrate that maternal undernutrition impairs the heart by modulating mitochondrial function and decreasing SIRT3 protein expression, which could be a feasible mechanism associated to later cardiovascular diseases. In these conditions, we further demonstrate that 4 weeks of moderate physical training protects the heart of animals submitted to a maternal protein restriction.

Financial support:

CNPq (408403/2016-0)

11.002 - EFFECT OF MODERATE PHYSICAL TRAINING ON THE OXIDATIVE BALANCE IN THE BRAINSTEM OF YOUNG RATS SUBMITTED TO MATERNAL PROTEIN RESTRICTION. BERNANRDO EM, PEREIRA AR, SILVA SCDA, BRAZ GRF, FERREIRA DJS, PEDROZA AADS, LAGRANHA CJ, - Laboratory of Exercise Biochemistry and Molecular Biology - UFPE Post-Graduate Program in Biochemistry and Physiology - UFPE 3Neuropsychiatry and Behavior Science Graduate Program - UFPE Federal University of Sao Francisco Valley - UNIVASF

Introduction:

Epidemiological and experimental studies show a link between malnutrition in the critical period of development and the predisposition to chronic noncommunicable diseases (NCDs) in adulthood. Although the biochemical and molecular mechanisms are not fully elucidated, several reports suggest that high levels of reactive oxygen species and oxidative stress in the brainstem are involved in the susceptibility to. On the other hand, physical exercise has been widely used as a tool in the fight against such diseases.

Aim:

To investigate the effects of a moderate physical training on the oxidative stress in the brainstem of rats submitted to maternal protein restriction.

Methods:

: Pregnant Wistar rats received either 17% casein (normal protein, N) or 8% casein (low protein, H) throughout pregnancy and lactation. At 30 days of life, offspring were subdivided into 4 group: normal protein sedentary (NS), low protein sedentary (HS), normal protein trained (NT) and low protein trained (HT). The NT and HT groups were submitted to a moderate exercise training on a treadmill during 4 weeks for 5 days / week and 60 min / day for 50% of the maximum capacity. At 60 days of life the animals were sacrificed, and the brainstem collected to the following analysis: Oxidative stress biomarkers (Malondialdehyde-MDA concentration and Carbonyl content), activity of antioxidant enzymes (Superoxide dismutase-SOD, Catalase-CAT and Glutathione-S-transferase-GST) and non-enzymatic antioxidant defense (Reduced glutathione-GSH and Total thiol groups-Sulfhydryl). The experimental procedures were in accordance to Brazilian Committee of Animal Experimentation and approval by UFPE Animal Care Committee (Process number: 23076.017806/2014-62). Data were analyzed by Two-way ANOVA with post-hoc Tukey test and expressed as percentage, considering significant values at $p < 0.05$.

Results:

Our data demonstrated an increase in carbonyls levels in HS group compared with NS group (NS:50.150 \pm 3.150, N=4; HS:66.367 \pm 3.650 mmol/gprot; $p=0.0109$), while exercise reverted this effect, comparing HS with HT (HS:66.367, N=6 vs. HT:31.467 \pm 1.538, N=6 650 mmol/gprot; $p=0.0001$). Regarding the enzymatic activities, the low protein diet downregulated SOD and CAT activities, (NS:7.808 \pm 0.602, N=6 vs

FeSBE Annual Meeting 2019

Poster Sessions and Abstracts

HS:5.080±0.9493, N=5 Umol/gprot; p=0,0464) and (NS:1.656±0.113, N=4 vs. HS:0.709±0.047, N=6 Umol/gprot; p=0.0001), respectively. The HS group also present lower levels of sulfhydryl content compared with the NS group (NS:0.104±0.005, N=5 vs. HS:0.078±0.003, N=6 mmol/gprot; p=0.0425). However, the moderate physical training offset the enzymatic impairment both in SOD (HS:4.488±0.919, N=6 vs. HT:10.491±1.097, N=7 Umol/gprot; p=0,0007) as in CAT (HS:0.709±0.047, N=6 vs. HT:2.098±0.250 N = 7 Umol/gprot; p = 0.0045). In the non-enzymatic antioxidant defense, the training also increased the total thiols -SH value (HS:0.078±0.003, N=6 vs. HT:0.091±0.002, N=7 mmol/prot; p=0.0078) and GSH levels (HS:6557±312.567,N=3 vs. HT:9110.593±677.892, N=3 µmol/gprot ; p=0,0109). We did not obtain significant differences in the MDA concentration, and in the activity GST.

Conclusion:

Our results show that a protein restriction in the critical period of development negatively impacts the oxidative balance in the brainstem, which could be a mechanism for vegetative functions-related diseases in later ages. Physical exercise, otherwise, seems to be an interesting strategy in the prevention of such pathologies.

Financial support:

CNPq (408403/2016-0)

11.003 - CONCURRENT PHYSICAL EXERCISE ASSOCIATED WITH PHOTOBIOBULATION MODULATES INFLAMMATORY INFLOW AND THE NUMBER OF ACTIVE CHONDROCYTES IN RHEUMATOID ARTHRITIS. LIMA R, Pedersen M, Brucieri L, Rocha TTS, Almeida AS, Andrade TAM, Esquisatto MAM, Bomfim FRC, Felonato M, - Programa de Pós-Graduação em Ciências Biomédicas - FHO

Introduction:

Characterized as an inflammatory autoimmune pathology, rheumatoid arthritis (RA) presents a systemic inflammation, which attacks the synovial membrane, causing damage and deformities to cartilage (JET et al, 2015). The synovial membrane affected by the presence of inflammatory cells, degrades the articular cartilage and compromises the function of chondrocytes (MOELANTS et al, 2013). Thus, treatments such as physical exercise and photobiomodulation (METSIOS et al., 2015) are used to improve the clinical condition.

Aim:

So, this work investigated the presence of chondrocytes and inflamed area in joint of animals with RA after non-drug therapy.

Methods:

For eight weeks, wistar rats were divided into 10 groups: CTL: control group with saline injection in joint; ZYM: group with injection of 200µg of zymosan in joint; ZYM+A: zymosan group submitted to the protocol of aerobic exercise with duration of 1h, 5 days/week with gradual overload increased weekly in 5% of the animal weight (NAVARRO et al., 2010); ZY+R: zymosan group submitted to the resisted exercise protocol with 4x10 jumps with 30 seconds rest, 3 days/week (MILARES et al., 2016; MUNIZ-REMO et al., 2005). The load was proportional to the body mass for each animal, starting at 20% of the body mass at 80%; ZYM+CON100%: zymosan group with concurrent exercise protocol (resisted and aerobic exercise) with 100% of total protocol volume; ZYM+CON50%: zymosan group with concurrent exercise protocol with 50% of the total volume of the protocol. All training protocols were subdivided into treatment with and without photobiomodulation with an 808nm gallium aluminum arsenide diode laser. The optical fiber was positioned perpendicular to the skin of the animal with power of 50mW, 1.4J of total energy for 56 seconds. The BASELINE group was used to verify the installation of the inflammatory process (72 hours). The animals were euthanized, and the knee was collected for histological analysis. The results were analyzed using the Variance Analysis Test (ANOVA/two way). When necessary, Tukey's post-hoc test was used, with a pre-established significance level of 5%. The study was approved by the FHO-UNIARARAS Ethics Committee (067/2018).

Results:

All groups presented an inflamed area in relation to control, however, among the groups, the animals of concurrent group 50% had lower inflamed area. The total number of chondrocytes in the femur did not present differences between the groups, while in tibia, the concurrent groups 100% and 50% laser presented number of cells similar to control group. Both therapies induced an increase in active chondrocytes in femur and tibia. Only the concurrent group 50% laser showed no difference in femur, while the concurrent groups 100% and 50% associated or not photobiomodulation showed no differences in tibia.

Conclusion:

The proposed treatments modulate the sinovial cell influx. The therapies with physical exercise protocols (aerobic and resisted) associated or not with photobiomodulation, as well as the concurrent physical exercise protocols without photobiomodulation, minimize the progression of pathology in femoral and tibial joint cartilage. Therefore, the association of concurrent physical exercise protocols and photobiomodulation seem not to be adequate for treatment of RA.

Financial support:

FHO-UNIARARAS

11.004 - MUSCLE OXIDATIVE STRESS IN RHEUMATOID ARTHRITIS: THE INFLUENCE OF EXERCISE AND LASER THERAPY PROTOCOLS. Pedersen M, Lima R, Brucieri L, Rocha TTS, Almeida AS, Andrade TAM, Esquisatto MAM, Bomfim FRC, Felonato M, - Programa de Pós-Graduação em Ciências Biomédicas - FHO

Introduction:

Rheumatoid arthritis (RA) is defined as an inflammatory disease of autoimmune etiology that destroys the joints. The inflammatory process responds with intense formation of reactive oxygen species and free radicals. These mediators trigger oxidative stress that amplifies the inflammation. It is known that different physical exercise protocols and laser therapy modulate pro and anti-inflammatory cytokines (VIACAVALI et al., 2014).

Aim:

Taking into consideration how much the protocols could induce muscle damage, this study evaluated the oxidative stress in experimental model of RA treated with physical exercise and laser therapy.

Methods:

For eight weeks, Wistar rats were divided into 10 groups: CTL: control group with saline injection in joint; ZYM: group with injection of 200 µg of zymosan in joint; ZYM + A: zymosan group submitted to protocol of aerobic exercise with duration of 1h, 5 days / week with increased weekly load in 5% of the animal weight (NAVARRO et al., 2010); ZY + R: zymosan group submitted to resistance exercise protocol with 4x10 jumps with 30 seconds rest, 3 days / week (MILARES et al., 2016; MUNIZ-REMO et al, 2005). The load was proportional to the body mass for each animal, starting at 20% of the body mass at 80%; ZYM + CON100%: zymosan group with concurrent exercise protocol (resistive and aerobic exercise) with 100% of total protocol volume; ZYM + CON50%: zymosan group with concurrent exercise protocol with 50% of total protocol volume. All training protocols were divided into treatment and without photobiomodulation with a laser diode of gallium arsenide-aluminum808nm. The optic fiber was positioned perpendicular to the skin of the animal with power of 50mW, 1.4J of total energy for 56 seconds. The animals were euthanized, and the knee was collected for histological analysis. The results were analyzed using the Variance Analysis Test (ANOVA/two way). When necessary, Tukey's "post-hoc" test was used, with a significance level of 5%. The study was approved by the Ethics Committee of FH O-UNIARARAS (067/2018).

Results:

The animals of the concurrent group 100% presented increased levels of Tbars in relation to other groups. Therefore, regarding the levels of the Sh group, the animals of zymosan group presented lower levels when compared to control group. In relation to the trained groups, the

FeSBE Annual Meeting 2019

Poster Sessions and Abstracts

aerobic group presents lower levels when compared to aerobic group. The groups 50% and resisted with laser present increased levels of the Sh group when compared to resisted and concurrent groups 50%, respectively. The concurrent group 100% presented increased levels of Sh when compared to concurrent group 100% laser.

Conclusion:

In the experimental RA model, treatment with 100% concurrent physical exercise induces oxidative stress, whereas the protocol of aerobic physical exercise induces greater muscle antioxidant activity. In association with laser therapy, all physical exercise protocols stimulate the production of muscle antioxidant activity. Thus, taking into consideration the best therapy directed to physical exercise protocol, the aerobic protocol seems to exert a better effect in reducing muscle fatigue caused by the pathology.

Financial support:

FHO-UNIARARAS

11.005 - RESISTANCE TRAINING PREVENTS THE DEVELOPMENT OF PULMONARY ARTERIAL HYPERTENSION IN RATS EXPOSED TO SECONDHAND SMOKE. Moreno ACR, Oliveira TO, Nai GA, Seraphim PM, - Patologia - UNOESTE Fisioterapia - UNESP Educação Física - UNESP

Introduction:

Smoking is one of the greatest threats to public health. Exposure to secondhand smoke is associated with more than 50 diseases, most notably pulmonary emphysema. Resistance training is an excellent option of treatment for patients with pulmonary diseases, as well as, is an effective form of exercise to improve health. However, little is known about the effects of high-intensity resistance training on the cardiac, hepatic and skeletal muscle of rats exposed to cigarette smoke.

Aim:

The aim of this study was to evaluate the effect the resistance training in rats exposed to second-hand smoke cigarette: 1) in the anatomopathological alterations in heart, liver, trachea, lungs, and muscle, 2) on the gene expression of mitochondrial markers of skeletal and cardiac muscles.

Methods:

Thirty-two Wistar male rats were divided into four groups: Sedentary Control (SC), Sedentary Smoker (SS), Exercised Control (EC) and Exercised Smoker (ES). SS and ES were exposed to the smoke of four cigarettes for 30 minutes twice daily, five days a week. EC and ES climbed on a vertical ladder with progressive load, once a day, five days a week. Both interventions were performed for 16 weeks at the same period. After euthanasia, blood was collected to measure fasting glycemia, total cholesterol, HDL, and triglycerides. Heart, trachea, lung, liver and gastrocnemius muscle were collected for anatomopathological analysis. Gene expression analysis of mitochondrial, dynamics and biogenesis, markers was performed by the RT-PCR assay in the heart and gastrocnemius muscle.

Results:

SC showed a higher body mass compared to all other groups ($p < 0.05$), EC group showed a higher body mass compared to smoking groups ($p < 0.05$). ES presented reduced gain of body mass compared to SS ($p < 0.05$), which was associated to reduced food intake ($p = 0.0005$). ES showed HDL reduction compared to EC ($p = 0.02$). Pulmonary emphysema (SS and ES vs SC and EC, $p < 0.0001$) and pulmonary artery thickness enlargement (SS vs SC and EC; ES vs SC, $p = 0.003$) were found in the smoking groups. In the heart, there was increase in the wall thickness of the right ventricle in SS ($p < 0.0001$). In the liver, it was observed increase of resident macrophages in SS and ES (vs. SC, $p = 0.002$). In the skeletal muscle, ES presented reduction of muscle fibers (ES vs SC and EC, $p = 0.0002$). Higher levels of Fis1 were found in the gastrocnemius muscle of SS vs SC ($p = 0.05$), without changes on the Mfn2 levels, indicating an imbalance in the mitochondrial dynamic. Increased mRNA level of Ppargc1a was observed in the heart of ES compared to SS ($p = 0.01$).

Conclusion:

We concluded that although it did not prevent Emphysema and HP, the Resistance Training has prevented pulmonary arterial hypertension in the smoking rats probably due to improvement of the oxidative capacity in the heart, since Ppargc1a mRNA levels were increased. This could result in the prevention of the increased right ventricle. However, in the skeletal muscle, the Resistance Training seems to reduce the muscle fiber size in smoking rats.

Financial support:

This study was supported by the Conselho Nacional de Desenvolvimento Científico e Tecnológico - Brasil (CNPq)

11.006 - EFFECT OF AEROBIC EXERCISE TRAINING ON IMMUNOLOGICAL CELLS PROFILE IN MICE. Machado LAF, Voltarelli VA, Brum PC, - Departamento de biodinâmica do movimento humano - Universidade de São Paulo

Introduction:

It is well known that aerobic exercise (AE) can induce different immune system outcomes, depending on its intensity and duration. Such responses may be immunoprotective (e.g. improving vaccination response), immunopathological (e.g. increasing allergic or autoimmune responses), or immunoregulatory/inhibitory (e.g. anti-inflammatory effect). However, most studies have focused on the acute effects of AE (effects of a single AE session), performed in both moderate and high intensities, while robust evidences for chronic effects of AE (effects of repeated AE sessions – also known as aerobic exercise training – AET) on immune cells are still scarce. In addition, many studies that addressed these questions were conducted in humans, which restricts the analysis of the immune system to peripheral blood cells.

Aim:

Considering this, the present study aimed to evaluate the effect of a moderate intensity AET protocol on immune cells distribution in a major lymphoid organ, the lymph node.

Methods:

To test this, 3 months old male Balb/c mice were submitted to a moderate intensity AET (60% of maximal aerobic capacity – determined by a previous exhaustion test - 5 days/week, 1 hour/day, in a treadmill) for 1 month. At the end of the AET protocol, a new exhaustion test was performed in order to evaluate the exercise training efficiency. After 48 hours of the last exhaustion test, animals were sacrificed by cervical dislocation under isoflurane anesthesia (the 48 hours after the test were chosen to avoid possible acute effects of the last exercise session on the results). Experimental groups were divided into control and exercise trained mice (AET). Inguinal lymph nodes (LNs) were harvested and then homogenized using a 70 μ m cell strainer for leukocytes isolation. After that, population of dendritic cells, macrophages (types M1 and M2), natural killer cells (NK), and T lymphocytes (TCD4+, TCD8+, regulatory T cells – Treg) were evaluated by flow cytometry. This study was approved by Animal Ethics Committee from School of Physical Education and Sport of University of São Paulo (CEUA/EEFE-USP nº 2018/03).

Results:

AET group presented a significant increase in NK+ and TCD8+ effector memory cells population in LNs when compared to sedentary animals. On the other hand, AET significantly decreased the percentage of dendritic cells and naive TCD4+ cells in this tissue. No significant changes were found for CD4+/CD8+ ratio, macrophages (M1 and M2), and Treg cells between groups.

Conclusion:

The data suggest that moderate intensity AET modulates the distribution of immunological cells in lymph nodes of trained mice towards a cytotoxic/effector immune profile. Therefore, these findings support the fact that AET could be used as a potential strategy in the prevention of diseases that require a proper functioning of the immune system, such as viral and bacteriological infections and cancer.

Financial support:

CNPQ

FeSBE Annual Meeting 2019

Poster Sessions and Abstracts

11.007 - DIVERSE MITOCHONDRIAL EFFECTS OF HIGH-INTENSITY EXERCISE IN WILD-TYPE AND ALZHEIMER'S DISEASE GENETIC MICE MODEL. Ferrari GD, Dechandt CRP, Alberici LC, - Departamento de Física e Química - FCFRP Departamento de Bioquímica e Imunologia - FMRP

Introduction:

Physical exercise is considered a primary intervention in many neurological diseases due to its ability to modify up to 82% of brain areas. In Alzheimer's disease (AD), the hippocampus is one of the most compromised areas of brain, being a major target for interventions seeking to improve hippocampal neurogenesis, synaptic plasticity and mitochondrial function. However, research analyzing the effects of physical exercise and mitochondrial bioenergetics in AD models are scarce, leaving a gap in our knowledge on changes underlying this mechanism. In this regard we aim to assess the changes in mitochondrial function, biogenesis and energy substrate use in a genetic AD mice model after high intensity training.

Aim:

To assess the changes in mitochondrial respiration, biogenesis and energy substrate use in a genetic AD mice model hippocampus after high intensity training.

Methods:

Triple transgenic mice (3xTG-AD) were submitted to an 8-week aerobic exercise on a treadmill. Soleus muscle PGC-1 α mRNA expression confirmed the effectiveness of the protocol. Hippocampal mitochondrial function was assessed through high resolution respirometry with tissue homogenate and the results were adjusted by Citrate Synthase (CS) unities. CS activity was used to determine mitochondrial biogenesis and qRT-PCR of GLUT3, LDH-A and MCT-2 were performed in order to analyze changes in glucose transport and metabolism. Data normal distribution was confirmed by Shapiro-Wilk test, Student's T test was performed to verify statistical changes and a p<0.05 was considered significant.

Results:

High resolution respirometry analyses showed that WT mice had lower baseline values in all respiration rates, when compared to 3xTG (337.4 \pm 18.5 and 511.7 \pm 56.2 - OXPHOS; 81.2 \pm 14.6 and 126.0 \pm 12.0 - LEAK; 663.5 \pm 86.1 and 921 \pm 72.9 ETS). Exercise increased all respiratory rates in WT and decreased them in 3xTG mice (OXPHOS +25% and -20%; LEAK +66% and -44%; ETS +54% and -48% in WT and 3xTG, respectively). Surprisingly CS activity was initially higher in WT than in 3xTG mice (0.47 \pm 0.07 and 0.37 \pm 0.12 μ mol/min/ μ g protein) and decreased after exercise in WT by 56% without changes in 3xTG mice. RT-qPCR showed that the 3xTG mice have a 2,7-fold increase in GLUT3 mRNA levels when compared to WT and less than half (46%) its LDH-A gene expression. After the exercise program no changes were observed in the WT group; GLUT3 levels were slightly reduced in AD mice (-26%), without statistical significance. However, LDH-A levels increased in the transgenic mice with high intensity exercise (46% to 143% when compared to WT). MCT-2 mRNA levels remained stable across all groups.

Conclusion:

Our data shows that high-intensity exercise may influence hippocampal mitochondrial phosphorylation capacity on normal and AD affected brains, but with contrasting effects. In WT hippocampus the training protocol reduced mitochondrial content but improved its function, while on the 3xTG mice the opposite was observed. Additionally, on WT hippocampus there were no changes in gene expression of the glycolytic pathway. Only AD brains with elevated glucose transporter expression presented an increase on lactate dehydrogenase mRNA levels, after exercise, suggesting a possible change in lactate metabolism.

Financial support:

Fundação de Amparo à Pesquisa do Estado de São Paulo (FAPESP) e Coordenação de Aperfeiçoamento de Pessoal de Nível Superior (CAPES)

13 - Cell differentiation, growth and death

13.001 - FATTY ACIDS Ω -3 PREVENT NON-ALCOHOLIC STEATOHEPATITIS (NASH) AND STIMULATE ADIPOGENESIS IN MESENCHYMAL CELLS OF ADIPOSE TISSUE AND ADIPOCYTES 3T3-L1. Antraco VJ, Sá RDCC, Simão JJ, Farias TSM, Cruz MM, Silva VS, Abdala FM, ALONSO-VALE MIC, - Departamento de Ciências Biológicas - Universidade Federal de São Paulo - UNIFESP

Introduction:

The mesenchymal cells derived from the WAT [adipose tissue-derived stromal cells (ADSC)] contained in the cellular fraction of the vascular stroma (EV) can differentiate into adipose cells with a beige phenotypic profile, with remarkable consequences on energy metabolism. It is of great relevance to the development of studies aimed at understanding the cellular and molecular mechanisms involved in the remodeling of WAT in obesity models.

Aim:

Based on the beneficial effects of ω -3 fatty acids on the reduction of adipocyte mass, adipocyte metabolism and adipocyte hypertrophy prevention demonstrated by our group previously, the present study proposes a therapeutic approach with fish oil [FO, (EPA/DHA 5: 1)], in mice submitted to obesity, in order to understand a possible role in directing ADSC extracted from the subcutaneous WAT [inguinal region, (WATing)] of these animals. Given the considerable impact of obesity on human health, it is of great relevance to the development of studies aimed at understanding the cellular and molecular mechanisms involved in the activation of factors that may interfere with the remodeling of WAT.

Methods:

Thus, proliferation and adipogenesis processes in these cells and in pre-adipocytes of the 3T3-L1 lineage were addressed in the present study. For this, 8-week male C57Bl/6j mice were induced to obesity through the ingestion of an HF diet for 8 weeks. Subsequently, these animals received FO by gavage (2 g/kg, 3 times per week, for 8 weeks). Body mass, food intake, plasma profile, tissue mass, and adiposity were analyzed. The subcutaneous WAT was removed, and the cells were isolated. EV cells containing ADSC were separated from the adipocytes. The ADSC and 3T3-L1 cells were cultured and the proliferation potential was estimated by MTT assay. Adipogenic potential was estimated by expression analysis of genes encoding PPAR γ 2, C/EBP α , perilipin, adiponectin, Glut-4, ATGL, HSL, lipin, LPL, DGAT1, FAS, ACC1, FABP4 by RT-PCR in real-time after induction of the cells to the differentiation (for 8 days) and by the accumulation of lipids in the adipocytes by oil red O.

Results:

The data showed that the consumption of the HF diet resulted in obesity of the animals. Compared to the HF group, the treatment with FO reduced the body mass, as well as the plasma concentration of TAG, total cholesterol, glucose, VLDL, LDL (concomitant to the increase of HDL), plasma transaminases (AST and ALT), alkaline phosphatase and gamma-GT such as liver mass and TAG content in this organ. In addition, FO decreased the mass of the WAT, but increased the cellularity (hyperplasia), and caused a drastic reduction in the volume (hypertrophy) of the adipocytes. We evidenced an increase in the proliferation of ADSC from the FO group in relation to the other groups; these data corroborate the results obtained after treatment (3T3-L1 and ADSC extracted from animals receiving CO diet) in vitro with EPA and 5:1 EPA/DHA association. Similarly, there was an increase in lipid accumulation in the FO group, data that also corroborate the in vitro treatment of the cells (3T3-L1 and ADSC) with EPA (alone or in combination with DHA). These data corroborate the increased gene expression of adipogenic transcriptional factors, and the late markers of adipocyte differentiation observed.

Conclusion:

We conclude the FA ω -3 exert an attenuating effect on body mass, dyslipidemia and hepatic steatosis induced by HF diet, as well as on adiposity, decreasing adipocyte hypertrophy; the data also suggest that

FeSBE Annual Meeting 2019

Poster Sessions and Abstracts

these FA increase WATing hyperplasia, as well as the recruitment (by increased proliferation and differentiation) of new adipocytes (white and/or beige), fundamental for the healthy expansion of WAT.

Financial support:

CAPES and FAPESP (2018/05485-6)

13.002 - AZADIRACHTA INDICA MODULATED INFLAMMATION AND FAVORED TISSUE FORMATION IN WOUND HEALING IN DIABETIC RATS. EUGÊNIO AN, Silva ACC, Torrezan M, Rodrigues AL, Mariano SS, Poletti S, Gaspi FG, Esquisatto MAM, Mendonça FAS, Aro AA, Andrade TAM, SANTOS GMT, - Programa de Pós-Graduação em Ciências Biomédicas - Centro Universitário da Fundação Hermínio Ometto - FHO

Introduction:

Alternative methods that aid complications associated with diabetes wound healing are important for tissue restoration. Azadirachta indica may be innovation in the healing of diabetic wounds due to its healing properties.

Aim:

To analyze tissue repair of wounds in diabetic and non-diabetic rats submitted to treatment with A. indica.

Methods:

30 non-diabetic animals and 30 diabetics induced by alloxan (45 mg/kg, intravenous) were used, with presented glycemia above 200mg/dL. The lesions were performed through punch (1.5 cm diameter) with anesthetized animals (ketamine/xylazine – 3.0/1.0 mg/kg). The animals were divided into: (S) non-diabetic, treated with carbopol gel; (N) non-diabetic, treated with A. indica+carbopol gel; (DM-S), treated with carbopol gel; (DM-N), treated with A. indica+carbopol gel. The lesions were photographed on the initial day (0d) and on the euthanasia days (2, 7 and 14 post-injury) for analysis of wound healing rate (WHR= initial area - final area/initial area). In these periods samples were collected for histomorphometric analysis: inflammatory infiltrate, fibroblasts and percentage of collagen; and for biochemical analysis: dosage of myeloperoxidase (MPO), N-Acetylglucosaminidase (NAG), Hydroxyproline (HO-Pro) and Glycosaminoglycans (GAGs), quantified and calculated by ImageJ software. The results (mean±standard error) were analyzed by Two-Way ANOVA and Tukey post-test ($p < 0.05$). (CEUA-UNIARARAS: 025/2017).

Results:

N (0.22 ± 0.02) presented higher WHR of the lesions than DM-N (0.06 ± 0.07) on the 2nd experimental day. DM-S presented higher quantification of inflammatory infiltrate than N in 2nd day: (DM-S: 292.9 ± 47.52 ; N: 152.3 ± 12.74) and 7th day: (DM-S: 286.2 ± 27.4 , N: 106.5 ± 18.2); on 14th day the groups S (229.4 ± 25.1), DM-S (300.7 ± 57.6) and DM-N (219.3 ± 35.4) had values higher than N (80.20 ± 11.87). As for MPO, DM-S (0.84 ± 0.02) and DM-N (0.83 ± 0.05) showed higher quantification on the 2nd experimental day and on the 14th day lower (0.10 ± 0.02 ; 0.11 ± 0.013 , respectively) when compared to S (2nd day: 0.48 ± 0.13 , 14th day: 0.36 ± 0.04). In relation to NAG, S (0.121 ± 0.005) was higher than DM-N (0.109 ± 0.004) on the 7th day. In relation to fibroplasia, DM-N (140.7 ± 6.8) presented higher quantification than the other groups on the 2nd day (S: 28.45 ± 4.25 , N: 53.47 ± 4.27 , DM-S: 28.78 ± 1.44); on the 7th day N (146.1 ± 24.1) presented lower values than the other experimental groups (S: 251.5 ± 32.62 ; DM-S: 268.5 ± 25.73 ; DM-N: $296, 8 \pm 21.78$) and on the 14th day the DM-N group (228.9 ± 7.920) was greater than DM-S (146.2 ± 2.849). Collagenase was higher in N (53.47 ± 4.27) and DM-N (44.02 ± 1.74) than S (28.45 ± 4.25) and DM-S (28.78 ± 1.44) on 2nd day. On 14th day, N (68.74 ± 3.41) was higher than S (49.67 ± 5.05). DM-N presented higher HO-Pro quantification in the 2nd (DM-N: 70.68 ± 12.45 , S: 29.66 ± 11.87) and 7th day (DM-N: 45.06 ± 5.412 ; S: 7.14 ± 1.31) when compared to S. On the 14th day (DM-N: 99.68 ± 10.96) was higher when compared to N (51.68 ± 4.393). Regarding the quantification of GAGs, there was no difference between the groups.

Conclusion:

A. indica, in addition to favoring the contraction of the wound, presented anti-inflammatory effect and benefited the fibroplasia and collagenesis, mainly in diabetic rats, in this experimental model. This indicates that it may help in the treatment of this type of lesion and in the presence of this pathology, constituting a therapeutic alternative.

Financial support:

HERMINIO OMETTO FOUNDATION

13.003 - CLONING OF METACASPASE YCA1 WITH N-TERMINAL DELETION. Prado IRS, Reis TS, Araujo LH, Souza LFLP, Marcondes MF, Machado MFM, - Centro Interdisciplinar de Investigação Bioquímica - UMC Departamento de Biofísica - UNIFESP

Introduction:

Metacaspases are cysteine proteases orthologs of the caspases, found only in simple eukaryotes and promotes cell death by apoptosis. In *Saccharomyces cerevisiae* is found a single metacaspase (YCA1), that modulates programmed cell death, and also is involved in cell cycle and remodeling protein aggregates. Interestingly, despite acting as protein stabilizer to prevent protein aggregation of other proteins in vivo, YCA1 presents a N-terminal region rich in hydrophobic residues that's responsible for YCA1 aggregation in experimental assays.

Aim:

Obtain the recombinant truncated-YCA1 (tYCA1) with a deletion of 86 aminoacids from the N-terminal region.

Methods:

The tYCA1 gene was amplified by Taq DNA polymerase with specific oligonucleotides that contain sequences to recognize NheI and EcoRI restriction enzymes. The amplified product and pET-28a(+) plasmid vector were digested by NheI and EcoRI. tYCA1 gene was incorporated on pET-28a(+) with an enzyme T4 Ligase. The tYCA1 amplicon was inserted by heat-shock into *E. coli* DH5 α , this clone was incubated on 37°C during 18 hours in a shaker. Screening for the positive clones was carried out by colony PCR using T7 primers. Plasmid minipreps of positive clones were performed. BL21(DE3) was transformed with plasmid minipreps products. tYCA1 expression was induced with 0,25 mM IPTG for 16 hours at 20°C. The pellet was lysed by lysozyme and this material was purified by affinity chromatography using a HisTrap-Ni²⁺ sepharose FF column in a Akta Pure and the elution was performed in different concentrations of imidazole (0-500 mM), in sequence a desalting column HiPrep™ 26/10 was used to exclude imidazole of the medium. The obtained proteins were analyzed by SDS-PAGE with 15% of acrylamide.

Results:

Amplification of tYCA1 gene was analyzed by 1% agarose electrophoresis and presented a single band with ~1120 bp corresponding of tYCA1 gene. Digestion by NheI and EcoRI endonucleases of the YCA1 gene and the pET-28a(+) vector were confirmed by 1% agarose electrophoresis, presenting bands of 1120 pb and 5366 pb, respectively, the digest material was purified and the insertion of tYCA1 gene and pET28a(+) was performed by T4 DNA ligase. This product was inserted into DH5 α strain and the cloning was confirmed by PCR using T7 primers in a 1% agarose electrophoresis. A mini-prep of the positive clones was obtained and transfected into the BL21(DE3) strain for expression of tYCA1. tYCA1 was expressed and confirmed by 15% acrylamide SDS-PAGE, confirming the presence of a 35 kDa band related to truncated metacaspase in a non-processed form and a small unit of 25 kDa corresponding on a processed form of tYCA1. For purification of tYCA1 we used a Ni-sepharose affinity column, the protein was shown to be pure after treatment with 300 mM imidazole, the data was confirmed by SDS-PAGE gel.

Conclusion:

The tYCA1 of *S. cerevisiae* was cloned, expressed and purified and will be used for biochemical characterization.

Financial support:

FAPESP, CNPq and FAEP

FeSBE Annual Meeting 2019

Poster Sessions and Abstracts

13.004 - CLONING OF THE METACASPASE OF PARACOCCIDIOIDES BRASILIENSIS WITH DELETION OF THE N-TERMINAL PORTION. Souza LFLP, Santos TR, Machado MFM, Machado MFM, - Centro Interdisciplinar de investigação bioquímica - UMC Biofísica - Unifesp

Introduction:

Metacaspases are cysteine-peptidases found in lower eukaryotes, these enzymes are similar to caspases and are closely correlated with cell death. Paracoccidioides brasiliensis a pathogenic fungus encodes only one metacaspase (PbMCA). Studies involving metacaspases demonstrate that many residues of glutamine and asparagine in the N-terminal portion lead to the formation of inclusion bodies, which hinders their biochemical characterization. Objective: Clone the PbMCA with deletion of the N-terminal portion.

Aim:

Clone the PbMCA with deletion of the N-terminal portion.

Methods:

tPbMCA (truncated PbMCA) gene was amplified using gene-specific primers with HotStar HiFidelity DNA polymerase, the PCR product was purified with kit (Promega) and digested with the NheI and EcoRI restriction enzymes, later, it was directionally inserted into the pET-28a(+) vector, which was also digested with the same enzymes. Thermal shock was procedure to introduced tPbMCA clone in E.coli DH5 α strain, the transformation was confirmed by colony PCR, using T7 primers. Alkaline lysis was procedure and was sequenced by Sanger technique. The clone was introduced into the competent bacterium BL21 (DE3), the transformation was also analyzed by colony PCR. After confirmation of cloning without the presence of mutation, the protein was expressed with 0.25 mM IPTG, the material was lysed with lysozyme and then purified by nickel resin column affinity chromatography, varying the concentrations of 0 to 500 mM imidazole, purification was available by SDS-PAGE with 15% of acrylamide.

Results:

Amplification of the tPbMCA gene was analyzed by 1% agarose electrophoresis that's presents a band with ~1100 bp. Digestion of the tPbMCA gene and pET28a(+) was analyzed by 1% agarose electrophoresis and presenting bands of 1100 bp and 5369 bp, respectively. After ligation, the recombinant DNA was introduced into the DH5 α strain and confirmed by colony PCR with T7 primers, 1% agarose electrophoresis showed the presence of 5 positive colonies, the plasmid was extracted by alkaline lysis and with this material sequencing was performed, through this we realized that cloning was performed without the presence of mutations. Positive colonies were then transfected into BL21 (DE3) strain and also confirmed by colony PCR, verifying that four colonies were positive. Expression of tPbMCA was analyzed on SDS-PAGE with 15% acrylamide, where a band around 40 kDa was visualized, indicating that the protein was successfully expressed, after expression the tPbMCA was purified by Ni²⁺-sepharose chromatography, that was analyzed by SDS-PAGE where it is found that the protein came out pure with 300 mM imidazole concentration.

Conclusion:

tPbMCA was cloned, expressed and purified successful, our next objective was testing the activity of this enzyme and procedure a biochemical study of tPbMCA soluble protein

Financial support:

FAPESP, CNPq and FAEP

13.005 - OBTAINING OF CANDIDA ALBICANS METACASPASE WITH N-TERMINAL DELETION (tCaMCA). Reis T, Trujillo MNR, Souza LF, Marcondes MF, Machado MFM, - Centro Interdisciplinar de Investigação Bioquímica - UMC Departamento de Biofísica - UNIFESP

Introduction:

Metacaspases are cysteine proteases present in simple eukaryotes. The metacaspases presents substrate specificity that contained basic amino acid at P1 position and your activity was calcium dependent. CaMCA

presents a hydrophobic N-terminal that promotes the aggregation of this enzyme, produced the CaMCA with N-terminal deletion could possibility in vitro biochemical characterization of this enzyme.

Aim:

Obtain recombinant tCaMCA metacaspase with the N-terminal deletion for future biochemical analysis of CaMCA.

Methods:

pET28a(+) vector (was chosen to cloning tCaMCA. Amplification of tCaMCA gene was perform with specific primers and HotStar HiFidelity DNA Polymerase in a PCR reaction. pET28a(+) plasmid and the PCR product were digested with NheI and EcoRI, these material was binding by T4 ligase. After ligation process tCaMCA clone was transformed by thermal shock in E. coli DH5 α strain, and positive colonies were select by PCR and this material was sequenced by Sanger's method. Positive colony was chosen, and an alkaline lysis was performed, this material was transformed in an E. coli BL21(DE3) strain and a PCR was made to choose a positive clone. tCaMCA was expressed using 0.25 mM of IPTG for 16 hours in 20 $^{\circ}$ C, the material obtained was purified with nickel-sepharose column (GE Lifescience) in different imidazole concentrations (0 - 500 mM).

Results:

Amplification of tCaMCA gene was availed with a 1% agarose electrophoresis. The material obtained with PCR and pet28a(+) was digest with NheI and EcoRI restriction enzymes, the digestion material was purified and with T4 ligase we performed the insertion of the DNA insert into the plasmid. The recombinant tCaMCA clone was transformed in an E.coli DH5 α strain by thermal shock and a positive clones was selected by kanamycin resistance, in order to confirm a transformation we procedure a PCR with T7 specific primers, a agarose 1% gel confirm the presence of CaMCA gene into pet28a(+) vector. The DH5 α contained CaMCA constructor was grow overnight at 37 $^{\circ}$ C, and a alkaline lysis was performed in order to obtained a high numbers of copies of the plasmid, these material was used to transformed a E.coli BL21(DE3) strain and DNA sequencing showed that tCaMCA clone did not presents any mutation. tCaMCA was expressed on 20 $^{\circ}$ C using 0.25 mM of IPTG, a SDS-PAGE on 15% acrylamide was performed and we could observed a two major protein bands, one with around 38 kDa that's corresponding a non-processed form of tCaMCA and other with around 28 kDa that's correspond a processed form of tCaMCA. For purified of tCaMCA we used a Ni-sepharose affinity collumn, the protein was shown to be pure after treatment with 300 mM imidazole, the data was confirmed by SDS-PAGE gel.

Conclusion:

tCaMCA was cloned, expressed and purified successful, our next objective was testing the activity of this enzyme and procedure a biochemical study of tCaMCA soluble protein.

Financial support:

FAPESP, CNPq and FAEP

13.006 - CELLULAR RESPONSES IN NEUROBLASTOMA CELLS UNDER DIFFERENT CONDITIONS OF STRESS IN VITRO. Cogo SC, Brehm FA, Thomazini MEO, Mondini G, Elifio-Esposito S, - Laboratório Experimental Multiusuário - PUCPR

Introduction:

To survive under stress conditions, cells require mechanisms that enable to detect changes in the environment, introduce necessary responses, and resist. Tumor cells can overcome stress and modulate their fundamental intracellular processes in pro-survival responses. Neuroblastoma (NB) is a pediatric solid tumor of the sympathetic nervous system found in the medulla of the adrenal gland or along the paravertebral ganglion in the abdomen, chest, pelvis, or neck. NB cell lines reflect the high heterogeneity of NB tumors and are interesting models to investigate the effect of stress in cellular survival.

Aim:

FeSBE Annual Meeting 2019

Poster Sessions and Abstracts

The present study aims to analyze neuroblastoma cell lines responses under growth factor deprivation, hypoxia, and chemotherapeutic incubations.

Methods:

The study was carried out in three human neuroblastoma cell lines: SK-N-SH, SH-SY5Y, and CHLA-20. Cells were submitted to different stress conditions in vitro. Growth factor deprivation (incubation with DMEM supplemented with FBS 0.5%), hypoxia (1% and 5% O₂), and by the incubation with the topoisomerase inhibitor topotecan, for 24, 48, and 72h. Viability was assessed by the methylene blue assay. Apoptosis was determined by flow cytometry with the staining with Annexin V/7AAD kit, and 7AAD was used for cell cycle evaluation. The presence of acidic vesicles, for the suggestion of autophagy, was determined with acridine orange, also by flow cytometry.

Results:

SH-SY5Y cell line was the most resistant, as cells were able to grow even at the lowest FBS concentrations after 72 hours. Cell cycle analysis demonstrated no significant change in hypoxia and FBS deprivation, and the apoptosis assay showed the same. Treatment with topotecan induced a modest apoptosis response with 16% of cells positive for annexin-V. At the same conditions, SK-N-SH and CHLA-20 cells were more susceptible over time in all of the stress conditions assayed, with a reduction of 50% of viable cells in 24h in hypoxia 1%, compared with normoxia ($p < 0.05$), or FBS deprivation for 72h, compared with FBS 10% ($p < 0.001$). Treatment with topotecan presented 81% of annexin-V positive cells and a cell cycle arrest at the S-phase. Cell cycle analysis for SK-N-SH and CHLA-20 in hypoxia at 1% of O₂ showed a sub-G₀ increase, representing DNA fragmentation of SK-N-SH cells, and arrest in G₁-phase for CHLA-20. Under FBS deprivation, both cell lines showed the same significant increase of the G₁ phase when exposed to 0.5% concentration of fetal bovine serum in 48h, when compared with other concentrations and different times.

Conclusion:

The study revealed evidence of resistance of the SH-SY5Y to apoptosis as compared to the other neuroblastoma cell lines in different conditions, suggesting the activation of intracellular mechanisms to avoid apoptosis under stress conditions.

Financial support:

CAPES/COFECUB (15/2016), CAPES (PROSUC, código de financiamento 001), CNPq (PIBIC/PUCPR), Fundação Araucária - Paraná (PBA 03/2016).

13.007 - INFLUENCE OF IL-1B AND TNFA ON MOUSE MYOBLAST CELLS TRANSITION BETWEEN PROLIFERATION AND DIFFERENTIATION EVENTS. Alvarez AM, Silva NC, Pereira CO, Chudzinski-Tavassi AM, Teixeira C, Moreira V, - Pharmacology - UNIFESP Centre of Excellence in new Target Discovery - Instituto Butantan Pharmacology Laboratory - Instituto Butantan

Introduction:

Proliferation and differentiation of muscle quiescent cells (satellite cells) are essential steps for the beginning of muscular tissue regeneration after injury. C2C12 myoblasts cells have been recognized as relevant tools to study the molecular mechanisms involved in proliferation and differentiation of satellite cells, in a more advanced stage of muscle regeneration. It has been reported that inflammatory cytokines such as IL-1 β and TNF α are involved in myogenesis and induce the production of IL-6, an important mediator of proliferation and differentiation of muscle cells. However, the roles of IL-1 β and TNF α in skeletal muscle regeneration are still controversial.

Aim:

This study aims to investigate the roles of these cytokines in muscular regeneration, by analyzing their effects on proliferation and also in expression of myogenic transcriptional regulatory proteins involved in skeletal muscle differentiation.

Methods:

Murine skeletal muscle cell line C2C12 from ATCC was cultured in growth medium (DMEM - FBS 10%). For the experiments, cells were plated in 96-wells plates coated with 2% gelatin and then i) cultured for 48 h to study effects in proliferative state or ii) cells were washed with PBS 1x at 5th day and further cultured in differentiation medium (DMEM - HS 2%) for 72 h to study their progression to differentiation stage. At these time points, cells were incubated with each cytokine (10 ng/ml) for 24 h. Cell viability was determined by MTT and LDH assays; cell proliferation by BrdU incorporation; quantification of PGE₂ and IL-6 release was performed by EIA, and expression of the transcription factors evaluated by High Content Screening (HCS).

Results:

Any of the studied cytokines were able to interfere with C2C12 viability in both proliferated and differentiated cells. Treatment of cells with IL-1 β increased proliferation of myoblast cells and induced release of PGE₂ ($p < 0,05$) in comparison with untreated control cells. As expected, both IL-1 β and TNF α increased IL-6 release. In proliferated cells, the expression of the transcription factors PAX7 and MyoD were lower than that of Myf-5 ($p < 0,05$). Interestingly, myogenin expression was higher than that of the other transcription factors. Upon stimulation with either TNF α or IL-6, a reduction of the expression of PAX7, MyoD and myogenin was detected. In the stages that precede cell differentiation, myogenin expression was higher than that of MyoD ($p < 0,05$), but stimulation of cells with the studied cytokines did not modify the expression of any of the transcription factors in comparison with control cells.

Conclusion:

Our data confirm previous reports on the stimulatory effect of IL-1 β in myoblast proliferation and release of IL-6, and demonstrate for the first time the ability of this cytokine to induce the release of PGE₂ from satellite cells. In addition, a link between TNF α and release of IL-6 can be suggested, since both cytokines displayed an inhibitory effect on expression of the transcription factors MyoD and myogenin at the proliferative stage. This can explain their reported effects on differentiation process. Together, our data allow to improve the current evidence for the role of IL-1 β / TNF α /IL-6 axis in the regulation of skeletal muscle regeneration.

Financial support:

FAPESP/GSK

13.008 - E-NTPDASES INHIBITION REGULATES PROLIFERATION BY PI3K AND ERK PATHWAY AND MODULATES CELL DEATH OF RAT RETINAL PROGENITORS. Repossi MG, Pereira LA, Velloso JCC, Ullrich H, Ventura ALM, Fragel-Madeira L, - Department of Neurobiology - UFF institute of exact and nature sciences - UNILAB Institute of Chemistry - USP

Introduction:

Ectonucleotidases (E-NTPDases) are enzymes of plasma membrane that rapidly break nucleotides into nucleosides. Adenine nucleotides have an important role on retinal development, performing several functions through P₂ receptors.

Aim:

Based on this, our aim was to analyze the function of E-NTPDases in vivo during the retina development.

Methods:

Lister hooded rats with four postnatal days (P4) were anaesthetized by hypothermia and intravitreal injections of ARL67156 200 μ M (E-NTPDases inhibitor) alone or combination with MRS2179 100 μ M (selective antagonist of P₂Y₁ receptor) were performed. Cell proliferation was assessed by Ki-67 immunolabeling and cell death by TUNEL assay.

Results:

Expression of E-NTPDases was evaluated by Real-Time PCR at P0, P3 and P5 rat retina. We identified a higher expression of E-NTPDase 1 at P3 and P5 rat retina (P0= 2.97 \pm 1.3; P3= 11.38 \pm 3; P5= 12.01 \pm 3.6), but not for NTPDase 2, 3 or 8, suggesting that E-NTPDase 1 is a possible

FeSBE Annual Meeting 2019 Poster Sessions and Abstracts

candidate for the action of adenine nucleotides on neuroblasts proliferation. Treatment with ARL at P4 rats for 24 hours increased proliferating cell number by approximately 30% compared to control, in an age that cellular proliferation rate is low. However, P2Y1 receptor blockage reversed this effect (control= 4734.4 ± 71.4; ARL= 6096 ± 150.9; ARL+MRS= 5113.4 ± 182.2). Also, we demonstrated that the effect of ARL was mediated by PI3K and ERK, but not by PKC pathway (control= 4069 ± 131; ARL= 6121 ± 140; ARL+U0126 (p-ERK inhibitor)= 4665 ± 93; ARL+LY294002 (PI3K inhibitor)= 4260 ± 65; ARL+Q (PKC inhibitor)= 5748 ± 66). Furthermore, considering that retina differentiation occurs from center to periphery we analyzed if this effect was similar at both regions. This increase on proliferation rate was observed both in the periphery and center of the retina, although P2Y1 blockage could not reverse this effect in the center (control: periphery= 5721.8 ± 131.5, center= 4074.2 ± 190.3; ARL: periphery= 7350.4 ± 233.9, center= 4933.2 ± 113.7; ARL+MRS: periphery= 5484.6 ± 227.7; center= 4829.2 ± 295). However, cell proliferation induction was not sustained 48 and 72 hours after ARL injection compared to control (control: 48 hours= 4549 ± 141; 72 hours= 3937 ± 125.9; ARL: 48 hours= 4826.7 ± 245.9; 72 hours= 3890.7 ± 209.1). We further analyzed if E-NTPDases blockade was inducing cell death. Results showed that after 24 hours ARL decreased cell death by 40%, but after 48 hours of treatment, there was an increase by approximately 70% on TUNEL positive cells compared to control (control: 24 hours= 692 ± 61 ; 48 hours= 668 ± 38; 72 hours= 459 ± 66; ARL: 24 hours= 421 ± 38 ; 48 hours= 730 ± 86; 72 hours= 736 ± 113).

Conclusion:

Our data suggest that ectonucleotidases blockage increased proliferation of rat retinal progenitors cells dependently partially of P2Y1 receptor by PI3K and ERK pathway and this raise was counterbalanced through cell death program.

Financial support:

Capes, FAPERJ, CNPq and Proppi-UFF.

13.009 - ELECTRICAL STIMULATION THERAPY FOR ENHANCING CALCIUM MATRIX FORMATION: IN VITRO STUDY. Albiazetti GC, Santarosa PC, Melo KM, Mendonça FAS, Caetano GF, - Graduate Program in Biomedical Sciences, University Center of Hermínio Ometto Foundation – FHO| UNIARARAS - FHO

Introduction:

Reducing surgical failures and restoring bone structure and function has been the goal of researches involving bone regeneration, once the prevalence of bone diseases and bone traumas have been increasing, especially for the elderly population. Different therapies have been proposed for the management of these complex clinical situations. Aiming to study a less invasive approach for bone repair and the recognition of bioelectricity's role in tissue healing, the therapeutic application of electrical stimulation provides a rationale, as the bone is a piezoelectric tissue. The exogenous application of electric current at physiological levels plays a role in cellular and molecular signaling pathways. The application intensity ranging from 10 to 20µA was reported to stimulate bone repair by triggering the cell surface, affecting membrane-receptor complexes, ion-transporting channels and alkaline phosphatase production for calcium deposition. In addition, it promotes bone formation through the activation of growth factors, such as vascular endothelial growth factor (VEGF), and mRNA expression of BMPs. Nevertheless, therapeutic acceptance requires further investigations.

Aim:

The objective of the study was to evaluate the osteoblast viability and the calcium content submitted to in vitro microcurrent application at 10µA of intensity.

Methods:

The experimental protocol was approved by the ethical committee of Hermínio Ometto Foundation (087/2018). Around 1x10⁴ osteoblasts

(UMR-106 rat osteoblast lineage-ATCC®CRL-1661™) in 1mL of culture media (DMEM high glucose, 10% fetal bovine serum) were seeded in 24-well plates, divided according to the period of electrical application: 0s, 30s, 60s, 90s, 120s, 150s, and 300s (the last one based on in vivo protocol of our research group), placing two metal electrodes coupled to a low-intensity transcutaneous electrical stimulator at 10µA in the well covered with culture media. The applications were performed in two different ways: daily and every other day. The mitochondrial activity of osteoblasts was determined using MTT colorimetric assay in order to evaluate the cell viability up to 7 days (plate reader at 540nm). Moreover, osteoblasts were cultured in osteogenic media (200µM of ascorbic acid, 10mM of β-glycerophosphate and 0.5µM of dexamethasone) to evaluate calcium content using alizarin red S (30min) followed by the addition of 10% acetic acid (plate reader at 450nm) after 3, 5 and 9 days.

Results:

The results show that none of the electrical stimulation periods at 10µA presented in vitro cytotoxicity (p>0.05). Initially, the assay to evaluate the calcium content in the extracellular matrix by the osteoblasts submitted to the electrical stimulation was conducted daily with the longest period of 150s. Osteoblasts submitted to 60s and 150s application presented 50% higher calcium content compared to the control group and the other groups (p<0.05). As 60s and 150s presented satisfactory results and considering 300s (in vivo animal model, every other day), the group submitted to 300s presented 50% higher calcium content than the 60s and 150s, and these two were 100% higher than the control group (0s) (p<0.05).

Conclusion:

The electrical stimulation every other day during 300s presented no cytotoxicity in osteoblast and stimulated greater calcium production.

Financial support:

FHO

15 - Optical and Mechanical Technologies for Health

15.001 - ATMOSPHERIC PLASMA CONTROL THE INFLAMMATION AND ENHANCED TISSUE FORMATION ON THE REPAIR OF CUTANEOUS BURNS IN DIABETIC RATS. Mariano SS, Silva JIS, Bagne L, Lopes BB, Tavares A, Andrade TAM, - Programa de Pós-Graduação em Ciências Biomédicas - Centro Universitário da Fundação Hermínio Ometto

Introduction:

Second degree burns are more difficult to treat when compared to other injuries, due to the production of mediators and proinflammatory cytokines. This become worse with associated pathologies, like diabetes. Atmospheric Plasma (AP) is ionized gas that has been a relevant and promising alternative to wound healing, even when associated to diabetes.

Aim:

To evaluate the inflammation and tissue formation of AP on repair of second degree burns in diabetes-induced rats.

Methods:

Approved by CEUA-FHO (nº 030/2017). Diabetes was induced in 48 Wistar rats (±300g) using 45mg/kg of aloxane, intravenous. The glycemia was measured 7 days post-induction and only animals with glycemia above 200mg/dL was included. One dorsal burn of 2.0cm in diameter were performed for 20 seconds at 120°C. The groups were: SHAM, burns typically treated every day with device switched off and AP, treatment by Atmospheric Plasma (35seconds/cm², 30kHz, 50W, 1.0L/min of argon gas). Samples were collected from the lesion area at the 2nd, 7th, 14th and 21st days (n=6/group/time) for immunohistochemistry analysis (IL-1β, IL-10 and IL-17), Western blotting (VEGF, collagen I and III) and histomorphometric analysis (collagen by Ponceau-stained). The results were analyzed by t-Student (among groups in the same days) and ANOVA One-way/Tukey (among days in the same groups) (p<0,05) (MED±SEM).

FeSBE Annual Meeting 2019

Poster Sessions and Abstracts

Results:

On the 7th and 14th days, the AP group (7d: 65.33±5.75; 14d: 68.61±4.90) showed a higher level of IL-1 β compared to SHAM (7d: 49.65±3.50; 14d: 50.56±3.49). About IL-10, the AP (2d: 16.45±1.99; 7d: 32.19±5.11; 14d: 47.92±4.77) was gradually higher than SHAM (2d: 6.17±0.73; 7d: 10.23±1.09; 14d: 1.25±0.21) from 2nd to 14th days. For IL-17, similar to IL-10, AP (7d: 84.45±3.90; 14d: 91.06 ±3.18) was higher than SHAM (7d: 60.54±0.30; 14d: 61.19±3.78), suggesting inflammation control. Regarding to VEGF, AP was effective to induced angiogenesis on 2nd day (1.07±0.01) compared to SHAM (0.73± 0.02) and the AP group showed a reduction of VEGF of 2nd (1.07±0.01), 7th (0.87±0.08), 14th (0.77±0.03) compared to 21st day (0.44±0.002). This anti-inflammatory and angiogenic profile, probably enhanced the tissue formation: AP group on 14th to 21st day presented higher collagen aggregates (14d: 67.36±9.22; 21d: 60.28±10.02) to SHAM (14d: 32.59± 4.35; 21d: 30.08±1.97). Moreover, AP group on 2nd day (1.25±0.03) was higher collagen III than SHAM (0.58±0.008), and AP-21st day (0.28±0.02) presented lower than AP-2th day (1.25±0.03) and AP-7th day (0.70±0.02). About collagen I, AP group was higher on 7th (1.10± 0.02) and 21st (1.42± 0.02) than SHAM (7d: 0.97±0.03; 21d: 0.97±0.01).

Conclusion:

Atmospheric Plasma showed anti-inflammatory activity and angiogenesis increased, that could contribute to enhanced the tissue formation.

Financial support:

FAPESP, HERMÍNIO OMETTO FOUNDATION.

15.002 - ATMOSPHERIC PLASMA IN REPAIR OF EXCISIONAL SKIN LESIONS AT DIABETES-INDUCED RATS. Alves N, Lima ACS, Hummel LH, Mariano SS, Luciano LM, França DR, Adriano LC, Lopes BB, Santos GMT, ANDRADE TAM, - Programa de Pós-graduação em Ciências Biomédicas - Centro Universitário da Fundação Hermínio Ometto (FHO)

Introduction:

Complications in wound healing associated with diabetes are increasing and the investigations for effective healing therapies is important. Atmospheric Plasma (AP) is ionized gas that has been a relevant and promising alternative to wound healing, even when associated to diabetes.

Aim:

To evaluate the effect of Atmospheric Plasma on the repair of excisional skin lesions in diabetes-induced rats.

Methods:

Approved by CEUA-FHO (nº 061/2017); Diabetes was induced in 48 Wistar rats (\pm 300g) using 45mg/Kg of aloxane, intravenous. The glycemia was measured 7 days post-induction and only animals with glycemia above 200mg/dL was included (fasting glycemia). Excisional skin lesions were performed using 1.5 cm diameter punch. The groups were SHAM: lesions treated topically every day with the device switched off and AP: treatment by Atmospheric Plasma (35seconds/cm², 30kHz, 50W, 1.0L/min of argon gas). The lesions were photographed at the beginning day 0) at the end of the follow-up (2nd, 7th, 14th and 21st days) to quantify the area of the lesion by ImageJ to later calculate the re-epithelialization by WHR-wound healing rate using the formula [initial area - final area / initial area]. Samples were collected from the lesion area at the 2nd, 7th, 14th and 21st days (n=6/group/time) to be subsequently analyzed by histomorphometry (HE and Gomori trichrome) regarding to inflammatory infiltrate, angiogenesis, fibroplasia, collagen and hair follicle. The results were analyzed by t-Student (among groups in the same days) and ANOVA One-way/Tukey (among days in the same groups) (p<0,05) (MED±SEM).

Results:

About the inflammatory infiltrate, AP-7d (308.8±20.29) was more effective than SHAM (176.20±25.60) and compared to AP-2d (128.0±38.60), AP-14d (70.18±13.48) and AP-21d (27.84±3.43). Moreover, AP (18.50 ± 2.12) was important to improve the

angiogenesis on 14th day compared to SHAM (10.28± 2.80) and to AP-21d (9.06±2.38). In relation to fibroplasia, AP on 7th (118.50±30.47) and 21st days (126.30±20.66) was higher than AP-2d (15.57±2.45). Moreover, AP on 14d (118.50±30.47) was lower fibroplasia than SHAM (196.40±37.54). Regarding to collagenesis, the AP group on the 14th (63.54±2.04) was lower than SHAM (71.88±2.73), and AP on 14th (63.54±2.04) and 21st days (72.32±3.35) were higher collagenesis than AP on 2nd (41.29±3.54) and 7th (45.76±3.54), respectively, showing that AP not presented better fibroplasia and collagenesis than SHAM, but higher than AP-2d. About hair follicle, the AP group on 2nd (7.83±0.86) and 14th days (11.33±1.16) showed more quantity compared to SHAM (2nd: 3.95±0.88; 14th: 7.93±0.84). This stimuli on all phases of wound healing, probably could contribute to reepithelialization of wounds: AP group on 14th day already presented all of the lesions reepithelialization (1.00±0.001) compared to SHAM (0.98±0.01).

Conclusion:

AP favored all phases of wound healing, even associated with the pathology of diabetes, besides the proliferation of hair follicle.

Financial support:

FAPESP, HERMÍNIO OMETTO FOUNDATION.

15.003 - LOW-LEVEL LASER IRRADIATION AND PLATELET RICH PLASMA DECREASE SYSTEMIC NITRIC OXIDE AND ARTICULAR INDUCIBLE NITRIC OXIDE SYNTHASE EXPRESSION. Gonçalves AB, Bovo JL, Mendes MF, Esquisatto MAM, Bomfim FRC, - Laboratório de Biologia Molecular - FHO-UNIARARAS Programa de Pós-graduação em Ciências Biomédicas - FHO-UNIARARAS

Introduction:

Rheumatoid arthritis is an autoimmune and inflammatory disease with a higher incidence among women causing local pain, edema and articular problems. For control of the inflammatory process, drugs or therapy may be used, the application of low-level laser (LLL), which associated or not with other therapies such as platelet rich plasma (PRP), decrease cell flow and increase vasodilation and local healing.

Aim:

The aim of this study was to evaluate the systemic levels of nitric oxide (NO) and inducible nitric oxide synthase (iNOS) protein expression in articular tissue of an experimental model of rheumatoid arthritis treated with LLL and PRP.

Methods:

This study was approved by CEUA-FHO 077/2017. Thirty female Wistar rats with 200g±10g, ad libitum food, maintained in 12-h light-dark cycles were distributed into five groups (n=6): A (control), B (Sham, untreated arthritis), C (arthritis+PRP), D (arthritis+LLL), E (arthritis+PRP and LLL). In addition, four male Wistar rats were used to obtain PRP from 20 mL of whole blood after successive buffered centrifugations. Arthritis induction was performed after anesthetic (Ketamine [0,3 mL/kg]-Xylazine [0,1 mL/kg]) in groups B, C, D and E with 200 μ g of Zymosan injected into the right knee of the animals. After 24 hours of induction, 50 μ L of PRP (800.000 platelets) in the intra-articular region was applied to the animals of group C and E, while in groups D and E the LLL was irradiated with the following parameters: λ =808nm, nominal power of 25mW, power density of 100mW/cm², fluence of 20J/cm², 0,02mm² of beam area, time of 33 seconds, total energy of 0,825J with punctual application in the right patellar region of the animals. After seven days of induction, animals were euthanized by anesthetic deepening associated with cardiac exsanguination to samples collection. Systemic nitric oxide (NO) production was quantified by the accumulation of nitrite in the serum samples with 50 μ L of serum that were incubated with an equal volume of Griess reagent (1% sulfanilamide, 0,1% naphthylene diamine dihydrochloride, 2.5% H₃PO₄) at room temperature for 10 min. The absorbance at 550 nm was determined with a microplate reader. iNOS expression was performed by immunohistochemical reaction, briefly, knee sections were

FeSBE Annual Meeting 2019

Poster Sessions and Abstracts

incubated in citrate buffer to antigen recuperation, incubated in primary antibody (anti-iNOS), washed with PBS, incubated with secondary antibody (anti-mouse) and stained with DAB. Statistical analysis was performed with ANOVA test and Tukey post-test with 5% of significant level ($p < 0.05$).

Results:

NO systemic evaluation showed mean \pm SD values were significant among the groups, A (3.402 \pm 1.287) x B (7.735 \pm 1.314) $p=0.0043$, B x C (3.061 \pm 0.9385) $p=0.0043$, B x D (3.061 \pm 1,722) $p=0.0087$ and B x E (2.551 \pm 0.7270) $p=0.0079$. In the present study, the expression of iNOS was significantly different, mean \pm SD, between the groups A (2.867 \pm 1.246) x B (7.933 \pm 1.280), B x C (5.133 \pm 1.598), B x D (4.2 \pm 1.699) and B x E (4.267 \pm 1.534) all differences with $p < 0.0001$.

Conclusion:

Treatments with PRP and LBI were effective to decrease the systemic NO and iNOS expression in the joint tissue and the association of the two treatments were more effective in reducing these markers of joint and systemic inflammation and degradation.

Financial support:

PIC FHO-UNIARARAS/Propesq

15.004 - PLATELET RICH PLASMA ASSOCIATED TO LOW-LEVEL LASER THERAPY IMPROVES KNEE JOINT FUNCTION IN AN EXPERIMENTAL MODEL OF ARTHRITIS IN RATS. Bomfim FRC, Gonçalves AB, Esquisatto MAM, Filho GJL, - Laboratório de Biologia Molecular - FHO UNIARARAS Cirurgia - UNIFESP-EPM Programa de Pós-graduação em Ciências Biomédicas - FHO-UNIARARAS

Introduction:

Joint inflammation is related to several arthritis diseases and can contribute to synovial and cartilage damage. The acute inflammation is observed in acute and chronic joint disorders which can lead the patient to joint and motor incapacity. Treatment of joint inflammation is based on anti-inflammatory drugs, although platelet rich plasma and laser therapy can be useful as non-drug treatment.

Aim:

The aim of this study was to observe the effects of platelet rich plasma (PRP) associated to low-level laser therapy on articular cartilage (CA) damage and collagen fibers formation.

Methods:

After approval of FHO-UNIARARAS Ethics Committee, number 077-2017, thirty-four Wistar rats, three month of age and 200g \pm 10g, were maintained under 12h light-dark cycles and free food. Four male animals were euthanized by anesthetic overdose (Ketamine [300 mg/kg]-Xylazine [30 mg/kg]) to total blood collection (20mL) to order the PRP (2mL) by consecutive centrifugations. Thirty female animals were assigned into five groups (n=6): Control, Sham (arthritis), PRP (arthritis and PRP), Laser (arthritis and laser) and PRP-laser (arthritis and both treatments). The arthritis induction was performed with 200 μ g of Zymosan injected on right knee of all animals of groups Sham, PRP, Laser, PRP-laser after anesthetic application of (Ketamine [100mg/kg]-Xylazine [10mg/kg]). The PRP application follow the same anesthetic and induction protocol of arthritis with a PRP dose of 800.000platelets/50 μ L that were injected in groups PRP and PRP-laser. Laser and PRP-laser groups received low-level laser irradiation with the following parameters, $\lambda=808$ nm, power of 25mW, power density of 100mW/cm², fluence of 20J/cm², 0.02mm² of beam area, time of 33 seconds, total energy of 0.825J with punctual application in the right knee by single dose method. Knee samples were collected after seven days by anesthetic overdose as described before. For CA thickness (μ M) to evaluate the damage was performed Hematoxylin-Eosin stain and to evaluated the percentage of collagen fibers in area (% total area) was performed Picro-sirius red stain with and without polarized light. Statistical analysis was performed with ANOVA test and Tukey post-test with 5% of significant level ($p < 0.05$).

Results:

CA thickness, mean \pm SD, showed significant differences only between PRP-laser (141,8 \pm 10,10) and Sham (104,9 \pm 3,611) $p=0,0013$. Collagen fibers area (% area total) in mean \pm SD showed differences between Sham (60,07 \pm 1,604) and Control (22,13 \pm 2,120) $p < 0.0001$, Sham (60,07 \pm 1,604) and laser (54,40 \pm 1,778) $p=0,0149$ and Sham (60,07 \pm 1,604) and PRP-laser (51,53 \pm 2,686) $p=0,0091$.

Conclusion:

The association between the treatments improved and prevented the decrease of CA thickness and showed to be important to decrease the formation of collagen fibers which indicate fibrosis areas formation in synovial and CA region. The association between PRP and laser seems to be a promising therapeutic option and more studies are necessary to understand the function of laser as a PRP enhancer.

Financial support:

Propesq-FHO; CAPES-CNPq

16 - Gene and Cell Therapy, Omics Biology

16.001 - AT1A RECEPTOR SILENCING EFFECT IN MYOBLASTS AND FIBROBLASTS: FUTURE DIRECTIONS TO EXPLAIN MUSCLE FIBROSIS. Bartolomeo CS, Salles SMC, Ivanov GZ, Smaili S, Pereira GJS, Stilhano RS, - Ciências Fisiológicas - FCMSCSP Farmacologia - UNIFESP

Introduction:

Skeletal muscle injuries may be caused by direct trauma (laceration, contusions and distension) or indirect trauma (ischemia or neurological dysfunction). The process of injury and repair is similar in the most part of the cases, however the functional recovery of a muscle injury changes according to the type of the trauma. Although the most part of the muscle injuries have complete regeneration capacity without any intervention, severe muscle injuries leads to imperfect tissue regeneration with fibrotic tissue formation. Fibrosis leads to imperfect tissue regeneration, muscle contractures and chronic pain. In addition, this scar tissue formation tends to cause new injuries due to change in tissue nature and the loss of functionality. Angiotensin II (AngII) is an important hormone acting in the blood pressure regulation, however, recently it was described as having a pro-fibrotic role in skeletal muscle. Data from our group showed that the silencing of AT1a receptor led to an important fibrosis reduction in the skeletal muscle after laceration. However, it still unclear the role of AT1a receptor silencing effect in the muscle cells.

Aim:

We propose to evaluate the AT1ar silencing effect in the proliferation, differentiation and gene expression in fibroblasts and myoblasts from skeletal muscle.

Methods:

Myoblasts and fibroblasts were obtained by tibialis anterior muscle enzymatic digestion from C57Bl/6 mice (3 months) obtained from CEDEME-UNIFESP (CEUA nº 7169290118). We followed the replating protocol to obtain the cells of interest. For AT1a receptor silencing we used Agtr1a MISSION shRNA Plasmid DNA Mouse (Sigma), composed by 4 lentiviral plasmids coding different shRNAs for rAT1a. Myoblasts were differentiated into myocytes through differentiation media (DMEM, 2% HS, 1% Penicillin/streptomycin). Five days after, we observed nucleus fusion and muscle cell contraction. For proliferation we counted the cells with trypan blue and for viability we used the MTT assay. In addition, we analyzed the myogenic (Myod1, Pax7 e Myf5) and fibrogenic (Tgfb1, Col1a1, Vim) gene expression using qRT-PCR.

Results:

The shRNA 575 showed the highest down-regulation of Agtr1a expression when compared to the others, therefore it was chosen for next experiments. After silencing, fibroblasts changed their morphology, presenting a cuboid format different of elongated format of fibroblasts treated with SC (Scramble). Also, they presented a reduction in the proliferation. The myoblasts did not show any changes in the morphology and proliferation. However, after differentiation in

FeSBE Annual Meeting 2019

Poster Sessions and Abstracts

myofibers, the shrAT1a group presented a higher number of fibers when compared to SC control. The gene expression analysis in myoblasts did not change after silencing. However, in fibroblasts it was observed a down-regulation in the gene expression after silencing.

Conclusion:

The pro-fibrotic effect of AngII is already well described in literature and we know the silencing of rAT1a leads to fibrosis reduction in skeletal muscle laceration models. However, it still necessary clarify the therapeutic effect of this silencing.

Financial support:

FAPESP

16.002 - ENRICHMENT OF CULTURE MEDIUM INCREASES THE PRODUCTION OF DOUBLE-STRANDED RNA (dsRNA) IN THE PROBIOTIC BACILLUS SUBTILIS. Dall'Agno L, Riet JG, Santos KO, CostaFilho J, Marins LFF, - Instituto de Ciências Biológicas - FURG Instituto de Oceanografia - FURG Departamento de Bioquímica - USP

Introduction:

RNA Interference (RNAi) is a conserved biological mechanism triggered by double-stranded RNA (dsRNA) that inhibits gene expression at the transcriptional level by degrading a complementary mRNA. This mechanism is known to naturally regulate gene expression in eukaryotes through silencing. In this way, it is considered an important tool in genetic studies. Production and administration of these dsRNAs for activation of RNAi mechanism have been carried out in *Escherichia coli* HT115 strain (which may have pathogenicity because it is a gram-negative bacterium) or commercial kits (making it an expensive tool). Thus, probiotic strains are an alternative in the production of the dsRNAs, since besides being harmless, they can present beneficial properties and are easy to genetically transform. Additionally, nutrient availability is known to be one of the strongest influences on the growth and size of bacterial cells and may correspond to the growth rate and increase in the production of molecules by genetically modified bacteria.

Aim:

Within this context, the present project had as objective to optimize the production of double-stranded RNA in *Bacillus subtilis* KMO analyzing different nutrients concentrations in the culture medium and cell size.

Methods:

Bacillus subtilis KMO strain was genetically engineered by the CRISPR/Cas9 method, containing a viral gene and bidirectional promoter induced in the stationary growth phase. Bacteria were cultured in Spizizen medium, with glucose and casein hydrolyzate. Three different nutritional concentrations of the medium were tested, each being considered an experimental group: normal concentration (N group) (0.5% glucose and 0.02% casein hydrolyzate), two times concentrated (2X group) and four times concentrated (4X group) in relation to the normal concentration. Cultures were performed in triplicate with 250 rpm agitation overnight at 37°C to reach the stationary phase and induction of the gene promoter used. The dsRNAs were extracted from the cells by the method already used in *Escherichia coli* HT115, adding lysozyme at 20 mg/mL. Samples were observed on 1% agarose gel, quantification was done by 1DscanEX software and statistical analysis by t-test ($p < 0.05$). Cell size was observed by optical microscopy and analyzed by ImageJ software.

Results:

Statistics related to the production of dsRNAs showed that between N and 2X groups there was no significant difference, although the mean indicated a three-fold increase in dsRNA production. In comparison of 2X group versus 4X, the data were significantly different with a two-fold increase in the double-stranded RNA production. In comparison between group N and 4X, a significant difference was obtained with a ten-fold increase in the production of dsRNAs. There was also a two-fold increase in cell size between treatments.

Conclusion:

With these results, we can observe that the use of an enriched medium with glucose and amino acids significantly increases the production of double-stranded RNA in probiotic *B. subtilis*. Thus, it can be used as an alternative for increasing the production of dsRNAs in a wide range of genetic studies.

Financial support:

FAPERGS e CAPES

16.003 - NEUTROPHILS ACTIVATED BY THE SNAKE VENOM LECTIN BJCUL INCREASE NEUROBLASTOMA CELLS MIGRATION IN VITRO. Rodrigues BS, Goetten JOLC, Elifio-Esposito S, - Biologia - PUCPR

Introduction:

Neuroblastoma (NB) is a pediatric tumor derived from precursor cells of the sympathetic nervous system, with 50% of cases presenting a high relapse rate with local or distant metastasis, mainly to the bone marrow. Components of the immune system are involved in metastasis, sheltering immunosuppressive, as well as pro-tumoral activities, which promote survival, invasion, and dissemination of malignant cells. BJCul is a dimeric C-type lectin isolated from *Bothrops jararacussu* venom that has shown immunogenic and anticarcinogenic actions in previous works.

Aim:

The aim of this study was to investigate the potential of BJCul activated neutrophils in affecting the migration and viability of human NB cells in vitro.

Methods:

Neutrophils isolated from peripheral blood were stimulated with BJCul (2.5 µg/ml) for 1h or 24h. The supernatant (conditioned medium, CM) was collected and transferred to an SK-N-SH NB cell culture plate. Neuroblasts were evaluated for viability by the methylene blue test, and migration by Scratch Wound Healing, in which mechanical scraping was performed on the monolayer. Cell migration was then observed by light microscopy for 2 days. Alternatively, neutrophils were co-cultured with the neuroblasts and both treated with BJCul, followed by the same analyzes.

Results:

Our results showed that BJCul did not affect the viability of SK-N-SH cells, but interfered both directly and indirectly in the migration of these cells. The CM of neutrophils treated with BJCul for 1h and 24h increased the migration of neuroblasts by 45% ($p = 0.002$) and 50% ($p = 0.009$), respectively, compared to the untreated control. Whereas the neuroblasts co-cultured of neutrophils in the presence of BJCul for 1h and 24h increased migration in 20% ($p = 0.0237$) and 45% ($p < 0.001$), respectively when compared to the untreated control.

Conclusion:

We conclude that CM and the direct association between immune cells stimulated by BJCul can increase the migratory potential of neuroblasts.

Financial support:

Fundação Araucária, CAPES.

16.004 - ACTIVATION OF RNA INTERFERENCE (RNAI) MECHANISM OF LITOPENAEUS VANNAMEI SHRIMP BY DSRNAS PRODUCED BY THE PROBIOTIC BACILLUS SUBTILIS: A POTENTIAL TOOL IN THE CONTROL OF VIRUSES IN SHRIMP FARMING. Graminho JR, Dall'Agno L, Santos KO, Filho JC, Wasielecky WJ, Marins LFF, - Instituto de Ciências Biológicas - FURG Instituto de Oceanografia - FURG Departamento de Bioquímica - USP

Introduction:

Crustacean farming is one of the fastest growing sectors of aquaculture in the world. This intensive production has led the emergence of viral diseases such as White Spot Syndrome Virus (WSSV) and Infectious Myonecrosis Virus (IMNV). The natural RNA interference (RNAi) mechanism can be used for degradation of complementary viral mRNA

FeSBE Annual Meeting 2019

Poster Sessions and Abstracts

through the use of double-stranded RNAs (dsRNA). One way of producing these dsRNAs is through commercial in vitro transcription kits or by the gram-negative bacterium *Escherichia coli* HT115. However, the synthetic production is expensive and the use of *E. coli* can generate some pathogenicity to consumers. An alternative is the use of probiotics such as *Bacillus subtilis* as a producer of dsRNA due to its beneficial properties to the animals, in addition to easy genetic manipulation.

Aim:

Therefore, the objective of this work was the production of dsRNA by *B. subtilis*, as well as the validation of these molecules in the activation of RNAi-related genes of *Litopenaeus vannamei* shrimp.

Methods:

B. subtilis KM0 was genetically engineered by CRISPR-Cas9 method for insertion of essential WSSV and IMNV genes, controlled by a bi-directional promoter for dsRNA production. *B. subtilis* was cultured at 37°C overnight. After dsRNA were extracted according to the protocol used for dsRNA extraction of *E. coli* HT115 with addition of lysozyme 20 mg/mL. The dsRNAs were verified in 1% agarose gel, quantified in spectrometer and standardized to 3 µg/mL. The validation of dsRNAs was based on two treatments with 150 L tanks, in triplicate, with adult animals of 10 g average weight. The animals were acclimated for one week prior to injection and the initial and final biometry was performed. The treatments were divided in two groups: a control in which they were injected intramuscularly with saline solution (third abdominal segment), and the treated group in which it was injected with the dsRNAs at 3 µg/g of shrimp weight. The animals were fed daily according to 5% of biomass. After one week, survival was observed and haemolymph collected from 18 animals per treatment to extract RNA from hemocytes. Evaluation of the expression of *Dicer2*, *Argonaute2* and *Sid1* genes were performed through qPCR. Statistical analyzes were performed using Student's t-test ($p < 0.05$).

Results:

After 7 days of injection, no mortality was observed. In addition, no difference was observed between treated and control groups, showing that growth was not affected by dsRNA injection. Regarding the gene expression, the *Dicer2* gene was not induced by dsRNA treatment. On the contrary, *Sid1* and *Argonaute2* genes were significantly induced (1.5 and 2 times, respectively) by the dsRNAs produced by the probiotic after the experimental period.

Conclusion:

It was concluded that a single injection of dsRNAs produced by *B. subtilis* was able to activate the genes *Sid1* and *Argonaute2* related to RNAi mechanism. These results are similar to the previously reported for dsRNAs produced by *E. coli* HT115 in *Litopenaeus vannamei*. Thus, this probiotic strain can be applied in the production of dsRNAs against viral agents in the crustacean farming.

Financial support:

CNPq, FAPERGS e CAPES

16.005 - MULTIFUNCTIONAL LIQUID-CRYSTALLINE NANOPARTICLES LOADING TRIPTOLIDE AND TNF- α siRNA TO IMPROVE GENE SILENCING THERAPY: EFFICIENCY IN CUTANEOUS AND CELLULAR DELIVERY IN VITRO. Silvestrini AVP, Praça FSG, Bentley MVLB, - Programa de Pós-Graduação em Ciências Farmacêuticas da Faculdade de Ciências Farmacêuticas de Ribeirão Preto - USP

Introduction:

Liquid-crystalline nanoparticles (LCN) have been shown to be an excellent drug delivery platform for therapy and diagnosis. Internal ordering properties and the ability to supply hydrophilic, lipophilic or amphiphilic molecules, as well as biocompatibility and multifunctionality are characteristics that allow their use in the treatment of cutaneous or systemic diseases. In particular, there is a great deal of interest in the delivery of topical therapeutic agents

because of the reduction of side effects and increased patient compliance.

Aim:

In this context, we hypothesized in this work that LCN would provide the co-delivery of triptolide (TP) and small interfering RNA (siRNA) TNF α molecules as an anti-sense therapeutic agent with objective of improving the topical treatment of inflammatory skin diseases.

Methods:

LCNs were obtained from bulk phase dispersion composed of monoolein, oleic acid, TP, polymer and aqueous phase (8:1:0.04:0.5:89.5, w/w/w/w/w). LCN-TP were characterized morphologically by polarized light microscopy (PLM) and atomic force microscopy (AFM). Physical-chemical characteristics were obtained through small angle X-ray scattering (SAXS), dynamic and electrophoretic light scattering, nanoparticle tracking analysis (NTA), encapsulation efficiency and electrophoretic assays with siRNA. In vitro studies in Franz diffusion cells were performed to evaluate drug release and permeation/retention cutaneous. Quantitative and qualitative data were obtained by high performance liquid chromatography and confocal microscopy, respectively. Cell viability and transfection studies in normal human keratinocyte cells (HaCaT) were performed by resazurin assays and flow cytometry.

Results:

LCN were previously identified as hexagonal phase by PLM which was confirmed by SAXS, with a ratio of 1:√3:√4 peaks. AFM revealed predominantly spherical particles, as well as visco-elasticity characteristics. The NLC-TP had mean hydrodynamic particle size of 163.5 ± 0.06 nm, polydispersity index about 0.15 ± 0.003 and positive surface charge around to 11.3 ± 0.65 mV. NTA studies showed 4.28 x 10¹³ nanoparticles/ml while drug encapsulation efficiency was 90.3 ± 2.53%. LCN showed to be able to complex with siRNA, and to release it integrally in assays. In the Franz cell, the release kinetics of TP in LCN followed the Higuchi model, and it was able to penetrate the deeper layers of the skin, when compared to the control. The region of higher fluorescence intensity confirmed the retention of LCN in the epidermis and dermis. In HaCaT cells the IC50 of LCN-TP-siRNA TNF α was equivalent to 0.1792 µM and 417 nM for TP and siRNA, respectively, while for the free TP it was 0.0787 µM which represented a 2-fold higher cytotoxicity. The rate of cell transfection was above 70% in 2, 6 and 12 hours of NLC treatment and maintaining cell viability at 95%.

Conclusion:

We conclude that the developed LCN presented physicochemical characteristics that were important to improve the penetration of the TP and siRNA in the target tissue. The cellular studies provided decreased drug cytotoxicity when it was loaded by the nanocarrier as well as high rates of cellular transfection of the payloads. Together, these data highlight the potential of this multifunctional nanoparticle developed herein as delivery nanosystem for TP and siRNA to improve the gene silencing therapy efficacy, and above all, make possible future in vitro and in vivo investigations.

Financial support:

This work was developed within the framework of National Institute of Science and Technology of Pharmaceutical Nanotechnology (INCT-Nanofarma), which is supported by Fundação de Amparo à Pesquisa do Estado de São Paulo (Fapesp, Brazil, grant #2018/08235-9) and Conselho Nacional de Pesquisa (CNPQ, Brazil, grant #465687/2014-8).

17 - Basic & Clinical Pharmacology

17.001 - IMMUNOMODULATORY ACTIVITIES FROM LEAVES EXTRACTS OF *ANNONA MURICATA* LINN. IN NEUTROPHILS AND MACROPHAGES. Saraiva AL, Justino AB, Franco RR, Silva HCG, Espindola FS, - Institute of Biotechnology - UFU

Introduction:

FeSBE Annual Meeting 2019

Poster Sessions and Abstracts

Natural products have been used by humans as source of therapeutic agent. Plants have received special attention as source of bioactive molecules since plants with extensive traditional use are a rich source of phytoconstituents that provide health benefits against various diseases. *Annona muricata*, a member of Annonaceae family and native to the warmest tropical areas in South and North America, had widespread popular use and presents an extensive set of phytoconstituents. In addition, *A. muricata* have showed antiinflammatory proprieties in experimental models of diseases.

Aim:

Here, through in vitro studies, we described new anti-inflammatory properties of two fractions from leaves of *A. muricata*.

Methods:

Crude ethanolic leaves extract was partitioned with solvents in increasing order of polarity: hexane, dichloromethane, ethyl acetate, n-butanol and water. Residual solvents and water were removed using rotary evaporator and lyophilization, respectively. Antiinflammatory effects of fractions were investigated in isolated neutrophils and in primary culture of bone marrow-derived macrophages (BMDM) from C57BL/6 mice. Neutrophils were isolated from bone-marrow through Percoll® (63% and 72%) density gradient centrifugation. BMDM were generated from differentiation of bone marrow cells were differentiated with L929-cells conditioned medium (LCCM). In all experiments, neutrophils and BMDM were pre-treated during 30 minutes with leaves fractions from *A. muricata*. ROS generation were induced by opsonized zymosan and detected through luminol oxidation. Following lipopolysaccharide (LPS- 1µg/mL) stimulus during 24h, IL-6 and TNF-α levels were determined in supernatant of BMDM culture through ELISA assay; expression of CD40 and CD80 were also evaluated through flow cytometry. Statistics were generated with One-Way ANOVA and Student-Newman-Keuls posttest for individual comparisons between groups. Animal procedures were approved by local ethics committee (protocol 032/18).

Results:

Analyzing ROS production by neutrophils, we performed a dose-response curve with each fraction at concentration of 1, 3 and 10 µg/mL. Ethyl acetate (EtOAc) and n-butanol (BuOH) fractions exhibited highest activity reducing ROS in a dose-dependent manner. Thus, we decided to study the effects of only EtOAc and BuOH fractions; at concentration of 3 µg/mL, EtOAc and BuOH reduced ROS production by BMDM after opsonized zymosan stimulus. Next, we evaluated the levels of cytokine secreted by BMDM upon LPS stimulation; pre-treatment with EtOAc and BuOH reduced the levels of IL-6 and TNF-α. Besides, we showed that EtOAc and BuOH reduced expression of CD40 following LPS stimulus.

Conclusion:

Although ROS generation is one of the main mechanisms that neutrophils and macrophages use against infections, excessive ROS contributes to tissue damage in inflammatory diseases. Thus, inhibitory effect of EtOAc and BuOH on ROS production could be exploited in the control of tissue damage associated to inflammation. TNF-α and IL-6 are secreted by macrophages to augment the inflammatory response. Besides, CD40 activation promotes further secretion of TNF-α and IL-6. Reduction of CD40 expression by EtOAc and BuOH could explain their effects on reduction of TNF-α and IL-6 secretion. Thus, our results suggest that EtOAc and BuOH extracts from leaves of *A. muricata* presents bioactive molecules which could be used for development of new antiinflammatory therapies.

Financial support:

CAPES, FAPEMIG

17.002 - PHOTOPROTECTIVE EFFECT OF THE BELLIS PERENNIS EXTRACT IN HUMAN KERATINOCYTES. Carvalho VMS, Covre JL, Lice I, Gil CD, - Morfologia e Genética - UNIFESP

Introduction:

Overexposure to ultraviolet (UV) radiation without suitable protection (i.e., sunscreen and clothing) has been implicated in mutagenesis and the onset of skin cancer. Furthermore, there are reports raising the question about a negative impact of specific UV filters on our environment causing among other things coral bleaching. There is need for more studies elucidating the benefit of photoprotective agents against UV with the aim to be environmentally safe at the same moment. In this regard, plant extracts represent a human friendly alternative formulation.

Aim:

This study was designed to evaluate the potential use of *Bellis perennis* extract (BPE) in cosmeceuticals as photoprotective factor, using an in vitro model of UVA-induced keratinocyte damage.

Methods:

HaCaT cells (human keratinocyte cell line) were incubated with BPE at 0.01, 0.1 or 1% in DMEM, and after 15 minutes they were submitted to UVA irradiation at 30, 60 and 90 min which resulted in accumulated doses of 5, 10 and 15 J/cm², respectively (CEP nº 9835191018). For comparative purposes, *Polypodium leucotomos* extract (PLE) were used as positive control of photoprotective effect. After 24 hours of UVA exposition, the cell viability assay was performed by MTT and LDH. Immunofluorescence analysis of cells was performed to study cleaved caspase 3 expression and reactive oxygen species detection (ROS). The toxicity of the plant extracts was also evaluated by the MTT assay at 24, 48 and 72 hours. Both plant extracts are standardized raw materials, certified by ANVISA (BPE - CAS 84776-11-4; PLE - CAS 76822-21-4) and were kindly given by Bio Farma compounding pharmacy (Promissão, Brazil).

Results:

Incubation of keratinocytes for 24-72 hours showed that both extracts at the three tested concentrations are non-cytotoxic. UVA radiation of the keratinocytes for 30, 60 and 90 min induced cell viability of 63%, 43% and 23%, respectively, showing that 60 min-timepoint as more suitable for our study. After 24 h of the last exposure to UVA (60 min), 1% BPE significantly increased cell viability compared to the cells exposed to UVA alone ($p < 0.05$). These findings were confirmed by the immunostaining of cleaved caspase-3 and ROS (biological markers of death and cell damage) in the cytoplasm of the keratinocyte, whose levels were significantly reduced after treatment with 1% BPE and 1% PLE in relation to UVA-radiated cells and without treatment ($p < 0.01$).

Conclusion:

Our in vitro results show photoprotective effect of 1% BPE on keratinocytes and support its use in the preventive treatment of sunburning and skin pathologies associated with UV-mediated damage.

Financial support:

FAPESP (2017/26872-5).

17.003 - CYTOTOXICITY OF EXTRACTS FROM LEAVES OF CASEARIA SYLVESTRIS AND THEIR MEDICAL POTENTIAL. Ambrosio FN, Lombello CB, Silva FD, - Centro de Ciências Naturais e Humanas - UFABC Centro de Engenharia, Modelagem e Ciências Sociais Aplicadas - UFABC

Introduction:

With a great potential not yet explored, the Brazilian flora biodiversity represents an opportunity for studies that seek identify new active compounds present in vegetal species. Extracts from the plant *Casearia sylvestris* (Cs) are utilized in popular medicine for diverse treatments, such as anti-inflammatory, snake bites and antiseptic. Searching into patents databank GooglePatent revealed that exist 29 patents about Cs and in Brazil, within the INPI database, this number drops to 9, which suggests an underexplored commercial potential.

Aim:

The objective of this work was to evaluate the cytotoxicity of different extracts from Cs as means to investigate the possibility for medical applications.

Methods:

FeSBE Annual Meeting 2019

Poster Sessions and Abstracts

Dry leaves of *Cs* were used for the preparation of the extracts and the solvents were water at 22° C (Cs-W), water at 70° C (Cs-HW), ethanol (Cs-Et) and methanol (Cs-Met). The solvents were removed by lyophilisation for the aqueous extract and rotoevaporation for the alcoholic extracts. The extracts were resuspended in distilled water for quantification. Cells from Vero lineage were selected for the in vitro cytotoxic essays and were cultivated with HAM-F10 medium at 37° C with 5% CO₂. In a multiple well plate, with cells at semi-confluence, the extracts were tested at the concentrations of 1000 µg/mL, 100 µg/mL, 50 µg/mL and 25 µg/mL. Additionally, DMSO (50 %, v/v) was used as positive control and non-treated cells as negative control. After 24 h of incubation, the cytotoxic potential of the extracts was evaluated by analysis of the cell morphology at an inverted phase contrast microscopy and by cell viability via MTT colorimetric assay.

Results:

The results showed that none of the extracts were cytotoxic at the tested concentrations, with no significant morphological changes and cell viability above 70% when compared to the negative control.

Conclusion:

In conclusion, aqueous and alcoholic extracts from the leaves of *C. sylvestris* did not exhibited cytotoxic activity at concentrations of 1000 µg/mL or lower, and so, further studies of their medical applications potential can be performed.

Financial support:

No financial support was available for this work until the present date.

17.004 - NEW DPP-4 INHIBITOR ATTENUATES METABOLIC DISTURBANCE AND IMPROVES CARDIOVASCULAR FUNCTION IN ZUCKER DIABETIC FATTY RATS. Montagnoli TL, Costa GC, Alencar AKN, DaSilva JS, Silva MMC, Alves BEO, Gamba LER, Lima LM, Barreiro EJ, Sudo RT, Zapata-Sudo G, - Programa de Pós-graduação em Farmacologia e Química Medicinal - UFRJ Programa de Pós-graduação em Cardiologia - UFRJ Programa de Pesquisa em Desenvolvimento de Fármacos - UFRJ

Introduction:

Diabetes mellitus type 2 is a chronic disease characterized by insulin resistance and systemic inflammation that leads to cardiac and renal complications. Drugs with hypoglycemic and anti-inflammatory action would be essential to slow the progression of the disease and reduce cardiovascular comorbidities. LASSBio-2090 is a new hybrid compound designed as dipeptidylpeptidase-4 inhibitor with anti-inflammatory property.

Aim:

Pharmacological effects were investigated after administration of LASSBio-2090 in Zucker diabetic fat (ZDF) rats.

Methods:

Protocols (CEUA 005/18) were approved by Animal Care and Use Committee at Federal University of Rio de Janeiro. Male and female Zucker diabetic fatty (ZDF) rats (24-32 wks old) were treated with LASSBio-2090 (100 µmol/kg/day i.p.) or DMSO during 14 days. Zucker lean (ZL) littermates received DMSO and were used as control group (n= 6). After two weeks, lipid profile was evaluated and cardiac function and morphology were analyzed by echocardiography. Hemodynamic parameters were recorded after introduction of a catheter into left ventricle (LV). Picro-sirius red staining and western blot were used to quantify collagen and inflammatory proteins expression (TNF-α/GAPDH, iNOS/GAPDH) in cardiac tissue. Statistical analysis was performed using one-way ANOVA and t-test.

Results:

ZDF rats showed elevation of plasma insulin from 0.25 ± 0.02 (ZL) to 0.44 ± 0.03 nM, cholesterol from 2.3 ± 0.2 (ZL) to 5.2 ± 0.5 mM and triglycerides from 0.3 ± 0.1 (ZL) to 1.1 ± 0.1 mM ($p < 0.05$). LASSBio-2090 attenuated metabolic syndrome in ZDF by reducing insulin to 0.26 ± 0.02 nM and cholesterol to 2.6 ± 0.1 mM ($p < 0.05$). ZDF showed increased filling pressure (E/e') of 38.2 ± 0.1 and LV end diastolic pressure (LVEDP) of 14.8 ± 1.8 mmHg when compared to 18.0 ± 1.2 and

5.0 ± 0.8 mmHg for ZL ($p < 0.05$). Cardiac output (CO) and ejection fraction (EF) were reduced in ZDF+DMSO from 130.0 ± 10.4 (ZL) to 70.6 ± 5.2 mL/min and from $62.6 \pm 2.2\%$ (ZL) to $45.4 \pm 1.8\%$ ($p < 0.05$), respectively. LV systolic pressure (LVSP) was also elevated from 92.4 ± 4.1 mmHg in ZL to 123.6 ± 4.7 mmHg in ZDF+DMSO ($p < 0.05$). LASSBio-2090 improved diastolic and systolic function by reducing E/e' to 17.7 ± 2.8 , LVEDP to 5.4 ± 1.8 mmHg, LVSP to 98.6 ± 10.0 mmHg and elevating CO to 139.1 ± 15.5 mL/min and EF to $61.2 \pm 1.4\%$ ($p < 0.05$). ZDF+DMSO rats had increased LV relative wall thickness (RWT) from 0.38 ± 0.01 to 0.48 ± 0.04 and collagen content from $4.0 \pm 0.2\%$ to $5.9 \pm 0.2\%$ ($p < 0.05$) and LASSBio-2090 reverted RWT to 0.29 ± 0.1 and collagen to $3.86 \pm 0.3\%$ ($p < 0.05$). LV in ZDF group showed elevated TNF-α/GAPDH (1.0 ± 0.2) and iNOS/GAPDH (1.4 ± 0.3) and LASSBio-2090 reduced protein densities to 0.5 ± 0.2 and 0.5 ± 0.2 ($p < 0.05$), respectively.

Conclusion:

LASSBio-2090 improved LV function and morphology and attenuated the inflammatory status induced by diabetes.

Financial support:

INCT/INOFAR, CAPES, CNPq, FAPERJ

17.005 - CLONING, EXPRESSION AND PURIFICATION OF CRK3 CYCLIN-DEPENDENT KINASE OF LEISHMANIA MAJOR. Paula ALM, Siqueira FS, Oliveira VC, Judice WAS, - Centro Interdisciplinar de Investigação Bioquímica - UMC

Introduction:

CRK3 is a cyclin-dependent serine/threonine kinase (CDK) protein that is active in the two life stages of the Leishmania major parasite, playing an important role in its cell cycle. It is present in the transition from G2 phase (mitosis staging phase) to M (mitotic phase) being responsible for catalyzing protein phosphorylation by transferring an ATP or GTP phosphate group or a hydroxyl group of the amino acid side chain threonine, serine or tyrosine residues because it has a catalytic domain where an ATP molecule is bound. Therefore, this binding is reversible and responsible for extra and intracellular stimuli, providing an efficient mechanism for the modulation of its activity. Because it is a CDK, it is inactive in its monomeric form, needing to be bound to cyclin 6 (CYC6) in order to be activated, to promote the phosphorylation of certain sites by proceeding with the normal functioning of the cell cycle.

Aim:

Our goal was perform the cloning, expression, and purification of the enzyme cyclin-dependent kinase of Leishmania major.

Methods:

The commercial cDNA genes of CRK3 and CYC6 were amplified by PCR and product was purified. The cDNA inserts and the pET 28 (a +) vector were digested with *Sla* I and *Xba* I). cDNA CRK3 and CYC6 inserts were ligated separately at pET 28 (a +) vector forming recombinant DNA plasmids. The plasmids pET28-CRK3 and pET28-CYC6 plasmids were introduced separately into competent DH5a bacteria and positive bacterial colonies were confirmed by PCR using T7 primers, and after amplified. BL21 (DE3) were cotransformed with pET28-CRK3 and pET28-CYC6 plasmids and positive colonies analyzed by PCR. Clones with both plasmids were submitted at protein expression induced by 0.8 mM of IPTG. The expression was analyzed by SDS-PAGE. The protein was purified by nickel column affinity chromatography and eluted with imidazole.

Results:

Gene amplification exhibited a single band containing ~ 1019 bp consistent with the size of the CRK3 gene and a single band containing ~ 995 bp matched to the size of the CYC6 gene. *Sla* I and *Xba* I digestion of the vector and the CRK3 gene was confirmed containing bands with ~ 966 bp, ~ 942 bp and ~ 5366 bp corresponding respectively to the digested CRK3, CYC6 and vector. Colony PCR confirmed the transformation of DH5α with plasmids. To expression of proteins, BL21 (DE3) were cotransformed with both plasmids and insertion confirmed by PCR. The coexpression of the protein was confirmed with 15%

FeSBE Annual Meeting 2019 Poster Sessions and Abstracts

acrylamide SDS-PAGE gel by the presence of a 38 kDa band related to CRK3 and a 35 kDa band related to CYC6.

Conclusion:

The clones of the *Leishmania major* CRK3 and CYC6 genes were successfully obtained. BL21 cotransformation was positive by agarose electrophoresis. Coexpression of CRK3 and CYC6 were confirmed in the SDS-PAGE analysis.

Financial support:

FAEP, FAPESP, CNPq, CAPES, OMEC

18 - Neuropsychopharmacology

18.001 - REPEATED ADMINISTRATION OF A SELENIUM-CONTAINING COMPOUND REVERSES LONG-TERM ALTERATIONS INDUCED BY LIPOPOLYSACCHARIDE IN MICE. Lourenço DA, Casaril AM, Domingues M, Bampi SR, Savegnago L, - Centro de Desenvolvimento Tecnológico - UFPEL Mainz Research School of Translational Biomedicine - JGU

Introduction:

Major depressive disorder affects more than 300 million people globally (WHO, 2017). Nevertheless, currently available pharmacological treatments have limited efficacy (Gartlehner et al., 2017), prompting the research of better antidepressant molecules. Intraperitoneal administration of lipopolysaccharide (LPS) - a highly validated animal model of depression-like behavior - leads to behavioral and neurochemical alterations (Kluger, 1991; Dantzer et al., 2011).

Aim:

In light with this, the aim of this study was to evaluate the ability of the selenium-containing compound 3-((4-chlorophenyl)selenanyl)-1-methyl-1H-indole (CMI) in reversing long-term behavioral and neurochemical alterations induced by LPS in mice.

Methods:

The CMI was synthesized according to Vieira et al. (2015) dissolved in canola oil and administered intragastrically at 1 mg/kg. LPS from *Escherichia coli* (0127:B8) (Sigma Aldrich, St. Louis, USA) was diluted in saline solution and administered by intraperitoneal route at 5 mg/kg. Experiments were conducted using male Swiss mice (25-30g), maintained at 22-25°C with free access to water and food, under a 12:12 light/dark cycle. The study was conducted in strict accordance with the recommendations of the Committee on the Care and Use of Experimental Animal Resources at the Federal University of Pelotas, Brazil (8331-2017). Animals were randomly divided into four experimental groups (n=6 mice/group). LPS was administered on day 0, and CMI was administered on days 23 to 29. On day 30, the behavioral tests were conducted. After that, mice were euthanized by cervical dislocation, followed by brain removal and isolation of the prefrontal cortex (PFC) and total hippocampus (HC) for analysis (Sunkin et al., 2013). The depression-like behavior was analyzed by the forced swimming test (FST), while cognitive impairment was evaluated by novel object recognition (NOR) test. Biochemical alterations were analyzed by thiobarbituric acid reactive species (TBARS) and evaluation of acetylcholinesterase (AChE) activity. Data were analyzed by two-way analysis of variance (ANOVA), followed by Tukey's post hoc test. Values were considered statistically significant when $p < 0.05$. The statistical analysis was accomplished using GraphPad Prism version 7.0 for Windows, GraphPad Software (San Diego, CA, USA).

Results:

As expected, LPS-treated mice exhibited increased immobility time in the FST; however, the administration of CMI for 7 days abolished the LPS-induced depressive-like behavior (LPS x CMI interaction, $F(1,20) = 44.6, p < 0.001$). The administration of CMI also reversed the cognitive impairment induced by LPS in the NOR test, as evidenced by a significant LPS x CMI interaction ($F(1,20) = 55.7, p < 0.001$). Additionally, the treatment with CMI reversed the increased lipid peroxidation in the PFC (LPS x CMI interaction, $F(1,20) = 55.9, p < 0.001$) and HC (LPS x CMI interaction, $F(1,20) = 11.1, p < 0.003$) of

challenged mice. LPS administration increased AChE activity in the PFC and HC, which was reversed by treatment with (LPS x CMI interaction, $PFC F(1,20) = 7.92, p < 0.01, HC F(1,20) = 12.9, p < 0.002$).

Conclusion:

Altogether, the present study showed that LPS administration at 5 mg/kg induced long-term alterations in behavior and neurochemical parameters. Repeated treatment with CMI for 7 days reversed these alterations, suggesting its antidepressant-like and antioxidant effects. Nonetheless, more studies are being conducted in order to investigate the molecular mechanism of action of this selenium-containing compound.

Financial support:

CAPES, CNPq, FAPERGS, UFPEL

18.002 - EFFECTS OF REPEATED KETAMINE EXPOSURE ON BEHAVIOR, ACETYLCHOLINESTERASE ACTIVITY AND CORTISOL IN ADULT ZEBRAFISH. Michelotti P, Marion JC, Franscescon F, Rosemberg DB, Pereira ME, - Departamento de Bioquímica e Biologia Molecular - Universidade Federal de Santa Maria (UFSM)

Introduction:

Ketamine is a non-competitive antagonist of N-methyl-D-aspartate (NMDA) glutamate receptor that induces analgesia and anesthesia. Although ketamine displays anxiolytic and antidepressant properties, it may induce pro-psychosis and hallucinogen effects, as well as stereotypic behaviors following acute administration at sub-anesthetic doses. Zebrafish (*Danio rerio*) is a small teleost widely used in behavioral neuroscience research. Because neurotransmitter and hormonal disorders are involved in neuropsychiatric conditions contributing to hallucinations, delusions, aggressive-like and anxiety, and stereotypic responses, we hypothesize a role of ketamine in modulating such behaviors.

Aim:

Thus, we investigated the effects of repeated exposure at sub-anesthetic concentrations of ketamine on aggression, locomotion, anxiety-like responses, as well as the brain acetylcholinesterase activity and whole-body cortisol levels in adult zebrafish.

Methods:

Adult short fin wild type (WT) zebrafish (*Danio rerio*) with 4-6 months-old and in a 50:50 (male: female) proportion was used. Animals were exposed to ketamine (2, 20 and 40 mg/L) for 20 minutes/day, for 7 consecutive days. Biochemical measures were performed at 8th day (n = 4-9), immediately after behavioral analyses. Locomotion, exploration, and anxiety-like behaviors were measured using the novel tank diving test (n = 11-16). Aggression was measured using the mirror-induced aggression task (n = 11-16). All behaviors were analyzed for 6 min using the ANY-Maze™ software. Results are expressed as a means ± standard error of the mean (S.E.M.) and differences between control and ketamine groups were determined using one-way ANOVA followed by Student-Newman-Keuls multiple comparison test. Significance was set at $p \leq 0.05$. All protocols were approved by the Ethics Commission on Animal Use of the Federal University of Santa Maria (protocol number 6894010616).

Results:

Ketamine did not alter aggression-, anxiety-like behavior, and locomotion in zebrafish. However, 40 mg/L ketamine elicited stereotypic behaviors, such as circular swimming when compared to other groups ($F(3,55) = 9.191, p < 0.0001$). Moreover, ketamine did not change acetylcholinesterase activity and whole-body cortisol content.

Conclusion:

In conclusion, we show that repeated ketamine exposure at sub-anesthetic concentrations does not change aggression- and anxiety-like responses in zebrafish. Although more studies are needed to elucidate the mechanisms underlying the effects of ketamine, 2 mg/L had a tendency to increase aggression (59%), whereas 20 mg/L ketamine showed a tendency to be anxiogenic and to reduce cortisol levels. Our

FeSBE Annual Meeting 2019

Poster Sessions and Abstracts

data corroborate the growing use of zebrafish in translational neuropsychiatric research as a model organism to investigate the effects of sub-anesthetic ketamine concentrations on behavioral and biochemical parameters.

Financial support:
CNPq, CAPES

18.003 - REDUCTION IN LONG-TERM POTENTIATION (LTM) AND INCREASE IN A2A RECEPTORS IN THE BLOOD OF OLD RATS AND DOGS ARE LINKED TO COGNITIVE DECLINE: A TRANSLATIONAL STUDY. Abrão GS, Pereira AAR, Toricelli M, Buck HS, Viel T A, - Farmacologia - USP

Introduction:

The characterization of biomarkers that indicate the cognitive status in the aging process is of great relevance for diagnosis and/or early treatment. It is already known that the increase of A2A receptor in the brain is related to cognitive deficits.

Aim:

The aim of this study was to verify whether A2A levels in the blood of rats can be linked to the loss of memory and levels of the same receptor in the brain. Also the same relationship was evaluated concerning dogs' aging, cognition and blood levels of A2A.

Methods:

Young (n=12, 3 months old) and old (n=12, 24 months old) female Wistar rats were submitted to the novel object recognition test to verify short and long-term memories. After that, they were anesthetized and the hippocampus was extracted. Cognition of young (n=10, 1-2 years old) and old (n=12, over 10 years old) dogs, both sexes, was evaluated using a questionnaire applied to the dogs owners (the greater the score, the worst the cognition). The blood (5 mL) was collected from the jugular vein. Density of proteins related to LTP and memory formation was evaluated by western-blotting and ELISA. Data were expressed as means \pm SEM and compared using Student-t test ($p < 0.05$). Ethical committee approved number ICB/USP: 2888070118.

Results:

Old rats presented loss in short and long-term memories (STM: -0.26 ± 0.06 ; LTM: -0.18 ± 0.07 , $p < 0.0001$), when compared to young. Besides, it was observed an increase of 2.06 fold in NMDA-R2B ($p < 0.0001$) and AMPA2-3-4 ($p < 0.001$) receptors (young: 0.29 ± 0.02 A.U. and 0.31 ± 0.03 A.U., respectively). Confirming the synapse stability and LTP disruption, reduction of 68.13% ($p < 0.0001$) in PSD-95 and 35.29% ($p < 0.01$) in synaptophysin levels was verified in old animals (young: 0.91 ± 0.09 A.U. and 0.85 ± 0.06 A.U., respectively) in addition to decrease of 38.80% ($p < 0.01$) in CAMK-IV and 29.08% in BDNF levels ($p < 0.05$) and 64.67% decrease in phosphoCREB/CREB relationship ($p < 0.01$) (young: 0.67 ± 0.06 A.U., 1054.00 ± 85.33 pg/ μ g and 1.34 ± 0.22 A.U., respectively). Also, a significant increase of 3.09 in pro-BDNF of old animals ($p < 0.0001$) (young: 0.23 ± 0.03 A.U.) was verified. Confirming the disruption in memory formation in old animals, density of A2A receptors was increased in 3.29 fold (young: 0.24 ± 0.05 A.U., $p < 0.001$). When analyzing BDNF and A2A receptors in rats' blood, an equivalent profile was confirmed: decrease of 50.07% in BDNF ($p < 0.001$) and increase of 2.34 fold in A2A receptors ($p < 0.001$) (young: 127.5 ± 14.25 pg/ μ g and 0.35 ± 0.04 A.U., respectively). Old dogs also presented significant decrease in cognition, as the score was 1.64 greater when compared to young animals ($p < 0.01$). Decrease of 78.01% in BDNF levels ($p < 0.05$) and increase of 6.96 fold in A2A receptors ($p < 0.0001$) was also verified (young: 2.82 ± 0.91 pg/ μ g and 0.25 ± 0.05 A.U.).

Conclusion:

LTP markers are altered in brains and blood of old rats and in the blood of old dogs. It is suggested, for the first time, that the increase in A2A receptor in the blood is also related to loss of memory in old animals, both rats and dogs. Those receptors could be taken as potential biomarkers of cognitive decline and maybe therapeutic targets for dogs with cognitive dysfunction.

Financial support:
CAPES, FAPESP

18.004 - THE ROLE OF LOCUS COERULEUS IN THE SPATIAL MEMORY IN A 6-OHDA ANIMAL MODEL OF PARKINSON'S DISEASE. Bustelli IB, Nunes TA, Oliveira LM, Caetano AL, - Departamento de Ciências Fisiológicas - FCMSCSP Instituto de Ciências Biomédicas - USP

Introduction:

Parkinson's disease (PD) is a chronic and progressive neurodegenerative disease, characterized by loss of dopaminergic neurons of the substantia nigra (SN). Patients with PD present non-motor preclinical symptoms such as changes in sleep, depression and autonomic nervous system dysfunction. Those non-motor symptoms use to show up before the classical motor symptoms in PD (tremor at rest, muscle stiffness, bradykinesia, hypokinesia, and changes in posture and balance), seems to be related to the neurodegeneration of the Locus coeruleus (LC). Data from the literature showed that ventral tegmental area (VTA) inputs the dorsal hippocampus promoted hippocampal reactivation during sleep and memory stabilization, but it has been verified that only 10% of this projection releases dopamine, suggesting that another area could be responsible for the activation of dopaminergic receptors in the hippocampus. Dopamine is removed from the hippocampal synapses by the norepinephrine transporter, indicating that it may be released by noradrenergic neurons. Although indirect action via VTA has not been ruled out, LC stimulation has been shown to increase dopamine levels in the prefrontal cortex, suggesting that LC efferences are not purely noradrenergic but also release dopamine in the dorsal hippocampus, improving implicit attention to spatial memory.

Aim:

Therefore, the aim of this study is to verify if selective lesion of LC is able to promote alterations in the spatial memory of rats submitted to a PD model.

Methods:

Male Wistar rats (250-300g) received bilateral injections of 6-hydroxydopamine (6-OHDA) or vehicle into the striatum ($24 \mu\text{g}/\mu\text{L}$) and LC ($24 \mu\text{g}/0.5\mu\text{L}$) or double injection (n=7/per group), approved by CEUA-FCMSCSP 014/16. The behavioral tests were analyzed by Morris Water Maze (MWM) and Object Localization (OL). In the end, a immunostaining was performed to quantify the lesion in the SN and LC.

Results:

Bilateral injection of 6-OHDA in the CPU elicited reduction of 65% and 80% catecholaminergic neurons in the SN (1074 ± 206 vs. vehicle: 376.5 ± 38 , $P < 0.05$) and LC (517 ± 365 vs. vehicle: 99 ± 4.24 , $P < 0.05$) respectively (t-student test). In the spatial memory, animals that received 6-OHDA into CPU, LC and the double injection groups showed deficit in learning and spatial memory compared to the control group (52.39s ; 46.21s ; 40.50s vs. vehicle: 21.71s ; $P < 0.0001$; Two-way ANOVA). The analysis of navigations parameters in MWM and OL did not show statistical differences.

Conclusion:

The hypotheses we have so far considering the double-injured group are 1) rats previously injured with 6-OHDA in CPU may had a decline in spatial memory after LC injury because of the deep depletion of catecholamines, or 2) LC lesion may have been an aggravating factor for spatial memory decline in rats with model of PD. Recent studies have shown that the activation of dopaminergic receptors facilitates the consolidation of spatial memory of rats and increases the stability of memory formed in extinction, thus the deficits in learning performance after the depletion of LC suggests that it provides catecholamines to the hippocampus. Our data suggest that the catecholamines released from LC are important to the spatial memory in a PD animal model.

Financial support:

FAPESP; FAP-FCMSCSP.

FeSBE Annual Meeting 2019

Poster Sessions and Abstracts

18.005 - ASSESSMENT OF OLIGOPEPTIDASES ACTIVITY IN BLOOD AND BRAIN OF ANIMAL MODEL FOR SCHIZOPHRENIA AIMING TO EVALUATE THE VALUE OF PERIPHERAL MEASUREMENTS PERFORMED IN CLINICS. NANI JV, Yonamine CM, Mari JJ, HAYASHI MAF, - Farmacologia - UNIFESP Psiquiatria - UNIFESP

Introduction:

Schizophrenia (SCZ) is a mental disorder with multifactorial origin, characterized by disturbances in cognition, regulation of the emotional state and/or behavior. Ndel1 (Nuclear distribution element like-1) and ACE (angiotensin I-converting enzyme) are oligopeptidases which cleave SCZ-related neuropeptides as the endogenous antipsychotic neurotensin (NT). Our group has demonstrated the possible important role of oligopeptidases in the etiology of SCZ in the last years, and significant differences in the activity of these oligopeptidases were found in SCZ patients compared to gender and age matched healthy controls (HCs). Spontaneously hypertensive rats (SHRs) was proposed by others as an animal model to study SCZ due to the presence of behavioral deficits that mimic SCZ-like symptoms, which were reversed by the treatment with typical and atypical antipsychotics employed in the clinic.

Aim:

Herein, a validated animal model for SCZ was used to confirm the power of predicting alterations of ACE and Ndel1 enzyme activity in the CNS based on measurements in peripheral blood.

Methods:

The activity of Ndel1 and ACE was determined in serum (and selected brain regions (namely prefrontal cortex, hippocampus, striatum, and nucleus accumbens) of SHR, which were then analyzed compared to control Wistar (NWR) animals, before or after dopaminergic manipulations (which included the treatment with typical (haloperidol) or atypical (clozapine) antipsychotics and/or administration of pro-schizophrenic drugs as the psychostimulants amphetamine and lisdexamphetamine). Parametric (Student's t test and two-way ANOVA) and nonparametric (Spearman's Rho) standard tests were applied accordingly to variables type and distribution.

Results:

Higher Ndel1 and ACE activity was observed in the blood of the SHR (5.8 ± 0.6 nM/min and 0.17 ± 0.06 μ M/min respectively) compared to untreated NWR (2.0 ± 0.7 nM/min and 0.11 ± 0.01 μ M/min respectively). In line with this, higher activity was observed in the brain of the SHR for Ndel1 (14.7 ± 1.0 nM/min) and ACE (7.80 ± 1.97 μ M/min) compared to untreated NWR (3.4 ± 1.1 nM/min for Ndel1 and 4.43 ± 1.49 μ M/min for ACE). In addition, treatment with typical and/or atypical antipsychotic, under conditions in which SCZ-like phenotypes reversion were demonstrated for SHRs, significant reduction of Ndel1 and ACE activity was observed in blood (4.5 ± 0.8 nM/min and 4.4 ± 0.4 nM/min for Ndel1; 0.10 ± 0.01 μ M/min and 0.11 ± 0.01 μ M/min for ACE) and brain of SHRs (3.7 ± 1.1 nM/min and 6.1 ± 2.0 nM/min for Ndel1; 3.26 ± 0.74 μ M/min and 1.88 ± 0.79 μ M/min for ACE) but not in control NWR strain.

Conclusion:

We confirmed here the validity of measuring the activity of Ndel1 and ACE oligopeptidases in the peripheral blood of SCZ patients to predict correlated changes in CNS. The observed modulation of specific brain areas by antipsychotics acting on dopamine and/or serotonin pathways also brings new insights for understanding the oligopeptidases role in SCZ pathophysiology and may suggest the importance of further exploitation of the convergence between dopamine and the neurodevelopmental determinants for SCZ.

Financial support:

FAPESP, CNPq, and CAPES.

19 – Toxicology

19.001 - ACUTE TOXICITY OF 2-CHLORINE-N-ARYLACETAMID DERIVATIVES IN MICE. AMORIM VR, Machado KC, Almeida AAC, Silva JN, Machado KC, Lavoratob SN, Alvesc RJ, FERREIRA PMP, - Department of Biophysics and Physiology - UFPI Pós-graduação em biotecnologia - UFPI Pós-graduação em Ciências Farmacêuticas - UFPI DEPARTAMENTO DE FARMACOLOGIA - UFMG DEPARTAMENTO DE FARMACOLOGIA - UFOB

Introduction:

Acetamides are organic substances classified as acetic acid amide and easily obtainable in larger quantities. Some derivatives have shown anticonvulsant, antidepressant, antimicrobial, anti-HIV and antituberculosis activity.

Aim:

Evaluate the acute toxicological activity in mice of three compounds derived from 2-chloro-N-arylacetamides [compound 1: 2-chloro-N- (4-chlorophenyl) acetamide, compound 2: 2-chloro-N- (4-bromophenyl) acetamide and compound 3: 2-chloro-N- (4-nitrophenyl) acetamide].

Methods:

The toxicity study was performed based on the OECD 423 intraperitoneally. The negative control received 5% DMSO and the positive control Diazepam 2 mg / kg. General behavioral parameters were observed by Hippocratic screening as well as evaluation of exploratory activity and motor coordination via open field, route rod and cross maze (Animal Experimentation Ethics Committee (202/16-UFPI). Significant differences between the different groups were determined by variance (ANOVA) followed by Student-Newman-Keuls, using the GraphPad Prism software, version 6.0, with a significance level of 5% ($p < 0.05$).

Results:

In the rotarod test it was observed that only in the groups of compound 1 (300 mg / kg: 2.8 ± 0.2 falls) and compound 3 (150 mg / kg: 2.4 ± 0.2 ; and 300 mg / kg: 2.8 ± 0.2 falls) caused increases in the number of falls compared to the negative control (1.0 ± 0.4). Compound 1 (300 mg / kg) caused a significant reduction in turnaround time to 46.8 ± 10.6 s compared to the negative control (173.8 ± 2.93 s). In the open field test, spontaneous locomotor activity, represented by the number of crossings, was reduced in the groups of compound 2 (150 mg / kg: 23.8 ± 5.5) and compound 3 (300 mg / kg: 22.8 ± 6.8) compared to the negative control (41.3 ± 6.9) ($p < 0.05$). In the elevated cross maze test, only compound 4 changed the Open Arm Entry number to 1.0 ± 0.3 entries, less than negative control (3.6 ± 0.4), compound 1 (300 mg / kg) and compound 3 (150 and 300 mg / kg) increased Open Arm Length of Stay (179.0 ± 16.7 , 196.2 ± 15.3 and 269.0 ± 10.4 s), as did diazepam (199.6 ± 27.3 s and 125.5 ± 14.0 s) when compared to the negative control. (100.2 ± 8.4 and 199.8 ± 8.4 s).

Conclusion:

The studied compounds caused apparent signs of systemic toxicity and muscle relaxation, as well as reduced locomotor activity and decreased number of entrances in the closed arms indicating a possible sedative action.

Financial support:

CAPES

19.002 - EVALUATION OF THE TOXICITY OF THE ESSENTIAL OILS OF OCIMUM GRATISSIMUM AND CYMBOPOGON NARDUS WITH POTENTIAL PULICIDAL ACTION IN EUKARYOTIC STUDY MODEL. Osorio RP, Grillo DCN, Chaves DSA, Souza MA, Santos JVB, Cid YP, Riger CJ, - Bioquímica - UFRJ Ciências farmacêuticas - UFRJ

Introduction:

Currently some substances are used to control the flea population in environments and animals; however, these synthetic substances can reach soil and rivers and cause damage to other species or to the biome of the region. Therefore, the use of natural substances that cause the same pulgicidal effect is an important tool in the fight against fleas.

FeSBE Annual Meeting 2019

Poster Sessions and Abstracts

From the results with the essential oils of *Cymbopogon nardus* and *Ocimum gratissimum* that showed ovicidal, larvicidal and adulticidal activity against fleas.

Aim:

In this study the toxicity of these oils was evaluated in a yeast strain *Saccharomyces cerevisiae* using it as a eukaryotic cell model in order to verify in a unicellular organism non-cytotoxic concentrations of the oils. Thymol, a natural anti-pest; and fipronil, a synthetic substance widely used as anti-pest, were used as positive controls and also as parameters of comparison.

Methods:

The study was performed by the number of viable *S. cerevisiae* cells and damage to cell membranes after incubation with the essential oils at the concentrations of 10 µg.mL⁻¹ and 100 µg.mL⁻¹ for a period of 24 and 48 hours and also the thymol and fipronil controls were used in the concentration of 100 µg.mL⁻¹. Cells were grown, incubated with the substances and plated on petri dishes containing culture medium YPD 2% solid for the cell viability assay and lysed and the peroxidized lipids quantified by the TBARS method. The results were determined through the average and standard deviation of at least three independent assays and expressed as a percentage as a function of the negative control. The ANOVA test was used as a statistical tool to validate group results and Tukey's post-test to compare individual values, with $p < 0.05$ in all the evaluated results.

Results:

In the analysis of cell viability in the 24 hour period, the essential oils and fipronil did not demonstrate a reduction in cellular viability, but thymol presented high toxicity with cellular viability of 48.20%. In the 48 hour period, only *Cymbopogon nardus* at the concentration of 100 µg.mL⁻¹ and thymol demonstrated a reduction in cell viability, with values of 85.22% and 18.42%, respectively. The results of lipid peroxidation levels are not yet conclusive, but present similarity with the results of cell viability. The oils presented lower toxicity than thymol, but greater toxicity than fipronil in the yeast model.

Conclusion:

In conclusion, the results obtained in this work are promising and qualify the essential oils of *C. nardus* and *O. gratissimum* as possible alternatives in flea control.

Financial support:

FAPERJ e CAPES

19.003 - ANALYSIS OF THE EFFECTS OF LONG-TERM EXPOSURE TO ALUMINUM HYDROXIDE IN BALB/C MICE. Castro TF, Kozima ET, Souza ABF, Matos NA, Bezerra FS, - Department of Biological Sciences - UFOP

Introduction:

Aluminum (Al) the third most abundant metal present in the earth and is widely used in the industry. This metal enters the human body through the gastrointestinal and respiratory tract. Chronic contact with aluminum may affect mainly the brain, liver, and kidneys, however, the study demonstrates toxic effects on lungs, cardiovascular system, and bones.

Aim:

Based on previous findings, this study aimed to evaluate the effects of long-term exposure to aluminum hydroxide on pulmonary, renal, hepatic and intestinal oxidative stress in adult mice.

Methods:

The Ethics Committee of the Federal University of Ouro Preto (UFOP) approved the experiments, according to the Protocol nº 2017/05. 24 Balb/c mice (8-9 weeks old) were divided into 3 groups (n = 8): control (CG), PBS (PBSG) and aluminum hydroxide (AHG). The PBS and HA groups received by orogastric gavage phosphate buffered saline (PBS) or aluminum hydroxide diluted in PBS (2.0M) three times a week for 6 consecutive months. Control group was submitted to the same experimental procedures, however without the administration of solutions. 24 hours after the last exposure the animals were euthanized

and blood, lung, kidneys, liver, and intestine were collected for biochemical analysis. Statistical analyses were performed using GraphPadPrism, data were expressed as mean ± SEM or median, minimum and maximum value and $p < 0.05$ was considered statistically significant.

Results:

In peripheral blood, the erythrocyte count (10⁶/mm³) was lower in AHG (9.52 ± 0.12) compared to CG (10.49 ± 0.13). Hematocrit (%) and hemoglobin (g/dL) and platelet count (10⁶/mm³) were lower in HAG(43.20 ± 0.40; 14.40 ± 0.13; 256.2 ± 8.13) when compared to GC (46.92 ± 2.08; 15.64 ± 0.33; 324.6 ± 12.91). Long-term exposure to aluminum promoted alterations in oxidative damage markers and activity of antioxidant enzymes in the lung, liver, kidneys, and intestine. In lungs the superoxide dismutase activity (SOD) (U/mg PTN) and catalase activity (CAT) (U/mg PTN) were lower in AHG (9.0 ± 1.48, 1.08 ± 0.18) compared to the CG (21.78 ± 3.89; 3.49 ± 0.67). The levels of carbonylated protein (nmol/mg PTN) were higher in HAG (21.93 ± 2.62) compared to CG (7.11 ± 1.64) and PBSG (9.25 ± 1.24). In liver, CAT activity in the animals exposed to aluminum (0.26 ± 0.04) was lower compared to CG (0.70 ± 0.11) and PBSG (0.79 ± 0.08), in addition, oxidized proteins levels were higher in the exposed animals (18.85 ± 2.79) compared to GC (5.83 ± 0.90) and PBSG (9.44 ± 1.30). In the kidney the oxidative damage was greater by an increase in the level of oxidized lipids (nmol/mg PTN) and proteins in AHG (1.91 ± 0.27; 27.09 ± 4.77) compared to CG (1.03 ± 0.06; 10.57 ± 1.61) In intestine catalase activity and oxidized protein levels were higher in AHG (0.65 ± 0.08; 34.24 ± 2.44) compared to CG (0.29 ± 0.05, 10.48 ± 1.61).

Conclusion:

Our results suggest that long-term exposure to aluminum hydroxide via orogastric gavage is able of triggering local effects as well as affecting other organs and blood.

Financial support:

CNPq, CAPES, FAPEMIG and UFOP

19.004 - THE TICK AMBLYOMMA SCULPTUM CRUDE SALIVA PROMOTES APOPTOSIS IN CASPASE 8-DEFICIENT-NEUROBLASTOMA CELLS. Nascimento TGFC, Júnior NF, Cavalheiro VL, Micheau O, Simons SM, Esposito SE, - Programa de Pós-Graduação em Ciências da Saúde - PUCPR Escola de Ciências da Vida - PUCPR Parasitologia - Instituto Butantan INSERM - UB

Introduction:

Neuroblastoma (NB) is a pediatric cancer with a wide range of clinical features. NB cells can be resistant to chemotherapy drugs, leading to widely different outcomes, ranging from spontaneous regression in low-risk disease, to a rate of 50% of death in high-risk patients. Resistance in NB cells might be due to the lack of Caspase 8 expression, which is an important characteristic of those cells. Several studies showed ticks saliva as a promising source of antitumor compounds. Hard tick *Amblyomma sculptum* saliva, specifically, presents antitumoral compounds affecting proliferation, cytoskeleton architecture stability, and cell death with characteristics of necrosis, as shown in previous works. The presence of agents inducing apoptosis is a significant bet since apoptosis plays a critical role in response to chemotherapy and it is not clear yet if the saliva could induce extrinsic or intrinsic pathways.

Aim:

This study aims to evaluate cell death induced by the hard tick *Amblyomma sculptum* saliva on neuroblastoma cell lines and to describe the pathway involved in this process.

Methods:

Cytotoxicity was tested in vitro in four different neuroblastoma cell lines (SK-N-SH, SH-SY5Y, Be-(2)-M17, CHLA-20) by the Methylene Blue assay, using a serial dilution of crude *A. sculptum* saliva from 20 µg/mL, for 72h. Apoptosis was analyzed in annexin-V stained cells by flow cytometry after incubation with crude saliva (10µg/mL) for 72h. To

FeSBE Annual Meeting 2019

Poster Sessions and Abstracts

determine the influence of caspases 1, 3, 8 and 9 in cell death, cells were treated for 30 min with the pan-caspase inhibitor Qvd (5µg/mL) before incubation with saliva. The expression of proteins involved in the apoptotic extrinsic and intrinsic pathways (caspases 10/9/8/3; BID, Mcl-1, Bcl-2, BAX) was determined by Western Blot.

Results:

All cell lines were susceptible to saliva in concentrations higher than 1 µg/mL. SK-N-SH, SH-SY5Y cells presented a rate of apoptosis of about 40%, which corroborates with what was found in the Methylene Blue assay that presented a reduction of viability in about 50%. Results after Qvd treatment showed that when the caspases are blocked cells do not die, suggesting the involvement of caspase-dependent cell death. Western Blot results demonstrated that all neuroblastoma cell lines lack caspase 10 and 8, except for SK-N-SH that presents down-regulation of caspase 8, suggesting that the apoptosis effect occurs by the intrinsic pathway.

Conclusion:

This work confirms the *A. sculptum* crude saliva as a promising source of antitumoral molecules, with the presence of apoptotic compounds, which act via the intrinsic pathway. It is a new perspective for the characterization of neuroblastoma cell lines susceptibility to new exogenous compounds

Financial support:

CAPES/COFECUB 16/2015 880/2017, Código 001; Fundação Araucária PBA 03/2016

19.005 - EVALUATION OF REPRODUCTIVE PARAMETERS OF FEMALE RATS TREATED WITH SULFASALAZINE DURING GESTATION AND LACTATION. Forcato S, Aquino ABO, Olanda LCN, Kiss ACI, Gerardin DCC, - Ciências Fisiológicas - UEL Fisiologia - UNESP-BOTUCATU

Introduction:

Glutamate is the major excitatory neurotransmitter in the brain, and it is suggested that its transmission facilitates motivated behaviors. The source of non-vesicular glutamate release is the system Xc. Sulfasalazine (SAS), drug commonly prescribed for the treatment of rheumatoid arthritis, has been indicated as the first line in treatment of chronic inflammatory bowel diseases in pregnant women for not presenting teratogenicity. It is known that SAS inhibits the system Xc and alters the motivation of rodents in behavioral experiments. Therefore, it could also interfere in the motivation of other behavior tests such as maternal behavior.

Aim:

To evaluate the fertility and maternal behavior of the female rats exposed to SAS during gestation and lactation periods.

Methods:

Wistar female rats were treated (n=10) with SAS 300mg/kg/day, by gavage from gestational day (GD) 0 until lactation day (LD) 21. During the gestational period dams received supplementation with folic acid (FA) 3mg/kg/day, (2h before of the treatment with SAS), since SAS inhibits folate uptake. Control dams (n=10) received carboxymethylcellulose (CMC, vehicle) by gavage at the same periods. Maternal body weight and feed consumption were determined weekly during the treatment. On LD 5 maternal behavior evaluation was performed. On LD 21 the rats were weighted, euthanized and the uterus and ovaries were removed and weighted and, the number of corpora lutea and implantation sites were counted to perform the fertility test. Results were considered statistically significant if $p < 0.05$ and compared by Analysis of co-variance (ANCOVA), ANOVA, Student t-test or Mann-Whitney U (CEUA/UEL: 10495.2018.13).

Results:

The body weight gain and feed consumption during the treatment, as well as, reproductive organs weight were similar between groups. In maternal behavior evaluation, ANOVA shows that SAS treatment induced a decrease in retrieving (CTR: 6.60 ± 2.07 ; SAS: $3.20 \pm 2.28^*$, $n=5$ /group). Furthermore, the Mann-Whitney U test showed that SAS

treatment induced a significant decrease in viability [CTR: 92.82(91.48-100); SAS: 81.67(76.24-94.23)*, $n=10$ /group] and, in post-implantation loss rate [CTR: 7.18(0-8.52); SAS: 18.33(5.77-23.76)*, $n=10$ /group].

Conclusion:

The pup retrieval is a parameter of maternal behavior motivation. It is suggested that the decrease in retrieving, as well as the alterations in fertility test in female rats, might be due to the inhibition of the system Xc, since the treatment with SAS induced infertility in men which is related to the toxic accumulation of reactive oxygen species (ROS), probably by the inhibition of the system Xc. However, more studies are necessary to confirm the hypothesis. Therefore, considering that SAS treatment during gestation and lactational periods is common, the results observed in this study could be a public health concern.

Financial support:

CAPES

19.006 - CLINICAL AND EPIDEMIOLOGICAL ASPECTS OF SCORPIONISM IN GOVERNADOR VALADARES AND ITS REGION FROM 2007 TO 2016. Ramiro LC, Alves LRM, Silva JGBPCP, Macedo LR, DeMatos IM, - Departamento de Ciências Básicas da Vida - Universidade Federal de Juiz de Fora - Campus Governador Valadares Departamento de Medicina - Universidade Federal de Juiz de Fora - Campus Governador Valadares Departamento de Economia - Universidade Federal de Juiz de Fora - Campus Governador Valadares

Introduction:

Scorpion envenomation is a frequent and sometimes fatal incident in tropical and subtropical countries. According to the Ministry of Health, approximately 8,000 scorpion envenomation cases are registered annually in Brazil. The *Tityus* genus is of medical importance in Brazil, and the common species are the *Tityus serrulatus*, *T. bahiensis*, *T. cambridgei*, and *T. trivittatus*, among which *T. serrulatus* raises more concern as accidents with such species tend to be more severe. The spatial distribution of this species encompasses some regions in Minas Gerais, São Paulo, Rio de Janeiro, Bahia, and Espírito Santo. Nevertheless, accidents with this type of scorpion are reported all over Brazil.

Aim:

This study aimed to describe and assess the scorpion accidents reported and treated in the Municipal Hospital of Governador Valadares, from January 2007 to December 2016, and calculate their incidence and mortality rate and identify factors that led to death.

Methods:

This retrospective and descriptive study was approved by the Ethics Committee of the Biological Sciences of the Federal University of Juiz de Fora – under the inscription number 1,698,173. Data were collected from all medical records of patients showing a diagnosis of scorpionism hospitalized in the Municipal Hospital of Governador Valadares from January 2007 to December 2016. The analysis of the medical records was authorized by written consent of the hospital's administration, upholding the confidentiality of patients. In the records, the date, city, and neighborhood where the incident occurred; patient's sex and age; characteristics of the accident; elapsed time between the sting and hospital admission; area of the sting, and main local and systemic manifestations were identified and evaluated during the hospitalization period.

Results:

During this period, 4,618 accidents occurred every month, with a high number of cases peaking in warm and rainy periods. Most accidents were classified as mild occurrences, and among the severe ones, there was a total of 12 deaths predominantly in the 1–14 age group. Local pain was reported in nearly 100% of the cases. Vomiting and diarrhea occurred in most cases showing systemic manifestations. Moreover, all cases that presented systemic complications were fatal, with the cause of death being acute pulmonary edema and/or shock. The elapsed time between the accident and medical care varied mostly between 0 and 3

FeSBE Annual Meeting 2019

Poster Sessions and Abstracts

h, and the upper limbs were the most affected area. Regarding sex, the majority of patients in the observed period were men.

Conclusion:

The results of this study are similar to those of other studies conducted in Minas Gerais and other regions in the country and constitute an important tool for the implementation of public policies to prevent and control scorpionism in Governador Valadares and its region and enhance the care provided to the victims of scorpion envenomation. Furthermore, this study provides important data for the development of educational campaigns aiming at the preventive control of scorpion stings.

Financial support:

The study did not have any funding other than my own.

19.007 - REPRODUCTIVE PARAMETERS OF MALE RATS EXPOSED TO SAS IN UTERO AND DURING LACTATION. Bilibio JO, Ferreira SF, Borges LI, Gerardin DCC, - Ciências Fisiológicas - UEL

Introduction:

According to the Developmental Origins of Health and Disease (DOHaD), the maternal exposure to drugs can affect the morphological and functional development of organs, which is related to the origin of late diseases. Sulfasalazine (SAS) is a drug indicated for the treatment of inflammatory diseases, such as rheumatoid arthritis, ulcerative colitis and Crohn's disease, being recommended as the first line of treatment for pregnant women due to not presenting teratogenicity. One of the adverse effects of SAS is the inhibition of intestinal and cellular folate uptake, therefore folic acid (FA) supplementation is recommended throughout pregnancy. It is known that both SAS and its metabolites cross the placenta and have been detected in the umbilical cord. Besides that, SAS metabolites were detected in the breast milk and in urine samples from the nursing infants. In men, exposure to SAS induces transient infertility characterized by reduced sperm count and motility and abnormal morphology of sperm cells; furthermore, it also decreases testosterone levels and increases luteinizing hormone (LH) levels. In Sprague-Dawley adult rats, this drug decreases the superoxide dismutase (SOD) and glutathione reductase (GR) in both testicular and epididymis leading to the toxic accumulation of reactive oxygen species (ROS).

Aim:

To evaluate reproductive parameters of the male offspring exposed to SAS during intrauterine and lactation periods.

Methods:

Wistar female rats (n=10) were treated with SAS 300mg/kg/day, by gavage, from gestational day (GD) 0 until lactation day (LD) 21. During the gestational period, dams received supplementation with FA 3mg/kg/day. The SAS and FA were dissolved in carboxymethylcellulose (CMC). The gavage with FA was 2h before the treatment with SAS. Controls dams (n=10) received CMC by gavage at the same period. The following parameters were observed in male pups: physical development, anogenital distance (AGD) and, installation of puberty. Moreover, at postnatal day 90, the rats were weighted, euthanized and the reproductive organs were removed and weighted. The vas deferens content was collected to perform sperm parameters: motility, concentration and sperm morphology. Results were considered statistically significant if $p < 0.05$ and compared by Analysis of covariance (ANCOVA), Student t-test or Mann-Whitney U (CEUA/UEL: 10495.2018.13).

Results:

The body weight, AGD, reproductive organs weight, as well as the installation of puberty were similar between groups. Furthermore, the treatment did not alter the sperm parameters, such as motility [CTR: 81.90±6.74; SAS: 80.20±5.43, n=10/group], concentration [CTR: 107.60±26.23; SAS: 104.20±25.61, n=10/group], abnormal head morphology sperm (%) [CTR: 12.25±2.57; SAS: 10.50±2.35, n=10/group]

or abnormal tail morphology sperm (%) [CTR: 1.00(0.87-2.5); SAS: 1.49(0.87-2.25), n=10/group].

Conclusion:

Although in the literature it is described that SAS alters fertility in men, the maternal exposure to SAS did not interfere in reproductive parameters of adult male offspring. More studies are required to investigate the effects of maternal exposure to SAS during critical periods of development.

Financial support:

CAPES; CNPQ

19.008 - TREATMENT WITH TOPIRAMATE DURING ADOLESCENCE: LATE REPERCUSSION ON THE REPRODUCTIVE ASPECTS OF MALE RATS. BORGES LI, Vidigal CB, Moura KF, Pereira MJD, Ceravolo GS, Franco MCP, Gerardin DCC- Departamento de Ciências Fisiológicas - UEL Departamento de Nefrologia - UNIFESP

Introduction:

Topiramate (TOP) is a drug for the treatment of epilepsy in children older than 2 years of age, adolescents and adults. Data in literature shows that adult Sprague Dawley rats treated with TOP through diet (100 mg/kg) over 60 days presented a decrease in reproductive organs weight, sperm motility, germ and Leydig cell numbers. The development of the reproductive system in rats begins during intrauterine life and extends up to 60 days after birth and is divided into four phases: neonatal (postnatal day (PND) 1-7), infant (PND 8-21), juvenile (PND 22-25) and peri-pubertal (PND 36-55 or 60), all these phases are vulnerable to disorders that alter the hormonal or genetic control.

Aim:

The objective of this study was to evaluate the late reproductive effects of TOP treatment during adolescence in male rats.

Methods:

Wistar male rats were divided into two groups (n=7/group): the control group (CTR) was treated with water, and the Topiramate group (TOP) was treated with TOP 41 mg / kg / day, by gavage, from PND 28 to 50. At adult life (PND 120) the following parameters were evaluated: reproductive organs weight, anogenital distance (AGD), motility, morphology and sperm count in the vas deferens. Results were considered statistically significant if $p < 0.05$ and compared by Student t-test. All procedures were approved by the Ethics Committee on the use of animals of UEL (CEUA / UEL 9379.2018.26).

Results:

The weight of testicles (g) (CTR: 1.49±0.27; TOP:1.42±0.20), epididymis (g) (CTR: 0.57±0.015; TOP: 0.55±0.17); prostate (g) (CTR: 0.46±0.031; TOP:0.47±0.021); seminal vesicle (g) (CTR: 1.43±0.031; TOP:1.42±0.075), and AGD were similar between groups, as well the sperm parameters such as motility, count in the vas deferens, and morphology.

Conclusion:

Although in the literature it is described that TOP alters reproductive parameters in adult male rats, the treatment during adolescence did not interfere in these parameters. Divergent results may be related to the treatment period, administration route and dose. However, complementary studies evaluating other reproductive parameters are necessary.

Financial support:

CAPES, CNPQ

19.009 - EVALUATION OF ANTIFUNGAL ACTIVITY OF OIL AND PROTEIN FRACTION FROM MORINGA OLEIFERA SEEDS AGAINST TRICOPHYTON TONSURANS. GUEDES CCDS, OLIVEIRA APSD, BUONAFINA MDS, ROCHA SKLD, SILVA SPD, COELHO LCB, NEVES RP, NAVARRO DMDAF, NAPOLEÃO TH, PAIVA PMG, - BIOQUIMICA - UFPE

Introduction:

FeSBE Annual Meeting 2019

Poster Sessions and Abstracts

Trichophyton tonsurans is a dermatophyte fungus of wide geographic distribution, being the etiological agent of tinea capitis, tinea corporis, tinea pedis and tinea unguium. The indiscriminate use of antifungals has led to the emergence of resistant strains; in addition, there is a concern about the side effects and toxicity of these agents as well as the hypersensitivity reactions of some patients. The search for natural compounds with antifungal activity may increase the number of options for therapeutic strategies.

Aim:

The present study aimed to investigate the antifungal activity of the oil and a protein fraction obtained from *Moringa oleifera* seeds against *T. tonsurans*.

Methods:

The oil was obtained through Soxhlet extraction and characterized by gas chromatography coupled to mass spectrometry (GC-MS). A water extract from moringa seeds was obtained by homogenizing the seed powder (10 g) with distilled water (100 mL) for 16 h at 4 °C. The protein fraction was obtained by treatment of the water extract with ammonium sulphate (60% saturation) for 4 h at 28 °C followed by centrifugation and dialysis of the precipitate against distilled water. The antifungal activity was determined by the broth microdilution method according to the Clinical and Laboratory Standards Institute (CLSI) protocol M38-A2. It was also evaluated the activity of mixtures of the oil and the protein fraction

Results:

The oil characterization showed the presence of some fatty acids being oleic acid the majority compound, representing about 66% of the total oil composition. When tested alone, the oil and the protein fraction inhibited the growth of *T. tonsurans* by 50% at 1024 µg/mL. When the two preparations were evaluated together, 50% inhibition of growth was detected for a mixture containing the oil at 512 µg/mL and the protein fraction at 8 µg/mL. The fractional inhibitory concentration (FIC) values were 0.5 and 0.007 for the oil and fraction, respectively. The fractional inhibitory concentration index (FICI) was 0.507, indicating an additive effect.

Conclusion:

Therefore, the oil and the protein fraction from *M. oleifera* seeds have potential to be evaluated in the control of *T. tonsurans* growth and showed improved antifungal effectiveness when in combination.

Financial support:

CAPES, CNPQ, FACEPE, UFPE

20 - Pain and Inflammation

20.001 - EXPERIENCING EARLY LIFE MATERNAL SEPARATION INCREASES PAIN SENSITIVITY IN ADULT OFFSPRING. Vieira JS, Silva ML, Giusti-Paiva A, Vilela FC, - Fisiologia Translacional - UNIFAL-MG

Introduction:

Maternal separation (MS) is a widely accepted model for studying long-term behavioral changes produced by events during early life and is considered an 'early stress' model. It is known that stress models can induce significant behavioral changes and change the sensitivity to pain.

Aim:

Therefore, our objective was to evaluate pain sensitivity, under different stimuli, in adult male and female rats submitted to MS.

Methods:

Animals (Wistar rats, n = 8 per group) were subjected to maternal separation from postnatal day (PND) 2-15 for 3h/day. Maternal behavior and litter weight were evaluated during this period. Sensitivity to pain was assessed in offsprings during adulthood by exposing them to stimuli, including formalin (5%; 20 µl), hot plate, and the electronic von Frey test, 4, 7, 10, and 24 h after the administration of saline or complete Freund's adjuvant (CFA; 100 µl) injection. The results were analyzed by two-way ANOVA followed by the Bonferroni post-test. All

the experimental procedures were tested by the CEUA ethics committee under number. 32/2016.

Results:

There was no difference between the groups (control and MS) regarding maternal behavior and litter weight. In the formalin test, there was an increase in the number of flinches (withdrawal response of formalin injected paw) in MS male offspring (from 34.38 ± 0.56 to 46.86 ± 0.71) in the 0-5 min time that remained until the 55-60 min (21.87 ± 0.51 for 31.00 ± 0.59, p <0.001) compared to the control group. About MS female offspring, in the 0-5 min time there was an increase in the number of flinches (from 30.00 ± 1.10 to 38.50 ± 1.45) which remained until the time 55-60 min (21.37 ± 0.56 for 31.88 ± 2.36, p <0.001) when compared to the control group. In the hot plate test there was a reduction in the latency time in the animals injected with CFA and with MS in male offspring (T7: 8.12 ± 0.58s for 5.62 ± 0.59s, T10: 6.00 ± 0.32s for 4.00 ± 0.37s, p <0.01) and in MS female offspring (T4: 11.50 ± 0.70s for 8.25 ± 0.52s, T7: 8.12 ± 0.58s for 5.75 ± 0.59s, T10: 6.00 ± 0.32 for 4.00 ± 0.37, p <0.01) compared to animals injected with CFA and not submitted to MS. In the electronic von Frey test, there was a reduction in the paw withdrawal threshold in the animals injected with CFA and with MS in male offspring (T7: 22.13 ± 1.44g to 16.86 ± 0.60g) which was maintained until T24 (19.01 ± 0.97g to 14.19 ± 0.67g; p <0.05) and in MS female offspring (T4: 20.17 ± 0.93g for 15.09 ± 0.86g) that remained until T24 (18.20 ± 0.57g for 12.37 ± 0.41g; p <0.001) when compared to the animals injected with CFA and not submitted to MS.

Conclusion:

Early maternal separation increases pain sensitivity in male and female offspring during adult life.

Financial support:

CAPES, Cnpq, FAPEMIG

20.002 - HIGH-INTENSITY DOWNHILL RUNNING EXERCISE INDUCES CHANGES ON NOCICEPTIVE THRESHOLD AND MECHANICAL MUSCLE HYPERALGESIA THAT IS PREVENTED BY NICOTINAMIDE RIBOSIDE SUPPLEMENT: PRELIMINARY RESULTS. Azambuja G, Crisol B, Barbosa LWT, Ropelle ER, Fusaro MCGO, - LABEDI - UNICAMP LABMEX - UNICAMP

Introduction:

Performance athletes are constantly submitted to high-volume and intensity training. Thus, muscle tissues have an environment of inflammation and oxidative stress that may lead to a high NAD⁺ consumption. These factors can decrease performance. Somatosensory system is sensitized by inflammation, in a such way that it can decrease nociceptive threshold and facilitate pain signaling. We hypothesized that in a high-intensity downhill running, nociceptive threshold could be decreased and the muscle pain be present. Nicotinamide Riboside (NR) supplement is a NAD⁺ precursor capable of increasing mitochondrial function and may be a strategy for muscle recovery in high-intensity exercise. There is no data showing that NR can prevent changing of nociceptive threshold and muscle pain.

Aim:

The aim of this study was to evaluate whether high-intensity downhill running decreases muscle nociceptive threshold and triggers mechanical muscle hyperalgesia. Also, if the NR prevents changing on these factors.

Methods:

To this end, 20 male C57BL/6J mice (CEMIB/UNICAMP, protocol: 5000-1/2018) were separated in groups: control, trained, downhill and downhill + NR. Treadmill running lasted eight weeks, five days/week. Aerobic training (60% Pmax) had two phases: 1^a) four weeks with gradually increased volume; 2^a) two weeks with the same volume. High-intensity downhill running had five phases: 1^a) four weeks with gradually increased volume; 2^a) one week with downhill running (-14%); 3^a) one week downhill with 70% Pmax intensity; 4^a) one week downhill

FeSBE Annual Meeting 2019 Poster Sessions and Abstracts

with 75% Pmax intensity; 5^a) one week downhill with 75% Pmax intensity, two sessions/day (4 hours interval). NR supplementation was through diet, 400 mg/kg/day/8 weeks. Randall-Selitto analgesymeter was used in gastrocnemius muscle, to measure nociceptive threshold and mechanical hyperalgesia, in grams (g). Measures were performed in last two weeks; before and 20 minutes after session; 72h after the end of the training. Mechanical muscle hyperalgesia was expressed by the difference (g) between pre and post session.

Results:

Results showed that, in the last week of exercise and 72h after, there was a decrease in muscle nociceptive threshold in downhill (34.49 g ± 1.09) and downhill + NR (36.6 g ± 1.16) groups, compared to control (41 g ± 1.45) and trained (40.13 g ± 0.76; One-way ANOVA, Tukey test, p<0.05). Decrease in muscle nociceptive threshold in downhill + NR was lower than in downhill (One-way ANOVA, Tukey test, p<0.05). There was mechanical muscle hyperalgesia in downhill (T1: 1.6 g ± 1.38; T2: 3.53 g ± 0.58; T3: 6.01 g ± 1.20) when compared to control (T1: -0.46 g ± 0.96; T2: 0.4 g ± 0.27; T3: 0.26 g ± 0.49) and trained in all time points (T1: 0.85 g ± 1.65; T2: 1.86 g ± 1.34; T3: 0.4 g ± 0.43; Two-way ANOVA, Bonferroni test, p<0.05). Interestingly, downhill + NR had no hyperalgesia in the last week (1.6 g ± 0.98) and 72h after the end, nociceptive threshold (37.15 g ± 1.04) was significantly higher than in downhill (34.35 g ± 1.34; Two-way ANOVA, Bonferroni test, p<0.05).

Conclusion:

In conclusion, high-intensity downhill running decreased muscle nociceptive threshold and triggered muscle pain, which were reduced by Nicotinamide Riboside supplementation.

Financial support:

Coordenação de Aperfeiçoamento de Pessoal de Nível Superior – Brasil (CAPES) – Finance code: 001; São Paulo Research Foundation - process number: 18/04192-5 and 18/07634-9

20.003 - DEPLETION OF MUSCLE MACROPHAGES AND PHYSICAL EXERCISES PREVENT THE TRANSITION OF ACUTE TO CHRONIC MUSCLE PAIN. Gomes BB, Azambuja G, Jorge CO, Rodrigues HL, Oliveira-Fusaro MCG, - Laboratory of Pain and Inflammation Research - UNICAMP

Introduction:

Muscle pain is a world health problem with high socio-economic impact. Several pain conditions are related to inflammation, which is a process modulated by immune cells. Macrophages are involved in acute pain, but their involvement in transition to chronic pain is unknown. Physical exercise is point out as a strategy to control muscle pain because of its anti-inflammatory effects.

Aim:

The aim of this preliminary study was to analyze if macrophages and/or physical exercise prevents transition of acute to chronic muscle pain.

Methods:

Male Swiss mice (2 months old) were used and all procedures were approved by ethics committee for animals at UNICAMP (protocol 4808-1). Carrageenan (100µg) was injected into gastrocnemius muscle to induce inflammatory pain and, 10 days later, PGE2 (1µg) was injected at the same local to reveal the state of chronic-latent hyperalgesia. Mechanical muscle hyperalgesia was quantified by Randall Selitto test in different time points. Macrophages was analyzed by muscle pretreatment with clodronate-encapsulated liposomes, which induce depletion of local macrophages (20µl, 4 days). Physical exercise was performed through swimming, in a volume of 50 min/day, 5 days/week, for 3 weeks, before carrageenan. Once a week, blood was collected to assay corticosterone levels by ELISA test because exercise-induced analgesia can be modulated by stress.

Results:

Pretreatment with Clodronate prior to carrageenan (n=6) reduced acute muscle hyperalgesia at 1h: 2.4g±0.38; 3h: 5.2g±0.47; 6h: 6g±0.36 and 24h: 5.5g±0.55 when compared to control group (n=4) (1h: 9.8g±0.24; 3h: 13.7g ±1.1; 6h: 14.7g±0.24; 24h: 10.9g±0.3) (p<0.001,

Two-way ANOVA, Bonferroni test). The chronic muscle hyperalgesia was also reduced at 1h: 3.9g±0.27; 4h: 6.5g±1.1; 24h: 8.5g ±1.6; 48h: 7.6g ±1.6; 168h: 9.78g ± 1.5) when compared to control group (1h: 13.2g±0.7; 4h: 15.1g±1.3; 24h: 15.4g±0.9; 48h: 14.9g±0.9; 168h: 14.7g±0.8) (p<0.001, Two-way ANOVA, Bonferroni test). To isolate acute from chronic muscle hyperalgesia, Clodronate was injected immediately before PGE2 in mice previously challenged by carrageenan. In this case, Clodronate did not reduce chronic pain at 1h and 4h (p>0.05), however, there were reduction at 24h: 7.3g±1.0; 48h: 7.3g±0.9; and 168h: 6.9g±0.1 (p<0.05, Two-way ANOVA, Bonferroni test). Swimming prevented acute (3h: 6.9g±0.5; 6h: 5.6g±0.5; 24h: 4.8g±0.5; 48h: 3.0g±0.5) and chronic muscle hyperalgesia (1h: 6.4g±0.4; 4h: 7.5g±0.3; 24h: 5.6g±0.4; 48h: 6.1g±0.7; 168h: 1g±0.3) (n=14) when compared to the sedentary animals (acute: 3h: 17±0.9; 6h: 16.6g±1.0; 24h: 10.2g±1.1; 48h: 5.9g±0.7; chronic: 1h: 13.2g±0.7; 4h: 15.1g±1.3; 24h: 15.4g±0.9; 48h: 14.9g±0.9; 168h: 14.6g±0.8) (p<0.05, Two-way ANOVA, Bonferroni test), without affect levels of corticosterone (1 week: 77,8ng/mL±19,2; 2 week: 28,8ng/mL± 6,0; 3 week: 34,6ng/mL± 11,6) when compared to the sedentary animals (1 week: 57,8ng/mL±8,8; 2 week: 40,7ng/mL±3,0; 3 week: 47,7ng/mL± 13,6) (p>0.05, Two-way ANOVA, Bonferroni test) (n=10).

Conclusion:

In conclusion, macrophages are involved in transition of acute to chronic muscle pain and in maintenance of it. In addition, physical exercise prevents transition of acute to chronic muscle pain. Therefore, we point out the control of macrophages and physical exercise as good strategies to prevent this transition. In future, we will analyze whether the exercise-induced prevention of chronic muscle pain is modulated by macrophages.

Financial support:

Coordenação de Aperfeiçoamento de Pessoal de Nível Superior - Brasil (CAPES) - Finance Code 001 and The São Paulo Research Foundation, FAPESP 17/17919-8

20.004 - EFFECT OF TDCS TREATMENT ON PERSISTENT PAIN AND NERVE REGENERATION IN NEUROPATHIC RATS. Jerônimo R, Paschoa AF, Lima GL, Campos ACP, Brunoni AR, Pagano RosanaL, - Division of Neuroscience - HOSPITAL SÍRIO-LIBANÊS School of Medicine - University of São Paulo

Introduction:

Transcranial direct current stimulation (tDCS) is an effective treatment for chronic neuropathic pain (NP); however, the mechanisms of action still not fully understood.

Aim:

Here, we evaluated the tDCS effect on the NP and on the nervous regeneration process in a peripheral neuropathy model.

Methods:

Male Wistar rats with chronic constriction injury (CCI) of the sciatic nerve or false-operated (FOP) were evaluated in nociceptive tests (mechanical hyperalgesia and allodynia). After 14 days of nerve injury, CCI rats were submitted to 10 sessions of bicephalic tDCS (250 µA/15 min - CCI + tDCS group). As controls, CCI or FOP rats were false-stimulated (250 µA/5 s). After 1 h of the last nociceptive test, 27 days after CCI or FOP, the sciatic nerve was collected and the expression of growth associated protein 43 (GAP-43) and of myelin basic protein (MBP) were evaluated by western blotting (CEUA-P 2017-02).

Results:

After 14 days of CCI, neuropathic animals showed the hyperalgesia (n= 5 per group; 50 ± 5.0 of CCI to 89 ± 2.2 of FOP, p < 0.0001) and allodynia (n= 5 per group; 0.59 ± 0.24 of CCI to 14.25 ± 5.59 of FOP, p < 0.05) phenomena, compared to the FOP group. tDCS treatment was able to revert these phenomena as well as to inhibit the MBP expression in the sciatic nerve of the CCI + tDCS animals, when compared to other groups (n= 4 per group; 85.28 ± 34.28 of CCI + tDCS, 166.77 ± 24.29 of CCI, 100.00 ± 39.63 of FOP, p = 0,0148). tDCS treatment was also able to

FeSBE Annual Meeting 2019

Poster Sessions and Abstracts

restored the GAP-43 expression in the sciatic nerve of CCI + tDCS rats compared to FOP rats (n= 4 per group; 71.29 ± 23.92 of CCI + tDCS, 126.31 ± 26.27 of CCI, 100.00 ± 29.15 of FOP, p = 0,0334).

Conclusion:

Our results showed that tDCS treatment reverses the NP, concomitantly with the suppression of the nerve regeneration process at a late stage, which could be contributing with the persistence of NP after peripheral nerve injury.

Financial support:

FAPESP; CAPES.

20.005 - P2X3 RECEPTORS OF SPINAL CORD DORSAL HORN ARE INVOLVED IN TRANSITION OF ACUTE TO CHRONIC MUSCLE PAIN. Jorge CO, Azambuja G, Gomes BB, Rodrigues HL, Oliveira-Fusaro MCG, - Laboratory of Pain and Inflammation Research (LABEDI) - UNICAMP

Introduction:

Mechanisms underlying transition of acute to chronic pain are poorly understood. Our preliminary study showed that P2X3 receptors of gastrocnemius muscle are involved in acute but not in chronic muscle pain. We also showed that physical exercise prevents transition of acute to chronic muscle pain

Aim:

Considering P2X3 receptors are expressed in nociceptive fibers of central nervous system, the aim of this study was to evaluate whether P2X3 receptors of spinal cord dorsal horn were involved in transition of acute to chronic muscle pain and, in this case, whether activation of P2X3 receptors reverse exercise-induced hypoalgesia

Methods:

Male Swiss mice (6 weeks-old) from CEMIB-UNICAMP were used and all experimental procedures were approved by the Ethics Committee in Animal Research of UNICAMP (4883-1). Carrageenan (100µg) was injected into gastrocnemius muscle to induce inflammatory pain and, 10 days later, PGE2 (1µg) was injected at the same local to reveal the state of chronic-latent hyperalgesia. Mechanical muscle hyperalgesia was measured by Randall-Selitto analgesymeter in different time points of acute (1-144h) and chronic pain (1-168h). Expression of P2X3 in dorsal root ganglia (L4-S1) at 6h and 48h after carrageenan and 24h after PGE2 was analyzed by Western Blotting. Physical exercise was performed through swimming, in a volume of 50 min/day, 5 days/week, for 3 weeks, before carrageenan. The involvement of P2X3 receptors was analyzed by using the selective P2X3 receptors antagonist, A317491, and the non-selective P2X3 receptors agonist, αβmeATP

Results:

Intrathecal pretreatment with A317491 (20µg) previously to carrageenan prevented the development of acute mechanical muscle hyperalgesia at 3h (5,03g±1,14), 6h (4g±1,54) and 24h (3,95g±0,5) (p<0.05, two-way ANOVA, Bonferroni test, n=4), and chronic mechanical muscle hyperalgesia at 4h: 5,35g±1,66; 24h: 3,92g±0,36; 48h: 3,27g±0,55; 168h: 3,25g±0,46 when compared to its vehicle, 0.9% NaCl (acute - 3h: 17.0g± 0.92g; 6h 16.6g ± 1.04g; 24h 10.2g ± 1.19g; chronic - 4h: 15.1g± 1.3g; 24h 15.4g ± 0.9g; 48h 14.9g ± 0.9g; 168h 14.6g ± 0.8g, n=9) (p<0.001, Two-way ANOVA, Bonferroni test). To isolate acute from chronic muscle hyperalgesia, A317491 was injected immediately before PGE2 in mice previously challenged by carrageenan. In this case, intrathecal A317491 (20µg) prevented development of chronic mechanical muscle hyperalgesia at 4h: 3,55g±0,55; 24h: 3,97g±1,26; 48h: 2,33g±0,27; 168h: 2,8g±0,33 (p<0.05, two-way ANOVA, Bonferroni test, n=5). There was reduction in expression of P2X3 receptors 6h after carrageenan (1,2au±0,40; p<0.05 T Test, n = 5) and no differences were found at 48h after carrageenan and 24h after PGE2 (p>0.05, T Test, n= 5). Intrathecal injection of αβmeATP (5µg) prior to PGE2 in exercised mice previously challenged by carrageenan reversed exercise-induced hypoalgesia at 1h: 9.3g±0.9; 4h: 12.1g±1.1; 24h: 10.5g±0.3; 48h: 9.7g±1.0; 168h: 9.8g±0.3 when compared to exercised control mice (1h: 6.4g±0.4; 4h: 7.5g±0.3; 24h:

5.6g±0.4; 48h: 6.1g±0.7; 168h: 1g±0.3, n=4) (p<0.05, Two-way ANOVA, Bonferroni test)

Conclusion:

In conclusion, P2X3 receptors of spinal cord dorsal horn but not of muscle tissue, are involved in transition of acute to chronic muscle pain and in exercise-induced hypoalgesia. Therefore, we point out P2X3 receptors of spinal cord dorsal horn as a pharmacological target to control chronic pain conditions in people who are sedentary or who practice regular physical exercises

Financial support:

Coordenação de Aperfeiçoamento de Pessoal de Nível Superior - Brasil (CAPES) - Finance Code 001 and The São Paulo Research Foundation, FAPESP 17/17919-8

20.006 - BIOLOGICAL EFFECT OF ANNEXIN A1-DERIVED TETRAPEPTIDE, ANXA19-12, IN AN EXPERIMENTAL MODEL OF ACUTE PERITONITIS. Lice I, Sanches JM, Correia-Silva RD, Icimoto MY, Moreira V, Gil CD, - Morfologia e Genética - UNIFESP

Introduction:

Annexin A1 (AnxA1) is a protein capable of mimicking the anti-inflammatory action of glucocorticoids by inhibiting the synthesis of eicosanoids and phospholipase A2. In addition, the regulatory action of AnxA1 and its mimetic peptides is mediated by formyl peptide receptors (Fpr), particularly Fpr2. This study evaluated the biological effect of the N-terminal AnxA1-derived tetrapeptide AnxA19-12 and its relationship with Fpr2 in murine model of acute peritonitis.

Aim:

This study evaluated the biological effect of the N-terminal AnxA1-derived tetrapeptide AnxA19-12 and its relationship with Fpr2 in murine model of acute peritonitis.

Methods:

Peritonitis was induced by intraperitoneal (i.p.) injection of 1 mL of 0.3% carrageenan solution, while the control mice received only saline. To determine the therapeutic efficacy of AnxA19-12, 15 minutes after carrageenan, animals were treated with 100 µg / animal, isolated or associated with WRW4 (10 µg/animal), diluted in 0.1 ml of sterile saline. For comparative purposes, specific agonist of Fpr2, WKYMVM (Pep; 100 µg/animal), was also administered i.p. alone or with WRW4 (CEUA nº 3308100518).

Results:

After 3 h of the i.p. of carrageenan, the animals had significant influx of neutrophils into the peritoneal cavity (9293 ± 1420 x 10³ cells/mL, p < 0.001), associated with high levels of the cytokines IL-1β, IL-6 and TNF-α (1897 ± 335, 8985 ± 1670 and 102 ± 14,94 pg/mL, respectively, p<0.01) in relation to the Control group. Pharmacological treatment with the AnxA19-12 and Pep associated or not with WRW4, despite not altering the levels of neutrophil influx, provoked a marked reduction of the mono-macrophage migration (AnxA19-12: 946 ± 182, Pep: 599 ± 60 x 10³ cells/mL) when compared to the Control group (2454 ± 213; p < 0.001). Additionally, peptide AnxA19-12 maintained high levels of IL-1β, IL-6 and TNF-α (2241 ± 734, 8197 ± 1582 and 75.86 ± 9,698 pg/mL, respectively) induced by i.p. of carrageenan, and its association with WRW4 did not show differences of IL-1β and TNF-α when compared to the Control group. On the other hand, treatment with Pep alone or associated with WRW4 did not alter the levels of IL-1β and TNF-α in relation to the Control group, while maintaining similar levels of IL-6 in relation to the Carrageenan group.

Conclusion:

Altogether, data show that AnxA19-12 is not effective in controlling neutrophil migration and production of inflammatory cytokines in the peritonitis model. Future studies may clarify its biological effect on the mono-macrophage lineage.

Financial support:

PBIC/CNPq; FAPESP

FeSBE Annual Meeting 2019

Poster Sessions and Abstracts

20.007 - STEPHALAGINE, A DERIVED APORPHINE ALKALOID, INDUCES ANTINOCICEPTIVE EFFECTS BY TRPA1 AND TRPV1 CHANNELS MODULATION IN MICE. Justino AB, Neves TV, Brum ES, Saraiva AL, Oliveira SM, Pivatto M, Espindola FS, Silva CR, - Instituto de Biotecnologia - UFU Departamento de Bioquímica e Biologia Molecular - UFMS Instituto de Química - UFU

Introduction:

Pain relief represents a critical unresolved medical need. Consequently, the search for new analgesic agents is intensively studied. Plant-derived alkaloids have previously demonstrated antinociceptive effects with suggested modulation of transient receptor potential (TRP) channels.

Aim:

This study aimed to investigate the antinociceptive properties of stephalagine, a Brazilian Savanna aporphine alkaloid from *Annona crassiflora* Mart. fruit peel, and its possible modulation of TRP channels.

Methods:

Male C57BL/6J/UFU mice, weighing 20–25 g at six weeks of age, were used in the experiments (CEUA/UFU-104/17, May 19th, 2018). Mice were pretreated with vehicle (10 mL/kg) or stephalagine (0.1, 0.3 and 1.0 mg/kg) by oral gavage, p.o. (in order to evaluate a systemic effect), 1 h prior to the intraplantar injection of 20 µL of cinnamaldehyde (1.3 µg/paw), capsaicin (1.6 µg/paw) or formalin 1% in the right hind paw, i.pl. (n=6/group). In another set of experiments, mice received vehicle (10 µL paw) or stephalagine (10 and 100 µg/paw) by intraplantar route, coinjected with cinnamaldehyde, capsaicin or formalin as described above (in order to evaluate a local effect) (n = 6/group). Animals were then evaluated for 30 min for the time spent licking the paw. Moreover, the stephalagine' effect was tested on capsaicin (20 µM) and cinnamaldehyde (30 µM) induced Ca²⁺ influx in spinal cord synaptosomes. SB-366791 (selective TRPV1 antagonist, 10 µM), A967079 (selective TRPA1 antagonist, 30 µM), were used as controls. In addition, *in silico* assessments of the absorption, distribution, metabolism and central nervous system permeability of stephalagine were carried out. Mice were also tested for locomotor coordination in a rotating bar (rotarod) and in an open field task after treated with 1 mg/kg of stephalagine, vehicle or 10 mg/kg of diazepam, used as a positive control.

Results:

When administered by oral route (1 mg/kg), stephalagine reduced the spontaneous nociception and paw edema induced by TRPV1 agonist, capsaicin (inhibitions of 68 ± 9% and 18 ± 4%, respectively), and the nociception induced by TRPA1 agonists, cinnamaldehyde (inhibition of 58 ± 6%) and formalin (inhibitions of 29% and 65% for the neurogenic and inflammatory phases), without altering the animals' locomotor activity observed by the number of crossing and rearing in the open field test, as well as number of falls on the rotarod test. The intraplantar administration of stephalagine (100 µg/paw) was not able to reduce spontaneous nociceptive response induced either by capsaicin, cinnamaldehyde and formalin. Furthermore, values of bloody-brain barrier permeability (BBB) and central nervous system permeability (CNS) were above 0.3 log BB and -2 log PS, respectively, indicating that stephalagine may act directly in the central nervous system. Furthermore, this alkaloid reduced the capsaicin- and cinnamaldehyde-mediated Ca²⁺ influx, indicating a possible modulation of TRPV1 and TRPA1 channels, respectively.

Conclusion:

Together, our results support the antinociceptive and anti-edematogenic effects of the aporphine alkaloid stephalagine, and suggest that these effects are triggered, at least in part, by TRPV1 and TRPA1 modulation.

Financial support:

Institucional - UFU

20.008 - LEVELS OF CUTANEOUS GALECTIN-9 ARE DOWNREGULATED BY DEXAMETHASONE TREATMENT IN ATOPIC DERMATITIS. Areias LL, Corrêa MP, Gil CD, - Morfologia e Genética - UNIFESP Departamento de Biotecnologia - UNESP

Introduction:

Galectin-9 belongs to a protein family characterized by a conserved carbohydrate recognition domain (CRD) of approximately 135 amino acids responsible for its binding to β-galactoside sugars. In experimental models of inflammation, Gal-9 has been pointed as an anti-inflammatory mediator. However, in relation to its mechanisms of action in allergy, Gal-9 can play a dual role, either regulating or activating the cellular response. In this context, Gal-9 is able to bind to IgE and prevent the formation of the antigen-antibody complex, preventing degranulation of the mast cells and release of pro-inflammatory mediators. *In vitro* studies Gal-9 is able to act as a chemoattractant factor for eosinophils.

Aim:

This study was designed to evaluate the expression pattern of Gal-9 and its relationship with inflammatory cells in ovalbumin (OVA)-induced experimental atopic dermatitis in mice.

Methods:

Male Balb/c mice were immunized on days 0 and 7 with a subcutaneous injection of 5 µg of OVA and 10 mg/mL of aluminum hydroxide adjuvant diluted in 200 µl of sterile saline. The skin of mice was challenged with drops containing 250 µg of OVA diluted in 50 µl of JOHNSON'S® baby oil on days 11, 14-18 and 21-24. In the last week (days 21-24), mice were treated with dexamethasone (Dex; 1 mg/kg) intraperitoneal, diluted in 0.1 ml of saline 15 minutes prior OVA challenge. Control groups were constituted by Naive (mice were not subjected to any procedures related to the AD model) and Sham (mice that received sterile saline and JOHNSON'S® baby oil alone). After 24 hours mice were euthanized to histological, immunohistochemical, immunofluorescence and western blotting analyses (CEUA 7067300817).

Results:

AD was characterized by epidermal hyperplasia and a marked influx of eosinophils (134±22.7 cells/mm²), mast cells (94±7.5) and CD207/langerin-positive cells (38±13) compared to control group (5±2.5, 32±1.6 and 5±3, respectively, P<0.01). Dex-treated mice exhibited skin thickness similar to control group, as well as produced a lower influx of these inflammatory cells into the dermis. Additionally, AD induced increased levels of Gal-9 in the skin, as evidenced by immunohistochemistry and western blot, especially localized in the epidermis and inflammatory cells. Gal-9 was co-localized with mouse mast cell protease 6 and eosinophil peroxidase in the cytoplasm of mast cells and eosinophils, respectively, as demonstrated by immunofluorescence analysis. Treatment with Dex reduced Gal-9 levels in the skin relative to the untreated AD group, an effect correlated with the reduction of inflammatory influx.

Conclusion:

Altogether, our results evidenced the participation of the Gal-9 protein in the pathogenesis of AD, constituting this protein as a relevant therapeutic target.

Financial support:

FAPESP (2017/10610-1 and 2017/26872-5)

22 - Cancer Signaling and Therapeutics

22.001 - BOTRYOSPHAERAN DECREASES THE WALKER-256 TUMOR DEVELOPMENT AND THE CANCER CACHEXIA SYNDROME IN WISTAR RATS. Martins KO, Geraldelli D, Ribeiro MC, Medeiros TC, Oliveira MF, Oliveira GA, Dekker RF, Barbosa-Dekker AM, Alegriani P, Queiroz EAIF, - Instituto de Ciências da Saúde - UFMT Programa de Pós-graduação em Ciências em Saúde - PPGCS - UFMT Departamento de Química - UEL

FeSBE Annual Meeting 2019

Poster Sessions and Abstracts

Programa de Pós-Graduação em Engenharia Ambiental (PPGEA) - UTFPR

Introduction:

Background: Cancer is a multifactorial disease, characterized by an uncontrolled growth of cells. Botryosphaeran, a (1→3)(1→6)-β-D-glucan, produced by the fungus *Botryosphaeria rhodina*, has been described to present antimutagenic, hypoglycemic and hypocholesterolemic effects. Furthermore, a previous study demonstrated that botryosphaeran exhibited a direct antiproliferative and pro-apoptotic effects related to the activation of AMPK and FOXO3a in MCF-7 cells (in-vitro). So, we hypothesized that botryosphaeran could decrease the tumor development in Wistar rats by a direct and/or indirect mechanism.

Aim:

Thus, the objective of this study was to analyze the botryosphaeran effects on tumor development in male Wistar rats and analyze the metabolic and hematologic profile of these animals.

Methods:

Methods: Study protocol was approved by the Ethics Committee under n°23108.973436/2018-54. Adult male Wistar rats were divided into two groups: Control Tumor-CT and Control Tumor Botryosphaeran-CTB, and received standard ration and water ad libitum throughout the experimental period. On the first day of the experiment, 1x10⁷ Walker-256 tumor cells were inoculated subcutaneously into the right flank of the rats, and concomitantly treatment with botryosphaeran (30mg/kg/day, via gavage, for 15 days) started. After the treatment, the animals were euthanized, and weight evolution, feed intake, adipose and muscle tissues weights, glucose and lipid profiles, and hemogram were analyzed. Moreover, tumor development and cachexia syndrome were measured, and the expression of proteins (Bax, Bcl-2, caspase-3, p27, p53 and FOXO3a) was determined by Western Blotting. The comparison between the groups was performed by Student's t-test and significant differences at p<0.05.

Results:

Results: Botryosphaeran significantly reduced tumor weight (OT=43.8±19.5g and OTB=12.5±9.0g#; #p<0.05) and the incidence of cachexia in the animals. Furthermore, the rats treated with botryosphaeran was not considered cachectic by the cachexia index (<10), demonstrating that this (1→3)(1→6)-β-D-glucan protected the animals from this condition. Botryosphaeran decreased the triglyceride and increased the HDL-cholesterol levels, and corrected the hypochromic macrocytic anemia, leukocytosis, lymphocytosis, and thrombocytopenia, presented by the CT group, improving the metabolic and hematologic conditions of these rats. CT and CTB groups presented neutrophilia and monocytosis, however, these parameters were significantly reduced in the CTB group. Finally, Bax (pro-apoptotic protein) expression was significantly higher in the CTB group demonstrating that botryosphaeran can be increasing the apoptosis of Walker-256 tumor cells by a direct or indirect mechanism.

Conclusion:

Conclusion: Botryosphaeran at a dose of 30 mg/kg/day was effective in reducing tumor development and cancer cachexia syndrome, increasing the Bax expression, and improving the metabolic and hematologic profiles of the animals contributing to a better prognosis.

Financial support:

UFMT and FAPEMAT

22.002 - PEPTIDE FROM POU DOMAIN OF TRANSCRIPTION FACTOR BRN2 IS INTERNALIZED AND INHIBITS CELL MIGRATION AND INVASION OF MURINE MELANOMA B16F10-NEX2. Cesar MCM, Souza VS, Paschoalin T, Mortara RA, Travassos LR, Arruda DC, - Núcleo Integrado de Biotecnologia - UMC Departamento de Microbiologia, Imunologia e Parasitologia - UNIFESP Unidade de Oncologia Experimental - UNIFESP Departamento de Biofísica - UNIFESP

Introduction:

Melanoma is a form of skin cancer that causes 55.000 deaths/year according to the World Health Organization. Melanoma originates from melanocytes mutations and causes very aggressive metastases. BRN2 transcription factor, an overexpressed protein in melanoma, is involved with cell differentiation, proliferation, migration and metastasis formation. Peptides from the transcription factor could act as competitors of the original binders to DNA and regulate protein expression, controlling cell metastasis. Currently, several groups showed that some peptides from transcription factors present antitumor activity, being a promising option for the development of new therapies.

Aim:

The present work aimed to determine whether peptide C9K derived from POU domain of BRN2 transcription factor is internalized, inhibits migration, invasion and induces protective effect in vivo.

Methods:

B16F10-Nex2 murine melanoma cells were treated with peptide C9K (0.5 mM) derived from BRN2 and peptide internalization and cell migration, invasion and internalization were determined. The wound-healing method was used to measure migration using four different time periods. Inhibition of cell invasion was determined using transwell inserts and matrigel. To verify the internalization of the peptide, cells treated with biotinylated C9K were fixed, permeabilized, stained with DAPI, Phalloidin-Rhodamine and Streptavidin Alexa-Fluor 488 and analyzed by confocal microscopy. For in vivo assay, melanoma cells were intravenously inoculated in C57Bl/6 male mice, which were treated intraperitoneally with 300 ug/day/mice of peptide. After treatment, mice were sacrificed and the lungs removed for nodule counting. For toxicity assay, mice were treated with 1 mg/day/mice of C9K for three consecutive days. After two days, animals were sacrificed and lungs, heart, kidneys, liver and spleen were removed to prepare histopathological slides. In vivo assays were approved by the Ethics Committee in Animal Use (CEUA) (Protocol 005/2015 and 003/2018). Statistical analyses were done using Student's test t.

Results:

Peptide C9K (0.5 mM) inhibited B16F10-Nex2 cell migration after 24 hours of incubation. Untreated cells migrated 0.5 mm while treated cells travelled 0.06 mm. At the same concentration, the peptide inhibited cell invasion in 24h of treatment. An average of 54 untreated cells invaded matrigel membrane compared to an average of 22 of treated cells. By confocal microscopy, we observed that C9K was internalized by melanoma cells. It was observed that C9K peptide colocalized with actin fibers and nuclei, remaining associated with both structures 24h after treatment. Furthermore, C9K showed in vivo protective effect inhibiting lung nodules development. Untreated mice C57Bl/6 showed an average of 381 nodules while treated ones presented an average of 120 nodules (p < 0.0001). Finally, C9K showed no toxic effects in mice treated with high concentration.

Conclusion:

B16F10-Nex2 cells internalized the peptide C9K derived from BRN2 transcription factor in 2h and remained associated with F-actin and nuclei for 24h. Peptide also inhibited cell migration and invasion at 24 hours and an in vivo protective effect, decreased lung nodules in treated mice. Therefore, C9K deserves further investigation as a potential tool for new therapies.

Financial support:

Capes and FAPESP.

22.003 - CELL CYCLE INTERFERENCE BY C15D PEPTIDE DERIVED FROM THE BRN2 TRANSCRIPTION FACTOR IN MURINE MELANOMA CELLS. Anastácio JM, Cunha FFM, Costa CA, Rodrigues T, Travassos LR, Arruda DC, - Núcleo Integrado de Biotecnologia - UMC Centro Interdisciplinar de Investigação Bioquímica - UMC Centro de Ciências Naturais e Humanas - UFABC Unidade de Oncologia Experimental - UNIFESP

Introduction:

FeSBE Annual Meeting 2019

Poster Sessions and Abstracts

Melanoma is a skin cancer originated from genetic mutations in melanocytes, which encode proteins of regulatory pathways that control cell proliferation, adhesion and death. The BRN2 transcription factor is expressed in melanocytes and overexpressed in melanoma. Recent studies showed that peptides derived from BRN2 transcription factors induce cell death, which make these molecules possible targets for cancer treatment.

Aim:

To determine peptide C15D interference in the cell cycle and inhibition of cell migration, being it derived from the transcription factor Brn-2 from murine melanoma cells.

Methods:

B16F10-Nex2 cells were incubated with C15D peptide for 24 and 48 h, at 0.06 to 1 mM. The cell viability was determined by Trypan blue exclusion test. Cells were pre-incubated with necroptose inhibitor (necrostatin), inhibitors of ROS (N-acetylcysteine), pancaspase (Z-VAD) and autophagy (3-methyladenine) and then, incubated with 1 mM of peptide C15D for 24 h and cell viability determined as indicated above. DNA degradation was performed by TUNEL assay at 1 mM of C15D treatment for 24 h. For hemolysis determination, human erythrocytes were treated with the C15D for 30 min and the absorbance measured in a spectrophotometer. To determine cell migration, the wound-healing method was used to measure migration in the presence of 0.5 mM peptide. The effect on the cell cycle was determined with cells incubated with the peptide for 0.25, 0.5 and 1.0 mM for 24 h. After treatment the cells were fixed with paraformaldehyde, permeabilized with saponin and treated with RNase, then stained with propidium iodide and analyzed in flow cytometry, in FL2 channel.

Results:

Treatment with 1 mM of the peptide decreased cell viability in 48% after 24 h and 43% after 48 h. C15D did not induce hemolysis in human erythrocytes. It was not possible to detect signs of cell death because the C15D peptide maintained its effect even in the presence of cell death inhibitors and did not induce DNA degradation. The peptide inhibited cell migration after treatment at 0.5 mM for 24 h. Treated cells migrated $0.11 \text{ mm} \pm 0.03$ while the untreated ones migrated $0.21 \text{ mm} \pm 0.01$. Moreover, C15D interfered in the cell cycle by inducing arrest in the G2 / M phase at 0.25 mM (10.7%), 0.5 mM (28.7%) and 1.0 mM (27.2) compared to the untreated control (1.14%).

Conclusion:

The C15D peptide induced cell cycle arrest in G2/M phase and showed inhibition of cell migration. Furthermore, C15D did not induce hemolysis in human blood cells, or DNA degradation in melanoma cells.

Financial support:

Capex and Fapesp.

22.004 - ASTAXANTHIN INDUCES AUTOPHAGY BY INCREASING INTRACELLULAR H₂O₂ LEVELS IN B16F10-NEX2 MELANOMA CELLS AND EXHIBITS ANTITUMOR ACTIVITY IN VIVO. Cunha FFM, Tonon AP, Travassos LR, Machado FC, Azevedo RA, Gadelha FR, Miguel DC, Grazia N, Arruda DC, - NIB - Universidade de Mogi das Cruzes Instituto de Química - USP Instituto de Biologia - Unicamp Unidade de oncologia experimental - Unifesp

Introduction:

The incidence of melanoma increases annually. This type of skin cancer can resist to current treatments, demonstrating the importance of having new drugs for its treatment. Astaxanthin, found in algae and marine animals, is a carotenoid that belongs to the xanthophyl family and presents a potent biological activity as compared to other carotenoids. The inhibitory effect of astaxanthin in the growth of different tumor cells, including colon, fibrosarcoma, breast, prostate cancer cells and fibroblasts, has been reported, making astaxanthin a promising agent in this field.

Aim:

Determination of astaxanthin cell death and mechanism of action in B16F10-Nex2 melanoma cells and its in vivo activity in a melanoma metastatic model.

Methods:

Astaxanthin was purified from *Haematococcus pluvialis*. B16F10-Nex2 cells were incubated with astaxanthin (0-80.0 μM , for 12 and 24 h) and viability was determined by MTT assay. The viability of non-tumor cells incubated with astaxanthin was also tested. The cytotoxic effect was evaluated in the presence of a reactive oxygen species (ROS) inhibitor (N-acetyl L-cysteine) and ROS production in treated B16F10-Nex2 cells was measured by dihydroethidium (DHE) assay. Moreover, H₂O₂ and superoxide anion production were assayed using Amplex red[®] and MitoSOX, respectively. Morphologic changes were observed by transmission electronic microscopy. The level of expression of autophagic proteins was determined by Western blotting. In addition, in vivo antitumor activity in the melanoma metastatic model was observed following treatment with astaxanthin administered by oral gavage in mice C57Bl/6. Ethics Committee on the Use of Animals (CEUA) approved the project. Protocol 020/2017. Statistical analysis: Student's test t and One-Way ANOVA.

Results:

Astaxanthin exerted cytotoxic effects in B16F10-Nex2 cells in vitro. EC₅₀ was $55.00 \pm 0.94 \mu\text{M}$ and $38.05 \pm 0.98 \mu\text{M}$, for 12 and 24 h, respectively. No toxicity was observed in non-tumor L929 fibroblasts and primary murine macrophages. The cytotoxic effect of astaxanthin in B16F10-Nex2 cells was partly inhibited in presence of N-acetyl L-cysteine. Melanoma cells treated with astaxanthin showed higher levels of ROS production, especially H₂O₂, but superoxide anion levels were similar to control. Vacuole formation was observed in treated cells. Increased expression of LC3I, LC3II and Atg12 proteins in treated cells was observed. Astaxanthin showed antimetastatic effects in vivo in the murine B16F10-Nex2 melanoma.

Conclusion:

We have shown that astaxanthin displays antitumor effects in vitro and in vivo with increased H₂O₂ intracellular levels and induces autophagy in B16F10-Nex2 cell line.

Financial support:

CAPES and FAPESP.

22.005 - ANTITUMOR EVALUATION IN VITRO OF NAPHTHOQUINONES MANNICH BASES FOR POSSIBLE TREATMENT OF OSCC. Souza MP, Forezi LSM, Wermelinger GF, Ferreira VF, Silva FC, Robbs BK, - Departamento de Ciências Básicas - UFF

Introduction:

Oral squamous cells carcinoma (OSCC) is the sixth most incident cancer in the world. There were 345,864 new cases and 177,384 deaths registered in 2018, the disease is more common in males older than 60 years, reaching women less. The survival rate for the OSCC is around 5 years and is considered the lowest between malignant neoplasms. Among drugs used more often for the treatment are carboplatin and cisplatin. However, in addition to the high costs of treatment side effects of nephrotoxicity, acquired resistance have been associated to this chemotherapeutics.

Aim:

the aim of the study was to evaluate the cytotoxic effect, selective and hemolytic activity of 18 naphthoquinones mannich bases compounds in OSCC and human fibroblasts cells lines.

Methods:

The 18 compounds synthesis occurred through the fusion of lausone to a Mannich reaction (MB1-18), which consists in aminomethylation of an activated carbon next to a carbonyl functional group employing an aldehyde and a primary or secondary amine with acid catalysis. Cytotoxicity and selectivity of the different compounds and controls were evaluated by MTT cell viability assays in OSCC (SCC9, SCC25) and normal human cells (fibroblast). Hemolysis assays were performed to

FeSBE Annual Meeting 2019

Poster Sessions and Abstracts

test the surfactant power of the compounds in sheep blood red cells (CECAL / Fiocruz). From the compounds dose-response curves and from the non-linear regression the concentration values required for the 50% inhibition of the cells (IC50) were calculated. The selectivity index (SI) was calculated as: IC50 of normal cells / IC50 of tumor cells, SI > 2 indicates that the compound is selective.

Results:

The 18 compounds showed dose dependent cytotoxicity; 4 compounds showed high selectivity: MB10 (IS: 2.6); MB11 (IS: 2.6); MB12 (IS: 3.3); MB17 (IS: 3.6), compared to controls, carboplatin (IS: 1.4) and lapachol (IS: 1.6) indicating that the compounds are more cytotoxic in tumor cells than in normal cells. Hemolysis assays indicated that the 18 compounds do not have hemolytic activity, with values to presenting less than 5% hemolysis indicating that they did not damage the membranes of the erythrocytes and could be used in animal testing.

Conclusion:

The results indicated that 4 of the 18 naphthoquinone mannich bases synthetic compounds have cytotoxic and selective potential in OSCC cells. In this context, further tests will be carried out to obtain the molecular mechanisms and in vivo toxicity of this possible therapeutic target for the treatment of OSCC.

Financial support:

CNPq; CAPES; FAPERJ, PROPPi/UFF.

22.006 - THERAPEUTIC ACTIVITY OF THE DICHLOROMETHANE FRACTION OF THE PIPER CERNUUM PLANT IN MICE WITH ORAL SQUAMOUS CELL CARCINOMA. Silva RC, Queiroz LN, Wermelinger GF, Macedo AL, Marinho RFN, Moreira DL, Valverde AL, Robbs BK, Robbs BK, - Departamento de Ciências Básicas - UFF Departamento de Química orgânica - UFF Departamento de Produtos Naturais - Fundação Oswaldo Cruz

Introduction:

Oral squamous cell carcinoma (OSCC) stands out as a public health problem in Brazil, being the 5th and 12th most common cancer among men and women respectively. Approximately 630,000 new patients are diagnosed annually worldwide with OSCC, resulting in more than 350,000 deaths. The OSCC's 5-year overall survival rate is approximately 60%. It has been discovered that plant species of the family Piperaceae have demonstrated bioactive properties that can act in many biological systems. Plants of the genus Piper L. have been widely used in traditional medicine to treat cancer or cancer-like symptoms, but little is known about their use / treatment of oral cancer. Data from our group demonstrated, in vitro, that dichloromethane partitions of the leaves of the Piper cernuum plant are cytotoxic and selective for OSCC cells and were not toxic to mice acutely.

Aim:

To evaluate the therapeutic activity, chronic toxicity and survival rate in the use of Piper Cernuum's dichloromethane fraction (PCDF) in OSCC models in vivo.

Methods:

Piper cernuum leaves (PC - leaves) were collected in January of 2015 in the Serra dos Orgãos, Guapimirim / RJ National Park (GPS 22 ° 29'36 `S 42 ° 59'54` W). After the preparation of the dichloromethane partition extract was carried out. With the authorization of CEAU / UFF982, the administration of carcinogen 4-Nitroquinoline 1-oxide (4NQO) was carried out in C57/BI/ 6 mice in the first 8 weeks after waiting for 8 weeks for tumor development that were confirmed visually. Subsequently, treatment for 8 weeks with intraperitoneal injection of preparation of PCDF, 30mg/kg, twice a week. These animals were divided into 2 groups: Histology, where after treatment were euthanized, with 24 weeks of experiment, to perform the histology; and the Survival Analysis group, where survival of the animals was observed for 50 weeks. The histology group was subdivided into a control group (n=4), a group that received PCDF (n=6), a group that received 4NQO

(n=6) and a group that received 4NQO + PCDF (n=6); the Survival Analysis group subdivided into a control group PCDF (n=6), the group that received 4NQO (n=10) and the group that received 4NQO + administration of PCDF (n=10); for reasons of statistical analysis the number of animals in this group was higher. Macroscopic and histopathological analysis of the tongue of these animals was performed. Survival was analyzed by a Kaplan-Meier curve in the GraphPadPrism 5 program.

Results:

There was a statistical difference in the survival curve with $p > 0.03$. Histological analysis of tumor progression revealed macroscopic and microscopic analysis between the groups 4NQO and 4NQO + PCDF in the number of tumors, indicating a possible therapeutic activity of this partition.

Conclusion:

Given the need for new drugs for the treatment of OSCC, the present study indicates PCDF as an important candidate for pharmacotherapy, since the results are promising. There is a need for further studies to determine the mode of action and active principles of PCDF which is being carried out by our group.

Financial support:

CNPq; CAPES; FAPERJ; PROPPi/UFF

22.007 - EVALUATION OF THE EFFECTS OF THE CAROTENOID FUCOXANTHIN ON LAMININ IN HUMAN GLIOBLASTOMA MULTIFORME CELLS. Krüger JV, Marques NF, Nedel CB, - Departamento de Biologia Celular, Embriologia e Genética - UFSC Departamento de Bioquímica - UFSC

Introduction:

Gliomas are tumors of Central Nervous System (CNS) that are originated from glial cells or its precursors. This type accounts for about 80% of the malignant neoplasms of the brain. One of the most common and aggressive gliomas is Glioblastoma Multiforme (GBM). Its treatment is very difficult, the standard treatment is surgery followed by radio and chemotherapy, and the median survival of the patients is about 14 months. The main compound used in chemotherapy is the Temozolomide (TMZ), an alkylant agent. However, TMZ causes many side effects and many types of gliomas present resistance mechanisms against it. Another cause of incidence is the high invasive GBM feature. For that, is necessary many extracellular matrix (ECM) components alterations, like laminin (LN), that is involved in the cell-ECM adhesion. Some types of LN are overexpressed in glioma cells and involved in its invasion. Fucoxanthin (Fx) is a carotenoid that have shown anticancer effects, including antimigratory, suggesting to be an interesting substance for future clinical use.

Aim:

The objective of this work was to evaluate the effects of Fx on LN on human GBM primary culture cells (GBM1).

Methods:

The effect of Fx on viability of GBM1 cells was carried out by the MTT assay, after 24 h of treatment, in three groups of cells: control (CTRL, with DMEM-F12); vehicle (VHC, DMEM-F12 + DMSO); and treated (DMEM-F12 + Fx 100µM). Then, a GBM cell adhesion assay was performed in the same three groups after 6 h, 12 h and 24 h. Finally, the distribution of LN in the ECM after 24 h was analyzed by immunocytochemistry in CTRL and treated groups. Statistical analysis was performed by one-way analysis of variance (ANOVA) followed by the Newman-Keuls test. Data were expressed as mean with standard error. The software used was GraphPad Prism 5 and values $p < 0.05$ were considered significant.

Results:

After 24 h, treatment with Fx 100µM reduced significantly cell viability by approximately 30% (CTRL – mean: 104.2, standard error (SE): 7.878; VHC – mean: 102.2, SE: 6.999; and Fx – mean: 70.89, SE: 5.397). Regarding cell adhesion, Fx did not cause alterations after 6 h and 12 h,

FeSBE Annual Meeting 2019

Poster Sessions and Abstracts

but decreased cell adhesion after 24 h (6 h: CTRL – mean: 0.3768, SE: 0.1994; VHC – mean: 0.2611, SE: 0.07034; treated – mean: 0.2576, SE: 0.05812; 12 h: CTRL – mean: 0.4977, SE: 0.1069; VHC – mean: 0.3579, SE: 0.04325; treated – mean: 0.3620, SE: 0.03467; and 24 h: CTRL – mean: 0.2484, SE: 0.005701; VHC – mean: 0.2468, SE: 0.009500; treated – mean: 0.1798, SE: 0.01375), with $n = 3$ in five times. The immunocytochemistry showed a decreased in LN staining after 24 h.

Conclusion:

These findings show that Fx decreases cell viability, cell adhesion and reduces LN staining, indicating the important role of LN in GBM viability and adhesion. LN may be important therapeutic targets, as well as Fx may be used as adjunctive treatment. However, immunocytochemistry has not been quantified and there are many other molecules in ECM and others that modulate it, so more studies need to be done.

Financial support:

CAPES, CNPq, INCT

22.008 - GLYPCAN-1 IN HUMAN GLIOBLASTOMA: IMPLICATIONS IN TUMORIGENESIS AND CHEMOTHERAPY. Listik E, Toma L, - Departamento de Bioquímica - Universidade Federal de São Paulo

Introduction:

Glioblastoma (GBM) is the most common brain malignant tumor, in which patients have a mean survival of 24 months. Scientific literature has indicated that glypican-1 (GPC1) is highly expressed in human GBM and correlates to low survival. GPC1 is a cell membrane proteoglycan with heparan sulfate chains, molecules that can bind morphogenic factors related to cancer.

Aim:

This work aim was to perform a knock-down of GPC1 in human U-251 MG human GBM cells and perform biological, biochemical and pharmacological assays to investigate GPC1 role in GBM tumorigenesis.

Methods:

The GPC1 gene silencing was induced with shRNA integrated by lentivectors, and monoclonal silenced cells lines were isolated by limited dilution. Further assays with RT-qPCR for GPC1 and related genes, flow cytometry for GPC1, cell viability, migration, proliferation, adhesion, clonogenicity, were performed. Furthermore, confocal microscopy to assess GPC1 localization in lipid rafts, against flotillin-1, and correlated proteoglycans, glypican-3 and syndecan-4, were also conducted. The generated cells were also submitted to susceptibility assay to temozolomide, a common antineoplastic drug for GBM. Silenced clones were compared against original U-251 MG and a negative viral transduction control.

Results:

RT-qPCR results reveal that the clones were silenced in more than 90% of GPC1 mRNA, in which they revealed altered expression of several heparan sulfate proteoglycans and reduced levels of metalloproteinases 2 and 9, indicating attenuation in tumor invasion. Flow cytometry analysis of GPC1 reveals that gene silencing not only reduced GPC1 expression of the clones but a mean of 20.5% of the cells ceases to synthesize the core proteins. The cell viability assay revealed that clones' growth was inhibited to a rate of up to 71% and proliferation to 51%. The migration capacity was diminished in 57% which correlates to the reduced ability of the clones in interacting with extracellular matrix substrates such as laminin, collagen IV and vitronectin. Clonogenicity assays demonstrate that GPC1 silencing reduces clone formation up to 75%. Confocal imaging corroborates that GPC1 is practically absent in silenced cells; nevertheless, the proteoglycan did not reveal much presence in lipid rafts (PCC = 0.05) or along syndecan-4 (PCC = 0.155) and glypican-3 (PCC = 0.2). However, syndecan-4 levels showed stability comparing silenced and control cell lines, yet glypican-3 revealed reduced levels in silenced clones. Finally, temozolomide's IC50 was up to 5 times lower in GPC1 silenced clones (1.57 mM) compared to U-251 MG (8.15 mM), revealing that the

reduced expression of GPC1 can make the cells susceptible to the antineoplastic drug.

Conclusion:

The results reveal how GPC1 may influence various aspects of GBM tumorigenesis, from tumor behavior and progression to influence in therapy. We seek to demonstrate not only some basic mechanisms of how this proteoglycan may integrate several biological aspects of GBM, but also introduce it as a target for future medicine.

Financial support:

FAPESP, CAPES, CNPq

22.009 - CHARACTERIZATION OF THE ANTITUMOR ACTIVITY OF THE PIPER CERNUUM SPECIES IN ORAL SQUAMOUS CELL CARCINOMA CELLS (OSCC). Machado TQ, Fonseca ACC, Macedo AL, Marinho RFN, Moreira DL, Valverde AL, Robbs BK, - Departamento de Ciências Básicas - Universidade Federal Fluminense

Introduction:

Oral squamous cell carcinoma (OSCC) is one of the 10 most common types of cancer. Plants of the genus Piper are used in traditional medicine to treat cancer, and they present a diversity of phytochemicals with cytotoxic potential.

Aim:

Analysis of cytotoxic potential and selectivity of Piper cernuum chromatographic partitions using three different oral squamous cell carcinoma (OSCC) cell lines, which are OSCC4, OSCC9, OSCC25; and fibroblasts.

Methods:

Methanol crude extract of P. cernuum leaves (CEPCL) and hexane, dichloromethane and ethyl acetate chemical partitions were produced (HPPCL, APPCL, DPPCL). Chromatographic partitions were prepared from the dichloromethane chemical partition of Piper cernuum. Partitions and fractions were tested by clonogenic and cell viability (MTT assay), using carboplatin as positive control. OSCC cell lines (SCC4, SCC9, SCC25) and primary human fibroblasts were used for all assays. From the dose-response curves of the compounds and from the non-linear regression the concentration values required for the 50% inhibition of the cells (IC50) (GraphPadPrism 5) were calculated. The selectivity index (IS) was calculated as: IC50 of normal cells/IC50 of tumor cells, an IS>2 indicates that the compound is selective. Acute toxicity tests were performed in mice according to the CEUA / UFF # 982 protocol.

Results:

In the clonogenic test, it was observed that CEPCL significantly reduced the cell density of the SCC9 line at all concentrations tested (1,5 and 25µg/mL) and reduced cell viability (IC50=106.3±0.06µg/mL) when compared to control (IC50=225.3±0.09µg/mL). Although all partitions showed cytotoxicity, the dichloromethane partition (DPPCL) was the most active (IC50≅47µg/mL). This partition induced reduction of cell number, induced membrane permeabilization (6.5 times more cells than control), was not hemolytic and not acutely toxic in mice. Seven chromatographic partitions of DPPCL were analyzed for its cytotoxicity where fractions 9 (IC50=40.25) and 12 (IC50=79.64) were the most active.

Conclusion:

After analysis it can be concluded that the extracts, partitions and fractions of P. cernuum were active against the cell lines of SCC9. In addition, chromatographic partitions of dichloromethane from Piper cernuum tested on OSCC9 cells had a significant inhibitory effect on the viability of oral squamous cells. The objectives will now be to determine which major substances are present in the most active and selective partitions and cell death pathway.

Financial support:

CNPq; CAPES; FAPERJ, PROPPI/UFF.

FeSBE Annual Meeting 2019

Poster Sessions and Abstracts

22.010 - ANALYSIS OF THE SELECTIVITY AND CYTOTOXICITY OF PIPER CABRALLANUM CHROMATOGRAPHIC FRACTIONS IN ORAL SQUAMOUS CELL CARCINOMA (OSCC). Wermelinger GF, Macedo AL, Moreira DL, Valverde AL, RobbsBK, RobbsBK, RobbsBK, - Departamento de Ciências Básicas - UFF Departamento de Química Orgânica - UFF Departamento de Produtos Naturais - Fiocruz

Introduction:

The oral squamous cell carcinoma (OSCC) brings together a heterogeneous group of malignant neoplasias, where in Brazil it makes up about 95% of the cases of cancer incidence and mortality of the mouth. In order to discover new drugs able to combat OSCC, we chose four species of the genus *Piper*, from Rio de Janeiro, for experimentation, since ethnobotanical studies indicate that plants of this genus have demonstrated function for cancer treatment.

Aim:

Phytochemical characterization and evaluation of chemopreventive and therapeutic biological activities in OSCC of chromatographic fractions of *Piper cabralanum* leaf.

Methods:

In an initial scan, using five species of the genus *Piper* (*P. mollicomum*, *P. arboreum*, *P. truncatum*, *P. cernuum* and *P. cabralanum*) using crude extracts and chemical fractions of methanolic, hexanic and ethyl acetate, were verified for its cytotoxicity and selectivity. Later the *P. cabralanum* was subjected to a chromatographic partitioning process, because in the previous tests presented selectivity index of 3.83. Subsequently, cell viability assays (MTT) were performed in SCC9 and fibroblast cells from primary cultures in order to verify the selectivity of the chromatographic partitions. Hemolytic assays were also performed using erythrocytes derived from fresh lamb blood.

Results:

In the initial tests performed, it was verified that *P. cabralanum* has a selectivity of 3.83, when compared the IC50 obtained in tumor cells and in the untransformed cells in the cellular viability assays. In the MTT assays the chromatographic fractions of *P. cabralanum* obtained the following IC50 in cells of the SCC9 line, where each number was assigned to a major partition: # 2 (42.75 µg / ml ± 0.070); # 3 (40.89 µg / ml ± 0.041); # 4 (42.72 µg / ml ± 0.063); # 5 (54.28 µg / ml ± 0.05); # 6 (46.82 µg / ml ± 0.034); # 12 (61.33 µg / ml ± 0.029); # 16 (53.71 µg / ml ± 0.055). In the untransformed cells the following concentrations of IC50: # 4 (97.17 µg / ml ± 0.10) were obtained; # 5 (54.28 µg / ml ± 0.04); # 12 (203.20 µg / ml ± 0.03), at the concentrations tested, the results obtained with the remaining fractions were ambiguous and are being repeated. Fraction 12 obtained IS of 3.31 and 4 of 2.27. In the hemolytic assay it was observed that no fraction induced significant hemolysis, except for 16 which obtained approximately 10%.

Conclusion:

After a scan in the chromatographic partitions, we can observe that partition 12 presents a good index of selectivity, besides not being hemolytic. The chemical analysis by MS / MS is being performed to determine the major compound.

Financial support:

CAPES; FAPERJ; CNPq; PROPPi/UFF

22.011 - CYTOTOXICITY AND SELECTIVITY OF THE EQUISETUM HYEMALE EXTRACT IN ORAL SQUAMOUS CELL CARCINOMA. Queiroz LN, Silva DPD, Pereira MTM, Pascoal ACRF, Robbs BK, - Departamento de Ciências Básicas - UFF

Introduction:

Cancer was the second leading cause of death in 2018 and oral squamous cell carcinoma (OSCC) stands out for the high mortality and low survival rate and low treatment evolution in the last 30 years. Therefore, the development of new treatments becomes necessary. Plants in the genus *Equisetum* are popularly used in the treatment of various diseases including cancer.

Aim:

Phytochemical analysis of the *Equisetum hyemale* stem, evaluation of the antiproliferative effect and determination of the cell death pathway induced by the extracts in the OSCC.

Methods:

Ethanol crude extract was prepared from the stem of *Equisetum hyemale* and clonogenic assays and cell viability assays were performed with MTT. Subsequently, the crude stem extract was partitioned into liquid/liquid fractions in hexane (EHH), dichloromethane (EHD) and ethyl acetate (EHA) and the MTT assay repeated. The IC50 was calculated by non-linear regression curve in the GraphPadPrism 5 program. Cell morphology was analyzed by microscopy and cell death analyzed in the propidium iodide (P.I) labeling assay. Hemolysis tests were performed with goat blood. The concentration of phenols and flavonoids were quantified based on controls of gallic acid and quercetin, respectively. SCC9 cells and primary human fibroblasts were used. Acute toxicity tests were performed on C57 Black/6J according to the CEUA/UFF #982 protocol. Liquid chromatography (Acquity HPLC) with mass spectrometer (TQD Acquity) was performed for the fractions.

Results:

Through the clonogenic assays and MTT assays with the crude extract IC50 of 200.6±0.09 µg/ml was calculated. In the cell viability assay with the partitions the IC50, EHA (64.5±0.072 µg/ml) was calculated and the EHH and EHD fractions did not reach 50% inhibition at the concentrations tested. As a positive control, Carboplatin chemotherapy (366.1±0.18 µg/ml) was used. To investigate the type of death the morphology of cells treated with EHA was analyzed by microscopy where lower numbers of cells, increased cytoplasm, and large amounts of granules and vacuoles were observed. The EHA partition was shown to be less hemolytic than the control, reduced the absolute number of cells in culture and induced its permeabilization of the tumor cells. The EHA fraction presented (0.41±0.17 µg/mg) phenol and (0.85±0.10 µg/mg) flavonoids. These partitions were selective when tested on normal primary fibroblasts and had no acute toxicity in mice. The LS / MS results are still under analysis.

Conclusion:

After analysis of the results it can be concluded that the *Equisetum hyemale* stem extract has a cytotoxic effect against oral squamous cells, with the EHA fraction being the most selective and non-toxic in vivo. Analysis of LC mass (LC-MS/MS) is being performed to identify possible active compounds.

Financial support:

CNPq; CAPES; FAPERJ, PROPPi/UFF.

22.012 - CYTOTOXIC POTENTIAL OF SYNTHETIC COMPOUNDS OF NAPHTHOQUINONES WITH ACRIDINE NUCLEUS IN ORAL SQUAMOUS CELL CARCINOMA (OSCC). Ouverney G, Zorzaneli BC, Fonseca ACC, Silva FC, Ferreira VF, Robbs BK, - Departamento de Ciências Básicas - UFF Departamento de Química Orgânica - UFF

Introduction:

Oral cancer that includes oral squamous cell is the fifth most prevalent in men in Brazil and in 2018 11.200 new cases were registered in the country. The use of traditional chemotherapy in the treatment, despite proven efficiency, have several side effects. The naphthoquinones, organic substances identified by the presence of cyclic diones conjugated by two connections C=C also exhibiting a naphthalene ring have proven cytotoxic potential. The production of substances containing acridine nucleus shows great antineoplastic potential. The formation of synthetic compounds containing naphthoquinones with acridine nucleus is an attractive planning strategy for new therapeutic agents.

Aim:

Conduct in vitro biological assays of cytotoxicity and selectivity of 15 synthetic naphthoquinone compounds fused to acridine nucleus in SCC9 human oral squamous cell carcinoma (OSCC) lineage and normal human fibroblasts.

FeSBE Annual Meeting 2019

Poster Sessions and Abstracts

Methods:

The compounds were synthesized by Drs. Fernando and Vitor group at Instituto de Química da Universidade Federal Fluminense. The synthesis is based on molecular hybridization to form new compounds maintaining acridine nucleus through reaction having as raw material 2-amino-1,4-naphthoquinone which provides different structural characteristics but preserving biological characteristics of the original substances. 15 compounds were obtained: NAC1-15. The SCC9 OSCC cell lineage and the normal human fibroblasts were submitted to MTT cell viability assay. The tumor cells were treated in at least 4 different concentrations, and fibroblasts were treated in twice the 50% inhibitory concentration of cell viability determined in SCC9 (2xIC₅₀). DMSO, Lapachol and Carboplatin were used as negative or positive controls.

Results:

The following IC₅₀ values were obtained in the assays in the SCC9 lineage with the compounds: NAC1 (14,69±0,011); NAC2 (51,57±0,189); NAC3 (14,71±0,126); NAC4 (5,86±0,1575); NAC5 (4,105±0,070); NAC6 (4,467±0,070); NAC7 (2,066±0,072); NAC8 (8,934±0,096); NAC9 (2,218±0,123); NAC10 (4,754±0,068); NAC11 (7,636±0,096); NAC12 (6,844±0,1415); NAC13 (7,206±0,086); NAC14 (5,906±0,145); NAC15 (3,323±0,132). Fibroblast tests were used to determine the selectivity of each compound. As used twice the concentration that kills 50% of the tumor cells, viability values higher than 50% in fibroblast would indicate that the compound is selective. Values higher than 70% indicate high selectivity. This test showed that compounds NAC5 (82% viability), NAC7 (73,68%), NAC3 (72,70%) and NAC9 (67,77%) are highly selective, while NAC4 (50,99%), NAC6 (53,72%), NAC8 (55,62%) and NAC10 (57,45%) are selective (viability > 50%).

Conclusion:

From the tests performed so far it is clear that some compounds have a great selective potential, being given continuity to those with IC₅₀ higher than 70% that will be tested on different tumor cell types and normal ones and assays to characterize cell death pathway will be performed.

Financial support:

CNPq; CAPES; FAPERJ, PROPPI/UFF.

22.013 - EVALUATION OF THE ANTITUMOR ROLE OF ISOLATED COMPOUNDS FROM PIPER RIVINOIDES FOR A POSSIBLE TREATMENT OF ORAL SQUAMOUS CELL CARCINOMA. Ribeiro AV, Fonseca ACC, Marques AM, Moreira DL, Robbs BK, - Departamento de Ciências Básicas - UFF Programa de Pós-Graduação Stricto Sensu em Odontologia - UFF Departamento de Produtos Naturais - Fiocruz

Introduction:

The oral squamous cell carcinoma (OSCC) stands out as a public health problem in Brazil due to its high incidence and low survival rate, despite advances in diagnosis and treatment. Therefore, the development of new drugs is urgent. Plants of the genus Piper are popularly used in the treatment of various diseases. These plants, as well as isolated neolignans (secondary metabolites), had their cytotoxic effect on tumor cells demonstrated, but the effect of the Piper rivinoides species on the treatment of OSCC is still unknown. The aim of this study was to perform the phytochemical analysis of the leaves of Piper rivinoides, evaluation of the antitumor effect and determination of the cell death pathway induced by the compounds in cell lines of oral cancer.

Aim:

The aim of this study was to perform the phytochemical analysis of the leaves of Piper rivinoides, evaluation of the antitumor effect and determination of the cell death pathway induced by the compounds in cell lines of oral cancer.

Methods:

The crude ethanolic extract was prepared from Piper rivinoides leaves. Then, the crude extract of the leaves was partitioned in liquid/liquid fraction in hexane. Of the hexane fraction, three neolignans were isolated: Conocarpan, Eupomatenoid-5 and Eupomatenoid-6. Cell

viability, compound stability and time curve assays were performed by MTT. The IC₅₀ was calculated by a non-linear regression curve in the GraphPad Prism 5 program. The release of reactive oxygen species (ROS) was investigated by DHR123 labeling. Pyknotic nuclei were analyzed to evaluate the type of cell death. At least 3 independent experiments were performed.

Results:

Viability assays showed that the three compounds were effective in inducing cell death in three different OSCC cell lines (SCC9, SCC4 and SCC25) compared to the standard chemotherapeutic agent Carboplatin. The mean IC₅₀ was 36.06µM for Conocarpan, 31.78µM for Eupomatenoid-5, 32.99µM for Eupomatenoid-6 and 200µM for Carboplatin. Through MTT assays, we found that Conocarpan is more stable than Eupomatenoid-5 and Eupomatenoid-6, resembling the high stability of Carboplatin; furthermore, we observed that the cytotoxic effect of the three compounds is time-dependent. There was no significant release of ROS for the three compounds compared to control (vehicle, DMSO). Moreover, results suggest that Conocarpan induce apoptosis due to the observation of pyknotic nuclei, but this data must be confirmed; there was no significant presence of pyknotic nuclei for Eupomatenoid-5 and Eupomatenoid-6 treatments compared to control (vehicle, DMSO).

Conclusion:

Among the purified neolignans from Piper rivinoides, Conocarpan was the most effective compound against OSCC cells, presenting high cytotoxicity and stability, and might be considered for future cancer therapy.

Financial support:

CNPq; CAPES; FAPERJ; PROPPI/UFF

23 - Regenerative Medicine and Developmental Biology

23.001 - NOVEL ROLE OF THE DROSOPHILA ROUGHEST CELL ADHESION PROTEIN IN MODULATING OVARIAN CONTRACTION ACTIVITY AND EGG CHAMBER MORPHOLOGY. Valer FB, Silva-Junior RMP, Spegorim GC, Ramos RGP, - Dept Biologia Celular e Molecular - USP Dept Clínica Médica - USP

Introduction:

Drosophila ovaries are formed by multiple cell types that make distinct contributions to their shape. Each ovary contains 15 strings of egg chambers in different developing stages from S1 to S14. Egg chambers, in turn, consist of 16 germ cells (GCs) surrounded by a monolayer follicular epithelium. Initially spherical, these structures elongate as they mature. This elongation is thought to occur through a 'molecular corset' mechanism, whereby structural elements within the epithelium become circumferentially organized perpendicular to the elongation axis and resist the expansive growth of the GCs to promote elongation. Another mechanism is provided by the contractile activity of the muscle sheaths that surround developing egg chambers. Although these two mechanisms provide good explanations about egg chamber elongation, they are not fully understood.

Aim:

Here, we uncover a novel role of cell adhesion molecule Roughest (Rst) in modulating contraction activity of the ovary, which can determine egg chamber morphology.

Methods:

Immunocytochemistry analysis; Gene expression by RT-qPCR; Kymographs using Fluorescence microscope

Results:

By immunocytochemistry, we first showed that Rst is expressed both in the basolateral region of the follicular epithelium and in the muscle sheaths. Analysing several available rst mutant alleles, we next showed that four of them are female sterile. rst mRNA quantification by RT-qPCR from 2-days old ovaries of the mutants indicate expression at 2 and 4 levels of magnitude less than controls. Finally, kymographs

FeSBE Annual Meeting 2019

Poster Sessions and Abstracts

measuring ovary contractions demonstrate that muscle sheaths of the mutants are hypo-contractile with impaired frequencies and this can lead to abnormal egg chambers shapes.

Conclusion:

Taken together, our data suggest a contribution of Rst to egg chamber elongation mechanisms by modulating muscle sheath contractility.

Financial support:

CAPES, FAPESP Grant 2018/18437-0

23.002 - DEVELOPMENT AND EFFICACY OF PLGA MICROPARTICLES CONTAINING CROTAMINE IN WOUND HEALING THERAPY. Pimentel VE, Gomes ABSP, Rodrigues TFS, Santana DS, Genari MC, Alfândega AAA, Aro AA, Caetano GF, Esquisatto MAM, Andrade TAM, Mazzi MV, - Protein and Peptide Characterization Laboratory - University Center of Hermínio Ometto Foundation (FHO)

Introduction:

Wound healing is a pathological process that ruptures the skin anatomical continuity and may cause infections. Crotonamine is a peptide present in the *C. durissus* terrificus snake venom. It has analgesic properties and myonecrotic effects. In addition, crotonamine belongs to the beta-defensin peptides and has such demonstrates antibacterial properties. Poly lactic-co-glycolic acid (PLGA) has been among the most attractive polymeric candidates used to devices for drug delivery and tissue engineering applications.

Aim:

Determine and characterize how PLGA microparticles, containing Crotonamine promotes wound healing.

Methods:

CEUA-UNIARARAS: 018/2018. Peptide-PLGA was prepared using the single emulsion/water. Skin permeation test was performed in vitro by using vertical Franz apparatus to assess passive diffusion of Crotonamine. For in vivo assay, forty-eight male Wistar rats (60 days, ~200g) were randomly divided into 4 groups (n=4) in each group, containing one vehicle control group (hydroxyethylcellulose gel), PLGA and CTM-PLGA (0.05%) groups. Cutaneous ulcers of 1.5 cm diameter were performed on the dorsum of the animals using histological punch and the lesions were treated daily. Samples of lesion / scar areas were collected after 2, 7 and 14 days (n = 4/group/ time) and analyzed for changes in histopathological parameters related to inflammatory infiltrate and blood vessels formation. Determination of ulcers healing index (UHI) was also assessed. Data were expressed as mean±SEM and statistical analysis used was ANOVA and Tuckey with p <0.05.

Results:

CTM and CTM-PLGA (0.05%) presented a wound healing ability in rats and this effect was time dependent. Results indicated that topical application of CTM (0.05%) on rats significantly accelerated wound closure compared with rats treated with vehicle control, and mainly for the second day. However, CTM group induced increased wound healing (WH) at the higher compared to CTM- CTM-PLGA group. The UHI of CTM and CTM-PLGA treated groups was 0.7 and 0.4 respectively versus 0.3 of the original size in control after the treatment for 2days. In contrast, all the groups (SHAM, PLGA, CTM and CTM-PLGA) showed similar UHI (0.6) after 7 and 14 days of treatment. Histopathological alteration showed angiogenic profile in CTM and CTM-PLGA groups. Higher number of blood vessel was observed in CTM group on the second day, when compared to the control group (SHAM=2±0.333 and CTM=3.4±0.1633). In addition, angiogenic profile was also observed in the CTM and CTM+PLGA groups when compared to SHAM (3.4±0.1633, 6±0.5963 and 6.1±0.5260, respectively) after the treatment for 14d. The inflammatory infiltrates was higher in CTM and CTM+PLGA groups when compared to SHAM group (67.00±4.351, 146.4±10.94 and 106.3±6.326, respectively) after the treatment for 14d.

Conclusion:

The results show that Crotonamine has healing power in the different treatment times, where the percentage of cicatrization was at 94.96%

and suggesting that, when conjugated to PLGA, it has a prolonged release effect, eliminating possible toxic effects and increasing your local action. In addition, our findings corroborate that Crotonamine has an angiogenic profile and suggesting an inflammatory modulation response alone or when conjugated to PLGA, providing new insights into the development of wound healing therapy.

Financial support:

FHO-Uniararas, CNPq

23.003 - EVALUATION OF THE BIOACTIVITY OF A BORATE-BASED BIOGLASS DEVELOPED WITH DIFFERENT CONCENTRATIONS OF PHOSPHORUS PENTOXIDE IN BONE REGENERATION. Almeida GHDR, Sousa BM, Gavazzoni A, Giroto C, Portes P, Sato F, Pedrochi F, Hernandez L, - Department of Morphological Sciences - State University of Maringá Department of Odontology - State University of Maringá Department of Physics - State University of Maringá Department of Clinical Analysis - State University of Maringá Department of Physics - Federal University of Maranhão

Introduction:

Bioglasses are bioactive materials widely used for orthopedic and dental purposes. The bioactivity of a bioglass is directly related to its chemical composition and, therefore, changes in its components are proposed to improve its properties in bone formation.

Aim:

The objective of this study was to evaluate in vitro by spectroscopic infrared via Fourier transform analysis, the physicochemical changes in the surface of the bioglass the borate with different phosphate concentrations in their chemical composition and evaluate, ex vivo, the process of bone regeneration of critical size defects in calvaria of rats after grafting with the materials.

Methods:

For the in vitro study, three formulations of borate-based bioglass with different percentages of phosphate in its composition were produced: 0% (BV0), 2% (BV2), 4% (BV4) and one silica-based (45S5). The bioglass was cut into discs for in vitro and ground to in vivo analysis. In vitro bioactivity studies were performed by immersing the disks in simulated body fluid (SBF) at the 14, 21 and 28 days intervals and measuring the infrared absorption via FTIR by a spectrophotometer equipped with Attenuated Total Reflection (ATR) accessory. For in vivo studies (CEUA protocol nº 4282010716), 96 male Wistar rats were used, which were divided into four groups according to the graft material. The rats were submitted to the surgical procedure for the manufacture of a critical size defect in the calvaria. Each defect received the graft of their respective material. Euthanasia of the animals occurred at 15, 45 and 60 days after surgery, and the calvaria was collected for histological study. The material underwent decalcification and histological processing for staining of H&E and Azan to evaluate the action of biomaterials on bone formation.

Results:

The in vitro study showed that the most significant changes occurred in BV0 samples. When compared to the 45S5 control, the BV0 bioglass was the one that presented the fastest dissolution and developed. The FTIR-ATR analysis also revealed that the layer formed in BV2 retained longer the shape of the bands originating from the borate bioglass, in order to overlap and attenuate the bands of phosphates and carbonates. In in vivo study, a dispersion of the granules interspersed by a very cellular and vascularized connective tissue was observed; deposition of bone matrix. At 60 days of observation, the tissue that filled the defect was denser than in previous periods and there was no evidence of an inflammatory response. The BV2 group had the highest frequency of bone islets among the borate groups, increased frequency of matrix deposition replacing the granule over time and less dissolution in vitro. These results suggest that the addition of 2% of phosphate in this formulation resulted in a more stable and more bioactive material compared to 4% borate and non-phosphate borate.

FeSBE Annual Meeting 2019

Poster Sessions and Abstracts

Conclusion:

Based on the in vitro and ex vivo analyzes, it can be concluded that different concentrations of phosphate altered the borate-based bioglass dissolution process and that a small addition of phosphate increased the stability of the biomaterial, resulting in a better bioactivity.

Financial support:

CNPq

23.004 - TRIB3 EXPRESSION AND TISSUE LOCALIZATION IN SKELETAL MUSCLE UNDER REGENERATION AND MYOGENESIS. Sougey WWD, Silvestre JG, Moriscot AS, - Anatomia - Universidade de São Paulo- USP

Introduction:

The skeletal muscle is an intensely recruited tissue, therefore susceptible to lesions that can compromise skeletal muscle fibers, leading to homeostasis breakdown, which might include disturbed insulin signaling. In this sense TRIB3 might be an important factor, since it is a potent AKT2 inhibitor and it has been shown to be involved in altered metabolic conditions such as insulin resistance and obesity. Here we hypothesized that the skeletal muscle under regeneration have altered levels of TRIB3 and that TRIB3 is involved in the regenerative and myogenic processes.

Aim:

The aim of this study is therefore to investigate the levels of expression and role of TRIB3 in the myogenic process by using C2C12 cells and skeletal muscle regeneration after injury.

Methods:

For that purpose, initially we cultured C2C12 cells in DMEM 10% FBS medium with addition of antibiotics at 37°C with 5% CO₂. Cultures were conducted to a confluence of ~50% (undifferentiated group; Und) and also ~80% confluence (control group 0; Con 0) and then differentiation was induced with 2% HS for 2 days (Diff 2) or 4 days (Diff 4). Subsequently cells were harvested and total RNA was isolated and used for gene expression measurements by RT-PCR. To investigate muscle regeneration, 16 adult male C57 / B16 mice (8 weeks of age, 30 ± 3g) were maintained in a 12/12h light/dark regimen and received food and water ad libitum. Regeneration was induced by injections of cardiotoxin (10µM) in the left Tibialis Anterior muscle, which was previously surgically exposed under anesthesia. Mice were killed by cervical dislocation and immediately TA and Soleus muscles were removed 1, 3 and 10 days post-injury. TA samples were cryopreserved and then processed for total RNA isolation and further TRIB3 gene expression measurement using RT-PCR. The RT-PCR results were analyzed using the -ΔΔCt method and statistic results were obtained using t-student test in comparison with control group, which did not receive cardiotoxin injection, or one-way ANOVA for nonparametric data and Dunns post-hoc for C2C12 samples analyses, always expressed in Mean ± SD. Soleus samples were frozen in hyper cooled isopentane and stored in liquid nitrogen for subsequent immunofluorescence analysis using anti-MHCI, anti-MHCII and anti-TRIB3 antibodies on muscle transversal cryosections. All experiments were approved by the Institute Of Biomedical Sciences Animal Experimentation Office Committee (6085260718).

Results:

We observed increased gene expression of TRIB3 in Con group when compared to Und group (~28 fold change, P<0.0005), decreased levels in Diff 2 group in comparison to Con group (~17 fold change, p<0,005) and no difference in TRIB3 expression between Diff4 and control groups. Using cardiotoxin-injured mice, we observed increased TRIB3 gene expression in 1, 3 and 10 days post-injury (~19, ~9 and ~5 fold changes respectively; p<0,05) compared with control. We also preliminarily observed, by immunofluorescence assay, that TRIB3 showed particular patterns of distribution comparing type I and type II fiber types apparently related to myosin heavy chain localization.

Conclusion:

Overall, these results suggest that TRIB3 is strongly regulated in C2C12 cells in differentiation and also in skeletal muscle tissue undergoing regeneration.

Financial support:

FAPESP

23.005 - THE USE OF HEPATIC ACELLULAR SCAFFOLD IN A RAT LIVER TRANSPLANTATION MODEL. Dias ML, Batista CMP, Cerqueira A, Secomandi VJK, Pinheiro LA, Goldenberg RCS, - Instituto de Biofísica Carlos Chagas Filho - UFRJ Hospital Universitário Clementino Fraga Filho - HUCFF

Introduction:

Liver transplantation is the only potentially curative treatment for patients facing end-stage hepatic disease. The surgical procedures include (i) orthotopic liver transplantation (OLT), in which the native liver is removed and replaced by the donor organ in the same anatomic position, (ii) heterotopic auxiliary liver transplantation (HALT) which involves implanting the new liver graft in a non-anatomical location and (iii) auxiliary partial orthotopic liver transplantation (APOLT) where a partial liver graft is implanted in an orthotopic position after leaving behind a part of the native liver. However, transplantation is mainly limited by the supply of transplantable donor organs resulting in increasing transplantation waiting lists. In this context, the creation of a bio-artificial liver might solve this clinical problem.

Aim:

The aim of this work was to optimize a surgical HALT technique to transplant decellularized liver scaffolds (DLS).

Methods:

Donor Wistar rats were heparinized, anesthetized and then submitted to transverse abdominal incision. The portal vein (PV) was separated and cannulated, Teflon tube was attached to the inferior vena cava (IVC) and fixed. Then the superior vena cava (SVC) was clamped. After removal, the donor liver was perfused via PV with 5 ml of custodiol solution (organ storage solution) supplemented with 10 µl of heparin (50 IU/ml) and placed in a cold saline bath for 5 minutes. Then, the livers were transferred to be perfused through portal vein using an infusion pump at 3 ml/min with water for 1 hour followed by 1% Triton X-100 for 2 hours and SDS 1% for 24h. After total decellularization, livers were washed with distilled H₂O for 2 days. To improve the DLS shape and the HALT performance, the matrix was perfused with 10 ml of rat blood diluted in 40 ml of custodiol solution for 1 hour and washed with 3 ml of phosphate saline solution (PBS). Then, the matrix was analyzed by H&E staining. Adult Wistar rats were used as recipients for HALT. Briefly, animals were heparinized and anesthetized by vaporized isoflurane. Then, under anesthesia animals were submitted to transverse abdominal incision and the left arterial and renal vein were clamped. After that, the nephrectomy of the left-side kidney was performed. The PV and IVC of the DLS were anastomosed to the recipient rats' left arterial and renal vein in an end-to-end anastomosis, respectively. Finally, the recipients' abdomens were closed.

Results:

After blood perfusion, the DLS shape resembled a native liver and H&E staining showed some cell retention on vessels of DLS. Active blood flow within the DLS was observed indicating that the PV and IVC of the scaffolds were able to sustain the arterial blood pressure when the circulation was re-established. No internal bleeding was observed prior to the rat abdomen closure. H&E staining and immunofluorescence analysis showed some cell retention on vessels and confirm CD31+ endothelial cells and Ki67+ cells 8 hours post HALT.

Conclusion:

Here, we performed a HALT surgical technique to transplant DLS. Also, our findings suggest that DLS were repopulated by recipient rat cells allowing cell attachment and proliferation. The decellularization protocol preserved the structural characteristics of the native microvascular network allowing blood perfusion and the

FeSBE Annual Meeting 2019

Poster Sessions and Abstracts

transplantation. In conclusion, our method is a promising approach of transplanting an engineered liver tissue for application in the hepatic regenerative medicine.

Financial support:

CNPq, Capes, FAPERJ, INCT-REGENERA, Ministério da Saúde

23.006 - THE INFLUENCE OF NATURAL RUBBER LATEX MEMBRANES WITH BIOTRANSFORMED SOYBEAN EXTRACT AND HYDROXYAPATITE ON THE GROWTH AND DIFFERENTIATION OF OSTEOBLASTS PRIMARY CULTURES. Torqueti AMR, Herculano RD, Faria AN, - Itajubá University Center - FEPI Biotechnology and Bioprocesses Dep., - UNESP Pharmaceutical Sciences - USP

Introduction:

Latex membranes (L) are a new green technology that can be used as a deposition system, as soybean phytoestrogens. These two technologies may be used to the treatment of bone fractures and loss. A biotransformed soybean extract (BSE) showed an improved gut absorption and activity on estrogen receptors, and were used to improve the membranes occlusion.

Aim:

The objectives of this research were to test this innovative technology for the development of natural latex membranes with BSE and hydroxyapatite. To test the safety of these products in contact with bone tissue by the in vitro evaluation of the growth and differentiation of osteoblasts.

Methods:

In order to develop a controlled delivery system for bone occlusion, it was used to improve the Latex membranes: with BSE adsorbed (L+BSE A); L with hydroxyapatite (LH); L with hydroxyapatite and BSE adsorbed (LH+BSE A). However, still there are no studies about its safety on bone cells. For this purpose, was investigated the toxicity of BSE on osteoblasts primary cultures at the concentrations of 0.5; 1, 4 and 6 µg/mL by the evaluation of osteoblasts viability, alkaline phosphatase activity, total proteins, and mineralized matrix formation. After this, the same tests were performed with the membranes.

Results:

The results showed that at concentrations below to 4 µg/mL of BSE its use on osteoblasts cultures were safe and used to develop the membranes. The analysis showed that L+BSE S and LH+BSE A increased the viability, matrix mineralization and ALP of osteoblasts cultures when compared to L membranes.

Conclusion:

This study concluded that L+BSE A and LH+BSE S increased the ALP, viability, and mineralization of osteoblasts cultures compared to L.

Financial support:

CNPq, CAPES, FAPESP, Pietro Ciancaglioni

23.007 - ROLE OF MIR-101A IN SKELETAL MUSCLE. Bento MR, Ribeiro FS, Silva WJ, MoriscotAS, - Anatomy - USP

Introduction:

The role of miR-101a in skeletal muscle is currently elusive, although important mRNAs related to muscle plasticity are putative targets, such as MuRF-1, MuRF2 and mTOR (obtained by in silico analysis). In this study we aimed to investigate the effect of miR-101a overexpression in C2C12 cells (in vitro) and C57bl/6 mice (in vivo).

Aim:

We aimed to investigate the effect of miR-101a overexpression in C2C12 cells (in vitro) and C57bl/6 mice (in vivo).

Methods:

C2C12 cells were seeded at a density of 80% confluence in proliferation medium (DMEM, 10% FBS and Penicillin and Streptomycin P/S Carlsbad, CA, USA). Then, they were transfected with 40nM of miR-101a mimic, using Lipofectamine 2000. After 24 hours, the medium was changed (DMEM, 2% HS and 1% P/S; Invitrogen, Carlsbad, CA, USA) and the cells

were induced to differentiation. After 5 days, the cells were fixed in 4% PFA and immunofluorescence assays were performed. The miR-101a was electrotransferred to the tibial anterior muscle for time course analysis of overexpression of this microRNA in the skeletal muscle. q-PCR was used to verify the efficiency of transgene expression of miR-101a. The cross-sectional area (CSA) of muscle fibers were determined with the ImageJ software (v. 1.45s, National Institutes of Health). (CEUA # 9910290318).

Results:

In vitro we observed that the miR-101a overexpression did not change the number eMHC positive cells, and myotube fusion index, but was able to severely reduce myotube diameter (~ 40%, p<0.05), as compared to control group. The miR-1 mimic, which is considered a 'gold standard' for skeletal muscle differentiation was used in parallel and was able to increase the number of eMHC positive cells and the myotube fusion index (~2 fold for both parameters), but myotube diameter was similar to control group. In vivo, electrotransfer elevated miR-101a expression (~5x, p<0.05), 4 days after electrotransfer, when compared to the Empty Vector and Naive groups. In addition, the histological analysis showed large areas with inflammatory infiltrate (~90% vs ~10% in EV group; p<0.05) 4 days after electrotransfer, and reduction of CSA in miR-101a overexpression muscles (~50%; p<0.05). Seven days after miR-10a expression vector electrotransfer, we observed that miR-101a kept elevated (~2-fold vs EV; p<0.05) when compared to the Empty Vector and Naive groups. However, miR-101a overexpression did not alter CSA seven days after electrotransfer, compared with EV.

Conclusion:

Overall, these results indicate that miR-101a overexpression drives decrease in CSA and promotes a histological condition compatible with an injured tissue.

Financial support:

FAPESP (#2015/04090-0) and CAPES

23.008 - BIOCELLULOSE MEMBRANE INCORPORATED WITH NANOSILVER PARTICULES STIMULATED ANGIOGENESIS AND COLLAGENESIS ON CUTANEOUS WOUND HEALING IN AN ANIMAL MODEL. Alves MTO, Munhoz LLS, Nascimento MGOF, Alves BC, Sábio RM, Barud HS, Bagnato VS, Andrade TAM, Aro AA, Caetano GF, - Graduate Program of Biotechnology in Regenerative Medicine and Medicinal Chemistry of the University of Araraquara (UNIARA), Araraquara, São Paulo, Br - UNIARA Graduate Program in Biomedical Sciences, University Center of Hermínio Ometto Foundation - FHO|UNIARARAS, Araras, São Paulo, Brazil. - FHO Institute of Physics of São Carlos (IFSC), University of São Paulo, São Carlos, São Paulo, Brazil. - USP

Introduction:

Studies involving natural substances have been increased in order to provide effective wound healing activity at low costs. During wound healing, tissue formation is an important phase to restore dermis and epidermis integrity. It is characterized by granulation tissue formation (fibroblasts and blood vessels) and collagen synthesis. Bacterial cellulose is bio-curative, acts as a support for cell proliferation and provide chemical and mechanical properties. Throughout medical history, silver is involved in wounds treatment due to anti-inflammatory, antimicrobial and healing activities.

Aim:

The objective of the study is to evaluate the application of the cellulose membrane and the cellulose membrane incorporated with nanosilver suspension and its biological stimulus on tissue formation during cutaneous wound healing in an animal model.

Methods:

The animal ethical committee of Hermínio Ometto Foundation approved the experimental protocol (CEUA/UNIARARAS-019/2018). All membranes were donated by the research group on biopolymers and

FeSBE Annual Meeting 2019

Poster Sessions and Abstracts

biomaterials of UNIARA. Seventy-two Wistar rats (300g) were anesthetized by intraperitoneal administration of ketamine and xylazine. Two circular full-thickness wounds were created on the dorsum region of each rat by using a histological punch (1.5cm diameter). The animals were distributed into three groups: SHAM (no treatment), MC (wounds treated with cellulose membrane) and MCP (wounds treated with cellulose membrane+silver). The animals were euthanized on the 2nd, 7th, 14th and 21st postoperative days. After fixation in buffered formaldehyde solution for 24 h and histological routine, the specimens (5.0 µm-thick cut) were stained with hematoxylin-eosin for cellularity and tissue structure evaluation; and Gomori's Trichrome for connective tissue and blood vessels evaluation using the optical microscope Leica DM2000 with camera LEICA® DFC-280 and ImageJ software. Moreover, the collagen content progression during wound healing was measured by biochemical assay by determination of hydroxyproline (absorbance values measured at 550nm). Statistical variations were determined using Two-way ANOVA and Bonferroni post-test with $\alpha=5\%$ using the GraphPad Prism 5 software.

Results:

The number of blood vessels was evaluated by histomorphometric analyses (200-x magnification). It can be observed that MCP had a higher number of blood vessels than SHAM and MC groups (26.1, 12.2, 12.8, respectively) on 2nd day ($p<0.05$). All groups presented a similar number of blood vessels during the other experimental periods. Although no differences were observed for the connective tissue formation, the MCP group presented mean of 138.4 mg of hydroxyproline/g of tissue, higher than SHAM group (90.9mg/g of tissue) and MC group (114.9mg/g of tissue) ($p<0.05$) on the 14th day (collagenesis). Even though it was also observed greater collagenesis in the MCP group on the 7th day, no differences were observed. Collagen is the major structural component of granulation tissue, strengthening the extracellular matrix and replacing the temporary fibrin matrix. The amino acid proline is part of the collagen fiber and hydroxyproline is used as a biochemical marker for tissue collagen as well as a positive indication of healing progression.

Conclusion:

Cellulose membrane and cellulose membrane incorporated with silver seem to favor the tissue organization. Cellulose membrane incorporated with silver accelerated the angiogenesis, the collagenesis and tissue remodeling.

Financial support:

University Center of Hermínio Ometto Foundation

23.009 - ANTI-INFLAMMATORY RESPONSE OF BIOCELLULOSE MEMBRANE INCORPORATED WITH SILVER ON CUTANEOUS WOUND HEALING IN ANIMAL MODEL. Alves BC, Munhoz LLS, Nascimento MGOF, Alves MTO, Sábio RM, Barud HS, Bagnato VS, Andrade TAM, Caetano GF, - Graduate Program in Biomedical Sciences, University Center of Hermínio Ometto Foundation – FHO|UNIARARAS, Araras, São Paulo, Brazil. - FHO Institute of Physics of São Carlos (IFSC), University of São Paulo, São Carlos, São Paulo, Brazil. - USP- São Carlos Graduate Program of Biotechnology in Regenerative Medicine and Medicinal Chemistry of the University of Araraquara (UNIARA), Araraquara, São Paulo, Br - UNIARA

Introduction:

Wound healing is a dynamic process to repair the structure of the injured tissue, divided into three overlapping phases: inflammation, tissue formation, and tissue remodeling. Studies involving potential natural healing substances have gained importance because of long treatment periods and high medical care costs. Bacterial cellulose (BC) is a renewable natural bionanomaterial. BC membranes show a 3D nanosized structure, large porosity, high water absorption capability and biocompatibility. Literature has evidenced efforts in improving the efficacy of BC membranes by adding silver nanoparticles in order to

prevent wound infection, as antimicrobial and antifungal properties. The use of BC membranes incorporated with silver nanoparticles on a pre-clinical model may provide data to its use for wound healing of chronic wounds.

Aim:

The objective of the study is to evaluate cellulose membranes prepared in silver nanoparticles suspension on cutaneous wound healing in an animal model.

Methods:

The animal ethical committee of Hermínio Ometto Foundation approved the experimental protocol (CEUA/UNIARARAS-019/2018). The research group on biopolymers and biomaterials of UNIARA donated the membranes to the in vivo evaluation. Seventy-two males Wistar rats (300g) were anesthetized by intraperitoneal injection of a combination of ketamine and xylazine. Two circular full-thickness wounds were created on the dorsum cervical region of each rat by using a histological punch (1.5 cm diameter). The animals were distributed into three groups: SHAM (no treatment), MC (wounds treated with cellulose membrane dressing) and MCP (wounds treated with cellulose membrane+silver dressing). The animals were euthanized on the 2nd, 7th, 14th and 21st postoperative days with an overdose anesthetic injection. The wounds were photographed separately before collecting samples of wounds/scars for histological and biochemical evaluation. The area of the wounds was calculated using the ImageJ software to analyze the re-epithelialization by the wound healing rate ($WHR = \text{initial area} - \text{final area} / \text{initial area}$). Samples fixed in buffered formaldehyde solution for 24 h were processed for histological analysis. The specimens (5.0 µm-thick) were stained with Hematoxylin and Eosin (HE). The myeloperoxidase (MPO) assay was used to evaluate the neutrophil infiltrate. Determination of macrophagic infiltrate was evaluated by N-acetylglucosamine assay (NAG). Statistical variations were determined using Two-way ANOVA and Bonferroni post-test with $\alpha=5\%$ using the GraphPad Prism 5 software.

Results:

No significant differences were observed among groups for reepithelization, according to the WRH. However, on the 7th day compared to both SHAM and MC groups, both biochemical assays showed that the MCP group presented 50% less neutrophil participation than SHAM and 42% less than the MC group ($p<0.05$). Moreover, the MCP group presented 28% fewer macrophages compared to SHAM and MC groups ($p<0.05$). From day 14 to 21, all groups presented similar decreasing of MPO (neutrophil) and NAG (macrophages).

Conclusion:

The results suggest the use of CB for the development of wound healing dressings and anti-inflammatory response of incorporated nanosilver on the cellulose membrane. The use of silver might play an important role to prevent infection and control de inflammatory phase of the cutaneous wound healing process.

Financial support:

University Center of Hermínio Ometto Foundation

23.010 - TREATED DENTIN FOR USE AS SCAFFOLD FOR STEM CELLS FROM HUMAN EXFOLIATED DECIDUOUS TEETH. Ferraraz DC, Lombello CB, Valle MD, Long SM, Ana PA, - Centro de Ciências Naturais e Humanas - UFABC Centro de Engenharia, Modelagem e Ciências Sociais Aplicadas - UFABC Odontologia - UMEPS

Introduction:

Tissue engineering presents three essential components: cells, scaffold and inducing factors. This field aims to cultivate cells in scaffolds, to restore damaged body parts. The cells used can be obtained from different sources such as, for example, the pulp of deciduous teeth. In the dental pulp are found the stem cells, which are of great importance for tissue repair and regenerative medicine. The chosen scaffold must have a biocompatible structure and may be a source of inductive

FeSBE Annual Meeting 2019

Poster Sessions and Abstracts

factors. Dentin is a mineralized connective tissue that can be used in tissue restoration due to its characteristics.

Aim:

This research evaluated the obtaining and characterization of stem cells from human exfoliated deciduous teeth (SHED) to study the use of treated dentin as scaffolds. The scaffolds were submitted to different treatments for demineralization and were characterized for the analysis of their properties.

Methods:

The cells were obtained from the pulp of deciduous teeth, by explant culture with the use of the enzyme trypsin. Cell characterization was first carried out through adhesion and morphology analysis using light microscopy and scanning electron microscopy (SEM). Cells were also evaluated by flow cytometry, with the antibodies CD45, CD34 and CD90. Finally, it was verified the ability to differentiate in osteoblasts, adipocytes and chondroblasts. The dentine scaffolds were obtained through the processing of human molar teeth. After preparation, the dentin was separated into four groups to perform the treatments: control (without treatment), treatment 1 (ethylenediamine tetraacetic acid), treatment 2 (ethylenediamine tetraacetic acid and citric acid) and treatment 3 (hydrochloric acid). To characterize the scaffolds, structure (SEM), chemical composition (Fourier transform infrared spectroscopy) and cytotoxicity (MTT assay) were evaluated. Afterwards, the cells were inoculated on the dentin for analysis of the cell-scaffold interaction.

Results:

With the results, it was verified that the obtained cells showed growth pattern, morphology and surface antigens characteristic of mesenchymal stem cells. The cells also exhibited the ability to differentiate in the three lineages. In the characterization of the scaffolds, it was observed that the treatments contributed to unblocking the dentinal tubules. It was also found that the demineralizing agents were efficient in removing the minerals from the dentin, exposing the organic part of the matrix (collagen). Treatment 3 presented the highest loss of the mineral portion, followed by treatments 2, 1 and control, according to the analyzes based on the FTIR. The cytotoxicity test demonstrated that treatment 3 caused a decrease in cell density (viability less than 70% of the stem cell culture). In the morphological evaluation of the cells in contact with the scaffolds, it was observed that the SHED developed normally in the dentin.

Conclusion:

Therefore, it was verified that the dentin presents characteristics favorable for the cell culture and the treatments 1 and 2 do not altered cellular development. To continue the evaluations, it will be studied how dentin treatments affect the osteogenic differentiation of the SHED, aiming at the application of the scaffold for bone tissue engineering.

Financial support:

Universidade Federal do ABC and Coordenação de Aperfeiçoamento de Pessoal de Nível Superior (Scholarship)

23.011 - BACTERIAL CELLULOSE HYDROGEL INCORPORATED WITH MONTMORILLONITE IMPROVED TISSUE REPAIR AFTER PRESSURE INJURY MODEL. Menegasso JF, Costa FV, Rabelo BD, Felipetti FA, Antonio RV, Dutra RC, - Department of Health Sciences (DCS) - UFSC Special Coordination of Physics, Chemistry and Mathematics (FQM) - UFSC

Introduction:

Pressure ulcer is defined as a skin lesion resulting from compression between bony prominences and external surface of the patients, which induce necrosis, pain and impairment of quality of life, mainly, in aging individuals. The search for new therapeutic targets for treatment of pressure injury is necessary, and has attracted attention of different researchers. Studies demonstrated that bacterial cellulose membrane has an important mechanical property preventing infection and injury.

Moreover, other studies have shown that montmorillonite has antibacterial properties and is effective in tissue repair. However, the specific mechanisms of bacterial cellulose hydrogel incorporated with montmorillonite action in pressure injury are not well-established.

Aim:

Herein, we investigated therapeutic effects of bacterial cellulose hydrogel incorporated to montmorillonite in the healing of pressure lesions in an animal model.

Methods:

Pressure injury model was induced in 30 male Swiss mice, randomly divided into three groups: control (n=9), bacterial cellulose hydrogel incorporated with montmorillonite (BCH-MMT) (n=9) and Dersani®, used as positive control (n=10). Animals were exposed to four cycles of cutaneous ischemia-reperfusion (I/R), imprisoning dorsal skin between two magnetic plates for 12 hours, followed by removal of the plaque to initiate formation of decubitus ulcer. All procedures used in the present were approved by the Animal Ethics Committee of the Universidade Federal de Santa Catarina (CEUA-UFSC, protocol number 4816200917). On days 5, 10 and 15 animals were euthanized and collected tegument tissue for later histological analysis. The data were analyzed using software R, and Bartlett or Shapiro-Wilk tests were used to verify assumptions deviation. A statistical comparison of the data was performed by one-way ANOVA followed by the Tukey test.

Results:

Histological analysis showed that, on days 5 and 10, tissue repair was similar in all groups. However, BCH-MMT (29469±29469 optical density) and Dersani® (23736±23736 optical density) showed complete re-epithelialization of epidermis and inhibited inflammatory cells when compared to control group (334105±54327 optical density) on day 15 after pressure injury induction.

Conclusion:

The application of BCH-MMT improved cutaneous tissue repair after pressure lesions induction in mice. Thus, the hydrogel showed great potential for biotechnological innovation, particularly considering the low cost of production and the easy therapeutic applicability.

Financial support:

CNPq; CAPES; FAPESC; INCT-INOVAMED; PGN-UFSC.

23.012 - THE INTERGENIC REGIONS BETWEEN THE DEVELOPMENTAL GENES KIAA0586, DACT1, AND DAAM1 CONTAIN SEVERAL CONSERVED NON-CODING ELEMENTS (CNES) WITH POTENTIAL REGULATORY ACTIVITY. Veiga FC, Janousek RG, Fontoura MA, Alvares LE, - Departamento de Bioquímica e Biologia Tecidual - UNICAMP Laboratório Nacional de Biociências - CNPEM

Introduction:

The identification of cis-regulatory elements over the past decades made it possible to associate mutations with several human diseases. Due to the great relevance of this kind of assessment, we intended to unveil possible mechanisms of expression control of three developmental neighbor genes, that are also related to human pathologies.

Aim:

This work aims to contribute to the understanding of KIAA0586, Dact1, and Daam1 genes regulation by identifying and characterizing DNA sequences (conserved non-coding elements, CNES) that may act as their possible regulators.

Methods:

Firstly, we did a literature search to compile KIAA0586, Dact1, and Daam1 developmental expression patterns and phenotypes caused by their disruption. Then, ECR Browser was used to compare the genomes of human, mouse and chicken in order to identify CNES in the locus comprehending Dact1 and flanking genes KIAA0586 and Daam1. To locate conserved transcription factors binding sites (TFBSs), CNES were subjected to the MultiTF software based on the TRANSFAC library. In addition, UCSC Genome Browser was used to verify the interactions

FeSBE Annual Meeting 2019

Poster Sessions and Abstracts

between mouse CNEs and specific proteins based on ChIP-Seq data applying all tracks for regulation analysis. Finally, CNE4, identified with the greatest regulatory potential by bioinformatic analyses, was amplified by PCR from *Mus musculus* genomic DNA and cloned into the vector pGL2-TK-Luc. The transcriptional activity of this CNE was tested in HEK293T cell culture. Luciferase activity was expressed as a ratio to the reporter gene expression supported by unmodified pGL2-TK-Luc (Fold Expression). Statistical significance was analyzed by the two-tailed Student's t-test ($p \leq 0.05$). Data were presented as mean \pm standard error of the mean (SEM) based on 3 independent experiments.

Results:

Data collection from the literature revealed that the genes encompassed in the genomic interval analyzed in this work share either similar expression patterns and/or phenotypes when mutated, suggesting that may be under the control of common regulatory elements. In addition, we identified eight CNEs in the intergenic region comprehending KIAA0586, *Dact1* and *Daam1* genes. The TFBSs analysis revealed great regulatory potential of the CNEs in developmental processes especially in neurogenesis, eyes, heart, skeleton, and genitourinary tract formation, myogenesis, and adipogenesis. UCSC Genome Browser BLAT supported the regulatory potential of the CNE4, which presented histone profiles highly significant to active regulatory regions. In HEK293T cell culture, the activity of the Luciferase reporter construct driven by the CNE4 was significantly higher than that observed in the control plasmid, demonstrating its enhancer characteristics.

Conclusion:

The CNEs identified among KIAA0586, *Dact1* and *Daam1* genes may be part of a Genomic Regulatory Block (GRB) that controls the expression of these developmental genes in a coordinated fashion. In addition, we demonstrated that a CNE acts as a cis-regulatory element. Although additional studies are needed to characterize the activity of this element during development, this research may serve as basis for identifying single nucleotide polymorphisms (SNPs) that may be related to developmental diseases.

Financial support:

CNPq

23.013 - FIBROBLASTS MIGRATION IN VITRO IS STIMULATED BY THE ELECTRICAL CURRENT APPLICATION. Silva DFD, Fujii LO, Chiarotti GB, Oliveira CA, Adrade TAM, Oliveira ALR, Mesquissatto MA, Mendonça FAS, Santos GMT, Aro AA, - Centro Universitário da Fundação Hermínio Ometto/FHO - Programa de Mestrado em Ciências Biomédicas - FHO/UNIARARAS

Introduction:

The participation of adjuvant therapies has been studied in the repair of lesions in different tissues. Several studies have demonstrated the beneficial effects of the application of electrical current on tissue repair, although the molecular mechanisms involved have not yet been fully elucidated.

Aim:

The aim of the present study was to analyze the effect of the application of the low intensity electric current (microcurrent) until the 4th day of the scratch assay.

Methods:

The parameter used for electrical current application was 10 μ A/90s established after the viability analysis of fibroblasts (NHI/3T3) at different application times (30s, 60s, 90s, 120s and 150s). It was also analyzed the electrical current effects on important genes involved in cell migration, extracellular matrix synthesis and remodeling, such as *Tgfb*, *Ctgf*, *Icam1*, *Igf1*, *Tnc*, *Tnm*, *Fmod*, *Fn1* and *Scx*. Thus, two groups were established: fibroblasts (F) and fibroblasts+microcurrent (F+MC).

Results:

Increase in cell viability was demonstrated in the F+MC group in comparison to the F group in the scratch closure on day 4. In the

molecular analysis, the application of the electrical current did not alter the gene expression profile on day 4 after the scratch assay, although it was observed only a few tendencies to lower expression of genes such as *Igf1*, *Tnc* and *Fmod* in the F+MC group in relation to the F group. It was not observed the gene expression of *Tnm* and *Icam1* in both groups.

Conclusion:

The application of electrical current modulated the cell viability and stimulated cell migration, although the genes involved were not identified on day 4 after the scratch assay. Further studies should be performed aiming to identify the molecular mechanisms involved in the response of fibroblasts after stimulation with the electrical current.

Financial support:

FHO/UNIARARAS

23.014 - GESTATIONAL EFFECTS OF GLYPHOSATE ADMINISTRATION IN MICE. Souza MOB, Júnior VAP, ZAVAN B, - Departamento de Biologia Celular e do Desenvolvimento - UNIFAL-MG

Introduction:

Annual pesticide consumption has increased significantly in recent years, with glyphosate being widely used in Brazilian crops. Responsible for about 40% of the total consumption of agrochemicals in Brazil, glyphosate has been shown to produce a number of adverse effects in both animal and human health. Gestation is a process that requires the occurrence of several changes that are essential for its proper course, such as trophoblastic invasion and vascular remodeling.

Aim:

This work aims to evaluate gestational parameters in mice after glyphosate administration, specifically on the biology of uNK cells, which are protagonists in the processes of uterine vascular remodeling.

Methods:

Pregnant female Swiss mice were divided in two experimental groups: those who received orogastric gavage of glyphosate (GLI - 50mg/kg) or the same volume in water (CON), between gestation day (GD) 1 and GD6; between GD1 and GD10; between GD1 and GD16; and those who received the treatment from GD1 until term. All experimental procedures were approved by the Ethics Committee on the Use of Animals of the Federal University of Alfenas (protocol nº 01/2018). Unpaired t test statistical analyzes were performed using GraphPad Prism 7 software and values of $p < 0.05$ were considered indicative of significance.

Results:

There were no changes in the embryo implantation rate between CON (99.38 \pm 2.9%) and GLI (91.15 \pm 7.1%) animals. The treatment did not interfere in the number of implantation sites observed after euthanasia in GD6 (GLI 12.2 \pm 0.9 vs CON 13.7 \pm 0.6), in GD10 (GLI 14.11 \pm 0.7 vs CON 13.4 \pm 0.4) and in GD16 (GLI 13.6 \pm 0.4 vs CON 13.89 \pm 0.6), but fell embryos presented mal formations or signs of teratogenesis. Treatment with GLI reduced the number of live births (7.75 \pm 1.25 vs 13.25 \pm 1.03, $p=0.0146$). The offspring weight at birth was higher in the GLI group (2.408 \pm 0.04) compared to the CON (2.144 \pm 0.04, $p=0.0003$). Treatment reduced the amount of subtype 1 uNK cells in region 1 (1.917 \pm 0.55 vs 5.2 \pm 1.29, $p=0.0430$), as well as subtype 2 in region 2 (0.8333 \pm 0.27 vs 2.6 \pm 0.63, $p=0.0263$), indicating reduction of immature uNK cells in the uterus concomitant with an increase of subtype 3 in region 3 (11.17 \pm 1.26 vs 4.933 \pm 1.59, $p=0.0068$).

Conclusion:

Glyphosate seems not to alter the implantation rate, nor the number of viable implantation sites until the GD16, however it seems to be related to bad fetal formations, resulting in liveborn pups reduction. Changes in uterine microenvironment seem to accelerate the uNK cells development, reducing the number of immature cells and increasing the number of mature cells. Ongoing studies will evaluate the effects of treatment on vascular remodeling and on the offspring physical development.

Financial support:

FAPEMIG

FeSBE Annual Meeting 2019

Poster Sessions and Abstracts

23.015 - WIDESPREAD TRANSCRIPTION REGULATION OF TLL IN THE SEGMENTATION CASCADE OF DROSOPHILA. Silva IR, Masuda LH, Gueller GC, Machado-Lima A, Andrioli LP, - Laboratório de Genética do Desenvolvimento - USP Laboratório de Bioinformática - USP

Introduction:

The segmentation cascade specifies the antero-posterior axis in *Drosophila* early in embryonic development. This cascade is formed by several transcription factors such as *tailless* (*tll*). *tll* is expressed in a cap at each end of the embryo and consistent with that, *tll* mutants exhibit defects in the formation of terminal structures of the body. However, *tll* genetic assays have also detected patterning defects in genes expressed in middle regions of the embryo.

Aim:

In this study, we investigated the existence of a widespread activity of *Tll* in the embryo.

Methods:

We first used a misexpression system that creates a *tll* ectopic expression domain that intersects the ventral portion of segmentation genes. In these assays we detected disturbances in the ventral regions of several expression patterns mostly consistent with a repression role of *Tll*. We further looked whether the misexpression effects could be due to the direct regulation of *Tll*. For that, we crossed *Tll* binding data from a ChIP-chip assay with the regulatory sequences of the affected expression patterns detected in the misexpression assays. We also cloned the full length cDNA of *tll* in a vector to express a recombinant protein in bacteria to further test *Tll* interactions in DNA binding in vitro assays.

Results:

The misexpression results confirmed previously inferred targets of *tll* regulation and revealed unsuspected targets. Crossing the ChIP-chip data with regulatory regions of the affected patterns in the misexpression system we confirmed possible direct regulation of *Tll* for the majority of them. We are now in the process of induction and purification of the recombinant protein that will be incubated with DNA regulatory regions and checked in DNA shift assays.

Conclusion:

Thus far, we detected a widespread and possibly direct role of *Tll* in the regulatory regions of segmentation genes. These results could imply *Tll* as key regulator avoiding the expression of thoracic and abdominal segmentation genes at terminal regions of the embryo.

Financial support:

FAPESP

23.016 - THE USE OF POLYCAPROLACTONE/HYDROXYAPATITE INTERCONNECTED POROUS SCAFFOLDS AS A BONE SUBSTITUTE AND ELECTRICAL STIMULATION THERAPY FOR BONE REGENERATION: EXPERIMENTAL STUDY. Helaeihil LV, Helaeihil JV, Lourenço CB, Camargo IX, Nalesso PRL, Huang B, Bartolo PJS, Santamaria-Junior M, Mendonça FAS, Caetano GF, - Manchester Biomanufacturing Centre, School of Mechanical, Aerospace and Civil Engineering, University of Manchester - UM Graduate Program of Orthodontics, University Center of Hermínio Ometto Foundation - FHO|UNIARARAS - FHO Graduate Program in Biomedical Sciences, University Center of Hermínio Ometto Foundation - FHO|UNIARARAS - FHO

Introduction:

Conventional treatments for bone regeneration/substitution are based on invasive approaches (autografts and allografts) and present several limitations, such as the need for secondary surgery, anatomic issues and rejection by the immune system. The use of synthetic grafts (scaffolds) produced by additive manufacturing technologies represents a viable approach for bone tissue engineering to support cell adhesion, proliferation and differentiation. Several research groups used poly(ϵ -caprolactone) (PCL) scaffold for bone regeneration however, it presents poor bioactivity. To overcome some limitations, PCL can be combined with hydroxyapatite (HA), an inorganic material widely used for

different medical applications since it provides osteoconductive property and presents a similar mineral structure to natural bone. As bone is a piezoelectric tissue, the exogenous application of electrical stimulation (ES) at physiological levels plays a role in cellular and molecular signaling pathways through the production of cytokines and growth factors.

Aim:

The objective of this work was to evaluate the use of polycaprolactone/hydroxyapatite scaffolds (PCL/HA) and electrical stimulation therapy for bone regeneration in an animal model.

Methods:

The experimental protocol was approved by animal ethical committee of Hermínio Ometto Foundation (CEUA/UNIARARAS-075/2017). PCL and PCL with 20% of HA interconnected porous scaffolds were printed using a screw-assisted additive manufacturing system (0/90° lay-down pattern). Seventy-two Wistar rats were submitted a 5mmx5mm critical-sized square defect using a sharp tip coupled to an ultrasound device under constant irrigation. The following groups were considered: SHAM (bone defect with no scaffold), SHAM+ES (bone defect with no scaffold + electrical stimulation), PCL, PCL+ES, PCL/HA and PCL/HA+ES. The electrical application (10 μ A/5min) was performed twice a week for 60 days. After euthanasia (30 and 60 days), samples were cross-sectioned and stained with hematoxylin-eosin and Masson-trichrome for histomorphometric evaluation (osteoclasts, blood vessels, connective and mineralized tissues) using ImageJ software. Data were processed using GraphPad_Prism software and analyzed by two-way ANOVA with post hoc Bonferroni's test (α =5% significance level).

Results:

The results showed that after 60 days the groups that received scaffolds showed a lower number of osteoclasts around the bone edges when compared to SHAM. Although the number of blood vessels was similar to all groups on the 30th day, PCL/HA and PCL/HA+ES groups presented higher vascular area (approximately 4.5% of area) compared to SHAM (1.8%), SHAM+ES (2%) and PCL (1.7%) groups. On the 60th day, PCL/HA+ES group presented 4% of vascular area compared to SHAM and SHAM+ES groups (1.8%). The connective tissue formation was similar to all groups on the 30th day, but on the 60th, all groups that received scaffolds in the bone defect presented higher connective tissue formation (around 90%) compared to SHAM (76%) and SHAM+ES (68%). Moreover, on the 30th day, PCL/HA and PCL/HA+ES groups presented higher mineralized tissue (16% and 13%, respectively) compared to SHAM (0%), SHAM+ES (1.5%), PCL (5%) and PCL+ES (0.5%).

Conclusion:

The use of interconnected PCL produced with 20% hydroxyapatite scaffolds is a promising approach to be used as a bone substitute, since it presented higher vascular area formation and stimulated higher mineralized tissue, as a positive indicator of bone formation.

Financial support:

FHO, CNPq and FAPESP (2018/21167-4)

23.017 - PCL/B-TCP INTERCONNECTED POROUS SCAFFOLDS AND ELECTRICAL STIMULATION THERAPY AS A TREATMENT FOR CRITICAL-SIZED BONE DEFECTS IN AN ANIMAL MODEL: HISTOMORPHOMETRIC EVALUATION. Helaeihil JV, Helaeihil LV, Lourenço CB, Camargo IX, Pulz RB, Huang B, Bártolo PJS, Mendonça FAS, Júnior MS, Caetano GF, - Graduate Program of Orthodontics, University Center of Hermínio Ometto Foundation - FHO|UNIARARAS - FHO Graduate Program in Biomedical Sciences, University Center of Hermínio Ometto Foundation - FHO|UNIARARAS - FHO Manchester Biomanufacturing Centre, School of Mechanical, Aerospace and Civil Engineering, University of Manchester, Manchester, United Kingdom - UM

Introduction:

Bone repair is a common and complicated clinical problem. When the defects are critical-sized caused by accidents, bone trauma, infections and tumors, the autografts and allografts are therapies used for bone

FeSBE Annual Meeting 2019

Poster Sessions and Abstracts

replacement but these treatments present several limitations. The use of synthetic grafts (scaffolds) produced by additive manufacturing technologies combined with biocompatible and biodegradable materials represents a viable approach for bone tissue engineering. Several research groups used poly(ϵ -caprolactone) (PCL) scaffold for bone regeneration, however, it presents poor bioactivity. PCL can be combined with β -TCP (tri-calcium phosphate), a ceramic material to provide osteoinduction property and stimulate the bone remodeling phase. As bone is a piezoelectric tissue, the exogenous application of electrical stimulation (ES) plays a role in cellular and molecular signaling pathways through the production of cytokines and growth factors for cell migration, differentiation and tissue formation.

Aim:

The objective of this work is to evaluate PCL scaffolds associated with 20% of β -TCP and electrical stimulation therapy for bone regeneration in an animal model.

Methods:

The experimental protocol was approved by animal ethical committee of Hermínio Ometto Foundation (CEUA/UNIARARAS-075/2017). PCL and PCL/ β -TCP interconnected porous scaffolds were printed using a screw-assisted additive manufacturing system (0/90° lay-down pattern). Seventy-two Wistar rats were anesthetized by intraperitoneal administration of 10% of ketamine hydrochloride (30 mg/Kg) and 2% of xylazine hydrochloride (10 mg/Kg) and submitted to a 5mm \times 5mm critical-sized square defect created using a sharp tip coupled to an ultrasound device under constant irrigation. The following groups were considered: SHAM (bone defect with no scaffold), SHAM+ES (bone defect with no scaffold + electrical stimulation), PCL, PCL+ES, PCL/ β -TCP and PCL/ β -TCP+ES. The electrical application (10 μ A/5min) was performed twice a week for 60 days. After euthanasia on the 30th and 60th days, samples were cross-sectioned of 4.0 μ m thick cut and stained with hematoxylin-eosin and Masson-Trichrome for histomorphometric evaluation (osteoclasts, blood vessels, connective and mineralized tissues) using ImageJ software. Data were plot using GraphPad Prism software and analyzed by two-way ANOVA with post hoc Bonferroni's test (α =5% significance level).

Results:

The results showed that, after 60 days, all groups treated with scaffolds presented a lower number of osteoclasts (PCL=12.3; PCL+ES=8.6; PCL/ β -TCP=9.4; PCL/ β -TCP+ES=8.6) in the bone edges when compared to SHAM (21) and SHAM+ES (21.2). Although PCL/ES presented a higher number of blood vessels (10) compared to PCL/ β -TCP and PCL/ β -TCP+ES (6.5) on the 30th day, PCL/ β -TCP presented higher vascular area (4.1%) compared to SHAM (1.8%), SHAM+ES (2%) and PCL+ES (1.7%). The connective tissue formation was similar to all groups on the 30th day, but on the 60th, all groups that received scaffolds in the bone defect presented higher connective tissue formation (around 90%) compared to SHAM (76%) and SHAM+ES (68%). Moreover, on the 60th day, PCL/ β -TCP+ES group presented higher mineralized tissue (6.8%) compared to SHAM, SHAM+ES (0%) and PCL/ β -TCP (1.3%).

Conclusion:

The use of PCL produced with 20% β -TCP interconnected porous scaffolds and electrical stimulation therapy stimulated angiogenesis and osteogenesis. The development of electroconductive ceramic biomaterials and the use of electrical stimulation therapy become an alternative approach in clinical treatments involving bone repair.

Financial support:

FHO, CNPq and FAPESP (2018/21167-4)

23.018 - THE USE OF ELECTROCONDUCTIVE CARBON NANOTUBES INTERCONNECTED POROUS SCAFFOLDS AND ELECTRICAL STIMULATION THERAPY FOR BONE REGENERATION: HISTOMORPHOMETRIC EVALUATION IN AN ANIMAL MODEL. Silva EP, Gonçalves LCF, Souza TFPS, Nalesso PRL, Pulz RB, Huang B, Bartolo PJS, Santamaria-Jr M, Mendonça FAS, Caetano GF, - 1Graduate Program in Biomedical

Sciences, University Center of Hermínio Ometto Foundation – FHO|UNIARARAS - FHO 2Manchester Biomanufacturing Centre, School of Mechanical, Aerospace and Civil Engineering, University of Manchester - UM 3Graduate Program of Orthodontics, University Center of Hermínio Ometto Foundation – FHO|UNIARARAS - FHO

Introduction:

Critical bone defects are considered one of the major clinical challenges in reconstructive bone surgeries, mostly because of the difficulty in achieving the regeneration process. Critical bone defects, characterized by absence of repair (spontaneously) in the expected time, require extremely invasive clinical procedures, such as autologous or heterologous transplantation. As an alternative approach, tissue engineering studies the development and application of biomaterials to act as a three-dimensional matrix (scaffolds), mimicking as a bone substitute to support bone regeneration. Polycaprolactone-based scaffolds (PCL) associated with the carbon nanotube (CNT) present scientific potential to be used in the bone tissue engineering for the development of durable, resistant and electroconductive structures. Biological evaluations in vitro provided data for the use of PCL scaffolds produced with 0.75% and 3% (percentage of weight) of carbon nanotube content to be considered for in vivo evaluation. Moreover, as the bone is a piezoelectric tissue, the exogenous application of electrical stimulation (ES) plays a role in cellular and molecular signaling pathways through the production of cytokines and growth factors for cell migration and cell differentiation.

Aim:

The objective of the present study was to evaluate the use of electrical stimulation and electroconductive PCL/CNT scaffolds (0.75% and 3%) for bone regeneration in an animal model.

Methods:

The experimental protocol was approved by the animal ethical committee of Hermínio Ometto Foundation (CEUA/UNIARARAS-002/2018). PCL and PCL/CNT interconnected porous scaffolds were produced by screw-assisted additive manufacturing system (0/90° lay-down pattern). Critical bone defects on the calvaria bone (5mm \times 5mm) were created in 96 Wistar rats using a sharp tip coupled to an ultrasound device. Eight groups were considered. SHAM-untreated bone defects; SHAM+ES-without treatment with electrical stimulation; PCL-PCL scaffold; PCL+ES; CNT0.75-PCL scaffold associated with 0.75% carbon nanotubes; CNT0.75+ES; CNT3-PCL scaffold associated with 3% carbon nanotubes and CNT3+ES. The electrical application (10 μ A/5min) was performed twice a week over 120 days. Regeneration of the bone defect was evaluated on the 60th and 120th post-operative by means of histomorphometric (blood vessels and total tissue formation), immunohistochemical (RANKL/OPG) and histochemical analysis (TRAP). Data were plot using GraphPad_Prism software and analyzed by two-way ANOVA with post hoc Bonferroni's test (α =5% significance level).

Results:

All groups that received scaffold as grafting presented a higher number of blood vessels compared to SHAM (n=4.5) and SHAM+ES (n=4). CNT0.75, CNT0.75+ES, CNT3 and CNT3+ES groups presented all of them approximately 7.5 blood vessels per analyzed histological image (p <0.05). Similar statistical results were observed on the 120th day. Moreover, higher percentage of total tissue formation (which includes the connective, osteoid and mineralized tissues) was observed in CNT0.75 (35%), CNT0.75+ES (35%), CNT3 (30%) and CNT3+ES (25%) groups compared to SHAM (20%) and SHAM+ES (18%) groups on the 120th day. The triad TRAP/RANKL/OPG evaluation showed greater osteoclasts activity (bone remodeling phase) in the defects with PCL+ES and both PCL/CNT+ES groups.

Conclusion:

The electrical stimulation combined with the use of both CNT scaffolds stimulated the angiogenesis and could have up-regulated growth factor that plays a role in osteogenesis and bone remodeling phase.

Financial support:

FHO and CNPq

FeSBE Annual Meeting 2019

Poster Sessions and Abstracts

23.019 - EARLY LESIONS OF ACUTE RENAL ISCHEMIA AND REPERFUSION INJURY: EFFECTS OF EXTRACELLULAR VESICLES SECRETED BY MESENCHYMAL CELLS. Lopes JA, Nossar LF, Sarmiento GC, Collino F, Lindoso RS, Vieyra A, - Carlos Chagas Filho Institute of Biophysics - UFRJ

Introduction:

In a recent study (Cellular Physiology and Biochemistry 52;1463-1483, 2019) we described late (72 h) effects of Acute Kidney Injury (AKI) in a rat model of ischemia/reperfusion (I/R), showing that injection of extracellular vesicles (EVs) secreted by human adipose mesenchymal cells (hADMSC) triggers processes that culminate in recovery. I/R-induced AKI is characterized by a rapid decline of renal function with intense ATP depletion and generation of reactive oxygen species (ROS), causing tissue oxidative damage.

Aim:

To investigate early mitochondrial and extramitochondrial lesional events (24 h after I/R), which could be possible targets of beneficial effects of EVs.

Methods:

Protocols approved by the Ethics Committee for the Use of Animals in Research/UFRJ (A02/16-61-15). We studied: (i) ROS formation, the expression of the cytokines IL-6 and TNF-alpha, the markers of renal lesion NGAL and KIM-1 (in vivo rat model); and (ii) induction of apoptosis (in vitro hypoxia/reoxygenation model using HK-2 cells). EVs were obtained from the supernatants of 12 h-hADMSC cultures. I/R was provoked by bilateral clamping of renal arteries for 30 min followed by 24 h-reperfusion, using 3 groups: SHAM, IR and I/R+EVs (subcapsular 2×10^9 EVs/kidney). Mitochondria were isolated from proximal tubules. ROS formation was evaluated fluorometrically by measuring the oxidation of Amplex[®]Red; markers by RT-PCR. HK-2 cells were submitted to hypoxia (HPX, 1% O₂, 24 h) followed by 24 h 21% O₂, without or with EVs (2×10^9 /1.5 ml well). Viable and apoptotic cells were quantified by cytometry.

Results:

(In vivo: n=4-7 different kidney pairs). I/R provoked a 30% increase in ROS formation after addition of succinate (P<0.0001), which was totally reversed in the I/R+EVs group. Even at a 10-fold lower level after addition of ADP, ROS increased 55% in I/R (P<0.0001) again fully reversed by EVs. With ATP synthesis blocked by oligomycin, the I/R-induced ROS (65% higher than CTR, P<0.0001) was cancelled by EVs, as well as the slow ROS formation encountered after addition of FCCP. I/R increased IL-6 more than 10 times, a level significantly reduced (50%) by EVs. The 2-fold increase in TNF-alpha was not modified by EVs. Neither the 15-fold NGAL increase, nor the 20-fold KIM-1 increase provoked by I/R, were reversed by EVs. (In vitro: EVs from n=9-16 cultures). Hypoxia increased early apoptosis (Annexin V+ cells) (2.3 ± 0.06 vs $1.9 \pm 0.03\%$ in CTR; P=0.0029), totally reversed by EVs. Late apoptosis (PI+ cells) was higher (10.3 ± 0.2 vs $3.1 \pm 0.1\%$ in CTR; P<0.0001) and reversal by EVs was partial, though significant (7.7 ± 0.2 ; P<0.0001 vs HPX).

Conclusion:

Intense ROS formation at mitochondrial complex I via reversal electron transfer from Complex II during succinate oxidation and huge formation of IL-6 and TNF-alpha are key events in the early I/R-induced renal lesions, demonstrated by the upregulation of NGAL and KIM-1. Whereas EVs totally reverse early oxidative damage, the lack of beneficial effect on TNF-alpha expression, and the partial decrease in IL-6 and in the elevated levels of late cell apoptosis levels at 24 h, indicate that vesicles trigger slow processes responsible for the decrease in lesion markers observed at 72 h.

Financial support:

CNPq, FAPERJ, CAPES, INCT of Regenerative Medicine/REGENERA

23.020 - DACT1 IS EXPRESSED DURING SKELETAL MUSCLE MYOGENESIS AND MODULATED IN HUMAN MUSCULAR PATHOLOGIES. Contriciani RE, Veiga FC, Castelucci BG, Alvares LE, - Departamento de Bioquímica e Biologia Tecidual - UNICAMP

Introduction:

DACT1 is a multifunctional protein that contains several structural domains, including an evolutionarily conserved N-terminal region related to the leucine-rich coiled-coil domain of dystrophins. In addition, Dact1 is expressed in somites of different vertebrates, suggesting that this molecule could play a role in skeletal myogenesis.

Aim:

Therefore, in this work we investigated whether Dact1 is involved in skeletal myogenesis and looked for possible modulation of Dact1 gene expression in human muscular pathologies.

Methods:

Skeletal myogenesis was studied in two in vitro systems: primary culture of chick myoblasts as a model for fetal myogenesis and murine myoblasts C2C12 culture, derived from satellite cells of adult mouse. qPCR and immunofluorescence assays were performed to investigate Dact1 gene expression and protein localization along skeletal muscle differentiation, which occurred during 120h in chicken and 240h in mouse. In addition, in situ hybridization (ISH) and immunofluorescence assays were performed in pectoral muscle of 11-day-old chick embryos, as well immunofluorescence in E14.5 skeletal muscle of mouse embryos. To investigate the modulation of Dact1 gene expression in human muscle diseases, we used Gene Expression Omnibus (GEO) datasets to collect expression data from human patients and the ShinyGEO application as a tool to compare expression levels among control and disease groups.

Results:

qPCR results revealed that Dact1 is expressed at later stages of chicken fetal myogenesis. In agreement, DACT1 protein was found in a highly organized distribution in the sarcoplasm of myofibers, in a pattern that resembles costamers. Also, this protein was found in the nucleus, where it forms small rosettes. The analysis of E11 pectoral tissue of chicken embryos confirmed the expression of Dact1/DACT1 in vivo. In mouse, we found increasing levels of Dact1/DACT1 in C2C12 differentiating cells, and confirmed Dact1 expression in skeletal muscle of E14.5 embryo. Finally, differential expression analysis of various human muscle diseases showed that Dact1 is up-regulated in patients with Duchenne Muscular Dystrophy (DMD) and Limb-Girdle Muscular Dystrophy type 2A (LGMD2A), while this gene is down-regulated in Acute Quadriplegic Myopathy (AQM) muscle biopsies.

Conclusion:

Our results confirm the involvement of DACT1 in skeletal myogenesis, indicating that this molecule may play important roles in this process. The modulation of Dact1 expression in muscular pathologies reinforces the need to deepen the studies on the role of this molecule aiming at future applications for human health.

Financial support:

CAPES / CNPq

23.021 - TOPICAL TREATMENT OF BIOCELLULOSE GEL WITH ALGINATE ON WOUND HEALING IN RATS. Nogueira JR, Mariano SS, Adriano LC, Santos GMT, Caetano GF, Barud HS, Sábio RM, Carbinatto FM, Bagnato VS, Andrade TAM, - Graduate Program of Biomedical Sciences - FHO University of Araraquara - UNIARA Seven Industry of Biotech Products Ltda - Seven Physics Institute of Sao Carlos - USP-IFSC

Introduction:

After a damage in the continuity of the tissue therapies can be implemented to improve it. Biological dressings, like biocellulose membranes, also known as Nexfill[®] (Seven), have been highlighted and shown promising results inducing tissue healing. This biomaterial affects the promotion of moist to the bed wound, it's a low-cost product that can be easy applied, also reducing pain in patients. At the

FeSBE Annual Meeting 2019

Poster Sessions and Abstracts

same time alginate is known for its application as a hemostatic agent, widely used during surgeries to prevent bleeding.

Aim:

To evaluate the effect of alginate-associated biocellulose gel on the healing of excisional wounds.

Methods:

Approved by CEUA-FHO (nº 010/2018). Sixty male Wistar rats ($\pm 300g$) were used in which dorsal lesions were performed with histological punch of 1.5 cm in diameter and were divided into 4 groups: SHAM: without treatment in the lesion; CONTROL: applied in the lesion with control gel (vehicle gel only); NEXFILL: treated with bacterial biocellulose gel and CB+AG: biocellulose gel with alginate. The groups were treated with 3 application per week ($n = 5$ rat/time/treatment). The wounds images were photographed on the day of the lesion (day 0) and at the end of each follow-up (2nd, 7th and 14th days post-injury). An area of therapy was quantified using the wound healing rate (WHR) using a formula (initial area-final area/initial area). Samples were collected from the lesion area at days 2, 7 and 14. ($n = 5$ animals/group/time) for histomorphometric analysis of inflammatory infiltrate, angiogenesis, fibroplasia and collagenase (HE and Gomori trichrome). In addition, biochemical measurements of MPO (myeloperoxidase - neutrophil) and NAG (N - acetylglicosaminidase - macrophage) were included and evaluated by ANOVA One - way/Tukey test (between groups in each experiment) ($p < 0.05$) (MED \pm SEM).

Results:

The CB+AG group presented control of the inflammatory response represented by the lower amount of inflammatory infiltrate on the 2nd day in relation to the Sham and Nexfill groups, while on the 7th and 14th days the Nexfill and CB+AG groups reduced the infiltrate in relation to Sham and Control gel. In addition, CB+AG presented lower MPO (on 2nd day) and NAG (on 2nd and 14th days) in relation to the other groups. Regarding angiogenesis, the CB+AG was characterized by the important production of vessels on the 2nd day in relation to Control gel and Nexfill and Sham-like, reducing this profile in the 7th and 14th days. In relation to fibroplasia, the CB+AG and Nexfill groups were distinguished by the greater amount of fibroblasts in relation to the other groups and throughout the follow-up. Regarding the collagenase, CB+AG presented higher than the Nexfill group in the 7th and 14th days, which combined with the other results probably contributed to the more evident reepithelization observed in the CB+AG group on the 7th day in relation to the Nexfill group.

Conclusion:

The association of bacterial biocellulose on gel with alginate favored the tissue repair in rats, despite not showing macroscopic visual differences.

Financial support:

HERMÍNIO OMETTO FOUNDATION

23.022 - DEVELOPMENT OF BIOCOMPATIBLE BIOINKS FOR 3D BIOPRINTING OF NEURAL TISSUE. Melo BAG, Rodrigues S, Porcionatto MA, - Departamento de Bioquímica - UNIFESP

Introduction:

3D bioprinting technology has great potential for engineering neural tissue due to its capacity to recreate organized and complex 3D architecture. However, there are still some challenges to overcome, including the development of hydrogels with structural and mechanical properties similar to the native matrix, with rheological properties that enable the bioprinting, and with capability to ensure neural cells viability during and after the process.

Aim:

In this work, we prepared a polymeric blend with optimal properties for 3D bioprinting neural stem cells (NSCs) and fabricate a neural tissue-like construct.

Methods:

The bioink consisted of fibrinogen, a Newtonian fluid with poor bioprinting capacity, which enzymatically crosslinks with thrombin forming fibrin fibers that contributes to cell attachment; gelatin, with sol-gel properties that favor the bioprinting process; and alginate, a natural copolymer with poor cell-adhesion capacity, but that through Ca^{2+} crosslinking, provides higher stability to the construct. Initially, printability was tested using polymeric solutions with different combinations of gelatin (5%, 7.5%, and 10%) and alginate (1%, 2.5%, and 4%), aiming to optimize the bioprinting process with a minimum concentration of gelatin. Afterward, bioprinted constructs were crosslinked in a 0.1 mol/L $CaCl_2$ bath for 30 min. Printable combinations were mixed to a 10 mg/mL fibrinogen solution prior to bioprint, and the rheological properties of each solution were evaluated. After bioprinting, alginate and fibrin were crosslinked in the $CaCl_2$ bath supplemented with 1 U/L of thrombin for 30 min. Mechanical properties were assessed after preparation and after 24 h at 37 °C. The morphology of hydrogels was evaluated by scanning electron microscopy (SEM). NSCs were extracted from 45 days C57BL/6 male mice (Ethics Committee number 9292090519) and added to the fibrinogen/gelatin/alginate bioink in the concentration of 106 cells/mL. After bioprinting, the constructs were transferred to a 24-well plate and cultured at 37 °C and 5% CO_2 . Cell attachment, spread, and viability were evaluated on culture days 1 and 7 using Live/dead reagents. Statistical analysis was made using one-way ANOVA with Tukey test, and $p < 0.05$ was considered significant.

Results:

Among gelatin-alginate combinations, those with gelatin 7.5% and 10% were printable. We selected gelatin 7.5%-alginate 2.5%, gelatin 7.5%-alginate 4% and gelatin 10%-alginate 2.5% for the following experiments. The three polymeric solutions presented Newtonian behavior, as verified by the power-law model applied to the viscosity vs shear rate curves, with the power-law index (n) being < 1 . The compressive modulus of gelatin 10%-alginate 2.5% presented high values after bioprinting (5 kPa) and low values after 24 h (2 kPa), indicating the diffusion of gelatin through the construct at 37 °C. SEM images showed that hydrogels were highly porous, especially those with the lowest concentration of alginate. NSCs attached and spread in the hydrogels and remained viable ($> 80\%$) on day 7, indicating that the bioprinting process and hydrogels microenvironment were favorable to maintain cell survival.

Conclusion:

Fibrinogen/gelatin/alginate blend showed to be a potential bioink for NSCs 3D bioprinting, which could represent a great advance in the neural engineering and contribute to future works on the development of neurodegenerative diseases treatments.

Financial support:

Fapesp, Processo 2018/23039-3 and INCT-CNPq, Processo 465656/2014-5.

23.023 - INFECTION OF HUMAN MUSCLE CELLS BY ZIKA VIRUS: ROLE OF LAMININ ISOFORMS AND THEIR RECEPTORS. GONZALEZ MN, ROCHA CDS, REIS RF, SAVINO W, Cruz DM, INGRIEDERER, - Laboratório de Pesquisa sobre Timo - Fiocruz

Introduction:

Muscle repair after degeneration, caused by trauma or disease, is physiologically ensured by proliferating myoblasts, derived from Satellite Cells that are muscular progenitors located beneath the Basal Lamina (BM) and the sarcolemma of muscle fibers. Laminin (LM) are trimeric ($\alpha\beta\gamma$) glycoproteins presenting several isoforms, and in the mature muscle, the LM isoforms 211 ($\alpha 2\beta 1\gamma 1$) and 221 are found surrounding the muscle fibers. However, our group identify other isoforms expressed by human myoblasts during proliferation, differentiation and fusion. Muscle cells are potential targets of several arboviruses such as Dengue-, Sindbis-, and Chikungunya-virus, that could be involved in the physiopathological course of the infection.

FeSBE Annual Meeting 2019

Poster Sessions and Abstracts

During the recent outbreak of Zika virus (ZIKV), myalgia was one of the most frequently reported symptoms.

Aim:

Here, we investigated the susceptibility of human muscle cells to ZIKV infection, and the role of LM isoforms in this process.

Methods:

We used an in vitro model of immortalized human myoblasts (LHCN-M2) cell line that can be differentiated into myotubes and were infected by clinical isolates of ZIKV-Rio-U1. Flow cytometry was used to detect infected cells (4G2), the $\alpha 6$ integrin and AXL (virus receptor) expression. Immunofluorescence was also used to detect infected cells (4G2), and to detect differentiated myoblasts (MyHC). Recombinant LM-511 (Biolamina) was used to treat human myoblasts.

Results:

We showed that myoblasts are productively infected by ZIKV. In contrast, myotubes were shown to be resistant to ZIKV infection, suggesting a differentiation-dependent susceptibility. Interestingly, we found a significant reduction in the infectivity of human myoblast by ZIKV when they were cultured on the LM-511 isoform, and also, a significantly decreased expression of their receptor, the $\alpha 6$ integrin. It is interesting to note that this isoform is expressed only in fused myoblasts. We further detected the membrane expression of AXL, a receptor for ZIKV, in human myoblasts and myotubes. But treating myoblasts with specific antibodies for AXL receptor and integrin $\alpha 6$ did not reduce the infectivity by ZIKV, suggesting that other receptor may be involved in virus entrance in these cells.

Conclusion:

Since myoblasts constitute the reservoir of stem cells involved in reparation/regeneration in the muscle tissue, muscle cells infection and viral-induced alterations observed here could constitute a valuable model to study host factors involved in myoblast infection by ZIKV.

Financial support:

Capes, FAPERJ, FIOCRUZ, CNPQ/Ciências sem Fronteiras, INCT-Neuroimunomodulação, FOCEM

23.024 - MACROPHAGE-MYOBLAST INTERPLAY AS THERAPY FOR SKELETAL MUSCLE REGENERATION. Reis RF, Jurberg AD, Savino W, Habib DCB, Riederer I, Cotta-de-Almeida Vinícius, - Laboratório de Pesquisas Sobre o Timo - Fundação Oswaldo Cruz

Introduction:

Skeletal muscle is able to regenerate new muscle fibers upon the activation of satellite cells. Following injury, these quiescent myogenic progenitors start to proliferate and then differentiate into new fibers. However, the use of stem cells for treating acute lesions or degenerative diseases runs into high cell death and impaired migration into the injured site. In this regard, numerous studies have shown that macrophages play key roles in muscle repair by providing trophic signals for muscle precursors and young fibers.

Aim:

The present work aims to investigate the impact of macrophage-derived signals during skeletal muscle regeneration.

Methods:

We used macrophages from human peripheral blood mononuclear cells to harvest macrophage-conditioned medium (MCM) and treat human CHQ or CL25 myoblasts for different time points (i.e. 1, 2, 5, and 7 days). Immunofluorescence assay, in which we evaluate the expression of molecules involved in myoblast differentiation such as the myosin heavy chain and myogenin. Moreover, we used immunofluorescence assay to verify the GDF11 and its ALK4/5/7 receptors expression.

Results:

Our findings suggest that MCM induced myoblast proliferation and inhibited cell differentiation when compared to non-conditioned medium. In addition, we found that macrophages, myoblasts, and myotubes produced the Transforming Growth Factor- β (TGF- β) superfamily member GDF11, which has been recently implicated in

skeletal muscle regeneration. Similarly, to MCM, treatment of myoblasts with recombinant GDF11 (rGDF11) increased cell proliferation and impaired cell differentiation in a dose-dependent manner. Moreover, blocking the TGF- β signaling branch by using the ALK4/5/7 type I receptor inhibitor SB-431542 stimulated myoblast differentiation after 3 and 6 days. We are currently dissecting the molecular mechanisms of GDF11 signaling on myoblast-macrophage interplay by generating mutant CRISPR/Cas9-based cell lines for each of those genes

Conclusion:

Ultimately, we expect that manipulation of macrophages may enhance skeletal muscle regeneration.

Financial support:

CAPES, FAPERJ, CNPq/Ciências sem Fronteiras, Fiocruz, IOC, INCT-NIT, FOCEM

23.025 - EVALUATION OF LAMININ-DERIVED PEPTIDES IN SURVIVAL, MIGRATION, PROLIFERATION, AND FUSION OF MUSCULAR CELLS: APPLICATION IN THERAPIES FOR MUSCULAR DYSTROPHIES. Horita SIM, Beghini DG, Riederer I, Henriques-Pons A, - Laboratório de Inovações em Terapias, Ensino e Bioprodutos - Fiocruz Laboratório de Pesquisa sobre o Timo - Fiocruz

Introduction:

Duchenne Muscular Dystrophy (DMD) affects 1 in 3600 to 6000 male births and is an X-linked recessive disorder. It is caused by mutations in the dystrophin gene, a protein that stabilizes the sarcolemma during muscle contraction. There is progressive muscle weakness and wasting in DMD, resulting in the loss of motor function, cardiorespiratory complications, and early death around the 20s. Cell therapy using myoblast transplantation is an alternative strategy for muscular disorders, in which the injected cells are able to fuse in dystrophic muscles, improving muscular strength and dystrophin expression. However, the injections of these cells in DMD patients presented some problems: high cell death, low proliferation, impaired migration, and host immune response, that decrease the efficacy of the therapy. Laminin-111(LM-111) was proposed as an effective protein-based therapy for DMD, as it prevents the pathology in mdx mice, a murine model for the disease. Furthermore, myoblast transplantation co-injected with laminin-111 improved the therapy efficacy in mdx mice. Partial proteolysis of extracellular matrix proteins, as laminin-111, produces peptides called matrikines, able to modulate cell activity. AG73, SIKVAV, and C16 are peptides derived from LM-111 with diverse biological functions in vivo and in vitro. In previous studies, the peptide AG73 improved myoblast adhesion, migration, and differentiation.

Aim:

In this study, we decided to investigate the biological activity of LM-111-derived peptides in myogenic cells and how these effects can contribute to pharmacological and cell therapy in the murine model of DMD. First, we analyzed the effect of LM-111 in myoblasts proliferation in vitro.

Methods:

Proliferation assay: We used C2C12 cell line in low serum condition in 10 μ g, 20 μ g, and 40 μ g of LM-111 per mL, using the CyQuant assay. Barium chloride-induced muscle injury. In the tibialis anterior (TA) of BALB/c mice, we injected 50 μ L of 1,2% barium chloride (BaCl₂). The muscles were harvested at 4 and 10 days post-injection, and by immunohistochemistry, we detected macrophages (F4/80), necrotic fibers (IgG positive fiber) and regenerating fibers (embryonic myosin heavy chain and centralized nuclei).

Results:

First, we analyzed the effect of LM-111 in myoblasts proliferation in vitro. We observed that the LM-111 treatment improved myoblast proliferation. At 4 days after injection, BaCl₂ treatment produced a robust inflammatory response and fiber damage with regenerating

FeSBE Annual Meeting 2019

Poster Sessions and Abstracts

fibers expressing eMyHC. Furthermore, we observed more centralized nuclei fibers at 10 days after injection, indicating muscle regeneration.

Conclusion:

In conclusion, we confirmed that LM-111 can improve myoblast proliferation in vitro, and BaCl₂ induced-injury is an alternative model for muscle regeneration and consequently, an in vivo model for muscle therapies.

Financial support:

CNPq e Papes/Fiocruz

23.026 - DEVELOPMENT OF TOOLS TO LABEL AND IMAGE PROLIFERATIVE CELLS AND NEURONS USING X-RAY IMAGING TECHNIQUES WITH SYNCHROTRON RADIATION. Vidal ISAB, Morão PP, Dias CSB, Pérez CA, Andrade HC, - Brazilian Biosciences National Laboratory - CNPEM Brazilian Synchrotron Light Laboratory - CNPEM

Introduction:

Zebrafish (*Danio rerio*) have been established as a robust model for vertebrate neural development due to the highly similarity in neuroanatomic and neurochemical pathways among vertebrates. Although zebrafish share a robust similarity to mammals' neurodevelopment, zebrafish have an exquisite ability to regenerate damaged neurons following spinal cord injury (SCI), while mammals fail to regenerate after injury in the central nervous system (CNS). Some components of the zebrafish spinal cord (SC) regeneration process are known, such as the necessity of quiescent ependymal cells (endogenous stem cells) activation, but little is known about the cellular mechanisms these cells undergo or the signalling pathways that activate them. Therefore, understanding the cellular behavior and manipulating signalling pathways that activate the stem/progenitor cells holds great promise in the treatment of SCI.

Aim:

To expand the horizons on what is known on this matter, the aim of this project is to develop tools to label and image newborn neurons and axonal process during SC regeneration in zebrafish using X-ray imaging techniques with Synchrotron Radiation. such as X-ray Fluorescence microscopy (XFM) and X-ray Computed Tomography.

Methods:

We performed BrdU incorporation in zebrafish larvae at 3 days post fertilization followed by immunohistochemistry against BrdU. We also performed immunohistochemistry against glial fibrillary acidic protein (GFAP) in adult SC sections. In both protocols we used a primary antibody against the protein of interest, a secondary antibody conjugated to horseradish peroxidase (HRP) and we developed an assay in which the HRP enzyme catalyzes 3,3'-diaminobenzidine (DAB) deposition and concomitantly the impregnation with nickel. This protocol enables the deposition of nickel in the same location of the antibody complex. We also transfected HEK 293T cells with APEX2, a peroxidase, and performed the DAB-Ni deposition/impregnation protocol.

Results:

Regarding the BrdU incorporation protocol we detected a high DAB-Ni deposition/impregnation using XFM. The regions with high nickel signal detected by XFM correlates with the regions with high concentration of proliferative cells labeled with BrdU and imaged using confocal microscopy. The immunohistochemistry against GFAP in adult zebrafish generated intense nickel deposition in the SC detected by XFM. The HEK 293T cells transfection with APEX2 produced an intense nickel signal following the DAB-Ni deposition/impregnation protocol. These data show that this protocol generates a specific signal that can be detected by XFM in different cell types and approaches.

Conclusion:

This assay is a promising successful tool that can be used to label proliferative cells and different cell types in a broad range of biological samples, giving them enough contrast/signal to be imaged by XFM with high specificity. We are currently on the process of generating a

zebrafish transgenic reporter line in which the islet1 regulatory region drives the expression on APEX2. This reporter line will enable the tracing of motoneuron regeneration in the adult SC in a non-destructive and tridimensional way using X-ray imaging techniques with Synchrotron Radiation.

Financial support:

24 - Vision and Ophthalmology

24.001 - GENETIC CHARACTERIZATION AND ESTIMATES OF THE SPECTRAL ABSORPTION PEAKS OF THE VISUAL PHOTOPIGMENTS OF THE RED EAR TURTLE (*TRACHEMYS SCRIPTA ELEGANS*) (TESTUDINE, EMYDIDAE). Corredor VH, Hauzman E, Ventura DF, - Departamento de Psicologia Experimental - USP

Introduction:

The red ear turtle *Trachemys scripta elegans* represents a consolidated model for the study of the visual system of vertebrates. Behavioral, electrophysiological, and microspectrophotometry (MSP) data revealed the presence of four cone types, with spectral sensitivity ranging from 370 to 700 nm, and one rod type. However, no study in the literature investigated the genetics of the visual photopigments in this species. Specific amino acids of the opsins associated with the retinal molecule, 11-cis-retinal or 11-cis-3,4-dehydroretinal, are responsible for tuning the spectral sensitivity of each opsin class. The association of the opsin with the 11-cis-3,4-dehydroretinal, found in *T. s. elegans*, causes a bathochromic shift of the spectral absorption peaks (λ_{max}) of the photopigments.

Aim:

To amplify and sequence the five opsin genes expressed in retinas of *T. s. elegans* and estimate the λ_{max} of the corresponding opsins, based on amino acids located at known spectral tuning sites, associated with the 11-cis-3,4-dehydroretinal chromophore.

Methods:

This study was approved by the Ethics Committee on Animal Research of the Institute of Psychology - University of São Paulo (IP-USP Protocol 544613117). One individual of *T. s. elegans* was euthanized with a lethal injection of sodium thiopental (100 mg/kg). After euthanasia the eyes were enucleated and preserved in RNA Later (Ambion) at 4°C. Total RNA was extracted and mRNA was converted to cDNA. Polymerase chain reactions (PCRs) were performed using primers designed from opsins of other reptiles. PCR products were purified and sequenced, and sequences were analyzed with BioEdit. The λ_{max} values were estimated based on the amino acids at spectral tuning sites, and the values were corrected considering the presence of the 11-cis-3,4-dehydroretinal, using the equation: $11\text{-cis } A_2 = (0,0022 * ([11\text{-cis } A_1] ^2)) - (0,8189 * x) + 384,31$.

Results:

The five opsin genes expressed in the retinas of *T. s. elegans* were amplified and sequenced. The estimated λ_{max} values were consistent with those presented in the literature. For the LWS we estimated a λ_{max} at ~616 nm, close to that measured from MSP and intracellular recording (IR) (617 and 620 nm, respectively). For the RH1 and RH2, the estimated λ_{max} at ~517 and ~518 nm, respectively, were also consistent with values obtained from MSP (518 nm). In the SWS1, the presence of the amino acid F86 indicates a UV sensitivity, with estimated λ_{max} at ~375 nm, a +3 nm difference from that obtained from IR and MSP (372 nm). For the SWS2 we estimated a λ_{max} at ~450 nm, which differs by 8-10 nm from the MSP and IR values (458 nm and 460 nm, respectively).

Conclusion:

The spectral sensitivity estimated for the five opsins were close to those described in the literature based on direct measurements. For the SWS1 and SWS2 photopigments the estimated values differed by +3 and -8 nm, respectively. Those differences can be due to the imprecise estimate of the shift caused by the 11-cis-3,4-dehydroretinal, or due to

FeSBE Annual Meeting 2019

Poster Sessions and Abstracts

the presence of specific amino acids with unknown effect on the opsins spectral tuning, such as residues M93, A109, and S118S in the SWS1, and residues T91, A109, and A116A in the SWS2.

Financial support:

FAPESP (2014/26818-2; 2014/25743-9), Capes and CNPq.

24.002 - LIPOPLEX FUNCTIONALIZATION WITH HYALURONIC ACID FOR AN EFFICIENT IN VIVO DELIVERY OF SIRNA TO THE RETINA. Ribeiro MCS, Miranda MC, Andrade GF, Gomes DA, Charrueau C, Escriou V, Silva-Cunha A, - Produtos Farmacêuticos - UFMG Bioquímica e Imunologia - UFMG Unité de Technologies Chimiques et Biologiques pour la Santé - UNIVERSITÉ PARIS DESCARTES Centro de Desenvolvimento da Tecnologia Nuclear - UFMG

Introduction:

Since the possibility of silencing specific genes linked to retinal diseases has become a reality with the use of small interfering RNAs (siRNAs), this technology has been widely studied in order to promote the treatment or even the cure of genetic eye disorders. Despite the recent advances, the clinical success of RNA interference in the retina is significantly limited by inherent anatomical and physiological ocular barriers. Moreover, the siRNA molecules cannot freely cross cell membranes due to their relatively large molecular weight and phosphodiester backbone. Therefore, new delivery systems are required to overcome these limitations and improve siRNA internalization into the retinal tissues.

Aim:

Develop a lipid-based nanocarrier (lipoplex) strategically coated with hyaluronic acid (HA) to promote a safe and efficient in vivo retinal delivery of siRNA by intravitreal injections.

Methods:

Different molecular weights of HA (8-15 kDa and 160-600 kDa) were evaluated for cationic lipoplex surface functionalization, and the obtained particles were characterized by dynamic light scattering and transmission electron microscopy. Electrophoresis and in vitro studies were also performed to evaluate if HA coating could interfere in the siRNA incorporation into lipoplex and their efficacy. Next, intravitreal administration of cationic and HA-lipoplex was investigated by electroretinography, clinical evaluation, confocal microscopy and histology of Wistar rat eyes. All in vivo experiments were approved by the Ethics Committee on Animal Research of UFMG (Comissão de Ética no Uso de Animais, CEUA-UFMG), under protocol 31/2019.

Results:

Cationic lipoplex had a Z-average diameter of 133.5 ± 1.2 nm and zeta potential of 71.1 ± 3.0 mV. Upon addition of HA (160-600 kDa), both size and zeta potential were statistically different compared to non-modified lipoplexes ($p > 0.05$), showing a Z-average diameter of 221.8 ± 9.2 nm and zeta potential of -34.2 ± 1.4 mV. These results and morphological characterization indicated an electrostatic binding between lipoplex and HA. In addition, our findings indicate that HA-lipoplexes were able to protect and introduce siRNA molecules (37,6 nM) in retinal cells without apparent cytotoxicity. Regarding in vivo studies, in contrast to the cationic lipoplex that was not able to penetrate deeper retinal structures, HA-coated lipoplexes showed a clear localization of fluorescent siRNA signal in the inner and outer retina. Moreover, both systems showed no apparent toxic effects to the retina after 7 and 14 days of intravitreal injections, according to electrophysiological functional exams, clinical evaluation, and histologic assays.

Conclusion:

Considering all results, the lipoplex coated with hyaluronic acid may represent a promising approach to promote the protection and transport of the siRNA to the retina.

Financial support:

CAPES (CAPES-COFEUCUB) e FAPEMIG

24.003 - SWS1 OPSIN GENE DUPLICATION CONFERS SENSITIVITY TO UV AND VIOLET LIGHT IN THE AQUATIC COLUBRID SNAKE HELICOPS MODESTUS. Hauzman E, Bhattacharyya N, ChangBSW, VenturaDF, - Psicologia Experimental - USP Ecology & Evolutionary Biology - UoFT Cell & Systems Biology - UoFT

Introduction:

Snakes rely on visual cues for foraging and prey capturing, but the spectrum of available light can differ between terrestrial and aquatic environments, particularly at short wavelengths. Visual pigments (opsins) form the first step in the sensory transduction cascade in the eye, with short wavelength vision being mediated via the sws1 opsin gene. The spectral absorption peak (Smax) of the opsins depends on the interaction of a covalently-bound chromophore with specific amino acid side chains of the surrounding opsin protein. The SWS1 opsins Smax can vary from ultraviolet to violet. Most snake SWS1 possess an amino acid thought to confer UV sensitivity (F86), but this mechanism has yet to be experimentally investigated. It has been suggested that UV sensitivity in snakes may facilitate visualization of important signals such as pheromone trails and rodent urine traces. However, in aquatic environments, UV light poorly penetrates the water column. Unlike most snakes, sea snakes possess SWS1 with V86 and Smax in the violet, which may be an adaptation to aquatic environments. A previous study of the aquatic freshwater snake *Helicops modestus* suggested the unusual presence of two copies of the sws1 gene in this species. The sws1 opsin is highly conserved, and duplications are extremely rare.

Aim:

To investigate this possible sws1 duplication in *Helicops*, using sequencing and cloning approaches, codon-based computational analyses of selection, and experimental methods to express and purify the SWS1, and measure their Smax.

Methods:

We used PCR amplification followed by cloning into plasmid vectors to identify multiple copies of sws1 opsin genes. Multiple clones were isolated and sequenced and the sequences were used for phylogenetic reconstruction. We investigated the selection pattern of *Helicops* sws1 with a codon-based method, using codeml program from PAML4. We used random sites and clade models, and likelihood ratio tests to compare among nested models. To investigate spectral sensitivity, we expressed the sws1 variants in mammalian cell culture, immunoaffinity purified, and recorded the UV-visible spectra of the 11-cis retinal regenerated opsin using absorbance spectroscopy.

Results:

We found 2 sws1 variants in *Helicops* snakes, with each copy possessing different amino acids at site 86 (sws1a: F; sws1b: V). Phylogenetic analyses grouped the two variants in different clades, suggesting that the duplication may have preceded the divergence of species within this genus. Clade model analyses indicate that *Helicops* sws1 is evolving under positive selection. Sws1a is evolving under stronger purifying selection compared to sws1b. In vitro expression assays revealed that both opsins are functional and that SWS1a has Smax in the UV (358 nm), and SWS1b in the violet (407 nm).

Conclusion:

Our results indicate that sws1 gene duplication in *Helicops* is associated with functional divergence in wavelength sensitivity, and the evolution of a novel violet-sensitive pigment. Molecular evolutionary analyses indicate less functional constraints which lead to violet sensitivity in the duplicated copy. *Helicops* snakes predate fishes and amphibians in terrestrial and aquatic environments. The acquisition of violet sensitivity may be an adaptation to aquatic environments, although UV vision may be advantageous for biological tasks during endeavors in terrestrial environments.

Financial support:

FAPESP (2014/26818-2; 2014/25743-9; 2018/09321-8), Capes, CNPq.

FeSBE Annual Meeting 2019

Poster Sessions and Abstracts

24.004 - ALTERATION OF CANNABINOID RECEPTORS AND MICROGLIA THROUGH THE DEVELOPMENT OF THE RETINA IN A MURINE MODEL OF RETINITIS PIGMENTOSA. Senos DL, Fragel-Madeira L, - Neurobiologia - Universidade Federal Fluminense

Introduction:

Retinitis Pigmentosa is a hereditary neurodegenerative disease that causes death of photoreceptors, resulting in a progressive loss of vision. Despite advances, this disease remains without cure. For this study, we used the PDE6 β rd10/rd10 murine model, in which it is possible to mimic the progressive loss of photoreceptors as well as other characteristic processes, such as microglial infiltration through retinal layers and reactive gliosis. The endocannabinoid system has already been shown to be altered in other neurodegenerative models, such as Alzheimer and Parkinson diseases. In many cases its modulation have a neuroprotective effect. The presence of endocannabinoid system components in adult murine retina under physiological conditions was already studied but remains unknown during retinal development or pathological conditions such Retinitis Pigmentosa.

Aim:

This project aims to analyze the presence of endocannabinoid system components in a murine model of Retinitis Pigmentosa PDE6 β rd10/rd10 (rd10) and compare them to C57Black/6 (Bl6) mice in physiological conditions.

Methods:

Bl6 and rd10 mice at three postnatal days (P3), P5, P9, P15, P17, P19, P21, P23, P25 and P30 ages had their retinas processed for immunohistochemistry. In sequence retina were labeled to cannabinoid receptor type 1 (CB1), cannabinoid receptor type 2 (CB2) and Ionized calcium binding adaptor molecule 1 (Iba-1), a marker of microglial cells. Quantitative data was performed by ImageJ v1.51h and GraphPad Prisma v7.0, using a One-Way ANOVA and Tukey post-test or Two-Way ANOVA and Dunnett's post-test and p values less than 0.05 was considered significant. Ethics Committee on Animal Use (CEUA) protocol number 679/2015.

Results:

The presence of CB1 receptor expression in rd10 mice was similar at different ages during retinal development when compared to control animals, labeling throughout retina, mainly plexiform layers. CB2 receptor became more expressed according to retina development in rd10 mice when compared to Bl6 mice, presenting a immunostaining pattern similar to CB1 receptor, but at degeneration periods in rd10 mice, nuclear layers also appeared marked. When we analyzed the presence of microglia, we noted an increase on microglial infiltration in photoreceptors nuclei layer at P23 (48.6 \pm 6.93), with a subsequent decrease at P25 (46.3 \pm 13.3), whereas the number of microglia in total retina remained the same. According to literature data, the peak of microglial infiltration is at P21, however, in our experimental conditions, this peak was at P23.

Conclusion:

We can conclude that CB1 expression did not change while CB2 receptor is upregulated rd10 compared to control animals. The increase of CB2 expression coincided with increase of microglial infiltration and death of photoreceptors cells, suggesting a possible involvement of them into retinal neurodegeneration. Our next steps are to apply an eye drop containing a CB2 antagonist (AM630) and analyze its effects on disease progression.

Financial support:

Support: Capes, FAPERJ, CNPq and Proppi-UFF.

24.005 - EFFECT OF NEAR-INFRARED LIGHT THERAPY USING AN ALTERNATIVE METHOD IN ASSOCIATION WITH RETINA DEGENERATION BY LIGHT-STRESS MODEL.. Dourado LFN, Alves AP, Paiva MRB, Ajero U, Siqueira RC, Silva-Cunha A, - Pharmaceutical Products - Federal University of Minas Gerais Physics - Federal University of Minas Gerais Ophthalmology - Padre Albino University Center

Introduction:

Photobiomodulation is a process which lights specific wavelengths are absorbed by cells photoreceptor, activating pathways that promote biological changes inside the cell. Thus, has been seen as a potential therapy against several diseases. The photobiomodulation therapy involves the light incidence in the wavelength from 600 to 1000 nm in red or near-infrared (NIR). The red and NIR light has a long wavelength, which provides an advantage of greater penetration on tissues thickness, making them an ideal choice for the treatment of neural tissue.

Aim:

Thus, the aim of this work is twofold: first, we investigate the Chorioallantoic Membrane Model (CAM) exposure to NIR light for groups with different times of exposure and detect the morphological changes. And the second we investigated the toxicity and neurodegenerative effect by photobiomodulation therapy using the light with the wavelength in 670-nm applied in vivo model of blue LED induced retinal damage.

Methods:

In the CAM assay we used Light Emitting Diode (LED) light at 670 nm wavelength applied in blood vessels and vascular network topology was analyzed and measurement. In order to evaluate the toxicity effect for a long time, the eyes of rats were exposed and after the retinas examined by clinical evaluation, electroretinogram, and histological analysis. Also, to evaluate a possible ameliorates in retinal degeneration, the animals have been exposed to 2000 lux intensity of blue LED and sequentially they were treated with NIR per 30 days.

Results:

The results obtained in CAM assay suggest that the NIR was able to change the vascular network topology and was observed a reduction on vascularization. The ERG and clinical examination do not display significant changes about long exposure. In the light of lighth-stress study, we observe that the NIR-treated eyes showed an ameliorate in bipolar cell response (b-wave) and a discrete protective effect on photoreceptors cells (a-wave amplitude) when compared to the NIR-untreated group. Also, all retinal histological showed that the number of cells and relative structural organization of the retinal layers is more similar to the control than to the light-damage.

Conclusion:

These results suggest that NIR can promote reduction of vascularization in CAMs vessels and changes in network topology. The highlight of this finding is about the possible use of NIR in neovascularization diseases ocular. In vivo model, the NIR was capable to ameliorate the retina function and reduce the damages. Besides that, our results suggest that NIR is safe and contributes to the ameliorates retina function by retinal degeneration in vivo model.

Financial support:

CNPq, Capes, FAPEMIG.

24.006 - BLOCKADE OF FAAH ENZYME INDUCED NEUROPROTECTION IN A MURINE MODEL OF RETINITIS PIGMENTOSA. Magalhães CF, Fragel-Madeira L, - Neurobiologia - Universidade Federal Fluminense

Introduction:

Retinitis pigmentosa (RP) is a group of hereditary diseases that affect retina, manifested by degeneration of photoreceptors cells and its last step is blindness. There are some palliative treatments, but the disease still does not have cure. Endocannabinoid system has been shown to be neuroprotective in a variety of diseases. Two main enzymes that control endocannabinoid levels are fatty acid amide hydrolase (FAAH) and monoacylglycerol lipase (MAGL).

Aim:

We aimed to inhibit FAAH pharmacologically in a murine model of RP, PDE6 β rd10 mice, in order to neuroprotect the photoreceptors cells, achieved for manipulation of endocannabinoid levels. This project agrees with the Ethical Principles for Animal Experimentation and

FeSBE Annual Meeting 2019

Poster Sessions and Abstracts

obtained approval for implementation by Ethics Committee on Animal Use (CEUA) under protocol number 679/2015.

Methods:

We performed injections of URB597 either intraperitoneally (i.p. 0.3mg/kg – began at P13 and finished at P18 or P24) or intravitreally (i.v. 30nM/ 100nM/ 300nM – one injection at P18) and evaluated photoreceptor cells by immunofluorescence for recoverin, cell death by TUNEL assay, reactive gliosis using GFAP marker and microglial infiltration by immunofluorescence for Iba-1. All quantitative data were performed by GraphPad Prism v.7.00 using unpaired Student t test with Welch's correction and the p values less than 0.05 was considered significant.

Results:

URB597 i.p. injections increased the number of photoreceptors about 42% at P19 (postnatal day 19), whereas at P25 (postnatal day 25) this increase was 25%. Meanwhile, i.v. injections increased about 20% at concentrations of 30nM and 100nM but 300nM did not alter the number of photoreceptors cells at P19. Cell death decreased 50% after i.p. injections and 30% succeeding i.v. injection (30nM and 100nM). Analysis of glial cells revealed that i.p. injections did not alter GFAP fluorescence intensity. Furthermore microglial number in the ONL remained the same in both ages analyzed (P19 and P25). Despite this, we did not reject the involvement of glial cells with our treatment. We also sought verify which receptor was involved in the neuroprotection mediated by FAAH blockade. For this purpose, we used a receptor cannabinoid 1 (CB1) antagonist, AM281, in the concentration of 2.5mg/kg, 30 min before URB597 intraperitoneal administration. Preliminary results demonstrated an increased 20% of photoreceptors cells suggesting that CB1 receptor had a partial effect upon the retina neuroprotection.

Conclusion:

Due to its neuroprotective effect over the photoreceptors cells in rd10 mice, endocannabinoid system can be a new target of research in the context of retinitis pigmentosa.

Financial support:

Funding support was made by Capes, FAPERJ, CNPq and Proppi-UFF.

25 - Education, Science History and Philosophy, Science Communication

25.001 - DEVELOPMENT OF SKILLS IN PHYSIOLOGY LEARNING: STUDENTS' PERCEPTION OF THE PHARMACY COURSE OF A FEDERAL UNIVERSITY. Guimarães AF, Martins CS, Nunes AGP, Porawski M, Gutierrez LLP, - DCBS - UFCSPA

Introduction:

The Initiation to Teaching Program (PID) 'Ludic Practices (LP) in Physiology Learning' proposes an educational methodology based on the protagonism of the student through LP, developing skills, promoting educational challenges in a relaxed environment that extrapolates classroom. The hypothesis was whether playful tools would facilitate the learning and the development of skills and abilities of students Pharmacy course of Physiology of the Federal University of Health Sciences of Porto Alegre (UFCSPA), according to student perception.

Aim:

The aim of this study was evaluate students' perception in the development of skills and in their learning through LP.

Methods:

The data was collected by convenience sampling (students who accepted to participate voluntarily) during the 1st semester of 2018, in the Physiology I discipline of the Pharmacy Course of UFCSPA. At the beginning of the semester a lecture on skills, LP and active methodologies (AM) was ministered. During the semester, the students experienced LP in three levels of participation: a) as spectators of playful activities developed by the teachers (music, theater, history or

clinical case); b) interacting with a ludic practice and; c) constructing a ludic practice in groups (video or musical parody). The activities were related to the programmatic content of the Physiology I discipline. At the end of the semester, a questionnaire was applied with closed questions to evaluate the student's perception regarding the use of LP in learning and regarding the development of skills in communication area, interpersonal and intrapersonal relationships and in the confrontation of problem situations, in addition to the methodology used in the discipline (material developed, relevance, learning and preparation challenges by the teachers and instructors). The data obtained were organized in Excel® (version 2010), described in the form of absolute frequency and percentages. This research was approved by the Research Ethics Committee (CAE 82851518.3.0000.5345).

Results:

The sample consisted of 27 students. Preliminary data shows that 74% of students believe that LP helped learning and 59.2% reported improvement in performance. Regarding the development of skills, 70% of students perceived improvement in communication, 81.5% in interpersonal relations, 66% intrapersonal relations and 74% in solving problem situations. In the evaluation of the methodology of the subject, 85.18% considered the material used significant and relevant, 74.08% evaluated that the learning challenges were adequate and 100% indicated that teachers and monitors were prepared and available during the activities.

Conclusion:

The results shows that the students believe that ludic practices helped in the construction of learning and in the improvement of their performances, in addition to perceiving improvement in the proposed skills. In this way, we search to qualify the Physiology I discipline, building knowledge through LP and AM, contributing in the development of skills students to collaborate effectively in their professional qualification.

Financial support:

Não houve.

25.002 - A WORKSHOP AND A AND ROUND OF CONVERSATION ON SLEEP PHYSIOLOGY: EDUCATION AND SCIENTIFIC DISSEMINATION WITH CAREGIVERS OF PERSONS WITH DISABILITIES. Martins C, Saraiva AC, Silva CPL, Vargas GRT, Souza LL, Barschak AG, GUTIERREZ LLP, - DCBS - Universidade Federal de Ciências da Saúde de Porto Alegre

Introduction:

The extension project of the Federal University of Health Sciences of Porto Alegre (UFCSPA) entitled 'Supporting and Educating Families of Persons with Disabilities (PwD)' is developed in the São João Batista Rehabilitation Center (Porto Alegre, RS), a non-profit institution that serves PwDs from low-income families. The objective is to approach health education with the caregivers, including actions of scientific dissemination in Human Physiology area. Our aim is to improve the caregivers knowledge and instrumentalize them, as they face challenges related to the complexity of care. Thus, the work is focused at caregivers of PwDs, in the period in which they expect their family entity to be attended in the various health specialties that the Rehabilitation Center offers for free.

Aim:

The goal of this study was to offer a workshop and a round of conversation on Sleep Physiology, in which Human Physiology content and scientific dissemination actions in the area were addressed to caregivers of PwDs, drawing attention to their sleep quality (tested by the Sleepiness Scale of EPWORTH - ESS-BR) and what to do to sleep well.

Methods:

The activity occurred in a room offered by the Rehabilitation Center, under the approval of the Research Ethics Committee (CAE 75125417.8.0000.5345), on November 14, 2018, with 90 minutes duration. As an educational practice, workshop and round of

FeSBE Annual Meeting 2019

Poster Sessions and Abstracts

conversation techniques were used. We talked about Sleep Physiology and, as an action for scientific dissemination in this area, the Epworth Sleepiness Scale (ESS-BR) was applied. To that end, undergraduates and professors used material developed by the group, composed of brown paper and colored cards, where each participant had a color to accompany their scores on the scale. Afterwards, the caregivers received a folder containing information about sleep hygiene, its importance and physiology, and each item was discussed.

Results:

The material on Sleep Physiology was prepared and discussed in advance among the professors and undergraduate students involved in the project. The students trained the approach of education in Physiology to non-academic listeners aiming to be understood by the caregivers. Four UFCSPA students are involved in the project, as well as two pharmaceutical professors. The workshop and the round of conversation allowed caregivers to understand Sleep Physiology in daily context. Of the 15 PwD caregivers participants, only 9 were present in this activity. According to the Epworth Sleepiness Scale, 33.3% of the caregivers presented healthy sleep, 22.2% had to take care of their sleep, and 44.4% had inadequate sleep. Many of the caregivers linked their results to high demand for care of their loved ones. It was possible to guide them on the subject, as well as to solve doubts.

Conclusion:

Health professionals and students can provide, through actions such as these, the contact of these caregivers with contents developed in the academic context that directly interfere in the whole PwD family quality of life. In addition, the activity also allows students to consolidate their knowledge in Physiology area, enabling their application in everyday life.

Financial support:

Proext UFCSPA

25.003 - THE EPITHELIAL DOMINO AS DIDACTIC RESOURCE TO PROMOTE HISTOLOGY GAME-BASED LEARNING.. Lippi BK, Iar CSM, Santos MM, Negreiros NGS, Lellis-SantosC, - Departamento de Ciências Biológicas - UNIFESP

Introduction:

Histology is mostly taught using traditional methods like lecture and observation in microscopes. However, some contents are difficult to be learned because they are delivered passively, grounded on memorization and did not promote engagement.

Aim:

This study aimed to develop and analyze a game based on the playability of the domino game, here in called the Epithelial Domino. Ultimately, we expected to contribute to the histology education in high school and post-secondary education.

Methods:

The game reproduced the structure of a classical domino, and the contents of the tiles were distributed according to histologic images of representative epithelial tissues (EP), illustrations of the EP, images of the organs where the EP are located and functions of the EP. Science, Biology and Pharmacy undergraduate students were invited to play the game and evaluate its potential as a didactic resource (CAAE 82532018.5.0000.5505 - CEP/Unifesp 0065/2018). A semi-structured questionnaire and interviews with the students were used to gather qualitative and quantitative data.

Results:

The production of the epithelial domino required time and meticulous analysis in order to create an accurate and free of misconceptions game. The media to create the images of the tiles was Adobe Illustrator CC. The game was tested with 12 pairs of students (N=24), who enjoyed to play. The game took approximately 16 minutes to be accomplished, and no significant difference on the time of playing was observed between the group of students that have succeed their histology course compared to the students that did not follow or failed a histology

course. The students classified the game as very good (75%) and strongly agreed that the game might help to learn histology (87.5%); however, they considered the difficult level of the game as medium (50%) and hard (45.8). The Spearman's correlation analysis revealed a statistically significant negative correlation between the success in the histology course and the opinion that the game can help in the learning process ($r_s = -0.45$, $p < 0.05$) or the time spent to accomplish the game ($r_s = -0.52$, $p < 0.05$).

Conclusion:

The Epithelial Domino can promote the engagement of the participants on learning histology by associating the information visualized on the domino tiles. The Epithelial Domino is cost-effective, easy to play, and represents an alternative teaching method to histology classes.

Financial support:

Self-funded

25.004 - THE USE OF EDUCATIONAL EQUIPMENT FOR REVIEWING PRINCIPLES OF CARDIOVASCULAR PHYSIOLOGY IN EXERCISE PHYSIOLOGY CLASSES: A DIALECTICAL APPROACH. Oliveira DS, Carrascoza LS, Brito LC, Almeida N, Marques MS, Alves LS, Brum PC, - Biodinâmica do Movimento Humano - USP Reumatologia - USP

Introduction:

In the present study, we have built educational equipment to review principles of cardiovascular physiology for students enrolled at exercise physiology course, such as: heart as a pump, cardiovascular hemodynamics and cardiovascular autonomic control. These principles are essential for students to understand the cardiovascular responses to aerobic exercise (i.e. walking, cycling) taking into consideration changes in exercise intensity, duration and exercising muscle mass.

Aim:

Therefore, the aim of this study was to review key principles of Cardiovascular Physiology (CV) to better understanding of cardiovascular responses to exercise by using a dialectical transdisciplinary approach.

Methods:

Two classes (Morning Class (G1) n=32 ; Afternoon Class (G2) n=39) of undergraduate students of Exercise Physiology Course at the School of Physical Education and Sport, University of Sao Paulo (n=71) were randomly assigned into 4 groups where students rotate through a series of 4 stations (station rotation model), being: station S1) heart as a pump (reviewing concepts of preload, post-load and contractility using a system proposed by Rodenbaugh et al 1999), S2) hemodynamics (concept of serial and parallel conductance in vessels, using a system proposed by Smith 1999) , S3) sympathetic nervous system (heart rate (HR) response to the Stroop color and word test) and S4) parasympathetic (HR response during face immersion in cold water). To evaluate the efficacy of the proposed intervention, we used a cloud-based student response system (Socrative app) to launch a multiple-choice quiz with eight questions before (PRE) and after (POST) the student's station rotation. The questions were related to the basic principles of CV physiology, exercise physiology and its consequences in the cardiovascular system. The reports generated by Socrative app were analyzed using a Mann-Whitney test between groups (PRE vs. PRE; POST vs. POST; DELTAG1 vs. DELTAG2) and a Wilcoxon Signed Rank test within group (PRE vs. POST).

Results:

Comparing groups, the results suggest that G1 and G2 did not display the same baseline knowledge of the proposed theme, with G1 presenting higher scores than G2 at the condition PRE student's station rotation (35.03 ± 18.7 vs. 27.82 ± 17.0 ; $p = 0.04$; respectively). Independent of the differences in the baseline condition, the scores achieved by both groups after student's station rotation (POST condition) displayed no significant differences between G1 and G2 groups ($p > 0.05$). Of interest, there was an improvement in student knowledge after post-station rotation assessment when compared with

FeSBE Annual Meeting 2019 Poster Sessions and Abstracts

pretest (delta = score POSTtest - score PREtest) with 36.31 ± 18.38 and 43.28 ± 18.55 for G1 and G2 respectively, $p < 0.01$). Out of 71 students, only 5 (7%) obtained scores between 5 and 8 and 66 (93%) were below 5 corrected answers. These scores were improved in post-test by 80% (57) obtained scores between 5 and 8, while 24% (17) got scores more than 7 indicating a significant improvement in the knowledge gained.

Conclusion:

Our results suggest that the use of educational equipment for reviewing principles of cardiovascular physiology was effective to improve the comprehension of CV principles that are essential to a better understanding of the CV responses to exercise.

Financial support:

Fapesp: 2016/19771-5 to D.S.O., CAPES, CNPq

25.005 - PROMOTING EMOTIONAL ENGAGEMENT IN CELL PHYSIOLOGY LECTURES. Machado DS, Silva RAL, LELLIS-SANTOS C, - Departamento de Ciências Biológicas - UNIFESP

Introduction:

The emotional engagement of the students optimizes the process of teaching and learning. But in higher education it is difficult to promote emotional arousal during classes due to the large number of students and reduced contact-time.

Aim:

Aiming to create an emotional arousal during a lecture, we engaged students to reflect about the role of human body cells in pathophysiology contexts and promote transcultured learning through audiovisual stimuli.

Methods:

Students (N=98) were named as human body cells and encouraged to study their roles in human body homeostasis. Three weeks later they watched 2 highly emotional short videos presenting the life history of 2 different children with Zika virus-related microcephaly and their struggling mothers. Students were asked to write a letter to one of the mothers and content analysis was applied to classify their approaches (CAAE-UNIFESP 82532018.5.0000.5505).

Results:

The majority (82.7%) of the letters did not present conceptual errors. Among students that made mistakes, they wrote incorrect information about cell function or cell location in the human body. Approximately 54 % of the letters presented mixed profile of scientific/formal and emotional/informal writing. Most of the students showed empathy on how they would help to overcome the situation as being a cell of the sick kid. Among the six basic emotions expressed in the letters, derivative feelings of love (79.8%), sadness (17.9%) and fear (2.4%) were identified. The Kendall's Tau correlation analysis revealed a statistically significant negative correlation between the number of physiological concept errors and the level of love expression in the letters ($\tau\text{-}b = -0.29$, $p < 0.05$).

Conclusion:

Overall, students were creative, expressed their feelings triggered by the histories, and used discourses based on cell anatomy and physiology. Thus, emotional letters are a potential didactic strategy to promote emotional arousal in physiology courses.

Financial support:

Pró-Reitoria de Graduação da UNIFESP

FeSBE Annual Meeting 2019
Poster Sessions and Abstracts

Poster Session II - Sept.11.2019 - 16:00 -18:00 h

2 - Anatomy	001 - 007
4 - Cardiovascular Biology and Diseases	011 - 019
6 - Endocrine System	007 - 011
7 - Nutrition and Metabolism	018 - 034
8 - Renal Biology and Diseases	007 - 012
9 - Respiratory Biology and Diseases	006 - 009
10 - Neurobiology	015 - 028
11 - Physical Training Responses	008 - 014
12 - Biomembranes, Transporters and Signaling	001 - 005
13 - Cell differentiation, growth and death	010 - 018
16 - Gene and Cell Therapy, Omics Biology	006 - 009
17 - Basic & Clinical Pharmacology	006 - 009
18 - Neuropsychopharmacology	006 - 010
19 - Toxicology	010 - 018
20 - Pain and Inflammation	009 - 015
21 - Immunology	001 - 004
22 - Cancer Signaling and Therapeutics	014 - 026
24 - Vision and Ophthalmology	007 - 012
25 - Education, Science History and Philosophy, Science Communication	006 - 010
26- FeSBE Jovem	001 - 034

FeSBE Annual Meeting 2019

Poster Sessions and Abstracts

2 – Anatomy

02.001 - METABOLIC AND TESTICULAR EFFECTS OF COCOA POWDER SUPPLEMENTATION IN WISTAR RATS SUBMITTED TO EARLY WEANING. Lima JC, Cardoso LMF, Monnerat JAS, Pereira AD, Rocha GS, Fernandes-Santos C, Gregorio BM, - Anatomia - UERJ Nutrição e Dietética - UFF Ciências Básicas - UFF - campus Nova Friburgo

Introduction:

Early weaning can lead to metabolic and cardiovascular complications in adulthood, with important changes in the morphology of certain organs, such as the heart, kidneys, and liver. It is believed that the consumption of functional foods during lactation and postnatal life are able to prevent these effects. Cocoa is a functional food, rich in bioactive compounds, with beneficial actions on metabolism and cardiovascular health. It is unknown the early weaning directly affects the morphology of the testicles, and if the polyphenols present in cocoa preserve the morphology of this gonad.

Aim:

Therefore, the aim of this study was to evaluate the effects of metabolic programming, by early weaning, upon the body mass, metabolism and morphology of the testicles of Wistar rats supplemented or not with cocoa powder.

Methods:

This study was approved by the Ethics Committee for the Care and Use of Experimental Animals on registration: CEU / UFF 1032/2018. After approval, the animals were divided into four experimental groups (n = 6, each): Control Group (C) - animals with complete lactation (21 days post birth) and receiving commercial food (Nuvilab®) in postnatal life; Cocoa Control Group (CCa) - animals with complete lactation (21 days post birth) and receiving commercial food supplemented with 10% cocoa powder; Early Weaning Group (EW) - animals weaned on the 18th day of lactation and received commercial food in postnatal life; Early Weaning Cocoa Group (EWCa) - animals weaned on the 18th day of lactation and receiving commercial food supplemented with 10% cocoa powder. Food intake and body mass were evaluated daily and weekly, respectively. The animals were followed up until 90 days, at which time euthanasia occurred. At this time, blood was collected, centrifuged and frozen for biochemical analysis; and the testicles were removed for histomorphometric analysis. Data were analyzed by One-Way Anova with post-test of tukey, considering $p < 0.05$.

Results:

The EW and CCa groups presented an increase at 13% and 11% in body mass when compared to C group, respectively ($P < 0.05$). Corroborating with this result, the CCa group showed an augment in food intake in relation to C group ($\uparrow 14\%$, $P < 0.0005$). Regarding the biochemical parameters analyzed to date, early weaning caused hyperglycemia ($\uparrow 48\%$, $P < 0.0001$). Inversely, dietary supplementation with cocoa powder was able to reduce serum glycemia in the C ($\downarrow 23\%$) and EW ($\downarrow 49\%$) groups when compared to their counterparts ($P < 0.0001$). Concerning testicular morphology, the EW group presented a reduction in tubule diameter (18%) and seminiferous epithelium height (9%) when compared to C, whereas EWCa animals presented a significant elevation in these parameters (15%, $P < 0.0001$) when compared to EW group.

Conclusion:

Early weaning resulted in body mass elevation, hyperglycemia and important morphological changes in the testicles. In contrast, dietary supplementation with cocoa powder attenuated these effects on the metabolism and testicular histoarchitecture, proving to be a good nutritional treatment strategy.

Financial support:

FAPERJ

02.002 - EFFECT OF LEUCINE ON HDAC4 EXPRESSION IN THE SKELETAL MUSCLE OF RATS SUBMITTED TO HINDLIMB IMMOBILIZATION. ALVES PKN, OLIVEIRA ACD, GRAÇA FA, MORISCOT AS, - ANATOMIA - Universidade de São Paulo - USP

Introduction:

Skeletal muscle retains a high capacity to adapt to various conditions such as injury and mechanical load. When mechanical load is decreased, muscle tissue triggers a catabolic response resulting in muscle atrophy, which can be mediated by histone deacetylases (HDACs). HDACs in turn are able to induce transcription of critical skeletal muscle atrophy mediators (Atrogin-1 and Murf1). In this study we hypothesized that leucine can exert its anti-atrophic effects throughout HDACs. This hypothesis is supported by RNAseq assays, suggesting that the expected induction of HDAC4 by hindlimb immobilization is attenuated by leucine supplementation.

Aim:

Thus our objective was to investigate whether the anti-atrophic effect of leucine depends on the suppression of HDAC4 expression. We examined the impact of Leucine on cellular and tissue localization of HDAC4 and its target genes.

Methods:

Thirty-five male Wistar rats (~260g) were housed in standard conditions and divided into four groups: control (CG); leucine (GL); hindlimb immobilized (GI); immobilized and leucine (GIL). All groups were submitted to gavage with or without Leucine for seven days. These animals were euthanized, and soleus muscle was removed for analysis of HDAC4 tissue localization and gene expression, as well as gene targets involved in the atrophic process. Also, C2C12 cells, treated with dexamethasone and leucine for 24h were used to evaluate the effects of leucine on the expression and localization of HDAC4 in an atrophic model in vitro. The results are expressed in means \pm SD, and the analysis of variance (ANOVA) was performed to compare the groups, and the significance was 5%.

Results:

Initially, RNA-Seq analysis of rats hindlimb immobilized and supplemented with leucine for three days indicated an induction of HDAC4 expression during immobilization. In addition, leucine supplementation was capable of attenuating this effect (~1,1/Log 2). In vivo, we also found a marked increase of the atrophic gene targets and HDAC4 expression in GI, which was mitigated in GIL (HDAC4: ~7 fold vs 3.5 fold; Myog: ~2 fold vs ~0.7 fold; Atrogin-1: 1.8 fold vs 1.1 fold; GI vs GIL respectively; $p < 0.05$). Regarding the tissue location of HDAC4, we found that the frequency of positive nuclei was higher in the GI and decreased in the GIL (GI 33% vs GIL 18.5%; $p < 0.05$). In addition, our in vitro results also demonstrated increased expression of HDAC4 and atrophic gene targets after dexamethasone treatment, which was reduced in leucine treated group ($p < 0.05$). Concerning cell location, our preliminary findings suggest a nuclear accumulation of HDAC4 in myotubes treated with dexamethasone. In addition, in myotubes treated with dexamethasone and leucine we found a perinuclear location.

Conclusion:

Overall, these results provide further insight upon the anti-atrophic effects of leucine.

Financial support:

FUNDAÇÃO DE AMPARO À PESQUISA DO ESTADO DE SÃO PAULO - FAPESP

02.003 - EFFECT OF GLUTAMINE SUPPLEMENTATION ON SKELETAL MUSCLE REGENERATION IN RATS.. Baggio BR, Koike TE, Miyabara EH, - Anatomia - USP

Introduction:

Skeletal muscle has a great capacity of regeneration after injury, In this context, glutamine supplementation represents a viable strategy to improve skeletal muscle regeneration by accelerating muscle mass

FeSBE Annual Meeting 2019

Poster Sessions and Abstracts

recovery after injury, as evidences show that glutamine is capable of inducing an increase in protein synthesis and an inhibition of muscle proteolysis. However, the detailed mechanisms by which glutamine regulates muscle protein metabolism are still unknown. Furthermore, the effect of glutamine supplementation on skeletal muscle regeneration is not well understood

Aim:

The aim of this study was to analyze the effect of glutamine supplementation on regenerating soleus and extensor digitorum longus (EDL) muscles from young rats.

Methods:

Wistar rats (2 months old) were randomly divided into two groups, without or with glutamine supplementation (daily, via gavage, 1 g/kg) and analyzed at 10 days after cryolesion. The glutamine supplementation started immediately after cryolesion. Body and muscle weights were analyzed. Histological aspects of the regeneration of the previously injured soleus and EDL muscles stained with hematoxylin and eosin were evaluated through measurement of muscle cross-sectional area, myofiber cross-sectional area and quantification of regenerating myofibers with centralized nuclei. For statistical analysis, the t-student test was used for the comparison between two groups and analysis of variance (ANOVA) followed by the Tukey test (parametric) for the multiple comparison between more than two groups. The analyzes were considered statistically significant when $p < 0.05$. This project was approved by the Committee on Ethics in the Use of Animals (CEUA, ICB/ USP) registered under protocol No. 71/2017.

Results:

Body weight and cross-sectional area of soleus and EDL muscles were unaltered with glutamine supplementation. Soleus muscle weight from cryolesioned group decreased compared to that from control group (30.8%). There were no differences in muscle weight from other groups. There was a decrease in the cross-sectional area of regenerating myofibers from cryolesioned soleus and EDL compared to their controls (6.4 and 4.1, respectively). In the cryolesioned supplemented group, there was an increase in the cross-sectional area of regenerating myofibers from soleus and EDL compared to those from the cryolesioned group (1.75 and 1.5, respectively). The number of regenerating myofibers with centralized nuclei in cryolesioned soleus and EDL muscles was unaltered with glutamine supplementation.

Conclusion:

Overall, the results suggest that glutamine accelerates muscle regeneration by increasing the size of regenerating myofibers. These results may inspire the study of future strategies to improve skeletal muscle recovery after injury models.

Financial support:

CAPES

02.004 - EVIDENCE THAT THE β_2 -ADRENOCEPTOR IS INVOLVED ON MYOGENIC DIFFERENTIATION BY REGULATING MTORC1 SIGNALING. Koike TE, Baggio BR, Miyabara EH, - Anatomia - USP

Introduction:

Skeletal muscle regeneration occurs after injury, which is followed by inflammation process and subsequent satellite cell activation and proliferation. After, most of these cells differentiate and recompose the injured skeletal muscle tissue. Previous studies showed the importance of β_2 -adrenoceptor (Adrb β_2) in structural and functional regeneration of skeletal muscle, however the mechanisms involved on that are not well understood.

Aim:

The aim of this study was to investigate the influence of Adrb β_2 on terminal muscle differentiation phase during muscle regeneration, through in vivo and in vitro analyses.

Methods:

Two-month-old male mice FVB (wild-type) and knockout for Adrb β_2 were used. In vivo analysis: tibialis anterior (TA) muscles from Adrb β_2

knockout (β_2 KO) and FVB mice were cryolesioned and analyzed after 10 days. The muscle cross-sections analyzed after 10 days post-cryolesion were used to detect embryonic myosin heavy chain (MyHCe) positive myofibers. In vitro analysis: for the terminal differentiation assay, skeletal muscles from both hindlimbs of β_2 KO and FVB mice were injured 3 days earlier (through needle injuries). On the day of myoblast isolation, injured skeletal muscles were digested with collagenase and dispase. Pre-plating was then performed for the elimination of fibroblasts, followed by the inclusion of the myoblasts in proliferation medium. After reaching 80% confluence, myoblasts were maintained in differentiation medium for 2 days and then subjected to immunostaining or western blot (WB) of phosphorylated p70S6K, a component of the PI3K/AKT/mTORC1 pathway. The primary antibodies used for immunostaining and WB were: mouse anti-desmin; rabbit anti-p70S6K (Ser 371) and rabbit anti-MyHCe. The corresponding secondary antibodies used were: donkey anti-rabbit (TRITC); goat anti- mouse (FITC). For statistical analysis, the t-student test was applied for the comparison between two groups and analysis of variance (ANOVA) followed by the Tukey test (parametric) for the multiple comparison between more than two groups. The analyzes were considered statistically significant when $p < 0.05$. This project was approved by the Committee on Ethics in the Use of Animals (CEUA, ICB/ USP) registered under the protocol No. 106/2017.

Results:

There was a lower percentage of regenerating myofibers positive to MyHCe in TA muscles from β_2 KO mice (59.32%) when compared to that from FVB group (72.38%). The expression of phosphorylated p70S6K in differentiating myoblasts from β_2 KO group decreased (70.9%) when compared to that from the FVB group. The percentage of desmin positive myoblasts expressing phosphorylated p70S6K was 45.6% lower in β_2 KO group, when compared to that from FVB group.

Conclusion:

The results suggest that the Adrb β_2 is involved on myogenic differentiation by regulating mTORC1 signaling.

Financial support:

FAPESP

02.005 - STRUCTURAL ANALYSIS OF THE BULBOSPONGIOSUS MUSCLE IN PATIENTS WITH BULBAR URETHRAL STRICTURES. Alves EF, Procopio IM, Gallo CBM, Sampaio FJB, Favorito LA, - Anatomia - UERJ

Introduction:

Bulbospongiosus (BS) muscle covers the bulbar urethra and its function is the expulsion of seminal fluid and urine from the urethra. Bulbar urethroplasty can evolve with ejaculatory dysfunction and post-micturitional dribbling, which has led to the preservation of this muscle during the surgical procedure. The hypothesis of the present study is that bulbar urethral stricture alters the morphology of BS muscle.

Aim:

The aim of the present study is to evaluate, by histochemical and immunohistochemical analysis, the BS muscle in patients with bulbar urethral stricture.

Methods:

From January 2016 to January 2019, 21 patients were submitted to surgical treatment and were divided into two groups: Control Group - 7 patients (mean=60.14 years old) submitted to perineal urethrostomy for hypospadias cripples and/or penile trauma; and Stricture Group - 14 patients (mean=62.00 years old) with bulbar urethral stricture submitted to open urethroplasty. Samples of BS muscle were obtained and fixed in 4% buffered formalin and paraffin embedding for perform histochemical and immunohistochemical techniques to evaluate muscle components. The histomorphometric analyzes were performed on photomicrographs using ImageJ software. Statistical analyzes were performed on GraphPad Prism 6 software, using the unpaired Student t test and the Mann-Whitney test, considering $p < 0.05$ as significant.

Results:

FeSBE Annual Meeting 2019

Poster Sessions and Abstracts

The diameter of muscle fibers did not present significant difference between the Control Group (41.71±14.63 µm) and the Stricture Group (40.11±8.59 µm), p=0.7668. When analyzing the collagen, we did not observe significant differences among the Control Group (10.63±5.37%) and the Stricture Group (10.83±4.55%), p=0.9296. The quantitative analysis of the elastic tissue fibers did not present significant difference between the Control Group (3.83±1.54%) and the Stricture Group (5.43±2.90%), p=0.2601. The quantitative analysis of the nerves did not present a significant difference between the Control Group (4.20±2.56%) and Stricture Group (5.41±2.12%), p=0.2621. When analyzing the vessels, we observed significant differences among the Control Group (5.11±1.98%) and the Stricture Group (3.57±1.32%), p=0.0460.

Conclusion:

Bulbar urethral stricture led to a significant decrease of vessels in the BS muscle without other significant structural changes. These findings tend to reinforce the preservation of the BS muscle during urethroplasties.

Financial support:

CAPES, CNPq and FAPERJ.

02.006 - METABOLIC AND PROSTATIC EFFECTS OF COCOA POWDER SUPPLEMENTATION IN WISTAR RATS SUBMITTED TO EARLY WEANING. Procopio-Oliveira CA, Cardoso LMF, Monnerat JAS, Pereira AD, Rocha GS, Fernandes-Santos C, Gregorio BM, - Anatomia - UERJ Nutrição e Dietética - UFF Ciências Básicas - UFF - Nova Friburgo

Introduction:

Early weaning can impair metabolic functions and to predispose the fetus and/or offspring to greater risk of developing metabolic diseases and chronic diseases in adulthood. It is believed that the consumption of functional foods during lactation and postnatal life are able to prevent these effects. Cocoa is a functional food, rich in polyphenols, that presents anti-inflammatory and antioxidant properties. However, it is unknown if early weaning affects the prostate morphology and whether cocoa preserves its morphology.

Aim:

The aim of this study was to evaluate the effects of metabolic programming, by early weaning, upon the body mass, metabolism and morphology of the prostate of Wistar rats supplemented or not with cocoa powder.

Methods:

This study was approved by the Ethics Committee for the Care and Use of Experimental Animals on registration: CEU / UFF 1032/2018. After approval, the animals were divided into four experimental groups (n = 6, each): Control Group (C) - animals with complete lactation (21 days post birth) and receiving commercial food (Nuvilab®) in postnatal life; Cocoa Control Group (CCa) - animals with complete lactation (21 days post birth) and receiving commercial food supplemented with 10% cocoa powder; Early Weaning Group (EW) - animals weaned on the 18th day of lactation and received commercial food in postnatal life; Early Weaning Cocoa Group (EWCa) - animals weaned on the 18th day of lactation and receiving commercial food supplemented with 10% cocoa powder. Food intake and body mass were evaluated daily and weekly, respectively. The animals were followed up until 90 days, at which time euthanasia occurred. At this time, blood was collected, centrifuged and frozen for biochemical analysis; and the prostate was removed for histomorphometric analysis. Data were analyzed by One-Way Anova with post-test of tukey, considering p <0.05.

Results:

The CCa and EW groups presented an increase at 15% and 13% in body mass when compared to C group (P<0.0001), respectively. Corroborating with this result, the CCa group showed an augment in food intake in relation to C group (↑14%, P <0.0001). Regarding the biochemical parameters analyzed until now, early weaning caused hyperglycemia (↑86%, P<0.0001). However, dietary supplementation with cocoa powder was able to reduce serum glycemia in the C (↓24%,

P<0.0001) and EW (↓58%, P<0.0001) groups when compared to their counterparts (P <0.0001). Concerning prostate morphology, the EW group presented a reduction in epithelial height (↓16%, P <0.0001) compared to C group, whereas the EWCa group presented a significant elevation in this variable (↑15%, P <0.0001) in relation to EW animals. When studying the smooth muscle density, early weaning decreased this parameter in comparison to C group (↓14%, P <0.0001), while powdered cocoa supplementation was able to augment the amount of smooth muscle in EWCa animals (↑15%, P <0.0001).

Conclusion:

Early weaning resulted in body mass elevation, hyperglycemia and important morphological changes in the prostate. In contrast, dietary supplementation with cocoa powder attenuated these effects on the metabolism and prostatic histoarchitecture, proving to be a good nutritional treatment strategy.

Financial support:

CAPES, FAPERJ

02.007 - EFFECTS OF CHRONIC STRESS IN FOOD PREFERENCE, TESTICULAR MORPHOLOGY AND SPERM PARAMETERS OF WISTAR ADULT RATS.. Lima JC, Procopio-Oliveira CA, Marchon RG, deMacedo CR, Maia ARB, deSouza DB, Sampaio FJB, Gregorio BM, - Anatomia - UERJ

Introduction:

Stress is a health problem that affects millions of people, and is related to the dynamics of the modern lifestyle. Exposure to prolonged stress exerts a destructive effect on tissues, inhibiting various bodies activities and negatively influencing cell proliferation and differentiation. In addition, chronic stress is associated with metabolic disturbances and changes in energy homeostasis, which may cause changes in food behavior in humans and animals. Recently, it has been shown that dietary factors are able to influence the response to chronic stress, and that highly palatable foods (comfort food) are able to attenuate this response. However, this type of diet compromises the testicular morphology and the production of spermatozoa, which added to the stress can be one of the causes of male infertility.

Aim:

The aim of this work was to study the effects of chronic stress (by restriction) on food preference and testicular morphology in adult Wistar rats.

Methods:

This study was approved by the Ethics Committee for the Care and Use of Experimental Animals on registration: CEUA 004/2019. After approval, the animals were divided into four experimental groups (n = 6, each): Control group (C)- standard chow (Nuvilab®); Control Comfort Food Group (CF)- standard chow + comfort food (Froot Loops®); Chronic stress Group (S)- standard chow with chronic stress; Chronic stress comfort Food (SCF)- standard chow + comfort food with chronic stress (Froot Loops®). At 3 months of age, food supply and stress were initiated. The chronic stress was induced by restriction (animals were contained in a polypropylene tubes for 2 hours, 7x / week, for 8 weeks). Body mass and food intake were checked daily. At the euthanasia, blood was collected, centrifuged and frozen for biochemical analysis; and the testicles were removed for histomorphometric analysis. Data were analyzed by One-Way Anova with post-test of tukey, considering p <0.05.

Results:

The CF group was heavier than the SCF group (P <0.005). Corroborating this result, food intake in S and SCF groups was lower than C group (↓ 23% and ↓ 26%, P <0.0001, respectively). However, when evaluated food preference, the CF and SCF groups presented high consumption (↑ 24% and ↑ 58%, P <0.0001) of the comfort food in comparison to standard diet, being the comfort food intake higher in the SCF group (↑ 19% P <0.0001). There was no significant difference between groups regarding glycemia. In the testes, there was no difference in the

FeSBE Annual Meeting 2019

Poster Sessions and Abstracts

seminiferous epithelium height and in the seminiferous tubule diameter. The viability of the spermatozoa was the same among the groups.

Conclusion:

Chronic stress was able to reduce food intake and to stimulate the preference for highly palatable foods. However, the morphology of the testicles and the viability of the spermatozoa were preserved.

Financial support:

CAPES, FAPERJ

4 - Cardiovascular Biology and Diseases

04.011 - A NOVEL P38-ALPHA MAPK INHIBITOR (LASSBIO-1824) REVERSES SU5416/HYPOXIA-INDUCED PULMONARY ARTERIAL HYPERTENSION IN RATS. Silva GF, Alencar AKN, Silva JS, Silva MM, Freitas RC, Montagnoli TL, Fraga CAM, Sudo RT, Zapata-Sudo G, - PROGRAMA DE PESQUISA EM DESENVOLVIMENTO DE FÁRMACOS - UNIVERSIDADE FEDERAL DO RIO DE JANEIRO (UFRJ)

Introduction:

Pulmonary arterial hypertension (PAH) is a disease characterized by pulmonary vascular remodeling with subsequent right ventricular (RV) failure.

Aim:

This work investigated the effects of a new p38-alpha mitogen-activated protein kinase (p38- α MAPK) inhibitor, named LASSBio-1824, on the hypoxia + SU5416-induced PAH (SuHx) model in rats.

Methods:

All experiments were conducted in accordance with the Animal Care and Use Committee at the Universidade Federal do Rio de Janeiro (under number 039/19). PAH was induced in male Wistar rats (180-220 g) that were exposed to 3 weeks of hypoxia and i.p. injections of a vascular endothelial growth factor receptor (VEGFR) antagonist (SU5416; 20 mg/kg/week). Control rats were exposed to normoxia (room air at 21% O₂), while the hypoxia groups were exposed to chronic normobaric hypoxia (10% O₂) in a ventilated acrylic chamber. At day 21 of protocol, Doppler echocardiography was used to image the pulmonary artery (PA) outflow waveform profile, and PAH establishment was confirmed by change in the shape of the PA waveform. After disease onset, animals were divided into three groups: Control + vehicle (DMSO), SuHx + vehicle and SuHx + LASSBio-1824 (50 mg/kg/day). All substances were administered by oral gavage for two weeks.

Results:

Pulmonary acceleration time (PAT; ms) was reduced from 33.2 \pm 2.7 (control) to 22.7 \pm 1.1 in SuHx + vehicle group ($p < 0.05$) and restored to 29.6 \pm 1.9 in SuHx + LASSBio-1824 group ($p < 0.05$ vs. PAH rats treated with vehicle). RV systolic pressures (mmHg) were increased from 22.2 \pm 1.5 (control) to 47.2 \pm 3.6 (SuHx + vehicle; $p < 0.05$) and reduced to 18.0 \pm 2.9 (SuHx + LASSBio-1824; $p < 0.05$). The medial wall thickness (%) of distal pulmonary arterioles ($< 50 \mu\text{m}$) was measured by immunohistochemistry for alpha smooth muscle actin (α -SMA) and was increased from 62.5 \pm 5.6 in control rats to 78.0 \pm 7.9 in PAH animals ($p < 0.05$), but reduced to 54.4 \pm 2.3 in SuHx + LASSBio-1824 group ($p < 0.05$). Acetylcholine (ACh)-induced maximal relaxation (%) in pulmonary arteries from PAH rats was reduced from 67.5 \pm 2.1 (control) to 49.63 \pm 5.6 (PAH group; $p < 0.05$). LASSBio-1824 beneficially increased the response to ACh to 73.7 \pm 4.1 ($p < 0.05$ vs. PAH group). The immunohistochemistry for c-fos protein, a product of the p38 pathway, showed that PAH rats had an increase of ratio between myocyte nuclei (%) marked and total nuclei (%), from 20.2 \pm 4.2 (control) to 38.0 \pm 0.5 (SuHx group; $p < 0.05$), and LASSBio-1824 significantly reduced this ratio to 24.0 \pm 2.3 ($p < 0.05$). The lung expression (a.u.) of inducible nitric oxide synthase, a pro-inflammatory protein, increased from 0.31 \pm 0.01 (control) to 0.57 \pm 0.02 in SuHx + vehicle group ($p < 0.05$) and it was

normalized by the treatment with LASSBio-1824 (0.31 \pm 0.10; $p < 0.05$ vs. PAH rats).

Conclusion:

LASSBio-1824 represents an important approach for the future treatment of PAH which improves the underlying remodeling and inflammation processes in the cardiopulmonary system.

Financial support:

CNPq, FAPERJ, CAPES.

04.012 - PROTECTIVE EFFECT OF EGG WHITE HYDROLYSATE ON CARDIOVASCULAR DAMAGE INDUCED BY CADMIUM IN RATS. PinheiroJúnior JEG, Moraes PZ, Cavalini TI, Pinton S, Peçanha FM, Vassallo DV, Miguel M, Santos FW, Wiggers GA, - Bioactivity and Food Analysis Laboratory - CIAL Departments of Physiological Sciences - UFES/EMESCAM Postgraduate Program in Biochemistry - UNIPAMPA

Introduction:

Egg white represents most part of the egg and is used as a food ingredient that when processed by enzymatic hydrolysis has biological potential and can be configured as a functional food. Natural compounds such as bioactive peptides derived from egg white can prevented or alleviate the effects of toxic metals in the cardiovascular system.

Aim:

The aim is to investigate the effects of egg white hydrolysate on cardiovascular damage induced by exposure to cadmium chloride (CdCl₂) in rats.

Methods:

Three-month-old male Wistar rats (± 300 g) were divided into four groups and treated for 14 days: a) Untreated (Control - distilled water ip), b) Cd (Cadmium Chloride - CdCl₂ - 1mg/kg ip) c) EWH (egg white hydrolyzate, 1 g/ kg/day per gavage), d) CdEWH (CdCl₂ plus EWH). Blood pressure (BP) was measured by caudal plethysmography and vascular reactivity was studied in mesenteric resistance arteries (MRA) in an organ-bath system. Dose-response curves for acetylcholine (ACh) and noradrenaline (NE) were performed and the possible involved vascular pathways investigated. Biochemical assay of reactive oxygen species (ROS), lipid peroxidation, total antioxidant capacity and activity of superoxide dismutase (SOD) were measured in plasma. We also measured in situ production of superoxide anion by DHE and COX-2 detection by immunofluorescence. The results are expressed as mean and SEM, compared by ANOVA followed by the Bonferroni test with significance level of $p < 0.05$.

Results:

The EWH prevented: a) the increased SBP observed after Cd exposure (Untreated: 119.1 \pm 2.1; Cd: 148.7 \pm 5.3 *; EWH: 124.4 \pm 2.9; CdEWH: 123.2 \pm 3.2# mmHg; n=10 *vs Ct and #vs Cd); b) the increased vasoconstrictor response to NE (Rmax of the concentration response curve to NE: Untreated: 97.4 \pm 2.3; Cd: 117.9 \pm 4.9*, EWH: 101.9 \pm 2.4, CdEWH: 98.2 \pm 4.5#) c) the endothelium vasoconstrictor - modulation and nitric oxide bioavailability involvement (E-: Untreated: 35.3 \pm 6.1; Cd: 2.6 \pm 0.4*; EWH: 22.3 \pm 6.2; CdEWH: 31 \pm 8.6#; L-NAME: Untreated: 34.9 \pm 6.0; Cd: 1.1 \pm 3.8*; EWH: 14.5 \pm 6.8; CdEWH: 28 \pm 11.4#, % dAUC) d) the increased ROS production from NAD(P)H oxidase (Apocynin: Untreated: 5.1 \pm 5.6; Cd: 44.1 \pm 6.4*; EWH: 3.0 \pm 3.1; CdEWH:17.3 \pm 7#, % dAUC) and contractile prostanoids from COX (Indomethacin: Untreated: 11.2 \pm 5.3; Cd: 58.6 \pm 8.1*; EWH: 7.9 \pm 5.0; CdEWH: 30.4 \pm 5.6#, NS 398: Untreated: 8.1 \pm 4.3; Cd: 53.6 \pm 6.9*; EWH: 1.2 \pm 5.1; CdEWH: 24.4 \pm 2.1#, % dAUC) e) the increased of the participation of the renin-angiotensin system (Losartan: Untreated: 2.1 \pm 3.1; Cd: 30.3 \pm 4.1*; EWH: 3.7 \pm 2.9; CdEWH: 11.3 \pm 3.1#, % dAUC) f) the increased plasmatic ROS production, lipid peroxidation, increased SOD activity, as well as the imbalance on antioxidant capacity after Cd exposure and g) prevented the increase of superoxide anion and COX-2 in situ. CEUA/UNIPAMPA: 013/2019.

Conclusion:

FeSBE Annual Meeting 2019

Poster Sessions and Abstracts

EWH prevented the toxic damage induced by CdCl₂ in the cardiovascular system.

Financial support:

Brazilian Government (Conselho Nacional de Desenvolvimento Científico e Tecnológico – CNPq 307399/2017-6); CAPES and by the Spanish Government [MINECO - AGL2017-89213-R and SAF2015-69294-R]

04.013 - EFFECT OF VITAMIN C ON CARDIORENAL SYNDROME TYPE 3: PARTICIPATION OF NITRIC OXIDE SINTETASES (NOS). Santos RSN, Carneiro-Ramos MS, - Centro de Ciências Naturais e Humanas - Universidade Federal do ABC

Introduction:

Cardiorenal syndrome is a pathophysiological disorder between heart and kidney that occurs when the acute or chronic dysfunction of one organ induces acute or chronic dysfunction in the other. It is known that the Nitric Oxide (NO) plays an important role in cardiovascular functions both in pathological and non-pathological conditions. Acute Kidney Insufficiency is responsible for systemic inflammation releasing inflammatory factors and ROS (reactive oxygen species), as nitric oxide (NO). High levels of ROS are linked to lipids, proteins, carbohydrates, nucleic acids destruction. On the other hand, the antioxidant system plays an important role to balance the production and destruction of ROS, such as peroxidases, glutathione and exogenous molecules like vitamin C (ascorbic acid). However, there are no evidences relating ascorbic acid on the CRS type 3 development in mice.

Aim:

To evaluate the role of ascorbic acid on the modulation of NOS expression in heart tissue during the cardiorenal syndrome type 3 induced by renal ischemia/reperfusion (I/R) protocol.

Methods:

All procedures were approved by Ethical committee of UFABC (CEUA/UFABC No 5745260918). C57BL/6 male mice were subjected to surgical occlusion of left renal pedicle for 60 min followed for reperfusion for 8 and 15 days, combined or not with Vitamin C (57mg/Kg/ day – d.w.). The animals were divided in 3 groups: Vehicle (only treat with vitamin C for 23 days), Pre treatment Vit C + I/R (8 days of Vit C treatment since surgery day and 15 days of reperfusion) and Post treatment Vit C + I/R (15 days of reperfusion followed by 8 days of Vit C treatment). Morphometric analyses were performed using as parameters kidneys weight, heart weight and body weight or tibia length ratios. To evaluate kidney injury, creatinine and urea levels was performed. Real time PCR was performed to analyze NOS's gene expression. Data were expressed as mean ± standard deviation (SD) and statistical analyzes was performed using ANOVA and Test t student, P value < 0,05 was considered statistically significant.

Results:

The renal parameters indicated a decrease on left kidney weight in both groups submitted to I/R compared to vehicle animals (p<0,05). Creatinine and urea levels did not alter in I/R animals whose received Vitamin C and vehicle group. The Pre treatment of Vitamin C was able to preserve the Heart Weight/Body Weight ratio (mg/g) compared to vehicle animals (5,72 ± 0,41 vs 6,01 ± 0,43). Cardiac iNOS and nNOS gene expressions were not different between I/R+ vitamin C (Pre or Pos) and Vehicle, but cardiac eNOS gene expression decreased in both groups submitted to I/R combined to Vitamin C treatment (0,35 ± 0,57 and 0,30 ± 0,64 vs 1,00 ± 0,46, respectively).

Conclusion:

The results suggest that vitamin C was able to modulate NOS in heart tissue, indicating an important action of NO in the heart and protection of renal function.

Financial support:

FAPESP 2015/19107-5

04.014 - BIOACTIVE PEPTIDES DERIVED FROM EGG WHITE HYDROLYSATE REDUCE VASCULAR DAMAGE PROMOTED BY CADMIUM EXPOSURE IN AORTA. Moraes PZ, PinheiroJúnior JEG, Rodrigues MD, Ronacher M, Santos FW, Peçanha FM, Vassallo DV, Martinez CS, Miguel M, Wiggers GA, - Campus Uruguaiana - Universidade Federal do Pampa Instituto de Investigación en Ciencias de la Alimentación - CIAL/CSIC Departamento de Fisiología - UFES

Introduction:

Cadmium (Cd) is a heavy metal and exposure to humans is due to the consumption of drinking water, food and cigarette smoke. Its deleterious effects affect various organic systems including the cardiovascular system. In contrast, functional foods derived from animal proteins with bioactive properties have been investigated as an alternative treatment for heavy metal damage derived from oxidative stress and inflammatory process.

Aim:

We aim to investigate whether egg white hydrolyzate (EWH), a functional food, may prevent or reverse cardiovascular damage caused by exposure to Cd.

Methods:

Male Wistar rats were divided into four groups and treated for 14 days: a) Untreated (Control - distilled water ip); Cd (Cadmium Chloride - CdCl₂ - 1mg/kg ip) c) EWH (egg white hydrolysate, 1 g/ kg/day per gavage), d) CdEWH (CdCl₂ plus EWH). The vascular reactivity in conductance artery (aorta) was evaluated in an organ-bath system and the possible involved vascular pathways investigated. Dose-response curves for acetylcholine (ACh), phenylephrine (Phe) and sodium nitroprusside (SNP) were performed. We evaluated the participation of reactive species (NADPH oxidase inhibitor, apocynin) and cox-2 derived prostanoids (the selective COX-2 inhibitor, NS 398) in the contractile response to Phe. Biochemical assay of reactive oxygen species (ROS), lipid peroxidation (TBARS), total antioxidant capacity (FRAP) were measured in aorta. Also Protein expression of COX-2 (Western Blotting) was evaluated in the aorta, measured in situ production of superoxide anion by DHE and COX-2 detection by immunofluorescence. The results are expressed as mean and SEM, compared by ANOVA followed by the Bonferroni test with significance level of p<0.05 (*vs Ct and #vs Cd). CEUA/UNIPAMPA: 013/2019.

Results:

Co-treatment with EWH prevented the increase vasoconstrictor response to Phe (R_{max} of the concentration response curve to Phe: (Untreated: 84.8±1.4; Cd: 101.6±1.9*, EWH: 90.5±1.4, CdEWH: 91.6±3.5#) induced by Cd-exposure. These effects are related mainly to reduction of oxidative stress mediated by NADPH oxidase (Apocynin: Untreated: 38.2±6.1; Cd: 66.6±4.1*; EWH: 40.7±10.2; CdEWH: 30.1±2.2#, % dAUC), the inhibition of prostanoids derived from COX-2 (NS398: Untreated: 42.7±5.1; Cd: 62.4±2.9*; EWH: 37.1±4.8; CdEWH: 40.7±2.7#, % dAUC) and the reduction of expression of COX-2 in aorta. EWH prevents to increased of reactive species level (ROS level: Untreated: 47.8±3.1; Cd: 81.1±5.6*; EWH: 36.2±5.6; CdEWH: 54.8±3.2#, FU) and induce reduction of lipid peroxidation (TBARS: Untreated: 11.5 ± 1.0; Cd: 20.4 ± 2.6* ; EWH: 6.3±2.2; CdEWH: 14.8±0.8#, nmol MDA/mL) in aorta of rats Cd-exposed. We also observed that co-treatment with EWH prevents increased COX-2 (Untreated: 38.9±3.9; Cd: 98.9±9.8 *; EWH: 47.9±5.0; CdEWH: 62.6±4.2#, AU) and increased of the superoxide anion in situ.

Conclusion:

EWH could be considered as an alternative for the treatment of cardiovascular damage induced by Cd.

Financial support:

Supported by the Brazilian Government (Conselho Nacional de Desenvolvimento Científico e Tecnológico – CNPq 307399/2017-6; CAPES; PROBIC FAPERGS/UNIPAMPA and by the Spanish Government [MINECO - AGL2017-89213-R and SAF2015-69294-R].

FeSBE Annual Meeting 2019

Poster Sessions and Abstracts

04.015 - EVALUATION OF TRANSCRIPTION FACTORS FOR MITOCHONDRIAL BIOGENESIS IN THE HEART OF FEMALE RATS SUBMITTED TO A LOW-PROTEIN DIET FOR TWO GENERATIONS. Lemos MDTB, Bernardo EM, Lima FAS, Pedroza AAS, Braz GRF, Silva SCA, Lagranha CJ, - Biochemistry and Physiology - UFPE Neuropsychiatry and Behavior Science - UFPE Laboratory of Biochemistry and Exercise Biochemistry - UFPE

Introduction:

According to the World Health Organization, by 2030, almost 23.6 million people will die from cardiovascular diseases (CVD). Nutritional insults during early life affects maternal mitochondria and changes could be expected to extend into the next generation since females are responsible for the passage of mitochondrial DNA to the offspring. However, there is a lack in literature concerning the second generation effects of a maternal low-protein diet on cardiac and mitochondrial biogenesis in young female rats.

Aim:

To evaluate the effects of a maternal protein restriction on transcription factors for mitochondrial biogenesis in the heart of second generation female rats

Methods:

The present study followed the recommendations of the Brazilian Ethics Committee for Animal experimentations and has been approved for Local Ethics Committee of Federal University of Pernambuco (protocol nº: 0026/2017). Pregnant Wistar rats (n=8) were divided into two experimental groups according to the diet: Normoprotein (NP, 17% casein) and Low-protein (LP, 8% casein). The diet was maintained during gestation and lactation. At 30 days of age, part of the offspring were euthanized and the heart collected for the molecular analyzes, animals F1 (first generation), and the other half received commercial chow until 80 days of age. At this age, rats were mated to the second generation (F2) according to the diet: Re-exposed - LP (F2) and not re-exposed (fed with commercial chow, Labina - F2L). Female pups constituted the F2 generation, and at 30 days of age cardiac tissue was collected to RT-PCR analysis: AMP-activated protein kinase (AMPK), Peroxisome proliferator-activated receptor gamma coactivator 1-alpha (PGC-1 α) and Mitochondrial transcription factor A (TFAM). Data were expressed as Mean \pm SEM and compared using two-way ANOVA with GraphPad Prism 6.0 software; significance was kept in 5% ($p < 0.05$) for all analysis.

Results:

Our data showed a decrease in gene expression of AMPK in F1-LP (F1-NP=1 \pm 0.04; n=6 and F1-LP=0.35 \pm 0.026; n= 5; $p < 0.0001$) and in F2L-LP compared with F1-LP (F1-LP=0.35 \pm 0.026; n= 5 and F2L-LP= 0.04 \pm 0.017; n= 5; $p < 0.0001$). The PGC-1 α expression increased in the F1-LP generation compared with control group (F1-NP= 1 \pm 0.5; n=6 and F1-LP=4.6 \pm 0.6, n= 6; $p < 0.0001$) and decrease in F2 with re-exposition of diet (F2-NP= 11.45 \pm 0.5; n= 6 and F2-LP= 9 \pm 0.5, n= 6; $p = 0.026$). The TFAM expression did not differ among groups

Conclusion:

Our results suggest that the nutritional insult during two generations did not affect cardiac tissue of young female rats. We believe that the presence of estrogen promotes protection in female rats by positive modulation in the gene expression of mitochondrial biogenesis.

Financial support:

FACEPE and CNPq

04.016 - CAN INDOXYL SULFATE, AN UREMIC TOXIN, LEAD TO CARDIAC HYPERTROPHY AS WELL AS THE ISCHEMIA-REPERFUSION LESION DOES?. Fogaça F, Carneiro-Ramos MS, - Centro de Ciências Naturais e Humanas - UFABC

Introduction:

The cardiorenal syndrome is described as a systemic inflammatory status in which different clinical conditions promote cardio and renal disfunctions. It is known that the renal chronic disease (RCD) and the

renal insufficiency (RI) and its inflammatory components can lead to damage in the heart tissue. One of the possible paths that may worsen the cardiac condition is the risen levels of uremic toxins, such as Indoxyl Sulfate (IS) that is a common toxin in patients going through dialysis. Previous studies have shown that IS has a hypertrophic role in cardiomyocytes cell culture by the activation of the MAPKs (Mitogen-Activated Protein Kinases) and NF κ B (Nuclear factor kappa-B) pathways. Our hypothesis is that we can mimic an acute kidney injury without the ischemia-reperfusion surgery commonly used by our group.

Aim:

The objective of this research is to investigate the role of Indoxyl Sulfate in the development of the cardiorenal syndrome.

Methods:

Indoxyl sulfate (Sigma-Aldrich) of 100 mg/kg/day was intraperitoneally injected to 12-week old C57BL/6 mice every day for seven days. Control animals were injected with the same volume of vehicle (saline 0,9%). After seven days of the last injection, the animals went through euthanasia, the blood was taken for post analyses and the heart, kidneys, and tibia harvested. During the days of experiment, food and water intake and their weight were measured and recorded daily.

Results:

The groups (Vh and IS) showed no differences in neither water nor food intake, the weight was also preserved in the groups. Kidney weight/body weight ratio didn't change after IS treatment. However, heart weight/tibia length ratio was ~17% higher in the IS treated group than the vehicle group ($p < 0,05$).

Conclusion:

: In summary, IS is showing to be an important target to be studied as a regulation factor for the development of cardiac hypertrophy after acute kidney injury. Our results indicate that IS may have an important role in the development of cardiac hypertrophy and it may be used as a model that imitates the acute kidney injury in a less invasive way than the ischemia and reperfusion surgery.

Financial support:

FAPESP 2015/19107-5

04.017 - PERIVASCULAR ADIPOSE TISSUE AGGRAVATES SEPSIS-INDUCED VASOPLEGIA: ROLE OF NO AND PROSTACYCLIN. Awata WMC, Gonzaga NA, Borges VF, Cunha FQ, Cárnio EC, Tirapelli CRT, - Farmacologia - Universidade de São Paulo - USP Fisiologia - Universidade de São Paulo - USP

Introduction:

Sepsis induces vascular hyporesponsiveness to vasoconstrictile agents. Perivascular adipose tissue (PVAT) displays anti-contractile action in various blood vessels. However, little is known about the effects of sepsis in the modulatory action of PVAT.

Aim:

Evaluate the effect of experimental (lethal) sepsis in the modulatory action that PVAT on the vascular tone and the possible mechanisms underlying such response.

Methods:

Male Wistar rats (250-300 g) were randomized in 2 groups: 1) Sham: the cecum was exteriorized without ligation and puncture; 2) CLP: lethal sepsis was induced using the cecal ligation and puncture (CLP) model. The thoracic aorta with or without PVAT (PVAT+ and PVAT-, respectively) was isolated 6 h after CLP surgery for functional and biochemical assays. Concentration-response curves for phenylephrine were obtained. In the absence or after incubation (30min) with one of the following drugs: L-NAME (non-selective inhibitor of NOS), carboxy-PTIO (NO scavenger), 1400W (selective inhibitor of iNOS), 7-nitroindazole (7-NI, selective nNOS inhibitor), ODQ (guanylyl cyclase inhibitor), tiron (superoxide anion scavenger), catalase (enzyme that decomposes H₂O₂), apamin (low conductance Ca²⁺-activated K⁺ channel inhibitor), charybdotoxin (high conductance Ca²⁺-activated K⁺ channel inhibitor), 4-aminopyridine (voltage-sensitive K⁺ channel

FeSBE Annual Meeting 2019

Poster Sessions and Abstracts

inhibitor), glibenclamide (ATP-sensitive K⁺ channel inhibitor), indomethacin (non-selective COX inhibitor) or RO1138452 (selective prostacyclin IP receptor antagonist). [CEUA #2017.5.86.22.9]. Two-way ANOVA followed by Bonferroni test ($p < 0.05$) was used to compare the results.

Results:

In PVAT- aortas sepsis decreased the contraction (in mN) induced by phenylephrine, when compared to sham. In PVAT aortas CLP induced a more pronounced reduction of phenylephrine-induced contraction (PVAT-: Sham: 10.6 ± 0.1 , $n=10$; CLP: $7.8 \pm 0.4^*$, $n=9$; PVAT+: Sham: 7.6 ± 0.3 , $n=10$; CLP: $3.8 \pm 0.5^*$, $n=12$). The increased anti-contractile effect of PVAT in the septic condition involves the participation of NO since this response was not found in arteries after incubation with L-NAME (14.9 ± 1.1 , $n=7$), carboxy-PTIO (15.6 ± 1.1 , $n=14$), 7-NI (8.1 ± 1.1 , $n=7$) and 1400W (10.8 ± 0.6 , $n=6$). Similar results were found in the presence of ODQ (9.9 ± 1.0 , $n=9$) and apamin (6.2 ± 0.6 , $n=5$). Besides that indomethacin (6.7 ± 0.7 , $n=13$) and Ro1138452 (6.3 ± 0.3 , $n=5$) reversed the hypocontractility mediated by PVAT in aortas from CLP rats. Tiron, catalase, 4-aminopyridine, charybdotoxin and glibenclamide did not alter phenylephrine-induced contraction in the CLP group. Increased generation of O₂^{•-} (RLU/mg protein) was detected in PVAT from CLP rats ($672.1 \pm 65^*$, $n=6$), when compared to PVAT of the Sham group (447.3 ± 41 , $n=7$). Conversely, CLP did not affect the concentration of H₂O₂ in PVAT. Increased prostaglandin (PG) I₂ levels were detected in PVAT from CLP rats ($27.7 \pm 7.2^*$, $n=7$), when compared to PVAT of the Sham group (11.4 ± 3.8 , $n=6$), but no alteration in PGE₂ levels was found. In situ quantification of O₂^{•-} and nitric oxide (NO) using fluorescent dyes revealed that sepsis increased the levels of both in PVAT.

Conclusion:

Lethal sepsis increases the anti-contractile action of PVAT by a mechanism that involves the activation of the NO-cGMP pathway and the opening of Ca²⁺-dependent K⁺ channel of low conductance. PGI₂ also contribute to the increased anti-contractile effect displayed by PVAT during sepsis.

Financial support:

CAPEs

04.018 - PREVIOUSLY EXERCISE TRAINING IN OVARECTOMIZED RATS SUBMITTED TO MYOCARDIAL INFARCTION DECREASES THE LEVELS OF DIMETHYLAMINE IN THE LEFT VENTRICLE. Ruberti OM, Viana LR, Marcondes MCG, Delbin MA, Rodrigues B, - Biologia Estrutural e Funcional - Unicamp

Introduction:

Dimethylarginines are known to be the result of the degradation of methylated proteins. Asymmetric dimethylarginine (ADMA) is metabolized via hydrolytic degradation in citrulline and dimethylamine by the enzyme dimethylarginine dimethylaminohydrolase (DDAH). The activity or expression of this enzyme may contribute to the pathogenesis of endothelial dysfunction, suggesting that this component is a cardiovascular risk marker.

Aim:

The aim of this study is to evaluate the impact of aerobic physical training (AT) performed prior to myocardial infarction on the expression of dimethylamine in rats submitted to ovariectomy.

Methods:

Female Wistar rats were ovariectomized and divided into four randomized groups: sedentary sham (SS), sedentary + MI (SI), AT + sham (TS), AT + myocardial infarction (TI). Exercise training was performed on a treadmill (60 to 75% of the maximum running speed) in ovariectomized rats before the MI. The maximal exercise test (MET) data were presented at the moments: pre (before aerobic training protocol), post (after aerobic training protocol) and final (after IM or SHAM surgery).

Results:

After 8 weeks of AT, the MET was increased at the post moment (2.40 ± 0.09) compared to the pre moment (1.44 ± 0.09) and decreased MET at the final moment (1.21 ± 0.09) compared to the post moment (2.40 ± 0.09) in TI group. Dimethylamine was significantly increased in the SI group (0.028 ± 0.007) compared to the SS group (0.007 ± 0.001) and decreased in the TS (0.003 ± 0.001) and TI (0.004 ± 0.000) groups in relation to the SI group.

Conclusion:

These results suggest that aerobic physical training may have a protective effect on cardiovascular diseases such as MI.

Financial support:

Capes, CNPq e FAPESP

04.019 - ETHANOL WITHDRAWAL INDUCES CARDIAC OXIDATIVE STRESS THROUGH AT₁-DEPENDENT MECHANISMS. Assis VO, Gonzaga NA, Pereira LC, Brigagão C, Tirapelli CR, - Departamento de Farmacologia - USP

Introduction:

The abrupt interruption of ethanol consumption in heavy drinkers lead to cardiovascular, physiological and behavioral changes that are collectively known as Ethanol Withdrawal Syndrome. We have shown that ethanol withdrawal (EW) induces activation of the rennin-angiotensin system (RAS) with further increase in blood pressure and vascular oxidative stress. These responses were prevented by losartan, a selective antagonist of AT₁ receptors. The molecular mechanisms underlying the cardiac effects of EW are not well defined. Understanding that ethanol withdrawal increases the circulating levels of angiotensin II and that this peptide may increase cardiac oxidative stress under distinctive circumstances, we hypothesized that EW would induce deleterious effects in the heart via angiotensin II/AT₁ receptors.

Aim:

To investigate a possible role for angiotensin II/AT₁ receptors in the cardiac effects induced by EW.

Methods:

Male Wistar rats (250g) were divided in 6 groups: Control: animals received water ad libitum for 21 days and daily gavage (DG) of vehicle (CV) or losartan (LST-10mg/kg/day - CL); Ethanol: animals were treated with ethanol 9% (v/v) for 21 days and DG of vehicle (EV) or LST (EL); Ethanol Withdrawal: animals were treated in the same way that ethanol group for 21 days and after that ethanol was removed and the animals received water ad libitum until the 23rd day. During EW period (48h) rats received DG of vehicle (EWW) or LST (EWL). At the end of the treatment, blood and cardiac tissue (left ventricle) were collected for biochemical analysis. The activity of creatine kinase-MB (CK-MB) was measured by colorimetric assay, while the levels of superoxide anion (O₂⁻) were detected by chemiluminescence of lucigenin. The expression of the following proteins was detected by Western Immunoblotting: eNOS, ECA, AT₁ and AT₂ receptors, Nox1, Nox2 and Nox4, SOD1, SOD2 and SOD3. The activity of catalase was determined by spectrophotometry and SOD activity was determined by a commercially available kit. Two-way ANOVA followed by Bonferroni was used to compare the results. $P < 0.05$ was considered as significant.

Results:

EW did not affect serum activity of CK-MB. On the other hand, EW increased O₂⁻ generation in the left ventricle (RLU/mg protein; $n=8$) (CV= 77 ± 4 ; CL= 66 ± 4 ; EV= 78 ± 4 ; EL= 71 ± 5 ; EWW= $108 \pm 5^*$; EWL= 69 ± 5) and losartan prevented this response. Neither ethanol nor losartan affected the expression of eNOS, ECA, AT₁ and AT₂ receptors, Nox1, Nox2 and Nox4, SOD1, SOD2 and SOD3. EW increased catalase activity in the left ventricle (U/mg protein; $n=4-7$) (CV= 12 ± 1 ; CL= 20 ± 3 ; EV= 16 ± 2 ; EL= 20 ± 2 ; EWW= $25 \pm 1^*$; EWL= 19 ± 1) and losartan prevented this response. EW did not affect SOD activity in the left ventricle.

Conclusion:

EW increases cardiac oxidative stress via AT₁ receptor activation.

Financial support:

CNPq and FAPESP

FeSBE Annual Meeting 2019

Poster Sessions and Abstracts

6 - Endocrine System

06.007 - EFFECTS OF OBESITY INDUCED BY HYPERCALORIC DIET AND ITS TREATMENT WITH EXENATIDE ON THE MUSCARINIC CHOLINERGIC NEUROTRANSMITTER IN THE RAT HIPPOCAMPUS.. Silva MFP, Alves PL, Vendrame RFA, Silveira PF, Abdalla FMF, - Farmacologia - IBU

Introduction:

Molecular cloning studies have revealed the existence of five distinct muscarinic acetylcholine receptor (mAChRs) subtypes (M1 to M5), which interact, via a G protein-regulated process, with multiple effector systems. The M1, M3 and M5 subtype couple primarily to PLC-mediated phosphoinositide hydrolysis. In the hippocampus, the modulation of excitatory transmission by mAChRs seems particularly relevant to learning and memory processing. Experimental studies has been shown that obesity-associated with hypercaloric diet impair learning and memory in rodents, suggesting a strong association between obesity and cognitive dysfunction. However, the mechanisms are not understood fully.

Aim:

The aim of this study was to investigate the possible effects of obesity induced by hypercaloric diet and its treatment with exenatide, an antiobesogenic drug derived from *Heloderma suspectum* venom, on the affinity, density, subtypes and intracellular signaling pathways linked to activation of mAChRs in rat hippocampus.

Methods:

Male Wistar rats were divided into three groups: control (CT), obese induced by hypercaloric diet (DIO) and DIO treated with exenatide (DIO+E). The experimental procedures were approved by the Research Ethics Committee of the Butantan Institute (# 22381003/17). In the hippocampus obtained from animals CT, DIO and DIO+E were performed: I- [3H]QNB binding to determine the affinity (KD) and density (Bmax) of mAChRs; II- Expression of each mAChR subtype (M1 to M5) by immunoprecipitation assays and III- Determination of [3H]inositol phosphates accumulation.

Results:

Specific binding analysis showed that the affinity did not differ among CT, DIO and DIO+E. In contrast, the density of mAChRs obtained in DIO animals (62.2 ± 12.1 , n=4) was lower than that obtained from CT rats (184.8 ± 12.4 , n=3). The density of mAChRs from DIO+E (194.0 ± 21.4 fmol/mg protein, n=3) was similar when compared with CT rats (P<0.05). Immunoprecipitation assays induced a decrease in the expression of M1 and M3 subtypes of DIO animals (0.6 ± 0.2 , n=7 and 0.2 ± 0.1 fmol/mg protein, n=7) when compared to respectively CT (8.9 ± 0.7 , n=6 and 2.8 ± 0.9 fmol/mg protein, n=8). Treatment with exenatide (DIO+E) recovered the expression of the two subtypes (4.5 ± 0.2 , n=3 and 2.2 ± 0.5 fmol/mg protein, n=3, respectively M1 and M3), similar to CT. (P<0.05). On the other hand, the M2, M4 and M5 subtypes did not differ among CT, DIO and DIO+E. Carbachol caused a concentration-dependent increase in the accumulation of [3H]inositol phosphates in the 3 experimental groups. The magnitude of the maximal response to carbachol was lower in DIO group (7.6 ± 4.9 , n=5) when compared to the CT and DIO+E animals (respectively 28.9 ± 4.9 , n=5 and $25.3 \pm 8.1\%$ above basal, n=5), which did not differ from each other (P<0.05).

Conclusion:

Our results indicate that obesity induced by hypercaloric diet strongly influences the expression and intracellular signaling coupled to M1-M3 subtypes. The exenatide reversed these effects, suggesting an important role on hippocampal muscarinic cholinergic system. This action of obesity might be a key step mediating cellular events important for learning and memory.

Financial support:

FAPESP AND CAPES

06.008 - INFLUÊNCIA DO EXERCÍCIO FÍSICO NAS REAÇÕES DE OXIDAÇÃO E REDUÇÃO NO SANGUE DE MULHERES OBESAS. Nascimento C, Peixoto MS, Boa LFF, Faria CC, Costaa TSF, Ferreira ACF, Carvalho DP, Fortunato RS, - Laboratório de Fisiologia e Sinalização Redox - UFRJ

Introduction:

Oxidative stress is involved in the pathophysiology of obesity, which can lead to damage in biomolecules. Physical exercise is a non-pharmacological strategy for the prevention and treatment of this disease, but its effects on redox homeostasis and DNA damage in obese individuals are conflicting.

Aim:

Thus, the aim of the present study was to determine the effect of 16 weeks of combined physical exercise on oxidative stress biomarkers and DNA damage of obese women. 18 obese women performed a combined physical training program (resistive and aerobic training), 3 times per week, for 16 weeks.

Methods:

Body weight, body mass index (BMI), body fat percentage, fat free mass, waist circumference, glycemia, glycated hemoglobin, LDL, HDL and total lipids, as well as serum levels of TSH, T3, free T4 and leptin were evaluated. We also measured the serum superoxide dismutase (SOD) activity, plasma 8-isoprostane levels, as well as DNA and chromosomal damage.

Results:

We observed significant reductions in the anthropometric variables comparing pre and post-training: body weight (p <0.001), BMI (p <0.001), fat percentage (p <0.05) and waist circumference (p <0.001). In addition, we observed a significant increase in HDL (p <0.01). Plasma levels of 8-isoprostane (p <0.05) and DNA damage (p <0.01), as assessed by the comet test, increased after physical training without significant changes in chromosomal damage.

Conclusion:

Thus, despite having positive effects related to body composition, this type of exercise should be prescribed with caution to obese women, due to its effects on redox homeostasis and DNA damage.

Financial support:

FAPERJ

06.009 - MIFEPRISTONE ACTIONS ON GLUCOSE HOMEOSTASIS AND HEPATIC ESTEATOSIS IN MSG OBESITY. Rocha LA, Junior JAS, Oliveira KM, Araújo TR, Ribeiro RA, - RJ - UFRJ

Introduction:

Hypothalamic obesity induced by neonatal monosodium glutamate (MSG) treatment in rodents induces hypercorticosteronemia which contributes to insulin resistance and hepatic steatosis.

Aim:

Evaluate whether mifepristone (MIF) treatment, a glucocorticoid (GR)-II receptor antagonist, could improve glucose homeostasis and hepatic steatosis in obese MSG mice.

Methods:

Male Swiss mice received MSG [4 g / kg body weight (PC)] subcutaneously (sc) during the first five days of life. At 30 or 60 days of age, MSG mice were treated daily with MIF 80 mg /kg BW [MIF30 group or MIF60, respectively] or vehicle [5% DMSO in corn oil without tocopherol; groups MSG30 and MSG60, respectively] for 30 days. Treatment with MIF or vehicle were also performed on MSG mice at 90 days [MIF90 and MSG90 groups, respectively], for 15 days. After the treatment, glucose (ipGTT) and glucagon tolerance tests (ipGluTT) were performed. After euthanasia, fat pads and liver were collected for adiposity and steatosis evaluation, respectively. Data were analyzed by Shapiro-Wilk normality test followed by Student t test or Mann-Whitney test (P < 0.05; CEUA UFRJ-Macaé approval: MAC054).

Results:

At the end of the treatments, MIF30 and MIF90 mice presented total glycemia during ipGTT (18895 ± 1764 and 20837 ± 2505 mg/dL.min-1)

FeSBE Annual Meeting 2019

Poster Sessions and Abstracts

and total hepatic glucose output in response to glucagon (4018 ± 1313 and 5793 ± 1030 mg/dL.min⁻¹) similar to MSG30 (16783 ± 2989 and 4967 ± 1230 mg/dL.min⁻¹) and MSG90 (26316 ± 2715 and 4677 ± 904 mg/dL.min⁻¹), respectively. But, MIF60 mice exhibited lower glycemia at 60 min (270 ± 21 mg/dL) and in the total glycemia during the ipGTT (16771 ± 1307 mg/dL.min⁻¹), when compared with MSG60 (479 ± 37 mg/dL and 33275 ± 4848 mg/dL.min⁻¹, respectively). However, the hepatic glucose production in MIF60 mice (7296 ± 896 mg/dL.min⁻¹) was similar to MSG60 (6836 ± 1007 mg/dL.min⁻¹). In addition, all MIF and MSG mice groups exhibited similar brown adipose tissue (MIF30: 6 ± 1 , MIF60: 8 ± 1 , MIF90: 8 ± 1 mg/g PC versus MSG30: 4 ± 1 , MSG60: 9 ± 3 , MSG90: 8 ± 2 mg/g PC, respectively) and epididymal fat pad weights (MIF30: 33 ± 3 , MIF60: 44 ± 3 , MIF90: 41 ± 12 mg/g PC and versus MSG30: 4 ± 1 , MSG60: $36 \pm 4.30 \pm 4$ mg/g PC, respectively). Regarding liver steatosis, the majority of MIF60 and MIF90 mice (80%) displayed mild steatosis (grade 1), while MSG60 and MSG 90 mice showed moderate hepatic steatosis (grade 2).

Conclusion:

MIF treatment improved glucose tolerance when administered from 60 days of age in MSG mice, but hepatic steatosis may be ameliorated if MIF treatment was started at 60 or 90 days of age in these rodents.

Financial support:

FAPERJ and CAPES

06.010 - BISPHENOL-A CONSUMPTION IMPAIRS ENDOCRINE PANCREAS PROLIFERATION IN MENOPAUSAL FEMALE MICE THAT FED ON A HIGH-FAT DIET. Oliveira KM, Figueiredo LS, Araújo TR, Freitas IN, Silva JN, Carneiro EM, RIBEIRO RA, - Laboratório de Fisiopatologia - UFRJ-MACAÉ Obesity and Comorbidities Research Center - UNICAMP

Introduction:

Bisphenol-A (BPA) is a constituent of several utensils and food packing, but some studies indicate that it has estrogenic, antiestrogenic and antiandrogenic actions that can impair glucose metabolism.

Aim:

Herein, we evaluated the effects of BPA consumption on glucose homeostasis and endocrine pancreatic morphofunction in ovariectomized (OVX) mice that fed on a high-fat diet (HFD).

Methods:

Menopause was induced in adult Swiss female mice through ovariectomy and after 14 days the females in anestrus were submitted or not to HFD or normolipid diet (CTL group), associated or not with 1 µg/mL BPA in their drinking water (HBPA or CBPA groups) for 3 months. Data were analyzed by Kolmogorov-Smirnov normality distribution test and compared using parametric (ANOVA followed by Newman-Keuls) or non-parametric tests (Kruskal-Wallis followed by Dunns; $P < 0.05$).

Results:

HFD females displayed higher body weight (BW; 58.7 ± 1.9 g) and increased mesenteric (40.4 ± 2.1 mg/g BW) and parametrial fat pads (45.8 ± 4.1 mg/g BW), when compared to CTL (46.2 ± 1.3 g, 19.6 ± 1.6 and 33.1 ± 2.6 mg/g BW, respectively). These obesity parameters in HBPA females (63.2 ± 1.2 g, 40.2 ± 4.4 and 45.6 ± 3.4 mg/g BW) were similar to HFD. In addition, HFD female were hyperglycemic (101.4 ± 5.5 mg/dL), hyperinsulinemic (0.7 ± 0.1 ng/mL), insulin resistant (HOMA-IR= 3.8 ± 0.7) and glucose intolerant (34366 ± 3077 mg/dL.min⁻¹), in comparison with CTL (82.9 ± 4.9 mg/dL, 0.1 ± 0.1 ng/mL, 22016 ± 1632 mg/dL.min⁻¹ and HOMA-IR= 0.5 ± 0.02 , respectively). These glucose homeostasis parameters in HBPA (105.8 ± 4.9 mg/dL, 32544 ± 2362 mg/dL.min⁻¹, 0.7 ± 0.2 ng/mL and HOMA-IR= 5.7 ± 1.3) did not differ from HFD. Isolated islets from HFD group hypersecreted insulin at 11.1 and 22.2 mM glucose (2.6 ± 0.3 and 4.6 ± 0.6 ng/islet.h), when compared to CTL (1.2 ± 0.2 and 2.4 ± 0.3 ng/islet.h). At these conditions the insulin released by HBPA islets was similar to HFD (2.7 ± 0.2 and 3.8 ± 0.6 ng/islet.h). HFD and CTL pancreases exhibited similar islet (9410 ± 814 and 9689 ± 899 µm², respectively) β- (7641 ± 695 and 8137 ± 801 µm²) and non-β cell (1759 ± 143.5 and 1436 ± 114.8 µm²) areas.

However, HBPA pancreases had higher islet (16002 ± 1282 µm²), β- (13559 ± 1137 µm²) and non-β cell (2707 ± 189 µm²) areas, than HFD. HFD regimen induced islet proliferation since the ratio of islet-cells immunolabeled for Ki67 was 126% higher. But, HFD regimen associated with BPA intake reduced Ki67 immunolabeled cells in HBPA islets, when compared to HFD. HFD islets displayed an enhancement of 137% in glucagon mRNA expression, in comparison with CTL islets. However, HBPA islets exhibited reductions of 66% and 68% in pancreatic and duodenal homeobox 1 (PDX)-1 and Neurogenin-3 (Ngn)-3 mRNAs, respectively, but an increase of 95% in tumor necrosis factor (TNF)-α gene expression, when compared to HFD islets

Conclusion:

BPA consumption associated with HFD regimen induced endocrine pancreatic tissue hypertrophy and impairs islet-cell proliferation in OVX mice. These effects are probably linked with reductions in the transcript factors, PDX-1 and Ngn-3, and in part due to augmentation of the pro-inflammatory gene, TNF-α, in HBPA islets.

Financial support:

FAPERJ and CAPES

06.011 - EFFECTS OF COMBINED ORAL CONTRACEPTIVE CONTINUOUS ADMINISTRATION UPON ADIPOSITY, GLUCOSE TOLERANCE AND HEPATIC STEATOSIS IN FEMALE MICE THAT FED ON A HIGH-FAT DIET. Chaves JO, Aguiar GS, Silva SC, Junior JAS, Figueiredo LS, Santos JJ, Blanc HNH, Ribeiro RA, - Laboratório de fisiopatologia - Universidade Federal do Rio de Janeiro

Introduction:

Hormonal contraceptives are widely used by women to prevent pregnancy, but its continuous use can impair glucose homeostasis, hepatic function and lipid metabolism.

Aim:

Herein, we evaluated the effect of continuous administration of a combined oral contraceptive (ACO) composed by ethinyl estradiol (EE) and drospirenone (DRSP) on obesity development, glucose tolerance and hepatic steatosis in female mice that fed on a high-fat diet (HFD).

Methods:

Adult female Swiss mice consumed a normolipid diet or HFD together with a daily gavage of 0.2 mL of distilled water [vehicle; control (CTL) and CH65 groups, respectively] or a solution containing 0.6 µg EE and 60 µg DRSP during 65 days [combined oral contraceptive (ACO) and AH65 groups, respectively]. After 35 days of treatment half of CTL and ACO females were also submitted to HFD (CH30 and AH30 groups). Data were analyzed by Shapiro-Wilk and compared by parametric (Student's t-test or ANOVA) or non-parametric tests (Mann-Whitney test or the Kruskal-Wallis, $P < 0.05$; CEUA UFRJ-Macaé certificate n.º: MAC039).

Results:

ACO treatment did not change body weight (BW: ACO 32 ± 1 and CTL 33 ± 1 g). HFD increased BW in CH30 (38.6 ± 1.8 g) and CH65 females (41.0 ± 2.1 g), when compared to CTL. But, HFD consumption together with ACO treatment only increased BW in AH30 group (37.3 ± 0.8 g). Furthermore, HFD consumption led to increases of 223% and 247% in periovarian fats and augments of 199% and 195% in mesenteric fats in CH30 and CH65, respectively, in comparison with CTL. Interesting, AH30 females displayed augments of 222%, 225% and 205% in the parametrial, periovarian and mesenteric fat pads, respectively, while AH65 females only increased the periovarian fat store (198%), when compared to ACO. No modifications were observed in glucose tolerance, since the total glycemia during the test in ACO (15223 ± 2618 mg/dL.min⁻¹) was similar to CTL (11390 ± 1623 mg/dL.min⁻¹) females. HFD regimen did not change this parameter in vehicle (CH30 13094 ± 2086 and CH65 15405 ± 2449 mg/dL.min⁻¹) or ACO-treated females (AH30 12942 ± 2618 and AH65 11202 ± 1454 mg/dL.min⁻¹). HFD ingestion increased triglyceride and cholesterol plasma levels only in CH65 (91 ± 9 and 124 ± 18 mg/dL), when compared to CTL (54 ± 4 and

FeSBE Annual Meeting 2019

Poster Sessions and Abstracts

59±11 mg/dL). However, HFD and ACO administration did not change these parameters in AH30 (80±9 and 101±22 mg/dL, respectively) and AH65 groups (71±7 and 101±19 mg/dL), in comparison with ACO (55±6 and 75±15). Despite no alterations in hepatic lipid accumulation were observed between ACO and CTL females, the HFD consumption led to moderate hepatic steatosis in 100% of the CH30 females and severe steatosis in 100% of CH65 females. In contrast, the combination of HFD with ACO seems to prevent/decrease lipid deposition in hepatocytes, since in AH30 group, 50% of the females did not exhibit steatosis and 50% displayed moderate hepatic steatosis. Also, 67% of AH65 females did not have steatosis (grade 0), and the remaining (33%) displayed mild hepatic steatosis.

Conclusion:

Therefore, continuous administration of EE and DRSP, especially when started with the introduction of the HFD regimen, prevented obesity development and modifications in plasma lipid profile, and attenuated hepatic steatosis induced by HFD.

Financial support:

FAPERJ and PIBIC-CNPq-UFRJ.

7 - Nutrition and Metabolism

07.018 - COMBINED EFFECTS OF METFORMIN AND LYCOPENE ON BIOCHEMICAL PARAMETERS AND BIOMARKERS OF OXIDATIVE STRESS IN STREPTOZOTOCIN-DIABETIC RATS. Figueiredo ID, Lima TFO, Inácio MD, Costa MC, Assis RP, Brunetti IL, Baviera AM, - Department of Clinical Analysis - UNESP

Introduction:

Oxidative stress has an important role in the establishment of the complications of diabetes mellitus (DM). Treatment of DM includes insulin and oral antidiabetic agents, with metformin being widely prescribed. However, there is a growing interest in the use of natural bioactive compounds as complementary therapy, because their additive benefits on the effects of classical therapy, and also because their antioxidant potentials. Lycopene appears as an interesting option; studies have shown several benefits of lycopene in combating the symptoms and complications of DM.

Aim:

In the present study, we evaluated the changes in biochemical parameters and biomarkers of oxidative stress in diabetic rats treated with yoghurt enriched with metformin or lycopene, alone or in mixtures.

Methods:

Male Wistar rats (150 ± 10 g) received streptozotocin (40 mg/kg i.v) for induction of DM. The animals were divided into 6 groups (8 rats/group): normal, treated with yoghurt (NYOG); diabetic treated with: yoghurt (DYOG); 4U insulin (DINS); 250 mg/kg metformin (DMET); 45 mg/kg lycopene (DLYC); metformin + lycopene (DLYCMET) for 30 days. Glycemia were monitored weekly; levels of cholesterol, triglycerides and cholesterol-HDL were determined at the beginning (day 0) and in the end (day 30) of the experiment. After 30 days, the activity of the antioxidant enzyme paraoxonase 1 (PON1, plasma), the levels of alanine aminotransferase (ALT, plasma) and protein carbonyls (PCO, plasma and liver), and the activities of superoxide dismutase (SOD, liver) and catalase (CAT, liver) were determined. The results were expressed as mean ± standard error and considered statistically different with $p < 0.05$ (One-Way ANOVA followed by Student-Newman-Keuls).

Results:

At day 0, diabetic rats had glycemia values of approximately 400 mg/dL; at day 30, all treated diabetic rats had decreases in glycemia (DINS = 93.2 ± 12.3, DMET = 399.8 ± 43.8, DLYC = 398.8 ± 36.2, DLYCMET = 263.7 ± 34.2, mg/dL) when compared to DYOG (534.5 ± 29.2 mg/dL); the glycemia reduction in DLYCMET rats was higher than those of the isolated treatments. Treatments with metformin and/or lycopene

reduced the plasma levels of cholesterol and triglycerides; in DLYCMET rats, the cholesterol reduction (44%) was higher than the isolated treatments (DLYC = 30%; DMET = 24%). No treatment improved the cholesterol-HDL. After 30 days, DYOG animals showed decrease in PON1 activity, and all treatments increased the PON1 activity. The ALT levels were increased in plasma of DYOG rats, suggesting hepatocyte damage, and all treatments were able to decrease the ALT levels; the decrease in ALT levels in DLYCMET (67%) was higher than DLYC (56%). Plasma and liver PCO levels were increased in DYOG, and all treatments decreased PCO. In liver of DYOG rats, the activities of SOD and CAT were decreased. Metformin did not improve SOD activity, while metformin+lycopene increased SOD, aggregating antioxidant value to this combined therapy.

Conclusion:

The treatment of diabetic rats with yoghurt enriched with metformin+lycopene improved the glycemic control, dyslipidemia, reduced the biomarkers of oxidative stress, and improved the antioxidant defenses, evidencing the potential of this combination in combating diabetic complications.

Financial support:

FCFAR/UNESP, CAPES, CNPq, FAPESP

07.019 - EFFECTS OF CURCUMIN AND AMINOGLUCANIDINE, ALONE OR COMBINED, IN PHYSIO-METABOLIC MARKERS, GLYCOXIDATIVE STRESS AND NEUTROPHILS FUNCTION IN DIABETES MELLITUS EXPERIMENTAL. Lima TFO, Costa MC, Figueiredo ID, Inácio MD, Assis RP, Baviera AM, Brunetti IL, - Department of Clinical Analysis - UNESP

Introduction:

Combination of compounds with different mechanisms of action to manage diabetes mellitus (DM) and its complications is promising because these compounds can have additive benefits to control the several disturbances observed in the disease, especially of glycoxidative stress. Curcumin incorporated into yoghurt, alone or in mixtures with others compounds, had antidiabetic and antioxidant activities; therefore, its combination with aminoguanidine, a potent inhibitor of advanced glycation end products (AGEs) formation, can promote benefits.

Aim:

This study evaluated the changes in physiological and metabolic markers of glycoxidative stress, and neutrophils function in diabetic rats treated with yoghurt enriched with curcumin and/or aminoguanidine.

Methods:

Male Wistar rats (150 ± 10 g) received streptozotocin (40 mg/kg i.v) for induction of DM. The animals were divided into 6 groups (8 rats/group): normal, treated with yoghurt (NYOG); diabetics treated with: yoghurt (DYOG), 4U insulin (DINS), 90 mg/kg curcumin (DC), 50 mg/kg aminoguanidine (DA) and curcumin+aminoguanidine combination (DCA) for 45 days. Body weight were monitored weekly and glycemia every 15 days. After 45 days, blood levels of glycated haemoglobin (HbA1c) and plasma levels of fructosamine, cholesterol, triglycerides, thiobarbituric acid reactive substances (TBARS), protein carbonyl groups (PCO), AGEs and activity of paraoxonase 1 (PON1) were determined, as well as the activities of phagocyte NADPH oxidase (NOX2) and myeloperoxidase (MPO) in peritoneal neutrophils. The results were expressed as mean ± standard error and considered statistically different with $p < 0.05$ (One-Way ANOVA followed by Student-Newman-Keuls).

Results:

At day 0, diabetic rats presented glycemia values of approximately 400 mg/dL; at day 45, in relation to DYOG (561.3±16.2 mg/dL), DINS presented reduction in glycemia (102.1±9.6 mg/dL), and DC, DA and DCA (473.2±7.7; 504.6±17.4; 479.6±14.2, mg/dL, respectively) presented inhibition of glycaemic levels progression. After 45 days (vs DYOG, 226.9±9 g) treatment with curcumin+aminoguanidine promoted a great body weight gain (269.4±11 g); this profile was similar that of

FeSBE Annual Meeting 2019

Poster Sessions and Abstracts

curcumin (271.9±14 g) and better than that of aminoguanidine (254.1±14 g). Curcumin and/or aminoguanidine treatments reduced HbA1c (DYOG= 18.6±0.28, DC= 15.0±0.58, DA= 17.1±0.30, DCA= 17.0±0.37, %), fructosamine (DYOG= 209.9±18, DC= 168.5±12, DA= 163.6±8, DCA= 172.6±7, µmol/L), cholesterol (DYOG= 70.0±1.8, DC= 60.9±2.2, DA= 61.4±2.7, DCA= 58.3±2.3, mg/dL), triglycerides (DYOG= 215.8±24.7, DC= 148.8±19.0, DA= 137.1±19.1, DCA= 126.0±13.7, mg/dL), TBARS (DYOG= 11.57±0.38, DC= 10.46±0.30, DA= 10.68±0.35, DCA= 9.09±0.27, µmol/L), PCO (DYOG= 0.42±0.02, DC= 0.29±0.03, DA= 0.30±0.02, DCA= 0.33±0.02, nmol/mg protein) and fluorescent AGEs (DYOG= 259.6±50, DC= 112.6±30, DA= 133.6±30, DCA= 156.7±10, UA/mg protein), as well as increased the activity of PON1 (DYOG= 852.8±29, DC= 1244±89, DA= 1224±95, DCA= 1267±81, U/L). DCA rats showed a greater reduction in TBARS levels than the isolated treatments. Curcumin+aminoguanidine treatment was more effective in neutrophil migration (89%) than the curcumin alone (32%) and similar that of aminoguanidine (81%). Neutrophils from DCA rats showed a greater reduction in generation of reactive oxygen species than the isolated treatments: NOX2 activity by lucigenin-dependent chemiluminescence (DCA= 7.99x105±1.28x105, DC= 1.59x106±2.67x105, DA= 1.30x106±1.45x105, integrated light emission) or by cytochrome c reduction (DCA= 1.91x10⁻⁷±3.35x10⁻⁸, DC= 3.23x10⁻⁷±4.73x10⁻⁸, DA= 3.04x10⁻⁷±3.59x10⁻⁸, µmol/min); MPO activity by taurine chloramine generation (DCA= 9.85±0.92, DC= 12.53±1.54, DA= 15.53±1.32, µmol/L) and oxidative burst by luminol-dependent chemiluminescence (DCA= 1.47x107±1.09x106, DC= 1.86x107±1.80x106, DA= 2.15x107±1.73x106, integrated light emission).

Conclusion:

The treatment of diabetic animals with yoghurt enriched with curcumin and aminoguanidine reduced the markers of glycoxidative stress and improved neutrophil function, evidencing the beneficial potential of this combination for diabetic complications.

Financial support:

FCFAR/UNESP, CAPES, CNPq, FAPESP

07.020 - CALORIC RESTRICTION REPROGRAMS LIPID BIOSYNTHESIS-RELATED GENE EXPRESSION IN HYPERTENSIVE RATS FED WITH HIGH FAT DIET. Razo UB, - Graduate program in Biomedical Sciences - FHO

Introduction:

The main causes of obesity and hypertension are related to diet. Therefore, a possible form of treatment is caloric restriction (CR) that acts to reduce oxidative stress by decreasing oxygen consumption and stimulating intracellular signaling pathways regulating glucose, lipid, and protein metabolism.

Aim:

To investigate whether the effects of CR alters the expression of genes involved in lipogenesis and cholesterol biogenesis to improve blood lipid profiles and hypertension in rats fed with high fat diet (HFD).

Methods:

The studies were approved by the Animal Use Ethics Committee (protocol 042/2016). The experiments employed 17 male Wistar rats (weight 180-200g). Hypertension was induced according to the 2-kidney, 1-clip (2K1C) model and the animals were divided into 3 experimental groups: Sham (n=5), fed with normolipid diet ad libitum; OH (n=6), hypertensive, HFD ad libitum for 12 weeks; OHR (n=6), hypertensive, HFD for 8 weeks followed by 40% CR for 4 weeks. The systolic blood pressure (SBP) was measured by tail plethysmography and after the experimental period was performed biochemical assays in the serum and the total RNA was isolated from the liver and cDNA was performed. Semiquantitative analysis of the expression of lipid biosynthesis-related genes were performed by RT-PCR. The data were presented as mean±standard error and the differences between the groups were evaluated using ANOVA followed by the Bonferroni, adopting a significance level of P <0.05.

Results:

In the HOR group, despite the excessive lipid load, the animals consumed less food due to the CR, so body weight (494±12g) was similar to that of the Sham (544±13g) and lower than OH group (624±22g). The SBP (mmHg) was also reduced in the HOR group (169±4) vs OH (232±13), with values similar to those of the Sham group animals (140±5). The total cholesterol (242±33 mg/dL) and LDL-c levels (183±30 mg/dL) were higher in the OHR animals than in the Sham (194±9; 102±9) and OH (185±22; 98±19) groups, respectively. These effects showed that CR down-regulates the LDLr gene (Sham=1.1±0.1, OH=1.1±0.1, OHR=0.7±0.05) and up-regulates of HMG-CoAR (Sham=1.0±0.04, OH=0.7±0.03, OHR=0.9±0.07) and SREBP-2 (Sham=0.9±0.04, OH=0.9±0.07, OHR=1.2±0.05) genes. Caloric restriction decreased the expression of lipogenic genes such as SREBP1-c (0.5±0.1), FAS (0.7±0.1), ACC1 (0.6±0.04) e SCD1 (0.4±0.04) in the OHR rats as compared to Sham (0.9±0.1; 1.1±0.1; 0.9±0.05; 0.7±0.03) and OH (0.9±0.1; 1.1±0.1; 0.8±0.03; 0.6±0.04), respectively. In addition, the gene expression of PPAR γ was higher in the liver of OH animals (1.1±0.04) than in the Sham (0.4±0.05), but was lower in the OHR (0.6±0.1). In contrast, the expression of SREBP-1a, gene that contributes to lipolysis, was higher in OHR animals than in others group (Sham=0.2±0.01, OH= 0.2±0.02, OHR= 0.4±0.03). These data are consistent with biochemical assays that show increase NEFA (Sham=0.3±0.03; OH=0.4±0.05; OHR= 0.6±0.1 mmol/L) and decrease in triglycerides in the OHR group (mg/dL 177±5 vs Sham=301±3 and OH=260±13).

Conclusion:

Caloric Restriction attenuates 2K1C-induced hypertension, reprograms lipogenesis and cholesterol biogenesis-related gene expression, and induces a compensatory phase observed by alterations in blood lipid profiles of rats on a high fat diet.

Financial support:

This research was supported by Fundação Hermínio Ometto/FHO

07.021 - IMPACT OF CARCINOGEN ADMINISTRATION IN FEMALE OFFSPRING WHOSE DAMS WERE SUBMITTED TO DIETARY PROTEIN RESTRICTION. Fonseca ARB, Zapaterini JR, Camargo ACL, Colombelli KT, Junior LAJ, Barbisan LF, - Departamento de Morfologia - UNESP

Introduction:

Breast cancer is the second most common type and its incidence is increasing in women. Epidemiological and experimental studies suggest that nutritional changes during pregnancy and in early life predispose the newborns to several chronic diseases, including breast cancer.

Aim:

Using female Sprague-Dawley rats (a strain susceptible), we investigated the development of the mammary gland and the risk for N-methyl-N-nitrosourea (MNU)-induced mammary tumors in female offspring whose dams were submitted to protein restriction, as well as the time-point of carcinogen administration.

Methods:

Pregnant females were fed a control diet (CD group, 17%) or a low-protein diet (LP group, 6%) from gestational day 1 (GD 1) until the postnatal day (PND) 21. After weaning, all female offspring were fed a control diet until PND 250. At PND 28 or 35, female received a single dose of MNU (25 mg/kg) and 24 hours after carcinogen administration were euthanized (PND 29 or 36). Abdominal mammary glands were removed for developmental analysis (whole mount), cell proliferation (Ki-67 marker) and apoptosis (cell morphology). After MNU administration, females were followed for body weight evolution and the appearance of mammary tumors. Latency, incidence and mean number of tumors were analyzed among groups. Mammary gland development, body weight and tumor development data were analyzed by ANOVA or Kruskal-Wallis tests (p<0.05), while the incidence of tumors was evaluated using the Kaplan-Meier test (p<0.05).

Results:

FeSBE Annual Meeting 2019

Poster Sessions and Abstracts

In PND 21, 28 and 35, the mean body weight of LP animals was significantly lower (~55, 44% and 33%) than the control animals in the same time-points ($p < 0.001$). After prepubertal period, this difference was reduced to less than 5% in all MNU-initiated groups. At PND 28, LP group (PND 28) presented a smaller length (~ 17%) and width (~ 56%) of the mammary gland ($p < 0.001$) in relation to the control group. In PND 35, no difference was observed in the length, width, area, perimeter or number of terminal end buds in the mammary glands in both groups. Cell proliferation index did not differ between the groups at PND 29 or 36, while the apoptosis index was higher in the LP group (PND 36) than in the control group ($p < 0.001$). Tumor incidence was significantly higher in the LP initiated at PND 35 than in the control group in same time point ($p = 0.020$). Tumor latency was lower in LP groups than in the control groups (5 weeks).

Conclusion:

The findings indicate that maternal LP did alter early in life body weight gain and favor the process of mammary carcinogenesis when MNU is administered after a catch-up growth of mammary gland development (PND 35), altering the apoptosis response after carcinogen administration.

Financial support:

Supported by CNPq (421307/2016-1) and FAPESP (2018/06067-3; 2018/19432-1).

07.022 - LEAN BODY MASS IS UNRELATED WITH RESTING METABOLIC RATE IN SEDENTARY WOMEN TREATED WITH BREAST CANCER.. Wittee ELC, Mello LS, Tibúrcio JPS, Vasconcelos CMT, Ferreira NF, Filho DMP, Neiva CM, - Departamento de Educação Física - UNESP

Introduction:

Breast cancer is the most common type of cancer among women, representing almost 25% of all diagnoses. Physical conditioning has been touted as a positive contributing factor, capable of reducing pain symptoms, fatigue, mood disorders and sleep disorders, contributing to the patient's comfort. In addition, physical fitness alters the resting metabolic rate (RMR), avoiding excess of body fat, osteopenia, sarcopenia, improving different physical abilities, such as muscle strength and cardiorespiratory fitness, as well as the increased lean body mass.

Aim:

Thus, the present study had as its objective, to investigate the relationship between the variables of the RMR and body composition, with a view to understanding the role of body composition on the function of body systems in a resting state among women undergoing breast cancer rehabilitation.

Methods:

18 sedentary women were selected (50.5 ± 12.69 years; 72.2 ± 12.69 kg; 1.63 ± 0.08 cm), belonging to the N.G.O Breast friends (Amigas do Peito - Bauru-SP). The number of local ethical committee is CAAE : 89092618.9.0000.5398 (UNESP Bauru /SP) All of the participants were submitted to the evaluation of RMR, employing CPET (Quark, COSMED) to obtain the basal daily caloric expenditure ($\text{kcal} \times \text{day}^{-1}$). The protocol consisted of a fasting evaluation of 10 hours, with measurements in the waking position (standing) for 10 minutes and lying in dorsal decubitus for 20 minutes, with the mean value obtained by the weighted average of each procedure. The body composition test was performed by dual-energy X-Ray absorptiometry (DXA-Hologic), obtaining lean body mass (LBM) for the whole body. The data was treated within the normality of Shapiro-Wilk and the multiple linear regression method, which evaluated the relationship between primary variable (RMR and LBM). Significance level adopted at $p \leq 0.05$.

Results:

The results expressed that RMR (1692.70 ± 299 $\text{kcal} \times \text{day}^{-1}$; 95%CI: 1436 – 1692 $\text{kcal} \times \text{Day}^{-1}$) was poorly associated with the variable LBM (31171 ± 11251 , 26 kg;) The level of association presented between RMR and LBM was ($r = 0.38$ $p = 0.05$), revealing that lean mass influence

was not important, being LBM a variable that is known for increasing RMR, proving in sedentary women the opposite. The deterministic power was ($R^2_{aj} = 0.489$, $p = 0.05$ and $EPE = 214,233$ $\text{kcal} \times \text{Day}^{-1}$) concluding that breast cancer treated women LBM was not able to predict RMR once the level of physical activity is almost zero and there is a prevalence of sedentarism.

Conclusion:

Thus, we can admit the RMR of sedentary women does not seem to relate to the lean body mass, probably for presenting a low rate of O₂ consumption. Such findings underscore the importance of the inclusion of physical conditioning program in women undergoing breast cancer rehabilitation.

Financial support:

CNPq

07.023 - QUERCETIN REDUCES HEPATIC INFLAMMATION AND REDOX IMBALANCE IN C57BL/6 MICE EXPOSED TO CIGARETTE SMOKE. Rocha DFA, Júnior PAM, Oliveira MÂDGS, Souza ABF, Castro TF, Araújo NPS, Matos NA, Bezerra FS, Cangussú SD, - Departamento de Ciências Biológicas - UFOP

Introduction:

Liver diseases represent an important focus of attention in view of the multiple functions of the liver in the body. Most avoidable risk factors for the body, such as smoking, are a source of reactive oxygen species and can lead to liver diseases. Studies have shown that quercetin, a natural antioxidant, has been shown to play an important antioxidant and anti-inflammatory role in some liver diseases.

Aim:

This study aimed to evaluate the effects of quercetin administration in C57BL/6 mice exposed to cigarette smoke (CS).

Methods:

The Ethics Committee of the UFOP approved the experiments (Protocol 2015/20). Sixty C57BL/6 mice (8-10 weeks old) were divided in 5 groups ($n=10$): control (CG), quercetin (QG), propylene glycol (PG), cigarette smoke (CSG), quercetin and CS (QCSG), propylene glycol and CS (PCSG). Animals from CG, QG, and PG were exposed to ambient air while CSG, QCSG, and PCSG were exposed to CS to 12 commercial cigarettes a day for sixty days, in an inhalation chamber. QG and QCSG received by orogastric gavage 10 mg/kg/day diluted in 200 μL of propylene glycol. PG and PCSG received by orogastric gavage 200 μL of propylene glycol. Twenty-four hours after, the animals were euthanized and blood and hepatic tissue samples were removed for morphological, morphometric and biochemical analyzes. Statistical analyses were performed using GraphPad Prism software version 5.00 for Windows 7. Data were expressed as mean \pm SEM and $p < 0.05$ was considered statistically significant.

Results:

There was a greater influx of inflammatory cells (number of cells/field) into the liver of animals exposed to CS (29.43 ± 2.246) compared to the other groups (CG: 16.51 ± 0.11 ; QG: 16.83 ± 0.49 ; PG: 18.39 ± 0.42 ; QCSG: 14.82 ± 0.52). Biochemical parameters revealed an increase in the activity of superoxide dismutase (SOD) (U/mg PTN) in CSG (115.4 ± 5.85) compared to CG (90.74 ± 4.73), QG (93.26 ± 5.43), PG (88.01 ± 5.00) and QCSG (81.42 ± 5.36). Catalase activity (CAT) (U/mg PTN) was higher in the CG (0.29 ± 0.03) when compared to the CSG (0.13 ± 0.03) and when compared to the QCSG (0.145 ± 0.02). The group exposed to CS showed a lower ratio (0.34; 0.41; 1.41) between reduced and oxidized glutathione (GSH/GSSG) compared to QG (5.25; 6.06; 9.04), QCSG (3.19; 6.61; 10.64). The levels of lipid peroxidation (nmol/mg PTN) were higher in CSG (2.07 ± 0.50) compared to CG (0.34 ± 0.02), QG (0.32 ± 0.03), PG (0.25 ± 0.02) and QCSG (0.28 ± 0.04). Protein oxidation (nmol/mg PTN) was higher in CSG (17.64 ± 0.83) compared to the other groups (QG: 12.27 ± 1.35 ; PG: 10.55 ± 1.17 ; QCSG: 11.37 ± 1.13 ; PCSG: 13.08 ± 0.74).

Conclusion:

FeSBE Annual Meeting 2019

Poster Sessions and Abstracts

Our data indicate that exposure to cigarette smoke generates an influx of inflammatory cells into the hepatic parenchyma and promotes damage and oxidative stress. On the other hand, the administration of quercetin led to a decrease in cellular influx and promoted an improvement in damage and oxidative stress generated by cigarette smoke exposure.

Financial support:

CNPq, CAPES, FAPEMIG and UFOP

07.024 - EFFECTS OF N-BUTANOL FRACTION OF SIOLMATRA BRASILIENSIS (COGN.) BAILL ON GLYCOXIDATIVE CHANGES IN AN IN VITRO MODEL SYSTEM OF PROTEIN GLYCATION. Kaga AK, Talpo TC, Motta BP, Inácio MD, Lima TFO, Santos CHC, Carvalho MG, Brunetti IL, Baviera AM, - Department of Clinical Analysis - UNESP Department of Chemistry - UFRRJ

Introduction:

Chronic hyperglycemia in diabetes mellitus accounts for the development of diabetic complications; both the protein glycation and the increased formation of advanced glycation end-products (AGEs) play important role. In this sense, it is important the search for natural preparations having potential to prevent and/or to attenuate the various disturbances observed in diabetes mellitus, allowing the advances in the prospection of phytochemicals as new candidates for complementary therapies or dietary supplementations for diabetic complications. Recently, using an in vitro model system of protein glycation, we observed that both the hydroethanolic extract and the ethyl acetate fraction of *Siolmatra brasiliensis* (Cogn.) Baill stems inhibited the formation of fluorescent AGEs, the oxidation of tyrosine and tryptophan amino acid residues, and the protein crosslinking formation (dos Santos, *Fitoterapia*, 133: 109-119, 2019).

Aim:

The present study was performed to explore the in vitro antiglycation potential of the n-butanol fraction of *Siolmatra brasiliensis* stems.

Methods:

The in vitro model system of protein glycation was performed by the incubation of bovine serum albumin (BSA, 10 mg/mL) in the presence of glucose (Glu, 0.5 M), sodium azide (0.02%) in 0.1 M phosphate buffer (pH 7.4), at 37°C for 30 days. Incubations were made in the absence or presence of n-butanol fraction of *Siolmatra brasiliensis* (n-BFSb, 62.5, 125, 250, 500 µg/mL) or aminoguanidine (AG, 1 mM, anti-AGE agent). After 10, 20 and 30 days of incubation, aliquots were used for the analysis of fluorescent AGEs (exc 355 nm; em 430 nm). After 30 days, markers of tyrosine [dityrosine (exc 330 nm; em 415 nm)] and tryptophan oxidation [N'-formylkynurenine (exc 325 nm; em 434 nm), kynurenine (exc 365 nm; em 480 nm)] were assessed. The results were expressed as mean ± standard error and considered statistically different with p<0.05 (One-Way ANOVA followed by Student-Newman-Keuls).

Results:

n-BFSb, at all tested concentrations, but mainly at 500µg/mL, was able to inhibit the formation of fluorescent AGEs, after 10 (BSA+Glu: 40932±19; 500µg/mL n-BFSb: 15645±425; AG: 15323±501, arbitrary units), 20 (BSA+Glu: 62868±803; 500µg/mL n-BFSb: 23976±239; AG: 24315±365, arbitrary units) and 30 days (BSA+Glu: 72313±630; 500µg/mL n-BFSb: 29271±87; AG: 25317±442, arbitrary units). In comparison with BSA alone, BSA+Glu showed increased levels of dityrosine, N'-formylkynurenine, and kynurenine, while incubations in the presence of n-BFSb reduced their levels in a concentration-dependent response.

Conclusion:

n-BFSb is able to inhibit the glycoxidative changes in an in vitro model system of protein glycation. These findings highlight *Siolmatra brasiliensis* as a promising species to be further studied as a complementary therapy for diabetic complications.

Financial support:

FCFAR/UNESP, CNPq, CAPES.

07.025 - DELETION OF MICRORNA-22 ATTENUATES DIET-INDUCED OBESITY IN FEMALE MICE. Silva TO, Fonseca RIB, Júnior JD, Wang D, DinizGP, - Anatomy - USP Physiology and Biophysics - USP Cardiology - Harvard Medical School

Introduction:

In the last two decades, the prevalence of overweight and obesity has increased in several countries, including in Brazil. Obese individuals have several cardiovascular and metabolic diseases, which are influenced by sexual dimorphism. Recent studies have shown that microRNA-22 (miR-22) is involved in the control of cardiac remodeling. In addition, a recent study from our laboratory revealed that miR-22 mediates some metabolic dysfunctions observed in obesity, such as dyslipidemia and increase of adipose tissue in male mice fed high fat (HF) diet. Considering that miR-22 is regulated by sexual dimorphism, and that it targets the estrogen receptor α and Sirt1, we hypothesized that miR-22 deletion may affect cardiac and metabolic alterations associated to obesity.

Aim:

In this sense, our goal is to investigate the role of miR-22 in obesity-induced metabolic disorders in female mice.

Methods:

Female wild type (WT) and knockout (KO) mice for miR-22, selected by genotyping, were treated with control or HF diet with condensed milk (HF+CM) for 16 weeks. The body weight gain was monitored weekly. After the treatment, we performed the analysis of body composition by magnetic resonance imaging and intraperitoneal glucose tolerance test (IGTT) (Protocol 097/13/ CEUA). For comparisons between multiple groups we used two-way ANOVA, followed by Bonferroni post-test, using GraphPadPrism v6.0 (p < 0.05).

Results:

WT female mice treated with HF+CM diet demonstrated an increase in body weight gain compared to their respective controls. However, KO female mice fed HF+CM diet showed an attenuation in body weight gain compared to WT mice fed HF+CM diet. In addition, fat mass was increased in HF+CM diet-treated WT female mice compared to their respective controls. However, KO mice fed HF+CM showed reduced fat mass compared to WT mice fed HF+CM diet. Furthermore, IGTT analysis demonstrated that both WT and KO mice fed HF+CM exhibited glucose intolerance compared to their respective controls.

Conclusion:

The HF+CM diet induced some obesity-related metabolic dysfunctions in female mice, such as increased body weight gain and fat mass, as well as glucose intolerance. However, deletion of miR-22 attenuated the body weight gain and fat mass gain induced by HF+CM diet, suggesting that miR-22 mediates, at least in part, some obesity-induced metabolic disorders in female mice.

Financial support:

FAPESP; CAPES.

07.026 - QUERCETIN ATTENUATES ACUTE LUNG INFLAMMATION IN A MURINE MODEL EXPOSED TO CIGARETTE SMOKE. Matos NA, Araújo NPS, Souza ABF, Castro TF, Cangussú SD, Menezes RCA, Bezerra FS, - Department of Biological Sciences - UFOP

Introduction:

Cigarette smoke (CS) is highly toxic and is the main risk factor for airway inflammation, oxidative stress, the decline in lung function and development of Chronic Obstructive Pulmonary Disease (COPD). Quercetin is a potent dietary antioxidant that displays anti-inflammatory activities.

Aim:

Therefore, this study aimed to evaluate the effects of quercetin administration on markers of oxidative stress and inflammation in short-term CS exposure in mice.

Methods:

FeSBE Annual Meeting 2019

Poster Sessions and Abstracts

The Ethics Committee of the Federal University of Ouro Preto approved the experiments, according to the Protocol nº 2015/20. Fifty male C57BL/6 mice, 8-10 weeks old, were divided into five groups: control group (CG), vehicle propylene glycol group (PG), quercetin group (QG), cigarette smoke group (CSG), and quercetin + cigarette smoke group (QCSG). For five consecutive days, CSG and QCSG were exposed to 4 cigarettes, 3 times a day using a CS inhalation chamber. QG and QCSG received 10 mg/kg/day of quercetin via orogastric gavage one hour before being exposed to CS or ambient air. After 24 h of the last exposure, mice were anesthetized, the trachea was cannulated to assess pulmonary function. After mice were euthanized, bronchoalveolar lavage fluid (BALF) and lungs were collected for histological, stereological and biochemical analyses. Statistical analyses were performed using Graph PadPrism, data were expressed as mean \pm SEM or median, minimum and maximum value and $p < 0.05$ was considered statistically significant.

Results:

In lung function, CS promotes changes in the pattern of breathing included the respiratory rate (RR, bpm) (91.8 ± 15.82) and the tidal volume (VT, mL) (1.14 ± 0.10) compared to CG (172.2 ± 6.42 and 0.51 ± 0.02 , respectively). Surprisingly, quercetin (QGCS) prevented these variations in VT (0.63 ± 0.08) compared to CSG. In BALF, the influx of inflammatory cells ($\times 10^3/\text{mL}$) increased in CSG (356.0 ± 19.5) compared to CG (113.3 ± 9.1), and there was a decrease in QCSG (256.0 ± 14.8) compared to CSG. Quercetin (QCSG) promoted a reduction in the number of macrophages (215.4 ± 16.1), lymphocytes (9.27 ± 0.82) and neutrophils (28.0 ± 5.1) compared to CSG (macrophages 113.4 ± 8.3 ; lymphocytes: 21.0 ± 2.7 ; neutrophils 35.4 ± 7.9). The damage in lung parenchyma was evaluated by carbonylated proteins (nmol/mgPtn) and TBARS (nm/mgptn), both increased in CSG (26.14 ± 3.71 and 4.01 ± 0.23 , respectively) compared to those in CG (12.22 ± 2.16 and 1.85 ± 0.20 , respectively). However, QCSG showed a reduction in carbonylated proteins (11.44 ± 2.42) and TBARS (1.84 ± 0.17) concentration compared to CSG. SOD and CAT activities decreased in CSG (21.21 ± 1.09 and 1.01 ± 0.07 , respectively) compared to CG (30.34 ± 1.74 and 1.4 ± 0.04 , respectively). However, there was an increase of SOD and CAT activity in QCSG (30.03 ± 1.49 and 1.67 ± 0.15 , respectively) compared to CSG. In the stereological analysis, the volume density values of alveolar air space ($V_v[a]$) were increase in CSG ($60.79[56.25-66.88]$) compared to CG ($42.19[38.44-52.50]$), and the volume densities of alveolar septa ($V_v[sa]$) were decrease in CSG ($39.22 [33.13-43.75]$) compared to CG ($58.75[47.50-61.56]$). However, quercetin administration promotes a decrease of $V_v[a]$ ($44.07[35.31-45.94]$) and increase of $V_v[sa]$ ($55.94[54.06-64.38]$) compared to CSG.

Conclusion:

Quercetin was able to reduce lung inflammation and oxidative stress, and prevented an increase in tidal volume and histological pattern changes of pulmonary parenchyma in a short-term cigarette smoke exposure in mice.

Financial support:

CNPq, CAPES, FAPEMIG and UFOP.

07.027 - NEONATAL SEROTONINERGIC MANIPULATION IN OVERFED RATS: SHORT-TERM EFFECTS ON CARDIAC OXIDATIVE STRESS. Lima FAS, Lemos MDTB, Silva SCA, Braz GRF, Lagranha CJ, - Laboratory of Biochemistry and Exercise Biochemistry - UFPE Graduate Program in Neuropsychiatry and Behavior Sciences - UFPE

Introduction:

Studies have suggested that obesity promotes oxidative stress and mitochondrial dysfunction, in addition to increasing susceptibility as cardiovascular diseases. Several studies have demonstrated the antioxidant role of Fluoxetine treatment, which reduces body weight in lean and obese animals and positively modulates oxidative balance.

Aim:

To evaluate, at 22 days of age, the effects of neonatal overfeeding in the heart of Wistar male rats submitted or not to a SSRI treatment during suckling period.

Methods:

At 3rd postnatal day (PND), male newborns between 6-8g were randomly assigned according to the nutritional insult: Normofed group (N, $n = 9$ per dam) and Overfed Group (O, $n = 3$ per dam). Similarly, pharmacological treatment was performed as follow: N group received vehicle solution (NaCl 0.9%) - NV group or Fluoxetine (10mg/b.w.) - NF group, as well as O group, divided in OV group (vehicle) or OF group (fluoxetine). All groups were treated daily subcutaneously until PND 21. At PND 22, the heart was collected for the following biochemical analysis: oxidative stress biomarkers (malondialdehyde-MDA and carbonyl content), enzymatic antioxidant defense (Superoxide dismutase-SOD activity, catalase activity and Glutathione-S-transferase-GST activity), non-enzymatic antioxidant defense (Reduced glutathione-GSH and oxidized glutathione-GSSG and Sulfhydryl groups). Data were analyzed using GraphPad Prism 5[®] software and two-way ANOVA test was used for comparison between groups, with $p \leq 0.05$. The project was approved by CONCEA and local ethics committee of the Bioscience Center of UFPE (0024/2018).

Results:

Our results showed that OV group had an increase in MDA levels compared to NV group (96.5%, $n=4$ a 7, $p < 0.0001$), and a decrease between OF and OV (31%, $n=4$ a 7, $p = 0.0071$). Related to carbonyl levels we found an increase between the OV and NV groups (103.63%, $n=3$ a 4, $p = 0.0003$) and a decrease between the OF and OV groups (28.37%, $n=3$, $p = 0.0267$). We found a decrease in SOD and CAT activity in the OV group compared to NV (34.83%, $n=5$, $p = 0.0036$; 77.42%, $n=3$ a 4, $p = 0.0004$, respectively). Regarding GST activity, the OV group significantly decreased (57.46%, $n=4$, $p = 0.0002$) compared to the NV group and OF group had a significant increase (73.59%, $n=4$, $p = 0.0290$) compared to OV group. GSH content had an increase (49.5%, $n=5$, $p = 0.0005$) in OF compared to OV group. REDOX state increased by 85.46% ($n=4$ a 5, $p = 0.0034$) in OF compared to OV.

Conclusion:

The results cover the hypothesis that the evaluation immediately after the pharmacological insult modulates positively the oxidative balance of the cardiac tissue, which is in agreement with the previous study of our research group.

Financial support:

CNPq

07.028 - HYPERLIPIDIC DIET CAUSES PHENOTYPICAL AND FUNCTIONAL ALTERATIONS IN THE PREGNANT UTERUS OF PARENTAL AND F1 GENERATIONS. Salles ÉSL, Calstron PF, Zavan B, Paffaro AMA, Caixeta ES, Junior VAP, - Cellular and Developmental Biology - Federal University of Alfenas

Introduction:

About 90% of uterine Natural Killer cells (uNK) express N-acetyl-D-galactosamine in their granules and membrane which could be stained by Dolichos biflorus agglutinin (DBA) lectin (DBA+uNK). DAB+uNK has a high angiogenic potential and no cytotoxicity in normal pregnancy. It is known that a high-fat diet consumption during pregnancy could change offspring physiology as a phenomenon called fetal programming.

Aim:

This study aimed to investigate the effect of a high-fat diet in DBA+uNK from mothers (F0) and their offspring (F1).

Methods:

Fifty SWISS mice were mated, gestation day (gd) 1 was considered the day of vaginal plug observation (Ethics approval-656/2015). Pregnant F0 received control (MCD; $n=15$) or High-fat diet (MHF, $n=15$) to obtain F1 or were killed at gd10 to implantation sites (IS) collection. Two days after birth, F1 was fostered by a control mother. Eight weeks after birth, females from each F1 (F1CD, $n=10$, and F1HF, $n=10$) were mated

FeSBE Annual Meeting 2019

Poster Sessions and Abstracts

to IS collection at gd10. The weight gain, perigonadal white adipose tissue (WAT) morphometry, presence of DBA+uNK and perforin+ cells, presence of cleaved caspase-3+ cells and perforin expression were analyzed in F0 and F1 generations. Data were analyzed by ANOVA two-ways and unpaired t-test and Chi-square test ($p \leq 0.05$).

Results:

A higher weight was found in the MHF (MCD=12,3g, DP= 2,9; MHF=16,6g, DP= 2,8; $p < 0.05$) after the 14thgd and in the 10thgd of F1HF (F1CD=5,6g; F1HF=6,8g; $p < 0.05$). Pregnant F1 also exhibited a WAT larger area (F1CD=3935,91 μm^2 , DP= 1,5; F1HF=6062,72 μm^2 , DP= 1,5; $p < 0.05$). uNK cells low reactivite to lectin DBA (DBA low uNK) was observed concomitantly to the reduction of uNK perforin reactivity and high incidence of caspase-3+ cells in MHF and F1HF. There was no difference in the perforin expression in MHF (MCD=0,826, E=0,1; MHF=0,566, E=0,09; $p > 0.05$), but it was lower in F1HF (F1CD=0,998, E= 0,02; F1HF=0,714, E=0,01; $p < 0.05$). A higher number of females with pregnancy loss was observed in F1HF (F1CD= 0, DP=0,0; F1HF= 11, DP= 4,9; $p < 0.05$).

Conclusion:

Thus, it can be concluded that consumption of a high-fat diet during pregnancy triggers not only changes in the maternal uterine environment but also promotes the fetal programming event, generating in the offspring changes very similar to those observed in the mothers who consumed the diet.

Financial support:

FAPEMIG and CAPES

07.029 - AN HPLC METHOD FOR THE DETERMINATION OF ADENOSINE DIPHOSPHATE: AN IMPORTANT MARKER OF HEXOKINASE ACTIVITY IN METABOLIC DISEASES. Santos RB, Santos RS, Otsuka FAM, Trindade DJ, Matos HR, - Departamento de Fisiologia - UFS

Introduction:

Hexokinases play a vital role in the cellular uptake and utilization of glucose. As such, they are of fundamental importance to all cells. By catalysing the ATP-dependent phosphorylation of glucose to yield glucose-6-phosphate, hexokinases control the first step of glucose metabolism, thereby sustaining the concentration gradient that permits facilitated glucose entry into cells and initiating all major pathways of glucose utilization.

Aim:

Our objective was to develop and validate highly sensitive and selective HPLC-PDA assays allowing the determination of ADP, which are useful for the hexokinase activity determination.

Methods:

Samples were analyzed by high performance liquid chromatography with photodiode array detector (HPLC-PDA) using an ACE C18 analytical column (250 x 4.6 mm) for chromatographic separation. Optimal detection was achieved based on isocratic elution with a mobile phase consisting of a sodium phosphate monobasic buffer-methanol 5% mixture.

Results:

All calibration functions were linear for ADP in both matrices over wide analytical ranges. The main advantages of our methods are the small volume of sample required for the analyses and simple and fast extraction procedures. The methods met all requirements of specificity, sensitivity, linearity, stability, precision and accuracy generally accepted in bioanalytical chemistry. The central difference between the HPLC-PDA method proposed here and enzyme-coupled spectrophotometric method for the determination of hexokinase activity was that the former only need one-step of enzyme-coupled assay and not NADP+ and G6PD. Because of the critical role of hexokinase in cellular metabolism, we believe that the HPLC-PDA method described here will potentially serve as a biological marker for the understanding of these pathological conditions.

Conclusion:

Determination of hexokinase activity in patients will allow characterization of their metabolic state in many diseases, as cancer and diabetes, under specific conditions at a defined time.

Financial support:

INCT-REDOXOMA and CNPq

07.030 - PYCNOPORUS SAGUINEUS EXTRACT INCREASE LIPID SYNTHESIS IN ADIPOSE TISSUE ON DIABETIC RATS. Dentz MCV, Rocha DS, Ohlweiler R, Maschio J, Girelli V, Model JFA, Vogt ÉL, Fontana RC, Camassola M, Jahn MP, Kucharski LC, - Laboratório de Metabolismo e Endocrinologia Comparada - UFRGS Laboratório de Fisiologia e Farmacologia - UCS Laboratório de Enzimas e Biomassas - UCS

Introduction:

Diabetes mellitus is a pathogenesis associated at increased risk of development of cardiovascular diseases, resulting in damage health, decreased quality of life and generation of economic costs. The search for treatments that represent lower costs of production and less adverse effects is often done through the study of natural products. The mushroom *Pycnoporus sanguineus*, popularly known as orelha-de-pau, is endemic of South America and there are no records of its utilization in popular medicine or consumption as food item. However, recent studies identified that the extract produced from the basidiomas of this fungus have hypolipidemic activity, being able to decrease serum levels of triglycerides, total cholesterol and non HDL cholesterol in diabetic rats.

Aim:

The objective of this study was to evaluate the effect of *P. sanguineus* extract on carbohydrates and lipids metabolism, searching understanding of how the extract acts to promote lipid homeostasis in diabetic rats.

Methods:

The extract was obtained from *P. sanguineus* basidiomas (lineage 14G) by distillation in water and 70% ethanol and then freeze-drying. Forty male Wistar rats, 60 days old, were divided in healthy or diabetic, and then treated or not with the extract, creating four groups: control treated with H₂O (C), control treated with extract (CE), diabetic treated with H₂O (D) and diabetic treated with extract (DE). Diabetes was induced with streptozotocin (65 mg/Kg i.p.) and the treatment with *P. sanguineus* extract was performed for 30 days through gavage (10 mg/Kg/day). After this period, the animals were euthanized and blood was collected and used for analysis of lipid profile, glucose and hepatic damage. The retroperitoneal adipose tissue (RAT) was used to evaluate the capacity of glucose oxidation into CO₂ and lipid synthesis. Morphometric parameters also were measured: total body mass (TBM), mass variation and liver, retroperitoneal adipose tissue and epididymal adipose tissue index. The experiments were approved by UFRGS's CEUA (number 31195). Parametric data were tested by two-way ANOVA and Tukey post hoc test. Nonparametric data were tested by Kruskal Wallis and Dunn's post hoc. Values of $p < 0.05$ were considered significant.

Results:

In diabetic animals the treatment was able to increase weight gain (D: 9.00 \pm 4.85 g and DE: 34.30 \pm 6.5 g), glucose oxidation (D: 5.57 \pm 1.08 $\mu\text{mol/g/h}$ and DE: 17.6 \pm 3.26 $\mu\text{mol/g/h}$) and lipogenesis (D: 86.35 \pm 17.97 $\mu\text{mol/g/h}$ and DE: 206.6 \pm 29.49 $\mu\text{mol/g/h}$) in RAT ($p < 0.05$).

Conclusion:

Based on these results, the changes promoted in RAT metabolism by treatment with extract are able to generate as clinic outcomes a serum lipids homeostasis and improvement of dyslipidemia in diabetes. These data suggest that the extract may act modulating PPARs. The PPAR γ , specifically, acts regulating the expression genes that promotes fat storage, increasing lipid oxidation in skeletal muscle and adipose tissue. Therefore, this study showed that the treatment with *P. sanguineus* extract changes the metabolism at tissue level and can result in changes in lipids homeostasis on blood, being important evaluate their modulation about PPARs expressed in adipose tissue.

Financial support:

CNPq

FeSBE Annual Meeting 2019

Poster Sessions and Abstracts

07.031 - ROLE OF THE BETA 3 ADRENERGIC RECEPTOR IN THE OXIDATIVE STRESS. Fragoço MB, Araújo A, Paixão C, Júnior ED, Fiorino P, Ribeiro MO, Angelis K, Farah VMA, - Laboratório de Fisiologia Farmacológica Cardiovascular e Renal - Universidade Presbiteriana Mackenzie Laboratório de fisiologia do exercício - UNIFESP Laboratório de neurobiologia e metabolismo energético - Universidade Presbiteriana Mackenzie

Introduction:

The β 3-adrenergic receptor (AR- β 3), has attracted attention in the field of research for its role in adipose tissue, especially in lipolysis and thermogenic control. However, AR- β 3 is also involved in the production of nitric oxide (NO), one of the major factors that modulates oxidative stress. Oxidative stress significantly alters the response of various metabolic pathways, leading to the development of chronic metabolic diseases through the unbalance between oxidant and antioxidant agents.

Aim:

Evaluate the role of AR- β 3 in hepatic oxidative stress.

Methods:

Adult male mice (26g - 29g) were divided into two groups (n=8/group): wild-type (WT) and β 3-adrenergic receptor knockout mice (KO β 3). The animals were euthanized by a mixture overdose of Ketamine and Xylazine and the liver was collected to measure the oxidative stress. The lipid peroxidation and protein oxidation were quantified by chemiluminescence method and carbonyl detection respectively. The unspecific non enzymatic antioxidant capacity was measured through the Ferric Reducing Ability of Plasma (FRAP). The activity of the anti oxidant enzymes Superoxide Dismutase (SOD) and Catalase (CAT) were assessed, as well as NADPHoxidase and hydrogen peroxide. The results were analyzed by Student's t test and are presented as mean \pm standard error of the mean. A p value equal to or less than 0.05 was considered statistically significant. All the procedures were approved by the ethics committee of the Mackenzie Presbyterian University (Process N $^{\circ}$ 151/01/2017).

Results:

Our results showed that the lack of the AR- β 3 caused an increase in lipid peroxidation (WT=1083 \pm 114 vs. KO β 3=2422 \pm 136 cps/mg) and in protein oxidation (WT=9.4 \pm 0.3 vs. KO β 3=10.2 \pm 0.4 mg/ml). Moreover, KO β 3 showed an increase of hydrogen peroxide (WT=6.1 \pm 0.4 vs. KO β 3=9.4 \pm 0.6 μ M H₂O₂). However, there were no alterations observed in the activity of CAT (WT = 9.4 \pm 0.8 vs. KO β 3=10.9 \pm 1.3 nmol/mg) and SOD (WT=18.1 \pm 1 vs. KO β 3=16.7 \pm 0.7 U₅₀₀/mg). In addition, the activity of NADPH oxidase (WT=0.5 \pm 0.03 vs. KO β 3=0.7 \pm 0.03 um/min/mg) was increased in KO β 3 when compared to WT.

Conclusion:

Taken together, our data showed that the lack of the AR- β 3 leads to an hepatic oxidative stress state, characterized by an excessive production of oxidizing agents, along with no alteration in the antioxidant defense. In this regard, our results suggest a protective role of the AR- β 3 against the development of hepatic oxidative stress.

Financial support:

Mackpesquisa

07.032 - SUPPLEMENTATION WITH MUCUNA PRURIENS L. CHANGES PARAMETERS OF GLUCOSE METABOLISM IN OBESE RATS. Tavares RL, deSouza DM, deVasconcelos MHA, Dorand VAM, D'Oliveira AB, Aquino JS, - DEPARTAMENTO DE NUTRIÇÃO - UFPB

Introduction:

Obesity is a disease associated with several comorbidities, such as insulin resistance (IR), a change in the ability to use insulin and glucose, involved in the pathophysiology of type 2 diabetes. Among the strategies to treat obesity is the use of herbal medicines. *Mucuna pruriens* (MP) stands out for its nutritional composition, phytochemistry and use in traditional medicine, but its effect on obesity has not yet been studied.

Aim:

to evaluate the effect of MP supplementation on some parameters of glucose metabolism of obese rats.

Methods:

The experiment protocol was approved by the Committee on Ethics in Animal Use (n. 4657230418). Thirty-two Wistar rats (\pm 40 days old), were randomized into: healthy non supplemented group (GS) or obese (non-supplemented) group. The GS consumed only commercial feed and GO consumed cafeteria diet and commercial feed for 8 weeks. Then, the groups were randomized into healthy non supplemented (GS), healthy supplemented with MP (GSMP), obese not supplemented (GO) and obese supplemented with MP (GOMP). Supplementation with 750 mg of the MP extract/kg/ day (diluted in 2 mL) started at the eighth week and lasted another eight weeks. Untreated groups received 2 mL of saline via gavage. Glucose (GTT) and insulin (ITT) tolerance tests were performed before and after supplementation, by incision at the animal's tail tip for glycemia measurement at times 0, 30, 60, 90 and 120 min in both tests. Glucose solution (2g/kg) was administered orally the GTT and 0.75 IU insulin/kg, diluted in 0.9% saline, via intraperitoneal to the ITT.

Results:

After the induction of obesity, higher glycemia was observed in the GO compared to GS over time (p<0.05) in GTT and ITT. For GTT, the GOMP group presented lower glycemia (p<0.05) at times 0 (101.98 \pm 3.10mg / dL) 30 (142.28 \pm 15.36mg / dL), 60 (161.66 \pm 13.40mg / dL) 90 (142.82 \pm 6.74mg / dL) and 120 minutes (131.97 \pm 10.29mg / dL) compared to GO. For ITT, glycemia of the GOMP group reduced (p<0.05) at time 0 (112.29 \pm 5.39mg / dL) and 120 minutes (128.86 \pm 8.82mg / dL) compared to GO.

Conclusion:

cafeteria diet altered the glucose metabolism, with greater resistance to glucose and insulin. However, obese animals supplemented with MP reduced glycemic levels, which indicates greater glucose tolerance and lower insulin resistance.

Financial support:

none

07.033 - COCONUT OIL EFFECTS ON PROSTATE AGING: PRELIMINARY MORPHOLOGICAL ANALYSIS. Guerra LHA, Zucão MI, Tamarindo GH, Taboga SR, Vilamaior PSL, - Departamento de Biologia - UNESP

Introduction:

Benign prostatic hyperplasia (BPH) is a disease associated with a hormonal imbalance that occurs among the aging process and affects more than fifty percent of men over fifty years of age. That said, BPH is a common condition that has a considerable impact on drug development and has been an object of study in the last decades in order to reduce BPH treatment side effects. In this context, complementary and alternative medicines such as phytotherapy emerge as a treatment option for BPH, among them coconut oil that has been shown to interfere with testosterone-induced BPH. However, much uncertainty still exists about the relationship between coconut oil effects and aging.

Aim:

The aim of this work was to explore the relationship between the consumption of coconut oil during aging and BPH in terms of prostatic morphology

Methods:

Adult male gerbils (*Meriones unguiculatus*) (100 days old) were divided into two groups: Intact control (IC) (ventral prostate collected at 460 days old) and coconut oil (CO) (animals received 0,1ml of coconut oil via gavage 5 times a week for 1 year and ventral prostate collected at 460 days old). Prostates were weighted for biometric analysis, fixed in paraformaldehyde, clarified in xylol and embedded in paraffin for histological analysis (n=6) or frozen in liquid nitrogen (n=6); the slides were stained with Hematoxylin-Eosin for general morphologic,

FeSBE Annual Meeting 2019

Poster Sessions and Abstracts

morphometric and stereological analyses. In addition, Oil red O staining was performed for tissue lipid quantification and localization. The quantitative data were submitted to statistical analysis (unpaired t-test for parametric data or Mann-Whitney test for nonparametric data).

Results:

The biometric analysis showed that coconut oil does not alter body weight and ventral lobe, but promotes a decrease in the weight of the prostate complex. General morphological analysis revealed that the presence of high-grade NIPs appears to be more common in the intact group in addition to the presence of many cells of the immune system in the lumen. The stereological analysis showed that coconut oil treatment did not promote changes in the relative frequency of the epithelium, stroma, lumen, and vessels, despite morphometry has shown that this oil promotes a thickness decrease in the secretory epithelium. The techniques using Oil red O revealed that the secretory cells accumulate lipid in the basal portion, however, we did not observe differences in their amount between the groups.

Conclusion:

Although our results are preliminary, they point to a potential anti-inflammatory and protective action for BPH, however, further analysis is required to confirm this coconut oil action.

Financial support:

CAPES/CNPq

07.034 - SUPPLEMENTATION WITH COCONUT OIL (COCOS NUCIFERA L.) CHANGES PARAMETERS OF GLUCOSE METABOLISM OF OBESE RATS. Vasconcelos MHA, D'Oliveira AB, Dorand VAM, Tavares RL, Junior EUT, Dutra MLV, Aquino JS, - DEPARTAMENTO DE NUTRIÇÃO - UFPB

Introduction:

In contemporary society, the high consumption of caloric foods and low nutritional value has been related to the etiology of obesity, due to its relationship with consequent endocrine and metabolic disorders. Dietary intervention with dietary improvement, exercise and supplementation has been investigated for the reduction of body weight. In this sense, the biological and functional efficacy of coconut oil (*Cocos nucifera* L.) is being studied because it is rich in medium chain fatty acids and antioxidants. However, researchers have warned about answers yet to be elucidated, with preliminary and contradictory results, and the benefits that prolonged consumption of coconut oil could exert on metabolism are not fully evidenced in the literature.

Aim:

This study evaluated the effect of extra virgin coconut oil (EVCO) supplementation on glucose parameters of obese Wistar rats.

Methods:

The procedures were approved by ethical committee of animal research (nº 6345230418/2018). Thirty-two rats (± 40 days old) were initially randomized into: not supplemented Healthy Group (HG) and not supplemented Obese Group (OG). Throughout 8 weeks the HG consumed commercial feed and the OG consumed commercial feed and a cafeteria diet. After this period, the groups were reallocated in: not supplemented Healthy Group (HG); Healthy Group supplemented with coconut oil (HGCO); not supplemented Obese Group (OG) and Obese Group supplemented with coconut oil (OGCO), their respective diets remained the same until the end of the experiment. As of the 8th week and on OGCO and HGCO received the supplementation with EVCO (3000 mg/body weight kg/day – 3,3mL) by gavage, while OG and HG received 2,0mL of distilled water in the same period. In the glucose tolerance test (GTT) the oral administration of glucose solution was performed (2g/kg) with fasted animals. In the insulin tolerance test (ITT) intraperitoneal administration of insulin was performed (0,75IU/kg) with fed animals. Glycemia was measured at 0, 30, 60, 90 and 120 min in both tests.

Results:

In the obesity induction period, higher levels of glycemia were observed in the OG at all time lapses: 0 min (113.36 \pm 10.29 mg/dL), 30 min

(167.44 \pm 9.96 mg/dL), 60 min (172.22 \pm 9.61 mg/dL), 90 min (160.88 \pm 10,60 mg/dL) and 120 min (151.11 \pm 9.73 mg/dL) of the GTT, as well as in the time lapses 0 min (114.80 \pm 4.87 mg/dL), 30 min (92.92 \pm 5.95 mg/dL), 60 min (76.58 \pm 5.47 mg/dL), 90 min (92.18 \pm 8.53 mg/dL) and 120 min (119.50 \pm 9.59 mg/dL) of the ITT compared to HG ($p < 0.05$). After the supplementation period, the OGCO had lower glycemia levels in time lapses 90 min (104.20 \pm 16.42 mg/dL) and 120 min (108.83 \pm 15.94 mg/dL) in the GTT compared with the OG ($p < 0.05$). However, in the ITT, the glycemia was only lower in the time lapse of 0 min (OGCO=107.60 \pm 8.65 mg/dL versus OG=131.50 \pm 5.89 mg/dL). The glycemia of HG and HGCO over time was similar, be on the GTT or in the ITT ($p > 0.05$).

Conclusion:

consumption of cafeteria diets reduced glucose and insulin tolerance; however, the supplementation with coconut oil improved glucose tolerance but was not able to minimize insulin resistance in obese rats

Financial support:

none

8 - Renal Biology and Diseases

08.007 - DOXYCYCLINE TREATMENT RECOVERS THE RENAL FUNCTION OF WISTAR RATS IN EXPERIMENTAL INTOXICATION WITH BOTHROPS JARARACUSSU VENOM. Silva PAS, Ferreira MAR, Melo PA, LARALS, - Programa de Pós-graduação em Farmacologia e Química Medicinal - Universidade Federal do Rio de Janeiro

Introduction:

Snakebite envenoming is one of the most neglected tropical diseases. In Brazil, Bothrops snakes are responsible for approximately 90% of reported snakebites representing a major public health problem in our country. Acute kidney injury (AKI) is a serious complication of ophidian accidents and the leading cause of death in patients who survive the initial effects of venom. A study conducted in our laboratory by Cortes et al., (2018) showed that doxycycline prevented AKI induced by the renal ischemia/reperfusion process. Our working hypothesis is that the pharmacological repositioning of doxycycline can be applied in the treatment of AKI induced by Bothrops jararacussu venom.

Aim:

The main objective of this study was to evaluate whether treatment with doxycycline reverses renal injury caused by experimental intoxication with Bothrops jararacussu venom.

Methods:

Male Wistar rats were randomly assigned to three different groups. Control (Ctrl): animals received saline solution 0.9% NaCl intramuscularly (im); Bothrops jararacussu (Bj): animals received 3.5 mg/kg Bj (im) venom; Bothrops jararacussu+Doxycycline (Bj+Dc): animals received 3.5 mg/kg Bj (im) venom and 2 h after intoxication were treated with 3.0 mg/kg Dc intraperitoneally (ip). Renal physiological parameters were evaluated by colorimetric kits, (Na⁺+K⁺)-ATPase by Western Blotting, enzymatic activity and immunofluorescence. Statistical analysis was performed using the One-Way ANOVA and Tukey post-test.

Results:

Results are reported as mean \pm standard error of the mean. All procedures were carried out in accordance with the standards of good research practice and approved by the Ethical Committee on Animal Use (CEUA) of the CCS of UFRJ under number 103/18. The results obtained in this study allowed us to conclude that experimental intoxication with Bj venom (3.5 mg/kg) promoted tissue damage in the renal cortical region (score 3) in 24 h associated with decreased glomerular and tubular function that promoted proteinuria and polyuria. Treatment with doxycycline 2 h after experimental intoxication reversed renal damage in the following parameters: cortical lesion (Ctrl 0,25 \pm 0,1 Bj 2,75 \pm 0,14 Bj+Dc score 0.5 \pm 0.2), increase in urinary volume (Ctrl 4 \pm 0,42 Bj 13 \pm 1.9 and Bj+Dc 5 \pm 0.3

FeSBE Annual Meeting 2019

Poster Sessions and Abstracts

mL in 24 h), an increase in the glomerular filtration rate (Ctrl 321 ± 26 Bj 698 ± 131.8 and Bj+Dc 351.4 ± 38.3 $\mu\text{L}/\text{min}$) and a decrease in the urinary creatinine/plasma creatinine ratio (Ctrl 92 Bj 43 and Bj+Dc 87), plasma urea nitrogen (Ctrl 52 ± 4.8 Bj 86.7 ± 5.4 and Bj+Dc 62.9 ± 3.2 mg/dL), filtered load Na^+ (Ctrl 65 ± 22.8 Bj 204.4 ± 19.4 and Bj+Dc 54.7 ± 11.6 mEq $\mu\text{L}/\text{min}$), Na^+ excretion (Ctrl 0.2 ± 0.1 Bj 0.6 ± 0.1 and Bj+Dc 0.1 ± 0.03 mEq/L) marked proteinuria (given by the ratio between proteinuria and urinary creatinine). Doxycycline treatment prevented the increase of the (Na^{++}K^+)-ATPase protein content induced by the intoxication (Ctrl 100 ± 5 Bj 166.5 ± 13.5 and Bj+Dc 84.3 ± 8.0 u.a.) and the decrease of the enzyme activity in the kidney cortex (Ctrl 963 ± 177.5 Bj 444.8 ± 61.01 and Bj+Dc 1036 ± 33.65 nmolPi/mg/min). In addition, Bj provoked translocation of the enzyme from this basolateral membrane to the luminal membrane being inhibited by the treatment as seen through immunofluorescence.

Conclusion:

Taken together, the results demonstrate that doxycycline may be a potential pharmacological alternative in the treatment of AKI induced by Bothrops intoxication.

Financial support:

CAPES, CNPq e FAPERJ.

08.008 - EVALUATION OF BIOMARKERS OF OXIDATIVE DAMAGE AND ANTIOXIDANT DEFENSES IN SERUM OF PATIENTS WITH CHRONIC KIDNEY DISEASE UNDERGOING HEMODIALYSIS. Marques MB, Lima TFO, Assis RP, Guaratti M, Costa MC, Saheb JL, Brunetti IL, Baviera AM, - Department of Clinical Analysis - UNESP Regional Center of Hemodialysis - DAVITA

Introduction:

The goal of hemodialysis (HD) is to remove uremic solutes and to reduce the symptoms related to uremic syndrome, improving the quality of life of individuals with chronic kidney disease (CKD). However, oxidative stress has been demonstrated in HD patients because of loss of antioxidants during HD and due to the production of free radicals by leukocyte activation through contact with dialysis membrane, contributing to the pathophysiology of cardiovascular diseases.

Aim:

In the present study, we evaluated biomarkers of renal function, oxidative damage and antioxidant activity in serum of healthy individuals and individuals with CKD, before and after one HD session.

Methods:

All subjects signed the informed consent form, approved by the local ethics committee (protocol number: 76859617.4.0000.5426). Serum samples from controls, healthy individuals (no clinical history of CKD or any other pathology) were obtained from the Hemonúcleo Regional de Araraquara, SP; serum samples from patients with CKD undergoing HD (for at least 3 months, prescription of 3-times/week HD procedure) were obtained from the Centro Regional de Hemodiálise de Araraquara, SP. Samples from CKD patients were collected before (pre-HD) and after (post-HD) a HD session. Serum samples were used for analysis of renal function biomarkers (creatinine and urea), biomarker of lipid peroxidation (TBARS, thiobarbituric acid reactive substances), protein oxidative damage (PCO, protein carbonyls), estimation of fluorescent advanced glycation end products (AGEs), and the activities of antioxidant enzymes catalase (CAT), glutathione peroxidase (GSH-Px) and paraoxonase 1 (PON1). The results were expressed as mean \pm standard error and considered statistically different with $p < 0.05$ (One-Way ANOVA followed by Student-Newman-Keuls).

Results:

HD patients had high serum levels of creatinine and urea (15 and 4 times, respectively) in comparison to controls; one session of HD was sufficient to reduce creatinine (65%) and urea (70%). Serum TBARS levels in pre-HD patients (18.12 ± 1.36 μM) were higher than values of controls (10.99 ± 0.33 μM); however, after the HD session, serum TBARS levels significantly decreased in CKD patients (13.01 ± 0.64 μM).

Serum fluorescent AGEs levels in CKD patients (pre-HD) were significantly higher (8 and 32 times, respectively) than values in control group; HD reduced AGEs (31%) when compared with pre-HD. Both pre-HD and post-HD samples had increased levels of PCO (51% and 54%, respectively) in comparison with controls. The activities of CAT, GSH-Px and PON1 were decreased (43%, 51% and 31%, respectively) in serum from pre-HD patients, when compared with controls; no significant differences were found in the activities of these enzymes after HD session.

Conclusion:

HD patients have high levels of biomarkers of oxidative damage and low activities of antioxidant enzymes when compared with controls, indicating oxidative stress, which can be associated with the uremic environment, inflammatory status, diabetes mellitus, hypertension and the HD procedure itself. However, one session of HD was sufficient to decrease the serum levels of uremic solutes, TBARS, and AGEs, suggesting that HD promotes benefits to CKD individuals not only by reducing uremic toxins, but also attenuating oxidative stress and then HD can contribute to prevent the complications of CKD.

Financial support:

FCFar/UNESP, CAPES

08.009 - RENAL EFFECTS OF QUERCETIN ADMINISTRATION IN A MURINE MODEL EXPOSED TO CIGARETTE SMOKE. Oliveira MAGS, Souza ABF, Júnior PAM, Castro TF, Araújo NPS, Matos NA, Bezerra FS, Cangussú SD, - Departamento de Ciências Biológicas - UFOP

Introduction:

Nephropathies represent an important focus of attention given the multiple functions of the kidney in the body. Most avoidable risk factors for the organism (drugs, irradiation, and smoking) are sources of reactive oxygen species and nitrogen, lead to cytotoxicity and may lead to multiple nephropathies. Cigarette smoke (CS) contains approximately 5000 chemical components with adverse effects on almost all organs of the body, even those that do not have direct contact with the smoke, as is the case with the kidney. Studies have shown that quercetin, a natural antioxidant, has been shown to play an important antioxidant and anti-inflammatory role in some kidney diseases.

Aim:

This study aimed to evaluate the effects of quercetin administration in a murine model exposed to cigarette smoke (CS).

Methods:

The Ethics Committee of the UFOP approved the experiments (Protocol nº 2015/20). Forty five C57BL/6 mice (8-10 weeks old) were divided in five groups: control (n=7) (CG), quercetin (n=8) (QG), propylene glycol (n=7) (PG), cigarette smoke (n=8) (CSG), quercetin and CS (n=8) (QCSG). Animals from CG, QG, and PG were exposed to ambient air while CSG and QCSG were exposed to CS to 12 commercial cigarettes a day for five days, in an inhalation chamber. QG and QCSG received by orogastric gavage 10 mg/kg/day diluted in 200 μL of propylene glycol. PG received by orogastric gavage 200 μL of propylene glycol. Twenty-four hours after, the animals were euthanized, and blood and kidney tissue samples were removed for morphological, morphometric and biochemical analyses. Statistical analyses were performed using GraphPad Prism software version 5.00 for Windows 7. Data were expressed as mean \pm SEM and $p < 0.05$ was considered statistically significant.

Results:

The morphological analysis detected a predominance of the edematous areas, inflammatory cells and congestion in the peritubular vessels into the kidney of animals exposed to CS compared to quercetin administration animals. Biochemical parameters revealed an increase in the uric acid levels (mg/dL) in the plasma of animals exposed to CS (5.61 ± 0.34) compared to CG (3.89 ± 0.25), QC (4.20 ± 0.23), PG (4.39 ± 0.34) and QCSG (4.44 ± 0.18). There was an increase in the activity of

FeSBE Annual Meeting 2019

Poster Sessions and Abstracts

catalase (CAT) (U/mg PTN) in CSG (3.096 ± 0.822) compared to CG (1.60 ± 0.06) and QCSG (1.29 ± 0.11). However, there was no significant difference in the superoxide dismutase activity (SOD) (U/mg PTN) (CG: 7.383 ± 2.753 ; QG: 7.328 ± 0.54 ; PG: 7.468 ± 0.753 ; CSG: 7.019 ± 0.658 ; QCSG: 7.159 ± 0.634); and there was no significant difference in the carbonylated protein (nmol/mg PTN) (CG: 3.78 ± 0.37 ; QG: 3.84 ± 0.35 ; PG: 4.72 ± 0.52 ; CSG: 4.53 ± 0.53 ; QCSG: 5.13 ± 0.43) between the groups.

Conclusion:

Our data suggest that short-term exposure to CS promotes oxidative stress and renal injury. However, the administration of quercetin has been shown to be able to reduce renal injury and redox imbalance induced by exposure to cigarette smoke.

Financial support:

CNPq, CAPES, FAPEMIG and UFOP

08.010 - ALAMANDINE TREATMENT PROTECTS RENAL FUNCTION OF WISTAR RATS FROM BILATERAL KIDNEY ISCHEMIA-REPERFUSION (I/R). Silva HM, Côrtes AL, Silva RC, Silva PAS, Santos RAS, Morcillo LSL, Gonzalez SR, - ICB - UFRJ ICB - UFMG Campus Macaé - UFRJ

Introduction:

Renal ischemia reperfusion (I/R) is the main risk factor for acute renal injury (AKI), promoting glomerular and tubular changes. It has been shown the inappropriate increase in intrarenal angiotensin II early after ischemia which is associated with tissue inflammation and tubular damage. Alamandine (Ala) is formed from angiotensin A or directly from angiotensin-(1-7). Ala produces vasodilation and a long-lasting anti-hypertensive action in spontaneously hypertensive rats, through activation of its specific receptor MrgD.

Aim:

We aimed to determine whether different intraperitoneal doses of Ala prevents renal function decay during bilateral kidney I/R and the involvement of renin angiotensin system (RAS).

Methods:

Adult male Wistar rats (200-300 g) were divided into 4 groups (n = 5 each, UFRJ-CEUA 137/13): (1) Control; (2) I/R: ischemia was performed by application of vascular clamp in the renal peduncle for 30 min followed by 24 h of reperfusion; (3) I/R+ALA: different doses of Ala was administered intraperitoneally during I/R procedure (0.025, 0.050, 0.1, 1, 10 and 50 mg/Kg). During the 24 h reperfusion period, the rats were individually allocated in metabolic cages for collection of urine. After reperfusion, the animals were euthanized for blood and kidney collection. Primary Na⁺ transporters activities were measured on the kidney cortex homogenate by the ³²Pi released in the absence and in the presence of the specific pump inhibitor in the presence of varying concentrations of Ala (from 2 pg/mL to 2 mg/mL). Proteins content of RAS were quantified by western blot analysis

Results:

We observed that body weight and plasma Na⁺ concentration did not change in experimental conditions. Ala treatment did not change the decreased water intake observed in the I/R rats. Ala (1 mg/Kg) prevented (1) the 57 % increase in urine volume, (2) the 3-times increase in proteinuria, (3) the 2-times increase in blood urea nitrogen accumulation and (4) abolished the increase in the Na⁺ excretion in the urine in the I/R rats. Glomerular filtration rate decay was partially blocked (GFR in $\mu\text{l}/\text{min}$: 176 ± 25 in I/R and 380 ± 70 in I/R+ALA 1 mg/Kg), however ALA at the same dose protected the urine creatinine reduction (Urinecr in mg/24h: 74 ± 4.5 in CTRL; 35 ± 9.0 in I/R and 70 ± 3.2 in I/R+ALA 1 mg/Kg). Ala did not change the (Na⁺+K⁺)ATPase activity, but Ala concentrations higher than 2 $\mu\text{g}/\text{mL}$ inhibit Na⁺-ATPase activity. I/R promotes increase in protein expression of prorenin receptor (PRR) and renin precursor (70 %) e (50 %), respectively. 100 $\mu\text{g}/\text{kg}$ of ALA protected the kidney from the RAS impairment.

Conclusion:

ALA treatment prevented the reduction of renal function caused by I/R. ALA acts on renal glomerular function and also avoids the change in tubular modulation of the Na⁺ during I/R. The most effective lower Ala dose with no additional effect to renal function decay is 1 mg/Kg. The molecular mechanism of renal protection by ALA is due to SRAA inhibition.

Financial support:

Cnpq

08.011 - RENIN-ANGIOTENSIN SYSTEM AND ACETYLATIONS: KEY ELEMENTS IN CARDIORENAL ALTERATIONS PROVOKED BY CHRONIC MALNUTRITION IN MALE ADULT RATS. Muzi-Filho H, Jannuzzi LB, Bouzan ACS, Alves-Bezerra DS, Pereira-Acacio A, Sarmiento GC, Vieyra A, - Carlos Chagas Filho Institute of Biophysics - UFRJ

Introduction:

BACKGROUND: Chronic malnutrition (CM) affects ~1 billion people worldwide, frequently associated with arterial hypertension (AH) and cardiorenal syndrome (CS), with Renin-Angiotensin System (RAS) and Na⁺ body balance alterations. The mechanisms by which CM affects Na⁺ balance in AH and CS are unknown. The imbalance between histone acetyltransferases (HATs) and deacetylases (HDACs) promotes AH. Valproic acid (Val, HDAC pan-inhibitor) reverses the AH caused by CM. Losartan (Los, the Angiotensin II type 1 receptor blocker/AT1R) stimulates the activity of HDACs, regardless of nutritional status, reversing the HAT/HDAC imbalance. However, the signaling pathways involved are unknown.

Aim:

The leading hypothesis in this study was that CM upregulates RAS and promotes renal and cardiac HAT/HDAC imbalance, together with alterations in the Na⁺ pump responsible for the fine-tune of Na⁺ transport, thus provoking AH in male adult rats. Taking together, the above observations suggest that processes that culminate in AH, CS and Na⁺ imbalance share same signaling pathways alterations. Therefore, the administration of Los and Val could reverse AH and CS.

Methods:

METHODS: Experimental design was approved by the Ethics Committee on the Use of Animals in Research from UFRJ (007-16 and 012-19). Eight groups of male rats between weaning (at 28 days) and 90 days of age (young adults) were used: CTR (only commercial diet), CTR+Los (commercial diet+30 mg/kg Los, daily from weaning), CTR+Val (commercial diet+100 mg/kg Val, daily from 70th day of age), CTR+Los+Val (combined), CM (receiving a deficient diet that mimics eating habits in vast and impoverished regions from developing countries, the 'Regional Basic Diet'), CM+Los, CM+Val and CM+Los+Val. The abundance of acetyl histone H3 and histone deacetylases HDAC2, HDAC4 and sirtuin 1 (SirT1), as well as the activity of Na⁺-ATPase insensitive to ouabain and protein kinases A and C in proximal tubules from renal cortex (RC) and cardiomyocytes from left ventricle (LV) were investigated.

Results:

RESULTS: CM upregulated Na⁺-ATPase from RC (75%, $P < 0.0001$, n=6), but downregulated this pump from LV (30%, $P < 0.0001$, n=6). In both organs, the Los+Val combination restored Na⁺-ATPase activity at control levels ($P > 0.9999$ vs. CTR). CM increased the PKC/PKA activity ratio (central regulatory ratio in the AT1R signaling pathway) in RC (75%, n=4), which was reverted by the Los+Val combination. When compared with CTR, CM upregulated acetyl histone H3 in RC (25%, $P = 0.0237$, n=6) and LV (15%, $P = 0.0160$, n=6), and downregulated renal HDAC4 (15%, $P = 0.0192$, n=6) and cardiac SirT1 (15%, $P = 0.0152$, n=6). CM upregulated the abundance of HDAC2 in LV (85%, $P < 0.0001$, n=6) despite the inhibition of total HDAC activity previously observed (85%, $P < 0.0001$, n=5).

Conclusion:

CONCLUSION: CM alters the HAT/HDAC balance by (1) upregulation of acetyl histone H3 and downregulation of HDAC activity and abundance

FeSBE Annual Meeting 2019

Poster Sessions and Abstracts

and (2) by raising the PKC/PKA activity ratio, two modifications likely involved in the stimulation of renal Na⁺-ATPase and Na⁺ reabsorption. Since the Los+Val combination reverses these effects and decreased blood pressure even below CTR levels (CM 144±2 vs. CM+Los+Val 101±2 mmHg, P<0.0001; CTR 124±1 mmHg; n=18-22). Thus, the combination of the two pharmacological approaches could be an option for the AH and CS treatment.

Financial support:

FINANCIAL SUPPORT: CNPq, FAPERJ, INCTs, FINEP, CAPES

08.012 - TEMPOL PROTECTS PARAQUAT-INDUCED CHANGES IN RENAL ATP-DEPENDENT NA⁺ TRANSPORT AND TISSULAR RENIN-ANGIOTENSIN SYSTEM. Cirilo MAS, Santos VBS, Lima NKS, Muzi-Filho H, Vieyra A, Paixao AD, Vieira LD, - Instituto de Biofísica Carlos Chagas Filho - UFRJ Departamento de Fisiologia e Farmacologia - UFPE

Introduction:

Acute kidney injury (AKI) occurs as a rapid decline in renal filtration that leads to metabolic waste accumulation and hydroelectrolytic balance disorders. Paraquat (1,1'-Dimethyl-4,4'-bipyridinium dichloride) exposure is a situation known to induce AKI through reactive oxygen species (ROS) production, however, its pathophysiology is not fully elucidated.

Aim:

Thus, we evaluated in rats whether AKI-induced by paraquat leads to altered proximal Na⁺ reabsorption and altered content of renin-angiotensin system (RAS) components and whether these changes are dependent on ROS production.

Methods:

Adult male Wistar rats (n=15; 300-340 g) were submitted to AKI by intraperitoneal administration of paraquat (PQ; 20 mg/kg). Part of these rats was previously treated with tempol (10 mg/kg, in tap water; n=7) during seven consecutive days. Control group (n=8) received administration of NaCl 0.9% (1 mL/kg, i.p.). The rats were placed in a metabolic cage to urine collection, and 24 hours after PQ exposure, they were submitted to indirect systolic blood pressure (SBP) evaluation by plethysmography. Then, the rats were anesthetized (ketamine and xylazine, 80 and 10 mg/kg, i.p.) for collection of kidneys and blood sample. In the kidneys, it was evaluated the lipid peroxidation (thiobarbituric acid reactive substances), ROS levels (dihydroethidium oxidation) and NADPH oxidase activity (lucigenin chemiluminescence). Moreover, renal samples were used to measurement of ouabain-sensitive (Na⁺+K⁺)ATPase and furosemide-sensitive Na⁺-ATPase activities, as well as, to immunoblotting of RAS components. The Committee for Ethics in Animal Experimentation of UFPE (n^o 0013/2017) approved the experimental procedure. The difference between group means was analyzed using one-way ANOVA followed by Tukey test.

Results:

PQ exposure led to a loss of body weight (7%, P<0.05), as well as, decreased water intake (30%, P<0.05) and increased diuresis (100%, P<0.001). It was also observed lower creatinine clearance (50%, P<0.01) in the Paraquat group in comparison to control rats, as well as increased (10%, P<0.05) SBP and heart rate. Concerning renal oxidative stress, we observed that PQ exposure led to an elevation of lipid peroxidation (75%, P<0.05), ROS levels (80%, P<0.05) and NADPH oxidase activity (20-80%, P<0.05) in both, cortex and medulla. The (Na⁺+K⁺)ATPase activity was higher (60%, P<0.01) in cortex-cortices from the PQ group than in the control group, while in the medulla, the pump activity was lower (40% P<0.05). The opposite was observed in Na⁺-ATPase activity, i.e. the activity was reduced in cortex-cortices (50%, P<0.001) and increased (40%, P<0.05) in medulla obtained from PQ-exposed rats. In addition, PQ induced elevation in cortex-cortices protein content of prorenin (50%, P<0.05), renin (100%, P<0.01), isoform 1 (40%, P<0.05) and 2 (50%, P<0.05) of angiotensin-converting

enzyme, and angiotensin II type 1 receptor (100%, P<0.01). These alterations were prevented by previous tempol treatment.

Conclusion:

PQ exposure led to a prominent urinary fluid loss that may occur due to impaired Na⁺ reabsorption induced by ROS, which may be a risk factor to vascular collapse. Moreover, paraquat led to the stimulation of cortical ATP-dependent Na⁺ transport and upregulation of pro-hypertensive RAS components that may act as an acute compensatory response.

Financial support:

FACEPE, CNPq.

9 - Respiratory Biology and Diseases

09.006 - EXOGENOUS SURFACTANT ATTENUATES VENTILATOR-INDUCED LUNG INJURY IN HEALTHY RATS. Paula LC, Chirico RN, Castro TF, Candido LS, Bezerra FS, Matos NA, - Department of Biological Sciences - UFOP

Introduction:

Mechanical ventilation (MV) is essential to maintain adequate gas exchange in surgery procedure, and it was common consent to use of large tidal volume to improve oxygenation and re-open collapsed lung units. However, this maneuver may be an inflammatory stimulus in the lungs.

Aim:

Once pulmonary surfactant has anti-inflammatory properties and acts as a therapeutic agent preventing alveolar collapse, this study aimed to investigate the intranasal effects of exogenous surfactant administration on ventilator-induced lung injury in healthy Wistar rats.

Methods:

The Ethics Committee of the Federal University of Ouro Preto approved the experiments, according to the Protocol n^o 2018/06. Male Wistar rats (8-10 weeks old), were divided into 4 groups: Control group (CG) and group pretreated with bovine surfactant (SURVANTA[®]) by intranasal instillation (BSG) were exposed to ambient air. Others rats were anesthetized, paralyzed, tracheotomized and then submitted to MV (Inspira Advanced Safety Ventilator, Harvard Apparatus) with the following ventilatory parameters: VCV mode, high tidal volume 12 mL/kg, PEEP of 3 cmH₂O, Respiratory Rate: 80 bpm, I:E ratio of 1:2 and Inspired Oxygen Fraction of 21%, during 1 hour, named MVG and the last group were pretreated with SURVANTA[®] (1 mL/kg) one hour before MV (MVBSG). After the experimental protocol, rats were euthanized, arterial blood, bronchoalveolar lavage fluid (BALF) and lung tissue were collected for analysis. Data were expressed as mean ± SEM and were analyzed by One-way ANOVA followed by the Tukey's post-test were used for statistical analyses and p <0.05 was considered statistically significant.

Results:

In BALF, the influx of total leukocytes (x10³/mL) was higher in the MVG (22.50±2.37) compared to controls, CG (9.60±0.58) and BSG (12.75±0.64). Exogenous surfactant MVBSG promoted a decrease in leukocytes (10.17±0.68) compared to MVG, specifically macrophages, lymphocytes and neutrophils. The biochemical parameters showed: the SOD enzyme activity (U/mg ptn) increased in MVG (34.61±3.24) when compared to CG (15.35±1.94) and BSG (17.74±3.19), in MVBSG we observed decrease (14.58±1.76) the activity compared to MVG; Catalase (CAT) activity (U/mg ptn) increased in MVG (2.91 ± 0.34) when compared to CG (1.42±0.24) and BSG (1.48±0.17), however we observed a decrease in the CAT activity in the MVBSG (1.91±0.12) when compared to MVG; The analysis of Thiobarbituric Acid Reactive Substances (TBARS) (nmol/ mg ptn) showed an increase in lipid peroxidation in MVG (1.13±0.13) when compared to CG (0.75±0.07), interestingly, pretreatment with SURVANTA[®] promoted decrease in TBARS concentration (MVBSG: 0.71±0.05) induced by MV (MVG: 1.13±0.13); in the last one, the levels of protein oxidation (nmol/mg ptn)

FeSBE Annual Meeting 2019

Poster Sessions and Abstracts

increased in MVG (8.94 ± 0.86) when compared to CG (4.52 ± 0.81) and BSG (4.27 ± 0.85), and pretreatment with surfactant decreased the protein carbonyl in MVBSG (3.59 ± 0.48) when compared to MVG. In the analysis of arterial blood gases, we observed that pO_2 (mmHg) was higher in MVG (136.3 ± 3.07) and MVBSG (135.5 ± 3.30) compared to CG (80.54 ± 4.17); and about $SatO_2$, we observed an increase in MVG (99.20 ± 0.20) and MVBSG (99.00 ± 0.00) when compared to CG (89.24 ± 4.09).

Conclusion:

Surfactant was able to reduce lung inflammation and oxidative stress induced by mechanical ventilation with high tidal volume in animals without previous lung disease.

Financial support:

CNPq, CAPES, FAPEMIG, UFOP and Nova Biomedical Corporation.

09.007 - COMPARATIVE STUDY BETWEEN VOLUME AND PRESSURE CONTROLLED VENTILATORY MODES IN PATIENTS SUBMITTED TO MECHANICAL VENTILATION. Bandeira ACB, Horta JGA, Almeida MR, Matos NA, Castro TF, Perucci LO, Talvani A, Bezerra FS, - Departamento de Ciências Biológicas - UFOP

Introduction:

Mechanical ventilation (MV) is an important tool in the treatment of critical patients and aims to promote adequate gas exchange. In patients submitted to MV, the maintenance of gas exchange brings consequences in the organism and its systems. It is believed that both high positive pressure and inspired oxygen fractions above 21% cause oxidative stress. This can cause the appearance of degenerative processes of the organic biomolecules and, consequently, cell death and insufficiency.

Aim:

This study aimed to analyze the oxidative effects of MV in volume controlled (VCV) and pressure controlled (PCV) modes on pulmonary and systemic inflammatory response in adult humans.

Methods:

The study was approved by the Ethics Committee of the Federal University of Ouro Preto (UFOP) according to Protocol # 2.166.790. Patients of both sexes, aged between 18 and 90 years, that were under mechanical ventilation, were divided into two experimental groups: PCV (n=9) or VCV (n=6) mode, in the first 24 hours after orotracheal intubation. After the experimental protocol, the tracheal aspirate, the serum and the ventilatory and hemodynamic parameters of the patients were collected. Statistical analyses were performed using GraphPad Prism software version 5.00 for Windows 7. Data were expressed as mean \pm SEM or median (interquartile interval) and $p < 0.05$ was considered statistically significant.

Results:

Analyzing the tracheal aspirate, we observed that the VCV mode induced more intense inflammatory response to promote an increase of neutrophil ($\times 10^3/\text{mL}$ cells) (0.245 ± 0.02) when compared to the PCV mode (0.123 ± 0.02). Also, in the tracheal aspirate, there was a significantly higher level of IL-33 (pg/mL) in patients submitted the VCV mode (0.806 ± 0.18) when compared PCV mode (0.283 ± 0.10). In blood plasma, there was a significantly higher concentration of IL-33 (pg/mL) on patients in the PCV mode (1.435 ± 0.19) when compared to VCV mode (0.658 ± 0.15). No significant difference was observed between the ventilator modes about IL-17 levels in samples of the tracheal aspirate and blood plasma, as well as, no significant differences were also observed in relation to the hematimetric parameters, the values of blood gases and the parameters of ventilatory mechanics in different ventilatory modes studied.

Conclusion:

VCV mode induced a pulmonary inflammatory response by neutrophil recruitment and higher levels of IL-33 in patients submitted to MV.

Financial support:

CNPq, CAPES, FAPEMIG, UFOP and Nova Biomedical Corporation.

09.008 - RESPIRATORY AND GESTATIONAL PARAMETERS OF OBESE MICE AFTER CHRONIC ADMINISTRATION OF β_2 ADRENERGIC AGONIST. Zavan B, Santos ALT, Lourenço LO, Paffaro JrVA, Soncini R, - Departamento de Biologia Celular e do Desenvolvimento - Unifal-MG Departamento de Ciências Fisiológicas - Unifal-MG

Introduction:

Obesity, whose spread and prevalence are alarming, compromises physiological patterns of breathing by changing volumes, frequency, inflammatory/immune status, smooth muscle tone, among others. One of the most frequently prescribed bronchodilators for low airflow or increased resistivity crisis (so common in obese patients) is the Salbutamol, a β_2 -adrenergic agonist. A physiological situation that is also capable of changing normal patterns of pulmonary ventilation is pregnancy, but little is known about the respiratory patterns of obese individuals during gestation, nor about the effect of the main drug prescribed for chronic obstructive pulmonary diseases on gestational parameters.

Aim:

To evaluate the effect of prolonged use of salbutamol on respiratory and gestational parameters in obese pregnant mice.

Methods:

Over nutrition-induced obesity by litter size reduction method was done. Obese or control female mice were treated subcutaneously with salbutamol (0.2mg/kg) or saline from the first day of gestation (GD1) until the day of interest: GD6, GD10, GD16 or until term. The ventilatory mechanics, pulmonary histology and gestational parameters such as quantity and quality of embryo implantation sites, stereological analysis of uterine Natural Killer cells (uNK), glycemic rate and weight gain of pregnant females and their offspring were evaluated. Two-way ANOVA, with post-test of Bonferroni was applied and values of $p < 0.05$ were considered indicative of significance.

Results:

The litter size reduction resulted in greater weight gain when compared to the normal litter, which persisted throughout the gestation in obese females when compared to the control females. Obesity resulted in higher glycemic indexes in GD6 (339 ± 33.1 vs 167 ± 18.7 mg/dL) and increase in adipose tissue in GD10 (2.29 ± 0.3 vs 0.59 ± 0.1 g). The analysis of ventilatory mechanics in GD6 and GD10 showed that obese individuals presented increased total resistance (5.31 ± 1.2 vs 3.62 ± 0.8 ; 6.25 ± 1.5 vs 3.49 ± 0.7 cmH₂O.s.m.L⁻¹), airway resistance (2.2 ± 0.4 vs 1.77 ± 0.3 ; 2.36 ± 0.5 vs 1.5 ± 0.2 cmH₂O.s.m.L⁻¹) and elastance (87.14 ± 16.4 vs 53.26 ± 9.4 ; 74.8 ± 16.1 vs 53.66 ± 8.7 cmH₂O.s.m.L⁻¹) after nebulization of methacholine (100mg/mL). Chronic treatment with salbutamol seems to prevent increases of total resistance (2.88 ± 0.3 , 1.48 ± 0.1 cmH₂O.s.m.L⁻¹) and elastance (49.5 ± 8.2 , 54.7 ± 9.2 cmH₂O.s.m.L⁻¹). Salbutamol treatment reduces pulmonary blood vessels luminal area (3438 ± 414.4 vs 8083 ± 1094 μm²) and its total cross-section area (8435 ± 773.4 vs 14869 ± 1764 μm²), whereas obesity seems to reduce the airway cross sections area (8023 ± 636.4 vs 13018 ± 1299 μm²) and total area (16101 ± 1780 vs 27340 ± 3715 μm²). Obese group receiving saline alone presented reduced luminal area of cross-sectioned arteries (990.4 ± 119.6 vs 1882 ± 243.6 μm²), but not in obese subjects who were treated with salbutamol (1659 ± 192 μm²). Stereological analysis of uNK cells at GD10 indicates a reduction of subtype 2 in obese individuals treated (3.44 ± 1.2 vs 9.93 ± 1.3 cell/area) or not (2.86 ± 1.2 vs 7.57 ± 0.8 cell/area) with salbutamol, and a reduction of subtype 4 (2.13 ± 0.1 vs 4.4 ± 0.6 cell/area) in obese subjects treated with salbutamol. It was observed the tocolytic effect of salbutamol, which delayed delivery in non-obese individuals. The offspring analysis suggests fetal weight reduction (0.4 ± 0.01 vs 0.51 ± 0.02 g) and placental weight gain (0.17 ± 0.01 g vs 0.14 ± 0.01 g) in obese who did not receive chronic treatment with salbutamol.

Conclusion:

Chronic treatment with salbutamol during gestation of obese mice improves respiratory parameters after bronchoconstriction-challenge, prevents exaggerated vasoconstriction of uterine spiral arteries in

FeSBE Annual Meeting 2019

Poster Sessions and Abstracts

obese individuals, and interferes with fetal and placental weight, but at the dose used, salbutamol did not have a tocolytic effect in obese mice. Studies are being conducted to elucidate the effect of salbutamol on the physical and neurological parameters of offspring.

Financial support:
CAPES e FAPEMIG

09.009 - VASCULAR REMODELLING IN AN ASTHMA MODEL IN MICE TREATED WITH ANTI-IL17 AND / OR RHO-KINASE INHIBITOR. Santos TM, Riguetti RF, Campos EC, Rezende BG, Saraiva-Romanholo BM, Camargo LN, Fukuzaki S, Prado CM, Leick EA, Martins MA, Tibério IFLC, - Ciências Médicas, Faculdade de Medicina da Universidade de São Paulo - FMUSP Hospital Sírío Libanês, Faculdade de Medicina da Universidade de São Paulo - FMUSP Department of Biological Sciences, Federal University of São Paulo - (UNIFESP) University City of São Paulo, Faculdade de Medicina, Universidade de São Paulo - UNICID/FMUSP

Introduction:

IL17 and Rho-kinase may play a critical role in regulating inflammatory and remodeling responses in inflammatory lung diseases.

Aim:

To study the effects of anti-IL17 and/or Rho-kinase inhibitor treatments on vascular changes in mice with chronic allergic inflammation.

Methods:

We used 64 BALB/c mice with pulmonary inflammation induced by ovalbumin that were treated with anti-IL-17A (7.5/µg/dose-ip) and/or Rho-kinase inhibitor (Y-27632-10mg/kg-intranasal) administered 1h before each ovalbumin challenge (22, 24, 26 and 28/days). Control animals were inhaled with saline. At the end of protocol, lungs were removed, morphometric analysis was performed to quantify vascular inflammatory, remodeling and oxidative stress responses. The Research Ethics Committee of the Hospital das Clínicas of the Faculty of Medicine of the University of São Paulo approved the present study (Case nº 064/15).

Results:

OVA-Rhoi and OVA-anti-IL17 decreased all parameters (dendritic cells, CD4+, CD8+, IL-1β, IL-2, IL-4, IL5, IL-6, IL-10, IL13, IL17, TNF-α, Rho-Kinase1, Rho-Kinase2, NFκB, TIMP1, MMP9, MMP12, iNOS, FOXP3, TGFβ, biglycan, decorin positive cells/104µm², collagen fibers and fibronectin, PGF2α contents) compared to OVA(p<0.05). Association of both treatments (OVA-Rhoi and OVA-anti-IL17) induced a decrease in: CD4+(2.3±0.6), CD8+(9.2±1.4), IL-1β(8.5±1.2), IL-2(4.5±0.9), IL-4(0.6±0.1), IL5(1.8±0.7), IL-6 (0.3±0.1), IL-10(3.2±1.1), IL13(2.4±0.8),IL17(2.9±0.6), Rho-Kinase1 (1.6±0.3), Rho-Kinase2 (1.1±0.4),NFκB(2.0±0.7),TIMP1(3.1±0.7),MMP9(9.3±1.0),MMP12(4.2±0.9), iNOS(6.0±1.3), FOXP3(1.0±0.6), TGFβ(1.4±0.4), decorin(8.2±1.2) positive cells/104µm² and collagen fibers(12.1±1.5%),PGF2α (21.7±1.6%) contents in vessel walls compared to OVA group (p<0.05). OVA group data: (CD4+: 5.5±0.4, CD8+: 40.8±3.3, IL-1β: 35±6.5, IL-2: 9.8±0.9, IL-4: 9.2±1, IL5: 14.6±1.9, IL6: 5±0.9, IL-10: 7.8±1.2, IL13: 6.8±1.4, IL17: 12.1±0.9, Rho-Kinase1: 12±1, Rho-Kinase2: 9.6±1.8, NFκB: 6.3±1, TIMP1: 8.1±1.6, MMP9: 14.4±1.4, MMP12: 8.8±1.8,iNOS: 22.4±3.6, FOXP3: 7.1±1.8, TGFβ: 24.9±1.7, decorin: 20.6±3.3 positive cells/104µm²) and collagen fibers (21±1.7),PGF2α (31±2.1%) contents.

Conclusion:

Anti-IL17 or Rho-kinase inhibitor modulate vascular inflammation, remodeling and oxidative stress responses. The association of these drugs does not potentiate the control of these responses compared to isolated treatments in this asthma model.

Financial support:

FAPESP, CNPq, LIM20-HC-FMUSP

10 - Neurobiology

10.015 - ARGONAUTE 2 TRANSLOCATES TO NUCLEUS DURING THE RETINAL DEVELOPMENT, AND IT IS INVOLVED IN THE DIFFERENTIATION OF SPECIFIC NEURONAL SUBTYPES. Móvio MI, Walter LT, Kihara AH, - CMCC - UFABC

Introduction:

MicroRNAs (miRNAs) are small non-coding RNAs that control protein levels in post-transcriptional manner. The action of miRNAs depends on a well-orchestrated machinery that includes several elements. In this regard, it is particularly interesting the role of Argonaute-2 (AGO2), an essential protein in RNA-induced silencing complex (RISC).

Aim:

The main aim of this work was to characterize the role of AGO2 in retinal development.

Methods:

Long Evans rats in early post-natal (P0) and adult (P60) ages was provided by UFABC vivarium, kept in 12:12h dark-light cycle. Animals were euthanized using intraperitoneal urethane (25%) and decapitation. Retinas were harvested to describe AGO2 in the developing and adult retina using real-time PCR (n=6), ii) western blotting (WB, n=5) and immunofluorescence (IF) (n=6). We also employed Manders' and Spearman coefficient analyses (n=6) for AGO2-nucleous colocalization. To induce AGO2 knockdown, morpholino oligo (MO) or scramble control oligo (Ctl) were injected in P0 subretinal space, and retinas were harvested after 7 days for WB (n=8), IF (n=6), and hematoxylin-eosin staining (HE, n=6). All procedures were approved by UFABC Animal Care Ethics Committee (16/2014) and results were measured using descriptive statistics and compared by paired t-test.

Results:

PCR and WB revealed that both gene expression and protein levels of AGO2 are lower at P0 (PCR: 2⁻¹=0.5-fold expression; P<0.05; WB: P0: 0.57±0.07 vs P60: 1.18 ± 0.09 normalized optical density, P<0.01). IF and fractionated protein quantification showed no changes of AGO2 in cytosol, while in P60 AGO2 cumulates in nucleus (P0: 15.63±1.77 vs P60: 23.95±2.32, P<0.05). When AGO2+ cells were analyzed, results showed that AGO2 localization depends on cell differentiation state. In P0, Spearman analysis showed lower nuclear AGO2 in immature cells than in mature (-0.04±0.22 vs 0.25±0.18, p<0.05), while Manders' revealed no changes in nuclear AGO2 in differentiated ganglion cells. MO treatment caused reduction of 52% in AGO2 protein levels, which induced several changes in the retina, as reduction in the thickness of the inner nuclear layer (Ctl:17.37±1.25 vs MO:13.69±1.38, P<0.05), increase in PKCα+ bipolar cells (Ctl: 14.83 ± 1.39 vs MO: 18.58 ± 0.67, P<0.01), CR+ amacrine cells (Ctl: 4.58 ± 1.56 vs MO: 11.17 ± 2.19, P<0.05), and decrease in ChAT+ amacrine cells (Ctl: 5.50 ± 0.58 vs MO: 6.00 ± 0.71, P<0.05).

Conclusion:

Taking together, our results revealed that AGO2 translocates to nucleus during retinal development, and its presence is essential for coordinated formation of retinal cell layers and differentiation of retinal subtypes.

Financial support:

FAPESP (2017/26388-6)

10.016 - RELATIONSHIP BETWEEN THE CHOLINERGIC SYSTEM AND IL-2 IN NEONATAL RAT RETINAL CELLS MAINTAINED IN CULTURE. Colares TG, Araujo EG, - Neurobiologia - UFF

Introduction:

Previous work from our group showed that treatment of rat retinal cell cultures with IL-2, for 48h, increased the uptake of [3H]choline. It was also demonstrated that acetylcholine released from T cells regulates IL-2 secretion (Mashimo et al., 2016).

Aim:

FeSBE Annual Meeting 2019

Poster Sessions and Abstracts

The aim of this study was to investigate the effect of IL-2 on the levels of cholinergic receptors and if the cholinergic activation induced by carbachol treatment could regulate the levels and expression of IL-2 in rat retinal cell cultures.

Methods:

Retinas from Lister Hooded rats were dissected in calcium and magnesium-free salt solution. After, was carried out the process of chemical dissociation with trypsin 0,1%. Following, retinas were mechanically dissociated through a glass Pasteur pipette, and the cells were plated to Petri dishes or in coverslips placed in 24-well plates previously coated with poly-L-ornithine (25µg/mL). The cultures were maintained in 199 culture medium (containing 5 % fetal bovine serum, glutamine and antibiotics) in the presence or not of carbachol (25 µM) or IL-2 (50U/mL) and incubated at 37°C in a humidified atmosphere of 5 % CO₂ and 95 % air for 45min, 24h and 48h. To investigate the levels of cholinergic receptors and IL-2 by western blot, after the incubation period the total proteins were extracted and assayed by the Bradford method. Statistical analysis was determined by Student's t-test. To evaluate the expression of IL-2 and its co-localization in retinal ganglions cells by immunocytochemistry, the culture medium was removed and the cells were fixed with paraformaldehyde (2,5%). The analysis of the immunofluorescence images captured in the Leica deconvolution microscope was based on qualitative criteria. Procedures using animals were approved by local committee on Ethics and Animal Use (CEUA/UFF, project nº 294).

Results:

Our results demonstrate that treatment with IL-2, for 45min, leads to a decrease in M1 (CT=100%; IL-2=74%; EPM=2%), M2 (CT=100%; IL-2=64,49%; EPM=10,54%), M3 (CT=100%; IL-2=73,89%; EPM=5,29%) receptors levels and an increase in M4 receptor levels (CT=100%; IL-2=144,2%; EPM=9,58%) and M5 (CT=100%; IL-2=128,3%; EPM=5,78%). Analyzing the levels of $\alpha 7$ subunit we observed a decrease (CT=100%; IL-2=66,18%; EPM=7,04%). In the time period of 24h, we observed a reduction in M1 (CT=100%; IL-2=70%; EPM=4,04%), M3 (CT=100%; IL-2=59,02%; EPM=2,74%) and M5 (CT=100%; IL-2=64,15%; EPM=7,67%) receptors. However, M2 and M4 receptor levels did not change. The levels of the $\alpha 7$ subunit increased in 24h (CT=100%; IL-2=130,7; EPM=7,25%). In the time interval of 48h, we observed a decrease in M1 (CT=100%; IL-2=66,64%; EPM=4,73%), M2 (CT=100%; IL-2=59,01%; EPM=9,35%), M4 (CT=100%; IL-2=75,63; EPM=7,24%) receptors levels and an increase in M5 (CT=100%; IL-2=125%; EPM=2,81%) receptors and $\alpha 7$ subunit levels (CT=100%; IL-2=122,6%; EPM=9,69%). M3 receptor levels were not altered. The treatment with carbachol, for 45min (CT=100%; IL-2=164,7%; EPM=7,12%), 24h (CT=100%; IL-2=137,3%; EPM=8,51%) and 48h (CT=100%; IL-2=130,1%; EPM=5,91%) increases IL-2 levels. We also observed an increase in the intensity of labeling for IL-2 in cultures treated with carbachol, for 45 min.

Conclusion:

In conclusion, we may suggest that IL-2 modulates cholinergic receptors and that carbachol is able to regulate IL-2 levels with possible effects on the process of retinal tissue differentiation.

Financial support:

CNPq, CAPES, INCT - NIM e PROPPI-UFF.

10.017 - OUABAIN PROMOTES M2 MICROGLIA POLARIZATION AND UPREGULATION OF THE TRKB/BDNF PATHWAY IN RAT RETINAL CELL CULTURES. Oliveira ACR, Ventura JV, Giestal-de-Araujo E, - Neurobiologia - UFF

Introduction:

The retina is originated from the neural ectoderm and its development encompasses different phenomena including a programmed cell death (PCD), where approximately 50% of the neurons initially generated die. Retinal ganglion cell (RGC) progenitors are the first cells to leave the cell cycle and have a well-established PCD period (from P0-P10). In retinal cell cultures 50% of RGCs die after 48 hours. Microglial cells enter in the

retina during early development period and are naturally activated by PCD. Microglia polarization is classified in M1 (pro-inflammatory and neurotoxic) and M2 (anti-inflammatory and neuroprotective). Arginase-1 is a marker for M2 microglial phenotype. Ouabain (OUA) is a steroid glycoside with well-known immunomodulatory action. We previous demonstrated the trophic effect of 3nM OUA on RGC survival after 48h in culture; an effect mediated by cytokine production. OUA treatment also regulates microglial activation.

Aim:

The aim of this work is to investigate if OUA promotes M2 microglia polarization.

Methods:

Rats (P2) were killed, their retinas dissected, the cells dissociated, plated at 105 cels/cm² in Petri dishes and maintained in 199 medium (CT) or in the presence of medium and OUA in atmosphere of 5% CO₂ / 95% air at 37 ° C. Levels of proBDNF, BDNF, p75, pTrkB, arginase-1 and pCREB were determined by the Western Blot. The number of RGCs was obtained following the systematic count in light field microscopy. Experimental procedures with animals were approved by the UFF Ethics Committee on Animal Use (726/2016).

Results:

OUA increases Arginase-1 levels at 15 min and 48h (CT 100% - OUA 161% ± 6,7 n=3 p=0,001; CT 100% OUA 146% ± 5,3 n=3 p=0,001 respectively) and decreases at 24h (CT 100% OUA 65% ± 10,7 n=3 p=0,02). OUA regulates the levels of proBDNF in 15min (CT 100% OUA 136,1 ± 4,4 n=3 p=0,02), 24h (CT 100% OUA 130,0 ± 5,3 n=3 p=0,04), 48h (CT 100% OUA 83,4 ± 1,8 n=3 p=0,02) and the levels of BDNF in 15min (CT 100% OUA 88,66 ± 2,9 n=3 p=0,08), 24h (CT 100% OUA 61,8 ± 3,1 n=3 p=0,004), 48h (CT 100% OUA 139,5 ± 3,8 n=4 p=0,003). The blockade of MMP-9 decrease BDNF levels (CT 100% OUA 139,5 INIB 112,3 OUA+INIB 74,7 n=3 p=0,003) and increased the proBDNF levels (CT 100% OUA 83,4 INIB 134,4 OUA+INIB 188,5 n=3 p=0,001). Also the inhibition of MMP-9 completely abolished the effect of OUA on the RGCs survival. Moreover at 48h we observed an increase pTrkB (CT 100% OUA 125,0 ± 5,0 n=3 p=0,001) and a Preliminary results (n=2) indicate an increase of 32% in pCREB.

Conclusion:

Our results demonstrate that the OUA treatment promotes M2-microglial polarization and BDNF/TrkB signaling, leading to an increase in RGC survival.

Financial support:

CAPES, FAPERJ, CNPq, INCT-NIM.

10.018 - A UNIFYING HYPOTHESIS FOR THE EFFECTS OF HIPPOCAMPAL NEUROGENESIS ON ANXIETY, MEMORY AND PATTERN SEPARATION. França TFA, - Fisiologia - FURG

Introduction:

The generation of new neurons in the brain of adult mammals (known as hippocampal neurogenesis (HN)) has been a topic of intense research over the last two decades. Much of this research tried to unravel HN's functional significance, and a lot of evidence was gathered implicating HN in various behaviors related different hippocampus-dependent processes, including memory, anxiety and pattern separation. However, there are many open questions about the mechanisms behind HN's effects on behavior. Although there are many hypotheses to explain the effects of HN manipulation in different behaviors, there is a shortage of unifying hypotheses that can explain HN's effects on all of those behaviors at once.

Aim:

A particularly promising hypothesis emerged when researchers found that immature adult-born neurons recruit inhibitory interneurons in the dentate gyrus, and this was suggested as a possible mechanism behind HN's behavioral effects. My goal here was to provide a deeper analysis of this hypothesis, originally conceived to explain HN's effects on

FeSBE Annual Meeting 2019

Poster Sessions and Abstracts

pattern separation, to see if it can account for HN's effect on anxiety and memory as well.

Methods:

To see if immature neurons' effects on inhibitory circuits can account for the different behavioral effects of HN, I adapted the Hill equation, widely used in biochemistry, to build a very simple mathematical model to analyze the effects of HN manipulations in hippocampal representations, and I compared the model's dynamics with behavioral and electrophysiological evidence available in the literature.

Results:

The model showed that ablating HN increases the number of neurons recruited to represent a given memory and the increase is proportional to the intensity of the stimulus given to the hippocampus. Crucially, the additional neurons recruited when there is no HN have receptive fields that don't match the stimuli as well as the neurons recruited when there is HN. This adds noise to the hippocampal representations, thus impairing memory and pattern separation. In addition, the increased hippocampal activity caused by the removal of HN could lead to anxiety-related behaviors since the level of activity of hypothalamus-projecting neurons in the anterior hippocampus is linked to the behavioral expression of anxiety. By comparing the model's dynamics with the trends observed in the literature, I was able to explain some general patterns in the behavioral data and to isolate key factors determining the magnitude of HN's effects. One of those factors is the efficiency of the animals' inhibitory circuits, which has important implications for comparative studies. Between-species variations in the number and connectivity pattern of inhibitory interneurons in the hippocampus (like those that are known to exist between rodents – the animal models used in most HN studies – and primates) could lead to differences in the relative importance HN for adult animals of different species.

Conclusion:

The conclusions of the analysis suggest that HN's effects on inhibitory circuits can explain the impact of neurogenesis in both emotion and cognition and provide a framework to interpret future studies in different species. The work also suggests new experiments that could significantly advance our understanding of the mechanism behind HN's effects on behavior.

Financial support:

O presente trabalho foi realizado com apoio da Coordenação de Aperfeiçoamento de Pessoal de Nível Superior - Brasil (CAPES) - Código de Financiamento 001

10.019 - PHARMACOLOGICAL INHIBITION OF ENHANCER OF ZESTER HOMOLOG 2 (EZH2) MODULATES NEUROINFLAMMATORY RESPONSE AND PROMOTES BETTER MOTOR FUNCTION RECOVERY AFTER RAT SPINAL CORD INJURY.. Correia FF, Morena BC, Gonçalves FRC, Paschon V, Kihara AH, - Centro de matemática, computação e cognição - UFABC

Introduction:

Spinal cord injury (SCI) is a traumatic neurologic disorder with clinical relevance due to the disruption of neuronal communication between the central nervous system (CNS) and peripheral nervous system. After the primary injury, often caused by mechanical trauma, the condition could aggravate by local tissue inflammation. Nowadays, it is already known that epigenetic-related processes contribute to the spread of CNS damage. Epigenetic is often related to alterations in the chromatin structure which are capable to change the genetic expression without altering the DNA sequence and are mainly related to histones modifications through methyl and acetyl group addition. Within this context, global methylation and especially the methylation on lysine 27 of histone 3 produced by Enhancer of Zeste Homolog 2 (EZH2) was related to modulation of the inflammatory response and cellular death in CNS infections. However, the role of EZH2 after a neuronal injury is not well described.

Aim:

The aim of this project was to describe the role of EZH2 activity on inflammation progress and tissue regeneration through pharmacology inhibition (GSK343) one hour after rat SCI.

Methods:

To this end, we combined immunofluorescence (IF) analyses with motor function evaluation as provided by Basso, Beattie, and Bresnahan (BBB) test and grid scale. Results were compared by student test T or two-way repeated measures ANOVA followed by appropriate posthoc test. All procedures were conducted in accordance with CEUA (2066300916).

Results:

IF results in sections of the spinal cord revealed that after acute SCI (24h after injury) the number of CD86 positive cells changes in the white matter. When compared to controls (only vehicle) the treatment with GSK343 increases the number of CD86-positive cells (588 ± 251 vs. 1298 ± 150 ; N= 5; $P < 0.01$), while the pixel intensity analysis demonstrated a reduction on individual bright of this marker (0.01 ± 0.002 vs. 0.0078 ± 0.0013 ; N= 5; $P < 0.01$). Moreover, when compared to controls, GSK343 treatment after SCI increased the score in BBB test 6 weeks after injury (7.28 ± 1.68 vs. 14.55 ± 2.25 ; N= 9; $P < 0.05$), grid-scale ($0.0\% \pm 33.3$ vs. $83.33\% \pm 36.07$ vs.; N= 6; $P < 0.05$) and subBBB scale (4.28 ± 1.04 vs. 7.88 ± 1.50 ; N= 9; $P < 0.05$). In addition, 6 weeks after injury, IF results evidenced that when compared to controls, growth-associated protein 43 (GAP43) pixel intensity is higher in the rostral region of the spinal cord (8.64 ± 0.05 vs. 17.3 ± 1.95 ; N=3; $P > 0.01$).

Conclusion:

All these data suggest the participation of EZH2 in immunological innate response, especially on CD86 expression. Also, the presence of EZH2 may influence the adaptive response, which is related to the axonal regeneration and motor function recovery.

Financial support:

FAPESP

10.020 - SHORT-TERM EFFECTS OF LACTATE ADMINISTRATION ON THE BRAIN INFARCT IN NEONATAL RATS SUBMITTED TO HYPOXIA-ISCHEMIA. Andrade MKG, Tassinari ID, daRosa LA, Rodrigues TL, Fabres RB, Paz AH, deFraga LS, - Departamento de Fisiologia - UFRGS Departamento de Ciências Morfológicas - UFRGS

Introduction:

Neonatal hypoxia-ischemia (HI) is the main cause of mortality and morbidity in human neonates. Lactate (LAC) is a metabolic substrate which is receiving more attention due to its putative neuroprotective actions on the brain.

Aim:

Here, we aimed to investigate if lactate administration is able to reduce the infarct volume on the neonatal brain following HI.

Methods:

Seven-days-old (P7) male Wistar rats (n=4) were assigned to four experimental groups: HI (rats submitted to HI), HILac (rats submitted to HI that received LAC), SHAM (rats underwent fictitious surgery) and SHAMLac (SHAM rats that received LAC). HI rats underwent a surgery for ligation of the right common carotid artery followed by exposure to a hypoxic atmosphere (8% of oxygen) for 60 min at 33°C. LAC was administered intraperitoneally 30 minutes, 2 hours and 18 hours after HI. Animals were euthanized at P8 and their brains were sliced (3 mm thick) and stained with TTC (triphenyltetrazolium chloride) in order to evaluate the volume of brain lesion. The volume of brain infarct (ipsilateral to carotid occlusion) was expressed as a percentage of lesion relative to the volume of the hemisphere contralateral to the lesion. Data were analyzed by two-way ANOVA followed by Bonferroni and expressed as mean \pm SEM. This study was approved by the Institutional Animal Care and Use Committee of the Hospital de Clínicas de Porto Alegre (#18-0258).

Results:

FeSBE Annual Meeting 2019

Poster Sessions and Abstracts

Animals submitted to HI showed an infarct volume of $17.6 \pm 3.2\%$ in the brain hemisphere ipsilateral to carotid occlusion. However, HI animals which received LAC (HILac) showed a significant reduction to $6.0 \pm 1.9\%$ in the volume of infarct ($p < 0.05$). No visible lesions were detectable in the brains of SHAM animals (SHAM and SHAMLac groups).

Conclusion:

In summary, LAC administration reduced the brain damage suggesting a neuroprotective role of LAC in animals submitted to HI. This short-term effect of LAC could indicate LAC is protecting brain by acting as an energy fuel. Additional experiments are required to understand the mechanism of action by which LAC may be protecting the brain.

Financial support:

Conselho Nacional de Desenvolvimento Científico e Tecnológico (CNPq), Fundo de Incentivo à Pesquisa e Eventos do Hospital de Clínicas de Porto Alegre (FIPE/HCPA), Pró-Reitoria de Pesquisa (PROPEQ/UFRGS).

10.021 - MITOPHAGY- AND AUTOPHAGY-RELATED PROTEINS ARE REDUCED BEFORE PROTEIN AGGREGATION IN THE HIPPOCAMPUS OF A MOUSE MODEL OF ALZHEIMER'S DISEASE. Henrique AM, Ferrari MFR, - Departamento de Genética e Biologia Evolutiva - USP

Introduction:

Loss of protein quality control and the impairment of the autophagic pathway contribute to the cellular events that culminate in neurodegeneration. In view of this, the purpose of the present study is to evaluate the cellular quality control system in genetically modified mouse model for Down syndrome, which can also be used to study the Alzheimer's disease related to triplicated copies of important genes to this neurodegenerative disease. The experiments were conducted before and after the appearance of the protein aggregates that are characteristic of neurodegenerative diseases. To this end, levels of Pink1 (PTEN-Induced Kinase 1) and Parkin, two proteins widely associated with mitophagy, and C9orf72, associated with autophagy traffic, were analyzed in the hippocampi of 2- and 5-months old mice. It is noteworthy that Parkin acts as an indirect Pink1 promoter via the Presenilin 1, Presenilin 2 and Amyloid Intracellular Domain, and that Pink1 also acts upstream of Parkin by phosphorylating its Ubiquitin-like Domain, leading to its activation.

Aim:

The objectives of the study were to evaluate the cellular quality control system in these mice via the measurement of Pink1, Parkin and C9orf72 levels in the hippocampi before and after protein aggregation.

Methods:

The genetically modified animals of the B6EiC3Sn-Rb(12.Ts1716Dn)2Cje/CjeDnJ strain were genotyped and divided between control (down-) and experimental (down+) groups. The hippocampi of 5 mice of each group were extracted. Afterwards, protein extraction was made, followed by quantification. Using SDS-PAGE and western blotting techniques, the proteins in each sample were quantified. Anti-Pink1 (Abcam Ab23707), Anti-Parkin (Cell Signaling #2132) and Anti-C9orf72 (Santa-Cruz sc-138763) antibodies were used to label the correspondent proteins. Anti- β -actin (Santa Cruz sc-47778) was used as the loading control. The data were submitted to two-way ANOVA and Bonferroni statistical analyses. All methods were approved by the ethical committee (CEUA) of the Institute of Biosciences (USP) - protocol nº 271/2016.

Results:

Immunoblotting analyses revealed that the levels of Pink1 are reduced from 2-months control (2MC) to 2-months down (2MD) mice (-36%; $p < 0.05$; $n = 4$). The reduction is bigger when comparing 2MC to 5-months control and 5-months down (5MC; 5MD) (-39%; $p < 0.001$). Between the two 5-months old groups, however, no significant change is observed. Parkin also displays a reduction from 2MC to 2MD (-52%; $p < 0.01$; $n = 4$) and between 2M and 5M mice (-79%; $p < 0.0001$). The levels of C9orf72 were also reduced in 5MD in comparison to 5MC mice (-27%; $p < 0.05$; $n = 4$). Between other groups, however, no change was observed.

Conclusion:

This study demonstrated that the expression of the mitophagy-related proteins Pink1 and Parkin is reduced in Alzheimer's model mice in comparison to the control ones, indicating that there might occur a premature aging in the central nervous system of these animals. The autophagy-related protein C9orf72 is also reduced in the same mice in comparison to the control ones, but only between 5-months old mice.

Financial support:

FAPESP

10.022 - REGULATION OF CREB ACTIVITY DURING RETINAL DEVELOPMENT. Gomes-da-Silva NC, Paes-de-Carvalho R, - Departamento de Neurobiologia - UFF

Introduction:

CREB (cyclic nucleotide responsive element binding protein) is a nuclear transcription factor which is phosphorylated in its 133-serine residue by PKA or other kinases and is regulated by NMDA and AMPA ionotropic glutamate receptors. CREB activates certain gene sequences leading to an increase in transcription of anti-apoptotic proteins and growth factors such as BDNF (brain-derived neurotrophic factor). CREB functions are related to neurogenesis (cell proliferation, differentiation and survival) as well as to long-term synaptic potentiation and neural plasticity. In the retina, it was already demonstrated a stimulation of CREB phosphorylation by adenylyl cyclase-coupled receptors such as dopamine or adenosine receptors as well by glutamate AMPA or NMDA receptors.

Aim:

The aim of this work is to evaluate CREB activation by different neurotransmitter systems during development of the chick embryo retina and to study the signaling pathways involved.

Methods:

Retinas from 10 and 16 day-old White Leghorn chicken embryos were dissected in CMF and submitted to ex vivo studies preincubating for 10 minutes at 37°C in Hanks with 500 μ M RO-201724 (phosphodiesterase inhibitor) and 0.5U/ml of adenosine deaminase (to eliminate endogenous adenosine) and next incubating with Forskolin (50 μ M, direct activator of adenylyl cyclase), CGS21680 (50nM, adenosine A2a receptor agonist), Glutamate (1mM) or Dopamine (50 μ M) for 10 minutes. Samples were then processed for western blotting. To analyze CREB activity we used anti-phospho ser-133 and anti-total Creb antibodies. These experiments were carried out with the approval of the Animal Research Ethics Committee of the Fluminense Federal University (number 00146/09).

Results:

In E10 retinas, treatment with Forskolin promoted a dramatic increase of CREB phosphorylation ($562,1\% \pm 104,3$, $n = 5$). However, no significant effect was observed when incubating with CGS21680 or Dopamine ($126,3\% \pm 40,2$, $n = 2$ or $83,2\% \pm 24,2$, $n = 2$, respectively). On the other hand, glutamate promoted a small effect in this age ($166,9\% \pm 48,6$, $n = 5$). Surprisingly, in E16 Forskolin had a small inhibitory effect ($76,8\% \pm 3,2$, $n = 4$) while glutamate still promoted a similar significant stimulation ($171,1\% \pm 41,3$, $n = 3$).

Conclusion:

Several different ideas outcome from our present results. 1) Since Forskolin activates adenylyl cyclase and promotes cAMP accumulation in both E10 and E16, it appears that the coupling between activation of PKA and CREB phosphorylation is no longer present in older developmental stages as E16, suggesting that this pathway is important for early retinal developmental functions. Interestingly, dopamine, which promotes cAMP accumulation in E10, is not able to activate CREB in this developmental period. 2) Activation of glutamate receptors promotes CREB activation in both developmental stages.

Financial support:

CNPq, Faperj and UFF

FeSBE Annual Meeting 2019

Poster Sessions and Abstracts

10.023 - COMBINATION EFFECTS OF SULFASSALAZINE AND CAFFEIC ACID IN GLIOBLASTOMA CELL LINEAGES. Romano I, Carvalho MV, Santos GMB, Cossenza M, - Neurociências - UFF

Introduction:

Glioblastoma (GB) is the most common and lethal brain cancer. The median survival of patients diagnosis with this pathology are about 14 months. Now a days the main treatment for GB consist in the surgical resection of the tumor followed by radiotherapy and chemotherapy. Even after the treatment the tumor presents recidiva in all cases. There is no cure for GB. Sulfasalazine, an already used anti-inflammatory drug, are capable of decrease viability of GB in vivo and in vivo through inhibition of a cystine glutamate exchanger called xC⁻ and, consequently, decrease of glutathione (GSH) and increase of reactive oxygen species (ROS). Caffeic Acid (CFA) is one of the composes presents in coffee. There are evidences of the antitumoral effect of CFA through increase of ROS. This effects are already described in C6 GB cells in vivo.

Aim:

The main objective of this study is evaluating the combine effects of sulfasalazine and caffeic acid in GB lineages in vitro.

Methods:

Cell Culture: The U87MG GB Cell Linage was maintained in DMEM F-12 culture medium with 10% of fetal bovine serum in 37 degrees Celsius and 5% of CO₂ Time Course: The U87MG cells was treated with 1000µM of CFA, SAS and SAS+CFA for 24, 48 and 72 hours. In each time a photo was taken in a phase contrast microscopy (20x objective). The cells present in each field of the image was counted. Dose Response Effects: The U87MG cells was treated with 125, 250, 500, 1000 and 2000µM of CFA, SAS and SAS+CFA for 48 hours. In the end of the treatment the cells were stained with houesht and a photo using a fluorescence microscope was taken (20x objective). The stained nuclei were counted. ROS Assay: The U87MG cells was treated with 1000µM of CFA, SAS and SAS+CFA for 24 hours. In the end of the treatment the cells were stained with H₂DCFDA and a photo using fluorescence microscope was taken (20x objective).

Results:

Time Course Viability: The U87MG cells presented a decrease in viability in the treatments with SAS and SAS+CFA in all times. The combine treatment with SAS and CFA generated a greater drop in the viability of U87MG cells (n=3). Dose Response Effects: The treatment with SAS and CFA together presented a bigger decrease of the U87MG cells in all concentrations when compared with the treatment only with SAS (n=3). ROS Assay: The treatments with SAS and SAS+CFA increase the ROS levels in U87MG cells. The combine treatment with SAS+DHA present high levels of intracellular ROS when compared to SAS only (n=3).

Conclusion:

We observe that the treatment using SAS and CFA together are capable of decrease the cell viability of U87MG cells in vitro more than the treatment only with SAS in various concentrations. We also know that the combine treatment increase intracellular ROS more than the treatment with SAS only.

Financial support:

CAPES; CNPq, FAPERJ; Propri UFF

10.024 - CLUSTERIN PREVENTS ENDOPLASMIC RETICULUM STRESS DURING OVEREXPRESSION AND AGGREGATION OF A-SYNUCLEIN IN DOPAMINERGIC NEURONS. Queiroz EO, Sakugawa AYS, Ferrari MFR, - Genética e Evolução - IB

Introduction:

Alpha-synuclein (α -syn) is an important protein mainly involved in synaptic transmission between neurons through association with synaptic vesicles membranes. In Parkinson's disease (PD) α -syn can form aggregates and also associates with organelles, proteins, cytoskeleton, lipids, nucleic acid and others impairing cell physiology. Endoplasmic reticulum (ER) is sensitive to accumulation of misfolded

proteins becoming stressed, which triggers the Unfolded Protein Response (UPR) in order to restore normal cellular function by increasing levels of chaperones involved in proteins folding. Proteinopathy spreading is present in PD through exosome exocytosis, transfer through plasma membrane and nanotubes. Clusterin (CLU) is an extracellular chaperone, secreted by cells, involved in homeostasis, proteasis, inhibition of cell death pathways with a pro-survival signal and is found up-regulated during neurodegeneration, such as in Alzheimer's disease, and in cancer.

Aim:

Considering the α -syn cytotoxicity and its pathological roles on dopaminergic neurons, the purpose of the present study is to analyse the role of CLU on the levels of proteins associated to ER stress in dopaminergic neurons derived from SH-SY5Y cells.

Methods:

SH-SY5Y was plated in 24 well dish and differentiated into dopaminergic neurons during eleven days with all-trans retinoic acid. SH-SY5Y neuron-like cells were transfected with the following plasmids: Empty Vector (EV) and α -syn Wild Type (WT), A30P and A53T mutants. CLU was added in medium in a concentration of 1mg/ml during transfection period (48 hours). Soluble fraction of SH-SY5Y neuron-like protein extract was collected and analysed by Western Blot. In order to target UPR proteins GRP78, GADD153 and XBP-1 the following antibodies was used: GRP78 (BiP) (C-20) sc-1051 [1/1000], GADD153 (CHOP) H-5 sc-166682 [1/500] and XBP-1 Antibody (M-186) sc-7160 [1/500]. The data was analysed by Two Way ANOVA.

Results:

α -syn WT increases the levels of BiP 50% compared to control group, but CLU prevents that increase in expression of BiP in about 75% for WT and 30% for A53T. However, the sample expressing α -syn A30P does not change expression of BiP, but when treated with CLU its levels becomes higher in almost 50% compared to control group. α -syn WT increases the level of CHOP in about 30% compared to control, but the exposure to CLU decreases in 30% compared to the non treated α -syn WT sample. In α -syn A30P the levels of CHOP expression decrease in 50% when treated with CLU compared to non treated sample. XBP-1 is increased in 100% compared to control group in cells expressing α -syn A53T, but when treated with CLU decreases to 35% of the control group levels. CLU also decreases XBP-1 levels in α -syn WT and A30P samples to 57% and 22%, respectively.

Conclusion:

Expression of α -syn and its mutations causes ER-stress that is prevented by CLU exposure.

Financial support:

FUNDING SUPPORT: FAPESP 2018/12978-9

10.025 - OUABAIN MODULATES THE IL-6 LEVELS IN RETINAL CELL CULTURES: THE ROLE OF IL-1BETA, TNF-ALFA AND IL-10. Azevedo MA, Araujo EG, - Neurociências - UFF

Introduction:

Cytokines are small polypeptides involved in immune response. Interleukin 6 (IL-6) is a pro-inflammatory cytokine playing an important role in physiologic events such as proliferation, survival, differentiation and apoptosis. Previously, our group demonstrated that treatment of mixed retinal cell cultures with IL-6 [50ng/mL] increases retinal ganglion cell (RGC) survival. We also showed that ouabain (OUA) increases RGC survival; an effect mediated by interleukin-1beta (IL-1beta), tumor necrotic factor alfa (TNF-alfa) and IL-6. Corroborating this last data, treatment with TNF-alfa [0,5ng/mL] or IL-1beta [5ng/mL] increases RGC survival. Our group also showed that OUA treatment modulates cytokine levels (IL-6, IL-1 β , TNF- α and IL-10) in retinal cell cultures.

Aim:

The aim of this study was to investigate if the increase in IL-6 levels induced by OUA treatment depends on IL-1beta, TNF-alfa and IL-10.

Methods:

FeSBE Annual Meeting 2019

Poster Sessions and Abstracts

Neonatal rats were killed, their retinas dissected, treated with 0.1% trypsin and mechanically dissociated. Cells were plated and maintained in 199 medium with or without OUA, IL-1 β , TNF- α and IL-10 in atmosphere of 5%CO₂ and 95% air at 37°C. IL-6 levels and its receptor were determined by Western blot analysis. Experimental animal procedures were approved by the Ethics Committee on Animal-UFF (project).

Results:

Our results show that in the absence of TNF- α the levels of IL-6 following OUA treatment increased 146%(\pm 18,11) in 15 min and decreased 83% \pm 10,67 after 24h. However, in the absence of IL-1 β the levels of IL-6 elicited by OUA treatment decreased in 15 min and 24h (30% \pm 10,18 and 12% \pm 4,163 respectively). But in the absence of IL-10 the levels of IL-6 in OUA treatment decreased in 15 min (20% \pm 8,686).

Conclusion:

Our data indicate that OUA has an important role in modulating the levels of IL6 and interestingly, this effect involves IL-1 β , TNF- α and IL-10 suggesting a cooperative effect of these cytokines on the regulation of IL-6 levels in retinal cell cultures induced by OUA treatment.

Financial support:

CAPES, FAPERJ, CNPq, INCT-NIM.

10.026 - DUCHENNE MUSCULAR DYSTROPHY NOT COMPROMISE THE NERVOUS SYSTEM HOMEOSTASIS IN THE ACUTE PHASE OF THE DISEASE. Petrovich ACZ, Carvalho SC, Alves GA, Franco LS, CHIAROTTO GB, - SP - São Paulo - Fundação Herminio Ometto - FHO - Uniararas

Introduction:

Duchenne Muscular Dystrophy is a progressive and degenerative neuromuscular disease characterized by the absence of dystrophin protein. It is known that alterations in the muscle interface with the nervous system caused by chronic muscular degeneration processes can retrogradely affect the spinal cord microenvironment, specifically the alpha motoneurons. However, the exact phase of the disease these alterations begin on the central nervous system is not clear.

Aim:

In the present study, we investigate the possible alterations arising out Duchenne Muscular Dystrophy on the nervous system of mdx mice.

Methods:

For this, we used C57BL /10ScCr / Uni (control group = 5) and C57BL /10-Dmdmdx / PasUni (dystrophic group = 5) male mice. The experiment occurs between the second and fourth week of animal life. The weight, length body and the inverted screen test to evaluate the muscular force were monitored two times. With 30 days, the animals were euthanized and the lumbar spinal cord, brain, and sciatic nerve were dissected and processed for histological staining and immunofluorescence techniques to evaluate the inflammatory response. In addition, the anterior tibialis and quadriceps muscle was weight for evaluating muscular atrophy.

Results:

The results showed that DMD not compromise the weight gain and growth of mdx mice when compared with control animals. These data demonstrating that in the acute phase, the disease not alters the development stage of the animals. The inverted screen analysis showed loss of muscle force in dystrophic animals when compared to controls (p<0.05). However, the mass of anterior tibialis and quadriceps muscles not showed differences between the experimental groups. In this phase of DMD, was not observed neuronal death of alpha motoneurons and neuroinflammation. Sciatic nerve staining demonstrated the absence of infiltrating cells.

Conclusion:

Overall, the results showed that in the acute phase of DMD, the alterations in the muscle not compromise the development of animals and not affect the nervous system microenvironment.

Financial support:

PIC - Institucional Centro Universitário Herminio Ometto

10.027 - EFFECT OF OUABAIN ON THE MODULATION OF INFF LEVELS IN RETINAL CELLS OF NEONATAL RATS MAINTAINED IN CULTURE.. Souto AM, Giestal-de-Araujo E, - Neurobiologia - UFF

Introduction:

Ouabain is a cardiotonic steroid hormone that at high concentrations (μ M), acts as a selective blocker of the Na⁺/K⁺ ATPase pump, while at low concentrations (nM), it stimulates the sodium and potassium pump as a ligand. In this condition Na⁺/K⁺ ATPase pump acts as a receptor and when activated induces different cellular responses such as proliferation and survival. In our laboratory, it was observed that ouabain has a trophic effect on retinal ganglion cells; an effect modulated by different cytokines such as IL-1 β and TNF- α . In fact treatment with ouabain modulates the levels of these inflammatory cytokines in different time intervals (15 and 45min and 24and 48h).

Aim:

Based in these previous results the aim of this study was to investigate the role of ouabain modulating INF γ levels, in cultures of retinal cells of neonatal rats, at different time intervals. Our objective is to analyze the role of ouabain as an immunomodulatory agent in retinal cells.

Methods:

Cultures from the retinas of neonates rat (Lister Hooded) at P2 were used in our studies. Animals were killed by decapitation and their retinas dissected in calcium and magnesium-free salt solution. Cellular dissociation were performed in two steps: first cells were chemically dissociated with trypsin 0,1% and in the second step mechanically dissociated was made using a glass Pasteur pipette. Cells were plated in Petri dishes previously coated with poly-L-ornithine (25 μ g/mL). The cultures were maintained in 199 culture medium (containing 5 % fetal bovine serum, glutamine and antibiotics) in the presence or not of ouabain and incubated at 37°C in a humidified atmosphere of 5 % CO₂ and 95 % air. Cultures were treated with ouabain (3nM) at the times of 15, 45 minutes and 24 and 48 hours. Anti-INF γ antibody at the concentration of 0.5 μ g/ml, was used for Western blot analysis. Procedures using animals were approved by local committee on Ethics and Animal Use (CEUA/UFF, 726/16).

Results:

Preliminary data shows that OUA treatment induces an increase in INF γ levels in all time intervals studied. At 15 minutes a 42% increase was obtained (CT 100%; OUA 142% n = 2). At 45 minutes a 27% increase was observed (CT 100%; OUA 127% \pm 8,587 n = 4). At 24 and 48 hours a 43% and 47% increase respectively was identified (CT 100%; OUA 143% n = 2; CT 100%; OUA 147% \pm 13.51 n = 3).

Conclusion:

Our results demonstrate that ouabain modulates INF γ levels in retinal cell culture of neonatal rats, during all the times analyzed. The present results are in accordance with those obtained by our group indicating an immunomodulatory role of ouabain in the central nervous system, in particular in the retina.

Financial support:

CAPES, FAPERJ, CNPq, INCT-NIM.

10.028 - OUABAIN EFFECT ON THE REGULATION OF A7 NICOTINIC ACETYLCHOLINE RECEPTOR LEVELS: POSSIBLE ROLE REGULATING THE INFLAMMATORY RESPONSE IN RAT RETINAL CELL CULTURES.. Terra AM, Giestal-de-Araujo E, - Neurobiologia - UFF

Introduction:

Ouabain (OUA) is considered an immunomodulatory molecule regulating cellular differentiation, proliferation and survival as well as the inflammatory processes. Previous data from our group demonstrated that OUA increases retinal ganglion cells (RGCs) survival, an effect mediated by activation of PKC pathway and the release of interleukin-1 β (IL-1 β) and tumor necrotic factor α (TNF- α) by retinal cells. Furthermore, retinal cell cultures treatment with IL-6 also showed the same RGCs survival result. Other study showed that nicotine treatment also promotes RGCs survival, an effect mediated by α 7

FeSBE Annual Meeting 2019

Poster Sessions and Abstracts

nicotinic acetylcholine receptor ($\alpha 7$ nAChR). Moreover, $\alpha 7$ subunit levels were increased in cultures following PKC activation.

Aim:

Since ouabain induces PKC activation leading to RGCs survival and $\alpha 7$ nAChR has a neuroprotective role in RGC and its level is modulated by PKC; the aim of this study was to investigate if OUA treatment modulates the levels of this receptor. We also analyzed if OUA could modulate pro-inflammatory cytokines levels with the blockade of $\alpha 7$ nAChR.

Methods:

Lister Hooded rats (P2) were killed, their retinas dissected, and cells were chemically (0,1% trypsin) and mechanically dissociated and posteriorly plated at 105 cells/cm² in Petri dishes. Cultures were maintained in 199 medium (CT) or in medium with OUA, for different periods of time (15min, 24h and 48h), in atmosphere of 5%CO₂ and 95% air at 37°C. Levels of $\alpha 7$ nAChR, TNF- α and IL-6 were determined by Western Blot analysis. Experimental animal procedures were approved by the Ethics Committee on Animal-UFF (project 726/16).

Results:

Despite preliminary data, our results suggest that OUA treatment do not change $\alpha 7$ nAChR levels in 15min (CT=100% OUA=99,2% n=2); however it shows a decreasing tendency in 24h (CT=100% OUA=88,4% n=2) and then a slight increase in 48h (CT=100% OUA=123% n=2). In the neutralization experiments, in 15min, OUA treatment increased TNF- α levels (CT=100% OUA=152,9% \pm 12,9 n=8), whereas co-treatment of OUA and MLA abolished that effect (CT=100% O+M=87,5% \pm 18 n=8). However, the inverse happens in 24h, both OUA treatment and co-treatment of OUA and MLA decreased TNF- α levels (CT=100% OUA=48% O+M=51,3% n=2). In the case of IL-6 in 15min, both OUA treatment alone and co-treatment of OUA and MLA increased its level (CT=100% OUA=161% O+M=184,9% n=2).

Conclusion:

Our results indicate that OUA treatment modulates $\alpha 7$ nAChR levels in retinal cell cultures, suggesting that OUA can promote RGCs survival by regulating that receptor. In relation to cytokines, it seems that OUA treatment loses its effect over TNF- α levels under $\alpha 7$ nAChR blockade in 15min. However, interestingly, such blockade appears to have no effect in 24h and over OUA modulation of IL-6 levels, suggesting another regulation pathway.

Financial support:

CAPES, FAPERJ, CNPq, INCT-NIM.

11 - Physical Training Responses

11.008 - SWIMMING TRAINING INCREASES SPONTANEOUS PHYSICAL ACTIVITY AND BROWN ADIPOSE TISSUE OF OVARIECTOMIZED RATS. Pejon TMM, Faria VS, Gobatto CA, Fabrício V, Beck WR, - Ciências Fisiológicas - UFSCar

Introduction:

Ovarian estrogens production absence promotes increased body mass (BM), generally associated to spontaneous physical activity (SPA) and brown adipose tissue (BAT) reduction and changes in carbohydrate metabolism that could reflect in metabolic diseases. It is known that physical training (PT) acts on these parameters, however, little is known about the effects of moderate intensity swimming training in ovariectomized rats.

Aim:

To investigate the effect of 12 weeks swimming training on BAT, SPA, glycemic and muscular glycogen content of ovariectomized (OVX) rats.

Methods:

The experimental procedure was approved by the Ethics Committee on Animal Use (CEUA) of the Federal University of São Carlos (1556060417). We assessed 36 Wistar rats distributed in control (CG; n=9), ovariectomized (OG; n=9), exercised (EG; n=9) and exercised ovariectomized groups (OEG; n=9). At 90 days-old, OG and OEG animals

were subjected to bilateral ovariectomy. At 95 days-old, EG and OEG were subjected to aquatic environmental adaptation and at 102 days-old individually performed critical load test, which consisted of 4 maximal swimming efforts with a time to exhaustion between 2 and 10 minutes, to determine the critical load intensity (CLI-%BM). The PT was performed 5 times a week for 30 minutes daily with weekly readjustment of the load equivalent to 80% of the CLI. Biweekly animals were subjected to gravimetric analysis to obtain daily SPA. After 12 weeks of experiment, 150-250 milligrams of soleus were collected. The muscular tissue was digested in potassium hydroxide (30%) for application of the phenol/sulfuric acid method and determination of the glycogen content. The inter-scapular BAT was extracted to record the total mass. The blood was collected and centrifuged to obtain the serum used for glycemic analysis by means of a commercial kit. Data were expressed as mean \pm standard deviation, subjected to analysis of variance factorial ANOVA. Significance level was set at 5%.

Results:

Regarding BM (CG: 311.70 \pm 15.24; OG: 360.02 \pm 38.21; EG: 308.59 \pm 21.10; OEG: 346.70 \pm 38.36 g), OVX increased (F=216,22; p<0.01), and PT did not promote significant alteration (F=0,40; p=0.78). Concerning BAT relativized by BM (CG: 1.31 \pm 0.30; OG: 0.99 \pm 0.23; EG: 1.80 \pm 0.24; OEG: 1.53 \pm 0.27 mg/g of rat), PT increased (F=35,63; p<0.01), while OVX reduced it (F=11,51; p<0.01). PT increased the SPA (F=19,75; p<0.01) while OVX reduced such outcome (F=6,67; p<0.05). Blood glucose was not modified by OVX (F=0,06; p=0.08) while PT reduced it (F=27,10; p<0.01) (CG: 133.99 \pm 16.77; OG: 135.07 \pm 8.31; EG: 112.16 \pm 8.11; OEG: 108.81 \pm 19.97 mg/dL). OVX did not promote difference (F=1,31; p=0.26) in muscular glycogen (CG: 0.26 \pm 0.12; OG: 0.21 \pm 0.06; EG: 0.35 \pm 0.13; OEG: 0.31 \pm 0.16 mg/100mg), but PT increased it (F=5,66; p<0.05).

Conclusion:

The PT proved to be an efficient non-pharmacological tool for reducing impairments caused by OVX on SPA and BAT, beyond positively modulating carbohydrate metabolism even under such adverse situation.

Financial support:

CNPq

11.009 - THE POSITIVE EFFECT OF SWIMMING TRAINING OF MODERATE INTENSITY ON BONE MINERAL DENSITY PRESERVATION IN RATS SUBJECTED TO FOOD RESTRICTION.. Faria VS, Pejon TMM, Beck WR, - Ciências Fisiológicas - Universidade Federal de São Carlos

Introduction:

Food restriction (FR) is an effective way to reduce body mass, but it has been associated with bone mineral density (BMD) impairment. Physical training (PT), in addition to visceral fat (VF) reduction, has been positively linked to BMD maintenance or improvement. Nevertheless, little is known about the effects of swimming training at moderate intensity on bone tissue of rats subjected to FR.

Aim:

Thus, the present study investigates the protective effect of swimming training on bone mineral density in a FR scenario.

Methods:

The experimental procedure was approved by CEUA/UFSCar (1556060417). 40 Wistar female rats were divided into four groups: control group (Ct: n=10), food restriction group (FR: n=10), exercise group (Ex: n=9) and food restriction and exercise (FRE: n=11). After aquatic adaptation, the animals were submitted to the critical load test at 108 days-old, which consisted of 4 maximum efforts of 2 to 10 minutes to determine the critical load intensity (CLI) (% body mass, % BM). Ex and FRE underwent physical swimming training for 12 weeks, 5 days/week, 30 minutes/day, with intensity equivalent to 80% of CLI. The swim was individually conducted in cylindrical, opaque tanks (100cm x 30cm x 80cm, length, diameter and height of the water, respectively) and water temperature maintained at 31 \pm 1°C. Ct. Ex received standard food "ad libitum", whereas FR and FRE were

FeSBE Annual Meeting 2019

Poster Sessions and Abstracts

submitted to a 20% reduction in the food supply in relation to Ct, relativized by body mass and adjusted weekly. 48 hours after the last training session the absolute weight of the VF was obtained and the right femur was collected for biophysical analysis. Bone volume was obtained using wet weight, immersed weight and water density and BMD was calculated through Archimedes's principle. Data were expressed as mean±standard deviation, ANOVA two-way and Newman-Keuls post hoc tests were employed with $p<0.05$.

Results:

The absolute VF value of Ex, FR and FRE ($9.76\pm 2.54g$, $1.99\pm 0.71g$, $1.98\pm 0.82g$) were significantly reduced in relation to Ct ($18.51\pm 0.82g$, $p<0.01$). In addition, there was a significant reduction in the BMD of the FR ($0.64\pm 0.03g/cm^3$) when compared to the Ct and Ex groups (0.71 ± 0.04 , $0.69\pm 0.03g/cm^3$; $p<0.01$), whereas FRE (0.67 ± 0.04) did not present a significant difference in relation to Ct, Ex and FR (0.71 ± 0.04 , 0.69 ± 0.03 ; $0.64 \pm 0.03 g/cm^3$, $p>0.05$) at the end of 12 weeks intervention.

Conclusion:

Thus, moderate intensity swimming PT plays a protective role on BMD in a FR scenario.

Financial support:

CNPq

11.010 - THE BENEFICIAL EFFECT OF SWIMMING TRAINING ON MUSCULAR AND HEPATIC GLYCOGEN STORES OF RATS SUBJECTED TO FOOD RESTRICTION AND OVARIECTOMY.. Infante NA, Pejon TMM, Faria VS, Beck WR, - Ciências Fisiológicas - Universidade Federal de São Carlos - UFSCar

Introduction:

Estrogens exerts protective effects against corporal adiposity, through increases of energy expenditure and appetite suppression. Bilateral ovariectomy (OVX) has been related to improves visceral fat (VF), contributing to several diseases, development, such as systemic arterial hypertension, acute myocardial infarction and diabetes. Food restriction is considered beneficial means for fat reduction, however, this type of intervention may lead to a marked decrease in energy stores, mainly muscle and hepatic glycogen, essential for proper cells functioning. In turn, physical training stimulates VF loss and increase glycogen stores, preserving energy metabolism. However, there is not much literature on the influence of individualized aerobic moderate intensity swimming training on glycogen levels of ovariectomized rats subjected to food restriction.

Aim:

To analyze the effect of aerobic moderate intensity swimming training in a scenario of food restriction and ovariectomy on muscular and hepatic glycogen stores.

Methods:

The experimental procedure was approved by the CEUA/UFSCar (1556060417). Twenty female Wistar of – rats 90 days old - were equally divided into 2 groups: 1) Animals subjected to food restriction and ovariectomy (GRO) and 2) animals subjected to food restriction, ovariectomy and exercise (GROE). After two weeks of water adaptation, the animals were subjected to the critical load test, which consisted of 4 maximum efforts of 2 to 10 minutes to determine the critical load intensity (CCI) (%body mass, %BM). The GRO and GROE underwent physical swimming training (PT) for 12 weeks, 5 days/week, 30 minutes/day, with intensity equivalent to 80% of CCI. The swim was individually conducted in cylindrical, opaque tanks (100cm in length x 30cm in diameter x 80cm in water depth) and water temperature maintained at $31 \pm 1 ^\circ C$. Both groups were subjected to a 20% reduction of food supply, relativized by body mass and adjusted weekly. After 48 hours of the last training session, absolute weight of visceral fat (VF), gluteus and liver were obtained. For glycogen content determination, gluteus and liver were digested in 30% potassium hydroxide (KOH) and subjected to colorimetry by the phenol/sulfuric

method. Data were expressed as mean ± standard deviation and, t-test was used for independent samples ($p<0.05$).

Results:

Absolute VF value of GRO ($0.97 \pm 0.32 g$) was significantly reduced in relation to GRO ($2.56 \pm 1.50 g$, $p<0.01$; 37.89%). In addition, there was a significant increase in GROE muscle glycogen ($0.44 \pm 0.17 mg/100mg$) when compared to the GRO group ($0.20 \pm 0.15 mg/100mg$, $p<0.01$; 45.45%) and also in the GROE hepatic glycogen ($1.55 \pm 0.38 mg/100mg$) when compared to the GRO group ($0.94 \pm 0.65 mg/100mg$, $p<0.03$; 60.64%) at the end of 12 weeks of intervention.

Conclusion:

12-week of individualized moderate intensity swimming training plays a protective role on muscular and hepatic glycogen stores even in a scenario of food restriction associated to ovariectomy.

Financial support:

CNPq - Conselho Nacional de Desenvolvimento Científico e Tecnológico

11.011 - AEROBIC EXERCISE TRAINING POSITIVELY MODULATES BROWNING OF WHITE ADIPOSE TISSUE IN OBESE MICE. Sepúlveda-Fragoso V, Giori IG, Alexandre-Santos B, Fernandes T, Oliveira EM, Vieira CP, Conte-Junior CA, Ceddia RB, Nobrega ACL, Frantz EDC, Magliano DC, - Laboratory of Morphological and Metabolic Analyses - Fluminense Federal University Laboratory of Exercise Sciences - Fluminense Federal University Laboratory of Biochemistry and Molecular Biology of Exercise - University of São Paulo Department of Food Technology - Fluminense Federal University School of Kinesiology and Health Science - York University

Introduction:

The browning of white adipose tissue (WAT) has been suggested as a possible target for treatment of obesity and evidence shows it can be modulated through exercise training (ExT) and the Renin-Angiotensin System (RAS).

Aim:

This study aims to compare the browning effects of ExT and/or treatment with Enalapril on WAT of obese mice.

Methods:

C57BL/6 mice (3-mo-old) were fed a standard-chow (SC, $n=10$) or a high-fat (HF, $n=40$) diet for 16 weeks. At 8th week, HF group was randomly divided into: HF ($n=10$), HF-Enalapril (HF-E, $n=10$), HF-Training (HF-T, $n=10$) and HF-Enalapril-Training (HF-ET, $n=10$). Body mass (BM) was evaluated weekly and systolic blood pressure (SBP), fortnightly. At 16th week, plasmatic cholesterol, glycidic metabolism, body composition and inflammatory mediators were assessed. In WAT, stereology, protein and gene expression of RAS and browning components were also measured. Data presented as mean±SD and analyzed by one-way ANOVA with Holm-Sidak post-hoc test ($p<0,05$).

Results:

HF group showed increased final BM ($40.2\pm 4.5g$, $p<0.0001$) and final SBP ($179\pm 7mmHg$, $p<0.0001$) in comparison to SC ($30.6\pm 3.2g$ and $113\pm 3mmHg$, respectively). All interventions decreased final BM (HF-E: $29.1\pm 4.8g$, HF-T: $33.4\pm 1.8g$, HF-ET: $25.7\pm 2.7g$, $p<0.05$) and SBP (HF-E: $126\pm 2mmHg$, HF-T: $131\pm 2mmHg$, HF-ET: $120\pm 2mmHg$, $p<0.0001$) in comparison to HF. OGTT and IPITT showed insulin resistance and glucose intolerance on HF group when compared to SC ($+32.33\%$, $p<0.01$ and $+47.19\%$, $p<0.01$, respectively) and all interventions improved insulin resistance (HF-E: -45.35% , $p<0.0001$; HF-T: -26.92% , $p<0,01$; HF-ET: -44.36% , $p<0,0001$), but only trained groups reduced glucose intolerance (HF-T: -24.68% , $p<0,01$; HF-ET: -18.92% , $p<0,05$). DEXA showed an increase of 56,14% of body fat mass and decrease of 35.71% of lean mass on HF group in comparison to SC. HF-E and HF-ET were able to reduce fat mass (-28.90% , $P=0,05$; -35.10% , $P=0,01$, respectively) and increase lean mass ($+44.08\%$, $p=0.052$; $+53.73\%$, $P=0.013$) when compared to HF. Plasmatic analyses revealed an increase on HF in comparison to SC group of cholesterol ($294.7\pm 39.5mg/dl$, $p<0.01$), IL-6 ($+114.48\%$, $p=0.0169$), TNF- α

FeSBE Annual Meeting 2019 Poster Sessions and Abstracts

(+37.23%, $p=0.0531$), leptin (+595.28%, $p=0.0176$) and resistin (+244.76%, $p=0.0328$). Only trained groups were able to reverse cholesterol (HF-T:238.3 \pm 3.8mg/dL, $p<0,05$; HF-ET:230.3 \pm 32.7mg/dL, $p<0,05$) and IL-6 levels (HF-T:-42.53%, $p=0.0488$; HF-ET:-40.95%, $p=0.0573$). All interventions reduced TNF- α in comparison to HF (HF-E:-29.05%, $p=0.0496$; HF-T:-27.29%, $p=0.0535$, HF-ET:-33.00%, $p=0.0138$). Trained groups increased irisin levels in relation to SC (HF-T:+58.64%, $p=0.0193$; HF-ET:+51.41%, $p=0.0421$) and HF groups (HF-T:+61.79%, $p=0.0162$; HF-ET:+54.41%, $p=0.0366$). Morphometry showed inguinal WAT hypertrophy in HF group when compared to SC (+61.92%; $p<0.0001$) and all the interventions reversed adipocyte diameter (HF-E:-39.05%, $p<0,0001$; HF-T:-37.61%, $p<0,0001$; HF-ET:-36.89%, $p<0.0001$). Islets of browning on inguinal WAT were only found on trained groups. AT1R was increased in HF group when compared to SC (+51.4%, $p<0.05$) and all interventions were able to reverse (HF-E:-71%, $p<0.0001$; HF-T:-80%, $p<0.0001$; HF-ET:-73%, $p<0.0001$). MasR and ACE2 levels were increased in all treated groups in relation to HF (HF-E:+186%, $p<0.001$; HF-T:+116%, $p<0.05$; HF-ET:+355%, $p<0.0001$ and HF-E:+988.8%, $p=0.0051$; HF-T:+1181.2%, $p=0.0010$; HF-ET:+652.0%, $p=0.0557$, respectively). In comparison to HF, PGC-1 α , UCP1 and PPAR α were increased on trained groups (HF-T:+549.9%, $p=0.0013$, +308.5, $p=0.0003$ and +409.7%, $p<0.0001$, respectively; HF-ET:+388.8%, $p=0.0263$, +317.7%, $p=0.0005$ and +372.7%, $p=0.0002$, respectively) and PPAR β/δ and PPAR γ were elevated in all interventions ($p<0,0001$). PRDM16 was increased on trained groups in comparison to SC (HF-T:+180.3%, $p=0.0029$; HF-ET:+168.4%, $p=0.0061$), HF (HF-T:+592.7%, $p<0.0001$; HF-ET:+553.5%, $p<0.0001$) and HF-E (HF-T:+202.1%, $p=0.0012$; HF-ET:+188.7%, $p=0.0024$).

Conclusion:

ExT was able to improve metabolic impairments of obese mice and to induce browning of inguinal WAT through modulation of the RAS and mediators involved in this process.

Financial support:

FAPERJ, CAPES and CNPq

11.012 - ACUTE EFFECTS OF AEROBIC EXERCISE ON REDOX PARAMETERS IN WHITE ADIPOSE TISSUE. MATTA LP, COSTA TF, LIMAJUNIOR NC, BOA LFF, FARIA CC, BATISTA PKDSM, Pierucci APTR, FERREIRA CF, FORTUNATO RS, - CCS - UFRJ

Introduction:

It is known that redox changes can modulate physiological functions of white adipose tissue (WAT). To our knowledge there are no studies in the literature about the acute effect of AE on WAT redox homeostasis.

Aim:

Thus, the aim of the study was to evaluate the acute effect of AE on WAT redox parameters.

Methods:

Five groups of male wistar rats divided in control, and exercised 0, 30, 60, and 120 min euthanized after exercise. Retroperitoneal (WAT-r) and subcutaneous fat (WAT-s) were collected. Superoxide Dismutase (SOD), Catalase (CAT), Glutathione Peroxidase (GPX) and thiol groups were analyzed by spectrophotometry. NADPH oxidase (NOX) activity was evaluated by AmplexRed/HRP assay. ANOVA One-way with Tukey post-test was used for statistical analysis. Data are shown as Mean \pm SEM. Ethics Committee and Animal Use Protocol No:132/18.

Results:

In the WAT-r, NOX activity was increased 0 and 30 minutes after exercise (CTRL: 28.13 \pm 1.10 vs T0: 34.23 \pm 1.59 nmol of H₂O₂/hour/mg protein, $p<0.02$; CTRL vs T30: 29.42 \pm 1.74 nmol of H₂O₂/hour/mg protein $p<0.05$). NOX activity return to baseline levels after 2 hours of exercise (T0: 34.23 \pm 1.59 vs T120: 25.19 \pm 1.28 nmol of H₂O₂/hour/mg protein, $p<0.0004$; T30: 29.42 \pm 1.74 nmol of H₂O₂/hour/mg protein vs T120, $p<0.0001$). AE reduced CAT activity in all groups (CTRL: 0.98 \pm 0.03 vs T0: 0.82 \pm 0.016 U/mg protein, $p<0.001$; CTRL vs. T30: 0.85 \pm 0.012

U/mg protein, $p<0.0044$; CTRL vs. T60: 0.83 \pm 0.033 U/mg protein, $p<0.0010$; CTRL vs. T120: 0.79 \pm 0.019 U/mg protein, $p<0.0001$). No differences were observed for SOD and GPX activities. In WAT-s, NOX activity increased 30 and 60 minutes after exercise (CTRL-s: 22.52 \pm 0.80 vs T30-s: 31.3 \pm 0.65 nmol of H₂O₂/hour/mg protein, $p<0.0001$ and CTRL-s vs T60: 27.23 \pm 1.31 nmol of H₂O₂/hour/mg protein, $p<0.0474$). CAT activity decreased immediately after training (CTRL: 0.61 \pm 0.041 vs T0: 0.46 \pm 0.019 U/mg protein, $p<0.02$). After 30 and 120 minutes of the end CAT activity increased (T0 vs T30: 0.61 \pm 0.033 U/mg protein, $p<0.002$; T0 vs T2H: 0.68 \pm 0.03 U/mg protein, $p<0.0004$). No significant difference was observed between T30, T60 and T120 and in GPX activity. SOD activity decreased immediately after exercise (CTRL: 28.83 \pm 2.29 vs T0: 19.17 \pm 2.00 U/mg protein, $p<0.003$). However, it increased after 120 min when compared to T0 (T0 vs. T120: 30.3 \pm 1.02 U/mg protein, $p<0.0006$). Thiol groups levels of WAT-r were lower in T0 when compared to CTRL and T120 groups (CTRL: 2.98 \pm 0.23 vs T0: 1.96 \pm 0.22 nmol DTNB reduced/mg protein, $p<0.01$; T0 vs T120: 2.87 \pm 0.052 nmol DTNB reduced/mg, $p<0.03$), and in T30 and T60 in comparison to CTRL (CTRL vs T30: 1.85 \pm 0.19 nmol DTNB reduced/mg protein, $p<0.009$; CTRL vs T60: 1.92 \pm 0.18 nmol DTNB reduced/mg protein, $p<0.01$). Thiol group levels of WAT-s were lower at T0 until 60 min (CTRL: 2.70 \pm 0.241 vs T0: 1.58 \pm 0.106 nmol DTNB reduced/mg, $p<0.0005$; CTRL vs T30: 1.85 \pm 0.187 nmol DTNB reduced/mg, $p<0.009$; CTRL vs T60: 1.92 \pm 0.180 nmol DTNB reduced/mg, $p<0.01$). In WAT-s, T120 group were higher than T0, T30 and T60 (T0 vs T120: 2.61 \pm 0.044 nmol DTNB reduced/mg, $p<0.001$; T30 vs T120, $p<0.02$; T60 vs T120, $p<0.04$).

Conclusion:

AE alters WAT redox homeostasis generating a transitory prooxidative environment. We intend to evaluate the physiological consequences of our findings.

Financial support:

CNPq, FAPERJ

11.013 - DAILY RESISTANCE TRAINING REPERCUSSIONS ON SUBCUTANEOUS AND VISCERAL ADIPOCYTES MORPHOMETRIC AND NUMBER OF CELLS IN ADULT RATS. Oliveira DPL, ANTONIO-SANTOS J, DASILVAARAGAO R, - Pernambuco - Universidade Federal de Pernambuco

Introduction:

Resistance training is characterized by an application of external overload in the body or body segment. This type of training is related to gains in muscular strength and hypertrophy. However, there is no strong evidence on the relationship of this training and changes in adipose tissue.

Aim:

In view of this, the present study aims to analyze the repercussions of daily resistance training on subcutaneous and visceral adipocytes morphometric and number of cells in adult rats. Our hypothesis is that daily resistance training is able to maintain the number and reduce the size of subcutaneous and visceral adipocytes through lipolysis induced by physical exercise.

Methods:

Thirteen male Wistar rats were used at 60 days of age, divided into two groups: Control (C = 6) and Trained (T = 7). Trained group underwent resistance training in ladder, 5 days per week, for 8 weeks. During the training, body weight evolution was evaluated. After the training, animals were sacrificed and their fat pads (inguinal, epididymal, total visceral) removed, weighed and prepared for histological hematoxylin-eosin stain and morphometric analysis. Ethical committee approval number 0002/2017. Student's t-test or Mann-Whitney test were used to compare groups when appropriated.

Results:

Resistance training was effective to reduce body (C: 398.3 \pm 12.91g, T: 336.8 \pm 7.88g, $p<0.01$) and total visceral weights (C: 15.74 \pm 1.339g, T:

FeSBE Annual Meeting 2019

Poster Sessions and Abstracts

12.07 ± 1.072g, p <0.04). Trained group also presented a reduction in epididymal adipocyte perimeter (C: 210.4 [171.0 - 251.9]µm, T: 190.0 [156.5 - 227.2]µm, p <0.0001) and area (C: 2723 [1817 - 3963]µm²; T: 2144 [1429-3048]µm², p <0.0001), but with no difference in cell number (C: 265.6 ± 10.32; T: 286.6 ± 10.33, p = 0.154). However, resistance training increased subcutaneous adipocytes perimeter (C: 161.1 [131.5 - 195.8]µm, T: 163.9 [136.5 - 193.6]µm, p <0.0090), area (C: 1769 [1108-2625]µm², T: 1856 [1304-2542] µm², p <0.0004), and number (C: 289.3 ± 53.18, T: 337.1 ± 71.49, p <0.0003).

Conclusion:

Thus, we conclude that resistance training can modify body composition and adipocyte profile. Mainly, it was observed reduction in visceral adipocytes size and increasing in subcutaneous adipocytes number and size. Such changes can be considered a protection factor against noncommunicable diseases. Increased number of subcutaneous adipocytes may be related to a differentiation of brown or beige adipocytes. Thus, resistance training is an important agent for maintaining health.

Financial support:

FACEPE - Fundação de Amparo a Ciência e Tecnologia do Estado de Pernambuco

11.014 - SKELETAL MYOPATHY IN HEART FAILURE: CHANGES IN MUSCLE REGENERATION CAPACITY AND THERAPEUTIC EFFECTS OF AEROBIC PHYSICAL TRAINING. Vieira JS, Bacurau AVN, Cunha TF, Carrascoza LS, Dourado PMM, Brum PC, - Biodinâmica do Movimento Humano - Universidade de São Paulo Instituto do Coração - InCor-FMUSP

Introduction:

Heart failure (HF) is the common endpoint of most cardiomyopathies and other diseases of the circulatory system. In addition to functional impairment, patients with HF have an excessive loss of muscle mass that can culminate in cardiac cachexia, cachexia from heart disease, and aerobic exercise training (AET) is an efficient strategy to reverse this condition. Among the mechanisms responsible for this skeletal myopathy, little is known about the participation of the muscle regeneration process in skeletal muscle maintenance in HF

Aim:

Evaluate the therapeutic effect of AET on the deleterious alterations triggered by HF in the cardiovascular and skeletal muscle systems, as well as the role of changes in muscle homeostasis and regeneration regulators to the progression of myopathy.

Methods:

Wild type C57BL6 / J mice aged between 2-6 months with monocrotaline-induced (80mg/kg) HF were studied. The AET was performed 5x / week for 4 weeks at 60% of the maximum speed reached in a exercise test. The exercise tolerance by progressive test until the exhaustion. Cardiac function by echocardiography. The cross-sectional area (CSA) of the fibers and the satellite cells (SC) numbers by immunofluorescence. The diameter of cardiomyocytes, pulmonary edema and fibers regeneration by staining with hematoxylin-eosin. The variables were compared between the groups by two-way ANOVA, with Tukey post-hoc or Student's t-test. Significance level p <0.05

Results:

After 4 months of treatment, the HF group presented a greater reduction in the right and left ventricular shortening fraction (45.66667±0.40 vs 30.050±3.4, p<0.05), exercise intolerance (delta 69.350±14.3 vs -115.7±26.4, p<0.05), pulmonary edema (number of events 1.63±0.274 vs 6.03±3.4, p<0.05) and cardiac hypertrophy (µm 14.07±0.23 vs 14.81±0.19, p<0.05) associated with atrophy of type II fibers in the soleus (µm² 3179±225.4 vs 2499.8±127.9, p<0.05) and tendency to fiber atrophy of type IIb / X in the anterior tibial (TA) (µm² 2277.3±220.7 vs 1985.1±73.8, p<0.05) when compared to the control group. This atrophy is associated with reduction in satellite cells number (2.89±0.09 vs 2.58±0.107, p<0.05) and an increase in regenerating fibers (centralized nuclei/total number of fibers

0.34±0.045 vs 0.903±0.157, p<0.05). AET reversed effort intolerance (delta -44.9±46 vs 334.5±68.94, p<0.05), normalized cardiac (µm 16.6 ±0.282 vs 15.74±0.468, p<0.05) and type IIb / X fibers in TA (µm² 1935±57.23 vs 2195±80.85, p<0.05) trophism as also increased the number of SC (2.581±0.09 vs 2.987±0.17, p<0.05) reduced the number of regenerating fibers (0.903±0.157 vs 0.236±0.085, p<0.05).

Conclusion:

Animals treated with HF present pulmonary edema, cardiac dysfunction and hypertrophy, effort intolerance, as well as skeletal muscle atrophy, which is associated with changes in the muscle regeneration process. AET was efficient in reversing effort intolerance, cardiac hypertrophy as well as muscle atrophy by increasing satellite cells number and reducing muscle damage, thus appearing to be an interesting therapeutic strategy in HF.

Financial support:

FAPESP e CNPq

12 - Biomembranes, Transporters and Signaling

12.001 - THE ROLE OF THE V-ATPASE IN POLYCHAETE REGENERATION. FAÇANHA AR, - LBCT - UENF

Introduction:

Studies in vertebrate models (Xenopus and zebra fish) show that the activation of ionic transporters is crucial to differentiate responses in injured tissues that evolve to regenerative healing.

Aim:

The aim of this work was to study the induction of V-ATPases in the regenerative process of polychaetes (aelossoma). The hypothesis to be tested postulates a mobilization of the pumps for the injured regions, with the respective activation of electrochemical H⁺ gradients as an essential phenomenon for the restorative healing in invertebrates.

Methods:

The animals were cultured in mineral water, fed with spirulina and kept at room temperature. The proton fluxes were measured in the regenerative regions using an ion selective vibration probe specific to H⁺ ions. About 1000 animals were analysed, half of them submitted to random amputations of the posterior part. After 24 hours the microsomal fraction was obtained to verify the specific activity of the pumps.

Results:

The V-ATPase activity increased 2 to 3 times in animals that were amputated (control average activity: 9,84µmolPi/min and DEM: 1,56; 24hours after amputation average activity: 35,18µmolPi/min and DEM: 11,7), while no significant change was found for the Na⁺/K⁺ -ATPase (control average activity: 13,93µmolPi/min and DEM: 2,89; 24hours after amputation average activity: 26,14µmolPi/min and DEM: 17,6) and F-ATPase activities (control average activity: 1,51µmolPi/min and DEM: 0,48; 24hours after amputation average activity: 3,03µmolPi/min and DEM: 0,58). The proton fluxes suggest the activation of the V-type H⁺ pumps in the cell membranes of the regeneration sites.

Conclusion:

These data corroborate the hypothesis that electrochemical gradients generated by V-ATPases participate in the transduction of energy and ion signalling, driving the regenerative process in animal tissues.

Financial support:

UENF, CNPQ, CAPES, FAPERJ

12.002 - TITLE: BREAKING COPPER HOMEOSTASIS IN DIABETES MELLITUS I: INSULIN INCREASES CU-ATPASE (ATP7B) ACTIVITY. Silva RT, Borges TB, Silva GBO, Lowe J, - Biofísica - UFRJ

Introduction:

Copper homeostasis is essential for body performance, since this ion acts as a cofactor in several enzymes, such as superoxide dismutase, which participates in the neutralization of reactive oxygen species.

FeSBE Annual Meeting 2019 Poster Sessions and Abstracts

Expressed in the liver, ATP7B is the Cu-ATPase responsible for the excretion of copper accumulation, and mutations in the respective gene lead to Wilson's disease. Most of the studies in the literature show that animals and patients presenting type I or II diabetes mellitus display altered copper homeostasis, and it is accepted copper accumulation occurs in hepatic tissue. However, no evidence is available to clarify the molecular mechanisms that lead to copper excess and nor its consequences in this tissue.

Aim:

Determine ATP7B ATPase activity in the liver of rats submitted to treatment with streptozotocin compared to normal rats. Investigate whether in vitro alterations in ATPase activity are caused by the lack of insulin in the diabetic model.

Methods:

Wistar rats were submitted to a single dose of streptozotocin (65 mg kg⁻¹) in 50 mM sodium citrate pH 4.5 to induce type I diabetes mellitus. Control rats were given a sodium citrate buffer. Mass, glycemia and insulinemia were determined every 2-4 days. The animals were euthanized after 14 days (ethical use of animal protocol CEUA-CCS - IBCCF122). Livers were extracted for copper content analysis by atomic absorption spectrometry (AAS) and Golgi complex-enriched vesicles were obtained for enzymatic determination. Total proteins were determined according to Lowry (1951) and ATPase activity was obtained according to the Fiske-Subarow method (1925).

Results:

The diabetic group animals (STZ) presented higher copper content in hepatic tissue when compared to the control group (CTR) (CTR = 11.98 ± 0.63 versus STZ = 21.04 ± 1.90), confirming copper homeostasis changes. ATP7B protein content and enzymatic activity under 5 mM ATP conditions were not statistically different between groups. However, the ATPase activity curve versus ATP concentrations show statistically significant differences at low ATP concentrations (2 mM), with ATP7B activity in the STZ group lower than in the CTR group (CTR = 40.74 ± 1.86 versus STZ = 18.20 ± 1.72). In vitro, the addition of 10⁻⁵ M insulin led to ATP7B activity in the STZ animals at the same level as the control group (CTR without insulin = 25,195 ± 2,943 versus STZ without insulin = 15,205 ± 1,591 and CTR with insulin = 22,25 ± 3,899 versus STZ with insulin = 25,2575 ± 4,282).

Conclusion:

The absence of insulin in streptozotocin-induced diabetes mellitus model leads to decreased Cu(I)-ATPase activity, resulting in the breaking of copper homeostasis in the first 2 weeks of induction, as demonstrated by the accumulation of this metal in hepatic tissue. Future analyses with the glucagon are being carried out to evaluate its relevance in ATP7B activity. Keywords: copper, ATP7B, Diabetes mellitus

Financial support:

CNPq, FAPERJ, CAPES, PIBIC-UFRJ

12.003 - ANALYSIS OF THE INFLUENCE OF THE ENDOPLASMIC RETICULUM STRESS ON MATING OF SACCHAROMYCES CEREVISIAE. Jr MAF, - Instituto de Bioquímica Médica Leopoldo de Meis - UFRJ

Introduction:

In eukaryotes, endoplasmic reticulum (ER) stress can lead to the compromise of several biological processes. UPR (Unfolded Protein Response) is a type of response to this stress that aim to recover the cellular homeostasis. Ire1 is a protein present at the ER membrane capable of sensing different types of ER stresses and, through its protein kinase and endoribonuclease activities, mediates the unconventional splicing of HAC1 mRNA into the cytosol.

Aim:

Previous results indicated that yeast under ER stress present a decrease in mRNA of MFα1, a gene that encodes a pheromone responsible for sensitizing haploid cells MATa to mating. Our goal was to analyse the effect of ER stress and its influence on mating.

Methods:

Yeast *S. cerevisiae* haploid strains (MATα or MATa) were used as model in this work. The mating factor encoded by the MFA1 or MFα1 genes are responsible for the mating sensitization of these two populations. The Mating test was done by the addition of 50% haploid 'a' and 50% haploid type 'α', being cells 'a' (with resistance to geneticin) and 'α' cells (resistant to nourseotricina). The mating test evaluates the growth of diploids resistant to both antibiotics. ER stress was induced in three distinct ways: addition of DTT; addition of tunicamycin; or by galactose treatment of a strain deleted of the GAL7 gene (De-Souza et al, 2014). Yeast cells were cultured at 30°C in medium (1% yeast extract, 2% Bacto peptone) containing 2% glucose (YPD), 2% galactose (YPGal) or 2% glycerol (YPGly). The statistical test used was Paired t-Student.

Results:

The qRT-PCR results showed that 'a' cell did not show a decrease in MFA1 mRNA (n = 3; p = 0.6872). However, in α-type cells, we observed a significant decrease in MFα1 mRNA during stress exposure by the addition of tunicamycin in the growth medium (n = 4; p = 0.0052), as previously described (Tam et al., 2014)). The mating test suggests a decrease in mating efficiency in DTT-treated strains, tunicamycin, or strains that have UPR triggered by defects in galactose metabolism. We did not observe a clear decrease in yeasts treated with a stress that does not induce ER stress, such as addition of lithium in YPD medium.

Conclusion:

A decrease of MFα1 mRNA (but not MFA1) was observed in yeasts under ER stress. It has also been observed that there has been a decrease in the formation of diploid cells in strains that are under ER stress. We intend to investigate now how mating might be influenced by the ER stress.

Financial support:

CNPQ

12.004 - TITLE: AIRWAY SMOOTH MUSCLE EXPRESS THE "EXTRACELLULAR CAMP-ADENOSINE PATHWAY". Pacini ESA, Godinho RO, - Farmacologia - UNIFESP

Introduction:

Background: cyclic AMP (cAMP) is a universal intracellular second messenger involved in many biological processes, such as muscle contraction, cell proliferation and gene expression. In the respiratory tract, intracellular cAMP has a crucial role in the smooth muscle relaxation induced by β2-adrenoceptors (β2-AR)/Gs protein/adenylyl cyclase axis. In addition to its classical intracellular function, in many other tissues, cAMP works as an extracellular third messenger, which depends on its efflux and the extracellular conversion into AMP and adenosine by ecto-phosphodiesterase and ecto-5'-nucleotidase, respectively (Godinho et al., Front. Pharmacol. 6:58, 2015). Nevertheless, the existence and the relevance of the so-called "extracellular cAMP-adenosine pathway" in the respiratory tract is unknown.

Aim:

Thus, the aim of this study was to pharmacologically characterize the role of extracellular cAMP-adenosine pathway in the airway smooth muscle.

Methods:

Methods: tracheal rings obtained from adult male Wistar rats were mounted in an organ bath containing Krebs-bicarbonate buffer at 37°C, under optimal resting tension. After stabilization, tissues were subjected to different protocols. 1st Protocol: tracheas were stimulated with β2-AR agonist formoterol for 10, 30 and 60 min, the incubation medium and tissues were collected and cAMP was quantified using a time-resolved fluorescence resonance energy transfer (TR-FRET) immunoassay. 2nd Protocol: carbachol (CCh) precontracted tracheas were incubated with a) increasing concentrations of cAMP ± EHNA and uridine (adenosine deaminase and adenosine uptake inhibitors); b) cAMP ± AMPCP (ecto-5'-nucleotidase inhibitor), ± CGS-15943 (non-

FeSBE Annual Meeting 2019

Poster Sessions and Abstracts

selective adenosine receptor antagonist) or \pm DPCPX (A1 adenosine receptor antagonist) and c) 8-Br-cAMP. The isometric contraction forces were recorded and expressed as mean \pm S.E.M. All values were normalized as percentage of the responses obtained with 1 μ M or the EC30 of CCh. Animal Ethics Committee: CEUA #9987150714

Results:

Results: Stimulation of rat trachea with formoterol induced $72 \pm 7\%$ relaxation and increased by up to 110% and 252% the intra- and extracellular cAMP content, respectively (basal intra= 1.18 ± 0.3 and basal extra= 2.78 ± 0.19 pmol mg tissue $^{-1}$) (n=6-10). Exogenous cAMP evoked phasic contractions in a concentration-dependent manner with maximum amplitude of $19 \pm 6\%$ and potency of 3.7 ± 0.5 (n=6). Conversely, the membrane-permeable cAMP analog 8-Br-cAMP induced $43 \pm 3\%$ (n=6) relaxation of precontracted tracheas. Finally, preincubation of tracheas with EHNA + uridine increased by 3-fold ($50 \pm 1\%$, n=6) the maximum cAMP-induced contraction ($19 \pm 6\%$, n=6), whereas it was significantly reduced by AMPCP ($11 \pm 3\%$, n=6), CGS-15943 ($4 \pm 0.6\%$, n=5), or DPCPX ($6 \pm 1\%$, n=8) pretreatments.

Conclusion:

Conclusion: Our results strongly suggest that airway smooth muscle expresses the extracellular cAMP-adenosine pathway with contracting effects mediated by activation of adenosine A1 receptor. The observation that formoterol is able to trigger cAMP efflux indicates that the extracellular cAMP-adenosine pathway may play a role in balancing relaxant effects of β 2-adrenoceptor agonists in airway smooth muscle and may be involved in the tolerance observed after repeated administration of β 2-adrenoceptor agonists.

Financial support:

Financial Support: CAPES, CNPq and Fapesp.

12.005 - SUBLINGUAL AND NASAL PORCINE MUCOSAE AS BIOLOGICAL BARRIERS FOR IN VITRO PERMEATION MODELS. Araújo JSM, Xavier GGA, Franz-Montan MBL, - Ciências Fisiológicas - UNICAMP

Introduction:

Sublingual and nasal mucosae are promising administration pathways in topical drug delivery for local and systemic effects. They have advantages such as avoiding first-pass hepatic metabolism and gastrointestinal tract degradation and convenient drug administration. Due to its similarity with human tissues and wide availability in food industry, porcine structures have been used as biological barriers in in vitro permeation assays, which are important for the development of topical formulations. However, prior research has not implemented swine sublingual and nasal mucosae preparation protocols for in vitro studies.

Aim:

Therefore, this study aimed to standardize the preparation technique and to evaluate the histological integrity and similarity of the selected swine area to human tissues in order to use them as biological barriers in in vitro permeation models.

Methods:

Sublingual and nasal mucosa were obtained from different areas of swine oral and nasal cavity. The mucosae were gently detached from adjacent structures with Molt surgical curettes and blunt scissors, were fixed, sectioned and stained with hematoxylin and eosin. Finally, the photomicrographs were analyzed by two investigators in light microscope, which were compared to photomicrographs of human oral lining and respiratory tissues.

Results:

It was observed that the detachment method did not compromise epithelial integrity and some areas of swine tissues corresponded to human histological structural arrangement. Central underside of the tongue and floor of the mouth presented nonkeratinized stratified squamous epithelium; while extremities of underside of the tongue and floor of the mouth anterior area presented parakeratinized stratified squamous epithelium. In nasal cavity, internal area of swine snout

presented pseudostratified columnar epithelium, while anterior region of nasal vestibule and medial nasal septum presented simple cubic epithelium.

Conclusion:

While some areas of porcine nasal and oral cavity might anatomically correspond to human structures, specific areas of swine mucosa present histological arrangement correspondent to human tissues. Therefore, it is important to collect sublingual mucosa from central underside of the tongue and floor of the mouth for sublingual models, and obtain nasal mucosa from posterior region of swine snout in order to obtain epithelial tissues comparable to the intended human epithelial barrier for permeation assays. In addition, gentle handling and detachment with blunt surgical instruments did not compromise tissue integrity.

Financial support:

CNPq 140926/2019-4

13 - Cell differentiation, growth and death

13.010 - PALMITOLEIC ACID PROMOTES THE RECRUITMENT OF NEW ADIPOCYTES BY STIMULATING ADIPOGENESIS. Simão JJ, Cruz MM, Jaco VA, Silva VS, Sa RCR, Farias TM, Abdala FM, Vale MICA, - Ciências Biológicas - UNIFESP

Introduction:

Obesity is a public health problem and is related to the excessive accumulation of fat in white adipose tissue (WAT) that increase individual's risk of developing obesity-associated morbidities such as dyslipidemia, insulin resistance, type 2 diabetes mellitus, hypertension and cardiovascular disease. Studies show that palmitoleic acid (C16:1n7), a monounsaturated fatty acid (FA) found in macadamia and sea buckthorn pulp oil, has important metabolic effects on glucose and lipids metabolism in skeletal muscle and liver, improving glucose tolerance, insulin sensitivity and plasma lipid profile in obese and diabetic patients. Recently our research group demonstrated that this FA has also important effects on WAT, improving adipocytes metabolism.

Aim:

The objective of this research was to investigate the effect of FAs C16:1n7 and palmitic (saturated, C16:0) on adipogenesis and proliferation processes and our hypothesis is that palmitoleic acid may constitute a stimulus for adipogenesis.

Methods:

For this, 3T3-L1 pre-adipocytes were cultured in D'MEM in the presence (or absence) of 16:0 or 16:1n7 FAs diluted in ethanol at a concentration of 100 μ M [separately or in combination (final concentration C16:0 + C16:1n7 100 μ M, 1: 1)]. The proliferation potential was estimated by MTT assay. Adipogenic potential was estimated by expression analysis of genes encoding PPAR γ 2, C / EBP α , C / EBP β , perilipin, adiponectin and aP2 / FABP4 by RT-PCR in real-time after induction of the cells to the differentiation (for 6 - 8 days) and by the accumulation of lipids in the adipocytes by color analysis with oil red O and spectrophotometry. All statistical analysis was performed using GraphPad Prism. Statistical significance was defined as *p < 0.05 by ANOVA. Data are representative of at least three independent experiments.

Results:

We evidenced an increase ($\sim 3,5x$) in the proliferation of 3T3-L1 pre adipocytes from the C16:1n7 group in relation to the other groups. C16:1n7 also increased the expression of the major regulators of early adipogenesis: PPAR γ (24%, p<0,05) and C/EBP α (42%, p<0,01), such as the mRNA expression of adipocyte terminal differentiation markers: Fabp4 (38%, p<0,05), perilipin (83%, p<0,05) and Glut-4 (31%, p<0,05). When C16:0 was associated to the treatment, the effects promoted by C16:1n7 were preserved. However, C16:0 alone decreased AdipoQ (44%, p<0,05) and Glut4 (38%, p<0,05) gene expression, but this effect was prevented when C16:1n7 was associated to C16:0. We next

FeSBE Annual Meeting 2019

Poster Sessions and Abstracts

quantified the amount of lipids present in each group by staining the lipid droplets with oil red O, 6 days after cell differentiation. We noted that oil red O staining is significantly increased in the presence of C16:1n7 and the lipids content was 60% higher ($p < 0.05$) in this group (but not in C16:0 group), compared to control.

Conclusion:

We suggest that the palmitoleic acid stimulates adipogenesis favoring the recruitment of new adipocytes and exerts an attenuating effect on adipocyte hypertrophy (data not shown) fundamental for the healthy expansion of WAT in contrast to the pathological expansion of WAT that accompanies the hypertrophic obesity.

Financial support:

FAPESP 2018/05485-6 and CAPES

13.011 - STRUCTURAL ORGANIZATION OF THE DERMIS IN THE SKIN EXPERIMENTAL LESION OF WISTAR RATS AFTER TREATMENT WITH MICROCURRENT IN COMBINATION WITH TOPICAL APPLICATION OF THE ARNICA MONTANA L. GEL. Zacarias CA, Florenzano RFM, Leitão DPS, Pavan J, Santos LA, Neves LMG, Mendonça FAS, Andrade TAM, Esquisatto MAM, Santos GMT, - Programa de Pós-Graduação em Ciências Biomédicas - FHO

Introduction:

An interesting research field is the investigation of the treatment of tissue injuries using alternative therapies.

Aim:

The aim of this study was to evaluate the effects of microcurrent application alone or in combination with the topical application of Arnica montana L. on the dermis organization during skin wound healing in Wistar rats.

Methods:

Forty-eight animals (~200g) were randomly distributed in four groups ($n=20$): C (control: lesion with no treatment), MC (microcurrent application), ARN (A.montana gel) and MC+ARN (A.montana gel and microcurrent). The gel consisted of 10% Natrosol, 0.2% Nipagin, 5% propylene glycol, and water qsp. Animals from all groups were anesthetized and linear incision wound was induced in the dorsal skin. The incision was not sutured. The microcurrent (10 μ A/2min) was applied by placing two metal electrodes with a spherical tip (10mm) on the wound. For treatment with A.montana, about 20mg of the gel formulation was applied. The treatments were started 24h after surgical intervention and were continued daily for 10 days. The procedures were performed daily at the same time and in the same way. After 2, 6 and 10 days of treatment, the animals were euthanized and the lesion regions were removed and processed for histomorphometric and ultrastructural analysis. The quantitative data were compared by ANOVA and Tukey's post-test ($p < 0.05$). CEUA-FHO Protocol n.058/2018.

Results:

Animals of the MC (21.1 \pm 2.7x104 μ m²) and MC+ARN (25.1 \pm 2.8) groups presented a larger repair area on the 10th days than the C (17.2 \pm 2.2) and the ARN groups (20.9 \pm 3.1). In relation to the total number of cells, significantly larger numbers were observed for the MC (6th: 602.1 \pm 91.8 in; 10th:891.7 \pm 69.8) and MC+ARN (6th:605.3 \pm 89.8, 10th:894.3 \pm 71.8) groups on the 6th and 10th days of treatment. The total number of newly formed vessels on the 6th and 10th days was similar to MC and MC+ARN groups compared to control on the 6th day. However, MC+ARN group (4.8 \pm 0.4 in 104 μ m²) presented a significantly larger number of newly formed vessels on the 10th day. The level of birefringence collagen fibers, quantified under polarized light, in relation to the total area was higher in MC (6th:69.3 \pm 6.3% of 104 μ m², 10th:86.6 \pm 9.4) and MC+ARN (6th:71.6 \pm 8.4, 10th:88.6 \pm 8.2) groups on the 6th and 10th days of treatment. The ultrastructure of active fibroblast was an elongated or stellate cell with cytoplasm containing numerous organelles, particularly well-developed endoplasmic reticulum. This cell was in close contact with collagen bundles. The

quiescent fibroblasts, detected at 10th day only in all groups, progressively lost their rough endoplasmic reticulum and modified their chromatin to heterochromatin. The content of proteoglycans ultrastructural markings did not present difference among the groups in all experimental times. The collagen fibrils diameters were similar among the groups at 2 and 6 days. However, at 10 days, the groups C (12.6 \pm 2.4nm) and ARN (13.8 \pm 3.3) presented the higher values than the others.

Conclusion:

The application of A.montana was effective on experimental wound healing when compared to control, but differences in the parameters studied were only observed when these treatments were combined with microcurrent application.

Financial support:

FHO

13.012 - CYTOTOXICITY AND PHYTOTOXICITY ASSAYS OF SILVER NANOPARTICLES. Ambrosio BN, Ambrosio F, Lombello R, Rolim WR, Seabra AB, Lombello C, - Center for Engineering, Modeling and Applied Social Sciences - UFABC Center for Natural and Human Sciences - UFABC

Introduction:

Silver nanoparticles are used for different cosmetic, pharmaceutical and biomedical purposes. However, the safety of application of these nanoparticles still shows controversial data.

Aim:

The objective of this project is to characterize cytotoxicity, in animal cells of the Vero line, and the phytotoxicity of silver nanoparticles.

Methods:

In this work, silver nanoparticles (NPs) were obtained through the reduction of silver, using green tea extract as both reducing and capping agent. The NPs test dilutions were: 10, 30 and 50 μ g/ml, for cytotoxicity and an added 1000 μ g/ml for the phytotoxicity tests. Vero cells (CCIAL 057) were used for the cytotoxicity test (adapted from ISO 10993-5). The NPs were inoculated directly onto the cell monolayers, in the described concentrations. The cell morphology was observed by inverted phase contrast microscopy after 24 hours. For the quantitative evaluation, the MTT assay was performed. For the phytotoxicity tests, it was made the germination test, 200 seeds of Lactuca sativa were placed in 4 Petri dishes, with filter paper moistened with 1 mL of NPs solution, at the different test concentrations. Observations were made in the period of 7 days. For the root apical meristem phytotoxicity test, roots with 1 cm were removed from the bulbs of the onion and transferred to glass containers with distilled water and NPs solution in the concentrations of 10, 30, 50 and 1000 μ g/mL. Then, they were fixed in Carnoy solution (3:1 ethanol and acetic acid, v/v) and transferred to 70% ethanol. The root tip was crushed with acid hydrolysis (1M HCl) and colored with Acetic Orcein 2%.

Results:

The cytotoxicity tests demonstrated the non cytotoxicity of NPs. Morphology and quantitative findings were in accordance. Vero cells showed normal morphology pattern, and viability above 88% for all the NPs concentration tested. For the statistic evaluation, none of the concentrations tested had a significative variation in relation to the negative control. For the seed growth, the germination index was above 72%, (74% in the concentration of 10 μ g/mL, 74% in 30 μ g/mL, 72% in 50 μ g/mL and 84% in 1000 μ g/mL), compared to 78.% control condition. In the highest concentration tested, the root apical meristem of onions showed more anomalies, such as polyploid nucleus, especially in the prophase. The percentage of the division index with 10 μ g/mL was 2.9% which is close to the control percentage, that is 2.7%. The other results were 2.4% in 30 μ g/mL, 1.6% with 50 μ g/mL and 2% with 1000 μ g/mL.

Conclusion:

FeSBE Annual Meeting 2019

Poster Sessions and Abstracts

The first results indicate the non cytotoxicity of Vero cells exposed to concentrations up to 50 µg/ml. Phytotoxicity of the NPs tested in concentrations up to 1000 µg/ml did not result in decrease of seed germination and in root apical meristem mitotic index, although the NPs in the highest concentration polyploid nucleus were observed in the meristematic tissue.

Financial support:

No financial support was provided for this work.

13.013 - PARKIN IS KEY FACTOR FOR MIOGENESIS AND DIFFERENTIATION PROCESS IN C2C12 CELLS. Severino MB, Esteca MV, Tamborlin L, Luchessi AD, Baptista IL, - Biologia - Unesp; Laboratório de Biologia Celular e Tecidual - Unicamp; Laboratório de Biotecnologia - Unicamp;

Introduction:

Recently, mitophagy and mitochondrial biogenesis were pointed as determinant during cell differentiation process in muscle cells. There are the hypotheses that combined phenomena plays key role in the differentiation process. The myoblasts require low energy, being constituted by mitochondria mainly glycolytic. The moment that cell start to proliferate and fuse, to give rise to myofibers, undergo an overload in the production of ATP. This process requires more efficient mitochondria, with oxidative activity. Thus, the performance of mitophagy pathways, especially the Parkin pathway, could play an important role in the differentiation process.

Aim:

The aim of this study, was manipulate the intracellular levels of Parkin, through expression plasmids to investigate the differentiation process in muscular cells C2C12.

Methods:

C2C12 cells was transfected with Parkin-flag DNA, and flag DNA as control group, with PEI protocol. The analysis was performed in 0h of differentiation, supply with 10% of SFB, and 48h, 96h and 144h after differentiation, supplemented with 2% of HS. We analyzed proteins of mitophagy and miogenics regulatory factors (MRFs) by western blotting; Using hematoxylin eosin staining we determine the cell number and fusion index. Finally, we performed immunofluorescence staining for visualization of parkin mitophagy dynamics.

Results:

HE staining showed that Parkin-flag DNA group presented higher number of cells compared to flag DNA group. However, this difference was decreasing during differentiation process (0h $p=0,00003^{****}$; 48h $p=0,004^{**}$; 96h $p=0,039^{*}$; 144 $p=0,09$), pointing that Parkin possibly had an protector against apoptosis, and could also to decrease the proliferative activity of this cell, since the number of cells in the flag DNA group increased faster than in the Parkin-flag DNA group. In addition, the Parkin-flag DNA group showed a higher fusion index (48h $p=0,042^{*}$; 96h $p=0,038^{*}$; 144h $p=0,02^{*}$), indicating that the differentiation process could be advanced in these cells. Western blotting analysis confirmed the observations made in HE staining, the mitophagy process starts even before the cell has been induced to differentiate, 24 hours after transfection. Moreover, we have noted an interesting effect in MRFs proteins, linking the mitophagy process with the activity of this group of proteins, especially Myod and Myogenin, explaining the acceleration of the differentiation process. Immunofluorescence showed a reorganization of the mitochondrial network. It was also possible to note that Parkinflag DNA transfection accelerated the mitochondrial reorganization process compared to flag DNA group.

Conclusion:

Our results reforced the idea that mitophagy process is a key for differentiation process of muscle cells (C2C12), with a crucial role of Parkin in the differentiation process, probably through removing low efficient mitochondria. Those results, in addition to the gene therapy

approach used here, raise the possibility to use the Parkin pathway as a target in myopathies and injury conditions.

Financial support:

Fapesp, Capes, CNPq, FAEPEX/UNICAMP

13.014 - EFFECT OF EUGENOL COMPOUNDS ON ACTIVITY OF METACASPASE-2 OF TRYPANOSSOMA BRUCEI. Araujo LH, Reis T, Marcondes MF, Veloso MP, Chagas TAB, Machado MFM, - Interdisciplinary Investigation Research Center - UMC Biophysical Department - UNIFESP Pharmaceutical Science Department - UNIFAL

Introduction:

Programmed cell death in mammalian cell has been associated with the action of cysteine proteases called caspases that are peptidases that cleave specifically at aspartic acid residues at the P1 position of their substrates. Metacaspases (MCAs) are associated caspase peptidases that were identified in plants, fungi and protozoa but interestingly metacaspases hydrolyze their substrates at basic residues in the P1 position. Five MCAs genes (TbMCA1-5) were describe in Trypanossoma brucei genome. The activity of TbMCA2 was described to be strictly Ca^{2+} -dependent, requiring about 1 mM $CaCl_2$ for the maximum activity. Research on activity modulator on TbMCA2 could provide a new therapeutic strategy for sleep disease.

Aim:

Screening of eugenol compounds as modulator of TbMCA2 activity

Methods:

TbMCA2 clone was kindly donate by Prof. Dr. Jeremy Mottram at York University and was expressed in a BL21(DE3) with induction 0.5 mM of IPTG. TbMCA2 purification was evaluated with Ni^{2+} -sepharose column in an Akta Purifier System (GE-Healthcare) with imidazole gradient (0-500 mM) and was eluted in a presence of 300 mM of imidazole. purification was observed with on SDS-PAGE with 15% of acrylamide. TbMCA2 activity was carried using a commercial substrate with sequence Z-RR-MCA in a spectrofluorometer Hitachi F2600 with $\lambda_{EM} = 380$ nm and $\lambda_{EM} = 460$ nm in a buffer with Tris 50 mM, NaCl 100 mM, $CaCl_2$ 1 mM DTT 2.5 mM at pH 8.0 at 25°C with constant agitation, the data was obtained on AFU/min, and refers a 100% of activity at TbMCA2. After that 19 eugenol compounds were assayed with a 10 µM in the same condition and a reminiscent activity was obtained compared with TbMCA2 activity without a presence of compounds.

Results:

Screening of eugenol compounds showed that two compounds were presents a fully inhibition effect on TbMCA2 activity in 10 µM concentration and four compounds were presenting an inhibition effect of TbMCA2 (compounds TB-01, TB-08, TB-11 and TB-14) all compounds was effective to inhibit around 70 – 90% of TbMCA2 activity. At this moment the dissociation constants for these four compounds was performed.

Conclusion:

TbMCA2 is a cysteine peptidase involved at programmed cell death, research of new compounds that could be modulated TbMCA2 activity it's interesting as a new therapeutic target for the infections of T.brucei. In this present work we are screening 19 eugenol compounds that's present TbMCA2 modulator effect as an inhibitor of this enzyme activity. The mechanism studies of these molecules on TbMCA2 activity could provide new strategies for T.brucei treatment.

Financial support:

FAPESP, CNPq and FAEP

13.015 - INVESTIGATING THE EXISTENCE OF AN ANTERIOR REPRESSION MECHANISM IN THE BLASTODERM OF DROSOPHILA. Baltruk LJ, Andrioli LP, - Ciências da Natureza - USP

Introduction:

At the beginning of Drosophila melanogaster development, the egg is a syncytial environment in which regulatory proteins are free to diffuse in

FeSBE Annual Meeting 2019

Poster Sessions and Abstracts

a cytoplasm shared by all nuclei. Therefore, interactions among nuclei can be directly accomplished by transcriptional factors without the interference of cell membrane and the necessity of cell signaling messengers. During the syncytial blastoderm, a cascade of transcriptional factors sets the information responsible for the antero-posterior axis specification and the division of the body in segments. The cascade comprises three hierarchical levels formed by gap, pair-rule and segment polarity genes. In the laboratory we study the segmentation cascade in the anterior region of the embryo. There, stripes, the typical expression pattern of pair-rule genes are not formed.

Aim:

According to our previous results, a mechanism comprised by the combined activity of gap repressors prevents the formation of pair-rule stripes in the anterior blastoderm. Here we tested this hypothesis simultaneously removing the activity of three previously characterized repressors (sloppy-paired (slp-), tailless (tll-) and kuckebein (hkb)) of the pair-rule striped pattern.

Methods:

To test the hypothesis we generated triple mutant embryos in genetic assays and detected effects in the striped pattern of pair-rule genes doing in situ hybridizations.

Results:

First, we established strains simultaneously defective in slp-, tll-, hkb. This was possible recombining tll- and hkb- alleles in the same chromosome. To confirm these lines, we collected embryos and used them for in situ hybridization assays. We were able to detect the expected genotypes including triple mutant embryos with severe disturbance in the expression pattern of pair-rule genes. We are now collecting more embryos to hybridize with other gap gene probes to better understand the severe effects we detected in the striped pattern of pair-rule genes in triple mutant embryos.

Conclusion:

As we expected, triple mutant embryos showed more drastic effects compared to single or even double mutant embryos as we will discuss.

Financial support:

FAPESP

13.016 - CYSTOGENESIS IN VITRO: DEVELOPMENT OF A MODEL WITH EPITHELIAL CELL DERIVED SPHEROIDS ASSOCIATED TO FIBROBLASTS. Brand LM, Laureno NK, Bernardi L, Visioli F, Lamers ML, Rados PV, - Patologia - UFRGS Ciência Morfológica - UFRGS

Introduction:

Radicular cysts represent 60-75% of tooth periapical pathologies. These lesions results from periapical tooth inflammatory processes induced by dental caries. Histologically, they are defined as a pathologic cavity totally lined by an epithelium circumscribed by a fibrous capsule. The whole mechanism of cyst establishment, growth, maintenance and regression is still unclear, since the interplay of inflammatory process and epithelium response are not yet fully understood. Our research group developed cyst-like structures in vitro using culture of spheroids of epithelial cells in a 3D collagen matrix. These cyst-like structures presented a gradual growth until day 15. Also, on the third day of growth, it was observed a cavity with epithelial lining morphology, similar to a pathological human radicular cyst.

Aim:

Based in this model, the aim of this research is to evaluate the role of connective cells in cyst progression.

Methods:

Cell spheroids were generated using cell lines of epithelial origin (HaCat) at a concentration of 1×10^5 transferred to 96-well plates of low adhesiveness (1.5% agarose). After 24 hours, the spheroids were collected, embedded in a 3D collagen matrix (1.8 mg / ml) with fibroblasts at different concentrations (5×10^4 , 1×10^5 and 2×10^5) and transferred to 24 well plates previously covered with polymerized

collagen and maintained by up to 21 days. Images were obtained and the spheroids collected for histological analysis on days 1, 3, 7, 14 and 21.

Results:

We observed the development of cyst-like structures in all experimental conditions. However, the concentration of 1×10^5 fibroblasts presented the best concentration for the continuity of the experiments, since 5×10^4 fibroblasts did not involve the structure and with 2×10^5 fibroblast induced contraction of collagen matrix.

Conclusion:

Herein we optimized the model of in vitro cysts in order to perform mechanistic assays to unveil the pathobiology of periapical lesions.

Financial support:

CAPES, CNPQ, FAPERGS, UFRGS

13.017 - HAEMOGLOBIN EXPRESSION IN PROSTATE CELLS: HYPOXIA OR DHT SIGNALLING? Barbutti I, Carvalho HF, - Biologia Celular e Estrutural - UNICAMP

Introduction:

Haemoglobin genes are usually expressed in erythroid cells, where the genes are tightly regulated by a number of mechanisms, including the expression of a specific pool of transcription factors. Ectopic haemoglobin expression has been found in other tissues, such as alveolar epithelial cells, and shown to be induced by hypoxia, which leads to HIF-1 α and HIF-2 α increase and, consequently, GATA1, GATA2, NF-E2, KLF1 and CP2 expression (Am. J. Respir. Cell. Mol. Biol. 44:439, 2011). Our laboratory has also found haemoglobin expression in prostate cells, cells in which dihydrotestosterone (DHT) signalling is of extreme importance. But the means in which haemoglobin expression is modulated indicate a possible hypoxia pathway.

Aim:

Thus, it is our aim to characterize whether haemoglobin expression in prostate cells is due to hypoxia or DHT signalling.

Methods:

The non-tumorigenic epithelial prostate cell line RWPE1 was cultured under the following conditions: 2D (treated/untreated with DHT) and 3D in matrigel (treated/untreated with DHT). To check whether hypoxia/HIF-1 α were capable of modulating haemoglobin expression, 2D cells were also cultured under hypoxia/CoCl₂ treatments. All cells were submitted to RNA extraction for qRT-PCR analysis of haemoglobin and erythroid transcription factors expression; and immunofluorescence for analysis of subcellular localization of HBA.

Results:

HBA2, HBA1 and HBE were found in 2D cultured RWPE1, and its expression increased in 3D cultured RWPE1 (2-, 5- and 3-fold, respectively), regardless of the presence/absence of dihydrotestosterone (DHT). In 2D cultured cells (treated/untreated with DHT), HBA was present in the nucleus. In 3D culture, however, the lack of DHT changed HBA subcellular localization: cells in the center of the spheroid presented higher amounts of HBA, localized mainly on the cytoplasm, whereas cells in the periphery presented the same nuclear localization as 2D cells. DHT treatment abolished HBA cytoplasmic localization. Interestingly, 2D cells cultured under hypoxia had increased HBA2, HBA1 and HBE expression (51-, 119- and 450-fold, respectively) compared to 2D cells not submitted to hypoxia. CoCl₂ treatment also increased HBA2, HBA1 and HBE expression, (9-, 7- and 16-fold, respectively), although it did not change HBA subcellular localization in DHT treated/untreated cells. The increase in haemoglobin expression was not accompanied by alterations in levels of the erythroid transcription factors GATA1, GATA2, KLF1, p45 (NF-E2), FOG1 or TAL1 in any culture.

Conclusion:

HBA2, HBA1 and HBE are expressed in RWPE1 cells, and its expression increase in 3D culture. Spheroids untreated with DHT present both cytoplasmic (center cells) and nuclear (peripheric cells) localization of

FeSBE Annual Meeting 2019

Poster Sessions and Abstracts

HBA, whereas DHT treatment abolishes HBA cytoplasmic localization. CoCl₂ treatment increases HBA2, HBA1 and HBE mRNA expression, but does not change subcellular localization of HBA. Thus, it is possible that the DHT signalling is more important for HBA expression in these cells than hypoxia, although the mechanisms behind the gene regulation remain elusive and require more study.

Financial support:

FAPESP

13.018 - MESENCHYMAL STEM CELLS X FIBRIN SEALANT: CONTROL OF THE INFLAMMATORY PROCESS IN EXPERIMENTAL PERIODONTITIS. Viganó LB, Santamaria Jr M, Aro AA, Felonato M, - Programa de Pós-Graduação em Ciências Biomédicas - Centro Universitario da Fundação Herminio Ometto

Introduction:

Periodontal diseases comprise a wide variety of inflammatory and immunological conditions. It is characterized by the destruction of the tissues that support the teeth, the periodontal (Suaid, 2010; Kinane, 2017). Among the treatments used, the objective is to remove the bacterial plaque and modulate the inflammatory response. However, they are not able to regenerate the periodontium, neoform alveolar bone or even produce a new insertion for the fibers of the periodontal ligament. An alternative would be cellular therapy through the application of mesenchymal stem cells derived from adipose tissue (CTMA), due to its immunomodulating properties and the proven paracrine effects during the treatment of various types of lesions. (Zuttion, 2013).

Aim:

The aim of this study was to evaluate the evolution of periodontitis through the therapy with the isolated CTMA and associated with fibrin sealant, a biological scaffold of animal origin used to maintain the CTMA in the injured region for longer.

Methods:

We used 36 Wistar rats, submitted to ligature placement in the first right upper molar for induction of periodontitis for 8 weeks. The animals were divided into 3 groups: SHAM, SF (Fibrin Sealant) and CT+SF (CTMA and fibrin sealant) and evaluated in the 3rd, 7th and 14th days after induction of CTMA. CTMA-GFP were obtained from the inguinal region of rats Lewis-GFP and cultivated until the 5th passage, following for the application in the rats of the groups CT+SF. The analysis of the migration of the CTMA-GFP was performed for the tissues affected by periodontitis in the 3rd, 7th and 14th days.

Results:

Before the in vivo application, the in vitro characterization of the CTMA-GFP was performed regarding its potential for osteogenic and adipogenic differentiation, in which calcification points were observed in the extracellular medium, as well as intracellular lipid droplets. In the cell migration analysis, CTMA-GFP were not observed in the gingiva, bone and ligament. The bone, number of blood vessels decreased on the 3rd day in the CT + SF group when compared to the other groups. In both gingival tissue and in the bone, the inflammatory infiltrate was lower in all periods (3rd, 7th and 14th days) in the SF and CT + SF groups when compared to Sham. The number of fibroblasts showed no difference between the groups and in both tissues.

Conclusion:

The preliminary results of this study suggest that the fibrin sealant or fibrin sealant associated with CTMA applied to experimental periodontitis had the same performance on tissues in inducing reduction of the inflammatory process, acting as Anti-inflammatory drugs in the pathology.

Financial support:

FHO-Fundação Herminio Ometto

16 - Gene and Cell Therapy, Omics Biology

16.006 - OBTENTION OF RECOMBINANT DICTYOSTELIUM DISCOIDEUM PARACASPASE: CLONING, EXPRESSION AND PURIFICATION. Trujillo MNR, Reis TS, Machado MFM, - Centro Interdisciplinar de Investigação Bioquímica - UMC

Introduction:

Caspases, metacaspases and paracaspases contains a histidine/cysteine (His/Cys) catalytic dyad. Paracaspases are found in metazoans and in the amoebozoan Dictyostelium discoideum. Studies suggest that metacaspases act on contractile vacuole of D. discoideum. Also, metacaspase is highly expressed during the Acanthamoeba castellanii encystment. Therefore, it is possible that paracaspase is involved in the differentiation of sporogenous of D. discoideum. D. discoideum are an excellent model to investigate the evolutionary mechanism of the programmed cell death (PCD) in a simple eukaryotic cells, a biochemical study of D. discoideum paracaspase could elucidate this enzyme could participate on PCD event on this amoeba.

Aim:

The purpose was to clone, expressed and purified a D. discoideum paracaspase (DdPCP) in Escherichia coli expression system.

Methods:

DH5 α was transformed with pMK-RQ plasmid containing insert encoding DdPCP gene. Miniprep product was used as template for PCR. pET28a and PCR product were treated with XhoI and NdeI. DdPCP gene and pET28a were ligated using T4 DNA ligase. DH5 α was transformed with ligation product. Screening for the positive clones was carried out by colony PCR using T7 primers. Plasmid minipreps of positive clones were performed. BL21(DE3) was transformed with plasmid minipreps products. PCR with T7 primers was carried out. Induction of expression was performed using of IPTG 0.25 mM for 16 hours in 20°C, the material obtained was purified with nickel-sepharose column (GE Lifescience) in different imidazole concentrations (0 - 500 mM).

Results:

PCR amplification of DdPCP gene contained a restriction sites by XhoI and NdeI was performed and was analysed in a 1% agarose electrophoresis. PCR product and pET28a(+) was digested with XhoI and NdeI, the digestion material was purified and the insertion of DdPCP gene on pET28a(+) was performed with T4 ligase. These material was transformed by thermal shock in an E. coli DH5 α strain, and a colony PCRs indicated that the amplicon was inserted between T7 promoter and T7 terminator of pET28a. The amplicon of DdPCP in DH5 α was grown at 37°C, and an alkaline lysis was performed and with these material a E. coli BL21(DE3) was transformed by thermal shock. DdPCP was expressed on 20°C using 0.25 mM of IPTG, a SDS-PAGE on 15% of acrylamide was performed and indicated IPTG-induced expression of ~45.0 kDa protein. For purified of DdPCP we used a Ni-sepharose affinity column, the protein was shown to be pure after treatment with 300 mM imidazole, the data was confirmed by SDS-PAGE gel.

Conclusion:

Results shows that Ddpcp was produced and purified using a E. coli expression system. Future studies of Ddpc may contribute to the biochemical characterization of this enzyme.

Financial support:

FAPESP, CNPq and FAEP

16.007 - DEVELOPMENT OF A SMARTPHONE-COUPLED MICROFLUIDIC SYSTEM TO PRODUCE ALGINATE MICROGELS WITH ENCAPSULATED NANOPARTICLES. Cinel VDP, Taketa TB, Carvalho BG, DelaTorre LG, Han SW, - Biophysics - Unifesp Bioprocess and Materials Engineering - Unicamp

Introduction:

Gene Therapy consists on the delivery of exogenous genetic material into a patient to treat diseases. One of the greatest challenges today is how to control delivery of vectors that carry therapeutic genes in a way

FeSBE Annual Meeting 2019

Poster Sessions and Abstracts

to prevent acute burst release and achieve long-term delivery. The advent of droplet microfluidic technology allowed us to produce reproducible, small and homogeneous microgels to be utilized as a vector carrier. For microgel production, a microscope is coupled in a microfluidic device to monitor flux of liquids and microgels.

Aim:

Here, we show a simple method to monitor the flow of microfluidic device using a smartphone, which is easier to use and has a lower cost than a microscope.

Methods:

Firstly, the alginate microgel production system was coupled with a smartphone equipped with a slow-motion recording device of 720 p and 240 fps in a regular optic microscope instead of a high-end digital microscope. The produced microgels were characterized by bright field microscopy and scanning electronic microscopy (SEM). Next, we encapsulated fluorescent latex nanoparticles with 0.03 μm (Millipore) in the alginate microgels. Different production conditions were evaluated to determine the best flow rates and the appropriated mass proportions of nanoparticles to alginate microgels. Finally, the encapsulation efficiency of nanoparticles in the microgels was analyzed by fluorescence spectroscopy.

Results:

The smartphone-coupled microfluidic system allowed us to monitor the flow rates for the microgels formation in real time inside of a flow hood, enabling us to produce sterile alginate microgels. The best flow rates for the alginate and oil syringes were 1 and 3 $\mu\text{L}/\text{min}$, respectively, forming an average size of $123 \pm 4 \mu\text{m}$ for 1.2 % alginate microgels, and $116 \pm 5 \mu\text{m}$ for 1.2 % alginate microgels encapsulated with nanoparticles. The 1:10 mass proportion of nanoparticles for alginate allowed the generation of a more stable microfluidic flow, producing monodispersed microgels with the SD of 5 μm . The SEM imaging revealed a spherical and homogeneous morphology of the microgels, confirming the expected sphericity. In our system, the average encapsulation efficiency of 3 experiments done in triplicate was $79 \pm 19.2 \%$.

Conclusion:

The technology used in this work has allowed a more portable setup of the required equipment for droplet microfluidics tests, enabling us to establish a microfluidic system inside a flow hood to produce sterile, spherical, homogeneous and biodegradable microgels in the microscale. Furthermore, we achieved an encapsulation efficiency high enough to recover most of the initial nanoparticle mass utilized in the encapsulation process. By allowing the efficient encapsulation of nanoparticles, this platform is a promising for gene therapy delivery. Next, we will evaluate the encapsulation efficiency and the release profile of viruses encapsulated in microgels and its further applications in gene therapy.

Financial support:

CAPES, CNPQ, Fapesp

16.008 - ADIPOSE-DERIVED MESENCHYMAL STEM CELLS IMPROVED STRUCTURAL ORGANIZATION OF THE INJURED CALCANEAL TENDON. Leite FG, FRAUZ K, Teodoro LFR, Aro AA, - Pos Graduação em Ciências Biomédicas - UNIARARAS Departamento de Biologia Funcional e Estrutural - UNICAMP

Introduction:

Cell therapy using adipose-derived mesenchymal stem cells (ADMSC) is promising for the treatment of tendon injuries due to their paracrine and immunomodulatory potential.

Aim:

Considering the high incidence of tendon injuries, which present a slow and complex healing process, the aim of the present study was to evaluate the effect of ADMSC application on the calcaneal tendon repair on the 14th, 21st and 45th days after injury.

Methods:

Thus, the analysis of gene expression was performed for Col1a1, Col3a1, Fmod, Tnc, Bgn, Sdc4, Fn, Ctgf, Vegf, Igf1, Egr1, Mxk, Smad2 and Smad3. On the 45th day after tendon transection, the analyses of the collagen organization and of the proteoglycans distribution in the extracellular matrix (ECM) were also performed. Lewis rats were divided in 7 groups: tendon without transection (N); Transected tendons (T14, T21 e T45); transected tendons + ADMSC (TC14, TC21 e TC45).

Results:

The ADMSC increased the genes expression of the Col1a1 and Tnc on the 14th day, as well as of the Tnc, Ctgf e Mxk on the 45th day. Lower amount and distribution of the proteoglycans were observed in the TC45 group in relation to the T45 group. Higher birefringence indicating higher collagen fibers organization was observed in the TC45 group.

Conclusion:

Our results demonstrated that the ADMSC increased the genes expression of Col1a1, Tnc, Ctgf and Mxk, contributing with a higher collagen fibers organization. Thus, the ADMSC application on the tendon repair can be promising, and new studies should be carried out to analyze the effects of this major tissue reorganization on tendon biomechanics in later times of the healing process.

Financial support:

Fundação Hermínio Ometto-UNIARARAS

16.009 - TRANSCRIPTIONAL PROFILE DURING MUSCLE CELL ATROPHY INDUCED BY MIR-155. Lopes LO, Freire PP, Cury SS, Moraes D, Oliveira JS, Oliveira G, Fernandez GJ, Dal-Pai-Silva M, Carvalho RF, - Morfologia - Unesp

Introduction:

Regulatory molecules, such as microRNAs (miRNAs), are involved in the control of gene expression in several muscular diseases. The miRNAs act in an orchestrated way to control biological functions. An emergent cooperative property of miRNAs is the regulation of transcriptional and epitranscriptional events that may determine muscle phenotype. Moreover, miRNA-mediated control of gene expression in skeletal muscle involves mRNAs that encode transcription factors, kinases, and phosphatases. Previous global miRNA expression studies in muscle diseases have identified an increased expression of miRNA miR-155 in muscular dystrophies and muscle cell atrophy; however, the overall functionality of the miR-155 in skeletal muscle cells is not yet known.

Aim:

We aimed to identify the potential direct and indirect target transcripts of miR-155 in C2C12 muscle cells.

Methods:

C2C12 myoblasts were transfected for 15 hours with the miR-155 mimetic molecule or with the respective negative control and, subsequently, these myoblasts were differentiated into myotubes for 120 hours. After this period, we performed transcriptome (RNA-Seq) and morphometric analyses. Subsequently, we identified all potential miR-155 targets transcripts using the computational algorithms miRWalk and miRTarBase. These data were compared to the transcriptional profile of miR-155 treated myotubes. The tool X2K Web was used to construct networks of transcription factors, proteins, and kinases predicted to regulate the differentially expressed genes. The data were compared using parametric or non-parametric tests. We considered a 5% difference as statistically significant.

Results:

The overexpression of miR-155 in skeletal muscle cells changed the transcriptional profile of C2C12 myoblasts and myotubes. The myotubes treated with miR-155 changed the expression of 359 genes (166 up-regulated, and 193 down-regulated; p-value < 0,05 and fold change > 1.5). These differentially expressed genes were associated with inflammation, cell cycle dysregulation, and apoptosis. The transcriptional factors E2F4, SIN3A, and FOXM1 were predicted to regulate genes associated with phosphorylation during cell proliferation

FeSBE Annual Meeting 2019

Poster Sessions and Abstracts

and differentiation, disruption of the sarcomere, and apoptosis. The kinases MAPK14, CDK4, and HIPK2 were predicted to regulate genes associated with activation and transcriptional repression, cell cycle progression, inflammatory response, and fibrogenesis.

Conclusion:

Our results show that miR-155 contributes to C2C12 muscle cell atrophy by controlling, directly and indirectly, a set of genes that include transcriptional factors and kinases controlling key biological functions in muscle cells.

Financial support:

This study was supported by a grant from the São Paulo Research Foundation (FAPESP) (grant #2018/23923-0).

17 - Basic & Clinical Pharmacology

17.006 - EFFECTS OF CHALCOGENOQUINOLONES IN MODULATION OF THE ACTIVITY OF CYSTEINE PROTEASES FROM LEISHMANIA MEXICANA. Iorio JFD, Stefani HA, Rodrigues T, Judice WAS, - Centro Interdisciplinar de Investigação Bioquímica - UMC Faculdade de Ciências Farmacêuticas da USP - USP Centro Ciências Naturais E Humanas - UFABC

Introduction:

Leishmania mexicana has a considerably higher cysteine protease activity in the amastigote form than in the promastigote form, favoring the survival of the amastigote in the macrophages of the mammalian host, making them important targets for the development of antileishmanial drugs. The class of CPBs in L. mexicana exists as multiple isoforms, encoded by a tandem array of 19 genes numbered in cpb1-cpb19. The CPB2.8 has Asn60, Asp61 and Asp64 whereas CPB3 has Asp60, Asn61 and Ser64, and CPB18 substitutes His84 for Tyr84. Chalcogenoquinolones are compounds that contain selenium in its structure and has attracted attention due to its biological properties, have neuroprotection, antipsychotic and anti-trypanosomatid effects.

Aim:

Characterization of chalcogenoquinolones compounds with potential inhibitory activity on cysteine proteases of trypanosomatids rCPB2.8, rCPB3 and rH84Y involved as virulence factors in leishmaniasis.

Methods:

Screening of inhibition was done using two fixed concentrations (10 μ M and 100 μ M) for each compound (25 chalcogenoquinolones). Compounds that showed inhibition of activity greater than 50% were selected to determine the inhibitory potential (IC₅₀). Assays were performed in 100 mM sodium acetate buffer (20% glycerol, 0.04% triton X-100, 5 mM DTT) pH 5.5 with enzymatic preactivation for 5 min at 37 °C. The activity of the enzymes (rCPB2.8, rCPB3.0 and rH84Y) was followed in λ Ex=360nm and λ Em=480nm in Hitachi-F2700 spectrofluorometer, in quartz cuvette using Z-FR-MCA as probe. The inhibitory potential was determined using increasing concentrations of each molecule and the IC₅₀ values determined by non-linear regression.

Results:

From the inhibition screening, four compounds (15, 18, 23 and 25) were selected at rCPB2.8, and IC₅₀ values determined were 3.6 \pm 0.8 μ M, 12.9 \pm 0.3 μ M, 54.0 \pm 1.6 μ M, 31.0 \pm 0.9 μ M, respectively. At inhibition of rH84Y the compounds 7, 8, 15, 18 and 23 were selected, which presented IC₅₀ values of 3.3 \pm 0.1 μ M, 8.7 \pm 0.05 μ M, 12.34 \pm 0.04 μ M, 20.19 \pm 0.5 μ M and 25.7 \pm 0.7 respectively. Enzyme rCPB3 where effectively inhibited by the compounds 7, 15, 18 and 23 from the screening assay, which presented IC₅₀ values of 4,56 \pm 0,08 μ M, 5,24 \pm 0.407 μ M, 6,38 \pm 0.18 μ M and 5,11 \pm 0.28 μ M respectively.

Conclusion:

The compounds 15, 18 and 23 were effective in the inhibition of three cysteine proteases, which could be related to the hydrophobicity of the compounds. Substitutions of the amino acid residues of the enzymes provided increased inhibitory capacity, since compound 23 was approximately two fold more potent in inhibiting rH84Y than rCPB2.8.

The ester in the structure of the molecule may have provided an interaction with the tyrosine residue at position 84 of the enzyme. However, compounds 15 and 18 were less potent in inhibiting rH84Y when compared to rCPB2.8.

Financial support:

FAEP, FAPESP, CNPq, CAPES, OMEC

17.007 - PHYTOCHEMICAL, CYTOTOXIC, ANTIOXIDANT AND MICROBIAL ACTIVITY OF GARCINIA BRASILIENSIS MART. (CLUSIACEAE) LEAVES ALCOHOL EXTRACT. Souza HR, Guandalini RB, Silva JM, Possebon L, Costa SS, Iyomasa-Pilon MM, Moreno AH, Girol AP, - Pós-Graduação - UNESP Ciências Básicas - UNIFIPA

Introduction:

In Brazil, the Garcinia brasiliensis species stands out in popular medicine by its anti-inflammatory and healing properties. Flavonoids and tannins, products of secondary plant metabolism which present biological activities of pharmacological interest, have already been identified in the G. brasiliensis leaves. However, these components may also present cell cytotoxicity.

Aim:

To quantify the presence of total polyphenols (flavonoids e tannins) and to evaluate the antioxidant and microbiological activities and also the cytotoxicity profile of the G. brasiliensis leaves crude alcoholic extract, or it's fractions, to develop topical formulation for wounds in the future.

Methods:

Leaves were collected in July/2019 of a G. brasiliensis specimen (exsiccata in the Irina Delanova Gemtchujnicov (BOTU) herbarium, number 33511). 20 g of dried and crushed leaves were infused for 24h in 100 mL of 70% alcohol. After, the alcohol was evaporated with rotary evaporator under reduced pressure at 45 °C to obtain the crude extract (PE). Subsequently, fractions were made by mixing hexane (HF) and ethyl acetate (EAF) in equal proportion to the PE for 24 h. After removing the solvents from the organic portion obtained the separated products were rediluted in water. In PE, HF and EAF quantitative colorimetric tests of flavonoids and polyphenols were performed using quercetin and gallic acid, respectively, as standards for the concentration curve. The antioxidant activity was verified by DPPH assay. An in vitro cytotoxic study was made using a glycosylated solution (5%) of erythrocytes, (4%) with 2.5, 5, 7.5 e 10% concentrations of PE, HF, EAF. We also proceed the in vivo cytotoxicity analysis by the chorioallantoic membrane (CAM) assay. 50 μ l of PE and EAF at 10%, were injected in fertilized Gallus gallus eggs, incubated at 37.5°C and relative humidity at 50% for 72h. Then, the egg shell was removed for evaluation of the vascularization in the CAM. Control eggs were injected with saline (0.9%). Microbiological test was performed with Staphylococcus aureus culture on BHI medium (dilution of 1.105, McFarland scale) and applied on Müller Hinton agar with PE and EAF embedded discs at concentrations of 20, 50 e 100 %.

Results:

The PE, HF and EAF presented, respectively, 7.8; 0.054 and 5.38 μ g/mL of flavonoids; 18.42; 0.0508, and 5.08 μ g/mL of polyphenols, 23.35; 14.2 and 84.01 % of antioxidant activity. In this way, HF showed less biological activity than PE and EAF. Also, the tannins were most likely excluded for the EAF fraction. The in vitro cytotoxic assay showed that PE was more cytotoxic than the fractions. But in CAM assay, both PE and EAF did not interfered in the embryos development or altered the vascularization of the CAM. The microbial assay indicated that only PE at 50 and 100% presented inhibition halo of bacterial growth of 0.3 and 0.5 cm, respectively.

Conclusion:

Our results showed higher biological and antioxidant activities for PE and EAF as well as their safety at the concentration of 10%. These findings highlighted the potentiality of the use of G. brasiliensis leaves extract for new drugs formulations.

FeSBE Annual Meeting 2019

Poster Sessions and Abstracts

Financial support:

Centro Universitário Padre Albino (UNIFIPA). Note.: postgraduate project in progress, the results presented are partial.

17.008 - INVOLVEMENT OF VOLTAGE-GATED ION CHANNELS IN THE EX VIVO AND IN VIVO EFFECTS OF CROTAMINE ON SKELETAL MUSCLE. Porta LC, Lima SC, Lima AC, Campeiro JD, Meurer Y, Teixeira NB, Duarte T, Oliveira EB, Picolo G, Godinho RO, Silva RH, Hayashi MAF, - Farmacologia - UNIFESP Departamento de Fisiologia - UFRN Laboratório Especial de Dor e Sinalização - IBU Departamento de Bioquímica e Imunologia - USP-RP

Introduction:

Crotamine, is a polypeptide from the venom of the South American rattlesnake *Crotalus durissus terrificus* "cascavel", which promotes a peculiar hind limbs paralysis, which seems important for the immobilization and capture of prey, and therefore, for this snake feeding advantage. However, little is known about the molecular mechanism of action involved in this paralysis described only in rodents up to now. In this work, aiming to clarify the mechanism(s) underlying the hind limbs paralysis triggered by crotamine, we have concomitantly performed ex vivo and in vivo assays to confirm the involvement of voltage-gated ion channels in this best-known toxic effect of this snake cationic polypeptide.

Aim:

Evaluate the involvement of voltage-gated sodium and potassium channels in the effect elicited by crotamine on skeletal muscles, employing in vivo and ex vivo assays.

Methods:

The contraction of diaphragm of adult male Swiss mice was evaluated ex vivo under transmural electrical stimuli, with 2 ms of duration, frequency of 0.1 Hz and supramaximal voltage, in the presence of crotamine and/or voltage-gated potassium (KV) channel blockers. Behavioral evaluation (namely open field, sucrose splash and hind limb immobilization tests) was performed employing C57/BL6 mice receiving crotamine and/or voltage-gated Na⁺ (NaV) or KV channel activators/blockers by intraperitoneal (i.p.) route.

Results:

Concentration-dependent positive inotropic effect (17-46 %) was observed for 3-10 nM crotamine. In addition, the KV channel blocker 4-aminopyridine (4-AP, 1 μM) increased by approximately 20% the crotamine-positive inotropic effect in this ex vivo experiment. In vivo administration of crotamine, reduced by about 40% the distance traveled by the animals in the open field and also reduced by 48% the total grooming period in the sucrose splash test. Also, 4-AP potentiated crotamine effect, reducing by 50% the distance travelled in open field test, compared to the effect of crotamine alone. The time-lapse to observe the hind limb paralysis was also dose-dependent, and higher doses allowed observing mice paralysis faster than when using lower doses. For instance, paralysis was observed after 7 min for 1.2 mg/kg, and after 3 min for 2 mg/kg of crotamine, i.p. Moreover, the paralysis effect and the animal death triggered by crotamine were both influenced by the KV channel blocker 4-AP, while the NaV channel blocker tetrodotoxin (TTX) affected the time for paralysis provoked by crotamine and NaV channel activator veratridine (VTD). Finally, TTX also delayed the death of animals due to the administration of crotamine or VTD.

Conclusion:

We show here that 4-AP can potentiates the crotamine effects on skeletal muscle as observed in either ex vivo or in vivo experiments. Also, the NaV channel activator/blocker influenced the time for paralysis and death of the animals triggered by crotamine. Taken together, we established the involvement of voltage-gated NaV and KV channels in hind limb paralysis induced by crotamine. These data may contribute to develop new methods for the treatment of muscular

dysfunctions or symptoms in ophidian envenomation by crotamine-positive rattlesnakes.

Financial support:

CAPES, CNPq and FAPESP.

17.009 - COMPARISON OF THE PHYTOCHEMICAL, ANTIOXIDANT, CYTOTOXIC AND MICROBIOLOGICAL PROFILES OF AQUEOUS AND ETHANOLIC EXTRACTS OF GARCINIA BRASILIENSIS LEAVES. Yoshikawa AH, Dairou H, Possebon L, Souza HR, Moreno AH, Girol AP, - Laboratório Multidisciplinar - UNIFIPA

Introduction:

Plants extracts present compounds with high anti-inflammatory and antimicrobial potential. However, it is important to characterize their actions and establish safe and effective dosages. Among the promising plant extracts we highlight those obtained from *Garcinia brasiliensis*, popularly known as bacupari.

Aim:

To compare the crude aqueous and ethanolic extracts obtained from *G. brasiliensis* leaves in relation to the phytochemical, antioxidant, cytotoxic and microbiological profiles for future pharmacological studies.

Methods:

G. brasiliensis leaves (exsicata in the Irina Delanova Gemtchujnicov (BOTU) herbarium, number 33511) were dried at 40°C until constant weight and ground by the turbolysis. Both final crude extracts were at 20% concentration. The aqueous extract (AE) was obtained by infusion (20g in 100 mL of boiling water) and the ethanolic extract (EE) was obtained by percolation (20g in 100 mL of 70% alcohol), then alcohol was evaporated and the extract diluted in physiological solution. The phytochemical analyses were performed by different colorimetric reactions for the identification of tannins (ferric chloride, lead acetate, copper acetate, glacial acetic acid and Wasicky reactive); flavonoids (aluminum chloride, ferric chloride, sodium chloride) and alkaloids (Heiber, Bourchardot, Mayer, Dragendorff). The antioxidant activity was verified by DPPH assay. Different concentrations of both extracts (2%,4%,6%,8% and 10%) were evaluated for cytotoxicity in vitro using a glycosylated solution of erythrocytes, followed by absorbance reading in the spectrophotometer (540nm). For microbiological evaluations, the microorganisms *Escheria coli*, *Staphylococcus aureus* and *Klebsiella pneumoniae* (dilution of 1.105, McFarland scale) were incubated in Petri dishes at 37 °C for 24h with discs moistened in different concentrations of the *G. brasiliensis* extracts (4%, 6%, 12%, 25%, 50%, 75% e 100%). After this period the halos of these discs were measured and compared to the Ampicillin antibiotic.

Results:

In both extracts the phytochemical reactions identified the presence of tannins (AE and EE: ferric chloride positive; EE: copper acetate and specific gallic tannins positive), flavonoids (AE and EE: ferric chloride and sodium chloride positive) and alkaloids (AE and EE: Bourchardot and Dragendorff positive). The antioxidant activity of AE was 69.2% and that of EA was 64.4%. In the citotoxicity test AE showed low hemolysis rate even at 10% concentration (1,064 absorbance), but relative hemolysis was already detected at 4% concentration in EE (1,194 absorbance), compared to the positive hemolysis control (1,775 absorbance). None of the extracts inhibited the *Escheria coli*. Only EE presented inhibition halos for *Staphylococcus aureus* at 50% (0,1 cm), 75% (0,3 cm) and 100% (0,5 cm) and for *Klebsiella pneumoniae* at 4%,6%,12%,25% (0,1 cm) and 50% (0,2 cm).

Conclusion:

Both extracts present important biological profiles. EE present more chemical compounds and antimicrobial activity but also higher cytotoxicity. These results stimulate future studies on pharmacological application of the *G. brasiliensis* extracts.

Financial support:

FeSBE Annual Meeting 2019

Poster Sessions and Abstracts

Centro Universitário Padre Albino (UNIFIPA). Note: Scientific initiation project in progress, the results presented are partial.

18 - Neuropsychopharmacology

18.006 - ACUTE ANTIDEPRESSANT EFFECTS OF DIFFERENT KETAMINE ISOMERS IN RATS SUBMITTED TO MATERNAL SEPARATION ANIMAL MODEL: A PILOT STUDY. Beanes G, Carneiro B, Marques G, Melo YV, Carvalho G, Réus GZ, Lacerda ALT, Quarantini L, Santana RC, - Biorregulação - UFBA Neurociências e Saúde Mental - UFBA Psiquiatria - UNIFESP Universidade Federal da Bahia - UFBA Programa de Pós-Graduação de Medicina e Saúde - UFBA

Introduction:

Background: Major depressive disorder (MDD) is a chronic, recurrent and disabling mental disorder with a high prevalence worldwide. Conventional treatment for MDD produces low response rates and it is associated to tolerability issues and treatment resistance in about thirty percent of patients [1]. Maternal separation is a validated animal model that promotes neurological and behavioral changes such as those presented in depressed individuals. This is a widely animal model used to study new antidepressant drugs, such as ketamine [2]. A subanesthetic dose of ketamine has shown promising results as a new therapeutic option for MDD [3]. However, the most studies have investigated its racemic form of (R,S)ketamine. It is still not clear whether ketamine enantiomers, R(-)ketamine and S(+)-ketamine, would be equivalent to the standardized racemic one. Moreover, there is a lack of data about which presentation of ketamine is the most effective antidepressant.

Aim:

Objective: To investigate the acute antidepressant effects of ketamine enantiomers and their racemic form in rats subjected to maternal deprivation model.

Methods:

Methods: An experimental preclinical study was performed with 30 male Wistar rats. They were randomized into seven experimental groups: non-deprived with placebo and other six deprived split into control and intervention groups. The protocol number CEUA 1638100518 was approved by the Ethic Committee on Animal Use of the Federal University of Bahia (Health Sciences Institute) (CEAU/ICS, UFBA). The enantiomers and doses used were (R,S)ketamine (10mg/kg), S(+)-Ketamine (10mg/kg), and R(-)ketamine (5,10 or 20mg/kg). The analyses of the type-depressive behavior were performed through grooming time in the splash test and immobility time in the forced swimming test. The differences between the experimental groups were examined with the Mann-Whitney U-Test for independent samples.

Results:

Results: Maternal deprivation seems to increase anhedonic-like and depressive-like behaviors. The mean of grooming time was lower in the deprived ($68,9 \pm 3,3$) as compared to the control group ($71,5 \pm 19,6$), both treated with saline. Similarly, the mean immobility time was higher in the deprived group ($182,8 \pm 29,5$) than in the control group ($139,6 \pm 18,6$) both treated with saline, however ($p > 0,05$). Additionally, in deprived rats, ketamine treatment was associated to increases in grooming time ($73,7 \pm 12,1$ vs. $68,9 \pm 3,3$), ($p > 0,05$). S(+)-Ketamine (10mg/kg) was more efficacious in treatment of anhedonic-like behavior as compared to R(-)ketamine (20mg/kg). Ketamine ($142,5 \pm 53,6$) also tends to revert the immobility behavior present in deprived rats when compared to those treated with placebo ($182,8 \pm 29,5$), ($p > 0,05$). S(+)-Ketamine (10mg/kg) was more efficacious for treating immobility in private rats, followed by R(-)ketamine (10 mg/kg) and (R,S)ketamine (10 mg/kg). R(-)ketamine (5 or 20 mg/kg) seems not to be effective in reducing the time of immobility.

Conclusion:

Conclusion: Present results suggest that Ketamine is effective for reversing the anhedonic and depressive-like behaviors of rats subjected

to maternal deprivation. For both parameters evaluated, S(+)-Ketamine seems to be more effective than both R(+)-Ketamine and R,S-Ketamine in doses studied.

Financial support:

PIBIC - UFBA, FAPESB e PPSUS

18.007 - EXPLORING THE OBJECT DISCRIMINATION TEST IN ZEBRAFISH AT DIFFERENT RETENTION INTERVALS. Stefanello FV, Fontana BD, Ziani PR, Müller TE, Mezzomo NJ, Rosemberg DB, - Bioquímica e Biologia Molecular - Universidade Federal de Santa Maria

Introduction:

The object discrimination test allows the testing of different memory retention periods. However, few behavioral endpoints have been measured in fish and retention is often assessed using a single parameter (time spent in object area). Importantly, other behaviors may reflect interaction of the zebrafish with the objects, which can vary depending on the retention period.

Aim:

Here, we explore the behavioral repertoire of zebrafish in the object discrimination task after distinct retention times (1 and 24h) in the presence or absence of scopolamine.

Methods:

Animals were individualized in house tanks and then habituated for 3 consecutive days to the experimental tank. Training session was performed for 10 min using two identical nonpreferred objects (black cube and sphere). After the retention interval (1 or 24 hours), a familiar object was replaced by a novel object (test session, 10 min). To characterize putative interaction-like behaviors, fish were tested in the absence or presence of scopolamine (1 hour before the test session). Fish were also tested in a novel tank to assess locomotion and anxiety-like behaviors. Preference percentages were calculated as follows: time of exploration of novel object/time of exploration of familiar object + time of exploration of novel object x 100. All protocols were approved by the Ethics Commission on Animals Use of the Federal University of Santa Maria (protocol number 2220181215). Data normality and homogeneity of variances were analyzed by Kolmogorov-Smirnov and Bartlett's tests, respectively. Behavioral endpoints measured across the habituation phase were analyzed by repeated-measures analysis of variance (ANOVA), whereas object preference and behaviors measured in the novel tank diving test were assessed by two way ANOVA. Post hoc comparisons were made using the Student-Newman-Keuls multiple range test when necessary. Object discrimination in each session was analyzed using Student's t-test.

Results:

Animals showed a significant reduction in distance traveled ($F(34, 68) = 14.18$; $p < 0.0001$) and erratic movements ($F(34, 68) = 2.422$; $p = 0.001$) after 3 days of habituation to the test apparatus. The shape and position of the object inside the tank had no effect on behavior. After the 1 hour retention interval, zebrafish spent more time ($t = 2.781$, $df = 46$, $p = 0.0078$) but presented reduced circular-like investigation near the novel object ($t = 2.328$, $df = 46$, $p = 0.0244$). After the 24 hours interval retention, zebrafish spent more time ($t = 2.099$, $df = 36$, $p = 0.0429$) and performed more rapid investigations in the novel object ($t = 2.169$, $df = 36$, $p = 0.0368$). Scopolamine abolished these phenotypes, as well the increased time spent in the novel object area during the test session, without changing locomotion and vertical activity in the novel tank test.

Conclusion:

Overall, we described two novel interaction-like behaviors (circular-like investigation and rapid investigation), which are sensitive to scopolamine and differ depending on the memory retention interval. Because isolation and scopolamine do not affect locomotion and anxiety-related behaviors, the behaviors measured predict potential temporal differences on the exploratory pattern of fish in the object discrimination test.

Financial support:

CAPES, CNPq

FeSBE Annual Meeting 2019

Poster Sessions and Abstracts

18.008 - ANTIDEPRESSANT EFFECT OF DIOCLEA VIOLACEA LECTIN ADMINISTERED IN RATS SUBMITTED TO CEREBRAL ISCHEMIA/REPERFUSION INJURY. CUNHA PLO, NETA MSBDF, LIMA LAR, LOPES MJP, SANTOS VFD, TEIXEIRA CS, FACUNDO HDTF, LIMA ISP, NOBRE MEP, - Research Laboratory in Neuroscience and Neuroprotection-LAPENN - Federal University of Cariri-UFCA Department of Morphology - Federal University of Ceará - UFC Laboratory of physiology, biochemistry and pharmacology - Estácio FMJ Laboratory of molecular and structural biology - LaBEM - Federal University of Maranhão - UFMA

Introduction:

Leguminous lectins are proteins of non-immunologic origin, able to recognize and bind specifically and reversibly to carbohydrates of cell surfaces. It has been described that lectins present anti-inflammatory, antidepressant, and anti-ischemic activities. A study demonstrated the antidepressant effect of lectin isolated from *Canavalia brasiliensis* seeds (ConBr). The lectin of *Dioclea violacea* (DVL) presents structural similarity with the ConBr.

Aim:

The present study aimed to evaluate the antidepressant effect of the lectin extracted from the seeds of *Dioclea violacea* (DVL) administered to rats submitted to cerebral ischemia/reperfusion injury.

Methods:

All experimental procedures were approved by the Committee on the Ethical Use of Animals at the Federal University of Cariri (Protocol nº003/2019). Male Wistar rats (280–300 g) were divided into five groups (n=4 a 8): the sham group (Sh), I/R non-treated group (I/Rn) and I/R treated with DVL at concentrations of 0.1, 0.5 e 1.0 µg/µL. Animals were anesthetized with ketamine hydrochloride (90mg/Kg, ip) and xilasin (10 mg/kg, ip) and then were submitted to stereotaxic surgery to intracerebroventricular (icv) administration of DVL in the lateral right ventricle according to a stereotactic orientation (Squishy: 1.2 ± 0.4 mm, depth: 3.2 ± 0.4 mm, straight to the middle sagittal plane: 1.4 ± 0.2 mm), fifteen minutes before bilateral occlusion of the carotid arteries. Sh and I/Rn animals were administered with saline (1 µl, icv). Animals were submitted to the cerebral ischemia model by bilateral occlusion of the carotid arteries for 30 minutes, followed by reperfusion. Animals in the Sham group received the same surgical process, except occluding common carotid arteries. After 24 h, animals were submitted to tests screening for alterations in locomotor activity (open field test), and forced swimming test (FST). Animals were decapitated and 10% homogenates from striata were used for the determination of dopamine (related to the generation of hydrogen peroxide) in HPLC. The data were analyzed by One-way ANOVA, followed by the Student-Newman-Keuls as a post-hoc test. The results were considered significant at p < 0.05.

Results:

Ischemia (I/Rn, 4.6±1.1, n=8) significantly decreased locomotor activity at 47,7% in relation to the sham group (Sh, 8.8±0.6, n=5) and this effect was reversed by DVL 0.1 (11.6±0.5, n=5) and DVL 0.5 (11.8±1.1, n=8). In the forced swimming test, the immobility time for DVL 0,1 (35.0±6.4, n=5) and DVL 0,5 (43.1±7.9, n=8) groups significantly decreased in contrast to the group I/Rn (79.9±12.8, n=7). DVL 0,5 (2.6±0.1, n=4) induced alterations in striatal monoamine contents, decreasing dopamine (DA) levels as compared to the group I/Rn (3.6±0.2, n=4).

Conclusion:

Our results showed that DVL reversed the changes of locomotor activity and forced swimming test promoted by ischemia, as well as prevented the increased of the dopamine levels in striatal areas, showing a potential neuroprotector and antidepressant effect of DVL, since dopamine oxidation by monoamine oxidases is one of the major mechanisms of harmful hydrogen peroxide generation in the brain.

Financial support:

Pro-Rectory of Research and Innovation - PRPI / Federal University of Cariri - UFCA

18.009 - ANTIOXIDANT EFFECT OF DIOCLEA VIOLACEA LECTIN ON CEREBRAL ISCHEMIA-REPERFUSION INJURY IN RATS. NETA MSBDF, CUNHA PLO, LIMA LAR, LOPES MJP, SANTOS VFD, TEIXEIRA CS, FACUNDO HDTF, LIMA ISP, NOBRE MEP, - Research Laboratory in Neuroscience and Neuroprotection-LAPENN - Federal University of Cariri-UFCA Department of Morphology - Federal University of Ceará - UFC Laboratory of physiology, biochemistry and pharmacology - Estácio FMJ Laboratory of molecular and structural biology - LaBEM - Federal University of Maranhão - UFMA

Introduction:

Lectins are proteins that specifically bind to carbohydrates and form complexes with molecules and biological structures containing saccharides, without altering the covalent structure of the glycosyl ligands. Because of the ability to interact with cellular glycans, these proteins may exhibit various biological activities, such as antioxidant, anti-inflammatory, antinociceptive, antidepressant and anti-ischemic activity.

Aim:

The objective of this study was to evaluate the effect of the lectin extracted from the seeds of *Dioclea violacea* (DVL) on the reduction of oxidative stress in cerebral ischemia-reperfusion injury in rats.

Methods:

The experimental procedures were approved by the Ethics Committee on Animal Research of Federal University of Cariri (nº 003/2019). Wistar male rats aged 9 weeks and weighing 280-300 g were anesthetized with ketamine hydrochloride (90 mg/kg, i.p.) and xylazine (10 mg/kg, i.p.). After anesthesia the animals underwent stereotactic surgery for intracerebroventricular (i.c.v.) administration of DVL at concentrations of 0.1, 0.5 and 1.0 µg/µL, with a constant volume of 1 µl, fifteen minutes before the induction of cerebral ischemia. The animals were submitted to the cerebral ischemia model by bilateral carotid occlusion for 30 minutes, followed by reperfusion. Five experimental groups were evaluated: (Sh) Sham; (I/Rn) ischemia; (I/R+DVL0.1) ischemia + DVL 0.1µg/µL; (I/R+DVL0.5) ischemia + DVL 0.5µg/µL, (I/R+DVL1.0) ischemia + DVL 1.0µg/µL. After 24 hours of the surgical procedure, the animals were euthanized by guillotine decapitation and the striatum (ST), hippocampus (HP) and pre-frontal cortex (PFC) were dissected for preparation of homogenates and determination of concentrations of nitrite and thiobarbituric acid reactive substances (TBARS). The data were analyzed by ANOVA and Newman-Keuls as the post hoc test. The results were considered significant at p<0.05.

Results:

The evaluation of the nitrite concentration in the hippocampus (169.0±4.6; n=3) and in the striatum (150.1±15.2; n=5) was about 2.2 times higher in animals submitted to ischemia in relation to the concentration of nitrite obtained in the Sham group (HP: 77.2±22.9, n=3, ST: 69.2±8.9, n=4). In the pre-frontal cortex, the increase was 4 times higher (79.8±10.5; n=4) than the Sham (19.9±5.9; n=4). Treatment with DVL reduced nitrite levels in the three areas evaluated, mainly in HP, where the concentrations of 0.1 (11.1±1.4; n=3), 0.5 (3.4±0.9; n=3) and 1.0 µg/µL (9.8±4.6; n=3) were reduced to levels well below of Sham group. Similar result was observed in the striatum at the concentration of 0.5 µg/µL (23.2±10.3; n=4). Regarding TBARS, the results showed that cerebral ischemia increased the levels of TBARS in ST (490.6±45.5; n=4) and PFC (397.6±45.3; n=5) an increase of 1.7 and 1.5 times, respectively, in relation to the Sham group (ST: 285.5±50.6; n=4; PFC: 260.8±33.3; n=3). On the other hand, DVL was able to reduce the levels of TBARS in ST at concentrations of 0.1 (104.1±12.3; n=4) and 0.5 µg/µL (91.7±21.4; n=4).

Conclusion:

From the results it was possible to conclude that the DVL showed antioxidant effect, reducing nitrite and TBARS levels induced by ischemia-reperfusion injury, demonstrating a neuroprotective potential of this protein.

Financial support:

FeSBE Annual Meeting 2019

Poster Sessions and Abstracts

Pro-Rectoria of Research and Innovation - PRPI / Federal University of Cariri - UFCA

18.010 - NEUROPROTECTIVE EFFECTS OF TREHALOSE IN A MICE MODEL OF TRAUMATIC BRAIN INJURY. Oliveira VG, Strogulski NR, Dorneles W, Salimen M, Kopczynski A, Hansel G, PORTELA LV, - Bioquímica - UFRGS

Introduction:

Traumatic Brain Injury (TBI) is a leading cause of morbidity and mortality internationally. It is also a risk factor for neurodegenerative disorders, such as Alzheimer's disease, linked to accumulation of dysfunctional mitochondria and neurotoxic proteins, giving support to diffuse chronic damage. Autophagy is responsible for the clearance of such intracellular aggregates and is knowingly impaired posterior to TBI. Since autophagy is an inherently cytoprotective mechanism, and that neurotoxic aggregates and dysfunctional cerebral bioenergetics, chronically lead to cognitive impairment; here we aimed to investigate potential of autophagy induction with trehalose phosphate (TP), a mTOR-independent autophagy inducer, as a neuroprotective agent, posteriorly to a severe TBI in mice.

Aim:

Here we assess the cognitive, bioenergetic, and neurochemical outcomes of autophagy induction with trehalose phosphate in a mice model of severe TBI.

Methods:

C57BL6/J mice (90 days) were anesthetized and a 5 mm craniotomy was performed, posteriorly these mice were separated in 3 groups: a group submitted to a severe controlled cortical impact (tip diameter: 3mm, impact speed: 5.7m/s, AP: 0.0 mm; L: -3.0 mm, V: -2.0 mm), with ad libitum either to water (CCI group), or a 2% solution of trehalose phosphate (TRE group); and a group of mice submitted only to craniotomy and access to water (SHAM group). After 14 days, mice were euthanized, and biochemical analyses performed. Mitochondrial respiration parameters were assessed in ipsilateral hemispheres with an Oroboros® O2-k High resolution Oxygraph, H₂O₂ production was assessed with Amplex Red (Invitrogen), and mitochondrial membrane potential ($\Delta\psi_m$) with safranin-o (Sigma-Aldrich). Cell viability was evaluated with MTT assay. Immunoccontent of contralateral hippocampus neurotoxic pTauSer396 was assessed with western blotting. Cognitive performance was evaluated with Morris Water Maze (MWM). Statistical analysis was performed with Prism GraphPad 7, through One-Way Analysis of Variance (ANOVA); and statistical significance considered when $p < 0.05$.

Results:

Mitochondrial oxidative phosphorylation related O₂ consumption ($p = 0.0334$), Mitochondrial membrane potential variation ($p < 0.005$) and cell viability were reduced in CCI ($p < 0.0001$), and attenuated in TRE mice as compared to SHAM ($p = 0.0485$). Simultaneously, H₂O₂ production ($p < 0.0001$) and neurotoxic pTauSer396 immunoccontent ($p = 0.038$) were increased in CCI but not in TRE group as compared to SHAM. The attenuation of the neurochemical and bioenergetic outcomes of TBI by trehalose led to reduced cognitive damage, indicated in MWM by reduced time in the target zone only by CCI group ($p = 0.0001$) and not TRE ($p = 0.0225$).

Conclusion:

Our results suggest that the induction of autophagy may exert neuroprotective effects over severe TBI, that involve attenuation of bioenergetic and neurochemical damage. Further studies must be performed to further elucidate additional mechanisms for trehalose neuroprotective effect in TBI, as well as evaluate the cell-type specificity of the effects of trehalose in response to TBI.

Financial support:

CAPES, CNPq

19 – Toxicology

19.010 - EVALUATION OF TOXICITY AND ANTIOXIDANT ACTIVITY IN SACCHAROMYCES CEREVISIAE CELLS OF HEXANIC AND ALCOHOLIC EXTRATS OS GREEN PROPOLIS. Fonseca MW, Cardoso BS, Castro RN, Riger CJ, - Bioquímica - UFRJ

Introduction:

Reactive oxygen species (ROS) from metabolism may cause oxidative stress in several cell types of tissues affected by various pathologies. These ROS increase free radical concentration and can damage plasma membranes by lipid peroxidation and promote extravasation and entry of substances into cells; altering cellular homeostasis, increasing levels of oxidative stress and causing cell death. However, there are endogenous and exogenous substances with antioxidant properties, which can reduce stress in cells. Studies show that propolis has antioxidant activity and several compounds with these characteristics were detected and isolated in different extracts of propolis.

Aim:

The objective of this study is to evaluate the toxicity and antioxidant potential of ethanolic and hexane extracts of green propolis using Saccharomyces cerevisiae cells, a cellular eukaryotic model widely used in these studies.

Methods:

To test cell tolerance against extracts, the cells were cultured by lofting in 2% YPD (2% glucose, yeast extract 1%, peptone 2%) liquid medium. Then, a volume corresponding to 20 mg of cells was incubated in liquid medium with different concentrations of the extracts (25, 50, 100 and 200 $\mu\text{g}\cdot\text{mL}^{-1}$) for 1 hour, together with negative (non-stressed) and positive controls (stressed with 2.0 mM H₂O₂). After incubation, the cells were harvested, washed and the cell vitality assay was performed. In this assay resazurin (blue) was used, which when reduced yields resorufin (pink). The pink staining compound had fluorescence and its quantification was done at 534nm (excitation) and 590nm (emission). As resazurin is reduced according to cellular metabolism, if the cell metabolism is accelerated or normal its coloration will turn pink, and the slower its metabolism, the color will be blue and consequently less fluorescent. This can also be observed qualitatively. The antioxidant analysis was measured by the lipid levels peroxidized in the cell membranes through the TBARS method, maintaining the same parameters of the vitality test. However, there was preincubation with the extracts and subsequent stress with 2.0 mM hydrogen peroxide.

Results:

By the analysis of cellular vitality, the results revealed that the ethanolic extract is less toxic to the yeast cells than the hexane extract. The results are expressed as percentages compared to the negative control. In the experiments with ethanolic extract the four different concentrations presented values equal to 100%; while peroxide stress decreased cellular vitality to $91 \pm 6.94\%$. In the experiments with the hexane extract, we have the following results: $100 \pm 1.62\%$, $99 \pm 0.60\%$, $99 \pm 1.15\%$, $97 \pm 2.61\%$ in increasing order of extract concentration. The results of lipid peroxidation are still preliminary, but apparently the lowest concentration of the ethanolic extract has antioxidant activity. The values found are expressed as pmol MDA / mg cells and were 94.87 for cells without stress; 104.31 for cells under stress with H₂O₂; and 95.29 for the stress cells preincubated with the 25 $\mu\text{g}\cdot\text{mL}^{-1}$ extract.

Conclusion:

In conclusion, the ethanolic extract of green propolis maintains cellular vitality and has good perspectives on the antioxidant activity.

Financial support:

Coordenação de Aperfeiçoamento de Pessoal de Nível Superior - Capes

19.011 - HOW THE PRESENCE OF INORGANIC CONTAMINANTS IN THE MUNDAÚ LAGOON WATER (MACEIÓ-AL) CAN MODULATE THE OXIDATIVE STATUS IN BLOOD CELLS OF FISHERMEN? SILVA-FILHO RC, Pereira NS, Santos MC, Nunes ÁM, Lima TRLA, Pinto RS, Marinho CR,

FeSBE Annual Meeting 2019 Poster Sessions and Abstracts

Fernandes MP, Santos JCC, Leite ACR, - ²Laboratory of Instrumentation and Development in Analytical Chemistry - UFAL ³Research Group of Catalysis and Chemical Reactivity - UFAL ⁴Centro Universitário Cesmac - CESMAC ⁵Laboratory of Biochemistry and Exercise Biochemistry - UFPE ¹Laboratory of Bioenergetics (IQB-UFAL) - UFAL

Introduction:

Oxidative stress is related with various pathologies and can be mediated by the presence of inorganic contaminants (IC) in the organisms. The IC interacts with biomolecules and change cell redox balance. We hypothesized that the IC cause redox unbalance in blood cells of fishermen.

Aim:

Our objective was to evaluate the correlation between the IC in Mundaú Lagoon's (Maceió-AL) and the oxidative stress in fishermen.

Methods:

Mundaú Lagoon's water was collected and the IC concentration (Pb and Hg) were analyzed. The blood of men and women (\approx 48 years old) from the control (C, n = 9) and exposed (E, n = 11) group of the Mundaú Lagoon's water were collected through the isolation of mononuclear cells (PBMC) and erythrocytes. In PBMC we investigated the general ROS and mitochondrial superoxide production, while in erythrocytes were measured the oxidative stress biomarkers (general ROS production, lipid peroxidation and carbonyl protein), the antioxidant enzymes activity (superoxide dismutase (SOD), catalase (CAT), glutathione peroxidase (GPx) and S-transferase (GS-T)), membrane integrity and O₂ uptake. The study was approved by Ethics Committee (CAAE number 57998116.8.0000.501). The results were analyzed by unpaired Student t test, and expressed as mean \pm SDM, considering significant $p \leq 0.05$ for all results.

Results:

Firstly, we observed that the level of Pb (14 to 1230 $\mu\text{g L}^{-1}$) and Hg (0.012 to 1.56 $\mu\text{g L}^{-1}$) in water were higher, according to CONAMA. Next, we observed that general ROS production was 40% high in erythrocytes of fisherman, compared to control group (E= 0.64 \pm 0.13 vs C= 0.46 \pm 0.07 nmol oxidized DCF), but in PBMC general ROS showed no difference (E= 0.49 \pm 0.22 vs C= 0.60 \pm 0.24 nmol oxidized DCF), while in mitochondrial superoxide was observed a tendency of increased in exposed group (E= 3.78 \pm 1.01 vs C= 2.89 \pm 0.99 F.U.). The lipid peroxidation (E= 15.50 \pm 3.03 vs C= 7.77 \pm 2.64 nmol/mg protein MDA) and carbonyl (E= 66.20 \pm 13.27 vs C= 20.10 \pm 2.64 nmol/mg carbonyl protein) in exposed group were higher 99 and 205%, respectively. For the antioxidant enzymes, the results showed an increase of SOD (E= 0.72 \pm 0.33 vs C= 0.42 \pm 0.06 U/mg protein) and GS-T activity (E= 0.123 \pm 0.073 vs C= 0.017 \pm 0.007 U/mg protein), on the other side GPx showed a decreased activity (E= 0.018 \pm 0.003 vs C= 0.045 \pm 0.008 U/mg protein), in exposed group when compared to control group. CAT activity (E= 0.867 \pm 0.534 vs C= 0.614 \pm 0.428 U/mg protein) had no significant differences. Finally, the erythrocytes of exposed group showed membrane integrity compromised (E= 0.950 \pm 0.160 vs C= 0.354 \pm 0.180 slope) and 37% less of O₂ uptake capacity (E= 196 \pm 116 vs C= 310 \pm 72 nmol O₂/min/mg) when compared to control group.

Conclusion:

Our findings suggest that erythrocytes of fishermen has an impaired in oxidative status, membrane integrity damage and low capacity of O₂ uptake, all these results may be related to aquatic environment exposure, associated with high Pb and Hg.

Financial support:

PPSUS, FAPEAL and CNPq

19.012 - ETHYL ACETATE FRACTION OF CHRYSOBALANUS ICACO L. LEAF EXTRACT PRESENTS CYTOTOXIC ACTIVITY AND MIGRATION INHIBITION IN BREAST AND LUNG CANCER CELL LINES. Cruz LO, Araújo LBN, Cal BBF, Salviano Í, Soares BO, Gagliardi RF, Dantas FJS, Mencalha AL, Mencalha AL, - Biofísica e Biometria - UERJ Departamento de Botânica - UERJ

Introduction:

Plant species are used in traditional medicine and ethnopharmacological research for therapeutic purposes. *Chrysobalanus icaco* L., known as Icaco or Abajero, is widely used in Brazil due to its therapeutic effects, such as hyperglycemia regulation, anti-inflammatory, analgesic and to treat chronic diarrhea. Studies have also indicated effects on the decrease of cell proliferation in human colon cancer lines, the inhibition of proliferation and induction of apoptosis in the leukemia line, including those with resistance to multiple drugs.

Aim:

The aim of this study was to investigate the cytotoxic effect of the ethyl acetate fraction of the leaves extracts of *C. icaco*.

Methods:

The leaves were collected in the Dunes Park, Cabo Frio, RJ. The methanolic extract was prepared from the maceration of dry leaves in methanol (200 g.L⁻¹) and then fractionated with increasing polarity solvents (hexane, dichloromethane, ethyl acetate, and butanol) by column chromatography silica gel. The fractions were then subjected to rotary evaporation for the complete elimination of the solvents. Breast MDA-MB-231 and lung A549 cancer cell lines were incubated with the ethyl acetate fraction (0.5, 1 and 5 $\mu\text{g.mL}^{-1}$) for 24h. Cells viability was evaluated by WST-1 and Trypan blue exclusion assays and the effects on the migratory capacity was verified through the wound healing or scratch assay.

Results:

The cell viability was reduced in both tested cells was observed by 50% in MDA-MB-231 and 48% in A549 in ethyl acetate fraction treated cells compared to untreated cells. The migration capacity of both cell lines was decreased about 6% in MDA-MB-231 and 68% in A549, being the migration of lung cancer cells the most affected to the treatment.

Conclusion:

The ethyl acetate fraction contains compounds with antitumor potential against MDA-MB-231 and A549 cancer cells, and the identification of the compounds may aid in studies for the development of new drugs against cancer.

Financial support:

This work was supported by Carlos Chagas Filho Foundation for Research Support of Rio de Janeiro State (FAPERJ), National Council for Scientific and Technological Development (CNPq) and National Council for the Improvement of Higher Education (CAPES)/PROEX

19.013 - BOTRYOSPHAERAN AT THE DOSAGE OF 30 MG/KG/DAY DOES NOT ALTERED THE HEMATOLOGICAL AND METABOLIC PARAMETERS OF HEALTHY WISTAR RATS. Oliveira GA, Geraldelli D, Martins KO, Ribeiro MC, Medeiros TC, Oliveira MF, Dekker RF, Barbosa-Dekker AM, Alegranci P, Queiroz EAIF, Queiroz EAIF, - Instituto de Ciências da Saúde - ICS - Universidade Federal do Mato Grosso - UFMT

Introduction:

Background: Studies have been demonstrated that β -glucans, polymers of glucose, produced by bacterial and fungus, present important activities against various diseases, like diabetes, obesity and cancer. Botryosphaeran, a (1 \rightarrow 3)(1 \rightarrow 6)- β -D-glucan, produced by the fungus *Botryosphaeria rhodina*, has been described as an antimutagenic, antiproliferative, pro-apoptotic, hypoglycemic and hypocholesterolemic agent when analyzed at the dose of up to 12 mg/kg/day for 15 days. In addition, a previous study demonstrated that botryosphaeran (30 mg/kg/day, for 15 days) presents antimutagenic, hypoglycemic, hypocholesterolemic and antiatherogenic effects when evaluated in dyslipidemic Swiss mice (knockout mice for the LDL receptor (LDLr^{-/-})). However, further studies were necessary to evaluate the effects of botryosphaeran at the dose of 30 mg/kg/day in Wistar rats, and to confirm that this (1 \rightarrow 3)(1 \rightarrow 6)- β -D-glucan do not present any toxicological effect in healthy Wistar rats.

Aim:

FeSBE Annual Meeting 2019

Poster Sessions and Abstracts

The objective of the present work was to analyze the effects of botryosphaeran (30 mg/kg/day for 15 days) on hematologic and metabolic profiles of healthy Wistar rats.

Methods:

Methods: Adult male Wistar rats were divided into two groups: Control (C) and Control+Botryosphaeran (CB), and received standard ration and water ad libitum throughout the experimental period. CB animals were treated with botryosphaeran (30 mg/kg/day, via gavage), and the control group received saline solution. After 15 days of treatment, oral glucose tolerance test (OGTT) and intraperitoneal insulin tolerance test (IPITT) were performed. Later, the animals were euthanized and analyzed for weight evolution, feed intake, absolute and relative tissues weight (adipose tissue, lean mass, liver, spleen, kidneys and adrenal), fasting glycemia, lipid profile, alanine aminotransferase (ALT), aspartate aminotransferase (AST) and hemogram. The comparison between the groups was performed by Student's t-test and significant differences at $p < 0.05$. Study protocol was approved by the Ethics Committee under n°23108.973436/2018-54.

Results:

Results: Body weight, feed intake and the absolute and relative weights of tissues were not altered by botryosphaeran. The metabolic parameters, as fasting glycemia (g/dL; C=112.6±8.8 and CB=115.0±6.1; $p=0.6299$), OGTT, IPITT and lipid profiles, also did not alter. Furthermore, there was no difference in ALT (g/dL, C= 89.0 ± 15.5 and CB=112.8 ± 34.4, $p=0.244$) and AST levels between the groups. Still, botryosphaeran did not alter the hematological profile of the animals, maintaining the erythrogram, leukogram and plaquetogram, within the reference values and similar to those of the control group.

Conclusion:

Conclusion: Botryosphaeran, at a dose of 30 mg/kg/day for 15 days, did not present any toxicological effect in healthy Wistar rats maintaining the same metabolic and hematological profile of control animals.

Financial support:

UFMT E CAPES

19.014 - NANOEMULSION CONTAINING ESSENTIAL OIL FROM XYLOPIA OCHRANTHA MART. PRODUCES MOLLUSCIDAL EFFECTS AGAINST DIFFERENT SPECIES OF BIOMPHALARIA (SCHISTOSOMA HOSTS).. RANGEL LDS, Tietbohl LAC, Rocha LM, Santos JAA, Faria RX, - Laboratório de Avaliação e Promoção da Saude Ambiental - Fiocruz Laboratório de Toxoplasmoses e outras Protozooses - Fiocruz Laboratório de Tecnologia de Produtos Naturais - UFF

Introduction:

This work describes a chemical study of the essential oil from leaves of *Xylopia ochrantha*, an endemic Annonaceae species from Brazil, and its activity against *Biomphalaria* species. Considering its poor solubility in aqueous medium, the essential oil was nanoemulsified to evaluate its action on controlling some mollusc species of genus *Biomphalaria*, snail hosts of *Schistosoma mansoni* that causes schistosomiasis, which mainly affects tropical and subtropical countries.

Aim:

The main aims of this work were to analyse the chemical composition of essential oil from *X. ochrantha*, and to evaluate the effect of its nanoemulsion on molluscs of genus *Biomphalaria* and their oviposition.

Methods:

Chemical analysis was performed by gas chromatography coupled to mass spectrometry. Nanoemulsions were prepared by a low energy method and characterised by particle size and polydispersity index. Biological assays evaluating the mortality of adult species of *B. glabrata*, *B. straminea* and *B. tenagophila* and their ovipositions upon contact with the most stable nanoemulsion during 24 and 48 h were performed.

Results:

Chemical analysis by mass spectrometry revealed the majority presence of bicyclogermacrene and germacrene D in the essential oil. The

formulation with a hydrophilic-lipophilic balance (HLB) of 9.26 was the most suitable for the oil delivery system. This nanoemulsion caused the mortality in *B. tenagophila*, *B. straminea* and *B. glabrata* of different sizes at levels ranging from 50 to 100% in 48 h, at concentrations below 100 ppm, being. Additionally, the formulation could inhibit the development of deposited eggs, at concentrations below 78 ppm.

Conclusion:

Thus, these results suggest the use of nanoemulsified essential oil from *X. ochrantha* as a possible alternative in controlling some *Biomphalaria* species involved in the schistosomiasis cycle.

Financial support:

CAPES and FIOCRUZ

19.015 - BIOACTIVE PEPTIDES DERIVED FROM EGG WHITE REDUCED AGAINST CADMIUM-INDUCED DAMAGE IN THE REPRODUCTIVE SYSTEM OF RATS. Santos JES, Pinheiro Jr, Moraes PZ, Barbosa Jr F, Peçanha FM, Santos FW, Vassallo DV, Miguel M, Wiggers GA, - Programara de Pos Graduação em Bioquímica - UNIPAMPA Faculdade de Ciências Farmacêuticas de Ribeirão Preto - USP Conselho Superior de Investigações Científicas/ Instituto de Investigación en Ciencias de la Alimentación - CSIC/CIAL Departamento de Ciências Fisiológicas - UFES

Introduction:

Exposure to heavy metals promoted damage to the reproductive organs mainly through oxidative stress and inflammatory factors. Exposure to cadmium (Cd) is related to infertility, spermatogenesis and testicular degeneration in male rats. Different sources of food protein, such as egg white hydrolyzate, provide known bioactive peptides with antioxidant and anti-inflammatory properties that can reduce the damage promoted by metals. Since cadmium is a potent toxic agent especially to the reproductive system, strategies of attenuation or protection of this system by natural sources are important.

Aim:

We investigated the effects of EWH on cadmium-induced damage in sperm motility, spermatogenesis and oxidative stress

Methods:

Three-month-old male Wistar rats (± 300 g) were treated for 14 days: a) Untreated (distilled water ip), b) Cd (Cadmium Chloride – CdCl₂ – 1mg/kg ip) c) EWH (1 g/kg/day per gavage), d) CdEWH (CdCl₂ plus EWH). We analyzed Cd concentration on testis and epididymis, sperm motility, daily sperm production, sperm number and transit time in epididymis, sperm membrane integrity and the reactive oxygen species levels, lipid peroxidation and total antioxidant capacity in testis and epididymis. Motility and integrity of the spermatid membrane are expressed as median [minimum - maximum] and analyzed by the Kruskal - Wallis test and sperm data expressed as mean \pm SEM and analyzed by ANOVA, values of $p < 0.05$ were considered significant (*vs Untreated; #vs Cd).

Results:

EWH co-treatment prevented: I) increased deposition of the metal in the testis (Untreated: 0.04 \pm 0.02, Cd: 4.68 \pm 1.03*, EWH: 0.01 \pm 0.00, CdEWH: 1.850 \pm 0.25# μ g Cd/g/dry tissue). II) the decrease on sperm motility: motile with progressive movement [Untreated: 64.5 (43-78), Cd: 16.8 (37-8)*, EWH: 62 (53-82), Cd-EWH: 55.6 (23-69)#] and immotile [Untreated: 10.5 (1-17), Cd: 56 (28-70)*, EWH: 11 (4-24), Cd-EWH: 14.5 (9-34)#]. III) damage the sperm membrane [Untreated: 68 (53-86), Cd: 28 (22-53)*, EWH: 66 (51-86), Cd-EWH: 70 (60-78)#]. III) reduction on daily sperm production x106/testis/day [Untreated: 35.7 \pm 2.6, Cd: 4.5 \pm 1.3*, EWH: 32.2 \pm 21, Cd-EWH: 6.2 \pm 1.1#]. IV) damage in morphology [Untreated: 92 (90-95), Cd: 53 (48-60)*, EWH: 92 (90-94), Cd-EWH: 90.9 (88-93)#] and reduced the number of sperm with head amorphous [Untreated: 2 (2-4), Cd: 15 (12-18)*, EWH: 2 (1-4), Cd-EWH: 3.5 (1-5) #]. V) the increase on oxidative stress after cadmium exposure on testis, epididymis and plasm. VI) the reduction of GSH level in the testis and restored the SOD activity to level similar to the control.

Conclusion:

FeSBE Annual Meeting 2019

Poster Sessions and Abstracts

EWH could represent a powerful natural alternative to protect the male reproductive system against cadmium induced- toxicity.

Financial support:

Supported by the Brazilian Government (Conselho Nacional de Desenvolvimento Científico e Tecnológico – CNPq 307399/2017-6; CAPES) and by the Spanish Government [MINECO - AGL2017-89213-R and SAF2015-69294-R].

19.016 - ANTIOXIDANT POTENTIAL OF THE AQUEOUS EXTRACT OF PETROSELINUM CRISPUM (SALSA) IN SACCHAROMYCES CEREVISIAE CELLS. Santos KF, Epifanio NMM, Chaves DSA, Riger CJ, - Departamento de Bioquímica - UFRRJ Departamento de Ciências Farmacêuticas - UFRRJ

Introduction:

Oxidative stress is caused by an imbalance between oxidant species, such as reactive oxygen species (ROS) and the insufficient intracellular defense mechanisms. These species cause damage to cells and tissues, and may be precursors to a number of pathologies as neurodegenerative and circulatory diseases, as well as carcinomas. Due to this fact, several studies investigate the prevention of the production of this oxidative stress through substances that have antioxidant action capable of maintaining intracellular redox homeostasis. In our previous studies, apiin showed antioxidant activity in *S. cerevisiae* cells, and their glycosylated flavonoid is present in the aqueous extract of *Petroselinum crispum* (parsley). Considering that aqueous extract of parsley has approximately 6.0% apiin, it was interesting to verify the antioxidant action of the aqueous extract of parsley in the same cellular model of study in order to compare with the results of the apiin.

Aim:

Therefore, the aim of this study was to verify if non-cytotoxic concentrations of the aqueous extract of parsley would show, in *S. cerevisiae* cells, a protective antioxidant effect through the oxidative stress induced by hydrogen peroxide solution.

Methods:

Cell toxicity and viability assays in addition to membrane lipid damage were performed on yeast cells. In the toxicity assay, cells were incubated in YPD 2% (2% glucose, 2% peptone, 1% yeast extract) for 1 hour with 200 and 400 $\mu\text{L}\cdot\text{mL}^{-1}$ of the aqueous extract and then seeded onto plates of petri with YPD 2% solid medium and the colonies counted after 48 hours. The viability assay followed the same experimental standards, however the hydrogen peroxide addition step (1.0 mM) was added after treatment of the cells with both extracts concentrations. In the lipid peroxidation test, cells preincubated with the extract and under oxidative stress with H_2O_2 were lysed with glass beads, and the malonaldehyde formed in the peroxidation was determined spectrophotometrically (532 nm) in reaction with thiobarbituric acid.

Results:

The results showed that 200 and 400 $\mu\text{L}\cdot\text{mL}^{-1}$ were the highest non-cytotoxic concentrations to yeast cells, obtaining survival percentages of $81.67 \pm 4.16\%$ and $105.33 \pm 6.81\%$ respectively. The results of the antioxidant potential parsley extract by cell viability through the oxidative stress by hydrogen peroxide (1.0 mM) showed similar protection in both concentrations. Cells stressed with H_2O_2 had viability of $26.50 \pm 8.88\%$, and with preincubation with extracts increased to $54.25 \pm 20.67\%$ and $46.33 \pm 5.51\%$ respectively. Preliminary results of lipoperoxidation showed the parsley extract did not decrease the damages in the cell membranes caused by H_2O_2 , however greater reproducibility of the results is required.

Conclusion:

Petroselinum crispum aqueous extract at concentrations of 200 and 400 $\mu\text{L}\cdot\text{mL}^{-1}$ showed an antioxidant action on *Saccharomyces cerevisiae* cells, however, the lipoperoxidation tests were not conclusive need future investigations with different concentrations.

Financial support:

Faperj

19.017 - EFFECT OF EGG WHITE HYDROLYSATE INTAKE ON MESENTERIC ARTERIES OF IN RATS CHRONICALLY EXPOSED TO MERCURY CHLORIDE (HgCl_2). Rodrigues MD, Escobar AG, Piagette JT, Cavallini TI, Peçanha FM, Rizzetti DA, Vassallo DV, Miguel M, Wiggers GA, - Programa de Pós graduação em Bioquímica - UNIPAMPA Programa de Pós-graduação em Ciências Fisiológicas - UFES Consejo Superior de Investigaciones Científicas/ Instituto de Investigación en Ciencias de la Alimentación - CSIC/CIAL

Introduction:

Mercury (Hg) is widely present in the environment and its toxicity is related to alter the tonus and the vasoconstriction and vasodilation capacity, which is directly related to the increase in the oxidative stress produced by the metal. In this context, the Egg white hydrolysate (EWH) has antioxidant, anti-inflammatory and vasodilator properties and could be an efficient alternative for prevention or treatment in heavy metal poisoning.

Aim:

To investigate the potential beneficial effects of EWH intake on vascular reactivity disorders induced by chronic exposure to low concentrations of Hg in mesenteric resistance arteries (MRA) as well as to clarify the possible pathways involved in its effects.

Methods:

Male Wistar rats were treated for 60 days: a) intramuscular injections (i.m.) of saline solution 0.9% and tap water by gavage (Untreated); b) i.m. injections of mercury chloride – HgCl_2 , the 1st dose 4.6 $\mu\text{g}/\text{kg}$, and subsequent doses of 0.07 $\mu\text{g}/\text{kg}/\text{day}$, to cover daily loss and tap water by gavage (HgCl_2); c) i.m. injections of saline solution 0.9% and EWH from pepsin for 8 h diluted in tap water (1 g/kg/day), by gavage, (EWH) and d) both treatments (EWH+ HgCl_2). Systolic Blood Pressure (SBP) was analyzed by method of tail-cuff plethysmography. Vascular function was analyzed in isolated organ bath. Concentration-response curves to acetylcholine (ACh) and sodium nitroprusside (NPS) were performed. Vasoconstrictor response to noradrenaline (NE) in presence and absence of endothelium and in presence of a nitric oxide synthase (NOS) inhibitor (L-NAME), a non-selective cyclooxygenase (COX) inhibitor, an essential cofactor for NO synthesis (BH4), a NADPH oxidase inhibitor (VAS2870) and a superoxide dismutase mimic (TEMPOL) were analyzed. We measured in situ production of superoxide anion, NO release, vascular reactive oxygen species (ROS), lipid peroxidation, antioxidant capacity and NPSH levels in MRA. Results were expressed as mean and SEM, compared by one- or two-way ANOVA analysis followed by the Fisher post hoc test. ($P < 0.05$).

Results:

EWH: a) prevented the increased SBP, the endothelial dysfunction and the increased vasoconstrictor response to NE observed in MRA after prolonged HgCl_2 exposure; b) restored the NO-mediated endothelial modulation; c) inhibited the NAD(P)H oxidase-derived oxidative stress and the inflammatory pathways induced by the metal in these vessels, normalizing the antioxidant status.

Conclusion:

EWH seems to be able to counteract the vascular toxic effects of long-term exposure to HgCl_2 , which points to possible therapeutic effects based on functional food against a highly widespread environmental contaminant.

Financial support:

Supported by the Brazilian Government (Conselho Nacional de Desenvolvimento Científico e Tecnológico – CNPq 203440/2014-5 and 307399/2017-6; CAPES; PROBIC FAPERGS/UNIPAMPA) and by the Spanish Government [MINECO - AGL2017-89213-R and SAF2015-69294-R].

FeSBE Annual Meeting 2019

Poster Sessions and Abstracts

19.018 - CA²⁺-DEPENDENT MITOCHONDRIAL PERMEABILIZATION PROMOTED BY 4-ORGANOSELENIUM QUINOLINE. Lopes RM, Costa CA, Ferraz LS, Oliveira IM, Stefani HA, Rodrigues T, - Centro Interdisciplinar de Investigação Bioquímica - UMC Centro de Ciências Naturais e Humanas - UFABC Instituto de Química - USP

Introduction:

Selenium-based compounds are extensively studied for their biological activities, including anti-inflammatory, antioxidant and neuroprotective effects. Despite these protective effects, recent studies suggested that organochalcogens presented cytotoxicity against tumor cells in vitro, exhibiting antitumor potential. However, the underlying mechanisms related to the induction of cell death were not studied yet.

Aim:

Here, the effects of a 4-organoselenium (compound 4a) were investigated on isolated mitochondria and compared with a structurally related non-chalcogen derivative (compound 8f).

Methods:

Compounds used in this study were synthesized, purified, and characterized elsewhere (New J. Chem., 41:9884-9888, 2017). Melanoma SK-MEL-147 (BRAFV600E) cells (6.25x10⁴/cm²) were cultivated in DMEM high glucose and leukemia Jurkat cells (1x10⁵/mL) in RPMI 1640, both supplemented with 10% BFS and penicillin/streptomycin. Cell viability was evaluated by the MTT reduction assay. Experiments involving animals were previously approved by UMC Ethics Committee under protocol number 004/2018. Rat liver mitochondria were isolated by differential centrifugation. In order to characterize the mitochondrial permeabilization, oxygen consumption was analyzed using a Clark type electrode (Hansatech Instruments Ltd., USA), and mitochondrial potential and Ca²⁺ levels were evaluated fluorometrically using rhodamine 123 and calcium green 5N, respectively. Modulators were added prior the addition of compounds, as indicated.

Results:

After screening the cytotoxicity of twenty-five newly synthesized 4-functionalized-quinoline derivatives in cultured tumor cells, the most potent derivatives, namely compound 4a and 8f, were selected to have their effects studied in isolated mitochondria. Both compounds were able to dissipate the mitochondrial transmembrane potential ($\Delta\Psi$), which was accompanied by increased electron flow through the respiratory chain and matrix Ca²⁺ efflux, indicative of mitochondrial permeabilization. The calcium chelator EGTA prevented completely the $\Delta\Psi$ dissipation induced by both compounds, suggesting it is a Ca²⁺-dependent effect. However, the thiol reducer DTT only prevented the $\Delta\Psi$ dissipation induced by compound 8f, but not by 4a, indicating that mechanisms of permeabilization are different, despite the structural similarity.

Conclusion:

These results demonstrated that 4-organoselenium-quinoline derivatives induced a Ca²⁺-dependent mitochondrial permeabilization, which may be potentially associated to the cytotoxicity exhibited by these compounds.

Financial support:

CAPES and FAPESP

20 - Pain and Inflammation

20.009 - ACTION OF LOW LEVEL LASER THERAPY ON THE SYNOVIAL MEMBRANE OF THE KNEE JOINT IN ADULT RATS AFFECTED BY EXPERIMENTAL MICROCRYSTALLINE ARTHRITIS. Bartoli DMF, Felizatti AL, Bomfim FRC, Bovo JL, Amaral MEC, Aro AA, Esquisatto MAM, - Graduate Program in Biomedical Sciences - University Center of Herminio Ometto Foundation

Introduction:

Therapeutic use of phototherapy in inflamed tissues may be an important alternative in joint pathologies.

Aim:

The aim of this study was to evaluate the effects of low-laser-therapy using the Gallium Indium and Phosphorus - InGaAlP ($\lambda=670\text{nm}$) laser on the organization of synovia in experimental microcrystalline arthritis induced in the knee joint of adult male Wistar rats.

Methods:

Seventy-two animals (~200g) were distributed in three groups of twenty-four components: A (control), B (induced arthritis-ia), C (ia+670nm laser). Animals from groups were anesthetized and arthritis was induced (B and C) with the solution of 2mg of Na₄P₂O₇ in 0.5mL of saline solution and injected twice in the right knee at 24h intervals. Control group received saline solution only. The InGaAlP laser treatments (DE=13.5J/cm², power=30mW, total energy=0.27J, beam area=0.02cm² for 12s) were applied daily at a point in the patellar region of the right knee after 48h of induction. After 7, 14 and 21 days of treatment, the animals of the three groups were euthanized and the right knees were removed and processed for histomorphometric, immunohistochemical, ultrastructural and biochemical (dosages and WB) analyzes of the synovial membrane. The quantitative data were compared by ANOVA and Tukey's post-test (p<0.05).

Results:

The number of granulocytes was lower in group A (7d:4.1±0.9; 14d:5.2±0.7; 21d:4.6±1.1) in relation to the others in all experimental periods. At 14 and 21 days, the B (14d:45.9±3.8; 21d:56.8±4.2) presented the higher number of these cells. The number of fibroblasts was higher in group B (14d:39.3±4.2; 21d:45.2±4.9) in relation to the others at 14 and 21 days. The A and C presented similar values. The number of cells positively marked for the TUNEL assay was higher in group B (14d:16.8±2.7, 21d:21.5±3.1) than in the others only in 14 and 21 days. The area occupied by the birefringent collagen fibers was lower in group A (14d:43.2±3.8, 21d:40.9±4.9) at 14 and 21 days. The B and C presented similar values. The ultrastructural analysis of the synovial membrane at 21 days revealed in group B the presence of fibrous elements, associated with crystalline structures in the extracellular matrix. The concentration of glycosaminoglycans did not present significant difference among the groups in all experimental times. The hydroxyproline content was similar among the groups at 7 days. However, at 14 (121.2±6.9) and 21(129.7±16.2) days, the group B had higher values than the others. The content of non-collagen proteins was higher in B at 21 days than in the other groups. The expression for TNF- α at 21 days was higher in A and B than in C. For TGF- β , at 21 days, groups B and C presented values similar to and higher than A. For MMP-13, groups A and B had data similar and superior to C at 14 and 21 days. Regarding ADAMT-54, at 21 days, groups B and C presented data similar and inferior to A.

Conclusion:

The InGaAlP-670nm therapy reduced the inflammatory process and cell and extracellular matrix changes of the synovial membrane compared to the untreated group.

Financial support:

FHO.

20.010 - INVOLVEMENT OF INTRATHECAL TRPV1 RECEPTORS IN TRANSITION OF ACUTE TO CHRONIC MUSCLE PAIN. Rodrigues HL, Jorge CO, Azambuja G, Gomes BB, OLIVEIRA-FUSARO MCG, - Laboratório de Estudos da Dor e Inflamação - LABEDI - UNICAMP

Introduction:

Muscle pain is one of the most important reason of disability in the world. Currently, several mechanisms are known that modulate acute muscle pain. However, the mechanisms underlying transition of acute to chronic pain, as well as, the maintenance of chronic pain, are poorly understood. The members of the TRP family, specially the TRPV1 receptors, has been shown as interesting targets for the control of several pain conditions. TRPV1 receptors are expressed in afferent

FeSBE Annual Meeting 2019

Poster Sessions and Abstracts

nociceptive fibers and its activation affects the nociceptive signaling pathway to central nervous system.

Aim:

Therefore, the aim of this study was to analyze whether intrathecal TRPV1 receptors are involved in transition of acute to chronic muscle pain and in the maintenance of it.

Methods:

To this end, male Swiss mice (6-weeks-old) from CEMIB-UNICAMP were used and all experimental procedures were approved by the Ethics Committee in Animal Research of UNICAMP (4883-1/2018). A model of transition of acute to chronic pain (Dina et al., J Pain, 2008) was used. This model is performed by an injection of carrageenan (100µg) into right gastrocnemius muscle to induce inflammatory pain and, 10 days later, PGE2 (1µg) is injected at the same local to reveal the chronic-latent hyperalgesia. Mechanical muscle hyperalgesia was measured by Randall-Selitto analgesymeter in different time points of acute (1-144h) and chronic pain (1-168h). To evaluate the involvement of TRPV1 receptor, the selective TRPV1 receptor antagonist, AMG9810, was injected intrathecally.

Results:

The results showed that intrathecal injection of AMG9810 (15µg but not of 3µg/5µl, n=5) prior to carrageenan reduced acute muscle hyperalgesia at 3h (Mean±SEM: 5.25g± 1.0g), 6h (3.46g ± 0.59g) and 24h (6.26g ± 0.91g) when compared to intrathecal injection of its vehicle, 0.9% NaCl (n=9) (3h: 17.0g± 0.92g; 6h 16.6g ± 1.04g; 24h 10.2g ± 1.19g) (p<0.001, Two-way ANOVA, Bonferroni test). Nociceptive thresholds returned to baseline levels after 96 hours. The chronic muscle hyperalgesia was also reduced at 4h (8.8g ± 0.48g), 24h (8.3g ± 0.39g), 48h (5.11g ± 0.35g) and 168h (3.2g ± 0.18g) when compared to intrathecal injection of its vehicle, 0.9% NaCl (4h: 15.1g± 1.3g; 24h 15.4g ± 0.9g; 48h 14.9g ± 0.9g; 168h 14.6g ± 0.8g) (p<0.001, Two-way ANOVA, Bonferroni test). To isolate acute from chronic muscle hyperalgesia, AMG9810 was injected immediately before PGE2 in mice previously challenged by carrageenan. In this case, intrathecal AMG9810 (15µg but not of 3µg/5µl, n=4) reduced chronic muscle hyperalgesia at 4h (8.9g±0.9g), 24h (9g±0.3g), 48h (6.16±0.21g) and 168h (4g±0.12g) (p<0.001, Two-way ANOVA, Bonferroni test).

Conclusion:

Our results demonstrate that intrathecal TRPV1 receptors are involved in transition of acute to chronic muscle pain and in the maintenance of chronic muscle pain. Therefore, we point out TRPV1 receptors as a pharmacological target to control chronic pain conditions.

Financial support:

This study was financed in part by the Coordenação de Aperfeiçoamento de Pessoal de Nível Superior - Brasil (CAPES) - Finance Code 001 and the São Paulo Research Foundation (FAPESP) - 2017/17919-8

20.011 - EFFECT OF THE ANNEXIN A1 MIMETIC PEPTIDE ON CISPLATIN-INDUCED OTOTOXICITY RAT MODEL. Sena LS, Sanches JM, Azevedo MF, Sasso GRS, Gil CD, - Departamento de Morfologia e Genética - UNIFESP - Universidade Federal de São Paulo

Introduction:

Cisplatin is a widely used antineoplastic agent that is associated with bilateral and irreversible hearing loss in patients. The generation of reactive oxygen species (ROS) by cisplatin induces cochlear inflammation and cell apoptosis in the cochlea. Thus, therapeutic strategies that aim to reduce auditory dysfunction through the prevention of inflammation have been studied. We highlight annexin A1 (AnxA1), a protein capable of mimicking the anti-inflammatory action of glucocorticoids by inhibiting the synthesis of eicosanoids and phospholipase A2, affecting components of the inflammatory reaction.

Aim:

This study evaluated the effect of the pharmacological treatment with the mimetic peptide of AnxA1, Ac2-26, on cisplatin-induced ototoxicity in rat model.

Methods:

Male Wistar rats were distributed in the followed groups (n = 5 animals/group): Cis - received three intraperitoneal (i.p.) doses of cisplatin (10 mg/kg) per day (30 mg/kg in 3 days); Ac2-26 - received i.p. treatment with 1 mg/kg of Ac2-26, 15 minutes prior to cisplatin administration; Control - received sterile saline only. Rats were tested to distortion product otoacoustic emissions (DPOAE) before and after treatments in order to evaluate possible changes in the presence of emission, amplitude and signal noise ratio in the 2, 4, 6 and 8 kHz frequencies. After 6 hours of the last cisplatin or saline administration, animals were euthanized for histological, immunohistochemical and ultrastructural analysis of the inner ear (CEUA nº 2152170418).

Results:

Administration of cisplatin caused a reduction of 100% in the presence of DPOAE at 2 and 3 kHz frequencies and 80% at 4 kHz in the right and left ears. Pharmacological treatment with Ac2-26 maintained 100% of the DPOAE presence in both ears at 3 to 8 kHz frequencies and 80% at 2 kHz frequency. Histological analysis of the inner ear provided identification of all cellular elements in the three experimental groups. Stereocilia were observed on the internal and external hair cells` apical surfaces through scanning electron microscopy. Quantification of the bipolar neurons of the spiral ganglion evidenced cell death through significant reduction of cells in the Cis group (5818 ± 261 cells/mm²) in comparison to the Control group (7226 ± 206; p < 0.01), while the Ac2-26 treatment showed an increased number of cells (7327 ± 329; p < 0.01) than the Cis group. These neuron count findings were corroborated by the strong immunoreactivity to cleaved caspase-3, a cell death marker, in the neuron cytoplasm of the Cis group (p < 0.001 vs. Control), while poor immunoreactivity was detected in the neurons from the Ac2-26-treated group compared to the Cis (p < 0.001). Additionally, Cis and Ac2-26 groups were associated with increased levels (p < 0.001 vs. Control) of phosphorylated extracellular signal-regulated kinase in the bony labyrinth near to the spiral ganglion's bipolar neurons.

Conclusion:

DPOAE showed that Ac2-26 treatment reduced cisplatin-induced hearing loss in this experimental model. This peptide effect predicts a neuroprotective role, evidencing the AnxA1 as a potent therapeutic target in the inner ear ototoxicity.

Financial support:

FAPESP (2018/08764-3 e 2017/26872-5)

20.012 - GALECTINS AS POSSIBLE BIOMARKERS IN INFLAMMATORY SKIN DISEASES. Corrêa MP, Areias LL, Correia-Silva RD, Lice I, Sasso GRS, Gil CD, - Morfologia e Genética - UNIFESP Biologia - UNESP

Introduction:

Complex mechanisms of the immune responses involving chronic inflammation of the skin, such as psoriasis (Ps) and dermatitis, evidence the great challenge in their clinical diagnosis. In this way, the study of biomarkers is fundamental to better define these pathologies, which will contribute to a personalized therapy. In this context, we highlight galectins, proteins characterized by a conserved 135 amino acid sequence in the carbohydrate-recognizing domain, responsible for binding affinity to beta-galactoside sugars. In skin inflammation, the role of galectin-1, -3 and -9 has been shown in dermatitis and Ps, and they may act with pro or anti-inflammatory paper.

Aim:

This study evaluated the expression pattern of galectin-1, -3 and -9 in Ps and atopic dermatitis (AD) biopsies, as well as the immunomodulatory effect of these galectins on human keratinocyte HaCaT cells stimulated with cytokine-stimulated with TNF-α/IFN-γ or IL-17.

Methods:

FeSBE Annual Meeting 2019

Poster Sessions and Abstracts

Galectin expression was analyzed by immunofluorescence and immunohistochemistry in the skin biopsies with Ps, AD and control (clinically normal skin) from 10 patients. HaCaT cells were stimulated with TNF- α /IFN- γ or IL-17 at 10 or 100 ng/mL, respectively. Keratinocytes were cultured in DMEM medium and subjected to the following experimental conditions: control (medium), activated by the TNF- α /IFN- γ (10 ng/mL) or IL-17 (100 ng/mL) and treated or not the Gal-1, Gal-3 and Gal-9 at 100, 500 or 1000 ng/mL. After 24 hours, the cell viability assay was performed by MTT and the supernatants were collected to measure the levels of proinflammatory cytokines IL-6 and IL-8.

Results:

Ps and AD biopsies showed similar histological characteristics, such as epidermal hyperplasia and chronic inflammatory infiltrate in dermis, characterized by the presence of lymphocytes, mast cells and eosinophils, hyperkeratosis also evident in Ps. Both skin lesions showed Gal-1 and Gal-3-immunopositive inflammatory infiltrate. AD epidermis was characterized by a marked expression of Gal-3 and Gal-9 (especially nuclear), while Ps epidermis showed a marked Gal-1 level. All experimental in vitro conditions showed cell viability above 50%, except when administered 1000 ng/mL of Gal-9. Cytokine dosage in keratinocyte supernatants demonstrated that both stimuli increased the release of IL-6 (TNF- α /IFN- γ : 492 ± 8 and IL-17: 51 ± 12 pg/mL, $p < 0.01$ vs control) and IL-8 (1712 ± 244 and 576 ± 80 , respectively, $p < 0.01$ vs control). On the other hand, Gal-1 and Gal-3 treatments at lowest concentration (100 ng/mL) reduced IL-6 production in relation to the TNF- α /IFN- γ -stimulated cells. Otherwise, another tested concentrations of galectins under the TNF- α /IFN- γ stimulation were not effective in decreasing the IL-6 and IL-8 production. In addition, treatment with the three galectins under IL-17 stimulation showed an immunomodulatory effect on keratinocytes at the lowest concentration, especially for IL-6 release.

Conclusion:

Different expression pattern of Gal-1, Gal-3 and Gal-9 in Ps and AD suggest these galectins as biological markers of inflammatory skin diseases. In addition, in vitro assays evidenced the immunoregulatory roles of these galectin family members on keratinocytes and pointed them as interesting therapeutic tools for skin inflammation.

Financial support:

CAPES (Finance Code 001); FAPESP (2017/26872-5).

20.013 - ROLE OF THE ANNEXIN A1 PROTEIN IN THE REGULATION OF NLRP3 INFLAMMASOME IN NEUTROPHILS. Correia-Silva RD, Sanches JM, Lice I, Moreira V, Gil CD, - Morfologia e genética - UNIFESP

Introduction:

NLRP3 is the most studied member of the NOD (nucleotide-binding oligomerization domain)-like receptor family and forms a multiprotein inflammasome complex with the adaptor protein ASC and procaspase-1. This multiprotein is able to recognize several microorganisms through activation of cell surface receptors triggering a pro-inflammatory response with production of cytokines (IL-1 α , IL-1 β and TNF- α) and chemokines. The release of pro-inflammatory mediators induces the influx of immune cells and consequent inflammatory response, which may be protective or deleterious, depending on the degree of immune response and the substances involved. In this context, the annexin A1 (AnxA1) protein plays a significant role in the control of the inflammatory cascade, especially related to the regulation of IL-1 β , but its relationship with the NLRP3 pathway has not been established.

Aim:

This study evaluated the role of the endogenous and exogenous AnxA1 in the regulation of the NLRP3 inflammasome.

Methods:

C57BL/6 wild-type (WT) and AnxA1 knockout mice (AnxA1 $^{-/-}$) received intraperitoneal (i.p.) of 0.3% carrageenan and, after 3 hours, the

peritoneal lavage (neutrophil population > 95%) was collected. WT and AnxA1 $^{-/-}$ neutrophils were then stimulated with lipopolysaccharide (LPS), followed by NLRP3 agonists, nigericin or ATP. In addition, to check the exogenous effect of AnxA1, neutrophils were pretreated with the mimetic peptide of AnxA1, Ac2-26, and then given the NLRP3 agonists. The following analyzes were performed: release of lactate dehydrogenase (LDH) to detect cell viability and western blotting and Elisa to measure the release of IL-1 β and caspase-1 (CEUA nº 6493130318).

Results:

WT and AnxA1 $^{-/-}$ neutrophils do not undergo pyroptosis upon NLRP3 activation, as demonstrated by LDH assay. NLRP3-derived IL-1 β production by WT neutrophils (Nigericin: 631 ± 137 , ATP: 246 ± 29 pg/mL, $p < 0.01$ vs. unstimulated cells) was abrogated by Ac2-26 administration before nigericin (299 ± 28) and ATP (151 ± 11). Otherwise, no effect of Ac2-26 was showed on IL-1 β production by nigericin-stimulated AnxA1 $^{-/-}$ cells which cytokine production was less substantial (279 ± 60) in comparison to WT cells. In addition, the lack of endogenous AnxA1 was associated with no alteration in the IL-1 β production upon ATP stimulation. Nigericin and ATP-stimulated WT neutrophils, with or without Ac2-26 treatment, showed caspase 1 activation. On the other hand, ATP stimulation on AnxA1 $^{-/-}$ neutrophils AnxA1 $^{-/-}$ cells was positively correlated with caspase 1 activation.

Conclusion:

Altogether, our results indicate that exogenous AnxA1 regulates NLRP3-derived IL-1 β production by neutrophils, while the lack of endogenous AnxA1 interferes with NLRP3 activation.

Financial support:

Financial Support: FAPESP (2018/13544-2 and 2017/26872-5)

20.014 - STRENGTH EXERCISE ATTENUATES HYPERALGESIA AND LOCOMOTOR IMPAIRMENT INDUCED BY FIBROMYALGIA MODEL. Ferrarini EG, Gonçalves ECD, Lopes EC, Gonçalves C, Dutra RC, - Programa de Pós Graduação em Neurociências - UFSC Laboratório de Autoimunidade e Imunofarmacologia - UFSC

Introduction:

Fibromyalgia (FM) is a chronic condition causing pain and sleep disturbance, fatigue, depression, anxiety, mood disorders, irritable bowel and other symptoms, which negatively impact the quality of life. Although its etiology is still not well understood, FM is a neurobiological disease caused by abnormal processing of pain. The complexity of the syndrome is also reflected by the fact that pharmacological, non-pharmacological and cognitive behavioral treatments do not seem to be efficacious. Currently, there is a constant search for new therapeutic options that minimize the impact of FM on patients' quality of life. Moreover, there are recent evidence that physical exercises inhibit pain and fatigue symptoms in FM patients, although there is no consensus about the type, frequency, duration, and intensity of physical activity for this population. Furthermore, in the literature there are conflicting results on the effects of strength training.

Aim:

Herein, we evaluated the effects of strength exercise in hyperalgesia and locomotor activity induced by FM model.

Methods:

Female Swiss mice were used for FM induced by reserpine subcutaneous administration in a volume of 1 ml/kg and at a concentration of 0.25 mg/kg, once daily for 3 consecutive days and exercise protocols lasted four weeks. All experimental procedures were approved by UFSC Committee on the Ethical Use of Animals and were carried out in accordance with Brazilian regulations on animal welfare (CEUA/UFSC protocol number 2572210218).

Results:

Our data showed that strength exercise protocol consistently reduced spontaneous pain during FM model ($p < 0.001$). Furthermore, strength

FeSBE Annual Meeting 2019

Poster Sessions and Abstracts

exercise significantly reduced mechanical allodynia response ($p < 0.001$), and markedly attenuated hyperalgesia induced by cold stimulus ($p < 0.001$). Finally, strength exercise showed positive effect in locomotor activity ($p < 0.01$).

Conclusion:

In conclusion, our data suggest that strength exercise may represent an important non-pharmacological intervention for treatment of FM symptoms.

Financial support:

CAPES – DS and CNPq.

20.015 - POSSIBLE INVOLVEMENT OF INFLAMMATORY CYTOKINES (IL-1BETA AND TNF-ALFA) IN PAIN INDUCED BY RHOPALURUS ROCHAI VENOM. Battocchio EC, Oliveira FSR, Bertozzi MM, Ferraz C, Cândido DM, Junior WAV, Kwasniewski FH, - Departamento de Ciências Patológicas - UEL (Universidade Estadual de Londrina) Laboratório de Artrópodes - Instituto Butantan

Introduction:

Scorpionism is a health public issue in several countries including Brazil. Pain and inflammation with production of inflammatory cytokines (IL-1beta and TNF-alfa) were early described with the scorpion venoms including those from Tityus genus (mainly *T. serrulatus*, Buthidae family). Other Brazilian scorpions from the Buthidae family have few data about the biological activities of their venoms, as *Rhopalurus rochai*. This scorpion is found in cerrado and caatinga, with scarce information about accidents as well as the activity of its venom.

Aim:

To evaluate pain, and the participation of IL-1beta and TNF-alfa, induced by *Rhopalurus rochai* venom (Rrv).

Methods:

Experiments (under permission of CEUA-UEL - 21366.2015.72) were done with male Swiss mice ($n=6$ per group). Rrv (0.6, 1.2 or 2.4 microg/paw in 20 microL, sc) was injected and pain was evaluated by the number of flinches in 30 minutes and mechanical hyperalgesia (electronic von Frey method) at 0.5h, 1h, 3h and 6h after stimulus. IL-1beta and TNF-alfa productions were quantified by ELISA in skin section collected after 0.5h, 1h and 3h after Rrv injection (2.4 microg/paw). Groups of mice stimulated with Rrv injection (2.4 microg/paw) were pretreated with: NF-kB inhibitor (PDTC, 100 mg/kg, 100 microL, sc., 1h before); TNF-alfa blocker (etanercept, 10 mg/kg, 200 microL ip., 48h and 1h before); steroidal anti-inflammatory (dexamethasone, 2 mg/kg 10 microL by gavage, 1h before). Data from cytokines production and flinches were analyzed using one-way analysis of variance (ANOVA) and Tukey's post-test ($P < 0.05$). Data from mechanical hyperalgesia were analyzed using two-way analysis of variance (ANOVA) and Bonferroni post-test ($P < 0.05$). The results were expressed as mean and standard error mean (SEM).

Results:

Flinches induced by Rrv were reduced when mice were pretreated with PDTC, dexamethasone and etanercept (83 ± 13 ; 102 ± 10 ; 75 ± 20 ; respectively) in comparison with their respective positive controls (153 ± 5 for PDTC and dexamethasone, 122 ± 32 for etanercept). Rrv induced mechanical hyperalgesia at 0.6 and 2,4 microg and this dose was selected for the next experiments. IL-1beta and TNF-alfa were produced after Rrv injection, TNF-alfa at 0.5h ($211 \pm 21\%$), 1h ($227 \pm 20\%$) and 3h ($455 \pm 7\%$) and IL-1beta only at 3h ($2587 \pm 11\%$) both in pg/100 mg of paw tissue. Mechanical hyperalgesia induced by Rrv was decreased by pretreatment with PDTC at 0.5h ($32 \pm 7\%$), 1h ($39 \pm 9\%$), 3h ($40 \pm 8\%$); dexamethasone at 0.5h ($55 \pm 15\%$), 1h ($59 \pm 7\%$), 3h ($58 \pm 6\%$) and 6h ($42 \pm 6\%$); and with etanercept at 0.5h ($58 \pm 21\%$), 1h ($61 \pm 16\%$), 3h ($36 \pm 8\%$) and 6h ($27 \pm 5\%$).

Conclusion:

IL-1beta and TNF-alfa are produced and probably have a role in pain and hyperalgesic response induced by *R. rochai* venom.

Financial support:

Fundação Araucária (bolsa de Inclusão Social - Battocchio, E.C.).

21 - Immunology

21.001 - CELLULAR RESPONSE MODULATION IN RENOVASCULAR HYPERTENSION MODEL ASSOCIATE WITH CALORIC RESTRICTION AND PHYSICAL EXERCISE. Orzari LE, Valverde AP, Terciotti LG, Santos BR, Oliveira CA, Amaral MEC, Dalia RA, Bernardes D, Felonato M, - Programa de Pós Graduação em Ciências Biomédicas - Centro Universitário da Fundação Hermínio Ometto

Introduction:

Behavioral changes which includes caloric restriction and physical exercise may promote blood pressure control associated with favorable immune modulation in target organs.

Aim:

Evaluate the renal cellular inflammatory profile induced by caloric restriction and physical exercise in a renovascular hypertension.

Methods:

Twenty male Wistar rats submitted by 2K1C surgery (renovascular hypertension) and received hyperlipidic diet ad libitum from the hypertension development (15 days after surgery). After 8 weeks, the animals were submitted to 4 weeks of caloric restriction of 40% and/or physical exercise training in anaerobic threshold intensity, composing the groups R (restrict), T (training), RT (restrict-training). The control group (C) was composed by animals that were not submitted in therapeutics interventions. All animals were euthanized by the end of 14th week protocol and the right kidney (intact) and left kidney (clipped) samples, were collected and processed for biochemical tests for NAG and MPS and macrophages (F4/80+) and neutrophils (MPO) immunohistochemical markers.

Results:

The 2K1C protocol was efficient in promoting blood pressure increase (SBP = 200mmHg in the 5th experimental week), jointly with increase on macrophages (5x) and neutrophils (20x) infiltrate in clipped kidney compared to intact kidney. Macrophages immunostaining (F4/80+) was $10 \pm 3\%$ in intact kidney area and $40 \pm 3\%$ in clipped kidney area; neutrophil immunostaining (MPO) was $2 \pm 1\%$ in intact kidney area and $40 \pm 3\%$ in clipped kidney area. However, all groups that underwent the interventions in isolated or associated way presented arterial pressure reduction and reduction of number of neutrophils in clipped kidney in relation to the control group. Thus, at the 14th experimental week, the SBP in R group was 160 mmHg ($p < 0.05$ vs C), T group was 155 mmHg ($p < 0.05$ vs C) and, RT group, 150 mmHg ($p < 0.05$ vs C). Neutrophil immunostaining in R groups clipped kidney area was $5 \pm 1\%$ ($p < 0.05$ vs C); in T group area was $2 \pm 1\%$ ($p < 0.05$ vs C) and, in RT group area was $4 \pm 1\%$ ($p < 0.05$ vs C). However, the isolated physical training caused higher neutrophil activation by increasing MPO levels in clipped kidney (OD of MPO: $0,04 \pm 0,001$ for control group and $0,06 \pm 0,001$ for T group, $p < 0,01$, 05). Caloric restriction alone caused increased immunostaining to macrophages (F4/80+) as well as activation of these cells (NAG levels) in intact kidney (OD of NAG: $0,10 \pm 0,001$ for the control group and $0,25 \pm 0,001$ for R group: $p < 0,05$).

Conclusion:

The reduction of blood pressure caused by caloric restriction, physical exercise or both associated is accompanied by neutrophil infiltrate reduction to target kidney. However, the isolated therapies caused a compensatory inflammatory response. As this compensatory response is not activated by the association of therapies, it is suggested that this strategy be more efficient in immunological changes control that cooperate for the worsening of hypertension.

Financial support:

FHO-UNIARARAS

FeSBE Annual Meeting 2019

Poster Sessions and Abstracts

21.002 - TREATMENT WITH LASERTHERAPY MODULATES ACTIVATION OF NEUTROPHILS IN THE GASTROCNEMIUS MUSCLE OF ANIMALS WITH RHEUMATOID ARTHRITIS AFTER CONCURRENT PHYSICAL EXERCISE PROTOCOLS. Brucieri L, Lima R, Pedersen M, Sampaio TT, De AS, Moretti TA, Marretto MA, Costa FR, Felonato M, - Programa de Pós Graduação em Ciências Biomédicas - FHO

Introduction:

Rheumatoid arthritis (RA) is an autoimmune disease (ICD), characterized by the presence of chronic inflammation, which attacks the synovial membrane, leading to cartilage and bone destruction (GOELDNER, et al 2011). The pathology affects small and large joints (KHURANA and BERNEY, 2005), presenting deleterious effects on physical mobility and functional capacity. In the search for alternative treatments, physical exercise and lasertherapy (METSIOS et al., 2015) have been used because they provide favorable reactions to the control of the inflammatory process (BROSSEAU et al., 2005).

Aim:

Thus we verified whether different protocols of physical exercise associated or not with lasertherapy could alter the levels of the systemic and muscular inflammatory process.

Methods:

For eight weeks, Wistar rats were divided into 10 groups: CTL: control group with saline injection at the joint; ZYM: group with injection of 200 µg of zymosan in the joint; ZYM + A: zymosan group submitted to the protocol of aerobic exercise with duration of 1h, 5 days / week with increased weekly load in 5% of the animal weight (NAVARRO et al., 2010); ZY + R: zymosan group submitted to the resistance exercise protocol with 4x10 jumps with 30 seconds rest, 3 days / week (MILARES et al., 2016; MUNIZ-REMO et al, 2005). The load was proportional to the body mass for each animal, starting at 20% of the body mass at 80%; ZYM + CON100%: zymosan group with concurrent exercise protocol (resisted and aerobic exercise) with 100% of total protocol volume; ZYM + CON50%: zymosan group with concurrent exercise protocol with 50% of total protocol volume. All training protocols were subdivided into treatment with and without lasertherapy with an 808nm gallium-aluminum arsenide diode laser. The optic fiber was positioned perpendicular to the skin of the animal with power of 50mW, 1.4J of total energy for 56 seconds. The animals were euthanized, the blood and the muscle was collected for biochemistry analysis. The results were analyzed using the Variance Analysis Test (ANOVA / two way). When necessary, Tukey's post-hoc test was used, with a significance level of 5%.

Results:

In the peripheral blood the levels of NAG and MPO did not present differences. Regarding muscle, all physical exercise protocols induced increased macrophage activity (NAG) in relation to the control and zymosan groups. On the other hand, the neutrophil activity (MPO) was increased in the zymosan group when compared to the control group. Regarding exercise protocols, the groups concurrent 100% and 50% laser presented a decrease in this marker when compared to the concurrent groups 100% and 50%, respectively.

Conclusion:

We observed that the treatment of RA with proposed physical exercise protocols associated or not with lasertherapy stimulated pro-inflammatory muscular potential, based on the presence of macrophage and neutrophils activation markers. However, only concurrent physical exercise protocols associated with lasertherapy were able to modulate the muscle inflammatory process by stimulating anti-inflammatory effect by reducing markers of neutrophil activation.

Financial support:

Financial support: FHO-UNIARARAS

21.003 - PHYSICAL EXERCISE ASSOCIATED WITH CALORIC RESTRICTION PROMOTE REDUCTION OF CD4+ T LYMPHOCYTE INFLUX IN 2K1C ANIMALS SUBMITTED TO A HYPERLIPIDIC DIET. Santos BR, Orzari LE,

Valverde AP, Terciotti LG, Alves AA, Oliveira CA, Dalia RA, Andrade TAM, Amaral MEC, Mendes MF, - Programa de Pós Graduação em Ciências Biomédicas - Centro Universitário da Fundação Hermínio Ometto

Introduction:

The systemic arterial hypertension is responsible for some cardiovascular complications. The correlation between hypertension and obesity is favored by hyperlipidic diets, as the imbalance between the intake of diets with high lipid content and energy expenditure lead to the development of obesity. The clamping of one of the kidneys in the experimental model promoted a raise of the blood pressure. The immune system helps in both protection and potentiation of inflammatory responses. Caloric restriction and physical exercise are used as therapeutic treatment of hypertension, promoting an anti-inflammatory cells increase and a blood pressure decrease.

Aim:

Therefore, this study analyzed the profile of CD4+ T lymphocytes in the associated models of renovascular hypertension, hyperlipidic diet, caloric restriction and physical exercise.

Methods:

Wistar rats weighting from 180 to 200 grams were divided into 4 groups. Sham: hypertensive animals submitted to a hyperlipidic diet (n=6); R: hypertensive animals submitted to hyperlipidic diet and caloric restriction (n=6); T: hypertensive animals submitted to hyperlipidic diet and physical exercise; RT: hypertensive animals submitted to hyperlipidic diet, caloric restriction and physical exercise (n=6). A silver clip with a 0.2 mm opening over the left renal artery induced arterial hypertension. After the confirmation of the hypertensive state, the hyperlipidic diet composed of 45% of lipids was offered to the rats for 8 weeks ad libitum. During 4 weeks, the group of restricted animals had 40% caloric restriction compared to the amount ingested by the control animals. After 10 weeks of clip insertion, the trained groups were submitted to the swimming exercise for 4 weeks, tolerating progressive overloads of lead fixed to the chest. The protocol execution time was inversely proportional to the weight of the load. The animals were euthanized and the liver, right kidney and left kidney were collected for immunohistochemical analysis (CD4+). The results were analyzed by the variance test (two-wayANOVA) and Tukey post-test (p<0.05) expressed as average±standard error. The study was approved by the FHO-UNIARAS Ethics Committee (042/2016).

Results:

In relation to the area marked on the right kidney, the animals of the group R presented an increase of CD4+ when compared to Sham and T animals. The RT group animals had a smaller percentage of area than the groups Sham, R and T. On the other hand, there were no differences in the left kidney in the groups Sham, R, T and RT. Regarding the percentage of positive area for CD4+ T in the liver, T group showed a decrease when compared to Sham and R groups.

Conclusion:

According to this experiment, it is possible to suggest that in hypertension animals submitted to the hyperlipid diet, the increase in intensity and reduction in volume of physical exercise, caused a reduction in the lymphocytic profile in organs that presents inflammation, and the proposed model is capable of inducing control of the adaptive immunity present in hypertension.

Financial support:

FHO-UNIARARAS

21.004 - MODULATION OF GENE EXPRESSION RELATED TO LYMPHOCYTE DIFFERENTIATION BY GANODERMA LUCIDUM SUPPLEMENTATION IN ELDERLY WOMAN. Lobato TB, Iser-Bem PN, Alecrim AL, Passos MEP, Santos LC, Diniz VL, Machado O, Manoel R, Correia IS, Santos BJC, Pereira ACG, Poma SO, Mendes M, Silva EB, Levada-Pires AC, Hatanaka E, Cury-Boaventura MF, Hirabara SM, Borges FT, Pithon-Curi TC, Curi R, Gorjão R, - Interdisciplinary Postgraduate Program in Health Sciences - UNICSUL

FeSBE Annual Meeting 2019

Poster Sessions and Abstracts

Introduction:

Studies have shown that aging is associated with a decrease in the immune balance, leading to immunosenescence. Some compounds extracted from *Ganoderma lucidum* may modulate the immune response reestablishing the balance disturbed by aging. However, few studies have demonstrated the synergistic effect of this mushroom as a whole. It is not known if the association of these active compounds found in the mushroom promotes greater effectiveness when compared to the isolated components. In addition, there are few studies in human involving supplementation with *Ganoderma*.

Aim:

The aim of this study is to investigate the effects of *Ganoderma lucidum* in the regulation of genes involved with differentiation of circulating lymphocytes from elderly woman.

Methods:

In a double-blind randomized controlled clinical trial, 20 elderly women (66.6 ± 6.7 years) were supplemented with 2 g daily of *Ganoderma lucidum* and 20 woman (66.1 ± 8.0) with 2 g of starch (placebo) for 8 weeks. Anthropometric measures and body composition was evaluated by bioimpedance. Biochemical markers of hepatic and renal toxicity, total cholesterol, LDL, HDL, triglycerides and fasting glycemia were also evaluated by colorimetric methods. Lymphocytes were isolated and mRNA expression of IL-6, IL-10, TGF-beta, Foxp3, ROR-gama, GATA3, IL-35, INF-gama, TNF -alfa and T-bet were evaluated by real time PCR. $\beta 2M$ gene expression was used as constitutive gene. The $2^{-\Delta\Delta Ct}$ method was used to calculate the relative expression of described genes. For the comparison between the groups, the two-way ANOVA of repeated measures followed by the Sidak post-test was used. P value < 0.05 was used as a criterion of significance. This study was approved by Ethics Committee of Cruzeiro do Sul University (protocol number CE/UCS-010_2016).

Results:

Ganoderma supplementation did not change body composition parameters and plasma biochemical markers. Supplementation with *Ganoderma* promoted an increase in mRNA expression of the FOXP3 transcription factor (increase of 2.9 times) and of the cytokines IL-10 and TGF- β (3.35 and 3.76 times of increase, respectively) that are related to T regulatory cell function. The expression levels of these genes were higher in *Ganoderma* group when compared to placebo group in the post period of supplementation. However, IFN-gamma and T-BET gene expression that are related to Th1 profile were also increased by *Ganoderma* supplementation (increase of 3.9 and 2.16). In the same way, the levels of these genes were higher in *Ganoderma* when compared to Placebo after 8 weeks of supplementation. On the other hand, GATA-3 gene expression that is related to Th2 profile also increased after supplementation (2.63 times), but there is not difference between *Ganoderma* and Placebo group in post period in relation to this gene. ROR-gamma transcription factor and IL-6 gene expression that are related to Th17 were not altered.

Conclusion:

Our results demonstrated promising effects on the immunomodulation promoted by *Ganoderma lucidum* supplementation. The present study suggest that there is a modulation of Th1 cell function that probably is accompanied by T regulatory lymphocyte function improvement, maintaining the immune balance between inflammatory and anti-inflammatory cells.

Financial support:

FAPESP; CNPq and CAPES.

22 - Cancer Signaling and Therapeutics

22.014 - DETOXIFIED CROTOXIN INDUCES CELL CYCLE ARREST, REDUCTION OF MIGRATORY ABILITY AND ACTIVATION OF APOPTOSIS CASCADE IN HUMAN MALIGNANT MELANOMA CELLS. Giannotti KC, Pereira CO, Camargo L, Marques-Porto R, Chudzinski-Tavassi AM, Reid

P, Picolo G, - Laboratório Especial de Dor e Sinalização - IBU Centro de Excelência para Descobertas de Alvos Moleculares, CENTD - IBU Laboratório de Biologia Molecular - IBU Spotlight Innovation Inc. - SI

Introduction:

Crotoxin (CTX) from *Crotalus durissus terrificus* snake venom exhibits immunomodulatory and antitumor activities. In this sense, many studies have demonstrated that CTX exerts a striking antitumor effect in several types of tumor, such as cutaneous melanoma. Drugs available for the treatment of this disease are of low efficacy and induce many side effects, justifying the search for new molecules. Despite CTX actions on melanoma cells, its use is limited by its toxicity. In this sense, studies using the detoxified toxin are of great value.

Aim:

This study aims to investigate the antitumor effects of native and detoxified CTX on melanoma cells, evaluating: i) the cytotoxic effect, ii) the activation of caspases 3/7, iii) the induction of apoptotic bodies, iv) the interference on cells proliferation and cell cycle distribution and v) the interference on cells migration.

Methods:

SK-MEL-28 melanoma cells or HDF- α fibroblast cells (CEUAIB Nº 3215080818) were incubated with either DMEM (control) or native (12.5-100 $\mu\text{g/ml}$) or detoxified CTX (25-100 $\mu\text{g/ml}$) from 12 up to 72h. Cellular viability was evaluated by MTT assay. The activation of caspases 3/7 and cells proliferation index were analyzed by high content screening. The formation of apoptotic bodies was evaluated by Hoechst 33258 fluorescence analysis and cell cycle distribution was determined by flow cytometry. Finally, the migratory index of melanoma cells was analyzed by wound healing assay.

Results:

Our data showed that native and detoxified CTX reduced melanoma cells viability at all concentrations and periods of incubation tested. Both CTX forms, only at higher concentration, reduced only about 10% of normal cells viability, after 72h of incubation. Moreover, native and detoxified CTX activated caspases 3/7, suggesting that CTX in both forms activates the apoptotic cascade. Fluorescence analysis confirmed these data since apoptotic bodies were seen in cells incubated with these toxins after 48h. In addition, native and detoxified CTX reduced cells proliferation with percentage of reduction around 45% and 38%, respectively and induced cell cycle arrest at G2 phase. Finally, both CTX forms inhibited melanoma cells migration.

Conclusion:

These data reveal the potent antitumor activity of both native and detoxified CTX upon melanoma cells by activating apoptotic pathway and by modulating cells proliferation and migration. Thereby, these results suggest that crotoxin has potential to be used in the treatment of melanoma.

Financial support:

FAPESP

22.015 - MOLECULAR MECHANISM OF ACTION OF NEW 1,4-NAPHTHOQUINONES-1,2,3-TRIAZOL WITH CYTOTOXIC AND SELECTIVE EFFECT AGAINST ORAL SQUAMOUS CELL CARCINOMA. Chipoline IC, Fonseca ACC, Costa GRM, Souza MP, Rabelo VW, Queiroz LN, Almeida ECP, Souza TLF, Abreu PA, Pontes BACC, Ferreira VF, Silva FC, Robbs BK, - Departamento de Ciências Básicas - Universidade Federal Fluminense (UFF) Departamento de Química Orgânica - Universidade Federal Fluminense (UFF) UFRJ - Macaé - Universidade Federal do Rio de Janeiro Faculdade de Farmácia - Universidade Federal do Rio de Janeiro (UFRJ) ICB - Universidade Federal do Rio de Janeiro (UFRJ)

Introduction:

The oral squamous cell carcinoma (OSCC) is a public health problem in Brazil due to its high incidence and low survival rate, despite advances in diagnosis and treatment. Naphthoquinones, substances derived from quinones, had their cytotoxic effect on different cancers demonstrated.

Aim:

FeSBE Annual Meeting 2019

Poster Sessions and Abstracts

In the present study, 35 compounds of triazole naphthoquinones were synthesized and antitumor activity and molecular mechanisms evaluated in a series of assays including in vitro and in vivo models of OSCC and normal oral human cells.

Methods:

The 1,4-naphthoquinone-1,2,3-triazole substances were synthesized from a 1,3-dipolar cycloaddition reaction between aromatic azides and Cu (I) catalyzed alkynes. For synthesis of the propargylated naphthoquinones, a C3 alkylation reaction followed by an O-alkylation in 2-hydroxy-1,4-naphthoquinone and its derivatives. The aromatic azides were obtained with a very common reaction in the literature that passes through the intermediate diazonium salt, Sandmeyer reaction, followed by nucleophilic substitution by the azide group. Cell viability, compound stability and clonogenic assays were performed by MTT. The IC50 was calculated by a non-linear regression curve in the GraphPad Prism 5 program. The Selective Index (SI) of the compounds was also calculated. Acute toxicity tests were performed in mice according to the CEUA / UFF # 982 protocol. The release of reactive oxygen species (ROS) was investigated by DHR123 labeling. Microtubule instability was analyzed by the staining of α -tubulin. Pyknotic nuclei and caspase-3 staining were analyzed to evaluate the type of cell death. A possible molecular mechanism for compounds action was investigated using binding in silico technique.

Results:

Compounds 4A, 4B and 4J were able to induce cytotoxicity in three different cell lines of human OSCC (SCC4, SCC9 and SCC25) and were more toxic and selective to tumor cells ($SI < 2$) than classical and chemically similar controls (Carboplatin and Lapachol). Compound 4J showed the higher SI value. Besides, compounds 4A, 4B and 4J significantly reduced colony formation of SCC9 cells in the tested concentrations. Regarding compounds stability, while Carboplatin is stable after even 48h of incubation at 37°C, compounds effectiveness drops to around 50% after the same time. Hemolytic assay using compounds 4A, 4B and 4J at high concentrations showed no compound exhibited hemolysis higher than 5%, similar to controls. Among the three compounds, in vivo acute toxicity study showed that 4J was the only with no apparent limiting toxic effects on mice in the tested concentrations. Considering the before mentioned results, the investigation of cell death mechanisms was only conducted on compound 4J. This compound does not trigger ROS production, binds to DNA nor express cleaved caspase-3. On the other hand, compound 4J induces microtubule instability, pyknotic nuclei presence and inhibits topoisomerases and hPKM2 activities.

Conclusion:

Among the 35 synthesized triazole naphthoquinones, compound 4J was the most effective compound against OSCC cells, presenting high cytotoxicity ($\sim 35\mu\text{M}$), selectivity ($SI \sim 6$), comparable stability in vitro between compounds and lower acute toxicity on animals, and therefore might be considered for future cancer therapy.

Financial support:

FAPERJ, CNPq, CAPES, PROPPi/UFF

22.016 - BIOPROSPECTING OF NATIVE AND EXOTIC MARINE INVERTEBRATES AT ARRAIAL DO CABO: POSSIBLE ANTIFOULING AND ANTICANCER POTENTIAL. NDIAYE NCG, LOPES GPDF, Honorato J, Villarinho N, Altvater L, Martinez S, Silva S, Maia RC, Coutinho R, - Biotecnologia Marinha - MB/MS Biotecnologia Marinha - MB Coordenação de Pesquisa - MS Química - UFBA Laboratório de Biomedicina do Cérebro - IECPN Laboratório de biotecnologia de produtos naturais e sintéticos - UCS

Introduction:

Marine invertebrates are source of molecules that have different ecological functions and unique complexity. Bioprospecting aims to identify the application of these molecules and their isolation. Among these applications, molecules with antifouling and anticancer

properties are subject to bioprospecting in natural products. The hypothesis is that the cytotoxic activity of these products is capable of inhibiting fouling organisms less environmentally toxic compared to conventional paints. Besides, the same cytotoxicity property can be used against cancer cells, one of the most lethal diseases in the world.

Aim:

Therefore, the present study aimed to evaluate the antifouling and anticancer potential of crude extracts from six marine invertebrates at Arraial do Cabo, Rio de Janeiro, being: two exotic invasive species as *Tubastraea coccinea* and *Didemnum* sp.; two established exotic species as *Darwinella* sp. and *Chromonephtea braziliensis*; and two native species as *Palythoa caribaeorum* and *Phyllogorgia dilatata*.

Methods:

To produce de crude extracts from marine invertebrates, five different individuals were collected, fixed in ethanol 90% and triturated. Then homogenates were diluted in methanol (1:5) and evaporated using rotary evaporator for 4h at 50°C. To evaluate the antifouling activity of crude extracts, inhibition experiments were carried out with five species of marine biofilm forming bacteria, promoting biofouling: *Shewanella putrefaciens*; *Vibrio* estuarian; *Pseudoalteromonas elyakovii*; *Polaribacter irgensii* and *Pseudomonas fluorescens*. Bacteria was cultured in solid medium and filter disks were embedded with 7.5, 15, 30, 60 e 120 (mg/ml) of crude extracts diluted in methanol. The positive control consisted in riphancipin (1g/mL) and negative control was the diluent methanol. For the anticancer evaluation, the cell viability of the T98G and U251 human glioblastoma cells and the healthy human cell fibroblast cell line was analyzed by the acid phosphatase method in both monolayer and three-dimensional cell culture models. The cells were cultured with 100, 200, 400, 800 e 1000microg/mL, and 12.5, 25, 50, 100 e 200microg/mL for *Didemnum* sp. All bacterial inhibition and cell viability assays were analyzed by Kruskal-Wallis non-parametric statistical test followed by multiple comparisons to control by the Dunn's test. The values were expressed by the median and their distribution (min-max) and were considered significant when $P \leq 0.05$.

Results:

The species that stood out in the activity against bacteria were *T. coccinea* > *Darwinella* sp. > *C. braziliensis* > *P. dilatata*. However, none of them presented significant more antifouling activity than antibiotic, as positive control. The anticancer evaluation, crude extract from *Didemnum* sp. and *T. coccinea* were effective in both culture models (2D and 3D), showed selective citotoxic effect in both glioblastoma cell lines, without citotoxicity of human fibroblasts. The IC50 of the extracts was 120.6 and 432.8 (microg/mL) for T98G cells and 63.32 and 317.2 (microg/mL) for U251 cells, of *Didemnum* sp. and *T. coccinea*, respectively.

Conclusion:

It is suggested that the exotic invasive species *Didemnum* sp. and *T. coccinea* it is found in abundance and its' crude extracts promising for the development of biotechnological products with pharmaceutical applications. Future experiments as chemical profile will be performed to identify the active biocompounds in these crude extracts and to forward to in vivo scale for brain tumor therapeutic future approach.

Financial support:

FAPERJ, CNPq, CAPES, Ministério da Saúde

22.017 - BOTRYOSPHAERAN REDUCES TUMOR DEVELOPMENT AND IMPROVES THE METABOLIC PROFILE OF WALKER-256 TUMOR-BEARING OBESE RATS. Geraldelli D, Martins KO, Ribeiro MC, Medeiros TC, Oliveira MF, Oliveira GA, Dekker RF, Barbosa-Dekker AM, Alegranci P, Queiroz EAIF, - Programa de Pós-Graduação em Ciências em Saúde - UFMT Instituto de Ciências da Saúde - UFMT Departamento de Química - UEL Programa de Pós-Graduação em Engenharia Ambiental - UTFPR

Introduction:

FeSBE Annual Meeting 2019 Poster Sessions and Abstracts

Background: Studies have been demonstrated that obesity is an important risk factor for tumor development, and chronic low-grade inflammation, oxidative stress, insulin resistance and hyperinsulinemia are the mechanisms related to carcinogenesis in obesity. Botryosphaeran, a (1→3)(1→6)-β-D-glucan, produced by the fungus *Botryosphaeria rhodina*, has been described as a potential drug for the treatment of obesity and cancer due to its antimutagenic, antiproliferative, pro-apoptotic, hypoglycaemic and hypocholesterolaemic properties.

Aim:

Thus, the objective of this study was to evaluate the effects of botryosphaeran on Walker-256 tumor development in obesity and analyze the metabolic profile of these animals, under the hypothesis that botryosphaeran could reduce tumor development and improve its metabolic profile improving the insulin resistance.

Methods:

Methods: Study protocol was approved by the Ethics Committee under n°23108.973436/2018-54. Obesity was induced in male Wistar rats by ingestion of a high-fat high-sugar diet for 11 weeks. On 9th week, 1x10⁷ Walker-256 tumor cells were inoculated subcutaneously into the upper right flank of the rats and treatment with botryosphaeran started (30mg/kg, via gavage, for 15 days). Thus, the rats were divided into two groups: Obese Tumor (OT) and Obese Tumor Botryosphaeran (OTB). At the 11th week, weight evolution, feed-intake, adipose and muscle tissues weights, glucose and lipid profiles, and hemogram were analyzed. Moreover, tumor development, percentage of rats that developed tumor, and cachexia syndrome were measured, as well as the expression of proteins (Bax, Bcl-2, caspase-3, p27, p53 and FOXO3a) was determined by Western Blotting. The comparison between the groups was performed by Student's t-test and significant differences at p<0.05.

Results:

Results: Botryosphaeran reduced significantly the tumor weight (OT=36.1±19.4g and OTB=16.8±8.0g#; #p<0.05) and the weight loss (OT= -55.5±31.2g and OTB= -7.8±13.1g; #; #p<0.05), as well as, decreased the cachexia index in 35%, demonstrating that this (1→3)(1→6)-β-D-glucan was effective to reduce tumor development and neoplastic cachexia. Furthermore, botryosphaeran significantly decreased mesenteric fat, and increased lean mass (soleus muscle) and insulin sensitivity. OT group presented hypochromic macrocytic anemia and botryosphaeran corrected this parameter. In the leukogram, all groups showed leukocytosis, neutrophilia and monocytosis, suggesting activation of the innate immune system. Moreover, OT animals presented lymphocytosis, suggesting an adaptive immune response. There was no change in the expression of the evaluated proteins.

Conclusion:

Conclusion: Botryosphaeran reduced tumor development and neoplastic cachexia in obese animals, mechanism associated with decreased fat accumulation and improved insulin sensitivity, confirming the potential role of botryosphaeran in the management of cancers.

Financial support:

CAPES; UFMT

22.018 - IN VITRO EVALUATION OF CELL VIABILITY AND BETALAINS QUANTIFICATION OF NUTRACEUTICAL CACTI-NEA. BIZINELLI D, SANTOS NTH, FALDONI FLC, NAVARRO FF, - Farmácia - FHO

Introduction:

CactiNea characterized as the aqueous extract dehydrated of the fruit of *Opuntia ficus indica* has several metabolite compounds responsible for several therapeutic actions. Nutraceuticals are classified as foods that have health benefits, including the prevention and/or treatment of diseases, from isolated nutrients, dietary supplements to designed products, plant products and processed foods. Mutations in DNA have caused several diseases, among which we can mention the degenerative and cancer. Such changes can be induced by several

factors, including the compounds present in foods or in food supplements.

Aim:

The aim of this study was to quantify beta-lactam content and to evaluate the cellular viability of Cacti-Nea in the MDA-MB-231 cell line.

Methods:

The Ethics and Animal Use Committee of FHO approved this study, under number 002/2019. The total concentration of the beta-carmines pigments contained in Cacti-Nea was evaluated according to Cai et al. (2001). For this analysis, dilutions of the nutraceutical were performed in a mixture of methanol and water (80:20 v/v), to obtain an absorption value between 0.9 > A > 1.0. The determination of cytotoxicity of Cacti-Nea for MDA-MB 231 cells was done by the MTT test, according to the protocol established by Mosmann (1983), evaluating the cellular behavior against different concentrations of nutraceutical (0,5; 5; 50 e 500 µg/mL).

Results:

The evaluated nutraceutical CactiNea is distributed in Brazil by the company Galena®, the lot evaluated in the present study was 1803035402 with validity 30/06/2020. The concentration of total betalains and betaxanthines and betacyanins present in the Cacti-Nea were 0.074% ± 0.0884; 0.059% ± 0.015; 0.0995% ± 0.0774. The cytotoxicity of different concentrations of Cacti-Nea (0,5; 5; 50; 500 µg/mL) for MDA-MB231 cells was estimated by MTT cell viability test. It was observed that the concentrations of 0.5 and 5.0 µg/mL presented cellular viability higher than 70% (72.27% ± 4.71 and 77.22 ± 6.45, respectively), while the other concentrations had anti-proliferative dose-dependent effects, where 50 µg/mL had a viability rate of 51.63% ± 1.96 and 500 µg/mL 31.33% ± 2.43.

Conclusion:

The constant search of the population for functional foods requires intensive research on the development of nutraceuticals, the sample of CactiNea showed potential antiproliferative dose-dependent effect, through the cell viability assay performed with MTT, and the quantification of betalains demonstrated the presence of these bioactive compounds. Such results allow new functional studies to verify the implication of the consumption of this nutraceutical as a possible preventive way to the progression of tumor cells.

Financial support:

PIC/FHO

22.019 - THE EXPRESSION LANDSCAPE OF CACHECTIC FACTORS IN HUMAN CANCERS. Freire PP, Fernandez GJ, Moraes D, Cury SS, Dal-Pai-Silva M, Reis PP, Rogatto SR, Carvalho RF, - Surgery and Orthopedics - UNESP Morphology - UNESP Clinical Genetics - SDU

Introduction:

Cancer cachexia is a multifactorial syndrome characterized by muscle wasting, leading to a significant weight loss that impacts patient morbidity and survival. Cachexia is highly associated with specific tumor types, such as pancreatic, esophageal, gastric, lung, and liver, and the causes of variation in cachexia prevalence and severity are still unknown. While distinct circulating mediators (soluble cachectic factors) derived from tumor cells have been implicated with the pathogenesis of the syndrome, these associations were generally based on plasma concentration rather than tissue-specific gene expression levels across tumor types. The access to The Cancer Genome Atlas (TCGA) database has allowed the identification of gene expression profiles that correlate with survival following cancer prognosis in different tumor types.

Aim:

We hypothesized that tumor gene expression profiling of cachectic factors could reveal potential cancer-specific biomarkers of clinical outcome. Our aim was to characterize the molecular landscape of cachectic factors in human cancers with different susceptibilities to develop cachexia.

FeSBE Annual Meeting 2019

Poster Sessions and Abstracts

Methods:

We first combined uniformly processed RNA sequencing data from The Cancer Genome Atlas and Genotype-Tissue Expression databases to characterize the expression profile of secretome genes across 12 cancer types (4,651 samples) with different susceptibility to cachexia, as compared to their matched normal tissues (2,737 samples). Next, we systematically investigated the transcriptomic data to assess the tumor expression profile of 25 known cachectic factors and analyze the prognostic value of these factors in terms of predicting patient survival. We used Xena Functional Genomics tool to collect the gene expression information according to neoplastic cellularity (high purity vs. low purity tumors) to analyze whether cancer samples would cluster according to the tumor grade, leukocyte methylation percentage, tumor DNA hypermethylation, and purity class.

Results:

We comprehensively characterized the expression landscape of secretome genes across human cancers and identified potential mediators of cachexia within the tumor microenvironment. Cachectic factors presented a tumor-specific expression profile. The number of up-regulated cachectic factor genes in tumor compared to normal tissues was strongly correlated with the prevalence of cachexia and weight loss (average percentage) across tumor types; this finding could be useful to explain why specific cancer types are more likely to develop cachexia. In pancreatic adenocarcinoma, these up-regulated cachectic factor genes were also associated with tumors presenting low neoplastic cellularity and high leukocyte fraction. Furthermore, the distinct gene expression profile according to tumor type was significantly associated with poor prognosis.

Conclusion:

Our results present a biological dimension for exploration of tumor-secreted elements clinically relevant to cancer biology and may be useful to explain why specific cancer types are more likely to develop cachexia. In addition, the tumor-specific profile of cachectic factors may help the development of better-targeted therapies to treat cancer types highly associated with the syndrome.

Financial support:

FAPESP (18/19695-2 ; 13/50343-1); CNPq (141919-2016-7)

22.020 - INFLUENCE OF THE RENIN-ANGIOTENSIN SYSTEM ON THE PROLIFERATION OF LEUKEMIA CELLS. Souza PD, Dias J, Vieyra A, - Programa de Pós-graduação em Química Biológica - UFRJ Programa de Pós-graduação em Fisiologia e Biofísica Celular - UFRJ

Introduction:

The renin-angiotensin system (RAS) is classically described as a circulating endocrine system that is responsible for controlling blood pressure and volume/composition of body fluids. Today, other complex functions are recognized and they depend on different organ and tissue-based RAS. Some components of RAS in the bone marrow have been described or proposed to exist, and RAS seems to be crucial in the regulation of hematopoiesis in physiological and pathological conditions.

Aim:

In this study, we investigated the influence of RAS on leukemic cell proliferation and apoptosis in vitro.

Methods:

Cell culture: K562 human erythroleukemia cell line (ATCC) was grown in RPMI-1640 medium. Immunodetection of AT1R and AT2R and angiotensinogen (the substrate for Ang II formation) was performed using samples obtained from lysed K562 cells after 24 h-incubation at different concentrations of fetal bovine serum (0–20%). Cell viability (trypan blue exclusion) was assessed after treatment of the cultures with the AT1R and AT2R blockers, Losartan (0–1.0 mM) and PD123319 (0–1.0 mM) by counting the number of viable cells every 24 h. Cell death was evaluated by flow cytometry (Annexin V and Propidium iodide); morphologic modifications by optical microscopy (May-

Grünwald-Giemsa). Experimental design was approved by Committee on Research of the National Cancer Institute (no: 63952017.70000.5274)

Results:

AT1R, AT2R and angiotensinogen were detected and the presence of fetal bovine serum (FBS) did not influence their abundance. Losartan inhibited growth of K562 cultures (initially 2.5×10^5 cells/ml) in the range 0.2–1 mM, the most pronounced effect seen after 72 h: 16 ± 1 (CTR) vs $1.2 \pm 0.8 \times 10^5$ viable cells/ml (1 mM losartan) ($P < 0.0001$). PD123319 was also inhibitory; after 72 h: 17 ± 0.5 (CTR) vs $0.11 \pm 2.2 \times 10^5$ viable cells/ml (1 mM PD123319) ($P < 0.001$). Losartan led almost the entire cell population to apoptosis (early and late) after 72 h: CTR 5.7% vs 94.1% (1 mM losartan) ($P < 0.0001$). K562 cells showed morphological characteristics of apoptosis, such as chromatin condensation and nuclear fragmentation; in addition, there was a decrease in the number of nuclei in division. After 24 h the number of viable cells in the presence of 1 mM losartan decreased 53% with respect to CTR ($P < 0.0001$), with early and late apoptosis being barely detectable in both groups.

Conclusion:

The existence of Ang II receptors (AT1R and AT2R) and angiotensinogen demonstrates a resident RAS in K562 cells, which seems to play an important role in cell viability and proliferation. Inhibition by both blockers is suggestive that there is a crosstalk between AT1R- and AT2R-signaling for leukemia cells growth and proliferation. The accentuated inhibition of growing without apoptosis at early stages reveals an effect of receptors blockers on growing, which is previous to induction of cell death. Finally, since there was no influence of FBS we propose that the concerted stimulus of RAS components synthesis in K562 cells is independent of Serum Response Factor.

Financial support:

CNPq, FAPERJ, INCTs, FINEP, CAPES

22.021 - EFFECT OF DOCOSAHEXAENOIC ACID (DHA) IN RESISTANT AND NON-RESISTANT GLIOBLASTOMA CELLS. Silva JA, Colquhoun A, - Departamento de Biologia Celular e do Desenvolvimento - USP

Introduction:

Current therapeutic strategies for glioblastoma are surgery, chemotherapy and radiotherapy. However, such treatments fail due to the tumor's acquired resistance mechanisms, such as increased activity of multidrug resistance proteins (MRPs). Polyunsaturated fatty acids (PUFA) such as DHA are described as modulators of the expression of these proteins.

Aim:

To evaluate the role of DHA in resistant and non-resistant glioblastoma cells, verifying their effects upon tumor growth and chemotherapeutic response to Vincristine (VCR) or Temozolomide (TMZ).

Methods:

Drug resistant U87MG cell lines were produced with VCR or TMZ in different concentrations (0.4 nM and 25 μ M, respectively). Cell growth assays were performed using DHA (ω -3) in U87MG, TMZ-resistant (TMZ-R) and VCR-resistant (VCR-R) U87MG-derived cells. MRP activity was assessed through a Rhodamine 123 efflux activity assay in U87MG, TMZ-R and VCR-R before and after DHA treatment [100 μ M; 72h]. Cell growth assays were performed using DHA in U87MG, TMZ-R and VCR-R. Gene resistance expression was assessed through qRT-PCR before and after DHA treatment [100 μ M; 72h]. For statistical analysis in cell growth assay and activity assay ANOVA with Bonferroni post-test were used to evaluate the statistical significance. For qRT-PCR Student's t test was used.

Results:

The preliminary results showed that gene expression of ABCB1, ABCC1 and MGMT was increased in TMZ-R in comparison with U87MG ($p < 0.05$; $n = 3$, in duplicate; $p < 0.05$; $n = 3$, in duplicate; $p < 0.001$; $n = 3$, in duplicate, respectively). ABCC3 and MGMT were increased in VCR-R in

FeSBE Annual Meeting 2019

Poster Sessions and Abstracts

comparison with U87MG ($p < 0.05$, $n=3$, in duplicate; $p < 0.01$, $n=3$, in duplicate, respectively). In U87MG, cell numbers decreased when treated with DHA [150 μM] compared with Albumin (BSA) ($p < 0.05$; 72h; $n=3$, in triplicate). TMZ + DHA in all concentrations did not decrease the number of cells versus TMZ alone. The decrease in cell number was more evident with VCR + DHA [100 μM and 150 μM ; 72h] than VCR and VCR + BSA ($p < 0.01$ and $p < 0.001$, respectively; $n=3$, in triplicate). DHA did not decrease the number of VCR-R cells. In U87MG, the efflux activity of MRPs appears to be decreased in the presence of TMZ + DHA and VCR + DHA after 100 min ($n=2$, in duplicate) and the gene expression of ABCB1, ABCC1, ABCC3 and ABCC4 decreased in the presence of TMZ + DHA and VCR + DHA [100 μM] ($n=2$, in duplicate) but not in the presence of DHA alone [100 μM].

Conclusion:

Co-treatment with DHA and chemotherapies reveals differences between TMZ + DHA combination and VCR + DHA combination. VCR + DHA might be more effective to decrease cell number. However, TMZ or VCR + DHA can modify the gene expression of ABC Transporters in U87MG. The efflux activity in U87MG appears to be modified in the presence of drugs and DHA. Further analysis must be done to understand the association between the resistance phenotype and the response to these treatments.

Financial support:

FAPESP

22.022 - EVALUATION OF THE ANTIPROLIFERATIVE POTENTIAL OF CYMBOPOGON FLEXUOSUS ESSENTIAL OIL IN CERVICAL CARCINOMA CELLS. Lima CS, Junior JCT, Pereira MTM, Pascoal VDB, PASCOAL ACRF, - Saúde - UFF

Introduction:

Cymbopogon flexuosus, popularly known as lemongrass from the East, produces a valuable essential oil that is widely used in perfumeries, cosmetics, and pharmaceuticals. Citral, the main constituent of essential oil, is also used in the synthesis of vitamins A and E. This essential oil and some of its components are antiproliferative, antimutagenic and antioxidant potentials. Cervical cancer is one of the most common neoplasms in women of childbearing age worldwide. The etiology of cervical cancer is linked to several risk factors, such as poor personal hygiene, prolonged use of oral contraceptives, a plurality of sexual partners, smoking, among others. However, in almost all cases, it is caused by cellular changes induced by human papillomavirus (HPV) in case of persistent infections, transmitted during intercourse. To find efficient strategies for the treatment and combat of this pathology, studies that aim to ascertain the pattern involved in the carcinogenesis of this tumor type and the action of new therapies through in vitro evaluations are one of the main steps of this path. In this context, cell cultures prove to be an interesting model considering the wide range of methodologies available for toxicological evaluation.

Aim:

The present work was carried out to evaluate the antiproliferative potential of *C. flexuosus* essential oil in cervical carcinoma cells (HeLa) in vitro

Methods:

Cervical carcinoma cells (HeLa cells), were seeded in a 96-well plate and after 24h the oil that had previously been diluted in the medium at the concentrations of 3 to 250 $\mu\text{g} / \text{mL}$ dissolved in RPMI medium was applied, and then the plate was incubated for 48h. The plate was washed with PBS, the MTT was applied, and the plate was incubated for 4h. After that, the MTT solution was withdrawn, DMSO was applied, and the spectrophotometer read at 570 nm

Results:

This method evaluated the mitochondrial activity of viable cells in metabolizing tetrazolium salts. Cell viability was compared to cells treated with vehicle alone (100% cell viability). There was a decrease in cell viability, statistically significant, $p < 0.05$, ANOVA followed by Tukey)

at concentrations of 31 to 250 $\mu\text{g} / \text{mL}$, IC 50 = 33.94 $\mu\text{g} / \text{mL}$ (concentration capable of inhibiting cell growth by 50%).

Conclusion:

Our results demonstrate that *C. flexuosus* essential oil presented a source of products with antiproliferative activity on cervical carcinoma cells in vitro.

Financial support:

Olin Cosméticos

22.023 - DOCOSAHEXAENOIC ACID DECREASE PROLIFERATION OF BENIGN AND MALIGNANT CELLS VIA METABOLIC STRESS INDUCTION AND DYSREGULATION OF ANDROGEN PATHWAY. Tamarindo GH, Goes RM, - Biologia - UNESP IB - UNICAMP

Introduction:

Prostate cancer (PCa) is among the main causes of death worldwide, but most of available therapies are not effective. Cancer cells are metabolically different from normal phenotype which may represent a potential therapeutic strategy. Docosahexaenoic acid (DHA) is a polyunsaturated fatty acid omega-3 found in the human diet that has been reported to decrease cell proliferation and tumor growth in several cancers, including prostate. Such fatty acid modulates energy metabolism, induces mitochondria dysfunction and oxidative stress and regulates the expression of genes involved in androgen signaling, metabolism and cell proliferation. However, DHA role along PCa development and progression is far from being widely known.

Aim:

The present study evaluated the protective as well as therapeutic property of DHA associated to proliferation inhibition and cell metabolism modulation in vitro.

Methods:

PNT1A and 22rv1 cells, representative of benign hyperplasia and tumor condition, respectively, were incubated with DHA at 100 μM for 48h. This concentration and time of incubation was chosen based on metabolic activity determined by MTS assay. Cell number and viability index were assessed by counting and Trypan Blue exclusion test, respectively. Metabolic stress was determined by fluorescence intensity after incubation with BODIPY[®] and MitoSOX[®] dyes and confirmed with Transmission Electron Microscopy. ERK activation was evaluated by Western Blotting. Also, RT-qPCR microarrays were performed in three pooled samples and evaluated the expression of 258 genes related to androgen pathway. All assays were performed with cells from three consecutive passages at least. For statistical analysis, unpaired t-test was performed for parametric and non-parametric data (Mann-Whitney).

Results:

DHA decreased metabolic activity in PNT1A (43%) but increased in 22rv1 (65%). Also, this fatty acid decreased cell number in both lines (27%), but only reduced viability in PNT1A what was followed by ERK activation (about 53%). This evidence suggests that such omega-3 triggers distinct pathways towards cell growth and proliferation between cancer and benign stages, as cell cycle and cell death, respectively. DHA also led to metabolic stress in both lines by increasing lipid accumulation (3-fold PNT1A; 1.8-fold 22rv1) and superoxide anion production (1.6-fold PNT1A; 2.2-fold 22rv1), an indicator of mitochondria dysfunction. Such stress was confirmed in the ultrastructural analysis since damaged mitochondria as well as augmented lipid droplets content were detected and seems to affect the endoplasmatic reticulum-mitochondria interaction. In addition, DHA upregulated NROB1, PPARG, SNAI2, ADAMT51 and KLK3 genes whereas downregulated ESRRG, NR5A1, RARB, NROB2, AR, GUCY1A3, KLK2, IGFBP5, FOS, SPDEF and TMPRSS2 in PTN1A cells (2-fold at least). It is not fully understood their role in PCa development and progression, but their entry in STRING database revealed that, except for GUCY1A3, ADAMT51 and RARG, their products directly or indirectly participate of androgen pathway through binding or regulation of

FeSBE Annual Meeting 2019

Poster Sessions and Abstracts

androgen receptor. Regarding 22rv1, only NROB1 and IGFBP5 were upregulated whereas HDAC7 and RXRG, ORM1 and TIPARP downregulated (2-fold at least).

Conclusion:

In conclusion, DHA decreased cell proliferation in both cell lines by inducing metabolic stress and modulation of different genes in each cell line, most of them related to PCa.

Financial support:

CAPES (Finance Code 001) and FAPESP (2018/21891-4)

22.024 - NEUTROPHIL EXTRACELLULAR TRAPS (NETS) INCREASE THE PRO-TUMORAL PROPERTIES OF THE HUMAN BREAST CANCER MCF-7 CELL LINE. Cardoso KM, Almeida VH, Bagri KM, Mermelstein C, König S, Monteiro RQ, - Bioquímica Médica - UFRJ Histologia e Embriologia - UFRJ Diferenciação celular - UFRJ

Introduction:

Breast cancer is the most common malignancy in women around the world. While the localized tumor presents an excellent prognosis, high rates of mortality have been associated with metastasis, a process in which primary tumor cells may achieve distance sites and promote the formation of new tumors. A number of different host cells found in the tumor microenvironment seem to facilitate metastasis by a variety of mechanisms. Neutrophils may undergo a cellular program that leads to the extrusion of a web-like material named Neutrophil Extracellular Traps (NETs) that are composed by DNA and proteins such as elastase, histones and myeloperoxidase. NETs have been proposed as possible effectors in the tumor progression.

Aim:

Herein, we evaluated the effects of isolated NETs towards the human breast carcinoma MCF7 cell line.

Methods:

Neutrophils were isolated from the blood of health donors and further stimulated with PMA to generate NETs (ethics committee approval number 82933518.0.0000.5257). MCF7 cells were starved in serum-free medium for 10 hours followed by stimulation with NETs for 16 hours. After the treatment, samples were generated for real time PCR analysis, flow cytometry analyses, migration assays and immunocytochemistry.

Results:

Treatment of MCF7 with purified NETs for 16 hours promoted remarkable morphological changes in the tumor cells. In addition, incubation of MCF7 with NETs dramatically increased the migratory properties of the tumor cells. NETs also increased the mRNA expression of IL6, iL8 and MMP9 genes as assessed by real-time PCR analyses, which was approximately 10, 12 and 100-fold higher than the control condition, respectively. In order to evaluate if NETs could promote β -catenin translocation from the membrane to nucleus, we performed an immunocytochemistry assay. NETs were not able to change the cellular localization of β -catenin in MCF7 cells. On the other hand, the expression of the cancer stem cell marker, CD44, was upregulated upon incubation of MCF7 cells with NETs, as demonstrated by PCR and by flow cytometry analyses, 6 and 4-fold higher than the control, respectively. Collectively our data demonstrate that NETs increase the pro-tumoral properties of the human carcinoma MCF7 cell line.

Conclusion:

We conclude that NETs may participate in breast cancer progression.

Financial support:

Financial support by the Brazilian Cancer Foundation (Programa de Oncobiologia), CAPES, CNPq, Faperj.

22.025 - EVALUATION OF THE ANTIPROLIFERATIVE ACTIVITY OF CAMPOMANESIA GUAVIROBA IN CERVICAL CARCINOMA. Júnior JCT, Pascoal VDB, Pereira MTM, Salvador MJ, PASCOAL ACRF, - Programa de Pós Graduação em Biociências e Tecnologia de Produtos Bioativos -

UNICAMP Laboratório Multiusuário de Pesquisa Biomédica - UFF Programa de Pós-Graduação em Ciência e Biotecnologia - UFF

Introduction:

Plants are excellent sources of active substances used for the development of new medicines, and the Myrtaceae family presents some species used in folk medicine. Among them, the Campomanesia genus has already demonstrated some biological effects, such as antiproliferative, antioxidant and anti-inflammatory activity. Campomanesia guaviroba, although well distributed by the Atlantic Forest, has few studies on its physiological effects. Cervical carcinoma is the third most frequent among the Brazilian female population and may take many years to develop, as it is the result of persistent infection by some HPV subtypes of high oncogenic risk. Also of great importance is the development of a product that can be used even in stages in which the patient presents lesions or atypia.

Aim:

Evaluate the Antiproliferative Activity of Campomanesia guaviroba in Cervical Carcinoma.

Methods:

Leaves of C. guaviroba were collected in Campinas, SP, dried and pulverized and subjected to alcohol extraction. Then, the liquid-liquid partition was performed, obtaining the hexane and dichloromethane fraction. The antiproliferative potential of the dichloromethane fraction, derived from the raw extract of C. guaviroba leaves, was evaluated by culturing Cervical Carcinoma cells (HeLa) (2×10^4 células/mL), which were seeded in a 96-well plate with culture medium (RPMI-1640 supplemented with 10% fetal bovine serum, 1% glutamine and 40ug / ml gentamicin). The plate was maintained in an oven at 37 ° C and 5% CO₂ throughout the period. After 24 hours plating the cells were treated with C. guaviroba extract, previously diluted in the medium. After 48 hours of treatment, the MTT solution was applied, and the plate was incubated for 4 hours under the same oven conditions and spectrophotometrically read at 570 nm. Then, the dichloromethane fraction was analyzed for its content of total phenolic compounds using the colorimetric method Folin-Ciocalteu, using a standard curve taking as reference substance gallic acid. Finally, the quantification of total flavonoid compounds was carried out by spectrophotometric assay, which had quercetin as the reference substance. The evaluation of the antiproliferative potential and quantifications of phenolic compounds and flavonoids were performed in triplicate.

Results:

As a result, it can be observed that the concentration capable of inhibiting 50% of cell growth was 47.38 $\mu\text{g} / \text{mL}$, whereas 12.68 $\mu\text{g} / \text{mL}$ of total phenolics and 4.73 $\mu\text{g} / \text{mL}$ quercetin/mg flavonoids.

Conclusion:

The results indicate a potential antiproliferative activity of C. guaviroba in cervical carcinoma cells, and this activity may be related to phenolic compounds and among them, flavonoids. Thus, further studies should be performed to identify the significant compounds present in the species.

Financial support:

FAPESP, FAPERJ, CAPES

22.026 - TISSUE REPAIR OF ELECTROCAUTERIZATION INJURY: APPLICATION OF LED THERAPY ASSOCIATED WITH PHOTODYNAMIC THERAPY. Manoel CA, Mariano SS, Adriano LC, Ramos ES, Paolillo FR, Santos GMT, Bagnato VS, Andrade TAM, - Graduate Program of Biomedical Sciences - FHO Physics Institute of Sao Carlos - USP-IFSC

Introduction:

The electrocauterization produces cutaneous lesion through electric discharge generating desiccation, without hemorrhage, reaching deeper layers of the skin and forming crust that protects the tissue. It is mainly used for rejuvenation, removal of age spots and other applications. In this sense, the association of therapeutic techniques

FeSBE Annual Meeting 2019

Poster Sessions and Abstracts

such as LED therapy with Photodynamic Therapy has been developed aiming at better therapeutic responses and for tissue remodeling.

Aim:

To evaluate the effects of LED therapy with Photodynamic Therapy (PDT) in the healing process of cutaneous lesions induced by electrocauterization.

Methods:

This study was approved by CEUA-FHO (nº 068/2017). A total of 72 rats ($\pm 280g$) were used, which had the dorsal region trichotomized to be submitted to cutaneous lesions (2.0cm²) using the New Skin® electrocautery (MMOptics - São Carlos-SP), at 100mV intensity, LED therapy (660nm, 60s, dose of 6J, 3x / week, for 14 days, associated or not with Photodynamic Therapy). For photodynamic therapy 5-aminolevulinic acid (ALA, 6% concentration, PDT Farma®, Cravinhos-SP) was used to be applied to the lesion (single session) soon after the surgical procedure (associated or not to LED therapy). Thus, the experimental groups were: No injury: no lesion and treatment; Injury: no treatment in the lesion; Injury+LED: treated in the lesion with LED only; Injury+ALA: treated with ALA and Injury+ALA+LED: treated with ALA and LED, for 2, 7 and 14 days post-injury (n = 6 animals/time/treatment). After euthanasia, cutaneous biopsies were collected for histomorphometry (HE and Gomori trichrome) for quantification of inflammatory infiltrate, blood vessels, fibroblasts, collagen and thickness of the crust using ImageJ software. The results were analyzed by ANOVA Two-way / Bonferroni.

Results:

The Injury+ALA+ LED group on the 2nd day presented lower inflammatory infiltration in relation to the other groups and this profile was reduced during the follow-up. Regarding angiogenesis, on the 7th day, the Injury+LED and Injury+ALA+LED groups presented higher blood vessels in relation to the lesion and Injury+ALA groups, respectively. On the 14th day, the Injury+LED group was larger than the lesion and the Injury+ALA groups and the Injury+ALA+LED group was larger than the lesion group. As for fibroplasia, the Injury +ALA+LED group was highlighted by its important fibroplasia on the 7th and 14th days in relation to the other groups. Regarding collagenesis, on the 14th day, there was lower collagen formation in the Injury+LED group compared to the lesion. When the thickness of the lesion crust was smaller in the Injury+ALA+LED group compared to the Injury+ALA and Injury+LED groups. In addition, the lesion group had lower crust thickness compared to the Injury+ALA group.

Conclusion:

The association of ALA with LED was effective in favor of tissue repair in the injury induced by electrocautery.

Financial support:

HERMÍNIO OMETTO FOUNDATION, MMOptics, Physics Institute of Sao Carlos.

24 - Vision and Ophthalmology

24.007 - GALUNISERTIB EFFECTS ON THE GLIAL-MESENCHYMAL TRANSITION OF RETINAL MÜLLER CELLS. Silva RA, Matsuda M, Tikasawa PSA, Roda VMP, Costa GJL, Hamasaki DE, - Cell & Developmental Biology - USP Laboratory of Ophthalmology - USP

Introduction:

Among the ophthalmologic diseases that lead to retinal detachment are proliferative vitreoretinopathy, diabetic retinopathy and age-related macular degeneration. In more advanced cases, occurs the formation of a contractile membrane that might lead to the tissue contraction, causing macular distortion and detachment of the retina, or even blindness. It is known that retinal Müller glial cells, when undergo harmful stimuli, enter into gliosis, leading them to proliferate and migrate to form the epiretinal membrane. TGF- beta is a major signaling pathway that is closely related to membrane formation and the studies showed increased levels of TGF-pathway molecules. Galunisertib is a

drug that blocks the kinase of the ALK5 pathway reducing the pSMAD2 activation in cells and it has been recently used in some cancers to prevent metastasis and tumor invasion.

Aim:

To investigate the effect of galunisertib on the Müller glial-mesenchymal transition, specifically on: 1) glutamine synthetase (GS), a marker of Müller cells; 2) alpha-smooth muscle actin (α -SMA), a cytoskeletal protein indicative of myofibroblast differentiation; 3) cell migration.

Methods:

Human Müller glial cells line (MIO-M1), was obtained from Dr. A. Limb (UCL Institute of Ophthalmology London, UK). The cells were treated with 10 ng/mL TGF- β I or II for 24h and 48h with or without 10 μ M of galunisertib. The dose was determined by {[3- (4,5-dimethylthiazol-2yl) -2,5-diphenyl tetrazolium bromide] (MTT) assay. GS and α -SMA gene expression was quantified by real-time quantitative PCR, and protein expression by immunofluorescence. Wound- healing assay was applied to evaluate cell migration.

Results:

Treatment with 10 μ M galunisertib, TGF- β 1 or TGF- β 2 (10 ng/mL) did not reduce MIO-M1 cell viability. TGF- β 1 and β 2 downregulated GS immunofluorescence and mRNA levels (about 25-60%) at 24h and 48h. When galunisertib was also added, no significant differences were observed compared to the controls. TGF- β 1, but not TGF- β 2, upregulated α -SMA mRNA levels at 24h and 48h (about 40%). Galunisertib downregulated α -SMA mRNA (about 20-55%) compared to the controls at 24h and 48h. Wound-healing assay preliminary results showed a decreased migration of Müller cells.

Conclusion:

Our data suggests that galunisertib attenuate glial-mesenchymal transition of retinal Müller cells, and may be a possible candidate to prevent the formation of fibrocontractile membranes.

Financial support:

FAPESP, CNPQ and CAPES.

24.008 - CHARACTERIZATION OF MELANOPSPIN EXPRESSION IN OWL RETINAS.. Naman MJV, Assis LVM, Hauzman E, Castrucci AML, Ventura DF, Baron J, Bonci DMO, - Departamento de Psicologia Experimental - USP Departamento de Fisiologia e Biofísica - UFMG Departamento de Fisiologia - USP

Introduction:

Melanopsins are photopigments that belong to the G protein-coupled receptor family and are responsible for triggering several physiological responses of organisms to light, such as the pupillary light reflex, melatonin suppression, and regulation of the circadian rhythm in mammals. In this group, melanopsins are located within a subpopulation of intrinsically photosensitive retinal ganglion cells (ipRGC). However, the patterns of melanopsin expression differ among other vertebrate groups, and little is known about the gene expression and location in non-mammalian vertebrates. Owl species from the families Strigidae and Tytonidae are interesting models to investigate the melanopsin expression, based on the diversity of daily activity patterns among species, which includes diurnal, nocturnal, and cathemeral habits.

Aim:

This study aims to investigate the melanopsin genes and their pattern of expression in diurnal and nocturnal owls. To do so, we amplified, detected the expression and sequenced the melanopsin genes, OPN4x and OPN4m, from retinas of the nocturnal species *Megascops choliba* and *Asio clamator*, and the diurnal/crepuscular *Glaucidium brasilianum*. We used immunohistochemistry to localize the melanopsins in retinas of the diurnal *Athene cunicularia* and the nocturnal *Tyto alba*.

Methods:

Specimens were collected, euthanized, and the eyes were enucleated. For genetic analysis, one eye of each species was preserved in

FeSBE Annual Meeting 2019

Poster Sessions and Abstracts

RNA later® (Ambion) at 4°C. RNA extraction and cDNA synthesis were performed. Partial sequences of melanopsin genes expressed in the retina were amplified by polymerase chain reactions (PCR) using primers based on melanopsin sequences of *Gallus gallus* and *Tyto alba*. PCR products were purified and directly sequenced. Sequences were analyzed with BioEdit v7.2.5 and aligned with melanopsin sequences from other birds. Quantitative Real time PCR (qPCR) was used to detect the expression of melanopsin genes using primers of *Athene cucularia* sequence. For morphological analysis, eyecups were fixed in 4% paraformaldehyde for 2 hours, and then rinsed in 0.1M phosphate buffer at 4°C. The eyes were cryosectioned and slices were incubated with antibody raised in rabbit against *Gallus gallus* OPN4x1. This study was approved by the Ethics Committees of the Psychology Institute from University of São Paulo (5691140818) and Federal University of Minas Gerais (39/2011).

Results:

Partial melanopsin gene coding sequences (~600 bp), OPN4x and OPN4m, of *M. choliba*, *A. clamator*, and *G. brasiliense* were amplified and sequenced. Sequences were aligned with melanopsin genes from other birds using the Basic Local Alignment Search Tool, BLAST. The identity of OPN4x was 84%-95%, and of OPN4m was between 74%-96%, when compared with other bird species. Morphological analysis showed that the melanopsin OPN4x is located in the inner nuclear and ganglion cell layers of *Athene cucularia* and *Tyto alba* retinas.

Conclusion:

Our results indicate that both melanopsin genes, OPN4x and OPN4m, are expressed in retinas of owls. The successful identification of melanopsin in the different retinal layers opens up the possibility for future examination of the different functions that this protein may display in physiological responses of the organisms. Future investigations will focus on understanding melanopsin gene expression patterns in owls.

Financial support:

FAPESP (2014/26818-2) and CAPES (88882.333310/2019-1).

24.009 - THE INFLUENCE OF VISUAL FUNCTIONS ON SCHOOL PERFORMANCE OF CHILDREN. Silva FMC, Sousa MDR, Oliveira MC, Cortes MIT, Souza GS, Lacerda EMCB, - Laboratório de Neurociência e comportamento - Ceuma Centro de Ciências da Saúde - UFMA Centro de Ciências da Saúde - UNIFAP Núcleo de Medicina Tropical - UFPA

Introduction:

The state of Maranhão still has low Human Development Index (HDI), and low Basic Education Development Index (IDBE). Therefore, the search for mechanisms that contribute to the development of the region remains fundamental. We know that visual disturbances during the school year may hinder strategies for memorizing and acquiring information, compromising the performance of children. The lack of knowledge about visual health can confuse diagnoses of needs presented by students, being relevant to the implementation of public policies in the area of health and education.

Aim:

To evaluate the vision of school - age children and to correlate with school performance in the city of São Luís, Maranhão state.

Methods:

The work was approved by the CEP / CEUMA (protocol CAAE 68908517.1.0000.5084), and consists of an observational epidemiological cross-sectional analytical study. A total of 315 (630 eyes) were tested, 261 were included in the inclusion criteria, 54 were excluded by exclusion criteria in schools and 8 years of high school in São Luís - MA (northeastern Brazil) attending 40 years of schooling fundamental to the 10 high school, the age of children from 9 to 17 years. The testes were completed monocularly in both eyes. To obtain an assessment of visual acuity the FRACT (program FrACT3.9.9a.exe.zip) was used. The color vision using the Ishihara pseudo-isochromatic and the Lanthony D15 hue desaturation test. The analysis of the school

performance of the evaluations was used as one of the two most important in the discipline of Portuguese, mathematics, arts, sciences, history, geography and foreign language. Statistics: Pearson's linear correlation considering $\alpha = 0.05$.

Results:

The higher the visual acuity, the higher the children's score in all the disciplines evaluated ($p < 0.0001$, the r values were between 0.2525 and 0.3749). The lower the number of errors in the Ishihara the higher the children's score in all subjects studied ($p < 0.0001$, the r values were between -0.2291 and -0.0213). Except in Portuguese ($p > 0.05$). There was no correlation between the ICC of the Lanthony D15d test and the grades of the school report cards ($p > 0.05$).

Conclusion:

We observed that visual acuity influences visual performance, therefore public health attention is needed regarding the causes of possible reasons for altering the visual acuity of children.

Financial support:

Universal FAPEMA 31/2016 # 01086/2017. Scholarship in the Institutional Program of Scientific Initiation of the University CEUMA 2018.

24.010 - ALPHA-LIKE GANGLION CELLS IN THE RETINAS OF CUTIA (*DASYPROCTA AGUTI*) AND PACA (*CUNICULUS PACA*). Sampaio GSA, Souza GS, Yamada ES, - Núcleo de Medicina Tropical - UFPA Instituto de Ciências Biológicas - UFPA

Introduction:

Alpha ganglion cells comprise an important subtype of ganglion cells that are involved in motion detection. They have been described in several species such as cat (*Proc R Soc Lond B Biol Sci.* 212;157, 1981), dog and wolf (*J Comp Neurol*, 324; 590, 1992), giraffe (*J Comp Neurol*, 521; 2042, 2013) and potto (*Perodicticus potto*) (*Brain Behav Evol*, 87;4, 2016). Alpha-like ganglion cells are present in the retinas of both cutia (*Dasyprocta aguti*) and paca (*Cuniculus paca*), which are large south american rodents belonging to the *Hystrichomorpha* suborder. Cutia is diurnal while paca is nocturnal (*Vision Res.* 22; 1371, 1982; *Braz J Med Biol Res.* 22; 121, 1989; *Neuroscience.* 44; 325, 1991).

Aim:

Compare retinal alpha-like ganglion cell density and topography in *Cuniculus paca* and *Dasyprocta aguti*.

Methods:

Stained retinas from *Cuniculus paca* and *Dasyprocta aguti* were obtained from an existing collection from the Tropical Medicine Nucleus, which were obtained in the 80's, according to the legislation in force. We used three retinas of each species, stained by the Nissl method using cresyl violet. Alpha-like ganglion cells, classified according to shape, size and staining, were counted under an optic microscopy to obtain density of cells per area. The analysis of alpha-like ganglion cell topography and cell body size was performed using Axion Scope Zeiss.

Results:

Total alpha-like ganglion cell density in *Dasyprocta aguti* retina was $23,7 \pm 3,8$ per mm^2 and in *Cuniculus paca* was $7,2 \pm 0,35$ cells/ mm^2 showing that cutia presents a higher density of these neurons. Alpha-like ganglion cell density in dorsal retina of cutia present $15,67$ cells/ mm^2 and paca $2,53$ cells/ mm^2 , cutia ventral retina 11 cells/ mm^2 and paca $3,86$ cells/ mm^2 , cutia visual streak $27,67$ cells/ mm^2 and paca $8,82$ cells/ mm^2 ($P \leq 0,01$, ANOVA). Cell body size in the dorsal region was $360 \pm 50 \mu\text{m}^2$ in cutia, similar to that obtained to paca ($360 \pm 65 \mu\text{m}^2$). In ventral region we find difference between diurnal ($347 \pm 74 \mu\text{m}^2$) and nocturnal species ($695 \pm 110 \mu\text{m}^2$) analyze soma size ($P \leq 0,01$, T test). Temporal region show difference for *D. aguti* ($1600 \pm 226 \mu\text{m}^2$) and *C. paca* ($551 \pm 84 \mu\text{m}^2$) ($P \leq 0,05$, T test).

Conclusion:

The topography and density retina are influenced by the environmental and habits of animals.

Financial support:

CAPES; FAPESPA; UFPA.

FeSBE Annual Meeting 2019

Poster Sessions and Abstracts

24.011 - LIGHT ADAPTATION OF THE PSEUDO-RANDOM ELECTROGRAM.
Brasil A, Assis JB, Loureiro TMG, Souza GS, - Núcleo de Medicina Tropical - UFPA

Introduction:

Light adaptation is a set of mechanisms that occur in the visual system when exposed to light after a dark adaptation period. Studies have shown that full field electroretinogram (ffERG) amplitude increases as a function of the light adaptation time with or without variation in the latency. Since there is evidence that first and second order nuclei (kernels) are generated by different retinal circuits they could present specificities during adaptation then we used pseudo-random sequences to modulate full-field flashes to induce correlated retinal responses (kernels) with different temporal stimulus interactions.

Aim:

Therefore, the aim of the present study was to investigate the magnitude and time course of pseudo-random ffERG variation during light adaptation.

Methods:

Ten healthy subjects, from 19 to 52 years old ($26 \pm 10,11$ years) underwent 20 minutes of dark adaptation and then the ffERG was activated by pseudo-random flash sequences ($3 \text{ cd} / \text{m}^2$) - sequences-m (210-1 elements) controlled by Veris Science software and presented by a Ganzfeld dome. One state of the m-sequence showed the flash, while the other element showed the constant field of light adaptation ($30 \text{ cd}/\text{m}^2$). The base period of the m-sequence was 50 ms. Each stimulation sequence lasting 40 s was repeated at 0, 5, 10, 15 and 20 minutes of light adaptation. Relative amplitude and latency (corrected by values found at 0 min) of the 3 components (N1, P1, N2) of first- (K1) and second-order (K2) kernel at 5 time points were evaluated. An exponential model was fitted to the mean amplitude and latency data as a function of the light adaptation time in order to estimate the time course (τ) of the light adaptation for each component. All procedures applied in the present study are in accordance with the Helsinki principles and were approved by the Human Research Ethics Committee of the Tropical Medicine Center- Federal University of Pará, Brazil (nº 007/2011). Repeated measures ANOVA followed by Tukey post-test was applied to the amplitude and latency data, considering significant values of $p < 0.05$.

Results:

Regarding amplitude, both N1 K1 and N1 K2 presented amplitude increased between 0 min and 5 min (1.33 ± 0.17 ; 1.35 ± 0.04 , respectively), $p < 0.05$. For P1 K1 there was difference between time 0 min and the other time points (5min = 2.16 ± 0.64 ; 10min = 2.14 ± 0.56 ; 15min = 2.13 ± 0.78 ; 20min = 2.28 ± 0.84) as well as in N2 K1 (5min = 1.81 ± 0.39 ; 10min = 1.82 ± 0.32 ; 15min = 1.79 ± 0.48 ; 20min = 1.97 ± 0.54), $p < 0.05$. While P1 K2 and N2 K2 showed no significant variation along light adaptation as well as latency data for all the components ($p > 0.05$). The amplitude variation obtained from the function was 0.30 for N1 K1, 1.18 for P1 K1, 0.86 for N2 K1, 0.33 for N1 K2. The τ for those components were respectively: 0.23, 1.26, 1.82, 0.23 min.

Conclusion:

Pseudo-random ffERGs showed different mechanisms of adaptation to retinal light. Two possible short- (N1 K1 and N1 K2) and medium-term (P1 K1 and N2 K1) light adaptation mechanisms. Different cellular origins may explain the different light adaptation courses of pseudo-random ERG components.

Financial support:

CNPq 31748/2016-0

24.012 - GENETIC ANALYSIS OF THE VISUAL PIGMENTS OF THE ELAPIDAE SNAKES, MICRURUS CORALLINUS AND M. LEMNISCATUS.
Tashiro JH, Hauzman E, Ventura DV, - Departamento de Psicologia Experimental - USP

Introduction:

The outer retina of vertebrates is formed by rod and cone photoreceptors, which are photosensitive neurons. They contain the visual photopigments formed by a membrane protein, the opsin or rhodopsin, and a chromophore, the retinal. The amino acid composition at spectral tuning sites of the opsins is responsible for the location of the photopigment spectral sensitivity peak (λ_{max}). The group of snakes is highly diversified and their visual system has a number of adaptations to the species ecology and habitat. Previous studies revealed that daily activity pattern has influenced the retinal morphology, the evolution of the opsin genes and the spectral tuning of the opsins of diurnal and nocturnal snakes. The snakes from the Elapidae family, *Micrurus corallinus* and *M. lemniscatus*, are fossorial and semi-aquatic, respectively. Due to their fossorial and secretive behavior, snakes from the *Micrurus* genus are rarely found and little is known about the daily activity pattern and specific behaviors of the species. Genetic studies of the opsin genes and information on the opsins spectral tuning can improve our knowledge of the species behavior and ecological adaptations.

Aim:

To investigate the expression of the opsin genes LWS, RH1, and SWS1 in retinas of the coral snakes *M. corallinus* and *M. lemniscatus*, and to estimate the λ_{max} of the opsins based on the amino acid sequences.

Methods:

This project was approved by the Animal Ethics Committee of the Psychology Institute, University of São Paulo (CEUA-IPUSP nº 1805090417). One individual of each species was obtained at the Butantan Institute and euthanized with a lethal dose of the anesthetic Thionembutal (sodium thiobarbiturate, 100 mg/kg) associated with lidocaine (10 mg/kg). The retinas were preserved in RNA later® (Ambion) at 4°C. Total RNA was extracted and mRNA was converted to cDNA. The opsin genes LWS, SWS1, and RH1, were amplified by polymerase chain reactions (PCR) using specific primers for snake opsins. The PCR products were visualized by agarose gel electrophoresis, purified and directly sequenced, and sequences were analyzed with BioEdit v.7.2.

Results:

We amplified and sequenced the three opsin genes LWS, RH1, and SWS1 expressed in retinas of *M. corallinus* and *M. lemniscatus*. The estimated λ_{max} of the LWS opsin was $\sim 560 \text{ nm}$ for *M. lemniscatus* and $\sim 554 \text{ nm}$ for *M. corallinus* due to the substitution S164A. In both species, the presence of the residue F86 in the SWS1 opsin may generate sensitivity at the UV band, with λ_{max} at $\sim 360 \text{ nm}$. For the rhodopsin photopigment RH1, the substitution D83N found in both species may generate a λ_{max} at $\sim 494 \text{ nm}$.

Conclusion:

The variation of the estimated λ_{max} of the LWS opsin may be related to differences in the activity pattern and habitat occupied by each species. These differences may be more significant in mesopic periods. The spectral sensitivity at the UV range of the SWS1 photopigment may contribute to hunting strategies in low light conditions. The 6 nm blue shift of the rhodopsin λ_{max} was previously observed in other crepuscular and fossorial snakes.

Financial support:

2014/26818-2; 2014/25743-9; 2018/13910-9

25 - Education, Science History and Philosophy, Science Communication

25.006 - THE CORE CURRICULUM OF HUMAN EMBRYOLOGY SET BY A MULTIDISCIPLINARY DELPHI PANEL. Costa CFP, Pereira LAVD, - Departamento de Bioquímica e Biologia Tecidual - Unicamp

Introduction:

A modified Delphi method was employed to decide what should be the minimum knowledge base required for human embryology, in a democratic and research-based process.

FeSBE Annual Meeting 2019

Poster Sessions and Abstracts

Aim:

The aim of this investigation was to obtain consensus opinion on essential core curriculum topics of Human Embryology to medical undergraduate course.

Methods:

Ethical approval for this study was granted by the Research Ethics Committee at University of Campinas (Reference Nº CAAE 59382016.0.0000.5404). A two-round of modified Delphi method with seven phases was used to identify essential topics: (1) initial questionnaire developing from the research team, with topic selection and shrinking, (2) validation of the questionnaire by a pilot panel; (3) first round, where participants were asked to rate the relevance of each topic in a Likert scale and demographic data was collected; (4) consensus analysis and identification of demographic information; (5) second round, the participants the panel was asked to accept or reject the most relevant topics from the previous round, (6) consensus analysis and concluding screening process from the research team, (7) Multivariate clustering analysis and descriptive categorization analysis were carried.

Results:

(1) Three embryology textbooks were screened for topic selection. A set of 1577 raw items were identified. Synonymous or similar topics were unified, resulting in 679 topics. (2) Mean response time to questionnaire was 53 minutes. (3) Invitations were sent to 109 experts from eight institutions, and a total of 57 individuals participated in the first round (52.3%). Six of the participants left entire sections unanswered and their responses were excluded from the analysis. (4) The expert panel (n=51) was comprised by 49% women and 51% men, and their age ranged from 29 to 70 years old. The most frequent age group were both 55-59 years (20%) and 40-44 (20%). Within the panel, 78% were medical doctors, 14% biologists, 6% biomedical scientists and one was a nurse (2%). Following consensus analysis, out of a total of 679 topics in human embryology, 10% were considered essential (n=69), 32% important (n=215), 44% acceptable (n=300) and 12% not required (n=79). (5) 69 selected topics for round two are classified accordingly to the acceptance rate. Five topics reached an acceptance rate equal or inferior than 80% and were rejected. (6) The core recommended for Human Embryology topic selected by the Delphi panel, following the consensus analysis was comprised by 64 items. (7) The Delphi method was supported by validity evidence. None of the six demographic characteristics (gender, age group, degree, year of graduation, medical specialty, and year of the last specialization of respondents) could be significantly associated with the two clusters that were produced following the multivariate clustering analysis. However, the core list of medical doctors would have 64 topics while the non-medical doctors would have 204. The agreement between those two groups - kappa coefficient (0.0535) - was significantly low ($p < 0.0001$).

Conclusion:

This study can be a valuable tool for decision-making in what should be the embryology curriculum for undergraduate medical or other health courses, especially in Brazilian and other Latin American institutions.

Financial support:

Capes

25.007 - THE PEER-INSTRUCTION METHOD IS TIME-CONSUMING, BUT PROMOTES LEARNING IN PHYSIOLOGY CLASSES FOR LOW-INCOME STUDENTS. Sá VA, Cunha AV, Lellis-Santos C, - Ciências Biológicas - Unifesp

Introduction:

Active learning methodologies benefit underrepresented minority (URM) students to overcome the unsatisfactory academic performance in physiology education, but it is unknown why those methodologies are not common in K-12 education in Brazil.

Aim:

We evaluated the viability of implementing the peer-instruction (PI) method assisted by the Socrative application during science classes in a low-income school.

Methods:

This study was performed based on the action-research method. We applied the PI method during lectures of the animal locomotion unit to students of Padre Aldo da Tofoi Elementary School, which is located in the suburbs of São Paulo city (CAAE 12630219.0.0000.5505). The PI method was performed at the computer lab, and consisted of short content lecturing, presentation of the conceptual multiple-choice question, individual voting assisted Socrative, peer discussion, individual voting for the same question, resolution of the question by the instructor and presentation of the performance of the students in the voting phases. The school is located in an area with social vulnerability, and students present low-income background. We applied the mixed-method of educational research to analyze the characteristics of the students, their performance and the facilities of the school.

Results:

Approximately 80% of the students have smartphone, but only 55% of students are allowed to bring it to school. And the majority do not have internet service access. The implementation of the PI by the teacher was counterproductive because of insufficient infrastructure, absence or instability of the internet connection, and reduced number of computers. Otherwise, the receptivity and engagement of the students was high. Despite the adversities, students significantly improved their performance by 25% of correct answers (pre 56.7 ± 6.4 vs post 81.7 ± 4.5 , $p < 0.05$, $N=4$). Average time to complete the PI method for one question was 45 min.

Conclusion:

Although the students have highly appreciated the method, its application is time-consuming and requires adequate facilities. The PI method has a great potential to promote engagement and learning in low-income schools.

Financial support:

Self-funded

25.008 - LUDIC MODEL OF ATHEROSCLEROSIS FOR SCIENCE COMMUNICATION TO CHILDREN AND ADULT POPULATION. Teixeira AP, Santos SM, Torres VM, Ribeiro BR, Ribeiro LP, Fernandes-Santos C, - Ciências Básicas - UFF

Introduction:

Research communication is necessary to create a scientific culture since it contributes to building critical and reflexive thinking by the population. However, a significant distance exists between researchers and the population, that is attributed to the difficulty of communicating complex concepts in a simple and didactic manner. It restricts the knowledge to a few people, resulting in an uninformed population, especially regarding primary health care and prevention of disease onset. Diabetes mellitus is a condition that affects millions of people that is associated with the development of atherosclerosis, with high risk for cardiovascular events. Thus, it is essential to create strategies for science communication and popularization about daily events to improve the quality of life.

Aim:

To elaborate a ludic model to illustrate the process of atherosclerosis and the obstruction of blood vessels.

Methods:

To make the model it was used recycled material, of easy access and low cost (e.g., PET bottle, beads, and amoeba (gelatinous mass)) to represent the artery, red blood cells, and the fat plaque on its several stages from fat streaks to a large plaque obstructing the vessel lumen. Some informative sheets showing reference values for serum levels of blood lipids and the steps of fat plaque development were also exposed. The model was showed during the National Week of Science

FeSBE Annual Meeting 2019

Poster Sessions and Abstracts

and Technology (Semana Nacional de C&T) of 2018 of Nova Friburgo/RJ, at schools and public places.

Results:

The primary audience in public spaces were adults and the elderly ranging from 40-70 years. At schools, they were children and teenagers from 8-15 years. The audience could interact with the model, and it looked like a long and transparent pipe, with both extremities closed, and the public could see inside. Within it, the fat plaque development was represented, and as the person turned the model extremity upside down the red blood cells could run along with it, getting stuck at the extremity where the fat plaque was larger. In general, both adults and children were able to understand the concept of what is the fat plaque and why it could stop blood from running inside the vessel. Children were mostly attracted by the possibility to touch and interact with the model. Regarding the adults and the elderly, they reported family cases of stroke or heart attack, and that with the model, they could now understand what is going on during the atherosclerotic disease.

Conclusion:

The use of a ludic model of atherosclerosis for science communication to the population of Nova Friburgo/RJ has proven to be an effective strategy to the understanding of a complex concept such as vessel obstruction, blood clot, stroke, and heart attack. Science communication serves as a social empowerment tool regarding people's attitudes towards personal and family health care, and more initiatives for exchanging knowledge between researchers and the population must be stimulated.

Financial support:

None

25.009 - CONSCIÊNCIA NA CIÊNCIA: FIVE YEARS OF VACATION COURSE TO HIGH SCHOOL STUDENTS IN NOVA FRIBURGO/RJ. Torres VM, Farsura AF, Emerick AS, Carvalho CVAL, Amaral LF, Duarte LS, Stumbo MB, Marqui MB, Rufino MB, Barreira RM, Silva RPM, Moraes TM, Santos CF, - Departamento de Ciências Básicas - UFF Departamento de Ciências Básicas - UNESA

Introduction:

The vacation courses are offered in July to high school students by the Federal Fluminense University (UFF) in the Nova Friburgo/RJ campus since 2014. It is a strategy of science communication that allows students of having the opportunity to know the academic environment and to get in touch with scientific knowledge, as well as to meet the professors and undergraduate students. Another goal is to help them to choose their future career. Course's content is related to health science, e.g., neuroscience, nutrition, anatomy, cell biology, and microbiology.

Aim:

To analyze the public interest in the vacation courses along five years of existence.

Methods:

It was analyzed the data between 2014-2018 such as the courses offered, website access, course registration and divulgation, and the reports from students that helped to organize the courses as tutors. Website access (<http://conscienciencia.wixsite.com/punf>) was evaluated by the visitor counting tool Web-Stat, and the registration form reports (jotform.com).

Results:

The number of courses, collaborator professors and students registered increases every year. The project began with 3 courses, 7 professors and 90 vacancies, and it turned to 7 courses, 10 professors and 158 vacancies in 2018. The website received more than 9,800 visits from June 2014 to June 2018, and the peak of visits occurred during the registration period. Traffic origin was from visitors that already know the website address, from google search engine, or from visitors that were redirected from institutional websites from UFF. Compared to 2014, visits increased by 20% in 2015, reaching +175% in 2018.

Registration form visualization increases every year (614 in 2015; 1,393 in 2018), although only 20 to 30% is converted in an actual registration. The world heat map from the last 1,000 visits shows that most visitors are from the RJ state (mountain, metropolitan, and lake regions). Although most registrations received are of students living in Nova Friburgo and nearby districts and small cities, it is common to receive e-mails from people interested in the vacation courses that reside outside the mountain regions of RJ state (and also from undergraduate students), which agrees with the website world heat map. The project has gained visibility in the local press, and it likely helped to increase the number of visits to the website. Teachers from primary education have been helped to divulge the courses to their students. Commonly, students attend for 2-3 years to one among the offered courses, showing their great interest in them. Some of them are currently undergraduate students at UFF campus Nova Friburgo and help with course preparation as tutors and logistics.

Conclusion:

The project has gained high visibility over the past years, especially in Nova Friburgo, and the website visits and the number of registrations show great interest by the population. Despite the lack of funding, the project has managed to maintain a constant number of vacancies due to the voluntary collaboration of UFF professors and tutors.

Financial support:

None

25.010 - CONTRIBUTIONS OF THE TRAVELING SCIENCE CENTER SCIENCE UNDER TENTS TO NEUROSCIENCES DISSEMINATION.. Marcena IR, Alves GH, Santos RF, Rodrigues MCS, Frigel-Madeira L, - Neurobiologia - UFF Pós-graduação em Ciências e Biotecnologia - UFF Pós-Graduação em Ensino em Biotecnologia e Saúde - Fiocruz

Introduction:

The study of Nervous System has been growing and gaining prominence since the 90's, known as the "Brain decade". Therefore, it is necessary that findings obtained from these surveys be disseminated to the population. In addition to school environments, non-formal educational spaces, such as museums or science centers, are conducive to generation and transmission of knowledge to the general people. The Science Under Tents (CST) is a traveling science center, composed of playful and interactive activities based on four thematic axes (Nature, Humanities, Technology and Health), which holds scientific exhibitions in the state of Rio de Janeiro.

Aim:

Thus, considering the relevance of neurosciences and the importance of disseminating such knowledge, this study aimed to analyze the presence of neuroscience themes in CST activities.

Methods:

We analyzed 16 distinct activities occurred during exposures of CST in the first semester of 2019: (A) Anatomy, (B) Arthropods, (C) Braille, (D) Knowing your Cells, (E) Electroconductivity, (F) 3D Printer, (G) LIBRAS, (H) Microplastic, (I) Microscopy, (J) Robotic with Ozobot, (K) Sprouting Seed Paper, (L) Painting the Body, (M) Ramp, (N) Augmented Reality, (O) Virtual Reality, (P) Tangram. For accomplishment of this study, participant observation methodology was used, since the researcher also acted as mediator of the activities. The analysis sought to identify themes and aspects related to three areas of neuroscience: neuroanatomy, neurophysiology and neurohistology.

Results:

Of the analyzed activities, only five (A, I, L, N and O) addressed themes directly related to neuroscience. Of these, I and O discussed issues related to neurohistology; A and N addressed neuroanatomy; L and O discussed notions of neurophysiology. However, considering that all CST activities have mediators who talk with public about contents presented in the activities, it is possible that neuroscience themes can be discussed through adaptations in speech during mediation. Thus, we realize that we can work on concepts of neuroanatomy in activities B,

FeSBE Annual Meeting 2019 Poster Sessions and Abstracts

with debates about arthropod anatomy; in F, with presentation of anatomical models of different animals printed in 3D; and in G, addressing brain areas involved with language. Regarding neurophysiology, one can work on tactile perception in C; issues relating to the conduction of nerve stimulation in E; and mathematical logic and spatial perception in J and P. As far as Neurohistology is concerned, activity D can be explored through the conception of eukaryotic cells and can address neuronal aspects. However, activities H, K and M did not present an opportunity to address neuroscience-related topics requiring a more interdisciplinary reflection with experts from different areas of knowledge.

Conclusion:

Thus, it can be considered that CST has more than 30% of its exposure with activities directly related to neuroscience topics and has great potential to have about 80% of its exposure addressing this theme. Therefore, we believe that CST has contributed to the popularization of neurosciences in a significant way.

Financial support:

CNPq, CAPES, FAPERJ, PROEX-UFF

FeSBE Annual Meeting 2019
Poster Sessions and Abstracts

Poster Session III - Sept.12.2019 - 16:00 - 18:00 h

3 - Laboratory Animal Science.....	006 - 010
4 - Cardiovascular Biology and Diseases	020 - 029
6 - Endocrine System	012 - 017
7 - Nutrition and Metabolism.....	035- 051
8 - Renal Biology and Diseases	013 - 018
9 - Respiratory Biology and Diseases.....	010 - 013
10 - Neurobiology	029 - 042
11 - Physical Training Responses.....	015 - 020
13 - Cell differentiation, growth and death	019 - 027
14 - Nuclear Biosciences for Health.....	001 - 007
16 - Gene and Cell Therapy, Omics Biology	010 - 013
17 - Basic & Clinical Pharmacology.....	010 - 013
18 - Neuropsychopharmacology	011 - 014
19 - Toxicology.....	019 - 027
20 - Pain and Inflammation	016 - 022
21 - Immunology.....	005 - 009
22 - Cancer Signaling and Therapeutics	027 - 039
24 - Vision and Ophthalmology	013 - 018
25 - Education, Science History and Philosophy, Science Communication.....	011 - 014
26- FeSBE Jovem	001 - 034

FeSBE Annual Meeting 2019

Poster Sessions and Abstracts

3 - Laboratory Animal Science

03.006 - DEVELOPMENT AND TESTING OF A MECHANIZED APPARATUS FOR RODENT MODELS OF CHRONIC SLEEP DEPRIVATION. Tonon AC, Rossi AC, Sanches PRS, Cioato MJG, Garcez TNA, Campagnol D, Souza DOG, Hidalgo MPL, - Programa de Pós-Graduação em Psiquiatria e Ciências do Comportamento - UFRGS Laboratório de Cronobiologia e Sono - HCPA Laboratório de Engenharia Biomédica - HCPA Unidade de Experimentação Animal - HCPA Departamento de Bioquímica - UFRGS

Introduction:

The animal models currently used for sleep deprivation have important methodological limitations, especially for the research using long/chronic exposure. It is known that sleep deprivation itself represents a psychological stress. Nevertheless, some of the experimental models stand above average. That is the case of forced constant activity using rotating drums and the platform-over-water (flowerpot) methods. In addition, an important complicating factor of the available protocols is the need to have a researcher monitoring the animals because of the nature of the arousal stimulus use, i.e. potentially fatal outcomes or the need for direct gentle stimulation.

Aim:

The aim of this work was to develop a new mechanical equipment to be used for chronic sleep deprivation in rodent models.

Methods:

The system consists of a microcontroller that executes the control of 2 step motors responsible for the movement of two L-shaped rods inside a rectangular rat cage. These metal rods rotate at a programmable speed. Their tracks form two adjacent circumferences that cover almost the entire animal housing. Five adult male Wistar rats (90 days of age) were used for testing. Paired in two, animals were tested at intervals of 2 hours every 2 days for 2 weeks during the resting period (between the 6th and the 8th hour of the light phase). Different animals were paired at each testing. The rods rotated once every two minutes. The efficacy of the equipment was determined by 1) need for animal's evasion of the rods, with a resting time no greater than two minute and 2) uninterrupted operation of the equipment for 2 hours at 4 different times, without any modifications or adjustments to the equipment. Testing sessions were directly observed but also filmed and analyzed afterwards.

Results:

All animals stayed active in their resting period during the time of the experiments. The longer recorded period of resting was of 2 minutes (the time of an entire rod turn). Throughout the observations all animals were still able to feed themselves and drink water, as well as interact with each other. No animals were harmed or deadily trapped by the rods during the experiments.

Conclusion:

The development of this equipment permits an efficient and safe experiment for longer periods of sleep restriction or sleep deprivation without a need for constant watch. Since the rods' functionality is programmable, this apparatus can be activated at any time of the day for any desired period. Hence, this work has promising applicability for future animal and translational studies that aim to design experiments simulating "real-life" sleep deprivation protocols.

Financial support:

FIPE-HCPA, CNPq, CAPES

03.007 - INFLUENCE OF THE AQUEOUS EXTRACT OF NEEM (AZADIRACHTA INDICA) ON THE FERTILITY OF MALE WISTAR RATS.. Martins DS, Gaspi FOG, Cardoso CA, - Departamento de Medicina Veterinária - FZEA/USP Farmácia - FHO

Introduction:

Neem is a plant native to India belonging to the family Meliaceae, popularly known as Nim or Neem and has been used for centuries in the East as: medicinal plant (in the treatment of inflammation, viral

infections, hypertension and fever), shading plant, repellent, building material, fuel, lubricant, fertilizer and more recently as natural pesticide. Even though the use of bio-insecticides is still underpinned by organic food production, there is still a need for more research on each formulation, especially its action on organisms.

Aim:

The objective of research was to study the contraceptive capacity of the aqueous extract of Neem, adapted in Brazil, in the same concentrations and time used in the farming corn as bioinsecticide under the reproduction of male Wistar rats.

Methods:

For this study we used 20 Wistar rats divided into 4 groups composed of 5 animals each, being: G1 - 10,000ppm, G2 - 7,500ppm, G3 - 5,000 ppm and G4 - control with distilled water. The volume administered was standardized in 1 ml for each animal and administration was given by gavage for eight days. Statistical analysis of the obtained data were performed using ANOVA followed by Hartley Test and the results of motility and sperm viability were expressed as a percentage. After analyzing the results, it can be considered that the aqueous extract of Neem administered for eight days orally in the doses used presented low toxicity, but revealed contraceptive capacity, since it altered the motility and sperm viability in the highest administered dose.

Results:

At the dose of 10,000 ppm sperm motility was affected by 95%, and viability was 89.2%, while in the lowest dose the motility was affected by 1% and viability by 1.4% and at the dose of 7,500 ppm a motility was affected by 10% and viability by 2%. It was possible in this study to analyze the results of the aqueous extract of the Neem plant, of Indian origin and adapted in Brazil, in face of physiological processes, being able to consider that it has contraceptive capacity in males of reproductive age and low toxicity in the highest concentration versus time of indicated for use in maize crops in the country.

Conclusion:

It is therefore prudent to consider that even without causing toxic effects, exposure to this aqueous extract could cause even momentary contraceptive effects.

Financial support:

CAPES (Coordenação de Aperfeiçoamento de Pessoal de Nível Superior)

03.008 - IMPORTANCE OF ENVIRONMENTAL AND HEALTH MONITORING IN STUDIES WITH ZEBRAFISH. Ventura BH, Kertsz R, Paiva C, Cruz RJ, Garibaldi M, Godoy CMSC, Caetano C, Carvalho LR, - Laboratório de Controle Genético e Sanitário - USP Departamento de Endocrinologia - USP

Introduction:

With exponential growth of Zebrafish use in science, it comes the need to establish criteria that guarantee research quality. Zebrafish environmental control encompasses factors that can alter water quality leading to a decrease in animal weight and size and high mortality. Health monitoring is important to detect pathogens that may interfere with the experimental results. The protozoan *Pseudoloma neurophilia* (PN) is lodged in the brain and spinal cord causing behavioral disorders, weight loss and scoliosis. Lack of environmental and health control can directly affect behavioral and phenotypic studies. Since we created nr2e1 knock down through CRISPR Cas genomic edition in zebrafish, we had to make sure there was no environmental influence in the animal behavior. Fierce behavior was already described in mice and drosophila mutant, but in order to characterize its whole in zebrafish behavior and pituitary development, once mutant mice was associated to short body size, we had to rule out environmental influence before doing pituitary characterization.

Aim:

Standardize and monitor an ideal environment for animals. Research the main pathogens. Establish an optimal environmental and health criterion for working with mutant animals.

FeSBE Annual Meeting 2019

Poster Sessions and Abstracts

Methods:

We analyzed and standardize pH, Temperature, conductivity and Ammonia. The main pathogens affecting zebrafish, were investigated through PCR, culture, microscopy and histology. Fertility rate was calculated by the number of the fertilized eggs per female and the dead embryos was counted to provide the mortality ratio.

Results:

In periods where there were variations in environmental controls, the mortality was up to 100% of larval stage of mutant animals. With the strict control of analyzed parameters the mortality did not exceed 10% in healthy animals. By screening the pathogens we establish the sanitary status of our colony that presented PN in the majority of mutant animals. With the standardization of the environmental control, we obtained an increase in the fertility rate and survival of our animals. We have established unacceptable interferers to work with mutant animals, which guarantees us quality research with reliable results.

Conclusion:

Satisfactory and reproducible result in Zebrafish studies must have well-established and routine environmental and health monitoring of animals facilitating harmonization in the results of the surveys and the exchange of animals between institutions.

Financial support:

Biotério Central FMUSP e FAPESP

03.009 - RESEARCHERS AND THE 3R'S: FROM CONCEPT TO APPLICATION. Farah R, - CCBS - UPM

Introduction:

William M.S Russell and Rex L. Burch established an important contribution to practice in animal experimentation: the concept of the 3 R's (replace, refine and reduce), which innovates science, improving animal welfare. Such innovation is used globally and applied in order to guarantee a more humanized Science. In Brazil, Law Arouca (law nº 11.794/08) is the concretization the 3 R's principles. The hypothesis of this project is to demonstrate how the 3 R's improved the welfare of experimental animals.

Aim:

Thereby, the goal is to evaluate both high and low points identified by graduate students that apply such concept.

Methods:

After the ethical committee approval nº 3.164.509, a survey was applied, in which master's degree, PhD and Post-Doc of the health, biological and agrarian science areas students that use animals in their studies were asked to respond. Age, sex and public or private institution weren't considered on the survey. A total of 74 volunteers answered questions regarding their experience with animals, the 3 R's, animal welfare and animal pain. The method was applied through a survey answered by Google Doc Form, with transversal descriptive character. The answers were showed in percentage and analyzed by Microsoft Office Excel 2010.

Results:

The results show that volunteers have considerable experience with animals because 60.8% of them are PhD and Pos-Doc students and 51.4% have more than 5 years of experience with laboratory animals. About animal welfare, the data suggests that the researchers are sensible to animal suffering because almost 80% of them have concerned about animal welfare since before their post-graduation. Nonetheless, some probably don't understand what animal suffering is, because 16.2% don't believe that animals can suffer and other 16.2% answered that animals can suffer only physically or emotionally. Regarding the concept of 3 R's, 30% of the volunteers understand partially or don't know how to apply it and 2.7% don't understand the concept of 3 R's. Also, 15% of the volunteers hasn't received training about animal welfare. Based on the data obtained, we understand that 42.1% of the volunteers apply partially the 3 R's on their project. About the 3 R's application, fortunately 97.3% understand that refinement is

the way to reduce discomfort from noninvasive procedures, but they probably have difficulty understanding pain scale and/or how to control the pain, because only 29.8% use the association of analgesic opioids and anti-inflammatories. 41.2% of the volunteers classified their experiments as moderate pain, 19% as intense pain and 1.7% didn't know how to classify it. Finally, 9.5% responded they don't know about alternative methods for their research line, although researchers show interest in improving alternative methods, since 67.6% have interest in such improvement in their research line.

Conclusion:

This project intends to show that researchers are sensible to animal welfare, but there's a considerable gap between 3 R's concept and its application in the field. Therefore, constant training of researchers can help them practice the 3 R's and improve laboratory animal welfare.

Financial support:

None

03.010 - EFFECT OF MATERNAL PSYCHOSOCIAL STRESS ON SWISS MOUSE OFFSPRING BEHAVIOR. Gonçalves AM, Garavelli GY, Botezzelli VS, Junior VAP, Paffaro AMA, - Department of Cellular Biology and Development - UNIFAL-MG

Introduction:

Stress is a biological and psychosocial phenomenon that affects all individuals. In the psychosocial aspect, several daily situations are stress-generating factors. Pregnancy is a period of vulnerability of women, in which physical and physiological changes will occur, leading the body to a naturally stressed state, aggravated by external factors. However, it is unclear in the literature to what extent maternal stress can affect embryo / fetal development, interfering until adulthood.

Aim:

Thus, this study aimed to analyze the behavioral aspects of the offspring of Swiss mice from mothers submitted to two models of psychosocial stress during pregnancy.

Methods:

For this purpose, virgin Swiss mouse females were mated with males of the same strain and observation of the vaginal tampon marked the first day of gestation (dog). From 1 dog, the females were distributed in the three experimental groups: Social Confrontation (SC) in which the pregnant female was allocated in the same box with five more non-pregnant females, changed every three days; Overpopulation (O) in which the pregnant female was housed with ten other non-pregnant females in the same cage and Individual Housing (IH) as they are usually kept in animal testing facilities. Offspring were standardized on day of birth and reduced to 3 males and 3 females and randomly submitted to short and long term memory tests, elevated cross maze, open field, forced swimming, nest-seeking and social interaction. All procedures were approved by the Animal Research Ethics Committee of the Federal University of Alfenas (47/2017). Data analysis was performed using GraphPad Prism 5 software, adopting $p < 0.05$ as statistically significant.

Results:

The offspring of both groups subjected to stress (SC and O) were born with weight reduction in relation to the IH group and in the O group this reduction was maintained until puberty. A sex-specific pattern was observed related to increased anxiety and depressive behavior in young female offspring in the SC and O group. SC stress affected short and long term memory of male pups while O stress showed a milder effect on offspring of both sexes. Regarding the psychosocial behavior tests, it was observed in the Nest-seeking test the latency time of both stressed groups (O: $15.39 \pm 65.29''$; SC: $22.2 \pm 67.44''$) significantly lower compared to the IH ($86.33 \pm 83.10''$). Behavioral changes were also observed in the Socialization test, there was a significant difference between the time spent on the C side of the apparatus, between the SC groups ($3.02 \pm 2.95'$) and IH group ($0.85 \pm 0.26'$).

Conclusion:

FeSBE Annual Meeting 2019

Poster Sessions and Abstracts

Maternal psychosocial stress during pregnancy, in addition to affecting birth weight, causes significant changes in the behavior of young and adult mice in a sex-dependent manner. Female puppies present altered anxiety patterns while males are more likely to have memory loss and socialization difficulty.

Financial support:

Nenhum

4 - Cardiovascular Biology and Diseases

04.020 - SEX DIFFERENCES IN THE ANTICONTRACTILE EFFECT OF PVAT: DO TISSUE AMOUNT AND ANATOMICAL PROXIMITY MATTER?. Victorio JA, Davel AP, - Departamento de Biologia Estrutural e Funcional - UNICAMP

Introduction:

Perivascular adipose tissue (PVAT) is a fat depot that surrounds almost all vessels and exerts an important role in the control of vascular tone, presenting a physiological anticontractile effect. Recent studies have suggested that PVAT morphology and quantity differ between male and female sex, and this may impact the risk to develop cardiovascular diseases in men and women.

Aim:

In the present study we investigated whether or not PVAT anticontractile effect in resistance vessels is influenced by 1) PVAT-vessel attachment, 2) the amount of PVAT, and 3) sex differences.

Methods:

Six-month-old male (n=7) and female (n=10) C57Bl6/J mice (ethical committee protocol # 4914-1/2018) had their mesenteric resistance arteries (~150 µm) dissected and mounted on a wire myograph in three ways: with intact surrounding PVAT; free of surrounding PVAT; or free of surrounding PVAT but incubated with 35 mg PVAT for 1h. Vascular reactivity to acetylcholine and phenylephrine was evaluated. Statistical analysis: Student's t test and one-way ANOVA; *P<0.05.

Results:

Male and female presented the same vasodilatory response to acetylcholine in the absence of PVAT [Maximum effect (Emax): male= 93 ± 2.3% vs. female= 94 ± 1.8%; LogEC50: male= 7.0 ± 0.2 vs. female= 6.9 ± 0.1]. The presence of surrounding or incubated PVAT did not change the relaxation response to this agonist in both males and females. In the absence PVAT, Emax to phenylephrine was higher in females compared to males (Emax: male= 112 ± 2.7% vs. female= 124 ± 3.2%*; LogEC50: male=6.5 ± 0.2 vs. female= 6.8 ± 0.1). Surrounding PVAT exerted anticontractile effect in both male and female, that was significantly pronounced in females as showed by increased values of the difference between the area under the curves (dAUC) in females (male= 26±3.8% vs. female: 50±6.8%*). In contrast to surrounding PVAT, incubation with 35 mg PVAT in clean vessels induced an anticontractile effect only in females.

Conclusion:

While surrounding PVAT exhibited an anticontractile effect in both sexes, the equal amount of incubated PVAT decreased the phenylephrine-induced contraction only in females. Although surrounding PVAT was more efficient to induce anticontractile effect than incubated PVAT, a higher anticontractile action of PVAT in females compared to males were observed using both methods. These findings indicate that there are sex differences in the PVAT modulation of vascular tone, evidencing the protector effect of this tissue in the female sex.

Financial support:

FAPESP grants # 2018/00543-8 and # 2018/16505-8

04.021 - CARDIOVASCULAR RISK FACTORS ASSOCIATION WITH FASTING AND POSTPRANDIAL LIPEMIA IN MEN. Venturino-Perez P, Almeida DPR, Oliveira AT, Ribeiro BR, Perrut DGP, Roque IC, Silva ÍA, Ribeiro LP, Rufino MB, Saez GO, Rocha RC, Pinna RA, Santos SM, Germano FN, Fernandes-Santos C, - DEPARTAMENTO DE CIÊNCIAS BÁSICAS (FCB) - Universidade Federal Fluminense - SUBHO - UNESA (Nova Friburgo, RJ) - UERJ (Nova Friburgo, RJ)

Introduction:

Remnant cholesterol and triacylglycerol (TG)-rich lipoproteins are found in the blood mainly at the postprandial state and contribute to onset of atherosclerosis. Thus, to study the postprandial lipemia (PPL) is of utmost importance to identify and prevent cardiovascular (CV) risk factors and related diseases.

Aim:

To evaluate the relationship between CV risk factors in men with normal and altered PPL.

Methods:

Ethics Committee Approval CAAE 49864015.2.0000.56.26. Fifty-one adult men (21-60yr) were allocated into three groups, by combining fasting and postprandial serum TG obtained by an oral fat tolerance test (OFTT): 1) normal fasting TG and not responsive to OFTT (N/NR); 2) normal fasting TG but responsive to OFTT (N/R) and; 3) altered fasting TG and responsive to TTOG (A/R). Fasting TG was normal when <150 mg/dL and the ideal OFTT response was TG <220 mg/dL. After 8-10h fasting, blood was collected by venipuncture and the OFTT was performed. It consisted in ingesting a high fat meal containing 75g of lipids, 25g of carbohydrates and 10g of proteins. Venous blood was collected again 4h after the high fat meal. Blood pressure (BP), glycemia, lipid profile, insulin resistance (HOMA-IR), ultra-sensitive C-reactive protein (CRP), hepatic enzymes, anthropometric parameters, and atherogenicity indexes were evaluated. Data are presented as mean±S.D. Paired Student's t test, one-way ANOVA with post-hoc test of Dunn's, and Pearson's correlation test were performed (GraphPad Prism v.6.0).

Results:

Mean BP and postprandial glucose were higher in the A/R group compared to N/NR group (BP: A/R = 91.9±8.2 vs. N/NR = 102.1±18.6 mm Hg, P<0.05; glucose: A/R = 121.9±26.1 vs. N/NR = 102.4±20.4 mg/dL, P<0.05). The A/R group had increased non-HDLc compared to N/R group (P<0.05). VLDLc in the A/R group was increased compared to the other groups. Castelli index I (CI-I) was similar between N/NR and N/R groups; however, the A/R group presented CI-I of 5.0±1.2, indicating CV risk (+39% P<0.01, and +36% P<0.05, respectively, vs. N/NR and N/R). The atherogenic index of plasma (AIP) of the N/NR and N/R groups indicated low atherosclerotic risk, and it was elevated only in the A/R group (P<0.0001). The highest atherogenic coefficient (AC) was found in the A/R group when compared to N/NR and N/R groups (+53% P=0.01, and +50% P<0.05, respectively). Body mass index, body weight and waist circumference were similar among groups. HOMA-IR, AC and AIP were correlated with both fasting and postprandial TG.

Conclusion:

Men that are both responsive to the OFTT and have altered fasting TG present insulin resistance and display higher CV and atherogenic risk. However, the ones with normal fasting TG seems to be protected, even with altered OFTT response.

Financial support:

There isn't.

04.022 - "DIFFERENCES BETWEEN MESENTERIC AND PANCREATIC SMALL RESISTANCE ARTERIES REMODELING IN MICE FOLLOWING PROTEIN RESTRICTION". 1POSSEBOM I.R.*, 1GUIZONI, D.M., 1CARNEIRO E.M., 1DAVEL, A.P., 1DEPARTAMENTO DE FUNCIONAL AND MOLECULAR BIOLOGY, IB/UNICAMP.. Davel AP, - Departamento de fisiologia animal - UNICAMP

Introduction:

FeSBE Annual Meeting 2019

Poster Sessions and Abstracts

Protein malnutrition during early life stages is an important risk factor for the development of cardiometabolic diseases such as hypertension and type 2 diabetes in adulthood. Vascular remodeling is a common feature of several cardiovascular diseases. In essential hypertension, peripheral resistance arteries present an increase of wall/lumen ratio. The inward hypertrophic remodeling contributes to increase peripheral vascular resistance and to raise blood pressure. However, whether or not a protein restriction diet in the early stages of development is associated with a remodeling of resistance arteries is still not known.

Aim:

To evaluate the morphology and structural parameters of resistance arteries from the mesenteric and pancreatic vascular beds of mice fed a post-weaning protein-restricted diet.

Methods:

(Ethics Committee Approval # 4533-1) Male C57Bl/6J mice (28 day-old; n= 9-11 animals per group) were fed with a normal- (14% protein, NP) or a low-protein (6% protein, LP) diet for 90 days. Small mesenteric and pancreatic arteries (internal diameter < 300µm) were isolated and frozen (-80°C) in tissue-tek OCT. Transverse 10 µm thick slices were obtained in a cryostat and then stained with hematoxylin and eosin. Images were obtained with a microscope (DFC300FX) coupled to a camera. Morphometrical analysis was performed using Image J software to obtain the vessel internal and external perimeter and area. Then, internal and external radii (R_i and R_e) were calculated according to the formula perimeter= 2.π.R; internal diameter (ID) was obtained by 2xR_i; wall thickness as R_e - R_i; and the media cross-sectional area (CSA) as π (R_e² - R_i²). Statistical analysis: One-way ANOVA, followed by the Newman-Keuls test (*P<0.05).

Results:

In resistance mesenteric arteries, there was an increase in ID and in internal and external perimeter and area, while CSA and wall thickness did not significantly change in RP group compared with NP group. The wall thickness/ID ratio was decreased by low-protein diet in mesenteric arteries (NP=0.206 ± 0.02 vs. RP=0.137 ± 0.01*). In contrast to mesenteric arteries, resistance pancreatic arteries exhibited a reduction in ID and in internal and external perimeter and area in RP group compared with NP group. In addition, wall thickness (NP=12.3 ± 0.55 vs. RP=17.3 ± 1.91* µm) and the wall thickness/ID ratio (NP=0.141 ± 0.01 vs. RP=0.234 ± 0.02*) were both significantly increased by low-protein diet in pancreatic resistance arteries.

Conclusion:

In conclusion, the data suggest that post-weaning protein-restricted diet differently affect structure and morphology of mouse small vessels. While induced an outward eutrophic remodeling of mesenteric arteries, protein restriction induced an inward hypertrophic remodeling in pancreatic arteries. Therefore, protein restriction might result in different modulation of regional vascular resistance and blood flow.

Financial support:

PIBIC/CNPq; FAPESP grant #2014/01717-9.

04.023 - ALTERNATIVES OF ANTICHAGASIC THERAPEUTICS AGENTS BASED FROM SCORPION VAEJOVIS MEXICANUS SMITHI VENOM. Freire KA, Pedron CN, Monteiro ML, Martins AMC, Jr PIS, Oliveira VXJr, - Centro de Ciências Naturais e Humanas - UFABC Departamento de Análises Clínicas e Toxicológicas da Faculdade de Farmácia - UFC Laboratório Especial de Toxinologia Aplicada - IB

Introduction:

Chronic cardiomyopathy of Chagas` disease (CCDC) is considered a serious public health problem in the endemic areas of Latin America, representing one of the major causes of heart failure and sudden death. It is caused by persistent infection of *T. cruzi*, associated with inflammation mediated by adverse immune mechanisms. Chagas disease does not have effective medications in all stages of the disease, so the search for new alternatives with different modes of action is urgent. VmCT1 is a small amphipathic cationic peptide isolated from the

venom of the scorpion *Vaejovis mexicanus smithi* with potent antimicrobial action, but its protozoan activity has not yet been explored.

Aim:

In this study, we used a physicochemistry-guided peptide design strategy to identify determinant characteristics for the antiparasitic application of this potent AMP, analyzing the toxicity of its analogs. The VmCT1 analogs were designed to increase the net charge, simple substitutions of arginine were made on the hydrophilic side of the peptides, in order to verify its activity against the trypomastigote phase of *T. cruzi* protozoan.

Methods:

Peptides were synthesized by solid-phase method, using Fmoc strategy, purified by liquid chromatography, characterized by mass spectrometry and tested against trypomastigotes. Conformational studies were performed by circular dichroism assays and the cytotoxicity was tested in renal monkey cells and hemolytic test in human erythrocytes.

Results:

Substitutions on the hydrophilic face were made in positions with unchanged polar amino acid residues (Asn7 and Ser11). These changes in peptide structure and physicochemical features, such as net charge, hydrophobicity and polar angle, caused by the designed substitutions contributed to an enhanced antichagasic activity. The peptides VmCT1-NH₂, [R]7-VmCT1-NH₂ and [R]11-VmCT1-NH₂, showed significant IC₅₀ values, against trypomastigotes of 1.4, 1.2 and 1.0 µmol L⁻¹, respectively. Toxicity against LLC-MK2 cells was low, with IC₅₀ > 60 µmol L⁻¹ approximately. The hemolytic effect of these analogs increased 2-fold, compared to VmCT1-NH₂ that showed toxicity around 50 µmol L⁻¹. The results observed by CD assays suggest that these peptides tend helical conformations in vesicles and TFE / water (60%) and undefined conformations in water.

Conclusion:

VmCT1-NH₂ and its analogs [R]7-VmCT1-NH₂ and [R]11-VmCT1-NH₂ were actives against the trypomastigote form of the *T. cruzi* protozoan, with the increase of the net load, the analogs showed lower IC₅₀, contributing to a greater electrostatic attraction of the peptide with the parasite, increasing the antichagasic activity. The peptides showed tendency to α-helix conformation, suggesting to be important for the interaction with biomembranes. Arg-substituted analogs were more hemolytic against the zwitterionics membranes; however, the cytotoxicity was low for LLC-MK2 cells.

Financial support:

CAPES AND FAPESP.

04.024 - EFFECT OF TAURINE ON ENDOTHELIAL CELLS MIGRATION AND APOPTOSIS DURING AMINO ACID RESTRICTION. Mendonça KCP, Guizoni DM, Carneiro EM, Davel AP, - Departamento de Biologia Estrutural e Funcional - UNICAMP

Introduction:

Cardiovascular diseases (CVD) are the leading cause of mortality worldwide. Endothelial cell dysfunction is a common feature and a risk factor for CVD. Protein malnutrition is known to predispose to endothelial dysfunction and hypertension, although the mechanisms are not fully elucidated. Taurine, an amino acid with a vasodilatory and antioxidant action, has emerged as a potential therapeutic adjuvant for obesity and malnutrition comorbidities. Therefore, in the present study we hypothesized that taurine supplementation might be protective for the possible damage induced by amino acid restriction in endothelial cells.

Aim:

To evaluate the effect of taurine supplementation on the migration and apoptosis of endothelial cells during amino acid restriction *in vitro*.

Methods:

Bovine aortic endothelial cells (BAEC) grown to 80% confluence were exposed to a DMEM containing either 100% amino acids (100% aa) or

FeSBE Annual Meeting 2019

Poster Sessions and Abstracts

25% amino acids (25% aa) for 48h in the presence or absence of 3 mM or 30 mM taurine. Propidium iodide (PI) and Hoechst (HO) assay was performed to evaluate cell viability and apoptosis. Endothelial cell migration was evaluated by the Wound-healing assay and the wound was induced by a 200 μ L pipette tip. Protein expression of caspase-3, Sirt-3 and VEGF was determined in the cell lysate by Western-blotting. Statistical analysis: 1-way ANOVA with a Dunnet post-test (* $p < 0.05$). Values are mean \pm SEM.

Results:

Exposure to 25% aa induced apoptosis of endothelial cells, as suggested by increased PI/HO fluorescence (100% aa = 1.02 ± 0.14 vs. 25% aa = 1.88 ± 0.29). Treatment with 3 mM taurine did not impact cell death, but 30 mM taurine prevented the amino acid restriction-induced endothelial cell apoptosis. Regarding cell migration, cells incubated with 25% aa showed a reduced wound-healing area compared with 100% aa (100% aa = 0.137 ± 0.004 vs. 25% aa = 0.062 ± 0.012 mm²), which was not modified taurine treatment. Western-blotting analysis revealed that amino acid restriction increased expression of caspase-3 (100% aa = 1.0 ± 0.07 vs. 25% aa = 1.5 ± 0.20) which was prevented only by 30 mM taurine. VEGF expression was not altered either by amino acid restriction or taurine. Next, we evaluated the expression of Sirt-3, suggested to regulate angiogenesis. Endothelial cells exposed to 25% aa exhibited reduced Sirt-3 expression (100% aa = 1.0 ± 0.04 vs. 25% aa = 0.7 ± 0.06) and taurine did not reverse this effect.

Conclusion:

Our data show that amino acid restriction results in apoptosis and reduced migration of endothelial cells. The amino acid restriction-induced apoptosis was associated with an upregulation of caspase-3 which was prevented by taurine; however, taurine did not reverse the reduced migration and Sirt-3 expression induced by amino acid restriction. Therefore, the endothelial damage resulting from protein malnutrition might be partially prevented by taurine supplementation.

Financial support:

CAPES and FAPESP grant # 2014/01717-9.

04.025 - SEX DIFFERENCES IN THE VASODILATORY EFFECT OF THE SELECTIVE GPER AGONIST IN MESENTERIC RESISTANCE ARTERIES OF GONADECTOMIZED RATS. Peixoto P, Lemos VS, Bissoli NS, Santos RL, - Ciências Fisiológicas - UFES Fisiologia e Biofísica - UFMG

Introduction:

Non-genomic effects of estrogen, which include rapid vascular effects, have been attributed to the G protein-coupled estrogen receptor (GPER). However, the mechanism underlying the vascular effects modulated through GPER is not well known, especially in hormonal deprivation.

Aim:

We investigated the vascular function of GPER in mesenteric resistance arteries from gonadectomized rats of both sex.

Methods:

Wistar rats (12 weeks old) of both sexes were used. Gonadectomy was performed under anaesthesia with ketamine/xylazine. The rats were euthanized by decapitation without anaesthesia. Mesenteric third-order branches were isolated and mounted and concentration-response curves obtained by cumulative doses of the G-1 agonist (1 nM - 10 μ M) or vehicle (dimethyl sulphoxide) in phenylephrine-precontracted vessels. The vasodilatory effects of G-1 were assessed before and after removal of the endothelium or incubation for 30 min with nitric oxide synthase, cyclooxygenase, cytochrome P450 inhibitors or H₂O₂ enzymatic scavenger (L-NAME, INDOMETHACIN, CLOTRIMAZOLE and CATALASE respectively, alone or combined), PI3K-Akt pathway inhibitor (LY-294,002), selective inhibitor iNOS (1400W), selective inhibitor nNOS (L-NPA), potassium channel blocker (TEA), specific GPER antagonist (G36) and ER α and ER β antagonist (ICI 182,780). The data were analyzed by of two-way analysis of variance

followed by the Bonferroni post-hoc test. $p < 0.05$ was considered. The protocols were approved by CEUA-UFES (067/2017).

Results:

GPER agonist induced concentration-dependent relaxation of the mesenteric resistance arteries in both females (93.6 ± 0.8 %) and males (90.0 ± 1.3 %) gonadectomized, without sex difference. In the endothelium absence, the response to G-1 was decreased in both females (51.0 ± 1.0 %) and males (46.9 ± 1.9 %), but was not abolished. Vasorelaxation was attenuated in both groups in the presence of L-NAME (F: 68.5 ± 6.6 %, M: 81.2 ± 1.1 %), and this effect was more accentuated among the females. CATALASE (F: 72.1 ± 2.9 %, M: 90.6 ± 2.8 %) reduced response only in females. On the other hand LY-294,002 (F: 91.7 ± 2.1 %, M: 75.6 ± 3.5 %) and 1400W (F: 97.9 ± 0.8 %, M: 63.6 ± 5.4 %) reduced response only in males. 1400W in the endothelium absence restored response in males (F: 49.9 ± 5.6 %, M: 89.2 ± 3.5 %). INDOMETHACIN (F: 97.1 ± 1.0 %, M: 95.3 ± 0.6 %), CLOTRIMAZOLE (F: 92.4 ± 2.3 %, M: 92.2 ± 2.1 %), L-NPA (F: 88.3 ± 2.2 %, M: 84.8 ± 3.3 %) and TEA (F: 96.1 ± 1.4 %, M: 96.7 ± 0.5 %) did not reduced vasorelaxation in either group. Results of L-NAME + INDOMETHACIN (F: 76.6 ± 4.6 %, M: 88.6 ± 2.3 %), L-NAME + INDOMETHACIN + CLOTRIMAZOLE (F: 78.6 ± 7.6 %, M: 91.4 ± 3.1 %) and L-NAME + CATALASE (F: 69.3 ± 5.2 %, M: 75.5 ± 4.9 %) were similar to individual inhibition with L-NAME, among these only L-NAME + CATALASE was similar in both groups.

Conclusion:

These findings suggest that GPER modulated vascular relaxing through a different endothelial mediators and mechanisms that will vary according to sex. The results obtained in the present study provide new insight into the effects of oestrogen-induced responses via GPER on vascular function in hormonal deprivation.

Financial support:

CAPES

04.026 - EFFECTS OF SMOOTH MUSCLE CELLS DERIVED EXTRACELLULAR VESICLES ON VASCULAR CELLS. FRONY AC, deJESUSSOUZA M, BARJAFIDALGO C, MORAES JA, - Biologia Celular - UERJ Farmacologia - UFRJ

Introduction:

Several functional changes are observed in arterial wall components during atherosclerotic plaque development. Besides the endothelial dysfunction and phenotypic changes in vascular smooth muscle cells, during atherosclerosis occurs intense extracellular vesicles production by all cellular types involved on this process. These events are provoked by pro-inflammatory and pro-atherogenic mediators released in response to vessel injury, including angiotensin II (Ang II). Ang II is one of the main atherogenic mediators responsible by phenotypic modifications observed in vascular smooth muscle cells (VSMC) during atherosclerotic plaque formation. However, the effects of Ang II on the release of extracellular vesicles from vascular smooth muscle, as well as the possible effects of these vesicles on vascular cells remains to be fully elucidated.

Aim:

The general objectives of this work are to evaluate the characteristics of extracellular vesicles from VSMC stimulated by Ang II and elucidate their effects on different functions of VSMC.

Methods:

a7R5 (VSMC) were incubated with Ang II (100 nM) for 1 hour and the supernatant was collected and submitted to ultracentrifugation for extracellular vesicles purification. The protein analysis was performed by immunoblotting. Cellular migration was accomplished in modified Boyden chamber, and proliferation by MTT. ROS production was analyzed by DCF and lucigenin probes. Cell Invasion was measured through transwell assay. Statistical analysis was accomplished by two-way ANOVA.

Results:

FeSBE Annual Meeting 2019 Poster Sessions and Abstracts

In this work we show that Ang II was able to increase extracellular vesicles (EV) release (Untreated-M: 100/ Ang II-M:210 +/-SD: 9,8), being inhibited by NOX inhibitor (M:75 +/-SD: 13), showing a redox-dependent way. Furthermore, this process was decreased by ROCK inhibitor (M:88 +/-SD: 15), being dependent on ROCK/MLC pathway activation. Interestingly, these extracellular vesicles carry MMP9, p47phox (NOX2 subunit), flotillin and caveolin (cholesterol microdomains markers). We observed that extracellular vesicles decrease VSMC proliferation induced by AngII (Ang II-M:114 +/-SD: 8,8/ EV-M:95 +/-SD: 5,0). We also observed that these vesicles transfer MMP9 to non-activated VSMC, being able to be responsible for the increase of invasion that we observed through transwell assay (Untreated-M:100/ EV-M:120 +/-SD: 3,0). Finally, we observed that extracellular ROS production in non-activated VSMC was induced by these vesicles on a NOX2-dependent manner, which may be justified by the presence of p47phox in the extracellular vesicles.

Conclusion:

Our data indicate that VSMC-derived extracellular vesicles can directly affect vascular cells, which could lead to instability and poorer prognosis of atherosclerosis. This new approach could make it possible to develop new strategies for the treatment of atherosclerosis.

Financial support:

CAPES; CNPq; FAPERJ

04.027 - CHARACTERIZATION OF THE MOUSE LIENO-PANCREATIC ARTERY REACTIVITY. Guizoni DM, Carneiro EM, Davel AP, - Departamento de Biologia Estrutural e Funcional - UNICAMP

Introduction:

In the mammalian pancreas, the endocrine islets perfusion is considerably higher than that of the exocrine gland, with a positive correlation between endocrine islet activity and the pancreas blood flow. Interestingly, the blood flow to the pancreas has been reported to be reduced at hyperinsulinemic states as found in obesity and type 2 diabetes. Mouse pancreas blood supply is provided by the superior mesenteric artery and by celiac axis branches as the lieno-pancreatic artery (LPA) which accounts for the perfusion of the body and tail of the pancreas. Despite the importance of adequate blood supply for the endocrine pancreatic function, little is known about how the major arteries supplying the pancreas respond to vasoactive stimuli.

Aim:

To characterize the endothelium-dependent and independent vasodilation and the α -adrenergic mediated contraction of the mouse LPA. Potency and maximal responses (Emax) to the vasoactive substances were compared to the well-studied small mesenteric arteries (SMA).

Methods:

(CEUA: 4533-1) LPA and SMA from male C57Bl/6 mice (4-month-old) were isolated to perform concentration-response curves to acetylcholine (ACh), insulin, nitric oxide (NO)-donor sodium nitroprusside (SNP) and α 1-adrenergic agonist phenylephrine (Phe) in wire myograph. The participation of NO and endothelium-derived relaxing factors (EDHF) in the ACh-induced relaxation was assessed by incubation with 100 μ M L-NAME or 20 mM KCl, respectively. The potency ($pD_2 = -\log EC_{50}$) to the vasoactive substances was calculated by non-linear regression. eNOS expression was evaluated by Western-blot. * $P < 0.05$ vs. SMA (Student t-test).

Results:

The internal diameter of LPA and SMA were similar. ACh, insulin, and SNP induced relaxation in both arteries. However, the endothelium-dependent relaxation to ACh and to insulin were smaller in LPA that exhibited lower Emax (ACh: SMA= 96 \pm 1.2 vs. LPA= 81* \pm 4.4 %; insulin: SMA= 95 \pm 0.8 vs. LPA= 68* \pm 4.3 %) and potency (ACh: SMA= 7.9 \pm 0.2 vs. LPA= 7.0* \pm 0.3 %; insulin: SMA= 10.3 \pm 0.1 vs. LPA= 9.8* \pm 0.1) to both substances. L-NAME and KCl incubation reduced the ACh-induced relaxation in both arteries but relaxation of LPA was significantly less

affected by L-NAME (Emax: SMA= 39 \pm 7.9 vs. LPA= 72* \pm 10.9 %) while KCl incubation almost abolished the relaxation to ACh in LPA (Emax: SMA= 66 \pm 11.5 vs. LPA= 24* \pm 7.0 %). These data suggest a substantial participation of EDHF in LPA endothelium-dependent vasodilation rather than NO. In addition, eNOS expression (SMA= 0.6 \pm 0.05 vs. LPA= 0.4* \pm 0.05 a.u.) and the vasodilatory response to the NO donor SNP (Emax: SMA= 97 \pm 1.4 vs. LPA= 48* \pm 15.5 %) were both reduced in LPA compared to SMA. Contraction response to Phe was lower in LPA compared to SMA (Emax: SMA= 1.8 \pm 0.33 vs. LPA= 0.7* \pm 0.04 mN/mm).

Conclusion:

Vasodilatory and contractile responses of the LPA were significantly lower when compared to SMA, with a similar internal vessel diameter. In contrast to SMA, the endothelium-dependent vasodilatory response of LPA relies more on EDHF than on the eNOS/NO pathway. It is possible that the lower insulin-induced relaxation in LPA is an adaptive mechanism in the insulin-rich environment of the pancreatic islet. These findings characterize the physiological LPA reactivity, opening possibilities to future evaluation on cardiometabolic diseases.

Financial support:

FAPESP, Capes.

04.028 - CILOSTAZOL EXERTS BENEFICIAL EFFECTS IN PREVENTING THE EARLY STAGES OF ATHEROSCLEROSIS IN WISTAR RATS. Lopes RO, Autran LJ, Motta NAV, Lima GF, Brazão SC, Mendes ABA, Pereira NCA, Marques EB, Scaramelo CBV, Brito FCF, - Departamento de Fisiologia e Farmacologia - UFF Grupo de Pesquisa, Inovação e Desenvolvimento em Endocrinologia Experimental - UFRJ

Introduction:

Atherosclerosis is characterized as a chronic vascular inflammatory disease and considered one of the most important pathogenic mechanisms in cardiovascular events. The development of atherosclerosis involves endothelial dysfunction and inflammation. Cilostazol, a selective inhibitor of phosphodiesterase (PDE3), has been shown to have vasodilatory and antiplatelet action and beneficial effects on the prevention of atherosclerosis. Cilostazol was approved by FDA for treatment of intermittent claudication. Aiming to investigate the potential cardioprotective effect of cilostazol in development of atherosclerosis, we have investigated their vasodilatory, anti-inflammatory and antioxidant effects in a hypercholesterolemic animal model.

Aim:

The present study aimed to investigate the vasodilatory, anti-inflammatory and antioxidant activities of cilostazol in serum and heart tissue of hypercholesterolemic rats.

Methods:

The animal protocols were approved by the CEUA/UFF 858/2016. Adult male Wistar rats (200- 250g) were divided into four groups: control group (C), control group + cilostazol (C+Cil), hypercholesterolemic diet group (HC) and diet group + cilostazol (HC+Cil). The C and C+Cil groups were fed with standard chow diet and HC and HC+Cil groups with hypercholesterolemic diet. The treatment with cilostazol (30mg/kg) was performed from the 31st day to the 46th day. The animals were submitted to tail plethysmography for blood pressure measurement. In 46th day, after anesthesia with ketamine (100mg/kg) and xylazine (10mg/kg), blood samples and heart tissue were collected for molecular and biochemical analysis. Euthanasia was performed by exsanguination under anesthesia. Data were analyzed using one-way ANOVA and post-test Bonferroni ($p < 0.05$).

Results:

Cilostazol reduced the systolic blood pressure (HC+Cil: 120.5 \pm 0.89 mmHg x HC: 170.4 \pm 4.73 mmHg) and was able to reduce total cholesterol levels in serum (HC: 361.0 \pm 12.8 x HC+Cil: 219.2 \pm 30.70 mg/dL), triglycerides (HC: 186.9 \pm 17.7 x HC+Cil: 78.35 \pm 1.931mg/dL), cLDL (HC: 330.9 \pm 9.7 x HC + Cil: 169.5 \pm 30.39 mg/dl), cVLDL (HC: 45.0 \pm 4.6 x HC+Cil: 15.67 \pm 0.3861 mg/dl). In ELISA assays, HC group has

FeSBE Annual Meeting 2019

Poster Sessions and Abstracts

presented an increase of inflammatory cytokines: TNF- α (HC: 52.2 ± 4.4 x C: 34.7 ± 3.1 pg/ml), ICAM-1 (HC: 1080.0 ± 76.3 x C: 396.9 ± 34.9 pg/ml), IL-1 (HC: 43.3 ± 3.5 x C: 27.8 ± 1.8 pg/ml), IL-6 (HC: 170.9 ± 2.2 x C: 139.0 ± 6.1 pg/ml) and the treatment with cilostazol reduced these levels. PCR assay showed that cilostazol was able to reduce IL-6 expression. In Western Blotting assay (heart homogenate) was observed a decreased expression of NF- κ B (HC+Cil: 0.90 ± 0.01 x HC: 1.60 ± 0.07) while increased expression of I κ B- α (HC+Cil: 2.30 ± 0.09 x HC: 1.21 ± 0.30). In oxidative stress indicators, cilostazol was able to reduce lipid peroxidation (HC+Cil: 6.87 ± 0.83 x HC: 2.09 ± 0.93) as well as increase the expression of catalase (HC+Cil: 1.42 ± 0.04 x HC: 0.47 ± 0.08), SOD (HC+Cil: 3.80 ± 0.42 x HC: 1.73 ± 0.21) and Gpx (HC+Cil: 0.94 ± 0.07 x HC: 0.57 ± 0.06) in heart tissue. PCR assay and Western Blotting analysis showed that cilostazol increase Nrf2 expression in heart tissue (p<0.05).

Conclusion:

This study demonstrated the hypolipidemic, anti-inflammatory and antioxidant effects of cilostazol in a hypercholesterolemic model, concluding that cilostazol may have potential effects on preventing early stages of atherosclerosis.

Financial support:

CNPq, CAPES, PROPPI-UFF, FAPERJ.

04.029 - HEART AND DIAPHRAGM IMPROVEMENT BY PREGABALIN TREATMENT (MDX MICE). Franco LS, Silva GIP, Ferreira JS, Júnior LCG, Marques MJ, Carvalho SC, - Programa de pós Graduação em Ciências Biomédicas - FHO Biologia Celular e Estrutural - UNICAMP

Introduction:

The absence of dystrophin triggers the mdx muscle degeneration process by increasing inflammation and the influx of calcium ions (Ca²⁺) into the muscle fiber. In an attempt to minimize the damages, present in the dystrophic muscle fiber, drugs such as deflazacorte (DFZ) are used and in fact reduce the progression of the disease. However, the need for continued use of DFZ leads to harmful side effects to dystrophic patients. In view of this, we investigated pregabalin (PGB), which has Ca²⁺ + channel blocking activity and although it has potential to be administered to dystrophic patients, besides that its effects on dystrophinopathies are not known.

Aim:

Here, we analyzed the effects of PGB in dystrophic fibers of the mdx and normal mice.

Methods:

Mdx and normal mice (14 days old) received PGB (mdx-PGB or CTRL-PGB; n=8; 20 mg/kg body mass; daily oral gavage) or water (mdx or CTRL; n=8; 20 mg/kg body mass; daily oral gavage) for 16 days, after which the heart and diaphragm (DIA) were removed. We analyzed the PGB effects on signaling molecules of the inflammatory cascade (TNF- α , NF- κ B and TRAF6), sarcolemma stabilization (β -DG), oxidative stress (SOD1,2) and lipid peroxidation (4-HNE).

Results:

PGB was effective in reducing myonecrosis, leading to 37% decrease in creatine kinase (mdx; 1761.8 ± 266.4 U/L and mdx-PGB: 1114.1 ± 185.9 U/L) and 68% reduction in central nucleated fibers on DIA (mdx: 3.33 ± 0.77 % and mdx-PGB: 1.06 ± 0.40 %), as well as, inflammatory area (heart mdx: 0.12 ± 0.04 and mdx-PGB: 0.04 ± 0.01 %; DIA mdx: 1.15 ± 0.07 and mdx-PGB: 0.07 ± 0.02 %). Immunoblotting indicated that PGB were effective in reducing inflammatory markers (about two times) and improve sarcolemma stabilization (β -DG; 74% of increasing). The oxidative stress and lipid peroxidation was not influenced by PGB. In normal mice PGB treatment promoted the appearance of discrete areas of inflammation, increased molecules of the inflammatory cascade (TNF- α and NF- κ B in DIA) and reduced stabilization of the sarcolemma β -DG (4.8 times in heart and 40% in DIA).

Conclusion:

These results indicate that PGB may represent a good alternative to dystrophy sarcolemma stabilization and to normal tissue more study is needed to verifies the side effects

Financial support:

PIC/FHO

6 - Endocrine System

06.012 - TSH INDUCES MIRNA EXPRESSION CHANGES IN THYROID FOLLICULAR CELLS. Fuziwara CS, deSantalnez DC, Sousa ISMA, Saito KC, Kimura ET, - Departamento de Biologia Celular e do Desenvolvimento - USP

Introduction:

Goiter is an abnormal enlargement of thyroid gland that may be smooth and uniform, or presented as nodules. Thyroid nodules are very frequent in adult population, however, only a small fraction of these nodules is malignant (cancer), with a well-defined genetic alteration pattern. Interestingly, most thyroid nodule (>80%) comprise benign lesions with a poorly understood physiopathology. TSH is the main proliferative signaling pathway in thyroid follicular cells, and its over-secretion is a mitogenic stimulus in thyroid gland.

Aim:

In order to contribute to the understanding of benign goiter physiopathology, we aim to investigate the influence of miRNAs in TSH-induced goiter; since microRNAs are a new class of non-coding RNA that regulate protein levels post-transcriptionally by targeting mRNA, and its contribution in goiter development is yet unknown.

Methods:

Two months old female Wistar rats were treated with 0.05% methimazole in the drinking water ad libitum for 5 days to induce pharmacological goiter (MTZ group) by increase in TSH serum levels. Control animals were treated with water. Thyroid glands were removed after proper euthanasia for RNA and protein analysis. Gene and microRNA expression were analyzed from total RNA, while protein expression was analyzed with total protein in Western-blotting. This study complied with the guidelines of animal care of ICB-USP (CEUA 108/2016).

Results:

Treatment with methimazole induced TSH increase in blood and thyroid gland weight. We observed histological changes in thyroid gland such as reduction of colloid content, cell hypertrophy and increase in cell number. miRNA expression analysis showed induction of oncogenic miRNAs miR-21 (~300%), miR-146b (~200%) and miR-20a (~200%), but at the same time tumor-suppressor miRNAs let-7a (~60%) and let7f (~300%) were also induced compared to control group. Protein expression analysis reinforce proliferative effect of TSH showing CyclinD1 and PCNA increase in MTZ group. On the other hand, Smad4, a member of TGF β signaling cascade, is also increased in MTZ group.

Conclusion:

In this study we showed that TSH induces cell proliferation and expression of thyroid oncogenic miRNAs miR-21, miR-146b and miR-20a, and tumor-suppressor miRNAs let-7a and let-7f, in normal thyroid gland exposed to pharmacological goiter. This mitogenic effect indicates that tumor-suppressor miRNAs activation is insufficient to counteract the effect of TSH and oncogenic miRNAs in this model.

Financial support:

FAPESP: 2016/17129-4 ;CNPq 430756-2018-6

06.013 - AGING MORPHOLOGICAL CHANGES IN THE ADRENAL CORTEX OF THE MONGOLIAN GERBIL. ZUCÃO MI, ANTONIASSI JQ, GUERRA LHA, TABOGA SR, VILAMAIOR PSL, - Biologia - UNESP

Introduction:

The aging process in males is known by occasioning a hormonal imbalance due to the gradual reduction in the testicular testosterone

FeSBE Annual Meeting 2019

Poster Sessions and Abstracts

synthesis, which affects most of the organs sensitive to this hormone and, among them, the adrenal glands, which its cortex is responsible to synthesize and secrete steroidogenic hormones as mineralocorticoids, glucocorticoids, and androgens. The significant role played by this gland in the regulation of the reproductive system is recognized and it is also known that it is sensitive to the reduction of testosterone caused by castration, however, there is still very little understanding of its role in the andropause process. Moreover, Mongolian gerbils are experimental models for studies in reproductive biology and endocrine deregulation, their adrenal glands present a peculiar structure and suggest having more similar morphophysiology to the primates than others rodents, nevertheless yet, there are few investigations about the gerbils' adrenocortical physiology.

Aim:

Considering this, the purpose of this research is to describe the morphology of the aging process of the adrenal cortex of *Meriones unguiculatus* during, and possibly provide information for the set as an experimental model for studies in the reproductive and endocrine system, as well as in aging.

Methods:

In this research were used thirty gerbils (*Meriones unguiculatus*), they were maintained in laboratory conditions over the period of three, six, nine, twelve and fifteen months, according to the experimental group (n=6). They were weighed and euthanized and their adrenal was collected, weighed and fixed in paraformaldehyde 4%. The organs fixed were processed for histology and serial sections were performed and the middle ones were chosen for morphological analysis and were stained with Hematoxylin and Eosin and Gomori's trichrome. The sections were also stained with Gömöri's reticulin for collagen fibers analysis.

Results:

The biometrical analysis has shown a significant ($p < 0.05$) gradual increase in the body weight and in adrenal absolute weight. In the adrenals of the older groups, on the other hand, the relative weight just presents an increase in the eldest group (15m), highlighting the role of this gland at this stage of aging, when the sexual hormones are decreasing, as well as the morphometry has shown a larger length of all cortical areas. General morphological analysis showed in older groups larger connective tissue between cortex and medulla and increase of collagen fibers. Also, were visualized a larger amount of blood vessels and inflammatory cells. In the reticular zona were seen lipofuscin accumulation in animal with the age of 12 and 15 months, as well as regions with larger cells and clear cytoplasm, that may reflect the decrease in the metabolic activities of the cell, due to the senescence process.

Conclusion:

This study has found that at the age of 12 and 15 months the adrenal presents signs of senescence, it shows hypertrophy demonstrating a probable compensatory function to the low cell metabolism and to the androgens decrease. This finding is similar to the research in primates making it a possible experimental model for adrenal diseases and aging studies.

Financial support:

FAPESP 2014/26660-0 and CAPES

06.014 - ADIPOGENIC EFFECTS OF FEMBUTATIN OXIDE, CARBOSULFAN AND BITERTANOL IN CELL CULTURE. Bittencourt MB, Carneiro FD, Mendonça LS, Sant'Anna TBF, Rodrigues KD, Machado JAMM, Araujo BP, Neves FAR, Lacerda MG, Milton FA, - fcb - universidade federal fluminense

Introduction:

This study seeks to evaluate a possible correlation between the consumption of pesticides and obesity. 3 pesticides were selected: Bitertanol, carbosulfan and Fembutatin Oxide. They were purchased in pure form through Sigma-Aldrich. In each pesticide the study was

carried out with Hela cells of the plasmids PPARgamma for the evaluation of the activation or not of the receptors with the endocrine disrupters; In addition, the cell differentiation study with 3T3-L1 cells was carried out to verify the different concentrations of the pesticides that stimulated a greater differentiation in the treatment period (14 days).

Aim:

The research seeks to verify if there is a correlation between the pesticides used in national territory for food crops and the fat cell in the cells. through the verification of activation by endogenous receptor and the observation of greater lipogenic activity in the study of cell differentiation.

Methods:

3T3-L1 cells and Hela cells were selected for the studies. The pesticides were purchased in their pure form, produced by Sigma-Aldrich. They were selected based on the following criteria: greater use in national cultures, chemical groups and different classes among those already selected, their use in Europe and the United States, and greater ease of acquisition. The study of cell differentiation proves that different concentrations of the pesticide influence a greater differentiation of adipocytes in adipocytes compared to DMSO (negative control for differentiation) and rosiglitazone (positive control for differentiation). Cells are also seeded into each well of the 6 well plate. It is expected to reach 100% confluence and counts 2 days to start the differentiation treatment. On the first day we added the medium with insulin and dexametazone and treated house well, one with DMSO, another with rosi and the others with increasing concentrations of the pesticide. It was also done 48 well plates were plated and waited for 100% confluence. after which PPAR Gal, Gal luc and lipofectamine were added to the serum. After 5 hours, the endocrine disrupters were treated and the following day transfected and read after administration of the luciferase enzyme.

Results:

All the 3 agrototoxics tested generated a higher accumulation of cellular fat when compared to the nontoxic concentration of the agrototoxic with the negative control (DMSO) and remained below the activation of the positive control of activation (rosiglitazone). Already in the transfection study, only carbosulfan and fembutatin oxide showed activation for the PPARy responses greater than the control. The highest activation promoted by carbosulfan was 3.6 times in the concentration of 100µM and the oxide of fembutatina, of 4.7 times, in the concentration of 50µM. Both pesticides can be considered PPARy partial agonists compared to rosiglitazone, which induced about 60-fold activation.

Conclusion:

With the study it can be concluded that both carbosulfan and fembutatin oxide were shown to be partial agonists of the PPAR Gamma receptor. And the three showed greater differentiation activity in the wells with the highest concentrations of agrototoxics.

Financial support:

sem apoio

06.015 - MATERNAL HYPERGLYCEMIA ALTERS THE DISTRIBUTION OF LAMININ AND INTEGRIN AND THE PROLIFERATIVE ACTIVITY IN THE PANCREATIC ISLETS OF PRETERM FETUSES IN MICE. Dias CP, Morais MRPT, Silva CSB, Barrence FA, Zorn TMT, - Biologia Celular e do Desenvolvimento - Universidade de São Paulo

Introduction:

Although extracellular matrix (ECM) is directly involved in the morphogenesis and branching of the pancreas, little is it known about the effect of maternal hyperglycemia on the ECM during this organ development.

Aim:

Objectives: In the present study, we investigated the impact of short-term maternal diabetes (30-50 days) on the deposition pattern of the

FeSBE Annual Meeting 2019

Poster Sessions and Abstracts

peri-islet basement membrane components and $\alpha 3$ integrin chain of the developing pancreas and the endocrine cells' proliferative profile.

Methods:

Alloxan-induced diabetic female mice with no insulin replacement were mated with normoglycemic males between 30 and 50 days after induction. Fetuses were collected at E19.0. Fetal pancreas was dissected, processed and analyzed through hematoxylin and eosin staining and immunohistochemistry. All the experiments were conducted according to the Animal Ethics Committee of the Institute of Biomedical Sciences, Protocol 111/2016.

Results:

Compared to the control group, the quantification of the percentage of immunostaining area for panlaminin, $\alpha 1$ and $\gamma 1$ laminin chain showed reduction in the marking intensity in the pancreas of fetuses of hyperglycemic mothers. Panlaminin (control $6,3 \pm 2,7$ vs experimental $4,8 \pm 2,1$), $\alpha 1$ laminin chain (control $4,6 \pm 3,2$ vs experimental $2,7 \pm 1,5$) and $\gamma 1$ laminin chain ($29,3 \pm 9,2$ vs $19,3 \pm 4,4$). On the other hand, $\alpha 3$ integrin immunostaining showed an increase the percentage of compared to the control group (control $11,3 \pm 14,0$ vs experimental $24 \pm 13,5$). Proliferative index of endocrine cells was lower in 33% in the experimental group.

Conclusion:

Short-term maternal hyperglycemia (30-50 days) alters the development of the endocrine pancreas by modifying the deposition pattern of basement membrane molecules and the integrin associated with decreased islet proliferative activity cells.

Financial support:

CNPQ

06.016 - TSH INDUCES GENOMIC INSTABILITY AND OXIDATIVE STRESS IN MAMMARY TISSUE. Peixoto MS, Souza AV, Andrade IS, Giusbi CCE, Faria CC, Fortunato RS, - Laboratório de Fisiologia e Sinalização Redox - UFRJ

Introduction:

Breast cancer and thyroid dysfunctions have been associated since the 1960s. Studies demonstrated that breast cancer patients have a higher incidence of thyroid disease than would be predicted by chance alone, supporting a link between thyroid hormone signaling and breast malignancy. Despite many studies suggesting a biological correlation, the mechanism that links these two pathologies has not been elucidated, particularly in subclinical hypothyroidism. The possible interaction between the thyroid gland and the breast tissue can be explained by the presence of TSH receptors in the mammary gland. Some authors suggest that the action of TSH on mammary cells involving activation of proliferative processes and oxidative stress may explain its role in tumorigenesis.

Aim:

In the current study, we investigated the role of TSH on breast genomic instability and redox homeostasis.

Methods:

We used a non-tumorigenic human breast epithelial cell line, MCF10A, which underwent treatment with TSH at concentrations of 1, 10 and 20 mU/mL for 24h and 72h. Then, the proliferative state, the production of reactive oxygen species (ROS) and DNA damage were evaluated. For in vivo analysis, Thirty-two female Wistar rats from the Rio de Janeiro Federal University (UFRJ) were used (ethics committee 01200.001568/2013-87). For a period of 7 or 21 days, the animals were treated with 0,03% of methimazole (MMI) in water; which inhibits the enzyme thyroperoxidase, therefore lowering T4 levels and increasing TSH. Control groups were also used for each period. At the end of treatment, the animals were sacrificed by decapitation and mammary tissue was removed. Intracellular peroxide generation, antioxidant enzymes activities and oxidative stress markers assays were performed.

Results:

We showed that the TSH receptors are present in breast cells both in vitro and in vivo. When treated with TSH at 20 mU/mL, MCF10A cells showed a higher extracellular (C24h= $2,64 \pm 0,07$; T24h= $6,37 \pm 0,31$; C72h= $2,39 \pm 0,02$; T72h= $3,01 \pm 0,02$), intracellular (C24h= $1,00 \pm 0,06$; T24h= $2,57 \pm 0,80$; C72h= $1,00 \pm 0,26$; T72h= $3,60 \pm 1,20$) and mitochondrial ROS (C24h= $1,04 \pm 0,08$; T24h= $1,47 \pm 0,20$; C72h= $1,00 \pm 0,08$; T72h= $1,32 \pm 0,18$) production at 24h and 72h. Also, a higher DNA damage was observed in these cells demonstrated by an increased number of 53BP1 loci (C24h= $7,33 \pm 0,99$; T24h= $14,53 \pm 8,21$; C72h= $9,57 \pm 3,61$; T72h= $16,07 \pm 5,46$) and a higher comet tail DNA percentage (C24h= $5,41 \pm 0,42$; T24h= $10,59 \pm 1,14$; C72h= $4,98 \pm 0,90$; T72h= $9,72 \pm 1,55$). Next, we evaluated redox homeostasis in vivo. After 7 days, lower antioxidant enzyme activities (Catalase: C= $0,56 \pm 0,06$; T= $0,36 \pm 0,13$; SOD: C= $15,33 \pm 1,85$, T= $16,71 \pm 1,84$; GPx: C= $173,81 \pm 24,43$, T= $142,02 \pm 9,60$) and calcium-dependent H2O2 production (C= $3,32 \pm 0,72$; T= $1,97 \pm 0,88$) were detected in MMI group compared to control rats; while the levels of 4-Hydroxynonenal (HNE), a lipid peroxidation marker, were higher (C= $1,00 \pm 0,06$; T= $1,58 \pm 0,39$). A longer administration of MMI for 21 days increased the activities of antioxidant enzymes (Catalase: C= $0,08 \pm 0,01$; T= $0,28 \pm 0,08$; SOD: C= $16,91 \pm 11,79$, T= $21,03 \pm 1,68$; GPx: C= $125,70 \pm 24,24$, T= $107,12 \pm 20,24$) and maintained the levels of oxidative stress markers, reduced thiol (C= $56,61 \pm 5,36$; T= $58,30 \pm 21,06$) and HNE (C= $1,00 \pm 0,25$; T= $0,89 \pm 0,19$), similar in both groups.

Conclusion:

In conclusion, these results show that TSH induces DNA damage and oxidative stress in breast cells. Collectively, our data support the hypothesis that dysregulated TSH levels may increase the risk of breast cancer development and highlight a need to further investigate the role of sub-clinical hypothyroidism in breast cancer.

Financial support:

Coordenação de Aperfeiçoamento de Pessoal de Nível Superior (CAPES) and Conselho Nacional de Desenvolvimento Científico e Tecnológico (CNPq)

06.017 - GENE EXPRESSION ANALYSIS OF AMH AND ITS IMMUNODETECTION IN THE LAMBARI FISH ASTYANAX ALTIPTARANAE TESTIS. Camargo MP, Jesus LWO, Branco GS, Bogerd J, Nóbrega RH, Borella MI, - Departamento de Biologia Celular e do Desenvolvimento - USP

Introduction:

Spermatogenesis in fish is regulated by both - luteinizing (Lh) and follicle stimulating (Fsh) - hormones (endocrine regulation), as well as by growth factors (paracrine regulation). Among the factors regulated by Fsh, the Anti-Müllerian hormone (Amh) is a glycoprotein of the Beta-Transforming Growth Factor (TGF β) family secreted by Sertoli cells.

Aim:

To clarify the endocrine and paracrine regulation of the spermatogonial niche in native species, the Characiforme *Astyanax altiparanae* was used as a neotropical model species with economic and ecological importance.

Methods:

Real-time quantitative PCR (qPCR) was performed to analyze the transcription levels of amh in heart, spleen, muscle, intestine, stomach, brain, gills, ovary and testis (tissue screen) and during the reproductive cycle in males. The primers sense and anti-sense used were designed on the sequences previously obtained for *A. altiparanae*, and reagent PowerSYBR[®] Green Universal Master Mix (Applied Biosystems) was used. All the samples were analyzed with the Step One Plus Real-Time PCR System (Applied Biosystems). To immunohistochemistry (IHQ), affinity purified-Amh antisera were produced in rabbit using as epitope a peptide corresponding to amino acid residues 437-451 from *A. altiparanae*. Testes were collected and fixed in Paraformaldeide 4% solution, and serial and transverse sections were obtained (5 μ m). Endogenous peroxidase was inactivated using 3% hydrogen peroxide in

FeSBE Annual Meeting 2019

Poster Sessions and Abstracts

phosphate buffered saline (PBS, pH 7.4) and blocked in 5% goat serum and 0.1% bovine serum albumin (BSA) in PBS with 0.1% Tween (PBS-T). The material was incubated with rabbit anti-A. altiparanae Amh (1:800) diluted in 1% goat serum 0.1% BSA in 0.1% PBS-T. Next, sections were incubated with Super Picture Polymer (Invitrogen) conjugated to HRP, and the immunostaining was revealed with 3,3'-diaminobenzidine (DAB, Invitrogen).

Results:

The tissue screen indicates that there is a significant statistical difference in the testis when compared to the other organs from both males and females. Moreover, even at the lower level, there is also the expression of transcripts to amh in the heart, muscle and brain in both gender, as well as amh expression in the ovaries. The expression of amh during the reproductive cycle in males (characterized according to the seasons) showed that there is statistical difference when comparing the summer and autumn seasons, and when comparing autumn with winter also. The highest expression of amh was observed in autumn. The IHQ resulted in immunostaining Sertoli cells which involved both undifferentiated spermatogonia (Aund), as well as differentiated type A spermatogonia (Adiff).

Conclusion:

The results obtained in this study indicate that amh plays an important role in the regulation of the spermatogenesis and suggest that it has an inhibitory effect in the pathway of spermatogonial differentiation, keeping the initial cells in their undifferentiated state. These findings may generate subsidies to help understand the reproductive biology of this species and to understand how the spermatogenesis homeostasis occurs and how its aspects influence the self renewal and differentiation of spermatogonia undifferentiated, possible candidates for spermatogonia stem cell.

Financial support:

FAPESP #2017/10012-7

7 - Nutrition and Metabolism

07.035 - MATERNAL LOW PROTEIN DIET AND SUGAR CONSUMPTION DURING THE POSTNATAL LIFE LEADS TO PROSTATE CARCINOMA IN SITU IN OLD RATS. Silva CLF, Colombelli KT, Fioretto MN, Santos SAA, Constantino FB, Camargo ACL, Portela LMF, Mani F, Justulin LA, - Departamento de Morfologia - UNESP Departamento de Química e Bioquímica - UNESP

Introduction:

The intrauterine period of development is a high vulnerable window important for the offspring health. The low protein diet (LPD) offered to dams during perinatal period negatively affects male offspring reproductive organs. These effects can be worse in individuals submitted to LPD early in life associated with consumption of hypercaloric foods and sedentary lifestyle throughout postnatal life, as demonstrated by increased incidence of obesity, diabetes and hypertension. Our research group recently demonstrated that maternal LPD induced offspring prostate carcinogenesis in older rats.

Aim:

Here we aimed to analyze the postnatal sugar consumption effects in metabolic profile and histopathology of ventral prostate (VP) in aging rats submitted to maternal LPD.

Methods:

This study was approved by the Ethics Committee on Use of Animals – IBB (protocol 951). We used Sprague Dawley male rats born from dams that were fed with normal protein diet (17% protein) or low protein diet (6% protein) during gestation and lactation. These rats were divided in 4 experimental groups at postnatal day (PND) 21 (n=6/group), and fed with normal protein diet: Control (CTR) consumed normal water until PND 90; Control+sugar (CTR+SUG) consumed sugar solution (10% diluted in water) until PND 90; Gestational and Lactational Low Protein (GLLP) received normal water until PND 90; and

GLLP+SUG consumed sugar solution until PND 90. After PND 90 all animals received normal water. The animals were euthanized at PND 540, the blood was collected to metabolic analyses (triglycerides, total protein and glucose) and VP were collected, weighted and processed to histopathological and immunostaining analyses. The statistical analysis was performed using ANOVA and Student's T test.

Results:

There were no differences in blood samples among experimental groups for the triglycerides (122.0±77.2 mg/dL for CTR, 205.5±32.8 mg/dL for CTR+SUG, 200.5±24.3 mg/dL for GLLP and 101.8±49.5 mg/dL for GLLP+SUG), total protein (8.9±3.0 mg/dL for CTR, 7.0±1.4 mg/dL for CTR+SUG, 7.3±1.7 mg/dL for GLLP and 7.5±1.6 mg/dL for GLLP+SUG) and glucose (188.6±20.9 mg/dL for CTR, 202.5±16.8 mg/dL for CTR+SUG, 192.9±14.6 mg/dL for GLLP and 203.4±10.8 mg/dL for GLLP+SUG). The GLLP and GLLP+SUG groups had absolute and relative VP weight significantly higher compared to control group (absolute weight: 0.47±0.04 g for CTR, 0.62±0.04 g for GLLP and 0.61±0.003 g for GLLP+SUG; relative weight: 0.0008±0.05 g for CTR, 0.0012±0.08 g for GLLP and 0.0013±0.08 g for GLLP+SUG). Histopathological analysis identified epithelial atrophy, physiological and focal hyperplasia, epithelial dysplasia and prostatic intraepithelial neoplasia (PIN) in all experimental groups, frequently associated with aging process. The carcinoma in situ was only detected in CTR+SUG and GLLP groups. In areas of PIN and carcinoma in situ, we observed an increase in Ki-67 positive cells (1.5±1.3 % of positive cells in normal areas vs 5.0±1.1 % of positive cells in lesion areas) and in AR staining intensity.

Conclusion:

These results demonstrated that postnatal sugar consumption associated or not with maternal LPD causes negatively effects on prostate homeostasis and can be associated with development of carcinoma in situ with aging in rodent model.

Financial support:

FAPESP (2018/16183-0)

07.036 - EARLY IN VITRO AMINO ACID RESTRICTION LEADS TO IMPAIRMENT OF MITOCHONDRIAL METABOLISM AND REDUCTION OF PANCREATIC B CELL VIABILITY WHEN EXPOSED TO FATTY ACIDS. Araujo TR, Vettorazzi JF, Guimarães DSPSF, Carneiro EM, - Biologia Funcional e Molecular - UNICAMP

Introduction:

Nutritional deficiency during development stages increases disturbances in different tissues of rodents and humans, which could increase the susceptibility to some diseases development as Type 2 Diabetes Mellitus when associated with high fat-rich diets in adulthood.

Aim:

We evaluated alterations in mitochondrial metabolism and viability of pancreatic β cell lines subjected to amino acid restriction in association or not with fatty acids.

Methods:

INS-1E cells were maintained in RPMI-1640 medium containing 11.1 mM glucose, supplemented with 10% fetal bovine serum and 100% amino acid [aa] (CON) or 25% aa (Aar) for 48 h. After that, CON and Aar received 500 μ M oleate and palmitate (FA) medium for 48h. The results were analyzed by the Shapiro Wilk normality test and submitted to two-way ANOVA followed by Bonferroni with P<0.05 afterwards.

Results:

Exposure to FA increased mitochondrial biogenesis and activity in control cells as observed by the increase in mitochondrial density (1.5±0.1 RFI), protein levels of PGC-1 α (2.1±0.2) and mitochondrial complexes I (1.9±0.2) and IV (2.1±0.1) compared to control (1±0.1 RFI; 1±0.2; 1±0.2 and 1±0.2, respectively). AaR cells had reduced mitochondrial density (0.65±0.1 RFI) and protein levels of mitochondrial complexes I (0.6±0.1) and IV (0.55±0.1) compared to control (1.1±0.1 RFI; 1±0.2 and 1±0.2, respectively). The FA treatment reduced the protein levels of the mitochondrial complex III (0.58±0.1) without

FeSBE Annual Meeting 2019

Poster Sessions and Abstracts

altering mitochondrial density in AaR cells (1.2 ± 0.1). Furthermore, FA induced an increase in XBP1 gene expression (1.8 ± 0.2) in control cells. However, previously amino acids restricted cells showed an increase in ATF4 (3.3 ± 0.3), XBP1 (3.1 ± 0.2) BIP (1.7 ± 0.2) and ATF6 (1.9 ± 0.2) genes expression when exposed to FA compared to AaR (1.7 ± 0.2 ; 1.3 ± 0.1 ; 1.2 ± 0.2 and 1.1 ± 0.3). The FA treatment not only doubled AKT phosphorylation (pS437) in control cells (2.1 ± 0.2 and 1 ± 0.2), but also reduced in amino acids-restricted cells (1.8 ± 0.1 and 3.2 ± 0.4). Moreover, the FA exposition augmented the levels of cleaved caspase-3/total caspase (5.8 ± 1.2) and the BAX/Bcl-2 ratio (1.32 ± 0.1) and reduced 25 % of the viability in early amino acids restricted cells (1.6 ± 0.2 and 0.65 ± 0.2 , respectively). Molecular alterations were reflected in functional changes, as observed by an 78% increase in the insulin secretion stimulated by 22.2 mM of glucose in control cells exposed to FA and only 25% increase in early amino acids-restricted cells.

Conclusion:

Our results have shown that early amino acids restriction alters the response of pancreatic β cells exposed to fatty acids, leading to a decrease in mitochondrial biogenesis and function, as well as an elevation of reticulum stress biomarkers, which culminates in a higher apoptosis rate by activation of BAX and cleaved caspase-3. Besides, early amino acids restriction decreased insulin secretion in response to FA, a phenotype similar to that occurring in Type 2 Diabetes Mellitus.

Financial support:

Research funded by FAPESP.

07.037 - PON1 ACTIVITY AND PLASMA LIPID PROFILE IN RATS (RATTUS NORVEGICUS) NEONATES AND ADULTS, MALES AND FEMALES. Silveira D, Breigeiron MK, Trapp M, - Fisiologia - UFRGS Departamento de Enfermagem Materno-Infantil (DEMI) - UFRGS

Introduction:

Paraoxonase 1 (PON1) is an esterase related to the plasmatic high-density lipoprotein (HDL), and presents lower activity in neonates. Low plasma concentrations of PON1 are associated with inflammatory diseases and cardiovascular disorders in adult mammals.

Aim:

The aim of this work was to study the PON1 plasma activity and the plasma lipid profile in relation to age and sex in Rattus norvegicus.

Methods:

A total of 65 Wistar rats (*Rattus norvegicus* species) were used throughout the experiment, of which 21 were neonates 7 days of age, (10 females, P7F; 11 males, P7M); 24 were neonatal 14 days of age (11 females, P14F; 13 males, P14M); and 20 were adult rats 70 days of age (10 females, F; 10 males, M). Activity of PON1 (U/mL), concentrations (mg/dL) of HDL, Total Cholesterol (TC) and Triacylglycerol (TGC), as well as hepatosomatic (IHS) and liposomal indexes (ILS) were evaluated (g/g). This project was approved by UFRGS Ethical committee (n \circ 34595). Statistical Analysis: The normality of the data was verified by the Kolmogorov-Smirnov test. The parametric data were submitted to two-way ANOVA analysis followed by Bonferroni post hoc. Non-parametric data were evaluated by Menn Witney Kruskal-Wallis followed by Dunn test. The accepted significance was $P < 0.05$ and the tests were performed using the Prisma software version 6.0. The parametric data were as mean \pm standard error of the mean, and the non-parametric data as median and interquartile range.

Results:

PON1 activity was higher ($P < 0.05$) in adults (M 209.9 ± 10.7 ; F 258.5 ± 6.5) than in neonates (P7F 25.8 ± 1.4 ; P7M 23.9 ± 0.7 ; P14F 33.8 ± 1.6 ; P14M 36.1 ± 2.9), and in F compared to M ($P < 0.05$). HDL concentration was higher in adults (F 45.9 ± 2.7 ; M 35.0 ± 1.7) than in neonates (P7F 13.3 ± 1.1 ; P7M 17.5 ± 1.8 ; P14F 18.8 ± 1.8 ; P14M 18.2 ± 1.7), regardless of gender. In females there was a positive correlation between PON 1 activity and serum HDL concentration in neonates at 7 days. In males, however, there was a positive correlation between PON-1 and serum

HDL activity only in adult and P14. TC concentration was higher in neonates (P7F 165 ± 8.6 ; P7M 147.5 ± 4.7 ; P14F 163.2 ± 6.1 ; P14M 171.4 ± 3.6) than in adults (F 60.2 ± 3.0 ; M 54.2 ± 1.8). There was no significant difference in TGC among adults and neonates. However, P14M (142.3 ± 16.7) presented an increase in serum TGC when compared to P7M (82.7 ± 13.7). The hepatic TGC also did not differ between sexes or ages. Higher LSI and HSI ($P < 0.05$) were found in adults (LSI: F 0.75 ± 0.003 ; M 1.0 ± 0.005 ; HIS: F 3.7 ± 0.05 ; M 3.5 ± 0.05) when compared to neonates (LSI: P7F 0.17 ± 0.002 ; P7M 0.21 ± 0.002 ; P14F 0.30 ± 0.003 ; P14M 0.24 ± 0.009 ; HIS: P7F 2.9 ± 0.05 ; P7M 2.8 ± 0.07 ; P14F 2.5 ± 0.03 ; P14M 2.7 ± 0.08).

Conclusion:

The results demonstrate that the lipid profile of the neonates, especially P7 animals, differs between males and females. In addition, the plasma lipid profile is different between neonates and adults. The greater activity of PON1 enzyme in adults compared to neonates probably occurs because of the greater amount of HDL present in adults. Higher enzyme activity associated with high HDL values in females may be related to a protective profile for inflammatory diseases.

Financial support:

UFRGS

07.038 - LYCOPENE, CURCUMIN OR BIXIN INCORPORATED IN YOGHURT IMPROVE PHYSIO-METABOLIC AND/OR OXIDATIVE STRESS BIOMARKERS IN LIVER OF HIGH-FAT-DIET INDUCED OBESE MICE. Assis RP, Dubois MJ, Pilon G, Baviera AM, Marette A, Brunetti IL, - Department of Medicine, Cardiology Axis of the Quebec Heart and Lung Institute - ULaval Department of Clinical Analysis - UNESP

Introduction:

Obesity is a leading public health issue and a risk factor for several diseases, including diabetes mellitus, heart and vascular diseases. The search of natural active compounds that have beneficial effects against these disorders is a promising trend. In addition, food fortification, mainly of dairy products, has appeared as an interesting way to offer active compounds acting to reduce or prevent chronic diseases related with metabolic disturbances.

Aim:

This study evaluated the treatment of mice fed a high-fat diet with lycopene, curcumin or bixin into yoghurt, and their effects on physiological and biochemical parameters, oxidative stress and antioxidants biomarkers.

Methods:

Eight-week-old C57Bl/6J male mice were randomly divided into six groups (n=12/group) and treated for 8 weeks: LF, low-fat diet treated with water; HF, high-fat diet treated with water; HFY, high-fat diet treated with yoghurt; HFC high-fat diet treated with 90 mg/kg curcumin into yoghurt; HFL, high-fat diet treated with 45 mg/kg lycopene into yoghurt; HFB, high-fat diet treated with 5.5 mg/kg bixin into yoghurt (ethical approval 2015100-1, Laval University). Body weight, food and energy intake were assessed three times a week. Insulin tolerance test and oral glucose tolerance test, were performed at weeks 6 and 7, respectively. After 8 weeks, adiposity was evaluated by TD-NMR (Bruker \circledR), the mice were sacrificed and liver samples were collected for analysis of biochemical parameters (triglycerides), biomarkers of lipid oxidation and antioxidant enzymes (thiobarbituric acid reactive substances, TBARS; catalase, CAT; superoxide dismutase, SOD; glutathione peroxidase, GSH-Px) and inflammatory biomarkers (IL-6 and TNF- α). Data was expressed as mean \pm standard error and considered statistically different $p < 0.05$ (One-way ANOVA, Student-Newman-Keuls).

Results:

Throughout the 8 weeks, mice HF group showed significant increase in body weight gain and body fat mass (vs L group). Mice HF had minor food intake (in grams) vs LF and increase energy intake, these facts

FeSBE Annual Meeting 2019

Poster Sessions and Abstracts

support the establishment of obesity. All treatments induced a lower body weight gain (vs HF), especially HFL mice showed significant decrease in body weight gain vs HFY. In fact, lycopene-enriched yoghurt improved the insulin sensitivity and glucose tolerance in mice fed high-fat diet vs HF and HFY. HFY mice showed reduction in hepatic levels of triglycerides (32%) vs HF mice, however when the mice were treated with natural active compounds, the reduction in triglycerides became even more evident (HFL=46%, HFC=32%, HFB=31% vs HFY). The treatment with lycopene presented the greatest effect in the reduction of TBARS (HFL=31.2±0.12 vs HF=48,7±0.16; HFY=42.3±0.10, µmol/L/g tissue), while HFC and HFB (38.4±0.08 and 36.7±0.04, µmol/L/g tissue, respectively) presented significant difference only vs HF. The activities of antioxidant enzymes were reduced in HF and HFY vs L mice, however HFC, HFL and HFB mice showed increased the activities of CAT (HFL=67%, HFC=33% vs HFY; HB=56% vs HF), SOD (HFL=66%, HFC=37%, HFB=31% vs HFY) and GSH-Px (HFL=33%, HFC=41%, HFB=34% vs HFY). All treatments had no effect for IL-6, whereas the treatment with lycopene and bixin reduced TNF-α levels (HFL=15%; HFB=11% vs HFY).

Conclusion:

Lycopene, curcumin or bixin appear as interesting options as complementary therapies for the complications in liver associated with obesity.

Financial support:

FCFAr/UNESP, PDSE/CAPEs, IUCPQ/Laval Univeristy

07.039 - ENZYMIC STIMULATION OF ATP7B IN HEPG2 CELLS BY PALMITATE: ALTERED OXIDATIVE STRESS. Nossar LF, Milhm G, Cardoso LHD, Lowe J, - Ciências Biológicas (Biofísica) - UFRJ

Introduction:

Copper is a transition metal considered a micronutrient. In hepatocytes, copper is carried by metal chaperones and directed to various organelles and enzymes performing different functions as a co-factor of cytosolic and extracellular superoxide dismutases (SOD 1 and 3, respectively), which dismutate superoxide in hydrogen peroxide and O₂. In case of accumulation of this metal in the hepatocytes, copper is directed to the Golgi complex by ATP7B (copper ATPase) and its excess is transported to the bile duct, controlling the intracellular copper. Chronic consumption of high-fat diet, a situation experienced by 1.9 billion adults worldwide, can lead to the establishment of several degenerative pathologies such as hepatic steatosis. It is known that a high-fat diet stimulates a signaling pathway leading to the accumulation of diacylglycerol in the hepatocytes and activation of PKC. However, it is not clear the effect of this pathway in the copper homeostasis. The imbalance of cellular copper homeostasis could be involved in the in reactive oxygen species (ROS) production.

Aim:

Investigate the production of ROS and its side effect, through molecular markers of cell damage and a potential influence on mitochondrial ultrastructure, correlating with changes in copper metabolism caused by a modulation of ATP7B activity.

Methods:

Human hepatocarcinoma cell cultures (HepG2) were treated with 0.5 mM fatty acid palmitate for 14 h, mimicking the chronic high-fat diet in a cellular model. The cells were grown in DMEM medium (1 g/L glucose) with 10% fetal bovine serum, maintained at 37 °C incubator in 5% CO₂. 3 × 10⁴ cells/cm² were inoculated in 60 x 15 mm plates every 3-4 days. There were two experimental groups: control group (CTRL) and palmitate (PALM). In order to determine changes in copper transport, ATP7B activity was tested (expressed in nmol Pi x mg⁻¹ x min⁻¹), oxidative stress was observed by Western blot, evaluating protein content of SOD1, SOD2, SOD3, 4-HNE (lipid peroxidation marker), nitrotyrosine (protein nitrosylation) and carbonyl reductase 1/2/3 (cell damage). To analyze the potential damages caused by oxidative stress in mitochondrial ultrastructure, transmission electron microscopy (MET) was performed.

Results:

Results. The experiments showed an increase in the enzymatic activity of ATP7B from PALM group compared to the CTRL (CTR = 33 ± 0,6 versus PALM = 52 ± 1,1) with alteration on protein content of SOD 1, 4-HNE, nitrotyrosine and carbonyl reductase markers. Loss of mitochondrial cristae and intense matrix vacuolization were observed in PALM group.

Conclusion:

The results showed that the treatment of HepG2 cells with palmitate increases ATP7B activity, which results in imbalance of copper metabolism, resulting in a consequent alteration on ROS production. The alterations on MET analyses suggest that a high-fat diet could trigger mitochondrial ultrastructural damages in hepatocytes.

Keywords:

Steatosis, Reactive oxygen species, Liver, Superoxide dismutase.

Financial support:

CNPq, FAPERJ, CAPES.

07.040 - CONSEQUENCES OF SATURATED LIPIDS AND/OR CURCUMIN-ENRICHED MATERNAL DIET ON THE METABOLIC AND REPRODUCTIVE PARAMETERS OF ADULT MALE RATS. Reame V, Correia JT, Negrin AC, Pinto-Fochi ME, Amaro GM, Scarpelli TP, Góes RM, - IB (Instituto de Biologia) - UNICAMP Biologia - UNESP

Introduction:

Pre or peri-natal nutrition is critical for development, as it results in a lasting effect and may make the adult predisposed to certain chronic diseases. Previously data from our research group showed that maternal obesity associated with the excess of unsaturated lipids intake reduces the sperm production of rats at adulthood, highlighting that gestation and lactation phases are particularly sensitive.

Aim:

This study evaluated the effects of saturated lipids and/or curcumin-enriched maternal diet on the metabolic and reproductive parameters of adult male rats.

Methods:

Male Wistar rats at 12w old were used (10 animals/group), offspring of mothers without any treatment (C group), treated with a diet rich in saturated lipids (L group), or with standard diet and with curcumin/corn oil (Cm group), or with standard diet and corn oil only (O group), or with diet rich in saturated lipids and curcumin (LCm group). Curcumin was administered orally on alternate days (100mg/kg diluted in 0.1ml of corn oil) from 8th to 12th weeks of the mother's life when mating occurred, being continuous during gestation and lactation. Lipid profile, metabolic and sperm parameters, testicular histology, testosterone and estradiol serum levels and the activity of antioxidant enzymes were analyzed. The data were tested according to Kolmogorov-Smirnov assumptions of normality and homogeneity of variances in GraphPad Prism 6.1 software. The parametric data were compared applying one-way ANOVA followed by Tukey (post hoc) and the non-parametric data were compared by applying the Kruskal-Wallis test followed by the Dunn test (post hoc). Data were expressed as mean ± standard error and p <0.05 was considered statistically significant. CEUA Protocol: 140/2016.

Results:

Our data indicated that the diet rich in saturated lipids (L group), during pregnancy and lactation, in adult male offspring led to a slight increase in the diameter of the seminiferous tubules and impaired sperm motility. During pregnancy and lactation, corn oil (O group) decreased testicular weight, increased levels of enzymatic GPx activity, and impaired sperm motility in adult male offspring. Maternal supplementation with curcumin/corn oil (Cm group) increased body weight of adult male offspring and increased immobile sperm count. In the LCm group there was an increased weight body fat, visceral and epididymal fat deposits, testicular weight and adiposity index; however, these changes did not culminate in spermatid damage, since the number of spermatids per testis and DSP were not affected, the sperm

FeSBE Annual Meeting 2019

Poster Sessions and Abstracts

reserve was higher when compared to the group O, and motile spermatozoa were affected mildly, with the increase of spermatozoa without progressive movement. In addition, the enzymatic activity of GPx and SOD increased in these animals. The levels of glucose, triglycerides, total cholesterol and HDL were not altered among the groups.

Conclusion:

The combination of the three components studied here in the LCM group in the maternal diet, during the gestation and lactation periods, led to the programming of adiposity in adult male offspring. Although all the treated groups presented alterations in sperm motility, maternal curcumin intake reduced the harmful effects of the corn oil and saturated lipids in sperm motility at adulthood.

Financial support:

FAPESP(2015/15709-0)/CNPq(308367/2014-6)/CAPES.

07.041 - EFFECTS OF OBESITY INDUCED BY CAFETERIA DIET ON THE ACTIVITY OF THE DBA + LECTIN UTERINE NATURAL KILLER CELLS IN PREGNANT MICE. Amaral RP, Salles ÉSL, Paffaro VA, - Departamento de Biologia Celular e do Desenvolvimento - Universidade Federal de Alfnas

Introduction:

Obesity is a chronic disease considered a worldwide pandemic that has been affecting women at reproductive age. This can be mimicked using nutritional changes before and during pregnancy in animal models. That changes can be caused by foods Cafeteria Diet/Junk food which are able to generate knowledge about the interaction of food and intrauterine environment. Uterine Natural Killer (uNK) cells are the most common leucocytes in the intrauterine environment during pregnancy. These cells are present in the uterus of humans and rodents during gestation and have a very importante role in the production of angiogenic factors and, therefore, in the remodeling of spiral arteries and maintenance of uterine integrity, contributing to the normal development of decidua and placenta. The uNK's were characterized in four morphological subtypes as a function of their maturation stage, more undifferentiated subtype I, subtype II in differentiation, subtype III considered mature and subtype IV, morphologically senescent.

Aim:

This study aims to evaluate the effects of obesity induced by diet Cafeteria on an activity of uNKs during gestation mice.

Methods:

Fourteen swiss mice females were divided in two groups: Cafeteria Diet (CAF) and control diet (CON) and the effects of the Cafeteria Diet consumption 60 days before pregnancy and up to 10th gestation day (gd) were evaluated. Analysis of food intake, weight gain and Lee's Index were performed. The presence and morphology of uNK cells were evaluated using DBA (Dolichos biflorus agglutinin) cytochemistry.

Results:

The results showed that the cafeteria diet was able to induce obesity in the female mice before CAF gestation 5,338 g (+3,04 g) and CON 1,409 g (+3,23 g) ($p = 0,0119$) and during gestation CAF 9.094 (+ 2.15g) and control 5.557 (+ 1.21g) at 10th gd ($p < 0.0001$), and the Lee Index on the 60th day of consumption (dc) CAF 38.55 (+ 0.804g/cm) and CON 35.44 (+ 1.431g / cm) ($p < 0.0001$) at 10th gd CAF 41.34 (+ 1.555g / cm) compared to the control group 36.96 (± 1.391) ($p < 0.001$). In addition, the treatment altered the appearance of the cytoplasmic granules of uNK cells, which appeared to be void, demonstrating the cytotoxic potential of these cells against obesity induced by cafeteria diet.

Conclusion:

Thus, it can be concluded that the consumption of cafeteria diet before and during gestation triggers changes in the maternal uterine environment.

Financial support:

Fapemig

07.042 - METABOLIC SYNDROME HIGH-FAT DIET-INDUCED IN WISTAR RATS. Ohlweiler RVC, Dentz MCV, Rocha DS, Maschio J, Girelli V, Model JFA, Vogt ÉL, Jahn MP, Kucharski LC, - Laboratório de Metabolismo e Endocrinologia Comparada - UFRGS Laboratório de Fisiologia e Farmacologia - UCS

Introduction:

Metabolic syndrome (MetS) is a set of metabolic disorders, such as central obesity, hyperglycemia, hypertension and dyslipidemia. It is a disease primarily associated with lifestyle and it is estimated that a quarter of the world's population has MetS. In this context, the development of an animal model that mimetize this comorbidity in humans is important for pathophysiological studies.

Aim:

Thus, the aim of this study was to develop an animal model of MetS high-fat diet-induced that was capable to mimic the metabolic deterioration observed in humans carrying the disease.

Methods:

Twenty male Wistar rats, 60 days old, were allocated into two groups: normal diet (ND) containing 65% carbohydrates, 12% protein and 4.5% lipids; or high-fat diet (HFD), produced in our laboratory, containing 49% carbohydrates, 8.2% proteins and 31% lipids. Afterwards 60 days of high-fat diet treatment, the animals were euthanized and blood was collected for analysis of lipid profile, glucose, insulin and liver damage. Liver, retroperitoneal adipose tissue (RAT) and soleus muscle were excised for metabolic analysis. Lipogenesis and triglycerides concentration in the liver were assessed. Glucose oxidation, lipogenesis and lipolysis was evaluated in RAT. Glucose uptake was assessed in soleus. Morphometric data were estimated: total body mass (TBM), mass variation and hepatic, RAT and epididymal adipose tissue (EAT) indexes. The University's ethics committee approved the present study (number 31195). The parametric data were analyzed by unpaired T-test and the non-parametric by Mann-Whitney test and a $p < 0.05$ was adopted.

Results:

The high-fat diet induced dyslipidemia, increasing serum total cholesterol concentrations (ND: 59.78 ± 2.10 mg/dL and HFD: 71.00 ± 2.71 mg/dL) and triglycerides (ND: 71.62 ± 23.10 mg/dL and HFD: 221.16 ± 20.04 mg/dL), as well as hyperglycemia (ND: 130.44 ± 2.56 mg/dL e HFD: 174.70 ± 4.38 mg/dL) and hyperinsulinemia (ND: 3.39 ± 0.17 ng/mL and HFD: 4.82 ± 0.25 ng/mL). In the liver, both lipogenesis (ND: 36.55 ± 6.69 $\mu\text{mol/g/h}$ and HFD: 80.56 ± 14.31 $\mu\text{mol/g/h}$) and triglycerides concentration (ND: 1.05 ± 0.05 mg% and HFD: 2.06 ± 0.16 mg%) increased, suggesting development of hepatic steatosis. In RAT there was a decrease in glucose oxidation (ND: 7.23 ± 1.86 $\mu\text{mol/g/h}$ and HFD: 1.15 ± 0.28 $\mu\text{mol/g/h}$) and increased lipolysis (ND: 3.96 ± 0.66 mmol glycerol/L/g/h and HFD: 5.70 ± 0.24 mmol glycerol/L/g/h). To finish, in soleus, a decrease in glucose uptake was observed (ND: 2.07 ± 0.17 t/m and HFD: 1.55 ± 0.06 t/m). Modifications caused by high-fat diet in metabolism of RAT and soleus indicate development of insulin resistance. Although there were no increase in mass variation, there was an increase in mass of adipose tissues (RAT: 58% and EAT: 62%).

Conclusion:

Taking into account these results, it is possible to affirm that the high-fat diet did not only induced dyslipidemia, but also gave rise to hyperglycemia, hiperinsulinemia, changes in body composition and deleterious alterations in metabolism of the liver, RAT and muscle tissues, that characterize obesity, insulin resistance and pre-diabetes. After that, these results suggest the efficacy of the high-fat diet for the development of MetS.

Financial support:

CNPq

FeSBE Annual Meeting 2019

Poster Sessions and Abstracts

07.043 - PROTECTIVE EFFECT OF FUCOIDAN ON ENDOTHELIAL DYSFUNCTION AND ATHEROSCLEROSIS VIA SUPPRESSING OXLDL-INDUCED VASCULAR INFLAMMATION AND OXIDATIVE STRESS. Fernandes-Braga W, Aguilar EC, Dias MTS, Couto NF, Rezende L, Andrade LO, Navia-Pelaez JM, Capettini LSA, Alvarez-Leite JI, - Bioquímica e Imunologia - UFMG Morfologia - UFMG Farmacologia - UFMG

Introduction:

Atherosclerosis is characterized by chronic oxidative stress and inflammatory changes in the vascular tissue. Endothelial injuries caused by oxidized low-density lipoprotein (oxLDL) play a key role in this pathology. Previous studies have shown that fucoidan, a sulfated polysaccharide extracted from brown seaweed, is associated to beneficial effects on the prevention of atherosclerosis. However, the role of fucoidan in regulating vascular endothelial function and atherosclerosis is not well understood.

Aim:

In order to investigate the effect of fucoidan in atherosclerosis, we address the molecular mechanisms involved in protection against vascular cell damage.

Methods:

To test the anti-atherosclerotic effect of fucoidan, eight to ten-week-old male apolipoprotein E-deficient (ApoE^{-/-}) mice were fed during ten weeks with either a high-cholesterol diet (HCD) or standard diet (SD), with or without 1% of fucoidan. At the end of this period, blood samples were collected for biochemical analysis and the aortas for en face quantification of atherosclerotic lesions (Sudan IV staining). To investigate the effect of fucoidan on endothelial dysfunction induced by oxLDL, thoracic aortic rings from wild type mice and human endothelial cells (EA.hy926) were pre-incubated with fucoidan (1, 5 or 10 µg/mL), by 30 minutes before 4 hours of coincubation with oxLDL (50 µg/mL). After incubation, aortic rings were used to perform vascular reactivity studies. EA.hy926 cells were used to perform adhesion assay, and to analyze the cytokines production, adhesion molecules expression and intracellular reactive oxygen species (ROS) generation. Further, we also addressed the correlation between fucoidan and ROS/NF-κB signaling pathway. All animal experiments were approved by the Federal University of Minas Gerais Animals Care and Use Committee according to the Protocol n° 284/2016. Statistical analyses: One-way ANOVA followed by Tukey post-test was performed to compare groups, using the GraphPad Prism 7 software. All data were presented as mean ± standard deviation. Differences were considered statistically relevant at p<.05.

Results:

Fucoidan treatment significantly reduced the lesion area in aorta of ApoE^{-/-} mice fed on a high-cholesterol diet by 42% (HCD 7.61±1.48 vs. HCD+1%Fuc 4.39±1.95, p<.05), without changes between standard diet groups. This result was associated with a decrease in serum levels of total cholesterol (22%; 684.21±133.93 vs. 536.12±74.98, p<.01), triglycerides (35%; 150.52±42.56 vs. 97.80±38.34, p<.01) and non-HDL cholesterol fractions (21%; 663.27±132.73 vs. 512.16±74.77, p<.01). In ex vivo and in vitro studies, we observed that oxLDL reduced acetylcholine (ACh)-induced vasodilation in mouse aorta and increased the inflammatory responses of oxLDL-treated endothelial cells. But the pretreatment with fucoidan reversed oxLDL-induced endothelial dysfunction. Fucoidan reduced the oxLDL-induced monocyte adherence to endothelial cells, production of proinflammatory mediators (MCP-1, IL-6 e TNF), and the expression of adhesion molecules (P-Selectin and VCAM-1). In addition, fucoidan attenuated ROS generation and reduced the NF-κB signaling pathway (decreasing NF-κB phosphorylation).

Conclusion:

Our study demonstrated that fucoidan reduced atherosclerosis in ApoE^{-/-} mice suppressing oxLDL-induced vascular inflammation and oxidative stress. Thus, fucoidan showed a vasoprotective property, suggesting possible therapeutic effects in atherosclerotic diseases.

Financial support:

CAPES, CNPq and FAPEMIG.

07.044 - EVALUATION OF PHENOLIC PROFILE AND ANTIOXIDANT ACTIVITY OF PHENOLICS FERMENTED BY LACTOBACILLI. Braz MVC, Prudêncio ER, Castro RN, Riger CJ, - Bioquímica - UFRJ

Introduction:

Multiple lines of evidence suggest that diets rich in polyphenols may have neuroprotective effects that result in a lower risk of neurodegenerative disorders including Parkinson's Disease (PD). It is characterized clinically by bradykinesia, tremor at rest and postural stiffness. PD is associated with aging and presents accumulation of an intraneuronal protein generating Levy bodies, that leads to selective loss of dopaminergic neurons located in the region of the substantia nigra. Studies indicate that there is a relation of PD with the accumulation of reactive oxygen species (ROS) and mitochondrial dysfunction, contributing to processes that lead to cellular disorders, causing irreversible damage to neuronal regions. The polyphenolic compounds are well known for their ROS scavenging ability, the fact that they can reach the brain leads to the suggestion that they may alleviate neurodegeneration via additional protective mechanisms. Recent studies indicate that the antioxidant activity of phenolics can be modified by microbial fermentation, since the beneficial effects of phenolic compounds can be related, in part, to their metabolites.

Aim:

The objective of this study was to evaluate the influence of the incubation of phenolic compounds with probiotics on the antioxidant activity of these phenolics using *Saccharomyces cerevisiae* control and mutant cells.

Methods:

In order to evaluate if the fermentation influences the antioxidant activity of phenolics compounds, CAPE and mangiferin were exposed to probiotics with incubation by contact of 0.1 mM of CAPE and mangiferin with 10⁸ cells.L-1 of probiotic blend Babybiotic®. The phenolic profile was determined before and after fermentation by HPLC/DAD. The antioxidant activity was evaluated in *Saccharomyces cerevisiae* cells (2 mg) after treatment with 0.1 mM phenolics (fermented or not) for 2 hours. Then, cells were exposed to hydrogen peroxide (2.0 mM) for 1 hour, diluted, and plated in YPD medium (agar 2%, glucose 2%, yeast extract 1%, and peptone 2%). The results were compared with negative (non-stressed) and positive (only stressed with H₂O₂) controls.

Results:

Chromatograms obtained by HPLC indicate that 50% of CAPE was converted to its precursors caffeic acid and quinic acid, probably due to esterases produced by the bacteria. On the other hand, only 0.3% of mangiferin was converted into other products. In BY4741 strain (control strain) CAPE, fermented CAPE and mangiferin promoted increased viability, reaching about 60% survival, compared to 40% of the positive control. Fermentation decreased the activity of mangiferin, since this treatment did not promote tolerance to oxidative stress. When the Δctt1 strain was evaluated, CAPE maintained the survival of the positive control (60%) while the remaining treatments were slightly toxic (40% survival). Similar profile was observed in strain Δgsh1, with the difference that fermented mangiferin was highly toxic to cells, inhibiting yeast growth, while others were similar to peroxide-stressed cells (20% survival). The same methodology will be used to analyze the influence of mutant strain superoxide dismutase strain (Δsod1).

Conclusion:

The results show that phenolics behave in different ways according to the deletion in the defense system. In general, fermentation has retained antioxidant activity of CAPE, but reduces the activity of mangiferin. Although HPLC analysis has shown that only a small fraction of mangiferin has been modified, other components of bacterial metabolism may be influencing the antioxidant activity of the phenolics tested.

Financial support:

FAPERJ, CNPQ, CAPES

FeSBE Annual Meeting 2019

Poster Sessions and Abstracts

07.045 - SUPPLEMENTATION WITH ASCORBIC ACID PROMOTES RECOVERY OF MUSCLE GROWTH AND PHENOTYPE IN JUVENILE PACUS (PIARACTUS MESOPOTAMICUS) SUBMITTED TO FASTING. Magiore IC, Zanella BTT, Duran BOS, Valente JS, Salomão RAS, Mareco EA, Carvalho RF, Paula TG, Dal-Pai-Silva M, - Morfologia - UNESP Biologia - UNOESTE

Introduction:

Pacu (*Piaractus mesopotamicus*) is a fish with economic importance for Brazilian aquaculture and is a model to analyze muscle growth, due to its fast growth. Muscle phenotype is controlled by protein synthesis and degradation pathways, which can be modulated by extrinsic factors, including fasting. Physiological stress caused by low nutrient intake may trigger the production of reactive oxygen species (ROS), which cause cell damage if not controlled. To minimize the negative effects of this process, antioxidants such as ascorbic acid (AA) can be supplemented in the fish diet.

Aim:

In this work, we aimed to evaluate the AA supplementation effects on pacu skeletal muscle submitted to a stress situation (fasting). We hypothesized that the animals over supplemented with AA would show better growth parameters and recovery the muscle phenotype.

Methods:

Juvenile pacus (≈ 30 g; n=8/group) were grouped in: Control (continuous feeding) and three refeeding groups for 15 days with different AA levels, after 15 days of fasting: Low (100mg/kg), Regular (200mg/kg) and Over supplementation (400mg/kg); (ethical committee protocol 1050). Skeletal muscle samples were collected for histological and molecular analyses. Muscles samples were stained with hematoxylin and eosin; muscle fibers were measured and distributed into classes according to the diameters (μ m). Gene markers for myogenesis and metabolism were evaluated by RT-qPCR. Statistical analyses were performed using the ANOVA test ($p < 0.05$) for comparisons between groups.

Results:

Compared to the Control, the Low and Regular AA supplementation groups showed a higher number of fibers in the smallest diameter class (10–20 μ m) and a lower number in the largest class ($\geq 40\mu$ m), while the Over supplementation group showed a distribution pattern similar to Control. The expression of *pgc1a* (mitochondrial biogenesis) showed a 0.44-fold increase in the Regular and Over supplementation compared to the Low group. *Myod* expression (muscle cell proliferation) was 0.19-fold upregulated in the Over supplementation when compared to the Low and Regular supplementation groups, while *myogenin* (muscle cell differentiation) was 0.36-fold downregulated in the Regular and Over supplementation compared to the Control and Low groups. The expression of *mtor*, *rragc*, and *rps6kb1a* (muscle anabolism) were downregulated in the Low group compared to the other groups, with 0.32-fold decrease for *mtor* compared to the Control group, 0.29-fold decrease for *rragc* compared to the Over supplementation, and 0.24-fold decrease for *rps6kb1a* compared to the other groups. The *murf1a* (muscle catabolism) had a 0.36-fold decrease in all groups compared to Control, and the *mafxb* expression (muscle catabolism) was 0.57-fold downregulated in the Low group compared to the Control and Regular groups.

Conclusion:

Our data suggest that the animals fed with the lower level of AA failed to recover muscle metabolism, as seen by the generally reduced gene expression, while the fish over supplemented with AA obtained better conditions for muscle cell proliferation, recovering growth and muscle phenotype.

Financial support:

FAPESP 2019/06708-1, 2017/26346-1; CNPq 148108/2018-0

07.046 - EFFECT OF PHYSICAL TRAINING ON RETROPERITONEAL ADIPOSITY OF WISTAR RATS FED A HIGH-FAT DIET SINCE POST-WEANING. Komoni G, Pereira RO, Correia LA, Evangelista FS, Fiorino P, Farah V, - Laboratório de Fisiologia Metabólica Cardiovascular e Renal - UPM Departamento de Medicina - UNIFESP Escola de Artes, Ciências e Humanidades - EACH USP

Introduction:

High-fat diet may cause several morphological and functional modifications, especially when the high-fat intake begins in childhood. Data from our group showed that there was adipocyte hypertrophy and an increase in visceral adipose tissue weight of adult Wistar rats fed a high-fat diet since post-weaning. Furthermore, it is known that the aerobic exercise training (AET) is an alternative for the prevention and treatment of several metabolic diseases.

Aim:

The purpose of this study was to evaluate the potential of AET to prevent morphological alterations in the retroperitoneal adipose tissue induced by the high-fat diet intake since early period of life.

Methods:

Male post-weaned Wistar rats (50-60g) were separated into 4 groups (n=4/group): Normal diet Sedentary (NS, 3,5% lipids and 2,57 kcal/g), High-fat diet Sedentary (HS, 30% lipids and 3,81 kcal/g), Normal diet Trained (NT) and High-fat diet Trained (HT) and followed during 12 weeks. AET was performed since the 5th week of protocol and consisted of 8 week treadmill sessions of 60 minutes at 60% of maximal speed, 5 days/week. Individual food and caloric intake were evaluated by metabolic cage during the last 24 hours of the protocol. Glucose tolerance test (GTT) after glucose intraperitoneal injection (0,3mL/100g body weight) was performed at the 10th week of the protocol. Insulin tolerance test (ITT) calculated by the rate constant for the disappearance of plasma glucose (kITT) was evaluated at the 11th week. After euthanasia, retroperitoneal adipose tissue was collected, weighted, fixed with 4% buffered formaldehyde and embedded in paraffin. Sections from adipose tissue (6 μ m) were stained with Hematoxylin-Eosin. Digital images were taken (microscope Leica DM 1000) and analysed using Image Pro-Plus 4.1. Results were presented as mean \pm standard error of the mean. Statistical analysis were performed using two-way ANOVA and Tukey post-hoc test ($P \leq 0.05$). Ethics Committee of Mackenzie (166/03/2018).

Results:

The food intake was reduced in HS and HT compared to NS and NT (HS: 14 \pm 2; HT: 12 \pm 1; NS: 18 \pm 2; NT: 20 \pm 1 g). However, there was no difference in caloric intake. High-fat diet promoted glucose intolerance in HS (195 \pm 6 AUC/min) compared to NS group (160 \pm 9 AUC/min). AET was able to prevent glucose intolerance in HT (175 \pm 8 AUC/min). No difference was observed in ITT. The AET prevented the increase in retroperitoneal fat pad (HS: 1.7 \pm 0.1; HT: 1.1 \pm 0.3; NT: 0.3 \pm 0.1 vs. NS: 0.6 \pm 0.1 g/cm), the increase in adipocyte area (HS: 4207 \pm 260; HT: 3558 \pm 363; NT: 2353 \pm 146 vs. NS: 2549 \pm 144 μ m²) and the increase in adipocyte diameter (HS: 83 \pm 2; HT: 75 \pm 4; NT: 60 \pm 2 vs. NS: 64 \pm 2 μ m) induced by high-fat diet.

Conclusion:

The AET was able to prevent the morphological alterations in the adipocytes of the retroperitoneal adipose tissue of adult rats submitted to the high-fat diet since post-weaning.

Financial support:

CAPES, Mackpesquisa

07.047 - EFFECTS OF GUARANA ON RENAL MORPHOLOGICAL ALTERATIONS IN RATS WITH DIABETES MELLITUS. HISTOMORPHOMETRIC AND STEREOLOGICAL STUDY. Corrêa LBNS, Picanço JR, Abboud RS, Ribeiro ICA, Silva VAP, Boaventura GT, Chagas MA, - Morfologia - UFF Nutrição - UFF

Introduction:

FeSBE Annual Meeting 2019

Poster Sessions and Abstracts

Diabetes Mellitus is a severe pathology marked by hyperglycemia resulting in chronic complications among them the impairment of renal morphophysiology. Hyperglycemia promotes increased production of reactive oxygen species (ROS) that lead to renal dysfunction, especially diabetic nephropathy. The guarana contains high concentration of polyphenols, considered a potential antioxidant and may favor the inhibition of ROS.

Aim:

This study aims to observe the action of guarana on glycemic levels, body weight and renal morphology of diabetic rats.

Methods:

The study was approved by the Animal Research Ethics Committee of Federal Fluminense University (Protocol 972/2018). We used 28 Wistar rats divided into 4 groups: Control (CG), Diabetic control (DCG), Guarana (GG) and Diabetic Guarana (DGG) group. The Guarana groups received the dose of 5g/kg guarana in the commercial feed. Diabetic groups were induced after administration of streptozotocin (100 mg/kg) and confirmation of hyperglycemia 72 hours after injection. Glucose and body weight of the animals were evaluated weekly. At the end of 8 weeks of consumption, the rats were euthanized, and the left kidneys were collected and fixed, at first, Bouin for 5 hours and subsequently, in 10% formalin. The material was cross-sectional and processed in paraffin-embedded method, stained with Hematoxylin and eosin. Histological images were prepared for histomorphometric and stereological measurements. We evaluated the renal corpuscle (RCA), glomerular (GA) and capsular space (CSA) areas of 75 glomeruli of each kidney. The percentage of the volumetric density of glomerular (VvG) and tubular lesions of the cortical (VvTL) were analyzed using a M42 grid system. Statistical analyzes were obtained with oneway ANOVA, considering significant $p < 0.05$.

Results:

The glycemic levels of DCG and DGG were higher than CG and GG ($P < 0.0001$). The results between DGG (541.69 ± 27.78 mg/dL) and DCG (553.338 ± 27.74 mg/dL) were not significant. Control groups (CG and GG) gained body mass after 60 days of consumption compared to diabetic groups. The DCG and DGG did not present significant differences in relation to the body weight of the rats ($p > 0.05$). In the means of the glomerular areas, the DCG had mean RCA, GA and CSA inferior to the CG and GG ($P < 0.0001$). DGG showed a significant increase in RCA, GA and CSA compared to DCG ($P < 0.0001$), being not significant in relation to CG and GG ($p > 0.05$). The percentage of VvG was lower in DCG compared to the control groups ($p < 0.0001$). DGG showed an increase ($1.42 \pm 0.10\%$) in the percentage of significant glomerular density compared to DCG ($1.06 \pm 0.09\%$). Regarding the percentage of VvTL, the DCG presented a lower percentage ($2.5 \pm 0.52\%$) compared to the DGG ($2.74 \pm 0.38\%$), but not significant.

Conclusion:

Hyperglycemia and consequent diabetic nephropathy were observed in the study. Hyperglycemia and body weight were not altered by the use of guarana in the diabetic group. However, the administration of guarana promoted a significant improvement at the glomerular level, reducing the loss rate by about 25%. There was no action on the percentage of tubular lesions in cortical volume. Thus, the continuous consumption of guarana during diabetes favored renal physiology, decreasing glomerular loss.

Financial support:

Coordenação de Aperfeiçoamento de Pessoal de Nível Superior (CAPES)

07.048 - HYDROALCOHOLIC EXTRACT OF SYZYGIUM CUMINI LEAVES IMPROVES GLYCOLIPID METABOLISM OF RATS FED A HIGH-SUCROSE DIET. Vieira VA, Silva MU, Filho GHL, Melo GB, Costa TCL, Miranda JPN, Ribeiro NLX, França LM, Pinto BAS, Cappelli APG, Paes AMA, - Departamento de Ciências Fisiológicas - UFMA

Introduction:

Background: The highest consumption of foods rich in simple sugars (e.g. glucose and fructose), especially in childhood, is directly involved with the higher prevalence of the metabolic syndrome (MS) in the world. Insulin resistance is one of the main pathophysiological mechanisms of MS, since it favors the development metabolic pathologies such as dyslipidemias and type 2 diabetes mellitus. Polyphenols have been highlighted as an alternative for the treatment of these metabolic disorders. In this context, we have studied the plant species *Syzygium cumini*, a rich source of these compounds and traditionally used to control SM. However, there is a lack of studies that evaluate the effect of this species on animal models of human-like SM.

Aim:

Therefore, the objective of this work was to evaluate the effect of the hydroalcoholic extract of *Syzygium cumini* (EHSc) leaves on glycolipid disorders of rats fed a sucrose rich diet.

Methods:

Methods: For this, weaned Wistar rats were fed standard feed (CTR, $n = 7$) or sucrose-rich diet (DRS, $n = 14$) up to 90 days of age. The DRS group was then divided into 2 groups (DRS and SYZ). SYZ animals ($n = 7$) were treated (v.o) daily with EHSc (0.5 g / kg) for 4 weeks. The CTR and DRS animals ($n = 7$ each) will receive H₂O (0.1 ml / kg) for the same period. During and at the end of treatment, morphometry, serum biochemical profile and glycemic homeostasis by glucose (GTT) and insulin (ITT) tolerance tests were evaluated. All experimental protocols were approved by the UFMA Ethics Committee on Animal Use. Differences among groups were detected at a significance level of 5% ($p < 0.05$) through analysis of variance (ANOVA; Newman Keuls).

Results:

EHSc treatment (SYZ) reduced white adipose fat pads retroperitoneal ($0,92 \pm 0,09$ vs $1,57 \pm 0,08$), periepididymal ($1,27 \pm 0,07$ vs $1,75 \pm 0,06$) and mesenteric ($0,75 \pm 0,10$ vs $1,29 \pm 0,11$), when compared to untreated DRS group. Corroborating with these results, the SYZ group also improves glucose and insulin intolerances induced by excess consumption of sucrose.

Conclusion:

Conclusion: These data demonstrate that the treatment for 4 weeks with the EHSc extract is able to improve the glycolipid metabolism in high-sucrose diet-induced MS rats. Therefore, this work contributes to the validation of *S. cumini* leaves as a potential herbal medicine for the treatment of metabolic disorders induced by diets.

Financial support:

FAPEMA

07.049 - EFFECT OF HIGH-PROTEIN DIET ON GLYCOLIPID METABOLISM OF HIGH-SUCROSE DIET- INDUCED METABOLIC SYNDROME RATS: COMPARISON WITH THE EFFECT OF CALORIC RESTRICTION. PASSOSASC, Melo TM, Costa TCL, Coelho CFF, França LM, Paes AMA, PINTOBAS, - Ciências Fisiológicas - UFMA

Introduction:

Metabolic syndrome (MS) consists of a set of interconnected metabolic dysfunctions such as dyslipidemias and type 2 diabetes mellitus. The premature and excessive consumption of addition sugars has a direct impact on the high prevalence of MS. High-protein diets have been highlighted as a nutritional intervention in the treatment of MS. However, there is a lack of studies that evaluate the effect of this excessive consumption of proteins on MS, especially when compared to caloric restriction.

Aim:

We hypothesized in this study that High-protein diet intervention is capable to revert the deleterious effects induced by sucrose consumption. Thus, the present study investigates the effects of a high-protein diet and its comparison with the caloric restriction on the glycolipid metabolism of rats with MS induced by high-sucrose diet.

Methods:

FeSBE Annual Meeting 2019

Poster Sessions and Abstracts

For this, Wistar male rats with 30 days of life were divided into two groups: one fed with the standard chow (CTR, n=8); and other fed with standard chow and 30% sucrose solution (SS, n=22). At 4 months of age the SS group was divided in three new groups: one that sucrose solution was withdrawn (SS-CTR; n=7); other which continued to receive this solution (SS-SS; n=7); and other which received only the 45% high-protein diet (HP; n=8). These nutritional interventions were performed for 2 months. During and at the end of this intervention the morphometric, biochemical and insulin resistance profiles were evaluated. The results were expressed as mean \pm SEM and the statistical differences were determined when $p < 0.05$ by ANOVA (post hoc Newman-Keuls). All experimental protocols were approved by the Ethical Committee on the Use of Animals under No 23115.017437/2018-28.

Results:

The high-protein diet (HP group) revert the obesogenic phenotype induced by sucrose solution, characterized by reductions in body weight (485.7 ± 11.19 vs 625.5 ± 30.76 g; $p < 0.0001$), central obesity (333.6 ± 1.42 vs 347.2 ± 2.1 g/3/cm x 1000; $p < 0.01$), triglycerides levels (65.62 ± 11.34 vs 240.8 ± 39.73 mg/dL; $p < 0.0001$) glucose intolerance and insulin resistance (2.57 ± 0.31 vs 0.93 ± 0.27 kitt %/min; $p < 0.05$). Additionally, the sucrose solution withdrawal (SS-CTR group) promoted in a similar way reductions in body weight (486.3 ± 12.82 g; $p < 0.0001$), central obesity (334.9 ± 2.54 g/3/cm x 1000; $p < 0.01$), triglycerides levels (88.4 ± 11.4 mg/dL; $p < 0.0001$), glucose intolerance and insulin resistance (1.61 ± 0.29 vs 0.27 kitt %/min; $p < 0.05$). Finally, it is noteworthy that there were no differences between the higher protein intake (HP) and the sucrose solution withdrawal (SS-CTR) in all parameters evaluated.

Conclusion:

With these results, it was observed that there is no difference between protein supplementation and caloric restriction in animals with higher sucrose intake. Therefore, this study ratifies the importance of caloric restriction as a first-choice nutritional intervention for the treatment of metabolic disorders, mainly associated with high sugar intake.

Financial support:

Fundação de Amparo à Pesquisa e Desenvolvimento Tecnológico do Maranhão

07.050 - EFFECTS OF ORAL ADMINISTRATION OF EICOSAPENTAENOIC (EPA)-RICH OIL ON WOUND HEALING IN DIABETIC MICE.. Burger B, Candreva T, Sagiorato RN, Silva JR, Pacheco M, Consonni SR, Vinolo MAR, Rodrigues HG, - SP - Universidade Estadual de Campinas

Introduction:

Delayed wound healing is a common complication of diabetes. Tissue repair requires the migration and proliferation of cells into the wounded area to restore the original density of the tissue. It is known that omega-3 fatty acids (ω -3) have immunomodulatory effects in pathophysiological conditions. Recently, we showed that eicosapentaenoic acid (EPA)-rich oil delayed the wound healing in healthy mice. However, the effects are not clear on diabetic tissue repair.

Aim:

So, our aim was to evaluate the effects of oral administration of EPA-rich oil on wound healing in diabetic mice.

Methods:

Diabetes was induced by administration of streptozotocin during 5 consecutive days. Mice with the glycemia ≥ 240 mg/dL were considered diabetic. Mice were separated into: (C) Control; (D) diabetic and (ED) diabetic that received 50 μ L of EPA-rich oil. After 4 weeks of supplementation, a wound was induced in the dorsum of the animals, and the tissue was collected for histological, flow cytometry and ELISA analysis at different time points (Ethical committee approval number: 4975-1/2018). Statistical analyses were performed using GraphPad Prism 5. Significance of difference was analyzed using One-way ANOVA.

All data are presented as mean \pm SD and $p < 0.05$ was considered significant.

Results:

In diabetic (D) mice, it was observed a delay in wound closure at 3rd (26,6%) and at 7th (31%) days after wound induction in comparison with control group (C). Under qualitative histological analysis the D animals also presented a delayed in granulation tissue formation and an increase in inflammatory infiltrate and edema between muscular layers in comparison with C. Moreover, we observed 1,17-fold increase of CXCL2 and 68% augmentation of MMP9 concentrations in D in comparison with C-group. These pro-inflammatory effects were maintained until the tenth day post-injury. The oral administration of EPA-rich oil to diabetic mice reduced the epithelial gap, 3 days after wound induction, in comparison with D (D: $100 \pm 10,8$; ED: $76,9 \pm 15,2\%$ in relation to D). There was also an increase of M2 macrophages 1 day after wound induction in ED animals in relation to D. This anti-inflammatory effects was followed by a reduction in IL-1 β concentrations (39,6%) and an improvement of granulation tissue formation in ED in relation to D. After 10 days, diabetic animals presented a increase of pro-Inflammatory in relation to C group.

Conclusion:

Anti-inflammatory effects of EPA-with oil supplementation improved the wound healing in diabetic mice.

Financial support:

Financial support: FAPESP, CNPq and FAEPEX/UNICAMP. This study was financed in part by the Coordenação de Aperfeiçoamento de Pessoal de Nível Superior - Brasil (CAPES) - Finance Code 001`

07.051 - FRUCTOSE-INDUCED OBESITY AND INSULIN RESISTANCE: PHENOTYPIC AND METABOLIC FEATURES IN OUTBRED SWISS MICE. Barreira RM, Gonçalves LF, Fernandes-Santos C, - Departamento de Ciências Básicas - UFF

Introduction:

Obesity is a major risk factor for type 2 diabetes (T2D), cardiovascular diseases (CVD), and cancer. Several rodent models of obesity were developed to understand the metabolic pathways and histopathologic changes, and the inbred C57Bl/6 mice fed with a high-fat or a high-fat high-sucrose diet has been widely used and characterized as a model of obesity and diabetes. However, the acquisition of purified diets according to the American Institute of Nutrition (AIN93) recommendations might be a limitation since it can be expensive when the experiment requires a large number of mice or for long-term experiments that require phenotype induction and then mice treatment. Nowadays, there is a large body of evidence that in Humans sugar consumption promotes CVD and T2D, and that it would be caused by fructose. Thus, fructose offering to rodents might be an alternative to lower experiment cost, but literature is contradictory regarding its dose, time required for phenotype induction, and rodent strain.

Aim:

To standardize a rodent model of fructose-induced obesity and metabolic disturbances in an outbred mice strain (Swiss mice).

Methods:

After reviewing the literature, it was chosen to offer fructose for eight weeks in the drinking water at two concentrations (20% [F20] and 30% [F30]). Control (C), F20, and F30 groups (n=5/groups) Swiss female mice received tap water ad libitum (C) or fructose diluted in the drinking water. Water, food intake, and body weight (BW) were measured weekly. Glucose metabolism was analyzed by oral glucose tolerance (OGTT) and intraperitoneal insulin tolerance tests (IPITT). At euthanasia, blood was withdrawn, and tissues weighed. Data are expressed as mean \pm SD and 1-way ANOVA and Holm-Sidak's multiple comparisons ($p < 0.05$).

Results:

Average water intake for C group was 5.79 ± 1.01 mL/mouse, and it increased by 64% and 43% in F20 and F30 groups, respectively

FeSBE Annual Meeting 2019

Poster Sessions and Abstracts

($P < 0.0001$). Unexpectedly, water intake was smaller in F30 compared to F20 groups (-13%, $P < 0.01$). As a consequence, ΔBW was higher in F20 (11.8 \pm 3.06g) compared to both F30 (7.5 \pm 2.11g, $P < 0.05$) and C (2.9 \pm 1.09g, $P < 0.001$) groups. White ovarian (F20=4.14 \pm 1.02g vs. C=1.12 \pm 0.35g $P < 0.001$ and F30=2.07 \pm 1.20g, $P < 0.01$), inguinal (F20=2.30 \pm 0.61g vs. C=0.94 \pm 0.29g $P < 0.01$) and brown interscapular fat depots (F20=0.42 \pm 0.17g vs. C=0.17 \pm 0.05g $P < 0.01$, F30=0.24 \pm 0.04) also increased in F20 group. Although blood glucose was similar among groups, F20 mice were intolerant to glucose and displayed insulin resistance (OGTT AUC +27% $P < 0.01$ and IPITT AUC +42% $P < 0.05$ vs. C). Total cholesterol (165.3 \pm 20.8mg/dL vs. C=114.2 \pm 25.6mg/dL $P < 0.05$), LDL (139.5 \pm 23.8mg/dL vs. 95.7 \pm 24.4mg/dL $P < 0.05$), and HDL (10.0 \pm 2.7mg/dL vs. 5.4 \pm 2.2mg/dL) increased compared to C group. Only HDL also increased in the F30 group (10.1 \pm 1.9mg/dL). Finally, blood levels of triacylglycerol and hepatic enzymes (ALT, AST, GGT) were not changed by fructose consumption.

Conclusion:

Current data showed that 20% fructose in the drinking water for eight weeks is suitable for diet-induced obesity and disturbances of glucose and lipid metabolism. Also, fructose effect is dependent on water intake, since mice reject water with high fructose dose (30%). Next steps are to characterize the male phenotype and the histopathological and molecular changes in tissues enrolled in body metabolism.

Financial support:

CAPES

8 - Renal Biology and Diseases

08.013 - EFFECTS OF ANGIOTENSIN-(3-4) IN BODILY NA⁺ BALANCE, RENAL NA⁺-ATPASE RENAL AND BLOOD PRESSURE OF UNDERNOURISHED MALE RATS.. Acacio AP, Nossar LF, Sarmiento GC, Silva PA, Muzi-Filho H, Vieyra A, - Centro de Ciências da Saúde - UFRJ Programa de Pós Graduação em Biomedicina Translacional - Unigranrio

Introduction:

Chronic undernutrition (CU) results from insufficient intake of various nutrients, which are needed for the body's demands. It promotes structural and functional changes in organs and tissues, especially cardiovascular and renal injuries. Systemic arterial hypertension (SAH) is frequently observed, associated with upregulation of the Renin-Angiotensin System (RAS). In recent years, our laboratory characterized Ang-(3-4) - the smallest angiotensin-derived peptide - as a physiological counterregulator of Ang II effects mediated by type 1 receptor (AT1R). Ang-(3-4) is an allosteric activator of AT2R, with antihypertensive effects in the case of RAS upregulation and stimulation of AT1R signaling.

Aim:

The aim of this study was to investigate the effects of Ang-(3-4) on the changes that CU provokes in renal Na⁺ handling and SAH.

Methods:

Experimental design was approved by the Ethics Committee for the Use of Animals in Research at UFRJ (007-16). We used 4 groups of male rats from weaning (at 28 days) until 90 days of age (young adults): CTRL (commercial diet only), CTRL+Ang-(3-4) (commercial diet + 1 dose of 80 mg/kg Ang-(3-4) per gavage at day 89), CU (receiving a deficient diet that mimics dietary habits in vast impoverished regions of developing countries, the 'Basic Regional Diet'), and CU+Ang-(3-4).

Results:

We measured Na⁺ intake, [Na⁺]pl, daily urinary Na⁺ excretion (UVNa), and Na⁺-ATPase activity of renal proximal tubules and systolic blood pressure (SBP) (n=4-8 depending on the group) at 90 days. When compared to CTR, CU did not change Na⁺ intake ($P = 0.2548$) or [Na⁺]pl when compared to CTR ($P = 0.4028$), but reduces [Na⁺]ur (25%, $P = 0.0030$, n=5-7). In CU rats, Ang-(3-4) decreased Na⁺ ingestion and [Na⁺]pl (30%, $P = 0.0013$, and 20%, $P < 0.0001$, respectively), without modifications in UVNa ($P = 0.1612$). In CTR rats, Ang-(3-4) decreased Na⁺

ingestion and [Na⁺]pl only by 15% ($P = 0.0409$) and 10% ($P = 0.0156$), whereas it increased UVNa by 30% ($P = 0.0279$). CU presented with elevated SBP (in mmHg): 147 \pm 0.3 vs. 123 \pm 0.4 in CTRL ($P < 0.0001$). Ang-(3-4) reduced SBP to 133 \pm 0.6, ($P < 0.0001$) (n=9-24). Ang-(3-4) did not modify SBP in CTRL rats ($P = 0.9351$).

Conclusion:

Ang-(3-4) emerges as a powerful regulator of corporal Na⁺ handling by decreasing Na⁺ ingestion (acting on central nervous system) and increasing Na⁺ excretion (acting at renal tubular levels). Its single-dose hypotensor effect only in the hypertensive CU group, and its more accentuated influence in Na⁺ intake leading to intense hyponatremia, allows to propose - as we previously demonstrated with spontaneously hypertensive rats - that Ang-(3-4) actions via AT2R are potentiated when the AT1R pathway is upregulated.

Financial support:

CNPq, CAPES, FAPERJ, INCT, FINEP

08.014 - HYPOTENSIVE EFFECTS OF NPCDC, A NEW NATRIURETIC PEPTIDE, ARE MEDIATED BY INCREASED VASCULAR LEVELS OF NO AND INCREASED RENAL FRACTIONAL NA⁺ EXCRETION IN RATS SUBJECTED TO 5/6 NEPHRECTOMY. Aires RS, Sousa SM, Freitas AC, Lima ME, Lima NKS, Farias JS, Paixão AD, Vieira LD, - Departamento de Fisiologia e Farmacologia - UFPE Departamento de Bioquímica e Imunologia - UFMG

Introduction:

NPCdc is a synthetic natriuretic peptide originally obtained from *Crotalus durissus cascavella* venom. This peptide presents anti-hypertensive and natriuretic effects which could be beneficial in the cardiorenal syndrome.

Aim:

This study aimed to investigate the mechanism of action by which NPCdc induces hypotension in rats subjected to 5/6 nephrectomy, a model of chronic renal failure, and whether the effects are dependent of nitric oxide (NO) levels modulation and NADPH oxidase inhibition.

Methods:

The Committee for Ethics in Animal Experimentation at the Federal University of Pernambuco approved the experimental protocol (nº 23076.016262/2015-01). Male Wistar rats (300 \pm 20 g) were submitted to a fictitious surgery (sham group, n=17) or to 5/6 nephrectomy (5/6Nx group, n=19). After 15 days of surgery, the animals were anesthetized (thiopental, 60 mg/kg, i.p) and surgically prepared to the infusion of NPCdc (7.5 μ g/kg/min) and evaluation of parameters hemodynamics. The mean arterial pressure (MAP) was measured through a catheter inserted in the left femoral artery. The glomerular filtration rate (GFR) was assessed by inulin clearance. After renal hemodynamic evaluation, the kidneys and thoracic aorta were collected. In the kidney, it was evaluated the activities of ouabain-sensitive (Na⁺K⁺)ATPase and furosemide-sensitive Na⁺-ATPase in the proximal tubule. NADPH oxidase was evaluated in both renal cortex and aorta. In the aorta, it was investigated nitric oxide (NO) levels (by Griess Reaction), as well as the total and phosphorylated protein levels of neuronal (nNOS), endothelial (eNOS) and induced (iNOS) nitric oxide synthase. Differences between groups were analyzed using two-way ANOVA followed by the Holm-Sidak multiple comparisons test. Differences between groups were considered significant at $P < 0.05$.

Results:

Intravenous infusion of NPCdc decreased (13-21% $P < 0.01$) MAP and increased GFR (111-130% $P < 0.001$) in both groups sham and 5/6Nx. The fractional Na⁺ excretion (73% $P < 0.01$) was increased in the 5/6Nx group when compared to sham group. The peptide lowered (27% $P < 0.01$) proximal tubule (Na⁺-K⁺)ATPase activity only in sham group, while it increased (50-70%, $P < 0.01$) Na⁺-ATPase activity in both groups. On the other hand, NPCdc decreased (26-42%, $P < 0.05$) NADPH oxidase activity in aorta and kidney of 5/6Nx group but not in sham group. It was also observed that NPCdc induced elevation (66-166%, $P < 0.001$) of nitric

FeSBE Annual Meeting 2019 Poster Sessions and Abstracts

oxide levels in the aorta from both groups, however it did not alter the protein content of p-eNOS, p-nNOS, and p-iNOS.

Conclusion:

In the 5/6Nx group, NPCdc led to a decrease of arterial pressure that occurred in parallel to renal hemodynamic changes related to increased salt excretion, albeit it did not lowered (Na⁺-K⁺)ATPase activity. On the other hand, the peptide effects on the aorta seem to be mediated by elevation of NO bioavailability due to inhibition of NADPH oxidase activity. Collectively, these results point to a potential therapeutic application of NPCdc in cardiorenal syndrome.

Financial support:

FACEPE, CNPq and CAPES.

08.015 - ENDOTHELIAL FUNCTION PROFILES IN RESISTANCE ARTERIES IN TWO DIFFERENT MOUSE MODELS ORTHOLOGOUS TO AUTOSOMAL DOMINANT POLYCYSTIC KIDNEY DISEASE TYPE 1. Dourado VC, Rossoni LV, Onuchic LF, - Departamento de Fisiologia e Biofísica - Universidade de São Paulo Departamento de Clínica Médica - Universidade de São Paulo

Introduction:

Autosomal dominant polycystic kidney disease (ADPKD) is the most common monogenic kidney disease. Among the genetically resolved cases, ~85% are caused by mutations in the PKD1 (Polycystic Kidney Disease 1) gene while ~15% occur due to mutations in PKD2. Although the renal phenotype prevails in ADPKD, the disease is systemic, also including extra-renal manifestations. Hypertension is observed in 50-70% of patients before a significant reduction in renal function. Using a mouse model heterozygous for a Pkd1 null mutation (Pkd1^{-/-}), a previous study detected endothelial dysfunction in conductance arteries only at an old age (30 weeks). Endothelial function, however, has not been investigated in resistance arteries (RA) in this and other Pkd1-deficient animal models. This characterization may elucidate potential alterations in the regulation of peripheral vascular resistance in ADPKD.

Aim:

To characterize the phenotype of RA associated with ADPKD, with emphasis to endothelial function, using genetically-modified mouse models orthologous to ADPKD type 1.

Methods:

We evaluated two Pkd1-deficient models: normotensive non-cystic Pkd1^{+/-} mice (HT) and their corresponding wild-type controls (Pkd1^{+/+}, WT), and hypertensive cystic Pkd1^{cond/cond}:Nestin^{cre} mice (CY) and their corresponding non-cystic controls (Pkd1^{cond/cond}, NC). Both models were on the C57BL/6 background. All experiments were performed in male mice, sacrificed by cervical dislocation at 8-12 weeks under the Ethics Committee approval numbers 901/17 and 1233/19. Serum urea nitrogen (SUN) was measured using an enzymatic-colorimetric method. Cardiac (CMI) and renal mass index (RMI) refer to the ratios between cardiac mass (ventricles) or renal mass and body weight (BW). Rings of first branches of mesenteric RA (diameters: WT 214±5.1 vs. HT 204±12.3 μm; NC 188±5.02 vs. CY 186± 5.13 μm) were dissected and mounted on a wire myograph. Endothelium-dependent and -independent relaxation were analyzed by means of concentration-response curves to acetylcholine (ACh; 10⁻⁹-10⁻⁵M) and sodium nitroprusside (SNP; 10⁻¹¹-10⁻⁵M), respectively. Statistical analyzes: Student's t-test or two-way ANOVA (p<0.05 *vs. WT; #vs. NC).

Results:

BW, RMI, CMI and SUN did not differ between WT and HT mice. In contrast, SUN and RMI were higher in CY than NC animals (NC 23.0±0.9 vs. CY 36.3±2.0 mg/dL#; and NC 0.69±0.02 vs. CY 1.21±0.32%#, respectively). CMI and BW did not differ between these groups. No differences in ACh- and SNP-induced relaxation (Maximum response; MR) were observed between WT and HT animals (WT 94±1.05 vs. HT 93±1.55%; and WT 99±0.97 vs. HT 99±0.26%; respectively). CY mice, on the other hand, displayed impaired ACh-induced relaxation compared

to NC (NC 46±7.10 vs. CY 22±5.35%#), while no difference in SNP-induced relaxation was observed (NC 100±0.82 vs. CY 96±2.71%).

Conclusion:

Mosaic inactivation of both copies of Pkd1 led to endothelial dysfunction in RA, a phenotype not induced by Pkd1 haploinsufficiency at the evaluated age. Smooth muscle-mediated relaxation, however, was not affected by either Pkd1-deficiency profiles. The endothelial abnormality observed in cystic mice may be a primary dysfunction or secondary to chronic hypertension, a matter of current investigation. This analysis may significantly contribute to improve the elucidation of hypertension pathogenesis in ADPKD.

Financial support:

FAPESP, CNPq.

08.016 - ANGIOTENSIN-(3-4) REVERSES THE INCREASED ACTIVE SODIUM TRANSPORT IN PROXIMAL TUBULES AND THE HIGH BLOOD PRESSURE IN OVERWEIGHED RATS WITH DECREASED GLUCOSE TOLERANCE. Luzes R, Crisóstomo TTA, Lima-Gonçalves ML, lack RL, Genelhu VA, Francischetti E, Silva PA, Vieyra A, - Programa de Pós-Graduação em Biomedicina Translacional - UNIGRANRIO Programa de Pós-graduação em Química Biológica - UFRJ

Introduction:

The pandemic obesity represents a global health problem, being an important risk factor when associated with other comorbidities like hypertension. We investigated whether a chronic hyperlipidic diet causes alterations in blood pressure in combination with changes in renal Na transporting ATPases and altered glucose metabolism.

Aim:

Investigate whether angiotensin-(3-4) (Ang-(3-4)), the smallest angiotensin-derived peptide, could revert the hypertension and possible alterations in active Na transporters.

Methods:

Male Wistar rats received a high lipid diet (HL, 70% calories from fat) or control diet (CTR, 10% calories from fat) during 108 days from 58th day of life. In the last 2 days, the animals were housed in metabolic cages and received 4 oral doses of 80 mg Ang-(3-4)/kg body mass (BM). We measured BM, heart, liver, kidney, epididymal and perirenal fat weight, systolic blood pressure (SBP, pletismography), creatinine and glucose in plasma (commercial kits), renal (Na⁺+K⁺)-ATPase and Na-ATPase activities (Pi release by spectrophotometry), together with [Li]pIs and [Li]ur (to calculate Li clearance LiCl) (flame photometry). The Committee for Ethical Use of Animals at UFRJ (#101/16) approved the study.

Results:

After 108 days BM of HL rats was higher (477±6.9 g) than that of CTR (412±6.7 g, P<0.0001, n=40 each group). Epididymal fat, a visceral fat marker, was higher in HL (0.86±0.03 vs 0.53±0.02 g; P<0.0001; n=46, 45), with increased adipocytes mean area (3,539±442 vs 2,187±163 μm² in CTR; P=0.0208; n=5). Similar results were encountered in perirenal fat (2.25±0.01 g vs 1.55±0.03 g; P<0.0001; n=10 in HL; and 3,175±59 vs 2,307±38 μm² in CTR; n=7). HL presented with higher kidneys, heart and liver weights (2.6±0.08 vs 2.2±0.05 g, P=0.0008; 1.50±0.01 vs 1.29±0.02 g, P<0.0001; 13.7±0.2 vs 13.2±0.1 g, P=0.0142; n=7). After glucose overload, the HL group showed higher glucose levels after 15-30 min with higher AUC (18,621±306 vs 16,227±561 a.u.; P=0.0015; n=10). HL presented with upregulated (Na⁺+K⁺)-ATPase activity in renal proximal tubules (376±22 vs 260±7 nmol Pi/mg/min; P=0.0121; n=6 each group), which returned to CTR values after Ang-(3-4) administration (257±10; P>0.9999 vs CTR; n=5). The Na-ATPase activity was also higher: 83±3 vs 55±3; P<0.0001; n=6, and normalized to 55±2; P>0.9999 vs CTR; n=5 after Ang-(3-4). LiCl was lower in HL (141±5.4 vs 168±7.1 μl/min per 100 g BM; P=0.0131; n=8). HL group gradually developed higher SBP from day 40 of dietary exposure (140±0.8 vs 130±0.8 mmHg; P<0.0001; n=40 each group) without difference in heart rate (348±6.9 vs 339±5.2 bpm in CTR; P=0.3099; n=19). SBP dropped to 128±1.1 mmHg (n=20; P<0.0001 vs HL) after Ang-(3-4).

FeSBE Annual Meeting 2019

Poster Sessions and Abstracts

Conclusion:

The increased Na reabsorption at the level of renal proximal tubules and decreased delivery of fluid to distal segments, likely due to the upregulation of renal local RAS (previously demonstrated), is a key physiopathological event that culminates with elevated Ang-(3-4)-sensitive SBP and disrupted baroreflex. The decreased glucose tolerance and the previously communicated dyslipidemia are the metabolic components in overweighted rats that have exacerbated RAS activity.

Financial support:

CNPq, FAPERJ, FINEP, CAPES

08.017 - RENAL ISCHEMIA-REPERFUSION INJURY LEADS TO HYPERTENSION AND LATER CHANGES IN PROXIMAL TUBULE NA⁺ TRANSPORT AND RENIN-ANGIOTENSIN SYSTEM: ROLE OF NADPH OXIDASE. Lima NKS, Araújo WRS, Oliveira AG, Farias JS, Aires RS, Muzi-Filho H, Paixão AD, Vieyra A, Vieira LD, - Fisiologia e Farmacologia - UFPE Instituto de Biofísica Carlos Chagas Filho - UFRJ

Introduction:

Acute renal injury (AKI) is a risk factor for hypertension, which may involve the participation of reactive oxygen species (ROS), changes in proximal sodium reabsorption, and activation of the intrarenal renin-angiotensin system (RAS) as underlying mechanisms.

Aim:

In this study, we investigated in rats whether ischemia-reperfusion (IR)-induced AKI changes proximal tubule ATP-dependent sodium transport and intrarenal protein content of RAS components, as well as the role of NADPH oxidase in these alterations.

Methods:

Rats weighing 300-350 g were submitted to AKI by bilateral IR (n=24). The animals submitted to IR injury were maintained: i) without treatment (n=8); ii) under treatment with NADPH oxidase inhibitor apocynin (100 mg/kg, in drinking water) during 24 hours before and after IR (n=8); or iii) under daily treatment with apocynin (100 mg/kg, in drinking water) starting 24 after surgery (n=8). The control group was rats submitted to sham surgery (Sham, n = 8). During 4 weeks, the rats were submitted to the evaluation of serum creatinine levels and to an indirect evaluation of systolic blood pressure (SBP) by plethysmography. Then, the rats were anesthetized (ketamine and xylazine, 80 and 10 mg/kg, i.p.) for the collection of kidneys. In the kidneys, it was evaluated ROS levels (dihydroethidium oxidation) and NADPH oxidase activity (lucigenin chemiluminescence). Moreover, renal samples were used to measurement of ouabain-sensitive (Na⁺+K⁺)-ATPase and furosemide-sensitive Na⁺-ATPase activities, as well as, to immunoblotting of RAS components and PKC isoforms. The Committee for Ethics in Animal Experimentation of UFPE (nº11764/2015-37) approved the experimental procedure. The difference between group means was analyzed using one-way ANOVA followed by Tukey test.

Results:

After 24 hours of renal ischemia, it was observed 4-times higher levels of serum creatinine (P<0.001) in the IR group compared to sham, whereas IR group treated with apocynin creatinine levels were nearly a half than non-treated IR group. After 4 weeks of IR surgery, the rats submitted to IR injury presented higher SBP (10%, p<0.05) and higher levels of renal ROS (194%, p<0.01) than the Sham group. Moreover, in renal cortex from IR group, it was observed higher (Na⁺+K⁺)-ATPase activity (57%, p<0.01), and upregulation of (pro)renin (101%, p<0.05), renin (236%, p<0.01) and type 1 angiotensin II receptor (AT1R) (32%, p<0.05) compared to renal cortex from Sham animals. On the other hand, there was a decrease in Na⁺-ATPase activity (44%, p<0.05) and decrease in protein content of isoforms 1 (27%, p<0.05) and 2 (35%, p<0.05) of the angiotensin-converting enzyme, of type 2 angiotensin II receptor (AT2R) (32%, P<0.01), and of the isoforms α (25%, p<0.05) and ε (36%, p<0.05) isoforms of protein kinase C. These alterations were

prevented by both protocols of apocynin administration, except to the changes in PKCα immunodetection.

Conclusion:

Thus, we conclude that AKI-induced by IR may induce changes in sodium reabsorption and in the renal content of RAS components that are compatible with renal sodium retention and hypertension, and that NADPH oxidase activation may be a key factor in these changes.

Financial support:

CAPES, CNPq, FACEPE

08.018 - NITRIC OXIDE AND NITRIC OXIDE SYNTHASE ISOFORMS ARE MODULATED IN RENAL ISCHEMIA/REPERFUSION INDUCED CARDIAC HYPERTROPHY MODEL. Caio-Silva W, Junho CVC, Panico K, Pelegrino MT, Pieretti JC, Santos RSN, Seabra AB, Carneiro-Ramos MS, - Centro de Ciências Naturais e Humanas - UFABC

Introduction:

It is known that kidney injury by ischemia/reperfusion (I/R) leads to cardiac hypertrophy mediated by immune system. Besides, the Nitric Oxide (NO) can be produced by Nitric Oxide Synthase (NOS) and plays a key role in cell signaling in a several physiological and pathophysiological conditions in the heart and kidney. However, the role of NOS, in pathophysiological cardiac hypertrophy caused by renal I/R has yet to be clarified. In this study, we begin to investigate the NOS expression and NO levels in kidney after I/R protocol.

Aim:

The aim of this study was to analyse the modulation in the gene expression of NOS enzyme and the S-Nitrosothiol availability in the kidney using the renal ischemia/reperfusion induced cardiac hypertrophy model.

Methods:

C57BL/6 male mice were subjected to surgical occlusion of left renal pedicle for 60 min followed for reperfusion (I/R) for 8 and 15 days. Morphometric analyses were performed using as parameters kidneys weight and body weight, and vimentin mRNA as molecular kidney injury marker. Real time PCR was performed to analyze gene expression. To assess the bioavailability of NO in the form of S-Nitrosothiols we use an amperometric protocol for S-nitrosothiol with an NO specific sensor.

Results:

The mRNA expression of all the three isoforms was analyzed in the left kidney. The expression of endothelial NOS and neuronal NOS were downregulated after 8 days of reperfusion (p<0.05) and returned to basal levels after 15 days. The induced NOS (iNOS) isoform followed the same pattern as the others at 8 days. However, the iNOS mRNA levels increased significantly after 15 days of reperfusion when compared to sham group (p<0.05). In relation to the bioavailability of NO in the form of S-Nitrosothiols, the results showed that the left kidney 15 days I/R group presented a significant increase when compared to sham group. The right kidney presented no alteration on NO content.

Conclusion:

These results showed that renal I/R induced renal damage leads to NOS modulation remarkably to iNOS expression at 15 days of reperfusion. This modulation can promote an increase on NO bioavailability and contribute to oxidative stress dysregulation. Data herein suggest a possible mechanism that contributes to cardiac hypertrophy developmental.

Financial support:

FAPESP 2015/19107-5

9 - Respiratory Biology and Diseases

09.010 - TITLE: BLOCKAGE OF ADENOSINE RECEPTORS POTENTIATES B2-ADRENOCEPTOR-INDUCED RELAXATION IN AIRWAY SMOOTH MUSCLE. Pacini ESA, Freitas BA, Godinho RO, - Farmacologia - UNIFESP

Introduction:

FeSBE Annual Meeting 2019

Poster Sessions and Abstracts

Background: Previous work from our group has demonstrated that activation of skeletal muscle β 2-adrenoceptors (β 2-AR) increases the intracellular generation of cyclic AMP (cAMP) that is followed by the cyclic nucleotide efflux. Outside the muscle cell, cAMP is sequentially degraded by ecto-enzymes into AMP and adenosine, which in turn stimulates postsynaptic A1 adenosine receptors leading to a negative inotropic effect (Duarte T, et al., J Pharm Exp Ther, 341:820-8, 2012).

Aim:

Considering a) the central role of the β 2-AR/cAMP signaling cascade in airway smooth muscle relaxation, b) the elevated levels of bronchoconstrictor adenosine in the lung of asthma patients, and c) the tolerance to the bronchoprotective effects of β 2-AR after its regular use, in the present study we evaluated the possible efflux of cAMP from tracheal tissue in response to β 2-AR stimulation and its role in airway smooth muscle relaxation.

Methods:

Methods: Tracheal segments obtained from adult male Wistar rats were isolated and mounted in a tissue bath system containing Krebs-bicarbonate solution, under optimal resting tension, at 37°C. After a 60 min stabilization period, the tissues were subjected to different protocols: a) Carbachol (CCh) precontracted tracheas were incubated with increasing concentrations of rolipram, adenosine or fenoterol \pm CGS-15943, and the isometric contraction forces were recorded and analyzed. b) Tracheal rings were incubated for 60 min with 1 mM IBMX \pm 1 μ M fenoterol, and the extracellular cAMP collected from medium was measured using the Lance Ultra cAMP Kit (Perkin Elmer, USA). The isometric contraction forces were normalized and presented as percentage of the CCh EC30 response. Values were expressed as mean \pm S.E.M. UNIFESP animal Ethics Committee: CEUA #9987150714.

Results:

Results: Rolipram (PD4 inhibitor) or fenoterol (β 2-AR agonists) induced relaxation of tracheal smooth muscle in a concentration-dependent manner with distinct potencies (pEC50; rolipram = 8.2 ± 0.2 and fenoterol = 5.9 ± 0.1) and maximum responses (Emax; rolipram = $85 \pm 3\%$ and fenoterol = $85 \pm 2\%$) (n=3-5). In opposition, adenosine induced contraction of pre-contracted rat trachea with Emax of $60 \pm 1\%$ and pEC50 of $4.8 \pm 0.1\%$ (n=7). Pretreatment of tracheas with 20 μ M CGS-15943 (a nonselective adenosine receptor antagonist) shifted the concentration-relaxation curve to fenoterol 11-fold to the left (pEC50; fenoterol + CGS = 7.0 ± 0.2 , n=3-5). Stimulation of β 2-AR with fenoterol for 60 min increased by up to 550% the extracellular cAMP levels (basal = 1.52 ± 0.24 pmol/mg tissue, n=5-6).

Conclusion:

Conclusion: These results show that activation of β 2-AR induces the efflux of cAMP from tracheal cells. The ability of CGS-15943 to potentiate the relaxing effect of fenoterol indicates that the combination of β 2-AR agonists with adenosine receptor antagonists could have potential clinical use in the treatment of asthma and chronic obstructive pulmonary diseases.

Financial support:

Financial Support: CAPES, CNPq and Fapesp.

09.011 - PREVENTIVE AND THERAPEUTIC TREATMENT WITH GLYCINE AMELIORATES ACUTE LUNG INJURY INDUCED BY LPS IN MICE. Righetti RF, Santos TM, Camargo LN, Saraiva-Romanholo BM, Bezerra SKM, Hamaguchi SSS, Leick EA, Prado CM, Martins MA, Nogueira RS, Neto JCSC, Souza DA, Salu BR, Olivo MLV, Tibério IFLC, - Faculdade de Medicina FMUSP - FMUSP University City of São Paulo - UNICID Federal University of São Paulo - UNIFESP

Introduction:

The pathophysiology of acute lung injury (ALI) and acute respiratory distress syndrome (ARDS) results in heterogeneous lung collapse, edema-flooded airways and unstable alveoli. Glycine showed an important effect on neutrophilic inflammation, involved in ALI/ARDS.

Thus it may be a possible therapeutic target for the treatment of this disease.

Aim:

to investigate the mechanisms involved in the effect of preventive and therapeutic treatment of glycine in a model of LPS-induced acute lung injury (ALI).

Methods:

This study was approved by the Ethics Committee in the Use of Animals - University of São Paulo (São Paulo, Brazil), protocol 1030/2018. Thirty-two male Balb/c mice (6 weeks old- 25-30g) were divided into four groups: LPS, LPS-GP, LPS-GT groups received LPS (5mg/kg-intratracheally). SAL group received intratracheally saline solution (50 μ L). LPS-GP: received 1h before LPS administration a single dose of glycine (1 mg/kg-intraperitoneally). LPS-GT: received 6h after LPS administration a single dose of glycine (1 mg/kg-intraperitoneally). After 24h, we evaluated: exhaled nitric oxide (eNO), resistance (Rrs) and elastance (Ers) of the respiratory systems and bronchoalveolar lavage fluid (BALF) cells. Statistical significance between groups was assessed using one-way analysis of variance (ANOVA) followed by the Holm-Sidak and considered to be significant when p<0.05.

Results:

Preventive and therapeutic treatment in LPS-GP (15.0 \pm 2.7ppb) and LPS-GT (16.0 \pm 2.8ppb) groups decreased the eNO compared to LPS group (28.7 \pm 5.1ppb); p<0.05. Considering respiratory mechanics, LPS-GP (1.03 \pm 0.01 cmH2O/mL/s) and LPS-GT (0.97 \pm 0.04 cmH2O/mL/s) groups decreased the Rrs compared to LPS group (1.4 \pm 0.1 cmH2O/mL/s) and LPS-GP (50.1 \pm 3.7 cmH2O/mL) and LPS-GT (50.6 \pm 4.4 cmH2O/mL) groups decreased the Ers compared to LPS group (93.2 \pm 7.1 cmH2O/mL); p<0.05 for all comparisons. LPS-GP (10.4 \pm 2.3 x10⁴cells/mL) and LPS-GT (8.8 \pm 1.6 x10⁴cells/mL) groups decreased the total cells in BALF compared to LPS group (24.8 \pm 7.0 x10⁴cells/mL); p<0.05.

Conclusion:

Our results show that preventive and therapeutic treatment with glycine plays an important role in protecting the acute lung injury induced by LPS.

Financial support:

FAPESP (number 2017/06630-7); Coordenação de Aperfeiçoamento de Pessoal de Nível Superior - Brasil (CAPES) - Finance Code 001 and Conselho Nacional de Desenvolvimento Científico e Tecnológico (CNPq) (number 401452/2016-6).

09.012 - PLANT-DERIVED BAUHINIA BAUHINIODES KALLIKREIN PROTEINASE INHIBITOR (BBKI) REDUCES LUNG MECHANICAL ALTERATIONS AND INFLAMMATION ON EXPERIMENTAL MODEL OF ASTHMA-COPD OVERLAP SYNDROME (ACOS). Silva LLS, Barbosa JAS, João JMLG, Santos TM, Camargo LN, Campos EC, Galli TT, Saraiva-Romanholo BM, Brito MV, Bezerra SKM, Hamaguchi SSS, Leick EA, Martins MA, Prado CM, Olivo MLV, Tibério IFLC, Righetti RF, - Ciências Médicas - Universidade de São Paulo Ciências médicas - Universidade Federal de São Paulo

Introduction:

Asthma and chronic obstructive pulmonary disease (COPD) represent two major public health problems. However, there is a significant proportion of patients with a mixed asthma-COPD phenotype, is defined as asthma-COPD overlap syndrome (ACOS). Plant-derived Bauhinia Bauhinioides Kallikrein Proteinase inhibitor (BbKI) has been associated potent anti-inflammatory and anti-oxidant effects and represents a potential new therapeutic treatment for ACOS.

Aim:

To investigate the mechanisms involved in the effect of BbKI treatment in a model of ACOS.

Methods:

Committee in the Use of Animals - University of São Paulo (São Paulo, Brazil), protocol 1030/2018. Fifty-six male Balb/c mice (25-30g and 6 weeks old) were divided into six groups: C (saline), OVA (sensitized with

FeSBE Annual Meeting 2019

Poster Sessions and Abstracts

ovalbumin with 50µg i.p. on days 0 and 14 and inhalation with OVA on days 21, 23, 25 and 27), ELA (intratracheally elastase-25 U EPP/100g), ACOS (intraperitoneally and inhalation of ovalbumin associated with intratracheally elastase) and ACOS-BbKI (intraperitoneally and inhalation of ovalbumin associated with intratracheally elastase and treatment with BbKI-2mg/kg). At day 28, we evaluated: exhaled nitric oxide (eNO), resistance (Rrs) and elastance (Ers) of the respiratory systems and bronchoalveolar lavage fluid (BALF) cells. The increase of maximum response of resistance (%Rrs) and elastance (%Ers) of the respiratory system were considered and statistical significance between groups was assessed using one-way analysis of variance (ANOVA) followed by the Holm-Sidak and considered to be significant when $P < 0.05$.

Results:

After treatment with BbKI, ACOS-BbKI (9.8±3.4ppb) group decreased the eNO compared to ACOS group (41.0±5.1ppb); $p < 0.05$. ACOS-BbKI (260.7±31.5%) group decreased the %Rrs compared to ACOS group (625.15±81.05%) and ACOS-BbKI (110.3±28.8%) group increased the %Ers compared to ACOS group (36.43±4.8%); $p < 0.05$ for all comparisons. Considering bronchoalveolar lavage fluid, ACOS-BbKI (9.4±2.2 x10⁴cells/mL) group decreased the total cells in BALF compared to ACOS group (23.2±2.9 x10⁴cells/mL); $p < 0.05$.

Conclusion:

BbKI treatment reduces lung mechanical alterations and inflammation on experimental model of ACOS.

Financial support:

FAPESP (number 2017/06630-7); Coordenação de Aperfeiçoamento de Pessoal de Nível Superior - Brasil (CAPES) - Finance Code 001 and Conselho Nacional de Desenvolvimento Científico e Tecnológico (CNPq) (number 401452/2016-6).

09.013 - PLANT PROTEINASE INHIBITOR FROM ENTEROLOBIUM CONTORTISILIQUM (ECTI) TREATMENT ON EXPERIMENTAL MODEL OF ASTHMA-COPD OVERLAP SYNDROME (ACOS). Barbosa JAS, Silva LLS, João JMLG, Santos TM, Camargo LN, Campos EC, Galli TT, Saraiva-Romanholo BM, Bezerra SKM, Hamaguchi SSS, Prado CM, Martins ME, Olivo MLV, Leick EA, Righetti RF, Tibério IFLC, - Faculdade de Medicina FMUSP - FMUSP Universidade Cidade de São Paulo - UNICID Universidade Federal de São Paulo - UNIFESP

Introduction:

The asthma-chronic obstructive pulmonary disease overlap syndrome (ACOS) occurs in patients with fixed airway obstruction that defines COPD, with symptoms more typical of asthma with poor response to corticosteroid treatment. Proteinase inhibitor from Enterolobium contortisiliquum (Ecti) have been associated with anti-inflammatory activities and may represent a potential therapeutic treatment ACOS.

Aim:

To investigate the mechanisms involved in the effect of EcTI treatment in a model of ACOS.

Methods:

This study was approved by the Ethics Committee in the Use of Animals - University of São Paulo (São Paulo, Brazil), protocol 1030/2018. Fifty-six male Balb/c mice (6 weeks old, 25-30g) were divided into seven groups: SAL (saline solution), OVA (sensitized with ovalbumin; 50 µg i.p. on days 0 and 14 and inhalation with OVA on days 21, 23, 25 and 27), ELA (intratracheally elastase-25 U EPP/100g), ACOS (intraperitoneally and inhalation of ovalbumin associated with intratracheally elastase) and ACOS-EcTI (intraperitoneally and inhalation of ovalbumin associated with intratracheally elastase and treatment with EcTI-2mg/kg). At day 29, we evaluated: exhaled nitric oxide (eNO), resistance (Rrs) and elastance (Ers) of the respiratory systems and bronchoalveolar lavage fluid (BALF) cells. The maximum response of resistance (%Rrs) and elastance (%Ers) of the respiratory system were considered for the study and statistical significance between groups

was assessed using one-way analysis of variance (ANOVA) followed by the Holm-Sidak and considered to be significant when $P < 0.05$.

Results:

Treatment with EcTI in ACOS-EcTI (16.5±1.9ppb) group decreased the eNO compared to ACOS group (41.0±5.1ppb); $p < 0.05$. Considering respiratory mechanics, ACOS-EcTI (186.77±39.55%) group decreased the %Rrs compared to ACOS group (625.15±81.05%) and ACOS-EcTI (118.91±28.10%) group increased the %Ers compared to ACOS group (36.43±4.8%); $p < 0.05$ for all comparisons. ACOS-EcTI (5.4±1.0 x10⁴cells/mL) group decreased the total cells in BALF compared to ACOS group (23.2±2.9 x10⁴cells/mL); $p < 0.05$.

Conclusion:

Our results show that EcTI treatment plays an important role in protecting the lung mechanics and inflammation on experimental model of ACOS.

Financial support:

FAPESP (number 2017/06630-7); Coordenação de Aperfeiçoamento de Pessoal de Nível Superior - Brasil (CAPES) – Finance Code 001, Conselho Nacional de Desenvolvimento Científico e Tecnológico (CNPq) (number 401452/2016-6), LIM-20-HCFMUSP.

10 - Neurobiology

10.029 - VARIATIONS IN LIGHT SPECTRAL COMPOSITION AND ITS EFFECTS ON THE REST-ACTIVITY RHYTHM OF WISTAR RATS. Oliveira MAB, Scop M, Abreu ACO, Rossi AC, Sanches PRS, Díez-Noguera A, Calcagnotto ME, Hidalgo MP, - Programa de Pós Graduação em Psiquiatria e Ciências do Comportamento da Universidade Federal do Rio Grande de Sul - HCPA/UFRGS Departamento de Psiquiatria e Medicina Legal - UFRGS Departamento de Engenharia Biomédica - HCPA Department de Bioquímica e Fisiologia - UB Programa de Pós-graduação em Neurociências - UFRGS Laboratório de Cronobiologia e Sono - HCPA

Introduction:

Living beings had to develop the ability to predict and adjust physiology and behavior to recurring environmental events in order to survive on Earth. Recent evidence revealed that besides changes in irradiance, the light spectral composition could also stimulate the biological clock, assuring the body's synchronization to the external environment.

Aim:

Therefore, using a lighting system with the particularity of modulating its spectral composition during the day, we evaluated the effects of this dynamic light on the rest-activity rhythm of nocturnal rodents.

Methods:

Male Wistar rats (n=17) were exposed to different lighting systems since gestation, being raised also under the same conditions of a long photoperiod regime (16 h light: 8 h dark) with combined red-green-blue (RGB) lights. Groups differed with regards to the presence of variations in light spectral composition during the light phase (RGB-v) aiming to mimic daily changes in natural light, or not (RGB-f). After weaning, actimetry data were recorded continuously for rhythm characterization of spontaneous motor activity. The evaluation of rest-activity rhythm was performed on El Temps. Student t-test was used to compare independent samples and Watson-Williams test for circular data to compare acrophases. Differences with a $p < 0.05$ were considered statistically significant. Statistical analysis and graphs were performed with SPSS 18.0 software and GraphPad Prism 5.01 for Windows. All procedures were approved by the Institutional Research Ethics Committee on Animal Experimentation of Hospital de Clínicas de Porto Alegre (number 16-0044).

Results:

Animals exposed to RGB-v did not exhibit a reactive peak of activity after the light phase onset, suggesting that this group was able to detect the variations in lighting. Furthermore, RGB-v animals presented an earlier activity acrophase when compared to those under RGB-f

FeSBE Annual Meeting 2019 Poster Sessions and Abstracts

(RGB-v = 12:16 - "hh:mm", RGB-f = 13:02; $p < 0.001$), which might have been due to animals' capability to predict the arrival of the dark phase when exposed to variations in light spectrum. The Fourier and waveform analysis of daily patterns revealed that rodents in the RGB-v group were better synchronized to a circadian rhythm throughout the experiment. RGB-v showed higher values for interdaily stability (29.75 ± 6.5 , $n=9$) than did RGB-f ($t(15) = 2.74$, $p = 0.015$). Besides, the highest power content on the first circadian harmonic was reached earlier in the RGB-v group. The circadian index of the whole period, calculated by dividing the power of the first harmonic by the accumulative power of the first twelve harmonics, was higher in the RGB-v group ($t(15) = 3.47$, $p = 0.003$). Thus, we could consider that the rhythm of locomotor activity was earlier entrained to the light-dark cycle in the RGB-v rats.

Conclusion:

This research provides additional evidence for the effects of variations in the light spectrum on nocturnal rodents. Our findings suggest that animals might predict the onset of the activity phase due to its advanced acrophase when exposed to RGB-v, displaying better entrainment to a 24-h rhythm. Finally, this study raises interesting points with concerns to the potential of lighting systems that could help our body with circadian adaptation.

Financial support:

Fundo de Incentivo à Pesquisa e Eventos (FIPE) of HCPA (FIPE-HCPA #2016-0044), Luxion Iluminação, Coordenação de Aperfeiçoamento de Pessoal de Nível Superior (CAPES) - Finance Code 001, Fundação de Amparo à Pesquisa do Rio Grande do Sul (FAPERGS), Conselho Nacional de Desenvolvimento Científico e Tecnológico (CNPq), Financiadora de Estudos e Projetos (FINEP) - 1245/2013 and CNPq - 302620/2016-8, Instituto Nacional de Ciência e Tecnologia (INCT) -465671/2014-4 and Bolsa de Produtividade em Pesquisa - PQ - CNPq - 303707/2016-0.

10.030 - REGULATION OF ADENOSINE A1 RECEPTORS EXPRESSION BY NITRIC OXIDE IN CHICKEN EMBRYO RETINAS. Vaz LC, Haaidamus AB, Paes-de-Carvalho R, Pereira MR, - Neurobiologia - Universidade Federal Fluminense

Introduction:

Previous work shows that NO increases A1 receptors expression in PC12 cells or cortical neurons cultures. In addition, data from our group demonstrates that endogenous NO production reduces A2a receptor expression in mixed cultures from chick embryo retinas. Therefore, the aim of this work is to evaluate whether NO can also regulate adenosine A1 receptors expression in mixed retinal cultures.

Aim:

Thus, our objective is to investigate whether chronic treatment with L-arginine, a precursor for endogenous NO production, regulates the adenosine A1 receptors expression in mixed cultures.

Methods:

Mixed cultures from E8 retinas were treated on the first day of culture (C1) with L-arginine until C3. Thus, cells were processed for Western Blot or Real Time RT-PCR experiments. Statistical analyzes were performed by ANOVA followed by Bonferroni post-test or t test using Graph Pad Prism software. The results were expressed as mean \pm standard deviation for $n \geq 3$.

Results:

After 1mM L-arginine treatment for 48h, an increase of the A1 receptor protein levels was observed. This effect was blocked by pretreatment with 10 μ M of 7-NI, a neuronal NO synthase enzyme inhibitor (control 99.7 ± 8.1 , L-arginine 137.0 ± 5.2 , 7-NI 93.3 ± 19.4 , L-arginine \pm 7-NI 97.7 ± 13.3 , $n = 3$; * $p < 0.05$). Treatment with L-arginine also increased A1 receptor mRNA levels (control 1.0 ± 0.1 , L-arginine 3.5 ± 0.8 , $n = 2$).

Conclusion:

The results obtained in this work suggest that L-arginine is converted into NO by the neuronal NO synthase enzyme and increases the expression of A1 receptors in mixed cultures. These data may have an impact on neuroprotective mechanisms.

Financial support:

CNPq, CAPES, FAPERJ, PRONEX-MCT

10.031 - PLASMA LEVELS OF METABOLITES DIFFERENTIATE FIRST EPISODE PSYCHOSIS IN SCHIZOPHRENIA AND BIPOLAR DISORDER PATIENTS. Costa A, Joaquim H, Talib L, Gattaz WF, - Psiquiatria - HCFMUSP

Introduction:

Schizophrenia (SCZ) and bipolar disorder (BD) are serious psychiatric disorders and share several characteristics and the diagnosis yet is mainly clinical. The sooner they are identified, diagnosed and treated, the better the clinical prognosis. Therefore, the development of sensitive and accurate biomarkers is highly required. Lipids play an increasingly recognized role in the neuronal function and plasticity of the brain. Glycerophospholipids and molecules-like comprise 60% of the non-aqueous portion of the brain and in an even greater proportion of the dendrites and synapses. Other metabolites directly influence its functioning and remodeling, such as acylcarnitines, sphingolipids, cholesterol and other lipids. Since lipid metabolism is altered differently in neuropsychiatric diseases, alterations in the lipid profile of the membrane can allow a discrimination between subjects in first-episode psychosis (FEP).

Aim:

Thus, our aim was to determine plasma levels of metabolites of subjects in FEP and controls and find cutoff values that differentiate each group.

Methods:

Plasma samples were analyzed for 55 drug-naïve patients (28 SCZ and 27 BD) and 30 controls. The lipid profile was determined by mass spectrometry - Flow injection analysis, using AbsoluteIDQ p180® kit (Biocrates Life Sciences). Statistical analyzes were performed using a classification method - Classification And Regression Tree.

Results:

A cluster analysis revealed that a combination of phosphatidylcholines (PC aa C26:0, PC aa C38:4, PC aa C34:3) and acylcarnitine (C16-OH) could differentiate the patients according to diagnostic group. The accuracy of the method is 87,1%. Generally, lysophosphatidylcholines and phosphatidylcholines levels were higher in patients with schizophrenia and bipolar disorder compared to controls. Patients with bipolar disorder also presented higher lysophosphatidylcholines and phosphatidylcholines levels than patients with schizophrenia, while sphingolipid concentrations were higher in patients with bipolar disorder and lower in patients with schizophrenia compared to controls. No differences in acylcarnitine concentration were found between the groups.

Conclusion:

Our results suggest that the levels of some plasma metabolites differentiate subjects with SCZ, BD and controls. The levels of these metabolites can be a potential biomarker for psychosis, as well as a diagnostic marker for SCZ and BD. The findings from this study require further validation in BD and SCZ subjects, but suggest that the metabolome is a good tool to understand the pathophysiology of these disorders and presents potential diagnostic biomarkers.

Financial support:

FAPESP (2017/26291-2)

10.032 - ELECTROENCEPHALOGRAPHIC AND REPRODUCTIVE CYCLE EVALUATION IN A RAT MODEL OF EPILEPSY WITH SPONTANEOUS ABSENCE-LIKE SEIZURES. Fracote AT, Souza TS, Mariano JD, Batista GB, Souza GMA, Sabbag IM, Vaz B, Batista CM, Carvalho KC, Maciel GAR, Marcondes RR, Valle AC, - Patologia - USP Molecular and Structural Gynaecology - USP

Introduction:

FeSBE Annual Meeting 2019

Poster Sessions and Abstracts

Epilepsy Syndromes affects women differentially than men, in part due to differences in hormones. Idiopathic Generalized Syndromes (IGS) constitute one third of all epilepsies and are two to five times more common in woman (Savic, 2014). However, the mechanisms implicated in sex differences as well as its negative impact in female reproductive function are poorly understood. Epilepsy animal models have been fundamental for the understanding of physiopathology of epilepsy and may be an important tool to investigate interferences and correlation among epileptic seizures, hormonal cycles and reproductive abnormalities

Aim:

The aim of this study is to characterize the estrous cycles phases and the occurrence of spontaneous absence-like seizures in a GEAS rats (Generalized Epilepsy Absence Seizures Rats), a new genetic epilepsy model.

Methods:

Females GEAS (N=12) and control Wistar (N=12) rats were used. Mean weight was 286.12g and 231.04g, respectively. Vaginal smears were collected during 15 consecutive days for determination of estrous cycles. Additional 15 days of vaginal smears concomitantly with EEGs recordings of GEAS were collected after 10 days of electrodes implant or SHAM surgery. At the end of this period, rats were anesthetized and their weight and anogenital distance were measured for the characterization of female external genitalia. Animals were then euthanized and had their ovaries dissected and weighted. Interventions: Stereotaxic surgery for electrodes implants. Outcome Measures: estrous cycle, morphological measurements of reproductive tract and EEGs recordings.

Results:

Results: GEAS rats presented lower ovaries weight (0.0400±0.013 mg) than controls (0.0509±0.016 mg) (p=0.02) and increased anogenital distance (1.608± 0.13 cm) compared to controls (1.458±0.49 cm). Regarding estrous cycles, GEAS rats presented longer proportion of estrous phase time compared to controls (p=0.001). Seizures frequency and duration was higher on metaestrous compared to estrous phase (p=0.001 and p=0.007, respectively). No differences on number and duration of seizures was observed between proestrous and diestrous phases. Finally, the electrodes and sham surgery showed to have influence over the architecture sequence of the estral phases (p=0.07 and p=0.02), respectively.

Conclusion:

Conclusions: In our study, GEAS rats presented alterations in estrous cycles as well as higher frequency and duration of seizures during metaestrous phase. Furthermore, these animals presented morphological differences in the ovaries and in their reproductive tract that are similar to the ones found in androgenized female rats. These findings suggest that GEAS rats have intrinsic reproductive dysfunctions with alterations in seizures occurrence and may be an animal model to study the reproductive dysfunctions in epilepsy.

Financial support:

FFM-HCFMUSP

10.033 - EXPRESSION OF FAAH ENZYME IN A MOUSE MODEL OF RETINITIS PIGMENTOSA. Azevedo RF, Magalhães CF, Silva HP, Madeira LF, - Departamento de Neurobiologia - UFF Instituto de Biofísica - UFRJ

Introduction:

Retinitis pigmentosa (RP) is an inherited neurodegenerative disease of retina characterized by progressive loss of photoreceptor cells, corresponding to a decay in visual function. As in other degenerative central nervous system diseases, endocannabinoid system is an important therapeutic target for modulation. Its main ligands are anandamide and 2- arachidonoylglycerol, which are degraded by enzymes such as fatty acid amide hydrolase (FAAH). Previous work from our group showed that inhibition of FAAH in Pde6β rd10 mouse model

of RP slowed photoreceptor loss which starts around 17 postnatal days, suggesting that this system might be altered during the disease.

Aim:

We aimed to evaluate if FAAH enzyme expression was altered in Pde6β rd10 mice compared to healthy C57Bl/6 background.

Methods:

In order to assess FAAH localization in retina we detected this enzyme in retinal slices from rd10 and C57Bl/6 mice by immunofluorescence. We also determined FAAH localization in microglial cells by co-labeling FAAH with microglial marker Iba-1. Western-blotting was used to quantify protein expression of FAAH from protein extracts of retinas from rd10 and C57Bl/6 mice.

Results:

Overall, both in rd10 and C57Bl/6 mice we observed FAAH was present in all retinal layers, being more prominent on plexiform layers, possibly related to endocannabinoid system's role in modulating neurotransmission. At 15 postnatal days (P15) we observed presence of puncta of FAAH immunolabeling in inner nuclear layer of rd10 mice retina which were not present in C57Bl/6 retina. At P23 we observed in rd10 mice, cells labeled against FAAH directly above the outer nuclear layer, in photoreceptor outer segments layer. In order to verify if those cells were microglial cells, we co- labeled retinas against FAAH and Iba-1, showing an overlap between FAAH expression and invading microglia during photoreceptor degeneration. Protein expression of FAAH was determined, and a trend for increased FAAH expression in rd10 mice was observed, both during development and degeneration stages: P1 (Bl6= 0.34; Rd10= 0.88), P3 (Bl6= 0.61; Rd10= 0.64), P5 (Bl6= 0.24; Rd10= 0.76), P15 (Bl6= 0.37 ± 0.085; Rd10= 0.975 ± 0.262), P19 (Bl6= 0.585 ± 0.078; Rd10= 1.40), P21 (Bl6= 0.315 ± 0.078; Rd10= 0.645); P23 (Bl6= 0.33; Rd10= 0.58 ± 0.113; data expressed as mean ± SD).

Conclusion:

Results shown here suggest that there are changes on FAAH localization and protein levels in rd10 mice during development and degeneration of photoreceptor cells. Therefore, FAAH modulation might be an interesting therapeutic strategy for treatment of retinitis pigmentosa.

Financial support:

FAPERJ, CAPES, CNPq

10.034 - TOXOPLASMA GONDII AFFECTS NEUROGENESIS IN NEURO2A CELLS AND REDUCES PROLIFERATION, MIGRATION AND GLOGENESIS IN MOUSE NEUROSPHERES.. Pires LB, Barbosa HS, Santiago MF, Adesse D, - Laboratório de Biologia Estrutural - Fiocruz Laboratório de Neurobiologia Celular e Molecular - UFRJ

Introduction:

Toxoplasmosis is a worldwide spread zoonosis caused by *Toxoplasma gondii*, an obligate intracellular protozoan that affects all warm-blooded animals, including humans. The ability to transmigrate through the placental barrier and to replicate in different fetal tissues, without being affected by the immune system, makes *T. gondii* infection an important cause of prenatal complications. Vertical transmission may interfere with the fetal development, leading to abortions or several malformations, such as neurological defects, blindness and microcephaly. The parasite has a tropism for the Central Nervous System where tissue cysts are found within neurons. However, little is known about the impact of infection on the differentiation of neuronal cells that may lead to alterations in cortical neurogenesis.

Aim:

The aim of this project is to study the mechanisms involved in the pathogenesis of toxoplasmosis, focusing on neurogenesis and gliogenesis.

Methods:

To evaluate the impact of *T. gondii* on neurogenesis we used two in vitro models. Initially we used Neuro2a cells (N2a), a neuroblastoma cell line that have the potential to differentiate into neurons upon serum withdrawal. N2a were infected with *T. gondii* tachyzoites (ME-

FeSBE Annual Meeting 2019

Poster Sessions and Abstracts

49, type II) for 1 day and were induced to differentiate with serum withdrawal. As a second approach, neurospheres composed of neural progenitor cells, isolated from Swiss Webster mice, were also used. The proliferation of floating neurospheres was analyzed after 48 and 72 hours post infection. For differentiation assays, neurospheres were plated in glass coverslips coated with fibronectin and Poly-L-lisine, in differentiation medium (DMEM-F12 containing N2, B27 with retinoic acid and Glutamax). The migrated area was calculated after 48 and 120 hours and the immunoreactivity of different markers was analyzed by immunostaining.

Results:

The infection of N2a cells with *T. gondii* significantly decreased ($p < 0.05$) the rate of neurons ($3.8 \pm 0.8\%$ of uninfected and $1.2 \pm 0.5\%$ of infected, $N=3$, Student's *t* test). With our neurospheres differentiation assays, we observed that *T. gondii* infection significantly reduces the cumulative rate of migration by 12% ($p < 0.001$) at 120 hours (uninfected: 30.7 ± 3.5 , $N=9$ and infected: 18.7 ± 1.1 , $N=7$; $p < 0.001$, 2-Way ANOVA with Bonferroni post-test). We also verified alterations on gliogenesis, as observed by numbers of GFAP (intermediate filament, marker of glial cells)-positive cells per perimeter (uninfected: 74 ± 7 GFAP/mm, $N=9$ and infected: 54 ± 5 GFAP/mm, $N=15$). Additionally, it was demonstrated that *T. gondii* infection significantly decreased ($p < 0.01$) the proliferation of neural progenitor cells after 48 and 72 hpi, as observed by Ki67, a marker of cell proliferation (48h= uninfected: $39.8 \pm 2.1\%$ Ki67+ cells, $N=32$ and infected: $27.7 \pm 2.1\%$, $N=28$; 72h= uninfected: $38.5 \pm 2.1\%$, $N=48$ and infected: $27.0 \pm 2.0\%$, $N=39$).

Conclusion:

We conclude with the results found until this moment that *T. gondii* affects neuronal and glial differentiation, with reduction in progenitor cells proliferation and migration. This data will contribute with the understanding of the mechanisms by which this parasite affects cortical development in mice.

Financial support:

This work was supported by Fundação Oswaldo Cruz, CNPq (Edital Universal 2014 and PAPES VII) and FAPERJ

10.035 - PROTECTIVE EFFECT OF RESVERATROL AGAINST OXIDATIVE STRESS-INDUCED NEURONAL DEATH IN CHICK RETINA. Santos-Pereira R, Paes-de-Carvalho R, dosSantos-Rodrigues A, - Department of Neurobiology, Graduate Program of Neurosciences - UFF

Introduction:

Oxidative stress is a cytopathologic consequence of the imbalance between free radicals production and antioxidant intracellular system. Many studies suggest that oxidative stress-induced neuronal death plays an important role in the development of neurodegenerative diseases. Resveratrol is a polyphenolic compound present in the skin and seeds of more than 70 different plant species, including grapes, berries, tea, grains and peanuts. Many studies have reported that Resveratrol has neuroprotective properties, however, such mechanisms are still not well understood. In our study, we used the chick retina model, which is part of central nervous system (CNS) and is a great model for the study of CNS neurochemical interactions.

Aim:

In this work, we sought to investigate the intracellular effects triggered by resveratrol to modulate neuronal death induced by hydrogen peroxide (H₂O₂) in purified cultures of retinal neurons.

Methods:

Purified cultures of chick retinal neurons were obtained from 8-day-old chick embryos. In order to evaluate the effect of resveratrol on neuronal death induced by oxidative stress, pre-treatments with Resveratrol 10 μ M for 6h, 24h and 48h before treatment with H₂O₂ in different concentrations, which were performed for 24h to induce neuronal death. For the treatment with LY294002, a PI3K inhibitor, we incubated the cells 30 minutes before the onset of the incubation with

Resveratrol. After this treatment, the cell cultures were fixed and the cell viability was assessed by counting the fixed cells and the results were evaluated in the Prism 7.0 program.

Results:

We observed that the treatment for 24 h with H₂O₂ 1 μ M and 10 μ M induced a significant neuronal survival reduction ($52.9 \pm 8.7\%$ and $17.2 \pm 4.2\%$ relative to the control; $n=4$), respectively. Pre-treatments with 10 μ M Resveratrol for 6h, 24h and 48h significantly protected against neuronal death induced by 1 μ M H₂O₂ (6h: $96.1 \pm 6.7\%$; 24h: $105.7 \pm 12.7\%$ and 48h: $102.1 \pm 6.6\%$ relative to the control; $n=3$) and 10 μ M H₂O₂ (6h: $57.1 \pm 7.2\%$; 24h: $57.3 \pm 12.5\%$ and 48h: $102.1 \pm 6.6\%$ relative to control, respectively; $n=3$). After that, we tested if the resveratrol's effect on cellular survival was mediated by PI3K/Akt pathway. According to our results, the inhibition of PI3K did not block the protective effect of Resveratrol (Pre-treatment for 24h) against neuronal death induced by H₂O₂ 1 μ M and 10 μ M ($92.5 \pm 14.5\%$ and $68.4 \pm 14.5\%$ relative to control, respectively; $n=3$). This result shows that Resveratrol is not mediating its cellular survival through PI3K pathway activation.

Conclusion:

Our results indicate that long term treatment with Resveratrol has a neuroprotective effect against neuronal death induced by H₂O₂, which states this compound as a potential agent in the treatment of neurodegenerative diseases.

Financial support:

UFF

10.036 - CAFFEINE AS A POSSIBLE MODULATOR OF CHLORIDE CO-TRANSPORTER DURING RETINAL DEVELOPMENT.. Nascimento AA, Figueiredo DP, Silva RB, Calaza KC, - Neurobiologia - Universidade Federal Fluminense Fisiologia - UFFAL

Introduction:

Most visual deficits are due to eye problems and the retina plays a crucial role in the processing of visual information, as it is the only tissue responsible for translating light information. Gamma-aminobutyric acid (GABA) is the major inhibitory retinal neurotransmitter. However, studies have shown that during development, immature neurons respond to GABA with depolarization. This non-classical response is due to the chloride ion differential gradient throughout development which in turn depends on the expression of two chloride ion co-transporters: NKCC1 and KCC2. Exogenous chemical mediators are known to alter GABAergic signaling during development and may lead to morphological and functional changes in neurons. In this context, exposure to caffeine, a psychoactive agent present in various foods, beverages and medicines, has been shown to promote changes in nervous system development. Earlier results from our group showed that caffeine exposure (embryonic day 14- 16) increased the binding of 3H-MK801, a NMDA receptor pore binder, under unstimulated conditions (without exogenous 2 mM glutamate) but not with glutamate stimulation. Caffeine also promoted a decrease in KCC2 protein content. With these results, the group hypothesized that caffeine could be altering the response of cells to GABA, postponing to some extent the shift from depolarization to hyperpolarization.

Aim:

Thus, the objective of this work is to establish the ontogenesis of the chloride ion co-transporter KCC2 in the retina and to analyze the effect of in vitro caffeine exposure and its impact on retinal excitability.

Methods:

For this, we used embryonic (E) and post-hatched (PE) retinas of the White Leghorn species, according to CEUA/UFF protocol 820/2018. Retinas were subjected to Western blotting and immunostaining approach. Mixed retinal cell cultures, obtained from E10 embryo, were treated with caffeine from the fourth day of culture (C4) to C6 and imaging for fluorescent-calcium sensor (Fluo3-AM). Statistical analysis

FeSBE Annual Meeting 2019 Poster Sessions and Abstracts

was performed using GraphPad Prism software, using one sample t-test, ANOVA analysis of variance and Bonferroni's Multiple Comparison Test.

Results:

The ontogenesis analysis showed an increase in the retinal KCC2 protein content with developmental progress. The immunohistochemical approach showed a significant increase in all retinal layers, with even more robust change in both plexiform layers from E14. In retinal cell culture, caffeine exposure decreased 20% the KCC2 co-transporter. NMDA receptors showed greater depolarizing responses in caffeine-treated cultures (80%±2%).

Conclusion:

The data suggest that the chloride ion co-transporter KCC2 increases with retinal development with the shift occurring around E14. Caffeine decreased retinal KCC2 content as well as increased NMDA receptor responses. If there is a direct link between KCC2 modulation and change in retinal excitability is still to be determined.

Financial support:

CAPES, CNPq, FAPERJ, PROPPI/UFF

10.037 - CAN GENETIC DIVERSITY OF TOXOPLASMA GONDII AFFECT THE HOST BEHAVIOR?. Bezerra ECM, Santos SV, Santos TCC, Junior HFA, Meireles LR, - Protozoologia - USP Parasitologia - FCMSCSP

Introduction:

Behavioral manipulation is one of the main theoretical currents used to explain the behavioral changes present in rodents parasitized by *Toxoplasma gondii*. Several studies propose that protozoan parasitism causes metabolic, immunological and neuropathological changes that enable the development of changes in the behavior of infected individuals. However, some factors related to the development of behavioral manipulation are still not well elucidated, among them, the possible effect of the genotype of the infecting strain on behavioral modifications.

Aim:

In this work, we evaluated the effect of chronic infection by genetically distinct cystogenic *T. gondii* strains on the behavior of mice.

Methods:

Experimental infection models with ME-49 (type II) and VEG (type III) strains were developed in BALB/c isogenic mice for evaluation of humoral immune response by ELISA, real time PCR quantification of brain parasites and behavioral tests. Passive Avoidance, Open Field and Y - Maze aiming at, respectively, the assessment of learning - memory, locomotor activity and feline odor aversion.

Results:

Our data show that mice infected with the VEG strain showed higher immune response by ELISA assay than ME-49 infected animals in the two evaluation periods, 6 weeks ($p < 0.05$ - Anova) and 16 weeks ($p < 0.01$ - Anova). Furthermore animals infected with the VEG strain also showed higher parasitic colonization in the CNS than animals infected with the ME-49 strain after 16 weeks of infection ($p < 0.001$ - Anova). Regarding behavior, there was a more marked reduction in long-term memory retrieval capacity, demonstrated by the reduction of the aversive environment latency ($p < 0.5$ - Anova) and the higher number of aversive environment entries ($p < 0.01$ - Chi-square) and more prominent motor changes in animals infected with the VEG strain ($p < 0.001$ and $p < 0.01$ - Anova). In assessing feline odor aversion, we found that VEG strain infection induced a more marked behavioral change in the host in the early stages of infection than ME-49 strain infection, and this effect was observed both in the presence of urine pure cat ($p < 0.5$ and $p < 0.001$ - Anova) as the amino acid L-felinine ($p < 0.5$ - Anova).

Conclusion:

Our results suggest that the genotype of the infecting strain may influence the development of behavioral changes in infected animals by

T. gondii, making the host more susceptible and exposed to the predator, especially in infections caused by type III strains.

Financial support:

Laboratório de Protozoologia IMT-SP e Laboratório de Parasitologia FCMSCSP

10.038 - STUDY OF THE PARTICIPATION OF NITRERGIC NEUROTRANSMISSIONS IN THE INSULAR CORTEX IN CARDIOVASCULAR RESPONSES BY ACUTE RESTRAINT STRESS IN RATS.. Goulart MT, Crestani CC, Busnardo C, Corrêa FMA, ALVES FHF, - Health Sciences Department - UFLA Pharmacology Department - USP Department of Active Principles and Toxicology - UNESP

Introduction:

The insular cortex (IC) is a brain structure involved in the central control of the cardiovascular system. Cardiovascular responses were reported after electrical or chemical stimulation of IC. These responses could be the neural substrate by IC connections with structures that participate of the central control of the cardiovascular system, such as the nucleus dorsal vagus and the nucleus of solitary tract. Nitrgic neurotransmission in the central nervous system (CNS) is well established in the central control of cardiovascular system and its present in IC. The NO in CNS is a neuromodulator that acts by activating the guanylate cyclase (GC) cascade producing guanosine monophosphate cyclase (cGMP). Although some papers have shown the participation of some brain areas and neurotransmitters in the central control of cardiovascular activity during stress phases, the mechanisms and the possible areas of the brain that control the cardiovascular system during stress situations doesn't have totally elucidate. There are no studies showing the involvement of nitrgic systems present in IC in the modulation of cardiovascular activity during stress situations.

Aim:

The objective of the present work was investigate the involvement of nitrgic neurotransmissions into IC modulating the cardiovascular responses during the restraint stress in rats.

Methods:

Male Wistar rats had guide cannulas bilaterally implanted in the IC for drugs injection. Polyethylene catheter was implanted in the femoral artery for mean arterial pressure (MAP) and heart rate (HR) recording using a computerized acquisition system. The restraint stress was realized putting the animals in a small plastic cylindrical restraining tube (diameter= 6.5 cm and length=15 cm) during 30 minutes. It was used a selective nNOS inhibitor, N-Propyl (0.4 nmol / 100nL); a NO scavenger, Carboxi-PTIO (2 nmol / 100 nL); and a specific GC formation inhibitor, ODC (2 nmol / 100nL). The drugs were microinjected in the IC 10 minutes before the animals be submitted to acute restraint.

Results:

Acute restraint ($n=28$) caused significant increases in the MAP (before restraint: 92 ± 4 and restraint: 107 ± 6 mmHg, $t=3$, $p < 0.05$) and in the HR (before restraint: 345 ± 11 and restraint: 410 ± 12 bpm, $t=5$, $p < 0.005$). Administration of vehicle in the IC did not affect the changes in the MAP (Δ MAP: 15 ± 2 vs 16 ± 3 mmHg, $t=0.2$, $p > 0.05$) and HR (Δ HR: 72 ± 8 vs 69 ± 6 bpm, $t=0.6$, $p > 0.05$) to acute restraint. However microinjection of drugs cited above, increase the tachycardic responses during restraint stress $F(3, 14) = 4,106$, $P=0,0277$, with no changes in pressor responses $F(3, 14) = 0,6146$, $P=0,6168$.

Conclusion:

In conclusion our results show that the nitrgic neurotransmission into the IC modulate the tachycardic responses during restraint stress, without significant changes in blood pressure

Financial support:

FAPEMIG, FAPESP and CNPq

FeSBE Annual Meeting 2019

Poster Sessions and Abstracts

10.039 - M5 MUSCARINIC RECEPTOR ACTIVATION REGULATES CELL PROLIFERATION IN RETINAL CELL CULTURES OF NEONATAL RATS. THAYLINI QUERINO DOS SANTOS CONCEIÇÃO¹, LUIS EDUARDO GOMES BRAGA¹, ELIZABETH GIESTAL DE ARAUJO², 2, ALINE ARAUJO DOS SANTOS, ¹³ ¹POSTGRADUATE PROGRAM IN NEUROSCIENCE, UFF, NITERÓI, RJ. ²DEPARTMENT OF NEUROBIOLOGY, INSTITUTE OF BIOLOGY, UFF, NITERÓI, RJ ³ DEPARTMENT OF PHYSIOLOGY AND PHARMACOLOGY, BIOMEDICAL INSTITUTE, UFF, NITERÓI, RJ. Conceição TQS, Braga LG, Araujo EE, Rabelo AAS, DosSANTOS AA, - Departamento de Neurobiologia - UFF Departamento de Fisiologia e Farmacologia - UFF

Introduction:

Introduction: Previous results from our group have shown that phorbol myristate acetate (PMA), a protein kinase C (PKC) activator, stimulates cholinergic differentiation, including modulation of M1 and M3 muscarinic receptor levels, in retinal cells of neonatal rats maintained in culture for 48h. Regarding the M5 receptors (M5R), their main function described in the central nervous system is related to the control of dopamine release in the midbrain, and their actions on retina are not known yet.

Aim:

Objective: The aim of this study was to analyze whether PMA treatment also modulates M5R levels in retinal cell cultures and to evaluate the effect of M5 receptor activation using VUO238429, a positive allosteric agonist, on proliferation and viability of these cells kept in culture.

Methods:

Methodology: Retinal cell cultures were obtained from Lister-Hooded rats on postnatal day 2 (P2). Retinas were plated in 35mm Petri dishes or 96-well plates at a density of 105 cells / cm². Control cultures (maintained in medium 199) and treated with PMA (50ng / mL) and / or Vu0238429 (at different concentrations) were maintained at 37°C in 5% CO₂ and 95% air for 45min, 24h or 48h. Retinal cell samples were obtained and M5R levels were determined by the Western Blot technique. Cell proliferation was assessed by the [³H]-thymidine incorporation technique and cell viability by the MTT technique. The project was approved by the local Ethics Committee in Animal Use (CEUA nº 642/15). The values shown represent the mean ± standard error and are presented as a percentage of control. Statistical analysis was obtained by analysis of variance (one-way ANOVA). Data were considered significant when p < 0.05

Results:

Results: Treatment with PMA 50ng / ml increased intracellular M5R levels by 45 min (CT 100%, PMA 134.6 ± 4.71%, n = 3), 24 hours (CT 100%, PMA 165.1 ± 14.91%, n = 3) and 48 hours (CT 100%, PMA 174.2 ± 9.93%, n=3). Treatment with 0.5uM Vu0238429 for 48h decreased cell proliferation (CT 100%, Vu 0.5uM 64.93 ± 9.10%, n = 9). No decrease in cell viability was observed after 48h treatment with Vu0238429 at different concentrations (CT 100% ,Vu 0.25uM 136.92 ± 14.19%, Vu 0.5uM 119.71 ± 14.04%, Vu, 1.0uM 100.23±7.81%, Vu 1.5uM 112.31 ±10.68%, n = 4).

Conclusion:

Conclusion: The results suggest that M5R activation during retinal differentiation may be important in controlling cell proliferation and that PKC pathway regulates the levels of this receptor in the retinal cell cultures rats.

Financial support:

Financial support: CAPES, FAPERJ, PROPPI-UFF, INCT-NIM.

10.040 - SIGNALING OF REACTIVE OXYGEN SPECIES AND C-FOS PROTEIN EXPRESSION IN THE CEREBRAL CORTEX OF SWISS WEBSTER MICE OF THE MODEL SPONTANEOUS OF AGGRESSION (MSA). Felipe RM, Horita SIM, Barbosa RS, Brito CF, Araújo-Jorge TC, Oliveira GM, Fragoso VMS, - Laboratório de Inovações em Terapias, Ensino e Bioprodutos- LITEB - FIOCRUZ Laboratório de Biologia Celular - FIOCRUZ

Introduction:

Aggression is defined as an act that an individual intentionally harms or injures another own species. This aggressiveness can promote acts of violence, in humans. Using MSA, which uses regrouping as a stressor, was observed that some adult male Swiss Webster individuals exhibit highly aggressive behavior. Previous studies demonstrated that mice considered dominant, in chronic social stress, have a significant increase in c-Fos expression in Frontal Cortex. Stress can also induce an exacerbated increase ROS production in the cell. There are no studies correlating the effects of regrouping stress on the behavior of highly aggressive MSA animals with analysis of c-Fos protein and ROS production.

Aim:

Investigate the signaling and the influence of c-Fos protein expression and ROS production in cerebral cortex of the Swiss Webster mice subjected to stress of regrouping in adulthood, compared to control animals on the MSA.

Methods:

The experimental protocol was approved by the Oswaldo Cruz Institute's Ethics Committee on Animal Use under the license number (011/2014). Male Swiss Webster mice at 3 weeks of age were identified and divided in groups. 4th, 6th and 8th weeks of life, tail suspension test and pattern of level aggression was performed. 10th week the animals were regrouped. The 16th week, etogram and pattern of level aggression were performed and the regrouped animals were individually classified as harmonic (Har), subordinate (Sub), highly aggressive (AgR) and no regrouped (NR). All mice were euthanized and the brain tissue was removed for c-Fos protein quantification, and ROS production analysis in the cerebral cortex by immunohistochemistry and DHE assay, respectively. Data were analyzed by the one-way analysis of variance (ANOVA) non-parametric test (PRISM software). The significance level was 5%, p < 0.05. The quantitative analysis of the c-Fos protein, and analysis of ROS production was performed using ImageJ v1.41o software.

Results:

1) Grouping phase presents 23% mice hyperactive, 27% hypoactive and 50% median behavior. 2) Only AgR mice presented a significantly higher number of attacks of 9.9 ± 6.9 number of attacks / 30 min (p < 0.05) compared to the other categories and only Sub individuals presented lesion of 3.0 ± 0.9 cm² (p < 0.05), in regrouping phase. 3) AgR animals showed a significant percentage increase of c-Fos positive cells of 98.6 ± 0.7% (p < 0.01), compared to the other categories (NR: 80.3 ± 5.8; Har: 87.9 ± 2.5; Sub: 87.7 ± 8), NR animals showed significant increase of c-Fos negative cells of 19.7 ± 5.8% (p < 0.0001) compared to the other categories (Har: 12.1 ± 2.5; Sub: 12.3 ± 8.9; AgR: 1.4 ± 0.7%). 4) AgR animals showed a significant increase in ROS production of 42.1 ± 4.8 MFI (p < 0.05), comparing with the other categories (Har: 32.9 ± 4.1; Sub: 29.2 ± 16.9; NR: 32.1 ± 6.1 MFI).

Conclusion:

The stress of regrouping was able to significantly increase c-Fos and superoxide production in highly aggressive animals. This stress leads the cell to oxidative stress state and, AgR animals produce ROS exacerbated due to possible cell dysregulation. c-Fos protein may be overexpressed as a cellular mechanism to stimulate agent production antioxidants, to reduce the concentration of cellular ROS.

Financial support:

CAPES and FioCruz

10.041 - POST-WEANING AND LONG-TERM EXPOSURE TO HIGH-SUCROSE DIET ACCELERATES COGNITIVE AND MOTOR IMPAIRMENTS VIA HIPPOCAMPAL ENDOPLASMIC RETICULUM STRESS-RELATED APOPTOSIS IN RATS. PINTO BAS, MELO TM, FLISTER KFT, FRANÇA LM, COSTA TCL, MOREIRA VR, Pereira SRF, Debbas V, Laurindo FRM, PAES AMA, - Departamento de Ciências Fisiológicas - UFMA

Introduction:

FeSBE Annual Meeting 2019

Poster Sessions and Abstracts

The raise of metabolic syndrome (MS) to epidemic proportions has been correlated to the exponential increase of sugar consumption, especially among children. Notwithstanding, MS dysfunctions have also been associated to cognitive impairment and early development of dementias, although the mechanisms by which these interactions occur are still unclear.

Aim:

In this context, our study hypothesized that endoplasmic reticulum (ER) stress-activated pathways underlie the interconnection between long-term MS-dysfunctions and neurofunctional impairments.

Methods:

Weaned Wistar rats were fed with high-sucrose diet (25% sucrose, HSD, n = 7) until 90 and 180 days of life and compared to both age-matched control (CTR, n = 7) and middle-aged lean rats (OLD; 20 months old, n = 7), which were fed a regular chow (10% sucrose). Were assessed in those groups: MS-development; redox profile by TBARS; cognitive, behavioral and motor functions assessed by water maze, open field and rotarod, respectively; and hippocampal gene/protein expressions for ER stress adaptive (Ire1 α , Perk, Atf6, Grp78, Grp94, Pdi A2, Calnexin, Calreticulin) and apoptotic (Bcl2, Chop, Caspase, Parp1) pathways, as well as neuronal plasticity (Bdnf), antioxidant defense (Nrf2) and senescence (p53, p21). The results were analyzed by t test and ANOVA (Newman-Keuls). All procedures were approved by the Ethical Committee.

Results:

Sustained post-weaning exposure to HSD induced MS-phenotype, which was aggravated in a time-dependent manner, characterized by marked weight gain (454.1 ± 7.6 vs. 422.4 ± 5.4 g; $p < 0.01$), central obesity (Lee index: 106.9 ± 1.8 vs. 93.14 ± 1.1 g^{1/3}/cm³*1000; $p < 0.0001$), fasting hyperglycemia (454.1 ± 7.6 vs. 422.4 ± 5.4 mg/dL; $p < 0.0001$), hypertriglyceridemia (4.8 ± 0.26 vs. 4 ± 0.2 μ M; $p < 0.0001$), hepatic steatosis, insulin resistance (HOMA index: 5.9 ± 0.16 vs. 3.1 ± 0.36 ; $p < 0.001$) and oxidative stress (MDA: 147.1 ± 16 vs. 43.5 ± 4.4 mg/dL; $p < 0.01$) when compared to CTR. Besides, HSD showed motor deficit, anxiety and cognitive impairment when compared to CTR and compatible with OLD rats. Noteworthy, HSD presented hippocampal ER stress characterized by failure of all-tested markers of adaptive signaling and increased expression of precocious cell death, as well as reduced neuroplasticity and antioxidant defense, as well as accelerated senescence, a panorama very similar to that found in OLD rats.

Conclusion:

Collectively, data herein presented successfully show that post-weaning and prolonged intake of sucrose leads to MS and oxidative stress, deepened by sustained exposure, which in turn disrupt the ER homeostasis in hippocampus and trigger ER stress signaling pathways. In fact, the hippocampus of HSD young animals (3 months old) presented a transition from UPR-adaptive to pro-apoptotic signaling, while adult rats (6 months) had an ER stress pattern, marked by failure of any adaptive signaling and presence of apoptotic markers. That ER stress-derived apoptosis was related to hippocampal damages and directly contributed to accelerate neuronal aging and, subsequently, cognitive, motor and behavioral impairments. Finally, we established a relationship between cognitive decay and MS-driven hippocampal ER stress, shedding light into novel mechanistic pathways and opening up new venues for dietary interventions to prevent premature MS-related neuronal aging.

Financial support:

FAPEMA

10.042 - COGNITIVE DEFICIT, BUT NOT ANXIETY BEHAVIOR, IS PRESENT IN MIDDLE-AGED MICE WITH HIPOTHALAMIC OBESITY. Coelho CFF, Souza ILS, Souza Chagas VT, Ribeiro NL, Pinto BAS, Paes AMA, - Programa de Pós-Graduação Ciências da Saúde - UNIVERSIDADE FEDERAL DO MARANHÃO

Introduction:

Neonatal treatment with monosodium L-glutamate (MSG) induces hypothalamic lesions on median eminence, arcuate and ventromedial nuclei. Thus, MSG-treated rodents develop growth hormone (GH) and insulin-like growth factor 1 (IGF-1) deficiency and hyperinsulinemia at young ages, exhibiting early hypoglycemia and absent catch up growth. Therefore, they develop obesity, hyperleptinemia, type II diabetes mellitus and hypertriglyceridemia. Besides, six-month old MSG mice develop cognitive deficit and hyperphosphorylation of tau protein in hippocampus. As hyperinsulinemia and GH deficiency themselves are predisposing conditions to impaired cognition, we hypothesized that MSG mice could present deficit at earlier adult age.

Aim:

Once MSG hypothalamic damage causes many endocrinological disturbs, we sought to characterize behavioral patterns in adult MSG obese mice.

Methods:

Swiss mice pulps were treated with a 20% solution of MSG (4g/Kg day) or a 9% saline solution (0,1g/10g day) by subcutaneous injection for five intercalated days at the first ten days of life (n=8, for each group). Animals were weighted twice a week. Serum triglycerides, glycemia, TyG Index and Lee Index were assessed each 30 days of life, until 90 days old. Thereafter, Open Field Maze (OFM), Elevated Plus Maze (EPM), Forced Swim (FS) and Morris Maze (MM) were performed with 135-day old mice. Serum triglycerides, glycemia, TyG Index and Lee Index were assessed too. Statistical analysis was performed in Graphpad Prisma 7, Student test t or one-way ANOVA (Newman-Keuls post-test).

Results:

MSG mice had lower nasoanal length and weight at all ages MSG mice had a greater amount of adipose tissue and were obese since 30 days of life. MSG mice were hypoglycemic (Control: 127.70 ± 5.51 mg/dL; MSG: 102.30 ± 5.01 mg/dL) and hypotriglyceridemic (Control: 91.92 ± 12.13 mg/dL; MSG: 60.84 ± 3.95 mg/dL) at 30 days of age. MSG mice exhibited hypertriglyceridemia (Control: 110.90 ± 9.86 mg/dL; MSG: 172.20 ± 31.13 mg/dL) and peripheral insulin resistance (assessed by TyG) (Control: 91.92 ± 12.13 ; MSG: 60.84 ± 3.95) at 90 days, but hyperglycemia only at 135 days of age. In EPM, MSG mice shown fewer number of Rearing (Control: 16.7 ± 1.7 ; MSG: 10.4 ± 0.6), but no other parameter changed between groups (Figure 3). OFM confirmed that MSG mice had no anxious behavior compared control ones, nor number of traveled squares (Control: 62.5 ± 6.2 ; MSG: 64.0 ± 9.1), neither time in outer zone (Control: 239.6 ± 4.7 s; MSG: 224.5 ± 14.0 s). However, MSG mice had more fecal boli than control ones at the end of sessions (Control: 0.4 ± 0.4 ; MSG: 2.5 ± 0.7). In FS, MSG mice did not exhibit a depressive behavior. As latency as time in immobility were close for MSG and control mice. On MM, latency to reach the platform was lower in control mice since the first day of training (AUC Control: 50.8 ± 5.2 ; AUC MSG: 150.5 ± 14.7). MSG mice had a greater latency to target zone and fewer time in target zone (Control: 36.6 ± 3.9 s; MSG: 21.3 ± 3.3 s), which is related to cognitive impairment.

Conclusion:

MSG mice present early cognitive deficit, which can be associated to GH deficiency and early hyperinsulinemia. As these animals did not demonstrated any anxious behavior, anxiety symptoms could not be appointed as a contributing feature for cognitive impairment, despite the hypercorticosteronemia described for this model. Neither depressive behavior. Further studies are necessary to appoint what factors are more relevant for the disruption and decline of cognition in these mice.

Financial support:

FAPEMA, CNPq

FeSBE Annual Meeting 2019

Poster Sessions and Abstracts

11 - Physical Training Responses

11.015 - METABOLIC AND MOLECULAR SUBACUTE EFFECTS OF A SINGLE LOW-INTENSITY EXERCISE BOUT, PERFORMED ON FED OR FASTED STATE, IN OBESE MALE WISTAR RATS. Vogt ÉL, Dentz MCV, Rocha DS, Model JFA, Kowalewski LS, Sarapio E, Amaral M, Souza SK, Simões LAR, Girelli V, Ohlweiler R, Krause M, Vinagre AS, - Departamento de Fisiologia - UFRGS

Introduction:

Obesity is a chronic disease that induces several associated disorders such as diabetes, cardiovascular, kidney and neurodegenerative diseases. Inappropriate diet and sedentary lifestyle are the major factors that contribute to its development. Considering the potential benefits of exercise and diet to improve metabolic health, combined interventions, such as the practice of exercise during fasting has recently gained popularity, since this strategy may potentiate lipid mobilization. However, the majority of the research looking at the effects of this type of intervention, assess mainly the acute (immediately after) but not subacute effects (subsequent hours after the session) of exercise.

Aim:

Herein, we submit obese rats to a low-intensity exercise bout, in fed or fasted state, analyzing metabolic and molecular responses 12 hours after the exercise.

Methods:

Plasma, liver, heart and skeletal muscle samples were assessed for general metabolism and skeletal muscle for the immunecontent of HSP70 and SIRT-1. The animals were induced to obesity by a high-fat diet for twelve weeks, and the evolution of obesity and insulin resistance were assessed. Afterwards, the obese animals were allocated in one of four groups: fed control (FDC), 8h-fasted control (FSC), fed exercise (FDE) and 8h-fasted exercise (FSE). The exercise groups performed a single bout of treadmill exercise for thirty minutes and then were subjected to a twelve-hour recovery. The University's ethics committee approved the present study (number 34271). The analysis of plasma metabolites, triglycerides and glycogen in tissues were performed by colorimetric methods and the immunecontent was evaluated by western blotting.

Results:

In FSE, triglyceridemia decreased compared to FSC (69.87 ± 4.34 vs 248.8 ± 37.91 mg/dL). Cholesterolemia decreased in FSE compared to FSC (46.94 ± 2.92 vs 104.4 ± 12.86 mg/dL) and in FSE compared to FDE (46.94 ± 2.92 vs 86.43 ± 9.69 mg/dL). Hepatic triglyceride were not altered, however in the heart, FDE were higher than FDC (5.46 ± 0.23 vs 4.67 ± 0.13 mg/g tissue) and FSE were lower than FSC (4.51 ± 0.16 vs 5.25 ± 0.19 mg/g tissue). In soleus, FDC were higher than both FSC (3.08 ± 0.19 vs 2.26 ± 0.04 mg/g tissue) and FSE (3.08 ± 0.19 vs 2.47 ± 0.16 mg/g tissue), respectively. Glycogen concentrations in gastrocnemius and heart were not modified, though in the soleus FSC were lower than FDC (0.03 ± 0.007 vs 0.14 ± 0.02 mg/g tissue). Hepatic glycogen were lower in FDE compared to FDC (3.78 ± 0.81 vs 6.99 ± 0.48 mg/g tissue). In soleus muscle, the content of HSP70 (0.49 ± 0.06 vs 0.28 ± 0.01 AU) and of SIRT-1 (0.48 ± 0.07 vs 0.27 ± 0.04 AU) was increased in FSE when compared to FSC.

Conclusion:

Thus, our results indicate that a single low-intensity exercise bout induces beneficial effects to lipid metabolism in obese rats that last for up to twelve hours. In the next steps, we intend to analyze the effects of this exercise protocol after different recovery times.

Financial support:

CNPq

11.016 - EFFECTS OF THE VOLUNTARY MATERNAL PHYSICAL ACTIVITY ON HEPATIC METABOLIC ENZYMES OF THE ADULT OFFSPRING. Pachêco LS, Santos JWO, Pereira AR, Bernardo EM, Lima TRLA, Leandro CVG, Fernandes MP, - ¹Laboratory of General, Molecular and Exercise Biochemistry - Federal University of Pernambuco - UFPE ²Nutrition Post-Graduate Program - Federal University of Pernambuco - UFPE

Introduction:

The exposure to unregulated dietary factors might cause metabolic disorders, therefore, physical activity influences the promotion of beneficial adaptations to the organism.

Aim:

Evaluate the effects of the voluntary maternal physical activity on hepatic metabolic enzymes of the adult offspring.

Methods:

For this, Wistar rats were placed in voluntary physical activity cages (VPAC) for a period of 30 days, for adaptation. After this period, the rats were classified on three experimental groups: inactive, active and very active. Inactive: made <1.0 km.dia-1, within the time <20 min.dia-1 and caloric expenditure <10.0 kcal.dia-1; Active: made $>1.0 \leq 5.0$ km.dia-1, within the time $>20 \leq 120.0$ min.dia-1 and caloric expenditure of $>10.0 \leq 40.0$ kcal.dia-1; Very Active: made >5.0 km.dia-1, within the time >120.0 min.dia-1 and caloric expenditure of >40.0 kcal.dia-1. After the classification, the rats were mated, and when the presence of spermatozoa was detected in the vaginal cavity, the animals were individually reassembled in the VPAC. The cycle ergometers were locked at the 14th postnatal day. The animals received LABINA® diet until reaching the age of experimental protocol. At 70 days of age, animals were decapitated by guillotine to remove hepatic tissue. Subsequently, total body mass, liver tissue and key enzyme activity of the main bioenergetic pathways were evaluated: phosphofructokinase 1 (PFK-1), glucose-6-phosphate dehydrogenase (G6PDH), β -hydroxyacyl-CoA dehydrogenase (β -HAD), fatty acid synthase (FAS) and citrate synthase (CS). All experimental protocols were approved by the Ethical Committee of the UFPE (23076.017125/2017-47). Data were analyzed using One-way ANOVA, followed by the TUKEY multiple comparison post-test and expressed as mean \pm EPM. It was used $n=6-9$ animals for group, considering significant when $p<0.05$.

Results:

Our results showed no significant difference between the groups in relation to total body mass and liver. However, we verified increase on the PFK-1 activity in the offspring of active rats (157%, $p<0.001$) and very active (338%, $p<0.001$) when compared to animals of the inactive group. We also observed G6PDH activity increased in the offspring of active rats (65%, $p<0.05$) and very active (129%, $p<0.05$) when compared to the inactive group. β -HAD activity was increased in the offspring of active rats (277%, $p<0.05$) and very active (723%, $p<0.05$) when compared to the inactive group. In contrast, we observed FAS activity decreased in the offspring of active and very active rats (62%, $p<0.05$) when compared to the inactive group. In relation to Krebs cycle activity, it was observed CS activity increased in the offspring of active (23%, $p<0.05$) and very active rats (48%, $p<0.01$) when compared to offspring of the inactive group.

Conclusion:

Our results suggest that the benefits of voluntary maternal physical activity on the hepatic metabolism are passed to offspring.

Financial support:

CAPES and FACEPE

11.017 - MORPHOMETRIC ANALYSIS OF THE MYOTENDINOUS JUNCTION AND SARCOMERES IN OBESE RATS TRAINED. Grillo BAC, Rocha LC, Neto JP, Jacob CS, Ciena AP, - Educação Física - UNESP

Introduction:

The understanding of the influences that obesity causes in the myotendinous junction (MTJ), the main site of transmission of strength and incidence to sports injuries, few investigated, especially when

FeSBE Annual Meeting 2019

Poster Sessions and Abstracts

correlated with aerobic training, which promotes musculoskeletal changes.

Aim:

The aim of the study was to analyze morphometric alterations in the sarcomeres and ultrastructural components of the MTJ - anterior tibial muscle in experimental model of obesity and aerobic training.

Methods:

Wistar rats were divided into four groups (n=8): Sedentary (S), not submitted to any protocol; Trained (T), submitted to treadmill training; Obese (O), submitted to a hyperlipidic diet; Obese Trained (OT), submitted to a hyperlipid diet and to treadmill training. Obesity was induced by hyperlipidic diet (5,350 kcal/kg), maintained in O and OT groups for 60 days, and suspended in the OT at the beginning of the training. The T and OT Groups underwent treadmill running training, conducted for 40 minutes, with a constant velocity of 8m/min, total of 40 sessions. Through the transmission electron microscopy images, the lengths of invaginations, evaginations, basal lamina (components of the MTJ) and lengths of the sarcomeres (belly, proximal and distal) were measured by ImageJ® software, the statistical analysis was performed ANOVA two-way, Bonferroni post-test, with significance level $p < 0.05$ (CEUA-Nº1988).

Results:

The lengths (μm) of the proximal sarcomeres presented reduction in the T Group (1.7 ± 0.2) of 31% ($p < 0.0001$), in the OT Group (2.0 ± 0.2) 24% ($p < 0.0001$) in relation to the O Group (2.7 ± 0.3), and an increase in the OT Group by 17% ($p < 0.05$) compared to the T Group. In the distal sarcomeres, a reduction in O Group (1.6 ± 0.6) of 24% ($p < 0.0001$) was also observed and in the OT Group (1.7 ± 0.6) of 14% ($p < 0.05$) compared to the T Group (2.0 ± 0.7). The lengths of MTJ invaginations showed reduction in O Group (0.3 ± 0.1) of 58% ($p < 0.0001$), and increase in the OT (0.7 ± 0.5) Group of 126% ($p < 0.0001$) in relation to the O Group. The length of the evaginations also showed a reduction - 56% ($p < 0.0001$) in O Group (0.3 ± 0.2), and increase in the OT Group (0.6 ± 0.4) of 101% ($p < 0.001$) over the O Group. The basal lamina demonstrated greater increase (58%) in the T Group (0.09 ± 0.02) ($p < 0.01$) and in the OT Group (0.08 ± 0.03) of 77% ($p < 0.05$) compared to the O Group.

Conclusion:

The morphometric alterations of sarcomeres and MTJ components demonstrate plasticity in obesity experimental model, especially when associated with aerobic training. Ours results revealed that obesity promotes adaptations in the MTJ, consequently increases the predisposition to injury, since aerobic training is an effective means of reducing the changes in MTJ caused by obesity.

Financial support:

Fundação de Amparo à Pesquisa do Estado de São Paulo (FAPESP) Processo nº 2018/20962-5.

11.018 - ROLE OF AEROBIC EXERCISE TRAINING ON TUMOR-INFILTRATED IMMUNE CELLS. Voltarelli VA, Amano MT, Camargo AA, Brum PC, - Departamento de Biodinâmica do Movimento Humano - USP Centro de Oncologia Molecular - HSL

Introduction:

Despite the remarkable treatment progress in the last decades, cancer remains the second leading cause of death in the world. Therefore, strategies capable of attenuating tumor initiation, progression and aggressiveness are important for reducing incidence and mortality caused by cancer. Considering this, it is well known that aerobic exercise training (AET) promotes several beneficial adaptations in the body, and it has emerged as a possible strategy to attenuate tumor progression. However, the mechanisms underlining the beneficial effects of AET on tumor progression are still unclear.

Aim:

Therefore, this study intended to evaluate whether AET could positively modify the tumor microenvironment, favoring infiltration of

“antitumor” immune cells, and/or reducing the amount of “protumor” immune cells, consequently attenuating tumor progression.

Methods:

To test this, Balb/c mice were submitted to a moderate intensity AET (60% of maximal aerobic capacity, 5 days/week, 1 hour/day, in a treadmill) for 1 month before being inoculated with 1×10^6 CT26 colon carcinoma cells (subcutaneous injection). The AET protocol was maintained during tumor progression, and the last exercise session was performed 48 hours before animals were sacrificed (9 days after tumor cells inoculation). Tumor volume and body weight were measured daily. Experimental groups were divided into control (healthy sedentary mice), CT26 SED (sedentary tumor-bearing mice) and CT26 TR (trained tumor-bearing mice). Tumors were harvested at day 9 and digested with collagenase IV and DNase. After that, tumor leukocytes were separated by a Percoll gradient. Tumor-infiltrated dendritic cells, macrophages, natural killer cells (NK), and T lymphocytes were measured by flow cytometry. Statistical analysis: Anova One-way, Duncan post hoc, $p < 0.05$. Ethical committee approval: CEUA EEEF-USP 2017/02.

Results:

Tumor-bearing mice submitted to AET presented an attenuated tumor progression when compared with CT26 SED group, with significant reduction in tumor volume and mass (ex vivo). AET significantly increased the total amount of tumor-infiltrated leukocytes (CD45+), which included an increase in the percentage of NK cells, total, activated and effector memory CD8+ T cells, and effector memory CD4+ T cells in CT26 TR when compared to CT26 SED. Although there were no significant changes in the tumor amount of total and activated CD4+ T cells, the CD4+/CD8+ ratio was significantly reduced in CT26 TR comparing with CT26 SED mice, suggesting that the balance between CD4+ and CD8+ T cells in trained mice tumors favored a cytotoxic/effector T lymphocyte profile. Moreover, the percentage of tumor-infiltrated regulatory T cells (Tregs) in CT26 TR was significantly decreased when compared to CT26 SED mice. No significant changes were found for dendritic cells and macrophages (types M1 and M2).

Conclusion:

AET increases tumor-infiltrated amounts of cytotoxic/effector immune cells, such as NK and CD8+ T cells, while decreasing the percentage of Tregs in a colon cancer animal model. These data suggest that AET can attenuate tumor growth by modulation of tumor-infiltrated immune cells number and profile.

Financial support:

FAPESP

11.019 - RESISTANCE TRAINING REVERTS METABOLIC AND MORPHOMETRIC DISORDERS CAUSED BY HIGH-SUCROSE DIET IN MALE WISTAR RATS. Costa TCL, Passos ASC, Santos TC, Costa LL, Sousa OC, Abreu LP, França LM, Filho MAS, Pinto BAS, Paes AMA, - Departamento de Ciências Fisiológicas - UFMA Departamento de Educação Física - UFMA

Introduction:

The early exposure to diets rich in simple sugars and sedentary lifestyle have been associated to metabolic disorders such as obesity and dyslipidemias. In this context, the skeletal muscle (SM) can suffer losses of mass, strength and recovery capacity. These changes may be related to induction of the endoplasmic reticulum (ER) stress in SM. It is notorious that physical activity preserve and improve the lean mass. However, the molecular mechanisms of exercise training on ER stress in muscle is unclear. We hypothesized that RT may improve metabolism and decreased expression of ER markers in SM of obese rats.

Aim:

Thus, the aim of this study was to evaluate the effect of resistance training (RT) on body composition, glycolipid metabolism and ER stress in the SM of male rats fed high-sucrose diet.

Methods:

FeSBE Annual Meeting 2019

Poster Sessions and Abstracts

28 weaned male Wistar rats (ethical committee: 23115.018725/2017-19) were randomized into 2 groups: Control (CTR), fed standard chow, and High-Sucrose Diet (HSD), fed HSD (25% sucrose). At 17 weeks of life, each group was split into 2 new groups: CTR, CTR-T, HSD and HSD-T, where T means animals that performed RT protocol. In this protocol, the animals climbed 5 times a vertical ladder with 2 minutes rest between each climb, with 60% of the maximum weight attached to the tail, 3 times per week for 4 weeks. Body weight (BW), food intake, Lee index (LI), insulin resistance (TyG index) and the biochemical profile (triglycerides, cholesterol, fasting blood glucose) were assessed monthly and in the end of experiment. The SM of hind paws and adipose tissues were collected to analyze of morphometry and gene expression (qPCR). The results were analyzed by ANOVA (post-test Newman-Keuls).

Results:

HSD induced obesity (LI: $322 \pm 2,98$ vs. $310,8 \pm 1,77$ g% •cm⁻¹ •1000), hypertriglyceridemia ($171,6 \pm 24,5$ vs $76,81 \pm 16,01$ mg/dL), insulin resistance ($8,86 \pm 0,11$ vs $7,93 \pm 0,22$) and increase ER stress markers, especially PERK (FC $3,82 \pm 0,44$) and IRE1 α (FC $3,83 \pm 0,4$) when compared to CTR. In HSD-T there were reduction of periepididymal ($2,97 \pm 0,24$ vs. $2,35 \pm 0,12$ g/100g BW), mesenteric ($1,46 \pm 0,14$ vs. $1,09 \pm 0,1$ g/100g BW) and retroperitoneal ($3,31 \pm 0,2$ vs. $2,51 \pm 0,13$ g/100g BW) fat pads, and also prevented loss of lean mass in gastrocnemius ($1,21 \pm 0,01$ vs. $1,08 \pm 0,04$ g/100g BW) and EDL ($0,1 \pm 0,002$ vs. $0,08 \pm 0,003$ g/100g BW), when compared to HSD. Gene expression of PERK, ATF-6 and IRE1 α in HSD-T animals was similar to CTR. However, there was a decrease of CHOP (FC $1,06 \pm 0,18$ vs $4,06 \pm 0,61$) in HSD-T group in relation to HSD.

Conclusion:

This study reinforces that the early exposure to foods rich in sugars promotes metabolic alterations and also activation of ER stress in SM. In addition, it was demonstrated that RT avoids the body weight gain, decreases triglyceridemia and insulin resistance, and downregulates the ER stress pathways in the SM of HSD rats. Therefore, the RT is able to reverse the metabolic disorders caused by HSD and might be effective to avoid the damage caused by ER stress in the SM.

Financial support:

FAPEMA e CAPES

11.020 - PREGABALIN IMPROVE MUSCULAR FORCE IN MDX MICE BY ANDROGEN RECEPTOR MODULATION. Alves GA, Filho DDM, Franco LS, Ferreira JS, Júnior LCG, Carvalho SC, - Programa de pós Graduação em Ciências Biomédicas - FHO

Introduction:

In Duchenne muscular dystrophy (DMD), as well as, in its experimental model, mdx mouse, the dystrophin absence is the main cause of muscle degeneration. The exacerbated influx of calcium ions (Ca²⁺) is the most important event in DMD, and the androgen receptors are involved in the development and maintenance of muscle tissue. Pregabalin (PGB) is a Ca²⁺ channel blocking agent, and is a possible option in androgen therapy.

Aim:

Here, we analyzed the effects of PGB in androgen receptor (AR) of dystrophic fibers of the mdx and normal mice.

Methods:

In addition, analyzed their effects on markers of inflammatory cascade (TNF- α , NF- κ B and IL-6) and on regenerative process (MyoD and VEGF). Mdx and normal mice (14 days old) received PGB (mdx-PGB or CTRL-PGB; n=8; 20 mg/kg body mass; daily oral gavage) or water (mdx or CTRL; n=8; 20 mg/kg body mass; daily oral gavage) for 16 days, after which the brachial biceps (BB) were removed.

Results:

PGB was effective in reducing myonecrosis, leading to 37% decrease in creatine kinase (mdx; $1761,8 \pm 266,4$ U/L and mdx-PGB: $1114,1 \pm 185,9$ U/L) and 28% reduction in central nucleated fibers, as well as MyoD

marker (mdx: $0,73 \pm 0,06$ and mdx-PGB: $0,47 \pm 0,04$). The inflammatory area was reduced by 45% with PGB treatment (mdx: $1,39 \pm 0,20$ and mdx-PGB: $0,77 \pm 0,20$ %). Suspension force test showed a better improvement in muscle force and hanging time with PGB (muscle force in CTRL: $4,0 \pm 0,2$ N seg; in mdx: $0,5 \pm 0,1$ N seg*; in mdx-PGB: $1,2 \pm 0,2$ N seg**; p < 0,05; * compare to CTRL and ** compare to mdx). Immunoblotting indicated that PGB were effective in reducing TNF- α (35%) and IL-6 (57%). The AR (mdx: $0,38 \pm 0,08$ and mdx-PGB: $0,57 \pm 0,04$) and VEGF (mdx: $0,19 \pm 0,04$ and mdx-PGB: $0,33 \pm 0,04$) markers were significantly increased by PGB treatment. In normal mice PGB treatment increase the MyoD and decrease VEGF and do not modulated AR protein.

Conclusion:

These results indicate that PGB in dystrophic muscle increases androgen receptor and can improve muscle force

Financial support:

PIC/FHO

13 - Cell differentiation, growth and death

13.019 - CELL VIABILITY ASSAY OF GUSTAVIA AUGUSTA AQUEOUS EXTRACTS: A COMPARATIVE STUDY OF QUANTITATIVE METHODS. Rezende LR, Lombello CB, - CCNH - UFABC

Introduction:

Cell culture is a critical technique for the molecular biology, supplying an economical and fast-response model of analysis. Therefore, in vitro assessment of cellular viability is a fundamental measurement, being necessary in all cell culture situation, like pattern cell maintenance, or cytotoxicity assay. Several methods are based on a single technical approach for determining cell viability, however, the widely-practiced tests are based on different cell process, and shows variation on the test sensitivity, and specificity of the technique. In this way, this study proposes to investigate the behaviour of four widely used quantitative techniques (MTT, Trypan Blue, Neutral Red and Violet Crystal) in *Gustavia augusta* aqueous extracts. Vero cell lineage is indicated as cytotoxicity standard cell line by ISO 10.993.

Aim:

This job intended to establish a comparison between the quantitative methodologies most commonly used in cytotoxicity assays, using also the qualitative evaluation of morphological alterations. Were evaluated the cost of reagents, practicality of execution, standard deviation and similarity between the results.

Methods:

Assays with the Vero cells were performed in 96-well plate, in triplicate. The positive control used phenol at 0.25% and the negative control, culture medium. The Vero cells were cultured for 24 hours until confluence, then the test solutions were added and the morphology was observed after 24h, by inverted light microscopy with phase contrast. For cytotoxicity test, *Gustavia augusta* aqueous extract obtained by maceration and lyophilization concentrated, and used in concentrations of 1 to 100 μ g/ml in complete culture medium. The quantitative tests for cytotoxicity were performed according to methodologies described in the literature, following: MTT, Red Neutral, Violet Crystal and Trypan Blue.

Results:

The aqueous extract of *G. Augusta* showed signs of cytotoxicity at the concentration of 25 μ g/mL, with slight morphological changes. The concentration of 50 μ g/mL presented morphological alterations, with increase of the number of rounded cells. For this concentration only Trypan Blue and Violet Crystal assays showed marked cytotoxicity (V<70%), similar to the morphological observations. Significant presence of cell fragments and high rates of cells on suspension, indicating cytotoxicity, was observed in 75 μ g/mL. Neutral Red was the only test that did not indicate viability below 70% for this concentration. In 100 μ g/mL, morphology was similar to the positive

FeSBE Annual Meeting 2019

Poster Sessions and Abstracts

control, and all tests registered viability below 25%, according to the morphological cytotoxicity pattern.

Conclusion:

The morphological analysis and the Trypan Blue and Violet Crystal tests corroborated the results described in the literature for the cytotoxicity of *Gustavia augusta* aqueous extract, which demonstrates cytotoxicity from 50µg/mL. There was a statistically significant difference between the results of each test, with Neutral Red only registering cytotoxicity at 100µg/mL and MTT presented viability of less than 70% at concentrations of 75 and 100µg/mL. The Trypan Blue and Violet Crystal assays presented data with lower standard deviations, closer to that described in the literature for morphological cell behavior. Due to the ease protocol and low cost of the reagent, the Crystal Violet stood out as the most efficient technique.

Financial support:

CNPq

13.020 - STRUCTURAL AND FUNCTIONAL ORGANIZATION OF HUMAN UMBILICAL CORD ENDOTHELIAL CELLS IN RESPONSE TO TOXOPLASMA GONDII INFECTION. Pereira CSM, Araujo NS, Garcia MC, Rosa LPA, Barreto RFSM, Barbosa HS, - Biologia Estrutural - Fiocruz Biologia Celular - Fiocruz

Introduction:

Toxoplasmosis is a zoonotic disease caused by protozoan *Toxoplasma gondii*, an obligate intracellular parasite of the Apicomplexa phylum. This parasite affects about a third of the world population and it is of great medical and veterinary relevance. Congenital toxoplasmosis represents one of the most serious consequences of the acute infection of the pregnant woman, which can lead to irreversible neurological damage to the fetus. Endothelial cells of the umbilical vein (HUVEC) are inserted in the main route of vertical transmission of *T. gondii* during congenital toxoplasmosis. This work is justified because the use of HUVEC in experimental toxoplasmosis studies is limited to a few studies. Thus, the understanding of the physical and molecular passage of the parasite by the umbilical cord until reaching the embryo has not yet been elucidated.

Aim:

The hypothesis of work is: (i) HUVEC can act as a repository of the parasite throughout the infectious process in pregnant women through the establishment of cystogenesis; (ii) the success of the infection is dependent on the migration and functional integrity of HUVEC organelles, such as Weibel-Palade bodies (WPB) and lipid bodies (LB).

Methods:

HUVEC infected with tachyzoites of ME-49 strain were analyzed to verify the intracellular development of the parasite at the beginning of infection, during the multiplicative phase and cystogenesis. Thus, cultures were characterized morphologically by optical and transmission electron microscopy (TEM) and for the parasite-cell interaction the following parameters evaluated: kinetics of infection in HUVEC and the intracellular fate of the parasite.

Results:

Cultures of HUVEC maintained the morphological and functional phenotypic characteristics preserved as in vivo. Quantitative analyzes showed that *T. gondii* is able to invade and multiply actively in these cells. Qualitative analyzes as revealed by TEM, cytochemistry and immunolabeling indicated that HUVEC infection generates cellular activation and changes the dynamics of organelles in response to infection, among them Weibel-Palade bodies, glycogen granules and LB. In particular, it was observed a great recruitment and close interaction of LB to the PV membrane, to the vacuolar space and to the membrane of the parasite inside the PV at different times of infection. In addition, WPB and glycogen granules migrate to the region where the parasites are located. For the first time, tachyzoites-bradyzoites conversion and establishment of cystogenesis in HUVEC was demonstrated. Cysts formation, in this important route of infection to the fetus and can act

as a repository of parasites throughout the gestation potentiating, through the rupture of the cysts, re-infections.

Conclusion:

These results allow us to explore: (i) the cystogenesis in HUVEC; (ii) cellular response to parasitism during intracellular fate of the parasite: invasion, replication and cystogenesis, dosing cytokines; (iii) the use of brefeldin to clarify the dependence of the integrity of Golgi functions on parasite development, focusing on the Weibel-Palade corpuscles considering that its biogenesis occurs in the trans Golgi network. This work opens new perspectives for the study of the interaction of *T. gondii* and HUVEC in vitro and thus can elucidate the molecular mechanisms involved in congenital transmission.

Financial support:

CNPq, FAPERJ (Bolsa nota 10) e IOC-Fiocruz

13.021 - PARKIN PLASMID ELECTROPORATION IN SKELETAL MUSCLE TISSUE.. Gomes GH, Santos GP, Esteca MV, Tamborlin L, Luchessi AD, Baptista IL, - Laboratório de Biologia Celular e Tecidual - Universidade de Campinas laboratório de Biotecnologia - Universidade de Campinas laboratório de Biotecnologia - Universidade Estadual Paulista

Introduction:

The regenerative process of the skeletal striated muscle is highly regulated. Studies indicate that the removal of dysfunctional mitochondria plays a crucial role in the regenerative process of the muscle. Other studies indicate that Parkin is important during the process of mitophagy, so it may be important to the regeneration of muscle tissue. One of the ways of manipulating such a protein is to insert the plasmid for modification and genetic modification during a period of time. For greater success in the insertion of the plasmid it is necessary to use the technique of electroporation, which can increase cell permeability hundreds of times, and consequently facilitating the insertion.

Aim:

The objective is to standardize the in vivo electroporation technique, aiming the insertion of the plasmid pFLAG-CMV™ -5a Expression Vector, containing sequences for Parkin expression in the anterior tibial muscle in mice, thus allowing the study of how skeletal muscle regeneration function during overexpression of this protein.

Methods:

Ten wild-type animals (WT) were used for the experiment. The surgical procedure had exposure of the anterior tibial muscle to both legs of the animal by injecting 25µL (0.4U / µl in PBS) of the hyaluronidase enzyme and then resting for 30 minutes for pretreatment. Subsequently, 50 µg (2.5 µg / µl in 20 µl) of plasmid pFLAG-CMV™ -5a Expression Vector (ESE) and PBS were injected into the contralateral paw as control (EC). After these procedures pulses with duration of 20ms, voltage of 50V and frequency of 1Hz and pause of 980ms were given. The number of pulses is what distinguishes the two groups. The first group (G1) consisted of 5 pulses and the second (G2) of 8 pulses. Both groups were sacrificed within 7 days. We used the hematoxylin and eosin technique to analyze lesion levels, immunofluorescence, western blotting, localization and expression of Flag levels. All procedures were approved by CEUA (46871/2017). The data were compared using densitometry and image J.

Results:

We use the HE technique to detect injury levels since this procedure is invasive and causes a level of injury. We observed that the G2 group (8 pulses) causes more damage due to the greater space between the fibers, more cells of infiltrates and more nuclei centralized in the fibers (given in the quantification phase). We Using immunofluorescence, we observed that the percentage of transfected cells in the 8p (n = 5) and 5p (5n = 5) group was approximately 100%. We also analyzed the transfection efficiency using Western Blot where we found Flag 500% comparing with the control that does not present the plasmid and increasing parkin protein by 300%.

FeSBE Annual Meeting 2019

Poster Sessions and Abstracts

Conclusion:

Our results suggest that transfection efficiency does not depend on the amount of pulses, since both quantities presented approximately 100% efficiency, but as observed in the HE technique, the G2 group has more lesions, indicating that after 7 days the best group would be G1 induces less injury

Financial support:

FAPESP, Capes, CNPq e FAEPEX/UNICAMP

13.022 - IMPACT OF TOXOPLASMA GONDII INFECTION IN MYOGENESIS WITH CHANGES IN SECRETORY PROFILE. Vieira PC, Waghabi MC, Beghini DG, Barbosa HS, Adesse D, - Laboratório de Biologia Estrutural - Fiocruz Laboratório de Genômica Funcional e Bioinformática - Fiocruz Laboratório de Inovação em Terapias, Ensino e Bioprodutos - Fiocruz

Introduction:

Toxoplasma gondii is an intracellular parasite with a strong tropism for the skeletal muscle cells, in which it forms tissue cysts. The parasite is capable of crossing the transplacental barrier and infecting fetal tissues, causing congenital toxoplasmosis. Previous studies of our group showed development defects in a murine model of congenital toxoplasmosis, where the skeletal muscle presented atrophy and myositis. We have recently shown a disturbance on MRFs expression caused by T. gondii in skeletal muscle cells (SkMC) in vitro, with down-regulation of myogenin and MyoD expression and up-regulation of Myf5. Since infected cultures presents a different pattern of cytokine secretion, we hypothesized that changes in the inflammatory environment caused by T. gondii infection could be trigger the pathway responsible for myogenic loss.

Aim:

Investigate the molecular mechanisms that could interfere in the myogenic program during T. gondii SkMC infection.

Methods:

Myoblasts of C2C12 cell line were infected with ME49 strain of T. gondii 24 hours after plating. In order to induce myogenesis, 24 hours after infection, proliferation medium was replaced by differentiation medium, as documented in the literature. At 24 or 120 hours after induction, the conditioned medium was collected for cytokine/chemokine analysis profiling using Cytokine Bead Array for IL-6, IL-10, IL-12p70, IFN-, TNF and MCP-1 and ELISA for TGF- β 1. To evaluate the role of IL-6 in myogenic loss, Tocilizumabe (TCZ), an inhibitor of the IL-6 receptor (IL-6R) was used. Concomitant with the induction of myogenesis, cultures were treated with 10 μ g/ml of TCZ. After 120 hours of induction, the differentiation index as well as maturation of myotubes were accessed by MyHC immunostaining.

Results:

Cytokine evaluation revealed that pro-inflammatory IL-6 and MCP-1 were highly increased in T. gondii infected cultures. At the first point of analyses, IL-6 secretion of infected cells was increase in 20-fold in proliferating cells and 7-fold in cultures with myogenic induction ($p > 0.05$, $n = 4$). At the same point a 4-fold increase in MCP-1 secretion was observed ($p < 0.05$, $n = 4$). 120 hours after myogenesis induction IL-6 was still increased in infected cultures but only in proliferating medium (29-fold, $p < 0.01$). On the other hand, the anti-inflammatory TGF- β secretion was decreased about 3-fold in infected cells after 24 h and almost 50% in 120 h ($p < 0.01$, $n = 4$). Treatment with TCZ wasn't able to restore the levels of myogenesis, with similar differentiation index and myotube maturation between mock and TCZ-treated.

Conclusion:

Our data indicate that T. gondii leads SkMC to a pro-inflammatory phenotype, leaving cells unresponsive to activation of the myogenic differentiation program. Such deregulation may suggest muscle atrophy and molecular mechanisms similar to those involved in myositis observed in human patients, although IL-6 pathway might not be involved in this damage.

Financial support:

Instituto Oswaldo Cruz, Fundação Oswaldo Cruz, CNPq (BPP, Edital Universal 2014 and PAPES VII) and FAPERJ.

13.023 - IN VIVO ANALYSIS OF EFFECT BY HYDROGEN PEROXIDE (H2O2) ON SACCHAROMYCES CEREVISIAE GROWTH. Dalzoto LAM, Santos JM, Santos TR, Machado MFM, - Centro de Iniciação Científica - UMC

Introduction:

The maintenance of life takes place through a process called the cell cycle. Studies have demonstrated the involvement of specific proteases in the regulation of the cell cycle and programmed cell death (PCD). Metacaspases are cysteine proteases, with functional and structural similarity to mammalian caspases, showing marked differences in substrate cleavage specificity and their mechanism of activation. Caspases cleave their substrates after aspartic acid residues, while the metacaspases after basic residues (arginine or lysine). Studies has showed that YCA1 is involved in the regulation on the growth of S. cerevisiae and programmed cell death. PCD in S. cerevisiae was studied, so far PCD was associated with the accumulation of reactive oxygen species as the regulators of apoptosis in yeast.

Aim:

In vivo analyses on growth curve of S. cerevisiae with H2O2 in the wild-type (BY4742) and knockout of YCA1 (Δ yca1) strains.

Methods:

Growth curve was performed from a pre-inoculum containing 107 cells/ml harvested in YPD (yeast extract 1%, peptone 2% and dextrose 2%) medium at 30°C while shaking at 180 rpm. Cell death was evaluated with two distinct methodologies, by optical density at 660nm for 72 hours with a 12 hour interval r and by flow cytometry. The yeast underwent three types of growth: with culture medium replacement, without culture medium change and in the presence of different concentrations of H2O2 (0-2 mM) that was changed at every 12 hours for 72 hours.

Results:

When cultivated in a Δ yca1 batch system, they initiated their stationary phase after 70 hours of incubation, while the wild type strains remained around 48 hours, already growing in continuous flow after 72 hours of incubation, both wild type strains initiated the stationary phase, while the knockout remained in the exponential phase of growth, but the knockout shows an increase in cell number. The results shows that YCA1 metacaspase is involved as a positive PCD regulator in wild type strains when subjected to H2O2, causing apoptosis in S. cerevisiae independent of H2O2 concentration, was demonstrated by higher propidium iodide (PI) labeling, on the other hand the knockout strain shows a decrease in a PCD on a presence of low H2O2 concentration, demonstrated by the low marking for PI, since the absence of the metacaspase gene caused a cell protection against death process, but on saturated concentrations of H2O2, even the Δ yca1 strain shows a cell death rate.

Conclusion:

In this study we showed that the absence of YCA1 metacaspase provided a cell death resistance on S. cerevisiae when these cells are exposure in a different H2O2 concentrations.

Financial support:

FAPESP, CNPq and FAEP

13.024 - BEHAVIOR OF TRANSPLANTED HSPCS IN A BONE MARROW RECOVERY. Silva MCM, Oliveira NR, Menechino BSB, Corat MAF, - Laboratório de Desenvolvimento de Modelos Biológicos - Unicamp

Introduction:

It is unquestionable the importance of studying methodologies that can allow a better use of hematopoietic stem and progenitors cells (HSPCs) extracted from the organism, and cultured in vitro, aiming a transplantation and genetic manipulation of these cells for cure or improvement of symptoms of diseases. The process of blood cell

FeSBE Annual Meeting 2019

Poster Sessions and Abstracts

renewal called hematopoiesis occurs orchestrated in the bone marrow (B.M.) niches by complex cytokine signaling. This signaling promotes communication between different cell types in the bone marrow responsible for regulating quiescence, proliferation and differentiation of HSPCs. In this work we took the advantage of this complex signaling network and promoted by gamma irradiation an state of emergency for bone marrow regeneration, followed by transplantation of green fluorescent protein labeled HSPCs (GFP+).

Aim:

The hypothesis here is that damaged B.M. by irradiation would stimulate signaling to trigger HSPC proliferation and B.M recovery. Thereby we could identify preferential neighboring cells of GFP+ cells that might play a role in this proliferative process, which might be used in co-culture for ex vivo expansion of HSPCs.

Methods:

We extracted HSPCs cells from B.M. of GFP+ animals. We processed and selected them by cytometry to obtain Lin-Sca-1 + c-kit + GFP+ cells. These cells were transplanted into non-GFP pathogen-free (SPF) animals shortly after they were submitted to a lethal dose gamma irradiation. We performed post-transplant marrow analysis on the longitudinal sections by immunostaining of GFP label, as well as, Nestin, Jag-1 and LepR proteins. The literature describes Nestin, Jag-1 and LepR as likely medullary cell marker for cells involved with proliferative process of HSPCs.

Results:

Nestin marked few and very small cells. Which appeared to be surrounded by GFP+ cells. LepR followed a weak but specific labeling profile of some regions of the medullary parenchyma and multinucleated "giant" cells. Both, Nestin and LepR, did not seem to be a preferred niche marker of regeneration chosen by transplanted cells. However, the Jag-1 protein looked like to be labeled throughout the B.M.'s parenchyma and adjacent to most GFP+ cell.

Conclusion:

Although a preferred proliferation niche has not been identified, Jag-1+ cells were scattered all along the B.M. parenchyma and in large number, which seemed to play a role in a regenerative process. We are in the process of selecting the best JAG-1+ cell extraction methodology and intend to use them for in vitro co-cultivation in the next step to test their proliferative and survival potential for ex vivo expansion of HSPCs.

Financial support:

FAPESP

13.025 - COMBINATORY EFFECTS OF LAMININ ISOFORMS AND IGF-1 ON THE SURVIVAL, PROLIFERATION, AND DIFFERENTIATION OF HUMAN MYOBLASTS. Processi AM, González M, Savino W, RIEDERER I, - Laboratório de Pesquisa sobre Timo - Fiocruz

Introduction:

Skeletal muscle is constituted by postmitotic multinucleated muscle fibers, and in a small proportion, by undifferentiated progenitor cells called satellite cells (SC). After injury or disease, SC are activated, proliferate (called myoblasts from this stage) and differentiate, being able to fuse and regenerate the injured fibers. Myoblast transplantation has been used for the treatment of neuromuscular diseases, particularly for Duchenne Muscular Dystrophy (DMD). However, the results were unsuccessful, with death, early differentiation, and low proliferation of transplanted myoblasts. Laminin (LM) is a major basement membrane component that surrounds individual muscle fibers and is involved in different biological processes such as cellular proliferation, differentiation, and survival. LM is a heterotrimeric glycoprotein ($\alpha\beta\gamma$ chains), formed by 11 genes (5 α , 3 β , and 3 γ), which can combine to form different isoforms. Despite the LM isoforms 211 ($\alpha 2\beta 1\gamma 1$) and 221 are the only LMs surrounding mature muscle fibers, other isoforms are present during myoblasts proliferation and differentiation. Insulin-like growth factor type -1 (IGF-1) is one of the major soluble factors that regulate muscle proliferation and

differentiation. Moreover, IGF-1 is also implicated in the survival of different cell types, including myoblasts.

Aim:

To investigate how different LM isoforms, combined with IGF-1, can modulate the death, proliferation, and differentiation of human myoblasts in vitro.

Methods:

Human myoblasts CHQ (primary culture-derived cell line) and CL25 (immortalized cell line) were used in this work. Cell death was analyzed by flow cytometry, with annexin V and PI staining. Human recombinant IGF-1 (Preprotech) and the human recombinant laminin isoforms (111, 211, 411, 421, 511 and 521 - BIOLAMINA) were to treat human myoblasts. Immunofluorescence was used to analyze myoblasts differentiation (Myosin heavy chain and miogenin markers), and proliferation (KI67 marker). Student's t-test and Anova were used for Statistical analyses.

Results:

First, we characterized human myoblast death induced by hydrogen peroxide, and we observed that human myoblasts were not protected from death by the LM isoforms. Surprising, our preliminary results indicates that the combination of IGF-1 with LM isoforms exacerbated cell death. Further, we observed that IGF-1 and LM-111 enhanced myoblast proliferation and LM-511 increased the number of myoblasts in the cell cycle (KI67). The treatment with IGF-1 increased the number and the hypertrophy of muscle fibers in vitro.

Conclusion:

This study seeks to understand how the interplay between IGF-1 and the LM affects myogenesis, and we expect that this knowledge will contribute to design better therapeutic strategies for muscle regeneration.

Financial support:

Capes, FAPERJ, FIOCRUZ, CNPQ/Ciências sem Fronteiras, Brazilian National Institute of Science and Technology on Neuroimmunomodulation, FOCEM

13.026 - ANDROGEN REGULATION OF PROSTATE MITOCHONDRIAL OXYGEN CONSUMPTION. Teófilo FBS, Busanello ENB, Navarro CDC, Vercesi AE, Carvalho HF, - Biologia Estrutural e Funcional - Universidade Estadual de Campinas Patologia Clínica - Universidade Estadual de Campinas

Introduction:

Citrate is among the several components of prostatic fluid, where it is found in high concentrations as compared to other bodily fluids. Mechanistically, it is believed that citrate secretion by prostatic epithelial cells occur by the blockage of aconitase activity, which converts citrate into cis-aconitate and subsequently into isocitrate within the citric acid cycle. However, little is known about the mechanisms of citrate metabolism in the prostate and how it is concentrated in its secretion. Equally, little is known about mitochondrial functioning through prostatic development and under the different physiological states, known to be regulated by the androgens testosterone and dihydrotestosterone, via the androgen receptor (AR).

Aim:

Thus, the aim of this study was to verify the relationship between mitochondrial respiration rates and androgen regulation.

Methods:

For this purpose, we evaluated mitochondrial oxygen consumption in ventral prostate biopsies of prepubertal (5 weeks after birth; before the beginning of secretory activity), postpubertal rats (12 weeks after birth; considered as young adult) and castrated postpubertal rats (12 weeks after birth killed on Day 3 after castration) [n=4 each group, at independent experiments].

Results:

FeSBE Annual Meeting 2019

Poster Sessions and Abstracts

Here, we report an increase in mitochondrial respiratory rates in the postpubertal group in comparison with the prepubertal group: induced by the addition of ADP (oxidative phosphorylation, 26%); oligomycin (resting state, 20%); and FCCP (maximum respiratory rate, 24%). The castrated group showed a significant decrease of respiration rates stimulated by ADP (45%), oligomycin (47%) or FCCP (28%) in comparison with noncastrated postpubertal animals.

Conclusion:

These results suggest an association between androgen stimulation and oxygen consumption in rat ventral prostate.

Financial support:

Funding support: CNPq, FAPESP and CAPES.

13.027 - ACTIVATED MACROPHAGES INDUCE TUMOR CELLS APOPTOSIS. Berti AS, Carvalho HF, - Departamento de Biologia Funcional e Estrutural - UNICAMP

Introduction:

Androgens are important for prostate gland development and homeostasis. Androgen deprivation leads to the influx of immune cells, in particular, of different populations of macrophages. We have shown that prostatic epithelial cells cultured in the absence of androgenic stimulus led to the production of soluble factors that influence macrophage polarization and motility. Furthermore, LNCaP conditioned medium affects RAW 264.7 macrophage precursors to promote prostate epithelial cell death (J Cell Physiol 2019, 234:10).

Aim:

The objective of this work was to analyze if LNCaP conditioned medium in the absence of androgens results in macrophage activation and apoptosis of tumor epithelial cells.

Methods:

The coculture of Raw 264.7 and cancer cell lines (MCF-7 breast cancer cell, PANC-1 pancreatic cancer cell and TPC-1 thyroid cancer cell) was in complete medium, supplemented with 10% of LNCaP conditioned medium either in the presence or absence of R1881 for 24h. After 24h, cells were immunostained for caspase-9 and TUNEL.

Results:

We have observed that the absence of androgens in the macrophages and tumor cell lines results in an increased frequency of TUNEL (DNA-fragmentation) and cleaved caspase 9 double-positive cells.

Conclusion:

These observations suggest that soluble factor induce macrophage polarization and this, in turn, lead to the activation of intrinsic apoptotic pathway in tumor cells.

Financial support:

CAPES

14 - Nuclear Biosciences for Health

14.001 - EVALUATION OF THE SPATIAL RESOLUTION OF A SMALL ANIMAL PET TOMOGRAPH. Souza GCA, Gontijo RMG, Silva JB, Mamede M, Ferreira AV, - Serviço de Radiofármacos e Irradiações - CDTN/CNEN Departamento de Anatomia e Imagem - UFMG

Introduction:

Positron emission tomography (PET) is an important molecular imaging modality. Its application on preclinical research has increased during the last decades as a valuable tool for studying animal models of human disease and to contribute in the development of new radiopharmaceuticals or in studies of new applications of traditional radiopharmaceuticals. Thus, a consistent methodology for measuring performance parameters of the PET imaging is necessary to optimize the images, providing a better evaluation of the qualitative and quantitative analyzes. Empirically, the spatial resolution of the PET tomograph can be determined from the measurement of point or linear

sources and FWHM (Full Width Half Maximum) analysis of the respective linear profiles.

Aim:

The aim of this study was to evaluate spatial resolution of the small animal PET tomograph (LabPET 4 GE, Healthcare Technologies) of the Nuclear Technology Development Center, CDTN/CNEN, using two different methods.

Methods:

The first evaluation was developed by the authors using specific phantom (HotRod) which contains 6 groups of fillable channels with different diameters (0,6; 0,8; 1,0; 1,2; 1,5 e 2,0mm). The other one evaluation was made according NEMA NU-4-2008 publication, using a point source that consist of a small quantity of concentrated activity confined to no more than 0.3 mm in all directions, embedded in an acrylic cube of 10 mm extent on all sides. The Hot Rod phantom was filled with 60 MBq activity of 18F-FDG solution. Its PET image was acquired during 60 minutes. The image reconstruction parameters adopted were: MLEM-3D, 20 iterations and 46 mm transverse FOV. The reconstructed images were treated using the PMOD® software. In this step, graphs containing the line profile of the PET signal intensity along the different channels were generated for each of its groups. Afterwards, the graphs were treated using the PeakFit® software to obtain the half height (FWHM) widths of the peaks of interest. For the image acquisitions of point source, a positioner was developed and fixed to the bed of mice and both were aligned with the axial FOV center. The images were acquired in two steps, at the axial center of the FOV, and one-fourth of the center of axial FOV. For these two steps images were acquired at 0 mm, 5 mm, 10 mm, 15 mm, 25 mm (radial). For each position, PET images were acquired during 2 minutes. Image reconstruction parameters were the same used in previous test.

Results:

In the tests performed with the phantom, the spatial resolution is between 2 and 3 mm, while in the test using the point source its value is approximately $1 \pm 0,01$ mm in the tangential, coronal and axial axes. These values were obtained for the displacement of the source up to 15mm from its origin. For greater distance up to 25mm the spatial resolution value is approximately $2 \pm 0,01$ mm.

Conclusion:

The small animal PET tomograph of CDTN/CNEN has adequate spatial resolution – its value is compatible with the values reported in international studies performed on similar equipments.

Financial support:

FAPEMIG, CNPQ and CDTN/CNEN.

14.002 - EVALUATION OF RADIO-INDUCED DEATH AND MORPHOLOGICAL CHANGES IN HUMAN UMBILICAL CORD-DERIVED MESENCHYMAL STEM CELLS. RochaNeto JC, Rodrigues CG, Gaião WD, Silva JSO, Madeiros PL, Junior JAS, Lopes IMSS, Amaral RS, Aguiar J, Napoleão TH, Silva MB, Paiva PMG, Fernandes TS, BraynerCavalcanti M, - Departamento de Energia Nuclear - UFPE Departamento de Biofísica e Radiobiologia - UFPE Departamento de Histologia e Embriologia - UFPE Departamento Bioquímica - UFPE

Introduction:

Stem cells play a key role in the development and maintenance of tissues and have had a significant impact on the progress of many fields of biotechnology, including cell-based regenerative therapies, drug testing and screening, disease modelling, avoidance of side effects in radiotherapy and many other applications. Among stem cells, Mesenchymal Stem-Cells (MSCs) have high plasticity, immunosuppressive activity, and the ability to differentiate into many cell types. Consequently, they have become attractive for tissue engineering and cell therapy, with few reports about their sensitivity to ionizing radiation.

Aim:

FeSBE Annual Meeting 2019

Poster Sessions and Abstracts

The purpose of this work was to evaluate radio-induced morphological changes and death in human umbilical cord-derived MSCs (hUC-MSCs).

Methods:

Umbilical cords were obtained from newborns in accordance with Ethics Committee of CCS/UFPE (CAAE: 67002117.0.0000.5208). MSCs from Wharton's jelly (1×10⁶ cells) were irradiated with gamma rays (3 Gy). hUC-MSCs (passage 3) were cultured in DMEM/Ham's-F12 supplemented with fetal bovine serum and penicillin-streptomycin at 37 °C in 5% CO₂. Morphology analysis was performed using an inverted phase contrast microscope after 8 days of irradiation. The cytotoxicity was evaluated by MTT assay, after 8 days of incubation. The readings were performed in a spectrophotometer at 595 nm. The cell-death assay was measured by Dead Cell Apoptosis Kit (INVITROGEN) and analyzed using flow cytometer (BD Accuri C6) with cell counts of 70,000 events. The Wilcoxon test was used at a significance level of 5%.

Results:

The non-irradiated cells preserved their typical fibroblast-like morphology without nuclear alterations. Irradiated cells with typical senescence morphology were observed, i.e., larger, wider cells with many stress fibers and filopodial extensions were evident as signalling of the rearrangement of the cell culture. The mean percentages of radio-cytotoxicity by MTT assay of non-irradiated cells were normalized to 100%. For the irradiated samples, the mean percentages of the viable hUC-MSCs was 73.5% ± 1.1. When comparing the viabilities of the non-irradiated hUC-MSCs with the irradiated hUC-MSCs, a statistically significant difference was observed ($p < 0.05$). By flow cytometry, the percentages of viable cells from control and irradiated samples were 99.7% ± 3.7 and 96.3% ± 2.5 for non-irradiated and irradiated cells, respectively; early apoptotic cells were 1.5% ± 2.5 and 2.6% ± 2.0; late apoptotic cells were 0.5% ± 0.9 and 0.7% ± 0.6; and necrotic cells were 0.2% ± 0.3 and 0.3% ± 0.25. When comparing the apoptotic cells from control with the irradiated one, no statistical difference was observed.

Conclusion:

The first analysis by MTT would lead to the interpretation of cell death in the irradiated sample, but after flow cytometry analysis, the viability was quite high and the apoptosis and necrosis levels were quite low. With this, we conclude that cells instead of entering in the via of cell death, are indeed in mitotic delay. This was confirmed by the morphological visualization of cells, but further studies using more than one test, including cell cycle analysis, for elucidating such radiobiological issue.

Financial support:

Universidade Federal de Pernambuco

14.003 - THE ROLE OF THE POLYCOMB 2 REPRESSOR COMPLEX IN THE EPIGENETIC SIGNATURE OF TRANSCRIPTION FACTORS INVOLVED IN THE DIFFERENTIATION OF MESENCHYMAL CELLS DERIVED FROM OBESE MOUSE ADIPOSE TISSUE. Silva VS, Simao JJ, Abdala FM, Sá RDCC, Antraco VJ, Farias TSM, Alonso-Vale MIC, Armelin-Correa LM, - Ciências Biológicas - UNIFESP

Introduction:

Epigenetics modifications involving Polycomb Repressor Complex 2 (PRC2) are related to the differentiation potential of human AdSC (Adipose Derived Stromal Cells). AdSC are contained in the vascular fraction of white adipose tissue, are responsible for adipogenesis, a process that contributes to an expansion of adipose tissue by hyperplasia. The expansion of white adipose tissue by hyperplasia is considered healthier than the expansion by hypertrophy, considering that this process is associated with the inflammatory processes of the tissue in obesity. The deletion of Ezh2 in murine pre-adipocytes showed that PRC2 is crucial for the repression of genes involved in the Wnt / beta catenin signaling pathway which inhibits adipogenesis, dramatically decreasing differentiation capacity in adipocytes and inhibiting the expression of PPAR γ , CEBP α and also PRDM16,

although other transcription factors critical for adipogenesis, such as CEBP β , were not evaluated. The hypothesis regarding AdSC differentiation would be that obesity would alter the distribution of epigenetic marks of these cells, altering the expression of important transcription factors responsible for specific differentiation programs, which in turn would alter the differentiation potential of these cells.

Aim:

The objective of the present study is to analyze the composition of PRC2 in AdSC contained in the stromal cell fraction of adipose tissue, and its role in regulating the expression of critical transcriptional factors in AdSC of obese and non-obese mice.

Methods:

12 C57Bl/6j (8 weeks) male (CEUA N 3310050219) are being used, half of them are fed a control diet (CO) with controlled ingestion of macronutrients whereas obesity-induced animals ingest a hyperlipid diet (DHL) (59% of lipids) for 12 weeks. After euthanasia, the AdSC of the will be removed and isolated to characterize and quantify the expression of the different transcripts (RT-PCR) and the proteins (Western Blot) of the subunits of PRC2 (Ezh2/1, Eed, Suz12). AdSC from non-obese mice will be treated with UNC1999, an Ezh2 / 1 inhibitor to analyze possible change in expression of the transcription factors CEBP β , CEBP δ , Srebf1, AP-1, Klf4 and Klf15, NcoR2, Ddit3 and Foxo1. The dosage used of the Ezh2 / 1 inhibitor was tested on 3T3-L1 (pre-adipocyte) cells to verify their toxicity by the cells were cultured in D'MEM in the presence of two different 1 μ M and 3 μ M concentrations of UNC1999 diluted in DMSO, in addition to vehicle and control samples.

Results:

The dosages used in the treatment of 3T3-L1 cells were not toxic to cells. In addition, the animals are undergoing treatment to obtain their cells for the required tests.

Conclusion:

The dosages were non – toxic and will be used in the cells obtained from the tissues removed from the animals.

Financial support:

fapesp e capes

14.004 - USE OF SMALL ANIMAL PET/[18F]FDG IMAGING FOR TREATMENT RESPONSE ASSESSMENT IN 4T1 BREAST CANCER MODEL. Tomaz BC, Ferreira TH, Oda CMR, Barros AB, Silveira MB, - Unidade de Pesquisa e Produção de Radiofármacos - CNEN Faculdade de Farmácia - UFMG

Introduction:

Positron emission tomography (PET) is a non-invasive imaging technique for investigating molecular and biological process. The main PET radiopharmaceutical is [18F]fludeoxyglucose ([18F]FDG), an analog of glucose, which accumulates on cells with elevated metabolic glucose rate. In oncology, PET/[18F]FDG presents several applications, including therapy response evaluation.

Aim:

The aim of this work is to establish PET imaging protocols using [18F]FDG in 4T1 tumor-bearing mice for evaluating the effectiveness of a new agent for cancer therapy.

Methods:

The 4T1 cells were cultivated and prepared for inoculation (2.5 x 10⁶ cells) in the flank of Balb/c female mice (n=8). Animals of 5- 6 weeks old, with approximately 20 g, were provided by the Animal Facility of the Federal University of Minas Gerais (CEBIO/UFMG). The experiment was approved by the UFMG Committee on Animal Experimentation (182/2018). Animals were separated into two groups: control (n=3) and treated (n=5). The treatment was performed daily using a chemotherapeutic agent-loaded micelles internalized into macrophages. Each animal underwent two PET scans with [18F]FDG (approximately 12 MBq) at day 11 and day 22 post-inoculation, before and after treatment, respectively. Static images were obtained using a

FeSBE Annual Meeting 2019

Poster Sessions and Abstracts

small animal PET system, LabPET4 Solo. A phantom was also scanned to determine the calibration factor, which was applied to all image data. Semi-quantitative data analyses were performed using PMOD 3.706. The results, expressed in SUVmean \pm SD and in T/M (tumor-to-muscle ratio), were compared before and after treatment. Statistical significance between experimental values was determined by t testing and differences were considered significant at $p < 0.05$.

Results:

In the control group, T/M was 9.90 ± 0.90 at day 11 and 14.40 ± 1.72 on the last imaging day, indicating tumor growth. The treated group presented T/M of 12.20 ± 2.81 before treatment and 9.52 ± 2.45 after treatment without a significant reduction. Before treatment, the SUVmean for the tumor was similar in the control group and in the treated group, 2.13 ± 0.20 and 2.20 ± 0.31 , respectively ($p < 0.05$). At day 22, the mean [18F]FDG uptake was 1.62 ± 0.06 in the control group and 1.70 ± 0.42 in the treated group showing that treatment did not alter [18F]FDG accumulation ($p < 0.05$). A central area of necrosis was observed in the tumors of all animals. This could possibly have a significant impact on [18F]FDG uptake.

Conclusion:

The results indicate that PET/[18F]FDG might be a useful tool for monitoring treatment response. However, data were not conclusive about treatment effectiveness in this study. There was not a clear association between tumor regression and a decrease in [18F]FDG uptake in tumors after treatment. Imaging protocols were adequate, but treatment must begin in earlier stages of 4T1 tumor growth, avoiding necrosis. Our findings were important to establish experimental conditions and PET imaging protocols for future investigations of new therapy approaches.

Financial support:

PIBIC/Fapemig, CDTN, CNPq

14.005 - TELOMERES AND CENTROMERES IN THE ELUCIDATION OF GENOMIC RADIOSENSITIVITY. Filho JSO, Leitão MVSFS, Junior WJS, Fernandes TS, Bezerra MBCF, Filho PTN, Lopes IMSS, - Departamento de Histologia e Embriologia - UFPE Departamento de Biofísica e Radiobiologia - UFPE Departamento de Energia Nuclear - UFPE Departamento de Genética - UFPE

Introduction:

The organisms can suffer single and double strand breaks in their DNA as a result of exposure to ionizing radiation (IR). The DNA is organized with proteins forming chromosomes, and these have centromere and telomeres, which are complex structures composed of specific DNA. Telomeres are specialized structures protecting the ends of chromosomes, and are susceptible to breaks induced by IR. When broken ends are produced, these can be mis-repaired originating a ring chromosome, when the ends are from the same chromosome, or a dicentric, when two different chromosomes with broken ends are involved. The breaks pulled apart are the acentric fragments. The centromeres are more resistant to IR and occupy a much larger area of chromosomes. There are evidences that the sizes of telomeres are biomarkers of human exposure to ionizing radiation, in which the size of the telomere is inversely proportional to the radiation dose. Also, it is possible to consider that the radiosensitivity may be related to the organization of telomere sequences, compared to centromeres.

Aim:

the present work aimed to evaluate the length and the sequences of centromeres and telomeres and to correlate this parameters with the sensitivity to IR.

Methods:

The size of human chromosomes and centromeres was obtained from the data base Assembly from GenBank (National Institute of Health, USA) with the extension FASTA using the code CRCh38.p12. The size of telomeres was estimated from the alignment using the bwa with data obtained from the data base SRA in the date 22th april 2019 at 03:58

p.m. under the code DRR89363398 and using the files FASTA of each chromosome previously obtained as a reference, and the file obtained was followed by the use of motif_counter in order to obtain the size of telomeres.

Results:

The DNA sequences of centromeres are larger than the sequences of telomeres. This is a controversy to the "target theory", that considerer the susceptibility of the genome to its total volume. The analysis of base pairs showed centromeres with higher content of AT than GC (from 9 to 13% higher). This is indicative that probably, not only the higher condensation of this region is responsible for protecting it to IR action, but also corroborate with studies that showed a higher resistance of AT to IR compared to GC. Nevertheless, telomeres have 50% of AT and 50% GC, and its elevated sensitivity would be now explained by this simple argument, and the distribution of Gs and Cs would be also a possible susceptible site for IR clastogenic action. The data will be fully presented and discussed.

Conclusion:

It was shown a potential method for analysing DNA susceptibility to ionizing radiation, based on statistical analysis of centromeres and telomeres sequences and considering the bases more sensitive and more resistant to IR based on literature. Based on this, it is recommended that the target theory should be revised, and further studies for elucidating the role of DNA sequences organization and distribution throughout the human genome for radiosensitivity.

Financial support:

POLITEC

14.006 - THE 'BLACK BOX' GENOME OF DEINOCOCCUS RADIOURANS BECOMING GREYISH. Ladewig R, Ahmed NL, Kruger WMAV, Pascutti PG, Silva ML, Lage C, - Biologia Molecular & Estrutural - UFRJ - Universidade Federal do Rio de Janeiro

Introduction:

In the Deinococcaceae group are known to exist robust extremophilic bacterial species, as *Deinococcus radiodurans*. Attempts to better understand its robustness have specially focused on analyses of its responses against extreme doses of gamma radiation, to explain survival mechanisms of *Deinococcus radiodurans* against other stresses, as desiccation and heat. Even under simulated extraterrestrial environments it has thrived to deal with severe biological damages. *D. radiodurans* has many defensive mechanisms, and transcriptomes/proteomes made in response to gamma radiation and desiccation revealed that some genes and proteins had undefined functions, while others have never been expressed under those conditions. Therefore, it is expected that such gene products with obscure function can code for novel resistance proteins to these extreme conditions.

Aim:

To predict functional roles for 26 hypothetical proteins of *D. radiodurans*.

Methods:

Initially, dr_0491::kan and dr_2073::kan mutants were designed from R1 wild type *D. radiodurans*, transformed with the PGEMT-Easy vector carrying the genes interrupted by the kanR cassette, and confirmed by PCR of dr_0491+kanR and dr_2073+kanR marginal regions. The generated phenotypes will be analyzed by survival and qPCR to desiccation, heat, radiation exposure and oxidative stress. qPCR reactions will be performed after those treatments for a selected group of studied genes.

Results:

Our group identified 26 genes predicted by molecular modeling, coding possibly related proteins to those resistance functions. Among them, dr_0491 and dr_2073 code, respectively, a potentially heat-shock protein (acting on stress protection and protein folding control), and a putative shikimate kinase (acting on aromatic amino acids biosynthesis

FeSBE Annual Meeting 2019

Poster Sessions and Abstracts

in bacteria, fungi and plants). The dr_0491::kanR construction is finished, and dr_2073::kanR mutant is being generated. This mutant is currently at dr_2073::kanR verification stage. We were not able to generate any dr_0491::kanR mutant so far. As an unprecedented information, the dr_0491 gene, assigned as hypothetical in this species, was shown to be essential.

Conclusion:

dr_0491 and dr_2073 gene products can take part in protein restoration and aromatic amino acids biosynthesis to regenerate damaged proteins by radiation and/or other kinds of stress.

Financial support:

CNPq, CAPES

14.007 - PET IMAGING FOR EVALUATING TUMOR INFLAMMATION IN BREAST CANCER ANIMAL MODEL. Souza AM, Real CC, Junqueira MS, Souza LE, Marques FLN, Buchpiguel CA, Faria DP, - Oncologia - FMUSP Radiologia - FMUSP Oncologia e Radiologia - FMUSP

Introduction:

Breast cancer is the most prevalent tumor type among women in the world, excludes non-melanoma cancer, and its development goes through biochemical adaptations of the microenvironment. The interaction between microenvironment and inflammation influences tumor progression, with important participation of Tumor-Associated Macrophages (TAMs) (immunological cells recruited to phagocyte invasive material). 18F-FDG is a PET tracer used to detect tumor cells, by its glucose uptake, being able also to detect inflammatory infiltrate due to the increase of local metabolism. TAMs express 18 kDa translocator protein (TSPO) in the mitochondria 11C-(R)-PK11195 is a specific radiotracer for TSPO and associated with Positron Emission Tomography (PET), allows in vivo visualization of TSPO expression.

Aim:

Compare 18F-FDG and 11C-(R)-PK11195 as tools for measuring inflammatory tumor microenvironment by PET imaging.

Methods:

Ethics Committee 992/2018. Female Balb/c mice (n=27) were inoculated with 7x10⁴ 4T1 tumor cells in the upper right breast. Images were acquired in PET/CT for small animals Triumph® II Trimodality System (CA, EUA). For PET images 11C-(R)-PK11195 (50.7±38.5 MBq) and 18F-FDG (37.3±6.7 MBq) were administered intravenously in 27 and 6 mice, respectively. The images were acquired in three time points: 3 days, 1 and 2 weeks after cells inoculation (a.c.i.). PET images were reconstructed using OSEM 3D algorithm and Computed Tomography (CT) images were acquired and reconstructed by Filtered Back Projection and merged with PET images by PMOD™ software for anatomical information and assist in the design of the ROIs. Radioactivity tumor uptake was calculated.

Results:

Tumor size was non-measurable at 3 days, 28.4±16.5mm³ at 1 week and 135.1±157.3mm³ at 2 weeks. 11C-(R)-PK11195 tumor uptake decreased 23.3±76.4% (P=0.9) from 3 days to 1 week and decreased 120.4±199.1% (P=0.1) from 1 week to 2 weeks a.c.i. The tumor/muscle uptake ratio was 3.8±2.6 at 3 days, 1.9±1.0 at 1 week and 1.8±1.0 at 2 weeks a.c.i. 18F-FDG tumor uptake was decreased 35.4±39.3% (P=0.7) from 3 days to 1 week and increased 21.7±12.2% (P=0.2) from 1 week to 2 weeks. The tumor/muscle ratio was 3.9±0.8 at 3 days, 1.7±0.3 at 1 week and 2.4±1.0 at 2 weeks a.c.i.

Conclusion:

11C-(R)-PK11195 and 18F-FDG uptake was higher at 3 days a.c.i, even without measurable tumors, which suggest local inflammation, either due to physical injury (injection) or due to migration of inflammatory cells to the tumor microenvironment. 18F-FDG uptake decreased from 3 days to 1 week and increased from 1 to 2 weeks a.c.i., following the tumor growth, which can be associated with a changing from inflammation process to tumor cells metabolism. However, 11C-(R)-PK11195 uptake decreased from 1 to 2 weeks, being the tracer uptake

negatively correlated to tumor size, suggesting a more specificity of the tracer with inflammatory cells in the tumor environment than 18F-FDG. These findings correspond to the literature that cites the best use of 18F-FDG for glucose metabolism and it increased uptake in staging processes and more aggressive tumors, despite its quality marking initial tumors (Chudgar, 2016; Wyatt, 2010). Therefore, 11C-(R)-PK11195 may be an important tool to evaluate TAMs in breast cancer animal model, although histological analyzes are still under progress.

Financial support:

GE Healthcare

16 - Gene and Cell Therapy, Omics Biology

16.010 - OVEREXPRESSION OF MIR-29C AS A REGULATOR OF SKELETAL MUSCLE MASS. Silva WJ, Graça FA, Oliveira AC, Silvestre JGO, Alves PKN, Lima GS, Yan CYI, Miyabara EH, Labeit S, Wang D, Moriscot AS, - Department of cell biology and development - USP Institute for Integrative Pathophysiology - UM Department of cardiology - HMS Department of Anatomy - USP

Introduction:

The skeletal muscle is highly adaptable environmental challenges such as injury and changes in mechanical demands leading to hypertrophy or atrophy. Several pathways have been associated with skeletal muscle mass control such as AKT mTOR and more recently certain microRNAs (miRs) have also been implicated in either hypertrophy or atrophy. miRs are small RNA molecules (21-23nt) which can inhibit the mRNA of target genes either by blunting translation or by degrading mRNA. In this study we firstly screened for miRs potentially involved in the modulation of skeletal muscle mass and subsequently focused in the role of miR-29c.

Aim:

Identify and investigate microRNAs with potential to remodeling skeletal muscle mass. For that purpose, we have initially utilized an in-silico analysis, resulting in the identification of miR-29c as a regulator of muscle mass and then analyzed the effects of overexpression of this miR in the muscle.

Methods:

Adult male C57BL/6 mice (8-12 weeks old, 24.9 ± 1.1g) had the Tibialis Anterior muscle injected with 50µg of plasmid, pMIR29c or Empty Vector (EV, as a control group), then the muscle was electroporated (50V, 5 pulses, 20ms and 1 Hz). Divided by periods (n = 4-30 days). The muscle was submitted to tetanic strength test, histology, extraction of total RNA for qPCR and protein for Western Blot. C2C12 cells were induced to differentiation for 1-5 days and transfected with a mimic miR-29c or a mimic scrambled as a control (40nM each). For statistical analysis we used one-way ANOVA or paired t-test; p <0.05 vs EV or Scrambled). Procedures approved by the Brazilian College of Animal Experimentation CEUA-ICB/USP n°118.

Results:

Overexpression of miR-29c, 30 days after electroporation, increased muscle mass by 40%, with a corresponding increase in fiber cross-sectional area (~36%) and force (~40%). In addition, we also observed increase in serial sarcomere number (~31%). Satellite cell activity was increased by miR-29c overexpression as we measured percentage of positive nuclei for Pax7 (~2.5 fold) and MyoD (~2.0 fold). Mechanistically, the overexpression of miR-29c inhibited the expression of the muscle atrophic factors MuRF1 (0.5 fold), Atrogin-1 (0.5 fold), HDAC4 (0.4 fold) and Myostatin (0.5 fold), and also modulated the expression of genes related to protein synthesis: Akt (1.8 fold) and PI3k (1.5 fold) vs EV control groups. In the luciferase assays, we found the key atrogene MuRF1 as a direct target of miR-29c. In C2C12 cells, miR-29c mimics increased myogenesis (2.0 fold) and myotube diameter (~44%) vs scrambled control groups. Accordingly, the mRNA levels of myogenic markers were also increased: MyoD (0.5 fold) and MyoG (0.5 fold) vs scrambled control groups.

FeSBE Annual Meeting 2019

Poster Sessions and Abstracts

Conclusion:

The overexpression of miR-29c increases muscle mass and function, with increased satellite cells and inhibition of muscle atrophy related genes, in addition we found the key atrogene MuRF1 as a direct target of miR-29c. For skeletal muscle, miR-29c might represent an attractive entry point for treating skeletal muscle deficits in the skeletal muscle diseases where a combined improvement for trophicity and function would be beneficial.

Financial support:

This study was funded by grants: FAPESP 2012/22488-2; FAPESP 2015/24716-0; FAPESP 2015/04090-0; CNPq; NIH HL116919; Leducq Foundation 13CVD04

16.011 - COMBINATION OF LODENAFIL AND HUMAN MESENCHYMAL CELLS THERAPY REDUCES CARDIAC AND VASCULAR DYSFUNCTION IN SU5416/HYPOXIA-INDUCED PULMONARY ARTERIAL HYPERTENSION IN RATS. Silva MMC, Alencar AKN, Montagnoli TL, DaSilva JS, Silva GF, Mendez-Otero R, Coelho PMP, Vasques JF, Sudo RT, Zapata-Sudo G, - Programa de Pós-Graduação em Farmacologia e Química Medicinal - UFRJ Programa de Medicina Regenerativa - UFRJ Programa de Pós-Graduação em Cardiologia - UFRJ

Introduction:

Pulmonary arterial hypertension (PAH) is a disease with high morbidity/mortality characterized by an increased pulmonary pressure and right ventricle (RV) failure.

Aim:

The main purpose of this work is the investigation of the effects of the combination of lodenafil, a PDE5 inhibitor, and human mesenchymal stem cells (hMSCs) in an animal model of PAH.

Methods:

All protocols were approved by the Animal Care and Use Committee of Federal University of Rio de Janeiro. Wistar rats (180-250 g) were randomly divided into 2 groups, either kept under normoxia (n=6) or exposed to hypoxia (n=20) during 21 days plus weekly i.p. injection of 20 mg/kg of SU5416 (SuHx). After confirmation of PAH using echocardiography, the SuHx group was subdivided into 4 groups treated for 14 days with: 1. vehicle (DMSO 1 mL/kg, p.o.); 2. lodenafil (10 mg/kg, p.o.); 3. hMSCs (5.10⁵, i.v.); 4. lodenafil plus hMSCs. At the end of protocol, hemodynamic parameters were obtained using echocardiography. Vascular reactivity of pulmonary artery was evaluated in all experimental groups through isometric tension recording. Ratio of RV/ left ventricle+septum (LV+S) weight was determined to assess cardiac hypertrophy.

Results:

Pulmonary artery acceleration time (PAT) which was evaluated using wave doppler echocardiography was significantly reduced in SuHx group with 25.6 ± 2.3 ms when compared to normoxia with 39.0 ± 3.7 (p<0.01). Administration of either hMSC (34.4 ± 5.0 ms) or the combination lodenafil+hMSC (34.3 ± 1.5 ms) but not lodenafil improved this parameter. RV wall thickness detected through echocardiography was 0.68 ± 0.04; 0.86 ± 0.12; 0.93 ± 0.14; 0.58 ± 0.12; 0.46 ± 0.05 mm for normoxia, vehicle-treated, lodenafil-treated; hMSC-treated and lodenafil+hMSC-treated groups. These results indicated cardiac hypertrophy in animals with HAP and reduction with the treatment with hMSC and combination of lodenafil+hMSC. Similar results were observed after in vitro analysis of RV because increased RV/LV+S ratio of 60.8 ± 9.0% in HAP group was reduced to 17.3 ± 3.7 and 20.0 ± 1.8% after treatment with hMSC and lodenafil+hMSC. Impaired vascular reactivity was observed in pulmonary arteries from HAP animals with acetylcholine-induced maximal relaxation of 17.2 ± 3.5% in contrast to vessels from normoxic animals with 67.5 ± 2.1% (p<0.01). However, treatment with lodenafil, hMSC and lodenafil+hMSC improved vascular dysfunction because the response to acetylcholine was 52.4 ± 9.7; 73.6 ± 13.3 and 74.5 ± 1.7%, respectively (p<0.01).

Conclusion:

hMSC therapy and its combination with lodenafil reduced cardiac and vascular dysfunction in rats with PAH.

Financial support:

CNPq, CAPES, INCT/INOFAR, FAPERJ

16.012 - IDENTIFICATION OF MOLECULAR PATHWAY POTENTIALLY INVOLVED IN PROSTATE CARCINOGENESIS IN OFFSPRING RATS SUBMITTED TO MATERNAL LOW PROTEIN DIET: A GLOBAL INTEGRATIVE APPROACH. Camargo ACL, Constantino FB, Santos SAA, Colombelli KT, Fioretto MN, Portela LMF, Moreno CS, Lam WL, Carvalho RF, Justulin LA, - Department of Morphology - Sao Paulo State University (UNESP), Botucatu Department of Pathology - Emory University Department of Pathology - University of British Columbia

Introduction:

Adverse condition during intrauterine development can drive the origin of different diseases in offspring during postnatal life, a condition known as Fetal Programming (FP). Among the most prevalent disorders are obesity, diabetes, cardiovascular disease and some types of cancer. The intrauterine exposure to low protein diet (LPD) is one of the most studied rodent models of FP. Results from our group show that maternal LPD can be associated with delayed prostatic development in young offspring and prostate cancer (Pca) in older rats.

Aim:

Here, we investigated the global expression of microRNAs, mRNAs and proteins in young rats submitted to maternal LPD in order to identify possible molecular pathways deregulated early in life that could be involved in prostate carcinogenesis in older offspring.

Methods:

Male Sprague Dawley rats were divided in 2 groups: Control (CTR, n = 4), born from dams fed with normal protein diet (17% protein); Gestational and Lactational LPD group (GLLP): born from dams fed with LPD (6% protein) during gestation and lactation periods (n = 3). The offspring were euthanized on postnatal day 21 (PND21) and the ventral prostate (VP) was processed for RNA sequencing and protein mass spectrometry.

Results:

We identified 27 deregulated microRNAs (22 up-regulated and 5 down-regulated). In silico analyses were performed to identify predictive mRNA regulated by those differentially expressed microRNA using mirwalk tool. Integrative analyses were performed using data generated by RNA sequencing and protein mass spectrometry. We found 285 predicted targets of the deregulated microRNAs shared with our results of transcriptome and proteomic data. The enrichment analyses using KOBAs tool demonstrated from those predicted targets, 30 enriched terms related to estrogen, Hippo, p53, MAPK, PI3K-Akt and Ras signaling pathway. The protein-protein interaction network generated by String tool identified 14 targets that shared molecular actions. The cBioPortal and SurvExpress database were used to verify the expression of these targets in patients diagnosed with Pca using data from The Cancer Genome Atlas (TCGA). Our set of genes was presented in 64% (313/488) of the patients in TCGA (cBioPortal). The Kaplan-Meier generated by SurvExpress (hazard ratio=12.5 and p-value= =0.000358) analyses demonstrated that these 14 genes were associated with poor prognosis for patients with Pca.

Conclusion:

Our results demonstrated that maternal LPD disrupted the homeostatic pathways involved in prostatic development, leading to slow-growing prostate carcinogenesis observed in aging rats.

Financial support:

FAPESP (2017/014063-7; 2017/08715-0; 2017/08716-6), CNPq (310663/2018-0).

FeSBE Annual Meeting 2019

Poster Sessions and Abstracts

16.013 - EXPLORING THE ROLE OF HUMAN MESENCHYMAL STROMAL CELLS IN IMMUNOMODULATION AFTER CLONAL SELECTION AND CELLULAR ACTIVATION. daSilva KR, Evangelista LSM, Araujo VAA, Felix OMWO, Filho APS, Salomão R, Câmara NOS, deAlmeida DC, - Nefrologia - UNIFESP

Introduction:

Mesenchymal stromal cells (MSCs) are considered promising agents for treatment of immune-associated diseases. MSCs potentially support an immunomodulatory microenvironment able to minimize tissue damage promoting the resolution of inflammation process. However, MSC cultures are essentially multi-clonal with several cellular clones acting differentially in repair and immunosuppression.

Aim:

Thus, in this work, we intend to select several clones of human MSCs cultures and evaluate their molecular and functional pattern to elaborate a molecular classificatory signature for therapeutic use.

Methods:

Bone marrow MSCs cultures were conducted from 3 donors and by manual serial dilution (30, 10, 3 and 1 cells/well) in 96 well-plates, it was generated 9 clones.

Results:

For all clones, immunophenotype, morphological and in vitro immunosuppressive assays were performed and DNA and RNA were saved. For each donors few clones ($\approx 7,6\%$) grew in culture and were staggered (96 to 48 to 12 to 6 well-plates) until culture 25 cm² flasks. All selected clones (9) had fibroblastic-like morphology and presented the typical MSCs immunophenotype (positive for CD73 and CD90 e negative for CD14 and CD45). The immunosuppressive potential in co-cultures with T lymphocytes showed clones with distinct profile: i) naturally immunosuppressive clones and ii) non-naturally immunosuppressive clones. After activation with IFN- γ and TGF- β , these clones, interestingly, improved their immunomodulatory abilities.

Conclusion:

In the final of this study, we intend evaluate the global transcriptional (mRNA and miRNA) and DNA methylation profile of these different sub-clones, as well as, make use of bioinformatics and networks approaches to establish a functionally classifiable MSCs immunosuppressive signature. Hence, we believe elucidate some fundamental aspects about MSCs immunobiology for better application in clinical practice.

Financial support:

CNPq and FAPESP

17 - Basic & Clinical Pharmacology

17.010 - THE ROLE OF LIPID BODIES DURING CYSTOGENESIS OF TOXOPLASMA GONDII IN FELID EPITHELIAL CELLS. Rosa LPA, Garcia MC, Castro SL, Barbosa HS, - Biologia Estrutural - Fiocruz Biologia Celular - Fiocruz

Introduction:

Toxoplasma gondii, the causative agent of toxoplasmosis, is an obligate intracellular parasite with a cosmopolitan distribution. During the establishment of infection, T. gondii uses and exploits the host cell metabolism ensuring the success of its parasitism. One of the mechanisms used by the parasite for this purpose is the recruitment of organelles, including the host cell lipid droplets (LD) for their interaction with the parasitophorous vacuole (PV). LD maintains close association with the PV membrane, the vacuolar space and the parasite membrane during the different stages of intracellular protozoal development. Furthermore, during infection, T. gondii induces increased biogenesis of this organelle and positively modulates the production of some cytokines. Therefore, the hypothesis of work was, based on inhibition of host cell LD biogenesis by blocking the enzymatic activity of fatty acid synthase (FAS), an important enzyme of the fatty acid synthesis

pathway, could interfere with the host cell lipid metabolism, affecting the intracellular development of T. gondii.

Aim:

To test this hypothesis, feline renal epithelial cell line (CRFK) was used to interact with a T. gondii cystogenic strain (ME-49) followed by treatment with C75, as an inhibitor of FAS.

Methods:

Assays were analyzed by optical microscopy (staining, immunofluorescence and cytochemistry) and electron microscopy (transmission and scanning).

Results:

Our results showed that the biogenesis of LD was negatively modulated by treatment with the compound. In addition, rates of reinfection, proliferation and differentiation of tachyzoites were also altered in the presence of C75. Cells treated with the inhibitor showed lower reinfection rates after 4 days. These data were confirmed by the lower incidence of cells harboring multiple VP with a high prevalence of vacuoles containing only one parasite indicative of recent infection. As to the intracellular fate of the parasite we demonstrate that: (i) T. gondii is able to positively modulate the biogenesis of LD in CRFK; (ii) the inhibition of C75-induced FAS triggers alteration in the fatty acid synthesis of the host cell causing metabolic stress in the cellular microenvironment, which stimulates high rates of differentiation from tachyzoites to bradyzoites; (iii) inhibition of host cell lipid synthesis during the interaction of T. gondii-CRFK showed that the parasite loses its ability to establish cystogenesis

Conclusion:

Thus, this set of data suggests that CRFK lipid deprivation, generated by the treatment with C75, negatively impacts on cystogenesis, making this potential candidate for pharmacological tests during the chronic phase of toxoplasmosis.

Financial support:

CNPq, FAPERJ, CAPES, PAPES VI Fiocruz

17.011 - PHARMACOLOGICAL PROFILE OF NEW ADENOSINE RECEPTOR AGONIST IN RATS SUBMITTED TO EXPERIMENTAL MYOCARDIAL INFARCTION. Santos-Carlos B, DaSilva JS, Beltrame F, Montagnoli TL, Maia RC, Rocha MD, Barreiro EJ, Fraga CAM, Sudo RT, Zapata-Sudo G, - Programa de Pesquisa em Desenvolvimento de Fármacos - UFRJ Programa de Pós-graduação em Cardiologia - UFRJ

Introduction:

The management of acute myocardial infarction (MI) includes not only rapid diagnosis but also pain relief and achievement of myocardium reperfusion.

Aim:

Since not all patients have the benefit using conventional treatment, this work investigates the effects of a new compound named LASSBio-1860, which was described as a ligand of adenosine receptor in an experimental model of MI.

Methods:

Protocols were approved by the Animal Care and Use Committee at Federal University of Rio de Janeiro (# 103/17). MI was induced by ligation of the anterior descending coronary artery in male Wistar rats (180-200g) and confirmed using transthoracic echocardiography. The experimental groups were divided into Sham, MI and MI treated orally with either vehicle or 70 $\mu\text{mol/kg}$ of LASSBio-1860 for 7 days. At the end of the protocol, the following parameters were evaluated: hemodynamics, collagen deposition and expression of markers involved in inflammatory pathway (TNF- α , p38) and remodeling (ERK-1/2).

Results:

The increased filling pressure (E/e') and left ventricular end diastolic pressure (LVEDP) detected in the MI of 37.0 ± 3.7 and 18.2 ± 2.2 mmHg ($p < 0.01$) were reduced to 15.8 ± 5.5 and 14.1 ± 5.6 mmHg ($p < 0.05$) after treatment with LASSBio1860. Reduction of ejection fraction observed in MI to $27.9 \pm 4.8\%$ ($p < 0.01$) as compared to Sham ($64.3 \pm$

FeSBE Annual Meeting 2019

Poster Sessions and Abstracts

8.0%) was recovered to $43.9 \pm 6.1\%$ after treatment with LASSBio-1860 ($p < 0.05$). An increase of collagen content and TNF- α expression, as well as nuclear p38 labeling, were detected in the hearts of MI rats in relation to Sham and were reduced in MI-LASSBio-1860 group. In addition, the ratio of phospho-ERK-1/2 to total-ERK-1/2 was increased from 0.750 ± 0.003 in Sham to 0.890 ± 0.006 ($p < 0.5$) in MI, whereas the MI treated with $70 \mu\text{mol/kg}$ of LASSBio-1860 showed a marked reduction to 0.79 ± 0.01 ($p < 0.05$).

Conclusion:

The reduction of inflammatory response and cardiac remodeling induced by LASSBio-1860 could be involved in the improvement of cardiac function in MI.

Financial support:

CNPq, FAPERJ, CAPES, INCT-INOVAR.

17.012 - IN SILICO STUDIES AND ANTILEISHMANIAL ACTIVITY OF RAVENELIN B ISOLATED FROM FUNGUS EXSEROHILUM ROSTRATUM. Silva-Silva JV1, Pina JRS2, Souza CSF1, Fernandes JMP, Lima AHL3, Almeida-Souza F4, Marinho AMR2, Marinho PSB2, Calabrese KS, - 1 Laboratório de Imunomodulação e Protozoologia - FIOCRUZ 2 Laboratório de Química e Pesquisa - UFPA 3 Laboratório de Planejamento e Desenvolvimento de Fármacos LPD - UFPA 4 Pós-Graduação em Ciência Animal - UEMA

Introduction:

Over 1 billion people living in endemic areas at risk of infection for leishmaniasis in at least 98 developing countries in Africa, South-East Asia, and the Americas. Chemotherapy is the most important means of dealing with this infection. Nevertheless, only few effective drugs are available, and each one has a particular disadvantage. Toxicity and long-term regimens compromise most chemotherapeutic options, which decreases patient compliance and adherence to the treatment and consequently the emergence of drug-resistant strains.

Aim:

The aim of this study was evaluate the antileishmanial activity of a new xanone, not yet described in the literature, isolated from fungus Exserohilum rostratum, acquired from the species Phanera splendens (Kunth) Vaz, as potential inhibitor of trypanothione reductase.

Methods:

The compound ravenelin B (unpublished substance) was obtained from cultures of *E. rostratum* in rice, by chromatographic procedures and identified through spectral methods 1D and 2D nuclear magnetic resonance and mass spectrometry. Initially, docking simulations were performed to characterize the interactions of the compound ravenelin B with trypanothione reductase (PDB ID: 2JK6). Herein, the Moldock score algorithm was used as the score function. The cytotoxicity (CC50) against BALB/c peritoneal macrophage was determined by the thiazolyl blue tetrazolium bromide (MTT) method. The viability of *Leishmania amazonensis* promastigote forms was evaluated after 24 hours of treatment with a Neubauer chamber for IC50 determination. Intracellular amastigote analysis was performed on coverslips containing infected macrophages treated with compound ravenelin B for 24 hours, and then fixed in Bouin, stained with Giemsa and examined by light microscopy. The selectivity index was calculated by dividing the CC50 of the macrophages by the IC50 of the *Leishmania* forms. The nitrite quantification was performed by the Griess method. Statistical analysis were carried out with GraphPad Prism 6.01 software.

Results:

Docking result shows that the binding mode of ravenelin B into the active site of the trypanothione reductase is energetically favorable ($\Delta E_{\text{bind}} = -97.75 \text{ kcal.mol}^{-1}$) and three hydrogen bond interactions were observed with Lys60 and Thr335 residues. The ravenelin B compound showed activity against *L. amazonensis* (IC50 promastigote $0.08277 \pm 1.09 \mu\text{g/mL}$; IC50 intracellular amastigote $0.7040 \pm 1.24 \mu\text{g/mL}$). The analysis of the infection parameters revealed concentration-dependent activity, with a decrease in the number of amastigotes per 100 cells, in

the percentage of infected cells and in the mean number of amastigotes per infected cell. When cytotoxicity was evaluated (CC50 of $47.73 \pm 1.23 \mu\text{g/mL}$) it was possible to observe a lower effect when compared to amphotericin B (CC50 of $8.505 \pm 1.08 \mu\text{g/mL}$), thus increasing the selectivity of ravenelin B by the parasite (promastigote, IS 576.7, intracellular amastigote, IS 67.8) compared to reference drug (promastigote, IS 343.5, intracellular amastigote, IS 14.6). However, no change in nitric oxide production was observed nor in the normal or infected cells treated with ravenelin B.

Conclusion:

The interaction of ravenelin B with the trypanothione reductase observed in the in silico study may be a possible way to better elucidate the leishmanicidal activity observed in the in vitro study.

Financial support:

This study was financed in part by the Coordenação de Aperfeiçoamento de Pessoal de Nível Superior – Brasil (CAPES) – Finance Code 001. Just as the authors thank the Instituto Oswaldo Cruz/FIOCRUZ, the Fundação Amazônia de Amparo à Estudos e Pesquisas (FAPESPA), the Fundação de Amparo à Pesquisa e Desenvolvimento Científico e Tecnológico do Estado do Maranhão (FAPEMA) and the Conselho Nacional de Desenvolvimento Científico e Tecnológico (CNPq).

17.013 - DOES MUSCARINIC ACETYLCHOLINE RECEPTOR MODULATE CLUSTERIN EXPRESSION AND/OR SECRETION IN EPIDIDYMIUM?. Moreira TJ, Gontijo LS, Corrêa TL, Ribas JAS, Morales CR, Porto CS, Maróstica E, - Physiology and Pharmacology - UFF Pharmacology - UNIFESP Anatomy and Cell Biology - McGill

Introduction:

Previous studies from our laboratory demonstrated the expression of muscarinic receptor subtypes M1, M2 and M3 in the efferent ducts and rat epididymis (Siu et al., Cell Tissue Res 323:157, 2006) but their functions have not been elucidated.

Aim:

Considering that autonomic neurotransmitters may be involved in various functions of the male reproductive tract, including protein secretion (Ricker et al., J. Androl 17:117, 1996), the objective of this study was to evaluate the effect of cholinergic agonist and antagonists on clusterin (CLU) expression, a protein abundant in the epididymis and important for sperm maturation

Methods:

(CEUA-UFF 931/17) 60-day old male Wistar rats ($n=6/\text{group}$) were anesthetized (ketamine/xylazine-80/10 mg.Kg-1; i.p.) and treated (i.v.) with Ringer's solution (CO) or cholinergic agonist ($10 \mu\text{g}$ carbachol-CA), in the absence or presence of muscarinic antagonists: nonselective ($480 \mu\text{g}$ atropine-AT), M1-selective ($120 \mu\text{g}$ pirenzepine-PI), M2-selective ($120 \mu\text{g}$ methoctramine-ME); M3-selective ($50 \mu\text{g}$ darifenacin-DA). After 2 hours treatments, the epididymis were removed and dissected. Homogenates of the epididymis were prepared for western blotting assays, as well as the epididymis were fixated in Bouin's solution and processed for immunohistochemical assays with clusterin monoclonal antibody. Spermatozoa were also obtained from epididymis cauda for evaluation of membrane integrity and functionality. Values are mean \pm SEM, ANOVA one-way, Newman-Keuls post hoc test, $P < 0.05$.

Results:

There was not statistical difference among the different treated experimental groups (CA, AT+CA, PI+CA, ME+CA and DA+CA) in CLU protein expression in the caput epididymis, when compared to CO group. On the other hand, in the proximal cauda epididymis, atropine induced an immunostaining increase in the apical region and stereocilia, when compared to the CO. With methoctramine treatment the staining pattern was similar, but more intense than the non-selective antagonist. M3-selective antagonist darifenacin did not alter the CLU staining in this region, but an increase in tubular diameter was observed. Furthermore, western blot analysis showed that the

FeSBE Annual Meeting 2019

Poster Sessions and Abstracts

pirenzepine treatment increased CLU protein expression more than atropine and methocramine. Regarding the evaluation of sperm, membrane integrity and functionality were not altered in the groups treated with CA, AT+CA, PI+CA, ME+CA and DA+CA, when compared to CO group.

Conclusion:

Our preliminary data showed that the blockade of M1 and/or M2 subtypes muscarinic receptors increases CLU expression, suggesting the involvement of these receptors in the modulation of secretory processes and/or regulation of protein expression in this tissue. Further studies will be necessary to understand the physiological contribution of these receptors and clarify the function of their in the epididymis and, consequently, in the male gamete maturation. That can be an important issue to understand and treat (in)fertility and to develop new tools for the male contraception.

Financial support:

CNPq, CAPES, PROPI/UFF.

18 - Neuropsychopharmacology

18.011 - OMEGA-3 ADMINISTERED TO RATS DURING PREGNANCY AND LACTATION PROMOTES ANTIDEPRESSANTS EFFECT IN PUPPIES UNDERGOING CEREBRAL ISCHEMIA/REPERFUSION. FEITOSA PWG, ARAGÃO MO, XENOFONTE RSC, MOURA RDS, NETA MSBDF, LIMA LAR, LOPES JMP, LIMA ISP, NOBRE MEP, - Research Laboratory in Neuroscience and Neuroprotection-LAPENN - Federal University of Cariri-UFCA Department of Morphology - Federal University of Ceará – UFC Laboratory of physiology, biochemistry and pharmacology - Estácio FMJ

Introduction:

Perinatal asphyxia is due to inadequate fetal-neonatal oxygenation during peripartum, at birth or in the first minutes of life, and may result in an irreversible brain injury with neurophysiological dysfunction, including motricity, learning, memory and depression. Docosahexaepic acid (DHA) and eicosapentaepic acid (EPA) are omega-3 essential fatty acids that exhibit neuroprotective properties in the face of cerebral ischemia in adult rats.

Aim:

The present study aimed to evaluate the neurochemical and behavioral alterations of puppies submitted to cerebral ischemia/reperfusion of rats treated with omega-3 during pregnancy and lactation.

Methods:

All experimental procedures were approved by the CEUA/UFCA (nº005/2019). Female Wistar rats (180-200 g) were treated with omega-3 at doses of 5 and 10 mg/kg/day (po) and control received distilled water, 0.1 mL/100 g, during pregnancy and lactation. On the 14th postnatal day, puppies (males and females) were submitted to cerebral ischemia by occlusion of the left common carotid artery for 15 minutes followed by reperfusion. The false-operated group (Sham) was submitted to the surgical procedure, except for carotid artery clamping. The puppies (n=6-8) were divided into five groups: false-operated puppies (Sh, control) of untreated mothers, false-operated puppies of mothers treated with omega-3 at a dose of 10 mg/kg (Sh+W3-10), ischemic puppies of untreated mothers (I/Rn), ischemic puppies of mothers treated with omega-3 at doses of 5 (I/R+W3-5) and 10 mg/kg (I/R+W3-10). After 7 days postoperative, puppies were submitted to tests screening for alterations in locomotor activity (open field test), and forced swimming test (FST). Animals were decapitated and homogenates from striata were used for the determination of monoamines in HPLC. The data were analyzed by One-way ANOVA, Student-Newman-Keuls used as post-hoc test (significance $p < 0.05$).

Results:

Ischemia (37.4±2.2, n=23) did not alter the locomotor activity in relation to the control group (32.7±1.9, n=21). However, Sh+W3-10 (19.7±2.9, n=28) and I/R+W3-10 (12.9±2.1, n=23) groups presented a

decrease of 39.8% and 65.5% in relation to their controls (Sh and I/Rn), respectively. The antidepressant activity evaluated by the FST showed that ischemia (185.9±10.8, n=23) increased in 92% the duration of immobility in relation to the control (96.8±8.3, n=21) and the treatment with Omega-3 in both doses (I/R+W3-5, 92.4±6.7, n=32 and I/R+W3-10, 59.5±6.1, n=23) was able to reverse this behavior in a dose-dependent manner. The Sh+W3-10 group (67.8±8.1, n=26) presented a decrease of 30% in relation to the control. Cerebral ischemia decreases by 10 times the levels of dopamine (0.3794±0.1344, n=5) when compared to control (3.663±0.2831, n=4). The I/R+W3-5 (0.5731±0.1662, n=11) and I/R+W3-10 (0.2569±0.0666, n=9) groups didn't present reversal of this parameter. The dopamine values for the Sh+W3-10 group (0.2830±0.1039, n=6) also decreased in relation to control. The dihydroxyphenylacetic acid (DOPAC) levels decreased in 57.22% in the ischemic animals (0.4953±0.0508, n=5) in relation to the control (1.158±0.1313, n=3), being this reduction reverted in I/R+W3-5 (1.180±0.1460, n=9) and I/R+W3-10 groups (0.9681±0.0672, n=9).

Conclusion:

Omega-3 produced a decrease in the immobility time and reversal of the reduction of the DOPAC levels, but did not promote alteration in the levels of dopamine and locomotor activity, thus demonstrating an antidepressant activity and potential neuroprotective.

Financial support:

Pro-Rectory of Research and Innovation - PRPI / Federal University of Cariri - UFCA

18.012 - THE MODULATION OF COCAINE-CONDITIONED PLACE PREFERENCE BY NATURALLY OCCURRING AND SYNTHETIC INDOLE MOLECULES IN ENVIRONMENTALLY-ENRICHED MALE AND FEMALE RATS. Heidrich N, Biff TF, Feddern C, Silva IA, Fonseca AR, Golbspan S, Almeida FB, Fernandes PR, Biajoli MNG, Freese L, Barros HMT, - Farmacociências - UFCSPA

Introduction:

It was recently found by our group that, in addition to having a protective role in animal models of addiction, environmental enrichment (EE) has a protective effect against cocaine-induced neurotoxicity (Freese et al, 2018). Concurrently, indole molecules have been growing in interest as treatment for drug addiction in pharmacological testing.

Aim:

Here, we aim to verify whether the protective effects of EE and treatment with naturally occurring (ibogaine) or synthetic (SS7 and SS12) indole molecules affect preference for cocaine in male and female rats in the conditioned preference place protocol (CPP).

Methods:

Wistar male (n = 56) and female (n = 51) rats on postnatal day (PND) 21 were allocated in: standard housing (SH) or enriched housing (EH, n = 10/cage), made of polycarbonate transparent cages (80x40x50) with 2 floors and diversified objects (rearranged 3x/week). At PND 50, a classical CPP was initiated. Treatments were administered at PND 62 approximately 5 hours before testing: vehicle (VEH: DMSO 80% + saline 20%); ibogaine (IBO): 40 mg/kg; indole molecules SS7 and SS12: 10 mg/kg. Vaginal smear cytology was performed daily to verify the female estrous cycle. Experiments followed the guidelines of the International Laboratory Animal Science Council and were approved by UFCSPA's Ethics Committee for Research (#233/18). Results are presented as mean±S.E.M.

Results:

The estrous cycle distribution of female rats in the CPP day test was: diestrus = 46%, metestrus = 18%, proestrus = 16% and estrus = 20%. In the VEH group, we found that the EH seem to be able to decrease the time spent (seconds) in the cocaine-paired chamber in males (VEH/SH = 478±55 - VEH/EH = 441±73) and females (VEH/SH = 394±57 - VEH/EH = 312±52). In male rats, not considering housing factor, we found that IBO and SS12 decreased the time spent in the drug-paired chamber by

FeSBE Annual Meeting 2019

Poster Sessions and Abstracts

12% and 30%, respectively. In females, both IBO and SS12 treatment reduced time in relation to VEH by 6%. However, SS7 treatment increased time spent on drug-paired chamber by 12% in the female rats and had no effect in males.

Conclusion:

Interestingly, SS12 showed promising results, as seen above, contrasting to SS7, which showed an increase on time spent on the drug-paired chamber. IBO treatment acted as seen previously in the literature, decreasing the time spent on drug-paired chamber. We show here innovative results from new molecules developed in our university. We expect to show the definitive analyses as soon as we finish all in vivo experiments.

Financial support:

CNPq, CAPES, AMTEPA, UFCSPA

18.013 - ANTIDEPRESSIVE ACTION OF (+)-LIMONENE EPOXIDE IN MICE. Almeida AAC, Carvalho RBF, Amorim VR, Lopes LS, Ferreira PMP, - Pós-Graduação em Ciências Farmacêuticas - UNIVERSIDADE FEDERAL DO PIAUÍ/UFPI Pós-Graduação em Biotecnologia - UNIVERSIDADE FEDERAL DO PIAUÍ/UFPI Departamento de Biofísica e Fisiologia - UNIVERSIDADE FEDERAL DO PIAUÍ/UFPI Departamento de Química - INSTITUTO FEDERAL DE EDUCAÇÃO, CIÊNCIA E TECNOLOGIA DO PIAUÍ

Introduction:

(+)-limonene epoxide is a promising derived terpenoid for investigation of therapeutic potential, such as antioxidant, anxiolytic and anthelmintic activities.

Aim:

The aim of this study was to evaluate the antidepressant effects of (+)-limonene epoxide in mice, as well as to clarify its mechanism of action using pharmacological tools.

Methods:

Male Swiss mice were divided into experimental groups (n = 6 animals/group) and treated with 0.05% Tween 80 dissolved in 0.9% saline (vehicle; vo, vehicle group), imipramine 50 mg/kg, paroxetine 20 mg/kg, reserpine 0.25 mg/kg (i.p., positive control groups) and (+)-limonene epoxide at oral doses of 25, 50 and 75 mg/kg. Forced swimming and tail suspension techniques were used to evaluate antidepressant activity. Differences between groups were determined by analysis of variance (ANOVA) followed by Student-Newman-Keuls (p < 0.05). All experimental protocols and procedures were approved by the Animal Experimentation Ethics Committee of the Federal University of Piauí (#091/2014).

Results:

In the forced swim test, (+) - epoxide limonene reduced the immobility time relative to the vehicle group (196.5 ± 4.9 s) at all doses tested (25, 50 and 75 mg / kg): 53.6% (91.2 ± 4.8 s) 72.7% (53.7 ± 2.6 s) and 88.6% (22.3 ± 2.0 s), respectively (p < 0.05). However, only the 75 mg / kg dose significantly reduced the immobility time when compared to imipramine (48.7 ± 3.6 s) and paroxetine (73.0 ± 6.0 s) (p < 0.05). Reserpine promoted a significant 34.8% increase in immobility time (264.8 ± 5.1 s), while imipramine (48.7 ± 3.6 s) and paroxetine (73.0 ± 6.0 s) reduced the immobility time by 75.2 and 62.8%, respectively, when compared to the vehicle group (p < 0.05). In the tail suspension test the antidepressants used as positive controls, paroxetine (46.3 ± 3.1 s) and imipramine (35.2 ± 1.6 s), the three doses of (+)-limonene epoxide (25 mg/kg: 66.1 ± 2.4 s; 50 mg/kg: 43.5 ± 3.5 s; 75 mg/kg: 21.0 ± 3.0 s) were significantly reduced (76.2, 81.9, 74.0, 77.7, and 89.2%, respectively), the immobility time of the mice in relation to the vehicle group (195.3 ± 5.1 s). Reserpine increased the immobility time to 254.3 ± 5.3 s in relation to the vehicle group (p < 0.05), as predicted for such standard drug for the model of depression used. To try to elucidate the mechanism of action, reserpine, paroxetine or imipramine, each associated with (+)-limonene epoxide 75 mg/kg, were administered. These combinations also reduced immobility time of animals in both tests when compared to the group that received reserpine, paroxetine

or imipramine alone, suggesting a beneficial and synergistic action (p < 0.05).

Conclusion:

(+)-limonene epoxide shows antidepressant effects possibly associated with modulation of serotonergic and adrenergic pathways.

Financial support:

CAPES - Coordenação de Aperfeiçoamento de Pessoal de Nível Superior

18.014 - AYAHUASCA INDUCES OPPOSITE CHANGES IN THE EXPRESSION OF GLUR1 AND GLUR2/3 AMPA RECEPTORS IN THE PREFRONTAL CORTEX OF WISTAR RATS. Rocha G, Iyomasa-Pilon MM, Regalo SCH, Siéssere S, Hallak JEC, Rosa MLNM, - Department of Neuroscience and Behavior - USP-RP Department of Biochemistry - FACISB Department of Histology - USP-RP Department of Biochemistry - FAMECA Department of Neurosciences and Behavioral Sciences - USP-RP

Introduction:

The consumption of Ayahuasca beverage is usual in several Brazilian syncretic religions that have expanded to countries in Europe and North America. Usually the ingestion of Ayahuasca occurs 3 times a week. This beverage is made from an Amazonian psychoactive plant containing the serotonin (5-HT) agonist N,N-dimethyltryptamine (DMT) and monoamine oxidase-inhibiting alkaloids (harmine, harmaline and tetrahydroharmine), resulting in enhanced serotonergic activation. Apart from 5-HT, Ayahuasca has been reported to affect glutamatergic processes in some brain areas including prefrontal cortex (PFC), which plays an important role in affective behaviour, attention, working memory, among others.

Aim:

This work aimed at investigating whether the ingestion of Ayahuasca might induce alterations in the expression of glutamate AMPA receptors (GluR1 and GluR2/3) in the dorsolateral PFC of rats.

Methods:

Twelve groups of male Wistar rats (230-250g, n=5-8/each) were used. Six groups received 0.2 or 0.4ml/g of Ayahuasca beverage, only once (acute), 3 times/day for 3 days (subchronic) or once/day for 15 days (chronic). Six control groups received water at the same conditions. Sixty minutes after the last Ayahuasca ingestion the animals were anaesthetized, perfused and their brains sectioned (40µm) for immunohistochemistry detection of GluR1 or GluR2/3 subunits. The number of immunopositive cells (IC) was quantified, separately, in the superficial and deep layers of the PFC, bilaterally. Comparisons between control and Ayahuasca groups used ANOVA followed by Bonferroni, DMS and Duncan tests (p≤0.05).

Results:

For GluR1 either acute, subchronic or chronic ingestion of 0.2 or 0.4ml/g of Ayahuasca induced an increase in the number of IC in both superficial and deep layers of the PFC (6-21%, p<0.01) when compared to control groups. However, for GluR2/3 acute and subchronic treatments induced a decrease in the number of IC (7-15%, p<0.01) in both superficial and deep layers, while only the chronic ingestion of 0.2ml/g induced an increase (17-23%, p<0.01). No difference was found after chronic ingestion of 0.4ml/g. When the Ayahuasca groups were compared, the ingestion of 0.4ml/g always induced lower expression in both GluR1 and GluR2/3 than 0.2ml/g (7-18%, p<0.001).

Conclusion:

Considering the involvement of the PFC in several neurodegenerative and psychiatric disorders, the results found here suggest that glutamate might be a potential therapeutic target for the treatment of disorders where the glutamatergic dysfunction is associated with serotonergic system activation.

Financial support:

FACISB

FeSBE Annual Meeting 2019

Poster Sessions and Abstracts

19 – Toxicology

19.019 -THE EGG WHITE HYDROLYSATE INTAKE ALTERS THE DEPOSITION OF CADMIUM AND THE OXIDATIVE STRESS PRODUCED IN TARGET ORGANS. Silva GC, Pinheiro Jr JEG, Moraes PZ, Stasiaski JE, Barbosa Jr F, Trost ME, Peçanha FM, Vassallo DV, Miguel M, Wiggers GA, - Laboratório de Fisiologia Cardiovascular - UNIPAMPA Faculdade de Ciências Farmacêuticas de Ribeirão Preto - USP Laboratório de Patologia Veterinária - UNIPAMPA Ciências Fisiológicas - UFES Conselho Superior de Investigações Científicas - CSIC/CIAL

Introduction:

Cadmium (Cd) is a heavy metal with known toxic effects in different systems related to its high capacity to induce oxidative stress. Compounds derived from foods with bioactive properties are a promising alternative against oxidative damage caused by exposure to heavy metals. Egg white hydrolysate (EWH) has antioxidant and anti-inflammatory properties with a known effect on metals such as mercury and aluminum. However, its potential effects on exposure to cadmium have not yet been tested.

Aim:

The aim of our study was to evaluate the ability of egg white hydrolysate (EWH) to prevent the effects of exposure to Cd on target organs.

Methods:

Male Wistar rats were treated for 14 days with: 1) intraperitoneal injections (i.p.) of distilled water and tap water by gavage (Untreated); 2) i.p. injections of 1 mg/kg bw per day of CdCl₂ and tap water by gavage (Cd); 3) i.p. injections of distilled water and EWH from pepsin for 8h diluted in tap water (1g/kg/day) by gavage (EWH); 4) both treatments (CdEWH). At the end of the treatment, the distribution of the metal in the hepatic, renal, testis, epididymis, brain and heart tissues were analyzed. We also evaluated biochemical parameters of oxygen species levels (ROS), lipid peroxidation, total antioxidant capacity, GSH level, superoxide dismutase activity (SOD), catalase activity and histopathology. Data are expressed as mean and SEM and compared by ANOVA with significance level of $p < 0.05$ (*vs Untreated; #vs Cd).

Results:

Co-treatment with EWH is able to prevent: a) the deposit of the metal in testis (Untreated: 0.04 ± 0.02 ; Cd: $4.68 \pm 1.03^*$; EWH: 0.01 ± 0.01 ; CdEWH: $1.85 \pm 0.25^{\#}$ $\mu\text{g Cd/g dry tissue}$) and kidney (Untreated: 0.13 ± 0.07 , Cd: $98.34 \pm 13.10^*$, EWH: 0.19 ± 0.05 , CdEWH: $49.82 \pm 3.47^{\#}$ $\mu\text{g Cd/g dry tissue}$); b) the increased oxidative stress in kidney, liver, heart, testis, epididymis and plasma induced by Cd (TBARS liver: Untreated: 42.88 ± 0.02 ; Cd: $64.36 \pm 2.83^*$; EWH: 3.36 ± 1.25 ; CdEWH: $26.28 \pm 4.07^{\#}$; testis: Untreated: 10.04 ± 1.11 ; Cd: $17.14 \pm 1.87^*$; EWH: 11.65 ± 1.73 ; CdEWH: $8.31 \pm 1.59^{\#}$, nmol MDA/mL; SOD kidney: Untreated: 2038 ± 101.3 ; Cd: $3642 \pm 436.6^*$; EWH: 1923 ± 202.2 ; CdEWH: $2518 \pm 79.1^{\#}$; Plasma: Untreated: 0.012 ± 0.00 ; Cd: $0.286 \pm 0.00^*$; EWH: 0.010 ± 0.00 ; CdEWH: $0.016 \pm 0.00^{\#}$, SOD activity (UI); GSH level liver: Untreated: 40.32 ± 1.52 ; Cd: $59.64 \pm 5.85^*$; EWH: 46.22 ± 2.87 ; CdEWH: $35.85 \pm 3.82^{\#}$; Kidney: Untreated: 29.83 ± 1.81 ; Cd: $40.56 \pm 4.08^*$; EWH: 23.59 ± 1.11 ; CdEWH: $26.58 \pm 0.91^{\#}$; Testis: Untreated: 1.08 ± 0.04 ; Cd: $0.75 \pm 0.03^*$; EWH: 1.20 ± 0.06 ; CdEWH: $0.98 \pm 0.05^{\#}$, nmol GSH/g tissue); c) the testicular degeneration, reduction of the number of sperm in the epididymis and testis and the number of multinucleated cells in the testis on the histopathological examination.

Conclusion:

EWH may be an alternative to protect against damage from exposure to Cd.

Financial support:

Supported by the Brazilian Government (Conselho Nacional de Desenvolvimento Científico e Tecnológico – CNPq 307399/2017-6; CAPES) and by the Spanish Government [MINECO - AGL2017-89213-R and SAF2015-69294-R].

19.020 - MUTAGENIC POTENTIAL OF CANNABIS SATIVA INFUSION - MICRONUCLEOUS QUANTIFICATION USING TRADESCANTIA PALLIDA (TRAD-MCN). Silva JS, Lobo DJA, Yariwake VY, Lichtenfels AJFC, Veras MM, Guimarães ET, - Laboratório de Poluição Atmosférica Experimental do Departamento de Patologia - HCFMUSP

Introduction:

In 1753, the Swedish botanist Carolus Linnaeus coined the scientific term Cannabis sativa for marijuana (popularly known in Brazil as maconha). C. sativa is a member of the family Moraceae, which grows freely in several parts of the world, mainly in the tropical and temperate regions. Reports of its use (textile, medicine, religious) date more than 4000 years. Δ^9 -THC (tetrahydrocannabinol or THC) is the main psychoactive compound present in Cannabis, however there are more than 40 cannabinoids with potential therapeutic such as cannabidiol (CBD). Although there are several studies focusing on Cannabis toxic and therapeutic potential, the available evidence on the possible mutagenic effects of Cannabis-derived products is still inconclusive (BOWLES, et al, 2012) even more if we consider the different forms of use (edibles, smoking, infusion, extracts).

Aim:

Thus, our proposal was to assess a possible mutagenic effect of Cannabis, using a mutagenicity bioassay. This test (Trad-MCN) uses a plant Tradescantia pallida, to quantify the number micronuclei (MCN) as an indicator of DNA damage. Trad-MCN is routinely used in environmental studies and has proved to be efficient.

Methods:

We used 75 cutting of Tradescantia pallida (young inflorescences) collected at the Polo Cultural do Pacaembu, located in the Pacaembu district of São Paulo-SP, Brazil (latitude -23.5449S and longitude -46.6653W). The cuttings were divided into 5 groups of 15. We put these cuttings in beakers (base) containing Cannabis sativa infusions prepared in 3 concentration (0.25%, 0.50% and 1.0%), we also used a negative control (NC) (tap water) and a positive control (PC) (0.5% formaldehyde in tap water). To prepare the infusion, 4 g of the material were boiled into 200 ml of water for 15 minutes. After cooling, it was filtered as a stock solution, from which the concentrations used in the experiment were prepared. Briefly, the cutting were left immersed in tap water for 24 hours (adaptation period) and then exposed to the solutions described above for 8h (exposure period), followed by another 24 hours immersed in tap water (recovery period). After these steps, young inflorescences were fixed in acetic acid and alcohol solution (1:3). Samples were blind-encoded prior to preparation of the slides. The MCN were quantified at 300 tetrads per slide at 400X magnification by a trained biologist. Statistics were performed using SPSS and comparisons conducted by ANOVA test.

Results:

The results are presented as mean \pm standard deviation. The number of MCN was increased in group 1% (7.99 ± 2.6) compared to control NC (2.90 ± 1.01 , $p = 0.008$), surprisingly number of MCN in 1% group was similar to values obtained in PC group (7.67 ± 2.2 , $p > 0.05$). There is a clear dose/concentration effect, as the number of MCN in group 0,25% (3.63 ± 2.29) and 50% (3.58 ± 1.77) was reduced when compared to group 1% ($p = 0.035$).

Conclusion:

Our results indicate that infusion prepared using Cannabis sativa has a mutagenic potential and it seems to dose dependent. This is one of the first studies that has investigated the mutagenic potential of Cannabis sativa "teas" using a bioindicator, further studies using in vivo and in vitro methods are necessary.

Financial support:

LIM-HCFMUSP

FeSBE Annual Meeting 2019

Poster Sessions and Abstracts

19.021 - PLATELET ACTIVATING FACTOR (PAF) ANTAGONISM HAS DUAL EFFECT IN ACUTE LUNG INJURY (ALI) CAUSED BY SCORPION VENOM. Andrade FB, Myamoto JG, Jacob VV, Candido DM, Filho PP, Ferraz C, Junior WAV, Kwasiński FH, - Patologia Experimental - UEL Instituto Butantan - IB Imunologia - IFRJ

Introduction:

ALI with participation of inflammatory mediators as PAF and nitric oxide (NO) can be triggered by venoms from scorpions of Buthidae family, such as Tityus. We have reported that, despite important differences, T.serrulatus and T.bahiensis venoms (Tsv and Tbv) caused ALI in rats. PAF participation has been studied in ALI induced by Tsv, but neither studies involving Tbv nor inflammatory mechanisms about the physiopathology are clear.

Aim:

Here the participation of PAF was investigated in ALI induced by Tsv and Tbv.

Methods:

Male rats (200-250 g) received Tsv or Tbv (200 µg/kg, iv), following the indicated times they were killed by CO₂ inhalation, lung circulation was perfused with isotonic NaCl via a cannula in the pulmonary artery, and trachea (T), upper and inner bronchi (UB / IB), and lungs (L) were dissected. Edema (in 30 min, n=6 to 11) and hemorrhage (in 60 min, n=8 to 13) were investigated by Evans blue (EB) extravasation and cyanometahemoglobin concentration, respectively. After 4 h of envenomation the protein content (by Bradford method, n=4 to 7) and leukocyte influx (total and differential counts, n=5 to 11) in bronchoalveolar lavage (BAL), activity of myeloperoxidase (MPO, n=5 to 7) and nitrite as estimative of NO (adapted Griess method, n=5 to 7) production in lung homogenates were analyzed. To evaluate the impact of PAF, the rats were pretreated with the antagonist receptor WEB2170 (WEB, 5 mg/kg, iv) 30 min before the envenomation. Venoms and WEB were diluted in NaCl 0.9%. Basal data were obtained with the injection of NaCl 0.9%. The procedures were approved by the institutional ethics committee (16583.2013.29). Data were compared by one-way ANOVA and Tukey's post-hoc, or Kruskal-Wallis and Dunn's post-hoc, considering a significance level of $\alpha=0.05$. Results were expressed as mean \pm standard deviation of means.

Results:

Tsv and Tbv induced ALI characterized by EB extravasation (Basal: T 16.5 \pm 1.7; UB 20.2 \pm 1.0; IB 28.9 \pm 3.3; L 27.4 \pm 4.5. Tsv: T 30.8 \pm 3.5; UB 40.4 \pm 5.8; IB 66.9 \pm 8.8; L 118.6 \pm 8.5. Tbv: T 17.7 \pm 1.1; UB 30.2 \pm 2.6; IB 52.1 \pm 3.3; L 75.3 \pm 6.4); hemorrhage (Basal: T 2.7 \pm 1.1; UB 3.3 \pm 1.1; IB 3.9 \pm 1.4; L 6.2 \pm 2.0. Tsv: T 3.3 \pm 0.3; UB 3.8 \pm 0.3; IB 9 \pm 1.1; L: 17.6 \pm 2.6. Tbv: T 3.8 \pm 1.9; UB 4.6 \pm 2.1; IB 10.7 \pm 3.8; L 26.4 \pm 6); alveolar influx of neutrophils (Basal: 0.1 \pm 0.02; Tsv: 0.8 \pm 0.3; Tbv: 0.4 \pm 0.06); MPO activity (Basal: 6.3 \pm 1; Tsv: 18.8 \pm 2.1; Tbv: 14.8 \pm 1.8); protein in BAL (Basal: 0.3 \pm 0.1; Tsv: 1.1 \pm 0.2; Tbv: 0.7 \pm 0.1) and NO production (Basal: 11.3 \pm 0.9; Tsv: 24.2 \pm 1.7; Tbv: 39.4 \pm 4.3). EB extravasation was not modified by WEB, but it inhibited hemorrhage in Tsv (IB 4.4 \pm 0.6; L 10.4 \pm 2.8). Neutrophils influx in BAL induced by both venoms was inhibited by WEB (Tsv: 0.1 \pm 0.01; Tbv: 0.07 \pm 0.02), but in Tsv envenomed animals WEB reduced (by 60%) also total leukocyte and mononuclear counts. In contrast, protein content in BAL and MPO activity in lung homogenates were increased by WEB in ALI induced by Tsv (5.2 \pm 2.2) and Tbv (8.0 \pm 2.1). In envenomed groups, NO production in lungs was inhibited by WEB (Tsv 16.6 \pm 1.2; Tbv 24.9 \pm 0.5).

Conclusion:

PAF seems to have a role in ALI induced by Tsv and by Tbv, but promoting broader effect in Tsv envenomed rats.

Financial support:

CAPES

19.022 - DETERMINATION OF THE EFFECTS OF MI-D (MESOIONIC COMPOUND 4-PHENYL-5- [4-NITROCINAMOYL] -1,3,4-THIADIAZOLYL-2-PHENYLAMINE CHLORIDE) AT HISTOLOGICAL LEVELS OVER TUMORAL CELLS (HT29) EMPLOYING CHORIOALLANTOIC MEMBRANE (CAM). Stoltz IR, Rocha LT, Goetten JO, Esposito SE, Echevarria Á, Rodrigues ALV, Gonçalves PG, Lopes RL, Oliveira RF, Campelo PMS, Pires DC, Castro HT, Pereira LF, - Laboratório de Biologia Experimental - PUCPR Centro de Pesquisa em Oncologia Molecular - HCB Síntese de compostos heterocíclicos - UFRJ

Introduction:

Mesoionic compounds are studied in the search for antineoplastic drugs, its structure confers a biological activity. It was verified the MI-D reduces the phosphorylation efficiency of mitochondria. To evaluate the MI-D effects on angiogenic phenomena the Chorioallantoic Membrane was used. In consequence of its high vascularization, tumor cells grow easily on this vascular bed. Also CAM's collagen level can be used to tumoral analysis, besides growing factors are associated with increased activity of inflammatory agents that mediate collagen disposition. The extracellular matrix (ECM) of CAM act as a regulator of tissue function, its remodeling plays a role on generation of biochemical migration routes, associated with tumors.

Aim:

To Analyze the MI-D effects on tumor (HT29 cells by human colon carcinoma) over CAM's angiogenic or antiangiogenic properties, using macroscopic and histological procedures.

Methods:

All procedures approved by the institutional ethical committee, numbers 850/2016. For the tests, were used 60 fertilized eggs of Gallus gallus (Chácara Amazônia - metropolitan area of Curitiba). The eggs were cleaned and incubated (38°C ~75% humidity), after 9 days were opened. The test (N=60) was distributed in six groups: control, collagen control, negative control, positive control, MI-D control and MID + HT29 groups (10 eggs per group). Prior to CAM test, HT29 cells were cultured in supplemented RPMI 1640 growth medium. Cells were added to collagen on a density of 1x10⁷ and polymerized in a concentration of 200 µL using sterile PBS 1 x. Controls test were performed containing only collagen, collagen + MI-D (5 µM, 25 µM, 50µM) and collagen + HT29 cells. After inoculation, the eggs were closed with tape and incubated to more 3 days. After that the eggs were re-opened, analyzed macroscopically and photographed. To analyze the images it was used a software IMAGE PRO PLUS®, to determine the CAM depth and collagen levels. For the histological studies (H&E, Sirius Red) part of CAM with the tumor was removed, fixed during 10 minutes in Formalin 10%. The embryos were euthanized with 200 µL of Ketamine then fixed to morphological studies. The statistical study was based in the sample of 10 independent experiments, performing M \pm SEM, ANOVA and Tukey's test.

Results:

The tests containing MI-D and HT29 have shown significant decreasing of vessels (v) number in different concentrations against control. 15.74% for MI-D 5 µM (10.70 \pm 0.84 v/mm²), of 26.29% for MI-D 25 µM (9.49 \pm 0.25 v/mm²), and 36.61% with MI-D 50 µM (8.05 \pm 0.44 v / mm²). The thickness and depth of CAM shown significantly decrease among the experiments with MI-D, 60% with 5 µM, 30% with 25µM, and 28% with 50µM. The collagen levels have changed significantly on the presence of tumor only, and tumor + MI-D under the concentration of 25 µm and 50 µm.

Conclusion:

Both MI-D and HT29 tumor changes CAM's vascularization significantly, the MI-D by decreasing blood vessels, and HT29 by changing CAM's ECM and collagen distribution. This effect corroborated to the effects described in literature.

Financial support:

Pontifical Catholic University of Parana.

FeSBE Annual Meeting 2019

Poster Sessions and Abstracts

19.023 - EVALUATION OF DECAVANADATE SALTS ($[(V_{10}O_{28})_6]^{6-}; (NH_4)_2[Cu(H_2O)_6]_2[V_{10}O_{28}] \cdot 2H_2O$) IN THE DEVELOPMENT PROCESS OF HET-CAM VESSELS. Taborda-Rocha L, Stoltz IR, Pires DC, Rodrigues ALV, Leme LBP, Sá EL, Nunes GG, Pereira LF, - Laboratório de Biologia Experimental - PUCPR Química - UFPR

Introduction:

Vanadium compounds have been extensively studied due to their interaction with proteins and their potential application in medicinal chemistry. Among them, decavanadate, $[V_{10}O_{28}]^{6-}$, has demonstrated a wide medical application. The chicken embryo chorioallantoic membrane (CAM) is a tissue that forms a wide network of blood vessels being very useful to visualization and determination of biological phenomena of angiogenesis. Therefore, CAM is of relatively easy manipulation and is a good model to evaluate the effect of chemicals in the angiogenesis. The copper element plays an essential role in the biochemistry of aerobic organisms, being essential to catalyze a wide range of enzymes. Thus the presence of copper inserted in a decavanadate structure should improve his biological activity.

Aim:

Evaluation of decavanadate effects combined with a first transition metal element in the formation of blood vessels using chick embryo chorioallantoic membrane as a model.

Methods:

The decavanadates were prepared by a research group in the department of inorganic chemistry of UFPR, the products were characterized by spectroscopic and diffractometric methods. All animal procedures were pre-approved by the institutional ethical committee nº 850/2013 (1st version). The fertilized eggs of chicken (Leghorn variety) were incubated for 7 days. A window was opened in the shell and CAM injected with different concentrations (0.1, 0.5, 1.0, 5.0, 15 mL⁻¹) of the products and sealed with adhesive tape. Seven days later CAM was photographed with a digital camera coupled to a stereoscopic microscope (30 x magnification). CAM was removed and fixed with formalin 10% and analyzed to count the blood vessels and quantificate the vessels' caliber. The embryos were euthanized and fixed to further morphological studies. The pictures were analyzed with Image-Pro Plus® program. Statistical analyses were performed with mean±SEM, ANOVA and Tukey's test.

Results:

Assays with CAM revealed that solutions of copper decavanadate in concentrations above 15 µg.mL⁻¹ were lethal to the embryos, causing desmoplasia (opacity, degradation) and disintegration of CAM. The doses up to 15 µg.mL⁻¹ were not embryotoxic, but triggered an increasing of CAM's blood vessel density in a dose-dependent manner and also increasing the caliber of the vessels, as compared with the control. On the other hand, only the decavanadate was lethal at all concentrations evaluated.

Conclusion:

The studies have shown that the general response on CAM system was dose-dependent, resulting in an angiogenic and vasodilator effect. All concentrations above 15 µg.mL⁻¹ decreased the morphological development of the embryos, in this sense is possible to infer a toxic effect of decavanadate and copper decavanadate on the CAM. More assays should be conducted to verify its effects over CAM and on the embryo.

Financial support:

Pontifícia Universidade Católica do Paraná, Universidade Federal do Paraná (UFPR).

19.024 - SUBCHRONIC EXPOSURE TO MICROCYSTIN-LR IMPAIRS MITOCHONDRIAL FUNCTION IN MOUSE LUNGS. MESQUITA FMD, Pinto LMO, Oliveira DF, Trajano AP, Meirelles LS, AZEVEDO SMFO, Nascimento JHM, ZIN WA, - Centro de Ciências da Saúde - Universidade Federal do Rio de Janeiro

Introduction:

Microcystins (MCs) are cyanobacterial hepatotoxic cyclic peptides reported in human intoxication outbreaks. Among routes of exposure, ingestion is of paramount importance because these toxins might be present in drinking water. Although the lung is not the main MCs target, the toxin can reach the respiratory system after being ingested, absorbed and carried into the liver. Interestingly, mitochondria serve as relevant markers of intoxication in several organs. Moreover, mitochondrial dysfunction is usually associated to several pulmonary diseases.

Aim:

Thus, we aimed to assess lung mechanics and mitochondrial function after the administration of sublethal doses of MC-LR during 20 consecutive days.

Methods:

BALB/c mice were divided into two groups (n=7) exposed by oral gavage: TOX (30 µg MC-LR/kg/day in water) and CTRL group (water). The animals were then anesthetized, paralyzed and mechanically ventilated for the determination of lung mechanics. Further, other two groups (n= 7 in each) were exposed to assess mitochondrial function by analysis of the ADP-stimulated respiration, swelling, transmembrane potential, ROS and ATP production.

Results:

Lung mechanics did not significantly changed in animals exposed to MC-LR. However, mitochondrial ROS increased significantly, mitochondria mechanics did not significantly changed in animals exposed to MC-LR. However, mitochondrial ROS increased significantly, decrease of ATP production and mitochondrial respiration fell and the membrane depolarized. Conversely, not was observed mitochondrial swelling.

Conclusion:

Thus, mitochondrial damage markers revealed that under the present experimental conditions microcystin-LR affected cell bioenergetics and antioxidant defenses, even before jeopardizing lung function.

Financial support:

CNPq

19.025 - MICRONUCLEI FREQUENCY AND POLLEN ABORTION USING TRADESCANTIA PALLIDA FOR MONITORING AIR POLLUTION GRADIENTES IN SÃO PAULO CITY: NEW INSIGHTS. Oliveira VMS, Seriani R, Veras MM, Guimarães ET, - Laboratório de Poluição Atmosférica Experimental - Faculdade de Medicina, Universidade de São Paulo, São Paulo, SP, BR.

Introduction:

Air pollution is a mix of particles and gases. Monitoring levels of air pollutants is one the most important steps to improve air quality, this data is essential to a successful plan to reduce air pollution. Monitoring networks and equipment are expensive and may difficult the implementation of a quality control system. Luckily, there is less expensive and efficient methods using plants as bioindicators. Tradescantia pallida has been used in several studies - the micronucleus quantification test (Trad-MCN), which has been shown to be effective to detect the genotoxic action of pollutants. The Pollen Abortion (PA) test has also been shown to be very efficient for biomonitoring, but is used with other species (e.g. Cichorium intybus, Linaria vulgaris, Robinia pseudoacacia). Testing the feasibility of developing the PA test in T. pallida may allow an association between the two techniques in a single bioindicator, giving greater robustness to biomonitoring.

Aim:

Thus, objectives of the present study were to verify the viability of the AP test in the T. pallida, identify a possible correlation between the MCN and PA test and to check if there is a best inflorescence phase to use (Phase1: young, Phase-2:1-flower and Phase-3:>-flowers) and to check the feasibility of applying the two techniques in the same inflorescence.

Methods:

FeSBE Annual Meeting 2019 Poster Sessions and Abstracts

We used inflorescences of *Tradescantia* collected at two points, which represent regions with different levels of pollution: FMUSP-polluted and Polo-less polluted. Briefly, the sampled inflorescences were fixed in acetic acid/alcohol (1:3) immediately after collection. Thirty slides were prepared per group, and the number of micronuclei in young tetrads (MCN) and the pollen abortion rate (PA) in the same inflorescence were quantified. Criteria for determination of aborted pollen were morphology and coloration. Previously, we monitored the ambient levels fine (PM_{2.5}) particulate pollution to characterize the levels at each point (FMUSP: PM_{2.5}=0.028g/cm³; Polo: PM_{2.5}=0.018g/cm³). A MANOVA were performed to resolve the main effects (levels of air pollution) and to check if there are interaction effects (inflorescence phase), Test T was used to compare the test and the correlation between them was assessed by Spearman's rank coefficient (CC). Null hypotheses were rejected at a probability level of P=0.05.

Results:

Our results confirmed the efficiency of both tests to detect differences in the levels of air pollution (local point, $p < 0.0001$; test, $p < 0.001$). Number of micronuclei (FMUSP, 5.5 ± 7.8 ; Polo, 1.4 ± 1.04 , $p < 0.001$) and pollen abortion (FMUSP 8.2 ± 17.2 ; Polo 2.84 ± 1.2 , $p = 0.004$) were higher in the point located at FMUSP. Inflorescence phase is determinant to detect these differences (phase*local, $p = 0,006$). Young phase (phase1) is more sensitive, we observed that in the cleaner point the number of MCN were different depending on phase, however in the more polluted point differences in detection by phase were not seen. CC was 0.518 ($p < 0.001$).

Conclusion:

We considered the application of the PA test in *Tradescantia* (Trad-PA), feasible. Phase-1 was the most adequate for the application of MCN and PA techniques and both tests were efficient and correlated well to detect a pollution gradient between the two points.

Financial support:

LIM-HCFMUSP

19.026 - STUDY OF ACUTE SINGLE DOSE TOXICITY OF CROTAMINE IN WISTAR RATS: ANALYSIS OF BIOCHEMICAL, HEMATOLOGICAL AND HISTOPATHOLOGICAL PARAMETERS. Andrade AAR, Pimentel VE, Rodrigues TFS, Souza DA, Pereira JHC, Alves GA, Franco LS, Chiarotto GB, MAZZI MV, - Laboratório de Caracterização de Proteínas e Peptídeos - FHO

Introduction:

Crotamine (CTM), is a polypeptide with cell penetration ability and nuclear specificity. CTM has been studied as a biomolecule carrier and anti-tumor agent. However, studies have shown that the molecule has varied bioavailability for different organs and systems, including the CNS, which restricts its systemic use.

Aim:

The aim of the present work was to determine the short-term adverse effects of the Crotamine in Wistar rats using a single dose of different concentrations.

Methods:

CEUA-UNUARARAS: 011/2018. 45 males Wistar rats (60 days, ± 200 g) were divided into 5 groups (n=3) containing vehicle (saline), control group and CTM (25, 50 and 100 μ g). The animals were injected i.p with a single dose, monitored for all the days and analyzed after 2d, 7d and 14d. Hepatic and renal functions were analyzed to access (TGO, TGP, gamma GT, Urea, PT and APTT). ELISA assay was used for determination of TGF- β . Hematologic parameters (Erythrocytes, hemoglobin, hematocrits and Thrombocytes) and Leukogram were determined. The liver and kidneys were collected for oxidative stress analyzes (-SH groups) and histological analyzes. The data were analyzed ANOVA with Bonferroni post-hoc ($p < 0.05$) and were expressed by the mean.

Results:

The groups treated with lower dose of CTM (100 μ g/kg/day and 50 μ g/kg/day) showed no significant alteration in TGO compared to the

control (Control2d=65,33 \pm 1,45; CTM2d 100 μ g/kg/day=100,33 \pm 0,66; Control7d=63,00 \pm 0,57; CTM7d 50 μ g/kg/day=81,33 \pm 3,71; CTM7d 100 μ g/kg/day=95,33 \pm 2,33). The groups treated with CTM (100 μ g/kg/day, 50 μ g/kg/day and 25 μ g/kg/day) showed a significant decrease of TGP (U/L) in relation to the control (Control2d=54,33 \pm 2,33; CTM2d 100 μ g/kg/day=32,33 \pm 1,45; CTM2d 50 μ g/kg/day=32,33 \pm 1,45; CTM2d 25 μ g/kg/day=30,00 \pm 0,57; Control7d=54,33 \pm 2,33; CTM7d 100 μ g/kg/day=23,00 \pm 1,15; CTM7d 50 μ g/kg/day=22,66 \pm 0,88; CTM7d 25 μ g/kg/day=35,00 \pm 1,73; Control14d=39,33 \pm 0,88; CTM14d 100 μ g/kg/day=29,00 \pm 2,30; CTM14d 50 μ g/kg/day=31,33 \pm 3,18; CTM14d 25 μ g/kg/day=25,33 \pm 0,88). All the CTM doses did not caused significant differences in urea and gamma GT level (mg/dL) in relation to the control (Control2d=247,66 \pm 2,18; CTM2d 100 μ g/kg/day=225,00 \pm 10,4; CTM2d 50 μ g/kg/day=260,00 \pm 28,3; CTM2d 25 μ g/kg/day=246,66 \pm 16,37; Control7d=297,66 \pm 15,9; CTM7d 100 μ g/kg/day=238,33 \pm 8,68; CTM7d 50 μ g/kg/day=243,00 \pm 1,15; CTM7d 25 μ g/kg/day=230,33 \pm 2,60; Control14d=344,66 \pm 7,31; CTM14d 100 μ g/kg/day=265,00 \pm 16,52; CTM14d 50 μ g/kg/day=326,33 \pm 50,71; CTM14d 25 μ g/kg/day=389,66 \pm 64,83; Control2d=56,00 \pm 2,51; CTM2d 100 μ g/kg/day=49,33 \pm 4,25; CTM2d 50 μ g/kg/day=51,66 \pm 6,69; CTM2d 25 μ g/kg/day=56,33 \pm 5,89; Control7d=53,66 \pm 5,60; CTM7d 100 μ g/kg/day=58,33 \pm 4,63; CTM7d 50 μ g/kg/day=61,00 \pm 2,30; CTM7d 25 μ g/kg/day=58,00 \pm 3,60; Control14d=54,00 \pm 2,88; CTM14d 100 μ g/kg/day=54,33 \pm 3,28; CTM14d 50 μ g/kg/day=56,33 \pm 3,38; CTM14d 25 μ g/kg/day=55,66 \pm 7,31; respectively). No alterations of coagulation time (TP and TTPA) was observed at the 14th (Control=26,00; CTM 100 μ g/kg/day=28,66; CTM 50 μ g/kg/day=30,00; CTM 25 μ g/kg/day=24,66; Control=34,66; CTM 100 μ g/kg/day=35,33; CTM 50 μ g/kg/day=32; CTM 25 μ g/kg/day=35,33; respectively). On the same day of analysis, the CTM (100 μ g/kg/day and 50 μ g/kg/day) presented higher levels of TGF- β (pg/mL) in relation to the control (Control=285,00 \pm 55,79; CTM 100 μ g/kg/day=274,16 \pm 46,21; CTM 50 μ g/kg/day=286,66 \pm 45,72). In addition, no significant differences were observed in the SH groups of both hepatic and renal functions (Control=1,406 $\times 10^{-5}$; 100 μ g/kg/day=1,503 $\times 10^{-5}$; 50 μ g/kg/day=1,448 $\times 10^{-5}$; 25 μ g/kg/day=1,439 $\times 10^{-5}$; Control=2,714 $\times 10^{-6}$; 100 μ g/kg/day=5,88 $\times 10^{-6}$; 50 μ g/kg/day=5,293 $\times 10^{-6}$; 25 μ g/kg/day=7,883 $\times 10^{-6}$; respectively). There were no significant changes in hematological parameters (erythrocytes, hemoglobin, hematocrit and thrombocytes) and Leukogram pattern. The histopathological analysis showed no alterations in the inflammatory infiltrate and no hemorrhagic areas were identified, thus demonstrating the conservation of the cytological structure.

Conclusion:

These data suggest that sub lethal doses of CTM did not present systemic toxicity, using the acute single dose toxicity test, as protocol established by ANVISA and FDA for the development of new drugs.

Financial support:

FHO-Uniararas, CNPq

19.027 - ZEBRAFISH EMBRYO TOXICITY TESTING: THE CRITICAL ROLE OF CHORION MEMBRANE. Medeiros AMZ, Silva GH, Castro VL, Martinez DST, - Grupo de nanobiotecnologia e nanoeotoxicologia (NBT) - LNNano / CNPEM Laboratorio de biotecnologia e biosegurança - Embrapa Meio Ambiente CENA - USP

Introduction:

In 2013 the Organisation for Economic Co-operation and Development (OECD) test guideline (236) for fish embryo acute toxicity (FET) was adopted. Zebrafish (*Danio rerio*) embryo toxicity test (FET) is a modern alternative animal to toxicology assay and represents a refinement in the sense of the 3Rs principle. This model presents an exceptional set of characteristics. For example, the embryo transparency allows the visualization of early organogenesis and amenability to embryological manipulation. This feature enables to observe adverse effects of xenobiotics, such as external phenotype changes. A new challenge in this assay is the presence of chorion during the begin of the test.

FeSBE Annual Meeting 2019

Poster Sessions and Abstracts

However, larger molecules have reduced access to the embryo. The chorion membrane has pore channels with 0.5-0.7 mm in diameter, which partly isolate the embryo until the moment of hatching (48 – 72 hours after fertilization – hpf). In this sense, new protocols have been developed to allow the removal of this membrane and exposure directly the “naked” embryo.

Aim:

The aim of this study is to verify the influence of chorion barrier on zebrafish embryo toxicology test.

Methods:

In this work, a modified FET methodology was designed to use dechorionated embryos. The chorion of 24 hpf embryos was removed mechanically with tweezers. The embryos were exposed during 72h to AgNO₃. The eggs (n=10) were maintained in Petri dishes at 28°C and 14h:10h light: dark with 20 ml of solution. All the experiment was three times replicated. Chorionated embryos were also exposed to the same conditions to compare the influence of this biological barrier.

Results:

The median lethal concentration (LC50) observed was 69.8 (61.1 – 78.8) µg L⁻¹ for chorionated embryos. The removal of chorion increase the mortality at the presence of AgNO₃ and its LC50 was decreased to 38.1 (33.3 – 41.0) µg L⁻¹. Also, the exposure of the embryo without chorion exhibited high rates of deformation in phenotype (like pericardial edema, spinal curvature, lack of yolk sac absorbed, shortened body length) in comparison with chorionated embryos. The embryos of control groups (chorionated and dechorionated) did not show alterations in their phenotype or death. The presence of chorion can block the xenobiotics entrance, and in consequence, its removal allows the beginning of exposure in early stages. It can be suggested that sulfhydryl groups in chorion could absorb the Ag⁺ ions, and decrease their penetration into perivitelline space.

Conclusion:

These findings emphasize the pivotal role of chorion on embryo toxicity. Furthermore, it also may have an influence on other xenobiotics absorption by zebrafish, such as nanomaterials and microplastics. These data suggest that evaluation of toxicity of dechorionated in zebrafish is a more sensitive method than more traditional analyses.

Financial support:

National Council of Scientific and Technological Development (CNPQ)

20 - Pain and Inflammation

20.016 - IN VIVO STUDY OF FUCOSYLATED CHONDROITIN SULFATE AS A NEW THERAPEUTIC AGENT TO TREAT ASTHMA AND EOSINOPHILIC ESOPHAGITIS. Amaral MM, Motta JM, Lintomen L, Nascimento MT, Souza HSP, Pavão MSG, - - - UFRJ

Introduction:

Eosinophilic esophagitis (EoE) is a chronic disease characterized by the recruitment of eosinophils, resulting in inflammation of the esophageal tissue. Histologically, EoE causes basal layer hyperplasia, tissue remodeling, angiogenesis, fibrosis and induction of Th2 immune responses, among others. Moreover, there is evidence of association between EoE and airways inflammation, such as asthma. Fucosylated chondroitin sulfate (FucCS) isolated from the sea cucumber *Holothuria grisea* is a glycosaminoglycan analogue to heparin that presents anticoagulant, anti-inflammatory and antitumoral properties. Our group showed that the sulfation pattern of this polymer is directly related to its biological effects.

Aim:

The aim of this study is to investigate the potential use of the FucCS as an anti-inflammatory agent against EoE and asthma in mice.

Methods:

In order to test our hypothesis, FucCs was extracted and purified from the body wall of *H. grisea*, by methods previously described by our

group. Asthma and EoE were induced in C57Bl/6 mice by intraperitoneal administration of ovalbumin (OVA) at days 0 and 14 followed by intranasal administration for 7 days starting at day 15. FucCS was administered through intraperitoneal injection concomitant to the intranasal administrations of OVA. After euthanasia, the bronchoalveolar lavage fluid (BALF) was obtained from the animals and total cells quantified in a Neubauer chamber. Polymorphonuclear cells were also detected by microscopy using panoptic staining. To investigate the presence of eosinophils within the esophageal tissue, sirius red was used as a marker.

Results:

Data obtained showed increased number of total cells and the presence of polymorphonuclear cells in the BALF of animals challenged with OVA compared to control group. Moreover, administration of FucCS reduced the number of cells in the BALF in comparison to OVA-treated mice (approximately 55% less cells). Regarding the esophagus, our preliminary results suggest the presence of eosinophils in the basal layer of OVA-treated mice, which is the major marker of EoE. On the other hand, no eosinophils were found in both control and FucCS-treated mice.

Conclusion:

Finally, although in initial phase, this study indicates that the *H. grisea* FucCS seems to be effective in attenuating inflammation from asthma and EoE. Additionally, our group successfully developed a more efficient protocol to isolate this glycan from the sea cucumber.

Financial support:

CAPES, CNPq and FAPERJ.

20.017 - ATP-INDUCE PERITONITIS IN MICE. Pereira JS, Faria RX, - Laboratório de toxoplasma e outras protozooses - FIOCRUZ

Introduction:

A large number of plasma membrane receptors are involved in inflammatory processes. Among them the P2X7 receptor, which is an ionotropic purinergic receptor, is distinguished of the other P2 receptors for needing of high ATP concentrations for its activation. P2X7 receptor has been demonstrated to be an important modulator of many physiological and pathophysiological processes. Some dysfunction in the P2X7 receptor can generate an inflammatory process, therefore this receptor is a new pharmacological target for some inflammatory diseases, as rheumatoid arthritis and sepsis.

Aim:

Our aim is to evaluate the action of the P2X7 agonist to induce sterile peritonitis as an animal model for studying this receptor in vivo.

Methods:

We administered 34 mg/kg ATP i.p. for 1, 2, 3, and 4 hours in Swiss Webster male mice. Total cellularity and differential count were realized for evaluating the inflammatory process. These experiments were previously approved for the Ethics Committee with number L043/2018.

Results:

The time of treatment of 2 hours with saline induced an average of 3500000 leucocyte/mL; and the treatment with ATP reduced this cellularity to 2700000 leukocytes/mL.

Conclusion:

Based on the results obtained until now, the ATP treatment reduces the basal cellularity in the peritoneal cavity.

Financial support:

IOC, CIEE, FARPEJ, CNPQ

20.018 - ROLE OF EICOSANOIDS DERIVED FROM 5-,12-LIPOXYGENASE AND CYTOCHROME P450 ON FIBER CONSTITUTION DURING THE REPAIR OF SKELETAL MUSCLE. Damico MV, Godinho RO, Gil CD, Pacini ESA, Fortes-Dias CL, Moreira V, - Farmacologia - Universidade Federal de São Paulo (UNIFESP) Departamento de Morfologia e Genética - UNIFESP

FeSBE Annual Meeting 2019

Poster Sessions and Abstracts

Departamento de Pesquisa e Desenvolvimento - Fundação Ezequiel Dias

Introduction:

Skeletal muscle tissue contains fibers constituted by distinct isoforms of myosin heavy chain (MyHC) that confer upon them fast or slow contractile properties. The slow-twitch fibers (type I) have smaller cross-sectional area (CSA), contain slow-MyHC and are responsible for sustained contractions, whereas fast-twitch fibers (type II) have larger CSA, fast-MyHC that are recruited for forceful movements. During the muscle regeneration the slow fibers are first originated by regulation of transcription factors expressed distinctly in this process. In addition, the inflammatory response accompanies the process of tissue regeneration and some mediators have been described regulating the regeneration muscle events, like prostaglandins, eicosanoids derived from arachidonic acid (AA). However, the influence of eicosanoids from other AA metabolic pathways, such as 5- and 12-lipoxygenase (5-,12-LOX) or cytochrome P450 (CYP450) on skeletal muscle fiber repair has never been studied.

Aim:

The aim was to analyze the regulatory role of eicosanoids from 5-,12-LOX and CYP450 pathways on the constitution of muscle fibers (by CSA and fast MyHC analyses) and on muscle tissue contractile activity, during the regenerative process.

Methods:

Distinct groups of male Swiss mice (20g) received intramuscular injection (i.m.) of a myotoxin (CB) (7,5µg/animal/50µL) or saline (SS). After 30min and 48h from i.m. injection, distinct groups received oral administration: i)1% carboximetilcelulose (CMC); ii)MK-886 (3mg/kg/100µL), 5-LOX inhibitor; iii)Baicalein (20mg/kg/100µL), 12-LOX inhibitor; iv)SKF-525A (25mg/kg/100µL), CYP450 inhibitor. After 21 days from i.m. injection, gastrocnemius muscles were dissected for paraffin processing. Tissue sections of 4µm were stained with hematoxylin/eosin for CSA (µm²) analysis or incubated with fast-MyHC antibody (Sigma) for immunohistochemistry analysis (IOD). To evaluation of contractile activity, gastrocnemius were submerged in Tyrod buffer and connected to isometric voltage transducer coupled to PowerLab® amplifier. Muscles were submitted to fatigue protocol: 10min (train rate/duration: 0,2TPS/300ms); 5min (0,3TPS/300ms).

Results:

The analysis of fibers showed that SS/CMC muscle was constituted predominantly by fibers with 600µm² and fibers type II (68852±7885 IOD-expression fast-MyHC). Comparatively, animals CB/CMC showed high frequency of smaller fibers (200µm²) and low quantitated of fast-MyHC expression (32283±5281 IOD) (p<0,05). Groups CB/MK, CB/Baic and CB/SKF presented larger fibers (300, 300 and 400µm², respectively) and values of 44899±9246, 64925±10369, 72118±11988 IOD of fast-MyHC expression, when compared with CB/CMC animals. Fatigue protocol showed that CB/CMC animals presented increase of muscle contractile resistance (p<0,05) of 28% in comparison with SS/CMC. CB/MK group presented similar levels of muscle resistance to CB/CMC group. However, CB/Baic and CB/SKF groups presented less pronounced resistance than group CB/CMC, with values of 17 and 12%, respectively, and higher than contraction activity presented by SS/CMC animals (p<0,05).

Conclusion:

For the first time it was demonstrated that eicosanoids from 5-,12-LOX and CYP450 share distinct regulatory role in the development of skeletal muscle fiber after injury. The data suggest that lipid mediators derived from 12-LOX and CYP450 are responsible for development of slow fibers of type I, with smaller calibrate and low resistance to fatigue stimulus while mediators originated from 5-LOX pathway stimulate the development of larger and fast fibers (type II) with low resistance, during skeletal muscle regeneration process.

Financial support:

FAPESP, Capes and CNPq.

20.019 - THE EFFECT OF PHOTOBIO-MODULATION THERAPY IN THE PAIN, QUALITY OF LIFE AND MOBILITY OF PATIENTS WITH KNEE OSTEOARTHRITIS. Ferreira NL, Pinto NC, Ashmawi HA, Fumis RRL, Chacur M, - Department of Anatomy - USP Intensive Care Unit - Sirio-Libanes Hospital Laboratory of Experimental Anesthesiology - FMUSP Bright Photomedicine - IPEN

Introduction:

Osteoarthritis (OA) is a chronic-degenerative inflammatory articular disease known for its worn out of the cartilage joint, changes in soft tissues, bone widening, cartilage destruction, affecting peripheral and axonal joints, the knee joint being the most affected (KOA). Its traditional pharmacological treatment consists on the use of non-steroidal anti-inflammatory drugs (NSAID), however highly associated with serious side effects. In the last few years, many scientific data on PhotoBioModulation Therapy (PBM) has been showing its effect in the treatment and control of inflammatory processes and algic syndromes such as Chronic Back Pain and Post Herpetic Neuralgia, among other positive findings.

Aim:

The purpose of this clinical trial was to evaluate the effect of PBM in pain, quality of life and mobility of patients with KOA.

Methods:

This study was held with 18 patients, in which nine were set in a placebo control group and nine were set to the treated group; and it was approved by the Ethic Committee in Research (CEP) of Plataforma Brasil (CAAE:393744418.5.0000.0068) and it is registered in Clinical Trials.Gov (NCT03924128). For the treatment, we used radiant energy ranging from 13 up to 37 J with 850 nm of wave length, continuous wave exposure, with application time from 4 up to 8 minutes, twice a week, with a total of 10 sessions. To evaluate the pain intensity, we used the Visual Analog Scale (VAS) before each application throughout the treatment; to evaluate the patient's quality of life two questionnaires were applied: the Knee Injury and Osteoarthritis Outcome Score (KOOS) and the World Health Organization Quality of Life-Bref (WHOQOL-BREF); to evaluate the patient's mobility we did the Sit-To-Stand test and the Timed-Up and Go test. For the statistical analysis we used the Analysis of Variance (ANOVA) with two different variants (group and time), associated with T Test (Turkey). The significance level was set at p<0.05.

Results:

After the 4th session, we were able to see considerable decrease in patients pain and expressive improvements in both their quality of life and mobility after the treatment was over when compared to the control group.

Conclusion:

We can conclude that PBM was efficient in decreasing the patients pain, and was even more efficient in improving their quality of life and mobility in patients with KOA. Suggesting that PBM could be a good complementary therapy for patients with different pain syndromes, such as knee osteoarthritis. Acknowledgement: Bright Photomedicine.

Financial support:

FAPESP/CNPq

20.020 - HEME TRIGGERED RESPONSES IN MONOCYTES AS TARGETS TO DETECT AUTOLOGOUS BLOOD TRANSFUSION. Amorim CS, Magdalena J, Silva JAMG, Mirotti LC, Carneiro ACD, Pereira HMG, Martins MR, - Programa de Farmacologia e Química Medicinal - UFRJ Departamento de Biologia Celular e Molecular - UFF Laboratório Brasileiro de Controle de Dopagem - UFRJ

Introduction:

The oxygen carrying capacity of the body is a limiting factor of performance in most sports for long duration and endurance. It is known that oxygen consumption can be increased naturally through intense and frequent resistance training triggering an increase in red blood cells, however these adaptations are slowly acquired over many

FeSBE Annual Meeting 2019

Poster Sessions and Abstracts

years. In order to increase their ergogenic resource athletes resort to artificial inductors of erythropoiesis. Furthermore, the increased supply of oxygen can also be achieved by homologous or autologous blood transfusion. In homologous transfusion, red blood cells concentrate obtained from a compatible donor is infused into the athlete's circulation, while in autologous transfusion, blood is withdrawn from the athlete, being preserved (stored) and reinfused in its circulation. However, these methods are used with the same objective: to gain an unfair competitive advantage by increasing the exercise capacity through the manipulation of the composition of the blood and its components. Despite being less risky, autologous blood infusions cannot yet be detected directly by any current anti-doping method, becoming one of the biggest challenges of doping control.

Aim:

Therefore, our objective was to evaluate in monocytes challenged with previously stored red blood cells proteins involved in the heme metabolism process. Thus, the protein expression of heme oxygenase 1 (HO-1), ferritin and the Spi-C transcription factor were evaluated in monocytes previously co-cultured with red blood cells.

Methods:

Cell Co-culture; Western Blotting; Colorimetric assay and Cytometric analyses.

Results:

Western blotting showed that the storage of red blood cells induced increased of free heme release, triggering a significant increase in the expression of ferritin (Mean: Control: 1 ± 0.3092 ; treatment: 2.925 ± 0.2660) and Spi-C (Mean: Control: 0.965 ± 0.1600 ; treatment: 2.216 ± 0.4580) in monocytes when compared to non-stored blood. The latter was presented as a promising sensor in the detection of free heme. Significant changes in free heme (Day 0: $7.182 \mu\text{M} \pm 1.223$; Day 21: $72.01 \mu\text{M} \pm 15.19$) and hemoglobin (Day 0: $7.77 \mu\text{M} \pm 0.7515$ and $31.65 \mu\text{M} \pm 6.913$) concentration were detected by colorimetric assay. Furthermore, cytometric analyses revealed that the storage process increased the release of microparticles from red blood cells (Mean: Control: 0.9 ± 0.12 ; treatment: 2.61 ± 0.60).

Conclusion:

Our results demonstrated, through an ex vivo transfusion protocol, the long-term effects of the storage process on red blood cells, triggering an increase in the expression of ferritin and Spi-C on monocytes. Herein we demonstrate for the first time, that Spi-C can be a promising molecule in the detection of autologous blood transfusion, paving the way for the development of bioanalytical assays for the detection of autologous transfusion in athletes.

Financial support:

Partnership for Clean Competition (PCC)

20.021 - PHOTOBIMODULATION AS TREATMENT FOR INFLAMMATION AND MUSCLE PAIN. Oliveira CG, Giorgi R, Chacur M, - Anatomy - ICB/ USP Pathophysiology Laboratory - IB

Introduction:

Muscular injury often occurs in sports, falls and work, including the youth, adult and elderly population. This kind of injury causes impaired pain and muscle function, triggering important functional limitation. In recent years, the application of photobiomodulation therapy (PBM) has been shown to be an interesting strategy to accelerate the process of tissue regeneration and reduce the release of inflammatory mediators. Several articles in the literature demonstrate that PBM has therapeutic properties in various musculoskeletal disorders.

Aim:

This proposal aims to understand the effect of photobiomodulation, using low level laser therapy (LLLT) and light emitting diode (LED), in the chronic muscle injury model (myositis).

Methods:

For this, we performed behavioral tests, measuring nociceptive and edematogenic responses and histology of muscle fibers. Male Wistar

rats weighing 200-220 grams were divided into four groups: naive (control), CFA (injured), CFA + LLLT and CFA + LED, with three different energy intensities for both types of photobiomodulation, being LLLT 1.08J, 1.8J and 3J and for LEDs - 0.29J, 0.71J and 3J per session. FBM treatment was initiated six days after CFA injury, and had duration of 5 sessions on consecutive days. After the behavioral analysis, animals were euthanized, and muscle were collected for histology analysis. Statistical analysis was performed using GraphPad Software version 6, two-way ANOVA and Bonferroni post-test, the assumed significance level was $p \leq 0.05$.

Results:

Our results demonstrated an improvement of mechanical, tactile and edematogenic response using for both LLLT and LED. However, in relation to the response to the thermal stimulus, no improvement of the nociceptive picture of the animals was observed. In addition, we observed a greater amount of inflammatory infiltrate in the injured group (CFA) compared to the control group (naive) in the histological analyzes.

Conclusion:

We suggest a beneficial effect of the treatment with photobiomodulation, and may also propose as an adjuvant in the treatment of patients with muscle pain. Acknowledgement: Bright Photomedice

Financial support:

FAPESP and CNPq

20.022 - EFFECT OF NANOESTRUTURED COPAÍBA OIL IN THE ANTINOCICEPTION. Silva MC, Ferrarini SR, Silva KP, Berber RCA, Coimbra NC, DeOliveira R, - Instituto de Ciências da Saúde - UFMT Departamento de Farmacologia - USP

Introduction:

Copaiba (Copaifera Langsdorffii) is a native tree of South America and easily found in the region of the Amazonian rainforest. The oil extracted from that tree is widely used by the general population and several studies report that copaiba oil has anti-inflammatory, antiseptic, antimicrobial properties and also promotes antinociception. Thus, we hypothesized that copaiba oil causes an antinociceptive effect and that its nanostructured form may be more effective even at lower doses.

Aim:

The aim of the present work was to investigate the antinociceptive effect caused by nanostructured copaiba oil (CONano).

Methods:

Male Wistar rats (250grs) from the Central Laboratory of the Federal University of Mato Grosso were used. The copaibeira, from which the oil was extracted is located in the city of Itaúba, Mato Grosso, Brazil. Nociceptive thresholds were measured using the tail-flick test. Each animal was placed in a holding device and its tail was inserted into the heating sensor of an analgesimeter apparatus. The heating sensor operates in such a way that the progressive calorimetric elevation is automatically interrupted when the animal withdraws its tail from the apparatus. A small adjustment of current intensity could be performed at the beginning of the experiment to obtain three consecutive tail withdrawal latencies (TWL) between 2.5 and 3.5 seconds. The animals received CONano (0.5, 1 and 2 mg/kg) and copaiba oil (200mg/kg) by gavage, intraperitoneal injections of morphine (1mg / kg) or vehicle, and the TWL were recorded at 20,30,40,50,60 and 80 minutes after intragastric or intraperitoneal administration of drugs. Data were submitted to a two-way analysis of variance (MANOVA), followed by the Newman-Keuls post hoc test and significant differences were considered at $p < 0.05$.

Results:

Administration of CONano (2mg/kg - more effective dose) significantly increased the nociceptive thresholds at all times when compared to control [F(4,38) varying from 7.44 to 17.28; $p < 0.0001$] and there was no significant effect at intermediate and low doses (Newman-Keuls, $P > 0.05$)

FeSBE Annual Meeting 2019

Poster Sessions and Abstracts

in all cases). According to MANOVA, there was a significant effect of treatment [F(4,31) = 7.437; p<0.001], of time [F(8,248) = 23.93; p<0.0001] and of the interaction between treatment versus time [F(32,248) = 1.758; p<0.05]. There was a significant effect of copaiba oil (200mg/kg) in the time of 50 minutes [F(4,31) = 0.9232; p<0.0001] after gavage. Morphine caused a significant antinociceptive effect, considering that there was an increase in nociceptive thresholds at all times [F(4,31) varying from 1,758 to 23,93; p<0.0001].

Conclusion:

The data demonstrated that COnano at the dose of 2mg/kg increased the nociceptive thresholds significantly at all times, while free copaiba oil at the dosage of 200 mg/kg caused an increase only in the time of 50 minutes after intragastric ingestion. These findings suggest that nanostructured copaiba oil are more suitable for phytotherapy with analgesic properties.

Financial support:

FAPEMAT

21 - Immunology

21.005 - DOCOSAHEXAENOIC ACID SLOWS INFLAMMATION RESOLUTION AND IMPAIRS THE QUALITY OF HEALED SKIN TISSUE. Candreva T, Kühl CM, Burger B, Anjos MB, Consonni SR, Fisk H, Calder PC, Vinolo MA, Rodrigues HG, - Laboratório de Nutrientes e Reparo Tecidual - UNICAMP - FCA Departamento de Bioquímica e Biologia Tecidual - UNICAMP Human Development and Health - University of Southampton NIHR Southampton Biomedical Research Centre - University of Southampton Departamento de Genética, Evolução, Microbiologia e Imunologia - UNICAMP

Introduction:

Successful wound healing requires the sequence of inflammation, proliferation and maturation phases. Omega-3 (ω -3) fatty acids (FA) have anti inflammatory actions, but there is a lack consensus on their effects on cutaneous repair.

Aim:

In the present study, we used 2 different approaches to address the role of ω -3 FA on the cutaneous wound healing: 1) FAT-1 transgenic mice, capable of producing endogenous ω -3 FA; 2) orally supplemented wild-type (WT) C57BL/6 mice with fish oil (25 μ L/day for 4 weeks).

Methods:

All animal study protocols were approved by Ethics Committee (CEUA – 4175-1 and 4122-1) and by Biosafety Internal Committee (CIBIO – 370) of the Faculty of Applied Sciences/UNICAMP. For skin wounds, an area of 10 mm² of skin from the lumbar region of mice was shaved and then removed. After wound induction, skin tissues were collected at specified time points. For wound closure analysis, images of the wound area were measured using Image J software. Gas chromatography was performed to analyse the lipid composition in the serum and skin of mice. Inflammatory mediators were quantified by ELISA method and the myeloperoxidase (MPO) active was determined by measuring the absorbance at 450 nm. Histological slides of skin tissue were stained with haematoxylin and eosin (H&E) for morphological analysis and Sirius Red for collagen organization. Skin cells type were quantified by cytometry. Results are presented as mean \pm standard deviation of mean (SD). Comparisons between groups were performed using Student's t-test or two-way ANOVA using the Prism 7.0 software. Differences were considered significant for p<0.05.

Results:

FAT-1 mice had higher systemic (serum) and local (skin tissue) ω -3 FA levels, mainly docosahexaenoic acid (DHA) (25 % in serum and 30% in skin), in comparison to WT mice (n = 5 WT and 6 FAT-1). FAT-1 mice had increased myeloperoxidase (MPO) activity (34%; n = 5 WT and 4 FAT-1) and content of CXCL-1 (44%) and CXCL-2 (41%), and reduced IL-10 (53,5%) in the skin wound tissue three days after the wound induction (n = 10 WT and 13 FAT-1). Inflammation was maintained by an elevated

TNF- α (58,3%) concentration and presence of inflammatory cells and edema in the skin wound tissue of five days post-wounding (n = 5 WT and 8 FAT-1). Similarly, DHA group had increased TNF- α content (34%; n = 7 WT and 8 DHA) and CD45+F4/80+ cells (41%; n = 7 WT and 5 DHA) at the 3rd day after skin wounding. In both experimental models, the wound area was bigger during inflammatory phase (between one and ten days post-wounding). Finally, poor orientation of collagen fibers and structural aspects were observed in repaired tissue of FAT-1 mice, twenty-one post wounding (n= 3 WT and 6 FAT-1).

Conclusion:

Elevated DHA content, achieved in both FAT-1 and DHA group, slowed inflammation resolution and impaired the quality of healed skin tissue.

Financial support:

Supported by FAPESP, CNPq and FAEPEX/UNICAMP. This study was financed in part by the Coordenação de Aperfeiçoamento de Pessoal de Nível Superior - Brasil (CAPES) - Finance Code 001

21.006 - ALTERATIONS OF COX-2 PATHWAY: RISK OF DEVELOPING SCHIZOPHRENIA. PereiraCAC, Joaquim H, Talib L, GattazWF, - Psiquiatria - HCFMUSP

Introduction:

Several inflammatory processes in the schizophrenia still unclear, therefore, it's necessary to understand those processes and if they predispose the first episode psychosis. This study aims to assess the mechanisms that could be affected by the etiology of the disease like prostaglandins.

Aim:

To determine the levels of cytokines and inflammatory markers from COX-2 (Cyclooxygenase-2) pathway, namely, thromboxane B² (TXB₂), prostaglandins E² (PGE²) and F² α (PGF² α).

Methods:

Subjects were recruited and divided into two groups based on their performance on Prodromal Questionnaire: the lowest values were considered UHR (Ultra High Risk) and the highest values as controls. Cytokines (IL-1 β , IL-10, IL-6, GM-CSF, IL-5, IFN- γ , TNF- α , IL-2, IL-4 and IL-8) were quantified by immunofluorescence in Luminex[®] equipment. TXB₂, PGE² and PGF² α levels were measured using the ELISA assays.

Results:

Further analysis showed that PGE² levels were increased in UHR subjects compared to controls (p=0.01), although PGF² α and TXB₂ levels have no difference. No significant differences were found between all cytokines in the groups. A positive correlation was found between PGE² and PGF² α (ρ = 0.361; p=0.002) and TXB₂ (ρ =0.336; p=0.011). Also, a positive correlation between PGF² α and TXB₂ (ρ =0.341; p=0.013). Regarding cytokines, there was a positive correlation between IL-6 and IFN- γ (ρ =0.6; p<0.001).

Conclusion:

This finding while preliminary, suggests that inflammatory levels of PGE² are altered in UHR stage and might impair metabolism related to signal transduction, neurotransmission and altered immunological cascades. However, further studies related to the UHR and inflammatory mechanism are needed.

Financial support:

FAPESP (2018/11414-4)

21.007 - CHOLESTERYL ESTER TRANSFER PROTEIN (CETP) EXPRESSION MODULATES MITOCHONDRIAL FUNCTION AND REDOX STATE IN MICE PERITONEAL MACROPHAGES. Dorighello GG, Assis LHP, Vercesi AE, Oliveira HCF, - Patologia Clínica - UNICAMP Biologia Estrutural e Inmunologia - UNICAMP

Introduction:

Plasma cholesteryl ester transfer protein (CETP) activity diminishes HDL-cholesterol levels, which could increase atherosclerosis risk. However, clinical trials using CETP inhibitors showed no benefits on

FeSBE Annual Meeting 2019

Poster Sessions and Abstracts

mortality rates. Local tissue functions of CETP are not known. Experimental evidences suggest that CETP may also exhibit anti-inflammatory functions.

Aim:

The aim of this study is to investigate whether CETP expression affects mitochondrial function and oxidants production in macrophages, the central cell type in atherogenesis.

Methods:

We analyzed the redox status and the mitochondrial morphology and function in thioglycolate-elicited peritoneal macrophages from CETP expressing transgenic mice and from non-transgenic mice (non-Tg) (Committee for Ethics in Animal Experimentation, CEUA/UNICAMP, protocol # 4746-1/2017). The comparisons between the groups were analyzed by unpaired Student's t test and the level of significance was set at $P < 0.05$.

Results:

We observed that CETP expression promoted a reduction of 28% in the mitochondrial superoxide (mitosox) (100 ± 5 vs 72 ± 4 , % of non-Tg), but not in the total superoxide (DHE) production (100 ± 6 vs 106 ± 7 , % of non-Tg) and in the global oxidants (H2DCFDA) (100 ± 17 vs 101 ± 11 , % of non-Tg). In addition, mitochondrial H2O2 release was also 17% lower in CETP expressing macrophages (9.9 ± 0.5 vs 8.2 ± 0.5 , $\eta\text{M H}_2\text{O}_2/\text{min}/\text{DNA}$) and the non-mitochondrial H2O2 release was similar in both groups (11.3 ± 0.8 vs 11.2 ± 0.7 , $\eta\text{M H}_2\text{O}_2/\text{min}/\text{DNA}$). Regarding mitochondrial respiration rates, CETP expression increased 23% the maximal respiration rate (229 ± 16 vs 281 ± 14 , $\text{pM of O}_2/\text{min}/\text{DNA}$) and 65% the spare respiratory capacity (56.3 ± 8.8 vs 92.8 ± 10.3 , $\text{pM of O}_2/\text{min}/\text{DNA}$). In addition, the glycolytic reserve was 8% higher in macrophage expressing CETP (29.9 ± 0.4 vs 32.4 ± 0.4 , $\text{mpH}/\text{min}/\text{DNA}$), without differences in basal glycolysis (52.2 ± 2.0 vs 49.7 ± 1.2 , $\text{mpH}/\text{min}/\text{DNA}$). Besides the mitochondrial functional and redox alterations, the CETP expression also changed the morphology of mitochondrial network, as demonstrated by the predominance of the elongation characteristic (1.54 ± 0.002 vs 1.58 ± 0.007 , aspect ratio), suggesting a dynamic that favors mitochondrial fusion over fission.

Conclusion:

The CETP expression in macrophages reduces mitochondrial oxidants production, presented an increased maximal respiratory capacity and promotes a more elongated mitochondrial network. These CETP induced mitochondrial changes in macrophages may be relevant for human atherosclerosis and other immuno-metabolic diseases.

Financial support:

FAPESP and CNPq

21.008 - EVALUATION OF INTRAHEPATIC LYMPHOID SUBPOPULATIONS IN THE PROGRESSION OF NONALCOHOLIC FATTY LIVER DISEASE IN MOUSE MODEL. Guimarães JR, Martins NV, Beghini DG, Horita SIM, Cascabulho CM, Pons AH, Pons AH, - Laboratório de Inovações em Terapia, Ensino e Bioprodutos - FIOCRUZ/RJ

Introduction:

Non-alcoholic fatty liver disease (NAFLD) is currently the most common cause of liver disease, with 20-30% of prevalence in Western countries. NAFLD is considered the hepatic component of the metabolic syndrome and is characterized by steatosis, a relatively mild condition that can progress to steatohepatitis, fibrosis, cirrhosis and, ultimately, hepatocellular carcinoma. Many cellular subpopulation of the immune system play a role in the development of NAFLD, such as regulatory T cells (Treg), NKT cells, T lymphocytes, and others. However, the pathogenic mechanisms of NAFLD have not yet been clearly established. The understanding its pathogenesis is critical for the prevention and treatment of the disease and we are evaluating lymphoid subpopulations in mice submitted to a hyperlipidic diet and their correlation with biochemical and histological findings.

Aim:

Evaluation of lymphoid subpopulations in the liver of C57BL6 mice submitted to high fat diet and correlate biochemical, histological and immunological parameters.

Methods:

8 weeks old male C57BL/6 mice ($n=40$) were divided in two groups fed, respectively, with standard chow and high fat diet for 16 weeks. Liver, spleen, serum, and plasma samples were collected for biochemical, histological and immunological analyses. Hepatic enzymes, as well as cholesterol, triglycerides, and glucose levels were evaluated by spectrophotometry as biochemical parameters. Histological staining was performed to study the inflammatory infiltration, lipid inclusions, necrosis, and fibrosis. Cytokines were analysed by flow cytometry using CBA Mouse Inflammation kit. The profile of memory, activation and immunoregulatory function in intrahepatic lymphocytes were evaluated by flow cytometry. All procedures were approved by the Oswaldo Cruz Foundation Ethics Committee for Animal Use (CEUA) (L006 / 2015). Statistical significance was determined using the nonparametric Kruskal-Wallis test and the Mann-Whitney test when appropriate. Data are presented as means and standard errors and are considered statistically significant for $P \leq 0.05$.

Results:

In the histological evaluation it was concluded that at the time of 60 days only hepatic steatosis is observed, with no evidence of manifestation of steatohepatitis. It was found that TNF, IL-6 and MCP 1 cytokines showed greatest change in the group the high fat diet group when compared to standard chow group. Phenotypic changes of T cell subpopulations were observed in the high fat diet group when compared to standard chow group. All data were statistically significant when comparing the two groups ($P \leq 0.05$).

Conclusion:

Our data indicate that the hyperlipidic diet changes the biochemical, histological, and immunological parameters in the C57BL/6 mouse model. The phenotype of T cell subpopulations in the hepatic stroma is altered at 90 days of diet, with an increase in the percentage of lymphocytes expressing PD-1 immunoregulatory molecule. The interaction of PD-1 with its ligands induced lymphoid silencing. Adoptive transfer experiments are under way to evaluate the functional profile of these cells. This study is underway and further research will provide more information on the intrahepatic cell profile during the different stages in the mouse model of NAFLD.

Financial support:

CAPES and IOC.

21.009 - PREGABALIN IMPROVE INFLAMMATION AND SARCOLEMMA STABILIZATION OF MDX MICE. Gerotto Junior LC, Silva JF, Franco LS, Marques MJ, Carvalho SC, - Programa de Pós-graduação em Ciências Biomédicas - FHO Biologia Celular e Estrutural - UNICAMP

Introduction:

The lack of dystrophin in the skeletal muscles of the mdx mice and in Duchenne muscular dystrophy leads to progressive myonecrosis. The main secondary cause of myonecrosis is the exacerbated influx of calcium ions caused by sarcolemma rupture and malfunctioning of the calcium channels. Corticosteroids are the main choice for dystrophy therapy, but their side effects stimulate the search for alternatives. Pregabalin (PGB) is an anticonvulsant drug of calcium channel blocking property, and its effects on dystrophinopathy are unknown.

Aim:

Here, we analyzed the effects of PGB in dystrophic fibers of the mdx and normal mice analyzed their effects on signaling molecules of the inflammatory cascade (TNF- α and NF- κ B), as well as, sarcolemma stabilization (β -DG).

Methods:

Mdx and normal mice (14 days old) received PGB (mdx-PGB or CTRL-PGB; $n=8$; 20 mg/kg body mass; daily oral gavage) or water (mdx or

FeSBE Annual Meeting 2019

Poster Sessions and Abstracts

CTRL; n=8; 20 mg/kg body mass; daily oral gavage) for 16 days, after which the diaphragm (DIA) and tibialis anterior (TA) were removed.

Results:

PGB was effective in reducing myonecrosis, leading to 37% decrease in creatine kinase and 68% reduction in central nucleated fibers on DIA. Suspension force test showed a better improvement in muscle force and hanging time with PGB (muscle force in CTRL: 4.0 ± 0.2 N seg; in mdx: 0.5 ± 0.1 N seg*; in mdx-PGB: 1.2 ± 0.2 N seg**; $p < 0.05$; * compare to CTRL and ** compare to mdx). Immunoblotting indicated that PGB were effective in reducing TNF- α (TA) and NF- κ B (DIA and TA) and improve sarcolemma stabilization (β -DG). In normal mice PGB treatment promoted the appearance of discrete areas of inflammation, increased molecules of the inflammatory cascade (TNF- α and NF- κ B) and reduced stabilization of the sarcolemma β -DG in DIA: 39% and in TA: 47%.

Conclusion:

These results indicate that PGB may represent a good alternative to dystrophy treatment and to normal tissue more study is needed.

Financial support:

FAPESP #2017/24255-9

22 - Cancer Signaling and Therapeutics

22.027 - BIOLOGICAL ACTIVITY OF ISCT1-BASED ANALOGS AGAINST TUMOR CELLS. Oliveira CS, Andrade GP, Cerchiaro G, Pinhal MAS, Jr PIS, Jr VXO, - Centro de Ciências Naturais e Humanas - UFABC Laboratório Especial de Toxicologia Aplicada - IB Instituto de Farmacologia - UNIFESP

Introduction:

Cancer is a major health problem worldwide and the second leading cause of death in the world. Data from the World Health Organization show that in 2018 about 18 million new cases were registered in the world, with a death rate of around 10 million. Tumor cells present several mechanisms that confer resistance to current therapies, such as high drug efflux capacity and overexpression of detoxifying enzymes. Thus, there is a need to seek new approaches against tumor cells and antimicrobial peptides are being studied for this purpose.

Aim:

Antimicrobial peptides (AMPs) are molecules with low molecular weight, which may have positive net charge and amphiphilic characteristics. An important feature of most AMPs is the ability to disrupt and penetrate the cell membrane, which has raised interest in the use of these molecules in possible applications in the combat against cancer. IsCT1 is a short cationic peptide isolated from the *Opisthacanthus madagascariensis* scorpion venom that shows biological activity against Gram-positive and Gram-negative bacteria. Based on this AMP, four analogs with modifications of 2 to 4 amino acids residues (using alanine, phenylalanine, lysine and proline as motif) and net charge ranging from +2 to +6 were synthesized and tested for biological activity against human breast cancer cells and their effects (cytotoxicity) on human cells.

Methods:

The peptides were synthesized by the solid phase method, using the Fmoc strategy. Compounds were purified by HPLC and characterized by LC-ESI-MS. In vitro assays were performed to verify antitumor activity against MCF-7A human breast adenocarcinoma cell, cytotoxicity and hemolytic activity were analyzed using MCF-10A epithelial breast cell and fresh human erythrocytes, respectively. Conformational studies were performed by circular dichroism (CD) in water and solutions of PBS and TFE.

Results:

IsCT1 and its analogs did not present cytotoxicity activity against MCF-10A cell up to the concentration of 100 μ mol L⁻¹. However, IsCT1 proved to be quite hemolytic, inducing 75% lysis of erythrocytes (12,5 μ mol L⁻¹), the analog [A]1[K]3[F]5[K]8-IsCT1 presented moderate

hemolysis at concentration 50 μ mol L⁻¹ (19%) and the other synthesized analogs did not present hemolytic activity at the concentrations tested. Both IsCT1 and its analog [A]1[K]3[F]5[K]8-IsCT1 showed activity against MCF-7A cells (25 and 50 μ mol L⁻¹, respectively), unlike the other analogs. CD spectra showed that the peptides tend to adopt a helical structure in TFE solution, especially IsCT1 and [A]1[K]3[F]5[K]8-IsCT1, and exhibit a random coil structure in the other medium.

Conclusion:

IsCT1 and its analog [A]1[K]3[F]5[K]8-IsCT1 showed a higher tendency to α -helix structuring than other peptides, suggesting that the secondary structure may be an important factor in the interaction with MCF-7A cells and erythrocytes. The increase in the net charge do not showed be an important parameter in the interaction with the cell membrane eukaryotic both zwitterionic membrane as in MCF-10A cells, as for negatively charged, such as tumor cells and the erythrocyte. The peptides with addition of the proline residue showed the greatest reduction in hemolytic activity, however, they were also impaired in the activity against MCF-7A.

Financial support:

CAPES AND FAPESP.

22.028 - CONTRIBUTION OF TETRAHYDROBIOPTERIN THROUGHOUT TUMOR PROGRESSION: POSITIVE OR NEGATIVE REGULATOR OF MELANOMA GENESIS?. Soares JPM, Sousa RX, Icimoto MY, Machado FHM, - Department of Physiological Sciences - Santa Casa de São Paulo School of Medical Sciences Biophysics Department - Federal University of São Paulo

Introduction:

Melanoma is the most aggressive type of skin cancer, presenting a high rate of metastasis and consequently a high mortality. Melanomagenesis is associated with reactive oxygen species increase, among them the superoxide anion (O₂^{•-}) that can be produced by dysfunctional nitric oxide synthase (NOS). The activity of NOS in endothelial cells is regulated by integrated mechanisms, including the bioavailability of the tetrahydrobiopterin cofactor (BH₄).

Aim:

Evaluate if BH₄ modulates positively or negatively altered biological processes along melanoma progression that contribute to neoplastic development.

Methods:

Human melanocytes (NGM), radial growth melanoma (Wm1552), vertical growth melanoma (Wm1366 and Wm793) and metastatic (Lu1205 and Wm983) cell lines were used to analyze: i) GCHI expression by qPCR; ii) the amount of GTPCH-I protein by western blot; iii) amount of BH₄ and total biopterins by HPLC; iv) concentration of O₂^{•-} by fluorimetry; v) concentrations of nitric oxide by Griess reaction; vi) cell viability using MTT assay at times 24, 48, 72 and 96 hours and clonogenic capability on cells treated with different concentrations of BH₄ and DAHP (GTPCH-I enzyme inhibitor). Statistical analysis was performed using ANOVA followed by Tukey-Kramer test and Student t test; was considered significant $p < 0.05$.

Results:

Melanoma cell lines showed increased expression of the GCHI transcript and in the amount of GTPCH-I protein in relation to the melanocyte. Increased amount of BH₄ and total biopterins was observed in Wm983 cell line in relation to the melanocyte, while was observed a trend of decrease in Wm1552 lineage. In the functional assays, we observed an increase in the concentration of O₂^{•-} in the melanoma lines Wm1552 and Wm983 and a decrease of NO concentration in the cell line Wm1552. Treatment with BH₄ decreased the viability and the clonogenic capacity of Wm1552, whereas the treatment with DAHP reduced the viability and the clonogenic capacity of the Wm983 lineage. Treatment with BH₄ did not alter the viability of melanocytes.

FeSBE Annual Meeting 2019

Poster Sessions and Abstracts

Conclusion:

In the radial growth melanoma, which corresponds to the initial phase of melanoma development, our results suggest that BH4 functions as a negative modulator, because when cells were treated pharmacologically with BH4, reduced cellular viability and clonogenic capacity were observed. By the other hand, in metastatic melanoma cells, which corresponds to the later stage of melanoma, BH4 seems to function as a positive modulator, because when we treated Wm 983 lineage with the inhibitor of BH4 synthesis, DAHP, there was a decrease in viability and colonies formation. Thus, the results suggest that it is important to assess at which stage of melanoma progression the administered drugs have anti or pro tumor activity. Therefore, the synthesis of BH4 may be a novel therapeutic target, being inhibited in the treatment of metastatic melanoma, while it is stimulated in the early stages of melanoma development.

Financial support:

CAPES and FAPESP 2017/04352-0

22.029 - PEPTIDE L21R FROM THE BRN2 TRANSCRIPTION FACTOR CAUSES CELL DEATH IN MURINE MELANOMA CELLS. SIQUEIRA CRS, CUNHA FFM, TRAVASSOS LR, ARRUDA DC, - Unidade de Oncologia Experimental - UNIFESP Laboratório de Biologia Experimental do Câncer - UMC

Introduction:

Melanoma is a malignant tumor derived from transformed melanocytes responsible for a number of fatal cases in the metastatic form. Conventional therapy is not effective and there is limited success of recent immunotherapy procedures. The search for additional drugs that can improve the response to antibodies directed to immune checkpoints has been a recent effort. We have studied the effect of peptides derived from transcription factors, in particular the BRN2 protein. High expression levels of BRN2 have been found in melanoma cell lines and recent studies showed that peptides from this protein may cause tumor cell death. The L21R peptide, derived from BRN2 is presently studied.

Aim:

The present work aims at investigating the cell death mechanism induced by L21R peptide, derived from the Brn-2 transcription factor.

Methods:

The L21R cytotoxicity was studied in B16F10-Nex2 cells (104) plated in 96-well plates and incubated with L21R peptide at different concentrations for 24 h. Viability was determined by counting cells in a Neubauer chamber with Trypan blue. The ROS production by B16F10-Nex2 cells treated with L21R peptide 0.10 mM, for 24 h, was measured by dihydroethidium (DHE) assay. Moreover, chromatin condensation was observed by staining with Hoechst 33342. Cells treated with L21R peptide at 0.10 mM for 1 and 24 h or untreated, were incubated with Hoechst 33342 and analyzed by fluorescence microscopy. DNA degradation was observed by TUNEL assay. Cells treated with L21R peptide 0.10 mM for 24 h and incubated with DAPI were analyzed in the Cytell Cell Imaging System.

Results:

L21R peptide exerted cytotoxic effects in B16F10-Nex2 cells in vitro. EC50 was 0.07 mM. Melanoma cells treated with L21R showed increased levels of ROS production, DNA degradation and chromatin condensation.

Conclusion:

The L21R peptide showed antitumor effects and the cell death mechanism involved increase of reactive oxygen species and apoptosis markers such as chromatin condensation and DNA fragmentation.

Financial support:

FAPESP

22.030 - METABOLISM OF EXTRACELLULAR NUCLEOTIDES IN ORAL SQUAMOUS CELL CARCINOMA (OSCC) CELL LINES. Diel LF, Vasconcelos JM, Bertoni APS, Wink MR, Lamers ML, - Laboratório de Migração Celular - UFRGS Departamento de Ciências Morfológicas - UFRGS Laboratório de Biologia Celular - UFCSPA

Introduction:

Oral squamous cell carcinoma (OSCC) is the most frequent type of cancer in the oral cavity. There are several factors that act on adjacent cells leading to its reprogramming leading to growth, progression, invasion and formation of metastases. Extracellular nucleotides and nucleosides have emerged as important modulators of tumor microenvironment. Extracellular ATP is mainly hydrolyzed by ectonucleotidase CD39, generating AMP, which is hydrolyzed by ecto-5'-nucleotidase (NT5E/CD73) to adenosine. Studies show that CD73 is associated with a worse prognosis in HNSCC but the functionality of these both enzymes were poorly explored in OSCC.

Aim:

Our objective was to analyze the hydrolyzing capacity of ATP and AMP in two OSCC strains (CAL27 and SCC9), and the functionality of CD73.

Methods:

We investigated the hydrolysis of ATP, ADP e AMP by Malachite Green method in CAL27 and SCC9 cells, and in silico using GSE64557 and GSE6631 datasets. We also analyzed the expression of CD73 expression in CAL27 and SCC9 cells and in samples of HNSCC and adjacent normal tissue.

Results:

Specific activity was expressed as nmol of Pi released and the differential expression was analyzed by Paired Student's t test. SCC9 cells hydrolyzed ATP at a lower rate comparing to CAL27 cells (4.27+0.57 vs 17.20+0.63) while these cells have higher capacity of hydrolyze AMP than CAL27 cells (22.57+0.99 vs 15.47+2.60). By using APCP, a specific CD73 inhibitor, the ability of SCC9 and CAL27 cells to hydrolyze AMP were decreased, adding evidence that CD73 is a functional enzyme in these cells. Using in silico data we showed that these results are in accordance with genic profile in these cell lines were SCC9 cells had about 24% higher expression of NT5E than CAL27. Importantly, NT5E expression was significantly higher ($p=0.0096$) in samples of HNSCC (78.6+39.59) than in the adjacent normal tissue (53.73+9.693).

Conclusion:

CAL27 and SCC9 showed differences in ATP and AMP hydrolysis ability, this may be related to the malignant profile of the lines, CAL27 (low invasion) and SCC9 (high invasion). CD73 was shown to be functional in both strains. More studies are under way to evaluate the role of nucleotides on the proliferation and migration of these cells.

Financial support:

CAPES, FAPERGS

22.031 - OBESITY MODIFIES BREAST CANCER CELLS BEHAVIOR: ROLE OF EXTRACELLULAR VESICLES DERIVED FROM HUMAN ADIPOSE TISSUE. Andrade IR, Silva JAMG, Costa RMB, Silva SV, Matheus ME, Silva CSC, Souza AAP, Renovato-Martins M, Barja-Fidalgo TC, - Biologia Celular e Molecular - UERJ

Introduction:

Obesity, a chronic low-grade inflammatory disease, is one of the major public health concerns worldwide, because of its association with several diseases, including cancer. Evidences have shown that obese women present worse breast cancer prognosis. This effect can be mediated by extracellular vesicles (EVs), which are small membrane targets capable of transferring content derived from the origin cells to target cells.

Aim:

The aim of this study was to investigate the effect of soluble mediators and EVs secreted by obese adipose tissue (AT) upon breast cancer cells.

Methods:

FeSBE Annual Meeting 2019

Poster Sessions and Abstracts

AT explants were collected from lean and obese individuals, during plastic or bariatric surgeries, respectively. AT supernatant, herein called conditioned media (CM), and EVs (obtained by centrifugation of the CM) were used as stimuli (24h) on two different mammary adenocarcinoma cell lines: MCF-7 and MDA-MB-231. Cell proliferation was evaluated by MTT method, in the presence or absence of MAPK/ERK inhibitor (PD98059). Cell migration was evaluated by wound healing and cell invasion was evaluated by transmigration through gelatin coated transwell, both assays were performed in the presence or absence of PI3K/Akt inhibitor (LY294002). ERK and Akt phosphorylation and MMP expression were evaluated by immunoblotting. Angiogenesis of endothelial cells was analyzed by tubulogenic assay and the proteolytic activity of EVs and MDA-MB-231 cells, by zymography. Statistical analysis was performed using the one-way ANOVA with Sidak's multiple comparisons or Student t-test with GraphPad Prism.

Results:

Our results showed that CM and EVs derived from obese AT increased MCF-7 cells proliferation (CM- M: 1,4 +/-SE: 0,1; EVs-M: 1,3 +/-SE: 0,1,9; obese:control ratio), while increased migration (CM- M: 1,7 +/-SE: 2,1; EVs- M: 1,5 +/-SE: 0,06; obese:control ratio) and invasiveness (CM-M: 1,6 +/-SE: 0,2; EVs: M: 1,5 +/-SE: 0,56; obese:control ratio) on MDA-MB-231 cells. Moreover, CM and EVs derived from obese AT increased ERK phosphorylation on MCF-7 cells (CM- M: 2,6 +/-SE: 0,22; EVs- M: 2,1 +/-SE: 1,75; obese:control ratio) and EVs increased Akt phosphorylation on MDA-MB-231 (M: 3,7 +/-SE: 0,7; obese:control ratio). The MAPK/ERK inhibitor impaired MCF-7 cells proliferation (CM-M: 0,6 +/-SE: 0,08; EVs-M: 0,7 +/-SE: 0,07; obese with PD:obese ratio), whereas PI3K/Akt inhibitor prevented MDA-MB-231 migration (CM- M: 0,7 +/-SE: 2,5; EVs - M: 0,5 +/-SE: 0,07; obese with LY:obese ratio) and invasiveness (CM - M: 0,3 +/- SE: 3,3; EVs - M: 0,4 +/- SE: 2,9; obese with LY:obese ratio). Additionally, HMEC-1 cells stimulated with the supernatant derived from primed MDA-MB-231 cells (previously stimulated with the CM derived from obese AT) showed increased tubulogenic capacity (M: 4,5 +/-SE: 3,4; obese:control ratio). Furthermore, our data demonstrated that EVs derived from obese AT were enriched in bioactive MMP9 (M:15 +/-SE: 5,1; obese:control ratio) and leptin (M: 6,7 +/-SE: 0,63; obese:control ratio). Interestingly, MDA-MB-231 cells stimulated with CM and EVs derived from obese AT resulted in intensive gelatin digestion (CM-M: 2 +/- SE:0,34; EVs: M: 1,3 +/-SE: 0,42; obese:control ratio).

Conclusion:

Our results indicate that obese AT modulates breast cancer cells, triggering the increase of their malignancy by the secretion of molecules and EVs with pro-tumoral activities.

Financial support:

CAPES, CNPq, FAPERJ

22.032 - ANTI-TUMOR EFFECTS OF BENZIMIDAZOLES ON ORAL SQUAMOUS CELL CARCINOMA. Pazutti L, Campos PS, Menti LD, Schrekker HS, Lamers ML, - Patologia - UFRGS Ciências Morfológicas - UFRGS Química Orgânica - UFRGS

Introduction:

Oral cancer is related to high mortality rates and the development of new drugs might contribute to improve patients survival. Tridimensional cell culture has been widely used to test potential antitumoral substances for cancer since it mimics in vivo microenvironment than traditional 2D monolayer culture. Benzimidazoles are fundamental part of various synthetic and natural pharmacological compounds and recently have shown antitumor effects.

Aim:

In this study we evaluated the capacity of different cells to form tumor spheroid and develop an approach for drug screening in vitro.

Methods:

Cell spheroids were generated using normal cell line keratinocyte from adult human skin (HACAT) and low invasive (CAL27) and high invasive (SCC09) Oral Squamous Cell Carcinoma (OSCC) cell lines. The cells were seed at a concentration of 1×10^4 per spheroid in low adhesiveness (1.5% agarose) 96-well plates. After 24 hours, spheroids were treated with Imidazolium Salts in different formulations (NB7) in increase concentration (0, 2.5, 5, 10 and 20 μ g/ml) and it was cultivated for 96 hours. Images were obtained daily and we measured external (spreading) and internal (spheroid center) area using ImageJ Software.

Results:

The compound NB7 affected cell-cell adhesion in oral tumor spheroid in Cal27 (5 μ g/ml) and SCC09 (2.5 μ g/ml) with almost no effect on normal keratinocytes (HACAT). However, Cisplatin, main quimioterapic for oral cancer, exhibited high effect in both normal and tumor spheroid.

Conclusion:

Our results showed that this new compound might have a potential antitumor effect since it demonstrated highly selectivity for tumor cells when compared to the gold standard.

Financial support:

CAPES, CNPq, FAPERGS

22.033 - CELL CONTRACTILITY DRIVES MECHANICAL MEMORY OF ORAL SQUAMOUS CELL CARCINOMA. deCampos PS, Matte BF, Placone JK, Engler AJ, LAMERS ML, - Patologia Bucal - UFRGS Departamento de Ciências Morfológicas - UFRGS Department of Bioengineering - UCSD

Introduction:

Oral cancer is characterized as a stiff nodule in oral mucosa. This increase in tissue rigidity may affect tumor progression, since dense collagen clusters correlate with poor outcomes in some cancer types. We demonstrated that oral cancer cells acquire an aggressive phenotype and migrate faster when exposed to prolonged time on stiff substrate, and we hypothesized that cells develop a mechanical memory that might be dependent on contractile proteins.

Aim:

Our aim is to evaluate the mechanisms that drive mechanical memory in oral squamous cell carcinoma (OSCC).

Methods:

Human biopsies were staining by Immunohistochemistry for NMIIA, NMIIB and NMIIC at adjacent epithelia and center of the tumor. Western blottings were performed for NMIIA, NMIIB, NMIIC, E-cadherin, N-cadherin and tubulin in low (Cal27) or highly (SCC25) invasive OSCC cell lines. The OSCC cell line (Cal27) were seeded for 5 days in soft (0.48kPa) and stiff (20kPa) substrate made with polyacrylamide (PA) hydrogels. Also, in soft group (0.48kPa) the cells were treat with Lysophosphatidic acid (LPA - 10 μ M) and in stiff group with Blebbistatin (10 μ M) and after this we start the assays.

Results:

We observed that the non-muscle type II myosin (MII) isoform B showed higher levels in tumor adjacent epithelia and center of tumor in patient biopsies comparing to MIIA and MIIC, while the isoforms MIIA and MIIB were overexpressed in high invasive OSCC cell line. We plated OSCC cell lines for 5 days in soft (0.48kPa) and stiff (20kPa) substrate made with polyacrylamide (PA) hydrogels and observed that stiff substrate induces cell changes in cell morphology in low invasive OSCC cell line. Then, in the group soft (0.48kPa) we induced cell contractility with Lysophosphatidic acid (LPA - 10 μ M), while in the group stiff (20kPa) we blocked contractility with Blebbistatin (10 μ M) for 5 days. Cells from all groups (0.48kPa, 0.48kPa+LPA, 20kPa, 20kPa+Blebbistatin) were re-plated onto either soft or stiff substrate and imaged for analysis of migration performance. Low invasive cells exhibited increase in migration velocity after prolonged exposure to a stiff substrate when compared to soft exposure ($p < 0.0001$). Cells plated in initial stiff condition did not change migration velocity when exposed to soft substrate, indicating a mechanical memory of cells. Treatment with LPA enhanced migration velocity in collective migration ($p < 0.0001$)

FeSBE Annual Meeting 2019

Poster Sessions and Abstracts

when compare to the soft control condition, while blebbistatin treatment overcome "memory" induce by stiff niche in individual cell migration ($p < 0.001$). For analysis in a 3D environment, we repeated the same groups for 5 days treatment and performed spheroids that were seeded in collagen gel (1.8mg/ml). We observed that cells from stiff substrate had a significant increase in spheroid area ($p < 0.001$) when compare to spheroid formed to cells in soft condition. The treatment with Blebbistatin in stiff condition demonstrated decrease in area ($p < 0.0001$) when compare to stiff control, while LPA shows a trend to increase spheroid spread in soft substrate.

Conclusion:

Therefore our data suggest that contractility is necessary for cells to acquire a mechanical memory according to the stiffness of the substrate.

Financial support:

Capes, Cnpq, Fapergs, PpgOdo

22.034 - LAMININ 111-DERIVED PEPTIDE C16 INTERACTION WITH BETA 1 INTEGRIN IN BREAST CANCER CELLS. Mateus RS, JAEGER RG, - Biologia Celular e do Desenvolvimento - USP

Introduction:

Breast cancer is among the most frequent worldwide mortality. Tumor microenvironment assumes important role during cancer progression. Different cells enmeshed in the extracellular matrix (ECM) compose such microenvironment. Laminin-111 is a major ECM glycoprotein and presents different bioactive peptides influencing tumor biology. We have demonstrated that the laminin-derived peptide C16 (KAFDITYVRLKF, short arm of gamma 1 chain) regulates migration, invasion, and invadopodia formation in different cancer cells. Our findings indicate that regulatory mechanisms underlying C16 effects are related to beta 1 integrin.

Aim:

This prompted us to investigate the interaction between C16 peptide and beta 1 integrin in breast cancer cells.

Methods:

MDA-MB-231 and MCF-7 cells were grown in Dulbecco's modified Eagle medium with 10% fetal bovine serum. Cells were subjected to adhesion assays in multiwell plates coated with laminin 111, C16 (KAFDITYVRLKF) or C16Rv (control peptide FKLRVYTIDFAK). Flow cytometry addressed whether beta 1 integrin would be activated by C16. Cells were incubated with either C16 peptide or the reverse control C16Rv for 1, 6 and 8 hours. The 12G10 antibody detected activated beta 1 integrin. We also analyzed C16 subcellular localization using Nanogold-conjugated peptides. Interaction between rodamine-conjugated peptides and MDA-MB-231 and MCF-7 cells was studied through time-lapse confocal fluorescence microscopy and the number of vesicles was analyzed.

Results:

Cells were subjected to adhesion assays in multiwell plates coated with laminin 111, C16 (KAFDITYVRLKF) or C16Rv (control peptide FKLRVYTIDFAK). MDA-MB-231 cells showed increased adhesion to C16 peptide compared to controls. Depletion of beta 1 integrin by siRNA decreased cell attachment to C16. Flow cytometry addressed whether beta 1 integrin would be activated by C16. Cells were incubated with either C16 peptide or the reverse control C16Rv for 1, 6 and 8 hours. The 12G10 antibody detected activated beta 1 integrin. C16 increased beta 1 activation after 8 hours. We also analyzed C16 subcellular localization using Nanogold-conjugated peptides. Transmission electron microscopy (TEM) showed C16 decorating cell membrane and inside cellular vesicles. This result would suggest interaction of C16 and cell membrane. The presence of C16 inside vesicles would imply peptide endocytosis. Interaction between rodamine-conjugated peptides and MDA-MB-231 and MCF-7 cells was studied through time-lapse confocal fluorescence microscopy and the number of vesicles was analyzed. Our data showed that both C16 and control C16Rv interacted with cells.

However, C16 internalization was greater than the internalization of control peptide C16Rv over time. Moreover, C16 endocytosis decreased after treatment with dynamin inhibitor in MCF-7 cells. Colocalization analysis between LysoTracker dye with rodamine-conjugated C16 showed that only a small amount of peptide colocalize with lysosomes. This finding indicates that this peptide could be participating in integrins recycling pathway.

Conclusion:

In conclusion, our findings strengthened C16 adhesive role and indicate that adhesion could happen through interaction of C16 with beta1 integrin. Furthermore, this peptide activates beta 1 integrin. Taken together, TEM and time lapse results suggest that after membrane interaction and putative beta 1 activation breast cancer cells would internalize C16 peptide.

Financial support:

FAPESP (15/03393-9; 2016/20228-4)

22.035 - SLIT/ROBO NEURAL GUIDE PATHWAY GENES ARE INCREASED IN NEUROENDOCRINE PROSTATE CANCER. Santos NJ, Barquilha CN, Barbosa IC, Monção CCD, Mosele FC, Delella FK, Justulin Jr LA, Felisbino SL, - Department of Cell Biology - UNICAMP Department of Morphology - Sao Paulo State University

Introduction:

Prostate cancer (PCa) is the second most frequent and the second highest rate of morbidity and mortality among men. Studies highlight the role of neuroendocrine differentiation in the more advanced stages of tumor progression, metastasis and resistance to castration of CaP. Previous analyzes of transcriptomes of knockout mice revealed changes in the expression of related genes SLIT/ROBO neural signaling pathway. SLITs and ROBOs are also expressed in nonneuronal tissues, such as mouse lung and kidney. Several SLITs and ROBOs have also been found to be aberrantly expressed during the development of ovarian, endometrial, cervical, and in the reproductive system. The roles of SLIT/ROBO pathway in tumors should be further discussed, for which there are no more detailed studies in the PCa.

Aim:

The aims of this study were to analyze the gene expression of the SLIT/ROBO pathway (SLIT1, -2; -3; and ROBO1, -2, -3 and -4) in the CaP progression of knockout mice and to identify target genes for neuroendocrine CaP therapy.

Methods:

A meta-analysis of the gene expression of these 7 genes from the SLIT/ROBO pathway was performed in the different normal and tumor prostate lobes of the knockout mice for the Pten (Pten model) and Tp53 and Rb1 (p53/Rb model) genes, these transcripts have already been deposited in the database in the NCBI GEO database (GSE94574).

Results:

Gene expression analysis in animal models showed an overexpression of SLIT1 in high-grade tumors of the p53 knockout mice and an up-regulated progression in the Pten model. The ROBO2 gene was upregulated in the advanced tumor p53, whereas the ROBO4 expression was increased in the advanced tumor of the Pten model. There was no significant difference in the expression of ROBO1 and ROBO3 in both models. The levels of gene expression in the human CaP of SLIT1, SLIT3, ROBO3 and ROBO4 genes were increased in patients at high risk.

Conclusion:

We can conclude that SLIT1, ROBO2 and ROBO4 are associated with advanced CaP and more aggressive/invasive tumors of the neuroendocrine type, and potential new therapeutic targets for the treatment of PCa.

Financial support:

CAPES/CNPq

FeSBE Annual Meeting 2019

Poster Sessions and Abstracts

22.036 - CROSS-SPECIES ANALYSES PINPOINT THE ANTIOXIDANT ENZYME SULFIREDOXIN AS A POTENTIAL THERAPEUTIC TARGET FOR METASTATIC PROSTATE CANCER. Barquilha CN, Monção CCD, Santos NJ, Barbosa IC, Mosele FC, Justulin Jr LA, Felisbino SL, - Biologia Estrutural e Funcional - UNICAMP Morfologia - UNESP

Introduction:

Prostate cancer (PCa) is currently the second most frequent cause of death in men and its incidence has been increasing. Despite advancements in cancer therapies, new therapeutic approaches are still needed for treatment-refractory advanced metastatic PCa. Considering the role of antioxidant pathways in tumor initiation and progression, we hypothesized that the inhibition of oxidative stress-related genes could be an adjuvant strategy to treat cancer.

Aim:

Our aim was to search for a new therapeutic target for PCa among the antioxidant genes that were overexpressed in the tumor.

Methods:

We initially used a genetically engineered mouse model (Pb-Cre4; Ptenf/f) to collect prostate tumors in different phases of progression and search for differentially expressed genes in PCa. By transcriptome data (RNAseq) and protein expression analyses (immunohistochemistry) of the prostate samples from mice, we selected the gene of the sulfiredoxin enzyme (Srxn1) for functional validations. Subsequently, we performed analyses in published human database to investigate the gene expression pattern and the clinical relevance of the target SRXN1 in patients with PCa. We also used tissue microarrays (TMAs) of human prostate samples to validate the protein expression pattern of SRXN1 in PCa and its association with clinical data from patients, such as prognosis and survival. It was performed in vitro validations to analyze the protein and gene expression of SRXN1 in normal (RWPE-1 and PNT-2) and tumor prostate cells (LNCaP and PC-3). To better understand the modulation of SRXN1 expression in PCa, we independently exposed the prostate cells to testosterone (2, 10 and 20nM), flutamide (2, 10 and 20µM), fibronectin (1, 10 and 20µg/mL) and H₂O₂ (25, 75 and 125µM). In addition, to confirm our hypothesis, we inhibited the SRXN1 mRNA in PCa cells LNCaP (by siRNA), followed by analysis in tumor cell viability.

Results:

We observed a gene and protein overexpression of Srxn1 mainly in advanced-stage prostate tumors (poor-differentiated adenocarcinoma) from Pb-Cre4; Ptenf/f mice. Analyses of human databases and prostate TMAs demonstrated that SRXN1 is up-regulated in a subset of high-grade prostate tumors and correlates with aggressive PCa with worse prognosis and decreased survival. In vitro analyses showed that SRXN1 expression is higher in most PCa cell lines compared to normal prostate cell lines. Furthermore, siRNA-mediated downregulation of SRXN1 led to decreased viability of PCa cells. We also observed that protein and gene expression of this enzyme is differentially modulated by testosterone, flutamide, fibronectin and H₂O₂ in prostate cells lines, which have different stress response mechanisms and different metabolisms.

Conclusion:

Cross-species analyses indicate the antioxidant enzyme SRXN1 as a potential therapeutic target for advanced and metastatic PCa. Within the context of precision medicine, our results suggest that the use of specific SRXN1 inhibitors may be an effective strategy for the adjuvant treatment of castration-resistant PCa with SRXN1 overexpression. It is still necessary a better understanding of how SRXN1 expression is regulated in the different phases of PCa progression for the development of new therapeutic approaches using inhibitors to SRXN1.

Financial support:

FAPESP (2015/26097-6; 2016/09532-3; 2016/25945-6), CNPq (305391/2014-3; 132849/2017-8) and CAPES (001)

22.037 - CYCLOOXYGENASE AND MICROSOMAL PROSTAGLANDIN E SYNTHASE-1 INHIBITION DOWNREGULATE EXTRACELLULAR MATRIX PROTEINS AND INTEGRIN GENE EXPRESSION AND REDUCE CELL MIGRATION IN GLIOBLASTOMA. Goes LMS, Colquhoun A, - Department of Cell Biology and Development - USP

Introduction:

Glioblastoma (GBM) is the most common and lethal brain cancer with a survival rate of 14 months. GBM rapidly invade into the surrounding tissue, and current therapies are inefficient. Components of extracellular matrix (ECM) and integrins play crucial roles in GBM dissemination. High levels of cyclooxygenases (COXs) and their major product prostaglandin E₂ (PGE₂) are related to tumor aggressiveness and invasiveness. Microsomal prostaglandin E synthase-1 (mPGES1) is the main PGE₂ synthase.

Aim:

To observe the effects of COX-1/2 or mPGES1 inhibition or exogenous PGE₂ in cell migration, expression of ECM proteins and integrins in U87MG and T98G GBM cells.

Methods:

Dose-response curves for COX-1/2 inhibitor Ibuprofen (IBP), mPGES1 inhibitor CAY10526 and PGE₂ were performed. mRNA expression levels in cells treated with IBP (100 µM, 72h in U87MG) (200 µM, 72h, in T98G), COX-1 inhibitor SC560 (50 µM, 48h), COX-2 inhibitor NS398 (50 µM, 48h), CAY10526 (20 µM, 48h in U87MG) (25 µM, 48h in T98G) and PGE₂ (10 µM, 72h) were determined for laminin (LAM), type IV collagen (COL4), fibronectin (FN), vitronectin (VTN), and integrins: αV (ITGAV), α3 (ITGA3), α5 (ITGA5), β1 (ITGB1) and β3 (ITGB3). Scratch assays were performed with cells exposed to individual treatments to evaluate the motility of cells.

Results:

IBP reduced cell numbers in both U87MG [100 µM, 72h] and T98G [200 µM, 72h] cells in comparison with ethanol (EtOH) (p<0,001, n=3, in triplicate). CAY10526 reduced cell numbers in U87MG [20 µM, 48h] and T98G [30 µM, 48h] cells in comparison with dimethyl sulfoxide (DMSO) (p<0,05, n=3, in triplicate). In contrast, PGE₂ increased cell numbers in both cells [10 µM, 72h] in comparison with EtOH (p<0,001, n=3, in triplicate). RT-qPCR analysis demonstrated that U87MG cells treated with IBP and CAY10526 decreased LAM (p<0,05, n=3, in duplicate), VTN (p<0,01, n=3, in duplicate) and ITGAV (p<0,05, n=3, in duplicate) mRNA levels compared with drug vehicle controls EtOH or DMSO. Also, CAY10526 decreased gene expression of COL4 (p<0,05, n=3, in duplicate), FN (p<0,01, n=3, in duplicate), ITGA5 (p<0,01, n=3, in duplicate) and ITGB3 (p<0,05, n=3, in duplicate) in U87MG cells in comparison with DMSO. SC560, NS398 and CAY10526 decreased LAM, COL4 and ITGAV mRNA levels in T98G cells compared with EtOH or DMSO controls (p<0,05, n=3, in duplicate). T98G decreased FN, VTN and ITGA5 gene expression when treated with SC560 in comparison with EtOH (p<0,05, n=3, in duplicate). SC560, NS398 and CAY10526 decreased migration of U87MG and T98G cells compared with EtOH or DMSO (p<0,05, n=3, in duplicate), while PGE₂ increased migration in U87MG cells in comparison with EtOH (p<0,05, n=3, in duplicate).

Conclusion:

These data indicate that COX-1/2 and mPGES1 inhibition decreases cell growth, alters gene expression critical for GBM invasion, and also decreases GBM cell migration in vitro. This evidence points to potential application of COX-1/2 and mPGES1 inhibitors in GBM management.

Financial support:

Capes, FAPESP

22.038 - EFFECT OF EXERCISE TRAINING ON THE REGULATION OF MICRORNAS IN CANCER. Tobias GC, Gomes JLP, Oliveira EM, - Estudos Biotécnicos da Educação Física e Esporte - USP

Introduction:

Exercise training is a non-pharmacological strategy that improves well-being and health in different organs and systems. Several studies have

FeSBE Annual Meeting 2019

Poster Sessions and Abstracts

demonstrated that exercise training can slow down tumor growth in different animal models, and recent evidence indicate that regular physical activity decreases the incidence of 13 different cancers in humans. However, the mechanisms underlying these effects are not fully understood. MicroRNAs (miRs) are a class of small noncoding RNAs involved in cell homeostasis and carcinogenesis. Several miRs are aberrantly expressed in tumors, and their deregulation is linked to cancer progression and clinical outcome. Nevertheless, it is completely unknown whether exercise training can modulate deregulated miRs in cancer.

Aim:

The aim of this study was understanding the effect of exercise training on the regulation of microRNAs in cancer.

Methods:

To test this, Balb/c mice were submitted to a moderate intensity exercise training (60% of maximal aerobic capacity, 5 days/week, 1 hour/day, in a treadmill) for 2 months before being inoculated with 1x10⁵ CT26 colon carcinoma cells (subcutaneous injection). The exercise training protocol was maintained during tumor progression, and the last exercise session was performed 24 hours before animals were sacrificed (19 days after tumor cells injection). Tumor volume and body weight were measured daily. Experimental groups were divided into control (healthy sedentary mice), CT26 SED (sedentary tumor-bearing mice) and CT26 TR (trained tumor-bearing mice). Tumors were harvested at day 19 and the microRNA array was performed. Statistical analysis: Student t test, Anova One-way, and Two-way, Tukey post hoc, p<0.05

Results:

As expected, exercise training significantly reduced CT26 tumor growth when compared to CT26 SED mice. After that, tumors fragments from both sedentary and trained mice were grafted into new sedentary healthy mice, and it was observed that tumor fragments from trained mice grew less than tumor fragments originated from sedentary mice. After that, we generated primary CT26 cells from these tumor fragments and injected it into new sedentary healthy mice. We observed that primary CT26 cells from trained mice grew less than primary CT26 cells from sedentary mice. In addition, when mice were sacrificed individually when tumor volume reached approximately 600 mm³, exercise training reduced splenomegaly, the increase in liver mass, and the gastrocnemius mass loss promoted by the CT26 tumor. To understand the role of miRs on these aforementioned responses, we performed a microRNA array to identify differentially expressed miRs between sedentary and trained mice tumors. We found that exercise training promoted a global downregulation of miRs in the tumor compared to CT26 SED group, which was accompanied by reduced gene expression of Dicer and Xpo5, two important markers involved in miRs processing.

Conclusion:

Exercise training decreases CT26 tumor growth, and this effect can be associated with the global downregulation of tumor miRs, as well as with the decreased gene expression of Dicer and Xpo5.

Financial support:

FAPESP 2018/02351-9

22.039 - CHARACTERIZATION OF ENDOCANNABINOID SYSTEM IN HUMAN RETINOBLASTOMA CELL LINE. Paiva ACS, Fragel-Madeira L, - Departamento de Neurobiologia - UFF

Introduction:

Currently, endocannabinoid system has been widely studied for being involved in several physiological mechanisms, as well as in pathophysiological conditions. This system is present throughout the body and is composed of two classical receptors, the type 1 and 2 cannabinoid receptor (CB1r and CB2r), its endogenous ligands Anandamide (AEA) and the 2-arachidonoyl glycerol (2-AG) and its synthesis enzymes phospholipase D and DAG lipase. The degrading

enzymes of these ligands are fatty acid amide hydrolase (FAAH), monoacylglycerol lipase (MGL). In addition, this system has been very promising for the treatment of tumors, in part because of its neuromodulatory function. Among cancers that affect the nervous system, retinoblastoma is the most common intraocular tumor in childhood, which can lead to organ loss and still has very controversial treatment. Therefore, relationship between this neoplasia to endocannabinoid system could contribute to disease prognosis in the future.

Aim:

The objective of this project was to analyze the presence of CB1 and CB2 receptors, and FAAH enzyme in human retinoblastoma Y79 cell culture.

Methods:

Y79 retinoblastoma cells were cultured in 25 cm² bottles in RPMI 1640 medium supplemented with 10% fetal bovine serum, 1% L-glutamine, 100 U/ ml penicillin and 100 µg/ ml streptomycin at 37 °C in an atmosphere with 5% CO₂. The cells were kept in suspension with a maximum concentration of 2x10⁶ cells/ mL. Cells were processed for protein extraction for later western blotting analysis and also for immunofluorescence.

Results:

We found an intense peri-cytoplasmic labeling for CB1 and CB2 in Y79 cells by immunofluorescence showing a staining in retinoblastoma cell membranes. However, immunostaining for FAAH was weak and questionable by this technique. To confirm these expressions, western blotting followed by densitometric analysis was performed. Our results showed two bands for CB1r, corresponding to approximately 40 and 73 kDa, which expected molecular weight for CB1 is approximately 53 kDa. As already seen in other studies, we believe that these different weights are due to expression of the glycosylated and non-glycosylated CB1r, respectively. Meanwhile, for CB2r expression, we found four bands of approximately 40 kDa, 45 kDa, 60 kDa and 80 kDa, being expected the first two molecular weights. As already described, the glycosylated form of this protein is approximately 59 kDa. Therefore, we suggested 80 kDa band could be justified by receptor homodimerization, as seen in other studies as well. The band identified by FAAH immunostaining was weak, with molecular weight of approximately 63 kDa as expected. Taken together, these results confirmed presence of CB1, CB2 receptors and now also FAAH in retinoblastoma cells.

Conclusion:

The characterization of endocannabinoid system components in this retinoblastoma cell line allows further studies to establish a relationship between the expression of these components and the development of the disease and consequently possible therapeutic interventions.

Financial support:

Capes, CNPq, Faperj, Proppi-UFF.

24 - Vision and Ophthalmology

24.013 - QUANTIFICATION OF INFLAMMATORY CELLS AND EVALUATION OF THE ANTI-INFLAMMATORY PROTEIN ANNEXIN A1 IN EXPERIMENTAL AUTOIMMUNE UVEITIS. Costa SS, Montresor LB, Tencarte SR, Possebon L, Pilon MMI, Girol AP, - Biociências - UNESP and UNIFIPA Biociências - UNIFIPA

Introduction:

Uveitis is associated with several autoimmune diseases and is one of the leading causes of blindness in the world. Although there are different drugs used to treat uveitis, the side effects of these drugs limit their use. In recent years, the role of the anti-inflammatory protein annexin A1 (AnxA1) in ocular inflammatory processes has been investigated in vivo and in vitro, and point to AnxA1 as one of the essential mediators in the homeostasis of the inflammatory process.

Aim:

FeSBE Annual Meeting 2019

Poster Sessions and Abstracts

Evaluate the severity of the experimental autoimmune uveitis (EAU) by clinical and histopathological studies and leukocytes quantification in the aqueous humor (AqH)

Methods:

Lewis rats were divided into three groups: untreated-induced uveitis (EAU), EAU treated preventively (P) or therapeutically (T) and control (C) (n = 10 / each group) (CEUA 01/14). For the development of the EAU the animals were inoculated in the right paw with 100 µg of bovine IRBP in 100 µl of Freund's complete adjuvant emulsion. Simultaneously, an intraperitoneal (i.p.) injection containing 0.5 µg of the Bordetella pertussis toxin in 100 µl PBS was administered as an additional adjuvant. In the prevention protocol, the animals were treated daily by i.p. administration of 200 µg of the AnxA1 peptide (Ac2-26) in 200 µl of PBS from day 1 to day 13 post-immunization. Animals from the therapeutic protocol also received the peptide daily, but from day 8 to day 13 post-immunization. All EAU animals were euthanized 14 days post-immunization for an excessive dose of anesthetic. Animals without manipulation were used as a control group. The EAU severity was assessed daily, from day 1 post-immunization, with a slit lamp (biomicroscope). Each eye was graded following predefined classification criteria. AqH was collected by puncture of the anterior chamber of the eyes for analysis of inflammatory cells after Turk staining (1:10) in the Neubauer chamber. The values for quantification were demonstrated as mean ± standard error (S.E.M) and the statistical analyses performed by ANOVA and Bonferroni.

Results:

The clinical analyses with the slit lamp showed control eyes with normal aspects of vascularization, pupil size, and transparency of the anterior chamber. In contrast, untreated-EAU eyes showed increased blood of vessel number, redness, obscured pupil, greater opacity of the anterior chamber and significantly reduced red reflex. In the EAU groups treated with Ac2-26, the vascularization, pupil size, and transparency of the anterior chamber were reestablished to the normal parameters, observing a greater similarity between preventive and control groups. The quantitative analysis of AqH showed a large amount of leukocytes, predominantly lymphocytes, in the untreated-EAU (EAU: 33.30 ± 2.776 , $p < 0.001$ vs C: 11.25 ± 2.339) and significant reduction of these cells ($p < 0.001$) with administration of Ac2-26, especially in the therapeutically treated group (P: 10.70 ± 1.598 ; T: 2400 ± 0.4783).

Conclusion:

The administration of AnxA1 peptide promoted effective anti-inflammatory effects in this model of experimental autoimmune uveitis, with potential for therapeutic application.

Financial support:

CNPq and UNIFIPA

24.014 - EVALUATION OF EFFICACY OF BIODEGRADABLE SYSTEMS CONTAINING SIROLIMUS IN EXPERIMENTAL AUTOIMMUNE UVEITIS MODEL. Paiva MRB, Santos DVV, Fialho SL, Castro BFM, Cunha-Júnior AS, - Departamento de Oftalmologia e Otorrinolaringologia - UFMG Pesquisa e Desenvolvimento Farmacêutico - FUNED Departamento de Produtos Farmacêuticos - UFMG

Introduction:

Uveitis, an ocular inflammatory condition that affects the iris, ciliary body, choroid, and adjacent tissues (retina, optic nerve, and vitreous body) plays an important role in cases of blindness worldwide. Sirolimus (SRL), a potent immunosuppressive drug, has shown promising results in the treatment of ocular diseases. Despite its therapeutic potential, its clinical use is a major challenge due to low bioavailability and poor solubility. Poly (lactic-co-glycolic acid) (PLGA) is a biodegradable polymer commonly used for ophthalmic drug delivery due to its suitable characteristics such as biocompatibility, good mechanical properties, and improvement of the pharmacokinetic profile of the drug.

Aim:

In the present study, we investigated the therapeutic efficacy of SRL-PLGA intravitreal implant on experimental autoimmune uveitis rabbits.

Methods:

Experimental uveitis was induced by unilateral intravitreal injection of *Mycobacterium bovis* bacillus Calmette-Guérin in preimmunized New Zealand rabbits. Animals were randomly divided into two groups that received intravitreal SRL-PLGA or sterile saline (n = 6 per group). Inflammation was evaluated by clinical examinations using slit-lamp and indirect ophthalmoscopy for 35 days and histopathological examinations were also performed at the end of the study. Alterations of protein levels, determination of myeloperoxidase (MPO) and N-acetylglucosaminidase (NAG) activity were investigated either in the aqueous or vitreous humor. The experimental protocol was approved by the Ezequiel Dias Ethics Committee on Animal Use, protocol nº 112/2017.

Results:

Combined inflammatory score, anterior inflammatory score, anterior chamber cells, and vitreous haze, were smaller in the treated eyes than in the untreated eyes throughout the 35 days of follow-up. In addition, optic disc edema, dense inflammatory membranes, and retinal detachment were observed in untreated animals at the end of the study. Histopathologic examinations showed less severe inflammation and tissue disorganization in treated eyes after 35 days. The total aqueous and vitreous protein was higher in the control group than in the drug-treated group after 35 days after intravitreal challenge ($p=0.0046$ and 0.0037 , respectively). Similarly, MPO activity in the aqueous or vitreous humor was lower in animals treated with SRL-PLGA implants compared to the control group ($p=0.0023$ and 0.0002 , respectively). NAG activity in the vitreous humor was significantly less than untreated eyes ($p=0.0003$) and resembling healthy contralateral eye ($p=0.1980$).

Conclusion:

According to the results, the implants developed in this study reduced the eye inflammation and could overcome the difficulty of promoting a prolonged release of SRL in the posterior segment of the eye. Therefore, the intravitreal SRL-PLGA implants could be a promising alternative of treatment to autoimmune uveitis.

Financial support:

CAPES, CNPq, FAPEMIG

24.015 - VITREOUS COMPONENTS IN THE RETINA OF NEWBORN, ADULT AND AGING RATS.. Costa GJL, Matsuda M, Akamine PS, Roda VMP, Silva RA, Hamassaki DE, - Department of Cell and Developmental Biology - USP Department of Ophthalmology - USP

Introduction:

Age-related changes that occur in ocular tissues, such as liquefaction of the vitreous matrix, as well as vitreous traction, are important causes of vision loss. In this context, proliferative vitreoretinopathy and proliferative diabetic retinopathy are leading causes of blindness due to tractional retinal detachment, and effective treatments have not been established yet. In the past few years, microRNAs (miRNAs), small non-coding RNAs that act by translational repression and mRNA degradation were altered in these diseases (Usui-Ouchi et al., Plos One 11: e0158043, 2016). We have previously observed that miR-9, miR-16, miR-21 and miR-204 in retina and vitreous showed different expression pattern with aging. Our hypothesis is that miRNAs may change with aging and influence the vitreous matrix and the vitreoretinal interface.

Aim:

The aim of the present study was to determine the expression of some vitreous matrix components that are also predicted targets of miR-9, miR-16, miR-21 or miR-204, in the retina and vitreous of newborn, adult and aging rats.

Methods:

Newborn (postnatal day 1-3, n = 5), adult (2 months, n = 5) and aging (12 months, n = 4) Wistar rats were sacrificed by anesthesia overdose,

FeSBE Annual Meeting 2019 Poster Sessions and Abstracts

their eyes enucleated and retinas collected. Total RNA was isolated using Trizol, and expression of collagens type 6 alpha1 (Col6a1), Col9a1, Hyaluronan synthase 2 (Has2), matrix metalloproteinase 1 (Mmp1), and Mmp13 was analyzed by real-time quantitative PCR. This research was approved by the Ethics Committee on the Use of Animals (CEUA/ICB/USP/075/2015).

Results:

Retinas of newborn, adult and aging rats expressed Col5a3, Col6a1, Col9a1, Has2, Mmp1 and Mmp13. Except for Col5a3 and Has2, the predicted targets of miR-16, miR-21 and miR-204 showed low levels of mRNA expression in the retina and no significant differences in newborn, adult and aging rats. Col5a3 was expressed in lower levels in newborn, but in higher levels in adult and aging retinas. Similar expression profile was observed for miR-204 in the retina, but especially in the vitreous. Interestingly, Has2, a predicted target of miR-9, miR-16, and miR-204, showed high levels in the newborn retina, and a decreased expression in adult and aging ones. However, miR-9 and miR-16 exhibited the same pattern, showing a downregulation with aging in both retina and vitreous.

Conclusion:

Our results suggest that among the investigated vitreous matrix component, Has2 has the potential to be modulated by miRNAs, especially by miR-204. Thus, further studies are necessary to investigate whether miR-204 is involved in regulating hyaluronan synthesis, as well as in morphological and physiological vitreoretinal changes associated with progressive age.

Financial support:

FAPESP, CNPQ and CAPES

24.016 - DARK-ADAPTED ROD THRESHOLDS IN DUCHENNE MUSCULAR DYSTROPHY PATIENTS. Dias SL, Silva LA, Oliveira TA, Nagy BV, Zatz M, Pavanello R, Costa MF, Grossklaus LF, Barboni MTS, Ventura DF, - Psicologia Experimental - USP Centro de Pesquisa sobre o Genoma Humano e Células-Tronco - USP Neurociências e Comportamento - USP Setor de investigação de doenças neuromusculares - Unifesp

Introduction:

Duchenne Muscular Dystrophy (DMD) is an X-linked recessive genetic disease leading to alteration of dystrophin proteins (Dps) such as Dp427, which results in severe muscle impairment. Muscle loss is rapid and severe, many patients die by the end of the second decade of life due to cardiac and respiratory muscle failure. Moreover, Dps are required for the normal functioning of the central nervous system. The retina is site of expression of four Dps: Dp427, Dp260, Dp140 and Dp71. Previous studies have shown that the absence of Dps in the retina cause alterations in the electroretinogram (ERG) and visual functions such as color vision and temporal and spatial contrast sensitivity in patients with DMD.

Aim:

The aim of the present study is to investigate the dark-adaptation, using a non-invasive psychophysical test, in DMD patients (N = 16, ten downstream and six upstream to exon 30, mean age = 16.90 ± 4.03 years) and controls (N = 21, mean age = 22.08 ± 5.74 years).

Methods:

A short-protocol previously reported by our group (Nagy et al. 2017) to measure the rod-adaptation luminance level was used with the Roland Dark-Adaptometer system Ganzfeld stimulator. The protocol lasts 13 minutes to test rod-adaptation, 6 minutes test session and is performed with green stimulation to test for rod adaptation.

Results:

The investigation was performed with 21 healthy subjects and 16 subjects with DMD, ten downstream and six upstream to exon 30. DMD patients with genetic mutations affecting the protein Dp260 show higher rod-adaptation thresholds (mean = -3.00±0.58 log cd/m²) than DMD patients with genetic mutations sparing the protein Dp260 (mean

= -3.81±0.52 log cd/m²) and compared to controls (mean = -4.10±0.23 log cd/m²).

Conclusion:

In conclusion, lacking only Dp427 results in a conservation of rod-adaptation sensitivity in DMD patients while the lack of smaller Dps, such as the Dp260 (mainly expressed by the rods) in DMD patients cause impairment of the rod function, as it has been extensively demonstrated using ERGs, and also affects their dark-adaptation.

Financial support:

Financial support: FAPESP grant numbers 2016/22007-5 to MTSB and 2014/26818-2 to DFV; CNPq grant number 404239/2016-1 to MTSB and CNPq Productivity 1 A 309409/2015-2 to DFV.

24.017 - EVALUATION OF THE RETINAL TOXICITY OF MOMETASONE FUROATE AFTER INTRAVITREAL INJECTION. Lage NA, Paiva MRB, Silva-Cunha A, - Department of Pharmaceutical Products - UFMG

Introduction:

Uveitis is a spectrum of inflammatory disorders characterized by ocular inflammation and is one of the leading causes of preventable visual loss. In Brazil, uveitis is responsible for 15.7% of individuals institutionalized for visual rehabilitation and represents the second most frequent diagnosis in low-vision clinics. The corticosteroids have been widely used in the treatment of ocular inflammatory diseases since their development in the early 1950s and are still the first option for treatment.

Aim:

In the present study was evaluated the ocular toxicity of Mometasone Furoate (MF), a potent corticosteroid, which has high binding affinity to glucocorticoid receptors and a high potency in the inhibition of IL-1 and TNF α , cytokines evidently involved in the inflammatory process of uveitis.

Methods:

We conducted an experimental controlled study of 12 male Lewis rats, with protocol approved by Ethics Committee on Animal Use of the UFMG under protocol 238/2018. Single intravitreal injections of 10 μ l of each specific dose of MF (30, 90 and 290 μ g/ml) or phosphate buffer (PBS) were applied to both eyes per rat in each 3-rats group. The retinal toxicity was assessed by electrophysiological recordings (ERG), at baseline and at 3, 7 and 15 days after the intravitreal injection. ERG performed in compliance with the International Society for Clinical Electrophysiology (ISCEV) guidelines. The retinal histology was performed after the end of the follow-up period, were evaluated quantitatively as the thickness of the retina and its main layers, ganglion cells, internal nuclear layer and outer nuclear layer, using the Image J program. The data were analyzed using the GraphPad Prism[®]5 program through the two-way ANOVA and Bonferroni as a post-test.

Results:

ERG responses (amplitude and implicit time of a and b waves) showed no significant difference was between the control group (PBS) and the groups that received different concentrations of MF over the 15 days of follow up. There was also no significant difference between the different study times in each group, suggesting that there were no toxic effects on the retina. No remarkable difference in retinal histopathology was detected among the groups. There were also no signs of necrosis, fibrosis or presence of inflammatory infiltrate.

Conclusion:

Single intravitreal injection at dose until 290 μ g/ml of MF showed no toxic effects on the function or morphology of the retina of the animals and, therefore, may be considered safe for ophthalmic use. The MF could be evaluated as an alternative treatment of a variety of intraocular inflammatory conditions.

Financial support:

We would like to thanks CAPES, CNPq e FAPEMIG for the financial support

FeSBE Annual Meeting 2019

Poster Sessions and Abstracts

24.018 - A NOVEL UVEITIS MODEL INDUCED BY BCG IN RABBITS. Castro BFM, Vieira LC, Silva LM, Santos DVV, Fialho SL, Cotta OAL, Paiva MRB, Guerra MCA, Silva-Cunha A, - Faculty of Pharmacy - UFMG Faculty of Medicine - UFMG Pharmaceutical Research and Development - FUNED Cell Biology Laboratory - FUNED

Introduction:

Uveitis is a heterogeneous and complex group of conditions characterized by intraocular inflammation and presenting an important contribution to blindness worldwide, involving specially working-age population. It is responsible for 5 to 20% of cases of blindness in developed countries and up to 25% in developing countries. Animal models of uveitis have provided important insights into the etiology and pathogenesis of the disease, giving rise to a more complete understanding of mechanisms and concepts, some of which applicable to human uveitis. However, due to the difficulties involved in investigating such a complex disorder, there is still an unmet need for the development of different / new uveitis models, especially those suitable for testing new treatments.

Aim:

This work proposes a new uveitis model in rabbits since their eyes have been useful models for studying intravitreal pharmacokinetics of drugs and drug delivery systems, important for developing new therapies. The experimental uveitis model of our study was induced by *Mycobacterium bovis* Calmette-Guérin Bacillus (BCG), a live-attenuated strain.

Methods:

The experimental protocol consisted of two subcutaneous injection of BCG followed by two intravitreal injections of the same antigen. Ophthalmological examination, histopathological analysis and electroretinography (ERG) provided clinical assessment of presence/severity of intraocular inflammation and were performed two days after each intravitreal injection. Protein quantification in vitreous, N-Acetyl- β -D-Glucosaminidase (NAG) and myeloperoxidase (MPO) activity measurement in vitreous and retina, were done after the second intravitreal injection to evaluate the possible disruption of ocular barriers.

Results:

Inflammatory reaction concentrated in the anterior chamber was observed after the first intravitreal injection, evidenced by conjunctival hyperaemia and congestion of iris vessels along with the presence of cellular aggregates. The second intravitreal injection of BCG led to an inflammatory response involving also the posterior segment, marked by fibrin plaque and inflammatory precipitates covering the posterior lens capsule and increased vitreous haze. These findings were confirmed by histopathologic evaluation which showed the presence of a dense mixed inflammatory infiltrate in the anterior chamber, iris and ciliary body, in addition to congestion of iris vessels after the first intravitreal injection. While less inflammatory cells in the anterior chamber was observed after the second injection, a considerable increase in inflammatory cells in vitreous and superficial retina was noted. Quantification of protein levels showed a significant higher amount in vitreous of animals that received intravitreal injection of BCG (60 ± 8.1 mg/mL), compared to control groups, (3.59 ± 1.9 mg/mL). Likewise, when compared to control, MPO levels in vitreous and retina were about 6- and 5-fold higher, respectively, whereas NAG levels increased by about 2-fold in vitreous and 12-fold in retina. The maximal scotopic response of ERG exhibited no significant alteration in amplitude of a- and b- waves after the first intravitreal injection, corroborating the previous findings. After the second intravitreal injection, a significant decrease in a- and b-waves amplitude was seen, indicating potential damage to retinal cells.

Conclusion:

Altogether these results demonstrated a possible disruption of ocular barriers and induction of panuveitis in rabbits by BCG. It establishes a novel and low-cost experimental model of uveitis.

Financial support:

CNPq/MCT and FAPEMIG (Brazil).

25 - Education, Science History and Philosophy, Science Communication

25.011 - UNRAVELING MULTIPLE INTELLIGENCES IN THE TRAVELING SCIENCE CENTER SCIENCE UNDER TENTS. Capistrano RL, Alves GH, Azeredo TV, Correa RP, Fragel-Madeira L, - Neurobiologia - UFF Pós-graduação em Ciências e Biotecnologia - UFF Pós-Graduação em Ensino em Biociências e Saúde - Fiocruz

Introduction:

Science Under Tents (CST) is a traveling science center that brings to public various playful and interactive scientific activities based on four central axes (Health, Humanities, Nature and Technology). Understanding science in the world depends on how each person sees, experiences and learns about it. Linked to this reflection, Howard Gardner proposed that humans have eight types of intelligences that are directly related to learning.

Aim:

In this way, we seek to identify if CST works all multiple intelligences in its exhibitions in order to favor the scientific education of any type of public.

Methods:

For this work we evaluated activities presented at CST exhibition during the first semester of 2019. The methodology used was participant observation, in which the researcher was also a mediator in activities. A total of 11 activities were evaluated: Anatomy, Braille, 3D Printer, Libras, Microplastic, Microscopy, Seed Paper, Body Painting, Ramp, Augmented Reality (A.R.), Virtual Reality (V.R.). These activities were analyzed in order to identify 8 types of multiple intelligences: Logical-mathematical, Linguistic, Spatial, Corporal-kinesthetic, Naturalistic, Intrapersonal, Interpersonal and Musical.

Results:

After analysis we found that all activities of CST, because have mediators, corroborate with interpersonal intelligence, as they explore ways to relate to another person, can be between the mediator and the visitor or a discussion between other actors present in the activities. Spatial intelligence has been identified in seven activities (Anatomy, V.R., A.R., Ramp, Body Painting, Microscopy and 3D Printer) once they explore the notion of space, planes and dimensions. Intrapersonal intelligence was also identified in seven activities (Anatomy, Microscopy, V.R., A.R., Braille, Libras and Body painting), since these present contents that add personal knowledge, such as where organs are located until the understanding of one's own language. Logical-mathematical intelligence was identified in six activities (Anatomy, 3D Printer, Braille, R.A, Ramp and Libras), as these address logical associations, technology, geometric bases and interpretation of questions. Body-kinesthetic intelligence is worked on in Libras and V.R. activities, since both predict use of the body to develop them. Linguistic intelligence, on the other hand, was identified in Braille and Libras activities as they address language and communication skills as well as writing and code recognition. Naturalistic intelligence is present in Microplastic and Seed Paper activities, emphasizing the importance of environmental awareness and anthropic effects and their consequences for environment. Musical intelligence is the only one that was not identified in any of activities.

Conclusion:

In conclusion, it can be seen that CST comprises all multiple intelligences, especially interpersonal, but with exception of musical, thus needing to develop more arts-oriented activities. In addition, Libras, Anatomy, Braille and A.R. activities address the widest range of intelligences. Therefore, we intend to use them as a model for creation of new activities and/ or adaptations of mediation, especially those little explored intelligences. However, we need to deepen the discussion of multiple intelligences in CST in order to reach all types of audiences.

Financial support:

CNPq, CAPES, FAPERJ, PROEX-UFF

FeSBE Annual Meeting 2019

Poster Sessions and Abstracts

25.012 - A SUCCESSFUL EXPERIENCE USING FLIPPED CLASSROOM METHODOLOGY FOR BIOPHYSICS TEACHING. Alves GH, Penaforte DC, Thomasi BBM, Terra AM, Repposi MG, Dias MIC, Souza DDC, Fragel-Madeira L, - Neurobiologia - UFF Pós-Graduação em Ensino em Biociências e Saúde - Fiocruz Pós-graduação em Neurociências - UFF

Introduction:

Research in teaching has pointed to a growing demand for teaching methods that break with the traditional format. From this perspective, active methodologies are presented as an option because they value students' participation in the construction of knowledge. The flipped classroom (FC) is an active methodology that aims to change the paradigms of classroom teaching, changing its traditional organization. In this strategy, students have prior access to content of the course and classroom serves as a practical application of these concepts.

Aim:

Thus, we aimed to apply and evaluate the FC strategy during the Biophysics course for undergraduate in Biology at Fluminense Federal University.

Methods:

The course had a total workload of 110 hours, divided weekly into two days. Moodle platform was used as virtual learning environment, in which was provided video lessons, scientific articles, complementary texts, music, videos, that should be watched and studied before classroom. During face-to-face classes, the first hour was devoted to clarifying doubts. In the following hours students (n = 51) developed playful or interactive activities such as individual or group directed exercises, artistic activities, video editing, games, practical activities etc. The evaluation of the students was continuous, based on each activity developed and has collaboration of student teachers and monitors who worked together with the responsible teacher. Evaluation of the course and FC method was performed through an online form in the Google forms platform.

Results:

Students performed 20 activities throughout the course, 48 students were approved and 3 failed. The final average of the class was 7.4 not differing significantly from previous groups that worked with traditional method. The results obtained with evaluation (n = 36) showed that 53% of students found the FC method easier than traditional model, 25% found the same and 14% as difficult as. Regarding classroom dynamics, approximately 95% of students thought it was good or great. Comparing to traditional method, 78% of students found the assessment fairer and 30% better. When asked about complementary materials, 58% thought it helped a lot in the study and 28% only reasonably. Regarding the time of study out of class weekly, almost 70% answered that they studied between 2 and 4 hours, 11% between 4 and 8 hours and 17% less than 2 hours. When asked if methodology helped in the organization of studies, the majority (78%) answered yes and 86% reached learning expectations using FC. Finally, 92% of students considered participation of teaching students and monitors to be fundamental or necessary. We also could observe from answers that some students did not adapt to FC methodology.

Conclusion:

Thus, we concluded that, even though average class performance was close to that of traditional method, the use of FC methodology for biophysics teaching was more motivating and with fairer evaluations, allowing not only more meaningful but also more engaged and pleasurable learning. However, depending on the type of course and the distribution of workload, it must be considered for application of FC, a teaching support team, an adequate physical structure and extra classroom time planning.

Financial support:

CAPES, CNPq, UFF

25.013 - FERMENTATION THROUGH INVESTIGATIVE TEACHING: A POSSIBLE AND EFFECTIVE PEDAGOGICAL STRATEGY. Pacífico CM, Pinheiro SCV, Dias ACAA, - PROFBIO - UFPA

Introduction:

Cellular Metabolism is one of the most important themes in cytology, as it contributes to an understanding life in terms of organized and integrated physical, chemical and biological processes. However, because of its complexity, relating this content to the student's reality is a major challenge for the biology teacher, and teaching through an investigative approach to scientific literacy becomes a useful alternative to achieve this purpose. The present work aimed the theme of Fermentation and was applied to 34 first year high school students of the Escola Bosque Foundation, an agency linked to the Belém City Hall, state of Pará, Brazil.

Aim:

To conceptualize Fermentation and understand the chemical equations inherent in this process; Promote scientific literacy through the application of the scientific method; encourage student interest and participation.

Methods:

The following steps were: 1- Motivation and previous knowledge survey; 2- Problematization, hypothesis survey and alcoholic fermentation experiment; 3- Socialization of the results and presentation in the form of a seminar; 4- Systematization through theoretical class, and application of evaluative questionnaire; 5- Contextualization and deepening of the theme; 6- General discussion and final evaluation. The information obtained was organized into emphases that form categories of analysis according to the proposed objectives, followed by quantitative and qualitative analysis of the results using the IRAMUTEQ software.

Results:

76% of participants considered the activity quite or totally interesting; 25% felt quite or totally motivated; 52% were satisfied with their individual performance, 76% were quite or fully participative; for 84%, the activity contributed to the learning of biology; 76% said the activity improved their understanding of the concept of fermentation; 56% were motivated to learn more about the theme and 96% expressed the desire to repeat the activity. Regarding subject learning, it was found that 48% of the students associated the fermentation process with the need for sugar, 40% justified the growth of the bread mass with carbon dioxide release and 48% reported that the fermentation process is performed by fungi. During the experimental practice, it was observed that, despite the students' difficulties in constructing the script, this process was useful for exercising their vision and doing their science.

Conclusion:

The present work demonstrated that the investigative and experimental activity can improve students learning in complex biological concepts, such as fermentation, by visualizing the process in practice the student was able to better fix the content. As well as proved to be an effective strategy to promote the student's interest, participation and autonomy, developing skills necessary for scientific thinking and attitudes.

Financial support:

Capes

25.014 - WHAT IS "TIME" FOR BRAZILIANS? AGE AND CHRONOTYPE RELATE TO DIFFERENT CONCEPTUALIZATIONS OF TIME. Boni VHF, Garay LLS, Oliveira MAB, Idiart MAP, HIDALGO MP, - Departamento de Psiquiatria e Medicina Legal da Universidade Federal do Rio Grande do Sul - UFRGS Departamento de Física da Universidade Federal do Rio Grande do Sul - UFRGS

Introduction:

Since the beginning of our evolution, humans use time as reference for their social activities and to construct their history. Time assumes different meanings for people depending on culture and age and

FeSBE Annual Meeting 2019 Poster Sessions and Abstracts

language plays a definite role in the construction of the temporal dimension. In chronobiology, biological time is strongly associated with external cues, that can be environmental or social. The body can adapt to external changes and meet social requirements. Some studies, suggest that the concept of time changes with increasing age, as the adaptation to social relations is accompanied by regular activities at fixed times.

Aim:

Given these considerations, we aimed to evaluate the change in the concept of time in different age groups and chronotypes.

Methods:

This was a cross-sectional study where data were collected between December 2018 and May 2019 by voluntarily answers in a questionnaire containing 25 questions, entitled 'Study of the Concept of Time' prepared in the Online Search Platform and published in digital platforms. At the questions "What words come to your mind to answer the question?", "What is time?" all participants could provide more than one answer, to present the different answers in a hierarchical order (first to fourth) and optionally add more words. The Reduce Morningness-Eveningness Questionnaire was applied to check each participant's chronotype. The study was approved by the Research Ethics Committee of the Clinical Hospital of Porto Alegre (protocol 2018-00299). The data were analyzed in SPSS version 18.0 and Nvivo 11 and results were expressed as frequencies according to age groups and chronotype.

Results:

The sample consisted of 2172 Brazilian participants, mainly women (81%), with a mean age of 35 ± 14 years including different age groups such as adolescents (18-19), young adults (20-39), adults (40-59) and seniors (60-80). A total of 1806 distinct words were mentioned as being related to the concept of time. The most frequent words presented in the four were: 'Life' (17.2%), 'Hours' (14.3%), 'Clock' (13.1%), 'Present' (5.3%), 'Past' (4.4%) among adolescents; 'Life' (21.3%), 'Clock' (19.5%) among young adults; 'Life' (25.9%), 'Space' (4.6%), 'Clock' (4.0%), 'Fast' (3.4%) among adults; and 'Life' (29.8%), 'Passage' (9.9%), 'Hours' (4.0%), 'Past' (2.7%), 'Future' (2.8%) among seniors. In the chronotypes, the most frequent words presented in the four were: 'Life' (24.3%), 'Clock' (7.1%), 'Hours' (3.0%), 'Age' (2.9%), 'Past' (2.1%) among morning people; 'Life' (24.2%), 'Clock' (12.8%), 'Future' (2.4%); among intermediate chronotype; 'Life' (21.9%), 'Clock' (18.7%) among evening type.

Conclusion:

The results suggests, in adolescents, the concept of time is related to maturity, in young adults to adaptation to daily activities, in adults it was related to the accomplishment of daily routine and in the seniors, existence. In the morning chronotype it was related to the reflection of the use of moments, in intermediate, to the planning of the routine according to the events and the afternoon, the adaptation to daily activities.

Financial support:

FIPE

FeSBE Annual Meeting 2019

Author Index

A

AARESTRUP, B. J. V.	9.001	ALMEIDA, P. P.	7.016
AARESTRUP, F. M.	9.001	ALMEIDA, V. H.	22.024
ABBOUD, R. S.	7.047	ALMEIDA-SOUZA, F.4	17.012
ABDALA, F. M.	13.001, 13.010, 14.003	ALONSO-VALE, M. I. C.	14.003
ABDALLA, F. M. F.	6.007	ALTVATER, L.	22.016
ABESSA, D. M. S.	1.001	ALVARES, L. E.	23.012
ABRÃO, G. S.	18.003	ALVAREZ, A. M.	13.007
ABREU, A. C. O.	10.029	ALVAREZ-LEITE, J. I.	7.043
ABREU, L. P.	11.019	ALVES, A. A.	21.003
ABREU, P. A.	22.015	ALVES, A. P.	24.005
ACACIO, A. P.	8.013	ALVES, B. C.	23.008, 23.009
ACIOLI, L. T.	3.002	ALVES, B. E. O.	17.004
ADESSE, D.	13.022	ALVES, E. F.	2.005
ADESSE, D.	10.034	ALVES, F. H. F.	10.038
ADRADE, T. A. M.	23.013	ALVES, G. A.	10.026, 11.020, 19.026
ADRIANO, L. C.	15.002, 23.021	ALVES, G. H.	25.010, 25.011, 25.012
AGUIAR, G. S.	6.011	ALVES, L. R. M.	19.006
AGUIAR, J.	14.002	ALVES, L. S.	25.004
AGUILAR, E. C.	7.043	ALVES, M. T. O.	23.008, 23.009
AHMED, N. L.	14.006	ALVES, N.	15.002
AIRES, R. S.	8.014, 8.017	ALVES, P. K. N.	2.002, 16.010
AJERO, U.	24.005	ALVES, P. L.	6.007
AKAMINE, P. S.	24.015	ALVES-BEZERRA, D. S.	8.011
ALBERICI, L. C.	11.007	ALVESC, R. J.	19.001
ALBIAZETTI, G. C.	13.009	AMANO, M. T.	11.018
ALECRIM, A. L.	21.004	AMARAL, L. F.	25.009
ALEGRANCI, P.	19.013, 22.001, 22.017	AMARAL, M.	1.004, 11.015
ALENCAR, A. K. N.	4.011, 16.011, 17.004	AMARAL, M. E. C.	20.009, 21.001, 21.003
ALENCAR, A. M.	4.004	AMARAL, M. M.	20.016
ALEXANDRE-SANTOS, B.	11.011	AMARAL, R. P.	7.041
ALFÂNDEGA, A. A. A.	23.002	AMARAL, R. S.	14.002
ALLODI, S.	10.012	AMARO, G. M.	7.040
ALMEIDA, A. A. C.	18.013, 19.001	AMBROSIO, B. N.	13.012
ALMEIDA, A. S.	11.003, 11.004	AMBROSIO, F.	13.012
ALMEIDA, D. P. R.	4.021	AMBROSIO, F. N.	17.003
ALMEIDA, E. C. P.	22.015	AMORIM NETO, D. P.	10.013, 10.014
ALMEIDA, F. B.	18.012	AMORIM, C. S.	20.020
ALMEIDA, G. H. D. R.	23.003	AMORIM, V. R.	18.013, 19.001
ALMEIDA, L. F.	7.001	ANA, P. A.	23.010
ALMEIDA, M. C.	3.004	ANASTÁCIO, J. M.	22.003
ALMEIDA, M. M.	7.002, 7.003, 7.006, 7.010	ANDERSEN, J. K.	10.009
ALMEIDA, M. R.	9.007	ANDRADE, A. A. R.	19.026
ALMEIDA, N.	25.004	ANDRADE, C. B. V.	6.001
		ANDRADE, F. B.	19.021
		ANDRADE, G. F.	24.002

FeSBE Annual Meeting 2019

ANDRADE, G. P.	22.027	ASHINO, T. E. B.	9.004
ANDRADE, H. C.	23.026	ASHMAWI, H. A.	20.019
ANDRADE, I. R.	22.031	ASSIS, A. P.	7.001
ANDRADE, I. S.	6.016	ASSIS, J. B.	24.011
ANDRADE, L. O.	7.043	ASSIS, L. H. P.	21.007
ANDRADE, M. K. G.	10.020	ASSIS, L. V. M.	24.008
ANDRADE, T. A. M.	11.003, 13.002,13.011,	ASSIS, R. P.	7.017, 7.018, 7.019,
.....	21.003, 23.002,23.008,	7.038, 8.008
.....	23.009	ASSIS, V. O.	4.019
ANDREO, J. C.	3.001	ATELLA, G. C.	1.005
ANDRIOLI, L. P.	13.015, 23.015	AUTRAN, L. J.	4.028
ANGELIS, K.	7.031	AWATA, W. M. C.	4.017
ANJOS, M. B.	21.005	AZAMBUJA, G.	20.002, 20.003,20.005,
ANTONIASSI, J. Q.	6.004, 6.013	20.010
ANTONIO, R. V.	23.011	AZEREDO, T. V.	25.011
ANTONIO-SANTOS, J.	11.013	AZEVEDO, C. E. A.	7.014
ANTRACO, V. J.	13.001, 14.003	AZEVEDO, M. A.	10.025
ANTUNES, G. F.	10.010	AZEVEDO, M. F.	20.011
AQUINO, A. B. O.	19.005	AZEVEDO, R. A.	22.004
AQUINO, J. S.	7.034	AZEVEDO, R. F.	10.033
ARAGÃO, M. O.	18.011	AZEVEDO, S. M. F. O.	19.024
ARAÚJO, B. P.	6.014	AZZI, C. M.	3.003
ARAÚJO, E. E.	10.039		
ARAÚJO, E. G.	10.016, 10.025	B	
ARAÚJO, I. C.	7.014	BACURAU, A. V. N.	11.014
ARAÚJO, L. H.	13.003, 13.014	BAGGIO, B. R.	2.003, 2.004
ARAÚJO, N. S.	13.020	BAGNATO, V. S.	23.008, 23.009, 23.021
ARAÚJO, T. R.	7.036	BAGNATO, V.S.	22.026
ARAÚJO, V. A. A.	16.013	BAGNE, L.	15.001
ARAÚJO, A.	7.031	BAGRI, K. M.	22.024
ARAÚJO, B. J.	4.005	BALLESTREM, C.	4.004
ARAÚJO, J. S. M.	12.005	BALTRUK, L. J.	13.015
ARAÚJO, L. B. N.	19.012	BAMPI, S. R.	18.001
ARAÚJO, M. L. G.	1.006	BANDEIRA, A. C. B.	9.007
ARAÚJO, N. P. S.	7.023, 7.026, 8.009	BAPTISTA, I. L.	13.013, 13.021
ARAÚJO, T. G.	4.005	BARBISAN, L. F.	7.021
ARAÚJO, T. R.	6.009, 6.010	BARBONI, M. T. S.	24.016
ARAÚJO, W. R. S.	8.017	BARBOSA JR, F.	19.015
ARAÚJO-JORGE, T. C.	10.040	BARBOSA, H. S.	10.034, 13.020, 17.010
AREIAS, L. L.	20.008, 20.012	BARBOSA, I. C.	22.035, 22.036
ARMELIN-CORREA, L. M.	14.003	BARBOSA, J. A. S.	9.012, 9.013
ARMENTANO, G. M.	3.004	BARBOSA, L. W. T.	20.002
ARO, A. A.	13.002, 13.018,20.009,	BARBOSA, R. S.	10.040
.....	23.002, 23.008	BARBOSA-DA-SILVA, S.	4.002
ARO, A.A.	23.013	BARBOSA-DEKKER, A. M.	19.013, 22.001, 22.017
ARO, A.A.	16.008	BARBUTTI, I.	13.017
ARRUDA, D. C.	22.002, 22.003	BARCELLOS, J. F. M.	1.006
ARRUDA, D.C.	22.004	BARJA-FIDALGO, C.	4.026

FeSBE Annual Meeting 2019

BARJA-FIDALGO, T. C.	22.031	BIGUETTI, C. C.	3.001
BARON, J.	24.008	BILIBIO, J. O.	19.007
BARQUILHA, C. N.	22.035, 22.036	BISSOLI, N. S.	4.025
BARREIRA, R. M.	7.051	BITTENCOURT, M. B.	6.014
BARREIRA, R. M.	25.009	BIZINELLI, D.	22.018
BARREIRO, E. J.	4.008, 17.004, 17.011	BLANC, H. N. H.	6.011
BARRENCE, F. A.	6.015	BLOISE, E.	6.001
BARRETO, R. F. S. M.	13.020	BLOISE, F. F.	6.001
BARROS, A. B.	14.004	BOA, L. F. F.	6.008, 11.012
BARROS, H.M.T.	18.012	BOAVENTURA, G. T.	7.047
BARSCHAK, AG.	25.002	BOGERD, J.	6.017
BARTOLI, D. M. F.	20.009	BOMFIM, F. R. C.	11.003, 15.004, 20.009
BARTOLO, P. J. S.	23.016, 23.018	BOMFIM, F.R.C.	11.004
BARTOLOMEO, C. S.	16.001	BONCI, D. M. O.	24.008
BARUD, H. S.	23.008, 23.009, 23.021	BONI, V. H. F.	25.014
BATISTA, B. L. V.	9.001	BORDON, I. C.	1.001
BATISTA, C. M.	10.032	BORELLA, M. I.	6.017
BATISTA, C. M. P.	23.005	BORGES, A. C.	10.014
BATISTA, G. B.	10.032	BORGES, F. T.	21.004
BATISTA, P. K. D. S. M.	11.012	BORGES, L. I.	19.007, 19.008
BATTOCCHIO, E. C.	20.015	BORGES, T. B.	12.002
BAVIERA, A. M.	7.024	BORGES, V. F.	4.017
BÁRTOLO, P. J. S.	23.017	BOSQUE, B. P.	10.013, 10.014
BEANES, G.	18.006	BOTEZZELLI, V. S.	3.010
BECK, W. R.	11.008, 11.010	BOTTINO, C. F. S.	3.002
BEGHINI, D. G.	13.022, 21.008, 23.025	BOUZAN, A. C. S.	8.011
BELTRAME, F.	17.011	BOVO, J. L.	15.003, 20.009
BENIN, T.	7.012	BRAGA, L. G.	10.039
BENTLEY, M. V. L. B.	16.005	BRANCO, G. S.	6.017
BENTO, M. R.	23.007	BRAND, L. M.	13.016
BERBER, R. C. A.	20.022	BRASIL, A.	24.011
BERNANRDO, E. M.	11.001, 11.002	BRAYNER CAVALCANTI, M... ..	14.002
BERNARDES, D.	10.003, 21.001	BRAZ, G. R. F.	4.015, 7.027, 11.001,
BERNARDI, L.	13.016	11.002
BERNARDO, E. M.	4.015, 11.016	BRAZ, M. V. C.	7.044
BERTI, A. S.	13.027	BRAZÃO, S. C.	4.028
BERTONI, A. P. S.	22.030	BREHM, F. A.	13.006
BERTOZZI, M. M.	20.015	BREIGEIRON, M. K.	7.037
BEZERRA, E. C. M.	10.037	BRIGAGÃO, C.	4.019
BEZERRA, F. S.	7.023, 7.026, 8.009,	BRITO, C. F.	10.040
.....	9.001, 9.003, 9.005,	BRITO, F. C. F.	4.028
.....	9.006, 19.003	BRITO, L. C.	25.004
BEZERRA, F.S.	4.001, 9.007	BRITO, M. L.	7.016
BEZERRA, M. B. C. F.	14.005	BRITO, M. V.	9.012
BEZERRA, S. K. M.	9.011, 9.012, 9.013	BROTTO, M.	3.001
BHATTACHARYYA, N.	24.003	BRUCIERI, L.	11.003, 11.004, 21.002
BIAJOLI, M. N. G.	18.012	BRUM, E. S.	20.007
BIFF, T. F.	18.012		

FeSBE Annual Meeting 2019

BRUM, P. C.	11.006, 11.014,11.018, 25.004	CANGUSSÚ, S. D.	7.023, 7.026, 8.009, 9.003, 9.005
BRUNETTI, I. L.	7.017, 7.018, 7.019, 7.024, 7.038, 8.008	CAPETTINI, L. S. A.	7.043
BRUNONI, A. R.	20.004	CAPISTRANO, R. L.	25.011
BUCHPIGUEL, C. A.	14.007	CAPPELLI, A. P. G.	7.048
BUCK, H.	10.006	CARBINATTO, F. M.	23.021
BUCK, H. S.	10.007, 18.003	CARDOSO, B. S.	19.010
BUCK, S. H.....	10.008	CARDOSO, C. A.	3.007
BUONAFINA, M. D. S.	19.009	CARDOSO, K. M.	22.024
BURGER, B.	7.050, 21.005	CARDOSO, L. H. D.	7.039
BUSANELLO, E. N. B.	13.026	CARDOSO, L. M. F.	2.001, 2.006
BUSNARDO, C.	10.038	CARDOSO, T. S. R.	6.006
BUSTELLI, I. B.	18.004	CARNEIRO, A. C. D.	20.020
		CARNEIRO, B.	18.006
		CARNEIRO, E. M.	4.024, 4.027, 6.010
C		CARNEIRO, F. D.	6.014
CAETANO A. L.	18.004	CARNEIRO-RAMOS, M. S.	4.013, 4.016, 8.018
CAETANO, B. G.	7.008	CARRASCOZA, L. S.	11.014, 25.004
CAETANO, C.	3.008	CARREIRA, A. C. O.	3.003
CAETANO, G. F.....	23.017	CARRETTIERO, D. C.	3.004
CAIO-SILVA, W.....	8.018	CARVALHO, B. G.	16.007
CAIXETA, E. S.	7.028	CARVALHO, C. P. F.....	6.005
CAL, B. B. F.	19.012	CARVALHO, C. V. A. L.	25.009
CALABRESE, K. S.....	17.012	CARVALHO, D. P.	6.008
CALAZA, K. C.	10.036	CARVALHO, G.	18.006
CALCAGNOTTO, M. E.	10.029	CARVALHO, H. F.	13.017, 13.027
CALDER, P. C.	21.005	CARVALHO, K. C.	10.032
CALSTRON, P. F.	7.028	CARVALHO, L. R.	3.008
CAMARGO, A. A.	11.018	CARVALHO, M. G.	7.024
CAMARGO, A. C. L.	7.021, 7.035, 16.012	CARVALHO, M. V.	10.023
CAMARGO, I. X.	23.016, 23.017	CARVALHO, R. B. F.	18.013
CAMARGO, L.	22.014	CARVALHO, R. F.	1.002, 7.045, 16.012, 22.019
CAMARGO, L. N.	4.003, 9.009, 9.011, 9.012, 9.013	CARVALHO, S. C.	4.029, 10.026, 11.020, 21.009
CAMARGO, M. P.	6.017	CARVALHO, V. M. S.	17.002
CAMASSOLA, M.	7.030	CASARIL, A. M.	18.001
CAMPAGNOL, D.	3.006	CASCABULHO, C. M.	21.008
CAMPEIRO, J. D.	17.008	CASTELLI, J. Z.	7.009
CAMPELO, P. M. S.	19.022	CASTELO-BRANCO, R. C.	8.002
CAMPOS, A. C. P.	10.005, 10.010, 20.004	CASTELUCCI, B. G.	23.020
CAMPOS, E. C.	9.009, 9.012, 9.013	CASTELUCCI, P.	5.001
CAMPOS, J. M.	7.016	CASTRO, B. F. M.	24.014, 24.018
CAMPOS, P. S.	22.032	CASTRO, H. T.	19.022
CANATELI, C.	10.014	CASTRO, R. N.	7.015, 7.044, 19.010
CANDIDO, D. M.	19.021	CASTRO, S. L.	17.010
CANDIDO, L. S.	9.006		
CANDREVA, T.	7.050, 21.005		

FeSBE Annual Meeting 2019

CASTRO, T. F.	7.023, 7.026, 8.009,	COLOMBELLI, K. T.	7.021, 7.035, 16.012
.....	9.003, 9.005, 9.006,	COLQUHOUN, A.	22.021
.....	9.007, 19.003	CONCEIÇÃO, T. Q. S.	10.039
CASTRO, V. L.	19.027	CONSONNI, S. R.	7.050, 21.005
CASTRUCCI, A. M. L.	24.008	CONSTANTINO, D. B.	3.005
CAVALHEIRO, V. L.	19.004	CONSTANTINO, F. B.	7.035, 16.012
CAVALINI, T. I.	4.012	CONTE-JUNIOR, C. A.	11.011
CAVALLINI, T. I.	19.017	CONTRICIANI, R. E.	23.020
CÁRNIO, E. C.	4.017	CORAT, M A F.	13.024
CÂMARA, N. O. S.	16.013	CORDEIRO, A.	7.002, 7.008
CÂNDIDO, D. M.	20.015	CORDEIRO, A. M. T.	10.001
CÂNDIDO, L. S.	9.003, 9.005	CORDEIRO, B. O.	7.004
CEDDIA, R. B.	11.011	CORRALES, P.	6.003
CERAVOLO, G. S.	19.008	CORREA, C. L.	10.012
CERCHIARO, G.	22.027	CORREA, R. P.	25.011
CERQUEIRA, A.	23.005	CORREDOR, V. H.	24.001
CESAR, M. C. M.	22.002	CORREIA, B. R. O.	7.005
CHACUR, M.	20.021	CORREIA, F. F.	10.011, 10.019
CHACUR, M.	20.019	CORREIA, I. S.	21.004
CHAGAS, M. A.	7.047	CORREIA, J. T.	7.040
CHAGAS, T. A. B.	13.014	CORREIA, L. A.	7.014, 7.046, 8.003
CHAGAS, V. T.	10.042	CORREIA, M. C.	4.005
CHAMOLI, M.	10.009	CORREIA-SILVA, R. D.	20.006, 20.012, 20.013
CHANG B. S. W.	24.003
CHARRUEAU, C.	24.002	CORRÊA, F. M. A.	10.038
CHAVES, D. S. A.	19.002, 19.016	CORRÊA, L. B. N. S.	7.047
CHAVES, J. O.	6.011	CORRÊA, M. P.	20.008, 20.012
CHIAROTTI, G. B.	23.013	CORRÊA, T. L.	17.013
CHIAROTTO, G. B.	10.026	CORTES, A. L.	8.004
CHINTA, S.	10.009	CORTES, M. I. T.	24.009
CHIPOLINE, I. C.	22.015	COSENZA, M.	10.023
CHIRICO, R. N.	9.005, 9.006	COSTA FILHO, J.	16.002
CHRISTOFFOLETE, M.A.	7.011	COSTA, A.	10.031
CHUDZINSKI-TAVASSI, A. M.	13.007, 22.014	COSTA, A. V.	5.002
CID, Y. P.	19.002	COSTA, C. A.	19.018, 22.003
CIENA, A. P.	11.017	COSTA, CFP.	25.006
CINEL, V. D. P.	16.007	COSTA, E. D.	4.009
CIOATO, M. J. G.	3.006	COSTA, F. R.	21.002
CIRILO, M. A. S.	8.012	COSTA, F. V.	23.011
COELHO, C. F. F.	7.049, 10.042	COSTA, G. C.	17.004
COELHO, L. C. B. B.	19.009	COSTA, G. J. L.	24.007, 24.015
COELHO, P. M. P.	16.011	COSTA, G. R. M.	22.015
COGO, S. C.	13.006	COSTA, J. C. B.	7.006
COIMBRA, N. C.	20.022	COSTA, L. L.	11.019
COIMBRA, T. M.	7.001	COSTA, M. C.	7.017, 7.018, 7.019,
COLARES, T. G.	10.016	8.008
COLLETA, S. J.	6.004	COSTA, M. F.	24.016
COLLINO, F.	23.019	COSTA, N. S.	7.016

FeSBE Annual Meeting 2019

COSTA, R. M. B.	22.031	DANTAS, F. J. S.	19.012
COSTA, S. S.	9.002, 9.004, 17.007,	DAVEL, A P.....	4.022
.....	24.013	DAVEL, A. P.....	4.020, 4.024, 4.027
COSTA, T. C. L.	7.048, 7.049, 10.041,	DE ALMEIDA, D. C.....	16.013
.....	11.019	DE CAMPOS, P. S.....	22.033
COSTA, T.F.	11.012	DE FRAGA, L. S.	10.020
COSTAA, T. S. F.	6.008	DE JESUS SOUZA, M.	4.026
COTRIN, J. C.	4.002	DE LA TORRE, L. G.	16.007
COTTA, O. A. L.	24.018	DE MACEDO, C. R.	2.007
COTTA-DE-ALMEIDA, V.....	23.024	DE MATOS, I. M.	19.006
COUTINHO, R.....	22.016	DE MORAES SOBRINO PORTO, L.C.	4.001
COUTO, N. F.	7.043	DE OLIVEIRA, R.....	20.022
COVRE, J. L.....	17.002	DE SANTA INEZ, D. C.	6.012
CÔRTEZ, A. L.	8.010	DE SOUZA, D. B.	2.007
CRESTANI, C. C.	10.038	DE SOUZA, D. M.	7.032
CRISOL, B.	20.002	DE VASCONCELOS, M. H. A..	7.032
CRISÓSTOMO, T. T. A.	8.016	DE, A. S.	21.002
CRISTANTE, A. F.	10.011	DEBBAS, V.	10.041
CRUZ, B. O.	7.016	DECHANDT, C. R. P.	11.007
CRUZ, D. M.	23.023	DEKKER, R. F.	19.013, 22.001, 22.017
CRUZ, L. O.	19.012	DELBIN, M. A.	4.018
CRUZ, M. M.	13.001, 13.010	DELELLA, F. K.	22.035
CRUZ, R. J.	3.008	DELFINO, H. B. P.	6.002
CUNHA, A. V.	25.007	DELGADO, N. T. B.	4.007, 4.010
CUNHA, F. F. M.	22.003, 22.004, 22.029	DENTZ, M. C. V.	7.030, 7.042, 11.015
CUNHA, F. Q.	4.017	DIAS, A.C.A.A	25.013
CUNHA, P. L. O.	18.008, 18.009	DIAS, C. P.	6.015
CUNHA, R. S.	9.001	DIAS, C. S. B.	23.026
CUNHA, T. F.	11.014	DIAS, J.	22.020
CUNHA-JÚNIOR, A. S.....	24.014	DIAS, M. I. C.	25.012
CURI, R.	21.004	DIAS, M. L.	23.005
CURY, S. S.	16.009, 22.019	DIAS, M. T. S.	7.043
CURY-BOAVENTURA, M. F. ..	21.004	DIAS, S. L.	24.016
CUSTÓDIO, I. C.	3.001	DIAS-ROCHA, C. P.....	7.003, 7.006
		DIEL, L. F.	22.030
D		DINIZ GP.....	7.025
DA ROSA, L. A.	10.020	DINIZ, V. L.	21.004
DA SILVA ARAGAO, R.	11.013	DÍEZ-NOGUERA, A.	10.029
DA SILVA, J. S.	4.008	DO VAL-AMORIM, J.....	1.005
DA SILVA, K. R.....	16.013	DOMINGUES, M.	18.001
DAÏROU, H.	17.009	DORAND, V. A. M.....	7.032
DAL-PAI-SILVA, M.	1.002, 7.013, 7.045,	DORIGHELLO, G. G.	21.007
.....	16.009, 22.019	DORNELES, W.	18.010
DALIA, R. A.	21.001, 21.003	DOS SANTOS, A. A.....	10.039
DALL'AGNO, L.	16.002	DOS SANTOS-RODRIGUES, A.	10.035
DALL'AGNO, L.	16.004	DOURADO, L. F. N.	24.005
DALZOTO, L. A. M.	13.023	DOURADO, P. M. M.	11.014
DAMICO, M. V.	20.018	DOURADO, V. C.....	8.015

FeSBE Annual Meeting 2019

DUARTE, L. S.	25.009	FARIAS, T. S. M.	13.001,	14.003
DUARTE, T.	17.008		
DUBOIS, M. J.....	7.038	FARSURA, A. F.	25.009	
DURAN, B. O. S.	1.002, 7.013, 7.045	FASSARELLA, L. B.	7.010	
DUTRA, M. L. V.	7.034	FAVARO, D. I. T.....	1.001	
DUTRA, R. C.	20.014, 23.011	FAVORITO, L. A.....	2.005	
D`OLIVEIRA, A. B.	7.032	FEDDERN, C.	18.012	
E				
ECHEVARRIA, Á.	19.022	FEITOSA, P. W. G.	18.011	
ELIFIO-ESPOSITO, S.....	16.003	FELIPETTI, F. A.	23.011	
ELIFIO-ESPOSITO, S.	13.006	FELIPPE, R. M.	10.040	
EMERENCIANO, A. K.	1.001	FELISBINO, S. L.	22.036	
EMERICK, A. S.	25.009	FELIX, O. M. W. O.	16.013	
ENGLER, A. J.	22.033	FELIZATTI, A. L.	20.009	
EPIFANIO, N. M. M.	19.016	FELONATO, M.	11.003, 21.001	
ESCOBAR, A. G.	19.017	FERNANDES, J. M. P.	17.012	
ESCRIOU, V.	24.002	FERNANDES, M. P.	11.016, 19.011	
ESPINDOLA, F. S.	17.001	FERNANDES, M. S. D. S.	11.001	
ESPOSITO, S. E.	19.004, 19.022	FERNANDES, P.	6.006	
ESQUISATTO, M. A. M.	11.003, 11.004, 13.002,	FERNANDES, P. R.	18.012	
.....	13.011, 15.003, 15.004,	FERNANDES, T.	11.011	
.....	20.009, 23.002	FERNANDES, T. S.	14.002	
ESTECA, M. V.	13.013, 13.021	FERNANDES-BRAGA, W.	7.043	
EUGÊNIO, A. N.	13.002	FERNANDES-SANTOS, C.	2.001, 7.051, 25.008	
EVANGELISTA, F. S.	7.014, 7.046, 8.003	FERNANDEZ, G. J.	16.009, 22.019	
EVANGELISTA, L. S. M.	16.013	FERRARAZ, D. C.	23.010	
EVANGELISTA, S. R.	10.008	FERRARI, G. D.	11.007	
F				
FABRES, R. B.	10.020	FERRARI, M. F. R.	10.024	
FABRÍCIO, V.	11.008	FERRARINI, E. G.	20.014	
FACUNDO, H. D. T. F.	18.008, 18.009	FERRARINI, S. R.	20.022	
FAÇANHA, A. R.	12.001	FERRAZ, C.	19.021, 20.015	
FALDONI, F. L. C.	22.018	FERRAZ, L. S.	19.018	
FARAH, R.	3.009	FERRAZ, M. S. A.	4.004	
FARAH, V.	7.014, 8.003	FERREIRA, A. C. F.	6.008	
FARAH, V. M. A.	7.031	FERREIRA, A. V.	14.001	
FARIA, A. N.	23.006	FERREIRA, C.F.	11.012	
FARIA, C. C.	6.008, 6.016, 11.012	FERREIRA, D. J. S.	11.001, 11.002	
FARIA, D. P.	14.007	FERREIRA, J. S.	4.029, 11.020	
FARIA, R. X.	19.014	FERREIRA, M. A. R.	8.007	
FARIA, S. C.	1.003	FERREIRA, N. F.	7.022	
FARIA, V. S.	11.008, 11.009, 11.010	FERREIRA, N. L.	20.019	
FARIA, R. X.	20.017	FERREIRA, P. M. P.	18.013, 19.001	
FARIAS, J. S.	8.014, 8.017	FERREIRA, S. F.	19.007	
.....		FERREIRA, T. H.	14.004	
FARIAS, T. M.	13.010	FERREIRA, V. F.	22.005, 22.012, 22.015	
			
		FIALHO, S. L.	24.014,	24.018
			
		FIGUEIREDO, D. P.	10.036	

FeSBE Annual Meeting 2019

FIGUEIREDO, I. D.	7.017, 7.018, 7.019	FRANCO, L. S.	4.029, 10.026, 11.020,
FIGUEIREDO, L. S.	6.010, 6.011	19.026, 21.009
.....		FRANCO, M. C. P.	19.008
FILHO, A. P. S.	16.013	FRANCO, R. R.	17.001
FILHO, D. D. M.	11.020	FRANÇA, D. R.	15.002
FILHO, D. M. P.	7.022	FRANÇA, L. M.	7.048, 7.049, 10.041,
FILHO, G. H. L.	7.048	11.019
FILHO, G. J. L.	15.004	FRANÇA, T. F. A.	10.018
FILHO, J. C.	16.004	FRANSCESCON, F.	10.002, 18.002
FILHO, J. S. O.	14.005	FRANTZ, E. D. C.	11.011
FILHO, M. A. S.	11.019	FRANZ-MONTAN, M.B.L.	12.005
FILHO, P. P.	19.021	FRAUZ, K.	16.008
FILHO, P. T. N.	14.005	FREESE, L.	18.012
FIORETTO, M. N.	7.035, 16.012	FREIRE, K. A.	4.023
FIORINO, P.	7.014, 7.031, 7.046,	FREIRE, M. A. M.	10.004
.....	8.003	FREIRE, P. P.	16.009, 22.019
FISK, H.	21.005	FREITAS, A. C.	8.014
FLISTER, K. F. T.	10.041	FREITAS, B. A.	9.010
FLORENZIANO, R. F. M.	13.011	FREITAS, I. N.	6.010
FOGAÇA, F.	4.016	FREITAS, J. J.	3.005
FOGUEL, D.	10.012	FREITAS, R. C.	4.011
FONOFF, E. T.	10.005	FRONY, A. C.	4.026
FONSECA, A. C. C.	22.009, 22.012, 22.013,	FUJII, L. O.	23.013
.....	22.015	FUKUZAKI, S.	9.009
FONSECA, A. R.	18.012	FUMIS, R. R. L.	20.019
FONSECA, A. R. B.	7.021	FUSARO, M. C. G. O.	20.002
FONSECA, F. L. A.	4.006	FUZIWARA, C. S.	6.012
FONSECA, M. C.	10.014	FÜRSTENAU, C. R.	4.005
FONSECA, M. W.	19.010		
FONSECA, R. I. B.	7.025	G	
FONTANA, B. D.	18.007	GADELHA, F. R.	22.004
FONTANA, R. C.	7.030	GAGLIARDI, R. F.	19.012
FONTES, C. C.	6.005	GAIÃO, W. D.	14.002
FONTES, K. N.	6.001	GALLI, T. T.	9.012, 9.013
FONTOURA, M. A.	23.012	GALLO, C. B. M.	2.005
FORCATO, S.	19.005	GAMA, P.	5.002
FOREZI, L. S. M.	22.005	GAMBA, L. E. R.	17.004
FORTES-DIAS, C. L.	20.018	GARAVELLI, G. Y.	3.010
FORTUNATO, R. S.	6.008, 6.016	GARAY, L. L. S.	25.014
FORTUNATO, R.S.	11.012	GARCEZ, T. N. A.	3.006
FRACOTE, A. T.	10.032	GARCIA DE LA SERRANA, D..	1.002
FRAGA, C. A. M.	4.011, 17.011	GARCIA, M. C.	13.020, 17.010
FRAGEL-MADEIRA, L.	13.008, 24.006	GARIBALDI, M.	3.008
FRAGOSO, M. B.	7.031	GASPI, F. G.	13.002
FRAGOSO, V. M. S.	10.040	GASPI, F. O. G.	3.007
FRANCHINI, K. G.	10.014	GATTAZ WF.....	21.006
FRANCISCHETTI, E.	8.016	GATTAZ, W. F.	10.031
		GAVAZZONI, A.	23.003

FeSBE Annual Meeting 2019

GENARI, M. C.	23.002	GONÇALVES, P. G.	19.022
GENELHU, VA.	8.016	GONSALEZ, S. R.	8.010
GERALDELLI, D.	19.013, 22.001, 22.017	GONTIJO, L. S.	17.013
GERARDIN, D. C. C.	19.005, 19.007, 19.008	GONTIJO, R. M. G.	14.001
GERMANO, F. N.	4.021	GONZAGA, N. A.	4.017, 4.019
GEROTTO JUNIOR, L. C.	21.009	GONZALEZ, M. N.	23.023
GIANNOTTI, K. C.	22.014	GONZÁLEZ, M.	13.025
GIESEN, J. A. S.	4.009	GORJÃO, R.	21.004
GIESTAL-DE-ARAUJO, E.	10.017, 10.027, 10.028	GOSMANN, G.	7.012
GIL, C. D.	17.002, 20.006, 20.008,	GOULART, M. T.	10.038
.....	20.012, 20.013	GÓES, R. M.	7.040
GIORGI, R.	20.021	GÓMEZ, M. G. M.	6.003
GIORI, I. G.	11.011	GRAÇA, F. A.	2.002, 16.010
GIRELLI, V.	7.030, 7.042, 11.015	GRAMINHO, J. R.	16.004
GIROL, A. P.	9.002, 17.007	GRAUS-NUNES, F.	7.007
GIROTO, C.	23.003	GRAZZIA, N.	22.004
GIUSBI, C. C. E.	6.016	GREGORIO, B. M.	2.001, 2.007
GIUSTI-PAIVA, A.	20.001	GRIENDLING, K. K.	10.005
GLAUSER, J. S. O.	7.007	GRILLO, B. A. C.	11.017
GOBATTO, C. A.	11.008	GRILLO, D. C. N.	19.002
GODINHO, R. O.	9.010, 12.004, 17.008,	GROSSKLAUS, L. F.	24.016
.....	20.018	GUANDALINI, R. B.	17.007
GODOY, C. M. S. C.	3.008	GUARATTI, M.	8.008
GOES, L. M. S.	22.037	GUEDES, C. C. D. S.	19.009
GOES, R. M.	22.023	GUELLER, G.C.	23.015
GOETTEN, J. O.	19.022	GUERRA, J. F. C.	4.005
GOETTEN, J. O. L. C.	16.003	GUERRA, L. H. A.	6.013, 7.033
GOLBSPAN, S.	18.012	GUERRA, M. C. A.	24.018
GOLDENBERG, R. C. S.	23.005	GUIMARÃES, A. F.	25.001
GOMES, A. B. S. P.	23.002	GUIMARÃES, D. S. P. S. F. ...	7.036
GOMES, B. B.	20.003, 20.005, 20.010	GUIMARÃES, E. T.	19.020, 19.025
GOMES, C. A. B. A.	10.012	GUIMARÃES, J. R.	21.008
GOMES, C. F. R.	7.002	GUIZONI, D. M.	4.024, 4.027
GOMES, D. A.	24.002	GUTIERREZ, L. L. P.	25.001
GOMES, D. S.	8.005	GUTIERREZ, LLP.	25.002
GOMES, G. H.	13.021		
GOMES, H. R.	6.001	H	
GOMES, J. L. P.	22.038	HABIB, D. C. B.	23.024
GOMES-DA-SILVA, N. C.	10.022	HAIIDAMUS, A. B.	10.030
GOMES-LEAL, W.	10.004	HALLAK, J. E. C.	18.014
GONÇALVES, A. B.	15.003, 15.004	HAMAGUCHI, S. S. S.	9.011, 9.012, 9.013
GONÇALVES, A. M.	3.010	HAMANI, C.	10.005
GONÇALVES, C.	20.014	HAMASSAKI, D. E.	24.007, 24.015
GONÇALVES, D. A. P.	7.001	
GONÇALVES, E. C. D.	20.014	HAN, S. W.	16.007
GONÇALVES, F. R. C.	10.019	HANSEL, G.	18.010
GONÇALVES, L. C. F.	23.018	HATANAKA, E.	21.004
GONÇALVES, L. F.	7.051		

FeSBE Annual Meeting 2019

HAUZMAN, E.	24.003, 24.008, 24.012	JAEGER, R. G.	22.034
.....		JAHN, M. P.	7.030, 7.042
HAYASHI, M. A. F.	17.008	JANNUZZI, L. B.	8.011
HAYASHI, M.A.F.....	18.005	JANOUSEK, R. G.	23.012
HECK, L. C.	7.001	JERÔNIMO, R.	20.004
HEIDRICH, N.	18.012	JESUS, L. W. O.	6.017
HELAEHIL, J. V.	23.016, 23.017	JOAQUIM, H.	10.031, 21.006
HELAEHIL, L. V.	23.016, 23.017	JOÃO, J. M. L. G.	9.012, 9.013
HENRIQUE, A. M.	10.021	JORGE, C. O.	20.003, 20.005, 20.010
HENRIQUES-PONS, A.....	23.025	JOSS-MOORE, L.	7.002
HERCULANO, R. D.	23.006	JOVIANO, W. R.	1.001
HERNANDES, L.	23.003	JR, M. A. F.	12.003
HERNANDES, M. S.	10.005	JR., P. I. S.	4.023, 22.027
HIDALGO, M. P.	3.005	JR., V. X. O.	22.027
HIDALGO, M. P. L.	3.006	JUDICE, W. A. S.	17.005
HIDALGO, M.P.	25.014	JUDICE, W.A.S.	17.006
HIRABARA, S. M.	21.004	JUNHO, C. V. C.	8.018
HIX, S.	4.006	JUNIOR, E. U. T.	7.034
HOLZER, S.	4.006	JUNIOR, H. F. A.	10.037
HONORATO, J.	22.016	JUNIOR, J. A. S.	6.009, 6.011, 14.002
HORITA, S. I. M.	10.040, 21.008, 23.025	JUNIOR, J. C. T.	22.022
HORTA, J.G.A.	9.007	JUNIOR, L. A. J.	7.021
HORTA, N. A. C.	6.006	JUNIOR, V. A. P.	3.010, 7.028
HUANG, B.	23.016, 23.017, 23.018	JUNIOR, W. A. V.	19.021, 20.015
HUMMEL, L. H.	15.002	JUNIOR, W. J. S.	14.005
		JUNIOR, W. R.	6.001
I		JUNQUEIRA, M. S.	14.007
IACK, R. L.	8.016	JURBERG, A. D.	23.024
IAR, C. S. M.	25.003	JUSTINO, A. B.	17.001, 20.007
ICIMOTO, M. Y.	20.006, 22.028	JUSTULIN JR, L. A.....	22.035, 22.036
IDIART, M.	3.005	JUSTULIN, L. A.....	16.012
IDIART, M. A. P.	25.014	JUSTULIN, L. A.....	7.035
IMPÉRIO, G. E.	6.001	JÚNIOR, E. D.	7.031
INÁCIO, M. D.	7.017, 7.018, 7.019,	JÚNIOR, J. C. T.	22.025
.....	7.024	JÚNIOR, J. D.	7.025
INFANTE, N. A.	11.010	JÚNIOR, L. C. G.	4.029, 11.020
INGO RIEDERER	23.023	JÚNIOR, M. S.	23.017
IORIO, J. F. D.	17.006	JÚNIOR, N. F.	19.004
ISER-BEM, P. N.	21.004	JÚNIOR, P. A. M.	7.023, 8.009
IVANOV, G. Z.	16.001	JÚNIOR, V. A. P.	23.014
IYOMASA, M. M.	9.004	KAGA, A. K.	7.024
IYOMASA-PILON, M. M.	17.007, 18.014	KERTSZ, R.	3.008
		KETTELHULT, I. C.	7.001
J		KETTELHUT, I. C.	6.002
JABLONKA, W.	1.005	KIHARA, A. H.	10.011, 10.015, 10.019
JACO, V. A.	13.010	KIKUCHI, D. S.	10.005
JACOB, C. S.	11.017	KIMURA, E. T.	6.012
JACOB, V. V.	19.021	KISS, A. C. I.	19.005

FeSBE Annual Meeting 2019

KOGA, B. A. A.	3.003	LELLIS-SANTOS, C.	25.005
KOIKE, T. E.	2.003, 2.004	LELLIS-SANTOS, C.	25.003
KOMONI, G.	7.046, 8.003	LEME, L. B. P.	19.023
KOPCZYNSKI, A.	18.010	LEMOS, M. D. T. B.	4.015, 7.027
KOWALEWSKI, L. S.	11.015	LEMOS, V. S.	4.009, 4.025
KOZIMA, E. T.	19.003	LEONARDI, B.	7.012
KÖNIG, S.	22.024	LEONI, G. H.	10.003
KRAUSE, M.	11.015	LEVADA-PIRES, A. C.	21.004
KREPISCHI, A. C. V.	10.014	LICE, I.	17.002, 20.006, 20.012, 20.013
KRIEGER, J. E.	4.004	LICHTENFELS, A. J. F. C.	19.020
KRUGER, W. M. A. V.	14.006	LIMA JUNIOR, N.C.	11.012
KRÜGER, J. V.	22.007	LIMA, A. C. S.	15.002
KUCHARSKI, L. C.	7.030, 7.042	LIMA, A. H. L.3.....	17.012
KUROKI, M. A.	10.005, 10.010	LIMA, Á. C.	17.008
KÜHL, C. M.	21.005	LIMA, C. S.	22.022
KWASNIEWSKI, F. H.	19.021	LIMA, F. A. S.	4.015, 7.027
KWASNIEWSKI, F.H.	20.015	LIMA, G. F.	4.028
L			
LABEIT, S.	16.010	LIMA, G. L.	20.004
LACERDA, A. L. T.	18.006	LIMA, G. S.	16.010
LACERDA, E.M.C.B.	24.009	LIMA, I. S. P.	18.008, 18.009, 18.011
LACERDA, M. G.	6.014	LIMA, J. C.	2.001, 2.007
LADEWIG, R.	14.006	LIMA, L. A. R.	18.008, 18.009, 18.011
LAGE, C.....	14.006	LIMA, L. M.	17.004
LAGE, N. A.	24.017	LIMA, M. E.	8.014
LAGRANHA, C. J.....	7.027	LIMA, N. K. S.	8.012, 8.014, 8.017
LAGRANHA, C. J.	4.015, 11.001, 11.002	LIMA, R.	11.003, 11.004, 21.002
LAM, W. L.	16.012	LIMA, R. R.	10.004
LAMERS, M. L.	13.016, 22.030	LIMA, S. C.	17.008
LAMERS, M.L.	22.033	LIMA, T. F. O.	7.017, 7.018, 7.019, 7.024, 8.008
LANZETTI, M.	4.001	LIMA, T. R. L. A.	11.016, 19.011
LARA, L. S.	8.005	LIMA-GONÇALVES, M. L.	8.016
LARA, L.S.....	8.004	LINDOSO, R. S.	8.004, 23.019
LARA. L. S.....	8.007	LINTOMEN, L.	20.016
LASSENÈ, B.	10.005	LIPPI, B. K.	25.003
LAURENO, N. K.	13.016	LISTIK, E.	22.008
LAURINDO, F. R. M.	10.041	LOBATO, T. B.	21.004
LAUTHERBACH, N. E. S.	7.001	LOBO, D. J. A.	19.020
LAVORATOB, S. N.	19.001	LOMBELLO, C.	13.012
LEANDRO, C. V. G.	11.016	LOMBELLO, C. B.	13.019, 17.003, 23.010
LEICK, E. A.	4.003, 9.009, 9.011, 9.012, 9.013	LOMBELLO, R.	13.012
LEITÃO, D. P. S.	13.011	LONG, S. M.	23.010
LEITÃO, M. V. S. F. S.	14.005	LOPES, B. B.	15.001, 15.002
LEITE, A.C.R.....	19.011	LOPES, E. C.	20.014
LEITE, F. G.	16.008	LOPES, G. P. D. F.	22.016
LELLIS-SANTOS, C.....	25.007	LOPES, I. M. S. S.	14.002, 14.005
		LOPES, J. A.	23.019

FeSBE Annual Meeting 2019

LOPES, L. O.	16.009	MANI, F.	7.035
LOPES, L. S.	18.013	MANOEL, C.A.	22.026
LOPES, M. J. P.	18.008, 18.009, 18.011	MANOEL, R.	21.004
LOPES, R. L.	19.022	MARCENA, I. R.	25.010
LOPES, R. M.	19.018	MARCHON, R. G.	2.007
LOPES, R. O.	4.028	MARCON, J. L.	1.006
LOUREIRO, T. M. G.	24.011	MARCONDES, M. C. C. G.	4.018
LOURENÇO, C. B.	23.016, 23.017	MARCONDES, M. F.	13.003, 13.005, 13.014
LOURENÇO, D. A.	18.001	MARCONDES, R. R.	10.032
LOURENÇO, L. O.	9.008	MARECO, E. A.	1.002, 7.013, 7.045
LOWE, J.	7.039	MARETTE, A.	7.038
LOWE, J.	12.002	MARI, J. J.	18.005
LUCHESSI, A. D.	13.013, 13.021	MARIANO, J. D.	10.032
LUCIANO, L. M.	15.002	MARIANO, S. S.	13.002, 15.001, 15.002,
LUZES, R.	8.016	23.021
		MARIANO, S.S.	22.026
M		MARINHO, A. M. R.2	17.012
M.ESQUISSATTO, M. A.	23.013	MARINHO, C. R.	19.011
MACEDO, A. L.	22.006, 22.009, 22.010	MARINHO, P. S. B.2	17.012
MACEDO, L. R.	19.006	MARINHO, R. F. N.	22.006, 22.009
MACHADO, D. S.	25.005	MARINS, L. F. F.	16.002, 16.004
MACHADO, F. A.	5.001	MARION, J. C.	10.002, 18.002
MACHADO, F. C.	22.004	MARÓSTICA, E.	17.013
MACHADO, F.H.M.	22.028	MARQUES, A. M.	22.013
MACHADO, J. A. M. M.	6.014	MARQUES, E. B.	4.028
MACHADO, K. C.	19.001	MARQUES, F. L. N.	14.007
MACHADO, L. A. F.	11.006	MARQUES, G.	18.006
MACHADO, M. F. M.	13.003, 13.004, 13.014,	MARQUES, M. B.	8.008
.....	13.023, 16.006	MARQUES, M. J.	4.029, 21.009
MACHADO, M.F.M.	13.005	MARQUES, M. S.	25.004
MACHADO, O.	21.004	MARQUES, N. F.	22.007
MACHADO, T. Q.	22.009	MARQUES-PORTO, R.	22.014
MACHADO-LIMA, A.	23.015	MARQUI, M. B.	25.009
MACIEL, G. A. R.	10.032	MARRETTO, M. A.	21.002
MADEIRA, L. F.	10.033	MARTINEZ, C. S.	4.014
MADEIROS, P. L.	14.002	MARTINEZ, D.S.T.	19.027
MAGALHÃES, C. F.	10.033, 24.006	MARTINEZ, R.C.R.	10.010
MAGDALENA, I. J.	20.020	MARTINEZ, S.	22.016
MAGIORE, I. C.	7.013, 7.045	MARTINS, A. M. C.	4.023
MAGLIANO, D. C.	7.016, 11.011	MARTINS, C.	25.002
MAHAMOUD, R.	3.001	MARTINS, C. S.	25.001
MAIA, A. R. B.	2.007	MARTINS, D. S.	3.007
MAIA, J.	10.009	MARTINS, F. F.	7.005
MAIA, R. C.	17.011, 22.016	MARTINS, I. C.	4.005
MALERBA, H.	10.006	MARTINS, K. O.	19.013, 22.001, 22.017
MALERBA, H. N.	10.007	MARTINS, M. A.	4.003, 9.009, 9.011,
MALNIC, G.	8.002	9.012
MAMEDE, M.	14.001	MARTINS, M. E.	9.013

FeSBE Annual Meeting 2019

MARTINS, M. R.	20.020	MEURER, Y.	17.008
MARTINS, N. V.	21.008	MEZZOMO, N. J.	18.007
MASCHIO, J.	7.030, 7.042	MICHEAU, O.	19.004
MASUDA, L.H.....	23.015	MICHELOTTI, P.	10.002, 18.002
MATEUS, R. S.	22.034	MIGUEL, D. C.	22.004
MATHEUS, M. E.	22.031	MIGUEL, M.	19.019
MATOS, H. R.	7.029	MIGUEL, M.	4.012, 4.014, 6.003,
MATOS, N. A.	7.023, 7.026, 8.009,	19.015, 19.017
.....	9.003, 9.005, 9.006,	MILHM, G.	7.039
.....	19.003	MILTON, F. A.	6.014
MATOS, N.A.	9.007	MIRANDA, C. S.	7.004
MATSUDA, M.	24.007, 24.015	MIRANDA, J. P. N.	7.048
MATSUMOTO, M. A.	3.001	MIRANDA, M. C.	24.002
MATTA, L. P.	11.012	MIRANDA, R. A.	7.008, 7.010
MATTE, B. F.	22.033	MIROTTI, L. C.	20.020
MAZZI, M. V.....	23.002	MIYABARA, E. H.	2.003, 2.004, 16.010
MAZZI, M.V.....	19.026	MIYAKAWA, AA.....	4.004
MEDEIROS, A. M. Z.	19.027	MODEL, J. F. A.	7.030, 7.042, 11.015
MEDEIROS, I. P. M.	1.003	MONÇÃO, C. C. D.	22.035, 22.036
MEDEIROS, T. C.	19.013, 22.001, 22.017	MONDINI, G.....	13.006
MEIRELES, L. R.....	10.037	MONNERAT, J. A. S.	2.001, 2.006
MEIRELLES, L. S.	19.024	MONTAGNOLI, T. L.	4.011, 16.011, 17.004,
MELLO, B. P.	8.004	17.011
MELLO, L. S.	7.022	MONTEIRO, I. M. L. V.	7.007
MELO, B. A. G.	23.022	MONTEIRO, M. L.	4.023
MELO, G. B.	7.048	MONTEIRO, R. Q.	22.024
MELO, K. M.	13.009	MONTEIRO, V. R. S.	6.001
MELO, M. M.	1.005	MONTRESOR, L. B.	24.013
MELO, P. A.	8.004, 8.006, 8.007	MORAES, D.	16.009, 22.019
MELO, T. M.	7.049, 10.041	MORAES, J.A.	4.026
MELO, Y. V.	18.006	MORAES, P. Z.	4.012, 4.014, 19.015
MENCALHA, A. L.	19.012	MORAES, PZ.....	19.019
MENDES, A. B. A.	4.028	MORAES, T. M.	25.009
MENDES, M.	21.004	MORAIS, M. R. P. T.	6.015
MENDES, M. F.	15.003, 21.003	MORALES, C. R.	17.013
MENDEZ-OTERO, R.	16.011	MORALES-GAMBA, R. D.	1.006
MENDONÇA, F. A. S.	13.002, 13.009,13.011,	MORÃO, P. P.	23.026
.....	23.013, 23.016,23.017,	MORCILLO, L. S. L.	8.001, 8.010
.....	23.018	MOREIRA, D. L.	22.006, 22.009,22.010,
MENDONÇA, K. C. P.	4.024	22.013
MENDONÇA, L. S.	6.014	MOREIRA, T. J.	17.013
MENECHINO, B. S. B.	13.024	MOREIRA, V.....	13.007
MENEGASSO, J. F.	23.011	MOREIRA, V.	20.006, 20.013
MENESES, D. D.	10.013	MOREIRA, V. R.	10.041
MENEZES, R. C. A.	7.026	MORENA, B. C.	10.011, 10.019
MENTI, L. D.	22.032	MORENO, A. C. R.	11.005
MERMELSTEIN, C.	22.024	MORENO, A. H.	9.002, 17.007, 17.009
MESQUITA, F. M. D.	19.024	MORENO, C. S.	16.012

FeSBE Annual Meeting 2019

MORETTI, T. A.	21.002	NEVES, L. M. G.	13.011
MORGAN, H. J. N.	6.002	NEVES, R. P.	19.009
MORISCOT A S.....	23.007	NEVES, T. V.	20.007
MORISCOT, A. S.	2.002, 16.010	NOBRE, M. E. P.	18.008, 18.009, 18.011
MORTARA, R. A.	22.002	NOBREGA, A. C. L.	11.011
MOSELE, F. C.	22.035, 22.036	NOGUEIRA, J. R.	23.021
MOTTA, B. P.	7.024	NOGUEIRA, R. S.	9.011
MOTTA, J. M.	20.016	NOSSAR, L. F.	7.039, 8.013, 23.019
MOTTA, N. A. V.	4.028	NÓBREGA, R. H.	6.017
MOURA, C. C. P.	7.008, 7.010	NUNES, A. G. P.	25.001
MOURA, K. F.	19.008	NUNES, Á. M.	19.011
MOURA, R. D. S.	18.011	NUNES, G. G.	19.023
MÓVIO, M. I.	10.015	NUNES, T. A.	18.004
MUNHOZ, L. L. S.	23.008, 23.009		
MUZI-FILHO, H.....	8.011	O	
MÜLLER, T. E.	18.007	OCIO, J. A. U.	6.003
MYIAMOTO, J. G.	19.021	ODA, C. M. R.	14.004
		OHLWEILER, R.	7.030, 11.015
N		OHLWEILER, R. V. C.	7.042
NAGATO, A. C.	4.001, 9.001	OLANDA, L. C. N.	19.005
NAGY, B. V.	24.016	OLIANI, S. M.	9.002
NAI, G. A.	11.005	OLIVA, A. H.	3.001
NALESSO, P. R. L.	23.016, 23.018	OLIVEIRA, A. C.	16.010
NAMAN, M. J. V.	24.008	OLIVEIRA, A. C. D.	2.002
NANI, J.V.....	18.005	OLIVEIRA, A. C. R.	10.017
NAPOLEÃO, T. H.	14.002, 19.009	OLIVEIRA, A. G.	8.017
NASCIMENTO, A. A.	10.036	OLIVEIRA, A. L. R.	23.013
NASCIMENTO, C.	6.008	OLIVEIRA, A. P. S. D.	19.009
NASCIMENTO, J. H. M.	19.024	OLIVEIRA, A. R. L.	10.003
NASCIMENTO, M. G. O. F. ...	23.008, 23.009	OLIVEIRA, A. T.	4.021
NASCIMENTO, M. T.	20.016	OLIVEIRA, C. A.	21.001, 21.003, 23.013
NASCIMENTO, T. G. F. C.	19.004	OLIVEIRA, C. C.	10.010
NASCIMENTO-SALES, M.....	7.011	OLIVEIRA, C. G.	20.021
NAVARRO, C. D. C.	13.026	OLIVEIRA, C. S.	22.027
NAVARRO, D. M. D. A. F.	19.009	OLIVEIRA, D. F.	19.024
NAVARRO, F.F.....	22.018	OLIVEIRA, D. P. L.	11.013
NAVEGANTES, L. C. C.	7.001	OLIVEIRA, D. S.	25.004
NAVEGANTES, L.C.C.....	6.002	OLIVEIRA, D.A.S.....	7.004
NAVIA-PELAEZ, J. M.	7.043	OLIVEIRA, E. B.	17.008
NDIAYE, N. C. G.	22.016	OLIVEIRA, E. M.	11.011
NEDEL, C. B.....	22.007	OLIVEIRA, F. S. R.	20.015
NEGREIROS, N. G. S.	25.003	OLIVEIRA, G.	16.009
NEGRIN, A. C.	7.040	OLIVEIRA, G. A.	19.013, 22.001, 22.017
NEIVA, C.M.....	7.022	OLIVEIRA, G. M.	10.040
NETA, M. S. B. D. F.	18.008, 18.009, 18.011	OLIVEIRA, H. C. F.	7.009, 21.007
NETO, J. C. S. C.	9.011	OLIVEIRA, I. M.	19.018
NETO, J. P.	11.017	OLIVEIRA, J. F.	10.014
NEVES, F. A. R.	6.014	OLIVEIRA, J. S.	16.009

FeSBE Annual Meeting 2019

OLIVEIRA, K. M.	6.009, 6.010	PAIVA, P. M. G.....	19.009
OLIVEIRA, L.	7.007	PAIXAO, A. D.	8.012
OLIVEIRA, L. M.	18.004	PAIXÃO, A. D.	8.014, 8.017
OLIVEIRA, L. R.	10.008	PAIXÃO, C.	7.031
OLIVEIRA, L. S.	7.008	PANICO, K.	8.018
OLIVEIRA, M. A. B.	3.005, 10.029, 25.014	PAOLILLO, F.R.....	22.026
OLIVEIRA, M. A. G. S.	8.009	PASCHOA, A. F.	20.004
OLIVEIRA, M. Â. D. G. S.	7.023	PASCHOA, A. F. N.	10.005
OLIVEIRA, M. C.	24.009	PASCHOALIN, T.	22.002
OLIVEIRA, M. F.	19.013, 22.001, 22.017	PASCHON, V.	10.011, 10.019
OLIVEIRA, N. R.	13.024	PASCOAL, A. C. R. F	22.022, 22.025
OLIVEIRA, R. F.	19.022	PASCOAL, A. C. R. F.	22.011
OLIVEIRA, S. M.	20.007	PASCOAL, V. D. B.	22.022, 22.025
OLIVEIRA, T. A.	24.016	PASCUTTI, P. G.	14.006
OLIVEIRA, T. O.	11.005	PASSOS A. S. C.....	7.049
OLIVEIRA, V. C.	17.005	PASSOS, A. S. C.	11.019
OLIVEIRA, V. G.	18.010	PASSOS, M. E. P.	21.004
OLIVEIRA, V. M. S.	19.025	PAULA, A. L. M.	17.005
OLIVEIRA, V.X. JR.	4.023	PAULA, L. C.	9.005, 9.006
OLIVEIRA-FUSARO, M. C. G ..	20.010	PAULA, T. G.	7.013, 7.045
OLIVEIRA-FUSARO, M.C.G	20.003, 20.005	PAVAN, J.	13.011
OLIVO, M. L. V.	9.011, 9.012, 9.013	PAVANELLO, R.	24.016
ONUCHIC, L. F.....	8.015	PAVÃO, M.S.G.....	20.016
ORTIGA-CARVALHO, T. M.....	6.001	PAZ, A. H.	10.020
ORZARI, L. E.	21.001, 21.003	PAZOS-MOURA, C. C.	7.003, 7.006
OSORIO, R. P.	19.002	PAZUTTI, L.	22.032
OTSUKA, F. A. M.	7.029	PEÇANHA, F. M.	4.012, 4.014, 6.003, 19.015, 19.017
OUVERNEY, G.	22.012	PEÇANHA, FM	19.019
P		PEDERSEN, M.	11.003, 11.004, 21.002
PACHECO, M.	7.050	PEDREIRA, J. G. B.	4.008
PACHÊCO, L. S.	11.016	PEDROCHI, F.	23.003
PACINI, E. S. A.	9.010, 12.004, 20.018	PEDRON, C. N.	4.023
PACÍFICO, C. M.	25.013	PEDROZA, A. A. D. S.	11.001, 11.002
PAES, A. M. A.	7.048, 7.049	PEDROZA, A. A. S.	4.015
PAES, A.M.A.....	10.041	PEIXOTO, M. S.	6.008, 6.016
PAES, A.M.A.....	10.042	PEIXOTO, P.	4.025
PAES-DE-CARVALHO, R	10.035	PEJON, T. M. M.	11.008, 11.009, 11.010
PAES-DE-CARVALHO, R.	10.022, 10.030	PELEGRINO, M. T.	8.018
PAFFARO JR. V.A.....	9.008	PENAFORTE, D. C.	25.012
PAFFARO, A. M. A.	3.010, 7.028	PEREIRA CAC.....	21.006
PAFFARO, V. A.	7.041	PEREIRA, A.	10.004
PAGANO, R. L.	10.005, 10.010	PEREIRA, A. A. R.	18.003
PAGANO, ROSANA L.	20.004	PEREIRA, A. C. G.	21.004
PAIVA, A. C. S.	22.039	PEREIRA, A. D.	2.001, 2.006, 7.016
PAIVA, C.	3.008	PEREIRA, A. R.	11.001, 11.002, 11.016
PAIVA, M. R. B.	24.005, 24.014, 24.017,	PEREIRA, C. O.	13.007, 22.014
.....	24.018	PEREIRA, C. S. M.	13.020

FeSBE Annual Meeting 2019

PEREIRA, G. J. S.	16.001	PIRES, D. C.	19.022, 19.023
PEREIRA, H. M. G.	20.020	PIRES, L. B.	10.034
PEREIRA, J. H. C.	19.026	PITHON-CURI, T. C.	21.004
PEREIRA, J. S.	20.017	PIVATTO, M.	20.007
PEREIRA, L. A.	13.008	PLACONE, J. K.	22.033
PEREIRA, L. C.	4.019	POLETINI, M. O.	6.006
PEREIRA, L. F.	19.022, 19.023	POLETTI, S.	13.002
PEREIRA, LAVD.....	25.006	POMA, S. O.	21.004
PEREIRA, M. D.	7.015	PONS, A. H.....	21.008
PEREIRA, M. E.	10.002	PONS, A. H.	21.008
PEREIRA, M. J. D.	19.008	PONTES, B. A. C. C.	22.015
PEREIRA, M. T. M.	22.011, 22.022, 22.025	PORAWSKI, M.	25.001
PEREIRA, M.R.....	10.030	PORCIONATTO, M. A.....	23.022
PEREIRA, N. C. A.	4.028	PORTA, L. C.	17.008
PEREIRA, N. S.	19.011	PORTELA, L. M. F.	7.035, 16.012
PEREIRA, R. O.	7.014, 7.046, 8.003	PORTELA, L. V.....	18.010
PEREIRA, S. R. F.	10.041	PORTES, P.	23.003
PEREIRA-ACACIO, A.....	8.011	PORTO, C. S.	17.013
PEREZ, P. L. V.	3.002	PORTUGAL, R. V.	10.014
PERRUT, D. G. P.	4.021	POSSEBON, L.	9.002, 9.004, 17.007,
PERUCCI, L. O.	9.007	17.009, 24.013
PETROVICH, A. C. Z.	10.026	PRAÇA, F. S. G.	16.005
PÉREZ, C. A.	23.026	PRADO, C. M.	4.003, 9.009, 9.011,
PIAGETTE, J. T.	6.003, 19.017	9.012, 9.013
PICANÇO, J. R.	7.047	PRADO, I. R. S.	13.003
PICOLO, G.	17.008, 22.014	PRADO, P. F. V.	10.014
PIERETTI, J. C.	8.018	PRIETO, M. C.	8.005
PIERUCCI, A. P. T. R.	11.012	PROCESSI, A. M.	13.025
PILON, G.	7.038	PROCOPIO-OLIVEIRA, C. A... 2.007	
PILON, M. M. I.	9.002, 24.013	PROCOPIO-OLIVEIRA, C. A... 2.006	
PIMENTEL, V. E.	19.026, 23.002	PROCÓPIO, I. M.	2.005
PIMENTEL-COELHO, P. M. ...	6.001	PRUDÊNCIO, E. R.	7.015, 7.044
PINA, J. R. S.2.....	17.012	PULZ, R. B.	23.017, 23.018
PINHAL, M. A. S.	22.027		
PINHEIRO JR 19.015		Q	
PINHEIRO JR, JEG..... 19.019		QUARANTINI, L..... 18.006	
PINHEIRO JÚNIOR, J. E. G. ... 4.014		QUEIROZ, E. A. I. F. 19.013, 22.001, 22.017	
PINHEIRO, L. A. 23.005		QUEIROZ, E. O. 10.024	
PINHEIRO, S. C. V. 25.013		QUEIROZ, L. N. 22.006, 22.011, 22.015	
PINNA, R. A. 4.021		QUINTAS, L. E. 8.001	
PINTO B. A. S. 7.049			
PINTO, B. A. S. 7.048, 10.041, 10.042, 11.019		R	
PINTO, L. M. O. 19.024		RABELO, A. A. S. 10.039	
PINTO, N. C. 20.019		RABELO, B. D. 23.011	
PINTO, R. S. 19.011		RABELO, V. W. 22.015	
PINTO-FOCHI, M. E. 7.040		RACHID, T. L. 7.004, 7.005	
PINTON, S. 4.012		RADOS, P. V. 13.016	
		RAMIRO, L. C. 19.006	

FeSBE Annual Meeting 2019

RAMOS, E. S.....	22.026	ROBBS, B. K.	22.006, 22.009,22.011,
RAMOS, R. G. P.....	23.001	22.012, 22.013, 22.015
RANE, A.	10.009	ROCHA NETO, J.C.	14.002
RANGEL, L. D. S.	19.014	ROCHA, B. S.	4.008
RAPOSO, H. F.	7.009	ROCHA, C. D. S.	23.023
RATTES, I. C.	5.002	ROCHA, C. P. D.	7.010
RAZO, U. B.	7.020	ROCHA, D. F. A.	7.023
REAL, C. C.	14.007	ROCHA, D. S.	7.030, 7.042, 11.015
REAME, V.	7.040	ROCHA, G.	18.014
REGALO, S. C. H.	18.014	ROCHA, G. S.	2.001, 2.006
REGINATTO, M. W.	6.001	ROCHA, L. A.	6.009
REID, P.	22.014	ROCHA, L. C.	11.017
REIS, N. G.	7.001	ROCHA, L. M.	19.014
REIS, P. P.	22.019	ROCHA, L. T.	19.022
REIS, R. F.	23.023, 23.024	ROCHA, M. D.	17.011
REIS, T.	13.005, 13.014	ROCHA, R. C.	4.021
REIS, T. G.	3.003	ROCHA, S. K. L. D.	19.009
REIS, T. S.	13.003, 16.006	ROCHA, T. T. S.	11.003
REIS-GOMES, C. F.....	7.003	ROCHA, T.T.S.	11.004
RENOVATO-MARTINS, M.	22.031	RODA, V. M. P.	24.007, 24.015
REPOSSI, M. G.	13.008, 25.012	RODRIGUES, A. L.	13.002
REZENDE, B. G.	9.009	RODRIGUES, A. L. V.	19.022
REZENDE, L.	7.043	RODRIGUES, B.	4.018
REZENDE, L. R.	13.019	RODRIGUES, B. S.	16.003
RÉUS, G. Z.	18.006	RODRIGUES, C. G.	14.002
RIBAS, J.A.S.....	17.013	RODRIGUES, H. G.	21.005
RIBEIRO, A. V.	22.013	RODRIGUES, H. L.	20.003, 20.005, 20.010,
RIBEIRO, B. R.	4.021, 25.008	RODRIGUES, HG.....	7.050
RIBEIRO, F. S.	23.007	RODRIGUES, K. D.	6.014
RIBEIRO, I. C. A.	7.047	RODRIGUES, M. C. S.	25.010
RIBEIRO, L. P.	4.021, 25.008	RODRIGUES, M. D.	4.014, 19.017
RIBEIRO, M. C.	19.013, 22.001, 22.017	RODRIGUES, S.	23.022
RIBEIRO, M. C. S.	24.002	RODRIGUES, T.	17.006, 19.018, 22.003
RIBEIRO, M. O.	7.031	RODRIGUES, T. F. S.	19.026, 23.002
RIBEIRO, N. L.	10.042	RODRIGUES, T. L.	10.020
RIBEIRO, N. L. X.	7.048	RODRIGUEZ, G. A.	3.005
RIBEIRO, R. A.	6.009, 6.010	ROGATTO, S. R.	22.019
RIBEIRO-SILVA, J. C.	4.004	ROLIM, W. R.	13.012
RIEDERER, I.	13.025, 23.024	ROMANELLI, M.A.	8.006
RIET, J. G.	16.002	ROMANO, I	10.023
RIGER, C. J.	7.015, 7.044, 19.002,	RONACHER, M.	4.014
.....	19.010, 19.016	ROPELLE, E. R.	20.002
RIGHETTI, R. F.	4.003, 9.011, 9.012,	ROQUE, I. C.	4.021
.....	9.013	ROSA, L. P. A.	13.020, 17.010
RIGONATI, C. A. M.	5.002	ROSA, M. L. N. M.	18.014
RIGUETTI, R. F.	9.009	ROSEMBERG, D. B.	10.002, 18.002, 18.007
RIZZETTI, D. A.	6.003, 19.017	ROSENBERG, C.	10.014
ROBBS B.K.	22.010	ROSSI, A. C.	3.006, 10.029

FeSBE Annual Meeting 2019

ROSSONI, L. V.	8.015	SANTOS, G.M.T.	13.002
ROUVER, W. N.	4.007, 4.009, 4.010	SANTOS, J. A. A.	19.014
RUBERTI, O. M.	4.018	SANTOS, J. C. C.	19.011
RUFINO, M. B.	4.021, 25.009	SANTOS, J. E. S.	19.015
RUIZ, A.	10.006	SANTOS, J. J.	6.011
		SANTOS, J. M.	13.023
S		SANTOS, J. V. B.	19.002
SA, R. C. R.	13.010	SANTOS, J. W. O.	11.016
SABBAG, I. M.	10.032	SANTOS, K. F.	19.016
SAEZ, G. O.	4.021	SANTOS, K. O.	16.002, 16.004
SAGIORATO, R. N.	7.050	SANTOS, L. A.	13.011
SAHEB, J. L.	8.008	SANTOS, L. C.	21.004
SAITO, K. C.	6.012	SANTOS, L. C. T.	10.010
SAKUGAWA, A. Y. S.	10.024	SANTOS, L. N.	1.001
SALES, D. C.	6.005	SANTOS, M. C.	19.011
SALIMEN, M.	18.010	SANTOS, M. M.	25.003
SALLES, É. S. L.	7.028, 7.041	SANTOS, N. J.	22.035, 22.036
SALLES, S. M. C.	16.001	SANTOS, N. T. H.	22.018
SALOMÃO, R.	16.013	SANTOS, R. A. S.	8.010
SALOMÃO, R. A. S.	7.013, 7.045	SANTOS, R. B.	7.029
SALU, B. R.	9.011	SANTOS, R. F.	25.010
SALVADOR, M. J.	22.025	SANTOS, R. L.	4.007, 4.009, 4.010,
SALVIANO, Í.	19.012	4.025
SAMPAIO, F. J. B.	2.005, 2.007	SANTOS, R. R.	10.012
SAMPAIO, G. S. A.	24.010	SANTOS, R. S.	7.029
SAMPAIO, T. T.	21.002	SANTOS, R. S. N.	4.013, 8.018
SANCHES, J. M.	20.006, 20.011	SANTOS, S. A. A.	7.035, 16.012
SANCHES, P. R. S.	3.006, 10.029	SANTOS, S. M.	4.021, 25.008
SANTAMARIA JR. M.	13.018	SANTOS, S. V.	10.037
SANTAMARIA-JR, M.	23.018	SANTOS, T. C.	11.019
SANTAMARIA-JUNIOR, M. ...	23.016	SANTOS, T. C. C.	10.037
SANTANA, A. C. M.	7.005	SANTOS, T. M.	4.003, 9.009, 9.011,
SANTANA, D. S.	23.002	9.012, 9.013
SANTANA, R. C.	18.006	SANTOS, T. R.	13.004, 13.023
SANTAROSA, P. C.	13.009	SANTOS, V. B.	1.002
SANTIAGO, M. F.	10.034	SANTOS, V. B. S.	8.012
SANTOS, A. L. T.	9.008	SANTOS, V. F. D.	18.008, 18.009
SANTOS, B. J. C.	21.004	SANTOS-CARLOS, B.	17.011
SANTOS, B. R.	21.001, 21.003	SANTOS-PEREIRA, R.	10.035
SANTOS, C. F.	25.009	SANTOS-SILVA, M.A.	4.001
SANTOS, C. H. C.	7.024	SANT`ANNA, T. B. F.	6.014
SANTOS, D. V. V.	24.014, 24.018	SARAIVA, A. L.	17.001
SANTOS, F. W.	4.012, 4.014, 19.015	SARAIVA, AC	25.002
SANTOS, G. B.	10.011	SARAIVA-ROMANHOLO, B. M.	9.009, 9.011, 9.012,
SANTOS, G. M. B.	10.023	9.013
SANTOS, G. M. T.	13.011, 15.002, 23.013,	SARAPIO, E.	11.015
.....	23.021	SARMENTO, G. C.	8.011
SANTOS, G. P.	13.021	SARNI, R. O. S.	4.006

FeSBE Annual Meeting 2019

SASSO, G. R. S.	20.011	SILVA, G. H.	19.027
SATO, F.	23.003	SILVA, G. I. P.	4.029
SAVEGNAGO, L.	18.001	SILVA, G. M. F.	3.002
SAVINO, W.	13.025, 23.023, 23.024	SILVA, H. C. G.	17.001
SÁ, E. L.	19.023	SILVA, H. M.	8.010
SÁ, R. D. C. C.	13.001, 14.003	SILVA, H. P.	10.033
SÁ, V. A.	25.007	SILVA, I. A.	18.012
SÁBIO, R. M.	23.008, 23.009, 23.021	SILVA, I. R.	23.015
SCARAMELO, C. . B. V.	4.028	SILVA, Í. A.	4.021
SCARPELLI, T. P.	7.040	SILVA, J. A. M. G.	20.020, 22.031
SCHIMIDT, T. C. G.	3.002	SILVA, J. B.	14.001
SCHOEPS, D. O.	4.006	SILVA, J. F.	21.009
SCHREKKER, H. S.	22.032	SILVA, J. G. B. P. C. P.	19.006
SCOP, M.	10.029	SILVA, J. I. S.	15.001
SEABRA, A. B.	8.018, 13.012	SILVA, J. M.	9.004, 17.007
SECOMANDI, V. J. K.	23.005	SILVA, J. N.	6.010, 19.001
SENA, L. S.	20.011	SILVA, J. R.	7.050
SENO, M. D. J.	10.010	SILVA, J. S.	4.011, 19.020
SEÑOS, D. L.	24.004	SILVA, J. S. O.	14.002
SEPÚLVEDA-FRAGOSO, V. ...	11.011	SILVA, J.A.	22.021
SERAFIM, S. C.	1.005	SILVA, J.R.M.C.	1.001
SERAPHIM, P. M.	11.005	SILVA, K. M.	5.002
SERIANI, R.	19.025	SILVA, K. P.	20.022
SEVERINO, M. B.	13.013	SILVA, L. A.	24.016
SIÉSSERE, S.	18.014	SILVA, L. F.	3.005
SILVA, A. C. C.	13.002	SILVA, L. L. S.	9.012, 9.013
SILVA, A. C. L.	9.003	SILVA, L. M.	24.018
SILVA, A. C. R.	3.001	SILVA, M. B.	14.002
SILVA, A. F.	7.005	SILVA, M. C.	20.022
SILVA, B. L.	4.001	SILVA, M. C. M.	13.024
SILVA, B. S.	8.002	SILVA, M. F. P.	6.007
SILVA, C. L. A.	6.002	SILVA, M. L.	20.001
SILVA, C. L. F.	7.035	SILVA, M. M.	4.011
SILVA, C. R.	20.007	SILVA, M. M. C.	16.011, 17.004
SILVA, C. S. B.	6.015	SILVA, M. U.	7.048
SILVA, C. S. C.	22.031	SILVA, N. C.	13.007
SILVA, CPL.	25.002	SILVA, P. A.	8.013, 8.016
SILVA, D. F. D.	23.013	SILVA, P. A. S.	8.006, 8.007, 8.010
SILVA, D. P. D.	22.011	SILVA, R. A.	24.007, 24.015
SILVA, E. B.	21.004	SILVA, R. A. L.	25.005
SILVA, E. P.	23.018	SILVA, R. B.	10.036
SILVA, F. C.	4.005, 22.005, 22.012,	SILVA, R. C.	8.001, 8.010, 22.006
.....	22.015	SILVA, R. H.	17.008
SILVA, F. D.	17.003	SILVA, R. P. M.	25.009
SILVA, F. M. C.	24.009	SILVA, R. T.	12.002
SILVA, G. B. O.	12.002	SILVA, S.	22.016
SILVA, G. C.	19.019	SILVA, S. C.	6.011
SILVA, G. F.	4.011, 16.011	SILVA, S. C. A.	4.015, 7.027

FeSBE Annual Meeting 2019

SILVA, S. C. D. A.	11.001, 11.00	SOUZA, A. M.	14.007
SILVA, S. P. D.	19.009	SOUZA, A. V.	6.016
SILVA, S. V.	22.031	SOUZA, C. S. F.1	17.012
SILVA, T. G.	4.004	SOUZA, D. A.	9.011, 19.026
SILVA, T. I. P.	4.002	SOUZA, D. D. C.	25.012
SILVA, T. O.	7.025	SOUZA, D. O. G.	3.006
SILVA, V. A. P.	7.047	SOUZA, F.C.	1.001
SILVA, V. S.	13.001, 13.010, 14.003	SOUZA, G. C. A.	14.001
SILVA, W. A. B.	10.012	SOUZA, G. M. A.	10.032
SILVA, W. J.	16.010, 23.007	SOUZA, G. S.	24.009, 24.011
SILVA-CUNHA, A.	24.002, 24.005, 24.017,	SOUZA, H. R.	9.002, 17.007, 17.009
.....	24.018	SOUZA, H. S. P.	20.016
SILVA-FILHO, R.C.	19.011	SOUZA, I. L. S.	10.042
SILVA-JUNIOR, R. M. P.	23.001	SOUZA, L. E.	14.007
SILVA-SILVA, J. V.1	17.012	SOUZA, L. F.	13.005
SILVA-VEIGA, FM	7.004	SOUZA, L. F. L. P.	13.003, 13.004
SILVEIRA, D.	7.037	SOUZA, L. L.	7.008
SILVEIRA, M. B.	14.004	SOUZA, LL.	25.002
SILVEIRA, P. F.	6.007	SOUZA, M. A.	19.002
SILVEIRA, W. A.	7.001	SOUZA, M. M.	1.003
SILVESTRE, J. G.	23.004	SOUZA, M. O. B.	23.014
SILVESTRE, J. G. O.	16.010	SOUZA, M. P.	22.005, 22.015
SILVESTRINI, A. V. P.	16.005	SOUZA, P. D.	22.020
SIMAO, J. J.	14.003	SOUZA, R. F.	5.001
SIMÃO, J. J.	13.001, 13.010	SOUZA, S. K.	11.015
SIMIONATO, G. B.	3.001	SOUZA, T. F. P. S.	23.018
SIMONS, S. M.	19.004	SOUZA, T. L. F.	22.015
SIMÕES, L. A. R.	1.004, 11.015	SOUZA, T. S.	10.032
SIQUEIRA, C. R. S.	22.029	SOUZA, V. S.	22.002
SIQUEIRA, F. S.	17.005	SOUZA-MELLO, V.	7.004
SIQUEIRA, R. C.	24.005	SOUZA-MELLO, V.	4.002, 7.005
SMAILI, S.	16.001	SPEGIORIM, G. C.	23.001
SOARES, B. O.	19.012	SPIESS, D. A.	6.001
SOARES, J. P. M.	22.028	STASIASKI, JE	19.019
SOGAYAR, M. C.	3.003	STEFANELLO, F. V.	18.007
SONCINI, R.	9.008	STEFANI, H. A.	17.006, 19.018
SOUGEY, W. W. D.	23.004	STEPHEN, M.	6.001
SOUSA, B. M.	23.003	STILHANO, R. S.	16.001
SOUSA, I. S. M. A.	6.012	STOCKLER-PINTO, M.B.	7.016
SOUSA, M. D. R.	24.009	STOLTZ, I. R.	19.022, 19.023
SOUSA, O. C.	11.019	STROGULSKI, N. R.	18.010
SOUSA, R. X.	22.028	STUMBO, M. B.	25.009
SOUSA, S. M.	8.014	SUANO-SOUZA, F. I.	4.006
SOUTO, A. M.	10.027	SUDO, R. T.	4.008, 4.011, 16.011,
SOUZA, A. A. P.	22.031	17.004, 17.011
SOUZA, A. B. F.	7.023, 7.026, 8.009,		
.....	9.003, 19.003	T	
SOUZA, A. F. P.	7.008	TABOGA, S. R.	6.013, 7.033

FeSBE Annual Meeting 2019

TABORDA-ROCHA, L.	19.023	TROST, ME	19.019
TAKETA, T. B.	16.007	TRUJILHO, M. N. R.	13.005, 16.006
TALIB, L.	10.031, 21.006		
TALPO, T. C.	7.024	U	
TALVANI, A.	9.007	ULLRICH, H.	13.008
TAMARINDO, G. H.	7.033		
TAMBORLIN, L.	13.013, 13.021	V	
TASHIRO, J. H.	24.012	VALE, M. I. C. A.	13.010
TASSINARI, I. D.	10.020	VALENÇA, S. S.	4.001, 8.004
TAVARES, A.	15.001	VALENTE, J. S.	7.013, 7.045
TAVARES, R. L.	7.034	VALER, F. B.	23.001
TAVARES, R.L.	7.032	VALLE, A. C.	10.032
TEIXEIRA, A. P.	25.008	VALLE, M. D.	23.010
TEIXEIRA, C.	13.007	VALVERDE, A. L.	22.006, 22.009, 22.010
TEIXEIRA, C. S.	18.008, 18.009	VALVERDE, A. P.	21.001, 21.003
TEIXEIRA, N. B.	17.008	VARGAS, GRT	25.002
TENCARTE, S. R.	24.013	VASCONCELOS, C. M. T.	7.022
TEODORO, L.F.R.	16.008	VASCONCELOS, J. M.	22.030
TEÓFILO, F. B. S.	13.026	VASCONCELOS, M. H. A.	7.034
TERCIOTTI, L. G.	21.001, 21.003	VASQUES, J. F.	16.011
TERRA, A. M.	10.028, 25.012	VASSALLO, D. V.	4.012, 4.014, 19.015,
THOMASI, B. B. M.	25.012	19.017
THOMAZINI, M. E. O.	13.006	VASSALLO, DV	19.019
TIBÉRIO, I F L C.....	4.003	VAZ, B.	10.032
TIBÉRIO, I. F. L. C.	9.011, 9.012	VAZ, L. C.	10.030
TIBÉRIO, I.F.L.C.	9.009, 9.013	VEIGA, F. C.	23.012, 23.020
TIBÚRCIO, J. P. S.	7.022	VEIGA, F. M. S.	7.007
TIETBOHL, L. A. C.	19.014	VELLOSO, J. C. C.	13.008
TIKASAWA, P. S. A.	24.007	VELOSO, M. P.	13.014
TIRAPELLI C.R. T.....	4.017	VENDRAME, R. F. A.	6.007
TIRAPELLI, C. R.	4.019	VENETUCCI, F.	10.010
TOBIAS, G. C.	22.038	VENTURA D. F.	24.003
TOMA, L.....	22.008	VENTURA, A. L. M.	13.008
TOMAZ, B. C.	14.004	VENTURA, B. H.	3.008
TONON, A. C.	3.005, 3.006	VENTURA, D. F.	24.001
TONON, A. P.	22.004	VENTURA, D. V.....	24.012
TORICELLI, M.	10.007, 18.003	VENTURA, J. V.	10.017
TORICELLI, M. P.	10.008	VENTURINO-PEREZ, P.	4.021
TORQUETI, A. M. R.	23.006	VERAS, M. M.	19.020, 19.025
TORRES, V. M.	25.008, 25.009	VERCESI, A. E.	13.026, 21.007
TORREZAN, M.	13.002	VETTORAZZI, J. F.	7.036
TRAJANO, A. P.	19.024	VIANA, L. R.	4.018
TRAPP, M.....	7.037	VICTORIO, J. A.	4.020
TRAVASSOS, L. R.	22.002, 22.003,22.004,	VIDAL, I. S. A. B.	23.026
.....	22.029	VIDIGAL, C. B.	19.008
TREVENZOLI, I. H.....	7.003, 7.006	VIEIRA, C. P.	11.011
TREVENZOLI, IH	7.010		
TRINDADE, D. J.	7.029	VIEIRA, J. S.	20.001

FeSBE Annual Meeting 2019

VIEIRA, L. C.	24.018	YAN, C. Y. I.	16.010
VIEIRA, L. D.....	8.014, 8.017	YARIWAKE, V. Y.	19.020
VIEIRA, L.D.....	8.012	YONAMINE, C. M.	18.005
VIEIRA, P. C.	13.022	YOSHIKAWA, A. H.	9.004, 17.009
VIEIRA, V. A.	7.048		
VIEL, T, A.....	18.003	Z	
VIEL, T.....	10.009	ZACARIAS, C. A.	13.011
VIEL, T. A.....	10.007	ZANELLA, A. P.	6.005
VIEL, T.....	10.006	ZANELLA, B. T. T.	1.002, 7.013, 7.045
VIEYRA, A.....	8.013	ZANON, N. M.	7.001
VIEYRA, A.	8.011, 8.012, 8.016,	ZAPATA-SUDO, G.	4.011, 16.011, 17.004
.....	8.017, 22.020, 23.019	ZAPATERINI, J. R.	7.021
VIGANÓ, L.B.	13.018	ZATZ, M.	24.016
VILAMAIOR, P. S. L.	6.004, 6.013, 7.033	ZAVAN, B.	7.028
VILELA, F. C.....	20.001	ZIANI, P. R.	18.007
VILLARINHO, N.	22.016	ZIMMER, A. R.	7.012
VINAGRE, A. S.	1.004, 11.015	ZIN, W. A.....	19.024
VINOLO, M. A.	21.005	ZORN, T. M. T.	6.015
VINOLO, M. A. R.	7.050	ZORZANELLI, B. C.	22.012
VISIOLI, F.	13.016	ZUCÃO, M. I.	6.013, 7.033
VISNIAUSKAS, B.	8.005		
VITORINO, L. C.	10.012		
VIZIN, R. C. L.	3.004		
VOGT, É. L.	1.004, 7.030, 7.042,		
.....	11.015		
VOLTARELLI, V. A.	11.006, 11.018		
W			
WAGHABI, M. C.	13.022		
WAJSENZON, I. J.	10.012		
WALTER, L. T.	10.015		
WANG, D.	7.025, 16.010		
WANG, H.	7.002		
WASIELESKY W. J.	16.004		
WERMELINGER, G. F.	22.005, 22.006, 22.010		
WIGGERS, G. A.....	4.014		
WIGGERS, G.A.....	6.003		
WIGGERS, GA	19.015, 19.019		
WINK, M. R.	22.030		
WITTEE, E. L. C.	7.022		
WOYAMES, J.	7.008		
X			
XAVIER, G. G. A.	12.005		
XAVIER, N. B.	3.005		
XENOFONTE, R. S. C.	18.011		
Y			
YAMADA, E. S.	24.010		